Annulated Quinoline- and Quinoxaline-Functionalized NHC- Ru(II)-Complexes: Catalytic Evaluation towards the C-H Bond Activation, Oxidation of Olefins and Annulation Reactions

A dissertation submitted to the

Indian Institute of Technology Guwahati

in partial fulfilment for the degree of

Doctor of Philosophy

Submitted by

Monuranjan Konwar

Roll no.: 186122020

Supervisor: Dr. Animesh Das

Department of Chemistry

Indian Institute of Technology Guwahati

Guwahati, Assam-781039

TH-3565_186122020

TH-3565_186122020

Dedicated

To

My Mother

TH-3565_186122020

INDIAN INSTITUTE OF TECHNOLOGY GUWAHATI
Department of Chemistry
Guwahati, Assam-781039, INDIA

STATEMENT

I, hereby declared that the work comprised in this thesis entitled "***Annulated Quinoline- and Quinoxaline-Functionalized NHC- Ru(II)-Complexes: Catalytic Evaluation towards the C-H Bond Activation, Oxidation of Olefins and Annulation Reactions***" is the outcome of the research work carried out by me under the supervision of **Dr. Animesh Das, Department of Chemistry, Indian Institute of Technology Guwahati, India**, for the award of the degree of Doctor of Philosophy.

In harmony with the general practice of reporting scientific observations, due acknowledgements have been made if the work is established on the findings of other investigators.

Monuranjan Konwar

Guwahati
September, 2024

Monuranjan Konwar
Roll No: 186122020
Department of Chemistry
IIT Guwahati, Assam, India-781039

TH-3565_186122020

INDIAN INSTITUTE OF TECHNOLOGY GUWAHATI
Department of Chemistry
Guwahati, Assam-781039, INDIA

Dr. Animesh Das,
Associate Professor, Department of Chemistry

E-mail: adas@iitg.ac.in
Phone: +91-361-2583478

CERTIFICATE

This is to certify that the work incorporated in the thesis entitled "***Annulated Quinoline- and Quinoxaline-Functionalized NHC- Ru(II)-Complexes: Catalytic Evaluation towards the C-H Bond Activation, Oxidation of Olefins and Annulation Reactions***" which is being submitted to the Indian Institute of Technology Guwahati for the award of Doctor of Philosophy in Chemistry by **Mr. Monuranjan Konwar** (Roll No: 186122020) was carried out by him under my supervision at this institute. The work presented in his thesis is original and that has not been submitted elsewhere for a degree.

Guwahati
September, 2024

Dr. Animesh Das
(Thesis Supervisor)
Associate Professor
Department of Chemistry
IIT Guwahati, Assam, India-781039

TH-3565_186122020

TH-3565_186122020

Acknowledgements

I would like to extend my heartfelt gratitude to all the wonderful people who have supported and helped me directly or indirectly throughout my PhD journey. Without their contributions, this thesis would not have become a reality.

First and foremost, I would like to extend my deepest respect and sincere gratitude to my supervisor Dr. Animesh Das for his guidance, constant encouragement, unstinting inspiration and amicable cooperation during my thesis work. I owe special gratitude to him for introducing me to the field of organometallic chemistry. I am constantly motivated by his commitment to research and hard effort to get through challenging times and to complete my work. I express my deepest respect to him not only for his guidance throughout my PhD career but also for his motivation and inspiration toward my future endeavours. I am also grateful to Madam Dr. Manideepa Saha for her constant support and encouragement.

I would like to acknowledge all my doctoral committee members Prof. Chandan K. Jana (Chairman), Dr. Shyam P. Biswas and Dr. Krishna Pada Bhabak for their timely evaluation, insightful comments and valuable suggestions which helped me to improve my research work. I also want to thank Dr. Pavan K. Kancharla for his valuable advice on improving my thesis work. I would like to thank Prof. Jubaraj B. Baruah, Prof. Biplab Mondal, Prof. Subhendu S. Bag and Prof. Subhas C. Pan for the informative and interesting courses they taught me as a part of my coursework. I also extend my thanks to all other faculty members of the Department of Chemistry for their help and support.

I am grateful to Dr. Babulal Das and my friends Sandeep Kumar and Somnath Paik for helping me analyze the single crystal XRD data for publication. I also thank Mr. Imdadul Islam and all the NMR operators for promptly recording my NMR data whenever I made an urgent request for it. I also want to thank all the non-teaching staff of our department for their cooperation and help during my research work. My sincere thanks to all the staff of Central Instrument Facility (CIF), North East Centre for Biological Sciences and Healthcare Engineering (NECBH), IIT Guwahati, especially to Mr. Bhashkar for HRMS analysis, and all the student operators for the instrumental facilities required for my research. I sincerely acknowledge IIT Guwahati for the financial support without which it would have been very difficult to complete my work.

I am extremely fortunate to have talented, enthusiastic and friendly lab mates during my PhD tenure. I am very much grateful to my seniors Dr. Bikash Kumar Sarmah and Dr. Dipanjan Bhattacharyya for mentoring me during the initial phase of my research period. I would like to extend my special thanks to Dr. Bikash Kumar Sarmah, who has guided and instructed me on everything from cleaning glass apparatus to setting up extremely delicate reactions. I sincerely thank our post-doctoral fellow Dr. Sekhar Nandi for his guidance and valuable advice. I am extremely grateful to my colleague Priyanka Adhikari for all of her assistance, support, and talks, which made even my unproductive days far easier than they could have been. I have some wonderful lab juniors Siddhartha, Rahul, Kritartha, Nitumoni, Kamal, Tapashi, Asish, Anit, Nitish, Manash and Sonali. I want to thank all of them for their love, support, and cooperation and for creating a homely atmosphere inside the lab. In particular, I would like to

TH-3565_186122020

acknowledge Nitumoni Hazarika for his constant support and help, without which it would have been impossible to finish my work properly. I also wish to thank all the project students Nand Kishor, Dipankar, Ranjit, Shivani, Ramakant, Vivek, Himanshu, Pallab, Nayan, Soumya, Arpan, Mayur and Neel. I would like to mention Shivani Rathi and Vivek Kumar Agrahari, especially for their help in my research work.

I am grateful to all of my teachers for their contributions to my education at different stages. Without them, I would not have been able to reach this stage of life. I would like to thank all of my teachers at Dhemaji Higher Secondary School, Salt Brook Academy, Cotton College and Tezpur University for their contributions to my passion for Chemistry.

I want to express my gratitude to my childhood and school friends. Especially I want to acknowledge school friends Palash, Manuranjan, Sarag, Kalpa, Debapatim, Bitul, Sankar, Manuj, Prasanta, and Bitupan; College friends Krishna Kanta, Himadri, Raja, Krisangi, Sikha, Pranajl, Partha, Manisha, Shilpa, and Manash. I acknowledge all my PhD batchmates; Rahul, Shankhadeep, Sagnik, Sandeep, Vinay, Bittu, Samir, Rinki, Sabina, Debojyoti, Chan, Indraneel, Tirupati, Hrishikesh, Tanumoy, Sujay, and Sourav for making my days memorable in IITG. I also want to thank my seniors, colleagues, and juniors, especially Chiranjib da, Monikha baa, Jinnat di, Tushar da, Raj da, Sounak da, Sulendar da, Debojit da, Shubhomoy da, Nikita ba, Namita baa, Nimisha baa, Partha da, Raktim, Gunanka, Barsha, Dipankar and Abhijeet.

I have some wonderful people in my life who have always supported me at difficult times, and words cannot explain how much I appreciate them. I deeply thank Bikoshita, Rabu, Mrinmoy, Rajdikshit, Suravi, Sanjib, and Prangovinda from the core of my heart.

My heartfelt gratitude goes to my mother (maa), my late father (deta), sister (baa), brother (bhaiti), and brother-in-law (vindeo) who have always supported and motivated me through all of my ups and downs. Without their good wishes, immense patience, and great sacrifice, I would have not been able to complete my doctoral studies. Thank you, Maa, for all the unconditional love, and sacrifices you made. I express my great respect for my uncles and aunts, especially Bhaskar mama for their love and support. It would be unfair if I do not mention the names of my cousins Juri, Monikha, Abhigyan, Pragyashree, Amilee, Pratiksha, and Kalpa. Without their well wishes and blessings, I would not have been able to reach this stage and complete my doctoral studies. I would like to express my greetings to all my relatives and other family members.

It's tough to fit all the names into a single paper; any absence in this brief acknowledgment does not imply a lack of appreciation.

Finally, I bow down to the almighty God for blessing, protecting, and guiding me throughout this period. I could never have accomplished this without the faith I have in the almighty.

Sincerely,
Monuranjan

TH-3565_186122020

TH-3565_186122020

Table of Contents

		Page No.
Chapter 1	***A Brief Introduction to Cyclometalated Complexes and its Application in Organic Synthesis***	1
	1.1. Cyclometalated complexes	2
	1.2. Fundamental principles	2
	1.3. Mechanistic aspects of cyclometalation	5
	1.4. Synthesis of different cyclometalated complexes	6
	1.4.1. Cyclometalated palladium complexes	6
	1.4.2. Cyclometalated rhodium complexes	8
	1.4.3. Cyclometalated ruthenium complexes	11
	1.4.3.1. C^P type ruthenacyclo complexes	12
	1.4.3.2. C^N type ruthenacyclo complexes	12
	1.4.3.3. C^C type ruthenacyclo complexes	16
	1.5. Catalytic application of cyclometalated ruthenium complexes	18
	1.5.1. Amidation of alcohol	18
	1.5.2. *N*-alkylation of amines	19
	1.5.3. (Transfer)hydrogenation reaction	20
	1.5.4. Alcohol oxidation	22
	1.5.5. C–H activation/annulation reactions	23
	1.6. Summary	25
	1.7. Objective and outline of this thesis	26
	1.8. References	29
Chapter 2	***Selective Oxidation of N-Substituted Tetrahydroquinolines to Lactams by Cyclometalated Ruthenium Catalysis***	35
	2.1. Introduction	36
	2.2. Design strategy	39
	2.3. Results and discussion	40
	2.3.1. Synthesis and characterization of cyclometalated ruthenium complexes	40
	2.3.2. Optimization of reaction conditions	42
	2.3.3. Substrate scope	45
	2.3.4. Post-synthetic modification	49
	2.3.5. Scale-up reaction	49
	2.3.6. Mechanistic investigation	50
	2.3.6.1. Radical trapping experiment	50
	2.3.6.2. Isotope labeling experiment	51
	2.3.6.3. Deuterium scrambling experiments	51
	2.3.6.4. Kinetic Hammett studies	52
	2.3.6.5. Kinetic Isotope Effect (KIE) studies	52
	2.3.6.6. Spectroscopic characterization of intermediate	53
	2.3.6.7. Role of water in oxidation reaction	54
	2.3.7. Computational studies	55
	2.4. Summary	57

TH-3565_186122020

	2.5. Experimental section	57
	2.6. References	108
Chapter 3	***Cyclometalated Ruthenium Complex as a Highly Efficient Catalyst for Selective Oxidative Cleavage of Olefins to Carbonyls***	112
	3.1. Introduction	113
	3.2. Present work	115
	3.3. Results and Discussion	116
	3.3.1. Synthesis and characterization of cyclometalated ruthenium complexes	116
	3.3.2. Optimization of reaction conditions	118
	3.3.3. Efficiency of the catalytic reaction	123
	3.3.4. Scope of the reaction	125
	3.3.5. Impact of annulated backbone in the catalysis	130
	3.3.6. Mechanistic investigation	131
	3.3.6.1. Effect of added para-cymene and different arenes	131
	3.3.6.2. Spectroscopic characterization of active catalyst **Ru-1-I1**	133
	3.3.6.3. Spectroscopic characterization of high-valent ruthenium(VI)-dioxo species	134
	3.3.6.4. UV-Vis spectroscopic studies for the metallacycle species	138
	3.3.7. Kinetic studies	139
	3.3.8. Computational studies	143
	3.3.9. Proposed mechanism	144
	3.4. Summary	145
	3.5. Experimental section	145
	3.6. References	195
Chapter 4	***Ruthenium(II)-Catalyzed Oxidative C-H Activation/Alkyne Annulation Using Quinoline-Functionalized NHC as a Directing and Functionalized Group***	198
	4.1. Introduction	199
	4.2. Present work	201
	4.3. Results and discussion	201
	4.3.1. Optimization of reaction conditions	201
	4.3.2. Substrate scope	205
	4.3.3. 1 mmol scale reaction	209
	4.3.4. Post-synthetic modification	210
	4.3.5. Photophysical properties	210
	4.3.6. Mechanistic investigation	211
	4.3.6.1. Proof of intermediate **Ru-1**/**Ru-5** in the catalytic cycle	211
	4.3.6.2. Insertion of alkyne into M−C bonds of **Ru-1**/**Ru-5**	212
	4.3.6.3. Proof of ruthenium(0) sandwich species **Ru-6** in the catalytic cycle	213
	4.3.6.4. Kinetic studies	215
	4.3.7. Proposed mechanism	218
	4.4. Summary	219
	4.5. Experimental section	219
	4.6. References	289

TH-3565_186122020

Chapter 5	***Carboxylic Acid Assisted Ru(II)-Catalyzed Annulation of Imidazo[1,5-a]quinoline with Alkynes via Double C−H Activation: A Direct Route to Functionalized Quinolizines***	292
	5.1. Introduction	293
	5.2. Present work	294
	5.3. Results and Discussion	295
	5.3.1. Optimization of reaction conditions	295
	5.3.2. Substrate scope	297
	5.3.3. Post-synthetic modification	300
	5.3.4. Recyclability and reusability of the catalytic system	301
	5.3.5. Photophysical properties	302
	5.3.6. Mechanistic investigation	305
	5.3.6.1. Control experiments	305
	5.3.6.2. Proof of intermediate **Ru-8** in the catalytic cycle	306
	5.3.6.3. Proof of protonated imidazo-quinolinium salt as an intermediate in the catalytic cycle	307
	5.3.6.4. Interaction of imidazoquinoline with carboxylic acid	307
	5.3.6.5. Kinetic studies	308
	5.3.6.6. Determination of regioselectivity of alkyne insertion into M−C bonds	309
	5.3.7. Proposed mechanism	310
	5.3.8. Computational studies	311
	5.4. Summary	312
	5.5. Experimental section	312
	5.6. References	349
Annexure I	***Selected ^{1}H and ^{13}C NMR spectra of the products (Chapter 2)***	353
Annexure II	***Selected ^{1}H and ^{13}C NMR spectra of the products (Chapter 3)***	361
Annexure III	***Selected ^{1}H and ^{13}C NMR spectra of the products (Chapter 4)***	386
Annexure IV	***^{1}H, ^{13}C and ^{19}F NMR spectra of the products* (Chapter 5)**	392
Annexure V	***The Cartesian coordinates (xyz) for all the optimized structures (Chapter 2)***	416
Annexure VI	***The cartesian coordinates (xyz) for all the optimized structures (Chapter 3)***	437
Annexure VII	***The cartesian coordinates (xyz) for all the optimized structures (Chapter 4)***	446
Annexure VIII	***The cartesian coordinates (xyz) for all the optimized structures (Chapter 5)***	456
	List of Publications	465
	List of Conferences	466

TH-3565_186122020

List of abbreviations

Ac	Acetyl
α	Alpha
Å	Angstrom
Ar	Argon
ACN	Acetonitrile
AIE	Aggregation-induced emission
*a*NHC	Abnormal *N*-heterocyclic carbene
APEX	Annulative π-extension
br.	Broad
β	Beta
BDE	Bond dissociation energy
BHT	Butylated hydroxytoluene
Bn	Benzyl
BTHQ	*N*-benzyl tetrahydroquinoline
Bu	Butyl
CCDC	Cambridge Crystallographic Data Centre
$CDCl_3$	Chloroform-*d*
CHEQ	Chelation enhanced quenching
CMD	Concerted metalation-deprotonation
Cy	Cyclohexyl
Cat.	Catalyst
^oC	Degree Celsius
d	Doublet or day
dd	Doublet of doublet
DFT	Density functional theory
DG	Directing group
3,4-DHQ	3,4-Dihydroquinoline-2(1*H*)-one
DKIE	Deuterium kinetic isotope effect
EtOAc	Ethyl acetate
equiv.	Equivalent
ESI	Electrospray ionization
Et	Ethyl
EWG	Electron withdrawing group
EDG	Electron donating group
g	Grams
GC-MS	Gas chromatography-mass spectrometry
γ	Gamma
h	Hours
HOMO	Highest occupied molecular orbital
HRMS	High-resolution mass spectrometry

TH-3565_186122020

Hz	Hertz
MHz	Mega Hertz
i	Iso
ImQ	Imidazo[1,5-*a*]quinoline
ImQx	Imidazo[1,5-*a*]quinoxaline
FT-IR	Fourier transform infrared spectroscopy
J	Coupling constant
m	Multiplet
m	Meta
mg	Milligram
mL	Millilitre
mmol	Millimole
µw	Microwave
Mp	Melting point
LUMO	Lowest unoccupied molecular orbital
NHC	*N*-heterocyclic carbene
NMR	Nuclear magnetic resonance
o	Ortho
ORTEP	Oak ridge thermal ellipsoid plot program
p	Para
PEG	Polyethylene glycol
Ph	Phenyl
Py	Pyridine
Pr	propyl
ppm	Parts per million
q	Quartet
rt	Room temperature
s	Singlet
SET	Single electron transfer
TH	Transfer hydrogenation
THF	Tetrahydrofuran
TEMPO	2,2,6,6-tetramethyl-1-piperidinyloxy
t	Tert
THQ	Tetrahydroquinoline
TLC	Thin layer chromatography
TMS	Tetramethylsilane
TOF	Turnover frequency
TON	Turnover number
TS	Transition state
UV	Ultraviolet
XPS	X-ray photoelectron spectroscopy
XRD	X-ray diffraction

TH-3565_186122020

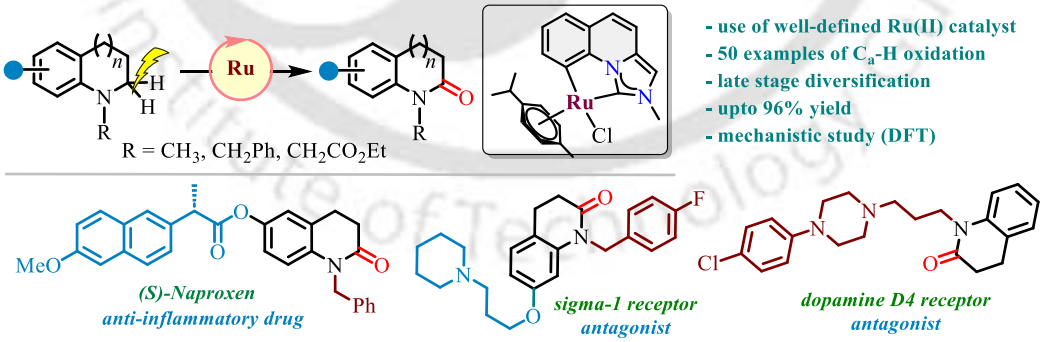
Abstract

The present thesis, entitled ***"Annulated Quinoline- and Quinoxaline-Functionalized NHC-Ru(II)-Complexes: Catalytic Evaluation towards the C-H Bond Activation, Oxidation of Olefins and Annulation Reactions"*** is divided into five chapters based on the results obtained from the experimental works performed during the complete course of the PhD research period.

Chapter 1 contains a brief overview of the diverse and rich chemistry of cyclometalated complexes. The synthesis, properties, reactivity, and application of these cyclometalated complexes in the catalytic fields are elaborately discussed. Especially the basic properties of C_{NHC}^C type ruthenacyclo complexes, their mechanism in catalytic reactions, and potential applications have been briefly presented.

Each of the following chapters (Chapter 2 to Chapter 5) contains an introduction, previous literature reports, present results and discussion, experimental section, and references along with the characterization data of the products including spectral data of the newly synthesized molecules.

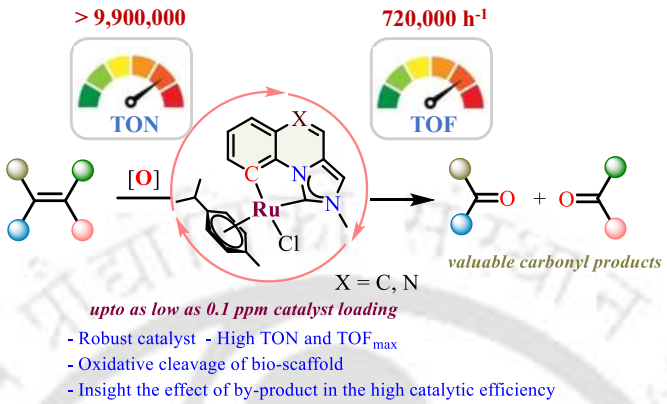
Chapter 2 reports a new rigid π-conjugated fused imidazo[1,5-*a*]quinoline (ImQ)-based cyclometalated ruthenium complex and its catalytic utility for selective oxidation of *N*-substituted tetrahydroquinolines to lactams. In the presence of α-methyl or reactive α-methylene C–H bonds, cyclic-α-methylene C–H bonds were selectively oxidized. This methodology has been successfully utilized in the late-stage functionalization and diversification of pharmaceuticals. The mechanistic study demonstrates that high-valent Ru(VI)-*cis*-dioxo species plays an important role in controlling selectivity. Detailed experimental and theoretical studies have been carried out to elucidate the reaction mechanism with the help of the deuterium kinetic isotope effect, kinetic Hammett studies, and DFT studies.



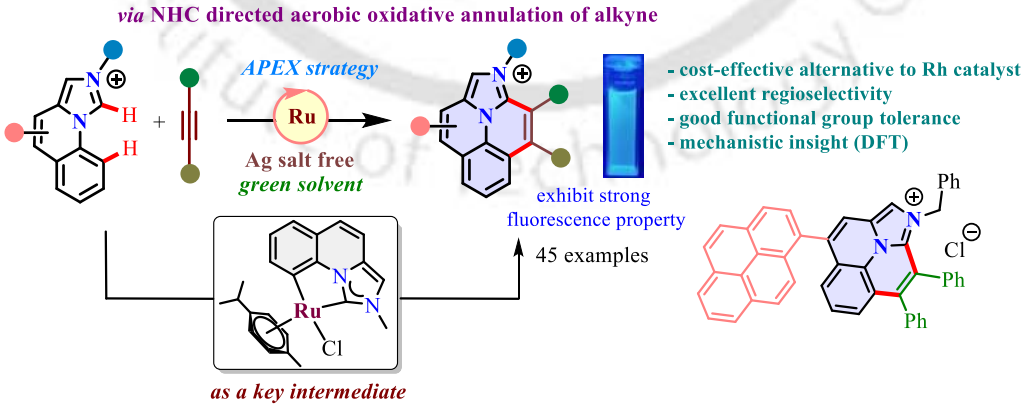
Chapter 3 demonstrates a highly efficient imidazo[1,5-*a*]quinoline (ImQ) and imidazo[1,5-*a*]quinoxaline (ImQx)-based cyclometalated ruthenium catalysts for olefin oxidation reactions. A strong σ-donating ability of both the carbanion donor site and NHC, paired with the rigid backbone and redox activity of ruthenium provided exceptionally high catalytic activity and a long lifetime for oxidative cleavage of olefin to the carbonyl compounds. Complex shows outperforming state-of-the-art systems reach turnover frequencies of 720000 h^{-1} and turnover numbers of several million. The catalyst tolerates numerous functional groups and applies to

TH-3565_186122020

challenging biomass, natural products, sugar, amino acid, and fatty acid-derived substrates. Based on kinetic studies, thermodynamic activation parameters, and DFT study, the mechanistic finding demonstrated that [3+2] cycloaddition reaction is the key step in the oxidation process. The effect of the by-product $NaIO_3$ in the unprecedented catalytic efficiency has been disclosed for the first time herein.



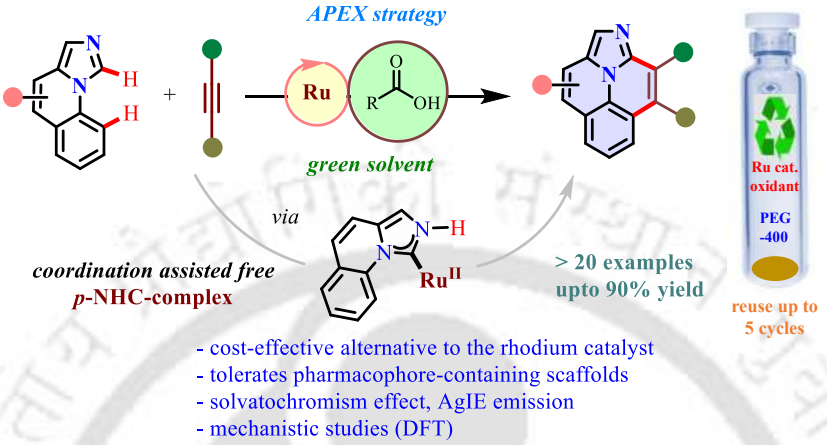
Chapter 4 describes the reactivity of the ImQ-based cyclometalated Ru(II)-complex **Ru-1**. The complex **Ru-1** is found as a key intermediate in the catalytic oxidative annulation reaction of imidazo[1,5-*a*]quinolin-2-ium salts with alkynes *via* *N*-heterocyclic carbene-directed C–H activation. Molecular oxygen has been explored as an economic and clean oxidant, an alternative to metal oxidants. The current protocol exhibits a wide range of substrate scope including bioactive (±)-*α*-tocopherol derivatives. Moreover, most of the products show strong fluorescence properties indicating their potential for making new light-emitting materials. Based on several control experiments, deuterium-kinetic isotope effect, and thermodynamic activation parameters the mechanistic finding demonstrated that fused imidazo-[1,5-*a*]quinolin-2-ium C(2)−H bond cleavage is the rate-determining step and ruling out the possibility of reductive elimination for controlling the rate of reaction. Furthermore, DFT calculation is also performed to support the proposed mechanism.



Chapter 5 reports a Ru(II)-catalyzed oxidative annulation of imidazo[1,5-*a*]quinoline with alkynes *via* double C−H activation to produce highly functionalized quinolizines where the key to the successful conversion is the addition of carboxylic acid as an additive. This reaction featured high efficiency and a relatively wide substrate scope, further has been successfully

TH-3565_186122020

utilized in the late-stage functionalization and diversification of annulated products. The reaction is highly chemoselective and regioselective. In addition, the use of biomass-derived solvent as a reaction medium, the catalyst can be recycled after five reaction cycles without loss of catalytic activity. Interestingly, most of the annulated products exhibit intense fluorescence emission at a broad range and their photophysical property could be tuned by restricting the intramolecular motion in aqueous media and showing AIE-active properties.



TH-3565_186122020

Chapter 1

A Brief Introduction to Cyclometalated Complexes and its Application in Organic Synthesis

TH-3565_186122020

1.1. Cyclometalated complexes

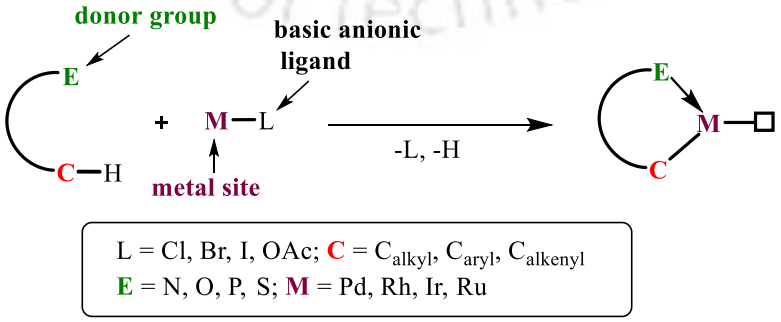
Cyclometalated complexes are organometallic compounds with a metal-to-carbon σ-bond stabilized by chelation brought about by intra-molecular coordination of the metalating organic ligand to the metal center. Since their first isolation in the mid-1960s, the scope and interest in these compounds have diversified into different areas including organic synthesis, catalysis, material science and life sciences.[1] Their rich reaction chemistry, metallomesogenic, and intriguing photo-physical properties have provided further impetus to the progress of this field.[2–4]

Kleiman and Dubeck isolated the first cyclometalated compound by the reaction of Cp_2Ni with azobenzene at 135 ºC.[5] Soon after, Cope and Siekman carried out the related reaction of azobenzene with $PdCl_2$ in methanol and K_2PtCl_4 in the dioxane-water mixture and obtained binuclear cyclometalated complexes.[6] These developments laid the foundation of one of the most important families of organometallic compounds.

Internally functionalized organic compounds containing neutral donor atoms (e.g. N, O, S, P, etc.) have been used for cyclometalation reactions leading to the formation of either four-electron bidentate or six-electron tridentate pincer C-anionic donor ligands. Cyclometalation is strongly preferred if the ligand forms five- or six-membered rings. Compounds with 3- and 4-membered cyclometalated rings are often unstable, while those with more than 6-membered rings can easily undergo reductive elimination.[7] In metalation reactions, aromatic sp^2 C−H bond activation is favoured over sp^3 C−H bonds. Ligands with lighter donor atoms are more easily cyclometalated than ligands with heavier hetero-donors.[8]

1.2. Fundamental principles

Cyclometalation reaction is usually involved in a two-step sequence. At first, the ligand is coordinated to the metal center by a hetero atom E (E = N, O, P, S, Se). This causes to alter the electron density at the metal center and aids to activate the C−H bond. The C−H bond of the coordinated ligand gets activated only when it falls within the metal coordination plane. A consequence of this C−H activation is closing the ring *via* the formation of a metal-to-carbon σ-bond. For a successful cyclometalation reaction, the metal precursor, the donor site E, and the C−H bond are also important.[9]



Scheme 1.1. Synthetic strategy for cyclometalation reaction

TH-3565_186122020

i) Use of metal precursor in cyclometalation reaction

The first step of cyclometalation, i.e., coordination of (hetero)atom to the metal center is possible only when the metal precursor provides an accessible site for bonding *via* M−E primary ligand interaction.[1a] Various types of metal precursors are known for bonding with the donor site E. They are mainly classified into three categories (i) In the presence of donor group, polymeric or dimeric complexes can easily be cleaved into monomeric species, e.g., [Ru (*p*-cymene)Cl_2]$_2$, [MCl(cod)]$_2$ (M = Ir, Rh); (ii) metal precursors having labile ligands such as [$PdCl_2$(NCMe)$_2$], [$PtCl_2$(SEt_2)$_2$] or [Ir(PPh_3)$_2H_5$]; (iii) -ate complexes, such as K_2PdCl_4 or K_2PtCl_4, in which one of the anionic ligands is easily replaced by a neutral ligand.[7,10]

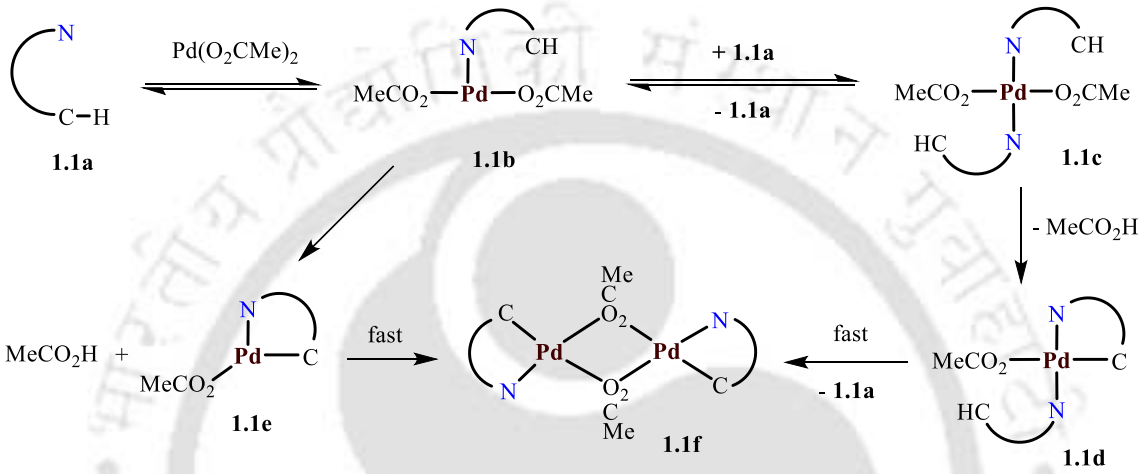
In the second step of cyclometalation, a strongly basic ligand at the metal center helped to activate the C−H bond.[10a] For instance, metal-bound halide, hydride, alkyl, alkoxide, and amide ligands considerably facilitate to activate the C−H bond by abstracting a proton from the metal-bound source and forming relatively less reactive hydrogen halide, hydrogen, alkane, alcohol, amine, respectively. One of the most studied ligands for cyclometalation reactions is the acetate (AcO^-) ligand as the AcO^- ligand has a flexible coordination mode and it can help to generate a vacant coordination site at the metal center.[7] Furthermore, weak conjugated acetic acid is formed in the C−H bond activation process, which does not interfere with the formed C−M bond. A cyclic transition state may also form by the bridging acetate ligand involving the metal center *via* one oxygen from the acetate group and the interaction of the other oxygen with the C−H bond of the ligand. This arrangement brings the metal close to the carbon and is involved in the C−H bond activation process.[11] Apart from these steric considerations, an electron density transfer occurs, since an increase of C–H•••O interaction weakens the C–H bond and concomitantly enhances the partial negative charge at the carbon center. Simultaneously, the M–O bond strength decreases and the C–O bond order increases which generates a more electropositive metal center. Finally, the C–H bond breaks, and the electron-deficient metal center forms a bond with the carbon center and forms a cyclometalated complex.

ii) Effect of the donor group E in cyclometalation reaction

In cyclometalation reaction, the influence of donor group E can be categorized based on its basicity and steric impact. The donor group generally follows the hard-soft acid-base principles described by Pearson.[12] When the donor atoms are hard, such in alkoxides, aryloxides, or amines, cyclometalation with high-valent early transition metals is most productive. On the other hand, soft transition metals, commonly the platinum group (Pt, Pd, Rh, Ru, Ir, and Os), prefer to bind with the phosphines and sulfides as soft Lewis bases. Contrary to this idea, there are several examples known in cyclometalation where relatively soft donor atoms bind with the hard metals (e.g., pyridine in zirconium (IV),[13] hard amine donors bind with soft palladium (II)).[14] On account of these mismatches, a novel kind of cyclometalation called the trans-cyclometalation reaction was developed where one ligand is exchanged with another ligand in the cyclometalation process. The process involves concurrent M–C bond making and M–C bond breaking. In the first step of the cyclometalation process, the metal precursor coordinates with the ligand **1.1a** through the donor atom to afford the complex **1.1b** (Scheme 1.2).[15,16]

TH-3565_186122020

Another donor group **1.1a** can coordinate to the vacant coordination site of complex **1.1b**, resulting in stable dimer-type coordination complexes **1.1c**. Cyclometalation takes place by removing weak conjugated acetic acid from **1.1c** to generate the complex **1.1d**. The coordinatively unsaturated complex **1.1e** can also be formed by abstracting a proton by the acetate anion from **1.1b**. If the M–E bond is very strong and stable, it hampers the ligand dissociation from complex **1.1c**, while a weak bond also shifts the equilibrium toward the right. The strength of the M–E bond is determined by both steric and electronic factors, and the relative importance of these elements may vary based on the nature of the donor group E.



Scheme 1.2. Mechanism of transcyclometallation process

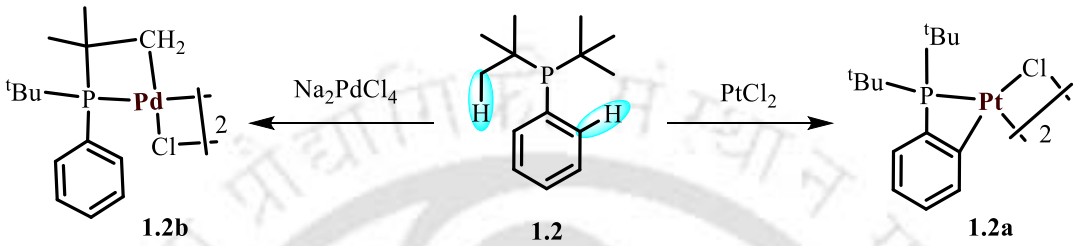
Steric factors largely affect the coordination of donor sites to the metal center. Large N-substituents in the amine as a donor site weaken the coordination ability of the metal center. For example, dimethylamino group (E = NMe_2) is particularly suitable for coordination, while NEt_2 groups coordinate more weakly and higher homologues groups like N^iPr_2 are unable to coordinate with the metal center due to the large shielding effect of the nitrogen atom.[17] Cyclometalation of primary amine-containing ligands is well-known in palladium chemistry. In contrast, soft donors like phosphines can effectively undergo metal coordination even when bulky substituent groups like P^tBu_3 are present.[18] In 1980, Shaw first identified the advantageous role of the steric bulky group in phosphorus where cyclometalation is favored by the sterically demanding phosphines because of the enthalpic and entropic factors.[19]

iii) Effect of the C–H bond in cyclometalation reaction

In the cyclometalation reaction, a five-membered ring is formed preferentially in a regioselective manner. This preference allows for predicting the five-membered product formation to a certain extent. If there is no possibility of the formation of the five-membered ring, both four- and six-membered metallacycles are formed in the cyclometalation reaction.[20] Examples of the smallest metallacycle, which consists of three atoms, have been also well-known and well-characterized.[13] On the other hand, up to eight-membered cyclometalated complexes are known in the literature.[21]

TH-3565_186122020

The effect of the C–H bond plays a crucial role in the cyclometalation process. In general, the activation of aromatic C(sp^2)–H bonds is preferred over C(sp^3)–H bond activation. Selectivity can be altered by the nature of the metal center and its auxiliary ligands. For example, cyclometalation of the phosphine PPh^{t}Bu$_2$ group with Pt(II) forms the four-membered *C,P*-metallacycle **1.2a** by the activation of C$_{aryl}$–H bonds,[22] but it also produces the palladacycle **1.2b** through the activation of C$_{alkyl}$–H bonds with Na_2PdCl_4 (Scheme 1.3).[23] The aromatic protons have higher kinetic lability than the protons in alkanes and alkenes, therefore C$_{aryl}$–H activation is frequently observed in the cyclometalation process.



1.2b **1.2** **1.2a**

Scheme 1.3. Reactivity of PPh^{t}Bu$_2$ with different metal center

By introducing substituent groups near the C–H bond, one can modify the lability of the C–H bond. If we introduce electron-withdrawing substituents in the *α*-position, the acidity of the C–H bond increases. Similarly, adding donor substituents at the arene ring facilitates a cyclometalation process that proceeds *via* an electrophilic C$_{aryl}$–H bond-activation mechanism.[1a,24] Steric congestion also plays an important role in the C–H bond activation process. There are several C–H bond activation processes are reported in which the ^{t}Bu group is located in close proximity to the metal center and this highly preorganized arrangement favours the C–H bond activation process by lowering the entropies of the system.

1.3. Mechanistic aspects of cyclometalation

Several outstanding pieces of literature have provided an overview of some of the mechanistic details of C–H bond activation in the cyclometalation process.[1a,24–26] Cyclometalated compounds can be prepared by several methods (i) adding low-valent metal complexes through oxidative addition, (ii) performing transmetalation reactions, and (iii) *σ*-bond metathesis. The most common method for synthesizing cyclometalated complexes is by C−H activation techniques. Acetate and carbonate group (CO_3^{2-} or $M'CO_3^-$) containing ligands are widely applied in this study. This anion performs two roles in the transition state: it acts as a ligand to the metal center and abstracts protons to complete the bond-activation process. Theoretical studies also suggest a possible agostic interaction at the initial stage of the bond-activation process.[11a]

For cyclometalation, oxidative addition is most frequently used in late-transition metals such as iridium (I), rhodium (I), and osmium (II) precursors.[27] Unlike agostic interactions, an oxidative addition occurs by transferring two electrons from the metal to the ligands by directly populating the antibonding σ* orbital of the C−H bond. This reaction remains a key paradigm for transition metal-catalyzed C−H activation of hydrocarbons.

TH-3565_186122020

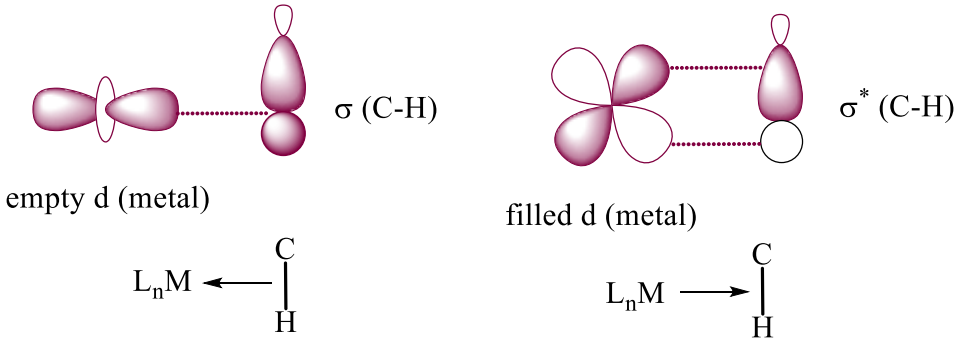
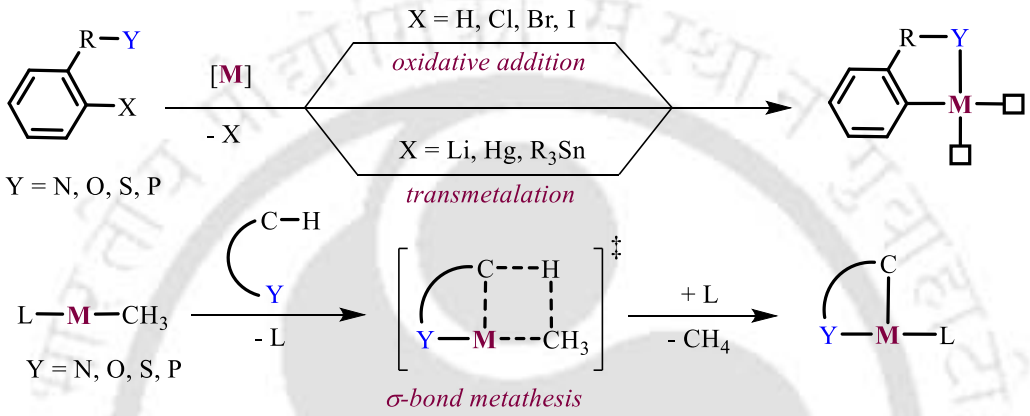


Figure 1.1. Representative MO diagram for synergic interactions

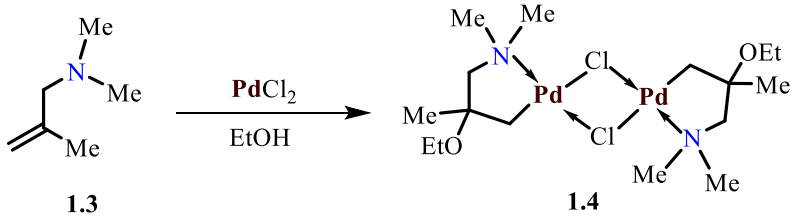


Scheme 1.4. Various synthesis methods for cyclometalated complex

1.4. Synthesis of different cyclometalated complexes

1.4.1. Cyclometalated palladium complexes

Palladium is one of the most studied transition metals as it forms cyclopalladated complexes with almost all types of ligands.[1a,1d,7] Cyclopalladation is an effective method for forming several bonds, such as carbon-carbon, carbon-oxygen, carbon-nitrogen, carbon-sulfur, carbon-phosphorus, and carbon-halogen bonds.[28] It is well known that the C−Pd bond can react with a variety of reagents to consistently produce functionalized products.[29–32] The versatility of palladium reagents comes from their tolerance to various functional groups and the selective reactivity of cyclopalladated intermediates at the C−Pd bond. The first example of the palladacycle with an (sp^3)C−Pd bond was reported by Cope *et al*. by the reaction of allylic amine **1.3** and $PdCl_2$ in an alcoholic medium to give the dimeric palladacycle complex **1.4** (Scheme 1.5).[33]



Scheme 1.5. First example of palladacycle complex

TH-3565_186122020

Many different kinds of palladacyclic compounds are still widely recognized today. Among them aliphatic palladacycles which have a characteristic σ-bond between palladium and a sp^3–hybridized carbon of the ligand (**1.5a-d**).[34,35] Cyclopalladated complexes with (sp^3)C–Pd bonds are classified into two types: benzylic (Figure 1.2B) and aliphatic (Figure 1.2C). The benzylic cyclopalladated complex (**1.5c**) connects the metal to a benzylic carbon, whereas in an aliphatic complex (**1.5d**) palladium is bonded to an aliphatic- sp^3-hybridized carbon. The organic moiety of benzylic and aliphatic cyclopalladated complexes can be an anionic four-electron (CY) or six-electron (YCY) donor (the latter type also known as pincer complex).[36,37] Although all YCY-type palladacycle complexes are mononuclear, CY-analogues can be mono, di, or trinuclear. In the di- and trinuclear complexes of CY-type palladacycles, the ligand can have *cis*- and *trans*-geometric isomers with halogen, acetate, or other bridging groups.[36,37]

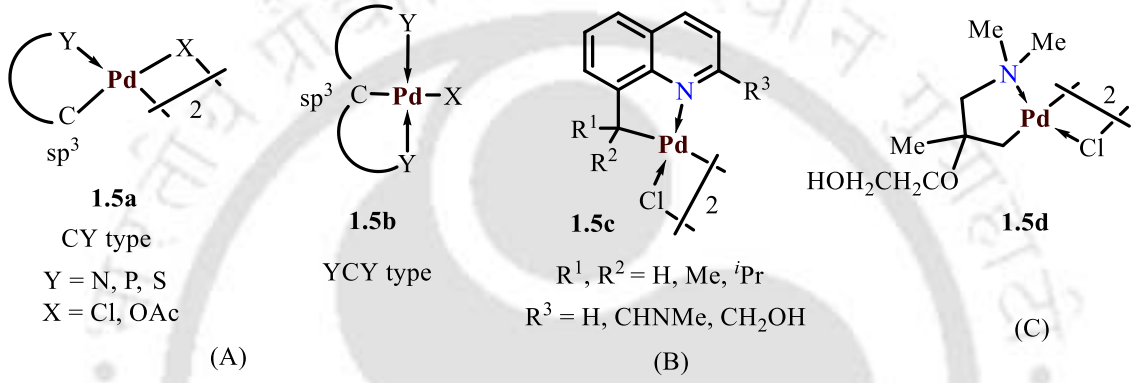


Figure 1.2. A) CY- and YCY-palladacycles, B) benzylic, and C) aliphatic palladacycle

Based on the donor heteroatom present in the ligand moiety, cyclometalated palladium complexes can be classified as CN-, CP-, CS-, and CO-type palladacycles. The donor atom Y contributes to the ring size of the cyclopalladated complex by delivering the palladium reagent to a specific C–H bond for palladation. CY-type benzylic palladacycles prefer to form five- or six-membered palladacycles[38,39] while aliphatic palladacycles can form three-[40,41] or four-membered rings.[42,43] CN-type palladacycles have imine, pyridine, quinoline, and aniline moieties as common directing groups. On the other hand, the CP-type complex is usually synthesized from aryl- or benzyl phosphines and generally forms a five-membered ring. CP-type palladacycle complex was first reported by Shaw *et al.* in 1972.[44] Since then, many research groups have reported the synthesis and application of these palladacyclic complexes in cross-coupling reactions.[38,45–48] Like phosphorous, soft donor sulfur atom can also act as a directing group to form a CS-type palladacycle complex. In 1989, Pfeffer *et al.* reported the synthesis of benzylic five-membered CS-type palladacycle **1.6c** from 2,6-dimethylthioanisole.[49] Although oxygen is a hard donor ligand, CO-type palladacyclic complexes were also reported. The benzylic CO-type complex **1.6d** was obtained by Lindsell and co-workers by the oxidation addition of 2-hydroxymethylbenzyl chloride with $Pd(PPh_3)_4$ in toluene.[50]

TH-3565_186122020

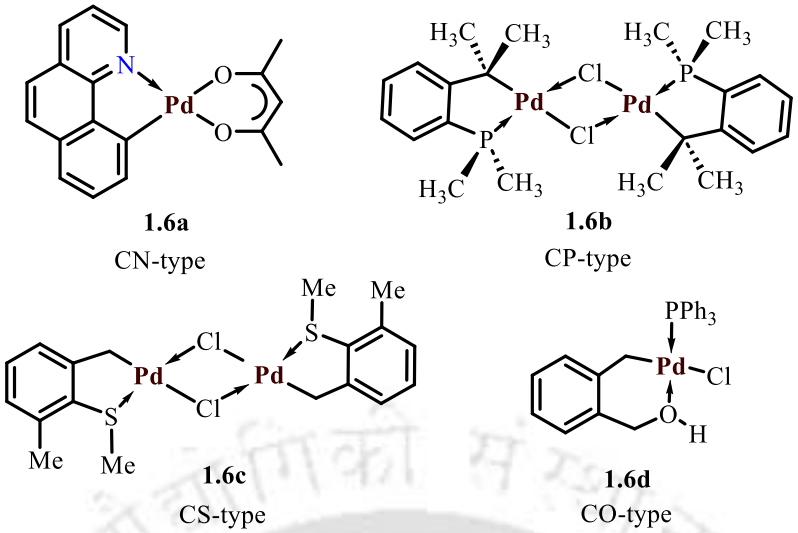
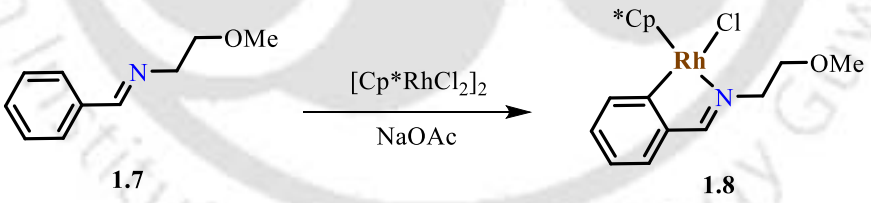


Figure 1.3. Selected examples of different cyclopalladated complex

1.4.2. Cyclometalated rhodium complexes

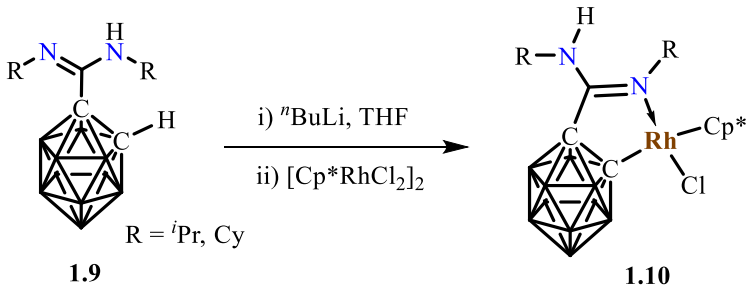
A range of rhodium complexes has been studied as a catalyst both in laboratory reactions and industrial processes. The cyclometalated rhodium complex has at least one rhodium-carbon bond which is stabilized by a ligand through intramolecular coordination of neutral donor atoms (N, C, O or P).[51–54] The cyclometalated species are often encountered as intermediates in $[Cp^*RhCl_2]_2$ catalyzed carbon-carbon or carbon-heteroatom bond-forming reactions.[55] In 2003, Davies and co-workers reported the first cyclometalated rhodium complex **1.8** using phenyl imine and $[Cp^*RhCl_2]_2$ in the presence of NaOAc (Scheme 1.6).[56] Later a series of *para*-substituted phenyl imines were investigated by Jones and co-workers.[57]



Scheme 1.6. First example of cyclometalated rhodium complex

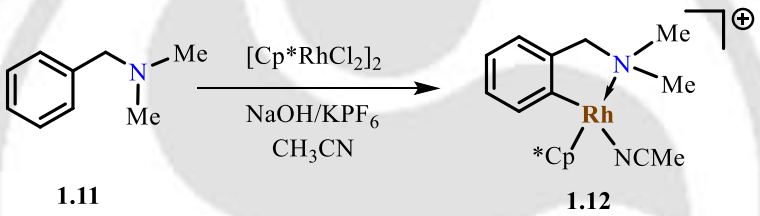
Jin and co-workers reported the variety of five-membered cyclometalated rhodium complexes based on 18- and 16-electron carboranylamidinate.[58] The half-sandwich rhodium complex **1.10** was made in a one-step reaction by the *in situ* formation of C-lithio-carboranylamidinate ligand on treatment with ^{n}BuLi, followed by the addition of $[Cp^*RhCl_2]_2$ in THF at room temperature (Scheme 1.7). In these processes, carboranylamidinate produced an unexpected *C,N*-coordination mode, rather than the ordinary *N,N*-mode.

TH-3565_186122020



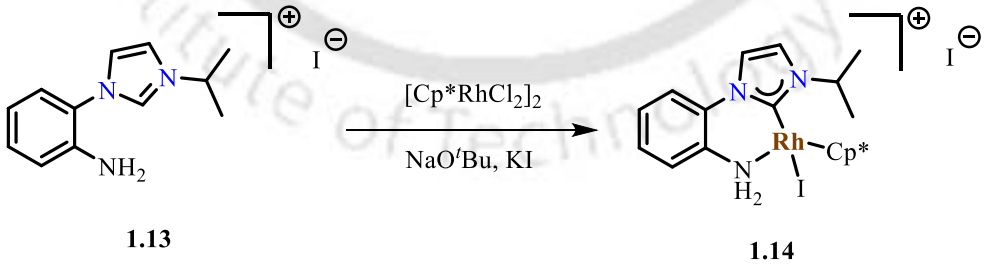
Scheme 1.7. Reaction of carboranylamidinate with [Cp*RhCl$_2$]$_2$

A series of cyclometalated complexes containing M–C bonds were reported by the reaction of imines with [Cp*RhCl$_2$]$_2$ in the presence of a base. Barloy, Pfeffer, and associates demonstrated that the cationic cyclometalated rhodium complex **1.12** can produced by the metalation of *N,N*-dimethylbenzylamine **1.11** and [Cp*RhCl$_2$]$_2$ with NaOH/KPF$_6$ (Scheme 1.8).[59] Half-sandwich metal chemistry usually employs *N*-heterocycles like pyridine, naphthyridine, benzo[*h*]quinoline, etc. These *N*-heterocycles can participate in rhodium-mediated cyclometalated C−H bond reactions.



Scheme 1.8. Reaction of *N,N*-dimethylbenzylamine and [Cp*RhCl$_2$]$_2$

Cross and co-workers reported the reactions of [Cp*RhCl$_2$]$_2$ with a primary-amine-functionalized imidazolium salt (Scheme 1.9).[60] The reaction of imidazolium salt **1.13** with [Cp*RhCl$_2$]$_2$ and NaO^{t}Bu/KI gave the amine-based six-membered cyclometalated *N*-heterocyclic carbene (NHC) salt, **1.14**.

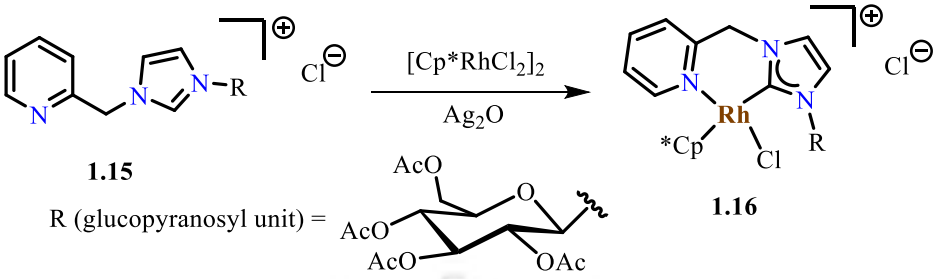


Scheme 1.9. NHC-based cyclometalated rhodium complex

Nishioka and co-workers provided an example of controlling the chirality around a metal center in chiral-at-metal complexes.[61] Diastereoselectivity was induced by the anomeric isomerism of sugar units into the ligands of metal complexes. The *S* and *R* configurations of the chiral-at-metal half-sandwich complex **1.16** were synthesized stereoselectively by employing chelate-type NHC ligands with *α*- and *β*-glucopyranosyl units (Scheme 1.10). The conformation of the

TH-3565_186122020

glucopyranosyl group in these complexes had an impact on the configuration of the metal center.



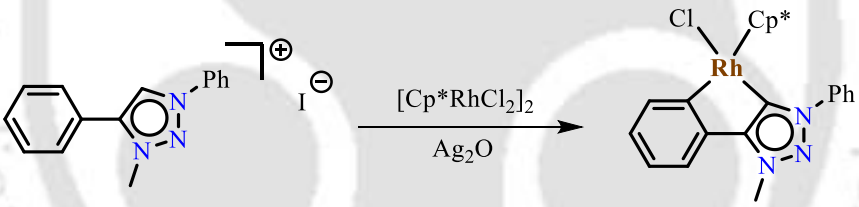
1.15

R (glucopyranosyl unit) =

1.16

Scheme 1.10. Diastereoselectively induced NHC-based cyclometalated rhodium complex

Recently, Peris and co-workers disclosed a series of cyclometalated [Cp*Rh(C^C)] complexes where the metal center binds with the ligand through *C,C*-coordination mode.[62] Cp*Rh(NHC) complexes can undergo facile intramolecular aromatic C–H activation and form cyclometalated [Cp*Rh(C^C)Cl] complexes **1.18**.[63] The 1,4-diphenyl-substituted 1,2,3-trizaolylidene silver complex of **1.17** underwent transmetalation with $[Cp^*RhCl_2]_2$ resulting in the spontaneous activation of the C–H bond of one phenyl ring and formed cyclometalated complex **1.18**. The aromatic C–H bond of the N-bound phenyl wingtip group of the triazolylidene can be activated selectively.

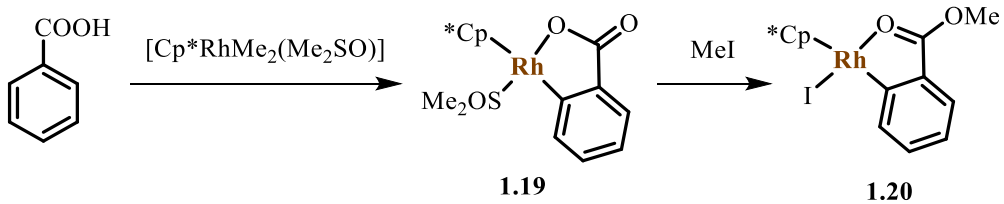


1.17

1.18

Scheme 1.11. Example of a cyclometalated [Cp*Rh(C^C)] complex

On the other hand, the isolation of cyclometalated [Cp*Rh(C^O)] intermediates is quite rare and difficult. Maitlis and co-workers first reported the cyclometalation of benzoic acid in the rhodium complex where the rhodium bonded with ligand through *C,O*-coordination mode (Scheme 1.12).[64] $[Cp^*RhMe_2(Me_2SO)]$ reacted with one equivalent of benzoic acid to form the desired complex **1.19** through cyclometalation. After being treated with methyl iodide, it produced the [Cp*Rh(C^O)] complex **1.20**, in which methyl was added to the benzoate oxygen and Me_2SO was replaced by iodide.



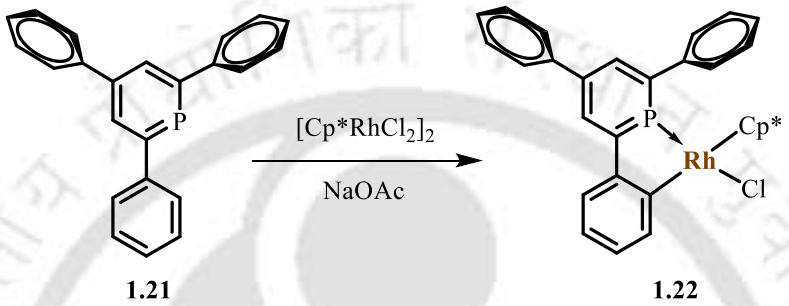
1.19

1.20

Scheme 1.12. Example of a cyclometalated [Cp*Rh(C^O)] complex

TH-3565_186122020

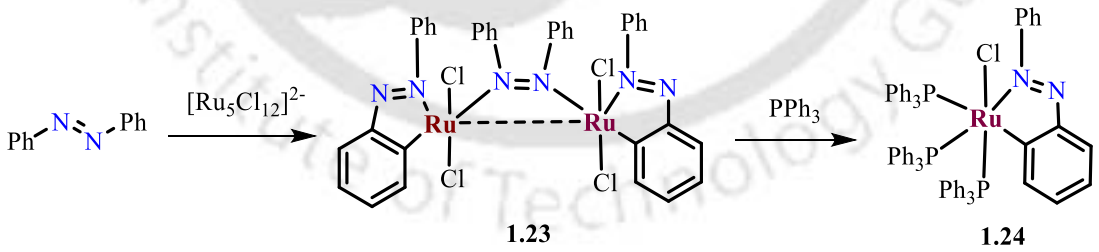
Phosphorus-containing cyclometalated complexes have been well studied in C–H activation chemistry with Cp*Rh complexes. The synthesis of cyclometalated [Cp*Rh(P^C)] complexes was demonstrated by Müller and colleagues.[65] The C–H activation of 2,4,6-triphenylphosphine **1.21** was achieved by using the half-sandwich Cp*Rh precursor with base NaOAc to get the five-membered complex (Scheme 1.13). The complexes were well-characterized and very stable under the applied reaction conditions. The phenyl group in the *ortho*-position of the phosphorus heterocycle gives additional kinetic stabilization of the metal complex. Cyclometalated rhodium complexes have been used as an anticancer agent and as catalysts in the oxidation of water in material science.



Scheme 1.13. Example of a cyclometalated [Cp*Rh(C^P)] complex

1.4.3. Cyclometalated ruthenium complexes

Cycloruthenation is a very broad and versatile field in organometallic chemistry. Cyclometalated ruthenium complexes have been used as catalysts in a variety of reactions, such as hydrogenation, olefin metathesis, reduction of ketones and aldehydes, and the formation of C–C bonds. Furthermore, they exhibit fascinating photophysical and electrochemical properties.[66,67] Some of the cyclometalated complexes also showed remarkable antitumor and anticancer activity.[68.69]



Scheme 1.14. Example of the first inorganic cyclometalated ruthenium complex

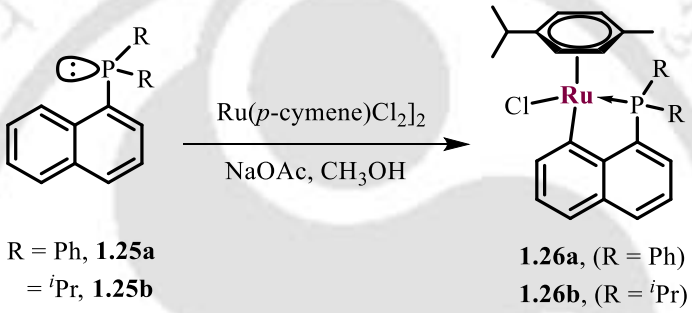
In cyclometalated ruthenium complex, the metal atom connects to the ligands by covalent C–M bonds and the species is stabilized by intramolecular coordination of one or two heteroatoms (O, N, S, or P) in the ligand system. In the last two decades, cycloruthenated complexes have been extensively studied, particularly in catalysis. In 1968 and 1969, the first inorganic ruthenium complex was reported independently by Levison and Robinson[70,71] and by Parshall, Knoth, and Schunn.[72] Later in 1970, Wilkinson *et al.* disclosed a reaction of $[Ru_5Cl_{12}]^{2-}$, a soluble subrogate of the fictitious $[RuCl_2]$, also known as "blue ruthenium chloride", with

TH-3565_186122020

azobenzene to form a bisruthenacyclic complex **1.23**, where ruthenium is in +3 oxidation state (Scheme 1.14).[73] This can be readily converted to Ru(II) species **1.24** by treating it with PPh_3.

1.4.3.1. C^P type ruthenacyclo complexes

In the C^P type cyclometalated ruthenium complex, the Ru metal is bonded with the bidentate ligand through *C,P*-coordination mode. Unlike the C^N type ruthenacyclo complex, there has been limited research on phosphine ligands in cyclometalation with $[RuCl_2(arene)]_2$ systems.[74] Owing to its ideal P-chelation, the C–H activation of 1-naphthyl phosphines occurs selectively at the peri position. Activating the peri C–H bond of 1-naphthyl phosphines is the most straightforward and common synthesis route to the C^P type ruthenacyclo complex. In 2017 Zhu and co-workers reported C^P type ruthenacyclo complexes **1.26a-b** by treating 1-naphthyl phosphine **1.25a-b** with $[RuCl_2(p\text{-cymene})]_2$ in the presence of base NaOAc.[75]

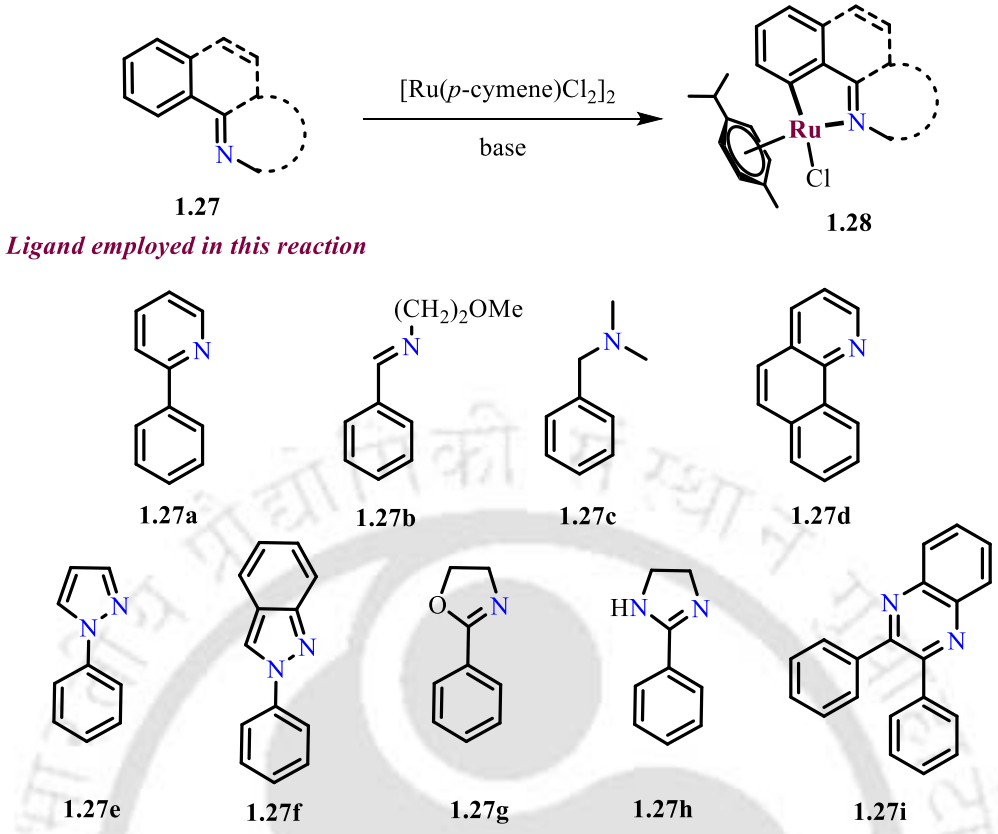


Scheme 1.15. Example of C^P type cyclometalated ruthenium complex

1.4.3.2. C^N type ruthenacyclo complexes

The C^N type ruthenacyclo complex is one of the most studied ruthenacyclo complexes, where the ruthenium atom bonded with the bidentate ligand through *C,N*-coordination mode. This type of ruthenacyclo complex can be synthesized by the coordination triggered-direct *ortho* C–H activation in the presence of a base. The (η^6-arene) di-μ-chloro-ruthenium precursors like $[Ru(p\text{-cymene})Cl_2]_2$, $[Ru(C_6H_6)Cl_2]_2$, $[Ru(C_6Me_6)Cl_2]_2$ are used for the synthesis of half-sandwich cycloruthenated compounds.[10d,76–78] A large variety of nitrogen-containing bidentate ligands such as benzylamine, arylimine, 2-phenyl pyridine, benzo[*h*]quinoline, azobenzene, 2-phenylindole derivatives, aryloxazolines, pyridyl naphthalimide are employed in this study (Scheme 1.16).

TH-3565_186122020



Scheme 1.16. Some selected examples of C^N-type cyclometalated ruthenium complexes

Introduction of NHC ligand in cyclometalation:

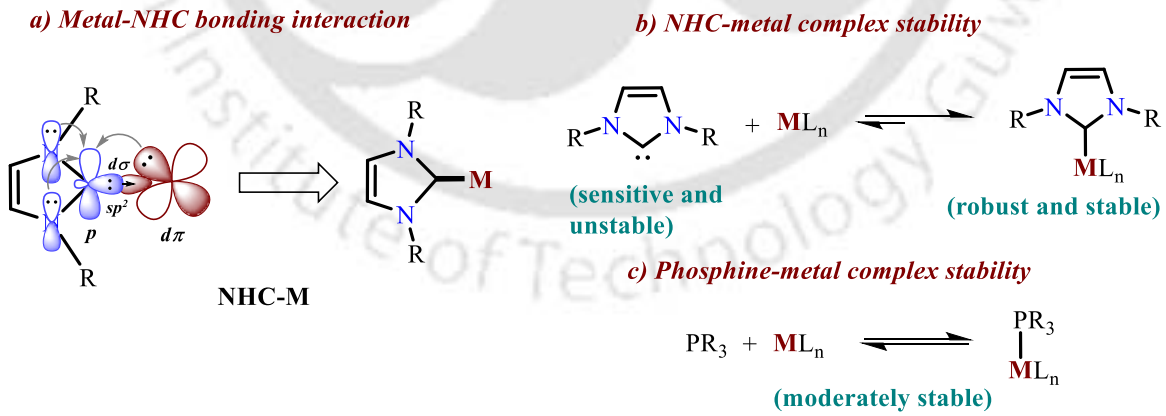


Figure 1.4. Representative metal-NHC bonding interaction

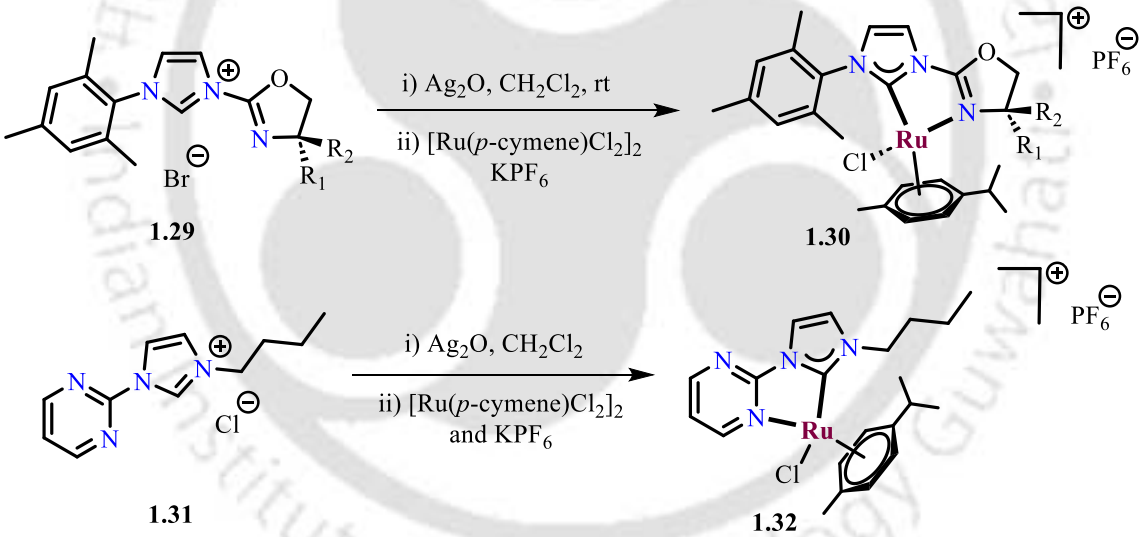
N-heterocyclic carbenes (NHC) are a new type of electron donor ligands that form dative metal-ligand linkages. From the frontier molecular orbitals (FMO) point of view, the sp^2 hybridized orbital (HOMO) on the carbon atom of the ligand acts as a σ-donor to the empty orbitals of

TH-3565_186122020

metal whereas the perpendicularly located vacant p-orbital (LUMO) acts as a π-acceptor from the metal bound to the carbon atom. NHCs are better sigma donors compared to phosphines and result in stronger metal-carbon bonds. The traditional donor ligands are quite labile in nature and cause destabilization of the complex over time.[2b,79–82] Therefore, replacing the traditional donor ligand with an NHC ligand can enhance the overall stability of the complexes. This is mainly due to the strong σ-donating properties of NHC ligands, which lead to the formation of stable metal-NHC complexes and facilitate the formation of long-lasting and efficient complexes.

C_{NHC}^N type ruthenacyclo complexes

In 2006, Gade *et al.* reported the first cyclometalated ruthenium complex **1.30** containing NHC ligands with oxazolinyl pendant arms (Scheme 1.17).[83] They synthesized the complex by coupling a chiral oxazoline unit with an *N*-heterocyclic carbene ring in a straightforward technique for creating chiral catalysts that used NHC as stereodirecting units. Likewise, ruthenium complex **1.32** was synthesized in a transmetalation pathway by Crabtree and co-workers.[84] Both complexes show versatility in catalyzing the transfer hydrogenation and the alkylation of both amines and secondary alcohols.



Scheme 1.17. Synthesis of C_{NHC}^N type ruthenacyclo complexes

Cross and Morris independently reported the same efficient strategy for the synthesis of primary amine functionalized cyclometalated complexes **1.33-1.34**.[60,85] They have studied that the bulky 2,6-diisopropylphenyl substituent on the amine can prevent the amine nitrogen from coordinating to the metal. Unlike this, the primary-amine functionalized imidazolium salt can exclusively react with [Ru(*p*-cymene)Cl_2]$_2$, Ag_2O, and KI to give the amine–NHC containing ruthenacyclo complex (Figure 1.5). Studies show that these amine-bound NHC complexes can efficiently act as catalysts in hydrogenation chemistry.

TH-3565_186122020

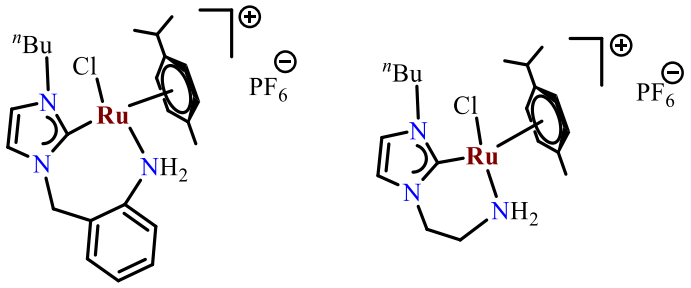
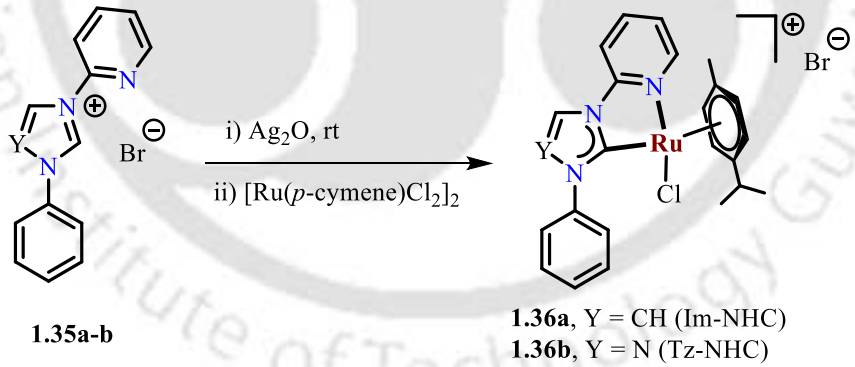


Figure 1.5. Primary amine functionalized C_{NHC}^N type ruthenacyclo complexes

The synthesis of imidazolydene-NHC (Im–NHC) and triazolydene-NHC (Tz–NHC)-based ruthenium(II)-complexes (**1.36a-b**) was recently reported by Choudhury *et al.*[86] This was achieved by first deprotonating the NHC-ligand precursors using Ag_2O as a mild base, which produced Ag-NHC intermediate, and then transmetalation to $[Ru(p\text{-cymene})Cl_2]_2$ (Scheme 1.18). They reveal that these ancillary NHC ligands (Im–NHC and Tz–NHC) containing ruthenium complexes efficiently work as catalysts to selectively oxidize alkenes and alkynes to the corresponding carbonyl compounds. The literature has extensively reported the extraordinary activity and selectivity of imidazolydene-based *N*-heterocyclic carbene containing ruthenium complexes in C–H bond activation chemistry. Very recently, Rit and co-workers have developed 1,2,3-traizol-5-ylidene(tz–NHC) chelating ligand containing C_{NHC}^N type Ru(II) complex.[87] These metal complexes can be significantly tuned for catalytic efficiency by changing the stereoelectronic profile of the ancillary carbene ligands in the hydride transfer chemistry of unsaturated compounds.



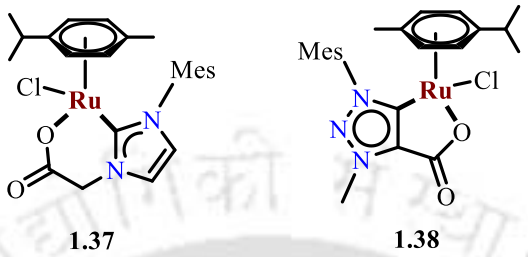
Scheme 1.18. Synthesis of Im–NHC and Tz–NHC based C_{NHC}^N type ruthenacyclo complexes

C_{NHC}^O type ruthenacyclo complexes

There are many complexes with NHC ligands with nitrogen donors reported, but very few examples of NHC ligands with oxygen donors are known. Albrecht *et al.* in 2009 reported a ruthenium(II) complex **1.37** by using bidentate chelating NHC ligands which have carboxylate in the wingtip of the ligand as a donor group.[88] The six-membered cyclometalated complex **1.37** was synthesized by following the transmetalation route from the corresponding Ag-NHC

TH-3565_186122020

intermediate. They revealed that the complex containing an NHC attached to a carboxylate group exhibited notable catalytic activity in homogeneous hydrogenation. The same group in 2014 reported a straightforward procedure to synthesize a donor-functionalized mesoionic triazolylidene ruthenium complex **1.38**.[89] The activity of the ruthenium complexes as catalyst precursors in alcohol oxidation and transfer hydrogenation is influenced by the introduction of donor functional groups into the triazolylidene skeleton.

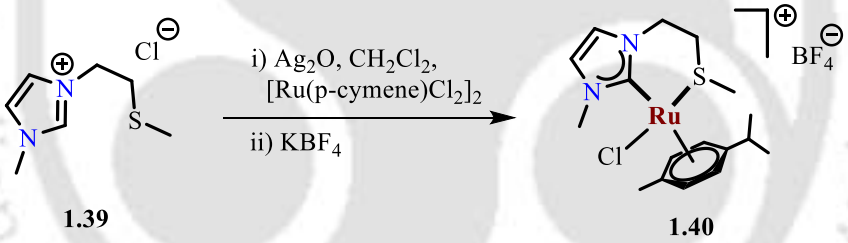


1.37 **1.38**

Figure 1.6. Example of C_{NHC}^O type ruthenacyclo complexes

C_{NHC}^S type ruthenacyclo complexes

C_{NHC}^S type ruthenacyclo complexes are very rare in organometallic chemistry. Albrecht synthesized an NHC-based ruthenacyclo complex **1.40** with sulfur as a donor atom (Scheme 1.19).[88] They prepared the complex with the known transmetalation pathways from the corresponding silver carbene complex.



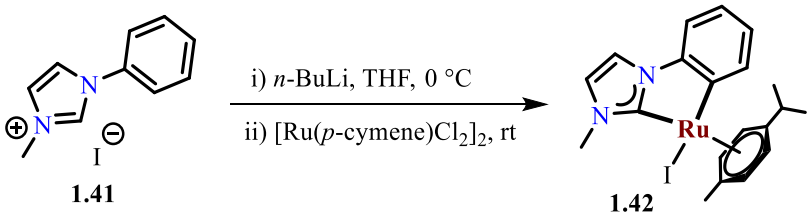
1.39 **1.40**

Scheme 1.19. Synthesis of C_{NHC}^S type ruthenacyclo complex

1.4.3.3. C^C type ruthenacyclo complexes

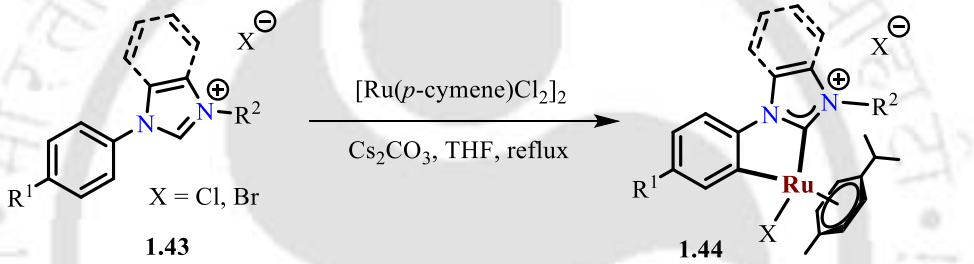
In the C_{NHC}^C type ruthenacyclo complexes, the ruthenium metal center coordinated with a carbanionic and a carbene moiety in the bidentate ligand. Over the past 10 years, C_{NHC}^C type ruthenacyclo complexes have been extensively studied and used for catalytic, photophysical and biological applications. The C_{NHC}^C type ruthenacyclo complexes can be synthesized by the following methods (a) modifying the size and nature of the linker, (b) varying the NHC donors and substituents at the ancillary ligands, and (c) alternating the solvent medium and/or metal precursors.[90] In 2009, Baiquan Wang first reported the preparation and reactivity of aryl-functionalized imidazolylidene cyclometalated Ru(II)-NHC complex **1.42**.[91] The imidazolylidene precursor, **1.41** was deprotonated at 0 ºC with *n*-BuLi and reacted with [Ru(*p*-cymene)Cl_2]$_2$ to afford the ruthenacyclo complex **1.42** (Scheme 1.20).

TH-3565_186122020



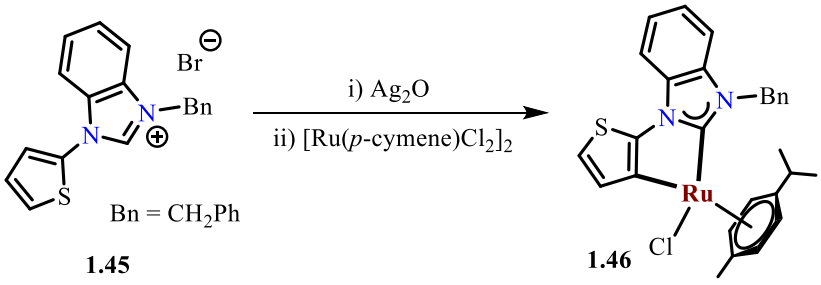
Scheme 1.20. First example of C_{NHC}^C type ruthenacyclo complex

A few research groups reported examples of C_{NHC}^C type ruthenacyclo complexes as an intermediate in NHC-directed alkyne annulation reactions. The same group in 2014 successfully developed a new and efficient strategy for synthesizing the NHC-based cycloruthenium complexes **1.44** by reacting aryl-substituted imidazolium salts **1.43** with [Ru(*p*-cymene)Cl_2]$_2$ under mild conditions (Scheme 1.21).[92] They have also shown that these compounds can react with alkynes in methanol *via* alkyne insertion followed by reductive elimination, producing novel imidazolium salts with high yields.



Scheme 1.21. Substituted phenyl imidazolium salt containing C_{NHC}^C type Ru complex

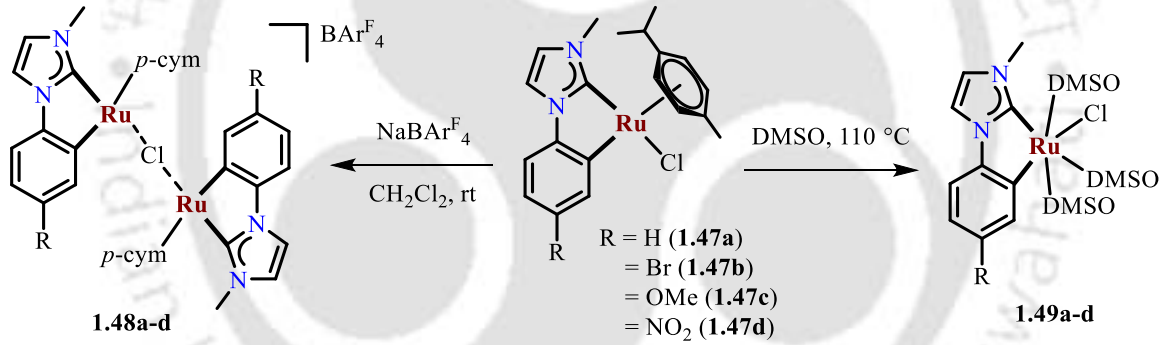
Huynh *et al*. synthesized and characterized cyclometalated Ru–thienyl–NHC complex **1.46** by treating thiophene containing imidazolium salt **1.45** with Ag_2O and subsequent addition of [Ru(*p*-cymene)Cl_2]$_2$ at ambient temperature.[93] The salt **1.45** first reacts with Ag_2O to generate a silver-carbene intermediate, and then a cyclometalated complex is formed *via* a transmetalation pathway (Scheme 1.22). It is anticipated that AgBr precipitation would facilitate the carbene transfer process. The chloride ligand will coordinate with the ruthenium center because AgBr has a greater formation constant than AgCl. In 2019, Strassner *et al.* reported a series of substituted phenyl-imidazo[1,5-*a*]pyridines as a C_{NHC}^C ligand in ruthenium(II) complexes.[94] The cyclometalated Ru-NHC complexes are formed following the transmetalation route from the respective silver carbenes and [Ru(*p*-cymene)Cl_2]$_2$ dimer.



Scheme 1.22. Synthesis of cyclometalated Ru–thienyl–NHC complexes

TH-3565_186122020

In 2016 Strassner demonstrated a one-pot synthetic method to develop different *ortho*-metalated Ru(II)-complexes (**1.47a-d**) with NHC ligands and studied the reactivity of the synthesized complexes.[95] These complexes were treated with sodium tetrakis[3,5-bis(trifluoromethyl)phenyl]borate salt in anticipation of generating a mono-cationic complex of formula $[(C_{NHC}\text{^}C)Ru(p\text{-cymene})]^{+}[BAr^{F}_{4}]^{-}$ by abstraction of the Ru-bound chloride ion. Remarkably, rather than the predicted mono-cationic complexes, the reaction produced the chloride-bridged dinuclear Ru-NHC piano stool complexes **1.48a-d** of formula $\{[(C_{NHC}\text{^}C)Ru(p\text{-cymene})]_2(\mu\text{-Cl})\}^{+}\{BAr^{F}_{4}\}^{-}$. Subsequently, the *p*-cymene moiety of the *ortho*-metalated Ru-NHC complexes can be replaced with the S-bound DMSO ligands to synthesize the corresponding dimethyl sulfoxide (DMSO) coordinated Ru-NHC complexes **1.49a-d**.[96] The geometry surrounding the Ru center changes (from facial to meridional) when the π-coordinated *p*-cymene ligand is replaced with three DMSO ligands, and the chloride moves into the *trans* position of the phenylic carbon atom. This can be explained by the weaker σ-donating chloride ligand being directed to be in the *trans* position by the more σ-donating carbanion's trans-effect. The *trans* position of the chloride ligand with respect to the carbenic carbon atom of the complex was also supported by DFT calculations. Furthermore, the synthesis of heteroleptic complexes with chelating ligands like bipyridine has also been reported by using these cyclometalated ruthenium complexes.



Scheme 1.23. Synthesis of cyclometalated Ru(II)-NHC complexes and their reactivity studies

1.5. Catalytic application of cyclometalated ruthenium complexes

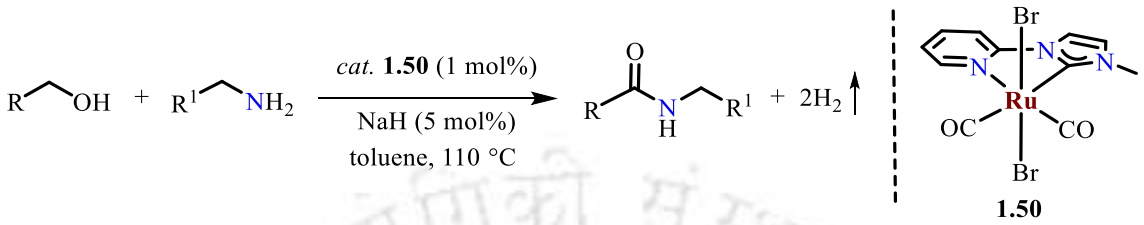
Cyclometalated ruthenium complexes have been successfully used as catalysts in several bond-forming reactions, such as amidation of alcohols, *N*-alkylation of amines, transfer hydrogenation, alcohol oxidation, and C–H activation/annulation reaction.

1.5.1. Amidation of alcohol

Amidation of alcohol is an active area of research due to the structural importance of these compounds in the agrochemicals and pharmaceutical industry. Amide linkage-containing compounds are the primary structural component of the biological world. Amide can directly be synthesized from commercially available cheap amines and alcohols by applying transition metal catalysis. Alcohol amidation catalyzed by transition metals is an environmentally benign and cost-effective method that produces only hydrogen as a byproduct.[97] Madsen introduced a ruthenium-based *N*-heterocyclic carbene (NHC) system for the amidation reaction of alcohols

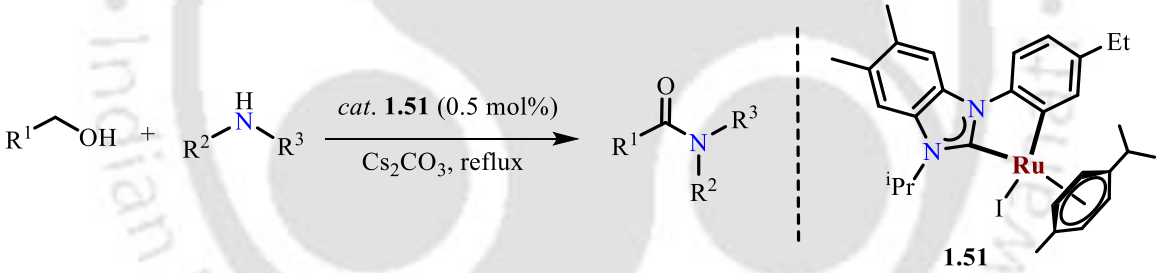
TH-3565_186122020

and amines.[98] Nowadays ruthenium-based cyclometalated NHC complexes have been extensively studied for this transformation. In 2014, Bera and co-workers reported a phosphine-free complex **1.50** containing two carbonyls and a pyridine-functionalized NHC and studied the catalytic activity for the acceptorless dehydrogenative coupling of alcohols and amines (Scheme 1.24).[99]



Scheme 1.24. Amidation of alcohol and amines using catalyst **1.50**

Pioneering work has been done by Verpoort *et al.* by using C_{NHC}^C bidentate NHC ruthenium complex **1.51**.[100] It was discovered that the phosphine-free bidentate Ru(II)-NHC catalytic system was the most effective for atom-economic alcohol amidation using amines. These complexes efficiently synthesize the amides at a relatively low catalyst loading of 0.5 mol%. They also exhibit great compatibility with various functional groups containing alcohols and amines, including *ortho*-substituted benzyl alcohols.



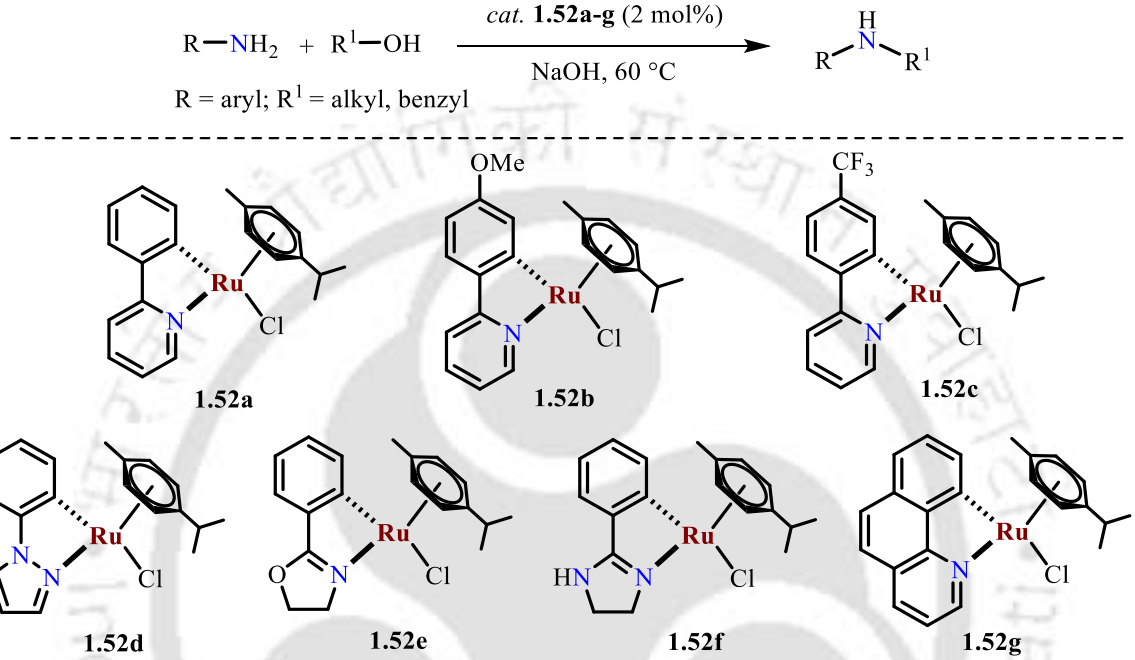
Scheme 1.25. Amidation of alcohol catalyzed by complex **1.51**

1.5.2. *N*-alkylation of amines

The selective *N*-alkylation of amines is frequently observed and is a significant chemical transformation in organic synthesis. The traditional methods of *N*-alkylation of amines mostly use waste-producing and hazardous alkylating chemicals such as formaldehyde and alkyl halides. Modern hydrogen autotransfer (also called hydrogen borrowing) reactions offer an attractive alternative to the *N*-alkylation of amines. It is a multi-step reaction sequence that begins with readily available, frequently affordable alcohols. In the first step of the reaction, the alcohol is dehydrogenated with the help of a transition metal catalyst and produces a more reactive aldehyde or ketone. The last stage of the reaction sequence uses the hydrogen that was extracted in the previous step to hydrogenate the intermediate product, which forms new C–N bonds, and produces water as the only stoichiometric by-product.[97b,101] The methylation of amines is very difficult since a higher energy barrier is required for the dehydrogenation of methanol as compared to the higher alcohols. In recent years, methylation of anilines has been

TH-3565_186122020

performed at high temperatures with the use of either molecularly defined complexes or heterogeneous materials. In the year 2021, Beller synthesized a series of new cyclometalated ruthenium complexes **1.52a-g** for this study.[102] Among them, complex **1.52f** bearing a phenyl imidazoline ligand was found to be an efficient catalyst for the *N*-methylation of anilines with methanol *via* a hydrogen autotransfer process. Other alkylating agents like aliphatic alcohols and benzylic alcohols were also tested and effectively afforded the *N*-alkylated product.



Scheme 1.26. *N*-alkylation of anilines with alcohols.

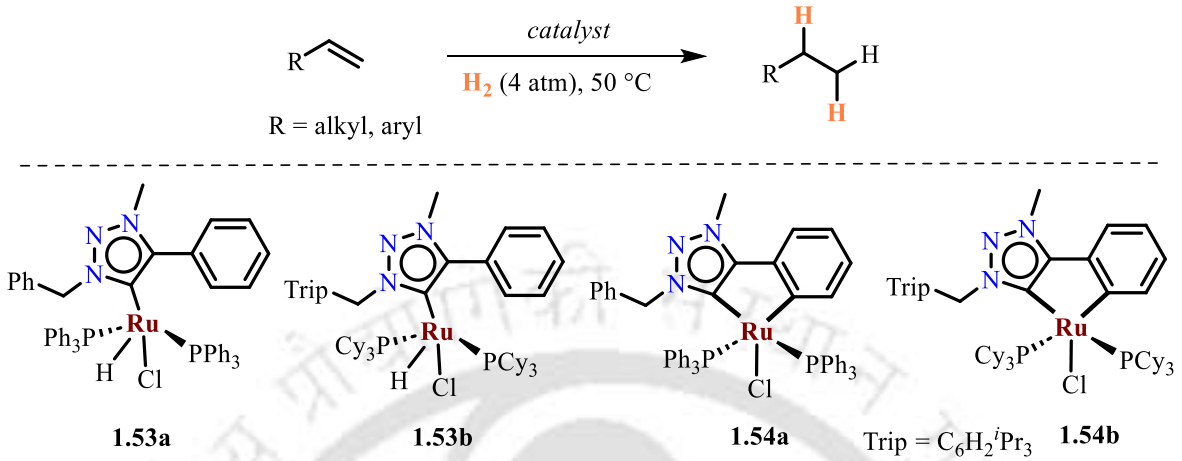
1.5.3. Transfer hydrogenation reaction

Hydrogenation is a chemical reaction between molecular hydrogen (H_2) and another compound or element, usually in the presence of a catalyst. The process typically constitutes the addition of pairs of hydrogen atoms to a molecule, often an unsaturated compound. Likewise, transfer hydrogenation (TH) is a chemical reaction involving the addition of hydrogen to a compound from a source other than molecular H_2. It is applied in laboratory and industrial organic synthesis to saturate organic compounds and reduce ketones to alcohol, and imines to amines. It avoids the need for high-pressure molecular H_2 used in conventional hydrogenation. Both processes efficiently occur at mild temperature and pressure conditions using cyclometalated ruthenium complexes.[103]

In 2016, Stephan and co-workers reported a series of mesoionic triazolylidene-based tzNHC Ru(II)-complexes **1.53a-b, 1.54a-b** which were greatly utilized for the hydrogenation of functionalized olefins.[104] During the synthesis of **1.54a-b**, non-orthometalated **1.53a-b** were found as the minor products (Scheme 1.27). The authors proposed that the initially formed non-orthometalated hydride complex **1.53a-b** follow an intramolecular C(sp^2)–H bond activation to provide the cyclometalated complex **1.54a-b** under the liberation of H_2. Cyclometalated

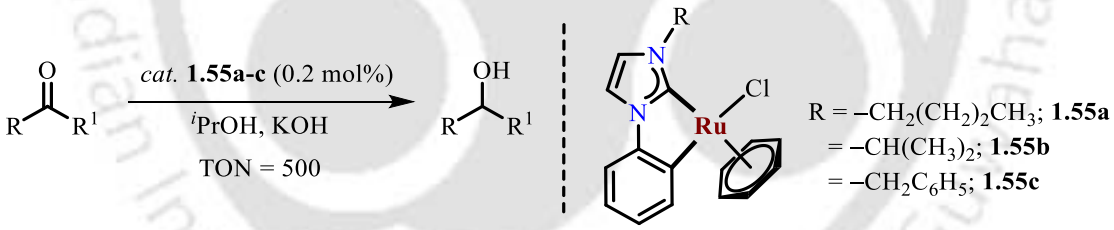
TH-3565_186122020

Ru^{II}-complex **1.54b** showed high activity compared to their non-orthometalated analogues. Further, the PCy_3 auxiliary ligand provided superior activity than PPh_3 probably due to the greater electron donating ability of PCy_3 than PPh_3.



Scheme 1.27. Hydrogenation of olefins by 1,2,3-triazolylidene-based Ru(II) complexes

Later in 2017, Malecki group reported half-sandwich Ru(II)-NHC complex **1.55a-c** from 1-phenyl imidazolium salts with various *N*-alkyl substituents.[105] The complexes were examined for catalytic transfer hydrogenation of ketones (Scheme 1.28). The complex containing the *n*-butyl wingtip, **1.55a** showed higher catalytic efficiency than the other wingtip. The activity difference is postulated due to steric effects imparted by the *N*-alkyl substituents.

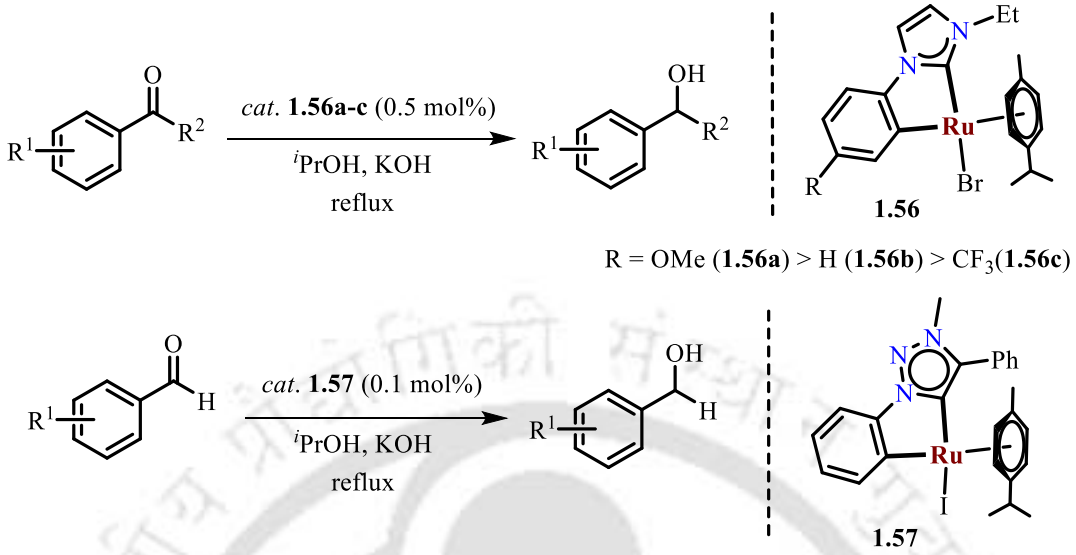


Scheme 1.28. Catalytic transfer hydrogenation of ketones to alcohols.

Then Rit *et al.* reported stereo-electronically tunable cyclometalated Ru(II)-NHC complexes **1.56a-c**, **1.57** in TH of carbonyl compounds or imines.[106] These are featured with various phenyl-based cyclometalated Ru(II)-NHC complex with planar ruthenacycles either with a bulky mesoionic carbene center or an imidazolylidene moiety with variable substituents at the *para*-position of the *N*-phenyl ring. The activity of the *p*-OMe substituted catalyst **1.56a** was found to be higher than the other complexes for ketone reduction whereas complex **1.57** bearing a triazolylidene ligand showed superior activity for aldehyde reduction, along with suppressing the formation of carboxylic acid by-product (Scheme 1.29). The mechanistic investigation suggested that a Ru(II)-H intermediate was involved in the catalytic cycle. Overall, the steric and electronic alteration of the catalyst significantly impacted transfer hydrogenation activity. Later, Gao and co-workers reported the polymer-supported cyclometalated Ru(II)-NHC

TH-3565_186122020

complexes for the transfer hydrogenation reaction of carbonyl compounds with greater efficacy.[107]

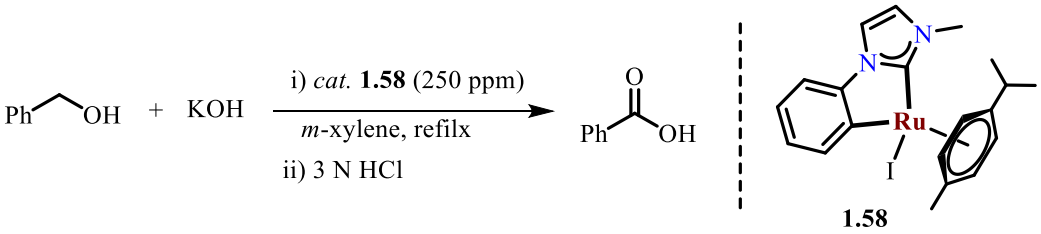


Scheme 1.29. C^C type Ru complexes in transfer hydrogenation reactions

1.5.4. Alcohol oxidation

In organic synthesis, carboxylic acid is a significant structure, particularly in the total synthesis of natural products and medicinal chemistry. However, the routine industrial manufacture of carboxylic acids uses aldehydes and a stoichiometric amount of oxidants, which results in waste and environmental issues.[108] Since the oxidation of primary alcohols into carboxylic acids is a basic and well-established process, many researchers have been motivated to carry out in-depth, methodical investigations. The dehydrogenation of alcohols to their corresponding aldehydes has been documented using a variety of transition metal catalysts; however, relatively fewer studies have been done on the direct conversion of alcohols to carboxylic acids or carboxylates through a dehydrogenative transformation in the absence of any oxidant. With this motivation, Verpoort and co-workers have synthesized several highly active bidentate Ru^{II}-NHC complexes for the dehydrogenative coupling of benzyl alcohol and hydroxide.[109] The corresponding complex showed a remarkably high activity with loading as low as 250 ppm and reaching TON of 32800. During the NMR study, several signals were observed in the range of −9.36 ppm to −7.81, indicating the key role of metal-hydride species in the catalytic cycle. In the mechanistic pathway first, the Ru-alkoxide intermediate was formed by the reaction of complex **1.58**, alcohol, and KOH. Then it undergoes *β*-hydride elimination to form a ruthenium-hydrido species. Once the first *β*-hydride elimination took place, the coordinated aldehyde of the Ru monohydride species interacted with H_2O/OH^- to generate another intermediate, which then produced another Ru monohydride species coordinated with the carboxylic acid. After that, this species replaces a ligand to deliver the required carboxylic acid and regenerate the active Ru-alkoxide catalyst.

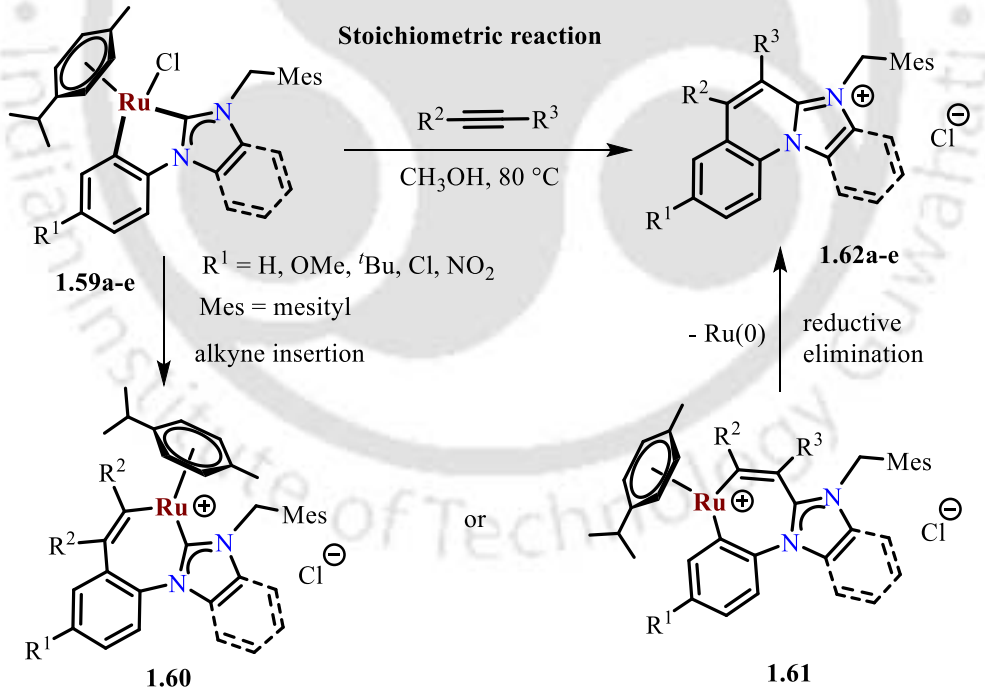
TH-3565_186122020



Scheme 1.30. Synthesis of carboxylic acids from alcohols

1.5.5. C–H activation/annulation reactions

Catalytic oxidative annulation reaction of alkyne *via* NHC-directed C–H bond activation is one of the fundamental reactions in organic chemistry since it produces polyaromatic compounds with hetero-atom effectively. These heteroaromatic scaffolds are important in pharmaceutical chemistry and materials science. NHC-based cyclometalated complexes are believed to be considered as key intermediates in the process. Initial study has been exemplified with the stoichiometric reaction between cyclometalated complex and alkyne. The reaction is involved with the insertion of alkynes to the corresponding NHC-based cyclometalated complex, followed by the reductive elimination to give the annulated product. Rhodium-based cyclometalated complexes are meticulously studied in this regard,[110] however cost-effective ruthenium-based cyclometalated complexes have not been systematically studied.



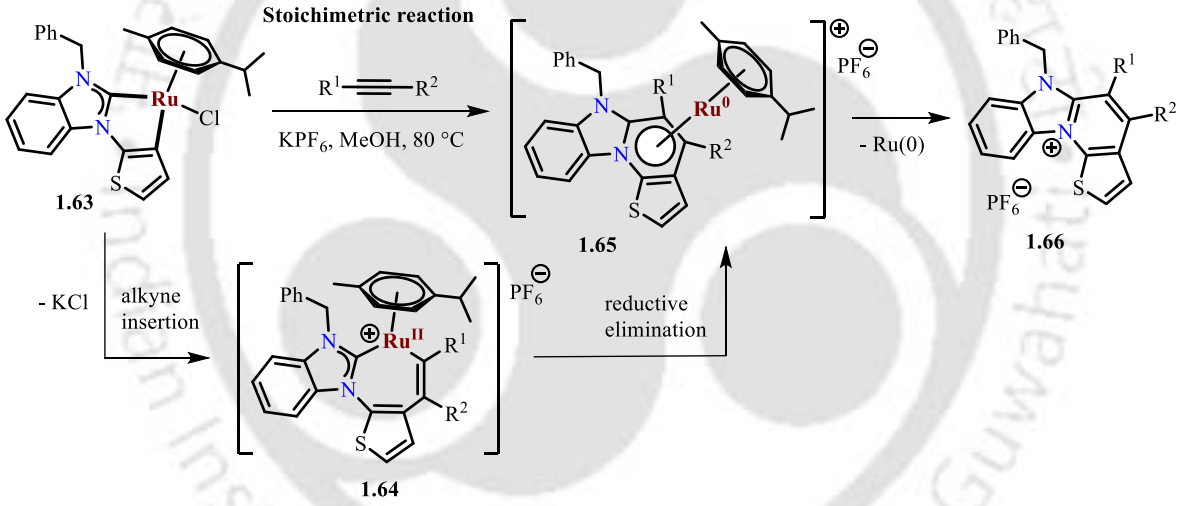
Scheme 1.31. Mechanism for alkyne insertion into NHC-based Ru(II)-complex

In 2014, Wang *et al.* first reported stoichiometric annulation reactions of alkyne with NHC-based cyclometalated ruthenium(II) complexes **1.59a-e** (Scheme 1.31).[92] The reaction is examined with a variety of aryl-substituted cycloruthenium complex **1.59a-e** and higher yields

TH-3565_186122020

were obtained for electron-donating groups on the phenyl ring compared to electron-withdrawing groups. Findings suggested that the alkyne insertion step is likely to be a slow process while the reductive elimination step is a relatively fast process.

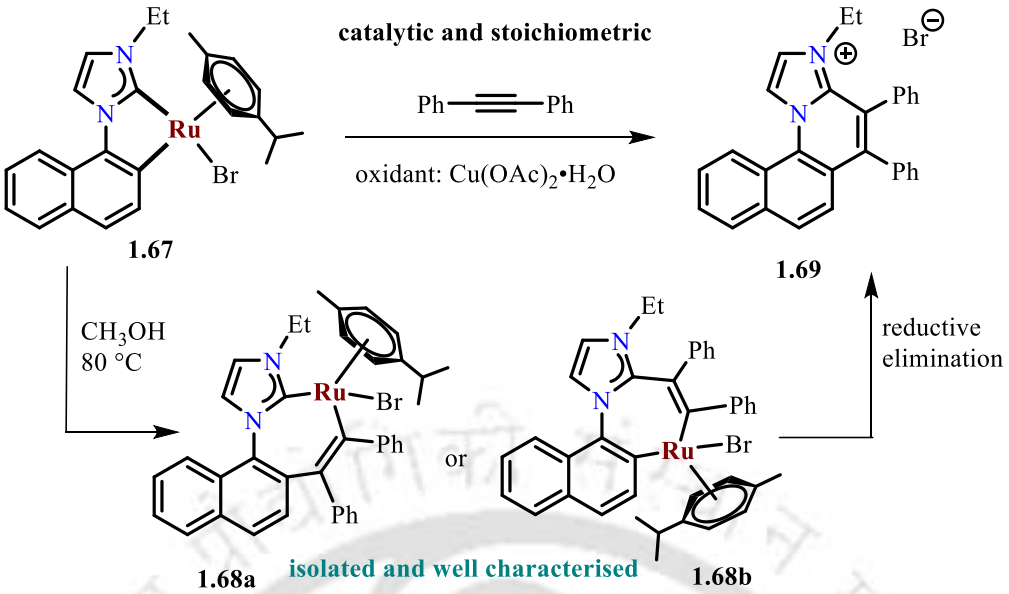
Later, in 2015, Huyhn and co-workers developed a series of cyclometalated ruthenium NHC complexes with thienyl moieties and investigated the thiophene annulation reaction *via* C–H bond functionalization.[93] *N*-benzyl substituted benzimidazolin-2-ylidene coordinated ruthenium-complex **1.63** was taken as a model substrate in the annulation reaction to evaluate its reactivity with different alkynes (Scheme 1.32). The reaction was examined with both symmetrical and unsymmetrical alkynes and used excess KPF_6 for promoting the reaction. The authors proposed that the aza-heterocyclic thiophenes **1.64** is formed as a result of alkyne insertion into the κ^2-*C,C* bound ditopic thienyl–NHC ligand. Then it is followed by intramolecular reductive elimination and formation of ruthenium(0) adduct **1.65**. Species **1.65** is particularly short-lived and quickly collapsed by eliminating the Ru(0) fragment to generate the final annulated aza-heterocyclic thiophene cation **1.66**. A black precipitate at the end of the reaction indicates evidence of ruthenium(0) in the catalytic process.



Scheme 1.32. Proposed pathway for the formation of aza-heterocyclic thiophenes

Since both the alkyne annulation reactions were executed in a stoichiometric manner (Scheme 1.31 and Scheme 1.32), the recent studies have been documented catalytically with naphthyl-derived orthometalated Ru(II)-NHC complexes using $Cu(OAc)_2 \cdot H_2O$ as an oxidant for catalytic application (Scheme 1.33).[111] Herein, the author is able to isolate the seven-membered diphenylethylene-inserted catalytic intermediate **1.68** from the reaction of Ru^{II}-NHC complex **1.67** with diphenylacetylene in a 1:1 ratio. It provides strong support for the reaction mechanism of annulation reactions involving azolium salts. This intermediate **1.68** slowly yields the corresponding annulated product **1.69** *via* reductive elimination. After the successful mono-annulation reaction, the bis-annulation reaction was documented with a limited example by simply varying the reaction parameters.

TH-3565_186122020



Scheme 1.33. Naphthyl-derived ortho-metallated Ru(II)-NHC complex for annulation

Despite these advances, reactions require the use of stoichiometric excess oxidants, such as copper(II) salts, thereby leading to the formation of a large amount of undesired copper-containing by-products. Thus, the method was restricted to scale-up synthesis. Therefore, in the context of green and sustainable chemistry, the development of operationally simple, easy, and straightforward methods with minimal chemical waste and good green metrics is highly desirable.

1.6. Summary

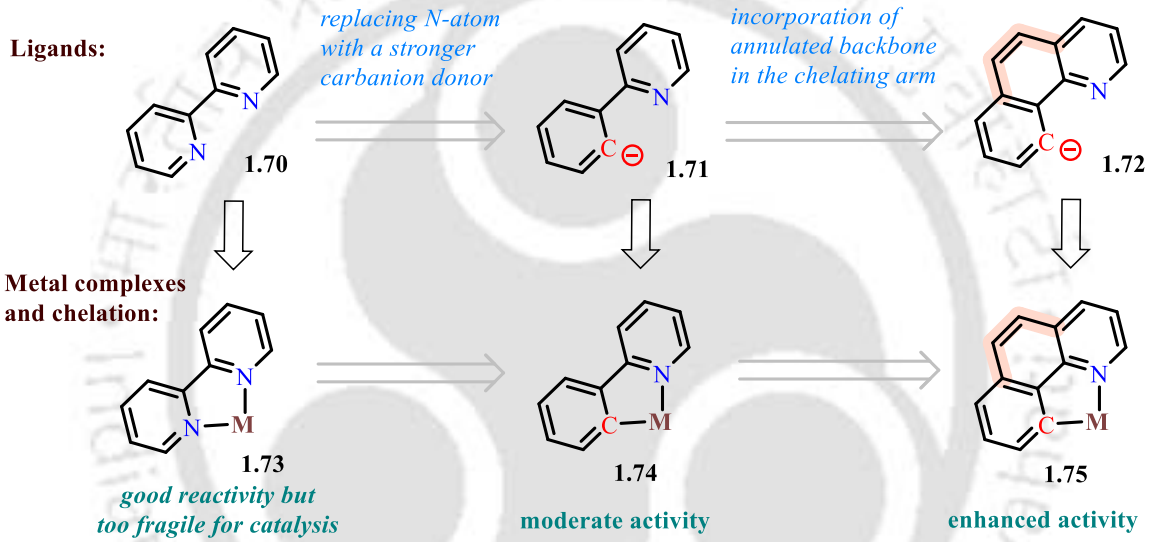
Since the early days after the successful isolation of cyclometalated complexes, they garnered immense attention due to the diverse range of catalytic, metallomesogenic and pharmaceutical activities. In the first step of the synthesis of these cyclometalated complexes, a metal center interacts with the ligand precursor through a (hetero)atom. Then a strongly basic ligand attached to the metal center abstracts a proton from the ligand, lying in the same plan as the metal center. This results in the formation of a new M–C bond to form the cyclometalated species. Notably, platinum group metals have been a popular choice, given their wide array of reactivities in different fields. Particularly, cycloruthenated complexes observe considerable attention not only for their contribution to the established processes like alcohol amination/oxidation, *N*-alkylation of amines, transfer hydrogenation, and C–H activation/annulation reaction but also for their immense potential in exploring new catalytic pathways. To enhance their reactivity, NHC compounds have emerged as versatile ligand systems, owing to their strong σ-donation ability. This results in a stable metal-organic complex suitable for catalysis.

TH-3565_186122020

1.7. Objective and outline of this thesis

1.7.1. Objective:

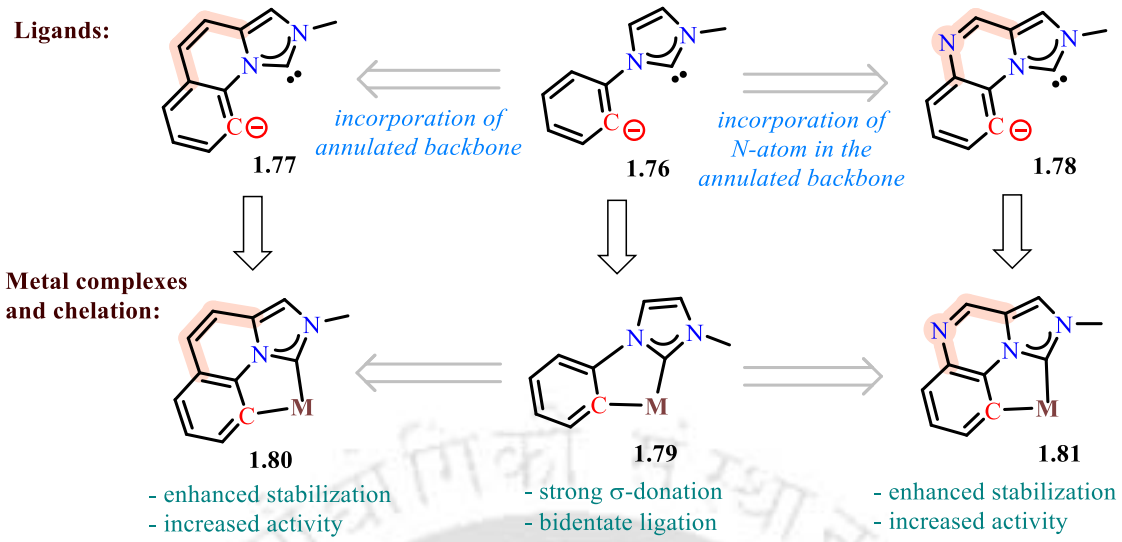
After a detailed investigation of the literature, it has been found that cyclometalated complexes are widely utilized in various organic transformations in particular oxidation chemistry. The blockbuster bidentate ligand bipyridine **1.70** is extensively used in homogeneous catalysis due to its chelate arm and N-donor atoms. However, they are too fragile under oxidative conditions. Their journey was initiated by replacing the N-donor atom with a stronger σ-donor carbanion **1.71**, followed by the incorporation of an annulated backbone in the chelating arm **1.72**, corresponding cyclometalated complexes (**1.73**–**1.75**) showed moderate to high activity in the catalysis (Scheme 1.34).



Scheme 1.34. Literature precedents with bidentate $C_{(carbanion)}$^N motif

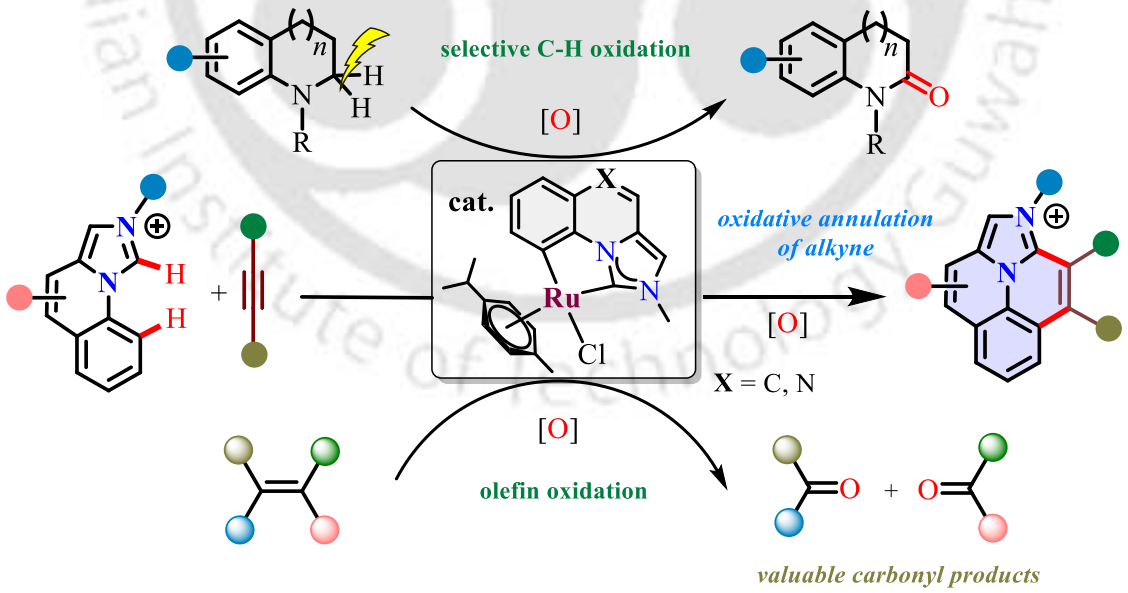
Later, cyclometalated complexes with *N*-heterocyclic carbene (NHC) ligands are found to be the most efficient catalyst possibly due to robust metal–C bonds and are less susceptible to decomposition under harsher conditions (Scheme 1.35).[112] Further, it has been proven that stronger σ-donating ability makes NHC superior candidates for oxidation chemistry. Herein I hypothesize that π-delocalization in the annulated systems may provide higher conjugational stability and enhanced σ-donating ability compared with their nonannulated analogues. Besides this, the nature of electrophilicity at the metal center is expected to be enhanced.

TH-3565_186122020



Scheme 1.35. Design strategy: bidentate ligands with $C_{(carbanion)}$^C_{NHC} motif and their metal complexes

Considering these facts, the present study is focused on the synthesis of cyclometalated ruthenium complexes bearing rigid π-conjugated fused imidazo[1,5-*a*]quinoline (ImQ) and imidazo[1,5-*a*]quinoxaline (ImQx) based NHC ligand, and study their usefulness towards (i) selective C–H oxidation of *N*-substituted tetrahydroquinolines to lactams (ii) selective oxidative scission of olefins to carbonyls (iii) and oxidative C–H activation and annulation of alkynes.



Scheme 1.36. Proposed catalytic reactions using NHC-based cyclometalated complex

TH-3565_186122020

1.7.2. Outline of this thesis:

The introduction chapter presents a brief overview of the diverse and rich chemistry of cyclometalated complexes. Synthesis, reactivity, and usefulness of cyclometalated complexes in the various organic transformations are extensively discussed. Particularly the basic properties of C_{NHC}^C type ruthenacyclo complexes and their reaction mechanism in catalytic reactions have been briefly presented.

In the second chapter, a new rigid π-conjugated fused imidazo[1,5-*a*]quinoline (ImQ)-based cyclometalated ruthenium complex was designed and its catalytic utility for selective oxidation of *N*-substituted tetrahydroquinolines to lactams has been demonstrated. Cyclic-α-methylene C–H bonds were selectively oxidized in the presence of α-methyl or reactive α-methylene C–H bonds. This protocol has been successfully utilized in the late-stage functionalization and diversification of pharmaceuticals. Detailed experimental and theoretical studies have been carried out to elucidate the reaction mechanism with the help of the deuterium kinetic isotope effect, kinetic Hammett studies, and DFT studies.

In the third chapter, a fused *π*-conjugated imidazo[1,5-*a*]quinoline (ImQ) and imidazo[1,5-*a*]quinoxaline (ImQx)-based cyclometalated ruthenium complexes **Ru-1** and **Ru-4**, respectively, are found to be a highly efficient catalyst for olefin oxidation. Both the ruthenium complexes showed excellent catalytic activity for the oxidative cleavage of olefins to carbonyls. The importance of an annulated backbone in catalysis is briefly discussed. To examine the efficacy of the catalytic reaction, the turnover numbers (TONs) and turnover frequencies (TOF) in the oxidation process are calculated. A broad range of substrates including biomass, natural product, sugar, amino acid, and fatty acid-derived substrates are successfully employed in the oxidative cleavage reaction. Detailed kinetic Hammett studies, thermodynamic activation parameters, several control experiments, and DFT studies are performed to establish the proposed mechanism. The effect of the by-product $NaIO_3$ on the catalytic efficiency has been disclosed for the first time herein.

In the fourth chapter, the reactivity of the ImQ-based cyclometalated Ru(II)-complex **Ru-1** with alkynes, and *tert*-butyl isocyanide has been examined. Corresponding Ru(II) complex **Ru-5** was found as a key intermediate in the catalytic oxidative annulation reaction of imidazo[1,5-*a*]quinolin-2-ium salts with alkynes. In the first part of this chapter, the oxidative annulation reaction of imidazo[1,5-*a*]quinolin-2-ium salts with alkynes *via* *N*-heterocyclic carbene-directed C–H activation to obtain *π*-conjugated fused imidazo[1,5-*a*]quinolin-2-ium derivatives is reported. Since this reaction required the use of stoichiometric copper(II) salt as an oxidant, thus leading to the formation of large amounts of undesired copper-containing by-products. To address this issue, in the next section, molecular oxygen has been employed as an economic and clean oxidant, an alternative to metal oxidants. Lastly, the reaction pathway has been demonstrated with the help of the deuterium kinetic isotope effect, thermodynamic activation parameters, and competitive experiments. Furthermore, DFT calculation is performed to support the proposed mechanism.

The last chapter demonstrates Ru(II)-catalyzed oxidative annulation of imidazo[1,5-*a*]quinoline with alkynes *via* double C−H activation to produce highly functionalized

TH-3565_186122020

quinolizines. The addition of carboxylic acid was found as a key reaction parameter for the successful conversion. This reaction featured high efficiency and a relatively wide substrate scope, further has been successfully utilized in the late-stage functionalization and diversification of annulated products. The reaction is highly chemoselective and regioselective. In addition, the use of biomass-derived solvent as a reaction medium, the catalyst can be recycled after five reaction cycles without loss of catalytic activity. Interestingly, most of the annulated products exhibit intense fluorescence emission at a broad range and their photophysical property could be tuned by restricting the intramolecular motion in aqueous media and showing AIE-active properties. Finally, the detailed mechanistic pathways of this reaction are investigated with the help of control experiments, deuterium kinetic studies, competitive experiments, and theoretical studies.

1.8. References

1. (a) Ryabov, A. D. *Chem. Rev.* **1990**, *90*, 403−424. (b) Trofimenko, S. *Inorg. Chem*. **1973**, *12*, 1215–1221. (c) Pfeffer, M. *Pure Appl. Chem.* **1992**, *64*, 335–342. (d) Dupont, J.; Pfeffer, M.; Spencer, J. *Eur. J. Inorg. Chem.* **2001**, 1917−1927. (e) Beletskaya, I. P.; Cheprakov, A. V. *J. Organomet. Chem.* **2004**, *689*, 4055−4082.

2. (a) Albrecht, M.; van Koten, G. *Adv. Mater.* **1999**, *11*, 171−174. (b) Severin, K.; Bergs, R.; Beck, W. *Angew. Chem., Int. Ed.* **1998**, *37*, 1634−1654. (c) Ryabov, A. D.; Sukharev, V. S.; Alexandrova, L.; Le Lagadec, R.; Pfeffer, M. *Inorg. Chem.* **2001**, *40*, 6529−6532. (d) Kurzeev, S. A.; Vilesov, A. S.; Fedorova, T. V.; Stepanova, E. V.; Koroleva, O. V.; Bukh, C.; Bjerrum, M. J.; Kurnikov, I. V.; Ryabov, A. D. *Biochemistry* **2009**, *48*, 4519−4527.

3. (a) Isozaki, K.; Takaya, H.; Naota, T. *Angew. Chem., Int. Ed.* **2007**, *46*, 2855−2857. (b) Hudson, S. A.; Maitlis, P. M. *Chem. Rev.* **1993**, *93*, 861−885. (c) Bruce, D. W.; Deschenaux, R.; Donnio, B.; Guillon, D. In *Comprehensive Organometallic Chemistry III*; Mingos, D. M. P., Crabtree, R. H., Eds.; Elsevier: Amsterdam, The Netherlands, 2007; Vol. 12, p 217.

4. (a) Dixon, I. M.; Collin, J.-P.; Sauvage, J.-P.; Flamigni, L.; Encinas, S.; Barigelletti, F. *Chem. Soc. Rev.* **2000**, *29*, 385−391. (b) Williams, J. A. G. *Chem. Soc. Rev.* **2009**, *38*, 1783−1801.

5. Kleiman, J. P.; Dubeck, M. *J. Am. Chem. Soc.* **1963**, *85*, 1544−1545.

6. Cope, A. C.; Siekman, R. W. *J. Am. Chem. Soc.* **1965**, *87*, 3272−3273.

7. Dupont, J.; Pfeffer, M., Eds.; Palladacycles: Synthesis, Characterization and Applications, Wiley-VCH, Verlag GmbH & Co. KGaA, Weinheim, 2008.

8. (a) Jones, W. D.; Feher, F. J. *Acc. Chem. Res.* **1989**, *22*, 91−100. (b) Pfeffer, M. *Inorg. Synth.* **1989**, *26*, 211–214.

9. Albrecht, M. *Chem. Rev.* **2010**, *110,* 576–623.

10. (a) Rothwell, I. P. *Acc. Chem. Res.* **1988**, *21*, 153−159. (b) Gomez, M.; Muller, G.; Rocamora, M. *Coord. Chem. Rev*. **1999**, *769*, 193–195. (c) Albert, J.; Granell, J.; Muller, G. *J.*

TH-3565_186122020

Organomet. Chem. **2006**, *691*, 2101–2106. (d) Djukic, J.-P.; Sortais, J.-B.; Barloy, L.; Pfeffer, M. *Eur. J. Inorg. Chem.* **2009**, *2009*, 817–853.

11. (a) Davies, D. L.; Donald, S. M. A.; Macgregor, S. A. *J. Am. Chem. Soc.* **2005**, *127*, 13754–13755. (b) Campora, J.; Lopez, J. A.; Palma, P.; Valerga, P.; Spillner, E.; Carmona, E. *Angew. Chem. Int. Ed.* **1999**, *38*, 147–151.

12. Pearson, R. G. *Chemical Hardness: Applications from Molecules to Solids*; Wiley-VCH: Weinheim, Germany, 1997.

13. Jordan, R. F.; Guram, A. S. *Organometallics* **1990**, *9*, 2116–2123.

14. Cope, A. C.; Friedrich, E. C. *J. Am. Chem. Soc.* **1968**, *90*, 909−913.

15. Ryabov, A. D.; Sakodinskaya, I. K.; Yatsimirsky, A. K. *J. Chem. Soc., Dalton Trans.* **1985**, 2629−2638.

16. Alsters, P. L.; Engel, P. F.; Hogerheide, M. P.; Copijn, M.; Spek, A. L.; Van Koten, G. *Organometallics* **1993**, *12*, 1831−1844.

17. van Beek, J. A. M.; van Koten, G.; Ramp, M. J.; Coenjaarts, N. C.; Grove, D. M.; Goubitz, K.; Zoutberg, M. C.; Stam, C. H.; Smeets, W. J. J.; Spek, A. L. *Inorg. Chem.* **1991**, *30*, 3059−3068.

18. Dunina, V. V.; Gorunova, O. N. *Russ. Chem. Rev.* **2005**, *74*, 871−913.

19. Shaw, B. L. *J. Organomet. Chem.* **1980**, *200*, 307.

20. Mohr, F.; Priver, S. H.; Bhargava, S. K.; Bennett, M. A. *Coord. Chem. Rev.* **2006**, *250*, 1851−1888.

21. Mata, J. A.; Chianese, A. R.; Miecznikowski, J. R.; Poyatos, M.; Peris, E.; Faller, J. W.; Crabtree, R. H. *Organometallics* **2004**, *23*, 1253−1263.

22. Mann, B. E.; Shaw, B. L.; Slade, R. M. *J. Chem. Soc., Dalton Trans.* **1971**, 2976.

23. Cheney, A. J.; Mann, B. E.; Shaw, B. L.; Slade, R. M. *J. Chem. Soc., Dalton Trans.* **1971**, 3833−3842.

24. Parshall, G. W. *Acc. Chem. Res.* **1970**, *3*, 139−144.

25. Canty, A. J.; van Koten, G. *Acc. Chem. Res.* **1995**, *28*, 406−413.

26. Vicente, J.; Saura-Llamas, I. *Comments Inorg. Chem.* **2007**, *28*, 39−72.

27. Harper, T. G. P.; Desrosiers, P. J.; Flood, T. C. *Organometallics* **1990**, *9*, 2523−2528.

28. Ng, J. K.-P.; Tan, G.-K.; Vittal, J. J.; Leung, P.-H. *Inorg. Chem.* **2003**, *42*, 7674−7682.

29. Dick, A. R.; Sanford, M. S. *Tetrahedron* **2006**, *62*, 2439–2463.

30. Dangel, B. D.; Johnson, J. A.; Sames, D. *J. Am. Chem. Soc.* **2001**, *123*, 8149–8150.

31. Sen, A. *Acc. Chem. Res.* **1998**, *31*, 550–557.

TH-3565_186122020

32. Stepanova, V. A.; Dunina, V. V.; Smoliakova, I. P. *J. Organomet. Chem.* **2011**, *696*, 871–878.

33. Cope, A. C.; Kliegman, J. M.; Friedrich, E. C. *J. Am. Chem. Soc.* **1967**, *89*, 287–291.

34. Dickmu, G. C.; Stahl, L.; Smoliakova, I. P. *J. Organomet. Chem.* **2014**, *756*, 27– 33.

35. McNally, A.; Haffemayer, B.; Collins, B. S. L.; Gaunt, M. J. *Nature* **2014**, *510*, 129–133.

36. Crabtree, R. H. *The Organometallic Chemistry of the Transition Metals*; 4th edn, John Wiley & Sons, Inc., Hoboken, New Jersey 2005.

37. Dupont, J.; Consorti, C. S.; Spencer, J. *Chem. Rev.* **2005**, *105*, 2527–2571.

38. Beller, M.; Fischer, H.; Herrmann, W. A.; Brossmer, C. US5831107A, 1998.

39. Lamb, J. R.; Stepanova, V. A.; Smoliakova, I. P. *Polyhedron* **2013**, *53*, 202–207.

40. Yoshida, G.; Kurosawa, H.; Okawara, R. *J. Organomet. Chem.* **1976**, *113*, 85– 89.

41. McPherson, H. M.; Wardell, J. L. *Inorg. Chim. Acta* **1983**, *75*, 37–43.

42. Goel, R. G.; Montemayor, R. *Inorg. Chem.* **1977**, *16*, 2183–2186.

43. Clark, H. C.; Goel, A. B.; Goel, S. *Inorg. Chem.* **1979**, *18*, 2803–2808.

44. Gill, D. F.; Shaw, B. L., *J. Chem. Soc., Chem. Commun.* **1972**, 65–66.

45. Beller, M.; Fischer, H.; Herrmann, W. A.; Oefele, K.; Brossmer, C. *Angew. Chem., Int. Ed. Engl.* **1995**, *34*, 1848–1849.

46. Herrmann, W. A.; Brossmer, C.; Reisinger, C.-P.; Riermeier, T. H.; Oefele, K.; Beller, M. *Chem. –Eur. J.* **1997**, *3*, 1357–1364.

47. Herrmann, W. A.; Brossmer, C.; Oefele, K.; Reisinger, C.-P.; Priermeier, T.; Beller, M.; Fischer, H. *Angew. Chem., Int. Ed. Engl.* **1995**, *34*, 1844–1847.

48. Falvello, L. R.; Fornies, J.; Martin, A.; Navarro, R.; Sicilia, V.; Villarroya, P. *Inorg. Chem.* **1997**, *36*, 6166–6171.

49. Dupont, J.; Beydoun, N.; Pfeffer, M. *J. Chem. Soc., Dalton Trans.* **1989**, 1715–1720.

50. Lindsell, W. E.; Palmer, D. D.; Preston, P. N.; Rosair, G. M.; Jones, R. V. H.; Whitton, A. J. *Organometallics* **2005**, *24*, 1119–1133.

51. Colby, D. A.; Bergman, R. G.; Ellman, J. A. *Chem. Rev.* **2010**, *110*, 624–655.

52. Omae, I. *Coord. Chem. Rev*. **2004**, *248*, 995−1023.

53. Ackermann, L. *Chem. Rev.* **2011**, *111*, 1315−134568.

54. Song, G.; Wang, G. F.; Li, X. *Chem. Soc. Rev.* **2012**, *41*, 3651–3678.

55. Han, Y.-F.; Jin, G.-X. *Chem. Soc. Rev.* **2014**, *43*, 2799−2823.

TH-3565_186122020

56. Davies, D. L.; Al-Duaij, O.; Fawcett, J.; Giardiello, M.; Hilton, S. T.; Russell, D. R. *Dalton Trans.* **2003**, 4132−4138.

57. Li, L.; Brennessel, W. W.; Jones, W. D. *Organometallics* **2009**, *28*, 3492−3500.

58. Yao, Z.-J.; Su, G.; Jin, G.-X. *Chem.–Eur. J.* **2011**, *17*, 13298–13307.

59. Sortais, J. B.; Pannetier, N.; Holuigue, A.; Barloy, L.; Sirlin, C.; Pfeffer, M.; Kyritsakas, N. *Organometallics* **2007**, *26*, 1856−1867.

60. Cross, W. B.; Daly, C. G.; Boutadla, Y.; Singh, K. *Dalton Trans.* **2011**, *40*, 9722−9730.

61. Shibata, T.; Hashimoto, H.; Kinoshita, I.; Yano, S.; Nishioka, T. *Dalton Trans.* **2011**, *40*, 4826−4829.

62. Segarra, C.; Mas-Marzá, E.; Benítez, M.; Mata, J. A.; Peris, E. *Angew. Chem., Int. Ed.* **2012**, *51*, 10841−10845.

63. Donnelly, K. F.; Lalrempuia, R.; Muller-Bunz, H.; Albrecht, M. *Organometallics* **2012**, *31*, 8414−8419.

64. Kisenyi, J. M.; Cabeza, J. A.; Smith, A. J.; Adams, H.; Sunley, G. J.; Salt, N. J. S.; Maitlis, P. M. *J. Chem. Soc., Chem. Commun.* **1985**, 770–771.

65. Broeckx, L. E. E.; Lutz, M.; Vogt, D.; Müller, C. *Chem. Commun.* **2011**, *47*, 2003–2005.

66. Maestri, M.; Balzani, V.; Deuschel-Cornioley, C.; von Zelewsky, A. *Adv. Photochem.* **1992**, *17*, 1–68.

67. Yam, V.WW.; Wong, K. M. C. In: Molecular Wires and Electronics. Topics in Current Chemistry, vol 257, 2005, Springer, Berlin, Heidelberg.

68. Lu, Y.; Zhu, D.; Gui, L.; Li, Y.; Wang, W.; Liu, J.; Wang, Y. *J. Nanobiotechnol* **2021**, *19*, 1–13.

69. Sun, Q.; Li, Y.; Shi, H.; Wang, Y.; Zhang, J.; Zhang, Q. *Molecules* **2021**, *26*, 4389–4409.

70. Levison, J. J.; Robinson, S. D. *Chem. Commun.* (London) **1968**, 1405−1406.

71. Levison, J. J.; Robinson, S. D. *J. Chem. Soc. A* **1970**, 2947–2954.

72. Parshall, G. W.; Knoth, W. H.; Schunn, R. A. *J. Am. Chem. Soc.* **1969**, *91*, 4990−4995.

73. Gilbert, J. D.; Rose, D.; Wilkinson, G. *J. Chem. Soc. A* **1970**, 2765–2769.

74. Díaz-Álvarez, A. E.; Vidal, C.; Suárez, F. J.; Díez, J.; Cadierno, V.; Crochet, P. *Organometallics* **2015**, *34*, 3670−3677.

75. Sun, R.; Chu, X.; Zhang, S.; Li, T.; Wang, Z.; Zhu, B. *Eur. J. Inorg. Chem.* **2017**, 3174−3183.

76. Arockiam, P. B.; Bruneau, C.; Dixneuf, P. H. *Chem. Rev.* **2012**, *112*, 5879−5918.

TH-3565_186122020

77. Findlay, M. T.; Domingo-Legarda, P.; McArthur, G.; Yen, A.; Larrosa, I. *Chem. Sci.* **2022**, *13*, 3335−3362.

78. Hafeez, J.; Bilal, M.; Rasool, N.; Hafeez, U.; Adnan Ali Shah, S.; Imran, S.; Amiruddin Zakaria, Z. *Arab. J. Chem.* **2022**, *15*, 104165.

79. Albrecht, M.; Lutz, M.; Spek, A. L.; van Koten, G. *Nature* **2000**, *406*, 970–974.

80. Peris, E. *Chem. Rev.* **2018**, *118*, 9988−10031.

81. Chen, C.; Liu, F. S.; Szostak, M. *Chem.−Eur. J.* **2021**, *27*, 4478−4499.

82. Zhao, Q.; Meng, G.; Nolan, S. P.; Szostak, M. *Chem. Rev.* **2020**, *120*, 1981−2048.

83. Poyatos, M.; Maisse-Francois, A.; Bellemin-Laponnaz, S.; Peris, E.; Gade, L. H. *J. Organomet. Chem.* **2006**, *691*, 2713−2720.

84. Gnanamgari, D.; Sauer, E. L. O.; Schley, N. D.; Butler, C.; Incarvito, C. D.; Crabtree, R. H. *Organometallics* **2009**, *28*, 321−325.

85. O, W. W. N.; Lough, A. J.; Morris, R. H. *Organometallics* **2009**, *28*, 6755−6761.

86. Gupta, S. K.; Sahoo, S. K.; Choudhury, J. *Organometallics* **2016**, *35*, 2462−2466.

87. Illam, P. M.; Donthireddy, S. N. R.; Chakrabartty, S.; Rit, A. *Organometallics* **2019**, *38*, 2610−2623.

88. Gandolfi, C.; Heckenroth, M.; Neels, A.; Laurenczy, G.; Albrecht, M. *Organometallics* **2009**, *28*, 5112−5121.

89. Delgado-Rebollo, M.; Canseco-Gonzalez, D.; Hollering, M.; Mueller-Bunz, H.; Albrecht, M. *Dalton Trans.* **2014**, *43*, 4462−4473.

90. Tiwari, C. S.; Illam, P. M.; Donthireddy, S. N. R.; Rit, A. *Chem.– Eur. J.* **2021**, *27*, 16581–16600.

91. Zhang, C.; Zhao, Y.; Li, B.; Song, H.; Xu, S.; Wang, B. *Dalton Trans.* **2009**, 5182–5189.

92. Ma, C.; Ai, C.; Li, Z.; Li, B.; Song, H.; Xu, S.; Wang, B. *Organometallics* **2014**, *33*, 5164−5172.

93. Xie, X.; Huynh, H. V. *Org. Chem. Front.* **2015**, *2*, 1598−1603.

94. Schleicher, D.; Tronnier, A.; Soellner, J.; Strassner, T. *Eur. J. Inorg. Chem.* **2019**, *14*, 1956–1965.

95. Schleicher, D.; Tronnier, A.; Leopold, H.; Borrmann, H.; Strassner, T. *Dalton Trans* **2016**, *45*, 3260−3263.

96. Schleicher, D.; Leopold, H.; Strassner, T. *J. Organomet. Chem.* **2017**, *829*, 101–107.

TH-3565_186122020

97. (a) Allen, C. L.; Williams, J. M. J. *Chem. Soc. Rev.* **2011**, *40*, 3405−3415. (b) Gunanathan, C.; Milstein, D. *Science* **2013**, *341*, 249. (c) Chen, C.; Verpoort, F.; Wu, Q. *RSC Adv.* **2016**, *6*, 55599−55607.

98. Dam, J. H.; Osztrovszky, G.; Nordstrøm, L. U.; Madsen, R. *Chem. −Eur. J.* **2010**, *16*, 6820−6827.

99. Saha, B.; Sengupta, G.; Sarbajna, A.; Dutta, I.; Bera, J. K. *J. Organomet. Chem.* **2014**, *771*, 124−130.

100. Wu, X.-J.; Wang, H.-J.; Yang, Z.-Q.; Tang, X.-S.; Yuan, Y.; Su, W.; Chen, C.; Verpoort, F. *Org. Chem. Front.* **2019**, *6*, 563−570.

101. (a) Hamid, M. H. S. A.; Slatford, P. A.; Williams, J. M. J. *Adv. Synth. Catal.* **2007**, *349*, 1555−1575. (b) Watson, A. J. A.; Williams, J. M. J. *Science,* **2010**, *329*, 635–636. (c) Irrgang, T.; Kempe, R. *Chem. Rev.* **2019**, 119, 2524−2549.

102. Piehl, P.; Amuso, R.; Spannenberg, A.; Gabriele, B.; Neumann, H.; Beller, M. *Catal. Sci. Technol.* **2021**, *11*, 2512−2517.

103. (a) Bolje, A.; Hohloch, S.; van der Meer, M.; Kosmrlj, J.; Sarkar, B. *Chem. −Eur. J.* **2015**, *21*, 6756−6764. (b) Hey, D. A.; Reich, R. M.; Baratta, W.; Kuhn, F. E. *Coord. Chem. Rev.* **2018**, *374*, 114−132.

104. Bagh, B.; McKinty, A. M.; Lough, A. J.; Stephan, D. W. *Dalton Trans*. **2015**, *44*, 2712−2723.

105. Balamurugan, G.; Ramesh, R.; Malecki, J. G. *Chemistry Select* **2017**, *2*, 10603−10608.

106. Bauri, S.; Donthireddy, S. N. R.; Illam, P. M.; Rit, A. *Inorg. Chem.* **2018**, *57*, 14582−14593.

107. Wang, R.; Qin, L.; Wang, X.; Chen, B.; Zhao Y.; Gao, G. *Catal. Commun.* **2020**, *138*, 105924.

108. Zweifel, T.; Naubron, J. V.; Grützmacher, H. *Angew. Chem., Int. Ed.* **2009**, *48*, 559−563.

109. Wang, Z. Q.; Tang, X. S.; Yang, Z. Q.; Yu, B. Y.; Wang, H. J.; Sang, W.; Yuan, Y.; Chen, C.; Verpoort, F. *Chem. Commun.* **2019**, *55*, 8591−8594.

110. Dutta, C.; Choudhury, J. *RSC Adv.* **2018**, *8*, 27881−27891.

111. Bauri, S.; Mallik, A.; Rit, A. *Organometallics* **2020**, *39*, 3362−3374.

112. (a) van der Boom, M. E.; Milstein, D. *Chem. Rev.* **2003**, *103*, 1759−1792. (b) Sanford, M. S.; Love, J. A.; Grubbs, R. H. *J. Am. Chem. Soc.* **2001**, *123*, 6543−6554. (c) Vivancos, Á.; Segarra, C.; Albrecht, M. *Chem. Rev.* **2018**, *118*, 9493−9586.

TH-3565_186122020

Chapter 2

Selective Oxidation of N-Substituted Tetrahydroquinolines to Lactams by Cyclometalated Ruthenium Catalysis

TH-3565_186122020

2.1. Introduction

3,4-Dihydroquinoline-2(1*H*)-one (3,4-DHQ) units are an important *N*-containing heterocycle present in numerous natural alkaloids,[1] marketed drugs,[2] and exhibit significant biological activities.[3] For example, several pharmaceuticals or therapeutically relevant natural compounds have 3,4-DHQ motifs such as aripiprazole (an antipsychotic medicine),[4a] vesnarinone (a cardiotonic agent),[4b] carteolol (a non-selective beta blocker),[4c] cilostazol (a phosphodiesterase-3 inhibitor)[2b,4d] and meloscine (an alkaloid).[4e] In a recent study, designed *N*-centered functionalized 3,4-DHQs are found as sigma-1 receptor antagonists[5a] for treating pain and dopamine D4 receptor antagonists[5b] for treating cancer. They are also useful intermediates that can be developed further to produce a variety of widely used heterocyclic compounds, including tetrahydroquinolines and octahydroquinolones.[6] From the medicinal chemistry perspective, the lactam motif reduces the hydrophilicity of secondary and tertiary ammonium species and provides an extra hydrogen bond acceptor site that may improve the therapeutic efficacy and decrease the toxicity of the drugs.

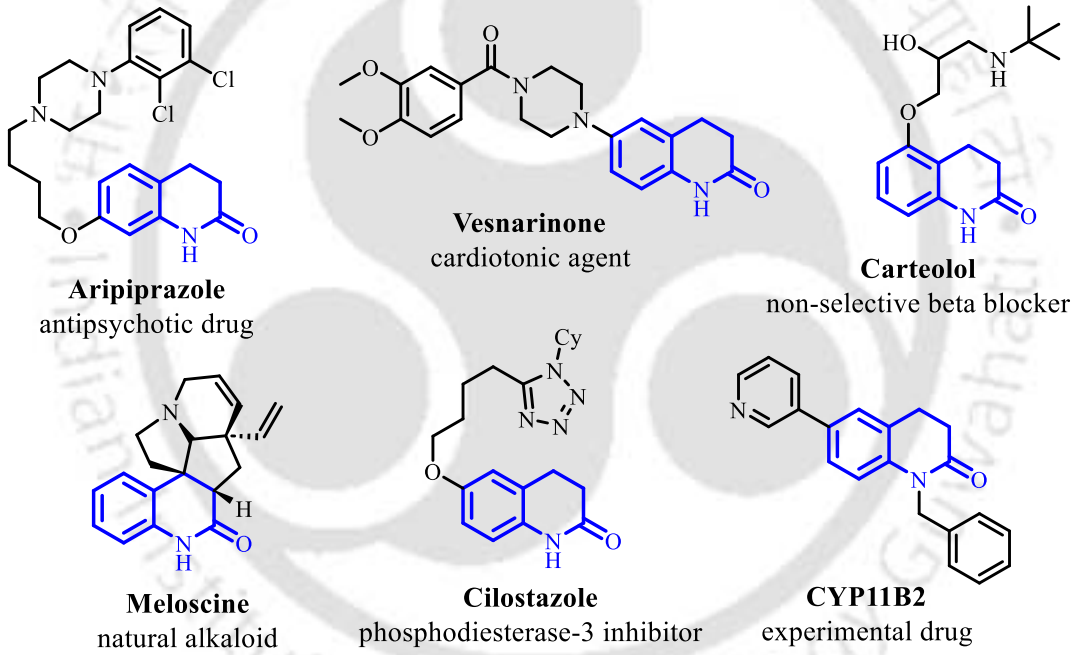
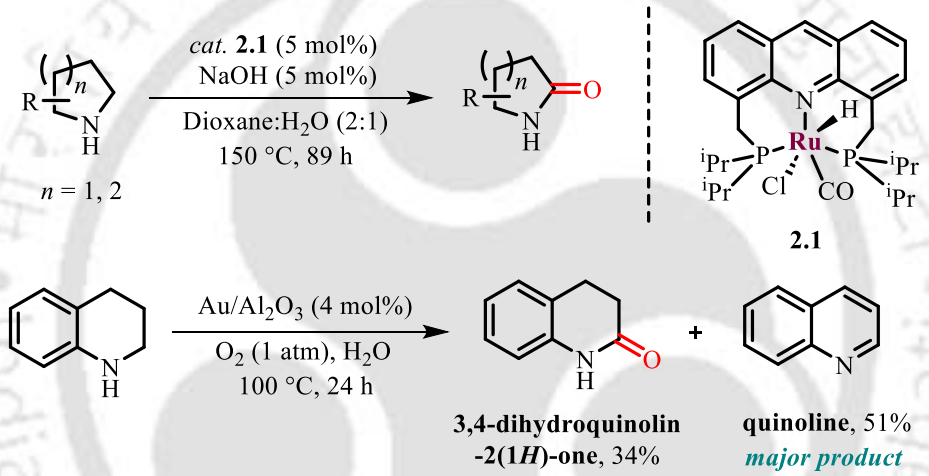


Figure 2.1. Representative marketed pharmaceuticals containing 3,4-dihydroquinoline-2 (1*H*)-one motif.

Over the past decades, various synthetic methods have been developed for 3,4-DHQ derivatives including Friedel–Crafts cyclization,[7–10] transition metal catalysis,[8] and radical reactions.[9] However, these strategies typically suffered from harsh reaction conditions, a narrow range of substrates, or required prefunctionalized substrates. Some elegant multi-step procedures such as retrosynthetic pathways, are alternative methods for constructing versatile synthons without requiring prefunctionalization of the substrate.[11] Despite these great achievements, many drawbacks still severely limit their applicability, including the utilization of heavy metals, stoichiometric hazardous oxidants, and expensive catalysts. The direct sp^3

TH-3565_186122020

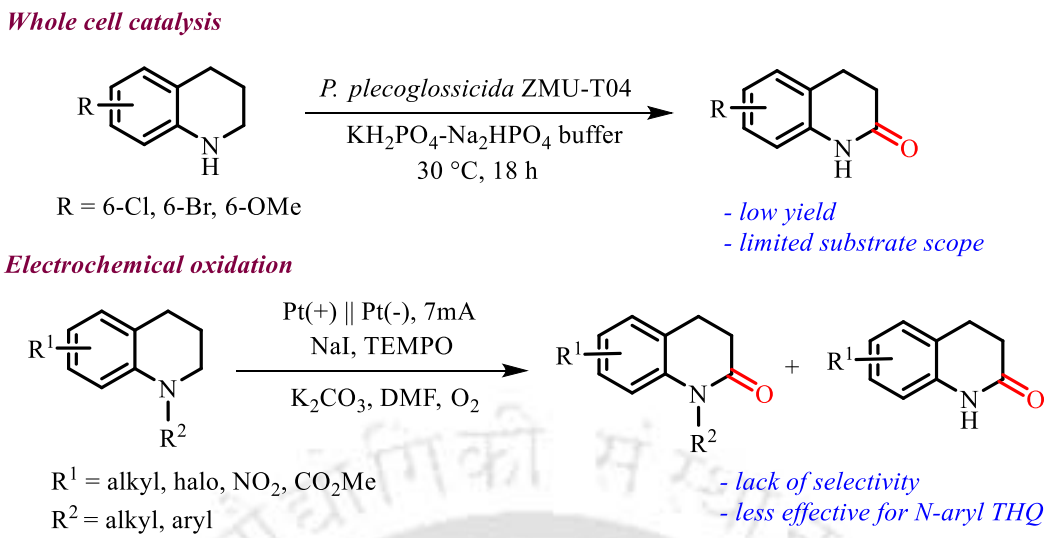
C–H bond oxidation of readily available tetrahydroquinolines to lactams is one of the most direct and atomically economical methods to access 3,4-DHQs with synthetic ease.[12] This method has the potential to be applied in large-scale synthesis. However, only a handful of examples have been reported in this regard.[13] The pioneered contribution was accomplished by the Milstein group, who demonstrated the catalytic oxidation of tetrahydroquinoline to the corresponding 3,4-dihydroquinolone using Ru-pincer catalyst **2.1** and NaOH.[13a] To achieve this transformation, the reaction requires a very high temperature of up to 150 ºC and a prolonged reaction time of 3 days. However, the efficiency of the process is limited by the use of air-sensitive catalysts and only a few substrates work in this procedure. Later Mizuno's group reported the oxidation of tetrahydroquinoline to lactam mediated by gold nanoparticles supported on alumina (Au/Al_2O_3) with molecular oxygen as an oxidant.[13b] In the oxidation of tetrahydroquinoline to lactam, quinoline was found as a major product *via* oxidative aromatization, hence hampering the selectivity of the process.



Scheme 2.1. Lactam formation from cyclic amines

Alternatively, Chen's group reported the above-mentioned motif by using whole cell biocatalysis.[13c] They demonstrated a procedure for the *α*-oxidation of cyclic amines by using *P. plecoglossicida* ZMU-T04 as a biocatalyst in KH_2PO_4/Na_2HPO_4 buffer solutions. Although whole cell biocatalysis was used for this conversion, its range of substrates is limited. During their study, it was found that *N*-methyl substituent bearing benzo-fused cyclic amine afforded formamide product solely instead of corresponding lactam since the α-methyl group is more reactive than the α-methylene group. The electrochemical oxidative condition is also reported for this transformation.[13d] He *et al.* developed a method for the synthesis of 3,4-dihydroquinolones through indirect electrochemical oxidation of tetrahydroquinolines. However, the method is less effective for the oxidation of *N*-aryltetrahydroquinolines, and it is less selective for the C2-oxidation of *N*-alkyl substituted tetrahydroquinolines since in each case *N*-alkyl bond cleaved product 3,4-DHQs was generated as a by-product. The overall study suggests that it is a very challenging task to find *N*-substituted tetrahydroquinolines with selective C–H oxidation at the α-methylene positions in the presence of a myriad of other functionalities.

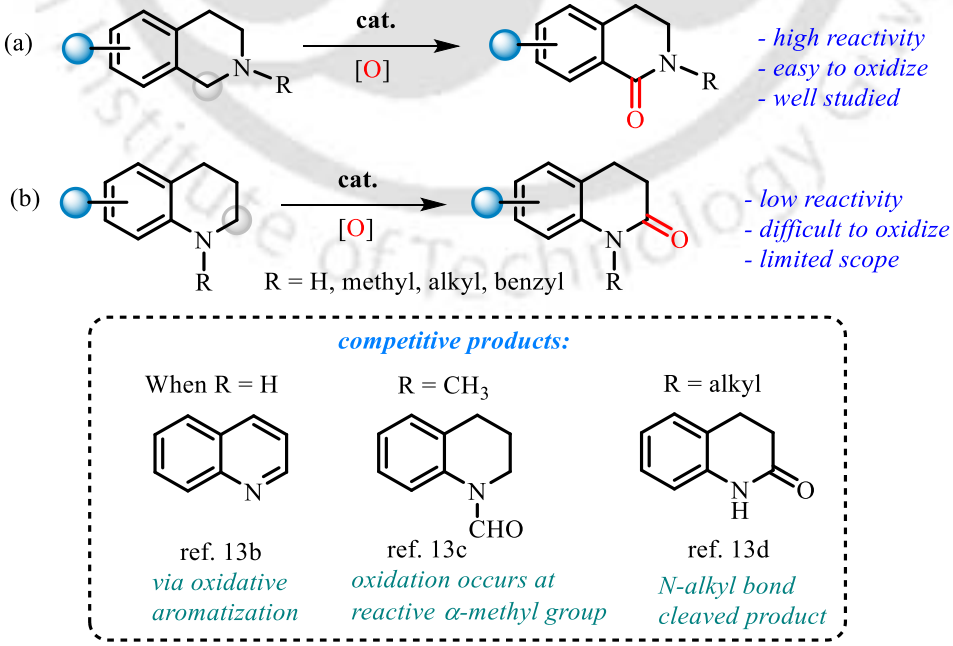
TH-3565_186122020



Scheme 2.2. Different synthetic procedures for the oxidation of cyclic amines

Synthetic challenges:

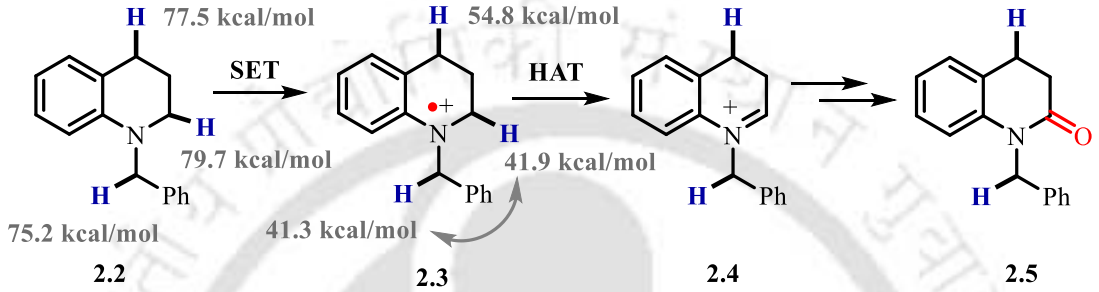
It is worth mentioning that substantial progress has been made in the direct synthesis of 3,4-dihydroisoquinolone derivatives *via* C1 oxygenation of *N*-substituted tetrahydroisoquinolines. Since C1 is located at the *α* position of N in tetrahydroisoquinoline and the benzyl position at the same time, it has high reactivity and is somewhat easy to oxidize under the reaction conditions. On the other hand, C2 of tetrahydroquinoline is only located at the *α* position of N and not the benzyl position, so its reactivity and intermediate stability are quite low. In addition, the oxidation of the benzylic carbon could be a probable competitive pathway and hence, the C2 oxygenation of THQ is considered more challenging. It is even more difficult with *N*-benzyl tetrahydroquinolines (BTHQs).



Scheme 2.3. C–H Oxidation of *N*-substituted tetrahydroisoquinoline and *N*-substituted THQ

TH-3565_186122020

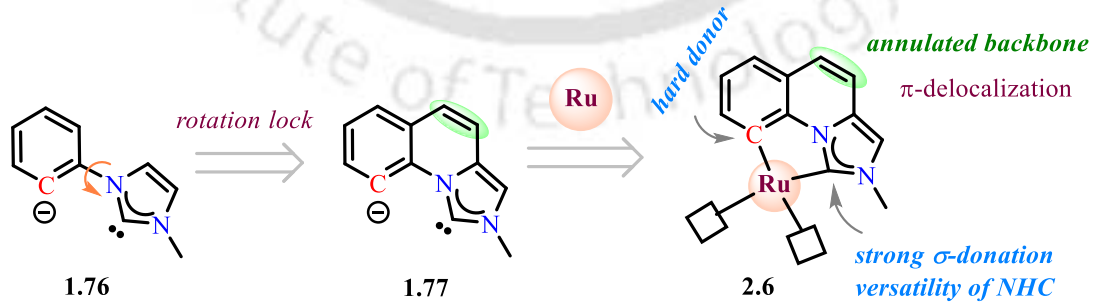
To demonstrate the hypothesis, preliminary calculations were carried out using BTHQs. The results have shown that the bond dissociation energy (BDEs) of C2−H (79.7 kcal/mol), C4−H (77.5 kcal/mol), and benzylic (75.2 kcal/mol) C−H bonds are very comparable (Scheme 2.4). Therefore, it is difficult to precisely predict the selectivity of C−H functionalization, in particular for structurally complex organic molecules. In the formation of a nitrogen centered radical cation **2.3** *via* a single electron transfer (SET) process, the BDE of the C2−H bond is significantly decreased (79.7 vs 41.9 kcal/mol). The BDE of the C2−H bond is almost similar to the benzylic C−H bonds of **2.3** (41.3 kcal/mol). Hence, controlling the selectivity bearing nearly resembling BDEs of C−H bonds is a challenging task.



Scheme 2.4. BDEs of different C−H bonds of *N*-benzyl tetrahydroquinolines

2.2. Design strategy

As mentioned in Chapter 1 (section 1.7.1), NHC-based cyclometalated complexes are known to be effective and long-living catalysts in various organic transformations primarily due to their strong metal-$C_{(NHC)}$ and metal-$C_{(carbanion)}$ bonds.[14] Also it has been shown that the stronger σ-donating ability of NHCs and carbanion donor site make it superior candidates in oxidation chemistry. In this context, I have designed a rigid π-conjugated fused imidazo[1,5-*a*]quinoline (ImQ)-based NHC-ligand **1.77** where rotational flexibility is restricted by the incorporation of an annulated backbone. The rigid system makes sure of directed metal binding. An electron-rich Ru(II)-complex **2.6** could be a superior catalyst for C−H oxidation chemistry in terms of both efficiency and selectivity.



Scheme 2.5. Design strategy

To obtain more information about the designed ligand system, DFT calculations were carried out between annulated and non-annulated NHC ligands at the B3LYP/6-31g(d,p) level of theory (Figure 2.2). Theoretical data suggests that annulated NHC ligand **2.8** (−5.55 eV/ −1.39

TH-3565_186122020

eV) has a higher HOMO energy and a lower LUMO energy than the corresponding non-annulated NHC ligand **2.7** (−6.01 eV/ −0.64 eV), thus decreasing the HOMO and LUMO energy gap (ΔE for **2.7**: 5.37 eV, ΔE for **2.8**: 4.16 eV). Also, it was found that carbanionic annulated NHC ligand **1.77** (+0.11 eV/ +2.49 eV) has a lower HOMO and LUMO energy gap (ΔE for **1.77**: 2.38 eV, ΔE for **1.76**: 2.65 eV) with respect to carbanionic non-annulated ligand **1.76** (−0.18 eV/ +2.47 eV). The theoretical data suggested that carbanionic annulated NHC ligand system **1.77** provides higher conjugational stability and enhances *σ*-donating ability compared with their nonannulated analogues.

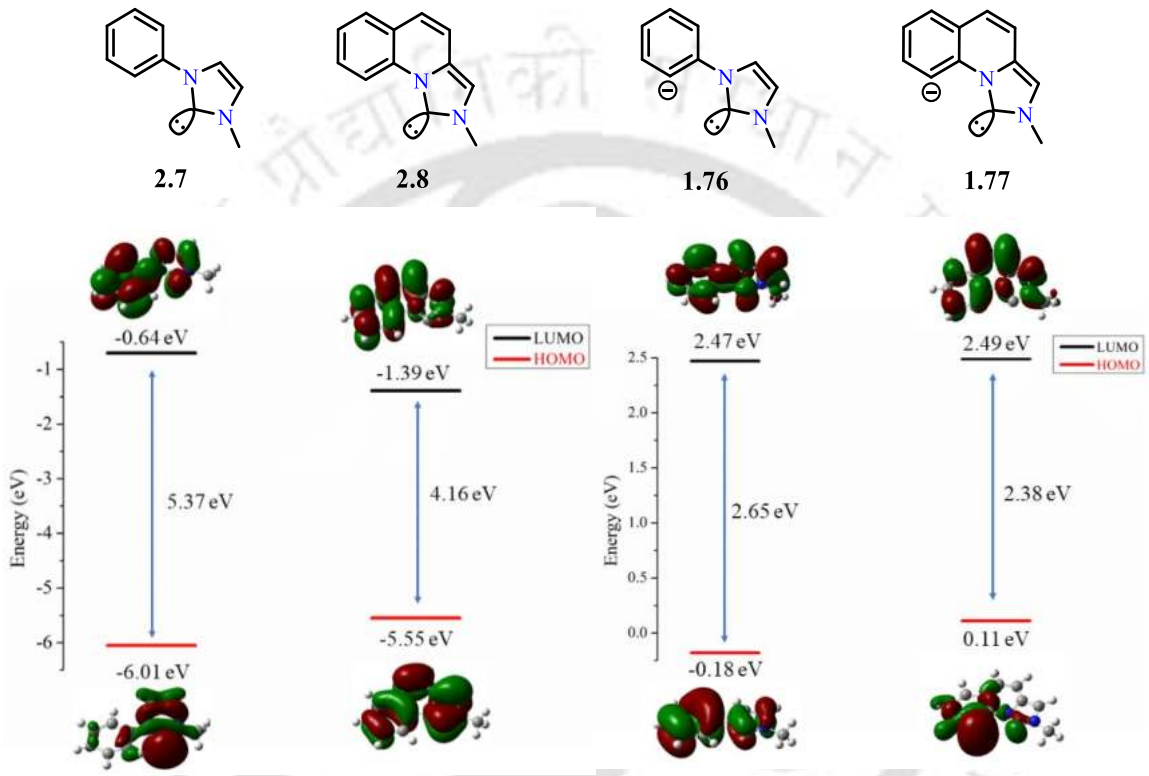


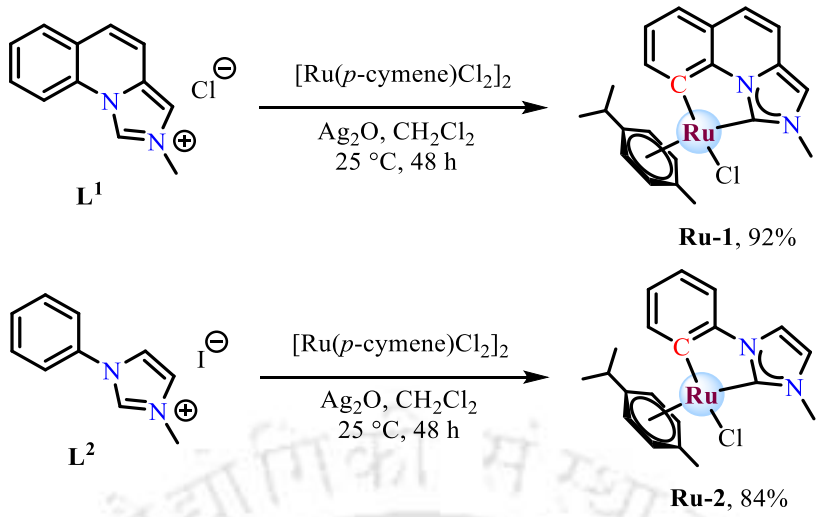
Figure 2.2. HOMO-LUMO energy profile for the ligands

2.3. Results and discussion

2.3.1. Synthesis and characterization of cyclometalated ruthenium complexes

The potential fused imidazo[1,5-*a*]quinoline-based ligand precursor $\mathbf{L^1}$ was prepared starting from cheap and readily available 2-formyl quinoline by a one-pot condensation reaction with methyl amine under an acidic medium at room temperature in 87% yield (experimental section 2.5.4). The ligand $\mathbf{L^2}$ was synthesized from phenyl imidazole following an earlier reported procedure.[15] The cyclometalated complexes **Ru-1** and **Ru-2** were synthesized *via* a one-pot transmetalation route by reacting the ligands with Ag_2O and $[RuCl_2(p\text{-cymene})]_2$ in the presence of dry CH_2Cl_2 at room temperature (Scheme 2.6). All the ruthenium complexes were fully characterized by NMR (^1H and ^{13}C) and ESI-mass spectrometry (experimental section 2.5.4). The complex **Ru-2** is already reported in the literature.[16] The formation of complex

TH-3565_186122020



Scheme 2.6. Synthesis of cyclometalated ruthenium complexes

Ru-1 is supported by the complete disappearance of the acidic imidazolium −NC*H*N− protons (10.44 ppm) from the ligand $\mathbf{L^1}$ and the presence of the characteristics Ru(II)-coordinated C_{NHC} signal at 176.8 ppm. A reasonably upfield-shifted C_{NHC} resonance in **Ru-1** suggests the presence of a relatively more electron-rich C_{NHC} in annulated complex **Ru-1** than in non-annulated cyclometalated analogue **Ru-2**. Then successful cyclometalation of the fused phenyl ring is indicated by the loss of an aromatic proton at the C9*H* position (*ortho* to the quinoline N-atom) and the presence of cyclometalated carbon signals at 160.8 ppm in the ^{13}C spectrum for **Ru-1**. Further, four different signals (in the region of 5.44−5.68 ppm) for the aromatic ring and two different signals (in the region of 0.74−0.91 ppm) for the methyl groups of the isopropyl substituent in the *p*-cymene moiety, attributing the loss of η^6 -ligand mirror symmetry along the axis of the substituents. The composition of complex **Ru-1** was further supported by ESI mass spectrometry, the main intensity peak at *m/z* 417.0907 for the $[M\text{-}Cl]^+$ ion is in good agreement with the simulated isotopic distribution patterns. A single crystal of the complex **Ru-1** was obtained by slow diffusion of petroleum ether into a solution of the complex in CH_2Cl_2 at room temperature. The X-ray crystal structure of the complex is shown in Figure 2.3. The complex adopts a typical piano-stool geometry and exhibits a distorted pseudo-octahedral coordination sphere around the ruthenium center which is occupied by the bidentate chelate ligands, halide, and planar *p*-cymene. The NHC ligand is coordinated to the metal center as a bidentate chelate motif *via* neutral carbenic and anionic carbon atoms in **Ru-1**, forming a planar five-membered metallacycle. Furthermore, it was found that the Ru−C_{NHC} bond length (2.044 Å) is slightly shorter than that of Ru−C_{aryl} bonds (2.081 Å) possibly due to π-back-donation from the metal center. To understand the steric profile of a chelating ligand, two important geometrical parameters-bite angle and yaw angle are measured. The bite angle and yaw distortion angles at the NHC/aryl ligand are measured to be 78.4° and 14.7°/9.8°, respectively, for **Ru-1**. These values are slightly higher than their non-annulated analogue **Ru-2** (76.65° and 9.1°/5.5°). These larger bite angles and an increase of yaw distortion in chelate rings are likely to indicate more conformational strain and a result of steric necessity in the annulated backbone.

TH-3565_186122020

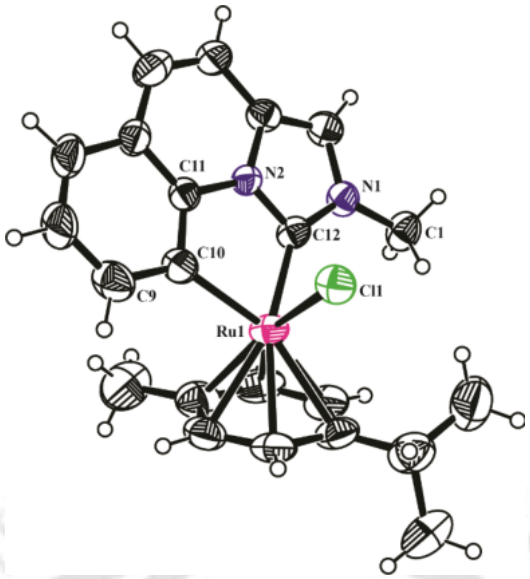
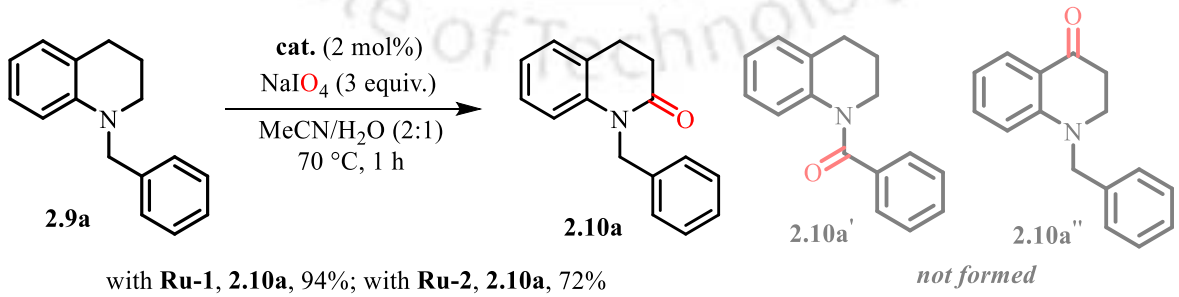


Figure 2.3. Molecular structure of complex **Ru-1** (thermal ellipsoid 30% probability level) with important atoms labeled.

2.3.2. Optimization of reaction conditions

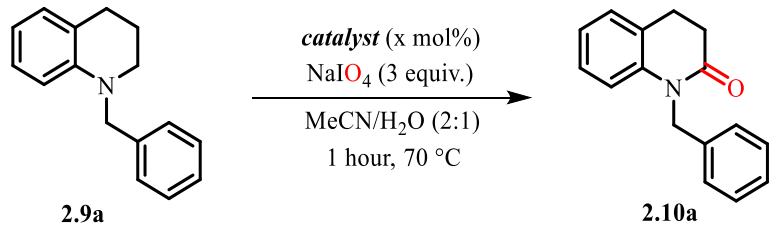
The optimization studies were initiated with *N*-benzyl tetrahydroquinoline, **2.9a** as the model substrate for the oxidation of *N*-substituted tertrahydroquinolines. The catalytic applicability of complexes **Ru-1** and **Ru-2** towards the oxidation of *N*-benzyl tetrahydroquinoline was investigated. **Ru-1** showed superior catalytic activity compared to **Ru-2** (see details in Table 2.1). The 1-benzyl-3,4-dihydroquinolin-2(1*H*)-one, **2.10a** was obtained in 94% yield using 2 mol% **Ru-1** complex under the reaction condition with 3 equiv. of $NaIO_4$, CH_3CN/H_2O (2:1) for 1 h at 70 °C. Notably, no *α*-benzylic (**2.10a'**) or C4-benzylic sp^3 C–H bond oxidized product (**2.10a''**) was formed in the reaction condition, showing excellent selectivity of **Ru-1**. Other metal catalysts such as RuO_2, RuO_4, CrO_3, $RuCl_3{\bullet}xH_2O$, $[Ru(p\text{-cymene})Cl_2]_2$ were also checked in this catalytic transformation. Only **Ru-1** was found to be the most efficient catalyst for this oxidation reaction. Control experiments suggest the necessity of the catalyst in this oxidation process.



Scheme 2.7. Ruthenium catalyzed selective oxidation of *N*-BTHQs.

Table 2.1. Screening of different catalyst[a]

TH-3565_186122020

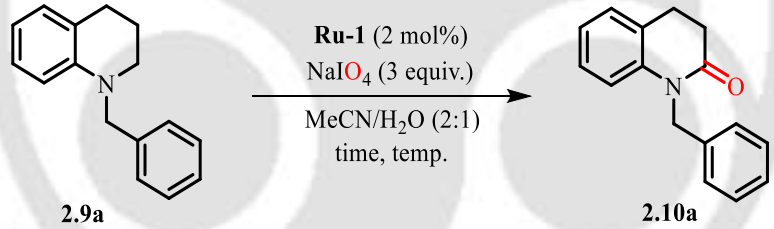


2.9a **2.10a**

Entry	Catalyst	Catalyst loading (mol%)	Yield [b] (%)
1	**Ru-1**	**2.0**	**94**
2	Ru-2	2.0	72
3	RuO_2	2.0	37
4	RuO_4	2.0	56
5	CrO_3	2.0	n.d.
6	$RuCl_3 \cdot xH_2O$	2.0	45
7	[Ru(*p*-cymene)Cl_2]	2.0	48
8	**Ru-1**	1.0	56
9	**Ru-1**	0.5	32
10	**Ru-1**	0.0	n.d.

[a] Conditions: **2.9a** (1 mmol), $NaIO_4$ (3 mmol), catalyst (x mol%) with CH_3CN/H_2O (v/v 2:1, total of 3 mL) were heated under air at 70 ºC for 1 hour in a screw-capped reaction tube. [b] isolated yields are reported. n.d. = not detected.

Table 2.2. Screening of time and temperature[a]



2.9a **2.10a**

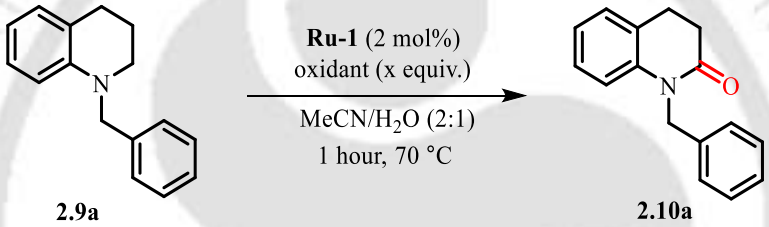
Entry	Time (h)	Temperature (ºC)	Yield [b] (%)
1	12	70	78
2	6	70	82
3	3	70	85
4	**1**	**70**	**94**
5	0.5	70	67
6	1	80	90
7	1	60	87
8	1	40	75
9	1	25	66
10	12	25	80
11[c]	1	70	91
12[d]	1	70	92

[a] Conditions: **2.9a** (1 mmol), $NaIO_4$ (3 mmol), **Ru-1** (2 mol%) with CH_3CN/H_2O (v/v 2:1, total of 3 mL) were heated in a screw-capped reaction tube under air at indicated time and temperature. [b] isolated yields are reported. [c]reaction was performed with oxygen-free solvents and under oxygen-free atmosphere. [d] reaction was performed under a molecular O_2 atmosphere.

TH-3565_186122020

For further optimization, reaction time and temperature were also checked for this transformation. The reaction required one hour for the complete conversion of the starting material (Table 2.2, entries 1−5). On reducing the reaction temperature, the yield of the reaction was also decreasing gradually (Table 2.2, entries 7−9). The results of the control experiment indicate that the oxidant is required for this catalytic transformation (Table 2.3, entry 1). The yield of the desired 1-benzyl-3,4-dihydroquinolin-2(1H)-one, **2.10a** was decreased with a lower amount of oxidant $NaIO_4$ (Table 2.3, entries 2 and 3) or a higher equivalent of $NaIO_4$ (Table 2.3, entry 5). Other oxidants such as H_2O_2, ^{t}BuOOH, *m*-CPBA, TBAPI, and molecular oxygen were less effective or not effective for this catalytic reaction (Table 2.3, entries 6−10). For further optimization, the reaction was examined with a series of other solvent combinations under identical reaction conditions (Table 2.4). Acetonitrile: water (2:1) was found to be the most efficient reaction medium in the current catalytic reaction. Therefore, I fixed the optimized reaction conditions as **2.9a** (1 equiv.), $NaIO_4$ (3 equiv.), **Ru-1** (2 mol%) at 70 °C for 1 hour in the solvent mixture of CH_3CN: H_2O (2:1).

Table 2.3. Screening of different oxidants [a]

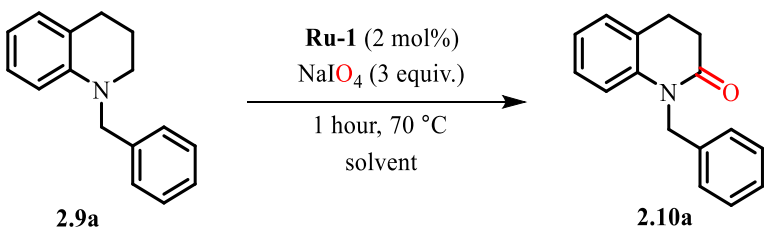


2.9a **2.10a**

Entry	Oxidant (equiv.)	Yield [b] (%)
1	$NaIO_4$ (0)	0
2	$NaIO_4$ (1)	30
3	$NaIO_4$ (2)	55
4	**$NaIO_4$ (3)**	**94**
5	$NaIO_4$ (4)	88
6	H_2O_2 (3)	22
7	^{t}BuOOH (3)	56
8	*m*-CPBA (3)	n.d.
9	TBAPI (3)	41
10	O_2 (1 atm)	n.d.
11[c]	O_2 (1 atm)	n.d.

[a] Conditions: **2.9a** (1 mmol), oxidant (x equiv.), **Ru-1** (2 mol%) with CH_3CN/H_2O (v/v 2:1, total of 3 mL) were heated under air at 70 ºC for 1 hour in a screw-capped reaction tube. [b] isolated yields are reported. [c]only CH_3CN as solvent. n.d. = not detected.

Table 2.4. Solvent optimization[a]



2.9a **2.10a**

TH-3565_186122020

Entry	Solvent (*v/v*)	Yield [b] (%)
1	CH_3CN: H_2O (1:1)	78
2	**CH_3CN: H_2O (2:1)**	**94**
3	CH_3CN: H_2O (3:1)	92
4	CH_3CN: H_2O (1:2)	88
5[c]	Only CH_3CN	12
6[d]	Dry CH_3CN	0
7	Only H_2O	<5
8	EtOAc: H_2O (2:1)	80
9	THF: H_2O (2:1)	85
10	DCE: H_2O (2:1)	52

[a] Conditions: **2.9a** (1 mmol), $NaIO_4$ (3 mmol), **Ru-1** (2 mol%) with indicated solvent mixtures were heated under air at 70 ºC for 1 hour in a screw-capped reaction tube. [b] isolated yields are reported. [c] wet CH_3CN is used. [d] dry CH_3CN is used.

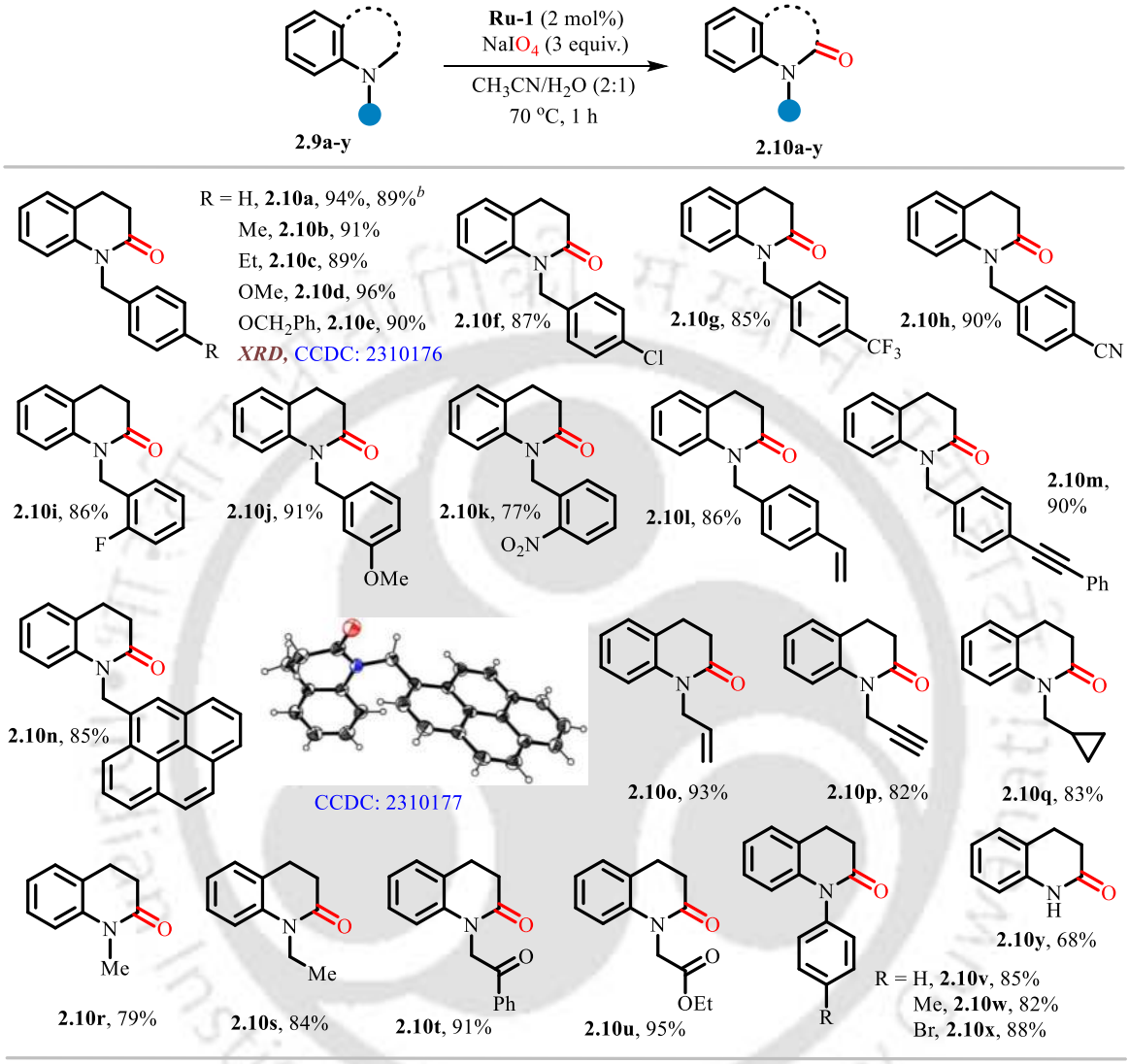
2.3.3. Substrate scope

After achieving the optimized reaction conditions, the scope of the oxidation reaction was explored with various *N*-substituted tetrahydroquinolines. The reaction seems fairly effective for a wide pool of substrates with high to good yields of the oxidized products at the C2 position. *N*-substituted tetrahydroquinolines having both electron-donating (e.g., −Me, −Et, −OMe, $-OCH_2Ph$) and electron-withdrawing (e.g., −Cl, $-CF_3$, and −CN) groups as substituents at the *para*-position in the benzyl moiety were efficiently reacted to obtain the desired products **2.10a-h** in good to excellent yield. Notably, the electron-donating substituents (Table 2.5, products **2.10b-e**) led to the desired products with higher yields compared to electron-withdrawing substituents (product **2.10f-h**). Similarly, substrates having *ortho*- and *meta*-substituents also produced the corresponding C2-oxidized product **2.10i-k** with a good yield. Interestingly the *ortho*-substituent $-NO_2$ group also survived these reaction conditions to give the oxidized product **2.10k** in 77% yield. Remarkably, the oxidation-sensitive benzylic C−H bond (**2.9e**) and C−C multiple bonds, such as **2.9l** and **2.9m**, were unaffected during the oxidation process, demonstrating the exceptional chemoselective nature of this protocol.[17] Although the reagent is strong enough to disrupt the least aromatic ring of pyrene,[17] it is selective enough to give **2.10n** in 85% yield, clearly revealing the effectiveness of the catalyst. The structural confirmation of **2.10e** and **2.10n** is unequivocally confirmed by single-crystal X-ray diffraction analysis. Additionally, substituents containing allyl, propargyl, and cyclopropyl groups were employed under the same reaction conditions to test the selectivity of the catalyst. The corresponding lactam **2.10o**, 93%, **2.10p**, 82%, and **2.10q**, 83%, respectively are formed, with no loss of functionality under the reaction conditions. In the case of *N*-methyltetrahydroquinoline **2.9r**, albeit the *α*-methyl group is more reactive than the *α*-methylene group, a desired C2 oxidized product **2.10r** was obtained in 79% yield. It should be noted that selective C2-oxidation occurs with **2.9t** and **2.9u** in the presence of reactive $-CH_2COPh$ and $-CH_2CO_2Et$ functionality, suggesting the chemoselective nature of the developed protocol. I have also tried to selectively oxidize the *N*-aryltetrahydroquinoline substrates, delightfully it gave the desired products **2.10v–x** in good yield. Next, non-

TH-3565_186122020

substituted tetrahydroquinoline was also found as a suitable candidate for the oxidation reaction, giving the product **2.10y** in 68% yield.

Table 2.5. Substrate scope of various *N*-substituted tetrahydroquinolines[a]

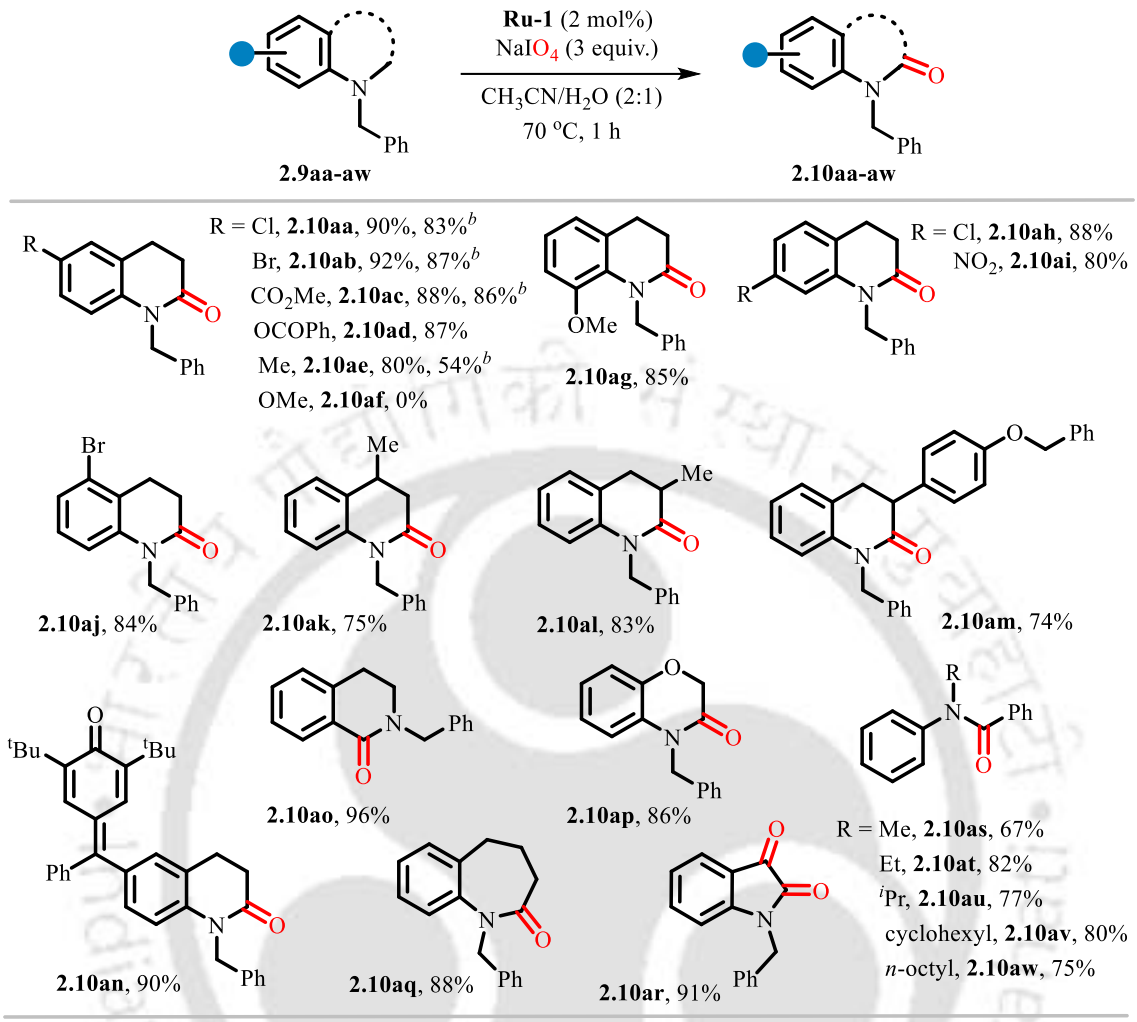


Reaction condition: [a] **2.9a-y** (0.5 mmol), **Ru-1** (2 mol%), $NaIO_4$ (3 equiv.), CH_3CN/H_2O (2:1) was heated at 70 °C in a reaction tube for 1 h, isolated yield. [b] 1 mmol scale.

To further evaluate the efficiency of this methodology, a variety of substituents in the benzo-fused ring were examined (Table 2.6). *N*-benzyltetrahydroquinoline bearing electron-withdrawing groups such as 6-Cl, 6-Br, 6-CO_2Me, 6-OCOPh, 7-Cl, 7-NO_2, and 5-Br groups, the expected products **2.10aa-ad**, **2.10ah-aj** were obtained in good yield. Sensitive functional group nitro (-NO_2) at the C7 position of the benzo-fused ring also survived under the reaction conditions and afforded a good yield of the desired product **2.10ai**. Similarly, BTHQs with electron-donating groups in the fused aromatic ring were investigated; these included 6-Me and 4-Me, which further yielded the desired products **2.10ae** and **2.10ak** in good yield. Compared to electron-donating groups, the electron-withdrawing group gave a higher yield. Surprisingly, I failed to obtain the desired oxidized product **2.10af,** when 6-methoxy-*N*-

TH-3565_186122020

Table 2.6. Substrate scope for different substituents containing benzo-fused ring[a]



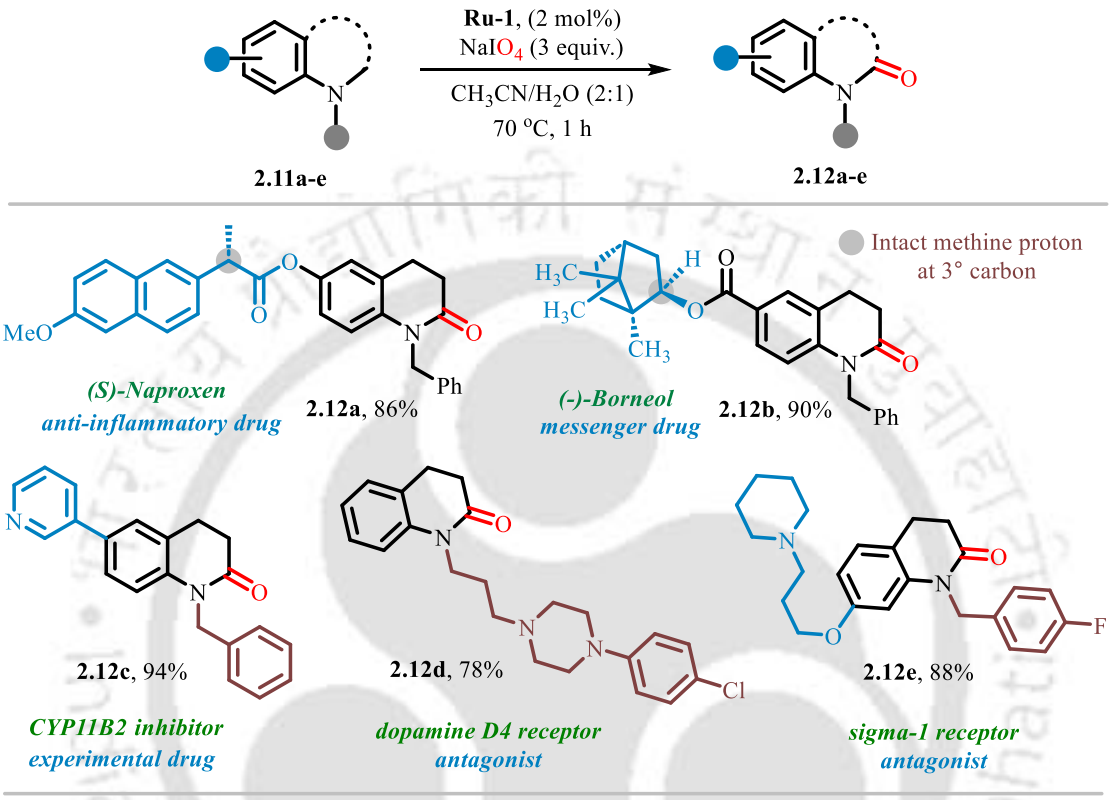
Reaction condition: [a] **2.9aa-aw** (0.5 mmol), **Ru-1** (2 mol%), $NaIO_4$ (3 equiv.), CH_3CN/H_2O (2:1) were heated at 70 °C in a reaction tube for 1 h, isolated yield. [b] at room temperature.

benzyltetrahydroquinoline (**2.9af)** was used as a substrate. On the other hand, 8-methoxy-*N*-benzyltetrahydroquinoline (**2.9ag**), afforded desired product **2.10ag** in 85% yield. This might be due to the electronic influence of -OMe at different positions of BTHQ. In comparison to 6-OMe, 8-OMe has a stronger electron-withdrawing induction effect for N, which may promote the C–H oxidation of **2.9ag**. Interestingly, substrates having substituents near the active site of a BTHQs moiety such as the C3 substituted BTHQs efficiently reacted to obtain the desired product **2.10al** and **2.10am** in 83%, and 74% yield, respectively, suggesting that the current protocol is not sensitive to the steric effect and shows excellent selectivity. Retaining halogen functional groups can be beneficial as it allows for further functionalization. In our study, the halogen substituents (5-Br, 6-Cl, 6-Br) remained intact giving the desired oxidized compounds in excellent yields. Although *para*-quinone methide is a potential acceptor in 1,6-nucleophilic conjugate addition reactions, a selective C2-oxidation was also effectively applied to *para*-quinone methide functionalized BTHQ derivatives **2.9an** to get the oxidized product **2.10an** in 90% yield. I was pleased to find that the scope of the reaction can be extended beyond quinoline and could easily react with other *N*-benzylic heteroarenes such isoquinoline, benzomorpholine,

TH-3565_186122020

tetrahydrobenzazepine, and indoline (products **2.10ao-ar**). It is noteworthy that the reaction of acyclic *N*-benzylic amine proceeded smoothly to deliver benzylic oxidized product **2.10as-aw** in moderate to good yield.

Table 2.7. Substrate scope of bioactive *N*-heterocycles *via* late-stage C–H oxidation[a]

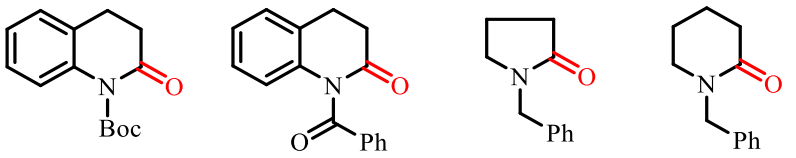


[a]Reaction condition: **2.11a-e** (0.5 mmol), **Ru-1** (2 mol%), $NaIO_4$ (3 equiv.), CH_3CN/H_2O (2:1) were heated at 70 °C in a reaction tube for 1 h, isolated yield.

Next, the scope of the reaction was expanded for the synthesis of different bioactive molecules. In light of the significance of the lactam motif in various biological and pharmaceutically relevant in complex molecular settings,[1–3] a substrate containing the nonsteroidal anti-inflammatory drug naproxen and the naturally occurring messenger drug (-)-borneol was successfully converted into lactam derivatives **2.12a**, and **2.12b** in 86% and 90% yield, respectively. To our delight, in both cases, methine proton at 3° carbon remained unaffected under the oxidation condition. Further highlighting the potential of this approach for practical uses, the current methodology was also used for the efficient synthesis of bio-active molecules *via* late-stage C–H oxidation, such as CYP11B2 inhibitor **2.12c** (94%),[3] dopamine D_4 receptor antagonist **2.12d** (78%),[5b] and sigma-1 receptor antagonist **2.12e** (88%).[5a] However, I failed to obtain the C2 oxidized product for *N*-Boc tetrahydroquinoline **2.13a**, *N*-Bz tetrahydroquinoline **2.13b**, *N*-benzyl pyrrolidine **2.13c**, and piperidine **2.13d** substrates (Table 2.8), suggesting the availability of nitrogen lone pair and benzo-fused ring structure is essential for this chemo-selective oxidation.

TH-3565_186122020

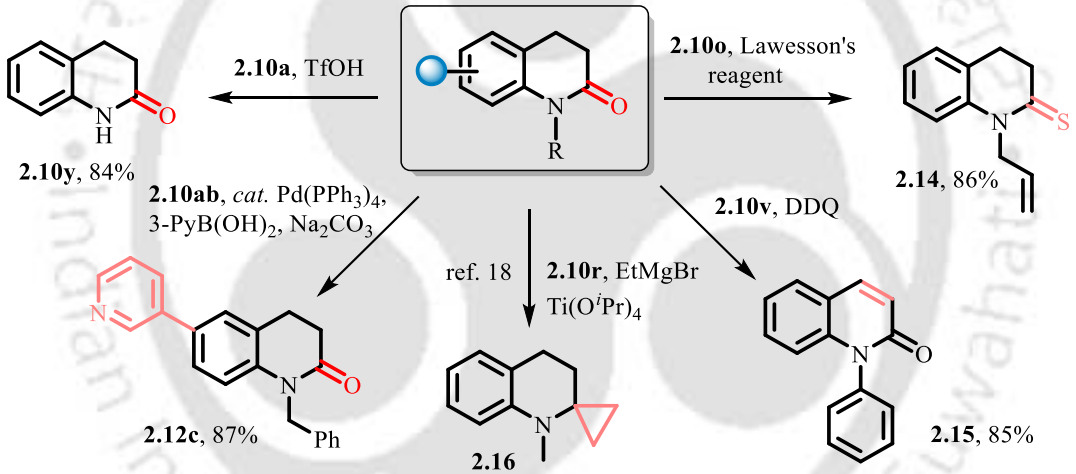
Table 2.8. Failed substrates for C2-oxidation of different *N*-substituted heterocycle



2.13a′, 0% **2.13b′**, 0% **2.13c′**, 0% **2.13d′**, 0%

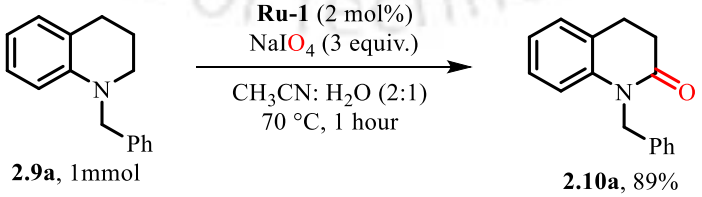
2.3.4. Post-synthetic modification

Furthermore, the lactam derivatives can easily transform into other useful molecules. For example, the debenzylation of **2.10a** was easily achieved by TfOH, providing **2.10y** in 84% yield. Using Lawesson's reagent, the C=O bond of **2.10o** could be converted to **2.14** with C=S functionality. The treatment of **2.10v** with DDQ delivers the dehydrogenation product **2.15** in 85% yield. Compound **2.16** can also be achieved *via* the reported condition.[18] The CYP11B2 inhibitor **2.12c** was achieved by using Pd-catalysed cross-coupling with **2.10ab**.



Scheme 2.8. Post-synthetic modification of lactam derivatives

2.3.5. Scale-up reaction



2.9a, 1mmol **2.10a**, 89%

Scheme 2.9. 1 mmol scale reaction of **2.9a**

The efficiency of this method was studied by scaling up the reaction in one mmol scale for bulk utilization. First, $NaIO_4$ (642 mg, 3 mmol) was taken in a screw-capped reaction tube and dissolved in water (2 mL). 1-benzyl-1,2,3,4-tetrahydroquinoline **2.9a**, (223 mg, 1 mmol), **Ru-**

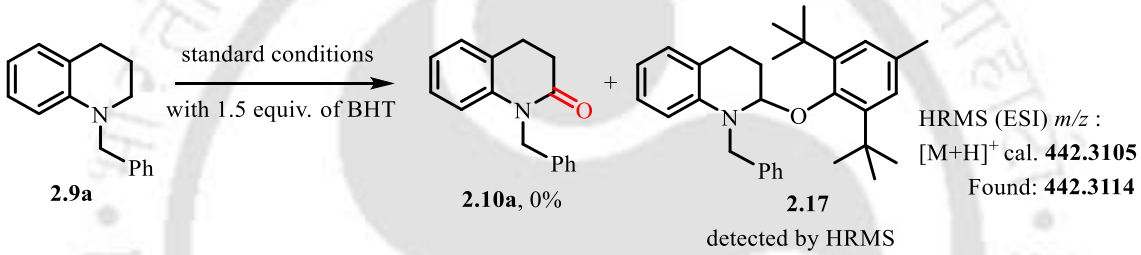
TH-3565_186122020

1 (2 mol%), and acetonitrile (4 mL) were added to the reaction tube and stirred the reaction mixture in a preheated oil bath at 70 ºC for 1 hour (Scheme 2.9). After the completion of the reaction, the crude product was purified to get the pure product **2.10a** as a white solid with an 89% yield. Hence, the process is overall very efficient from a practical perspective.

2.3.6. Mechanistic investigation

2.3.6.1. Radical trapping experiment

To get insight into the reaction pathway, I have performed a few control experiments. To verify whether the reaction undergoes a radical path or not I used the common radical scavenger 2,6-di-*tert*-butyl-4-methylphenol (BHT) in a radical trapping experiment. The reaction was completely suppressed in the presence of BHT. An analysis of the crude reaction mixture using ESI-mass spectrometry revealed the likely formation of **2.9a**-BHT-adduct, **2.17**. This suggests a potential radical pathway involved in the reaction, possibly with *α*-amino radical species as one of the key intermediates. (Scheme 2.10).



Scheme 2.10. Radical trapping experiment

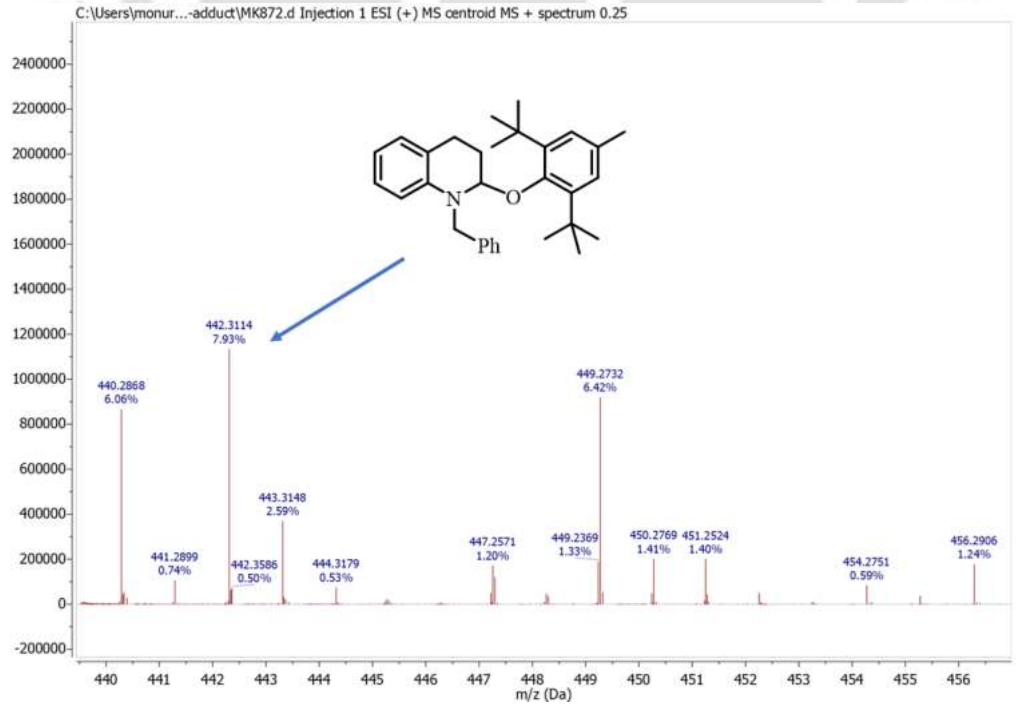
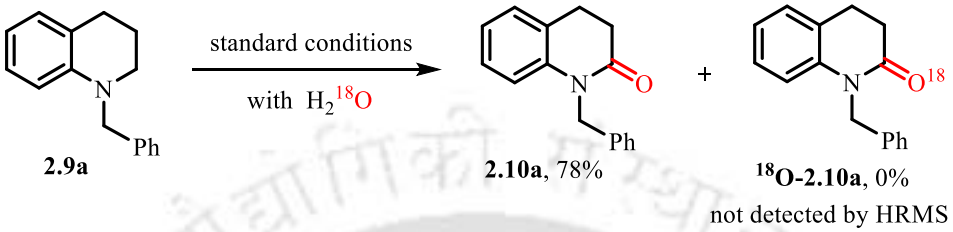


Figure 2.4. Mass spectrometry (HRMS) spectrum of the radical trapping experiments

TH-3565_186122020

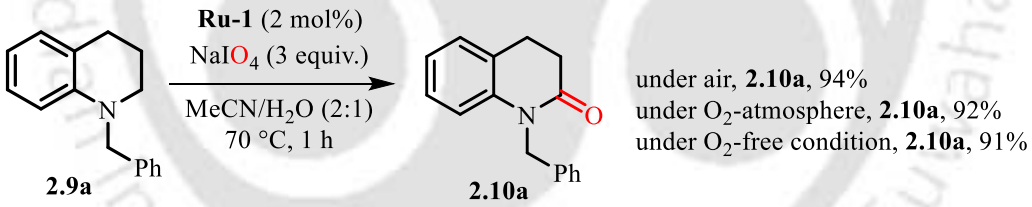
2.3.6.2. Isotope labeling experiment (source of carbonyl oxygen)

An isotope labeling experiment was performed to understand the source of the carbonyl oxygen in the product. When the reaction was conducted in the presence of $H_2{}^{18}O$ instead of H_2O, no ^{18}O incorporation product **^{18}O-2.10a** was detected in the ESI-mass spectrometry analysis, which ruled out the possible involvement of $H_2{}^{18}O$ acts as a nucleophile in the reaction (Scheme 2.11).



Scheme 2.11. Isotope labeling experiment with $H_2{}^{18}O$

A few control experiments were carried out to further confirm the source of carbonyl oxygen. Since the model reactions were carried out under an air atmosphere, air might be the source of carbonyl oxygen. To understand this, control experiments were performed with or without an O_2 atmosphere (Scheme 2.12). Results suggest that the source of the carbonyl group likely to be from periodate, ruling out the possible involvement of air since the yield of **2.10a** is almost comparable under air, under oxygen-atmosphere, and oxygen-free conditions (see Table 2.2, entry 4, entry 13, entry 14).

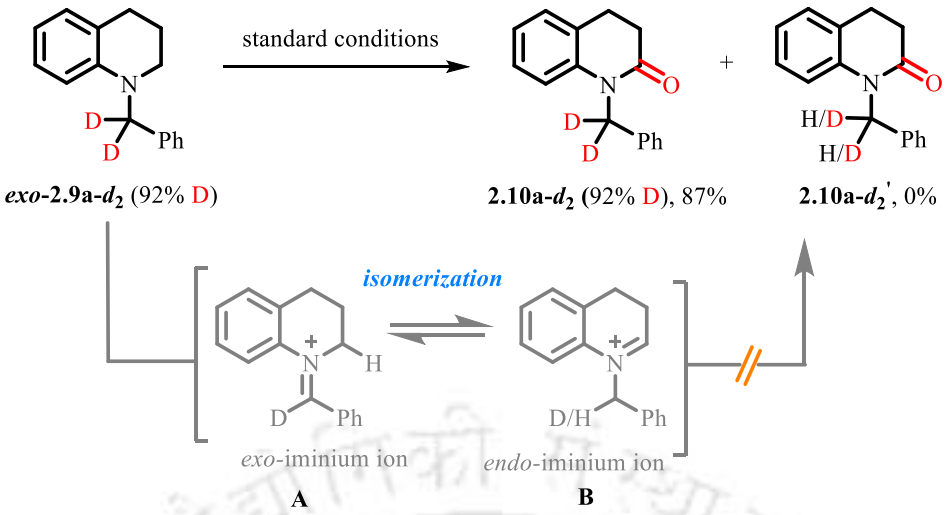


Scheme 2.12. Control experiments to know the source of carbonyl oxygen

2.3.6.3. Deuterium scrambling experiments

Since the *N*-benzyl group is more reactive than the *α*-methylene group, the *N*-benzyl group can first oxidize to generate the *exo*-iminium ion **A**, which further undergoes isomerization to give *endo*-iminium ion **B** and then leads to the desired product (Scheme 2.13). To probe whether the reaction proceeds through isomerization pathways or not, I have performed an experiment with ***exo*-2.9a-*d*$_2$** as a substrate under standard conditions, and no H/D scrabbling product **2.10a-*d*$_2'$** was observed. Only the C2 oxidized product **2.10a-*d*$_2$** was formed in 87% yield, which is likely to be ruled out the possible involvement of iminium ion isomerization.

TH-3565_186122020



Scheme 2.13. Deuterium scrambling experiments

2.3.6.4. Kinetic Hammett studies

To understand the electronic feature of the transition state in the reaction, a linear free energy analysis was performed using initial rates of various 6-substituted BTHQs under standard reaction conditions (Figure 2.5). The reaction rates are in the order CO_2Me >Cl>Br >H>Me. The least-squares fit to the plot of [log(k_X/k_H)] *vs*. Hammett σ^+ constant gave a straight line with a ρ^+ value of +2.39. A large positive ρ^+ value suggests the development of a negative charge in the transition state which is stabilized by the electron-withdrawing substituents.

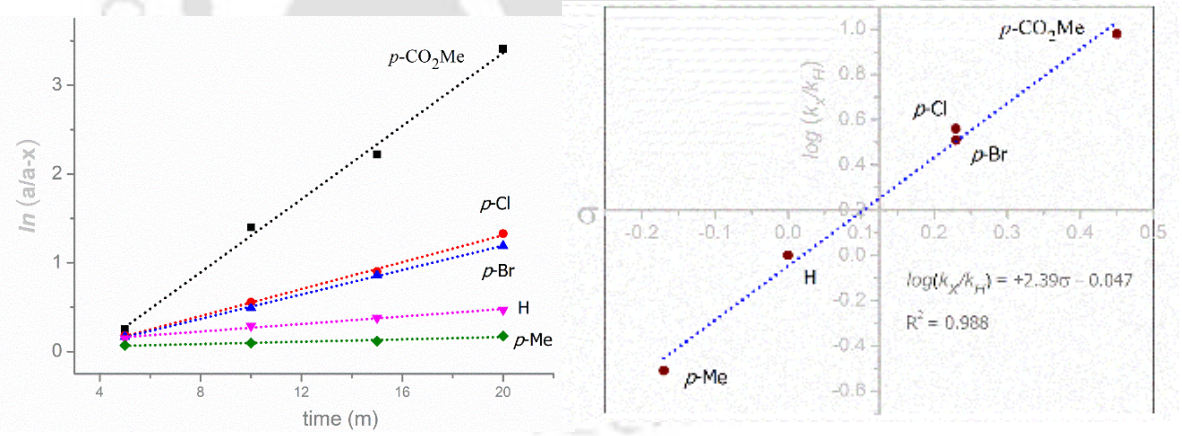


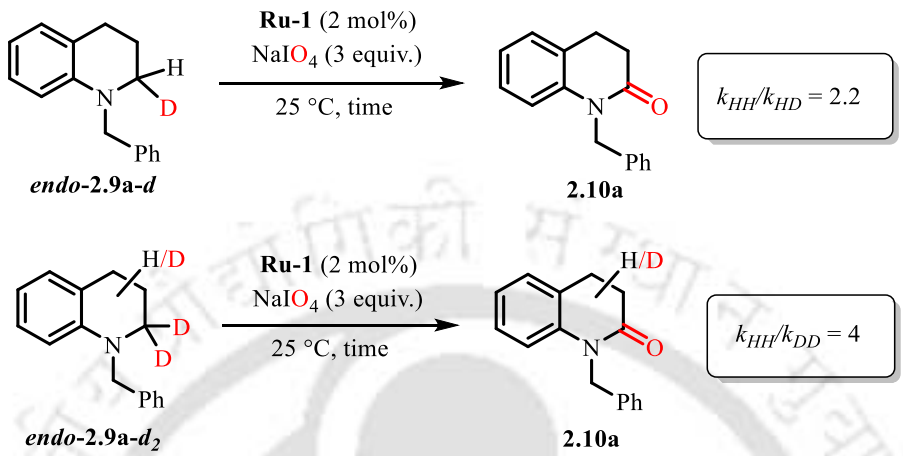
Figure 2.5. Kinetic profile for the initial rates of oxidation of 6-substituted BTHQs (left figure) and Hammett plot (right figure).

2.3.6.5. Kinetic Isotope Effect (KIE) studies

kinetic isotope effect (KIE) is a unique way to determine the mechanism of the reaction. The kinetic isotope effects were studied by performing three parallel reactions for the individual substrate **2.9a**, ***endo*-2.9a-*d***, and ***endo*-2.9a-*d*$_2$** respectively. The KIE based on independently determined production rates was large (k_{HH}/k_{DD} = 4, k_{HH}/k_{HD} = 2.2), revealing the α-methylene

TH-3565_186122020

C–H bond cleavage of **2.9a** as the turnover-limiting step (Scheme 2.14). This outcome is distinctly different from most other conventional amine oxidation processes,[12,19] which generally feature the electron transfer (ET) step from the amine to oxidant as the rate-limiting step, and enhancing the rate of the reaction by the EDGs.



Scheme 2.14. KIE experiments

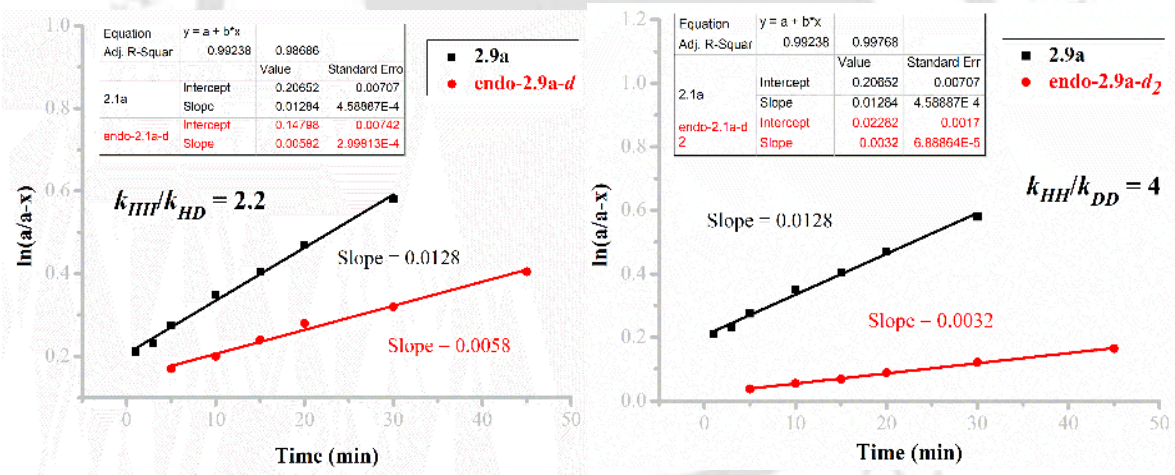


Figure 2.6. Plot of ln(a/a-x) *vs* time (min)

2.3.6.6. Spectroscopic characterization of intermediate

In order to gain insight into the proposed intermediates, one stoichiometric reaction was performed between complex **Ru-1** and $NaIO_4$ (aq.) (1:1 molar ratio) at room temperature in acetonitrile and the ESI-MS recorded immediately. The signal at *m/z* 314.9704 corresponds to cationic **Ru-1** *cis*-dioxo species i.e., [**Ru-1-I2**-Cl]$^+$ which may actively be involved in the catalytic process (Figure 2.7).

TH-3565_186122020

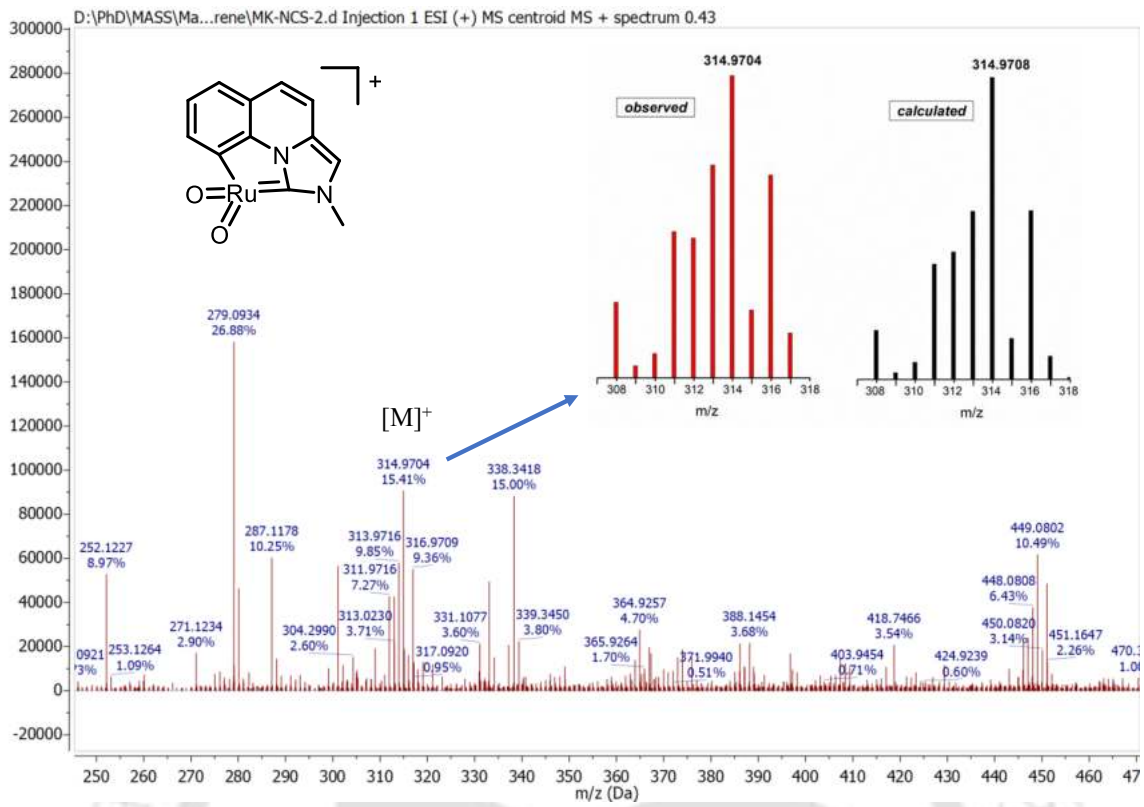


Figure 2.7. Mass spectrometry (HRMS) data of [**Ru-1-I2**-Cl]$^+$

2.3.6.7. Role of water in oxidation reaction

Since the reaction was conducted with a mixture of solvents CH_3CN: H_2O (2:1), the role of water in the oxidation process has been investigated. When the model reaction was conducted with freshly dry acetonitrile and completely moisture and oxygen-free conditions, no conversion of **2.9a** was acquired, indicating the important role of water in the catalytic process (Table 2.4, entry 6). On the other hand, in Table 2.3, it has been proven that the oxidant $NaIO_4$ plays an important role in the catalytic process. The oxidant is soluble in water, not in other organic solvents. In the reaction mechanism, (Figure 2.8), Ru(VI)-*cis*-dioxo species **Ru-1-I2**

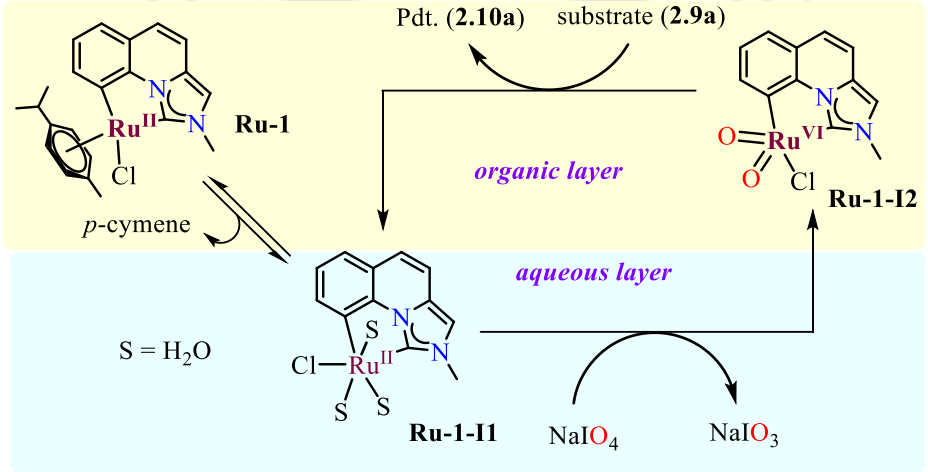


Figure 2.8. Catalytic cycle

TH-3565_186122020

(perhaps soluble in organic solvents) is readily reacted with the substrate and moves into the aqueous layer as **Ru-1-I1** (soluble in water), where it is oxidized back to **Ru-1-I2** by the oxidant. Overall, this is a biphasic system. The aqueous layer likely helps in complex oxidation (**Ru-1-I1** → **Ru-1-I2**), and the organic layer expedites substrate oxidation (**2.9a** → **2.10a**).

2.3.7. Computational studies

To gain further mechanistic insight into the mechanism, DFT calculations have been performed using the B3LYP-gd3bj/Def2SVP level of theory. Initially, single-electron transfer (SET) occurs from the electron-rich nitrogen atom of **2.9a** to the high valent Ru(VI)-dioxo species **Ru-1-I2**, forming a nitrogen radical cation species **int-1**. The process is energetically uphill (ΔG = 18.4 kcal/mol). The **int-1** is then transformed to α-amino radical ***endo*-int-2** in an exothermic manner (ΔG = 8.4 kcal/mol) with a proton transfer segment *via* **TS-1** with an energy barrier of 4 kcal/mol (Figure 2.9). Likewise, **int-1** can led to the formation of the α-amino radical species ***exo*-int-2** in an exothermic fashion (ΔG = 1.9 kcal/mol, Figure 2.10). Unfortunately, the transition state from **int-1** to ***exo*-int-2** could not be found. In both cases,

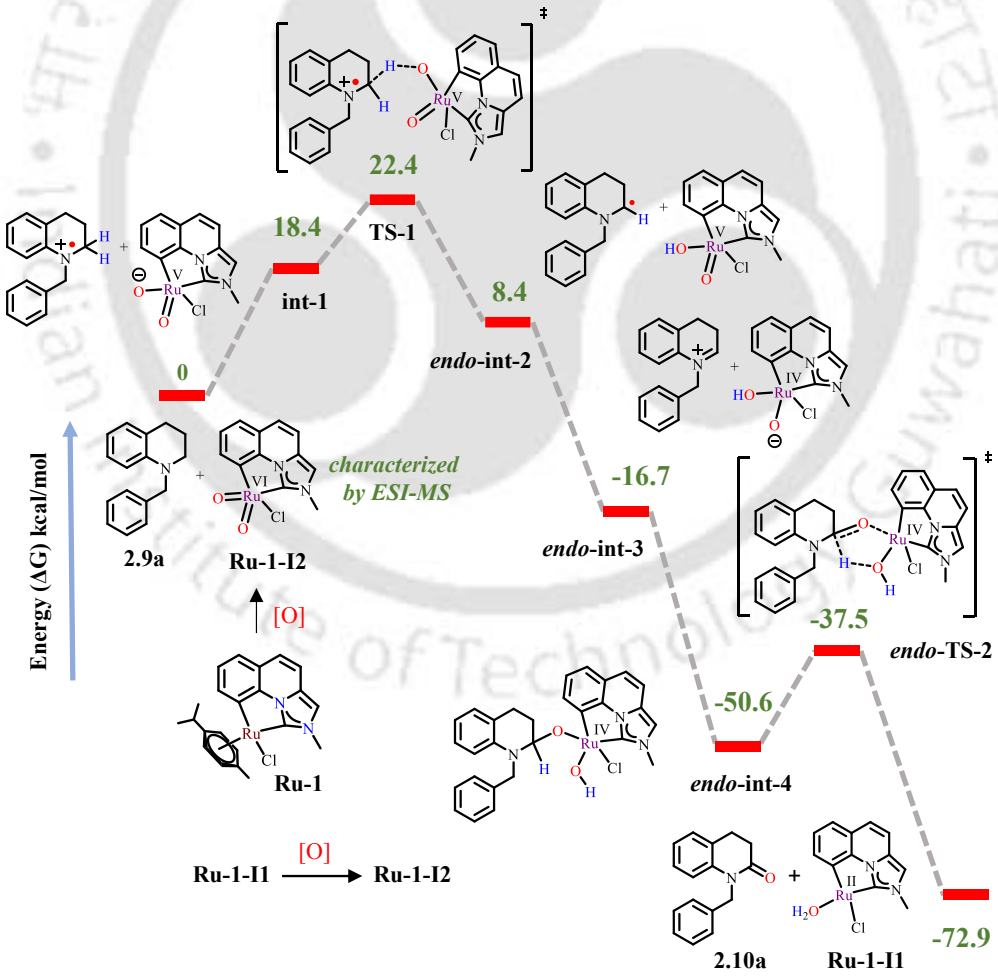


Figure 2.9. Energy profile diagram and proposed reaction pathway for the *endo*–α–CH_2 bond oxidation.

TH-3565_186122020

the corresponding α-amino radical species undergo subsequent SET to form iminium ion ***endo*-int-3** (ΔG = -16.7 kcal/mol) or ***exo*-int-3** (ΔG = -21.6 kcal/mol). These could then further be thermodynamically downhill with the formation of μ-oxo-bridged metal complex ***endo*-int-4** or ***exo*-int-4** (ΔG = -50.6 kcal/mol) respectively. Lastly, ***endo*-int-4** leads to the formation of the oxidized product **2.10a** and released complex **Ru-1-I1** in an exothermic fashion (ΔG = −72.9 kcal/mol) *via* intramolecular H-atom transfer with the ***endo*-TS-2** energy barrier of 13 kcal/mol. Similarly, ***exo*-int-4** can give the α-methylene oxidized product **2.10a'** and complex **Ru-1-I1** in an exothermic fashion (ΔG = −67.3 kcal/mol) *via* ***exo*-TS-2** with an energy barrier of 13.3 kcal/mol. A slightly lower energy barrier and higher exothermic reaction parameter possibly drives the selectivity towards *endo*–α–CH_2 bond oxidation over *exo*–α–CH_2 bond oxidation.

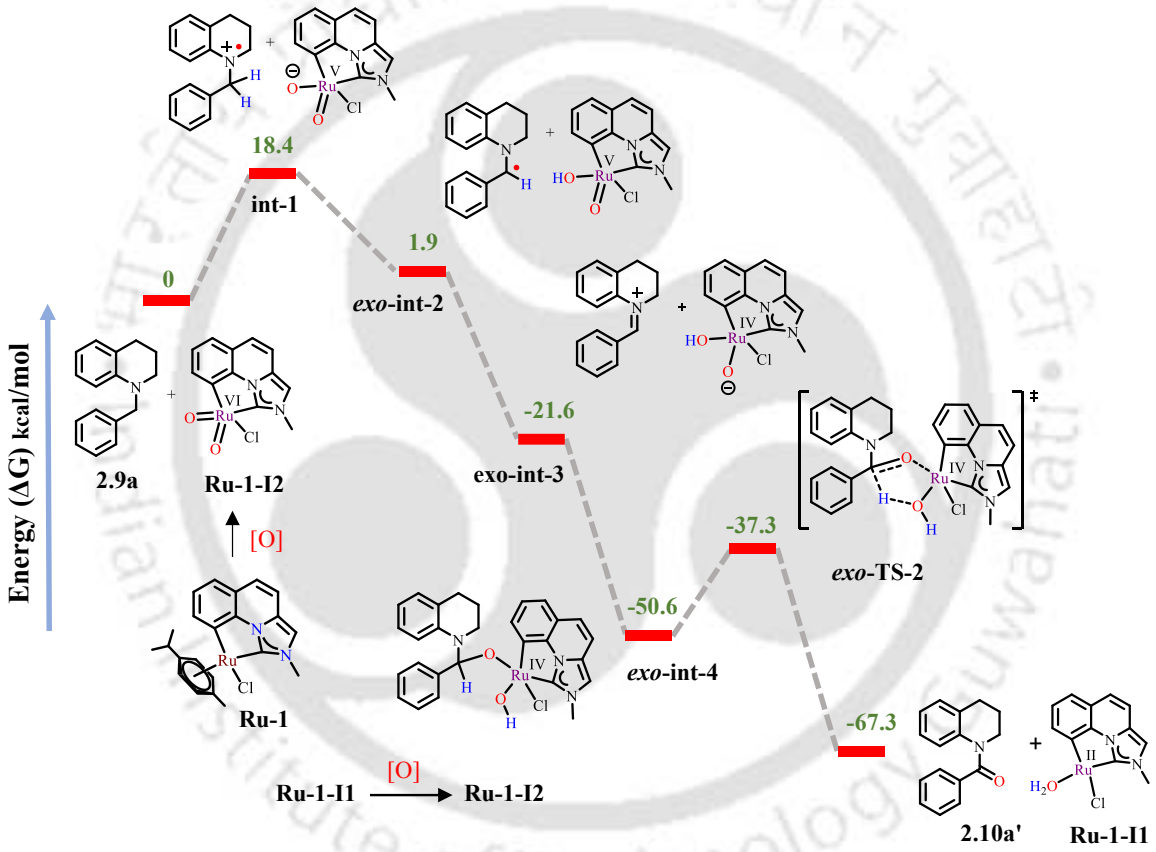


Figure 2.10. Energy profile diagram and proposed pathway for the *exo*–α–CH_2 bond oxidation

To elucidate the reason for higher reaction rates of the EWGs containing substrates in the oxidation reactions, BTHQ (**2.9a**), 6-CO_2Me-BTHQ (**2.9ac**) and 6-Me-BTHQ (**2.9ae**) are taken as model substrates to compute the energy barrier. The energy barrier was found to be in the order ***endo*-TS-2_6-Me** (14.2 kcal/mol) > ***endo*-TS-2** (13.0 kcal/mol) > ***endo*-TS-2_6-CO_2Me** (7.6 kcal/mol) with 6-substituted BTHQs, suggesting the reaction is kinetically favored with the EWGs (Figure 2.11). These findings are also in line with the Hammett correlation study where a higher reaction rate was observed with the electron-withdrawing substituents.

TH-3565_186122020

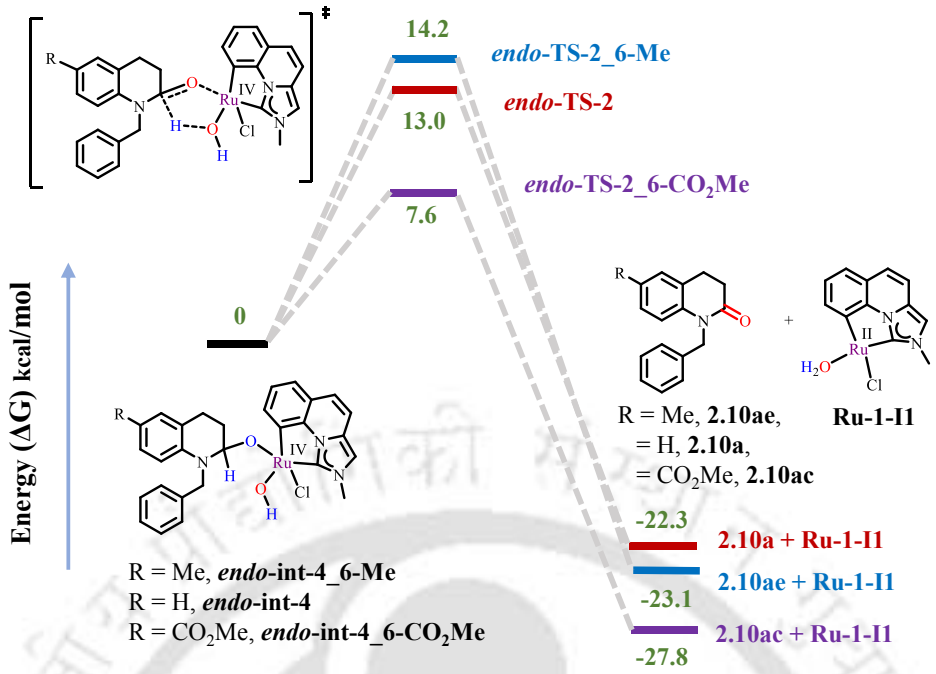


Figure 2.11. Energy profile diagram of the *endo*–*α*–CH_2 bond oxidation of different substrates.

2.4. Summary

In conclusion, I have developed an efficient annulated ImQ-based cyclometalated ruthenium complex **Ru-1**. The complex has remarkable catalytic activity in the Cα–H oxidation of *N*-alkylated tetrahydroquinolines to lactams with notable selectivity, as it suppresses the generation of the often-unwanted α-methyl-oxidized product formamide or the *N*-alkyl cleaved product 3,4-dihydroquinolin-2(1*H*)-one. The wide range of functional group tolerance and structural features encountered in pharmaceuticals is remarkable. Furthermore, this operationally simple reaction condition offers the oxidation of complex molecules at late stages. The synthesis of various biologically important medicinal compounds was also demonstrated. In addition, mechanistic and kinetic studies were executed to understand the reaction sequences to achieve the desired oxidized product. This study highlights the broad use of annulated NHC ligands in organometallic catalysis, particularly in oxidation chemistry.

2.5. Experimental section

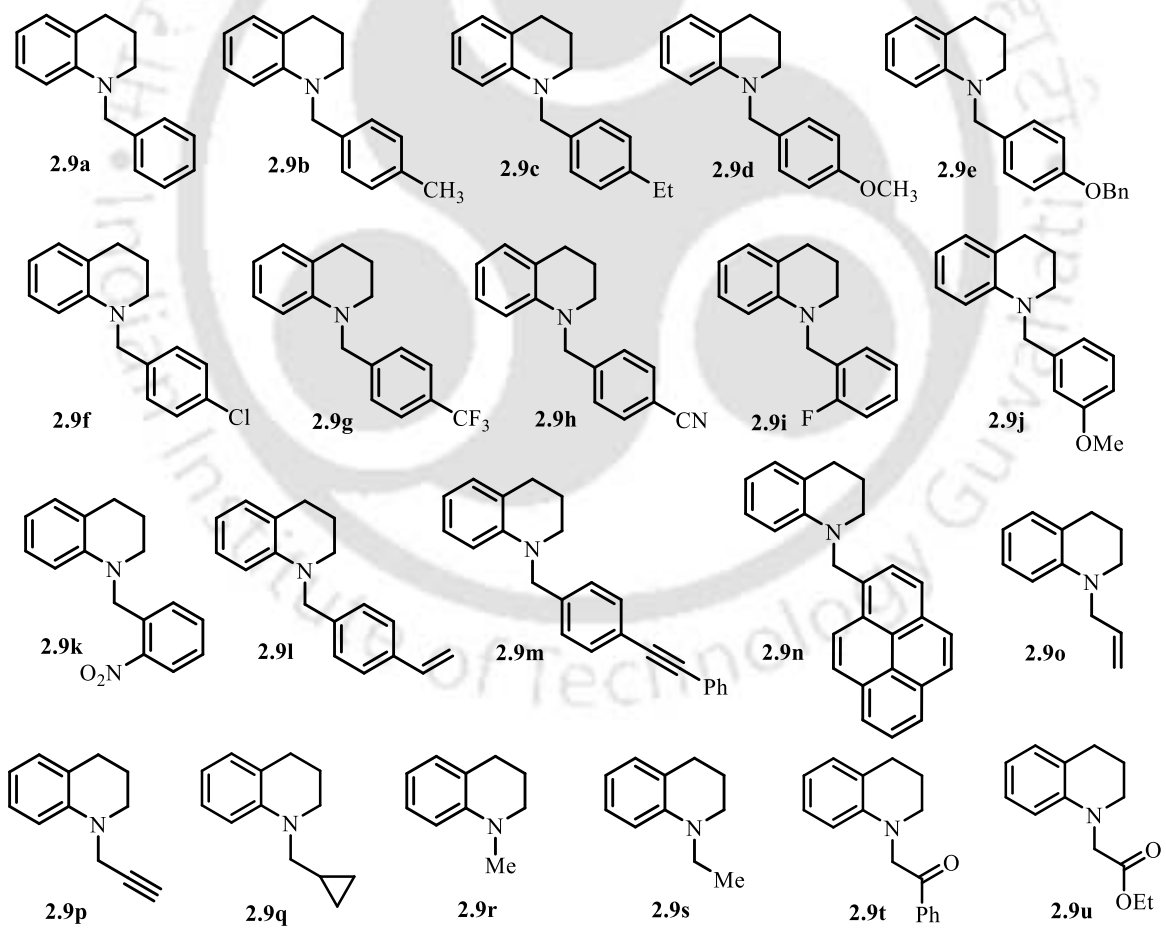
2.5.1. General information

All the reagents and chemicals were purchased from common commercial suppliers like Sigma-Aldrich, Alfa Aesar, Merck, Spectrochem, Avra Synthesis Pvt. Ltd., BLD Pharma and directly used as received without any further purification unless otherwise mentioned. *N*-substituted tetrahydroquinolines were prepared according to the literature reported procedures.[20-24] ^1H, ^{13}C NMR and ^{19}F spectra of the compounds were measured in $CDCl_3$ as a solvent by using TMS as an internal standard. Chemical shifts, δ (in ppm), were reported relative to TMS δ (^1H) 0.0 ppm, δ (^{13}C) 0.0 ppm, which was used as the internal reference. Otherwise, the solvent's residual proton resonance and carbon resonance $CHCl_3$, δ (^1H) 7.26

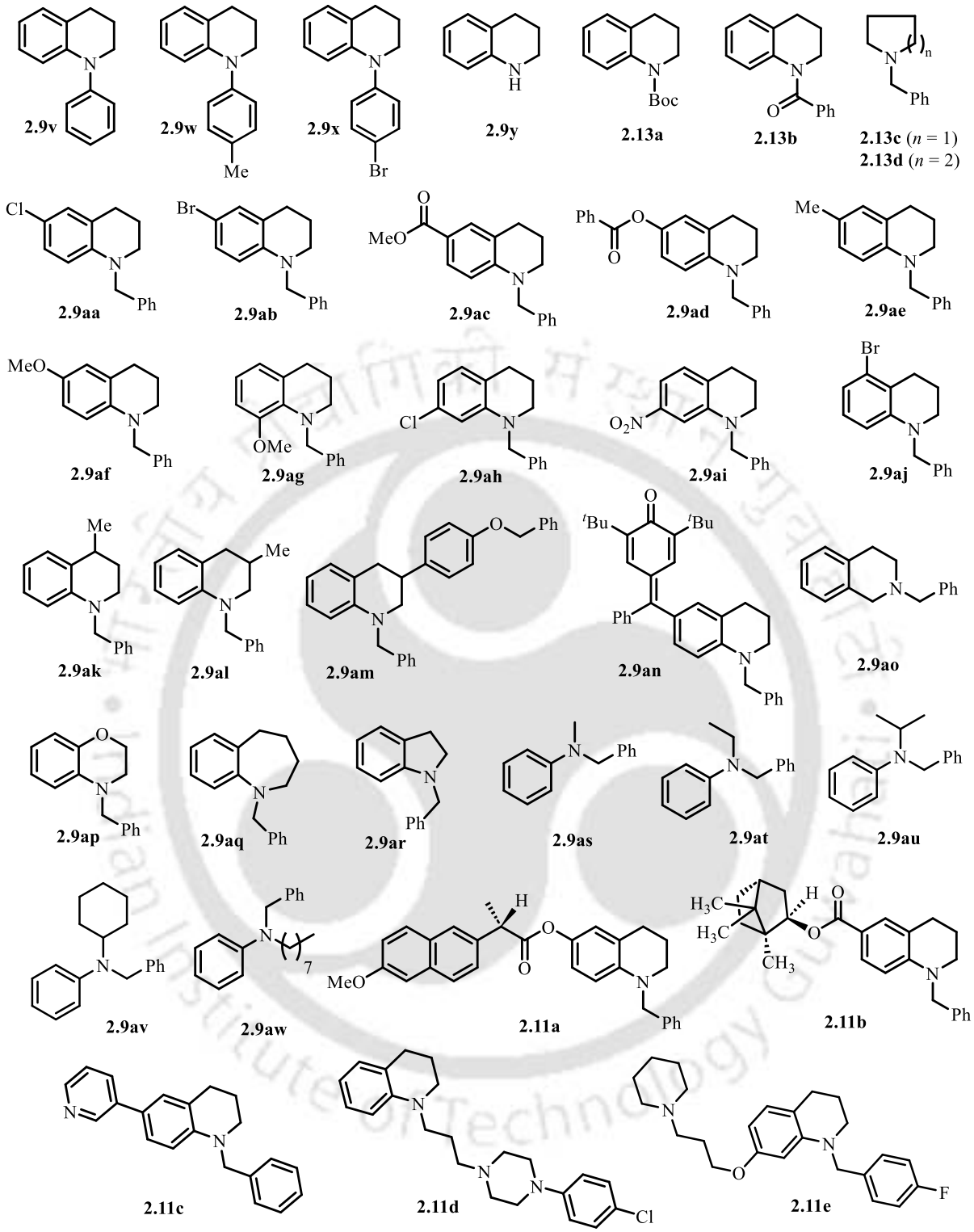
TH-3565_186122020

ppm, δ (^{13}C) 77.16 ppm were used for calibration. Bruker Avance III 600, 500 and 400 spectrometers were used to record the NMR spectra. Chemical shift (δ) values were reported in ppm and spin-spin coupling constant (J) was expressed in Hz and other data were reported as follows: s = singlet, d = doublet, dd = doublet of doublet, dt = doublet of triplet, t = triplet, m = multiplet, q = quartet, p = pentet, br = broad, and brs = broad singlet. MS (ESI-HRMS): Mass spectra were recorded on an Agilent Accurate-Mass Q-TOF LC/MS 6546. Merck silica gel 60-120 was used for column chromatography. All the starting *N*-substituted tetrahydroquinolines, ligands, catalyst and their oxidized products were characterized by spectroscopic methods and compared to literature wherever applicable, otherwise stated. All the oxidation reactions were carried out under air and in preheated oil baths unless otherwise mentioned. Completion of reactions was examined by thin layer chromatography carried out on pre-coated Merck silica gel-60 F_{254} aluminium plates with ultraviolet light (UV) or iodine as visualizing agents.

2.5.2. Substrates employed in the reaction



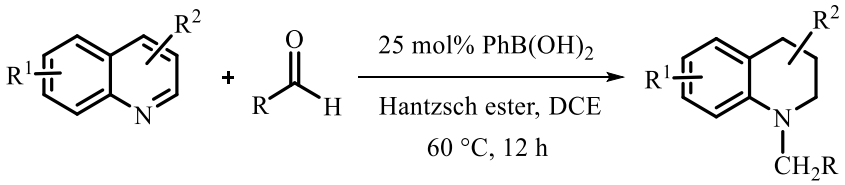
TH-3565_186122020



2.5.3. Experimental procedures for starting materials

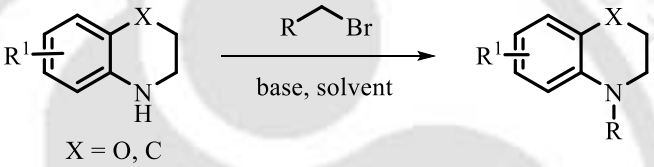
General procedure (GP-I)

TH-3565_186122020



In a reaction tube (15 mL), substituted quinoline (0.5 mmol), substituted aldehyde (0.5 mmol), Hantzsch ester (1.75 mmol), $PhB(OH)_2$ (25 mol%) and DCE (2 mL) were taken. Then the reaction tube was properly closed and placed in a preheated oil bath at 60 ºC for 12 h with continuous stirring. The reaction was monitored by thin layered chromatography (TLC) in petroleum ether and ethyl acetate solvent system. After completion of the reaction, the reaction tube was brought to room temperature, and the crude compound was purified through silica gel column chromatography. **2.9a-k**, **2.9m, 2.9n, 2.9t, 2.9aa-af, 2.9ak-an, 2.11a** and **2.11b** were prepared by following this method.[20]

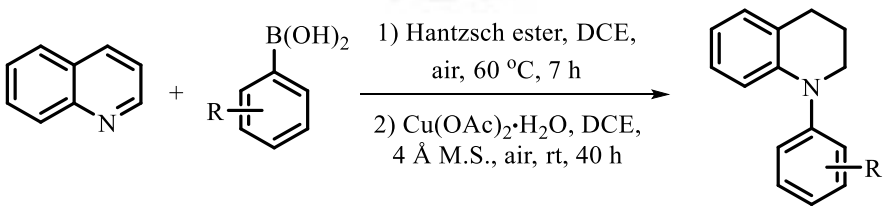
General procedure (GP-II)



A mixture of the corresponding tetrahydroquinoline (1.0 equiv.), base (2 equiv.), and alkyl halide (1.2 equiv.) in CH_3CN/DMSO was stirred for 12 h. The reaction was monitored by thin layered chromatography (TLC) in petroleum ether and ethyl acetate solvent system. After completion of the reaction, the reaction tube was brought to room temperature and the solvent was removed under reduced pressure, extracted with EtOAc and H_2O. The combined organic layers were dried over anhydrous Na_2SO_4 and evaporated in vacuo. The residue was purified by flash chromatography on silica gel using petroleum ether/ethyl acetate as the eluent to give the desired product.

- K_2CO_3 was used as a base[21] for **2.9o-r**, **2.9u, 2.9ag-aj, 2.9ao-aq, 2.9as-aw**.
- KOH was used as a base[22] for **2.9l**, **2.9s**.
- NaH was used as a base[23] for **2.9ar**.

General procedure (GP-III)

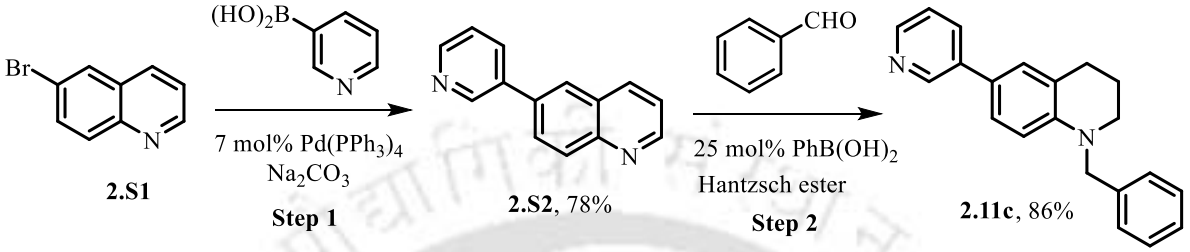


A mixture of quinoline (1 equiv.), Hantzsch ester (2.2 equiv.), arylboronic acid (0.3 equiv.) and DCE (2 mL) were added into a reaction tube (25 mL) equipped with a stirring bar. The reaction tube was properly closed and placed in a preheated oil bath at 60 °C with continuous stirring for 7 h. To the resulting mixture, arylboronic acid (0.7 equiv.), copper(II) acetate monohydrate

TH-3565_186122020

(0.7 equiv.) and 4 Å M.S. was added and stirred at room temperature for 40 h. After completion of the reaction, the reaction mixture was then passed through a bed of celite, the filtrate was collected and concentrated under reduced pressure. The crude reaction mixture was purified by column chromatography over silica gel using petroleum-ether or ethyl acetate/ petroleum-ether mixture as eluent. **2.9v**, **2.9w** and **2.9x** were prepared by following this method.[24]

Synthesis of compound 2.11c



Scheme 2.15. Synthesis of **2.11c**

Step 1: Synthesis of 6-(pyridin-3-yl)quinoline (**2.S2**)

An oven dried pressure tube was charged with 6-bromoquinoline **2.S1** (120 mg, 0.56mmol, 1 equiv.), pyridin-3-ylboronic acid (118 mg, 0.96 mmol, 1.67 equiv.), Na_2CO_3 (366 mg, 3.5 mmol, 6 equiv.), and $Pd(PPh)_4$ (46 mg, 7 mol%). toluene (1.5 mL), water (1 mL), and EtOH (0.5 mL) were added to the reaction mixture under a nitrogen atmosphere, and the mixture was refluxed at 120 °C for 24 h. The reaction mixture was then allowed to cool before being filtered through a celite plug. The resulting mixture was extracted with EtOAc and H_2O. The combined organic layers were dried over anhydrous Na_2SO_4 and evaporated in vacuo. The residue was purified by flash chromatography on silica gel using ethyl acetate/MeOH (v/v = 10/1, R_f = 0.3) as the eluent to give the desired product **2.S2** as a white solid (91 mg, 0.44 mmol, 78%).

^{1}H NMR (400 MHz, Chloroform-*d*): δ 8.97 – 8.82 (m, 2H), 8.65 – 8.62 (m, 1H), 8.21 – 8.17 (m, 2H), 7.97 – 7.88 (m, 3H), 7.43 – 7.38 (m, 2H). ^{13}C NMR (151 MHz, Chloroform-*d*): δ 150.6, 148.5, 148.1, 147.5, 136.4, 135.71, 135.67, 134.7, 130.1, 128.6, 128.3, 125.8, 123.7, 121.7. Spectral data is in accordance to the reported literature.[25]

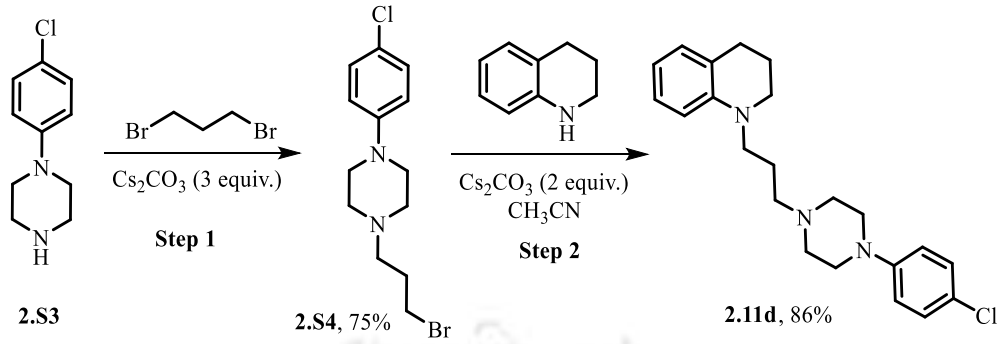
Step 2: Synthesis of 1-benzyl-6-(pyridin-3-yl)-1,2,3,4-tetrahydroquinoline (**2.11c**)

Compound **2.11c** was prepared according to the general procedure GP-I from **2.S2** (140 mg, 0.46 mmol). The title compound **2.11c** was isolated by using silica gel column chromatography with ethyl acetate/ pet ether (v/v = 1/4, R_f = 0.5) as the eluent to afford the desired product as a yellow solid (0.40 mmol, 118 mg, 86%).

^{1}H NMR (400 MHz, Chloroform-*d*): δ 8.78 (d, J = 2.4 Hz, 1H), 8.45 (d, J = 3.9 Hz, 1H), 7.79 (dt, J = 8.0, 2.0 Hz, 1H), 7.35 – 7.21 (m, 8H), 6.59 (d, J = 8.3 Hz, 1H), 4.54 (s, 2H), 3.43 (t, J = 5.7 Hz, 2H), 2.90 (t, J = 6.3 Hz, 2H), 2.09 – 2.03 (m, 2H). ^{13}C NMR (151 MHz, Chloroform-*d*): δ 147.5, 146.9, 145.8, 138.6, 136.9, 133.4, 128.8, 127.7, 127.1, 126.6, 126.0, 124.9, 123.6, 122.9, 111.5, 55.2, 50.1, 28.5, 22.4. HRMS (ESI) *m/z*: $[M+H]^+$ calculated for $C_{21}H_{21}N_2$: 301.1700; found 301.1705.

TH-3565_186122020

Synthesis of compound 2.11d



Scheme 2.16. Synthesis of **2.11d**

Step 1: Synthesis of 1-(3-bromopropyl)-4-(4-chlorophenyl)piperazine (**2.S4**)

1-(4-chlorophenyl)piperazine **2.S3** (300 mg, 1.5 mmol), 1,3-dibromopropane (3.1 g, 15.2 mmol) was taken in an oven dried reaction tube with Cs_2CO_3 (1.5 g, 4.5 mmol) and the resulting mixture was stirred at 35 ºC for 48 h. The reaction mixture was evaporated in a vacuum, and purified by using silica gel column chromatography with ethyl acetate/ pet ether (v/v = 7/20, R_f = 0.7) as the eluent to afford the desired product **2.S4** as a colourless oil (356 mg, 1.12 mmol, 75%).

^{1}H NMR (400 MHz, Chloroform-*d*): δ 7.19 (d, J = 9.0 Hz, 2H), 6.83 (d, J = 8.9 Hz, 2H), 3.48 (t, J = 6.6 Hz, 2H), 3.16 – 3.14 (m, 4H), 2.61 – 2.52 (m, 6H), 2.06 (p, J = 6.8 Hz, 2H). ^{13}C NMR (151 MHz, Chloroform-*d*): δ 150.0, 129.0, 124.6, 117.3, 56.5, 53.2, 49.3, 31.8, 30.1. Spectral data is in accordance to the reported literature.[26]

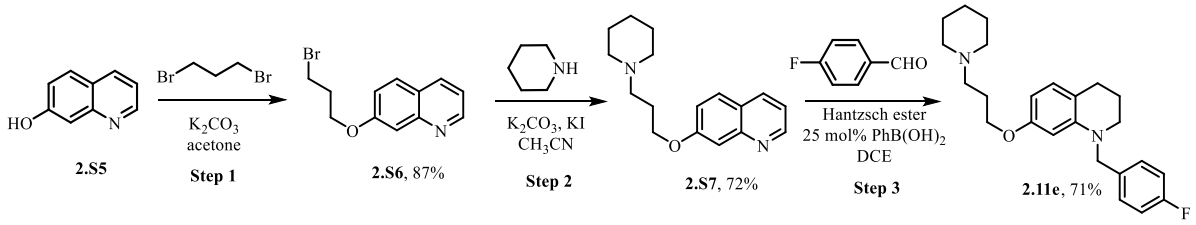
Step 2: Synthesis of 1-(3-(4-(4-chlorophenyl)piperazin-1-yl)propyl)-1,2,3,4-tetrahydro quinoline (**2.11d**)

To the mixture of **2.S4** (114 mg, 0.36 mmol) and Cs_2CO_3 (244 mg, 0.75 mmol) in acetonitrile (3.0 mL), THQ (40 mg, 0.3 mmol) was added, and the resulting mixture was stirred at 120 ºC for 24 h. The precipitate was filtered and the filtrate was concentrated in a vacuum. The residue was purified by column chromatography on silica gel using ethyl acetate/ pet ether (v/v = 1/20, R_f = 0.8) as the eluent to afford the desired product **2.11d** as a yellow solid (0.26 mmol, 95 mg, 86%).

^{1}H NMR (600 MHz, Chloroform-*d*): δ 7.34 – 7.24 (m, 1H), 7.08 – 6.95 (m, 3H), 6.79 (d, J = 7.4 Hz, 1H), 6.61 – 6.56 (m, 2H), 6.51 (t, J = 7.5, 1H), 5.89 – 5.83 (m, 1H), 5.23 – 5.15 (m, 1H), 3.89 – 3.87 (m, 1H), 3.64 (t, J = 6.2 Hz, 1H), 3.46 – 3.44 (m, 1H), 3.32 – 3.28 (m, 2H), 3.15 – 3.33 (m, 2H), 2.79 –2.76 (m, 5H), 2.09 – 2.02 (m, 1H), 2.00 – 1.97 (m, 4H), 1.65 – 1.59 (m, 1H). ^{13}C NMR (151 MHz, Chloroform-*d*): δ 133.7, 129.4, 129.1, 128.7, 127.2, 127.1, 126.7, 116.0, 115.9, 111.1, 110.7, 54.0, 50.2, 49.3, 43.1, 28.3, 27.8, 22.5, 22.3. HRMS (ESI) *m/z*: $[M+H]^+$ calculated for $C_{22}H_{29}ClN_3$: 370.2045; found 370.2044.

TH-3565_186122020

Synthesis of compound 2.11e



Scheme 2.17. Synthesis of **2.11e**

Step 1: Synthesis of 7-(3-bromopropoxy)quinoline (**2.S6**)

7-hydroxyquinoline (800 mg, 5.5 mmol), 1,3-dibropropane (2.3 g, 11 mmol) and K_2CO_3 (1.6 g, 11 mmol) was taken in a reaction tube with acetonitrile (5 mL) and reflux it for 12 h. After the completion of the reaction as confirmed by TLC, the reaction mixture was evaporated in a vacuum, and purified by using silica gel column chromatography with ethyl acetate/ pet ether (v/v = 3/10, R_f = 0.6) as the eluent to afford the desired product **2.S6** as a white solid (1.2 g, 4.8 mmol, 87%).

^{1}H NMR (600 MHz, Chloroform-*d*): δ 8.84 (dd, J = 4.3, 1.7 Hz, 1H), 8.07 (d, J = 8.9 Hz, 1H), 7.70 (d, J = 8.9 Hz, 1H), 7.44 (d, J = 2.5 Hz, 1H), 7.27 (dd, J = 8.1, 4.3 Hz, 1H), 7.20 (dd, J = 8.9, 2.6 Hz, 1H), 4.27 (t, J = 5.8 Hz, 2H), 3.64 (t, J = 6.5 Hz, 2H), 2.41 (p, J = 6.2 Hz, 2H). ^{13}C NMR (151 MHz, Chloroform-*d*): δ 159.8, 150.8, 150.0, 135.8, 129.0, 123.8, 120.0, 119.2, 108.3, 65.7, 32.3, 29.9. HRMS (ESI) *m/z*: $[M+H]^+$ calculated for $C_{12}H_{13}BrNO$: 266.0176; found 266.0180.

Step 2: Synthesis of 7-(3-(piperidin-1-yl)propoxy)quinoline (**2.S7**)

A reaction tube was charged with compound **2.S6** (580 mg, 2.2 mmol), piperidine (225 mg, 2.6 mmol), K_2CO_3 (610 mg, 4.4 mmol), KI (4 mg, 1 mol%) with acetonitrile (5 mL) and stirred at reflux condition for 12 h. After the completion of the reaction as confirmed by TLC, the reaction mixture was filtered and evaporated in a vacuum. The residue was purified by flash chromatography on neutral alumina using ethyl acetate/ pet ether (v/v = 1/4, R_f = 0.2) as the eluent to give the desired product **2.S7** as a white solid (428 mg, 1.6 mmol, 72%).

^{1}H NMR (400 MHz, Chloroform-*d*): δ 8.81 (dd, J = 4.4, 1.8 Hz, 1H), 8.04 (dd, J = 8.2, 1.8 Hz, 1H), 7.67 (d, J = 8.9 Hz, 1H), 7.41 (d, J = 2.4 Hz, 1H), 7.25 – 7.18 (m, 2H), 4.16 (t, J = 6.4 Hz, 2H), 2.53 – 2.49 (m, 2H), 2.41 (br, 4H), 2.08 – 2.01 (m, 2H), 1.59 (p, J = 5.6 Hz, 4H), 1.46 – 1.42 (m, 2H). ^{13}C NMR (126 MHz, Chloroform-*d*): δ 160.1, 150.5, 150.0, 135.6, 128.7, 123.5, 120.1, 118.9, 108.0, 66.8, 56.0, 54.7, 26.7, 26.0, 24.5. HRMS (ESI) *m/z*: $[M+H]^+$ calculated for $C_{17}H_{23}N_2O$: 271.1805; found 271.1808.

Step 3: Synthesis of 1-(4-fluorobenzyl)-7-(3-(piperidin-1-yl)propoxy)-1,2,3,4-tetrahydro quinoline (**2.11e**)

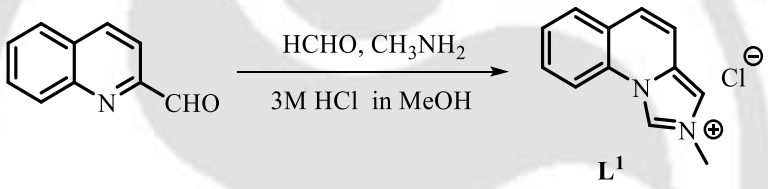
TH-3565_186122020

Compound **2.11e** was prepared according to the general procedure GP-I from **2.S7** (162 mg, 0.6 mmol). The title compound **2.11e** was isolated by using silica gel column chromatography with ethyl acetate/ pet ether (v/v = 1/20, R_f = 0.7) as the eluent to afford the desired product as a colourless oil (162 mg, 0.43 mmol, 71%).

^{1}H NMR (500 MHz, Chloroform-*d*): δ 7.23 – 7.21 (m, 2H), 7.00 (t, J = 8.7 Hz, 2H), 6.87 (d, J = 8.2 Hz, 1H), 6.16 (dd, J = 8.2, 2.2 Hz, 1H), 6.06 (d, J = 2.2 Hz, 1H), 4.42 (s, 2H), 3.99 – 3.97 (m, 2H), 3.67 – 3.65 (m, 2H), 3.31 (t, J = 5.6 Hz, 2H), 2.74 (t, J = 6.3 Hz, 2H), 2.15 – 2.11 (m, 2H), 1.99 – 1.96 (m, 2H), 1.29 – 1.26 (m, 8H), 0.90 – 0.86 (m, 2H). ^{13}C NMR (126 MHz, Chloroform-*d*): δ 158.5, 146.5, 129.6, 128.3, 128.2, 115.7, 115.6, 115.5, 101.4, 98.4, 64.3, 54.7, 49.8, 41.8, 32.5, 29.8, 27.6, 22.8, 22.7, 14.3. ^{19}F NMR (471 MHz, Chloroform-*d*): δ -116.4. HRMS (ESI) *m/z*: $[M+H]^+$ calculated for $C_{24}H_{32}FN_2O$: 383.2494; found 383.2498.

2.5.4. Synthesis of ligands and ruthenium complexes

Synthesis of ligands L^1:



L^1

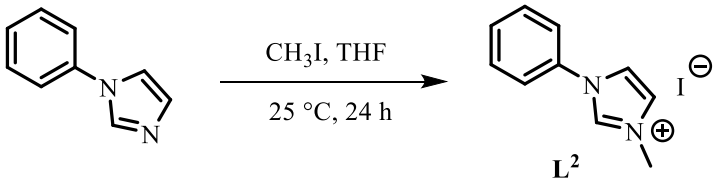
Scheme 2.18. Synthesis of **L^1**

To a solution of methylamine (1 equiv.) in dry methanol, formalin solution (1.5 equiv.) is added at room temperature and stirred for 15 minutes. At 0 ºC, 3M HCl in MeOH (1.5 equiv.) is prepared in another reaction tube (by adding acetyl chloride (1.5 equiv.) to the reaction tube containing methanol at 0 ºC), then added to the previous reaction mixture, followed by the addition of quinoline-2-carboxaldehyde (1 g, 1 equiv.) and stirred at room temperature for overnight. After completion of the reaction as confirmed by TLC, the crude reaction mixtures are concentrated and placed under a high vacuum. The solid formed was purified by neutral alumina column chromatography (ethyl acetate: methanol 10:1) to get a pure white solid (1.2 g, 87%).

^{1}H NMR (500 MHz, DMSO-d_6): δ 10.44 (s, 1H), 8.36 (d, J = 8.3 Hz, 1H), 8.19 (s, 1H), 7.99 (d, J = 7.7 Hz, 1H), 7.83 (t, J = 7.8 Hz, 1H), 7.71 (t, J = 7.5 Hz, 1H), 7.65 (q, J = 9.6 Hz, 2H), 4.16 (s, 3H). ^{13}C NMR (126 MHz, DMSO-d_6): δ 130.2, 129.5, 128.8, 128.7, 128.4, 128.0, 126.0, 124.0, 116.5, 116.3, 115.1, 36.9. HRMS (ESI) *m/z*: calcd. for $C_{12}H_{11}N_2^+$ [M^+] 183.0917; found: 183.0919.

Synthesis of ligands L^2:

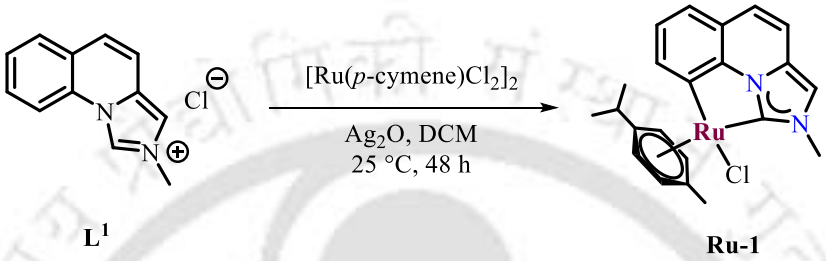
TH-3565_186122020



Scheme 2.19. Synthesis of **L²**

Ligand **L²** was synthesized in accordance with the reported literature procedure.[15]

Synthesis of Ru-1

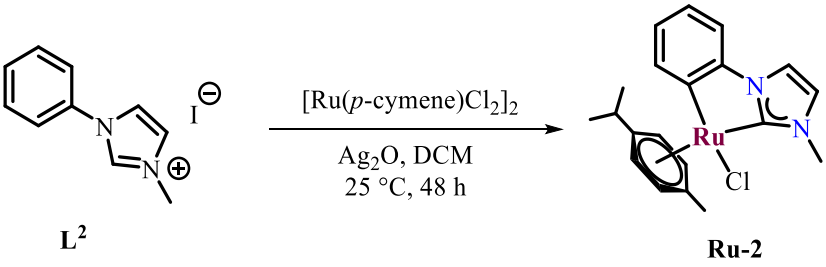


Scheme 2.20. Synthesis of **Ru-1**

In a reaction tube, ligand **L¹** (100 mg, 0.45 mmol, 1 equiv.) was added with [Ru(*p*-cymene)Cl_2]$_2$ (140.42 mg, 0.23 mmol, 0.5 equiv.). Ag_2O (159.38 mg, 0.68 mmol, 1.5 equiv.) was added to the reaction mixture, followed by dry CH_2Cl_2 (2 mL). The reaction mixture was stirred at room temperature for two days under dark conditions. The resulting yellow solution was filtered through a Celite plug and reduced under vacuum. The resulting crude was purified on neutral alumina column chromatography (ethyl acetate: pet ether 1:2). The major yellow band was collected, concentrated, and precipitated by the addition of Et_2O, which afforded the title complex as a yellow solid (194 mg, 92%).

^{1}H NMR (600 MHz, Chloroform-*d*): δ 8.17 (d, J = 7.0 1H), 7.19 (t, J = 7.4 Hz, 1H), 7.15 – 7.11 (m, 2H), 7.06 (s, 1H), 6.92 (d, J = 9.4 Hz, 1H), 5.68 (d, J = 5.8 Hz, 1H), 5.59 (d, J = 5.8 Hz, 1H), 5.45-5.44 (m, 2H), 4.33 (s, 3H), 2.29 – 2.24 (m, 1H), 2.02 (s, 3H), 0.91 (d, J = 6.9 Hz, 3H), 0.74 (d, J = 6.9 Hz, 3H). ^{13}C NMR (151 MHz, Chloroform-*d*): δ 176.8, 160.8, 141.4, 140.3, 127.5, 127.1, 125.2, 120.6, 120.3, 112.9, 111.9, 102.1, 100.6, 90.1, 88.2, 86.2, 84.0, 37.8, 31.1, 23.1, 22.0, 19.2. HRMS (ESI) *m/z*: calcd. for $C_{22}H_{23}N_2Ru$ $[M\text{-}Cl]^+$ 417.0905; found: 417.0907.

Synthesis of Ru-2

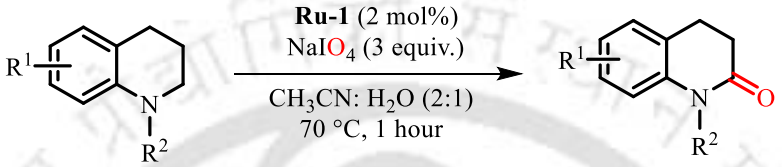


Scheme 2.21. Synthesis of **Ru-2**

TH-3565_186122020

The title complex was synthesized in accordance with the reported literature procedure.[16] ^{1}H NMR (600 MHz, Chloroform-*d*): δ 8.14 – 8.13 (m, 1H), 7.33 (m, 1H), 7.07 – 7.05 (m, 1H), 6.98 – 6.95 (m, 3H), 5.60 (d, J = 6.0 Hz, 1H), 5.56 (d, J = 5.9 Hz, 1H), 5.47 (d, J = 5.9 Hz, 1H), 5.39 (d, J = 5.9 Hz, 1H), 4.16 (s, 3H), 2.20 – 2.15 (m, 1H), 2.07 (s, 3H), 0.89 (d, J = 7.1 Hz, 3H), 0.75 (d, J = 6.9 Hz, 3H). ^{13}C NMR (151 MHz, Chloroform-*d*): δ 188.5, 163.1, 145.8, 141.7, 124.6, 122.4, 122.0, 114.3, 111.1, 104.8, 99.0, 92.8, 89.8, 87.9, 84.3, 37.9, 31.2, 23.2, 21.9, 19.1.

2.5.5. General procedure for the catalytic oxidation of tetrahydroquinolines (GP-IV)

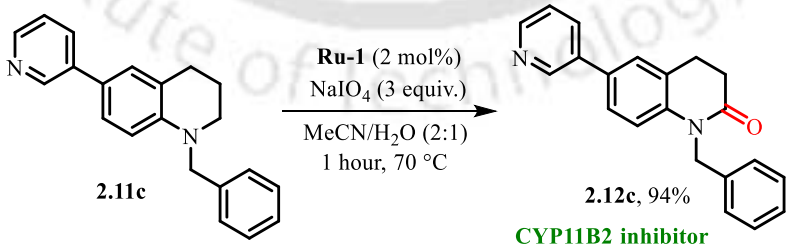


Scheme 2.22. Synthesis of lactam from amines

$NaIO_4$ (1.5 mmol, 3 equiv.) was taken in a screw-capped reaction tube and dissolved it in water (1 mL). The *N*-substituted tetrahydroquinolines (0.5 mmol, 1 equiv.), **Ru-1** (2 mol%), and acetonitrile (2 mL) were added to the reaction tube and stirred the reaction mixture in a preheated oil bath at 70 ºC for 1 hour. After the completion of the reaction as confirmed by TLC, the reaction mixture was worked up with CH_2Cl_2 and water. The organic layer was separated and the aqueous layer was again extracted with CH_2Cl_2 (two times, 5 mL). The combined organic layer was washed with brine solution (8 mL). The organic layer was separated and dried over anhydrous Na_2SO_4 and the solvent was evaporated under a vacuum. The crude product was purified through silica-gel column chromatography to get the pure product.

2.5.6. Synthesis of drug molecules

Synthesis of CYP11B2 inhibitor (2.12c)



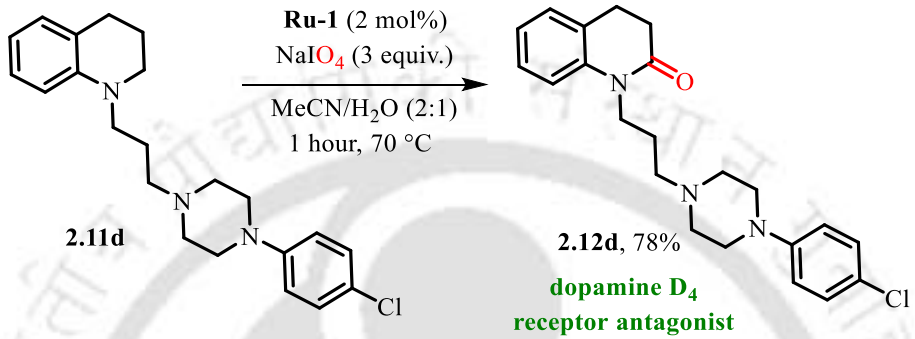
Scheme 2.23. Synthesis of **2.12c**

The compound **2.12c** was prepared following the general procedure GP-IV from **2.11c** (150 mg, 0.5 mmol). The title compound **2.12c** was isolated as a white solid using silica gel column chromatography with acetone/DCM (v/v = 1/10, R_f = 0.4) in 94% yield (148 mg, 0.31 mmol).

TH-3565_186122020

^{1}H NMR (400 MHz, Chloroform-*d*): δ 8.78 (d, J = 2.4 Hz, 1H), 8.55 (d, J = 6.4 Hz, 1H), 7.81 – 7.79 (m, 1H), 7.40 – 7.39 (m, 1H), 7.35 – 7.30 (m, 4H), 7.26 – 7.23 (m, 3H), 6.98 (d, J = 8.4 Hz, 1H), 5.22 (s, 2H), 3.09 – 3.05 (m, 2H), 2.86 – 2.83 (m, 2H). ^{13}C NMR (151 MHz, Chloroform-*d*): δ 170.5, 148.4, 148.0, 140.0, 136.9, 135.8, 134.0, 132.5, 128.9, 127.3, 127.2, 126.6, 126.5, 126.2, 123.7, 116.3, 46.2, 31.9, 25.8. Spectral data is in accordance to the reported literature.[27]

Synthesis of dopamine D4 receptor antagonist (2.12d)

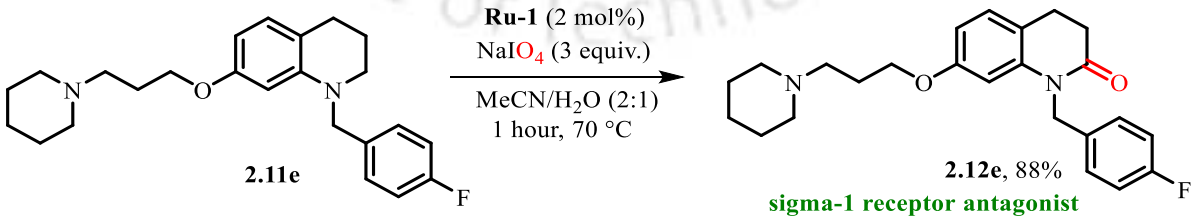


Scheme 2.24. Synthesis of **2.12d**

The compound **2.12d** was prepared following the general procedure GP-IV from **2.11d** (185 mg, 0.5 mmol). The title compound **2.12d** was isolated as a white solid using silica gel column chromatography with ethyl acetate/ pet ether (v/v = 1/10, R_f = 0.5) in 78% yield (150 mg).

^{1}H NMR (600 MHz, Chloroform-*d*): δ 7.23 (t, J = 7.8 Hz, 1H), 7.19 (d, J = 8.6 Hz, 2H), 7.16 (d, J = 7.4 Hz, 1H), 7.09 (d, J = 8.1 Hz, 1H), 7.00 (t, J = 7.4 Hz, 1H), 6.83 (d, J = 8.6 Hz, 2H), 4.01 (t, J = 7.4 Hz, 2H), 3.16 (t, J = 5.0 Hz, 4H), 2.90 – 2.88 (m, 2H), 2.65 – 2.63 (m, 2H), 2.60 (t, J = 5.0 Hz, 4H), 2.48 (t, J = 7.1 Hz, 2H), 1.88 (p, J = 7.3 Hz, 2H). ^{13}C NMR (151 MHz, Chloroform-*d*): δ 170.4, 150.0, 139.7, 129.0, 128.2, 127.5, 126.7, 124.6, 122.9, 117.3, 115.0, 55.7, 53.2, 49.2, 40.6, 32.0, 25.7, 24.8. Spectral data is in accordance to the reported literature.[27]

Synthesis of sigma-1 receptor antagonist (2.12e)



Scheme 2.25. Synthesis of **2.12e**

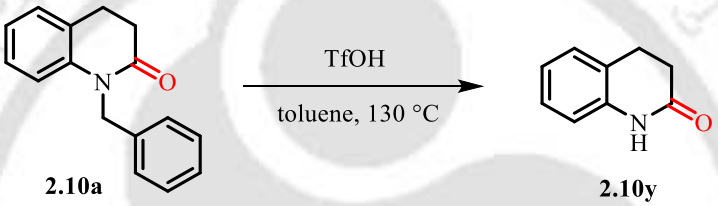
The compound **2.12e** was prepared following the general procedure GP-IV from **2.11e** (191 mg, 0.5 mmol). The title compound **2.12e** was isolated by using neutral alumina column

TH-3565_186122020

chromatography with MeOH/ethyl acetate (v/v = 1/20, R_f = 0.2) as the eluent to afford the desired product as a colourless liquid (174 mg, 0.44 mmol, 88%).
^{1}H NMR (500 MHz, Chloroform-*d*): δ 7.19 (dd, J = 8.6, 5.4 Hz, 2H), 7.03 (d, J = 8.2 Hz, 1H), 6.99 – 6.96 (m, 2H), 6.50 (dd, J = 8.3, 2.4 Hz, 1H), 6.42 (d, J = 2.4 Hz, 1H), 5.10 (s, 2H), 3.86 (t, J = 6.4 Hz, 2H), 2.89 – 2.86 (m, 2H), 2.75 – 2.72 (m, 2H), 2.40 – 2.35 (m, 6H), 1.87 (p, J = 6.6 Hz, 2H), 1.56 (p, J = 5.6 Hz, 4H), 1.44 – 1.40 (m, 2H). ^{13}C NMR (126 MHz, Chloroform-*d*): δ 170.8, 163.0, 161.0, 158.6, 140.7, 132.9 (C-F, $J_{C\text{-}F}$ = 3.1 Hz), 128.5, 128.3 – 128.2 (C-F, $J_{C\text{-}F}$ = 7.8 Hz), 118.5, 115.8 – 115.6 (C-F, $J_{C\text{-}F}$ = 21.6 Hz), 108.0, 103.7, 66.8, 55.9, 54.7, 45.6, 32.3, 26.8, 26.0, 24.8, 24.5. ^{19}F NMR (471 MHz, Chloroform-*d*): δ -115.7. HRMS (ESI) *m/z*: $[M+H]^+$ calculated for $C_{24}H_{30}FN_2O_2$: 397.2286; found 397.2294.

2.5.7. Post-synthetic modifications

Synthesis of 3,4-dihydroquinolin-2(1*H*)-one (2.10y)

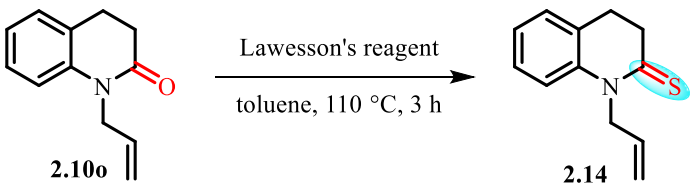


Scheme 2.26. Synthesis of **2.10y**

In a well-dried pressure tube, compound **2.10a** (237 mg, 1 mmol, 1 equiv.), trifluromethansulfonic acid (0.4 mL, 4.0 equiv.) was added with toluene (3 mL) and the reaction mixture was heated at 130 °C for 30 h. After the completion of the reaction as confirmed by TLC, the reaction mixture was neutralized with aqueous $NaHCO_3$, extracted with EtOAc, and washed with brine solution. The organic layer was separated and dried over anhydrous Na_2SO_4 and the solvent was evaporated under a vacuum. The crude product was purified through silica-gel column chromatography with acetone/DCM (v/v = 1/50, R_f = 0.4) to afford the desired product **2.10y** as a brown solid (124 mg, 0.84 mmol, 84%).

^{1}H NMR (600 MHz, Chloroform-*d*): δ 8.72 (brs, 1H), 7.18 – 7.15 (m, 2H), 7.00 – 6.97 (m, 1H), 6.81 (d, J = 7.8, Hz, 1H), 2.97 (t, J = 7.5 Hz, 2H), 2.66 – 2.63 (m, 2H). ^{13}C NMR (151 MHz, Chloroform-*d*): δ 172.1, 137.4, 128.1, 127.7, 123.8, 123.2, 115.6, 30.9, 25.5. Spectral data is in accordance to the reported literature.[28]

Synthesis of 1-allyl-3,4-dihydroquinoline-2(1*H*)-thione (2.14)



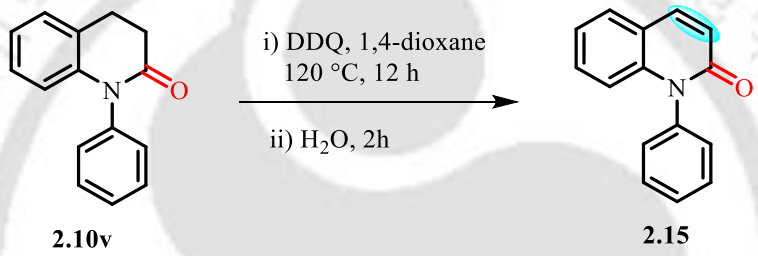
Scheme 2.27. Synthesis of **2.14**

TH-3565_186122020

An oven-dried reaction tube was charged with compound **2.10o** (90 mg, 0.48 mmol, 1 equiv.), Lawesson's reagent (98 mg, 0.24 mmol, 0.5 equiv.) and toluene (3 mL) and the reaction mixture were placed in a preheated oil bath to 110 ºC. After 3 h stirring, the reaction mixture was concentrated in vacuo and purified by column chromatography on silica gel with ethyl acetate/ pet ether (v/v = 1/10, R_f = 0.8) as the eluent to afford the desired product **2.14** as a pale-yellow oil (84 mg, 0.41 mmol, 86%).

^{1}H NMR (600 MHz, Chloroform-*d*): δ 7.27 – 7.23 (m, 1H), 7.19 – 7.17 (m, 2H), 7.09 (t, J = 7.4 Hz, 1H), 6.01 – 5.95 (m, 1H), 5.28 (d, J = 10.3 Hz, 1H), 5.21 – 5.17 (m, 3H), 3.24 – 3.21 (m, 2H), 2.84 – 2.82 (m, 2H). ^{13}C NMR (151 MHz, Chloroform-*d*): δ 200.6, 139.7, 131.2, 128.9, 127.9, 127.6, 124.7, 117.1, 116.9, 53.0, 42.4, 24.9. HRMS (ESI) *m/z*: $[M+H]^+$ calculated for $C_{12}H_{14}NS$: 204.0842; found 204.0830.

Synthesis of 1-phenylquinolin-2(1*H*)-one (2.15)



2.10v **2.15**

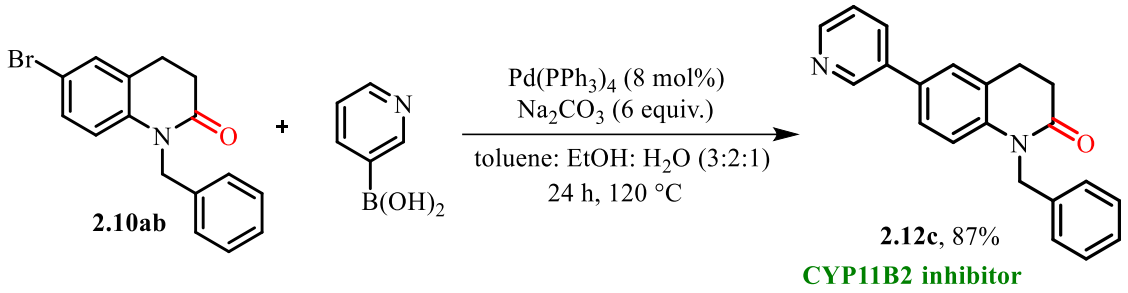
Scheme 2.28. Synthesis of **2.15**

A solution of compound **2.10v** (50 mg, 0.22 mmol, 1.0 equiv.) and DDQ (204 mg, 0.90 mmol, 4.0 equiv.) in 2 ml of 1, 4-dioxane were refluxed at 120 °C for 12 h. The reaction mixture was allowed to stir further by applying 2-3 drops of water. After 2 hours of stirring, the organic contents were extracted using chloroform, washed with brine, dried over anhydrous Na_2SO_4 and evaporated to dryness. Then the crude compound was purified by column chromatography on silica gel with ethyl acetate/ pet ether (v/v = 1/2, R_f = 0.3) as the eluent to afford the desired product **2.15** as a white solid (42 mg, 0.19 mmol, 85%).

^{1}H NMR (500 MHz, Chloroform-*d*): δ 7.78 (d, J = 9.6 Hz, 1H), 7.61 – 7.58 (m, 3H), 7.54 – 7.51 (m, 1H), 7.34 – 7.28 (m, 3H), 7.19 (t, J = 7.4 Hz, 1H), 6.78 (d, J = 9.5 Hz, 1H), 6.65 (d, J = 8.5 Hz, 1H). ^{13}C NMR (126 MHz, Chloroform-*d*): δ 162.4, 141.3, 139.9, 137.8, 130.33, 130.30, 129.0, 128.9, 128.4, 122.42, 122.36, 120.4, 116.1. Spectral data is in accordance to the reported literature.[29]

Synthesis of CYP11B2 inhibitor (2.12c) from 2.10ab

TH-3565_186122020



Scheme 2.29. Synthesis of **2.12c** from **2.10ab**

Following the reported literature procedure,[27] a well-dried Schlenk tube was charged with **2.10ab** (120.9 mg, 0.4 mmol, 1 equiv.), pyridin-3-ylboronic acid (83.6 mg, 0.68 mmol, 1.7 equiv.), Na_2CO_3 (255 mg, 2.4 mmol, 6 equiv.), and $Pd(PPh)_4$ (37 mg, 8 mol%). To this reaction mixture, toluene (1.5 mL), EtOH (1 mL), and water (0.5 mL) were added under a nitrogen atmosphere, and the mixture was refluxed at 120 °C for 24 h. After completion of the reaction, the reaction mixture was cooled, and filtered through a plug of celite. The resulting mixture was diluted with water and extracted with ethyl acetate. The combined extracts were dried over Na_2SO_4, concentrated, and purified by flash chromatography on silica gel (acetone/CH_2Cl_2, 1:10, R_f = 0.4) to afford the desired CYP11B2 inhibitors **2.12c** as a white solid in 87% yield (109 mg, 0.35 mmol).

2.5.8. Mechanistic investigation

a) Radical trapping experiment (Scheme 2.10)

The reaction was performed between **2.9a** (0.5 mmol) and BHT (1.5 equiv.) under standard reaction conditions following the general procedure GP-IV. After 1 h, some portion of the reaction mixture was taken out, filtered, and the high-resolution mass spectrometry (HRMS) was checked. The result indicates the likely formation of a **2.9a**-BHT adduct, **2.17**. Nevertheless, oxidized product **2.10a** was not isolated, and the reaction was completely suppressed. HRMS (ESI) *m/z*: $[M+H]^+$ calculated for $C_{31}H_{40}NO$: 442.3105; found: 442.3114.

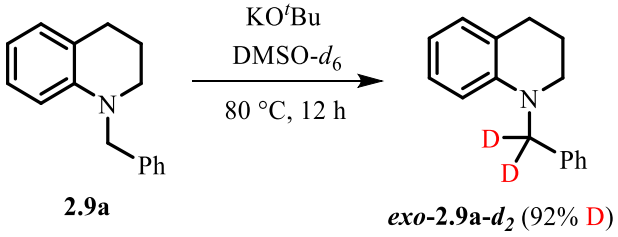
b) Isotope labeling experiment (Scheme 2.11)

$NaIO_4$ (0.3 mmol, 3 equiv.) was taken in a screw-capped reaction tube and dissolved with $H_2{}^{18}O$ (100 µL). To this, **2.9a** (0.1 mmol, 1 equiv.), **Ru-1** (2 mol%) and acetonitrile (200 µL) were added and the reaction mixture was stirred at 70 ºC for 1 hour. After completion of the reaction, the organic layer was separated and all the volatiles were removed under reduced pressure. The crude reaction mixture was purified by silica gel column chromatography using ethyl acetate and petroleum ether as eluent. The product **2.10a** was obtained in 78% yield. No ^{18}O incorporation product **^{18}O-2.10a** was detected by HRMS analysis.

c) Deuterium scrambling experiments (Scheme 2.13)

Synthesis of 1-(phenylmethyl-*d*$_2$)-1,2,3,4-tetrahydroquinoline (*exo*-2.9a-*d*$_2$)

TH-3565_186122020



Scheme 2.30. Synthesis of ***exo*-2.9a-d_2**

In an oven dried pressure tube, **2.9a** (180 mg, 0.8 mmol, 1 equiv.) was taken with KO^{t}Bu (27 mg, 0.24 mmol) in DMSO-d_6 (1 mL) and the reaction mixture was stirred at 80 °C under argon atmosphere for 12 h. After cooling the mixture to room temperature, workup was done with ethyl acetate and water, washed with brine, and dried over anhydrous Na_2SO_4. The crude reaction mixture was purified by silica gel column chromatography using ethyl acetate and petroleum ether as eluent to get the desired molecule ***exo*-2.9a-d_2** (159 mg, 88%).

^{1}H NMR (400 MHz, Chloroform-*d*): δ 7.29 – 7.21 (m, 5H), 6.97 – 6.93 (m, 2H), 6.58 – 6.54 (m, 1H), 6.50 – 6.48 (m, 1H), 4.43 (s, 0.16H), 3.34 – 3.32 (m, 2H), 2.81 – 2.78 (m, 2H), 2.01 – 1.97 (m, 2H). ^{13}C NMR (151 MHz, Chloroform-*d*): δ 145.7, 138.9, 129.1, 128.7, 127.3, 126.87, 126.86, 126.71, 126.69, 122.3, 115.9, 111.03, 111.01, 49.9, 28.3, 22.5. HRMS (ESI) *m/z*: $[M+H]^+$ calculated for $C_{16}H_{16}D_2N$: 226.1560; found 226.1564.

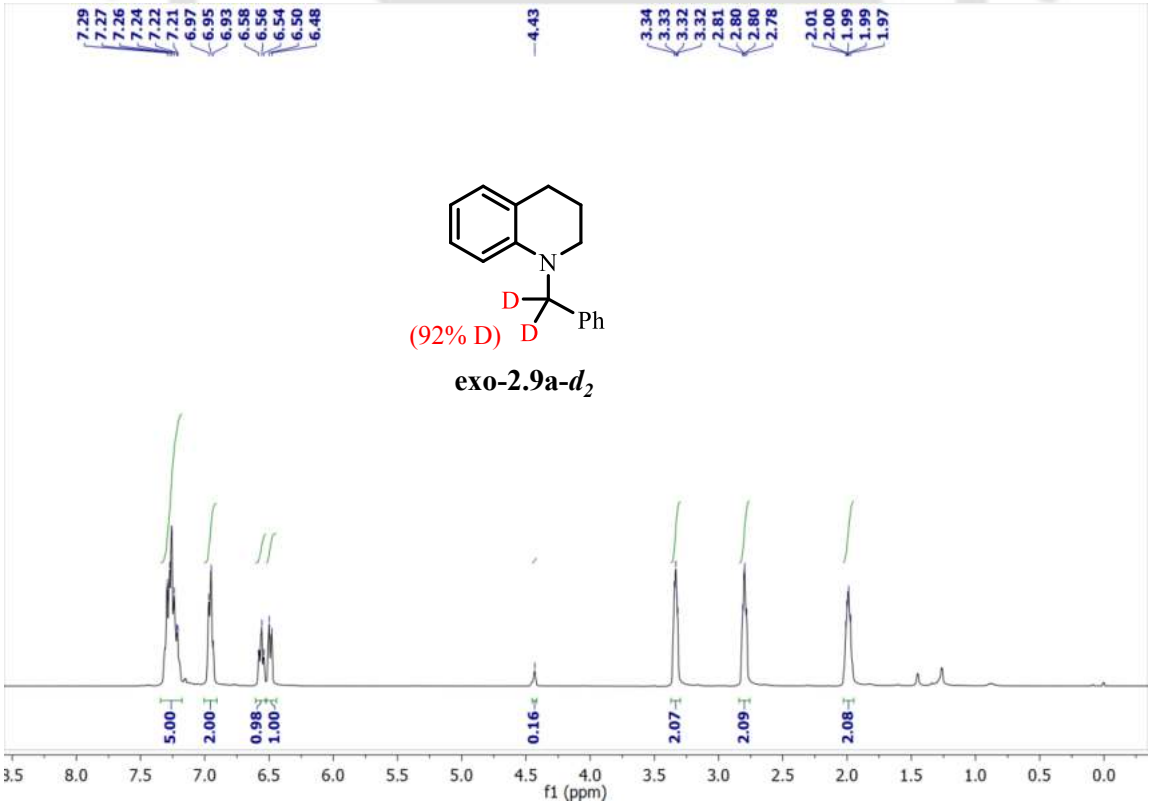


Figure 2.12. ^{1}H NMR spectrum of ***exo*-2.9a-d_2** ($CDCl_3$, 400 MHz, 298 K)

TH-3565_186122020

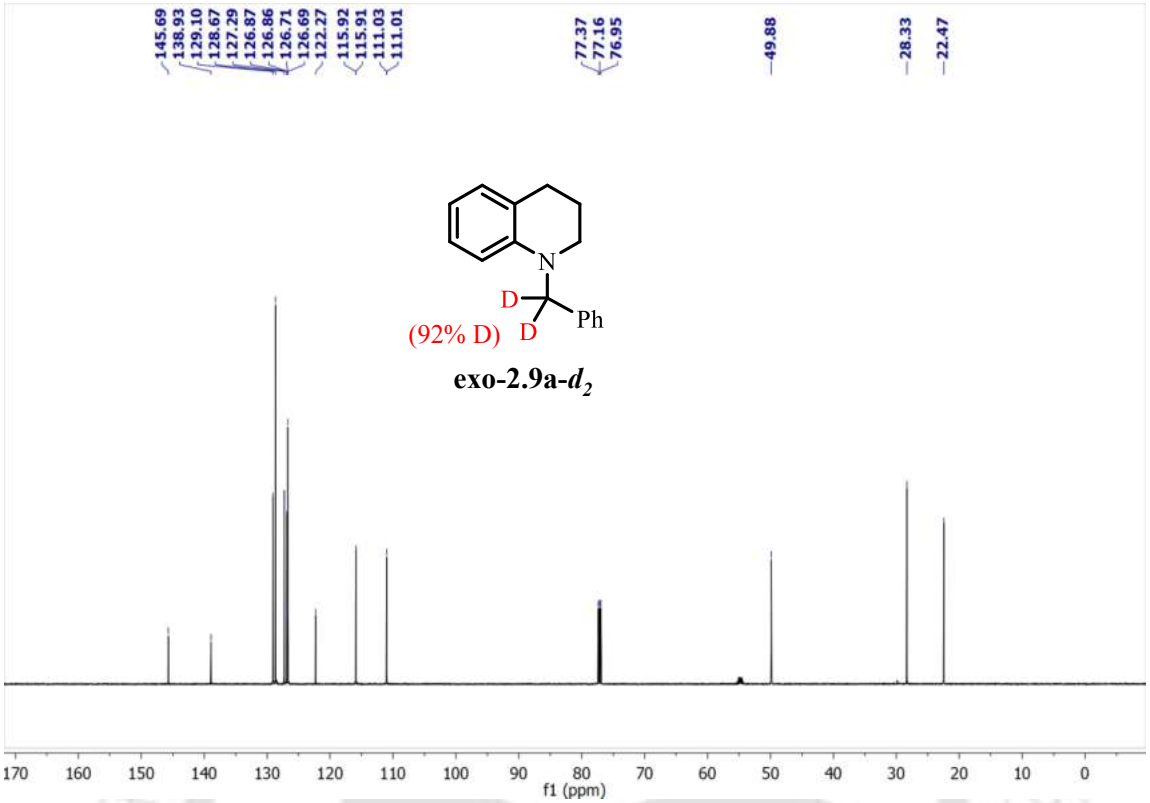
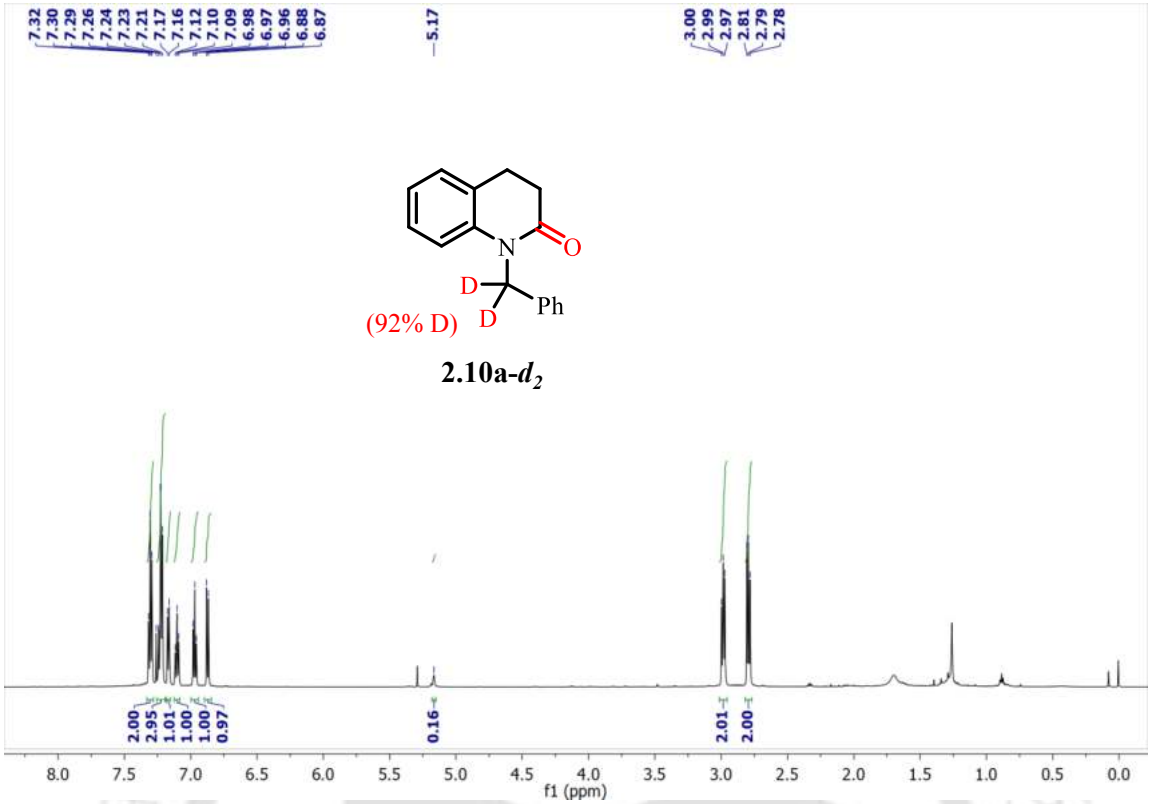


Figure 2.13. $^{13}C\{^{1}H\}$ NMR spectrum of ***exo*-2.9a-d_2** ($CDCl_3$, 151 MHz, 298 K)

Procedure: To study whether the reaction proceeds through the isomerization pathway, I have performed one experiment with deuterated ***exo*-2.9a-d_2** (65 mg, 0.29 mmol, 1 equiv.) as a substrate under standard reaction conditions following the general procedure GP-IV (Scheme 2.13). After completion of the reaction, the organic layer was separated and all the volatiles were removed under reduced pressure. The crude reaction mixture was purified by silica gel column chromatography using ethyl acetate/ pet ether (v/v = 1/5) as the eluent to afford the product **2.10a-d_2** (60 mg, 87%). No scrabbling H/D product of **2.10a-d_2'** was observed, ruling out the possible involvement of iminium ion isomerization.

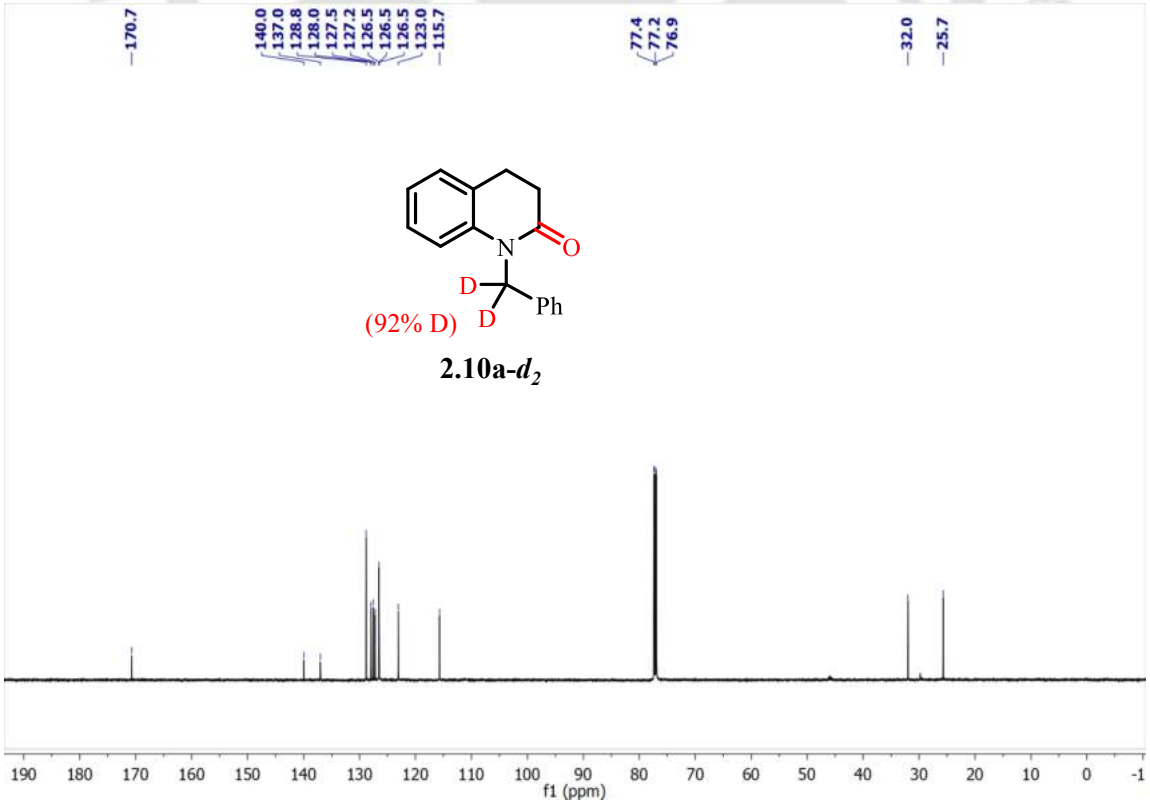
^{1}H NMR (600 MHz, Chloroform-*d*): δ 7.31 (t, J = 7.8 Hz, 2H), 7.24 – 7.21 (m, 3H), 7.17 (d, J = 7.4 Hz, 1H), 7.10 (t, J = 7.5 Hz, 1H), 6.97 (t, J = 7.4 Hz, 1H), 6.87 (d, J = 8.2 Hz, 1H), 5.17 (s, 0.16H), 3.00 – 2.97 (m, 2H), 2.81 – 2.78 (m, 2H). ^{13}C NMR (151 MHz, Chloroform-*d*): δ 170.7, 140.0, 137.0, 128.8, 128.0, 127.5, 127.2, 126.52, 126.50, 126.46, 123.0, 115.7, 32.0, 25.7. HRMS (ESI) *m/z*: $[M+H]^+$ calculated for $C_{16}H_{14}D_2NO$: 240.1352; found 240.1353.

TH-3565_186122020



2.10a-d_2

Figure 2.14. ^{1}H NMR spectrum of **2.10a-d_2** ($CDCl_3$, 600 MHz, 298 K)



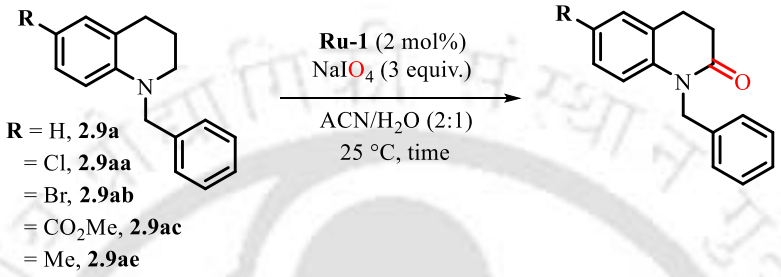
2.10a-d_2

Figure 2.15. ^{13}C{^{1}H} NMR spectrum of **2.10a-d_2** ($CDCl_3$, 151 MHz, 298 K)

TH-3565_186122020

d) Hammett studies

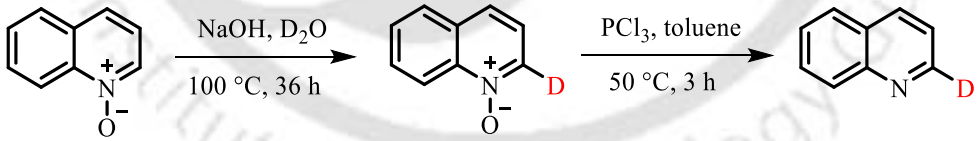
Procedure: A reaction tube was charged with well-dissolved $NaIO_4$ (3 equiv.) in 1 mL water. The *para*-substituted *N*-benzyltetrahydroquinoline derivatives (1 mmol) and **Ru-1** (2 mol%) were added to the tube with acetonitrile (2 mL). The reaction tubes were stirred at room temperature (25 °C) for the specified times. The progress of the reaction was analyzed by NMR using 1,3,5-trimethoxybenzene as an internal standard. All the reactions were carried out three times and the average conversion of the substituted *N*-benzyltetrahydroquinoline at different time intervals was plotted as ln(a/a-x) *vs* time (min).



Substrate	$k \times 10^{-3}$ (min^{-1})	k_X/k_H	log (k_X/k_H)	σ_p	ρ
p-CO_2Me (**2.9ac**)	199.8	9.42	0.98	0.45	**+2.39**
p-Cl (**2.9aa**)	75.8	3.59	0.56	0.23	
p-Br (**2.9ab**)	68.7	3.26	0.51	0.23	
H (**2.9a**)	21.1	1.00	0	0	
p-Me (**2.9ae**)	6.62	0.31	-0.51	-0.17	

e) Kinetic Isotope Effect (KIE) studies (Scheme 2.14)

Synthesis of quinoline-2-*d*



quinoline 1-oxide-2-*d* **quinoline-2-*d***

Scheme 2.31. Synthesis of **quinoline-2-*d***

Step 1: Quinoline *N*-oxide (750 mg, 5.2 mmol, 1 equiv.) was taken in a pressure tube with NaOH (517 mg, 2.5 equiv.) in D_2O (2 mL) and stirred at 100 ºC for 36 h. After cooling to room temperature, the reaction mixture was then extracted with ethyl acetate, washed with brine solution. The organic layer was separated and all the volatiles were removed under reduced pressure to get the crude **quinoline 1-oxide-2-*d*** (730 mg, 96%). The product **quinoline 1-oxide-2-*d*** was directly employed for the next step without further purification.

Step 2: In a round bottom flask, **quinoline 1-oxide-2-*d*** (490 mg, 3.3 mmol, 1equiv.) was taken with toluene (5 mL) and stirred at 0 ºC. To this, PCl_3 (690 mg, 1.3 equiv.) was added dropwise

TH-3565_186122020

and the reaction mixture was allowed to stir at 50 ºC for 3 h. After completion of the reaction, saturated $NaHCO_3$ solution was added and extracted with ethyl acetate. The organic layer was washed with brine solution and evaporated. The crude reaction mixture was purified by silica gel column chromatography with ethyl acetate/ pet ether (v/v = 1/5) to afford the desired product **quinoline-2-*d*** (309 mg, 72%).

^{1}H NMR (400 MHz, Chloroform-*d*): δ 8.88 (d, J = 2.4 Hz, 0.06H), 8.12 (d, J = 8.5 Hz, 1H), 8.07 – 8.05 (m, 1H), 7.74 (d, J = 8.2 Hz, 1H), 7.69 – 7.64 (m, 1H), 7.50 – 7.46 (m, 1H), 7.30 (d, J = 8.2 Hz, 1H).

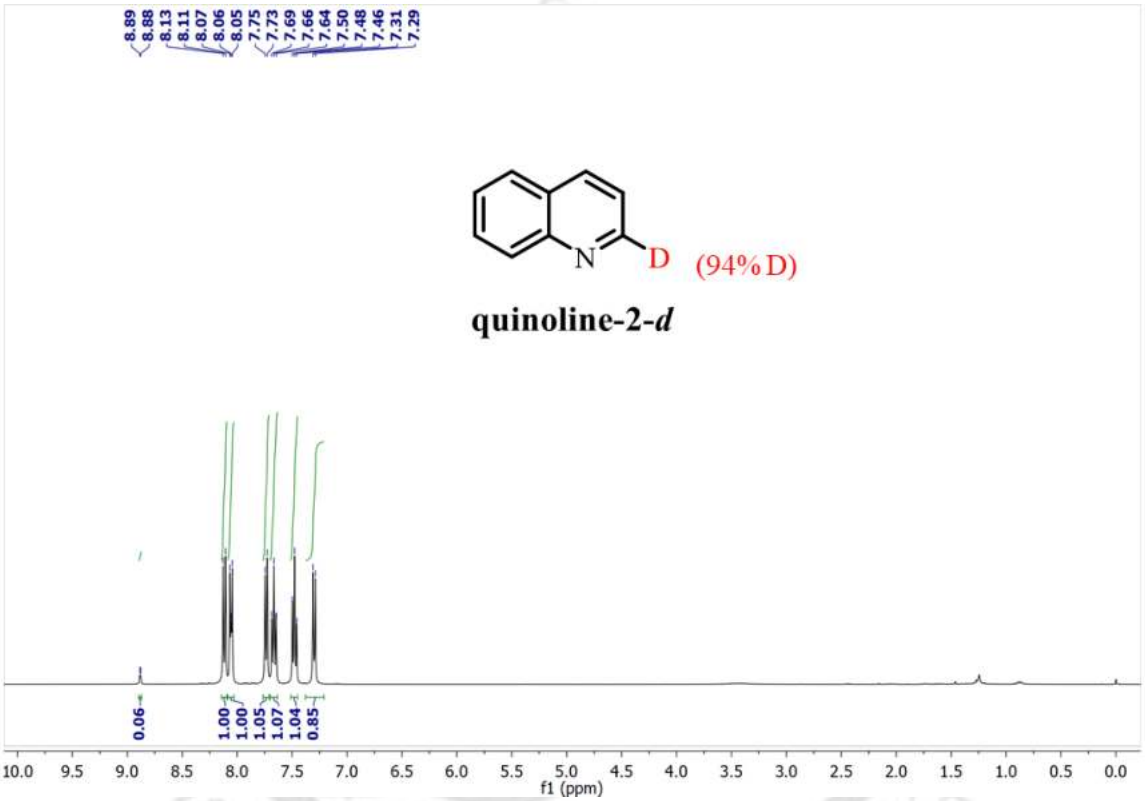
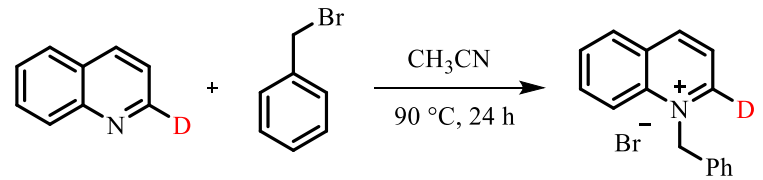


Figure 2.16. ^{1}H NMR spectrum of **quinoline-2-*d*** ($CDCl_3$, 400 MHz, 298 K)

Synthesis of 1-benzylquinolin-1-ium-2-*d* bromide



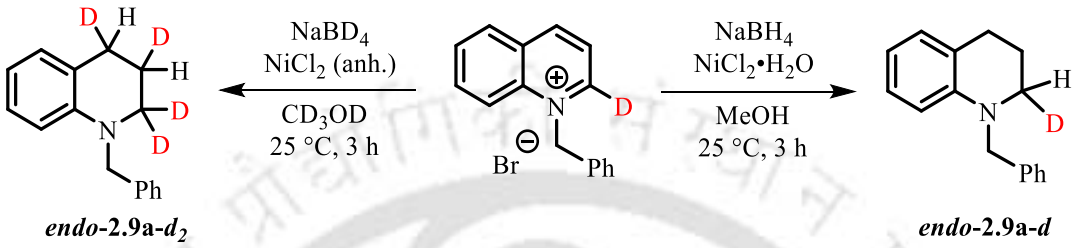
quinoline-2-*d* **1-benzylquinolin-1-ium-2-*d* bromide**

Scheme 2.32. Synthesis of 1-benzylquinolin-1-ium-2-*d* bromide

TH-3565_186122020

Following the general procedure GP-II, **quinoline-2-*d*** (310 mg, 2.4 mmol, 1 equiv.) was taken in a reaction tube with benzyl bromide (530 mg, 1.3 equiv.) in acetonitrile and stirred under reflux condition for 24 h to afford the desired salt as an off-white solid (657 mg, 91%). The product **1-benzylquinolin-1-ium-2-*d* bromide** was directly employed for the next step without further purification.

Synthesis of *endo*-2.9a-*d* and *endo*-2.9a-d_2



Scheme 2.33. Synthesis of ***endo*-2.9a-*d*** and ***endo*-2.9a-d_2**

In an oven dried round bottom flask, **1-benzylquinolin-1-ium-2-*d*** salt (200 mg, 0.6 mmol, 1 equiv.), $NaBH_4/NaBD_4$ (85 mg, 3 equiv.) were taken with $NiCl_2.H_2O/NiCl_2$ (130 mg, 1.5 equiv.) in $MeOH/CD_3OD$ (2 mL) respectively and allowed to stir at room temperature for 3 h. After completion of the reaction, the solvent was removed using a rotary evaporator and extracted with ethyl acetate and water. The crude reaction mixture was purified by silica gel column chromatography with ethyl acetate/ pet ether (v/v = 1/5) to afford the desired product.

endo*-2.9a-*d (112 mg, 83%). ^{1}H NMR (400 MHz, Chloroform-*d*): δ 7.31 – 7.19 (m, 5H), 6.95 (t, J = 7.3 Hz, 2H), 6.56 (t, J = 7.1 Hz, 1H), 6.49 (d, J = 8.4 Hz, 1H), 4.45 (s, 2H), 3.31 (m, 1.06H), 2.79 (t, J = 6.3 Hz, 2H), 1.98 (q, J = 6.1 Hz, 2H). ^{13}C NMR (151 MHz, Chloroform-*d*): δ 145.7, 139.0, 129.1, 128.7, 127.3, 126.8, 126.7, 122.3, 115.9, 111.1, 55.2, 28.3, 22.4. HRMS (ESI) *m/z*: $[M+H]^+$ calculated for $C_{16}H_{17}DN$: 225.1497; found 225.1499.

***endo*-2.9a-d_2** (106 mg, 78%). ^{1}H NMR (400 MHz, Chloroform-*d*): δ 7.31 – 7.19 (m, 5H), 6.95 (t, J = 7.3 Hz, 2H), 6.56 (t, J = 7.2 Hz, 1H), 6.49 (d, J = 8.4 Hz, 1H), 4.45 (s, 2H), 3.30 (m, 0.10H), 2.79 – 2.76 (m, 1H), 1.97 – 1.93 (m, 1H). ^{13}C NMR (151 MHz, Chloroform-*d*): δ 145.7, 139.0, 129.1, 128.7, 127.3, 126.8, 126.7, 122.2, 115.9, 111.0, 55.2. HRMS (ESI) *m/z*: $[M+H]^+$ calculated for $C_{16}H_{14}D_4N$: 228.1685; found 228.1688.

TH-3565_186122020

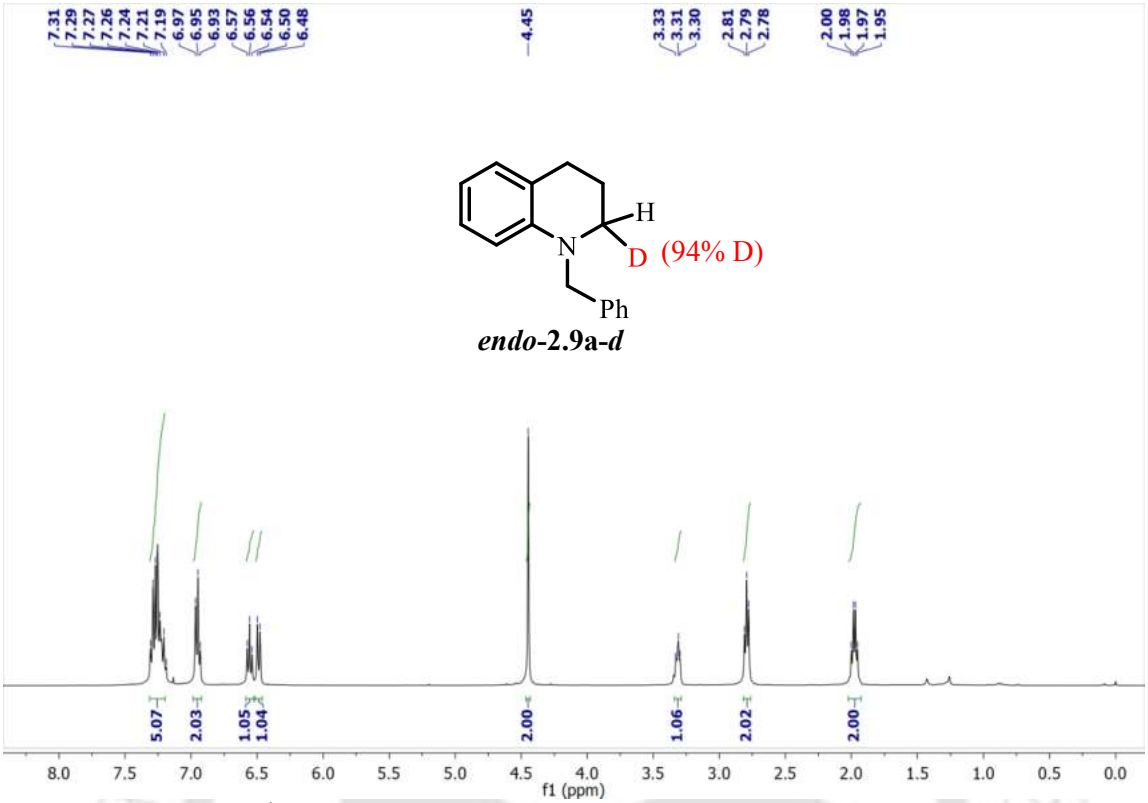


Figure 2.17. ^{1}H NMR spectrum of ***endo*-2.9a-*d*** ($CDCl_3$, 400 MHz, 298 K)

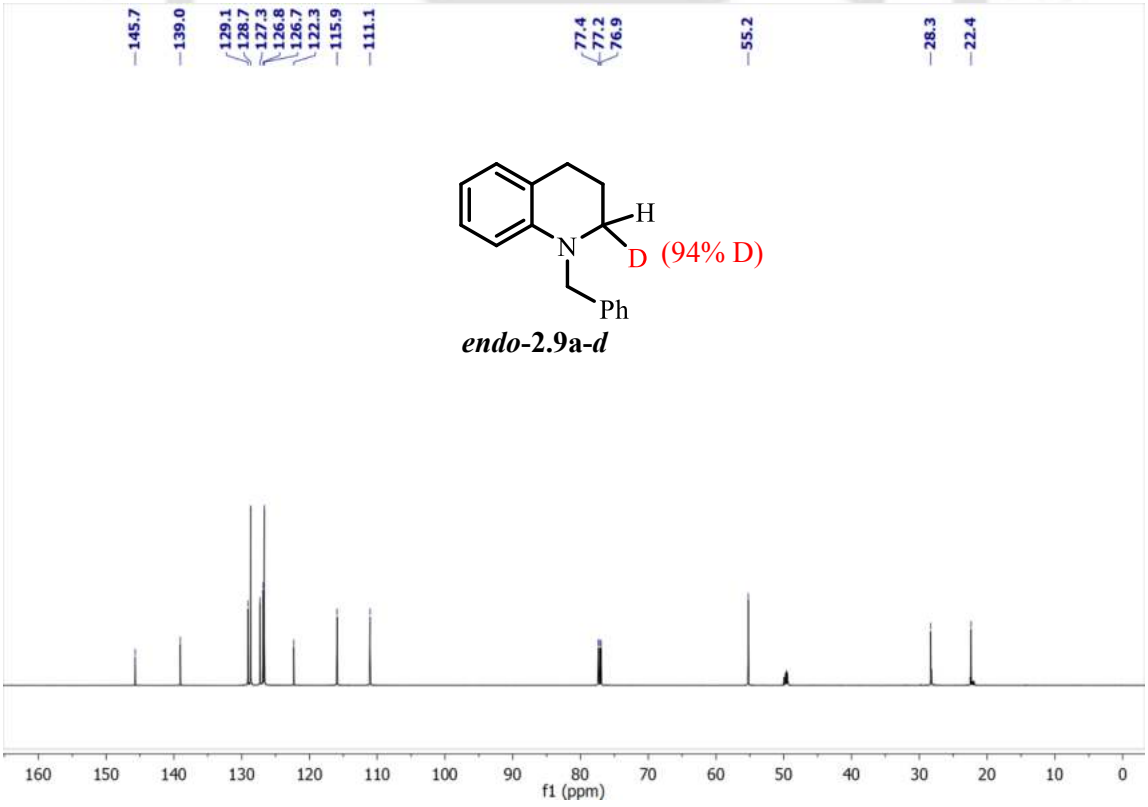


Figure 2.18. ^{13}C{^{1}H} NMR spectrum of ***endo*-2.9a-*d*** ($CDCl_3$, 151 MHz, 298 K)

TH-3565_186122020

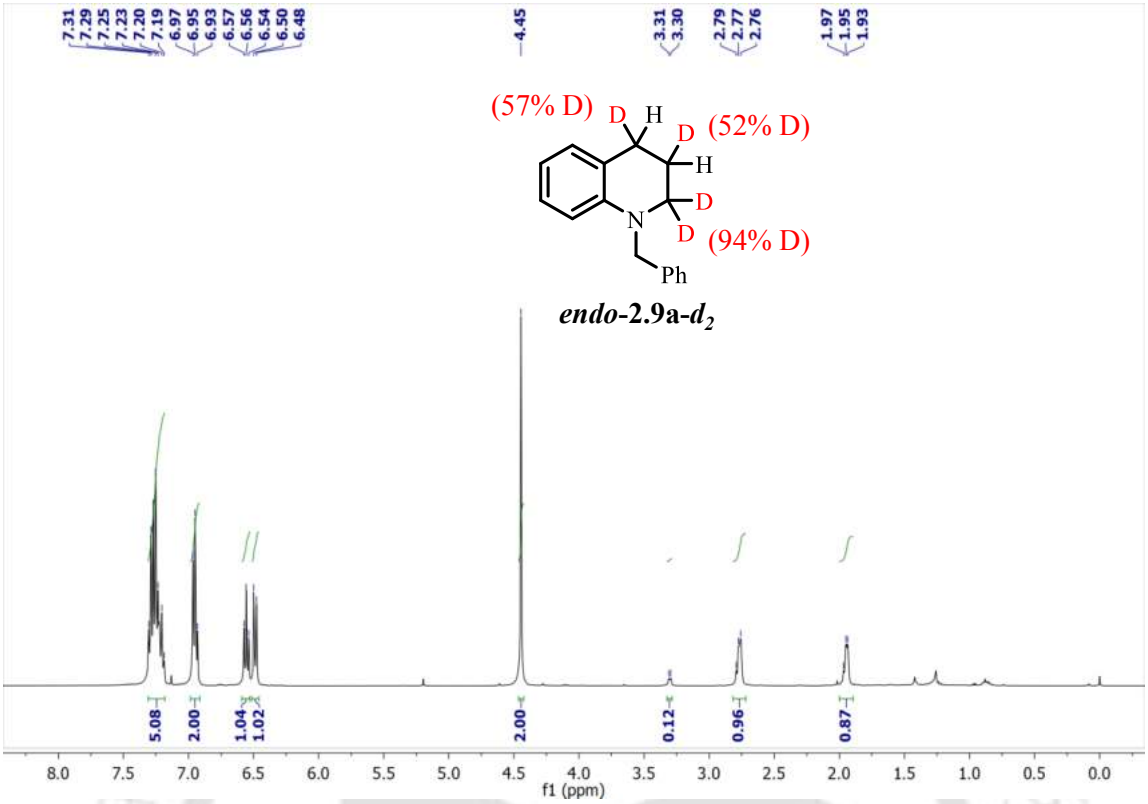


Figure 2.19. ^{1}H NMR spectrum of ***endo*-2.9a-d_2** ($CDCl_3$, 400 MHz, 298 K)

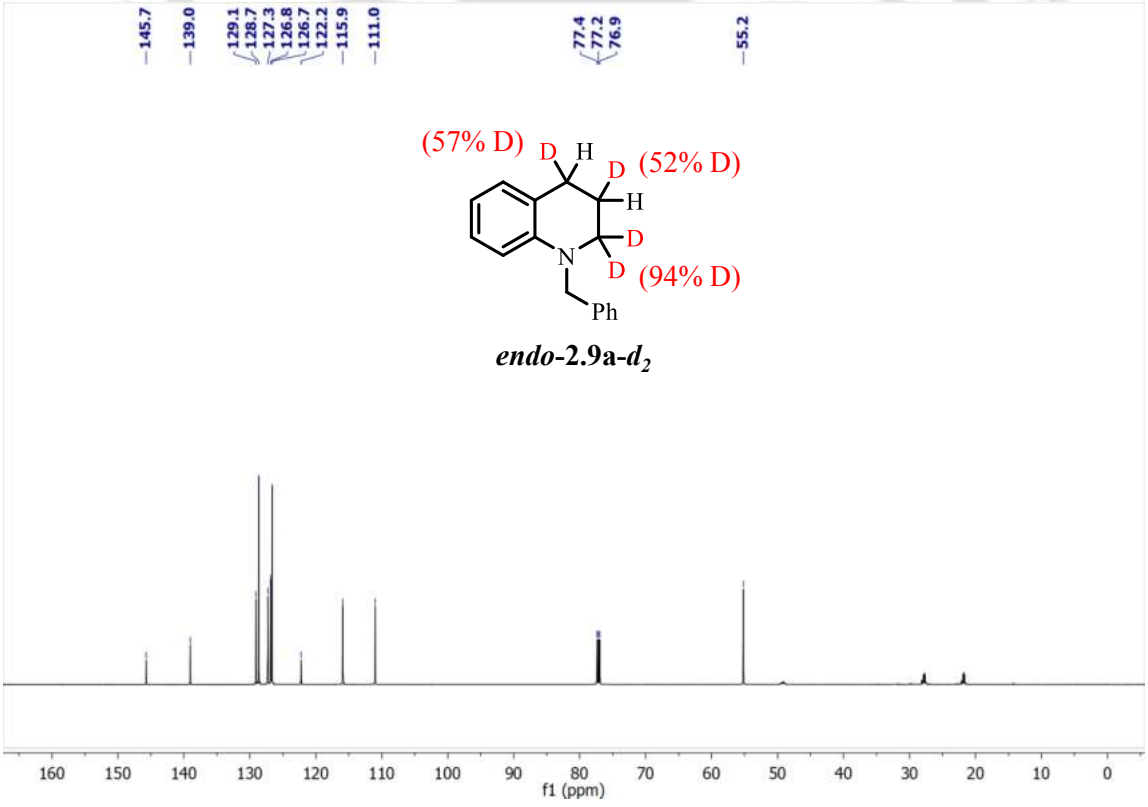


Figure 2.20. $^{13}C\{^{1}H\}$ NMR spectrum of ***endo*-2.9a-d_2** ($CDCl_3$, 151 MHz, 298 K)

TH-3565_186122020

Procedure: Three parallel reactions for the individual substrate **2.9a**, ***endo*-2.9a-*d***, and ***endo*-2.9a-*d*$_2$** respectively were carried out for KIE studies (Scheme 2.14). In a screw cap tube, $NaIO_4$ (3 equiv.) was charged with 1 mL water and dissolved it. To this, substrate (1 mmol), **Ru-1** (2 mol%), and acetonitrile (2 mL) were added and stirred the reaction mixture at room temperature (25 °C) for the specified times. The progress of the reaction was analyzed by NMR using 1,3,5-trimethoxybenzene as an internal standard. The ln(a/a-x) was plotted against time (min) to obtain the slope which gave the rate constant (k) for each case (Figure 2.6).

f) Intermediate trapping experiments

Procedure: To trap the intermediate, I have carried out one stoichiometric reaction between complex **Ru-1** (0.05 mmol) and aq. $NaIO_4$ (0.05 mmol) (1:1 molar ratio) at room temperature in acetonitrile, and immediately injected into the ESI-HRMS analysis; which showed a signal at m/z = 314.9704 corresponding to the cationic ruthenium dioxo species, [**Ru-1-I2**-Cl]$^+$ (see details in section 2.3.6.6).

2.5.9. Crystallographic data

Crystallographic data of Ru-1

Single crystals of compound **Ru-1** suitable for X-ray diffraction were obtained by slow evaporation of the saturated solution of the compound in CH_2Cl_2 at room temperature. X-ray crystallographic data were collected with a Bruker D8 VENTURE diffractometer. Structures were solved by direct methods using SHELXL-2014 software and Olex2 v1.5. All of the non-H atoms were refined anisotropically. The ORTEP diagram was obtained with ORTEP3 software with 30% thermal ellipsoid (see below, Figure 2.21). The crystallographic parameters and refinement data are listed in Table 2.9.

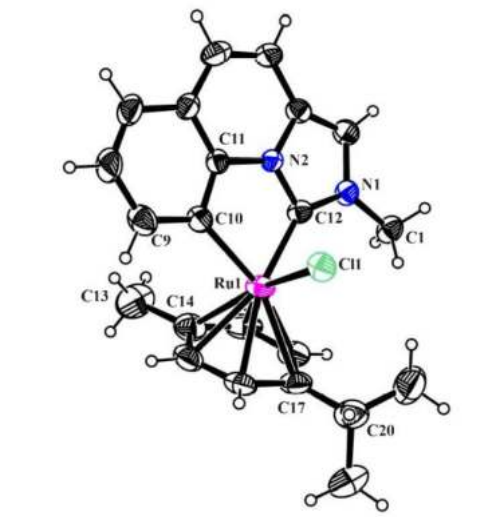


Figure 2.21. Molecular structure of compound **Ru-1** (thermal ellipsoid 30% probability level). Selected Bond lengths (in Å): Ru(1)–Cl(1) 2.4409(17), Ru(1)–C(10) 2.081(6), Ru(1)–C(12) 2.044(6), N(1)–C(12) 1.366(7), N(2)–C(12) 1.340(7). Selected Bond Angles (in °): C(10)–

TH-3565_186122020

Ru(1)–Cl(1) 87.24(17), C(12)–Ru(1)–Cl(1) 85.71(16), C(12)–Ru(1)–C(10) 78.2(2), N(2)–C(12)–N(1) 101.9(5), N(1)–C(12)–Ru(1) 143.6(4), N(2)–C(12)–Ru(1) 114.4(4).

Table 2.9. Crystal data and structure refinement for **Ru-1**

Identification code	MK389	
CCDC	2160136	
Empirical formula	$C_{22}H_{23}ClN_2Ru$	
Formula weight	451.959	
Temperature	296.15 K	
Wavelength	0.71073 Å	
Crystal system	triclinic	
Space group	P-1	
Unit cell dimensions	a = 12.486(2) Å	α = 86.156(5)°
	b = 12.796(2) Å	β = 85.187(5)°
	c = 13.774(2) Å	γ = 63.558(6)°
Volume	1962.5(6) $Å^3$	
Z	4	
Density (calculated)	1.530 g/cm^3	
Absorption coefficient	0.943 mm^{-1}	
F(000)	916.0	
Crystal size	0.29 × 0.24 × 0.21 mm^3	
2Θ range for data collection	3.8 to 54°	
Index ranges	$-16 \le h \le 16$, $-17 \le k \le 17$, $-18 \le l \le 18$	
Reflections collected	47619	
Independent reflections	8547 [R_{int} = 0.0808, R_{sigma} = 0.0812]	
Completeness to theta = 27.00°	99.6%	
Data/restraints/parameters	8547/0/477	
Goodness-of-fit on F^2	1.065	
Final R indexes [I>=2σ (I)]	R_1 = 0.0597, wR_2 = 0.1318	
Final R indexes [all data]	R_1 = 0.1046, wR_2 = 0.1523	
Largest diff. peak and hole	2.83 and -1.80 e $Å^{-3}$	

Crystallographic data of 2.10e

TH-3565_186122020

Single crystals of compound **2.10e** suitable for X-ray diffraction were obtained by slow evaporation of the saturated solution of the compound in CH_2Cl_2 at room temperature. X-ray crystallographic data were collected using Bruker D8 QUEST diffractometer. Data refinement and cell reduction were carried out by *APEX4*. Structures were solved by direct methods using Olex2 v1.5 and refined by a full-matrix least-squares method using Olex2 v1.5. All of the non-H atoms were refined anisotropically. The ORTEP diagram was obtained with ORTEP3 software with 30% thermal ellipsoid (see below, Figure 2.22). The crystallographic parameters and refinement data are listed in Table 2.10.

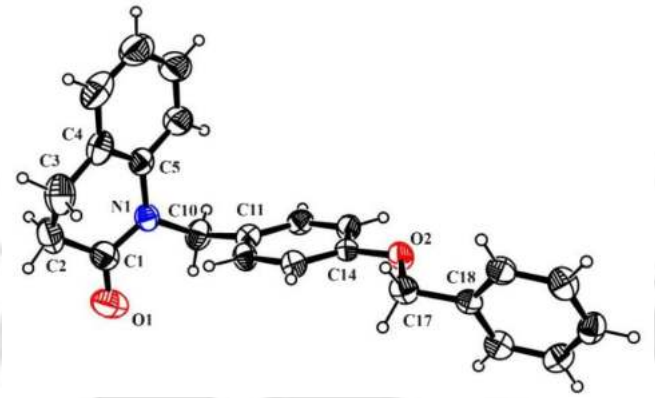


Figure 2.22. Molecular structure of compound **2.10e** (thermal ellipsoid 30% probability level). Selected Bond lengths (in Å): O(1)–C(1) 1.232(6), N(1)–C(1 1.371(6), N(1)–C(5) 1.423(6), N(1)–C(10) 1.450(6), C(1)–C(2) 1.492(8), C(2)–C(3) 1.505(8), C(4)–C(3) 1.491(8), C(11)–C(10) 1.507(6), O(2)–C(14) 1.370(5), O(2)–C(17) 1.432(5), C(18)–C(17) 1.493(6). Selected Bond Angles (in °): C(1)–N(1)–C(5) 121.2(4), C(10)–N(1)–C(5) 119.9(4), C(10)–N(1)–C(1) 118.8(5), C(11)–C(10)–N(1) 114.2(4), C(2)–C(1)–N(1) 116.5(5), C(3)–C(2)–C(1) 111.8(5), C(2)–C(3)–C(4) 111.0(5), C(17)–O(2)–C(14) 117.3(3), C(18)–C(17)–O(2) 108.1(3).

Table 2.10. Crystal data and structure refinement for **2.10e**

Identification code	MK-820_0m_a	
CCDC	2310176	
Empirical formula	$C_{23}H_{21}NO_2$	
Formula weight	343.429	
Temperature	297.00 K	
Wavelength	0.71073 Å	
Crystal system	monoclinic	
Space group	$P2_1/c$	
Unit cell dimensions	a = 8.2715(15) Å	α = 90°
	b = 5.5989(10) Å	β = 90.424(6)°
	c = 38.914(7) Å	γ = 90°

TH-3565_186122020

Volume	1802.1(6) $Å^3$
Z	4
Density (calculated)	1.266 g/cm^3
Absorption coefficient	0.080 mm^{-1}
F(000)	728.4
Crystal size	0.34 × 0.29 × 0.21 mm^3
2Θ range for data collection	4.18 to 50.3°
Index ranges	$-9 \leq h \leq 9, -6 \leq k \leq 6, -46 \leq l \leq 46$
Reflections collected	40103
Independent reflections	3202 [R_{int} = 0.1002, R_{sigma} = 0.0819]
Completeness to theta = 25.15°	99.2%
Data/restraints/parameters	3202/0/236
Goodness-of-fit on F^2	1.053
Final R indexes [I>=2σ (I)]	R_1 = 0.0846, wR_2 = 0.2132
Final R indexes [all data]	R_1 = 0.1491, wR_2 = 0.2407
Largest diff. peak and hole	0.39 and -0.40 e $Å^{-3}$

Crystallographic data of 2.10n

Single crystals of compound **2.10n** suitable for X-ray diffraction were obtained by slow evaporation of the saturated solution of the compound in CH_2Cl_2 at room temperature. X-ray crystallographic data were collected using Bruker D8 QUEST diffractometer. Data refinement and cell reduction were carried out by *APEX4*. Structures were solved by direct methods using Olex2 v1.5 and refined by a full-matrix least-squares method using Olex2 v1.5. All of the non-H atoms were refined anisotropically. The ORTEP diagram was obtained with ORTEP3 software with 30% thermal ellipsoid (see below, Figure 2.23). The crystallographic parameters and refinement data are listed in Table 2.11.

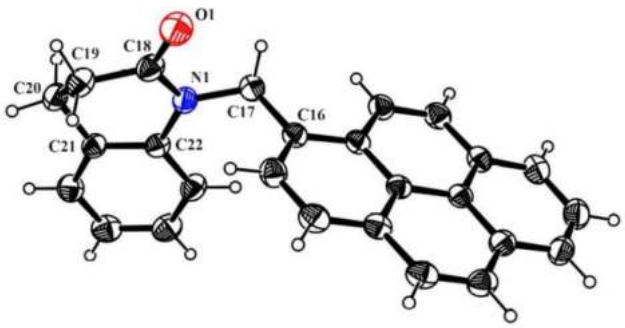


Figure 2.23: Molecular structure of compound **2.10n** (thermal ellipsoid 30% probability level). Selected Bond lengths (in Å): O(1)–C(18) 1.220(2), N(1)–C(17) 1.466(2), N(1)–C(18)

TH-3565_186122020

1.374(2), N(1)–C(22) 1.423(2), C(16)–C(17) 1.515(2), C(18)–C(19) 1.491(3), C(19)–C(20) 1.499(3), C(20)–C(21) 1.493(2), C(21)–C(22) 1.394(2). Selected Bond Angles (in °): O(1)–C(18)–N(1) 120.96(18), O(1)–C(18)–C(19) 122.83(17), N(1)–C(17)–C(16) 114.67(15), N(1)–C(18)–C(19) 116.19(16), C(18)–C(19)–C(20) 112.90(16), C(21)–C(20)–C(19) 110.01(15).

Table 2.11. Crystal data and structure refinement for **2.10n**

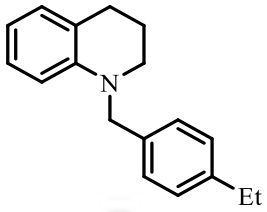
Identification code	SG_27_0ma_a	
CCDC	2310177	
Empirical formula	$C_{26}H_{19}NO$	
Formula weight	361.42	
Temperature	298.00 K	
Wavelength	0.71073 Å	
Crystal system	monoclinic	
Space group	$P2_1/c$	
Unit cell dimensions	a = 15.4528(7) Å	α = 90°
	b = 9.1085(4) Å	β = 114.4090(10)°
	c = 14.1231(6) Å	γ = 90°
Volume	1810.17(14) $Å^3$	
Z	4	
Density (calculated)	1.326 g/cm^3	
Absorption coefficient	0.080 mm^{-1}	
F(000)	760.0	
Crystal size	0.39 × 0.35 × 0.29 mm^3	
2Θ range for data collection	5.48 to 52.76°	
Index ranges	$-19 \le h \le 19$, $-11 \le k \le 11$, $-17 \le l \le 17$	
Reflections collected	43782	
Independent reflections	3693 [R_{int} = 0.0375, R_{sigma} = 0.0203]	
Completeness to theta = 26.38°	99.7%	
Data/restraints/parameters	3693/0/253	
Goodness-of-fit on F^2	1.073	
Final R indexes [I>=2σ (I)]	R_1 = 0.0463, wR_2 = 0.1029	
Final R indexes [all data]	R_1 = 0.0713, wR_2 = 0.1215	
Largest diff. peak and hole	0.17 and -0.18 e $Å^{-3}$	

TH-3565_186122020

2.5.10. Analytical data

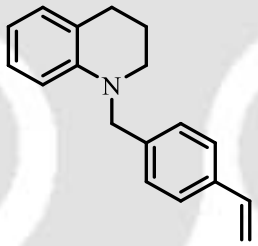
a) For starting materials

1-(4-ethylbenzyl)-1,2,3,4-tetrahydroquinoline (2.9c)



Following the general procedure GP-I, the title compound **2.9c** was isolated as a colourless oil using silica gel column chromatography with ethyl acetate/ pet ether (v/v = 1/20, R_f = 0.8) in 87% yield (109 mg). ^{1}H NMR (600 MHz, Chloroform-*d*): δ 7.18 (d, J = 8.0 Hz, 2H), 7.14 (d, J = 8.0 Hz, 2H), 6.97 – 6.95 (m, 2H), 6.56 (t, J = 7.4 Hz, 1H), 6.51 (d, J = 8.6 Hz, 1H), 4.44 (s, 2H), 3.35 – 3.33 (m, 2H), 2.80 (t, J = 6.4 Hz, 2H), 2.62 (q, J = 7.6 Hz, 2H), 1.99 (p, J = 5.8 Hz, 2H), 1.22 (t, J = 7.5 Hz, 3H). ^{13}C NMR (151 MHz, Chloroform-*d*): δ 145.8, 142.9, 136.2, 129.1, 128.2, 127.3, 126.7, 122.3, 115.8, 111.1, 55.0, 49.9, 28.6, 28.4, 22.5, 15.8. HRMS (ESI) *m/z*: $[M+H]^+$ calculated for $C_{18}H_{22}N$: 252.1747; found 252.1755.

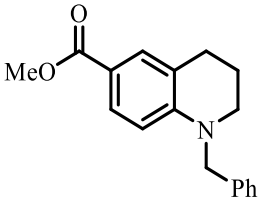
1-(4-vinylbenzyl)-1,2,3,4-tetrahydroquinoline (2.9l)



Following the general procedure GP-II, the title compound **2.9l** was isolated as a white solid using silica gel column chromatography with ethyl acetate/ pet ether (v/v = 1/50, R_f = 0.8) in 81% yield (101 mg). ^{1}H NMR (600 MHz, Chloroform-*d*): δ 7.35 (d, J = 8.1 Hz, 2H), 7.22 (d, J = 7.9 Hz, 2H), 6.96 (t, J = 7.6 Hz, 2H), 6.69 (dd, J = 17.6, 10.9 Hz, 1H), 6.57 (t, J = 7.3 Hz, 1H), 6.49 (d, J = 8.2 Hz, 1H), 5.71 (d, J = 17.6 Hz, 1H), 5.20 (d, J = 10.9 Hz, 1H), 4.45 (s, 2H), 3.36 – 3.34 (m, 2H), 2.81 (t, J = 6.4 Hz, 2H), 2.02 – 1.98 (m, 2H). ^{13}C NMR (151 MHz, Chloroform-*d*): δ 145.7, 138.8, 136.7, 136.4, 129.1, 127.3, 126.9, 126.6, 122.4, 116.0, 113.5, 111.1, 55.1, 50.0, 28.4, 22.5. HRMS (ESI) *m/z*: $[M+H]^+$ calculated for $C_{18}H_{20}N$: 250.1591; found 250.1594.

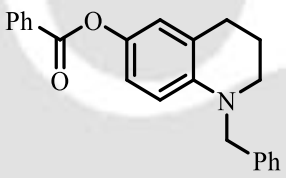
Methyl 1-benzyl-1,2,3,4-tetrahydroquinoline-6-carboxylate (2.9ac)

TH-3565_186122020



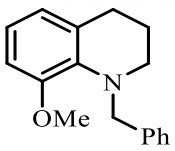
Following the general procedure GP-I, the title compound **2.9ac** was isolated as a white solid using silica gel column chromatography with ethyl acetate/ pet ether (v/v = 1/10, R_f = 0.7) in 78% yield (134 mg). ^{1}H NMR (400 MHz, Chloroform-*d*): δ 7.66 – 7.64 (m, 2H), 7.31 (t, J = 7.0 Hz, 2H), 7.24 – 7.19 (m, 3H), 6.46 (d, J = 9.4 Hz, 1H), 4.54 (s, 2H), 3.82 (s, 3H), 3.44 – 3.41 (m, 2H), 2.82 (t, J = 6.2 Hz, 2H), 2.03 – 1.97 (m, 2H). ^{13}C NMR (151 MHz, Chloroform-*d*): δ 167.6, 149.3, 137.7, 130.7, 129.8, 128.9, 127.2, 126.5, 121.3, 116.8, 109.8, 54.8, 51.5, 50.1, 28.2, 22.0. HRMS (ESI) *m/z*: $[M+H]^+$ calculated for $C_{18}H_{20}NO_2$: 282.1489; found 282.1484.

1-benzyl-1,2,3,4-tetrahydroquinolin-6-yl benzoate (2.9ad)



Following the general procedure GP-I, the title compound **2.9ad** was isolated as a colourless oil using silica gel column chromatography with ethyl acetate/ pet ether (v/v = 1/10, R_f = 0.8) in 84% yield (118 mg). ^{1}H NMR (600 MHz, Chloroform-*d*): δ 8.17 (d, J = 7.4 Hz, 2H), 7.60 (t, J = 7.4 Hz, 1H), 7.48 (t, J = 7.6 Hz, 2H), 7.33 (t, J = 7.6 Hz, 2H), 7.28 – 7.23 (m, 3H), 6.85 (d, J = 2.8 Hz, 1H), 6.79 (dd, J = 8.8, 2.8 Hz, 1H), 6.49 (d, J = 8.8 Hz, 1H), 4.48 (s, 2H), 3.37 (t, J = 5.7 Hz, 2H), 2.83 (t, J = 6.3 Hz, 2H), 2.03 (p, J = 6.0 Hz, 2H). ^{13}C NMR (151 MHz, Chloroform-*d*): δ 166.1, 143.8, 141.0, 138.9, 133.4, 130.21, 130.16, 128.8, 128.6, 127.0, 126.7, 123.2, 122.0, 119.9, 111.4, 55.6, 50.0, 28.4, 22.4. HRMS (ESI) *m/z*: $[M+H]^+$ calculated for $C_{23}H_{22}NO_2$: 344.1646; found 344.1650.

1-benzyl-8-methoxy-1,2,3,4-tetrahydroquinoline (2.9ag)

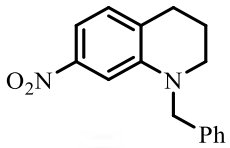


Following the general procedure GP-II, the title compound **2.9ag** was isolated as a colourless oil using silica gel column chromatography with ethyl acetate/ pet ether (v/v = 1/20, R_f = 0.8) in 90% yield (114 mg). ^{1}H NMR (400 MHz, Chloroform-*d*): δ 7.49 (d, J = 6.7 Hz, 2H), 7.35 – 7.31 (m, 2H), 7.27 – 7.23 (m, 1H), 6.85 (t, J = 7.8 Hz, 1H), 6.71 – 6.68 (m, 2H), 4.19 (s, 2H), 3.84 (s, 3H), 2.99 – 2.96 (m, 2H), 2.76 (t, J = 6.6 Hz, 2H), 1.79 – 1.74 (m, 2H). ^{13}C NMR (151

TH-3565_186122020

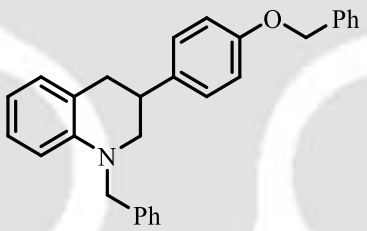
MHz, Chloroform-*d*): δ 152.1, 140.6, 137.6, 129.5, 128.8, 128.3, 126.9, 122.0, 120.9, 108.8, 57.8, 55.5, 47.4, 28.0, 17.9. HRMS (ESI) *m/z*: $[M+H]^+$ calculated for $C_{17}H_{20}NO$: 254.1540; found 254.1542.

1-benzyl-7-nitro-1,2,3,4-tetrahydroquinoline (2.9ai)



Following the general procedure GP-II, the title compound **2.9ai** was isolated as an orange solid using silica gel column chromatography with ethyl acetate/ pet ether (v/v = 1/10, R_f = 0.6) in 94% yield (126 mg). ^{1}H NMR (600 MHz, Chloroform-*d*): δ 7.39 (d, J = 8.2 Hz, 1H), 7.34 – 7.32 (m, 3H), 7.27 – 7.23 (m, 3H), 7.04 (d, J = 8.2 Hz, 1H), 4.54 (s, 2H), 3.42 (t, J = 5.8 Hz, 2H), 2.86 (t, J = 6.4 Hz, 2H), 2.02 (p, J = 6.1 Hz, 2H). ^{13}C NMR (151 MHz, Chloroform-*d*): δ 148.0, 146.1, 137.4, 129.5, 129.2, 129.0, 127.4, 126.7, 110.8, 104.9, 55.0, 49.5, 28.5, 21.6. HRMS (ESI) *m/z*: $[M+H]^+$ calculated for $C_{16}H_{17}N_2O_2$: 269.1285; found 269.1286.

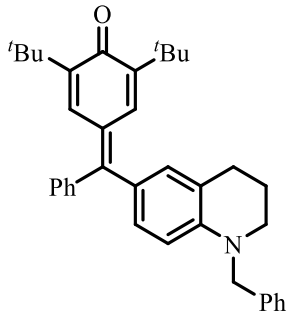
1-benzyl-3-(4-(benzyloxy)phenyl)-1,2,3,4-tetrahydroquinoline (2.9am)



Following the general procedure GP-I, the title compound **2.9am** was isolated as an orange solid using silica gel column chromatography with ethyl acetate/ pet ether (v/v = 1/10, R_f = 0.6) in 94% yield (126 mg). ^{1}H NMR (400 MHz, Chloroform-*d*): δ 7.47 – 7.20 (m, 10H), 7.14 (d, J = 8.6 Hz, 2H), 7.02 (t, J = 7.6 Hz, 2H), 6.93 (d, J = 8.6 Hz, 2H), 6.63 – 6.57 (m, 2H), 5.04 (s, 2H), 4.50 (s, 2H), 3.41 (d, J = 7.9 Hz, 2H), 3.23 – 3.16 (m, 1H), 3.04 – 2.95 (m, 2H). ^{13}C NMR (151 MHz, Chloroform-*d*): δ 157.7, 145.1, 138.9, 137.2, 136.0, 129.3, 128.73, 128.72, 128.3, 128.1, 127.6, 127.5, 127.0, 126.8, 122.3, 116.2, 115.1, 111.2, 70.2, 56.6, 55.4, 38.0, 35.9. HRMS (ESI) *m/z*: $[M+H]^+$ calculated for $C_{29}H_{28}NO$: 406.2166; found 406.2162.

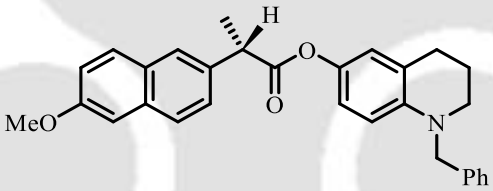
4-((1-benzyl-1,2,3,4-tetrahydroquinolin-6-yl)(phenyl)methylene)-2,6-di-tert-butylcyclohexa-2,5-dien-1-one (2.9an)

TH-3565_186122020



Following the general procedure GP-I, the title compound **2.9an** was isolated as an orange solid using silica gel column chromatography with ethyl acetate/ pet ether (v/v = 1/50, R_f = 0.6) in 79% yield (203 mg). ^{1}H NMR (600 MHz, Chloroform-*d*): δ 7.42 – 7.38 (m, 4H), 7.34 (t, *J* = 8.2 Hz, 2H), 7.28 – 7.26 (m, 5H), 7.01 (d, *J* = 2.5 Hz, 1H), 6.91 (d, *J* = 2.2 Hz, 1H), 6.86 (dd, *J* = 8.6, 2.2 Hz, 1H), 6.51 (d, *J* = 8.6 Hz, 1H), 4.56 (s, 2H), 3.46 (t, *J* = 5.6 Hz, 2H), 2.79 (t, *J* = 6.2 Hz, 2H), 2.06 – 2.02 (m, 2H), 1.30 (s, 9H), 1.21 (s, 9H). ^{13}C NMR (151 MHz, Chloroform-*d*): δ 186.0, 158.4, 147.3, 146.2, 146.0, 141.6, 138.0, 134.2, 133.2, 133.0, 132.9, 132.5, 129.2, 128.9, 128.0, 127.8, 127.3, 126.7, 121.4, 110.1, 55.1, 50.1, 35.4, 35.3, 29.8, 29.6, 28.2, 22.2. HRMS (ESI) *m/z*: $[M+H]^+$ calculated for $C_{37}H_{42}NO$: 516.3261; found 516.3262.

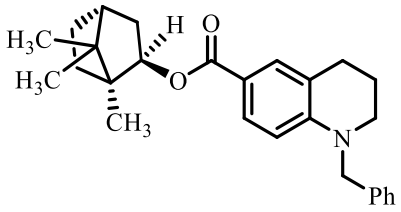
1-benzyl-1,2,3,4-tetrahydroquinolin-6-yl (*S*)-2-(6-methoxynaphthalen-2-yl)propanoate (2.11a)



Following the general procedure GP-I, the title compound **2.11a** was isolated as a colourless liquid using silica gel column chromatography with ethyl acetate/ pet ether (v/v = 1/10, R_f = 0.6) in 78% yield (176 mg). ^{1}H NMR (600 MHz, Chloroform-*d*): δ 7.74 – 7.70 (m, 3H), 7.48 (dd, *J* = 8.5, 1.9 Hz, 1H), 7.29 – 7.27 (m, 2H), 7.23 – 7.19 (m, 3H), 7.15 – 7.11 (m, 2H), 6.60 (d, *J* = 2.7 Hz, 1H), 6.57 (dd, *J* = 8.9, 2.8 Hz, 1H), 6.37 (d, *J* = 8.9 Hz, 1H), 4.41 (s, 2H), 4.03 (q, *J* = 7.1 Hz, 1H), 3.90 (s, 3H), 3.31 – 3.29 (m, 2H), 2.73 (t, *J* = 6.4 Hz, 2H), 1.97 – 1.93 (m, 2H), 1.65 (d, *J* = 7.2 Hz, 3H). ^{13}C NMR (151 MHz, Chloroform-*d*): δ 174.0, 157.8, 143.6, 141.0, 138.8, 135.6, 133.8, 129.4, 129.1, 128.7, 127.3, 126.9, 126.7, 126.4, 126.2, 123.0, 121.6, 119.5, 119.1, 111.3, 105.7, 55.6, 55.4, 49.9, 45.6, 28.3, 22.3, 18.7. HRMS (ESI) *m/z*: $[M+H]^+$ calculated for $C_{30}H_{30}NO_3$: 452.2221; found 452.2223.

(1*S*,2*R*,4*R*)-1,7,7-trimethylbicyclo[2.2.1]heptan-2-yl-1-benzyl-1,2,3,4-tetrahydroquinoline-6-carboxylate (2.11b)

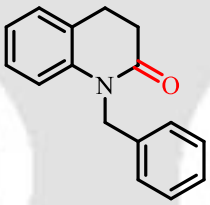
TH-3565_186122020



Following the general procedure GP-I, the title compound **2.11b** was isolated as a colourless liquid using silica gel column chromatography with ethyl acetate/ pet ether (v/v = 1/20, R_f = 0.7) in 85% yield (170 mg). ^{1}H NMR (600 MHz, Chloroform-*d*): δ 7.63 – 7.62 (m, 2H), 7.33 – 7.30 (m, 2H), 7.26 – 7.23 (m, 1H), 7.21 – 7.20 (m, 2H), 6.45 (d, J = 8.4 Hz, 1H), 4.84 (dd, J = 7.6, 4.0 Hz, 1H), 4.54 (s, 2H), 3.44 – 3.42 (m, 2H), 2.83 (t, J = 6.2 Hz, 2H), 2.03 – 1.99 (m, 2H), 1.89 – 1.81 (m, 2H), 1.75 (t, J = 4.2 Hz, 1H), 1.72 – 1.68 (m, 1H), 1.59 – 1.54 (m, 1H), 1.23 – 1.19 (m, 1H), 1.13 – 1.11 (m, 1H), 1.09 (s, 3H), 0.89 (s, 3H), 0.86 (s, 3H). ^{13}C NMR (151 MHz, Chloroform-*d*): δ 166.6, 149.1, 137.7, 130.6, 129.6, 128.9, 127.2, 126.4, 121.3, 117.6, 109.8, 80.6, 54.8, 50.1, 49.0, 47.1, 45.2, 39.1, 33.9, 28.2, 27.2, 22.0, 20.3, 20.2, 11.7. HRMS (ESI) *m/z*: $[M+H]^+$ calculated for $C_{27}H_{34}NO_2$: 404.2585; found 452.2587.

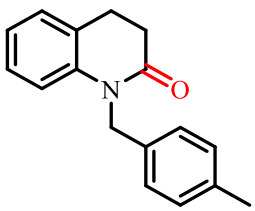
b) Analytical data of the products

1-benzyl-3,4-dihydroquinolin-2(1*H*)-one (2.10a)



Following the general procedure GP-IV, the title compound **2.10a** was isolated as a white solid using silica gel column chromatography with ethyl acetate/ pet ether (v/v = 1/10, R_f = 0.4) in 94% yield (112 mg). ^{1}H NMR (600 MHz, Chloroform-*d*): δ 7.30 (t, J = 7.5 Hz, 2H), 7.24 – 7.20 (m, 3H), 7.17 (d, J = 7.3 Hz, 1H), 7.10 (t, J = 7.3 Hz, 1H), 6.97 (t, J = 7.3 Hz, 1H), 6.86 (d, J = 8.2 Hz, 1H), 5.18 (s, 2H), 3.00 – 2.97 (m, 2H), 2.81 – 2.79 (m, 2H). ^{13}C NMR (151 MHz, Chloroform-*d*): δ 170.8, 139.9, 137.0, 128.9, 128.0, 127.6, 127.2, 126.5, 126.4, 123.1, 115.7, 46.3, 32.0, 25.6. Spectral data is in accordance to the reported literature.[30]

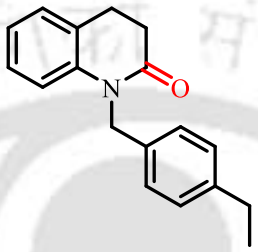
1-(4-methylbenzyl)-3,4-dihydroquinolin-2(1*H*)-one (2.10b)



TH-3565_186122020

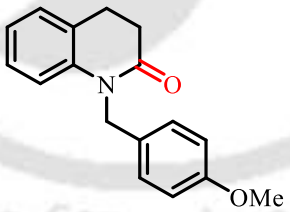
Following the general procedure GP-IV, the title compound **2.10b** was isolated as a colourless liquid using silica gel column chromatography with ethyl acetate/ pet ether (v/v = 1/5, R_f = 0.3) in 91% yield (114 mg). ^{1}H NMR (600 MHz, Chloroform-*d*): δ 7.16 (d, J = 8.8 Hz, 1H), 7.12 – 7.09 (m, 5H), 6.97 – 6.95 (m, 1H), 6.89 (d, J = 9.3 Hz, 1H), 5.14 (s, 2H), 2.98 – 2.96 (m, 2H), 2.79 – 2.77 (m, 2H), 2.30 (s, 3H). ^{13}C NMR (151 MHz, Chloroform-*d*): δ 170.7, 140.1, 136.8, 134.1, 129.5, 127.9, 127.5, 126.5, 123.0, 115.8, 46.1, 32.0, 25.7, 21.2. HRMS (ESI) *m/z*: $[M+H]^+$ calculated for $C_{17}H_{18}NO$: 252.1383; found 252.1386.

1-(4-ethylbenzyl)-3,4-dihydroquinolin-2(1*H*)-one (2.10c)



Following the general procedure GP-IV, the title compound **2.10c** was isolated as a colourless oil using silica gel column chromatography with ethyl acetate/ pet ether (v/v = 1/5, R_f = 0.4) in 89% yield (118 mg). ^{1}H NMR (400 MHz, Chloroform-*d*): δ 7.17 – 7.09 (m, 6H), 6.96 (t, J = 7.4 Hz, 1H), 6.90 (d, J = 8.1 Hz, 1H), 5.14 (s, 2H), 2.99 – 2.95 (m, 2H), 2.80 – 2.76 (m, 2H), 2.60 (q, J = 7.6 Hz, 2H), 1.20 (t, J = 7.6 Hz, 3H). ^{13}C NMR (151 MHz, Chloroform-*d*): δ 170.7, 143.2, 140.1, 134.3, 128.3, 127.9, 127.5, 126.53, 126.51, 123.0, 115.8, 46.1, 32.1, 28.6, 25.7, 15.7. HRMS (ESI) *m/z*: $[M+H]^+$ calculated for $C_{18}H_{20}NO$: 266.1540; found 266.1538.

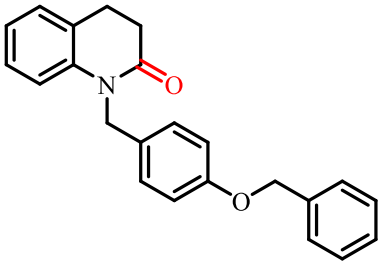
1-(4-methoxybenzyl)-3,4-dihydroquinolin-2(1*H*)-one (2.10d)



Following the general procedure GP-IV, the title compound **2.10d** was isolated as a yellow oil using silica gel column chromatography with ethyl acetate/ pet ether (v/v = 1/4, R_f = 0.4) in 96% yield (128 mg). ^{1}H NMR (400 MHz, Chloroform-*d*): δ 7.16 – 7.09 (m, 4H), 6.96 (t, J = 7.4 Hz, 1H), 6.91 (d, J = 8.0 Hz, 1H), 6.84 – 6.82 (m, 2H), 5.11 (s, 2H), 3.76 (s, 3H), 2.98 – 2.94 (m, 2H), 2.79 – 2.75 (m, 2H). ^{13}C NMR (151 MHz, Chloroform-*d*): δ 170.7, 158.8, 140.0, 129.2, 127.9, 127.8, 127.5, 126.5, 123.0, 115.8, 114.3, 55.4, 45.7, 32.1, 25.7. Spectral data is in accordance to the reported literature.[31]

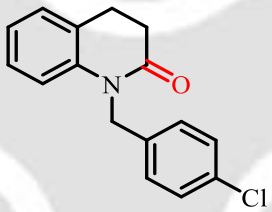
1-(4-(benzyloxy)benzyl)-3,4-dihydroquinolin-2(1*H*)-one (2.10e)

TH-3565_186122020



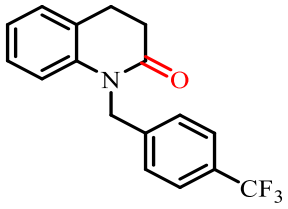
Following the general procedure GP-IV, the title compound **2.10e** was isolated as a white solid using silica gel column chromatography with ethyl acetate/ pet ether (v/v = 1/10, R_f = 0.4) in 90% yield (155 mg). ^{1}H NMR (600 MHz, Chloroform-*d*): δ 7.41 – 7.40 (m, 2H), 7.37 (t, J = 7.3 Hz, 2H), 7.33 – 7.30 (m, 1H), 7.17 – 7.14 (m, 3H), 7.13 – 7.10 (m, 1H), 6.97 (t, J = 7.8 Hz, 1H), 6.92 – 6.90 (m, 3H), 5.12 (s, 2H), 5.02 (s, 2H), 2.98 – 2.95 (m, 2H), 2.79 – 2.76 (m, 2H).^{13}C NMR (151 MHz, Chloroform-*d*): δ 170.7, 158.0, 140.0, 137.1, 129.5, 128.7, 128.1, 127.94, 127.86, 127.6, 127.5, 126.5, 123.0, 115.8, 115.2, 70.2, 45.7, 32.1, 25.7. HRMS (ESI) *m/z*: $[M+H]^+$ calculated for $C_{23}H_{22}NO_2$: 344.1646; found 344.1649.

1-(4-chlorobenzyl)-3,4-dihydroquinolin-2(1*H*)-one (2.10f)



Following the general procedure GP-IV, the title compound **2.10f** was isolated as a colourless liquid using silica gel column chromatography with ethyl acetate/ pet ether (v/v = 1/5, R_f = 0.44) in 87% yield (118 mg). ^{1}H NMR (600 MHz, Chloroform-*d*): δ 7.28 – 7.26 (m, 2H), 7.18 – 7.15 (m, 3H), 7.11 (t, J = 7.8 Hz, 1H), 6.98 (t, J = 7.4 Hz, 1H), 6.82 (d, J = 8.2 Hz, 1H), 5.14 (s, 2H), 2.99 – 2.97 (m, 2H), 2.80 – 2.77 (m, 2H). ^{13}C NMR (151 MHz, Chloroform-*d*): δ 170.7, 139.7, 135.7, 133.0, 129.0, 128.1, 128.0, 127.6, 126.5, 123.3, 115.5, 45.7, 32.0, 25.6. HRMS (ESI) *m/z*: $[M+H]^+$ calculated for $C_{16}H_{15}ClNO$: 272.0837; found 272.0840.

1-(4-(trifluoromethyl)benzyl)-3,4-dihydroquinolin-2(1*H*)-one (2.10g)

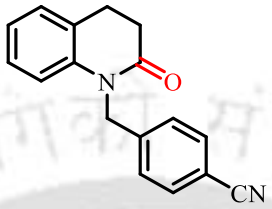


Following the general procedure GP-IV, the title compound **2.10g** was isolated as a white solid using silica gel column chromatography with ethyl acetate/ pet ether (v/v = 1/10, R_f = 0.5) in 85% yield (130 mg). ^{1}H NMR (600 MHz, Chloroform-*d*): δ 7.57 (d, J = 8.0 Hz, 2H), 7.33 (d,

TH-3565_186122020

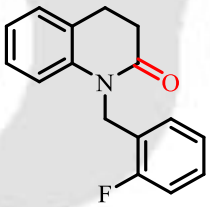
J = 8.0 Hz, 2H), 7.20 (d, *J* = 7.4 Hz, 1H), 7.12 (t, *J* = 7.8 Hz, 1H), 7.00 (t, *J* = 7.4 Hz, 1H), 6.79 (d, *J* = 8.2 Hz, 1H), 5.23 (s, 2H), 3.01 – 2.99 (m, 2H), 2.82 – 2.79 (m, 2H). ^{13}C NMR (151 MHz, Chloroform-*d*): *δ* 170.7, 141.4, 139.7, 128.2, 127.7, 126.8, 126.5, 125.9 (q, C-F, $^{1}J_{C\text{-}F}$ = 3.8 Hz), 123.4, 115.4, 46.0, 31.9, 25.6. ^{19}F NMR (565 MHz, Chloroform-*d*): *δ* -62.5. Spectral data is in accordance to the reported literature.[30]

4-((2-oxo-3,4-dihydroquinolin-1(2*H*)-yl)methyl)benzonitrile (2.10h)



Following the general procedure GP-IV, the title compound **2.10h** was isolated as a white solid using silica gel column chromatography with ethyl acetate/ pet ether (v/v = 2/5, R_f = 0.3) in 90% yield (118 mg). ^{1}H NMR (600 MHz, Chloroform-*d*): *δ* 7.60 (d, *J* = 8.3 Hz, 2H), 7.32 (d, *J* = 8.2 Hz, 2H), 7.20 (d, *J* = 7.6 Hz, 1H), 7.12 (t, *J* = 7.8 Hz, 1H), 7.00 (t, *J* = 7.4 Hz, 1H), 6.73 (d, *J* = 8.1 Hz, 1H), 5.22 (s, 2H), 3.01 – 2.99 (m, 2H), 2.81 – 2.78 (m, 2H). ^{13}C NMR (151 MHz, Chloroform-*d*): *δ* 170.7, 142.9, 139.5, 132.7, 128.3, 127.7, 127.3, 126.5, 123.5, 118.8, 115.2, 111.3, 46.1, 31.9, 25.6. Spectral data is in accordance to the reported literature.[30]

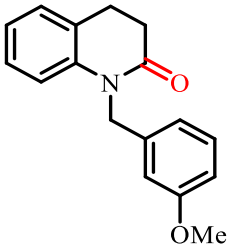
1-(2-fluorobenzyl)-3,4-dihydroquinolin-2(1*H*)-one (2.10i)



Following the general procedure GP-IV, the title compound **2.10i** was isolated as a colourless oil using silica gel column chromatography with ethyl acetate/ pet ether (v/v = 1/10, R_f = 0.4) in 86% yield (110 mg). ^{1}H NMR (600 MHz, Chloroform-*d*): *δ* 7.23 – 7.19 (m, 1H), 7.18 (d, *J* = 7.3 Hz, 1H), 7.13 (t, *J* = 7.8 Hz, 1H), 7.08 – 7.01 (m, 3H), 6.98 (t, *J* = 7.0 Hz, 1H), 6.84 (d, *J* = 8.2 Hz, 1H), 5.24 (s, 2H), 3.00 – 2.98 (m, 2H), 2.81 – 2.79 (m, 2H). ^{13}C NMR (151 MHz, Chloroform-*d*): *δ* 170.8, 161.4, 159.7, 139.6, 128.8 (d, C-F, $J_{C\text{-}F}$ = 7.8 Hz), 128.0 (C-F, $J_{C\text{-}F}$ = 5.1 Hz), 127.7, 126.5, 124.5 (d, C-F, $J_{C\text{-}F}$ = 3.4 Hz), 124.0, 123.9, 123.2, 115.6 – 115.4 (C-F, $J_{C\text{-}F}$ = 21.4 Hz), 40.0 (d, C-F, $J_{C\text{-}F}$ = 5.4 Hz), 32.0, 25.6. ^{19}F NMR (377 MHz, Chloroform-*d*): *δ* -118.6. HRMS (ESI) *m/z*: $[M+H]^+$ calculated for $C_{16}H_{15}FNO$: 256.1133; found 256.1129.

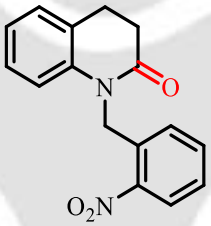
1-(3-methoxybenzyl)-3,4-dihydroquinolin-2(1*H*)-one (2.10j)

TH-3565_186122020



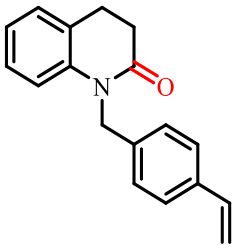
Following the general procedure GP-IV, the title compound **2.10j** was isolated as a pale-yellow oil using silica gel column chromatography with ethyl acetate/ pet ether (v/v = 1/4, R_f = 0.4) in 91% yield (122 mg). ^{1}H NMR (400 MHz, Chloroform-*d*): δ 7.24 – 7.20 (m, 1H), 7.16 (d, J = 7.3 Hz, 1H), 7.11 (t, J = 7.8 Hz, 1H), 6.99 – 6.95 (m, 1H), 6.88 (d, J = 8.2 Hz, 1H), 6.81 – 6.75 (m, 3H), 5.15 (s, 2H), 3.77 (s, 3H), 3.00 – 2.96 (m, 2H), 2.80 – 2.77 (m, 2H). ^{13}C NMR (151 MHz, Chloroform-*d*): δ 170.7, 160.1, 140.0, 138.8, 129.9, 127.9, 127.6, 126.5, 123.1, 118.8, 115.8, 112.4, 112.3, 55.3, 46.3, 32.0, 25.7. HRMS (ESI) *m/z*: $[M+H]^+$ calculated for $C_{17}H_{18}NO_2$: 268.1333; found 268.1328.

1-(2-nitrobenzyl)-3,4-dihydroquinolin-2(1*H*)-one (2.10k)



Following the general procedure GP-IV, the title compound **2.10k** was isolated as a yellow oil using silica gel column chromatography with ethyl acetate/ pet ether (v/v = 1/5, R_f = 0.4) in 77% yield (109 mg). ^{1}H NMR (600 MHz, Chloroform-*d*): δ 8.19 (dd, J = 8.2, 1.4 Hz, 1H), 7.52 (t, J = 7.6 Hz, 1H), 7.44 – 7.42 (m, 1H), 7.22 (d, J = 7.3 Hz, 1H), 7.14 – 7.11 (m, 2H), 7.02 (t, J = 7.4 Hz, 1H), 6.65 (d, J = 8.2 Hz, 1H), 5.53 (s, 2H), 3.06 – 3.03 (m, 2H), 2.84 – 2.81 (m, 2H). ^{13}C NMR (151 MHz, Chloroform-*d*): δ 170.7, 139.7, 134.2, 132.9, 128.3, 128.2, 127.8, 127.5, 126.5, 125.8, 123.6, 115.3, 45.1, 32.0, 25.6. HRMS (ESI) *m/z*: $[M+H]^+$ calculated for $C_{16}H_{15}N_2O_3$: 283.1078; found 283.1072.

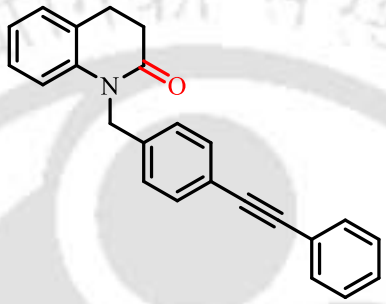
1-(4-vinylbenzyl)-3,4-dihydroquinolin-2(1*H*)-one (2.10l)



TH-3565_186122020

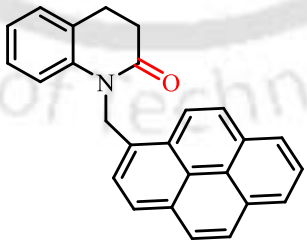
Following the general procedure GP-IV, the title compound **2.10l** was isolated as a yellow oil using silica gel column chromatography with ethyl acetate/ pet ether (v/v = 1/10, R_f = 0.3) in 86% yield (113 mg). ^{1}H NMR (400 MHz, Chloroform-*d*): δ 7.34 (d, J = 8.2 Hz, 2H), 7.18 – 7.15 (m, 3H), 7.10 (t, J = 9.4 Hz, 1H), 6.96 (t, J = 7.4 Hz, 1H), 6.86 (d, J = 8.0 Hz, 1H), 6.67 (dd, J = 17.6, 10.9 Hz, 1H), 5.70 (d, J = 18.4 Hz, 1H), 5.21 (d, J = 10.5 Hz, 1H), 5.17 (s, 2H), 3.00 – 2.96 (m, 2H), 2.81 – 2.77 (m, 2H). ^{13}C NMR (151 MHz, Chloroform-*d*): δ 170.7, 140.0, 136.8, 136.64, 136.55, 128.0, 127.6, 126.8, 126.7, 126.5, 123.1, 115.7, 113.8, 46.1, 32.0, 25.7. HRMS (ESI) *m/z*: $[M+H]^+$ calculated for $C_{18}H_{18}NO$: 264.1383; found 264.1385.

1-(4-(phenylethynyl)benzyl)-3,4-dihydroquinolin-2(1*H*)-one (2.10m)



Following the general procedure GP-IV, the title compound **2.10m** was isolated as a colourless oil using silica gel column chromatography with ethyl acetate/ pet ether (v/v = 1/5, R_f = 0.4) in 90% yield (152 mg). ^{1}H NMR (600 MHz, Chloroform-*d*): δ 7.52 – 7.50 (m, 2H), 7.47 (d, J = 8.2 Hz, 2H), 7.35 – 7.32 (m, 3H), 7.21 – 7.17 (m, 3H), 7.11 (t, J = 7.8 Hz, 1H), 6.98 (t, J = 7.4 Hz, 1H), 6.83 (d, J = 8.2 Hz, 1H), 5.19 (s, 2H), 3.00 – 2.98 (m, 2H), 2.82 – 2.79 (m, 2H). ^{13}C NMR (151 MHz, Chloroform-*d*): δ 170.7, 139.8, 137.5, 132.1, 131.7, 128.5, 128.4, 128.0, 127.6, 126.6, 126.5, 123.4, 123.2, 122.2, 115.7, 89.5, 89.3, 46.2, 32.0, 25.7. HRMS (ESI) *m/z*: $[M+H]^+$ calculated for $C_{24}H_{20}NO$: 338.1540; found 338.1542.

1-(pyren-1-ylmethyl)-3,4-dihydroquinolin-2(1*H*)-one (2.10n)

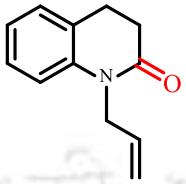


Following the general procedure GP-IV, the title compound **2.10n** was isolated as a white solid using silica gel column chromatography with ethyl acetate/ pet ether (v/v = 1/10, R_f = 0.4) in 85% yield (153 mg). ^{1}H NMR (400 MHz, Chloroform-*d*): δ 8.34 (d, J = 9.2 Hz, 1H), 8.24 – 8.19 (m, 3H), 8.07 – 8.00 (m, 4H), 7.66 (d, J = 8.0 Hz, 1H), 7.22 – 7.20 (m, 1H), 7.00 – 6.93 (m, 2H), 6.78 – 6.75 (m, 1H), 5.94 (s, 2H), 3.11 – 3.08 (m, 2H), 2.95 – 2.92 (m, 2H). ^{13}C NMR (151 MHz, Chloroform-*d*): δ 171.0, 140.1, 131.5, 130.9, 130.7, 129.5, 128.1, 128.0, 127.63,

TH-3565_186122020

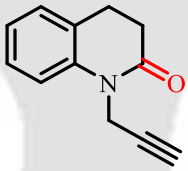
127.61, 127.3, 126.7, 126.2, 125.5, 125.4, 125.24, 125.15, 125.0, 123.4, 123.2, 122.1, 116.0, 44.8, 32.3, 25.8. HRMS (ESI) *m/z*: $[M+H]^+$ calculated for $C_{26}H_{20}NO$: 362.1540; found 362.1537.

1-allyl-3,4-dihydroquinolin-2(1*H*)-one (2.10o)



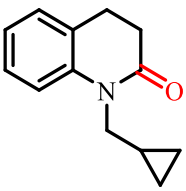
Following the general procedure GP-IV, the title compound **2.10o** was isolated as a colourless oil using silica gel column chromatography with ethyl acetate/ pet ether (v/v = 1/10, R_f = 0.4) in 93% yield (87 mg). ^{1}H NMR (400 MHz, Chloroform-*d*): δ 7.21 – 7.13 (m, 2H), 6.99 – 6.96 (m, 2H), 5.92 – 5.83 (m, 1H), 5.18 – 5.12 (m, 2H), 4.54 (d, J = 4.8 Hz, 2H), 2.91 – 2.87 (m, 2H), 2.67 – 2.64 (m, 2H). ^{13}C NMR (151 MHz, Chloroform-*d*): δ 169.8, 139.7, 132.5, 127.6, 127.2, 126.1, 122.7, 116.1, 115.2, 44.8, 31.6, 25.3. Spectral data is in accordance to the reported literature.[13d]

1-(prop-2-yn-1-yl)-3,4-dihydroquinolin-2(1*H*)-one (2.10p)



Following the general procedure GP-IV, the title compound **2.10p** was isolated as a colourless oil using silica gel column chromatography with ethyl acetate/ pet ether (v/v = 1/10, R_f = 0.4) in 82% yield (76 mg). ^{1}H NMR (400 MHz, Chloroform-*d*): δ 7.28 (t, J = 7.9 Hz, 1H), 7.22 – 7.16 (m, 2H), 7.05 – 7.02 (m, 1H), 4.68 (d, J = 2.5 Hz, 2H), 2.91 – 2.88 (m, 2H), 2.68 – 2.64 (m, 2H), 2.22 (t, J = 2.5 Hz, 1H). ^{13}C NMR (151 MHz, Chloroform-*d*): δ 169.8, 139.0, 127.9, 127.5, 126.2, 123.2, 115.1, 78.8, 71.8, 31.9, 31.6, 25.2. Spectral data is in accordance to the reported literature.[32]

1-(cyclopropylmethyl)-3,4-dihydroquinolin-2(1*H*)-one (2.10q)

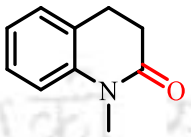


Following the general procedure GP-IV, the title compound **2.10q** was isolated as a pale-yellow oil using silica gel column chromatography with ethyl acetate/ pet ether (v/v = 1/5, R_f = 0.4) in

TH-3565_186122020

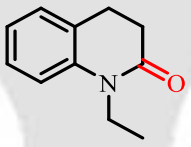
83% yield (84 mg). ^{1}H NMR (600 MHz, Chloroform-*d*): δ 7.26 – 7.24 (m, 1H), 7.17 (d, J = 7.3 Hz, 1H), 7.14 (d, J = 8.2 Hz, 1H), 7.02 – 6.99 (m, 1H), 3.88 (d, J = 6.8 Hz, 2H), 2.92 – 2.89 (m, 2H), 2.67 – 2.64 (m, 2H), 1.17 – 1.11 (m, 1H), 0.50 – 0.47 (m, 2H), 0.43 – 0.41 (m, 2H). ^{13}C NMR (151 MHz, Chloroform-*d*): δ 170.5, 140.0, 128.1, 127.4, 126.7, 122.7, 115.3, 45.9, 32.0, 25.7, 9.9, 4.2. Spectral data is in accordance to the reported literature.[13d]

1-methyl-3,4-dihydroquinolin-2(1*H*)-one (2.10r)



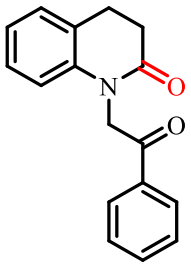
Following the general procedure GP-IV, the title compound **2.10r** was isolated as a pale-yellow oil using silica gel column chromatography with ethyl acetate/ pet ether (v/v = 1/4, R_f = 0.6) in 79% yield (64 mg). ^{1}H NMR (600 MHz, Chloroform-*d*): δ 7.28 – 7.25 (m, 1H), 7.17 (d, J = 7.3 Hz, 1H), 7.04 – 7.01 (m, 1H), 6.99 (d, J = 8.1 Hz, 1H), 3.37 (s, 3H), 2.92 – 2.90 (m, 2H), 2.67 – 2.65 (m, 2H). ^{13}C NMR (151 MHz, Chloroform-*d*): δ 170.5, 140.6, 127.7, 127.5, 126.2, 122.8, 114.7, 31.8, 29.6, 25.4. Spectral data is in accordance to the reported literature.[32]

1-ethyl-3,4-dihydroquinolin-2(1*H*)-one (2.10s)



Following the general procedure GP-IV, the title compound **2.10s** was isolated as a yellow oil using silica gel column chromatography with ethyl acetate/ pet ether (v/v = 1/10, R_f = 0.4) in 84% yield (73 mg). ^{1}H NMR (600 MHz, Chloroform-*d*): δ 7.26 – 7.23 (m, 1H), 7.17 – 7.15 (m, 1H), 7.03 – 6.99 (m, 2H), 4.00 – 3.97 (m, 2H), 2.90 – 2.86 (m, 2H), 2.65 – 2.62 (m, 2H), 1.27 – 1.25 (m, 3H). ^{13}C NMR (151 MHz, Chloroform-*d*): δ 170.1, 139.7, 128.1, 127.6, 126.7, 122.8, 114.8, 37.5, 32.0, 25.7, 12.9. Spectral data is in accordance to the reported literature.[33]

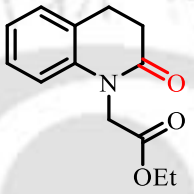
1-(2-oxo-2-phenylethyl)-3,4-dihydroquinolin-2(1*H*)-one (2.10t)



TH-3565_186122020

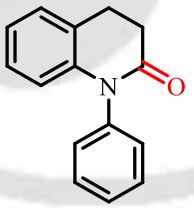
Following the general procedure GP-IV, the title compound **2.10t** was isolated as a yellow oil using silica gel column chromatography with ethyl acetate/ pet ether (v/v = 1/5, R_f = 0.5) in 91% yield (121 mg). ^{1}H NMR (400 MHz, Chloroform-*d*): δ 8.11 – 8.02 (m, 2H), 7.65 – 7.61 (m, 1H), 7.53 – 7.49 (m, 2H), 7.20 – 7.12 (m, 2H), 7.00 (t, *J* = 7.4 Hz, 1H), 6.63 (d, *J* = 8.0 Hz, 1H), 5.38 (s, 2H), 3.00 – 2.97 (m, 2H), 2.80 – 2.76 (m, 2H). ^{13}C NMR (151 MHz, Chloroform-*d*): δ 193.1, 171.1, 139.8, 135.0, 134.0, 130.3, 129.0, 128.2, 128.1, 127.6, 126.5, 123.2, 114.8, 49.5, 31.6, 25.5. HRMS (ESI) *m/z*: $[M+H]^+$ calculated for $C_{17}H_{16}NO_2$: 266.1176; found 266.1175.

Ethyl 2-(2-oxo-3,4-dihydroquinolin-1(2*H*)-yl)acetate (2.10u)



Following the general procedure GP-IV, the title compound **2.10u** was isolated as a colourless oil using silica gel column chromatography with ethyl acetate/ pet ether (v/v = 1/4, R_f = 0.6) in 95% yield (111 mg). ^{1}H NMR (600 MHz, Chloroform-*d*): δ 7.23 – 7.20 (m, 1H), 7.18 (d, *J* = 7.4 Hz, 1H), 7.02 (td, *J* = 7.4, 1.1 Hz, 1H), 6.75 (d, *J* = 8.0 Hz, 1H), 4.66 (s, 2H), 4.22 (q, *J* = 7.1 Hz, 2H), 2.96 – 2.94 (m, 2H), 2.73 – 2.70 (m, 2H), 1.26 (t, *J* = 7.1 Hz, 3H). ^{13}C NMR (151 MHz, Chloroform-*d*): δ 170.8, 168.8, 139.7, 128.1, 127.7, 126.4, 123.3, 114.5, 61.6, 44.5, 31.6, 25.5, 14.3. HRMS (ESI) *m/z*: $[M+H]^+$ calculated for $C_{13}H_{16}NO_3$: 234.1125; found 234.1124.

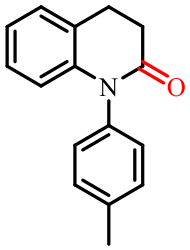
1-phenyl-3,4-dihydroquinolin-2(1*H*)-one (2.10v)



Following the general procedure GP-IV, the title compound **2.10v** was isolated as a colourless oil using silica gel column chromatography with ethyl acetate/ pet ether (v/v = 1/4, R_f = 0.35) in 85% yield (95 mg). ^{1}H NMR (600 MHz, Chloroform-*d*): δ 7.51 (t, *J* = 7.7 Hz, 2H), 7.42 (t, *J* = 7.4 Hz, 1H), 7.24 – 7.23 (m, 2H), 7.21 (d, *J* = 7.3 Hz, 1H), 7.06 – 7.03 (m, 1H), 7.00 – 6.98 (m, 1H), 6.36 (d, *J* = 8.1 Hz, 1H), 3.09 – 3.06 (m, 2H), 2.85 – 2.82 (m, 2H). ^{13}C NMR (151 MHz, Chloroform-*d*): δ 170.4, 141.8, 138.6, 130.0, 129.2, 128.3, 127.9, 127.3, 125.8, 123.1, 117.2, 32.4, 25.8. Spectral data is in accordance to the reported literature.[13d]

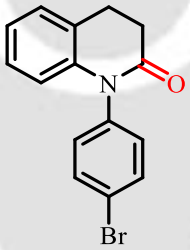
1-(*p*-tolyl)-3,4-dihydroquinolin-2(1*H*)-one (2.10w)

TH-3565_186122020



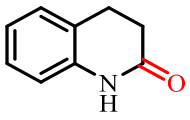
Following the general procedure GP-IV, the title compound **2.10w** was isolated as a white solid using silica gel column chromatography with ethyl acetate/ pet ether (v/v = 1/5, R_f = 0.6) in 82% yield (97 mg). ^{1}H NMR (600 MHz, Chloroform-*d*): δ 7.31 (d, J = 8.0 Hz, 2H), 7.20 (d, J = 7.3 Hz, 1H), 7.11 (d, J = 8.2 Hz, 2H), 7.04 (t, J = 7.4 Hz, 1H), 6.98 (t, J = 7.4 Hz, 1H), 6.38 (d, J = 8.0 Hz, 1H), 3.08 – 3.05 (m, 2H), 2.84 – 2.81 (m, 2H), 2.42 (s, 3H). ^{13}C NMR (151 MHz, Chloroform-*d*): δ 170.5, 141.9, 138.2, 135.8, 130.7, 128.8, 127.9, 127.2, 125.7, 123.0, 117.1, 32.3, 25.8, 21.4. Spectral data is in accordance to the reported literature.[8c]

1-(4-bromophenyl)-3,4-dihydroquinolin-2(1*H*)-one (2.10x)



Following the general procedure GP-IV, the title compound **2.10x** was isolated as off-white solid using silica gel column chromatography with ethyl acetate/ pet ether (v/v = 1/5, R_f = 0.5) in 88% yield (133 mg). ^{1}H NMR (600 MHz, Chloroform-*d*): δ 7.63 (d, J = 8.6 Hz, 2H), 7.22 (d, J = 7.3 Hz, 1H), 7.13 (d, J = 8.6 Hz, 2H), 7.06 (t, J = 7.5 Hz, 1H), 7.00 (t, J = 7.3 Hz, 1H), 6.37 (d, J = 8.0 Hz, 1H), 3.08 – 3.05 (m, 2H), 2.83 – 2.81 (m, 2H). ^{13}C NMR (151 MHz, Chloroform-*d*): δ 170.3, 141.4, 137.6, 133.2, 130.9, 128.1, 127.4, 125.9, 123.4, 122.2, 117.1, 32.3, 25.7. Spectral data is in accordance to the reported literature.[8c]

3,4-dihydroquinolin-2(1*H*)-one (2.10y)

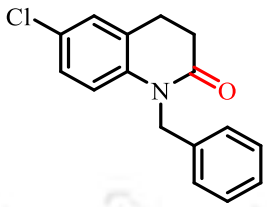


Following the general procedure GP-IV, the title compound **2.10y** was isolated as a white solid using silica gel column chromatography with ethyl acetate/ pet ether (v/v = 1/10, R_f = 0.4) in 68% yield (50 mg). ^{1}H NMR (400 MHz, Chloroform-*d*): δ 8.13 (brs, 1H), 7.20 – 7.16 (m, 2H), 6.99 (t, J = 6.9 Hz, 1H), 6.77 (d, J = 7.5 Hz, 1H), 2.97 (t, J = 7.4 Hz, 2H), 2.66 – 2.63 (m, 2H).

TH-3565_186122020

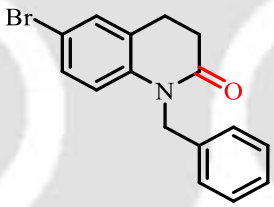
^{13}C NMR (151 MHz, Chloroform-*d*): δ 171.7, 137.3, 128.2, 127.7, 123.8, 123.3, 115.4, 30.9, 25.5. Spectral data is in accordance to the reported literature.[28]

1-benzyl-6-chloro-3,4-dihydroquinolin-2(1*H*)-one (2.10aa)



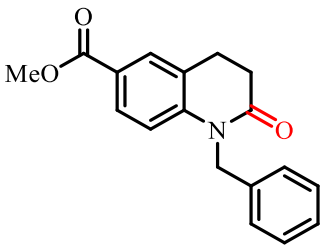
Following the general procedure GP-IV, the title compound **2.10aa** was isolated as an off-white solid using silica gel column chromatography with ethyl acetate/ pet ether (v/v = 1/5, R_f = 0.6) in 90% yield (122 mg). ^{1}H NMR (600 MHz, Chloroform-*d*): δ 7.30 (t, J = 7.5 Hz, 2H), 7.23 (t, J = 7.3 Hz, 1H), 7.19 (d, J = 7.6 Hz, 2H), 7.15 (s, 1H), 7.05 (dd, J = 8.7, 2.5 Hz, 1H), 6.78 (d, J = 8.7 Hz, 1H), 5.16 (s, 2H), 2.97 – 2.94 (m, 2H), 2.79 – 2.77 (m, 2H). ^{13}C NMR (151 MHz, Chloroform-*d*): δ 170.2, 138.6, 136.7, 128.9, 128.21, 128.17, 127.9, 127.4, 127.3, 126.5, 116.9, 46.2, 31.6, 25.5. HRMS (ESI) *m/z*: $[M+H]^+$ calculated for $C_{16}H_{15}ClNO$: 272.0837; found 272.0838.

1-benzyl-6-bromo-3,4-dihydroquinolin-2(1*H*)-one (2.10ab)



Following the general procedure GP-IV, the title compound **2.10ab** was isolated as a yellow oil using silica gel column chromatography with ethyl acetate/ pet ether (v/v = 1/5, R_f = 0.3) in 92% yield (145 mg). ^{1}H NMR (400 MHz, Chloroform-*d*): δ 7.32 – 7.28 (m, 3H), 7.26 – 7.17 (m, 4H), 6.73 (d, J = 8.6 Hz, 1H), 5.15 (s, 2H), 2.98 – 2.94 (m, 2H), 2.79 – 2.76 (m, 2H). ^{13}C NMR (151 MHz, Chloroform-*d*): δ 170.2, 139.1, 136.6, 130.8, 130.4, 129.0, 128.6, 127.4, 126.5, 117.3, 115.8, 46.2, 31.7, 25.5. Spectral data is in accordance to the reported literature.[33]

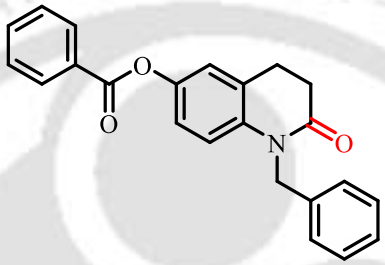
Methyl 1-benzyl-2-oxo-1,2,3,4-tetrahydroquinoline-6-carboxylate (2.10ac)



TH-3565_186122020

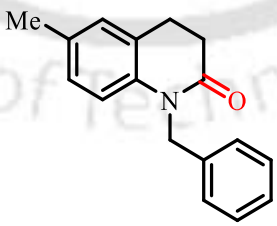
Following the general procedure GP-IV, the title compound **2.10ac** was isolated as a colourless oil using silica gel column chromatography with ethyl acetate/ pet ether (v/v = 3/10, R_f = 0.5) in 88% yield (130 mg). ^{1}H NMR (600 MHz, Chloroform-*d*): δ 7.85 (s, 1H), 7.78 (dd, *J* = 8.5, 2.0 Hz, 1H), 7.30 (t, *J* = 7.6 Hz, 2H), 7.23 (t, *J* = 7.5 Hz, 1H), 7.19 (d, *J* = 6.9 Hz, 2H), 6.90 (d, *J* = 8.5 Hz, 1H), 5.20 (s, 2H), 3.87 (s, 3H), 3.04 – 3.02 (m, 2H), 2.83 – 2.80 (m, 2H). ^{13}C NMR (151 MHz, Chloroform-*d*): δ 170.6, 166.6, 143.8, 136.5, 129.5, 129.3, 129.0, 127.4, 126.5, 126.2, 124.6, 115.4, 52.2, 46.2, 31.7, 25.5. HRMS (ESI) *m/z*: $[M+H]^+$ calculated for $C_{18}H_{18}NO_3$: 296.1282; found 296.1283.

1-benzyl-2-oxo-1,2,3,4-tetrahydroquinolin-6-yl benzoate (2.10ad)



Following the general procedure GP-IV, the title compound **2.10ad** was isolated as a yellow oil using silica gel column chromatography with ethyl acetate/ pet ether (v/v = 3/10, R_f = 0.4) in 87% yield (155 mg). ^{1}H NMR (600 MHz, Chloroform-*d*): δ 8.16 (d, *J* = 7.8 Hz, 2H), 7.62 (t, *J* = 7.9 Hz, 1H), 7.49 (t, *J* = 7.7 Hz, 2H), 7.31 (t, *J* = 7.5 Hz, 2H), 7.24 – 7.21 (m, 3H), 7.06 – 7.05 (m, 1H), 6.94 (dd, *J* = 8.8, 2.6 Hz, 1H), 6.89 (d, *J* = 8.8 Hz, 1H), 5.18 (s, 2H), 3.00 – 2.98 (m, 2H), 2.82 – 2.80 (m, 2H). ^{13}C NMR (151 MHz, Chloroform-*d*): δ 170.4, 165.4, 146.2, 137.8, 136.8, 133.8, 130.2, 129.4, 128.9, 128.7, 127.8, 127.3, 126.4, 121.3, 120.4, 116.5, 46.4, 31.6, 25.6. HRMS (ESI) *m/z*: $[M+H]^+$ calculated for $C_{23}H_{20}NO_3$: 358.1438; found 358.1442.

1-benzyl-6-methyl-3,4-dihydroquinolin-2(1*H*)-one (2.10ae)

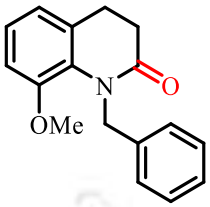


Following the general procedure GP-IV, the title compound **2.10ae** was isolated as a colourless liquid using silica gel column chromatography with ethyl acetate/ pet ether (v/v = 1/20, R_f = 0.4) in 80% yield (101 mg). ^{1}H NMR (600 MHz, Chloroform-*d*): δ 7.29 (t, *J* = 7.6 Hz, 2H), 7.23 – 7.20 (m, 3H), 6.98 (s, 1H), 6.90 (d, *J* = 8.4 Hz, 1H), 6.76 (d, *J* = 8.2 Hz, 1H), 5.16 (s, 2H), 2.95 – 2.93 (m, 2H), 2.78 – 2.76 (m, 2H), 2.26 (s, 3H). ^{13}C NMR (151 MHz, Chloroform-

TH-3565_186122020

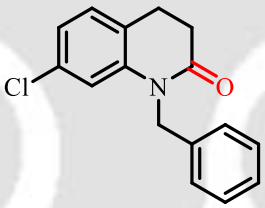
d): δ 170.6, 137.6, 137.2, 132.6, 128.8, 128.7, 127.9, 127.1, 126.5, 126.4, 115.6, 46.2, 32.1, 25.7, 20.6. HRMS (ESI) *m/z*: $[M+H]^+$ calculated for $C_{17}H_{18}NO$: 252.1383; found 252.1382.

1-benzyl-8-methoxy-3,4-dihydroquinolin-2(1*H*)-one (2.10ag)



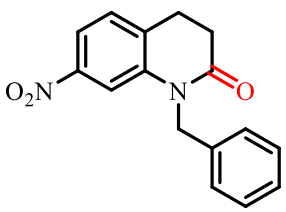
Following the general procedure GP-IV, the title compound **2.10ag** was isolated as a colourless oil using silica gel column chromatography with ethyl acetate/ pet ether (v/v = 1/50, R_f = 0.4) in 85% yield (114 mg). ^{1}H NMR (400 MHz, Chloroform-*d*): δ 7.21 – 7.18 (m, 2H), 7.14 – 7.12 (m, 3H), 6.96 (t, *J* = 7.7 Hz, 1H), 6.76 – 6.71 (m, 2H), 5.33 (s, 2H), 3.71 (s, 3H), 2.84 – 2.81 (m, 2H), 2.65 – 2.62 (m, 2H). ^{13}C NMR (151 MHz, Chloroform-*d*): δ 172.6, 150.1, 139.0, 132.2, 129.1, 128.2, 127.2, 126.7, 124.8, 120.0, 111.3, 55.6, 48.0, 33.1, 26.5. HRMS (ESI) *m/z*: $[M+H]^+$ calculated for $C_{17}H_{18}NO_2$: 268.1333; found 268.1329.

1-benzyl-7-chloro-3,4-dihydroquinolin-2(1*H*)-one (2.10ah)



Following the general procedure GP-IV, the title compound **2.10ah** was isolated as a colourless oil using silica gel column chromatography with ethyl acetate/ pet ether (v/v = 1/5, R_f = 0.4) in 88% yield (120 mg). ^{1}H NMR (400 MHz, Chloroform-*d*): δ 7.33 – 7.30 (m, 2H), 7.24 – 7.19 (m, 3H), 7.07 (d, *J* = 8.0 Hz, 1H), 6.93 (dd, *J* = 8.0, 2.0 Hz, 1H), 6.87 (d, *J* = 2.0 Hz, 1H), 5.14 (s, 2H), 2.96 – 2.92 (m, 2H), 2.78 – 2.75 (m, 2H). ^{13}C NMR (151 MHz, Chloroform-*d*): δ 170.4, 141.1, 136.5, 133.1, 129.0, 128.9, 127.4, 126.5, 124.8, 122.9, 116.0, 46.3, 31.8, 25.2. HRMS (ESI) *m/z*: $[M+H]^+$ calculated for $C_{16}H_{15}ClNO$: 272.0837; found 272.0838.

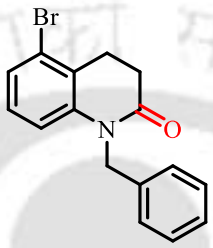
1-benzyl-7-nitro-3,4-dihydroquinolin-2(1*H*)-one (2.10ai)



TH-3565_186122020

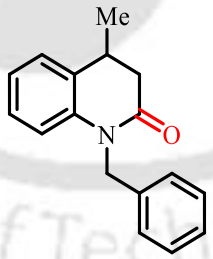
Following the general procedure GP-IV, the title compound **2.10ai** was isolated as a yellow solid using silica gel column chromatography with ethyl acetate/ pet ether (v/v = 1/5, R_f = 0.4) in 80% yield (113 mg). ^{1}H NMR (400 MHz, Chloroform-*d*): δ 7.84 – 7.79 (m, 2H), 7.35 – 7.30 (m, 3H), 7.27 – 7.23 (m, 3H), 5.24 (s, 2H), 3.10 – 3.06 (m, 2H), 2.85 – 2.81 (m, 2H). ^{13}C NMR (151 MHz, Chloroform-*d*): δ 169.8, 147.7, 140.8, 135.9, 133.6, 129.1, 128.6, 127.8, 126.9, 118.0, 110.6, 46.1, 31.1, 25.8. HRMS (ESI) *m/z*: $[M+H]^+$ calculated for $C_{16}H_{15}N_2O_3$: 283.1078; found 283.1075.

1-benzyl-5-bromo-3,4-dihydroquinolin-2(1*H*)-one (2.10aj)



Following the general procedure GP-IV, the title compound **2.10aj** was isolated as a yellow oil using silica gel column chromatography with ethyl acetate/ pet ether (v/v = 1/6, R_f = 0.45) in 84% yield (133 mg). ^{1}H NMR (600 MHz, Chloroform-*d*): δ 7.30 (t, *J* = 7.6 Hz, 2H), 7.24 – 7.21 (m, 2H), 7.18 (d, *J* = 7.6 Hz, 2H), 6.95 (t, *J* = 8.2 Hz, 1H), 6.83 (d, *J* = 8.2 Hz, 1H), 5.16 (s, 2H), 3.14 – 3.11 (m, 2H), 2.80 – 2.78 (m, 2H). ^{13}C NMR (151 MHz, Chloroform-*d*): δ 170.2, 141.4, 136.7, 128.9, 128.4, 127.3, 127.2, 126.41, 126.38, 123.7, 115.1, 46.6, 31.3, 25.5. HRMS (ESI) *m/z*: $[M+H]^+$ calculated for $C_{16}H_{15}BrNO$: 316.0332; found 316.0334.

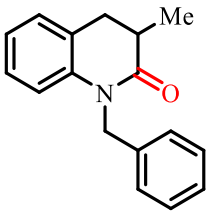
1-benzyl-4-methyl-3,4-dihydroquinolin-2(1*H*)-one (2.10ak)



Following the general procedure GP-IV, the title compound **2.10ak** was isolated as a yellow oil using silica gel column chromatography with ethyl acetate/ pet ether (v/v = 1/5, R_f = 0.35) in 75% yield (94 mg). ^{1}H NMR (400 MHz, Chloroform-*d*): δ 7.32 – 7.28 (m, 2H), 7.26 – 7.18 (m, 4H), 7.13 – 7.09 (m, 1H), 7.00 (t, *J* = 7.4 Hz, 1H), 6.89 (d, *J* = 8.1 Hz, 1H), 5.25 – 5.14 (m, 2H), 3.13 (sext, *J* = 6.8 Hz, 1H), 2.90 – 2.85 (m, 1H), 2.63 – 2.57 (m, 1H), 1.32 (d, *J* = 7.0 Hz, 3H). ^{13}C NMR (151 MHz, Chloroform-*d*): δ 170.1, 139.1, 137.2, 131.3, 128.8, 127.5, 127.2, 126.61, 126.57, 123.3, 115.8, 46.2, 39.3, 30.7, 19.6. Spectral data is in accordance to the reported literature.[8b]

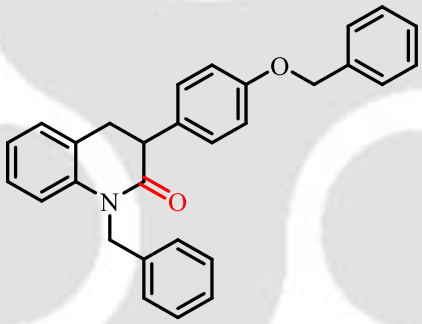
TH-3565_186122020

1-benzyl-3-methyl-3,4-dihydroquinolin-2(1*H*)-one (2.10al)



Following the general procedure GP-IV, the title compound **2.10al** was isolated as a colourless liquid using silica gel column chromatography with ethyl acetate/ pet ether (v/v = 1/20, R_f = 0.4) in 83% yield (104 mg). ^{1}H NMR (600 MHz, Chloroform-*d*): δ 7.30 (t, J = 7.6 Hz, 2H), 7.24 – 7.20 (m, 3H), 7.16 (d, J = 7.4 Hz, 1H), 7.12 – 7.09 (m, 1H), 6.98 – 6.95 (m, 1H), 6.86 (dd, J = 8.2, 1.0 Hz, 1H), 5.26 (d, J = 16.2 Hz, 1H), 5.08 (d, J = 16.2 Hz, 1H), 3.01 (d, J = 9.6 Hz, 1H), 2.82 – 2.75 (m, 2H), 1.34 (d, J = 6.5 Hz, 3H). ^{13}C NMR (151 MHz, Chloroform-*d*): δ 173.5, 139.9, 137.4, 128.9, 128.1, 127.5, 127.1, 126.5, 125.9, 123.0, 115.5, 46.6, 35.8, 33.6, 15.8. Spectral data is in accordance to the reported literature.[34]

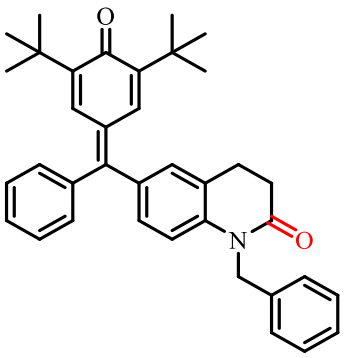
1-benzyl-3-(4-(benzyloxy)phenyl)-3,4-dihydroquinolin-2(1*H*)-one (2.10am)



Following the general procedure GP-IV, the title compound **2.10am** was isolated as a white solid using silica gel column chromatography with ethyl acetate/ pet ether (v/v = 1/5, R_f = 0.5) in 74% yield (155 mg). ^{1}H NMR (600 MHz, Chloroform-*d*): δ 7.42 (d, J = 7.6 Hz, 2H), 7.38 (t, J = 7.4 Hz, 2H), 7.32 (t, J = 7.3 Hz, 1H), 7.28 – 7.25 (m, 2H), 7.22 – 7.18 (m, 6H), 7.12 (t, J = 7.7 Hz, 1H), 6.98 (t, J = 7.4 Hz, 1H), 6.93 – 6.89 (m, 3H), 5.21 (s, 2H), 5.04 (s, 2H), 3.96 (t, J = 7.5 Hz, 1H), 3.28 (d, J = 7.5 Hz, 2H). ^{13}C NMR (151 MHz, Chloroform-*d*): δ 171.4, 158.1, 139.7, 137.3, 137.2, 130.7, 129.3, 128.8, 128.7, 128.3, 128.1, 127.7, 127.6, 127.2, 126.7, 125.7, 123.2, 115.6, 115.1, 70.2, 46.8, 46.2, 32.9. HRMS (ESI) *m/z*: $[M+H]^+$ calculated for $C_{29}H_{26}NO_2$: 420.1959; found 420.1961.

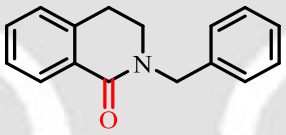
1-benzyl-6-((3,5-di-*tert*-butyl-4-oxocyclohexa-2,5-dien-1-ylidene)(phenyl)methyl)-3,4-dihydroquinolin-2(1*H*)-one (2.10an)

TH-3565_186122020



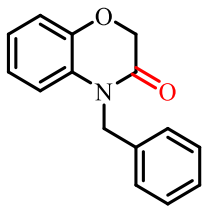
Following the general procedure GP-IV, the title compound **2.10an** was isolated as a yellow solid using silica gel column chromatography with ethyl acetate/ pet ether (v/v = 1/10, R_f = 0.5) in 90% yield (298 mg). ^{1}H NMR (400 MHz, Chloroform-*d*): δ 7.43 – 7.38 (m, 3H), 7.34 – 7.30 (m, 2H), 7.25 – 7.20 (m, 5H), 7.16 (d, *J* = 2.6 Hz, 1H), 7.09 (d, *J* = 2.6 Hz, 1H), 7.04 (s, 1H), 7.01 – 6.98 (m, 1H), 6.90 (d, *J* = 8.4 Hz, 1H), 5.22 (s, 2H), 2.99 – 2.96 (m, 2H), 2.85 – 2.81 (m, 2H), 1.24 (s, 9H), 1.21 (s, 9H). ^{13}C NMR (151 MHz, Chloroform-*d*): δ 186.2, 170.5, 155.2, 147.54, 147.46, 140.9, 140.8, 136.8, 135.4, 132.13, 132.08, 131.9, 131.8, 131.7, 129.8, 129.4, 128.9, 128.2, 127.4, 126.6, 126.0, 115.2, 46.4, 35.45, 35.40, 31.9, 29.7, 29.6, 25.5. HRMS (ESI) *m/z*: $[M+H]^+$ calculated for $C_{37}H_{40}NO_2$: 530.3054; found 530.3058.

2-benzyl-3,4-dihydroisoquinolin-1(2*H*)-one (2.10ao)



Following the general procedure GP-IV, the title compound **2.10ao** was isolated as a yellow oil using silica gel column chromatography with ethyl acetate/ pet ether (v/v = 1/4, R_f = 0.6) in 96% yield (114 mg). ^{1}H NMR (600 MHz, Chloroform-*d*): δ 8.15 (d, *J* = 7.7 Hz, 1H), 7.40 – 7.38 (m, 1H), 7.34 – 7.29 (m, 5H), 7.26 – 7.24 (m, 1H), 7.13 (d, *J* = 7.4 Hz, 1H), 4.78 (s, 2H), 3.45 (t, *J* = 6.6 Hz, 2H), 2.90 (t, *J* = 6.6 Hz, 2H). ^{13}C NMR (151 MHz, Chloroform-*d*): δ 164.6, 138.1, 137.4, 131.7, 129.3, 128.6, 128.4, 128.0, 127.4, 127.0, 126.9, 50.4, 45.4, 28.0. Spectral data is in accordance to the reported literature.[35]

4-benzyl-2*H*-benzo[*b*][1,4]oxazin-3(4*H*)-one (2.10ap)

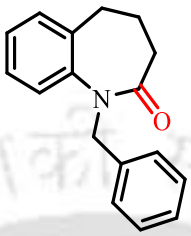


Following the general procedure GP-IV, the title compound **2.10ap** was isolated as a white solid using silica gel column chromatography with ethyl acetate/ pet ether (v/v = 1/10, R_f = 0.4)

TH-3565_186122020

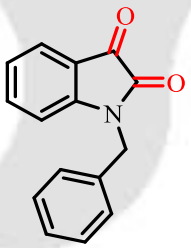
in 86% yield (103 mg). ^{1}H NMR (400 MHz, Chloroform-*d*): δ 7.34 – 7.31 (m, 2H), 7.27 – 7.24 (m, 3H), 7.01 – 6.94 (m, 2H), 6.92 – 6.87 (m, 2H), 5.17 (s, 2H), 4.73 (s, 2H). ^{13}C NMR (151 MHz, Chloroform-*d*): δ 164.9, 145.4, 136.0, 129.0, 128.9, 127.6, 126.7, 124.1, 122.9, 117.1, 115.9, 67.8, 45.1. Spectral data is in accordance to the reported literature.[36]

1-benzyl-1,3,4,5-tetrahydro-2*H*-benzo[*b*]azepin-2-one (2.10aq)



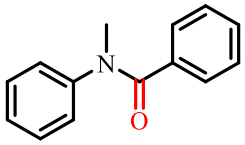
Following the general procedure GP-IV, the title compound **2.10aq** was isolated as a yellow oil using silica gel column chromatography with ethyl acetate/ pet ether (v/v = 1/5, R_f = 0.55) in 88% yield (110 mg). ^{1}H NMR (400 MHz, Chloroform-*d*): δ 7.24 – 7.20 (m, 6H), 7.18 (d, J = 7.8 Hz, 1H), 7.13 – 7.12 (m, 2H), 5.02 (s, 2H), 2.53 (t, J = 7.2 Hz, 2H), 2.35 (t, J = 7.0 Hz, 2H), 2.15 (brs, 2H). ^{13}C NMR (151 MHz, Chloroform-*d*): δ 173.4, 142.6, 138.0, 136.0, 129.4, 128.5, 128.2, 127.6, 127.4, 126.5, 122.9, 51.4, 33.3, 30.1, 29.1. HRMS (ESI) *m/z*: $[M+H]^+$ calculated for $C_{17}H_{18}NO$: 252.1383; found 252.1384.

1-benzylindoline-2,3-dione (2.10ar)



Following the general procedure GP-IV, the title compound **2.10ar** was isolated as a yellow oil using silica gel column chromatography with ethyl acetate/ pet ether (v/v = 1/10, R_f = 0.4) in 91% yield (108 mg). ^{1}H NMR (400 MHz, Chloroform-*d*): δ 7.61 (dd, J = 7.4, 1.3 Hz, 1H), 7.48 (td, J = 7.8, 1.4 Hz, 1H), 7.38 – 7.30 (m, 5H), 7.09 (t, J = 7.6 Hz, 1H), 6.78 (d, J = 8.0 Hz, 1H), 4.93 (s, 2H). ^{13}C NMR (151 MHz, Chloroform-*d*): δ 183.4, 158.4, 150.9, 138.4, 134.6, 129.2, 128.3, 127.6, 125.6, 124.0, 117.8, 111.1, 44.2. Spectral data is in accordance to the reported literature.[37]

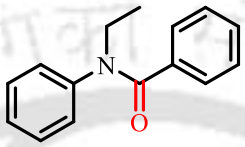
***N*-methyl-*N*-phenylbenzamide (2.10as)**



TH-3565_186122020

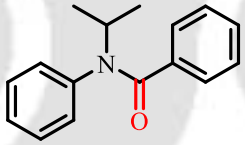
Following the general procedure GP-IV, the title compound **2.10as** was isolated as a yellow oil using silica gel column chromatography with ethyl acetate/ pet ether (v/v= 1/5, R_f = 0.3) in 67% yield (71 mg). ^{1}H NMR (600 MHz, Chloroform-*d*): δ 7.29 (d, J = 7.3 Hz, 2H), 7.15 – 7.12 (m, 3H), 7.09 – 7.03 (m, 3H), 6.99 (d, J = 8.4 Hz, 2H), 3.43 (s, 3H). ^{13}C NMR (151 MHz, Chloroform-*d*): δ 170.0, 144.4, 135.5, 129.1, 128.7, 128.2, 127.2, 126.4, 126.0, 37.8. Spectral data is in accordance to the reported literature.[38]

_N_-ethyl-_N_-phenylbenzamide (2.10at)



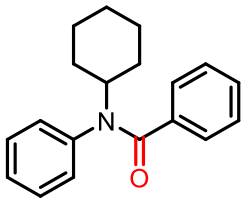
Following the general procedure GP-IV, the title compound **2.10at** was isolated as a colourless oil using silica gel column chromatography with ethyl acetate/ pet ether (v/v= 1/5, R_f = 0.35) in 82% yield (92 mg). ^{1}H NMR (600 MHz, Chloroform-*d*): δ 7.29 (d, J = 7.7 Hz, 2H), 7.20 – 7.16 (m, 3H), 7.13 – 7.11 (m, 3H), 7.01 (d, J = 7.9 Hz, 2H), 3.97 (q, J = 7.2 Hz, 2H), 1.22 – 1.20 (m, 3H). ^{13}C NMR (151 MHz, Chloroform-*d*): δ 170.1, 143.1, 136.2, 129.4, 129.0, 128.6, 127.8, 127.6, 126.5, 45.3, 12.9. Spectral data is in accordance to the reported literature.[39]

_N_-isopropyl-_N_-phenylbenzamide (2.10au)



Following the general procedure GP-IV, the title compound **2.10au** was isolated as a colourless oil using silica gel column chromatography with ethyl acetate/pet ether (v/v= 1/10, R_f = 0.3) in 77% yield (92 mg). ^{1}H NMR (600 MHz, Chloroform-*d*): δ 7.25 – 7.24 (m, 2H), 7.22 – 7.20 (m, 2H), 7.17 – 7.16 (m, 1H), 7.15 – 7.11 (m, 3H), 7.03 – 7.02 (m, 2H), 5.12 (brs, 1H), 1.21 (d, J = 6.8 Hz, 6H). ^{13}C NMR (151 MHz, Chloroform-*d*): δ 170.8, 139.7, 137.4, 130.8, 129.0, 128.7, 128.2, 127.7, 127.5, 47.7, 21.2. Spectral data is in accordance to the reported literature.[38]

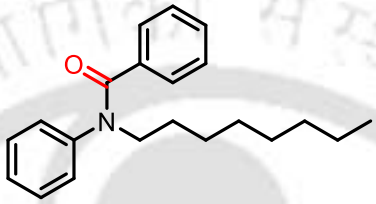
_N_-cyclohexyl-_N_-phenylbenzamide (2.10av)



TH-3565_186122020

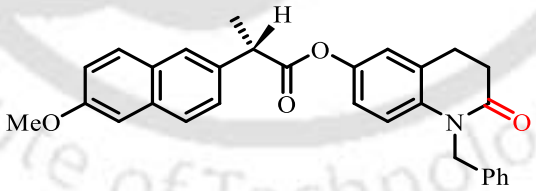
Following the general procedure GP-IV, the title compound **2.10av** was isolated as a white solid using silica gel column chromatography with ethyl acetate/pet ether (v/v= 1/10, R_f = 0.4) in 80% yield (112 mg). ^{1}H NMR (600 MHz, Chloroform-*d*): δ 7.22 – 7.18 (m, 4H), 7.17 – 7.15 (m, 1H), 7.14 – 7.09 (m, 3H), 7.01 – 7.00 (m, 2H), 4.72 (brs, 1H), 1.96 (d, J = 11.3 Hz, 2H), 1.77 (d, J = 13.6 Hz, 2H), 1.61 (d, J = 13.1 Hz, 1H), 1.47 – 1.42 (m, 2H), 1.25 – 1.23 (m, 1H), 1.21 – 1.19 (m, 1H), 1.00 – 0.93 (m, 1H). ^{13}C NMR (151 MHz, Chloroform-*d*): δ 170.7, 140.0, 137.5, 130.9, 128.9, 128.6, 128.2, 127.6, 127.5, 55.6, 31.8, 26.0, 25.5. Spectral data is in accordance to the reported literature.[38]

_N_-octyl-_N_-phenylbenzamide (2.10aw)



Following the general procedure GP-IV, the title compound **2.10aw** was isolated as a colourless oil using silica gel column chromatography with ethyl acetate/pet ether (v/v= 1/10, R_f = 0.35) in 75% yield (116 mg). ^{1}H NMR (600 MHz, Chloroform-*d*): δ 7.27 (d, J = 7.5 Hz, 2H), 7.19 (q, J = 7.6 Hz, 3H), 7.14 – 7.10 (m, 3H), 7.01 (d, J = 7.7 Hz, 2H), 3.92 – 3.90 (m, 2H), 1.62 (p, J = 7.4 Hz, 2H), 1.33 – 1.22 (m, 10H), 0.86 (t, J = 7.0 Hz, 3H). ^{13}C NMR (151 MHz, Chloroform-*d*): δ 170.3, 143.5, 136.4, 129.4, 129.1, 128.6, 127.8, 127.7, 126.5, 50.5, 31.8, 29.3, 29.2, 27.7, 27.0, 22.6, 14.1. HRMS (ESI) *m/z*: $[M+H]^+$ calculated for $C_{21}H_{28}NO$: 310.2166; found 310.2161.

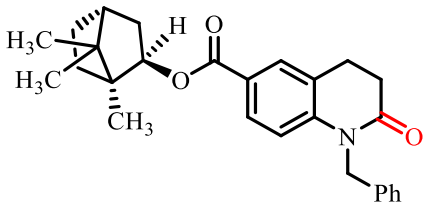
1-benzyl-2-oxo-1,2,3,4-tetrahydroquinolin-6-yl-(*S*)-2-(6-methoxynaphthalen-2yl) propanoate (2.12a)



Following the general procedure GP-IV, the title compound **2.12a** was isolated as a pale-yellow oil using silica gel column chromatography with ethyl acetate/ pet ether (v/v = 2/5, R_f = 0.4) in 86% yield (200 mg). ^{1}H NMR (600 MHz, Chloroform-*d*): δ 7.74 – 7.71 (m, 3H), 7.47 – 7.46 (m, 1H), 7.28 (t, J = 7.5 Hz, 2H), 7.21 (t, J = 7.3 Hz, 1H), 7.17 – 7.13 (m, 4H), 6.81 – 6.78 (m, 2H), 6.71 (dd, J = 8.8, 2.6 Hz, 1H), 5.13 (s, 2H), 4.06 (q, J = 7.1 Hz, 1H), 3.92 (s, 3H), 2.92 – 2.90 (m, 2H), 2.77 – 2.74 (m, 2H), 1.67 (d, J = 7.1 Hz, 3H). ^{13}C NMR (151 MHz, Chloroform-*d*): δ 173.5, 170.4, 157.9, 146.1, 137.7, 136.8, 135.1, 133.9, 129.4, 129.1, 128.9, 127.6, 127.5, 127.3, 126.5, 126.24, 126.16, 121.0, 120.1, 119.3, 116.4, 105.7, 55.5, 46.4, 45.6, 31.6, 25.6, 18.6. HRMS (ESI) *m/z*: $[M+H]^+$ calculated for $C_{30}H_{28}NO_4$: 466.2013; found 466.2011.

TH-3565_186122020

(1*S*,2*S*,4*R*)-1,7,7-trimethylbicyclo[2.2.1]heptan-2-yl 1-benzyl-2-oxo-1,2,3,4-tetrahydroquinoline-6-carboxylate (2.12b)



Following the general procedure GP-IV, the title compound **2.12b** was isolated as a colourless oil using silica gel column chromatography with ethyl acetate/ pet ether (v/v = 1/4, R_f = 0.45) in 90% yield (188 mg). ^{1}H NMR (600 MHz, Chloroform-*d*): δ 7.81 (brs, 1H), 7.74 (dd, *J* = 8.5, 2.0 Hz, 1H), 7.31 (t, *J* = 7.6 Hz, 2H), 7.24 (t, *J* = 7.4 Hz, 1H), 7.19 (d, *J* = 7.1 Hz, 2H), 6.90 (d, *J* = 8.6 Hz, 1H), 5.20 (s, 2H), 4.87 (dd, *J* = 7.8, 3.7 Hz, 1H), 3.05 – 3.02 (m, 2H), 2.83 – 2.80 (m, 2H), 1.91 – 1.83 (m, 2H), 1.78 (t, *J* = 4.2 Hz, 1H), 1.75 – 1.70 (m, 1H), 1.61 – 1.56 (m, 1H), 1.24 – 1.19 (m, 1H), 1.15 – 1.10 (m, 1H), 1.08 (s, 3H), 0.88 (d, *J* = 11.4 Hz, 6H). ^{13}C NMR (151 MHz, Chloroform-*d*): δ 170.6, 165.6, 143.7, 136.5, 129.3, 129.2, 129.0, 127.4, 126.4, 126.2, 125.4, 115.4, 81.6, 49.1, 47.1, 46.3, 45.2, 39.0, 33.8, 31.7, 27.2, 25.5, 20.3, 20.2, 11.7. HRMS (ESI) *m/z*: $[M+H]^+$ calculated for $C_{27}H_{32}NO_3$: 418.2377; found 418.2380.

2.5.11. Computational details

All calculations were performed using the Gaussian-16 program package in the gas phase.[40] The geometry optimizations were carried out using the Kohn-Sham hybrid-DFT B3LYP[41] level of theory in conjunction with Grimme's dispersion correction[42] (henceforth referred to as B3LYP-gd3bj). The standard double-ζ quality Def2SVP basis set was employed.[43] Method and basis set were selected based on a previous report on similar complexes.[44] The BDE was calculated by using M06-2X[45]/6-31G* level of theory. Frequency calculations at the same method and basis set were performed to distinguish transition state structures (one imaginary frequency) and minima structures (no imaginary frequency) on the potential energy surface. The transition states were verified by the intrinsic reaction coordinate (IRC) calculations, wherever necessary.[46] Free energies were calculated by using frequency calculations at 70 °C to match the experimental conditions.

Table 2.12. Free Energies (G) and Total Energies (E) of all the optimized structures given in Hartree along with the number of imaginary frequencies[a]

Species	Free energy (G)	Total energy (E)	# Imaginary Frequency (NImag)
endo cyclic pathway			
2.9a + Ru-1-I2	-1951.076767	-1951.4807598	0
int-1	-1951.047385	-1951.4485795	0
TS-1	-1951.041148	-1951.4383583	1
***endo*-int-2**	-1951.063459	-1951.4615215	0
***endo*-int-3**	-1951.103327	-1951.5050915	0

TH-3565_186122020

***endo*-int-4**	-1951.157448	-1951.5591717	0
***endo*-TS-2**	-1951.136603	-1951.5387009	1
2.10a + Ru-1-I1	-1951.192972	-1951.5977797	0
exo cyclic pathway			
2.9a + Ru-1-I2	-1951.076767	-1951.4807598	0
int-1	-1951.047385	-1951.4485795	0
***exo*-int-2**	-1951.073802	-1951.4780993	0
***exo*-int-3**	-1951.111217	-1951.5137091	0
***exo*-int-4**	-1951.157417	-1951.5627503	0
***exo*-TS-2**	-1951.136311	-1951.5379439	1
2.10a′ + Ru-1-I1	-1951.184085	-1951.5886086	0
substituent effect on the rate of the reaction			
***endo*-int-4**	-1951.157448	-1951.5591717	0
***endo*-TS-2**	-1951.136603	-1951.5387009	1
2.10a + Ru-1-I1	-1951.192972	-1951.5977797	0
***endo*-int-4_6-Me**	-1990.427764	-1990.8525507	0
***endo*-TS-2_6-Me**	-1990.405207	-1990.8291078	1
2.10ae + Ru-1-I1	-1990.464648	-1990.8920271	0
***endo*-int-4_6-CO_2Me**	-2178.837753	-2179.2786956	0
***endo*-TS-2_6-CO_2Me**	-2178.825587	-2179.2610444	1
2.10ac + Ru-1-I1	-2178.882135	-2179.3213757	0

[a](G) is calculated at 70 °C to meet the experimental conditions. All the figures were generated using (G) values. The transition state has one NImag and all the reactants, intermediates and products have zero NImag. All the calculations were performed at B3LYP-gd3bj/Def2SVP level of DFT.

2.6. References

1. El-Kashef, D. H.; Daletos, G.; Plenker, M.; Hartmann, R.; Mándi, A.; Kurtán, T.; Weber, H.; Lin, W.; Ancheeva, E.; Proksch, P. *J. Nat. Prod.* **2019**, *82*, 2460–2469.

2. (a) Taylor, R. D.; MacCoss, M.; Lawson, A. D. *J. Med. Chem.* **2014**, *57*, 5845–5849. (b) White, A. Cilostazol. *Pract. Diab. Int.* **2011**, *28*, 43–44.

3. Hu, Q.; Yin, L.; Hartmann, R. W. *J. Med. Chem.* **2012**, *55*, 7080–7089.

4. (a) Vardanyan, R.; Hruby, V. *in Synthesis of Best-Seller Drugs,* 2016. (b) Cavusoglu, E.; Frishman, W. H.; Klapholz, M. *J Card Fail.* **1995**, *3*, 249–257. (c) Matsuo, M.; Kuse, Y.; Takahashi, K.; Kuwahara, K.; Tanito, M.; Kaidzu, S.; Shimazawa, M.; Hara, H.; Ohira, A. *J. Pharmacol. Sci.* **2019**, *139*, 84−90. (d) Frishman, W. H.; Fuksbrumer, M. S.; Tannenbaum, M. *J. ClIn. Pharmacol.* **1994**, *34*, 795−803. (e) Guo, L.-W.; Zhou, Y.-L. *Phytochemistry.* **1993**, *34*, 563−566.

5. (a) Lan, Y.; Chen, Y.; Xu, X.; Qiu, Y.; Liu, S.; Liu, X.; Liu, B. F.; Zhang, G. *Eur. J. Med. Chem.* **2014**, *79*, 216−230. (b) Pavletic, P. Semeano, A.; Yano, H.; Bonifazi, A.; Giorgioni, G.;Piergentili, A.; Quaglia, W.; Sabbieti, M. G.; Agas, D.; Santoni, G.;Pallini, R.; Ricci-Vitiani, L.; Sabato, E.; Vistoli, G.; Del Bello, F. *J. Med. Chem.* **2022**, *65*, 12124−12139.

6. Schiwek, C. H.; Jandl, C.; Bach, T. *Org. Lett.* **2020**, *22*, 9468−9472.

TH-3565_186122020

7. (a) Chen, I.-L.; Wang, T.-C.; Chen, Y.-L.; Tzeng, C.-C. *J. Chin. Chem. Soc.* **2000**, *47*, 155−162. (b) Cherest, M.; Lusinchi, X. *Tetrahedron Lett.* **1989**, *30*, 715−718. (c) Wassmundt, F. W.; Padegimas, S. J. *J. Am. Chem. Soc.* **1967**, *89*, 7131−7132. (d) Tian, J.; Li, L.; Yan, X. L.; Chen, L. G. *J. Heterocyclic Chem.* **2014**, *51*, 1811−1813.

8. (a) Li, B.; Park, Y.; Chang, S. *J. Am. Chem. Soc.* **2014**, *136*, 1125−1131. (b) Hu, T.; Lückemeier, L.; Daniliuc, C.; Glorius, F. *Angew. Chem., Int. Ed.* **2021**, *60*, 23193−23196. (c) Zhang, L.; Sonaglia, L.; Stacey, J.; Lautens, M. *Org. Lett.* **2013**, *15*, 2128−2131. (d) Guan, M.-Y.; Pang, Y.-B.; Zhang, J.-Y.; Zhao, Y.-S. *Chem. Commun.* **2016**, *52*, 7043−7046. (e) Sun, W.; Ling, C.-H.; Au, C.-M.; Yu, W.-Y. *Org. Lett.* **2021**, *23*, 3310−3314.

9. Keum, H.; Jung, H.; Jeong, J.; Kim, D.; Chang, S. *Angew. Chem., Int. Ed.* **2021**, *60*, 25235−25240.

10. Griffiths, R. J.; Burley, G. A.; Talbot, E. P. A. *Org. Lett.* **2017**, *19*, 870−873.

11. (a) Hwang, Y.; Park, Y.; Kim, Y. B.; Kim, D.; Chang, S. *Angew. Chem., Int. Ed.* **2018**, *57*, 13565–13569. (b) Deng, T.; Mazumdar, W.; Ford, R. L.; Jana, N.; Izar, R.; Wink, D. J.; Driver, T. G. *J. Am. Chem. Soc.,* **2020***, 142*, 4456–4463. (c) Xie, L.-Y.; Duan, Y.; Lu, L.-H.; Li, Y.-J.; Peng, S.; Wu, C.; Liu, K.-J.; Wang Z.; He, W.-M. *ACS Sustainable Chem. Eng.* **2017**, *5*, 10407–10412.

12. (a) Mitchell, E. A.; Peschiulli, A.; Lefevre, N.; Meerpoel, L.; Maes, B. U. W. *Chem. - Eur. J.* **2012**, *18*, 10092–10142. (b) Tanaka, K.; Yoshifuji, S.; Nitta, Y. *Chem. Pharm. Bull.* **1988**, *36*, 3125–3129.

13. (a) Khusnutdinova, J. R.; Ben-David, Y.; Milstein, D. *J. Am. Chem. Soc.* **2014**, *136*, 2998–3001. (b) Jin, X.; Kataoka, K.; Yatabe, T.; Yamaguchi, K.; Mizuno, N. *Angew. Chem., Int. Ed.* **2016**, *55*, 7212–7217. (c) Zheng, D. J.; Zhou, X. J.; Cui, B. D.; Han, W. Y.; Wan, N. W.; Chen, Y. Z. *ChemCatChem.* **2017**, *9*, 937–940. (d) Tan, Y.-F.; Long, C.-J.; Guan, Z.; He, Y.-H. *Green Chem.* **2022**, *24*, 4581–4587.

14. (a) van der Boom, M. E.; Milstein, D. *Chem. Rev.* **2003**, *103*, 1759−1792. (b) Peris, E. *Chem. Rev.* **2018**, *118*, 9988−10031. (c) Chen, C.; Liu, F. -S.; Szostak, M. *Chem. Eur. J.* **2021**, *27*, 4478−4499. (d) Zhao, Q.; Meng, G.; Nolan, S. P.; Szostak, M. *Chem. Rev.* **2020**, *120*, 1981−2048. (e) Findlay, M. T.; Domingo-Legarda, P.; McArthur, G.; Yen, A.; Larrosa, I. *Chem. Sci.* **2022**, *13*, 3335–3362. (f) Simonetti, M.; Cannas, D. M.; Just-Baringo, X.; Vitorica-Yrezabal, I. J.; Larrosa, I. *Nat. Chem.* **2018**, *10*, 724–731. (g) Sanford, M. S.; Love, J. A.; Grubbs, R. H. *J. Am. Chem. Soc.* **2001**, *123*, 6543−6554.

15. Berding, J.; van Paridon, J. A.; van Rixel, V. H.; Bouwman, E. *Eur. J. Inorg. Chem.* **2011**, *15*, 2450–2458.

16. Schleicher, D.; Tronnier, A.; Leopold, H.; Borrmann, H.; Strassner, T. *Dalton Trans.* **2016**, *45*, 3260−3263.

TH-3565_186122020

17. Salzmann, K.; Segarra, C.; Albrecht, M. *Angew. Chem., Int. Ed.* **2020**, *59*, 8932−8936.

18. Grimm, M. L.; Suleman, N. K.; Hancock, A. N.; Spencer, J. N.; Dudding, T.; Rowshanpour, R.; Castagnoli, N., Jr.; Tanko, J. M. *J. Am. Chem. Soc.* **2020**, *142*, 2640−2652.

19. Boess, E.; Van Hoof, M.; Birdsall, S. L.; Klussmann, M. *J. Org. Chem.* **2020**, *85*, 1972−1980.

20. Adhikari, P.; Bhattacharyya, D.; Nandi, S.; Kancharla, P. K.; Das, A. *Org. Lett.* **2021**, *23*, 2437−2442.

21. Alcaide, B.; Almendros, P.; Alonso, J. M. *Chem. Eur. J.* **2003**, *9*, 5793−5799.

22. Zhao, D.; Wang, Y.; Zhu, M. X.; Shen, Q.; Zhang, L.; Du, Y.; Li, J. X. *RSC Adv.* **2013**, *3*, 10272−10276.

23. Yamamoto, Y.; Yamada, Y.; Sajiki, H.; Sawama, Y. *Bull. Chem. Soc. Jpn.* **2020**, *93*, 1419−1423.

24. Bhattacharyya, D.; Senapati, S. K.; Das, A. *Synlett.* 2023, *34*, 651−656.

25. Haibach, M. C.; Ickes, A. R.; Tcyrulnikov, S.; Shekhar, S.; Monfette, S.; Swiatowiec, R.; Kotecki, B. J.; Wang, J.; Wall, A. L.; Henry, R. F.; Hansen, E. C. *Chem. Sci.* **2022**, *13*, 12906–12912.

26. Biancalani, C.; Giovanni, M. P.; Pieretti, S.; Cesari, N.; Graziano, A.; Vergeli, C.; Cilibrizzi, A.; DiGianuario, A.; Colucci, M.; Mangano, G.; Garrone, B.; Polezani, L.; Dal Piaz, V. *J. Med. Chem.* **2009**, *52*, 7397−7409.

27. Yadav, S.; Kant, R.; Kuram, M. R. *Chem. Commun.* **2023**, *59*, 7088–7099.

28. Zubar, V.; Brzozowska, A.; Sklyaruk, J.; Rueping, M. *Organometallics* **2022**, *41*, 1743–1747.

29. Kumar, K. A.; Kannaboina, P.; Jaladanki, C. K.; Bharatam, P. V.; Das, P. *Chemistry Select* **2016**, *1*, 601–607.

30. Kang, W. J., Pan, Y., Ding, A., Guo, H. *Org. Lett.* **2023**, *25*, 7633–7638.

31. Winter, D. K.; Drouin, A.; Lessard, J.; Spino, C. *J. Org. Chem.* **2010**, *75*, 2610−2618.

32. Xie, D.; Zhang, S. J. Org. Chem. **2022**, *87*, 8757–8763.

33. Yang, X.; Wang, L.; Hu, F.; Xu, L.; Li, S.; Li, S. S. *Org. Lett.* **2021**, *23*, 358−364.

34. Cheng, H.; Lam, T. L.; Liu, Y.; Tang, Z.; Che, C. M. *Angew. Chem., Int. Ed.* **2021**, *60*, 1383−1389.

TH-3565_186122020

35. Kurouchi, H.; Ohwada, T. *J. Org. Chem.* **2020**, *85*, 876–901.

36. Zhan, C. J.; Jia, J.; Yang, B. C.; Huang, A. P.; Liu, Y. L.; Ma, C. *RSC Advances* **2012**, *2*, 7506–7512.

37. Abdelhamid, Y.; Kasten, K.; Dunne, J.; Hartley, W. C.; Young, C. M.; Cordes, D. B.; Slawin, A. M. Z.; Ng, S.; Smith, A. D. *Org. Lett.* **2022**, *24*, 5444−5449.

38. Gao, H.; Guo, L.; Zhu, Y.; Yang, C.; Xia, W. *Chem. Commun*., **2023**, *59*, 2771–2774.

39. Lu, S.; Zheng, T.; Ma, J.; Deng, Z.; Qin, S.; Chen, Y.; Liang, Y. *Angew. Chem. Int. Ed.* **2022**, *61*, No. e2022012.

40. Frisch, M. J.; Trucks, G. W.; Schlegel, H. B.; Scuseria, G. E.; Robb, M. A.; Cheeseman, J. R.; Scalmani, G.; Barone, V.; Petersson, G. A.; Nakatsuji, H.; Li, X.; Caricato, M.; Marenich, A. V.; Bloino, J.; Janesko, B. G.; Gomperts, R.; Mennucci, B.; Hratchian, H. P.; Ortiz, J. V.; Izmaylov, A. F.; Sonnenberg, J. L.; Williams-Young, D.; Ding, F.; Lipparini, F.; Egidi, F.; Goings, J.; Peng, B.; Petrone, A.; Henderson, T.; Ranasinghe, D.; Zakrzewski, V. G.; Gao, J.; Rega, N.; Zheng, G.; Liang, W.; Hada, M.; Ehara, M.; Toyota, K.; Fukuda, R.; Hasegawa, J.; Ishida, M.; Nakajima, T.; Honda, Y.; Kitao, O.; Nakai, H.; Vreven, T.; Throssell, K.; Montgomery, J. A., Jr.; Peralta, J. E.; Ogliaro, F.; Bearpark, M. J.; Heyd, J. J.; Brothers, E. N.; Kudin, K. N.; Staroverov, V. N.; Keith, T. A.; Kobayashi, R.; Normand, J.; Raghavachari, K.; Rendell, A. P.; Burant, J. C.; Iyengar, S. S.; Tomasi, J.; Cossi, M.; Millam, J. M.; Klene, M.; Adamo, C.; Cammi, R.; Ochterski, J. W.; Martin, R. L.; Morokuma, K.; Farkas, O.; Foresman, J. B.; Fox, D. J. *Gaussian 16*, Revision C.01, Gaussian, Inc., Wallingford CT, 2016.

41. (a) Becke, A. D. *J. Chem. Phys*, **1993**, *98*, 5648-5652. (b) Lee, C.; Yang, W.; Parr, R. G. *Phys. Rev. B.* **1988**, *37*, 785-789.

42. (a) Grimme, S.; Ehrlich, S.; Goerigk, L. J. *Comput. Chem*. **2011**, *32*, 1456–1465. (b) Grimme, S.; Antony, J.; Ehrlich, S.; Krieg, H. *J. Chem. Phys*. **2010**, *132*, 154104.

43. Weigend, F.; Alhrichs, R. *Phys. Chem. Chem. Phys*. **2005**, *7*, 3297–3305.

44. Pedrón, M.; Legnani, L.; Chiacchio, M.-A.; Caramella, P.; Tejero, T.; Merino, P. *Beilstein J. Org. Chem*. **2019**, *15*, 1552–1562.

45. Zhao, Y.; Truhlar, D. G. *Theor. Chem. Acc.* **2008**, *120*, 215–241.

46. Fukui, K. *Acc. Chem. Res.* **1981**, *14*, 363–368.

TH-3565_186122020

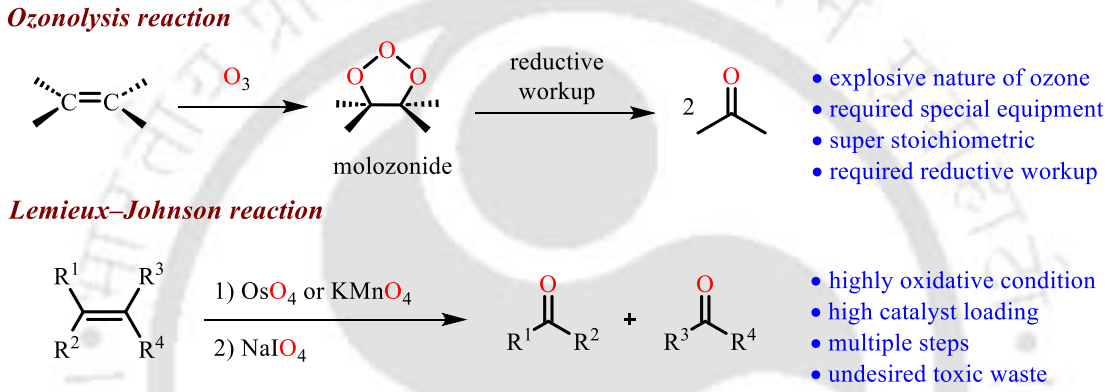
Chapter 3

Cyclometalated Ruthenium Complex as a Highly Efficient Catalyst for Selective Oxidative Cleavage of Olefins to Carbonyls

TH-3565_186122020

3.1. Introduction

The oxidative cleavage of C=C bonds to the corresponding carbonyl compounds is an important transformation in chemical and pharmaceutical processes.[1] The process is widely utilized in biomass processing and for the synthesis of drug molecules.[2] One of the most commonly used approaches is ozonolysis. However, the use of ozone is associated with several limitations such as the explosive nature of ozone, difficulty in controlling stoichiometry, require special equipment, and prerequisite reductive workup.[3] Lemieux and Johnson developed an alternative method safer than ozone by combining sodium periodate oxidant and osmium-based complex as catalysts.[4] Generally, the process requires high catalyst loading and its propensity to enter into rapid over-oxidation to produce the acid mostly.[5] Hence, the development of a mild, general, and selective method toward the oxidative cleavage of alkenes is highly desired.

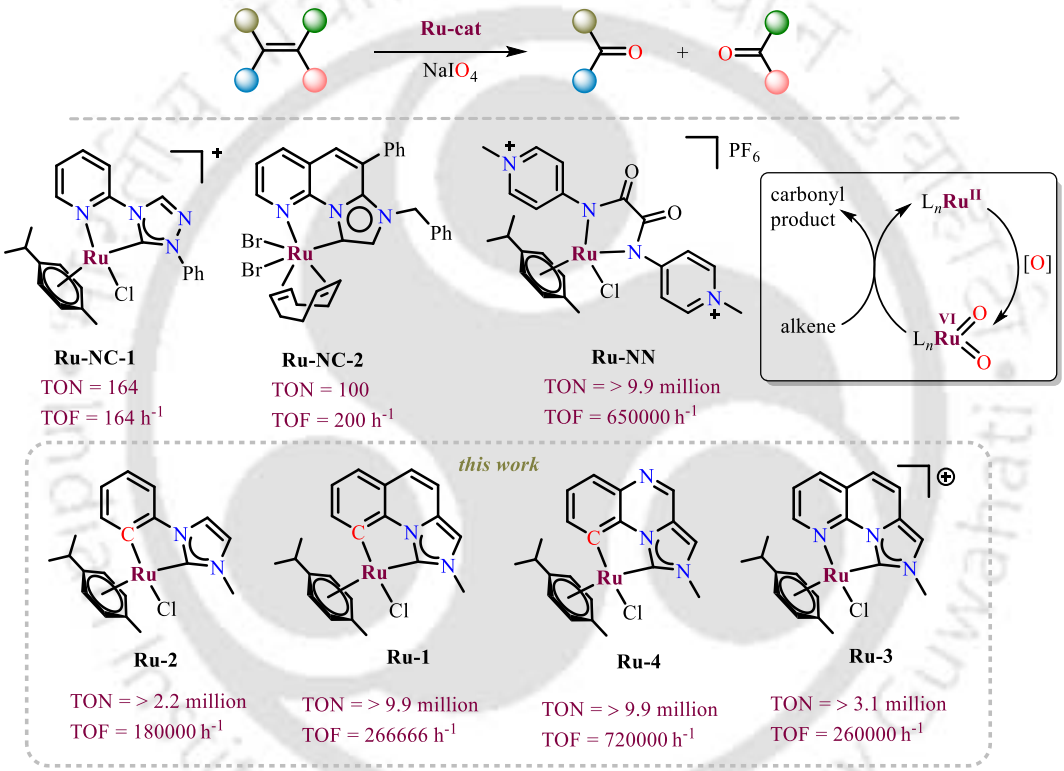


Scheme 3.1. Oxidative cleavage of C=C bonds by conventional methods

Transition-metal-catalyzed alkene scission reactions have been found as one of the prominent synthetic strategies in contemporary chemistry.[6,7] Among transition metal catalysts, ruthenium complexes have shown the most efficient to date due to their tunable oxidation states (-2 to +8), and high catalytic efficacy.[7] The use of catalytic amounts of ruthenium complex not only improves the chemoselectivity towards the formation of aldehyde but also prevents various side reactions such as epoxidation, dihydroxylation, and allylic oxidation. The bidentate ligand system with *N*-donor ligand greatly succeeded in this transformation (Scheme 3.2).[7b,7c] Choudhury *et al.* reported a Ru^{II}Im-NHC-based (Im-NHC = an imidazolydene-based *N*-heterocyclic carbene) complex **Ru-NC-1** to demonstrate the selective oxidation of alkenes and alkynes to the corresponding carbonyl compounds.[6d] They showed that the ancillary NHC ligand itself when properly modified, can impose a dramatic electronic bias at the Ru(II) center and accelerate the catalytic activity for the mentioned reaction. In 2014, Bera and co-workers developed an elegant catalytic system based on an imidazo [1,2-*a*] [1,8] naphthyridine-based abnormal *N*-heterocyclic carbene (*a*NHCs) ruthenium complex **Ru-NC-2** with C_{aNHC}^N motif.[7b] This complex exhibits excellent selectivity and efficiency towards highly functionalized sugar- and amino acid-derived substrates. The mechanistic insight suggests a catalytic cycle involving toggling between a low valent ruthenium (II) intermediate and a high-valent ruthenium (VI)-dioxo species. The stronger σ-donating ability of *a*NHCs in the

TH-3565_186122020

Ru-NC-2 was found to be a strategic motif to enrich this chemistry. Further, it was revealed that the σ-donating *a*NHC ligand enforces the Ru^{IV} center reasonably electron-rich which facilitates to undergo two-electron reduction and cleaves the C−C bond effectively. Very recently, Albrecht group reported a more efficient ruthenium bisPYA (bisPYA = N, N'-bis(pyridylidene)oxalamide) catalyst **Ru-NN** for olefin oxidation with remarkably high activity and long lifetime, obtaining turnover frequencies of 650000 h^{-1} and turnover numbers of several million.[7c] The important feature for the efficacy of the catalytic process is illustrated by the paired effect of a dynamic donor ability of the bisPYA ligand and redox activity of ruthenium. The extremely fast catalytic rates are postulated to arise by a high stabilization of both the $Ru^{VI}(=O)_2$ intermediate through a zwitter-ionic π-basic form of bisPYA ligand and also a high stabilization of Ru^{II}-precursors through the neutral π-acidic form of bisPYA ligand.



Scheme 3.2. Selected examples of efficient ruthenium catalysts for olefin oxidation and the present work. Given are the TON and TOF_{max} for the oxidation of styrene to benzaldehyde.

Based on the literature precedents,[8,9] herein I hypothesized that two active intermediates (L_nRu^{II} and $L_nRu^{VI}(=O)_2$) could be greatly stabilized by the ImQ-based cyclometalated ruthenium complex **Ru-1** and imidazo[1,5-*a*]quinoxaline (ImQx)-based cyclometalated ruthenium complex **Ru-4**. The salient features of the designed complexes are as follows; (i) π-delocalization in the annulated system may provide higher conjugational stability (ii) the nature of electrophilicity at the metal center is expected to be enhanced and is hoped to accelerate the rate of the reaction (iii) a strong σ-donating ability of NHC and carbanion donor site would stabilize the high-valent Ru^{VI}-dioxo species and further it may facilitate the two-electron reduction from L_nRu^{IV} to L_nRu^{II} in the C−C bond cleavage step. Therefore, it is anticipated to show high efficacy and selectivity in the catalytic process. To demonstrate the hypothesis,

TH-3565_186122020

preliminary calculations were carried out using B3LYP/6-31g(d,p) level basis set (Figure 3.1). HOMO-LUMO energy calculation for ImQ-based ligand precursor and complex **Ru-1** were discussed in Chapter 2. Here ImQx-based ligand **3**, and its ruthenium complex **Ru-4** are presented. Results suggested that low-lying LUMO and little effect of HOMO, resulting in decreasing HOMO-LUMO gap with respect to their nonannulated analogue **2.7** and complex **Ru-2**, respectively. Thereby, simply incorporating -N=CH- moiety in the ligand backbone provides higher conjugational stability compared to their nonannulated analogue.

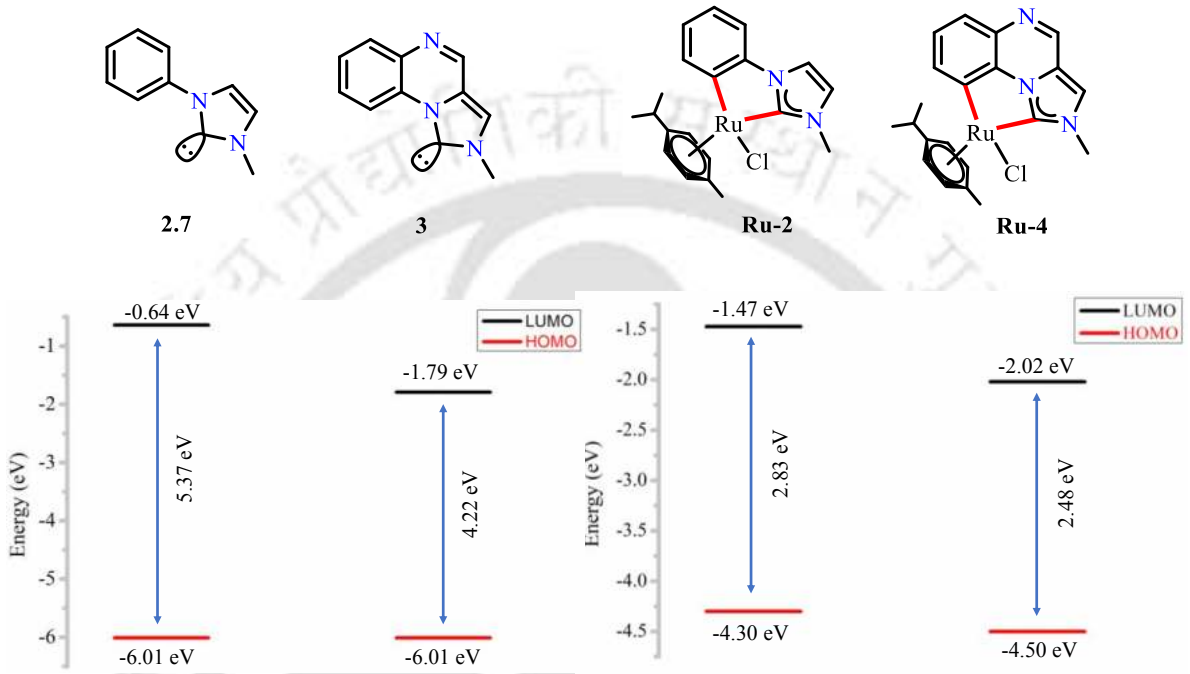
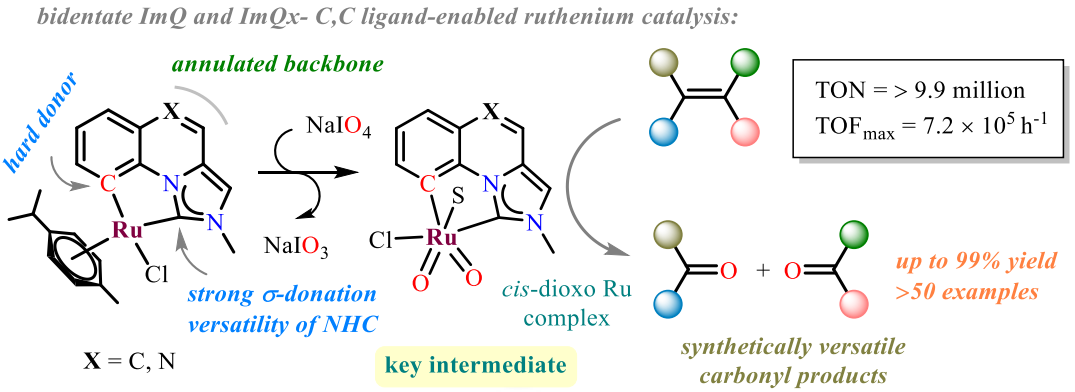


Figure 3.1. HOMO-LUMO energy profile for **2.7**, **3**, **Ru-2** and **Ru-4**

3.2. Present work

In this work, a highly efficient ruthenium-based catalyst for olefin oxidation has been demonstrated by employing a fused π-conjugated ImQ- and ImQx-based NHC ligand with bidentate $C_{(carbanion)}$^C_{NHC} motif. A strong σ-donating ability of both carbanion donor site and NHC, paired with rigid backbone and redox activity of ruthenium provided exceptionally high catalytic activity and long lifetime for oxidative cleavage of olefin to the carbonyl compounds. Complex **Ru-4** out-performs state-of-the-art systems that reach maximum TOF values of 720000 h^{-1} and turnover numbers of several million. Both the catalysts tolerate numerous functional groups and are applicable to challenging biomass, natural products, sugar, amino acid, and fatty acid-derived substrates. Detailed kinetic Hammett studies, thermodynamic activation parameters, several control experiments, and DFT studies are performed to establish the proposed mechanism.

TH-3565_186122020

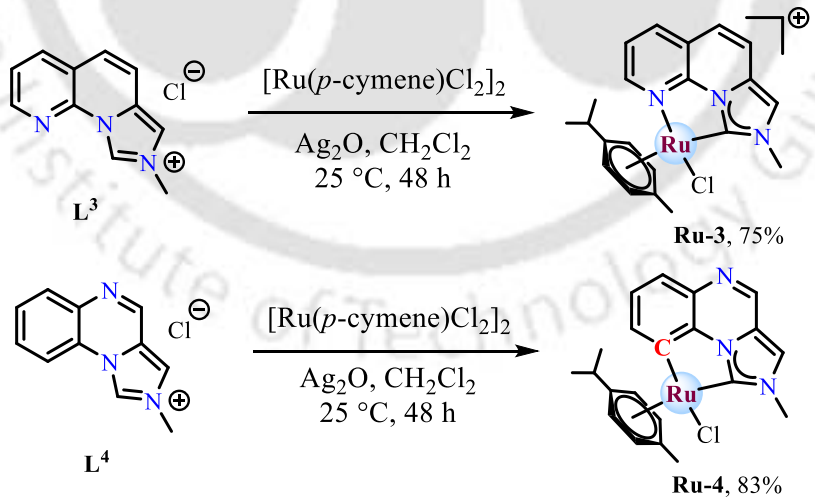


Scheme 3.3. ImQ and ImQx-based cyclometalated ruthenium complexes for olefin oxidation.

3.3. Results and discussion

3.3.1. Synthesis and characterization of cyclometalated ruthenium complexes

The synthesis and characterization of complex **Ru-3** and **Ru-4** are presented herein and for complex **Ru-1** and **Ru-2** are mentioned in Chapter 2 (section 2.3.1). ImQx-based cyclometalated ruthenium complex **Ru-4** was isolated in 83% yield *via* a one-pot transmetalation route by reacting ligand $\mathbf{L^4}$ with Ag_2O and $[RuCl_2(p\text{-cymene})]_2$ in the presence of dry CH_2Cl_2 at room temperature (see experimental section 3.5.3). It has been fully characterized by NMR, ESI-MS, and SC-XRD. Then, complex **Ru-3**, replacing the carbanion donor site with the isoelectronic N atom keeping the annulated NHC intact in the chelate arm, was synthesized by using a similar procedure starting from the corresponding ligand precursors $\mathbf{L^3}$ as shown in Scheme 3.4.



Scheme 3.4. Synthesis of cyclometalated ruthenium complexes

The presence of the characteristics Ru(II)-coordinated C_{NHC} signals (Table 3.1; reasonably upfield-shifted C_{NHC} resonance in **Ru-1** and **Ru-4** suggests the presence of a relatively more electron-rich C_{NHC} in the complexes than in nonannulated analogue **Ru-2**). Since low cost is required for the preparation of the ligand and its ruthenium complex, the process could be more

TH-3565_186122020

economically attractive than other state-of-the-art catalysts (see experimental section, Table 3.16−3.19). The composition of complexes **Ru-3** and **Ru-4** was further supported by ESI mass spectrometry, the main intensity peak at *m/z* 454.0626 (**Ru-3**) for the $[M]^+$ ion and at *m/z* 417.0906 (**Ru-4**) for the $[M\text{-}Cl]^+$ ion is in good agreement with the simulated isotopic distribution patterns.

Table 3.1. $^{13}C\{^1H\}$ NMR chemical shifts of C_{NHC} in the ruthenium complexes

entry	complex	C_{NHC} chemical shifts (ppm)
1	**Ru-1**	176.8
2	**Ru-2**	188.5
3	**Ru-3**	174.5
4	**Ru-4**	177.4

A single crystal of the complexes **Ru-3** and **Ru-4** were obtained by slow diffusion of petroleum ether into a solution of the complex in CH_2Cl_2 at room temperature. The X-ray crystal structure of the complexes is shown in Figure 3.2. Complex **Ru-4** adopts a typical piano-stool geometry and exhibits a distorted pseudo-octahedral coordination sphere around the ruthenium center which is occupied by the bidentate chelate ligands, halide and planar *p*-cymene. In all the cases, NHC ligand is coordinated to the metal center as a bidentate chelate motif with anionic carbon atoms or *N*-donor site, forming a planar five-membered metallacycle. Furthermore, it was found that Ru−C_{NHC} bond length (2.043Å) is slightly shorter than that of Ru−C_{aryl} bonds (2.103 Å) possibly due to π-back-donation from the metal center. To understand the steric profile of a chelating ligand, two important geometrical parameters-bite angle and yaw angle are measured. The bite angle and yaw distortion angles at the NHC/aryl ligand are measured to be 78.0° and 16.5°/8.3°, respectively, for **Ru-3** and 77.9° and 15.2°/9.1°, respectively, for **Ru-4**. These values are slightly higher than their non-annulated analogue **Ru-2** (76.65° and 9.1°/5.5°). This larger bite angle and an increase of yaw distortion in metallachelate indicate more conformational strain in the annulated backbone.

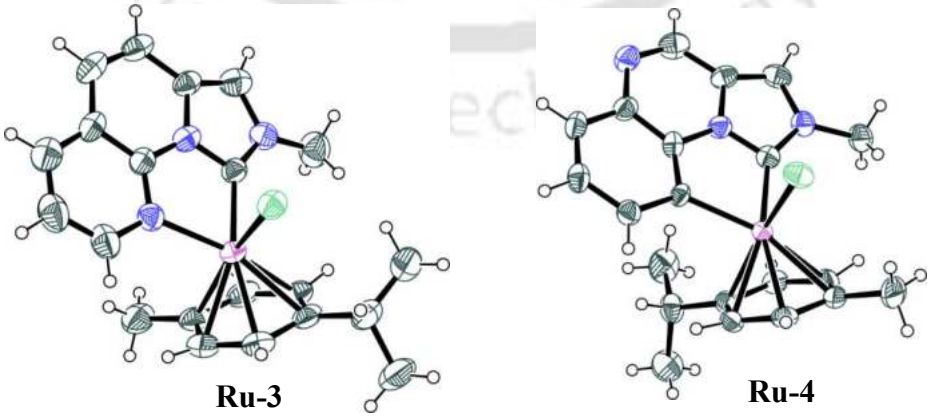


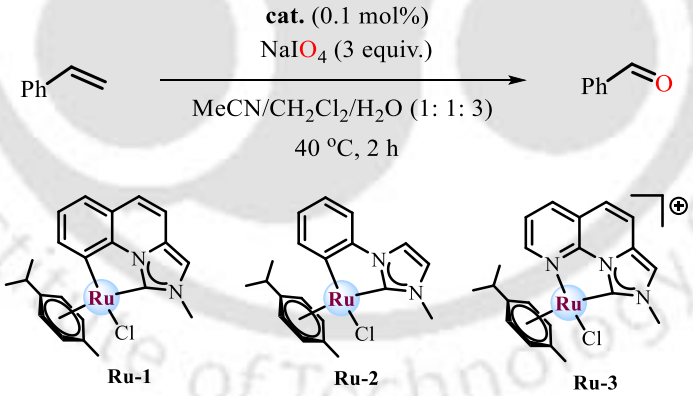
Figure 3.2. Molecular structure of complex **Ru-3** (CCDC: 2311869) and **Ru-4** (CCDC: 2342585) with thermal ellipsoid 40% probability level.

TH-3565_186122020

3.3.2. Optimization of reaction conditions

To inspect the catalytic applicability of the prepared ruthenium complexes **Ru-1**, **Ru-2**, and **Ru-3**, the optimization studies were initiated with styrene as a model substrate for the catalytic oxidation of olefin. **Ru-1** showed superior catalytic activity with respect to **Ru-2**, and **Ru-3** (Table 3.2). Initially, the reaction was examined at room temperature by using 3 equivalents of $NaIO_4$ in the deoxygenated solvent mixture of $CH_3CN/CH_2Cl_2/H_2O$ (1:1:3 *v/v*) with 1 mol% of **Ru-1** complex (Table 3.3). After 2 hours, complex **Ru-1** afforded 57% conversion to aldehyde (entry 1, Table 3.3). When the reaction temperature was slightly increased to 40 ºC, a quantitative conversion (> 99%) of styrene was achieved within 30 min (entry 5, Table 3.3). Further lowering the catalyst loading to 0.1 mol%, afforded a full substrate conversion within 2 hours (entry 9, Table 3.3). To our delight, no trace of over-oxidized acid was observed under the conditions. Nevertheless, the use of aerobic conditions or the use of larger quantities of oxidants (e.g., > 4 equiv. $NaIO_4$) led to a small amount of over-oxidized product (<10% acid). As a part of further optimization, the reaction was performed with other oxidants such as hydrogen peroxide, *tert*-butyl hydroperoxide, and molecular oxygen. These are found to be ineffective (Table 3.4). A blank reaction in the absence of **Ru-1** complex afforded only 5% conversion to benzaldehyde which reveals the importance of **Ru-1** complex in the catalytic reaction (entry 11, Table 3.3). Further see Table 3.5 and Table 3.6 for the effect of solvent mixtures and the effect of oxygen-free solvent and reaction environment, respectively. The solvent mixture $CH_3CN/CH_2Cl_2/H_2O$ (1:1:3 *v/v*) was found to be most effective for this transformation.

Table 3.2. Screening of different catalysts [a]

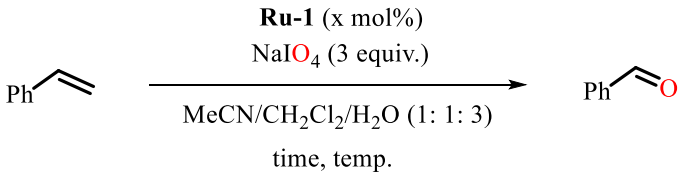


entry	**cat.** (0.1 mol%)	conversion (%)[b]	selectivity[b, c]
1	**Ru-1**	> 99 (98 %)	100
2	**Ru-2**	35	97
3	**Ru-3**	28	95
4	[Ru(*p*-cymene)Cl_2]$_2$	24	-
5	RuO_4	42 (38 %)	90
6	$RuCl_3$•xH_2O	16	88
7	-	5	-

[a]*Reaction conditions:* styrene (1 mmol), $NaIO_4$ (3 mmol) in solvent mixtures of MeCN/DCM/H_2O (1:1:3, 2.5 mL) at indicated time and temperature. Isolated yields are in parenthesis. [b]conversion/selectivity was determined by ^{1}H NMR spectroscopy relative to an external standard (anisole). [c]selectivity towards benzaldehyde (in %) *vs*. overoxidation to benzoic acid.

TH-3565_186122020

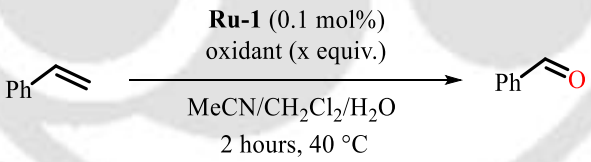
Table 3.3. Screening of loading catalyst, time, and temperature [a]



entry	catalyst loading (mol%)	time (h)	temperature (ºC)	conversion[b] (%)	selectivity[b, c]
1	1	2	25	57	-
2	1	2	35	84 (80 %)	100
3	1	2	40	> 99	100
4	1	1	40	> 99	100
5	1	0.5	40	> 99	100
6	0.5	0.5	40	> 99	100
7	0.1	0.5	40	30	100
8	0.1	1	40	72 (66%)	100
9	0.1	2	40	> 99 (98 %)	100
10	0.1	2	50	> 99	96
11	-	2	40	5	-
12	-	60	40	9	-

[a]*Reaction conditions:* styrene (1 mmol), $NaIO_4$ (3 mmol) in solvent mixtures of MeCN/DCM/H_2O (1:1:3, 2.5 mL) at indicated time and temperature. Isolated yields are in parenthesis. [b]conversion/selectivity was determined by ^1H NMR spectroscopy relative to an external standard (anisole). [c]selectivity towards benzaldehyde (in %) *vs*. overoxidation to benzoic acid.

Table 3.4. Screening of different oxidants [a]

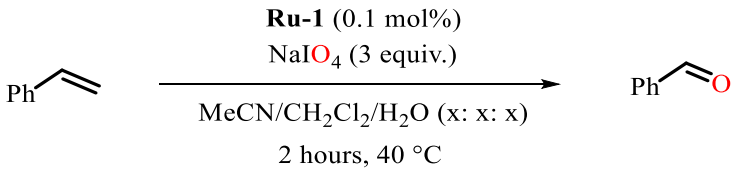


entry	oxidant (equiv.)	Time (h)	conversion (%) [b]	selectivity (%) [b,c]
1	$NaIO_4$ (0)	2	0	-
2	$NaIO_4$ (1)	2	28	97
3	$NaIO_4$ (2)	2	70	100
4	$NaIO_4$ (3)	2	> 99	100
5	$NaIO_4$ (4)	2	> 99	89
6	H_2O_2 (3)	2	38	-
7	^{t}BuOOH (3)	2	57	-
8	*m*-CPBA (3)	2	14	-
9	O_2 (1 atm)	2	8	-

[a]Conditions: styrene (1 mmol), catalyst **Ru-1** (0.1 mol%) in MeCN/ CH_2Cl_2/H_2O (1:1:3, 2.5 mL) at 40 ºC. [b]Conversion/selectivity determined by ^1H NMR spectroscopy relative to an external standard (anisole). [c]Selectivity towards benzaldehyde (in %) *vs*. overoxidation to benzoic acid.

TH-3565_186122020

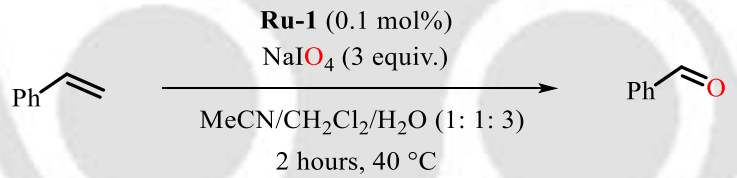
Table 3.5. Effect of solvent mixtures [a]



entry	$CH_3CN:CH_2Cl_2:H_2O$	conversion (%) [b]	selectivity (%)[b,c]
1	0:0:3	92	87
2	1:0:3	> 99	92
3	0:1:3	55	98
4	1:0:0	13	100
5	0:1:0	15	100
6	1:1:1	82	83
7	1:1:2	87	89
8	1:1:3	> 99	100
9	1:1:4	> 99	86

[a]*Reaction conditions:* styrene (1 mmol), catalyst **Ru-1** (0.1 mol%), $NaIO_4$ (3 mmol) in solvent mixtures of MeCN/DCM/H_2O (2.5 mL) at 40 ºC. [b]Conversion/selectivity determined by ^1H NMR spectroscopy relative to an external standard (anisole). [c]Selectivity towards benzaldehyde (in %) *vs.* overoxidation to benzoic acid.

Table 3.6. Effect of oxygen-free solvent and reaction environment [a]

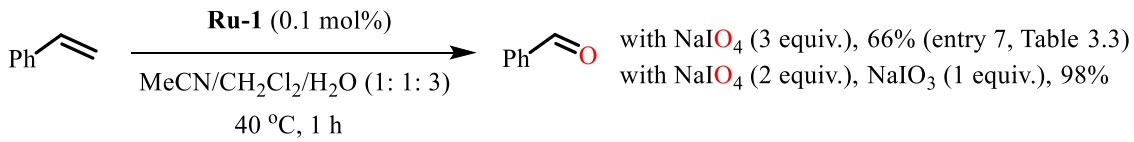


Entry	conditions	time (h)	conversion (%)[b]	selectivity (%)[b, c]
1	Aerobic	2	> 99	92
2[d]	Oxygen-free solvent	2	> 99	100
3[d]	Oxygen-free solvent and N_2 saturated mixture	2	> 99	100

[a]*Reaction conditions*: styrene (1 mmol), catalyst **Ru-1** (0.1 mol%), $NaIO_4$ (3 mmol) in MeCN/DCM/H_2O (1:1:3; 2.5 mL) at 40 ºC. [b]Conversion and selectivity (towards benzaldehyde in %) determined by ^1H NMR spectroscopy relative to an external standard (anisole). [c]Selectivity towards benzaldehyde (in %) *vs.* overoxidation to benzoic acid. [d]reaction mixture is subjected to a three-time freeze-thaw pump cycle.

Since $NaIO_3$ was identified as the by-product of the sacrificial oxidant at the end of the reaction, as confirmed by X-ray diffraction analysis, I was quite curious to know the effect of $NaIO_3$ in the catalytic reaction. When the reaction was carried out with a mixture of $NaIO_4$ (2 equiv.) and $NaIO_3$ (1 equiv.) instead of $NaIO_4$ (3 equiv.) under identical conditions, the reaction was completed within one hour and benzaldehyde was obtained in 98% yield (Scheme 3.5).

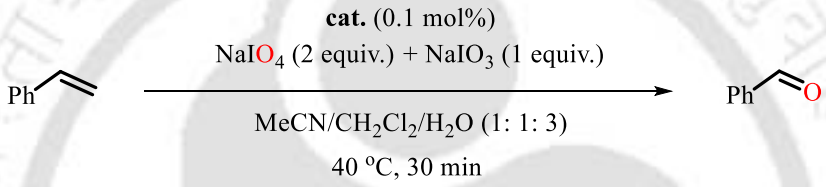
TH-3565_186122020



Scheme 3.5. Oxidation of styrene with a mixture of $NaIO_4$ (2 equiv.) and $NaIO_3$ (1 equiv.)

Further screening of the ruthenium complexes **Ru-1** to **Ru-4**, the activity of the complex **Ru-4** was found to be superior to the other complexes (Table 3.7). As a part of further optimization, the reaction was performed with other loading catalysts, time, and temperature (see Table 3.8−3.10 for detailed optimization studies). Best optimization was found to be **Ru-4** (0.1 mol%), $NaIO_4$ (2 equiv.), $NaIO_3$ (1 equiv.), at 40 °C for 30 minutes in $CH_3CN/CH_2Cl_2/H_2O$ (1:1:3, *v/v*) solvent mixture.

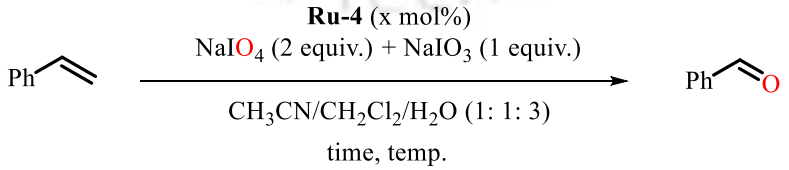
Table 3.7. Screening of different catalysts [a]



entry	**cat.** (0.1 mol%)	conversion (%) [b]	selectivity [b, c]
1	**Ru-1**	58	99
2	**Ru-2**	36	97
3	**Ru-3**	30 (28%)	99
4	**Ru-4**	**> 99 (97%)**	**100**
5	[Ru(*p*-cymene)Cl_2]$_2$	16	–
6	RuO_4	27	90
7	$RuCl_3$•xH_2O	10	–

[a]*Reaction conditions:* styrene (1 mmol), $NaIO_4$ (2 mmol) + $NaIO_3$ (1 mmol) in solvent mixtures of MeCN/DCM/H_2O (1:1:3, 2.5 mL) at indicated time and temperature. Isolated yields are in parenthesis. [b]conversion/selectivity was determined by ^{1}H NMR spectroscopy relative to an external standard (anisole). [c]selectivity towards benzaldehyde (in %) *vs*. over oxidation to benzoic acid.

Table 3.8. Screening of loading catalyst, time, and temperature [a]



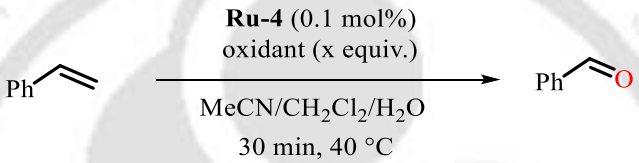
entry	catalyst loading (mol%)	time (min)	temperature (°C)	conversion [b] (%)	selectivity [b, c]
1	1	60	25	58	–
2	1	60	35	87	100
3	1	60	40	> 99	100
4	1	30	40	> 99	100

TH-3565_186122020

5	1	20	40	> 99	100
6	1	10	40	89	100
7	1	5	40	45	100
8	0.5	10	40	84	100
9	0.1	10	40	67	100
10	0.1	15	40	75	100
11	**0.1**	**30**	**40**	**> 99**	**100**
12	–	30	40	n.d.	–
13	–	26 h	40	4	–

[a]*Reaction conditions:* styrene (1 mmol), $NaIO_4$ (2 mmol) + $NaIO_3$ (1 mmol) in solvent mixtures of MeCN/DCM/H_2O (1:1:3, 2.5 mL) at indicated time and temperature. [b]conversion/selectivity was determined by ^1H NMR spectroscopy relative to an external standard (anisole). [c]selectivity towards benzaldehyde (in %) *vs*. over oxidation to benzoic acid.

Table 3.9. Screening of different oxidants. [a]

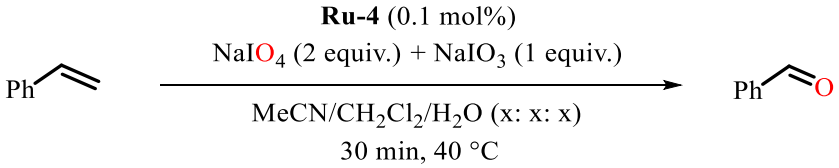


entry	oxidant (equiv.)	conversion (%) [b]	selectivity (%) [b, c]
1	$NaIO_4$ (0)	n.d.	–
2	$NaIO_4$ (1)	25	100
3	$NaIO_4$ (2)	58	100
4	$NaIO_4$ (3)	66	98
5	$NaIO_4$ (4)	68	94
6	$NaIO_4$ (3) + $NaIO_3$ (0.5)	80	99
7	$NaIO_4$ (3) + $NaIO_3$ (1)	> 99	99
8	$NaIO_4$ (2) + $NaIO_3$ (0.5)	76	100
9	**$NaIO_4$ (2) + $NaIO_3$ (1)**	**> 99**	**100**
10	$NaIO_4$ (2) + $NaIO_3$ (2)	> 99	100
11	$NaIO_4$ (1) + $NaIO_3$ (2)	30	–
12	$NaIO_4$ (1) + $NaIO_3$ (1)	24	–
13	$NaIO_3$ (3)	n.d.	–
14	H_2O_2 (3)	25	–
15	^{t}BuOOH (3)	43	–
16	*m*-CPBA (3)	n.d.	–
17	O_2 (1 atm)	n.d.	–
18	$NaIO_4$ (2) + $NaNO_3$ (1)	74	–
19	$NaIO_4$ (2) + KPF_6 (1)	60	–
20	$NaIO_4$ (2) + $NaBF_4$ (1)	52	–

[a]*Reaction conditions*: styrene (1 mmol), catalyst **Ru-4** (0.1 mol%) in MeCN/CH_2Cl_2/H_2O (1:1:3, 2.5 mL) at 40 ºC. [b]Conversion/selectivity determined by ^1H NMR spectroscopy relative to an external standard (anisole). [c]Selectivity towards benzaldehyde (in %) *vs*. over oxidation to benzoic acid.

TH-3565_186122020

Table 3.10. Effect of solvent mixtures. [a]



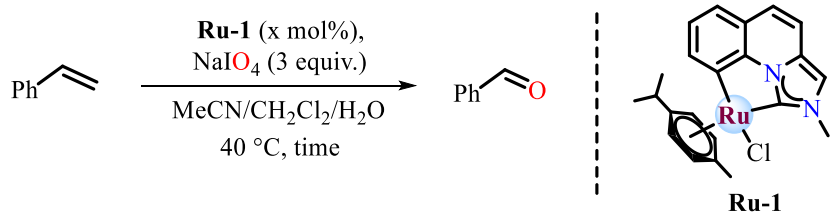
entry	CH_3CN: CH_2Cl_2: H_2O	conversion (%) [b]	selectivity (%) [b, c]
1	0:0:3	82	90
2	1:0:3	96	98
3	0:1:3	85	98
4	1:0:0	n.d.	–
5	0:1:0	n.d.	–
6	1:1:1	86	97
7	1:1:2	95	100
8	**1:1:3**	**> 99**	**100**
9	1:1:4	> 99	93

[a]*Reaction conditions:* styrene (1 mmol), catalyst **Ru-4** (0.1 mol%), $NaIO_4$ (2 mmol) + $NaIO_3$ (1 mmol) in solvent mixtures of MeCN/DCM/H_2O (x: x: x, total 2.5 mL) at 40 ºC. [b]Conversion/selectivity determined by ^1H NMR spectroscopy relative to an external standard (anisole). [c]Selectivity towards benzaldehyde (in %) *vs.* over oxidation to benzoic acid.

3.3.3. Efficiency of the catalytic reaction

To examine the efficacy of the catalytic reaction, turnover numbers (TONs) and turnover frequencies (TOF) were calculated in the oxidation process (Table 3.11). Complex **Ru-1** showed ultra-high catalytic activity and a long lifetime, reaching TONs and TOF of several million. By gradually lowering the catalyst loading from 1 mol% → 0.1 mol%→0.01 mol% → 0.001 mol% → 0.0001 mol%, a full conversion is achieved within acceptable range (30 h) (see Figure 3.3; time-conversion profiles with different concentrations of catalyst loading). Interestingly, the catalytic activity was preserved even with the catalyst loading as low as 0.1 ppm and reaching TONs of > 9900000 and TOF_{max} = 266666 h^{-1}. Control study in the absence of complex **Ru-1**, 9% conversion was obtained after 60 h, indicating the importance of the catalyst in the oxidation process.

Table 3.11. Effect of low catalyst loading for **Ru-1**[a]

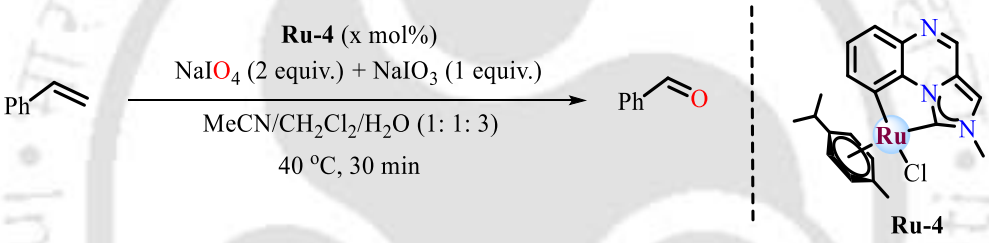


TH-3565_186122020

entry	**Ru-1** [mol%]	time [h]	conversion[b] (%)	selectivity[b,c] (%)	TON	TOF_{max} [h^{-1}][d]
1	1	0.5	> 99	100	> 99	276
2	0.1	2	> 99	100	> 990	750
3	0.01	4	> 99	96	> 9900	3100
4	0.001	10	> 99	92	> 99000	10250
5	0.0001	30	> 99	85	> 990000	45833
6	0.00001	60	> 99	77	>9900000	266666

[a]*Reaction conditions:* styrene (1 equiv.), complex **Ru-1**, $NaIO_4$ (3 equiv.) in $MeCN/CH_2Cl_2/H_2O$ (1:1:3; 1.5 mL), 40 ºC. [b]Conversion/selectivity was determined by ^1H NMR analysis relative to an internal standard (anisole). [c]Selectivity towards benzaldehyde *vs* over oxidation to benzoic acid. [d]Maximum turnover frequency TOF_{max} extracted from time-conversion profiles (Figure 3.3).

Table 3.12. Effect of low catalyst loading for **Ru-4**[a]



entry	**Ru-4** [mol%]	time [h]	conversion[b] (%)	Selectivity[b, c] (%)	TON	TOF_{max} [h^{-1}][d]
1	1	0.33	> 99	100	> 99	388
2	0.1	0.5	> 99	100	> 990	2800
3	0.01	2	> 99	97	> 9900	10600
4	0.001	7	> 99	95	> 99000	28500
5	0.0001	14	> 99	91	> 990000	155000
6	0.00001	26	> 99	88	> 9900000	720000

[a]*Reaction conditions:* styrene (1 equiv.), complex **Ru-4**, $NaIO_4$ (2 equiv.) and $NaIO_3$ (1 equiv.) in $MeCN/CH_2Cl_2/H_2O$ (1:1:3; 1.5 mL), 40 ºC. [b]Conversion/selectivity was determined by ^1H NMR analysis relative to an internal standard (anisole). [c]Selectivity towards benzaldehyde *vs* over oxidation to benzoic acid. [d]Maximum turnover frequency TOF_{max} extracted from time-conversion profiles (Figure 3.3).

Similarly, the turnover numbers (TONs) and turnover frequencies (TOF) for the complex **Ru-4** are also calculated for the oxidation reaction of styrene (Table 3.12). With 1 mol% catalyst loading the reaction was completed within 20 min. Interestingly, the catalytic activity was preserved even with the catalyst loading as low as 0.1 ppm and reaching TONs of > 9900000 and TOF_{max} = 720000 h^{-1}. This is the highest TOF value ever reported for the metal-catalyzed oxidative cleavage of olefins. Control reaction in the absence of complex **Ru-4**, only 4%

TH-3565_186122020

conversion was obtained in the same time frame, indicating the importance of the ruthenium complex in the oxidation process.

Time-conversion profile

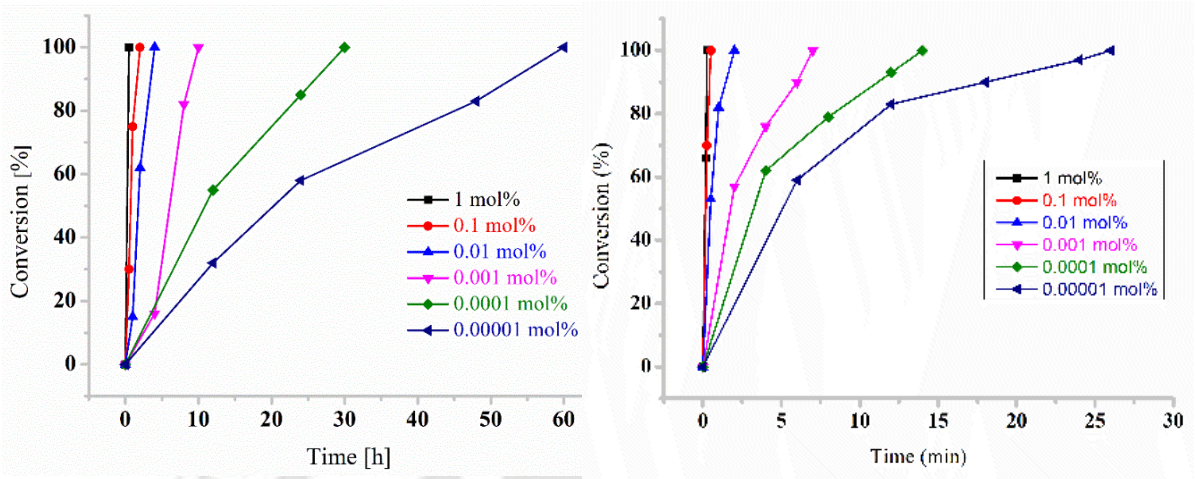


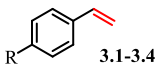
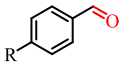
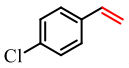
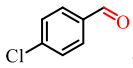
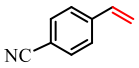
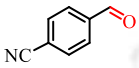
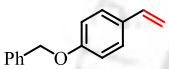
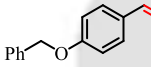
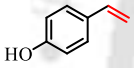
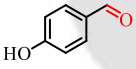
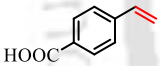
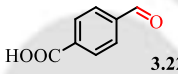
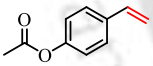
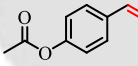
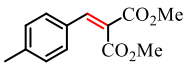
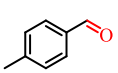
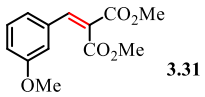
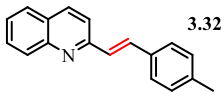
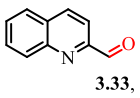
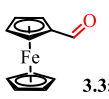
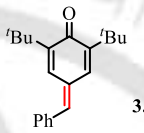
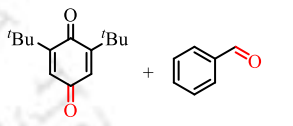
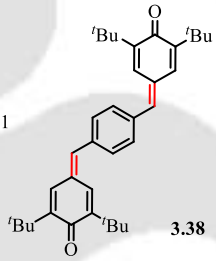
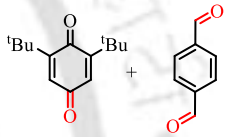
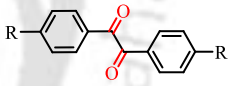
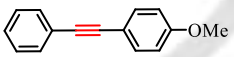
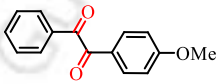
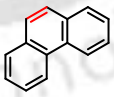
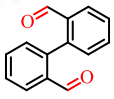
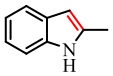
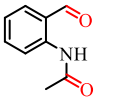
Figure 3.3. Time-conversion profiles of catalytic runs with different concentrations. Reaction conditions for **Ru-1**: styrene (1 mmol), complex **Ru-1** (x mol%), $NaIO_4$ (3 mmol) in $CH_3CN/CH_2Cl_2/H_2O$ (1:1:3; 5.0 mL) at 40 ºC (left figure). Reaction conditions for **Ru-4**: styrene (1 mmol), complex **Ru-4** (x mol%), $NaIO_4$ (2 mmol), $NaIO_3$ (1 mmol) in $CH_3CN/CH_2Cl_2/H_2O$ (1:1:3; 5.0 mL) at 40 ºC (right figure).

3.3.4. Scope of the reaction

The substrate scope of this reaction was examined using 0.1 mol% catalyst loading with both **Ru-1** and **Ru-4** complex under the following optimized reaction conditions (Table 3.3, entry 9 for **Ru-1** and Table 3.8, entry 11 for **Ru-4**). Initially, the reaction was explored with a series of terminal alkenes (Table 3.13). The electron-rich substituent containing styrene derivatives such as *p*-methyl-, *p*-methoxy, and *p*-*tert*-butylstyrene gave a quantitative yield of the corresponding aldehydes (> 94%, entries 1-4), however electron-deficient *p*-chlorostyrene and *p*-cyano styrene (entries 5 and 6) afforded slightly lower yields under the identical reaction condition. Likewise, the reaction of *m*-methoxy and *m*-chloro styrene gave the corresponding carbonyl product in good yield. It is worthy to mention that the oxidation-susceptible benzylic C−H bond (**3.17**), hydroxyl O−H bond (**3.19**), and base-labile groups (–CN, and $–OCOCH_3$) remained intact during the oxidation, showing the protocol chemoselective. Besides styrenes, polysubstituted olefins also successfully participated in the reaction to provide the desired products in moderate to good yield (entries 13-17, Table 3.13). Geminal olefins such as *α*-methyl styrene gave a higher yield for the corresponding product than the 1,1-diphenylethylene possibly due to steric effect (entries 13-14, Table 3.13). Interestingly, 2-styryl quinoline **3.32** led to the formation of desired products **3.33** and **3.6** in excellent yields (entry 18, Table 3.13). To our delight redox-active ferrocene moiety **3.34** is also

TH-3565_186122020

Table 3.13. Oxidation of substituted alkenes, alkynes and their derivatives[a]

entry	substrate	product and yield
1-4	R = H, Me, OMe, ^{t}Bu  **3.1-3.4**	 **3.5**, 100% (100%), 94%[b]; **3.6**, 99% (98%); **3.7**, 97% (98%); **3.8**, 94% (95%)
5	 **3.9**	 **3.10**, 91% (92%), 65%[b]
6	 **3.11**	 **3.12**, 90% (90%)
7	 **3.13**	 **3.14**, 90% (91%)
8	 **3.15**	 **3.16**, 87% (85%)
9	 **3.17**	 **3.18**, 80% (82%)
10	 **3.19**	 **3.20**, 81%, (83%)
11	 **3.21**	 **3.22**, 77% (80%)
12	 **3.23**	 **3.24**, 83% (86%)
13	 **3.25**	 **3.26**, 89% (90%)
14	 **3.27**	 **3.28**, 62% (68%)
15	 **3.29**	 **3.5**, 92% (92%)
16	 **3.30**	 **3.6**, 95% (96%)
17	 **3.31**	 **3.14**, 90% (92%)
18	 **3.32**	 **3.33**, 97% (99%) + **3.6**, 91% (92%)
19	 **3.34**	 **3.35**, 33%[c] (36%[c])
20	 **3.36**	 **3.37**, 80% (82%) **3.5**, 87% (88%)
21	 **3.38**	 **3.37**, 75% (78%) **3.39**, 71% (71%)
22-24	R = H, OMe, Cl  **3.40-3.42**	 **3.43**, 94% (95%); **3.44**, 96% (96%); **3.45**, 82% (84%)
25	 **3.46**	 **3.47**, 95% (95%)
26	 **3.48**	 **3.49**, 88% (91%)
27	 **3.50**	 **3.51**, 80%[d,e] (84%[d,e])

[a]Reaction conditions: substrate (1 mmol), **Ru-1** (0.1 mol%), $NaIO_4$ (3 mmol) in $MeCN/CH_2Cl_2/H_2O$ (1:1:3; 1.5 mL), 40 ºC, 2 h. Isolated yield. [b]with 1 ppm **Ru-1** catalyst loading. [c]Along with 48% of starting material was recovered. [d]with 1 mol% catalyst. [e]with reaction time = 6 h. The parenthesis yield represents the reaction conditions: substrate (1 mmol), **Ru-4** (0.1 mol%), $NaIO_4$ (2 mmol) and $NaIO_3$ (1 equiv.) in $MeCN/CH_2Cl_2/H_2O$ (1:1:3; 1.5 mL), 40 ºC, 30 min. Isolated yield.

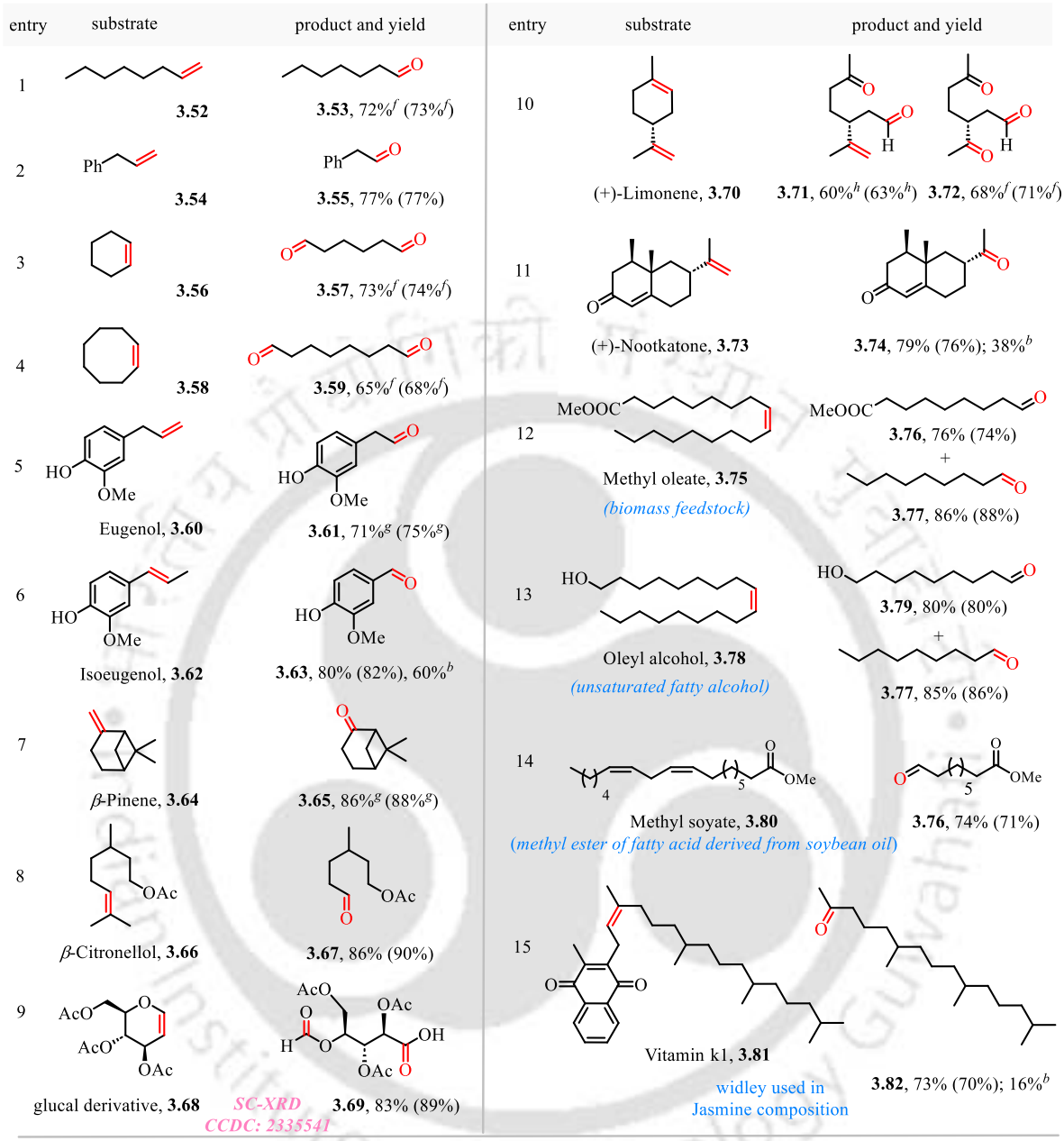
TH-3565_186122020

compatible with this method (entry 19). Though *para*-quinone methide is an acceptor in 1,6-nucleophilic conjugate addition reactions, only the exocyclic double bond was selectively oxidized under the reaction condition to provide the fission products **3.37** and **3.5** (entry 20, Table 3.13). Next, the reaction was examined on polysubstituted alkene **3.38** with multiple C=C double bond sites (entry 21, Table 3.13). Gratifyingly, 1,4-benzoquinone and terephthalaldehyde **3.39** were obtained with impressive selectivity. The scope of the reaction was further extended to a series of internal alkynes (entries 22-25, Table 3.13). Diarylacetylene delivers the corresponding diaryl 1,2-diketone in good yield. To our delight, when phenanthrene **3.48** was used as a substrate, the oxidative scission product biphenyl-2,2′-dicarbaldehyde **3.49** was obtained with excellent yield (entry 26, Table 3.13). Similarly, 2-methylindole **3.50** under identical conditions afforded *N*-(2-formylphenyl) acetamide **3.51** with good yield indicating the efficacy of the catalyst (entry 27, Table 3.13).

Synthetically challenging non-activated aliphatic alkenes were also found to be amenable to this method, giving scission products in good yields, but required longer reaction time for complete conversion (entry 1-4, Table 3.14). To further demonstrate the practical applicability of this process, I tried the oxidative cleavage of a wide range of natural products and their derivatives (entries 5-15, Table 3.14). Natural products having olefinic and phenolic groups such as eugenol **3.60**, (so called clove oil), and its isomer isoeugenol **3.62** were subjected to the standard reaction conditions, homovanillin **3.61**, and vanillin **3.63** were obtained in good yield. Notably, vanillin **3.63** is an important component in vanilla and is widely applied as a flavouring agent in foods, beverages, and pharmaceuticals.[10] Monoterpenes for instance *β*-pinene **3.64**, acetyl-*β*-citronellol **3.66** were also successfully employed and afforded the corresponding carbonyl compounds nopinone **3.65** and **3.67** in good yields. The resulting species nopinone **3.65** is a useful chemical intermediate for fragrance. Further, it has been useful as an important building block for the construction of nabilone,[11] a synthetic cannabinoid used to treat nausea and vomiting during cancer treatment, and the prostaglandin D2 (PGD2) receptor antagonist S-5751.[12] Though **3.65** was manufactured industrially from ozonolysis of **3.64**, a detailed safety study of the industrial ozonolysis has revealed the high risk of explosion and a runaway reaction in this multistep process (−57, −27, 0, and finally 25 °C).[12] Thereby, the present catalytic protocol may find a worthwhile alternative. Oxidative cleavage of olefins appended sugar units such as glucal derivative **3.68** afforded the corresponding formyl ester **3.69**, which could be important synthons for further structural amplification. The structure of the compound **3.69** was unambiguously confirmed by SC-XRD. Next, (+)-Limonene **3.70** was examined in our reaction condition as a typical monoterpene with two olefinic groups. To our delight, only endocyclic alkene scission product **3.71** was obtained selectively after 2 h, and a longer reaction time led to the formation of double cleavage product **3.72**. Hence, simply by varying the reaction parameter one can obtain monocleavage and di-cleavage products individually. (+)-Nootkatone **3.73**, a sesquiterpenoid, originates from the heartwood of yellow cedar and also underwent oxidative cleavage

TH-3565_186122020

Table 3.14. Oxidation of aliphatic alkenes, natural products and their derivatives[a]



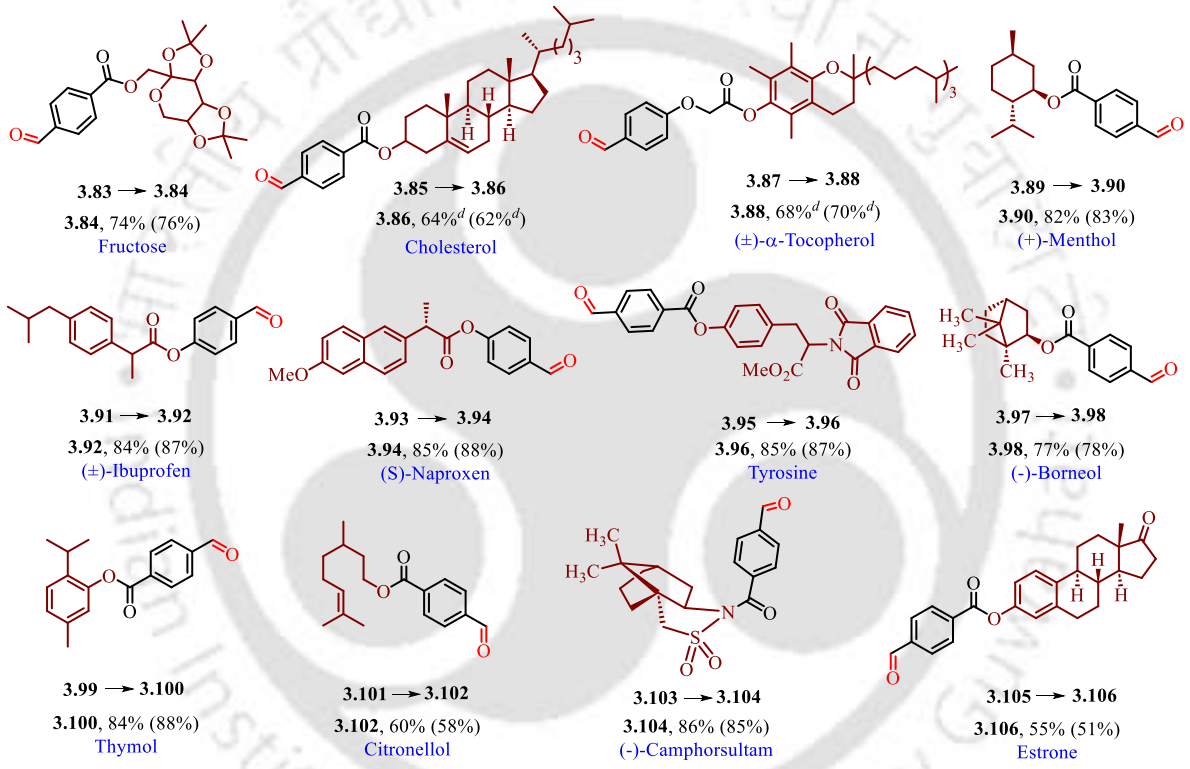
[a]Reaction conditions: substrate (1 mmol), **Ru-1** (0.1 mol%), $NaIO_4$ (3 mmol) in $MeCN/CH_2Cl_2/H_2O$ (1:1:3; 1.5 mL), 40 ºC, 2 h. Isolated yield. [b]with 1 ppm **Ru-1** catalyst loading. [f]with reaction time = 8 h. [g]yields are determined by GC analysis by using dodecane as an internal standard. [h]along with 32% starting material was recovered. The parenthesis yield represents the reaction conditions: substrate (1 mmol), **Ru-4** (0.1 mol%), $NaIO_4$ (2 mmol) and $NaIO_3$ (1 equiv.) in $MeCN/CH_2Cl_2/H_2O$ (1:1:3; 1.5 mL), 40 ºC, 30 min. Isolated yield.

to give the corresponding methyl ketone **3.74** in a highly chemoselective manner. Then, successful oxidative functionalization of abundant biomass feedstock[13,14] methyl oleate **3.75** to the corresponding aldehyde **3.76** and 1-nonanal **3.77** and unsaturated fatty alcohol **3.78** to 9-hydroxynonanal **3.79** and 1-nonanal **3.77**, indicating the usefulness of the current protocol under mild conditions. It is worth mentioning that resulting

TH-3565_186122020

9-hydroxynonanal **3.79** is extensively used in the manufacture of artificial lemon oil and its ester derivative **3.76** is also used in perfumery and flavors. Further effort has been devoted to the soybean oil-derived biodiesel[15] methyl soyate **3.80**, leading to the formation of aldehyde **3.76** in good yield. Notably, in both cases, neither the ester group (entry 14, Table 3.14) nor primary alcohol (entry 13, Table 3.14) moiety is affected by oxidative conditions, indicating excellent functional group tolerance. Next, fat-soluble vitamer so called Vitamin K1 **3.81** was tested under the optimized protocol and gladly gave valuable hexahydrofarnesyl acetone **3.82** with high efficiency. Compound **3.81** is considered as a member of sesquiterpenoids and used in jasmine compositions.[16]

Table 3.15. Scope of styrene derivatives design with biologically relevant motifs[a]



[a]Reaction conditions: substrate (1 mmol), **Ru-1** (0.1 mol%), $NaIO_4$ (3 mmol) in $MeCN/CH_2Cl_2/H_2O$ (1:1:3; 1.5 mL), 40 ºC, 2 h. Isolated yield. [d]with 1 mol% catalyst. The parenthesis yield represents the reaction conditions: substrate (1 mmol), **Ru-4** (0.1 mol%), $NaIO_4$ (2 mmol), and $NaIO_3$ (1 equiv.) in $MeCN/CH_2Cl_2/H_2O$ (1:1:3; 1.5 mL), 40 ºC, 30 min. Isolated yield.

Notably, this catalytic system showed remarkable activity not only in the conversion of styrene but also in the conversion of representative natural products **3.62**, **3.73**, and **3.81** by 1 ppm catalyst loading. Encouraged by the performance of the catalyst, we further expanded its scope using highly functionalized substrates with complex molecular settings. It suggests that the catalytic process is more beneficial than the ozonolysis technique.[3] A range of biologically relevant motifs (BRM) were targeted and were independently subjected to the optimized reaction conditions, afforded the corresponding aldehyde containing fructose **3.84**, cholesterol **3.86**, (±)-α-tocopherol

TH-3565_186122020

3.88, (+)-menthol **3.90**, (±)-ibuprofen **3.92**, (*S*)-naproxen **3.94**, protected tyrosine **3.96**, (-)-borneol **3.98**, thymol **3.100**, citronellol **3.102**, (-)-camphorsultam **3.104** and estrone **3.106** moiety without any structural (chemical and stereochemical) changes of the complex architecture (Table 3.15).

3.3.5. Impact of annulated backbone in the catalysis

To understand the effect of bidentate C_{NHC}^C ligand in oxidation chemistry, non-annulated C_{NHC}^$C_{carbanion}$ ligand $\mathbf{L^2}$ and control ligands with annulated C_{NHC}^N donor ligand $\mathbf{L^3}$ containing ruthenium complexes **Ru-2** and **Ru-3**, respectively were tested into the conversion of styrene using 1 mol% of catalyst loading under the reaction conditions.

As shown in the kinetic profiles in Figure 3.4, complexes **Ru-2** and **Ru-3** showed low activity in the first 30 minutes and the initial rate of the reaction was order of magnitude lower than the complex **Ru-1** under identical conditions. The difference in reaction rate is attributed to the effect of the ligand backbone in the corresponding complexes. Complex **Ru-1** is 5-fold faster than the non-annulated cyclometalated complex **Ru-2**. Complex **Ru-3** exhibited less activity in olefin oxidation possibly due to the weaker *σ*-donating ability of the nitrogen atom in C_{NHC}^N motif. Hence these results suggest that the combination of rigid *π*-conjugated fused imidazo[1,5-*a*]quinolin-2-ium framework and hard carbanion donor site greatly favour the oxidative cleavage of olefins possibly *via* the effective stabilization of high-valent ruthenium(VI)-*cis*-dioxo species in the catalytic process.

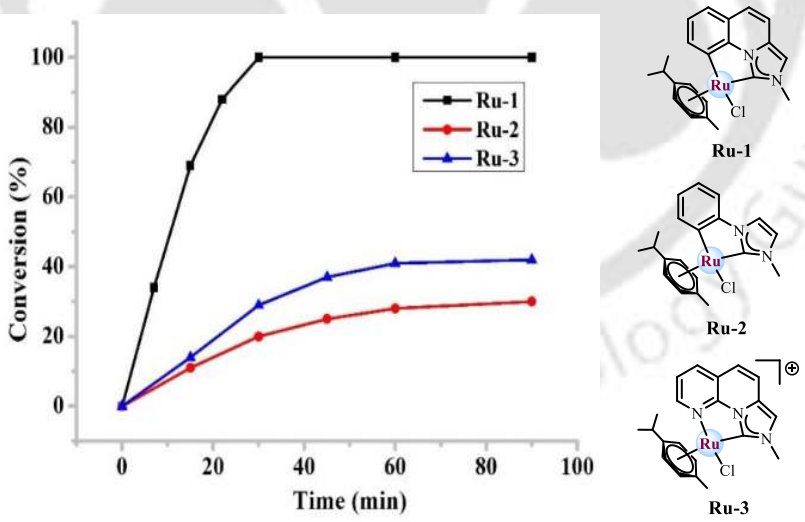


Figure 3.4. Comparison of time-conversion profiles for the olefin oxidation of styrene using different catalysts. *Reaction conditions:* styrene (1 equiv.), complex ***cat.*** (1 mol%), $NaIO_4$ (3 equiv.) in $MeCN/CH_2Cl_2/H_2O$ (1:1:3; 1.5 mL), 40 ºC. Conversion of styrene to benzaldehyde was determined by GC analysis relative to an external standard (anisole).

TH-3565_186122020

Similarly, to understanding the impact of bidentate C_{NHC}^$C_{carbanion}$ ligand **L**^{4} in the catalysis, non-annulated C_{NHC}^$C_{carbanion}$ ligand **L**^{2} and control ligand **L**^{3} with C_{NHC}^N motif containing ruthenium complexes **Ru-2** and **Ru-3**, respectively were tested in the conversion of styrene using 1 mol% of catalyst loading under the reaction conditions. The former indicates the importance of the annulated backbone in the ruthenium complex and the latter suggests the significance of the carbanionic donor site in the chelating arm (Figure 3.5). Kinetic studies suggest that a combination of rigid π-conjugated fused imidazo[1,5-*a*]quinoxalin-2-ium framework and hard carbanion donor site greatly favor the oxidative cleavage of olefins possibly *via* the effective stabilization of high-valent ruthenium(VI)-*cis*-dioxo species in the catalytic process.

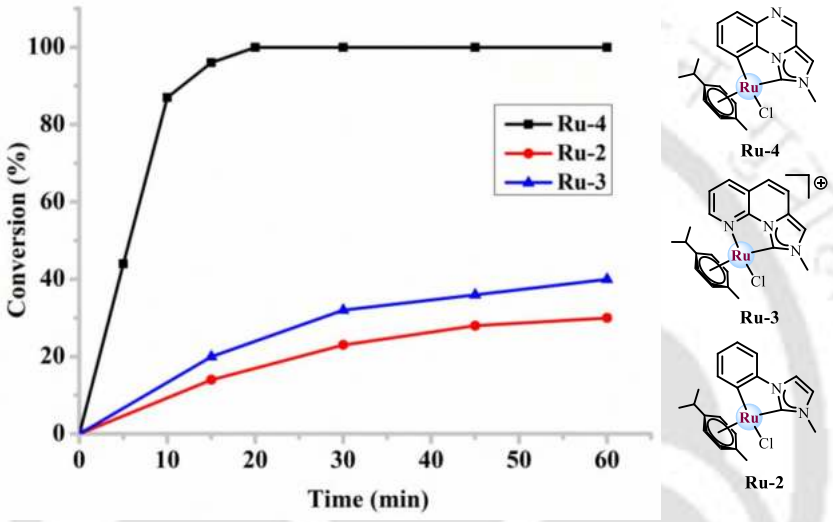


Figure 3.5. Comparison of time-conversion profiles for the olefin oxidation of styrene using different catalysts. *Reaction conditions:* styrene (1 equiv.), complex ***cat.*** (1 mol%), $NaIO_4$ (2 equiv.), $NaIO_3$ (1 equiv.) in MeCN/CH_2Cl_2/H_2O (1:1:3; 1.5 mL), 40 ºC. Conversion of styrene to benzaldehyde was determined by GC analysis relative to an external standard (anisole).

3.3.6. Mechanistic investigation

3.3.6.1. Effect of added *para*-cymene and different arenes

To check the effect of *para*-cymene dissociation on the catalytic activity of **Ru-1**, a control experiment was conducted by adding excess *para*-cymene into the reaction mixture (Figure 3.6) and monitoring the product formation. The yield of the aldehyde was decreased by adding *para*-cymene. A similar low yield of aldehyde was also obtained having electron-rich arenes. In contrast, the yield of the products was unchanged by adding electron-deficient arenes. These results suggest the possibility of reversible loss of *para*-cymene under the reaction conditions. It is worth mentioning that *para*-cymene was found to remain unreacted under the reaction conditions. In a similar

TH-3565_186122020

way for the complex **Ru-4**, the effect of added *para*-cymene and different arenes was also studied as shown in Figure 3.7.

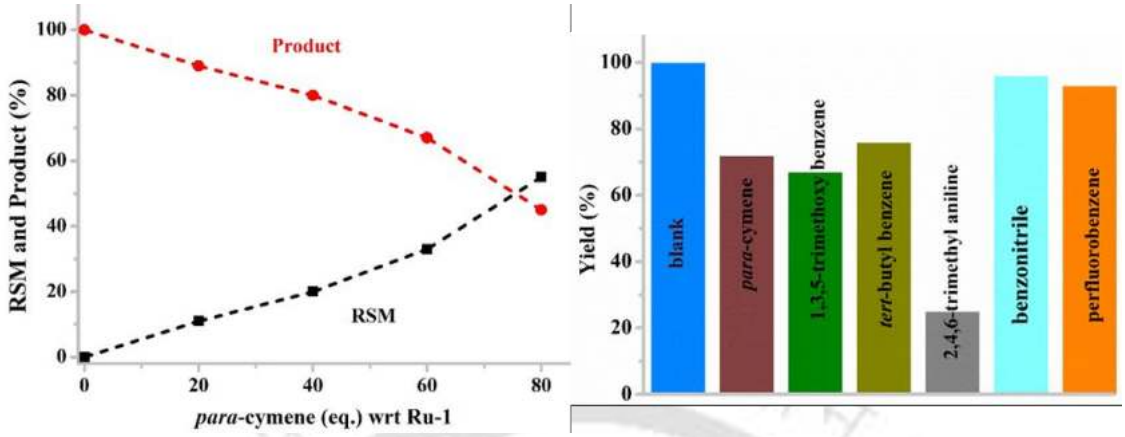


Figure 3.6. Effect of added *para*-cymene (left) and different arenes (right) on the oxidation of styrene (RSM = recovered starting material). *Reaction conditions:* styrene (0.4 mmol), *p*-cymene (x equiv.), **Ru-1** (0.1 mol%), $NaIO_4$ (1.2 mmol) in $CH_3CN/CH_2Cl_2/H_2O$ (1:1:3; 1.5 mL) at 40 °C for 2 h (for left figure). *Reaction conditions:* styrene (0.4 mmol), arenes (60 equiv. wrt to **Ru-1**), **Ru-1** (0.1 mol%), $NaIO_4$ (1.2 mmol) in $CH_3CN/CH_2Cl_2/H_2O$ (1:1:3; 1.5 mL) at 40 °C for 2 h (for right figure).

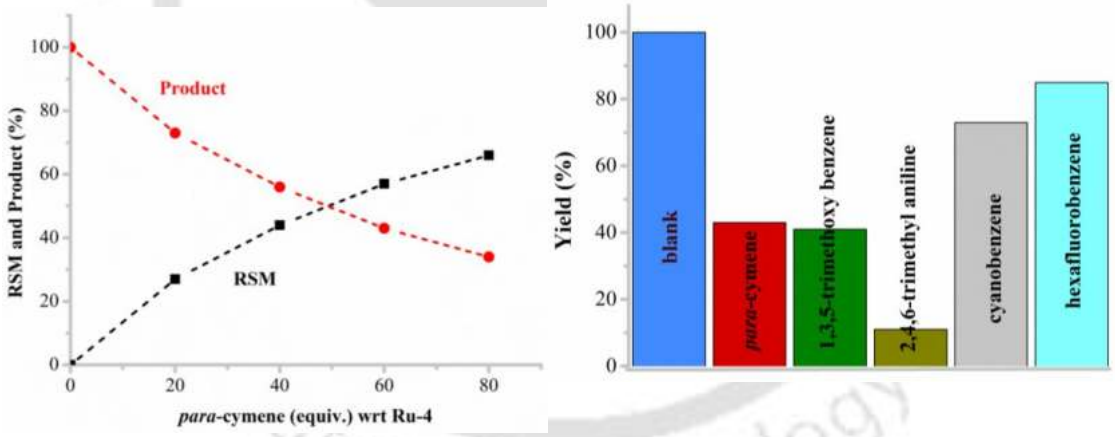
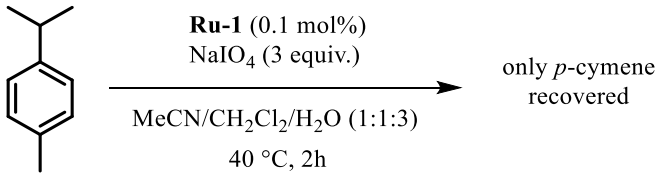


Figure 3.7. Effect of added *para*-cymene (left) and different arenes (right) on the oxidation of styrene (RSM = recovered starting material). *Reaction conditions:* styrene (0.4 mmol), *p*-cymene (x equiv.), **Ru-4** (0.1 mol%), $NaIO_4$ (0.8 mmol), $NaIO_3$ (0.4 mmol) in $CH_3CN/CH_2Cl_2/H_2O$ (1:1:3; 1.5 mL) at 40 °C for 30 min (for left figure). *Reaction conditions:* styrene (0.4 mmol), arenes (60 equiv. wrt to **Ru-4**), **Ru-4** (0.1 mol%), $NaIO_4$ (0.8 mmol), $NaIO_3$ (0.4 mmol) in $CH_3CN/CH_2Cl_2/H_2O$ (1:1:3; 1.5 mL) at 40 °C for 30 min (for right figure).

Fate of *para*-cymene under oxidative conditions

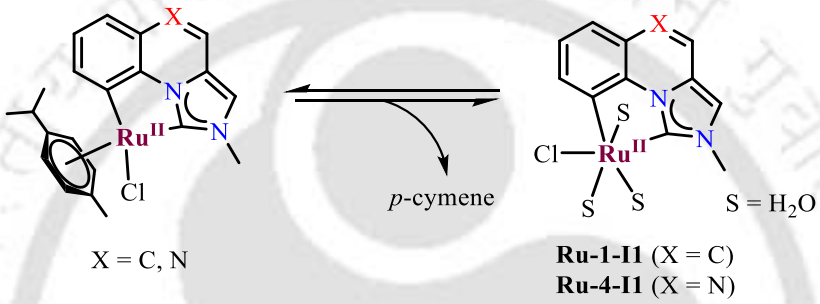
TH-3565_186122020



Scheme 3.6. Oxidation of *p*-cymene

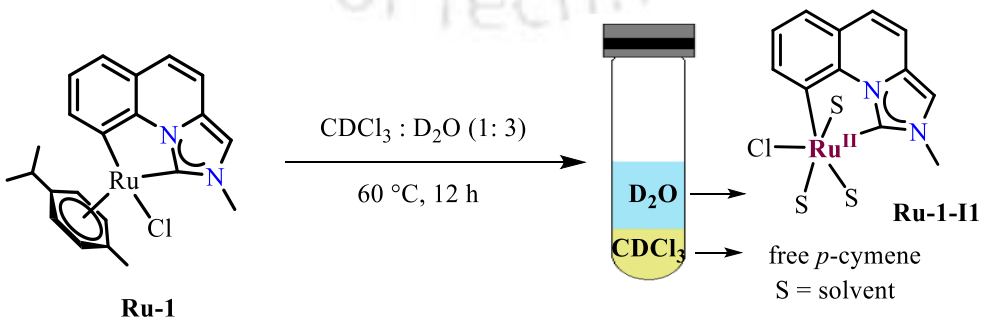
To understand the effect of free *para*-cymene in the conditions, I have performed the reaction with *para*-cymene under standard conditions. GC analysis shows that there were no any conversions and only the *para*-cymene was recovered.

These results suggest that possibly reversible loss of *para*-cymene under the reaction conditions and *para*-cymene was found to remain unreacted under the conditions.



3.3.6.2. Spectroscopic characterization of active catalyst Ru-1-I1

In order to characterize the active ruthenium (II) species in the catalytic process, I performed the reaction with **Ru-1** at 60 °C in a $CDCl_3$ /D_2O (1:3) solvent mixture, the free *p*-cymene was found in the $CDCl_3$ layer and failed to obtain solvent-coordinated active ruthenium(II) species in the aqueous layer due to broadness of the peaks in the ^1H NMR even after several trials. However, the corresponding species was confirmed by ESI-HRMS analysis which showed signals at *m/z* = 356.0448 $[M + CH_3CN + CH_3OH]^+$ and 397.1431 $[M + 2(CH_3CN) + CH_3OH]^+$, respectively, corresponding to the solvent coordinated ruthenium(II) species **Ru-1-I1** (Figure 3.8).



Scheme 3.7. Reaction of **Ru-1** with $CDCl_3$:D_2O mixture

TH-3565_186122020

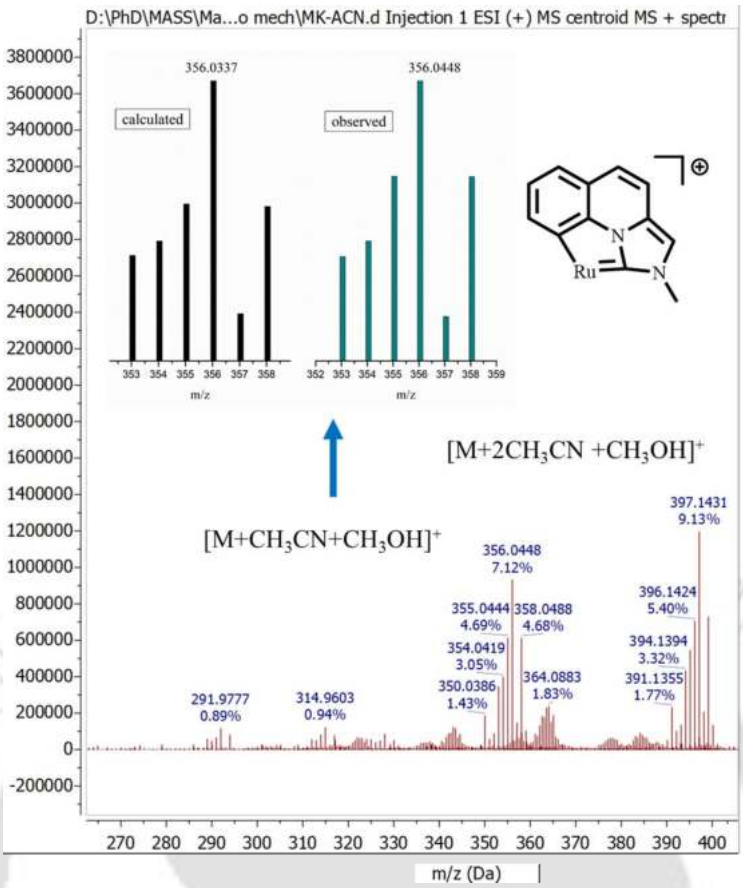
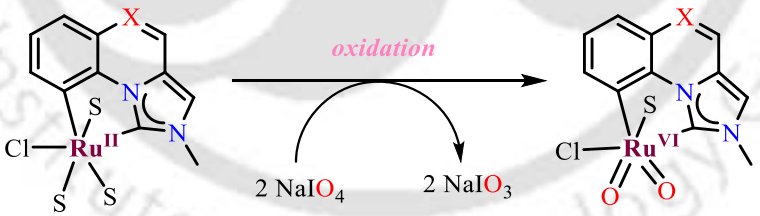


Figure 3.8. HRMS (ESI) spectrum of solvent coordinated Ru(II)-complex (**Ru-1-I1**)

3.3.6.3. Spectroscopic characterization of high-valent ruthenium(VI)-dioxo species



X = C, **Ru-1-I1**
X = N, **Ru-4-I1**

X = C, **Ru-1-I2**
X = N, **Ru-4-I2**

In order to gain further insight into the proposed intermediates, I performed a stoichiometric reaction between complex **Ru-1**, $NaIO_4$ (aq), and styrene (1:1:1.5 molar ratio) at room temperature in acetonitrile, and immediately injected into the ESI-HRMS; which showed a signal at *m/z* = 314.9703 corresponding to high-valent ruthenium(VI) dioxo species **Ru-1-I2**, $[Ru(\mathbf{L^1})(=O)_2]^+$ i.e. [**Ru-1-I2** – Cl]$^+$ (Figure 3.9). The presence of the parent moiety suggested the stability of the NHC-Ru backbone under catalytic conditions.

TH-3565_186122020

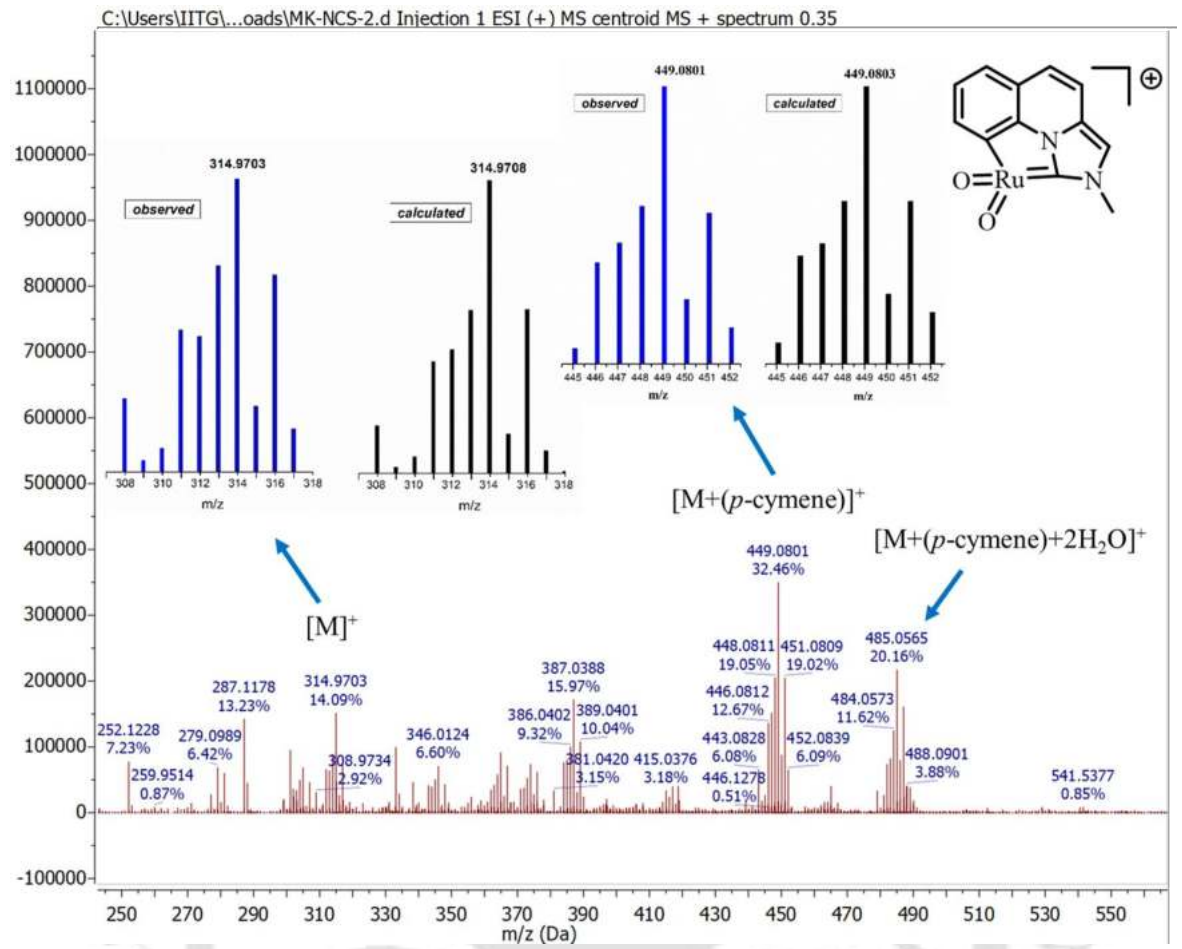


Figure 3.9. HRMS (ESI) spectrum of ruthenium(VI)-*cis*-dioxo species **Ru-1-I2** for **Ru-1**

Likewise for **Ru-4**, a stoichiometric reaction was performed between complex **Ru-4**, $NaIO_4$ (aq), and styrene (1:1:1.5 molar ratio) at room temperature in acetonitrile, and immediately injected into the ESI-HRMS; which showed a signal at *m/z* = 315.9662 corresponding to high-valent ruthenium(VI) dioxo species **Ru-4-I2**, $[Ru(\mathbf{L^4})(=O)_2]^+$ i.e. $[\mathbf{Ru\text{-}4\text{-}I2} - Cl]^+$ (Figure 3.10).

TH-3565_186122020

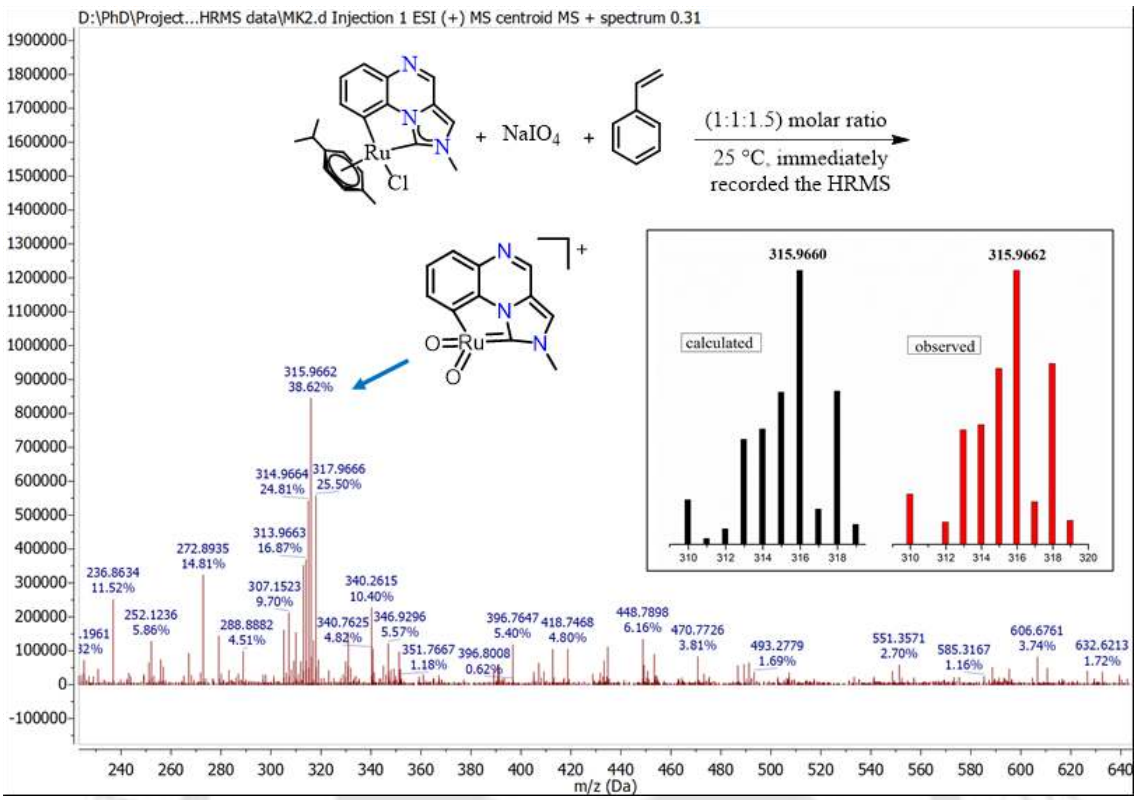
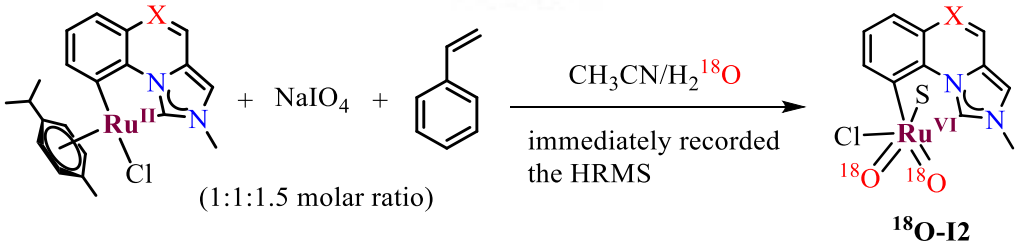


Figure 3.10. HRMS (ESI) spectrum of ruthenium(VI)-*cis*-dioxo species **Ru-4-I2** for **Ru-4**

^{18}O Isotope labeling experiment

To gain further insight into the Ru(VI)-dioxo intermediate **Ru-1-I2**, we carried out the reaction between complex **Ru-1**, $NaIO_4$ (aq), and styrene (1:1:1.5 molar ratio) in $H_2{}^{18}O$ and acetonitrile mixture at room temperature, and immediately analyzed the ESI-HRMS. The signal at *m/z* = 318.9782 corresponding to ^{18}O labeled high-valent ruthenium(VI) dioxo species **^{18}O-I2**, $[Ru(\mathbf{L^1})(=^{18}O)_2]^+$ was observed (Figure 3.11). Similarly for the complex **Ru-4**, the signal at *m/z* = 319.9729 corresponding to ^{18}O labeled high-valent ruthenium(VI) dioxo species **^{18}O-I2**, $[Ru(\mathbf{L^4})(=^{18}O)_2]^+$ was observed (Figure 3.12). The study suggests the exclusive incorporation of the ^{18}O label in the complex. Furthermore, the signal at *m/z* = 141.069 likely corresponds to ^{18}O labeled carbonyl compound ($PhCH^{18}O + H^+ + CH_3OH$).



Scheme 3.8. ^{18}O labeled water experiments

TH-3565_186122020

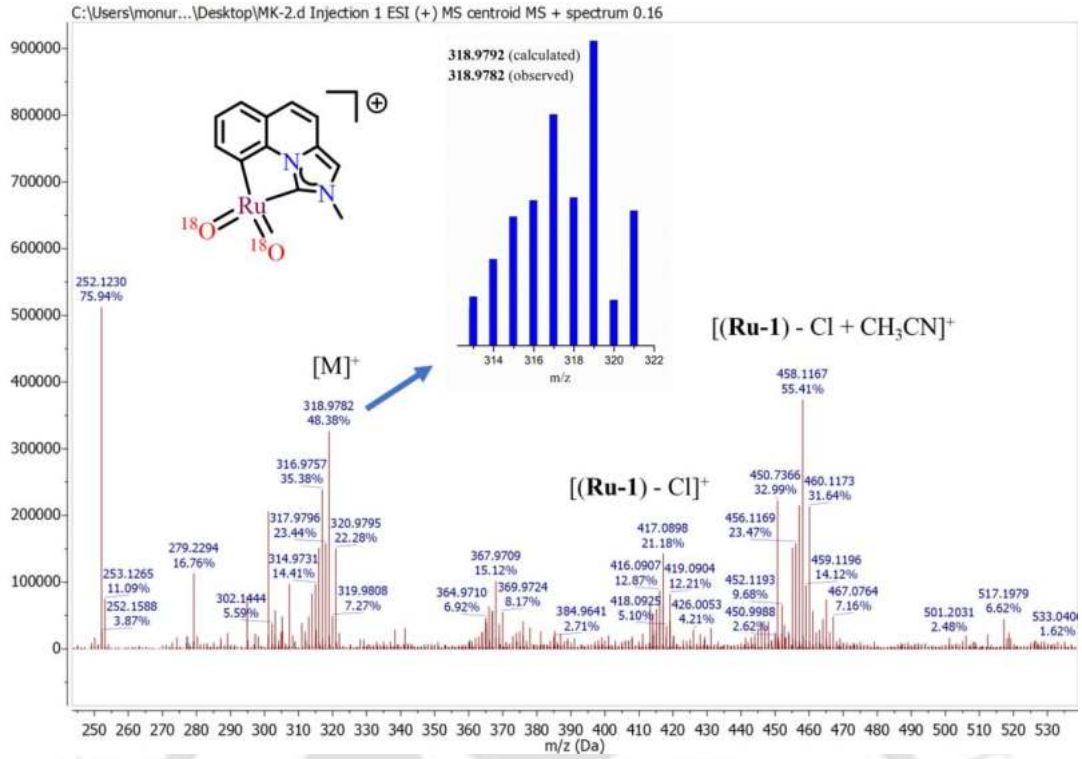


Figure 3.11. HRMS (ESI) spectrum of ^{18}O labeled Ru(VI)-dioxo species (**^{18}O-I2**) for **Ru-1**

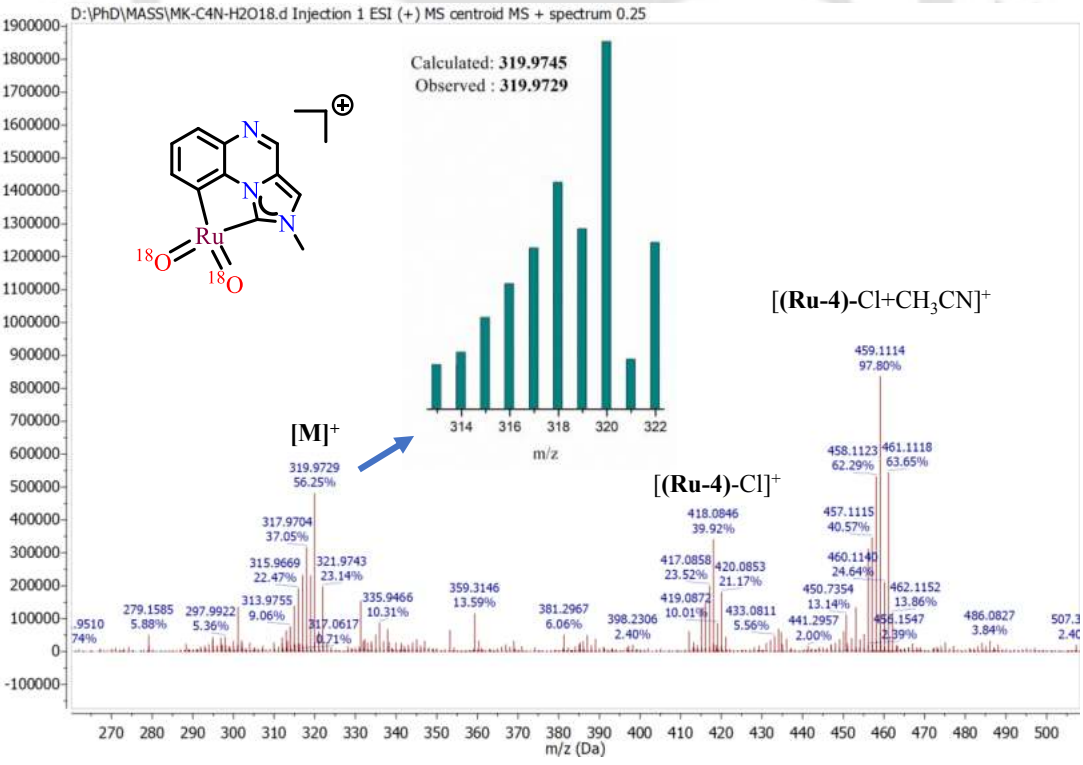


Figure 3.12. HRMS (ESI) spectrum of ^{18}O labeled Ru(VI)-dioxo species (**^{18}O-I2**) for **Ru-4**.

TH-3565_186122020

XPS study

Then XPS analysis was performed for the intermediate Ru(VI)-*cis*-dioxo species **Ru-1-I2** of **Ru-1**. We examined the oxidation state of Ru by analysis of Ru 3*d* by core-level X-ray photoelectron spectroscopy (XPS), which was fitted with spin-orbital split $3d_{5/2}$ and $3d_{3/2}$. Two sets of XPS peaks appeared at 283.0 and 285.1 eV for the binding energies of the $3d_{5/2}$ and $3d_{3/2}$ components, respectively, indicating that Ru is in the +6 oxidation state (Figure 3.13).[17]

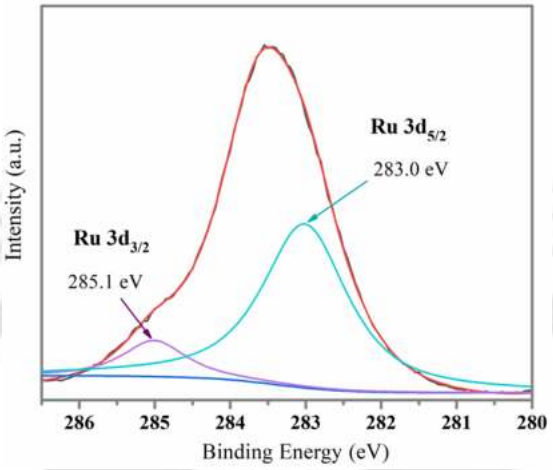


Figure 3.13. Binding energies of XPS spectra for the analysis of valent states of **Ru-1-I2**

Furthermore, this high-valent ruthenium(VI) dioxo species **Ru-1-I2** was characterized by IR. The presence of new absorption peaks at 764, 803, and 918 cm^{-1} suggests the symmetric and asymmetric stretching for the Ru(VI)-*cis*-dioxo intermediate (see the experimental section 3.5.7 for details).[7b]

3.3.6.4. UV-Vis spectroscopic studies for the metallacycle species

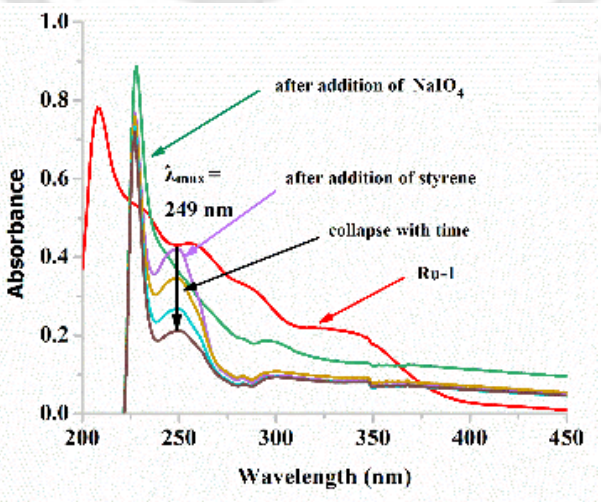


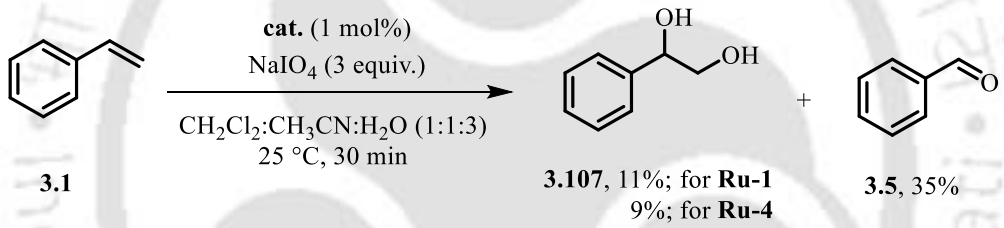
Figure 3.14. UV-Vis absorption spectra for **Ru-1** (red), after the addition of $NaIO_4$ (green) and after the addition of styrene (purple), and the collapse of the absorption maximum at ~249 nm with time.

TH-3565_186122020

To gain insight into the formation of a five-membered metallacycle intermediate by the reaction of alkene and ruthenium *cis*-dioxo species, a UV-Vis spectroscopic study was carried out (Figure 3.14). Adding styrene into the solution of complex **Ru-1** and $NaIO_4$, appeared a new band at λ_{max} = 249 nm. Based on the earlier reports[7a,18] we postulated the new band at λ_{max} = 249 nm for the five-membered metallacycle intermediate. The absorption maxima were gradually decreased over time. This might be due to the collapse of this metallacycle to the C–C cleaved product.

Proof for the formation of 1,2-diol

When styrene oxidation was carried out at room temperature with 1 mol% of **Ru-1** with a shorter reaction time (30 minutes), phenyl-1,2-diol **3.107** was intercepted at partial conversion and identified by ^1H and ^{13}C NMR, suggesting the possible involvement of 1,2-diol under the reaction conditions (Scheme 3.9). Since diols are known to react with $NaIO_4$ spontaneously with C–C bond cleavage, the study suggests that the ruthenium complex is mostly catalyzing diol formation. The same reaction was attempted for **Ru-4**, with a 9% yield of **3.107**.



Scheme 3.9. Isolation of 1-phenyl-1,2-ethanediol

3.3.7. Kinetic studies

Determination of the order dependency of catalyst precursor, $NaIO_4$ and alkene

To investigate the rate-determining step of the reaction in detail, a series of kinetic experiments were carried out and the order with respect to Ru(II) precatalyst (**Ru-1**), oxidant $NaIO_4$ and styrene was determined (see details in experimental section 3.5.8). The kinetic study revealed a first-order rate dependence on the concentration of Ru(II) precatalyst and styrene, respectively, and a zero-order rate dependency on the amount of oxidant. These data suggested that the concentrations of active catalytic species and the alkene are kinetically relevant, and oxidant $NaIO_4$ might not be involved in the rate-determining step.

TH-3565_186122020

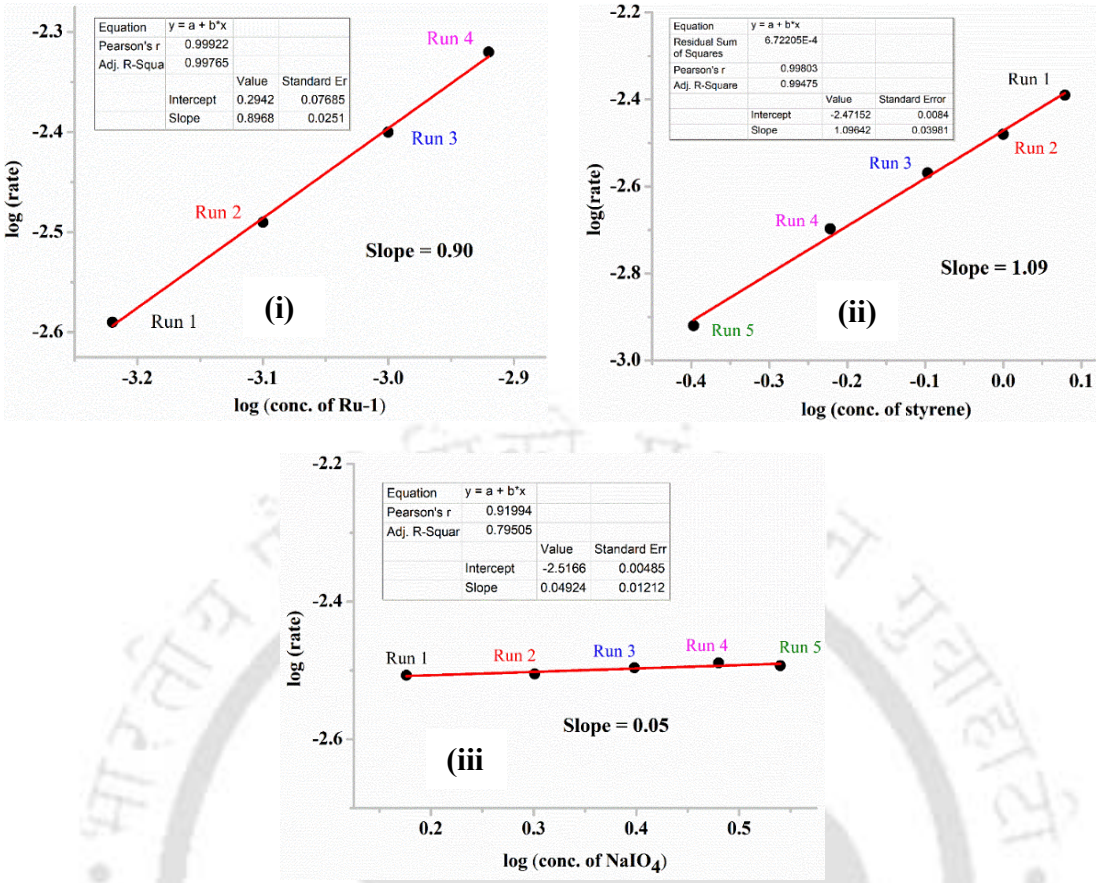
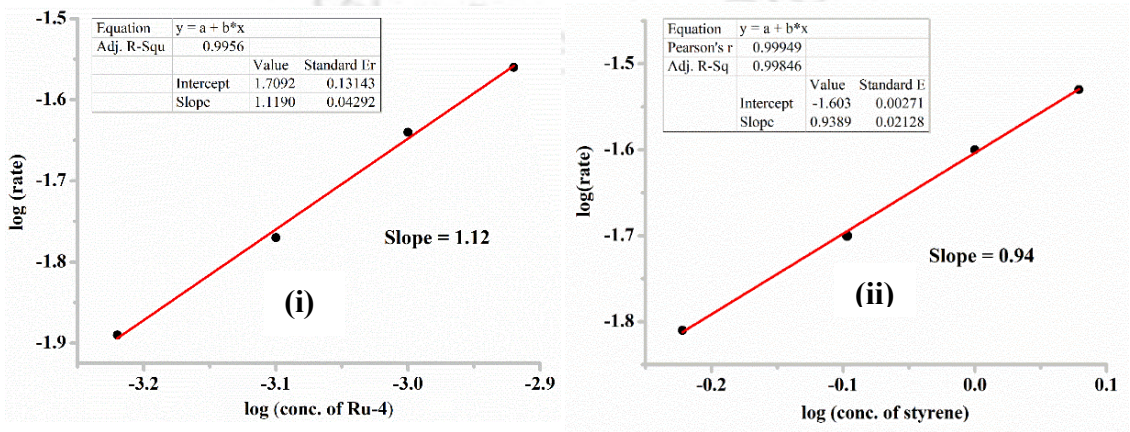


Figure 3.15. Dependence of initial rate (i) with respect to **Ru-1**, (ii) with respect to styrene and (iii) with respect to $NaIO_4$

Similarly, a series of kinetic experiments were also carried out for the complex **Ru-4** and the order with respect to Ru(II) precatalyst, $NaIO_4$, $NaIO_3$ and styrene was determined (Figure 3.16). The kinetic study revealed a first-order rate dependence on the concentration of Ru(II) precatalyst and styrene, respectively, and a zero-order rate dependency on the amount of oxidant $NaIO_4$. Nevertheless, the concentration of $NaIO_3$ has a certain impact on the kinetics because of a partial order of 0.3.



TH-3565_186122020

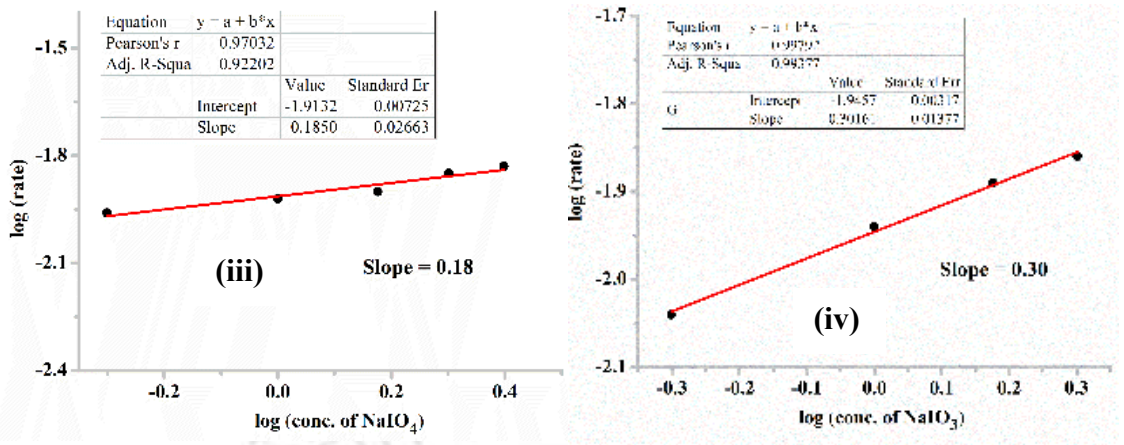


Figure 3.16. Dependence of initial rate (i) with respect to **Ru-4**, (ii) with respect to styrene, (iii) with respect to $NaIO_4$ and (iv) with respect to $NaIO_3$

Kinetic Hammett Studies

To study the electronic influence in the reaction, the Hammett correlation study was performed using various substituted styrenes under standard reaction conditions (Figure 3.17). A negative slope of -1.74 (for **Ru-1**) and -1.42 (for **Ru-4**) suggested the development of positive charge in the α-carbon atom of styrene in the transition state, which is stabilized by the electron-donating substituents (see details in the experimental section 3.5.8).

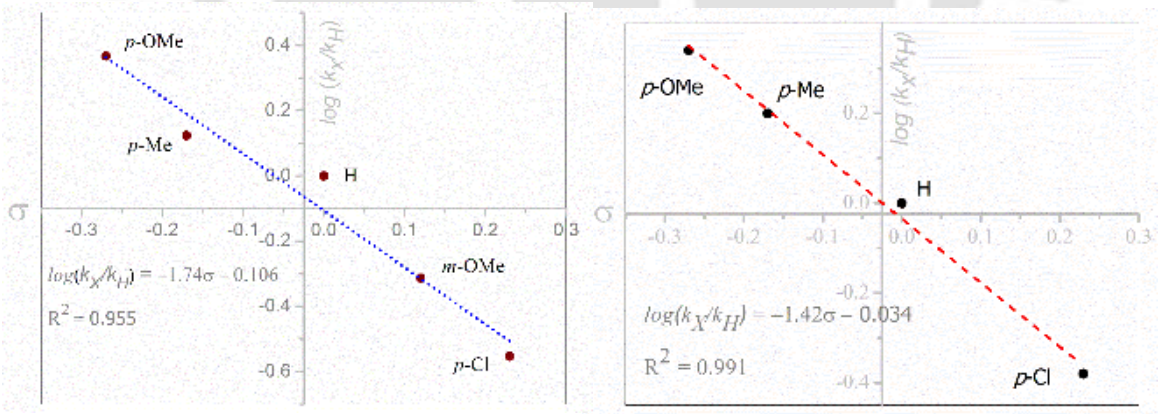


Figure 3.17. Hammett plot for **Ru-1** (left), **Ru-4** (right).

Entropy of activation

Further, the effect of temperature on the rate of the reaction was examined by using Eyring analysis. The Eyring plot of ln(*k*/*T*) versus 1/*T* in the temperature range of 10 °C to 40 °C was used to determine the activation parameters. The activation parameters were obtained using rate constants from these kinetic experiments and were found to be

TH-3565_186122020

$\Delta H^{\ddagger} = 11.14 \pm 0.7$ kcal mol^{-1} and $\Delta S^{\ddagger} = -32.1 \pm 2.3$ cal mol^{-1} K^{-1} for **Ru-1** (see details in experimental sections 3.5.8) and $\Delta H^{\ddagger} = 16.56 \pm 1.1$ kcal mol^{-1} and $\Delta S^{\ddagger} = -11.84 \pm 0.7$ cal mol^{-1} K^{-1} for **Ru-4** (see details in experimental sections 3.5.8). In both cases, the large and negative $\Delta S^{\ddagger}$ values suggested the involvement of an associative process in the turnover-limiting step and ruled out the possibility of reductive elimination in the rate of the reaction.[7a,7b] Based on the thermodynamic activation parameters and order dependence, one can postulate that the association possibly occurs with ruthenium-*cis*-dioxo complexes and alkenes.

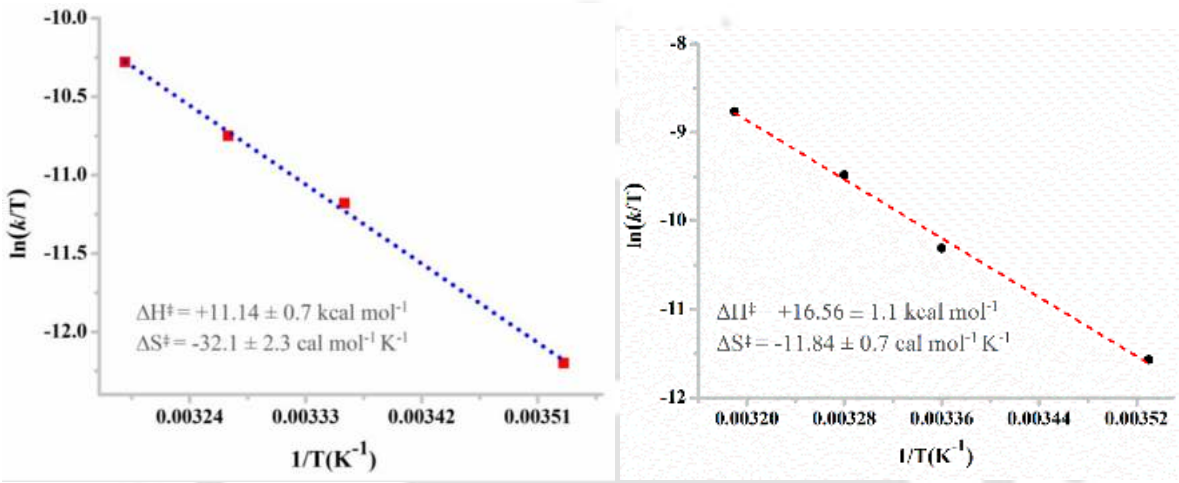


Figure 3.18. Arrhenius-Eyring plot for **Ru-1** (left), **Ru-4** (right).

Effect of by-product $NaIO_3$ on the rate of the reaction

Initial kinetic study was executed with 2 equiv. of $NaIO_4$ and compared the kinetic data to that with 1 equiv. $NaIO_4$ (i.e., 3 equiv. $NaIO_4$) and also in the presence of 1 equiv. $NaIO_3$ (i.e., 2 equiv. $NaIO_4$ and 1 equiv. $NaIO_4$). It was found that the rate of the reaction was increased by ~2.5-fold with $NaIO_3$.

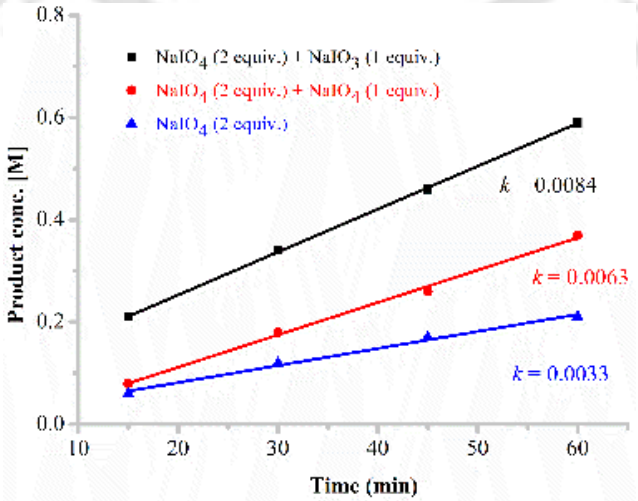


Figure 3.19. Effect of $NaIO_3$ on the reaction rate

TH-3565_186122020

3.3.8. Computational studies

To understand the pathway of the reaction mechanism, DFT calculation was carried out for the reaction catalyzed by the complex **Ru-1** (Figure 3.20). The initial optimized structure of Ru^{VI}-*cis*-dioxo intermediate **I2_Cl** undergoes concerted [3+2] cycloaddition reaction with ethylene to form five-membered Ru^{IV}-metalladioxo intermediate **I3_Cl** (ΔG = -35.5 kcal/mol) *via* **TS_Cl** with a $\Delta G^{\ddagger}$ of 15.7 kcal/mol. Subsequently, two-electron oxidation occurs across the C−C bond to provide formaldehyde-coordinated Ru^{II}-species **I4_Cl** (ΔG = -33.7 kcal/mol).

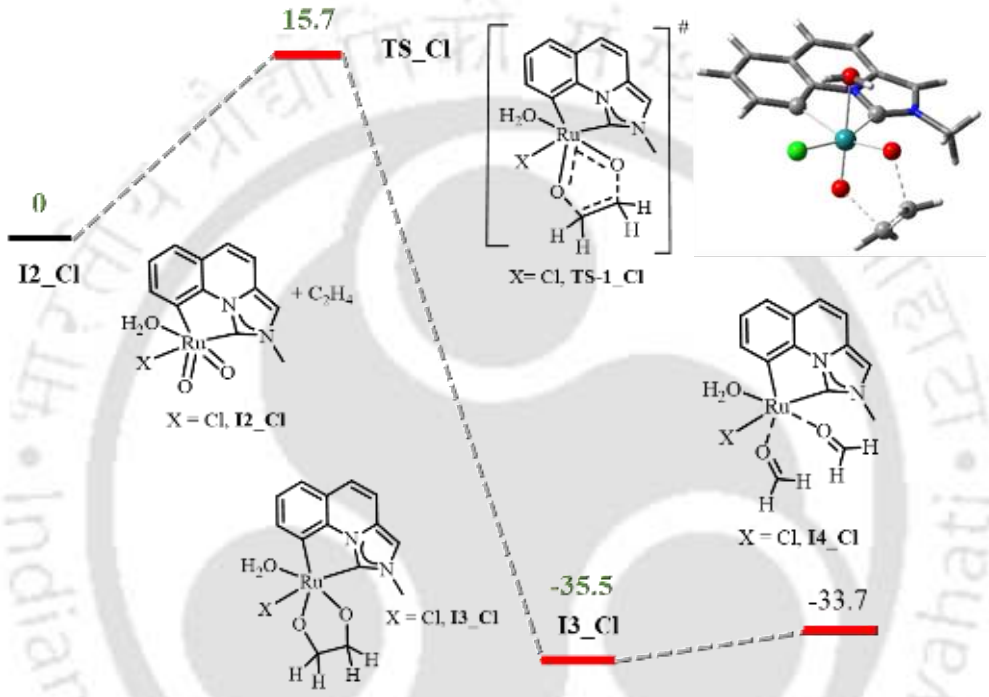


Figure 3.20. Computed reaction profiles for alkene oxidation catalyzed by **Ru-1**. Energies are shown in kcal/mol.

Furthermore, to gain insight into the effect of $NaIO_3$ in the reaction rate and to understand the pathway of the reaction mechanism catalyzed by the complex **Ru-4**, DFT calculation was carried out (Figure 3.21). The initial optimized structure of Ru^{VI}-*cis*-dioxo intermediate **I2_Cl** undergoes concerted [3+2] cycloaddition reaction with ethylene to form five-membered Ru^{IV}-metalladioxo intermediate **I3_Cl** (ΔG = -35.5 kcal/mol) *via* **TS_Cl** with a $\Delta G^{\ddagger}$ of 15.7 kcal/mol. Subsequently, two-electron oxidation occurs across the C−C bond to provide formaldehyde-coordinated Ru^{II}-species **I4_Cl** (ΔG = -34.4 kcal/mol). Likewise, with $NaIO_3$, the **I2_IO3** can form the metalladioxo intermediate **I3_IO3** in an exothermic fashion (ΔG = − 42.1 kcal/mol) *via* **TS_IO3** with an energy barrier of 12.0 kcal/mol, followed by produced the intermediate **I4_IO3** (ΔG = -41.6 kcal/mol). A lower energy barrier and higher exothermic reaction parameter possibly drive the reaction rate for $NaIO_3$.

TH-3565_186122020

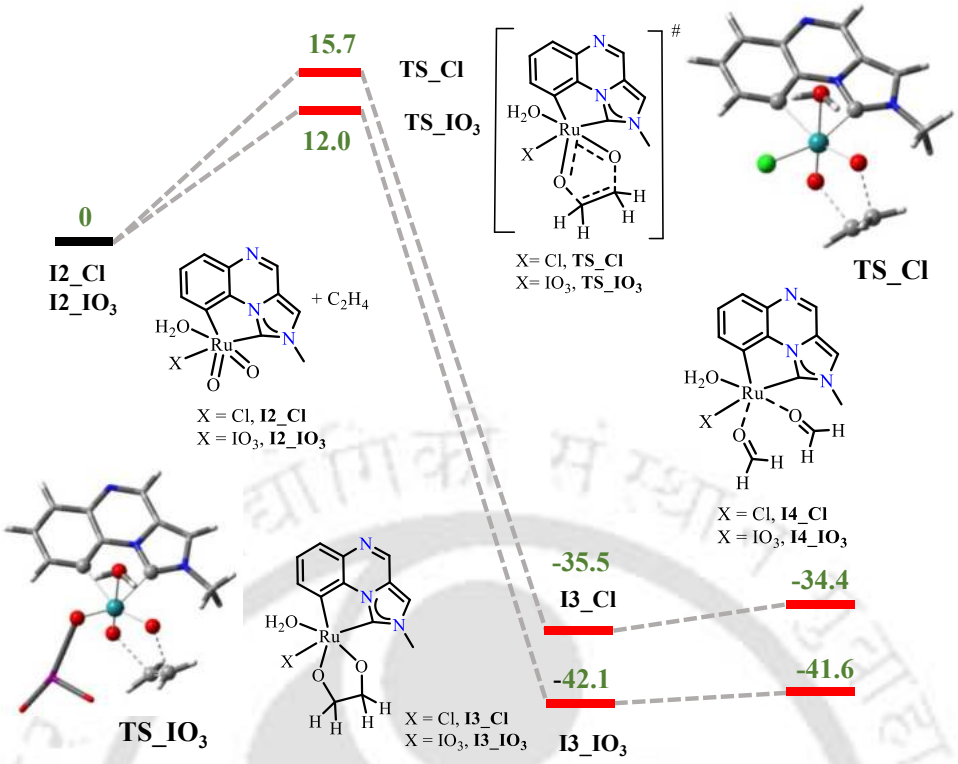
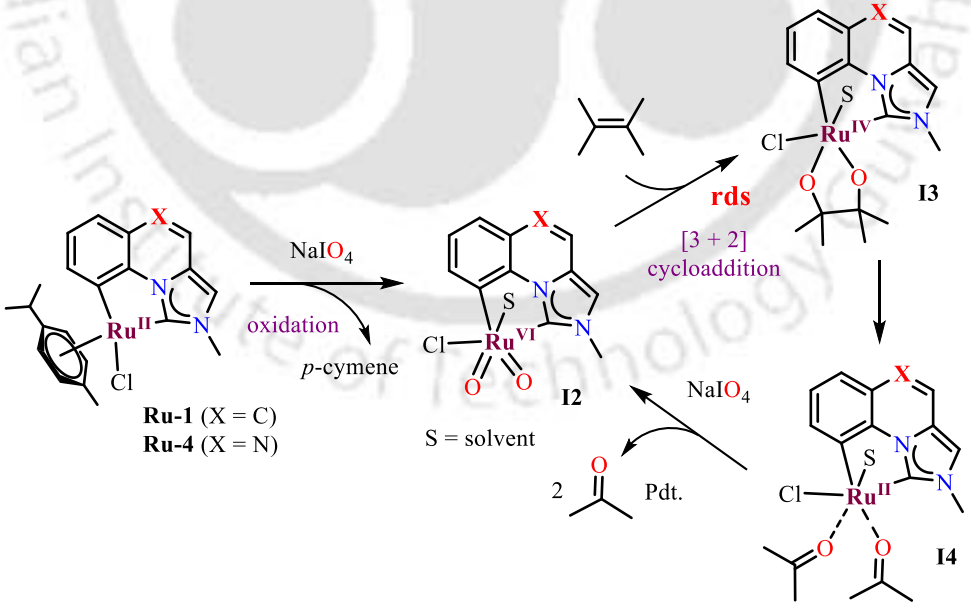


Figure 3.21. Computed reaction profiles for alkene oxidation catalyzed by **Ru-4** w/t $NaIO_3$. Energies are shown in kcal/mol.

3.3.9. Proposed mechanism



Scheme 3.10. Proposed mechanism for the catalytic olefin oxidation

Based on experimental findings and taking previous literature reports,[7] a plausible catalytic cycle is shown in Scheme 3.10. The reaction was initiated by a reversible loss

TH-3565_186122020

of *para*-cymene and the formation of a water-coordinated active Ru^{II} complex **I1**. Complex **I1** was then readily oxidized in the presence of periodate to form high-valent Ru^{VI}-*cis*-dioxo species **I2** and releases sodium iodate. The corresponding intermediate **I2** undergoes a concerted [3+2] cycloaddition reaction with an alkene to produce a Ru^{IV} cycloadduct **I3**. Owing to the strong σ-donating nature of the ligand, the Ru^{IV} center of the cycloadduct **I3** becomes reasonably electron-rich, thus allowing it to proceed in two-electron reduction and cleave the C−C bond to produce the desired carbonyl product.

3.4. Summary

In summary, annulated ImQ-based and ImQx-based cyclometalated ruthenium complexes **Ru-1** and **Ru-4**, respectively, showed unprecedented catalytic activity in the oxidative scission of olefins to carbonyl compounds, reaching turnover numbers of several million and turnover frequencies of 720000 h^{-1}. A simple incorporation of the annulated backbone, corresponding cyclometalated Ru(II)-NHC complexes display significantly outperform state-of-the-art systems. Study suggests that by simply incorporating -N=CH- moiety in the ligand backbone, complex **Ru-4** is 4-fold faster than its non-annulated analogue **Ru-2**. The functional group tolerance is outstanding. This protocol converts simple olefins to highly functionalized substrates including challenging biomass, natural product, sugar, amino acid, and fatty acid-derived substrates. On the basis of kinetic Hammett studies, thermodynamic activation parameters, several control experiments and DFT study, the mechanistic finding demonstrated that [3+2] cycloaddition reaction is the key step in the four-electron olefin oxidation process. In addition, this study underlines the use of by-product $NaIO_3$ in the catalytic efficiency.

3.5. Experimental section

3.5.1. General information

^{1}H, $^{13}C\{^{1}H\}$ and ^{19}F NMR spectra of the compounds were measured in $CDCl_3$ and DMSO-d_6 as a solvent by using TMS as an internal standard. Chemical shifts, δ (in ppm), were reported relative to TMS δ (^{1}H) 0.0 ppm, δ (^{13}C) 0.0 ppm, which was used as the internal reference. Otherwise, the solvent's residual proton resonance and carbon resonance $CDCl_3$: δ (^{1}H) 7.26 ppm, δ (^{13}C) 77.16 ppm; DMSO: δ (^{1}H) 2.5 ppm, δ (^{13}C) 39.52 ppm were used for calibration. Bruker Avance III 600, 500 and 400 spectrometers were used to record the NMR spectra. Chemical shift (δ) values were reported in ppm and spin-spin coupling constant (J) was expressed in Hz and other data were reported as follows: s = singlet, d = doublet, dd = doublet of doublet, dt = doublet of triplet, t = triplet, m = multiplet, q = quartet, p = pentet, br = broad, and brs = broad singlet. MS (ESI-HRMS): Mass spectra were recorded on an Agilent Accurate-Mass Q-TOF LC/MS 6546. GC analyses were performed on a PerkinElmer-Clarus 590 GC instrument fitted with Elite-1 column (30 m length, 0.32 mm ID) using the following method: Injection volume: 1 µL, inlet temperature: 280 °C, FID detector temperature: 280 °C, oven temperature: start at 60 °C hold time 1 min, ramp: 12 °C /min, upto 320 °C, Flow rate (carrier):

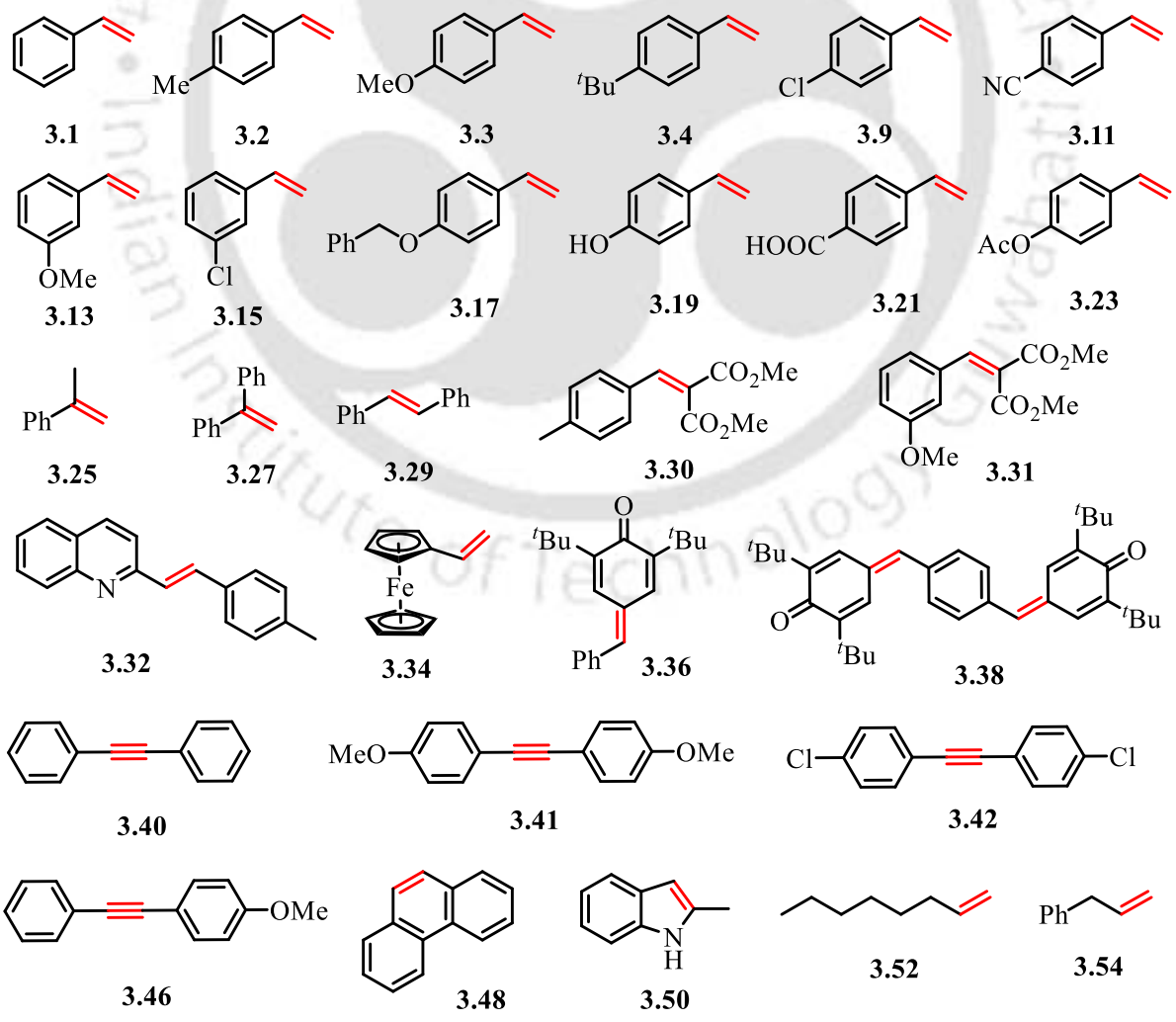
TH-3565_186122020

25 mL/min (N2). Merck silica gel 60-120 mesh and neutral alumina 60-325 mesh were used for column chromatography. All the starting material, ligands, catalyst and their oxidized products were characterized by spectroscopic methods and compared to literature wherever applicable, otherwise stated. All the reactions were carried out in a preheated oil bath unless otherwise mentioned. Completion of reactions was examined by thin layer chromatography carried out on pre-coated Merck silica gel-60 F254 aluminium plates with ultraviolet light (UV) or iodine as visualizing agents.

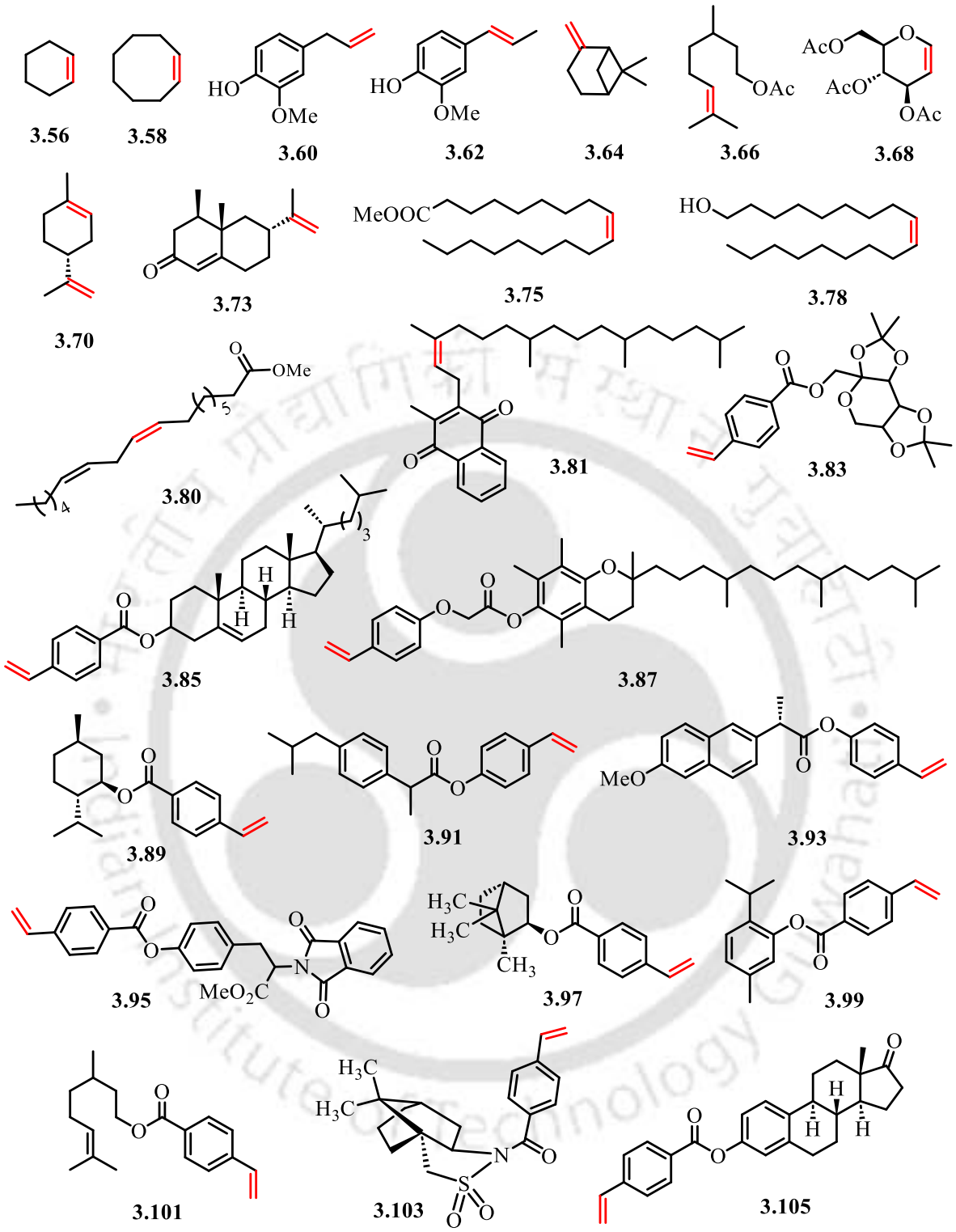
Materials:

Unless otherwise noted, all the reagents were obtained commercially and used without purification. Dichloromethane (CH_2Cl_2), acetonitrile (CH_3CN) and toluene were distilled over CaH_2. $[RuCl_2(p\text{-cymene})]_2$ and Ag_2O were purchased and used as received. Quinoline-2-carbaldehyde, Quinoxaline-2-carbaldehyde and 1,8-naphthyridine-2-carbaldehyde were purchased from BLD Pharm. All other reagents were purchased from various commercial sources and used as received. Analytical and spectral data of all the known compounds exactly match with the reported values.

3.5.2. List and preparation of different alkenes



TH-3565_186122020



All the alkenes and other unsaturated hydrocarbons were purchased from common commercial suppliers like Sigma-Aldrich, Alfa Aesar, Merck, Spectrochem, Avra Synthesis Pvt. Ltd., BLD Pharma and directly used as received without any further purification unless otherwise mentioned. Compounds **3.30-3.31**,[19] **3.32**,[20] **3.38**[21] and **3.66**[22] are synthesized by known procedures. Following the reported method,[23] the alkynes **3.41**, **3.42** and **3.46** were prepared. Following the reported method, the biologically relevant motifs containing styrene derivatives

TH-3565_186122020

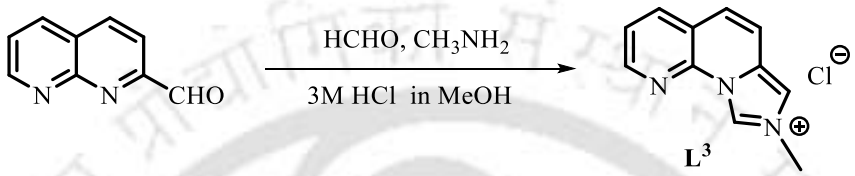
3.83,[24] **3.85**,[24] **3.87**,[25] **3.89**,[25] **3.91**,[26] **3.93**,[27] **3.97**[28] and **3.105**[28] were prepared. Compounds **3.95**, **3.99**, **3.101,** and **3.103** were prepared for the first time following a known procedure.[29]

3.5.3. Synthesis of ligands and ruthenium complexes

Synthesis of ligands

The synthesis of ligand $\mathbf{L^1}$ and ligand $\mathbf{L^2}$ was already discussed in Chapter 2 (see experimental section 2.5.4)

Synthesis of $\mathbf{L^3}$:

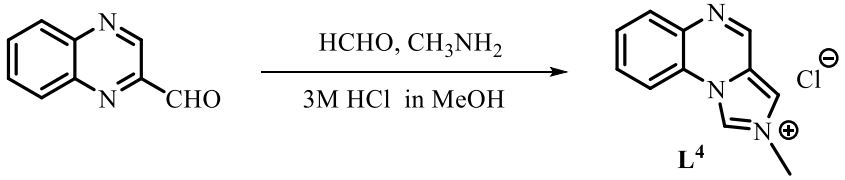


Scheme 3.11. Synthesis of ligand $\mathbf{L^3}$

To a solution of methylamine (1 equiv.) in dry methanol, formalin solution (1.5 equiv.) is added at room temperature and stirred for 15 minutes. At 0 ºC, 3M HCl in MeOH (1.5 equiv.) is prepared in another reaction tube (by adding acetyl chloride (1.5 equiv.) to the reaction tube containing methanol at 0 ºC), then added to the previous reaction mixture, followed by the addition of 1,8-naphthyridine-2-carbaldehyde (1 g, 1 equiv.) and stirred at room temperature for overnight. After completion of the reaction as confirmed by TLC, the crude reaction mixtures are concentrated and placed under a high vacuum. The solid formed was purified by neutral alumina column chromatography (ethyl acetate: methanol 3:2) to get a pure white solid (164 mg, 78%).

^{1}H NMR (500 MHz, DMSO-d_6): δ 10.52 (s, 1H), 8.84 (d, J = 4.5 Hz, 1H), 8.6 (d, J = 7.8 Hz, 1H), 8.36 (s, 1H), 7.86 (dd, J = 7.8, 4.8 Hz, 1H), 7.81 (d, J = 9.6 Hz, 1H), 7.71 (d, J = 9.6 Hz, 1H), 4.23 (s, 3H). ^{13}C NMR (126 MHz, DMSO-d_6): δ 149.5, 140.6, 138.5, 128.9, 128.6, 125.0, 124.9, 119.3, 117.6, 116.5, 37.1. HRMS (ESI) *m/z*: calcd. for $C_{11}H_{10}N_3^+$ [M^+]: 184.0870; found 184.0888.

Synthesis of $\mathbf{L^4}$:



Scheme 3.12. Synthesis of ligand $\mathbf{L^4}$

Ligand $\mathbf{L^4}$ was obtained in a similar method described above for $\mathbf{L^3}$, using quinoxaline-2-carbaldehyde as a starting material. After completion of the reaction as confirmed by TLC, the crude reaction mixtures are concentrated and placed under a high vacuum. The solid formed

TH-3565_186122020

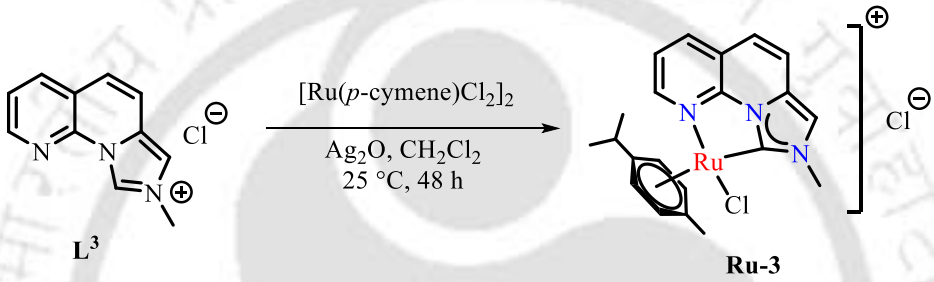
was purified by neutral alumina column chromatography (ethyl acetate: methanol 10:1) to get a pure white solid (1.1 g, 82%).

^{1}H NMR (600 MHz, DMSO-d_6): δ 11.30 (s, 1H), 9.52 (s, 1H), 8.93 – 8.71 (m, 1H), 8.24 – 8.00 (m, 4H), 4.42 (s, 3H). ^{13}C NMR (151 MHz, DMSO-d_6): δ 145.2, 135.7, 130.5, 130.45, 130.36, 129.8, 123.1, 122.6, 121.3, 116.8, 37.4. HRMS (ESI) *m/z*: calcd. for $C_{11}H_{10}N_3^+$ [M$^+$]: 184.0870; found: 180.0874.

Synthesis of ruthenium complexes

The synthesis of complex **Ru-1** and complex **Ru-2** was already discussed in Chapter 2 (see experimental section 2.5.4)

Synthesis of Ru-3:



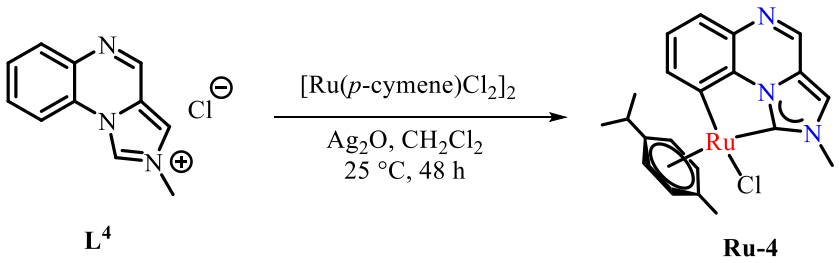
Scheme 3.13. Synthesis of complex **Ru-3**

In a reaction tube, ligand **L^3** (100 mg, 0.45 mmol, 1 equiv.) was added with [Ru(*p*-cymene)Cl_2]$_2$ (140.42 mg, 0.23 mmol, 0.5 equiv.). Ag_2O (156.38 mg, 0.68 mmol, 1.5 equiv.) was added to the reaction mixture followed by the addition of dry CH_2Cl_2 (2 mL). The reaction mixture was stirred at room temperature for two days under dark conditions. The resulting yellow solution was filtered through a celite plug and reduced under vacuum. The resulting crude was purified on basic alumina column chromatography (methanol: ethyl acetate 1:4). The major yellow band was collected, concentrated, and precipitated by the addition of Et_2O, which afforded the title complex as a yellow solid (180 mg, 75%). Slow diffusion of petroleum ether into a concentrated solution of complex **Ru-3** in CH_2Cl_2 gave yellow crystals suitable for X-Ray diffraction analysis.

^{1}H NMR (600 MHz, DMSO-d_6): δ 9.37 (d, J = 5.6 Hz, 1H), 8.46 (d, J = 7.8 Hz, 1H), 8.10 (s, 1H), 7.76 – 7.74 (m, 1H), 7.65 (d, J = 9.5 Hz, 1H), 7.48 (d, J = 9.5 Hz, 1H), 6.45 (d, J = 6.1 Hz, 1H), 6.37 (d, J = 6.2 Hz, 1H), 6.28 (d, J = 6.2 Hz, 1H), 5.90 (d, J = 6.1 Hz, 1H), 4.38 (s, 3H), 2.45 – 2.40 (m, 1H), 2.08 (s, 3H), 0.88 (d, J = 6.9 Hz, 3H), 0.84 (d, J = 6.9 Hz, 3H). ^{13}C NMR (151 MHz, DMSO-d_6): δ 174.5, 153.7, 145.2, 138.1, 127.3, 123.6, 123.2, 119.8, 118.4, 89.1, 87.7, 86.1, 81.4, 38.3, 30.5, 22.2, 21.9, 18.5. HRMS (ESI) *m/z*: calcd. for $C_{21}H_{23}ClN_3Ru$ [M]$^+$: 454.0624; found: 454.0626.

Synthesis of Ru-4:

TH-3565_186122020



L^4 Ru-4

Scheme 3.14. Synthesis of complex **Ru-4**

In a reaction tube, ligand $\mathbf{L^4}$ (100 mg, 0.45 mmol, 1 equiv.) was added with [Ru(*p*-cymene)Cl_2]$_2$ (140.42 mg, 0.23 mmol, 0.5 equiv.). Ag_2O (156.38 mg, 0.68 mmol, 1.5 equiv.) was added to the reaction mixture followed by the addition of dry CH_2Cl_2 (2 mL). The reaction mixture was stirred at room temperature for two days under dark conditions. The resulting yellow solution was filtered through a celite plug and reduced under vacuum. The resulting crude was purified on neutral alumina column chromatography (ethyl acetate: pet ether 1:2). The major yellow band was collected, concentrated, and precipitated by the addition of Et_2O, which afforded the title complex as a yellow solid (169 mg, 83%). Slow diffusion of petroleum ether into a concentrated solution of complex **Ru-4** in CH_2Cl_2 gave yellow crystals suitable for X-Ray diffraction analysis.

^{1}H NMR (400 MHz, Chloroform-*d*): δ 8.60 (s, 1H), 8.16 (d, J = 7.1 Hz, 1H), 7.44 (d, J = 8.0 Hz, 1H), 7.35 (s, 1H), 7.33 – 7.30 (m, 1H), 5.72 (d, J = 5.9 Hz, 1H), 5.62 (d, J = 5.9 Hz, 1H), 5.45 – 5.43 (m, 2H), 4.33 (s, 3H), 2.29 (hept, J = 6.9 Hz, 1H), 2.02 (s, 3H), 0.92 (d, J = 6.9 Hz, 3H), 0.75 (d, J = 6.9 Hz, 3H). ^{13}C NMR (151 MHz, Chloroform-*d*): δ 177.4, 160.8, 141.5, 140.6, 133.7, 133.4, 126.5, 123.9, 121.2, 115.5, 101.9, 101.5, 89.8, 88.1, 86.0, 83.8, 38.0, 31.1, 23.0, 22.0, 19.2. HRMS (ESI) *m/z*: calcd. for $C_{21}H_{22}N_3Ru$ $[M\text{-}Cl]^+$: 418.0857; found: 418.0858.

3.5.4. Cost for the synthesis of ligand L^1, L^4 and catalyst Ru-1, Ru-4

Table 3.16. Costs for the synthesis of the ligand precursor $\mathbf{L^1}$

Reagent	Amount used	Cost (INR)	Price per unit
quinoline-2-carboxaldehyde	1 g	322.4	INR 1612 / 5 g (BLD pharm)
methylamine	0.28 mL	0.112	INR 200 / 500 mL (Loba)
formalin solution	0.18 mL	0.118	INR 320 / 500 mL (Avra)
CH_3COCl	0.68 mL	0.986	INR 725 / 500 mL (Spectrochem)
MeOH	4 mL	0.304	INR 76 / 1 L (Finar)
Yield:	1.2 g (87%)	323.92	**INR 270 / 1 g**

Table 3.17. Used chemicals and costs for the synthesis of complex **Ru-1**

Reagent	Amount used	Cost (INR)	Price per unit

TH-3565_186122020

Ligand **L[1]**	0.5 g	135	INR 270 / 1 g
$Ru(p\text{-cymene})Cl_2]_2$	0.7 g	3025.82	INR 4322.6 / 1 g (Thermo Scientific)
Ag_2O	0.797 g	1155.33	INR 1449.6 / 1 g (Sigma Aldrich)
CH_2Cl_2	10 mL	1.36	INR 136 / 1 L (Thermo Scientific)
EtOAc	250 mL	41	INR 164 / 1 L (Finar)
Pet ether	90 mL	13.32	INR 148 / 1 L (Finar)
Et_2O	10 mL	12.18	INR 1218 / 1 L (Finar)
Neutral alumina	12 g	15.12	INR 1260 / 1 kg (SRL)
		4317.51	**INR 4497.4 / 1 g**, *before column*
Yield:	0.96 g (92%)	4399.13	**INR 4582.42 / 1 g**, *after column* (50.52 €, 55.48 US$, 43.27 £) (exchange rate per 1 Jan 2024)

Table 3.18. Costs for the synthesis of the ligand precursor **L[4]**

Reagent	**Amount used**	**Cost (INR)**	**Price per unit**
quinoxaline-2-carbaldehyde	1 g	3011	INR 3011 / 1 g (BLD pharm)
methylamine	0.28 mL	0.112	INR 200 / 500 mL (Loba)
formalin solution	0.18 mL	0.118	INR 320 / 500 mL (Avra)
CH_3COCl	0.68 mL	0.986	INR 725 / 500 mL (Spectrochem)
MeOH	4 mL	0.304	INR 76 / 1 L (Finar)
Yield:	1.1 g (82%)	3012.52	**INR 2738.65 / 1 g**

Table 3.19. Used chemicals and costs for the synthesis of complex **Ru-4**

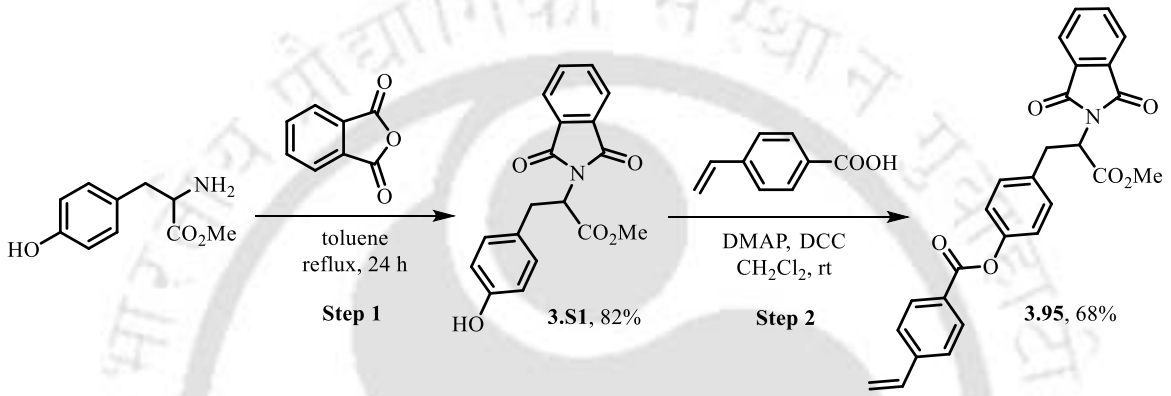
Reagent	**Amount used**	**Cost (INR)**	**Price per unit**
Ligand **L[1]**	0.1 g	273.86	INR 2738.65 / 1 g
$Ru(p\text{-cymene})Cl_2]_2$	0.140 g	605.16	INR 4322.6 / 1 g (Thermo Scientific)
Ag_2O	0.159 g	230.5	INR 1449.6 / 1 g (Sigma Aldrich)
CH_2Cl_2	2 mL	0.3	INR 136 / 1 L (Thermo Scientific)
EtOAc	250 mL	41	INR 164 / 1 L (Finar)
Pet ether	90 mL	13.32	INR 148 / 1 L (Finar)
Et_2O	10 mL	12.18	INR 1218 / 1 L (Finar)
Neutral alumina	10 g	12.6	INR 1260 / 1 kg (SRL)

TH-3565_186122020

		1109.82	**INR 6567 / 1 g**, *before column*
Yield:	0.169 g (83%)	1188.92	**INR 7035 / 1 g**, *after column* (79.09 €, 84.33 US$, 67.5 £) (exchange rate per 1 Jan 2024)

3.5.5. Synthesis of bioactive molecule-derived styrene derivatives

Synthesis of 4-(2-(1,3-dioxoisoindolin-2-yl)-3-methoxy-3-oxopropyl)phenyl 4-vinylbenzoate (3.95):



Scheme 3.15. Synthesis of compound **3.95**

Step 1: Synthesis of methyl 2-(1,3-dioxoisoindolin-2-yl)-3-(4-hydroxyphenyl)propanoate **(3.S1)**

A 50 mL round bottom flask equipped with a stir bar was charged with L-tyrosine, methyl ester (390 mg, 5.0 mmol, 1.0 equiv.), phthalic anhydride (755 mg, 5.1 mmol, 1.02 equiv.) and toluene (5 mL). The reaction mixture was heated to reflux for 24 h. The solvent was removed under a rotary evaporator. The crude material was absorbed into silica gel by dissolving in CH_2Cl_2 and removed the solvent with the help of a rotary evaporator. The resulting solid was purified by silica gel column chromatography (EtOAc/pet ether = 1/2) to get compound **3.S1** as a white solid (1.3 g, 82% yield).

^{1}H NMR (500 MHz, Chloroform-*d*): δ 7.77 – 7.76 (m, 2H), 7.69 – 7.67 (m, 2H), 6.99 (d, J = 7.8 Hz, 2H), 6.61 (d, J = 8.2 Hz, 2H), 5.66 (br, 1H), 5.10 (dd, J = 11.3, 5.2 Hz, 1H), 3.77 (s, 3H), 3.53 – 3.42 (m, 2H). ^{13}C NMR (126 MHz, Chloroform-*d*): δ 169.5, 167.8, 154.8, 134.4, 131.6, 130.1, 128.5, 123.7, 115.6, 53.6, 53.1, 33.9. HRMS (ESI) *m/z*: calcd. for $C_{18}H_{15}NNaO_5$ $[M+Na]^+$: 348.0843; found: 348.0868.

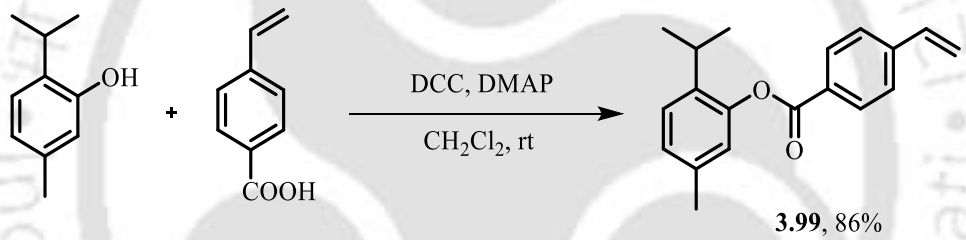
Step 2: Synthesis of 4-(2-(1,3-dioxoisoindolin-2-yl)-3-methoxy-3-oxopropyl)phenyl 4-vinylbenzoate **(3.95)**

TH-3565_186122020

To a 50 mL round-bottom flask 4-vinyl benzoic acid (127 mg, 0.78 mmol, 1 equiv.), compound **3.S1** (253 mg, 0.78 mmol, 1 equiv.), *N,N'*-dicyclohexylcarbodiimide (DCC, 177 mg, 0.86 mmol, 1.1 equiv.), and DMAP (19 mg, 0.16 mmol, 0.2 equiv.) were added. CH_2Cl_2 (4 mL) was then added and stirred at room temperature until the acid was consumed as monitored by TLC. Then, the solvent was removed under reduced pressure, and the residue was purified by column chromatography on silica gel (EtOAc/pet ether = 1/3) to afford the desired compound **3.95** as a white solid (240 mg, 68%).

^{1}H NMR (500 MHz, Chloroform-*d*): δ 8.09 (d, J = 8.4 Hz, 2H), 7.82 – 7.80 (m, 2H), 7.71 – 7.70 (m, 2H), 7.50 (d, J = 8.4 Hz, 2H), 7.24 (d, J = 8.5 Hz, 2H), 7.06 (d, J = 8.5 Hz, 2H), 6.77 (dd, J = 17.6, 10.9 Hz, 1H), 5.89 (d, J = 17.6 Hz, 1H), 5.41 (d, J = 10.9 Hz, 1H), 5.18 (dd, J = 11.0, 5.6 Hz, 1H), 3.79 (s, 3H), 3.65 – 3.56 (m, 2H). ^{13}C NMR (126 MHz, Chloroform-*d*): δ 169.4, 167.6, 164.9, 149.9, 142.7, 136.0, 134.4, 134.3, 131.7, 130.5, 130.0, 128.7, 126.4, 123.7, 121.9, 117.1, 53.2, 53.1, 34.2. HRMS (ESI) *m/z*: calcd. for $C_{27}H_{21}NNaO_6$ $[M+Na]^+$: 478.1262; found: 478.1254.

Synthesis of 2-isopropyl-5-methylphenyl 4-vinylbenzoate (3.99):



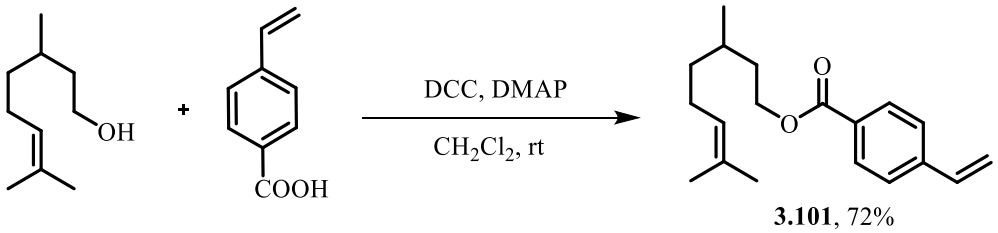
Scheme 3.16. Synthesis of compound **3.99**

4-Vinylbenzoic acid (198 mg, 1.33 mmol, 1 equiv.) was added to a mixture of thymol (200 mg, 1.33 mmol, 1 equiv.), DMAP (33 mg, 0.30 mmol, 0.2 equiv.), and *N,N'*-dicyclohexylcarbodiimide, DCC (302 mg, 1.5 mmol, 1.1 equiv.) in CH_2Cl_2 at room temperature and stirred overnight. Upon complete consumption of the starting material, the reaction mixture was filtered, concentrated on a rotary evaporator, and the residue was purified by flash column chromatography on silica gel (EtOAc/pet ether = 1/9) to yield the desired compound **3.99** as a colorless oil (321 mg, 86%).

^{1}H NMR (600 MHz, Chloroform-*d*): δ 8.17 (d, J = 8.4 Hz, 2H), 7.47 (d, J = 8.4 Hz, 2H), 7.21 (d, J = 8.0 Hz, 1H), 7.02 (d, J = 8.0 Hz, 1H), 6.94 (brs, 1H), 6.72 (dd, J = 17.6, 10.9 Hz, 1H), 5.85 (d, J = 17.6 Hz, 1H), 5.36 (d, J = 10.9 Hz, 1H), 3.07 (hept, J = 6.9 Hz, 1H), 2.30 (s, 3H), 1.21 (d, J = 7.1 Hz, 6H). ^{13}C NMR (151 MHz, Chloroform-*d*): δ 165.0, 148.2, 142.5, 137.1, 136.5, 135.9, 130.4, 128.7, 127.1, 126.4, 126.3, 122.9, 116.8, 27.3, 23.0, 20.8. HRMS (ESI) *m/z*: calcd. for $C_{19}H_{20}NaO_2$ $[M+Na]^+$: 303.1356; found: 303.1349.

Synthesis of 3,7-dimethyloct-6-en-1-yl 4-vinylbenzoate (3.101):

TH-3565_186122020

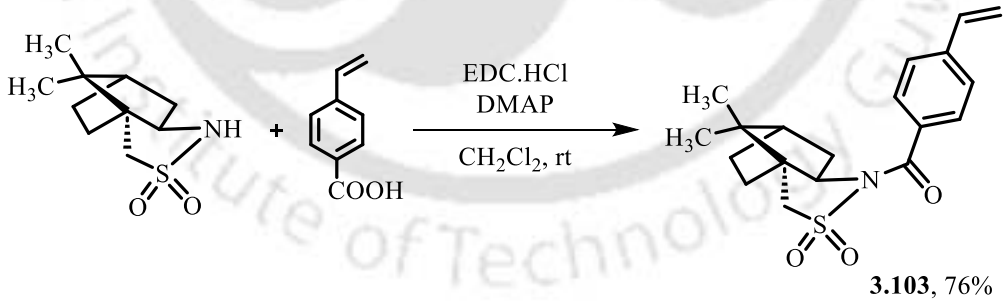


Scheme 3.17. Synthesis of compound **3.101**

4-Vinylbenzoic acid (259.3 mg, 1.75 mmol, 1 equiv.) was added to a mixture of citronellol (273 mg, 1.75 mmol, 1 equiv.), DMAP (42.8 mg, 0.35 mmol, 0.2 equiv.), and *N,N′*-dicyclohexylcarbodiimide, DCC (392 mg, 1.9 mmol, 1.1 equiv.) in CH_2Cl_2 at room temperature and stirred overnight. After completion of the reaction as confirmed by TLC, the reaction mixture was filtered, concentrated on a rotary evaporator, and the residue was purified by flash column chromatography on silica gel (EtOAc/pet ether = 1/9) to yield the desired compound **3.101** as a colorless oil (360 mg, 72%).

^{1}H NMR (600 MHz, Chloroform-*d*): δ 7.99 (d, J = 8.4 Hz, 2H), 7.44 – 7.43 (m, 2H), 6.75 – 6.71 (m, 1H), 5.85 – 5.82 (m, 1H), 5.36 – 5.34 (m, 1H), 5.11 – 5.09 (m, 1H), 4.39 – 4.31 (m, 2H), 2.07 – 1.95 (m, 2H), 1.84 – 1.78 (m, 1H), 1.67 (s, 3H), 1.60 (s, 3H), 1.59 – 1.54 (m, 1H), 1.43 – 1.37 (m, 1H), 1.26 – 1.21 (m, 2H), 0.97 (d, J = 6.6 Hz, 3H). ^{13}C NMR (151 MHz, Chloroform-*d*): δ 166.4, 141.9, 136.1, 131.3, 129.9, 129.8, 126.1, 124.7, 116.4, 63.5, 37.1, 35.6, 29.7, 25.8, 25.5, 19.6, 17.7. HRMS (ESI) *m/z*: calcd. for $C_{19}H_{26}NaO_2$ $[M+Na]^+$: 309.1825; found: 309.1817.

Synthesis of ((3a*R*)-9,9-dimethyl-2,2-dioxidohexahydro-1*H*,3*H*-3a,7-methanocyclohepta[*c*]isothiazol-1-yl)(4-vinylphenyl)methanone (3.103):



Scheme 3.18. Synthesis of compound **3.103**

A solution of *N′*-(3-dimethylaminopropyl)-*N*-ethylcarbodimide hydrochloride salt (EDC·HCl) (807 mg, 4.2 mmol, 3.0 equiv), 4-*N,N′*-dimethylaminopyridine (DMAP) (379 mg, 3.1 mmol, 2.2 equiv.) and 4-vinylbenzoic acid (228 mg, 1.5 mmol, 1.1 equiv) in CH_2Cl_2 (5.0 mL) was stirred under air. Camphorsultam (300 mg, 1.4 mmol, 1.0 equiv) was added in a small portion at 0 °C for 30 minutes and warmed to ambient temperature, and stirred for 12 h. Upon complete consumption of the starting material, the reaction mixture was washed with 10% aqueous $NaHCO_3$ and brine. The organic part was extracted with CH_2Cl_2 and dried over Na_2SO_4. The

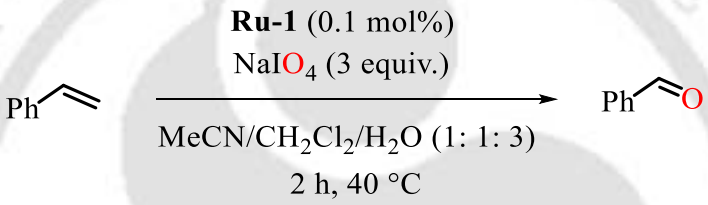
TH-3565_186122020

solvent was filtered and evaporated under reduced pressure. The crude residue was purified using column chromatography on silica gel (EtOAc/pet ether = 1/3) to get the desired compound **3.103** as a white solid (382 mg, 76%).

^{1}H NMR (500 MHz, Chloroform-*d*): δ 7.74 (d, J = 8.4 Hz, 2H), 7.46 (d, J = 8.4 Hz, 2H), 6.73 (dd, J = 17.6, 10.9 Hz, 1H), 5.84 (d, J = 17.5 Hz, 1H), 5.36 (d, J = 10.9 Hz, 1H), 4.19 (dd, J = 7.7, 4.8 Hz, 1H), 3.53 (d, J = 13.7 Hz, 1H), 3.42 (d, J = 13.7 Hz, 1H), 2.14 – 2.04 (m, 2H), 2.00 – 1.92 (m, 3H), 1.49 – 1.39 (m, 2H), 1.34 (s, 3H), 1.02 (s, 3H). ^{13}C NMR (126 MHz, Chloroform-*d*): δ 169.9, 141.9, 136.2, 133.0, 130.0, 125.9, 116.6, 66.2, 53.7, 48.2, 47.9, 45.2, 38.5, 33.3, 26.7, 21.4, 20.1. HRMS (ESI) *m/z*: calcd. for $C_{19}H_{23}NNaO_3S$ $[M+Na]^+$: 368.1291; found: 368.1296.

3.5.6. General procedure for oxidation of olefins

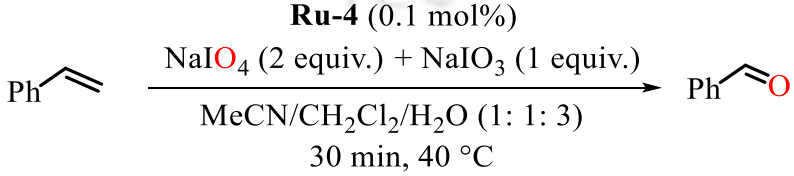
General procedure for the catalytic oxidative cleavage of olefins (GP-I)



Scheme 3.19. Oxidation of olefins catalyzed by **Ru-1**

Unsaturated hydrocarbon (1 mmol) and $NaIO_4$ (3 mmol) in a deoxygenated solvent mixture of $CH_3CN/CH_2Cl_2/H_2O$ (1:1:3 v/v; a total of 1.5 mL) were placed in a reaction tube and the reaction mixture was stirred at 25 ºC until $NaIO_4$ was completely dissolved. Complex **Ru-1** (0.1 mol%) was added to the reaction mixture and stirred in a preheated oil bath at 40 ºC for 2 h. The course of the reaction was monitored by TLC. At the end of the reaction, the product was extracted with CH_2Cl_2 and washed with H_2O. The organic layer was separated and dried over anhydrous Na_2SO_4 and the solvent was evaporated under a vacuum. The residue was purified by column chromatography on silica gel (petroleum ether/EtOAc) to get the desired product.

General procedure for the catalytic oxidative cleavage of olefins (GP-II)



Scheme 3.20. Oxidation of olefins catalyzed by **Ru-4**

Unsaturated hydrocarbon (1 mmol), $NaIO_4$ (2 mmol) and $NaIO_3$ (1 mmol) in a deoxygenated solvent mixture of $CH_3CN/CH_2Cl_2/H_2O$ (1:1:3 v/v; a total of 1.5 mL) were placed in a reaction tube and the reaction mixture was stirred at 25 ºC until $NaIO_4$ was completely dissolved. Complex **Ru-4** (0.1 mol%) was added to the reaction mixture and stirred in a preheated oil bath

TH-3565_186122020

at 40 ºC for 30 minutes. The course of the reaction was monitored by TLC. At the end of the reaction, the product was extracted with CH_2Cl_2 and washed with H_2O. The organic layer was separated and dried over anhydrous Na_2SO_4 and the solvent was evaporated under a vacuum. The residue was purified by column chromatography on silica gel (petroleum ether/EtOAc) to get the desired product.

3.5.7. Mechanistic studies

Effect of added *para*-cymene and different arenes

Procedure for the reaction catalyzed by Ru-1: Catalyst **Ru-1** (0.1 mol%), styrene (42 mg, 0.4 mmol) and $NaIO_4$ (103 mg, 1.2 mmol) were kept constant in a fixed volume of solvent $CH_3CN/CH_2Cl_2/H_2O$ (1:1:3 v/v; a total of 1.5 mL). The *para*-cymene was added to the reaction mixture varying from 0 to 80 equivalents with respect to the catalyst precursor. The reactions were carried out at 40 ºC for 2 hours. The yields of benzaldehyde were determined by GC analysis (using anisole as an internal standard). To check the effect of different arenes (both electron-deficient and electron-rich arenes), a similar procedure was undertaken and up to 60 equivalents of different arenes were added to the reaction mixture (Figure 3.6).

Procedure for the reaction catalyzed by Ru-4: For these experiments, catalyst **Ru-4** (0.1 mol%), styrene (52 mg, 0.5 mmol), $NaIO_4$ (214 mg, 1 mmol) and $NaIO_3$ (99 mg, 0.5 mmol) were kept constant in a fixed volume of solvent $CH_3CN/CH_2Cl_2/H_2O$ (1:1:3 v/v; a total of 1.5 mL). The *para*-cymene was added to the reaction mixture varying from 0 to 80 equivalents with respect to the catalyst precursor. The reactions were carried out at 40 ºC for 30 minutes. The yields of benzaldehyde were determined by GC analysis (using anisole as an internal standard). A similar procedure was undertaken to check the effect of different arenes (both electron-deficient and electron-rich arenes), and up to 60 equivalents of different arenes were added to the reaction mixture (Figure 3.7).

Spectroscopic characterization of high-valent ruthenium(VI)-dioxo species Ru-1-I2

Procedure for XPS analysis:

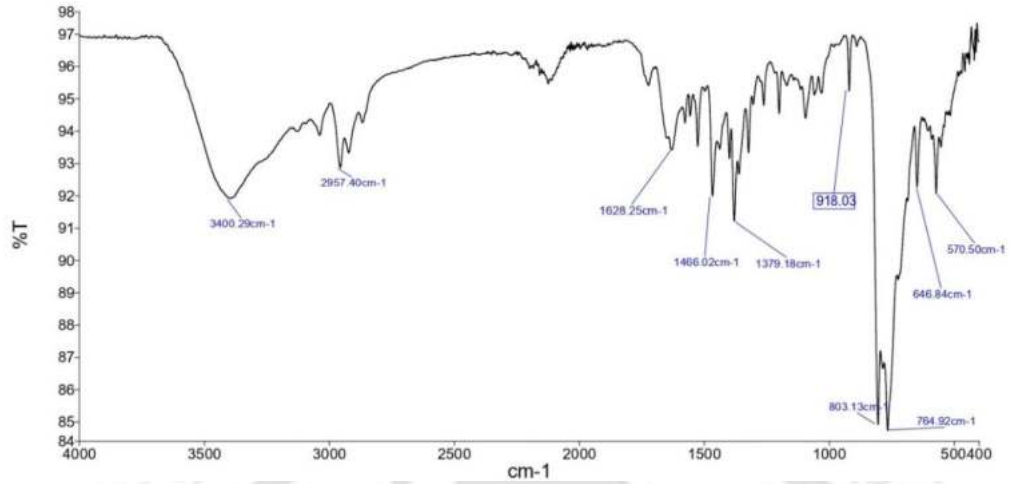
XPS analysis was performed for the intermediate Ru(VI)-dioxo species. The sample for XPS studies was prepared by reaction of complex **Ru-1** (3 mg, 1 equiv.), aq. $NaIO_4$ (1 equiv.) in acetonitrile (0.5 mL) at room temperature. We examined the oxidation state of Ru after the reaction of **Ru-1** with $NaIO_4$ by analysis of Ru 3*d* by core-level X-ray photoelectron spectroscopy (XPS), which was fitted with spin-orbital split $3d_{5/2}$ and $3d_{3/2}$. Two sets of XPS peaks appeared at 283.0 and 285.1 eV for the binding energies of the $3d_{5/2}$ and $3d_{3/2}$ components, respectively (Figure 3.13). These two peaks at higher binding energies confirm the presence of Ru in a +6 oxidation state. Observation is in accordance with the literature.[17]

IR studies:

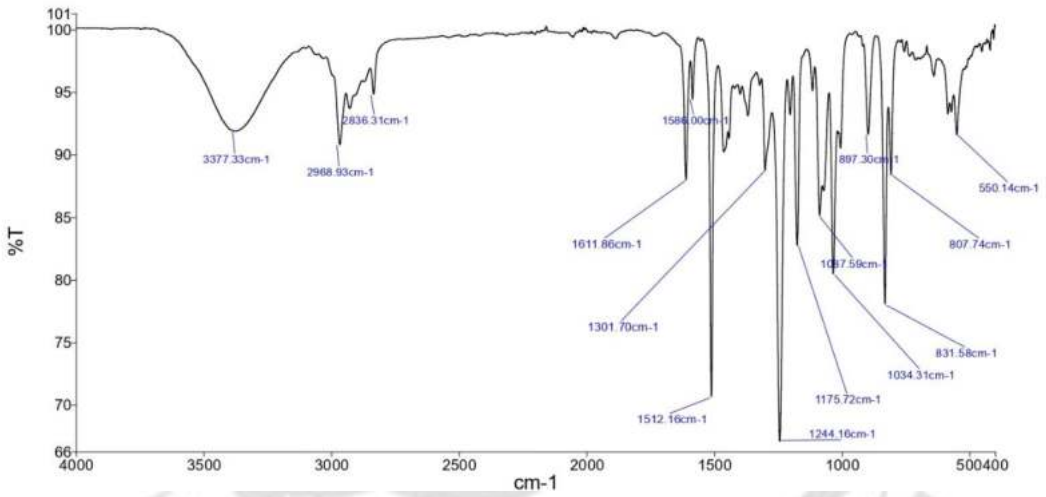
A stoichiometric reaction between complex **Ru-1** and $NaIO_4$ (aq) (1:1 molar ratio) at room temperature in acetonitrile was performed and immediately recorded the IR spectra. Similarly,

TH-3565_186122020

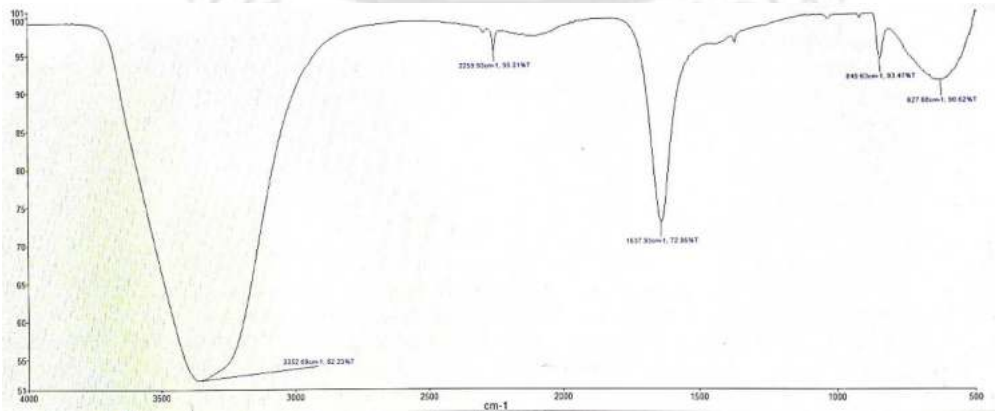
IR spectra for the reaction between **Ru-4** and $NaIO_4$ were also recorded and fall in the same range. Representative IR spectra for the reaction between **Ru-1** and $NaIO_4$ are shown in Figure 3.22.



(a) IR spectra for a reaction mixture of **Ru-1** and $NaIO_4$ (aq.) in CH_3CN.



(b) IR spectra of complex **Ru-1** in acetonitrile.



(c) IR spectra of $NaIO_4$ in an aqueous medium.

TH-3565_186122020

Figure 3.22. IR spectra of the reaction between complex **Ru-1** and $NaIO_4$ (aq.) at room temperature in CH_3CN (a), IR spectra of complex **Ru-1** in acetonitrile (b), and IR spectra of $NaIO_4$ in an aqueous medium (c).

UV-Vis spectroscopic studies for the metallacycle species

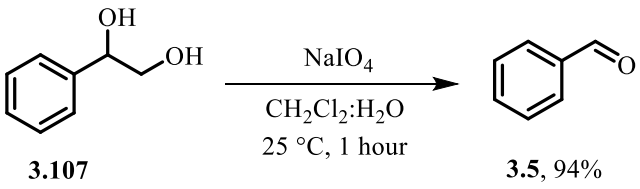
Procedure: To gain insight into the progress of the reaction, a UV-Vis spectroscopic study was carried out on a Cary 100 UV-Vis spectrophotometer using 1.0 cm quartz cuvettes at room temperature. A stock solution of $NaIO_4$ was made in H_2O and a stock solution of the complex **Ru-1** was made in acetonitrile. The total volume of each sample was kept constant at 2.5 mL (acetonitrile + water 1:3). The required amount of H_2O was added just before the addition of $NaIO_4$ solution to the respective sample. First, UV-Vis spectra were recorded only for pure complex **Ru-1**, then $NaIO_4$ solution was added to the sample followed by the addition of styrene (5 equiv.) to the same sample. Adding styrene into the solution of complex **Ru-1** and $NaIO_4$, appeared a new band at λ_{max} = 249 nm (Figure 3.14). Based on the earlier reports we postulated the new band at λ_{max} = 249 nm for the five-membered metallacycle. The absorption maxima were gradually decreased over time. This might be due to the collapse of this metallacycle to the C–C cleaved product. The finding is in accordance with Che's work for metallacycle intermediates.[7a,18]

Isolation of 1-phenyl-1,2-ethanediol (Scheme 3.9)

Procedure: Styrene (52.1 mg, 0.5 mmol, 1 equiv.) and $NaIO_4$ (321 mg, 1.5 mmol, 3 equiv.) were taken in a reaction tube with a deoxygenated solvent mixture of $CH_2Cl_2/CH_3CN/H_2O$ (1:1:3 v/v; a total of 1.5 mL) and stirred at room temperature until $NaIO_4$ was completely dissolved. Complex **Ru-1/Ru-4** (1 mol%) was added to the reaction mixture and stirred at 25 ºC for 30 minutes. At the end of the reaction, the product was extracted with CH_2Cl_2 and washed with H_2O. The organic layer was separated and dried over anhydrous Na_2SO_4 and the solvent was evaporated under a vacuum. Compound 1-phenyl-1,2-ethanediol was isolated along with benzaldehyde by column chromatography on silica gel with petroleum ether/ethyl acetate (v/v = 5:1, R_f = 0.50) as a white solid.

^{1}H NMR (600 MHz, Chloroform-*d*): δ 7.38 – 7.35 (m, 4H), 7.33 – 7.29 (m, 1H), 4.83 (d, J = 8.4 Hz, 1H), 3.79 – 3.75 (m, 1H), 3.69 – 3.65 (m, 1H), 2.59 (d, J = 3.1 Hz, 1H), 2.15 – 2.14 (m, 1H). ^{13}C NMR (151 MHz, Chloroform-*d*): δ 140.6, 128.7, 128.2, 126.2, 74.8, 68.2.

Control experiment with 1-phenyl-1,2-ethanediol



3.107 **3.5**, 94%

Scheme 3.21. Reaction of 1-phenyl-1,2-ethanediol with $NaIO_4$

TH-3565_186122020

Procedure: In a reaction tube, 1-phenyl-1,2-ethanediol (41.5 mg, 0.3 mmol, 1 equiv.) and $NaIO_4$ (96.3 mg, 0.45 mmol, 1.5 equiv.) were taken with CH_2Cl_2: H_2O (1:1) and stirred at room temperature for 1 hour. After completion of the reaction, the product was extracted with CH_2Cl_2 and washed with H_2O. The organic layer was separated and dried over anhydrous Na_2SO_4 and the solvent was evaporated under a vacuum. The product was isolated by column chromatography on silica gel with petroleum ether/ethyl acetate (v/v = 50:1, R_f = 0.90) as a colorless liquid (30 mg, 94%). Since the C-C bond in diol was easily cleaved by $NaIO_4$ in the absence of catalyst indicating the role of catalyst is crucial in the diol formation step.

3.5.8. Kinetic studies

(a) Determination of the order dependency of catalyst precursor, $NaIO_4$, and alkene for the reaction catalyzed by Ru-1

Styrene was used as a substrate for all the order determination experiments. The concentration of each of the reaction components (catalyst **Ru-1**, $NaIO_4$, and substrate) was varied in separate experiments (keeping the other components in fixed concentration) to evaluate the order of dependency with respect to catalyst precursor **Ru-1,** $NaIO_4$, and substrate (styrene).

i) with respect to catalyst (Ru-1): Four identical experiments were carried out following the standard catalytic reaction condition by varying the amount of catalyst loading of **Ru-1** from 0.06 mol% to 0.12 mol%. The amounts of styrene and $NaIO_4$ were kept constant in a fixed volume of solvent ($CH_3CN/CH_2Cl_2/H_2O$; 1:1:3; 1 mL). The reactions were carried out at 40 ºC for different time intervals. Accordingly, the concentration of the final product (benzaldehyde) was calculated at different times by GC analysis using anisole as an internal standard. All the reactions were repeated thrice, and the average data were plotted as product conc. *vs* time (min) in Figure 3.23. The rate of reaction at different loading catalysts of **Ru-1** was given below and used to plot the log(rate) *vs* log(conc.) (Figure 3.24) to determine the order of reaction with respect to catalyst (**Ru-1**).

Table 3.20. Experimental details

Entry	Styrene	$NaIO_4$	**Ru-1**
1	1 mmol	3 mmol	0.06 mol%
2	1 mmol	3 mmol	0.08 mol%
3	1 mmol	3 mmol	0.10 mol%
4	1 mmol	3 mmol	0.12 mol%

TH-3565_186122020

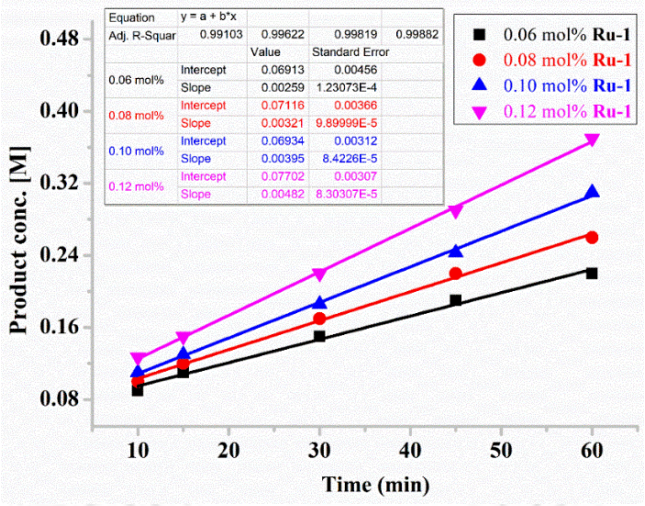


Figure 3.23. Determination of initial slopes for oxidation of styrene to benzaldehyde by taking different loading catalysts of **Ru-1**.

Table 3.21. Rate of the reaction at different loading catalysts of **Ru-1.**

Run	**Ru-1** (mol)	log (conc. of **Ru-1**)	Initial rate (M/min)	log (rate)
Run 1	6×10^{-4}	-3.22	2.6×10^{-3}	-2.59
Run 2	8×10^{-4}	-3.10	3.2×10^{-3}	-2.49
Run 3	1×10^{-3}	-3.00	3.9×10^{-3}	-2.41
Run 4	1.2×10^{-3}	-2.92	4.8×10^{-3}	-2.32

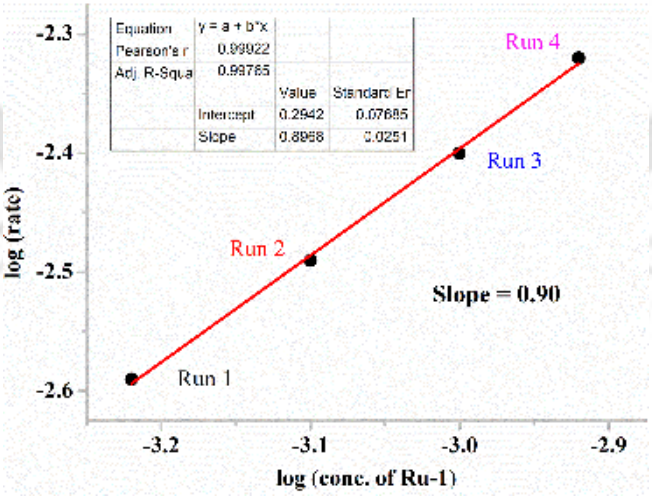


Figure 3.24. Determination of order of the oxidation of styrene to benzaldehyde with respect to catalyst (**Ru-1**).

ii) with respect to substrate (styrene): Five identical experiments were carried out following the standard catalytic reaction condition by varying the amount of substrate (styrene) from 0.4 mmol to 1.2 mmol. The amounts of **Ru-1** (0.1% mmol) and $NaIO_4$ (3 mmol) were kept constant

in a fixed volume of solvent ($CH_3CN/CH_2Cl_2/H_2O$; 1:1:3; 1 mL). The reaction was carried out at 40 ºC and the concentration of the final product (benzaldehyde) was calculated at different times by GC analysis using anisole as an internal standard. All the reactions were repeated thrice, and the average data were plotted as product conc. *vs* time (min) in Figure 3.25. The rate of reaction at different initial concentrations of styrene was given below and used to plot the log(rate) *vs* log(conc.) (Figure 3.26) to determine the order of reaction with respect to the substrate.

Table 3.22. Experimental details

Entry	Styrene	$NaIO_4$	**Ru-1**
1	0.4 mmol	3 mmol	0.1 mol%
2	0.6 mmol	3 mmol	0.1 mol%
3	0.8 mmol	3 mmol	0.1 mol%
4	1.0 mmol	3 mmol	0.1 mol%
5	1.2 mmol	3 mmol	0.1 mol%

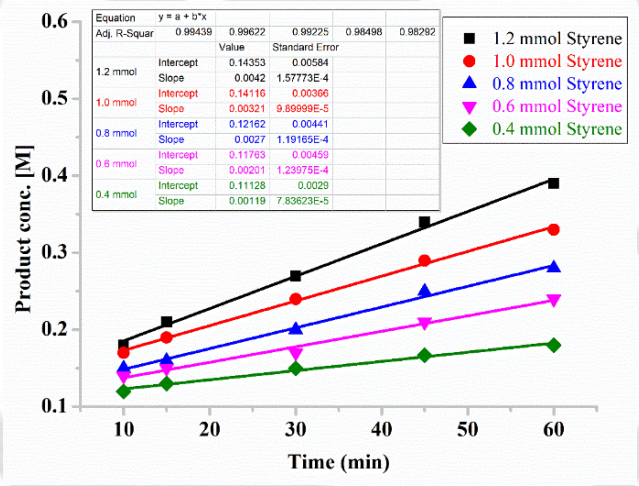


Figure 3.25. Determination of initial slopes for oxidation of styrene to benzaldehyde by taking different initial concentrations of styrene.

Table 3.23. Rate of the reaction at different initial concentrations of styrene.

Run	Styrene	log (conc. of styrene)	Initial rate (M/min)	log (rate)
Run 1	1.2 mmol	0.079	4.2×10^{-3}	-2.38
Run 2	1.0 mmol	0	3.2×10^{-3}	-2.49
Run 3	0.8 mmol	-0.097	2.7×10^{-3}	-2.57
Run 4	0.6 mmol	-0.222	2.0×10^{-3}	-2.69
Run 5	0.4 mmol	-0.398	1.2×10^{-3}	-2.92

TH-3565_186122020

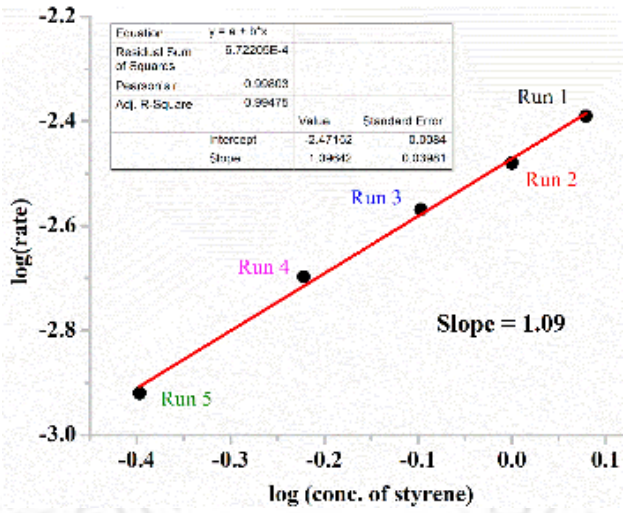


Figure 3.26. Determination of order of the oxidation of styrene to benzaldehyde with respect to substrate (styrene).

iii) with respect to oxidant ($NaIO_4$): Five identical experiments were carried out following the standard catalytic reaction condition by varying the amount of $NaIO_4$ from 1.5 mmol to 3.5 mmol. The amounts of **Ru-1** and styrene were kept constant in a fixed volume of solvent ($CH_3CN/CH_2Cl_2/H_2O$; 1:1:3; 1 mL). The reactions were carried out at 40 ºC and the concentration of the final product (benzaldehyde) was calculated at different times by GC analysis using anisole as an internal standard. All the reactions were repeated thrice, and the average data were plotted as product conc. *vs* time (min) in Figure 3.27. The rate of reaction at different concentrations of $NaIO_4$ was given below and used to plot the log(rate) *vs* log(conc.) (Figure 3.28) to determine the order of reaction with respect to $NaIO_4$.

Table 3.24. Experimental details

Entry	Styrene	$NaIO_4$	**Ru_1**
1	1 mmol	1.5 mmol	0.1 mol%
2	1 mmol	2.0 mmol	0.1 mol%
3	1 mmol	2.5 mmol	0.1 mol%
4	1 mmol	3.0 mmol	0.1 mol%
5	1 mmol	3.5 mmol	0.1 mol%

TH-3565_186122020

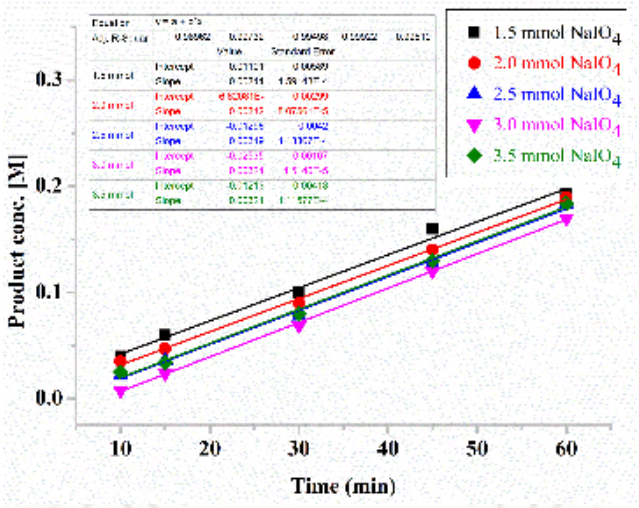


Figure 3.27. Determination of initial slopes for oxidation of styrene to benzaldehyde by taking different concentrations of $NaIO_4$.

Table 3.25. Rate of the reaction at different initial concentrations of $NaIO_4$.

Run	$NaIO_4$	log (conc. of $NaIO_4$)	Initial rate (M/min)	log (rate)
Run 1	1.5 mmol	0.18	3.11×10^{-3}	-2.507
Run 2	2.0 mmol	0.30	3.12×10^{-3}	-2.505
Run 3	2.5 mmol	0.39	3.19×10^{-3}	-2.496
Run 4	3.0 mmol	0.48	3.24×10^{-3}	-2.489
Run 5	3.5 mmol	0.54	3.21×10^{-3}	-2.493

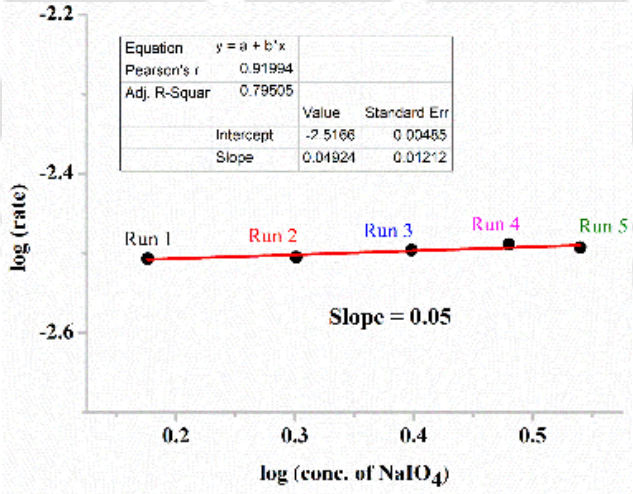


Figure 3.28. Determination of order of the oxidation of styrene to benzaldehyde with respect to $NaIO_4$.

(b) Determination of the order dependency of catalyst precursor, $NaIO_4$, $NaIO_3$ and alkene for the reaction catalyzed by Ru-4

TH-3565_186122020

Styrene was used as a substrate for all the order determination experiments. The concentration of each of the reaction components (catalyst **Ru-4**, $NaIO_4$, $NaIO_3$ and substrate) was varied in separate experiments (keeping the other components in fixed concentration) to evaluate the order of dependency with respect to catalyst precursor **Ru-4**, $NaIO_4$, $NaIO_3$ and substrate (styrene).

i) with respect to catalyst (Ru-4): Four identical experiments were carried out following the standard catalytic reaction condition by varying the amount of catalyst loading of **Ru-4** from 0.06 mol% to 0.12 mol%. The amounts of styrene, $NaIO_4$ and $NaIO_3$ were kept constant in a fixed volume of solvent ($CH_3CN/CH_2Cl_2/H_2O$; 1:1:3; 1 mL). The reactions were carried out at 40 ºC for different time intervals. Accordingly, the concentration of the final product (benzaldehyde) was calculated at different times by GC analysis using anisole as an internal standard. All the reactions were repeated thrice, and the average data were plotted as product conc. *vs* time (min) in Figure 3.29. The rate of reaction at different loading catalysts of **Ru-4** was given below and used to plot the log(rate) *vs* log(conc.) (Figure 3.30) to determine the order of reaction with respect to catalyst (**Ru-4**).

Table 3.26. Experimental details

Entry	Styrene	$NaIO_4$ + $NaIO_3$	**Ru-4**
1	1 mmol	2 mmol + 1 mmol	0.06 mol%
2	1 mmol	2 mmol + 1 mmol	0.08 mol%
3	1 mmol	2 mmol + 1 mmol	0.10 mol%
4	1 mmol	2 mmol + 1 mmol	0.12 mol%

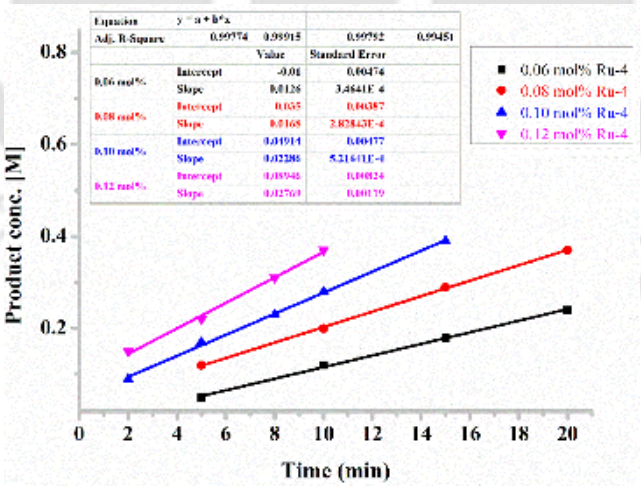


Figure 3.29. Determination of initial slopes for oxidation of styrene to benzaldehyde by taking different loading catalysts of **Ru-4**.

Table 3.27. Rate of the reaction at different loading catalysts of **Ru-4**

TH-3565_186122020

Run	**Ru-4** (mol)	log (conc. of **Ru-4**)	Initial rate (M/min)	log (rate)
Run 1	6×10^{-4}	-3.22	1.26×10^{-2}	-1.89
Run 2	8×10^{-4}	-3.10	1.68×10^{-2}	-1.77
Run 3	1×10^{-3}	-3.00	2.29×10^{-2}	-1.64
Run 4	1.2×10^{-3}	-2.92	2.77×10^{-2}	-1.56

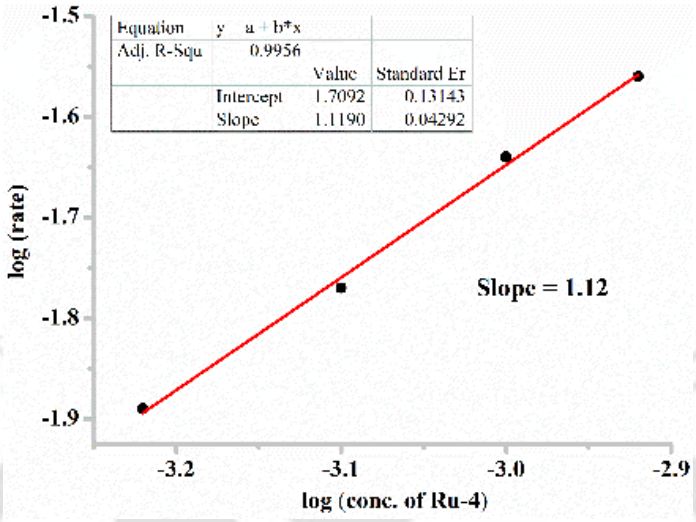


Figure 3.30. Determination of order of the oxidation of styrene to benzaldehyde with respect to catalyst (**Ru-4**).

ii) with respect to substrate (styrene): Four identical experiments were carried out following the standard catalytic reaction condition by varying the amount of substrate (styrene) from 0.6 mmol to 1.2 mmol. The amounts of **Ru-4** (0.1% mmol), $NaIO_4$ (2 mmol) and $NaIO_3$ (1 mmol) were kept constant in a fixed volume of solvent ($CH_3CN/CH_2Cl_2/H_2O$; 1:1:3; 1 mL). The reaction was carried out at 40 ºC and the concentration of the final product (benzaldehyde) was calculated at different times by GC analysis using anisole as an internal standard. All the reactions were repeated thrice, and the average data were plotted as product conc. *vs* time (min) in Figure 3.31. The rate of reaction at different initial concentrations of styrene was given below and used to plot the log(rate) *vs* log(conc.) (Figure 3.32) to determine the order of reaction with respect to the substrate.

Table 3.28. Experimental details

Entry	Styrene	$NaIO_4$ + $NaIO_3$	**Ru-4**
1	0.6 mmol	2 mmol + 1 mmol	0.1 mol%
2	0.8 mmol	2 mmol + 1 mmol	0.1 mol%
3	1.0 mmol	2 mmol + 1 mmol	0.1 mol%
4	1.2 mmol	2 mmol + 1 mmol	0.1 mol%

TH-3565_186122020

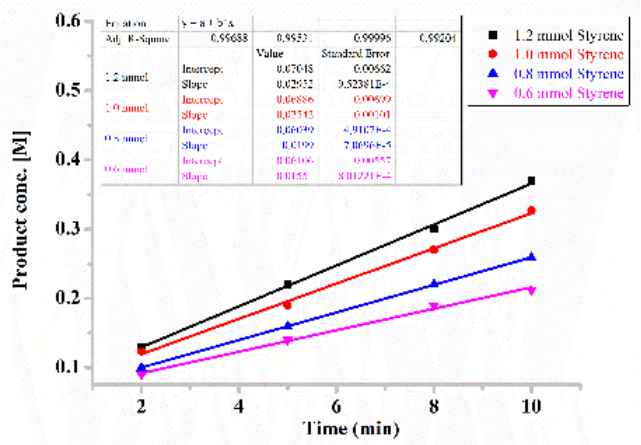


Figure 3.31. Determination of initial slopes for oxidation of styrene to benzaldehyde by taking different initial concentrations of styrene.

Table 3.29. Rate of the reaction at different initial concentrations of styrene

Run	Styrene	log (conc. of styrene)	Initial rate (M/min)	log (rate)
Run 1	1.2 mmol	0.079	2.95×10^{-2}	-1.53
Run 2	1.0 mmol	0	2.54×10^{-2}	-1.59
Run 3	0.8 mmol	-0.097	1.99×10^{-2}	-1.70
Run 4	0.6 mmol	-0.222	1.55×10^{-2}	-1.81

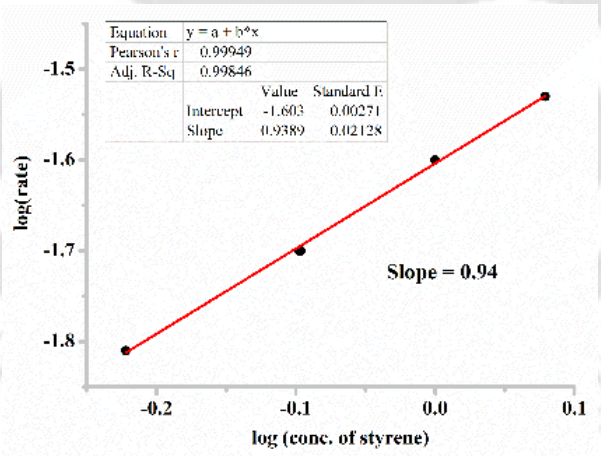


Figure 3.32. Determination of order of the oxidation of styrene to benzaldehyde with respect to substrate (styrene).

iii) with respect to oxidant ($NaIO_4$): Four identical experiments were carried out following the standard catalytic reaction condition by varying the amount of $NaIO_4$ from 1.0 mmol to 2.5 mmol. The amounts of **Ru-4**, $NaIO_3$ and styrene were kept constant in a fixed volume of solvent ($CH_3CN/CH_2Cl_2/H_2O$; 1:1:3; 1 mL). The reactions were carried out at 40 ºC and the concentration of the final product (benzaldehyde) was calculated at different times by GC analysis using anisole as an internal standard. All the reactions were repeated thrice, and the average data were plotted as product conc. *vs* time (min) in Figure 3.33. The rate of reaction at

TH-3565_186122020

different concentrations of $NaIO_4$ was given below and used to plot the log(rate) *vs* log(conc.) (Figure 3.34) to determine the order of reaction with respect to $NaIO_4$.

Table 3.30. Experimental details

Entry	Styrene	$NaIO_4 + NaIO_3$	**Ru-4**
1	1 mmol	1.0 mmol + 1 mmol	0.1 mol%
2	1 mmol	1.5 mmol + 1 mmol	0.1 mol%
3	1 mmol	2.0 mmol + 1 mmol	0.1 mol%
4	1 mmol	2.5 mmol + 1 mmol	0.1 mol%

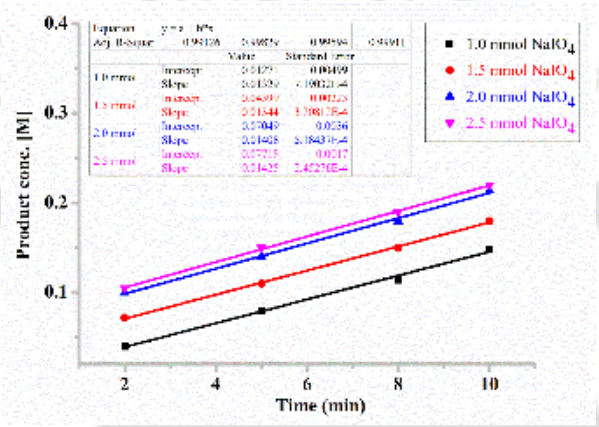


Figure 3.33. Determination of initial slopes for oxidation of styrene to benzaldehyde by taking different concentrations of $NaIO_4$.

Table 3.31. Rate of the reaction at different initial concentrations of $NaIO_4$

Run	$NaIO_4$	log (conc. of $NaIO_4$)	Initial rate (M/min)	log (rate)
Run 1	1.0 mmol	0	1.33×10^{-2}	-1.876
Run 2	1.5 mmol	0.176	1.34×10^{-2}	-1.872
Run 3	2.0 mmol	0.301	1.41×10^{-2}	-1.851
Run 4	2.5 mmol	0.398	1.43×10^{-2}	-1.845

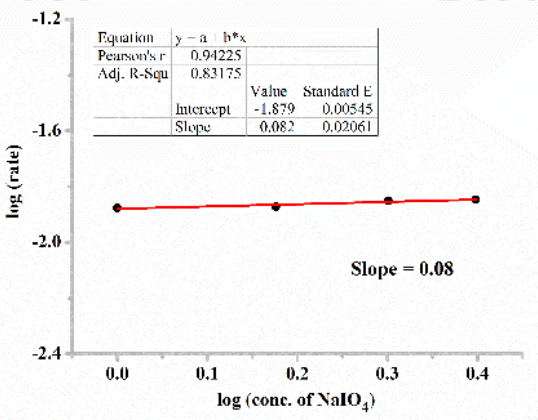


Figure 3.34. Determination of order of the oxidation of styrene to benzaldehyde with respect to $NaIO_4$.

iv) with respect to $NaIO_3$: Four identical experiments were carried out following the standard catalytic reaction condition by varying the amount of $NaIO_3$ from 0.5 mmol to 2.0 mmol. The amounts of **Ru-4**, $NaIO_4$ and styrene were kept constant in a fixed volume of solvent ($CH_3CN/CH_2Cl_2/H_2O$; 1:1:3; 1 mL). The reactions were carried out at 40 ºC and the concentration of the final product (benzaldehyde) was calculated at different times by GC analysis using anisole as an internal standard. All the reactions were repeated thrice, and the average data were plotted as product conc. *vs* time (min) in Figure 3.35. The rate of reaction at different concentrations of $NaIO_3$ was given below and used to plot the log(rate) *vs* log(conc.) (Figure 3.36) to determine the order of reaction with respect to $NaIO_3$.

Table 3.32. Experimental details

Entry	Styrene	$NaIO_4$ + $NaIO_3$	**Ru-4**
1	1 mmol	2 mmol + 0.5 mmol	0.1 mol%
2	1 mmol	2 mmol + 1.0 mmol	0.1 mol%
3	1 mmol	2 mmol + 1.5 mmol	0.1 mol%
4	1 mmol	2 mmol + 2.0 mmol	0.1 mol%

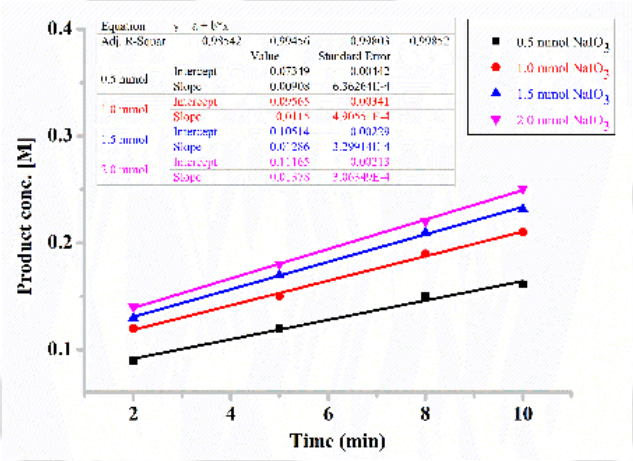


Figure 3.35. Determination of initial slopes for oxidation of styrene to benzaldehyde by taking different concentrations of $NaIO_3$.

Table 3.33. Rate of the reaction at different initial concentrations of $NaIO_3$

Run	$NaIO_3$	log (conc. of $NaIO_3$)	Initial rate (M/min)	log (rate)
Run 1	0.5 mmol	-0.301	0.91×10^{-2}	-2.04
Run 2	1.0 mmol	0	1.15×10^{-2}	-1.94
Run 3	1.5 mmol	0.176	1.29×10^{-2}	-1.89
Run 4	2.0 mmol	0.301	1.38×10^{-2}	-1.86

TH-3565_186122020

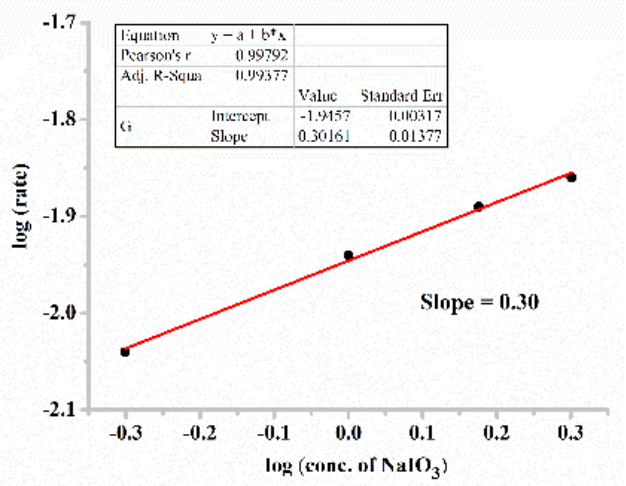
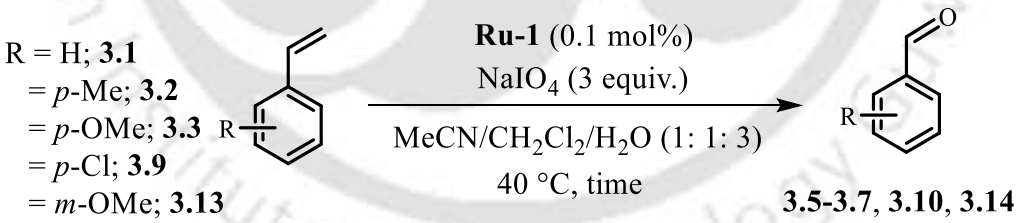


Figure 3.36. Determination of order of the oxidation of styrene to benzaldehyde with respect to $NaIO_3$.

(c) Kinetic Hammett Studies

Reaction conditions involving Ru-1: A reaction tube was charged with $NaIO_4$ (3 mmol) in a deoxygenated solvent mixture of $CH_3CN/CH_2Cl_2/H_2O$ (1:1:3 *v/v*; a total of 3.0 mL) and the reaction mixture was stirred at 25 ºC until $NaIO_4$ was completely dissolved. The substituted alkene derivative (1 mmol) and **Ru-1** (0.1 mol%) were added to the tube and stirred at 40 ºC for different time intervals. The progress of the reaction was monitored by GC analysis using anisole as an internal standard. All the reactions were carried out three times and the average conversion of the substituted alkene at different time intervals was plotted as ln(a/a-x) *vs* time (min).



substrate	k (min^{-1})	k_X/k_H	log (k_X/k_H)	σ_p	ρ
H (**3.1**)	0.0150	1.00	0	0	**-1.74**
p-Me (**3.2**)	0.0200	1.33	0.12	-0.17	
p-OMe (**3.3**)	0.0348	2.32	0.36	-0.27	
p-Cl (**3.9**)	0.0042	0.28	-0.55	0.23	
m-OMe (**3.13**)	0.0073	0.48	-0.31	0.12	

TH-3565_186122020

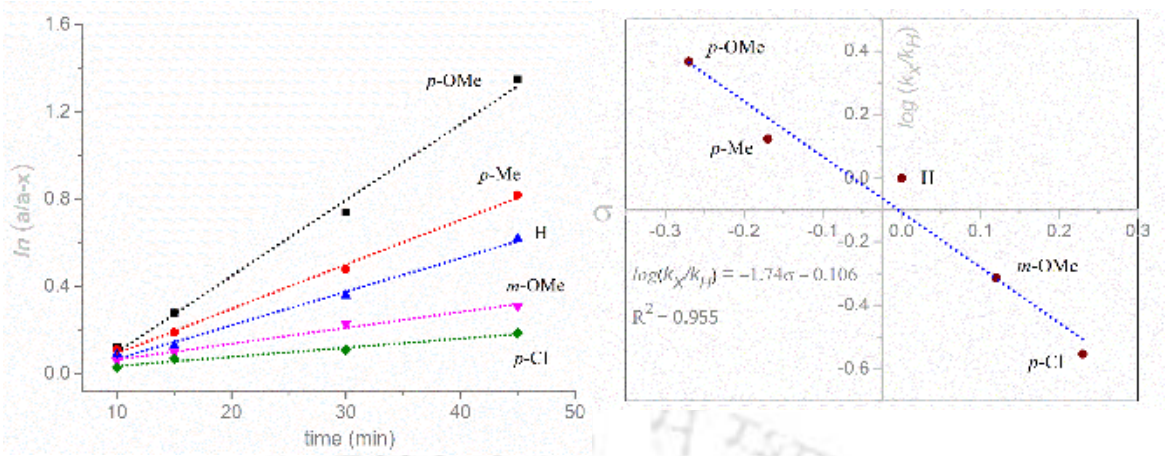
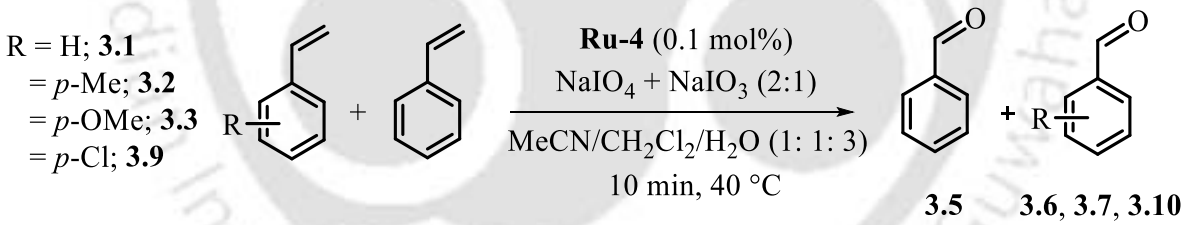


Figure 3.37. Determination of rate constant for different substituted alkenes by plotting ln(a/a-x) *vs* time (min) (left) and Hammett plot for **Ru-1** (right).

Reaction conditions involving Ru-4: In three different reaction tubes, a mixture of styrene, **1** (0.5 mmol), $NaIO_4$ (1 mmol), $NaIO_3$ (0.5 mmol) and **Ru-4** (0.1 mol%) were taken with a fixed volume of solvent ($MeCN/CH_2Cl_2/H_2O$; 1:1:3; 1 mL). To the respective reaction tube, substituted alkene **3.2** (0.5 mmol), **3.3** (0.5 mmol) and **3.9** (0.5 mmol) were added individually. The reaction tube was properly closed and placed in a preheated oil bath at 40 ºC with continuous stirring for 10 min. The ratio of yields (**3.5:3.6**), (**3.5:3.7**) and (**3.5:3.10**) were estimated using GC analysis with anisole as standard.



R		k_X/k_H	$\log(k_X/k_H)$	ρ
p-OMe	-0.27	2.20	0.34	**-1.42**
p-Me	-0.17	1.60	0.20	
H	0	0	0	
p-Cl	0.23	0.42	-0.38	

TH-3565_186122020

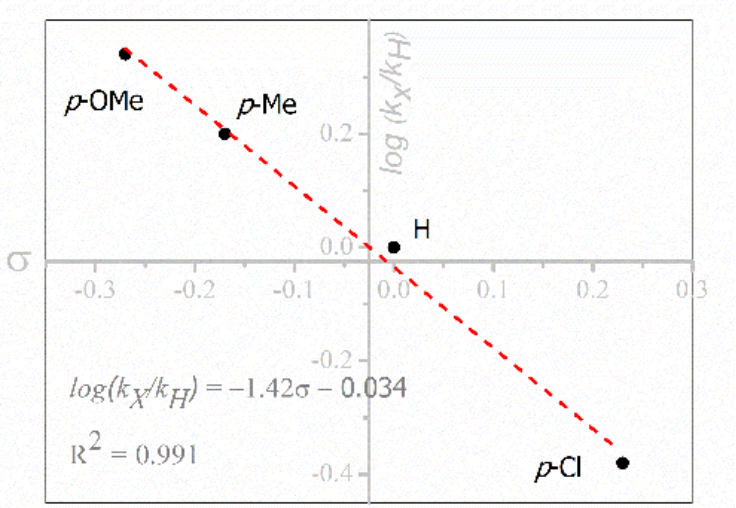


Figure 3.38. Hammett plot for **Ru-4**

(d) Entropy of activation

Further information was gathered by monitoring the rate of the reaction at temperatures between 10 and 40 °C for the oxidation reaction of styrene by using 0.1 mol% **Ru-1** catalyst. Individual rate constants obtained from these kinetic experiments were used to calculate the activation parameters. These were found to be $\Delta H^{\ddagger}$ = 11.14 ± 0.7 kcal mol^{-1} and $\Delta S^{\ddagger}$ = -32.1 ± 2.3 cal mol^{-1} K^{-1}. The large negative entropy of activation suggested the involvement of an associative process in the rate-limiting step.

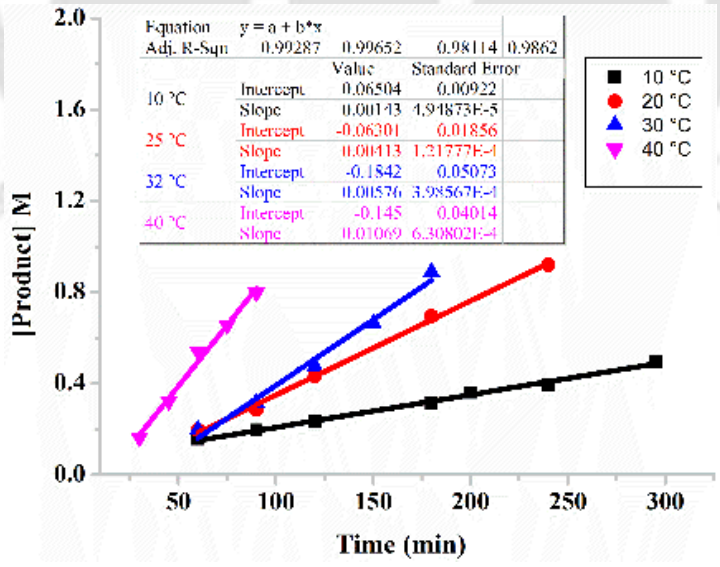


Figure 3.39. Product conc. [M] *vs* time plot at different temperatures

Activation enthalpy ($\Delta H^{\ddagger}$) and activation entropy ($\Delta S^{\ddagger}$) values were obtained from the slope and intercept of plots of ln(*k*/T) *vs* 1/T (Figure 3.40) by using the following equation:

$$\ln(k/T) = -\Delta H^{\#}/R.(1/T) + \ln(k_B/h) + \Delta S^{\#}/R$$

TH-3565_186122020

where k_B = Boltzmann constant, R = universal gas constant, and h = Planck's constant

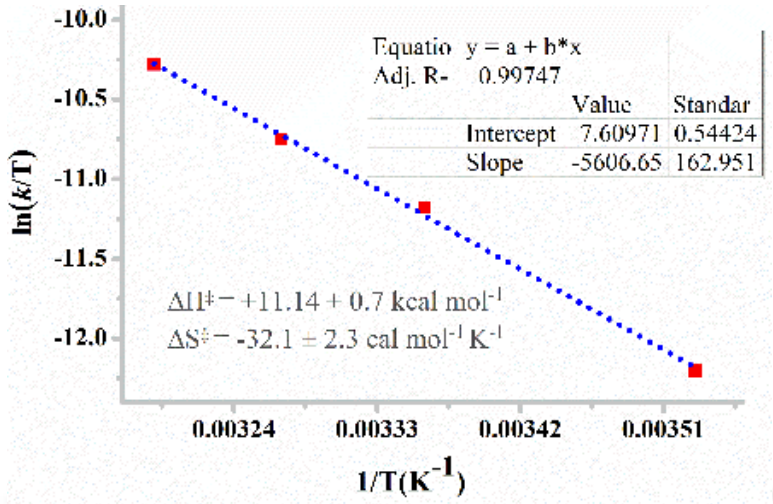


Figure 3.40. Arrhenius-Eyring plot

Similarly, using the catalyst **Ru-4**, the effect of temperature on the reaction rate was also studied by using Eyring analysis (Figure 3.41). The activation parameters were found to be $\Delta H^{\ddagger}$ = 16.56 ± 1.1 kcal mol^{-1} and $\Delta S^{\ddagger}$ = -11.84 ± 0.7 cal mol^{-1} K^{-1}. The results obtained are in accordance with the previous observation for complex **Ru-1**.

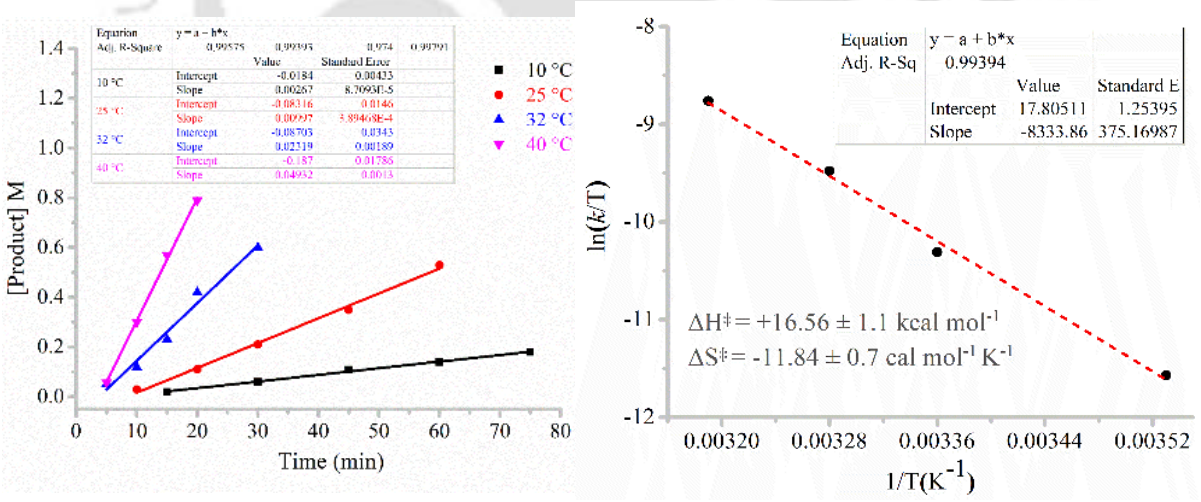


Figure 3.41. Concentration [Product] *vs* time plot at different temperatures (left) and Arrhenius-Eyring plot (right)

(e) Effect of by-product $NaIO_3$ on the rate of the reaction

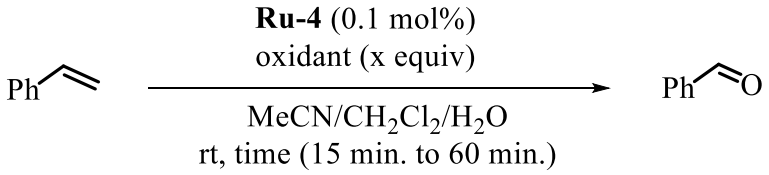
The initial kinetics were studied by performing three different experiments with

(i) 1 equiv. of $NaIO_3$ and 2 equiv. of $NaIO_4$

(ii) 3 equiv. of $NaIO_4$

TH-3565_186122020

(iii) 2 equiv. of $NaIO_4$



Scheme 3.22. Oxidation of styrene with different conc. of oxidant.

as an oxidant at room temperature. Figure 3.42 shows a ~2.5-fold increase in the reaction rate with $NaIO_3$ over its not adding $NaIO_3$ was observed.

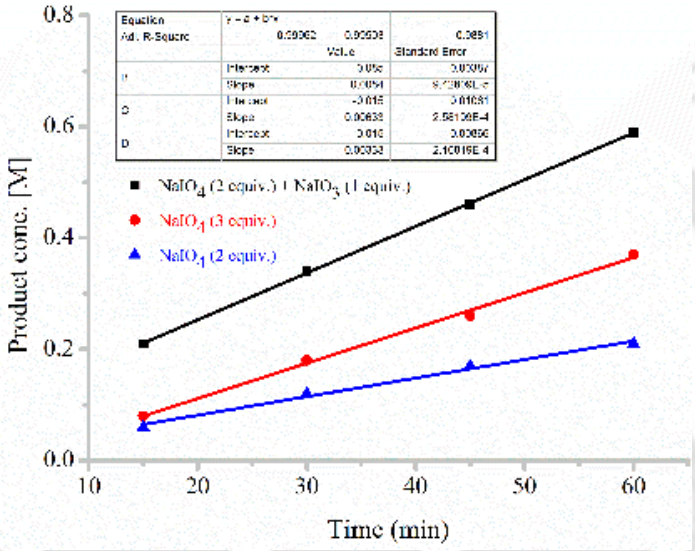


Figure 3.42. Kinetic plot of the above three reactions at different intervals of time.

3.5.9. Crystallographic data

The details crystallographic data of **Ru-1** and **Ru-2** are discussed in Chapter 2.

Crystallographic data of Ru-3

Single crystals of compound **Ru-3** suitable for X-ray diffraction were obtained by slow evaporation of the saturated solution of the compound in CH_2Cl_2 at room temperature. X-ray crystallographic data were collected with a Bruker D8 QUEST diffractometer. Data refinement and cell reduction were carried out by *APEX4*. Structures were solved by direct methods using Olex2 v1.5 and refined by a full-matrix least-squares method using Olex2 v1.5. All of the non-H atoms were refined anisotropically. The ORTEP diagram was obtained with ORTEP3 software with 40% thermal ellipsoid (see below, Figure 3.43). The crystallographic parameters and refinement data are listed in Table 3.34.

TH-3565_186122020

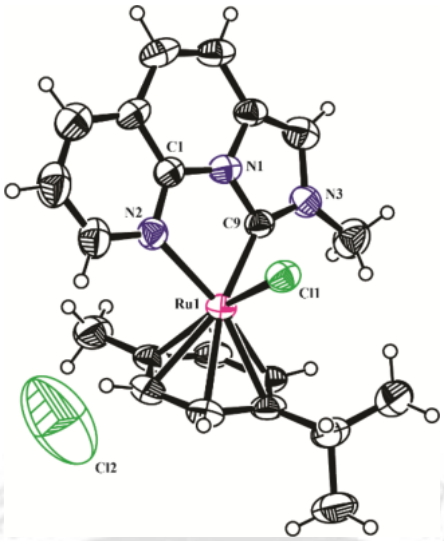


Figure 3.43. Molecular structure of compound **Ru-3** (thermal ellipsoid 40% probability level). Selected Bond lengths (in Å): Ru(1)–Cl(1) 2.4228(17), Ru(1)–N(2) 2.117(5), Ru(1)–C(9) 2.053(6), N(1)–C(9) 1.365(7), N(3)–C(9) 1.313(7). Selected Bond Angles (in °): C(9)–Ru(1)–N(2) 78.0(2), C(9)–Ru(1)–Cl(1) 115.4(2), N(2)–C(1)–N(1) 114.7(5), N(3)–C(9)–N1 103.6(5), N(2)–Ru(1)–Cl(1) 95.1(2).

Table 3.34. Crystal data and structure refinement for **Ru-3**

Identification code	MK655_2_0m_a	
CCDC	2311869	
Empirical formula	$C_{21}H_{31}Cl_2N_3O_4Ru$	
Formula weight	561.46	
Temperature	297(2) K	
Wavelength	0.71073 Å	
Crystal system	monoclinic	
Space group	C2/c	
Unit cell dimensions	a = 31.841(12) Å	α = 90°
	b = 12.162(5) Å	β = 90.505(11)°
	c = 13.100(5) Å	γ = 90°
Volume	5073(3) $Å^3$	
Z	8	
Density (calculated)	1.470 g/cm^3	
Absorption coefficient	0.859 mm^{-1}	
F(000)	2304.0	
Crystal size	0.26 × 0.24 × 0.2 mm^3	

TH-3565_186122020

2Θ range for data collection	4.738 to 50.078°
Index ranges	$-37 \leq h \leq 37, -14 \leq k \leq 14, -15 \leq l \leq 15$
Reflections collected	68360
Independent reflections	4478 [R_{int} = 0.0436, R_{sigma} = 0.0203]
Completeness to theta = 27.00°	99.6%
Data/restraints/parameters	4478/6/290
Goodness-of-fit on F^2	1.161
Final R indexes [I>=2σ (I)]	R_1 = 0.0534, wR_2 = 0.1396
Final R indexes [all data]	R_1 = 0.0762, wR_2 = 0.1685
Largest diff. peak and hole	1.06 and -0.86 e $Å^{-3}$

Crystallographic data of Ru-4

Single crystals of compound **Ru-4** suitable for X-ray diffraction were obtained by slow evaporation of the saturated solution of the compound in CH_2Cl_2 at room temperature. X-ray crystallographic data were collected using Bruker D8 QUEST diffractometer. Data refinement and cell reduction were carried out by *APEX4*. Structures were solved by direct methods using Olex2 v1.5 and refined by a full-matrix least-squares method using Olex2 v1.5. All of the non-H atoms were refined anisotropically. The ORTEP diagram was obtained with ORTEP3 software with 40% thermal ellipsoid (see below, Figure 3.44). The crystallographic parameters and refinement data are listed in Table 3.35.

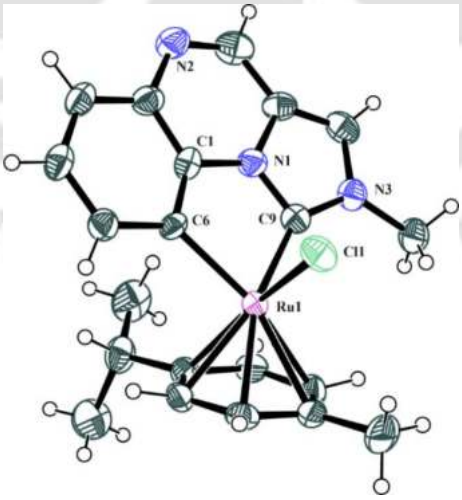


Figure 3.44. Molecular structure of compound **Ru-4** (thermal ellipsoid 40% probability level). Selected Bond lengths (in Å): Ru(1)–Cl(1) 2.4170(15), Ru(1)–C(6) 2.103(5), Ru(1)–C(9) 2.043(4), N(1)–C(9) 1.352(6), N(3)–C(9) 1.352(6). Selected Bond Angles (in °): C(6)–Ru(1)–Cl(1) 88.06(14), C(9)–Ru(1)–Cl(1) 84.65(18), C(9)–Ru(1)–C(6) 77.9(2), N(1)–C(9)–N(3) 102.1(4), N(1)–C(9)–Ru(1) 113.5(3), C(1)–C(6)–Ru(1) 114.4(4).

TH-3565_186122020

Table 3.35. Crystal data and structure refinement for **Ru-4**

Identification code	MK_C4N_0ma_a	
CCDC	2342585	
Empirical formula	$C_{21}H_{22}ClN_3Ru$	
Formula weight	452.93	
Temperature	299.00 K	
Wavelength	0.71073 Å	
Crystal system	orthorhombic	
Space group	$P2_12_12_1$	
Unit cell dimensions	a = 11.5141(12) Å	α = 90°
	b = 11.6166(12) Å	β = 90°
	c = 14.2119(14) Å	γ = 90°
Volume	1900.9(3) $Å^3$	
Z	4	
Density (calculated)	1.583 g/cm^3	
Absorption coefficient	0.975 mm^{-1}	
F(000)	920.0	
Crystal size	0.29 × 0.23 × 0.18 mm^3	
2Θ range for data collection	4.528 to 50.744°	
Index ranges	$-13 \leq h \leq 13, -13 \leq k \leq 13, -17 \leq l \leq 17$	
Reflections collected	44342	
Independent reflections	3456 [R_{int} = 0.0532, R_{sigma} = 0.0214]	
Completeness to theta = 25.372°	100%	
Data/restraints/parameters	3456/0/239	
Goodness-of-fit on F^2	1.090	
Final R indexes [I>=2σ (I)]	R_1 = 0.0277, wR_2 = 0.0566	
Final R indexes [all data]	R_1 = 0.0332, wR_2 = 0.0603	
Largest diff. peak and hole	0.51 and -0.37 e $Å^{-3}$	

Crystallographic data of 3.69

TH-3565_186122020

Single crystals of compound **3.69** suitable for X-ray diffraction were obtained by slow evaporation of the saturated solution of the compound in $CHCl_3$ at room temperature. X-ray crystallographic data were collected using Bruker D8 QUEST diffractometer. Data refinement and cell reduction were carried out by *APEX4*. Structures were solved by direct methods using Olex2 v1.5 and refined by a full-matrix least-squares method using Olex2 v1.5. All of the non-H atoms were refined anisotropically. The ORTEP diagram was obtained with ORTEP3 software with 40% thermal ellipsoid (see below, Figure 3.45). The crystallographic parameters and refinement data are listed in Table 3.36.

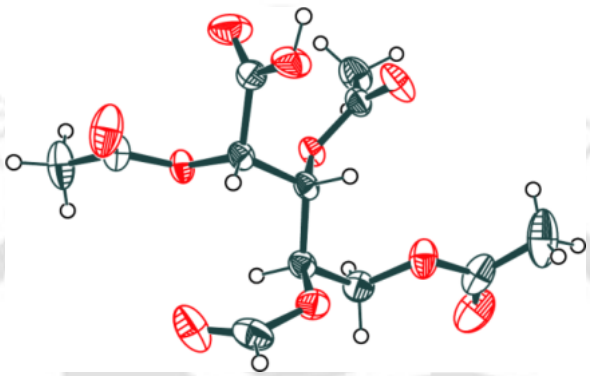


Figure 3.45. Molecular structure of compound **3.69** (thermal ellipsoid 40% probability level).

Table 3.36. Crystal data and structure refinement for **3.69**

Identification code	MK_861_0m_a	
CCDC	2335541	
Empirical formula	$C_{12}H_{16}O_{10}$	
Formula weight	320.25	
Temperature	297.00 K	
Wavelength	0.71073 Å	
Crystal system	monoclinic	
Space group	$P2_1$	
Unit cell dimensions	a = 8.0257(5) Å	α = 90°
	b = 7.7104(5) Å	β = 95.245(2)°
	c = 12.3665(8) Å	γ = 90°
Volume	762.05(8) $Å^3$	
Z	2	
Density (calculated)	1.396 g/cm^3	
Absorption coefficient	0.124 mm^{-1}	
F(000)	336.0	

TH-3565_186122020

Crystal size	0.39 × 0.34 × 0.25 mm^3
2Θ range for data collection	3.308 to 52.802°
Index ranges	-10 ≤ h ≤ 10, -9 ≤ k ≤ 9, -15 ≤ l ≤ 15
Reflections collected	19489
Independent reflections	3105 [R_{int} = 0.0266, R_{sigma} = 0.0194]
Completeness to theta = 26.401°	99.3%
Data/restraints/parameters	3105/1/205
Goodness-of-fit on F^2	1.077
Final R indexes [I>=2σ (I)]	R_1 = 0.0329, wR_2 = 0.0719
Final R indexes [all data]	R_1 = 0.0382, wR_2 = 0.0759
Largest diff. peak and hole	0.17 and -0.14 e $Å^{-3}$

3.5.10. Computational details

All calculations were performed using the Gaussian-16 program package in the gas phase.[30] Full geometry optimizations were carried out using M06L level[31] of theory and BS1 basis set. BS1 is defined as an SDD[32] basis set for Ru atom and 6-31G* Pople basis set for all other atoms. Frequency calculations at the same method and basis set were performed to distinguish transition state structures (one imaginary frequency) and minima structures (no imaginary frequency) on the potential energy surface. The transition states were verified by the intrinsic reaction coordinate (IRC) calculations, wherever necessary.[33] Free energies were calculated by using frequency calculations at 40 °C to match the experimental conditions.

Table 3.37. Free Energies (G) and Total Energies (E) of all the optimized structures given in Hartree along with the number of imaginary frequencies (for the oxidation reaction catalyzed by **Ru-1**)

Species	Free energy (G)	Total energy (E)	# Imaginary frequency (NImag)
I2_Cl	-1432.474707	-1432.6828133	0
TS_Cl	-1432.449725	-1432.6649475	1
I3_Cl	-1432.531265	-1432.7532325	0
I4_Cl	-1432.528403	-1432.7429202	0

[a](G) is calculated at 40 °C to meet the experimental conditions. All the figures were generated using (G) values. All the transition states have one NImag and all the intermediates have zero NImag. All the calculations were performed at the M06L level of DFT.

TH-3565_186122020

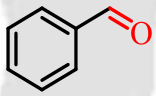
Table 3.38. Free Energies (G) and Total Energies (E) of all the optimized structures given in Hartree along with the number of imaginary frequencies (for the oxidation reaction catalyzed by **Ru-4**)

Species	Free energy (G)	Total energy (E)	# Imaginary frequency (NImag)
with Cl			
I2_Cl	-1448.519488	-1448.7153806	0
TS_Cl	-1448.494509	-1448.6976189	1
I3_Cl	-1448.576101	-1448.7860529	0
I4_Cl	-1448.574378	-1448.7771190	0
with $NaIO_3$			
I2_IO_3	-1225.137468	-1225.3366846	0
TS_IO_3	-1225.118383	-1225.3181672	1
I3_IO_3	-1225.204620	-1225.4110756	0
I4_IO_3	-1225.203685	-1225.4080851	0

[a](G) is calculated at 40 °C to meet the experimental conditions. All the figures were generated using (G) values. All the transition states have one NImag and all the intermediates have zero NImag. All the calculations were performed at the M06L level of DFT.

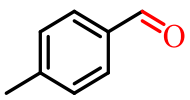
3.5.11. Analytical data of the products

Benzaldehyde (3.5)



The title compound **3.5** was isolated as a colorless liquid using silica gel column chromatography with petroleum ether/ethyl acetate (v/v = 50:1, R_f = 0.90) in 100% yield (106 mg) from GP-I; 100% yield (106 mg) from GP-II. ^{1}H NMR (500 MHz, Chloroform-*d*): δ 10.00 (s, 1H), 7.87 (d, J = 8.4 Hz, 2H), 7.63 – 7.60 (m, 1H), 7.51 (t, J = 7.9 Hz, 2H). ^{13}C NMR (151 MHz, Chloroform-*d*): δ 192.3, 136.4, 134.4, 129.7, 129.0.

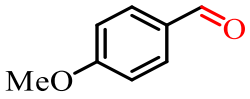
4-methylbenzaldehyde (3.6)



The title compound **3.6** was isolated as a colorless liquid using silica gel column chromatography with petroleum ether/ethyl acetate (v/v = 50:1, R_f = 0.80) in 99% yield (118.9 mg) from GP-I; 98% yield (117.7 mg) from GP-II. ^{1}H NMR (500 MHz, Chloroform-*d*): δ 9.95 (s, 1H), 7.77 (d, J = 8.3 Hz, 2H), 7.32 (d, J = 7.9 Hz, 2H), 2.43 (s, 3H). ^{13}C NMR (151 MHz, Chloroform-*d*): δ 191.9, 145.5, 134.2, 129.8, 129.7, 21.8.

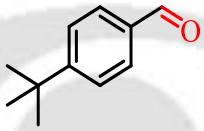
TH-3565_186122020

4-methoxybenzaldehyde (3.7)



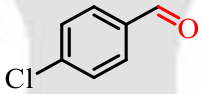
The title compound **3.7** was isolated as a colorless liquid using silica gel column chromatography with petroleum ether/ethyl acetate (v/v = 50:1, R_f = 0.80) in 97% yield (132.1 mg) from GP-I; 98% yield (133.4 mg) from GP-II. ^{1}H NMR (500 MHz, Chloroform-*d*): δ 9.83 (s, 1H), 7.79 (d, J = 8.8 Hz, 2H), 6.95 (d, J = 8.8 Hz, 2H), 3.83 (s, 3H). ^{13}C NMR (126 MHz, Chloroform-*d*): δ 190.9, 164.6, 132.0, 129.9, 114.3, 55.6.

4-(*tert*-butyl)benzaldehyde (3.8)



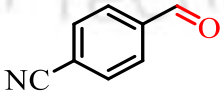
The title compound **3.8** was isolated as a pale-yellow liquid using silica gel column chromatography with petroleum ether/ethyl acetate (v/v = 40:1, R_f = 0.60) in 94% yield (152.5 mg) from GP-I; 95% yield (154.1 mg) from GP-II. ^{1}H NMR (500 MHz, Chloroform-*d*): δ 9.98 (s, 1H), 7.82 (d, J = 8.5 Hz, 2H), 7.55 (d, J = 8.5 Hz, 2H), 1.35 (s, 9H). ^{13}C NMR (126 MHz, Chloroform-*d*): δ 192.2, 158.6, 134.2, 129.8, 126.1, 35.5, 31.2.

4-chlorobenzaldehyde (3.10)



The title compound **3.10** was isolated as a pale-yellow solid using silica gel column chromatography with petroleum ether/ethyl acetate (v/v = 30:1, R_f = 0.60) in 91% yield (127.9 mg) from GP-I; 92% yield (129.3 mg) from GP-II. ^{1}H NMR (500 MHz, Chloroform-*d*): δ 9.98 (s, 1H), 7.82 (d, J = 8.4 Hz, 2H), 7.51 (d, J = 8.4 Hz, 2H). ^{13}C NMR (151 MHz, Chloroform-*d*): δ 191.0, 141.1, 134.8, 131.0, 129.6.

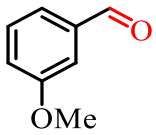
4-formylbenzonitrile (3.12)



The title compound **3.12** was isolated as a pale-yellow solid using silica gel column chromatography with petroleum ether/ethyl acetate (v/v = 10:1, R_f = 0.40) in 90% yield (118 mg) from GP-I; 90% yield (118 mg) from GP-II. ^{1}H NMR (500 MHz, Chloroform-*d*): δ 10.10 (s, 1H), 8.00 (d, J = 8.2 Hz, 2H), 7.85 (d, J = 8.2 Hz, 2H). ^{13}C NMR (151 MHz, Chloroform-*d*): δ 190.7, 138.9, 133.1, 130.0, 117.84, 117.77.

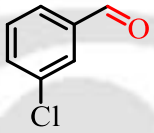
3-methoxybenzaldehyde (3.14)

TH-3565_186122020



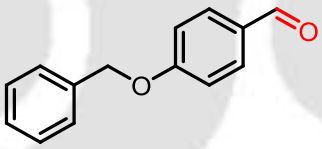
The title compound **3.14** was isolated as a white solid using silica gel column chromatography with petroleum ether/ethyl acetate (v/v = 20:1, R_f = 0.40) in 90% yield (122.5 mg) from GP-I; 91% yield (123.9 mg) from GP-II. ^{1}H NMR (600 MHz, Chloroform-*d*): δ 9.98 (s, 1H), 7.46 – 7.44 (m, 2H), 7.40 (s, 1H), 7.18 (d, J = 7.3 Hz, 1H), 3.87 (s, 3H). ^{13}C NMR (151 MHz, Chloroform-*d*): δ 192.3, 160.3, 138.0, 130.2, 123.7, 121.7, 112.2, 55.6.

1-chloro-3-vinylbenzene (3.16)



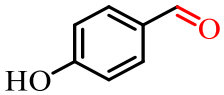
The title compound **3.16** was isolated as a colorless liquid using silica gel column chromatography with petroleum ether/ethyl acetate (v/v = 20:1, R_f = 0.40) in 87% yield (122.3 mg) from GP-I; 85% yield (119.5 mg) from GP-II. ^{1}H NMR (500 MHz, Chloroform-*d*): δ 9.98 (s, 1H), 7.85 (s, 1H), 7.76 (d, J = 7.6 Hz, 1H), 7.60 (d, J = 8.0 Hz, 1H), 7.48 (t, J = 7.8 Hz, 1H). ^{13}C NMR (126 MHz, Chloroform-*d*): δ 191.0, 138.0, 135.6, 134.5, 130.5, 129.5, 128.1.

4-(benzyloxy)benzaldehyde (3.18)



The title compound **3.18** was isolated as a white solid using silica gel column chromatography with petroleum ether/ethyl acetate (v/v = 10:1, R_f = 0.6) in 80% yield (169.8 mg) from GP-I; 82% yield (174 mg) from GP-II. ^{1}H NMR (400 MHz, Chloroform-*d*): δ 9.89 (s, 1H), 7.84 (d, J = 8.8 Hz, 2H), 7.45 – 7.34 (m, 5H), 7.08 (d, J = 8.7 Hz, 2H), 5.16 (s, 2H). ^{13}C NMR (151 MHz, Chloroform-*d*): δ 190.9, 163.9, 136.1, 132.1, 130.3, 128.9, 128.5, 127.6, 115.3, 70.4.

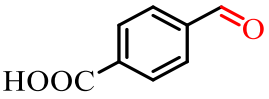
4-hydroxybenzaldehyde (3.20)



The title compound **3.20** was isolated as a brown solid using silica gel column chromatography with petroleum ether/ethyl acetate (v/v = 4:1, R_f = 0.50) in 81% yield (98.9 mg) from GP-I; 83% yield (101.3 mg) from GP-II. ^{1}H NMR (600 MHz, Chloroform-*d*): δ 9.87 (s, 1H), 7.83 (d, J = 6.8 Hz, 2H), 6.98 (d, J = 6.9 Hz, 2H), 6.32 (br, 1H). ^{13}C NMR (151 MHz, Chloroform-*d*): δ 191.5, 161.8, 132.7, 130.0, 116.2.

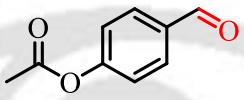
TH-3565_186122020

4-formylbenzoic acid (3.22)



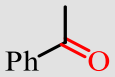
The title compound **3.22** was isolated as a white solid using silica gel column chromatography with petroleum ether/ethyl acetate (v/v = 3:2, R_f = 0.20) in 77% yield (115.6 mg) from GP-I; 80% yield (120 mg) from GP-II. ^{1}H NMR (600 MHz, Chloroform-*d*): δ 10.13 (s, 1H), 8.27 (d, J = 7.9 Hz, 2H), 8.00 (d, J = 7.9 Hz, 2H). ^{13}C NMR (126 MHz, Chloroform-*d* + DMSO-d^6): δ 191.4, 166.7, 138.4, 135.7, 129.8, 128.9.

4-formylphenyl acetate (3.24)



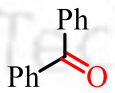
The title compound **3.24** was isolated as a colorless liquid using silica gel column chromatography with petroleum ether/ethyl acetate (v/v = 20:1, R_f = 0.40) in 83% yield (136.2 mg) from GP-I; 86% yield (141.2 mg) from GP-II. ^{1}H NMR (500 MHz, Chloroform-*d*): δ 9.97 (s, 1H), 7.90 (d, J = 8.7 Hz, 2H), 7.27 (d, J = 8.7 Hz, 2H), 2.32 (s, 3H). ^{13}C NMR (126 MHz, Chloroform-*d*): δ 190.9, 168.7, 155.3, 134.0, 131.2, 122.4, 21.1.

Acetophenone (3.26)



The title compound **3.26** was isolated as a colorless liquid using silica gel column chromatography with petroleum ether/ethyl acetate (v/v = 50:1, R_f = 0.40) in 89% yield (106.9 mg) from GP-I; 90% yield (108 mg) from GP-II. ^{1}H NMR (600 MHz, Chloroform-*d*): δ 7.96 (d, J = 7.4 Hz, 2H), 7.56 (t, J = 7.3 Hz, 1H), 7.46 (t, J = 7.6 Hz, 2H), 2.61 (s, 3H). ^{13}C NMR (151 MHz, Chloroform-*d*): δ 198.3, 137.3, 133.2, 128.7, 128.4, 26.7.

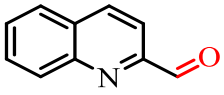
Benzophenone (3.28)



The title compound **3.28** was isolated as a white solid using silica gel column chromatography with petroleum ether/ethyl acetate (v/v = 20:1, R_f = 0.60) in 62% yield (113 mg) from GP-I; 68% yield (124 mg) from GP-II. ^{1}H NMR (600 MHz, Chloroform-*d*): δ 7.81 (d, J = 7.2 Hz, 4H), 7.59 (t, J = 7.4 Hz, 2H), 7.49 (t, J = 7.6 Hz, 4H). ^{13}C NMR (151 MHz, Chloroform-*d*): δ 196.9, 137.8, 132.6, 130.2, 128.4.

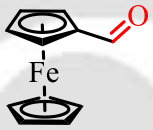
Quinoline-2-carbaldehyde (3.33)

TH-3565_186122020



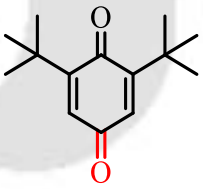
The title compound **3.33** was isolated as a yellow solid using silica gel column chromatography with petroleum ether/ethyl acetate (v/v = 9:1, R_f = 0.42) in 97% yield (152.5 mg) from GP-I; 99% yield (155.6 mg) from GP-II. ^{1}H NMR (500 MHz, Chloroform-*d*): δ 10.23 (s, 1H), 8.31 (d, J = 8.4 Hz, 1H), 8.25 (d, J = 8.5 Hz, 1H), 8.03 (d, J = 8.4 Hz, 1H), 7.90 (d, J = 8.2 Hz, 1H), 7.83 (t, J = 8.4 Hz, 1H), 7.69 (t, J = 8.2 Hz, 1H). ^{13}C NMR (126 MHz, Chloroform-*d*): δ 193.9, 152.7, 148.1, 137.5, 130.63, 130.58, 130.2, 129.3, 128.0, 117.5.

Ferrocene carboxaldehyde (3.35)



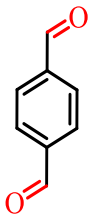
The title compound **3.35** was isolated as a yellow solid using silica gel column chromatography with petroleum ether/ethyl acetate (v/v = 5:1, R_f = 0.50) in 33% yield (70.6 mg) from GP-I; 36% yield (77.1 mg) from GP-II. ^{1}H NMR (400 MHz, Chloroform-*d*): δ 9.96 (s, 1H), 4.80 (t, J = 2.0 Hz, 2H), 4.61 (t, J = 2.0 Hz, 2H), 4.28 (s, 5H). ^{13}C NMR (151 MHz, Chloroform-*d*): δ 193.6, 79.5, 73.3, 69.8.

2,6-di-*tert*-butylcyclohexa-2,5-diene-1,4-dione (3.37)



The title compound **3.37** was isolated as a yellow oil using silica gel column chromatography with petroleum ether/ethyl acetate (v/v = 100:1, R_f = 0.95) in 80% yield (176.2 mg) from GP-I; 82% yield (180.6 mg) from GP-II. ^{1}H NMR (600 MHz, Chloroform-*d*): δ 6.50 (s, 2H), 1.28 (s, 18H). ^{13}C NMR (151 MHz, Chloroform-*d*): δ 189.3, 188.0, 158.1, 130.3, 35.7, 29.5.

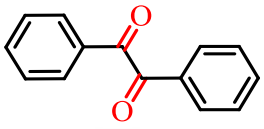
Terephthalaldehyde (3.39)



TH-3565_186122020

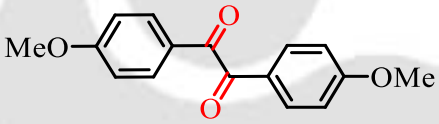
The title compound **3.39** was isolated as a white solid using silica gel column chromatography with petroleum ether/ethyl acetate (v/v = 10:1, R_f = 0.20) in 71% yield (95.2 mg) from GP-I; 71% yield (95.2 mg) from GP-II. ^{1}H NMR (500 MHz, Chloroform-*d*): δ 10.13 (s, 2H), 8.05 (m, 4H). ^{13}C NMR (126 MHz, Chloroform-*d*): δ 191.6, 140.2, 130.3.

Benzil (3.43)



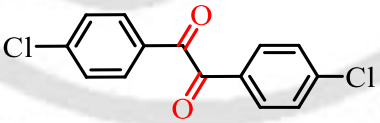
The title compound **3.43** was isolated as a yellow solid using silica gel column chromatography with petroleum ether/ethyl acetate (v/v = 50:1, R_f = 0.80) in 94% yield (197.6 mg) from GP-I; 95% yield (199.7 mg) from GP-II. ^{1}H NMR (500 MHz, Chloroform-*d*): δ 7.98 (d, J = 7.5 Hz, 4H), 7.66 (t, J = 7.5 Hz, 2H), 7.52 (t, J = 7.7 Hz, 4H). ^{13}C NMR (151 MHz, Chloroform-*d*): δ 194.7, 135.0, 133.2, 130.1, 129.2.

1,2-bis(4-methoxyphenyl)ethane-1,2-dione (3.44)



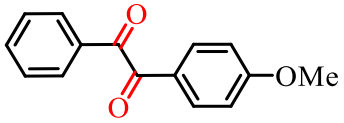
The title compound **3.44** was isolated as a yellow solid using silica gel column chromatography with petroleum ether/ethyl acetate (v/v = 9:1, R_f = 0.40) in 96% yield (259.5 mg) from GP-I; 96% yield (259.5 mg) from GP-II. ^{1}H NMR (500 MHz, Chloroform-*d*): δ 7.94 (d, J = 8.9 Hz, 4H), 6.96 (d, J = 8.9 Hz, 4H), 3.88 (s, 6H). ^{13}C NMR (151 MHz, Chloroform-*d*): δ 193.6, 165.0, 132.5, 126.4, 114.4, 55.8.

1,2-bis(4-chlorophenyl)ethane-1,2-dione (3.45)



The title compound **3.45** was isolated as a white solid using silica gel column chromatography with petroleum ether/ethyl acetate (v/v = 50:1, R_f = 0.30) in 82% yield (228.9 mg) from GP-I; 84% yield (234.4 mg) from GP-II. ^{1}H NMR (400 MHz, Chloroform-*d*): δ 7.92 (d, J = 8.6 Hz, 4H), 7.50 (d, J = 8.6 Hz, 4H). ^{13}C NMR (101 MHz, Chloroform-*d*): δ 192.5, 142.0, 131.4, 131.3, 129.7.

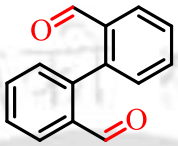
1-(4-methoxyphenyl)-2-phenylethane-1,2-dione (3.47)



TH-3565_186122020

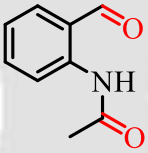
The title compound **3.47** was isolated as a white solid using silica gel column chromatography with petroleum ether/ethyl acetate (v/v = 6:1, R_f = 0.40) in 95% yield (228.3 mg) from GP-I; 95% yield (228.3 mg) from GP-II. ^{1}H NMR (500 MHz, Chloroform-*d*): δ 7.98 – 7.94 (m, 4H), 7.64 (t, J = 7.2 Hz, 1H), 7.50 (t, J = 7.6 Hz, 2H), 6.97 (d, J = 8.9 Hz, 2H), 3.88 (s, 3H). ^{13}C NMR (101 MHz, Chloroform-*d*): δ 195.0, 193.3, 165.1, 134.8, 133.3, 132.5, 130.0, 129.1, 126.2, 114.5, 55.8.

[1,1'-biphenyl]-2,2'-dicarbaldehyde (3.49)



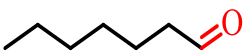
The title compound **3.49** was isolated as a light-yellow oil using silica gel column chromatography with petroleum ether/ethyl acetate (v/v = 50:4, R_f = 0.50) in 88% yield (185 mg) from GP-I; 91% yield (191.3 mg) from GP-II. ^{1}H NMR (500 MHz, Chloroform-*d*): δ 9.84 (s, 2H), 8.06 (dd, J = 7.8, 1.5 Hz, 2H), 7.67 (td, J = 7.5, 1.5 Hz, 2H), 7.60 (t, J = 7.8 Hz, 2H), 7.35 (d, J = 7.5 Hz, 2H). ^{13}C NMR (151 MHz, Chloroform-*d*): δ 191.2, 141.4, 134.7, 133.6, 131.8, 129.0, 128.7. Spectral data is in accordance to the reported literature.[34]

***N*-(2-formylphenyl)acetamide (3.51)**



The title compound **3.51** was isolated as a colorless oil using silica gel column chromatography with petroleum ether/ethyl acetate (v/v = 5:4, R_f = 0.20) in 80% yield (130.6 mg) from GP-I; 84% yield (137 mg) from GP-II. ^{1}H NMR (500 MHz, Chloroform-*d*): δ 10.95 (s, 1H), 8.73 (d, J = 8.5 Hz, 1H), 8.11 (d, J = 8.1 Hz, 1H), 7.60 (t, J = 8.6 Hz, 1H), 7.12 (t, J = 7.7 Hz, 1H), 2.26 (s, 3H). ^{13}C NMR (151 MHz, Chloroform-*d*): δ 171.2, 169.5, 142.2, 135.7, 131.8, 122.8, 120.6, 113.9, 25.7. Spectral data is in accordance to the reported literature.[35]

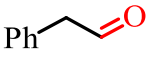
Heptanal (3.53)



The title compound **3.53** was isolated as a colorless liquid using silica gel column chromatography with petroleum ether/ethyl acetate (v/v = 50:1, R_f = 0.50) in 72% yield (82.2 mg) from GP-I; 73% yield (83.4 mg) from GP-II. ^{1}H NMR (500 MHz, Chloroform-*d*): δ 9.76 (s, 1H), 2.44 – 2.41 (m, 2H), 1.66 – 1.60 (m, 4H), 1.30 (m, 4H), 0.89 – 0.88 (m, 3H). ^{13}C NMR (151 MHz, Chloroform-*d*): δ 203.0, 43.9, 31.6, 28.9, 22.5, 22.1, 14.0.

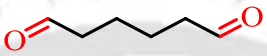
TH-3565_186122020

2-phenylacetaldehyde (3.55)



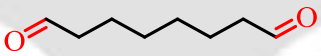
The title compound **3.55** was isolated as a colorless oil using silica gel column chromatography with petroleum ether/ethyl acetate (v/v = 9:1, R_f = 0.65) in 77% yield (92.5 mg) from GP-I; 77% yield (92.5 mg) from GP-II. ^{1}H NMR (400 MHz, Chloroform-*d*): δ 9.74 (t, J = 2.3 Hz, 1H), 7.39 – 7.35 (m, 2H), 7.32 – 7.30 (m, 1H), 7.22 – 7.20 (m, 2H), 3.68 (d, J = 2.5 Hz, 2H). ^{13}C NMR (151 MHz, Chloroform-*d*): δ 199.6, 132.0, 129.7, 129.1, 127.5, 50.7.

Adipaldehyde (3.57)



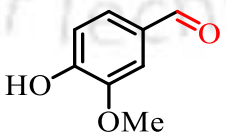
The title compound **3.57** was isolated as a colorless oil using silica gel column chromatography with petroleum ether/ethyl acetate (v/v = 2:1, R_f = 0.50) in 73% yield (83.3 mg) from GP-I; 74% yield (84.5 mg) from GP-II. ^{1}H NMR (600 MHz, Chloroform-*d*): δ 9.75 (t, J = 1.6 Hz, 2H), 2.47 – 2.45 (m, 4H), 1.66 – 1.63 (m, 4H). ^{13}C NMR (151 MHz, Chloroform-*d*): δ 202.1, 43.6, 21.6. Spectral data is in accordance to the reported literature.[36]

Octanedial (3.59)



The title compound **3.59** was isolated as a colorless oil using silica gel column chromatography with petroleum ether/ethyl acetate (v/v = 2:1, R_f = 0.50) in 65% yield (92.4 mg) from GP-I; 68% yield (96.7 mg) from GP-II. ^{1}H NMR (600 MHz, Chloroform-*d*): δ 9.75 (t, J = 1.8 Hz, 2H), 2.42 (td, J = 7.3, 1.8 Hz, 4H), 1.64 – 1.61 (m, 4H), 1.35 – 1.33 (m, 4H). ^{13}C NMR (151 MHz, Chloroform-*d*): δ 202.8, 43.9, 29.0, 21.9. Spectral data is in accordance to the reported literature.[36]

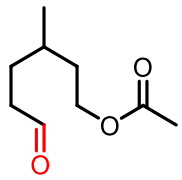
4-hydroxy-3-methoxybenzaldehyde (3.63)



The title compound **3.63** was isolated as a white solid using silica gel column chromatography with petroleum ether/ethyl acetate (v/v = 20:1, R_f = 0.40) in 80% yield (121.7 mg) from GP-I; 82% yield (124.7 mg) from GP-II. ^{1}H NMR (500 MHz, Chloroform-*d*): δ 9.82 (s, 1H), 7.43 – 7.42 (m, 2H), 7.04 (d, J = 8.5 Hz, 1H), 6.25 (brs, 1H), 3.97 (s, 3H). ^{13}C NMR (126 MHz, Chloroform-*d*): δ 191.0, 151.8, 147.3, 130.1, 127.6, 114.5, 109.0, 56.3. Spectral data is in accordance to the reported literature.[37]

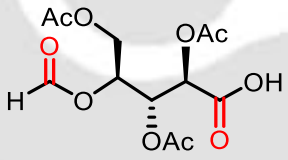
TH-3565_186122020

3-methyl-6-oxohexyl acetate (3.67)



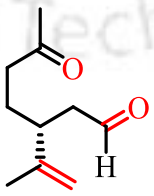
The title compound **3.67** was isolated as a yellow oil using silica gel column chromatography with petroleum ether/ethyl acetate (v/v = 4:1, R_f = 0.35) in 86% yield (148.1 mg) from GP-I; 90% yield (155 mg) from GP-II. ^{1}H NMR (600 MHz, Chloroform-*d*): δ 9.78 (s, 1H), 4.15 – 4.07 (m, 2H), 2.52 – 2.31 (m, 2H), 2.04 (s, 3H), 1.74 – 1.65 (m, 2H), 1.63 – 1.57 (m, 1H), 1.52 – 1.45 (m, 2H), 0.94 (d, J = 6.6 Hz, 3H). ^{13}C NMR (151 MHz, Chloroform-*d*): δ 202.4, 171.1, 62.5, 41.3, 35.1, 29.4, 28.6, 20.8, 19.0. Spectral data is in accordance to the reported literature.[38]

(2*R*,3*R*,4*S*)-2,3,5-triacetoxy-4-(formyloxy)pentanoic acid (3.69)



The title compound **3.69** was isolated as a colourless crystalline solid using silica gel column chromatography with petroleum ether/ethyl acetate (v/v = 10:1, R_f = 0.4) in 83% yield (265.8 mg) from GP-I; 89% yield (285 mg) from GP-II. ^{1}H NMR (400 MHz, Chloroform-*d*): δ 8.00 (s, 1H), 7.55 (br, 1H), 5.64 (dd, J = 8.7, 2.2 Hz, 1H), 5.38 – 5.35 (m, 1H), 5.22 (d, J = 2.2 Hz, 1H), 4.30 – 4.26 (m, 1H), 4.14 (dd, J = 12.6, 5.3 Hz, 1H), 2.12 (s, 3H), 2.05 (s, 3H), 2.01 (s, 3H). ^{13}C NMR (151 MHz, Chloroform-*d*): δ 170.9, 170.4, 169.9, 159.6, 69.8, 68.6, 67.7, 61.7, 20.6, 20.42, 20.35. Spectral data is in accordance to the reported literature.[39]

(*R*)-6-oxo-3-(prop-1-en-2-yl)heptanal (3.71)

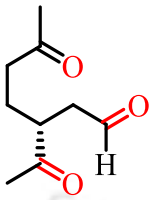


The title compound **3.71** was isolated as a colorless oil using silica gel column chromatography with petroleum ether/ethyl acetate (v/v = 2:1, R_f = 0.30) in 60% yield (100.9 mg) from GP-I; 63% yield (106 mg) from GP-II. ^{1}H NMR (600 MHz, Chloroform-*d*): δ 9.67 (s, 1H), 4.83 (s, 1H), 4.77 (s, 1H), 2.70 – 2.65 (m, 1H), 2.47 – 2.43 (m, 2H), 2.39 (t, J = 7.6 Hz, 2H), 2.13 (s, 3H), 1.72 (m, 1H), 1.64 (s, 3H), 1.62 – 1.61 (m, 1H). ^{13}C NMR (151 MHz, Chloroform-*d*): δ

TH-3565_186122020

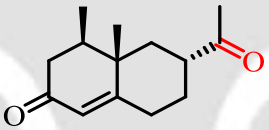
208.5, 202.0, 145.2, 113.4, 47.6, 41.1, 40.9, 30.2, 26.6, 18.5. Spectral data is in accordance to the reported literature.[40]

3-acetyl-6-oxoheptanal (3.72)



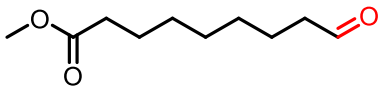
The title compound **3.72** was isolated as a pale-yellow oil using silica gel column chromatography with petroleum ether/ethyl acetate (v/v = 3:2, R_f = 0.10) in 68% yield (115.7 mg) from GP-I; 71% yield (120.8 mg) from GP-II. ^{1}H NMR (500 MHz, Chloroform-*d*): δ 9.71 (s, 1H), 3.08 – 3.03 (m, 1H), 2.95 – 2.90 (m, 1H), 2.43 – 2.40 (m, 3H), 2.25 (s, 3H), 2.13 (s, 3H), 1.93 – 1.88 (m, 1H), 1.73 – 1.71 (m, 1H). ^{13}C NMR (151 MHz, Chloroform-*d*): δ 210.2, 207.4, 200.2, 44.9, 44.8, 40.2, 30.1, 29.4, 24.5. Spectral data is in accordance to the reported literature.[40]

(4*R*,4*aS*,6*R*)-6-acetyl-4,4a-dimethyl-4,4a,5,6,7,8-hexahydronaphthalen-2(3*H*)-one (3.74)



The title compound **3.74** was isolated as a colorless oil using silica gel column chromatography with petroleum ether/ethyl acetate (v/v = 5:2, R_f = 0.30) in 79% yield (174 mg) from GP-I; 76% yield (167.4 mg) from GP-II. ^{1}H NMR (500 MHz, Chloroform-*d*): δ 5.70 (s, 1H), 2.72 – 2.67 (m, 1H), 2.49 – 2.43 (m, 1H), 2.36 – 2.33 (m, 1H), 2.22 – 2.18 (m, 2H), 2.13 (s, 2H), 2.04 – 1.94 (m, 4H), 1.41 – 1.33 (m, 1H), 1.19 (t, J = 13.1 Hz, 1H), 1.05 (s, 3H), 0.92 (d, J = 6.8 Hz, 3H). ^{13}C NMR (151 MHz, Chloroform-*d*): δ 210.5, 199.2, 168.6, 125.1, 46.7, 42.0, 40.2, 39.9, 38.8, 32.0, 28.4, 28.2, 16.7, 14.9. Spectral data is in accordance to the reported literature.[4b]

Methyl 9-oxononanoate (3.76)

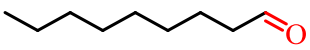


The title compound **3.76** was isolated as a colorless oil using silica gel column chromatography with petroleum ether/ethyl acetate (v/v = 5:1, R_f = 0.40) in 76% yield (141.6 mg) from GP-I; 74% yield (137.8 mg) from GP-II. ^{1}H NMR (400 MHz, Chloroform-*d*): δ 9.75 (s, 1H), 3.66 (s, 3H), 2.41 (t, J = 7.1 Hz, 2H), 2.29 (t, J = 7.4 Hz, 2H), 1.63 – 1.59 (m, 4H), 1.31 (brs, 6H). ^{13}C

TH-3565_186122020

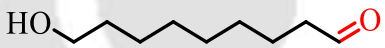
NMR (151 MHz, Chloroform-*d*): δ 202.6, 174.0, 51.3, 43.6, 33.8, 28.72, 28.68, 28.6, 24.6, 21.7. Spectral data is in accordance to the reported literature.[41]

Nonanal (3.77)



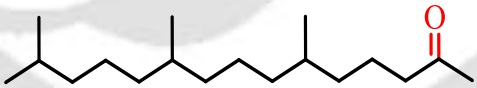
The title compound **3.77** was isolated as a brown oil using silica gel column chromatography with petroleum ether/ethyl acetate (v/v = 10:1, R_f = 0.60) in 86% yield (122.3 mg) from GP-I; 88% yield (125.2 mg) from GP-II. ^{1}H NMR (500 MHz, Chloroform-*d*): δ 9.75 – 9.74 (m, 1H), 2.40 (td, J = 7.4, 1.9 Hz, 2H), 1.64 – 1.58 (m, 2H), 1.28 – 1.26 (m, 10H), 0.86 (t, J = 6.4 Hz, 3H). ^{13}C NMR (126 MHz, Chloroform-*d*): δ 203.1, 44.0, 31.9, 29.4, 29.3, 29.2, 22.8, 22.2, 14.2. Spectral data is in accordance to the reported literature.[42]

9-hydroxynonanal (3.79)



The title compound **3.79** was isolated as a colourless oil using silica gel column chromatography with petroleum ether/ethyl acetate (v/v = 5:1, R_f = 0.40) in 80% yield (126.6 mg) from GP-I; 80% yield (126.6 mg) from GP-II. ^{1}H NMR (400 MHz, Chloroform-*d*): δ 9.76 (s, 1H), 3.63 (t, J = 6.6 Hz, 2H), 2.42 (t, J = 7.3 Hz, 2H), 1.62 – 1.54 (m, 4H), 1.34 – 1.27 (m, 8H). ^{13}C NMR (151 MHz, Chloroform-*d*): δ 203.2, 63.1, 44.0, 32.8, 29.4, 29.3, 29.2, 25.8, 22.2. Spectral data is in accordance to the reported literature.[43]

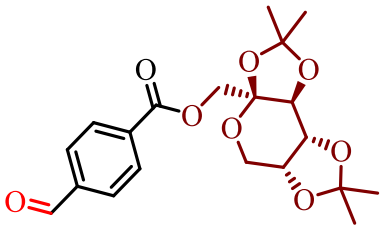
6,10,14-trimethylpentadecan-2-one (3.82)



The title compound **3.82** was isolated as a colorless oil using silica gel column chromatography with petroleum ether/ethyl acetate (v/v = 20:1, R_f = 0.60) in 73% yield (196 mg) from GP-I; 70% yield (188 mg) from GP-II. ^{1}H NMR (500 MHz, Chloroform-*d*): δ 2.39 (t, J = 7.5 Hz, 2H), 2.12 (s, 3H), 1.61 – 1.48 (m, 3H), 1.38 – 1.22 (m, 11H), 1.14 – 1.06 (m, 5H), 0.86 – 0.82 (m, 12H). ^{13}C NMR (151 MHz, Chloroform-*d*): δ 209.5, 44.3, 39.5, 37.5, 37.41, 37.35, 36.6, 32.9, 32.8, 30.0, 28.1, 24.9, 24.5, 22.8, 22.7, 21.6, 19.9, 19.7. Spectral data is in accordance to the reported literature.[6b]

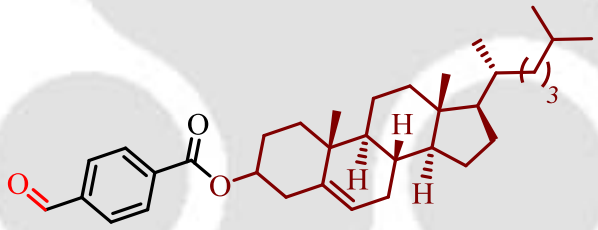
(2,2,7,7-tetramethyltetrahydro-3a*H*-bis([1,3]dioxolo)[4,5-b:4',5'-*d*]pyran-3ayl)methyl 4-formylbenzoate (3.84)

TH-3565_186122020



The title compound **3.84** was isolated as a white solid using silica gel column chromatography with petroleum ether/ethyl acetate (v/v = 5:1, R_f = 0.45) in 74% yield (290.4 mg) from GP-I; 76% yield (298.2 mg) from GP-II. ^{1}H NMR (600 MHz, Chloroform-*d*): δ 10.09 (s, 1H), 8.22 (d, J = 8.0 Hz, 2H), 7.94 (d, J = 8.0 Hz, 2H), 4.70 (d, J = 11.8 Hz, 1H), 4.63 (dd, J = 7.9, 2.7 Hz, 1H), 4.43 (d, J = 2.7 Hz, 1H), 4.35 (d, J = 11.8 Hz, 1H), 4.25 (d, J = 9.7 Hz, 1H), 3.95 – 3.93 (m, 1H), 3.80 – 3.78 (m, 1H), 1.54 (s, 3H), 1.44 (s, 3H), 1.35 – 1.33 (m, 6H). ^{13}C NMR (151 MHz, Chloroform-*d*): δ 191.7, 165.1, 139.4, 135.0, 130.5, 129.6, 109.3, 109.0, 101.6, 70.84, 70.78, 70.2, 66.1, 61.5, 26.6, 26.0, 25.6, 24.1. Spectral data is in accordance to the reported literature.[44]

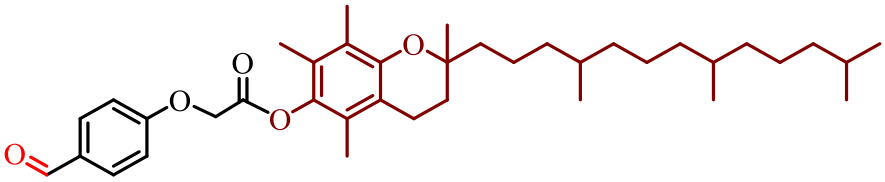
(8*S*,9*S*,10*R*,13*R*,14*S*,17*R*)-10,13-dimethyl-17-((*R*)-4-methylpentan-2-yl) 2,3,4,7,8,9,10,11,12,13,14,15,16,17-tetradecahydro-1*H*-cyclopenta[*a*]phenanthren-3-yl 4-formylbenzoate (3.86)



The title compound **3.86** was isolated as a white solid using silica gel column chromatography with petroleum ether/ethyl acetate (v/v = 13:1, R_f = 0.40) in 64% yield (332 mg) from GP-I; 62% yield (322 mg) from GP-II. ^{1}H NMR (400 MHz, Chloroform-*d*): δ 10.10 (s, 1H), 8.19 (d, J = 8.2 Hz, 2H), 7.94 (d, J = 8.2 Hz, 2H), 5.43 (d, J = 3.2 Hz, 1H), 4.93 – 4.85 (m, 1H), 2.48 (d, J = 7.9 Hz, 2H), 2.04 – 1.91 (m, 4H), 1.86 – 1.70 (m, 2H), 1.60 – 1.45 (m, 7H), 1.38 – 1.30 (m, 3H), 1.25 – 1.10 (m, 7H), 1.07 (s, 3H), 1.03 – 0.96 (m, 3H), 0.92 (d, J = 6.5 Hz, 3H), 0.87 (d, J = 1.8 Hz, 3H), 0.86 (d, J = 1.8 Hz, 3H), 0.69 (s, 3H). ^{13}C NMR (101 MHz, Chloroform-*d*): δ 191.9, 165.1, 139.5, 139.2, 136.0, 130.3, 129.6, 123.2, 75.5, 56.8, 56.3, 50.2, 42.5, 39.9, 39.7, 38.3, 37.1, 36.8, 36.3, 35.9, 32.1, 32.0, 28.4, 28.2, 28.0, 24.4, 24.0, 23.0, 22.7, 21.2, 19.5, 18.9, 12.0. Spectral data is in accordance to the reported literature.[45]

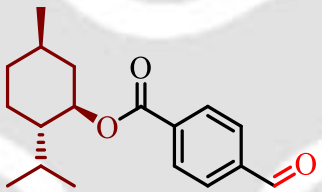
2,5,7,8-tetramethyl-2-(4,8,12-trimethyltridecyl)chroman-6-yl-2-(4-formylphenoxy) acetate (3.88)

TH-3565_186122020



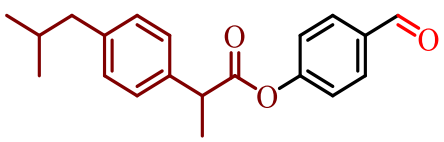
The title compound **3.88** was isolated as a yellow oil using silica gel column chromatography with petroleum ether/ethyl acetate (v/v = 10:1, R_f = 0.55) in 68% yield (403.1 mg) from GP-I; 70% yield (415 mg) from GP-II. ^{1}H NMR (600 MHz, Chloroform-*d*): δ 9.91 (s, 1H), 7.88 (d, J = 8.4 Hz, 2H), 7.12 (d, J = 8.4 Hz, 2H), 5.02 (s, 2H), 2.59 (t, J = 6.9 Hz, 2H), 2.10 (s, 3H), 2.02 (s, 3H), 1.97 (s, 3H), 1.83 – 1.74 (m, 2H), 1.57 – 1.51 (m, 3H), 1.49 – 1.44 (m, 2H), 1.41 – 1.37 (m, 3H), 1.29 – 1.21 (m, 10H), 1.16 – 1.08 (m, 6H), 0.88 – 0.85 (m, 12H). ^{13}C NMR (151 MHz, Chloroform-*d*): δ 190.8, 166.9, 162.6, 149.9, 139.9, 132.1, 131.0, 126.5, 124.8, 123.4, 117.7, 115.1, 75.3, 65.1, 39.5, 37.63, 37.60, 37.54, 37.49, 37.47, 37.4, 36.7, 32.87, 32.85, 32.8, 28.1, 24.90, 24.89, 24.5, 22.8, 22.7, 21.1, 20.7, 19.85, 19.78, 13.1, 12.2, 11.9. Spectral data is in accordance to the reported literature.[46]

(1*R*,2*S*,5*R*)-2-isopropyl-5-methylcyclohexyl 4-formylbenzoate (3.90)



The title compound **3.90** was isolated as a yellow oil using silica gel column chromatography with petroleum ether/ethyl acetate (v/v = 9:1, R_f = 0.40) in 82% yield (236.5 mg) from GP-I; 83% yield (239.4 mg) from GP-II. ^{1}H NMR (500 MHz, Chloroform-*d*): δ 10.10 (s, 1H), 8.19 (d, J = 8.3 Hz, 2H), 7.95 (d, J = 8.3 Hz, 2H), 4.96 (td, J = 11.0, 4.4 Hz, 1H), 2.14 – 2.12 (m, 1H), 1.96 – 1.91 (m, 1H), 1.74 (d, J = 12.4 Hz, 2H), 1.59 – 1.54 (m, 2H), 1.16 – 1.11 (m, 2H), 0.93 (t, J = 6.0 Hz, 7H), 0.79 (d, J = 6.9 Hz, 3H). ^{13}C NMR (126 MHz, Chloroform-*d*): δ 191.9, 165.2, 139.2, 136.0, 130.3, 129.6, 75.8, 47.4, 41.0, 34.4, 31.6, 26.7, 23.7, 22.2, 20.9, 16.6. Spectral data is in accordance to the reported literature.[47]

4-formylphenyl 2-(4-isobutylphenyl)propanoate (3.92)

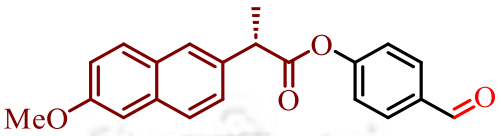


The title compound **3.92** was isolated as a colorless oil using silica gel column chromatography with petroleum ether/ethyl acetate (v/v = 10:1, R_f = 0.50) in 84% yield (260.7 mg) from GP-I; 87% yield (270 mg) from GP-II. ^{1}H NMR (500 MHz, Chloroform-*d*): δ 9.87 (s, 1H), 7.78 (d, J = 8.7 Hz, 2H), 7.29 (d, J = 8.2 Hz, 2H), 7.14 – 7.11 (m, 4H), 3.94 (q, J = 7.2 Hz, 1H), 2.45

TH-3565_186122020

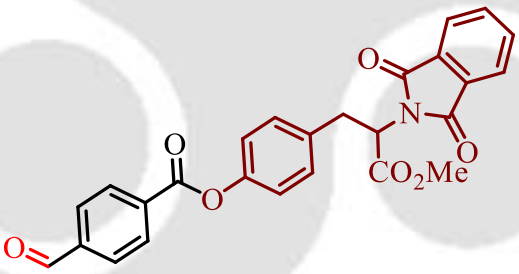
(d, J = 7.3 Hz, 2H), 1.85 (hept, J = 6.8 Hz, 1H), 1.58 (d, J = 7.3 Hz, 3H), 0.89 (d, J = 7.0 Hz, 6H). ^{13}C NMR (126 MHz, Chloroform-*d*): δ 190.6, 172.3, 155.4, 140.8, 136.8, 133.8, 130.9, 129.5, 127.1, 122.0, 45.1, 44.9, 30.0, 22.2, 18.3. Spectral data is in accordance to the reported literature.[48]

4-formylphenyl (*S*)-2-(6-methoxynaphthalen-2-yl)propanoate (3.94)



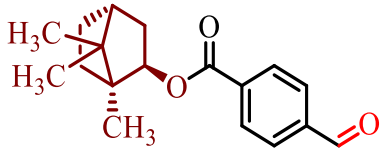
The title compound **3.94** was isolated as a colorless oil using silica gel column chromatography with petroleum ether/ethyl acetate (v/v = 8:1, R_f = 0.55) in 85% yield (284.2 mg) from GP-I; 88% yield (294.3 mg) from GP-II. ^{1}H NMR (500 MHz, Chloroform-*d*): δ 9.95 (s, 1H), 7.86 (d, J = 8.7 Hz, 2H), 7.78 – 7.74 (m, 3H), 7.50 (dd, J = 8.5, 1.8 Hz, 1H), 7.19 – 7.15 (m, 4H), 4.13 (q, J = 7.1 Hz, 1H), 3.93 (s, 3H), 1.71 (d, J = 7.2 Hz, 3H). ^{13}C NMR (126 MHz, Chloroform-*d*): δ 191.0, 172.6, 158.0, 155.7, 134.7, 134.1, 134.0, 131.2, 129.4, 129.1, 127.6, 126.3, 126.1, 122.3, 119.4, 105.8, 55.5, 45.7, 18.5. Spectral data is in accordance to the reported literature.[49]

4-(2-(1,3-dioxoisoindolin-2-yl)-3-methoxy-3-oxopropyl)phenyl 4-formylbenzoate (3.96)



The title compound **3.96** was isolated as a white solid using silica gel column chromatography with petroleum ether/ethyl acetate (v/v = 20:9, R_f = 0.75) in 85% yield (388.8 mg) from GP-I; 87% yield (398 mg) from GP-II. ^{1}H NMR (600 MHz, Chloroform-*d*): δ 10.12 (s, 1H), 8.30 (d, J = 8.3 Hz, 2H), 7.99 (d, J = 8.3 Hz, 2H), 7.81 (dd, J = 5.5, 3.1 Hz, 2H), 7.71 (dd, J = 5.5, 3.1 Hz, 2H), 7.26 (d, J = 8.5 Hz, 2H), 7.08 (d, J = 8.5 Hz, 2H), 5.19 (dd, J = 11.2, 5.3 Hz, 1H), 3.79 (s, 3H), 3.66 – 3.57 (m, 2H). ^{13}C NMR (151 MHz, Chloroform-*d*): δ 191.6, 169.3, 167.6, 164.1, 149.6, 139.7, 134.9, 134.6, 134.3, 131.7, 130.8, 130.1, 129.7, 123.7, 121.7, 53.2, 53.1, 34.2. HRMS (ESI) *m/z*: calcd. for $C_{26}H_{19}NNaO_7$ [M+Na]$^+$: 480.1054; found: 480.1051.

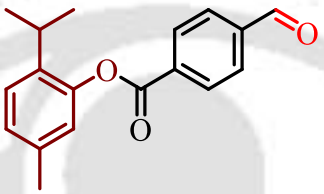
(1*S*,2*R*,4*R*)-1,7,7-trimethylbicyclo[2.2.1]heptan-2-yl 4-formylbenzoate (3.98)



TH-3565_186122020

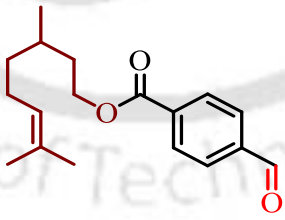
The title compound **3.98** was isolated as a white solid using silica gel column chromatography with petroleum ether/ethyl acetate (v/v = 12:1, R_f = 0.70) in 77% yield (220.5 mg) from GP-I; 78% yield (223.4 mg) from GP-II. ^{1}H NMR (500 MHz, Chloroform-*d*): δ 10.11 (s, 1H), 8.17 (d, *J* = 8.4 Hz, 2H), 7.96 (d, *J* = 8.4 Hz, 2H), 4.95 (dd, *J* = 7.1, 4.6 Hz, 1H), 1.94 – 1.92 (m, 2H), 1.82 (m, 1H), 1.78 – 1.73 (m, 1H), 1.63 (td, *J* = 12.6, 4.2 Hz, 1H), 1.27 – 1.22 (m, 1H), 1.18 – 1.16 (m, 1H), 1.14 (s, 3H), 0.95 (s, 3H), 0.90 (s, 3H). ^{13}C NMR (126 MHz, Chloroform-*d*): δ 191.6, 164.9, 139.1, 135.8, 130.0, 129.5, 82.3, 49.1, 47.0, 45.1, 38.8, 33.7, 27.0, 20.10, 20.08, 11.6. Spectral data is in accordance to the reported literature.[50]

2-isopropyl-5-methylphenyl 4-formylbenzoate (3.100)



The title compound **3.100** was isolated as a yellow oil using silica gel column chromatography with petroleum ether/ethyl acetate (v/v = 20:1, R_f = 0.80) in 84% yield (237.1 mg) from GP-I; 88% yield (248.4 mg) from GP-II. ^{1}H NMR (600 MHz, Chloroform-*d*): δ 10.05 (s, 1H), 8.28 (d, *J* = 8.3 Hz, 2H), 7.94 (d, *J* = 8.3 Hz, 2H), 7.17 (d, *J* = 8.0 Hz, 1H), 7.00 – 6.99 (m, 1H), 6.86 (br, 1H), 2.95 (hept, *J* = 6.9 Hz, 1H), 2.25 (s, 3H), 1.13 (d, *J* = 6.9 Hz, 6H). ^{13}C NMR (151 MHz, Chloroform-*d*): δ 191.6, 164.5, 148.0, 139.7, 137.1, 136.9, 134.6, 130.8, 129.8, 127.6, 126.7, 122.7, 27.4, 23.1, 20.9. HRMS (ESI) *m/z*: calcd. for $C_{18}H_{18}NaO_3$ $[M+Na]^+$: 305.1149; found: 305.1163.

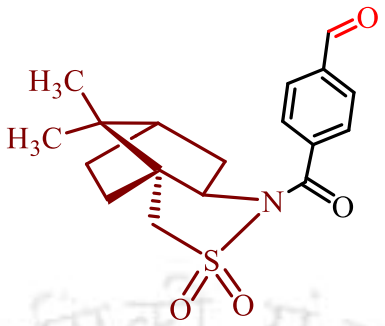
3,7-dimethyloct-6-en-1-yl 4-formylbenzoate (3.102)



The title compound **3.102** was isolated as a colorless oil using silica gel column chromatography with petroleum ether/ethyl acetate (v/v = 10:3, R_f = 0.60) in 60% yield (173 mg) from GP-I; 58% yield (167.3 mg) from GP-II. ^{1}H NMR (600 MHz, Chloroform-*d*): δ 10.08 (s, 1H), 8.16 (d, *J* = 8.3 Hz, 2H), 7.92 (d, *J* = 8.5 Hz, 2H), 5.07 (t, *J* = 6.2 Hz, 1H), 4.41 – 4.34 (m, 2H), 2.05 – 1.93 (m, 2H), 1.84 – 1.79 (m, 1H), 1.64 (s, 3H), 1.63 – 1.60 (m, 2H), 1.58 (s, 3H), 1.42 – 1.36 (m, 1H), 1.26 – 1.20 (m, 1H), 0.96 (d, *J* = 6.6 Hz, 3H). ^{13}C NMR (151 MHz, Chloroform-*d*): δ 191.7, 165.6, 139.2, 135.6, 131.5, 130.2, 129.5, 124.6, 64.2, 37.0, 35.5, 29.6, 25.8, 25.4, 19.6, 17.7. Spectral data is in accordance to the reported literature.[51]

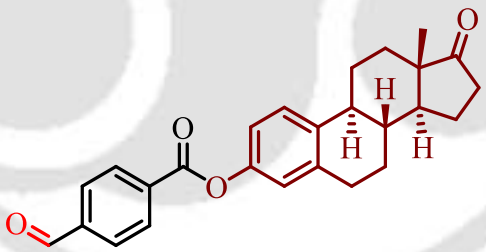
TH-3565_186122020

4-((3a*R*)-9,9-dimethyl-2,2-dioxidohexahydro-*1H,3H*-3a,7-methanocyclohepta[*c*] isothiazole-1-carbonyl)benzaldehyde (3.104)



The title compound **3.104** was isolated as a white solid using silica gel column chromatography with petroleum ether/ethyl acetate (v/v = 10:3, R_f = 0.50) in 86% yield (310.9 mg) from GP-I; 85% yield (307.2 mg) from GP-II. ^{1}H NMR (600 MHz, Chloroform-*d*): δ 10.08 (s, 1H), 7.94 (d, J = 8.3 Hz, 2H), 7.87 (d, J = 8.3 Hz, 2H), 4.17 (dd, J = 7.7, 4.9 Hz, 1H), 3.54 (d, J = 13.7 Hz, 1H), 3.43 (d, J = 13.7 Hz, 1H), 2.17 – 2.12 (m, 2H), 2.02 – 1.94 (m, 3H), 1.50 – 1.46 (m, 1H), 1.43 – 1.39 (m, 1H), 1.34 (s, 3H), 1.03 (s, 3H). ^{13}C NMR (151 MHz, Chloroform-*d*): δ 191.7, 169.1, 138.9, 138.8, 130.0, 129.3, 66.1, 53.7, 48.4, 48.0, 45.2, 38.5, 33.3, 26.6, 21.4, 20.0. HRMS (ESI) *m/z*: calcd. for $C_{18}H_{22}NO_4S$ $[M+H]^+$: 348.1265; found: 348.1273.

(8*R*,9*S*,13*S*,14*S*)-13-methyl-17-oxo-7,8,9,11,12,13,14,15,16,17-decahydro-6*H*-cyclopenta [*a*]phenanthren-3-yl 4-formylbenzoate (3.106)



The title compound **3.106** was isolated as a white solid using silica gel column chromatography with petroleum ether/ethyl acetate (v/v = 4:1, R_f = 0.30) in 55% yield (221.4 mg) from GP-I; 51% yield (205.3 mg) from GP-II. ^{1}H NMR (600 MHz, Chloroform-*d*): δ 10.14 (s, 1H), 8.35 (d, J = 8.0 Hz, 2H), 8.02 (d, J = 8.0 Hz, 2H), 7.35 (d, J = 8.5 Hz, 1H), 7.01 – 6.96 (m, 2H), 2.96 – 2.94 (m, 2H), 2.54 –2.50 (m, 1H), 2.45 – 2.42 (m, 1H), 2.35 – 2.31 (m, 1H), 2.19 – 2.13 (m, 1H), 2.09 – 2.03 (m, 2H), 2.00 – 1.98 (m, 1H), 1.66 – 1.61 (m, 3H), 1.55 – 1.48 (m, 3H), 0.93 (s, 3H). ^{13}C NMR (151 MHz, Chloroform-*d*): δ 191.7, 164.6, 148.7, 139.7, 138.4, 138.0, 134.8, 130.9, 129.8, 126.7, 121.6, 118.8, 50.6, 48.1, 44.3, 38.1, 36.0, 31.7, 29.6, 26.5, 25.9, 21.7, 14.0. Spectral data is in accordance to the reported literature.[49]

TH-3565_186122020

3.6. References

1. (a) Clayden, J.; Greeves, N.; Warren, S. G. *Organic Chemistry*, Oxford University Press, Oxford, **2012**. (b) Ruffoni, A.; Hampton, C.; Simonetti M.; Leonori, D. *Nature,* **2022**, *610*, 81–86.

2. (a) Rajagopalan, A.; Lara, M.; Kroutil, W. *Adv. Synth. Catal.* **2013**, *355*, 3321−3335. (b) Corma, A.; Iborra, S.; Velty, A. *Chem. Rev.* **2007**, *107*, 2411−2502.
3. (a) Bailey, P. S. *Chem. Rev.* **1958**, *58*, 925−1010. (b) Hassan, Z.; Stahlberger, M.; Rosenbaum, N.; Bräse, S. *Angew. Chem., Int. Ed.* **2021**, *60*, 15138−15152. (c) Caron, S.; Dugger, R. W.; Ruggeri, S. G.; Ragan, J. A.; Ripin, D. H. B. *Chem. Rev.* **2006**, *106*, 2943−2989. (d) Fisher, T. J.; Dussault, P. H. *Tetrahedron Lett.* **2017**, *73*, 4233−4258.
4. (a) Pappo, R.; Allen, D. S., Jr.; Lemieux, R. U.; Johnson, W. S. *J. Org. Chem.* **1956**, *21*, 478−479. (b) Travis, B. R.; Narayan, R. S.; Borhan, B. *J. Am. Chem. Soc.* **2002**, *124*, 3824−3825. (c) Whitehead, D. C.; Travis, B. R.; Borhan, B. *Tetrahedron Lett.* **2006**, *47*, 3797−3800.
5. (a) Rup, S.; Sindt, M.; Oget, N. *Tetrahedron Lett.* **2010**, *51*, 3123−3126. (b) Shing, T. K. M.; Tam, E. K. W.; Tai, V. W.-F.; Chung, I. H. F.; Jiang, Q. *Chem. Eur. J.* **1996**, *2*, 50−57. (c) Plietker, B. *J. Org. Chem.* **2003**, *68*, 7123−7125.

6. (a) Gonzalez-de-Castro, A.; Xiao, J. *J. Am. Chem. Soc.* **2015**, *137*, 8206−8218. (b) Huang, Z.; Guan, R.; Shanmugam, M.; Bennett, E. L.; Robertson, C. M.; Brookfield, A.; McInnes, E. J. L.; Xiao, J. *J. Am. Chem. Soc.* **2021**, *143*, 10005−10013. (c) Borrell, M.; Costas, M. *J. Am. Chem. Soc.* **2017**, *139*, 12821−12829. (d) Gupta, S. K.; Sahoo, S. K.; Choudhury, J. *Organometallics* **2016**, *35*, 2462−2466. (e) Chen, S.; Liu, Z.; Shi, E.; Chen, L.; Wei, W.; Li, H.; Cheng, Y.; Wan, X. *Org. Lett.* **2011**, *13*, 2274−2277. (f) Fan, P.; Su, S.; Wang, C. *ACS Catal.* **2018**, *8*, 6820−6826.
7. (a) Yip, W.-P.; Yu, W.-Y.; Zhu, N.; Che, C.-M. *J. Am. Chem. Soc.* **2005**, *127*, 14239−14249. (b) Daw, P.; Petakamsetty, R.; Sarbajna, A.; Laha, S.; Ramapanicker, R.; Bera, J. K. *J. Am. Chem. Soc.* **2014**, *136*, 13987−13990. (c) Salzmann, K.; Segarra, C.; Albrecht, M. *Angew. Chem., Int. Ed.* **2020**, *59*, 8932– 8936. (d) Bailey, A. J.; Griffith, W. P.; White, A. J. P.; Williams, D. J. *J. Chem. Soc., Chem. Commun.* **1994**, 1833–1834.
8. (a) van der Boom, M. E.; Milstein, D. *Chem. Rev.* **2003**, *103*, 1759−1792. (b) Peris, E. *Chem. Rev.* **2018**, *118*, 9988−10031. (c) Chen, C.; Liu, F. -S.; Szostak, M. *Chem. Eur. J.* **2021**, *27*, 4478−4499. (d) Zhao, Q.; Meng, G.; Nolan, S. P.; Szostak, M. *Chem. Rev.* **2020**, *120*, 1981−2048. (e) Findlay, M. T.; Domingo-Legarda, P.; McArthur, G.; Yen, A.; Larrosa, I. *Chem. Sci.* **2022**, *13*, 3335–3362.
9. (a) Sanford, M. S.; Love, J. A.; Grubbs, R. H. *J. Am. Chem. Soc.* **2001**, *123*, 6543−6554. (b) Hey, D. A.; Reich, R. M.; Baratta, W.; Kuehn, F. E. *Coord. Chem. Rev.* **2018**, *374*, 114–132. (c) Vivancos, Á.; Segarra, C.; Albrecht, M. *Chem. Rev.* **2018**, *118*, 9493−9586.
10. Arya, S. S.; Rookes, J. E.; Cahill, D. M.; Lenka, S. K. *Adv. Tradit. Med.* **2021**, *21*, 1.
11. (a) Stolle, A. *Eur. J. Org. Chem.* **2013**, *2013*, 2265−2278. (b) Archer, R. A.; Blanchard, W. B.; Day, W. A.; Johnson, D. W.; Lavagnino, E. R.; Ryan, C. W.; Baldwin, J. E. *J. Org. Chem.* **1977**, *42*, 2277–2284.
12. Hida, T.; Kikuchi, J.; Kakinuma, M.; Nogusa, H. *Org. Process Res. Dev.* **2010**, *14*, 1485–1489.
13. Corma, A.; Iborra, S.; Velty, A. *Chem. Rev.* **2007**, *107*, 2411−2502.
14. (a) Spannring, P.; Prat, I.; Costas, M.; Lutz, M.; Bruijnincx, P. C. A.; Weckhuysen, B. M.; Klein Gebbink, R. J. M. *Catal. Sci. Technol.* **2014**, *4*, 708–716. (b) Chen, J.; de Liedekerke Beaufort, M.; Gyurik, L.; Dorresteijn, J.; Otte, M.; Klein Gebbink, R. J. M. *Green Chem.* **2019**, *21*, 2436−2447.

TH-3565_186122020

15. Biswas, A.; Sharma, B. K.; Vermillion, K.; Willett, J. L.; Cheng, H. N. *J. Agric. Food Chem.* **2011**, *59*, 3066−3070.
16. Breitmaier, E. *Terpenes: Flavors, Fragrances, Pharmaca, Pheromones.* John Wiley & Sons, 2006.
17. Manrıquez, M. E.; Norena, L. E.; Wang, J. A.; Chen, L.; Salmones, J.; Gonzalez-Garcia, J.; Reza, C.; Tzompantzi, F.; Hernandez Cortez, J. G.; Ye L.; Xie, H. *Int. J. Photoenergy*, **2018**, *2018*, 1–12.
18. Che, C. M.; Yu, W. Y.; Chan, P. M.; Cheng, W. C.; Peng, S. M.; Lau, K. C.; Li, W. K. *J. Am. Chem. Soc*. **2000**, *122*, 11380–11392.

19. Novikov, R. A.; Timofeev, V. P.; Tomilov, Y. V. *J. Org. Chem.* **2012**, *77*, 5993−6006.

20. Yan, Y.; Xu, K.; Fang, Y.; Wang, Z. *J. Org. Chem.* **2011**, *76*, 6849−6855.

21. Akyildiz, V.; Lafzi, F.; Kilic, H.; Saracoglu, N. *Org. Biomol. Chem.* **2022**, *20*, 3570−3588.

22. Wang, T.-Z.; Pinard, E.; Paquette, L. A. *J. Am. Chem. Soc.* **1996**, *118*, 1309−1318.

23. Wu, H.-P.; Shao, C.-K.; Wu, D.; Jiang, L.; Yin, H.-Q.; Chen, F.-X. *J. Org. Chem.* **2021**, *86*, 5327−5335.

24. Tu, J. L.; Tang, W.; Xu, W.; Liu, F. *J. Org. Chem.* **2021**, *86*, 2929−2940.

25. Katta, N.; Zhao, Q. -Q.; Mandal, T.; Reiser, O. *ACS Catal.* **2022**, *12*, 14398−14407.

26. Liu, J. G.; Wu, S.; Yu, J. J.; Lu, C. X.; Wu, Z.; Wu, X. X.; Xue, X. S.; Zhu, C. *Angew. Chem., Int. Ed*. **2020**, *59*, 8195−8202.

27. Wu, C.; Hui, X.; Zhang, D.; Zhang, M.; Zhu, Y.; Wang, S. *Green Chem*. **2022**, *24*, 1103−1108.

28. Song, T.; Ma, Z.; Wang, X.; Yang, Y. *Org. Lett.* **2021**, *23*, 5917–5921.

29. Chen, L.; Jin, S.; Gao, J.; Liu, T.; Shao, Y.; Feng, J.; Wang, K.; Lu, T.; Du, D. *Org. Lett*. **2021**, *23*, 394−399.

30. Frisch, M. J.; Trucks, G. W.; Schlegel, H. B.; Scuseria, G. E.; Robb, M. A.; Cheeseman, J. R.; Scalmani, G.; Barone, V.; Petersson, G. A.; Nakatsuji, H.; Li, X.; Caricato, M.; Marenich, A. V.; Bloino, J.; Janesko, B. G.; Gomperts, R.; Mennucci, B.; Hratchian, H. P.; Ortiz, J. V.; Izmaylov, A. F.; Sonnenberg, J. L.; Williams-Young, D.; Ding, F.; Lipparini, F.; Egidi, F.; Goings, J.; Peng, B.; Petrone, A.; Henderson, T.; Ranasinghe, D.; Zakrzewski, V. G.; Gao, J.; Rega, N.; Zheng, G.; Liang, W.; Hada, M.; Ehara, M.; Toyota, K.; Fukuda, R.; Hasegawa, J.; Ishida, M.; Nakajima, T.; Honda, Y.; Kitao, O.; Nakai, H.; Vreven, T.; Throssell, K.; Montgomery, J. A., Jr.; Peralta, J. E.; Ogliaro, F.; Bearpark, M. J.; Heyd, J. J.; Brothers, E. N.; Kudin, K. N.; Staroverov, V. N.; Keith, T. A.; Kobayashi, R.; Normand, J.; Raghavachari, K.; Rendell, A. P.; Burant, J. C.; Iyengar, S. S.; Tomasi, J.; Cossi, M.; Millam, J. M.; Klene, M.; Adamo, C.; Cammi, R.; Ochterski, J. W.; Martin, R. L.; Morokuma, K.; Farkas, O.; Foresman, J. B.; Fox, D. J. *Gaussian 16*, Revision C.01, Gaussian, Inc., Wallingford CT, 2016.

31. Wang, Y.; Jin, X.; Yu, H. S.; Truhlar, D. G.; He, X. *PNAS* **2017**, *114*, 8487–8492.

32. Dolg, M.; Wedig, U.; Stoll, H.; Preuss, H. *J. Chem. Phys*., **1987**, *86*, 866–872.

33. Fukui, K. *Acc. Chem. Res.* **1981**, *14*, 363–368.

34. Liang, T.; Dong, G.; Li, C.; Xu, X.; Xu, Z. *Org. Lett.* **2022**, *24*, 1817−1821.

TH-3565_186122020

35. Gurawa, A.; Kumar, M.; Rao, D. S.; Kashyap, S. *New J. Chem.* **2020**, *44*, 16702−16707.

36. López, S.; Fernández-Trillo, F.; Castedo, L.; Saá, C. *Org. Lett.* **2003**, *5*, 3725−3728.

37. Bao, K.; Fan, A.; Dai, Y.; Zhang, L.; Zhang, W.; Cheng, M.; Yao, X. *Org. Biomol. Chem*. **2009**, *7*, 5084−5090.

38. Buntasana, S.; Hayashi, J.; Saetung, P.; Klumphu, P.; Vilaivan, T.; Padungros, P. *J. Org. Chem.* **2022**, *87*, 6525−6540.

39. Hillers, S.; Niklaus, A.; Reiser, O. *J. Org. Chem.* **1993**, *58*, 3169−3171.

40. Buntasana, S.; Seankongsuk, P.; Vilaivan, T.; Padungros, P. *Asian J. Org. Chem*. **2021**, *10*, 1141−1152.

41. Gung, B. W.; Dickson, H. *Org. Lett.* **2002**, *4*, 2517−2519.

42. Wertz, S.; Studer, A. *Adv. Synth. Catal.* **2011**, *353*, 69−72.

43. Song, Z.; Meng, S.; Wang, Q. *Chemistry Select* **2022**, *7*, e202202991.

44. Chen, Y. -X.; He, J. -T.; Wu, M. -C.; Liu, Z. -L.; Tang, K.; Xia, P. -J.; Chen, K.; Xiang, H. -Y.; Chen, X. -Q.; Yang, H. *Org. Lett.* **2022**, *24*, 3920−3925.

45. Liu, M. -S.; Shu, W. *ACS Catal.* **2020**, *10*, 12960−12966.

46. Bhattacharyya, D.; Sarmah, B. K.; Nandi, S.; Srivastava, H. K.; Das, A. *Org. Lett.* **2021**, *23*, 869−875.

47. Shee, M.; Singh, N. D. P. *Adv. Synth. Catal.* **2022**, *364*, 2032−2039.

48. Xie, H.; Breit, B. *ACS Catal.* **2022**, *12*, 3249−3255.

49. Zhang, S.; Perveen, S.; Ouyang, Y.; Xu, L.; Yu, T.; Zhao, M.; Wang, L.; Song, P.; Li, P. *Angew. Chem., Int. Ed.* **2022**, *61*, No. e202117843.

50. Fu, B.; Wang, L.; Yu, X.; Fang, X.; Mack, J.; Dingiswayo, S.; Nyokong, T.; Liang, X.; Xu, H. *Dyes Pigm.* **2021**, *195*, No. 109699.

51. Ou, J.; He, S.; Wang, W.; Tan, H.; Liu, K. *Org. Chem. Front.* **2021**, *8*, 3102−3109.

TH-3565_186122020

Chapter 4

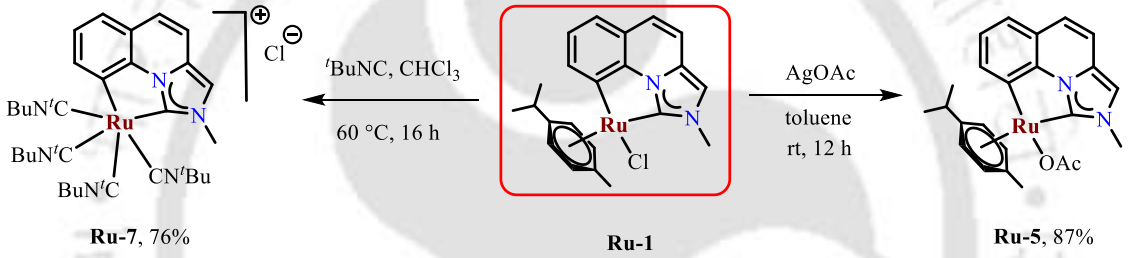
Ruthenium(II)-Catalyzed Oxidative C-H Activation/Alkyne Annulation Using Quinoline-Functionalized NHC as a Directing and Functionalized Group

TH-3565_186122020

4.1. Introduction

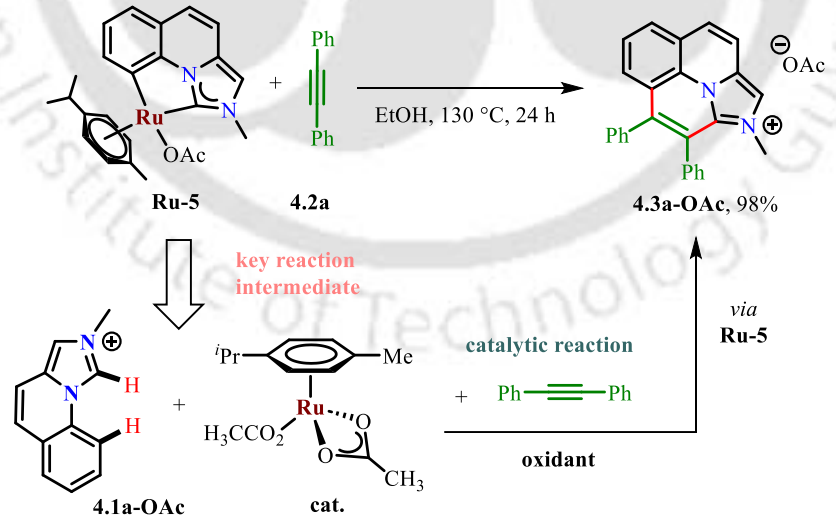
The chemistry of heteroaromatic compounds particularly nitrogen-containing molecules is a broad field with nearly two centuries of research. The focus of fused *N*-heterocyclic chemistry has expanded to include a wide range of areas in molecular biology, materials science, synthetic and physical organic chemistry, and natural product synthesis.[1] Additionally, the conjugated π-system displays significant photochemical and electrochemical properties, suggesting possible uses as organic semiconductors and materials for luminescence.[2]

In the previous two chapters (Chapter 2 and Chapter 3), I have discussed the catalytic utility of the synthesized cyclometalated ruthenium complex **Ru-1** in the selective C–H oxidation of *N*-heteroarenes and olefin oxidation. In this chapter, the reactivity of the cyclometalated complex **Ru-1** is initially inspected. The η^6-mode of *p*-cymene can easily be replaced by a strong σ-donor ^{t}BuNC ligand and formed cationic complex **Ru-7** in 76% yield (Scheme 4.1). On the other hand, the metal-bound Cl group is replaced by the acetate group using AgOAc to form **Ru-5** in 87% yield.



Ru-7, 76% **Ru-1** **Ru-5**, 87%

Scheme 4.1. Reaction of **Ru-1** with AgOAc and ^{t}BuNC



Ru-5 **4.2a** **4.3a-OAc**, 98%

4.1a-OAc **cat.**

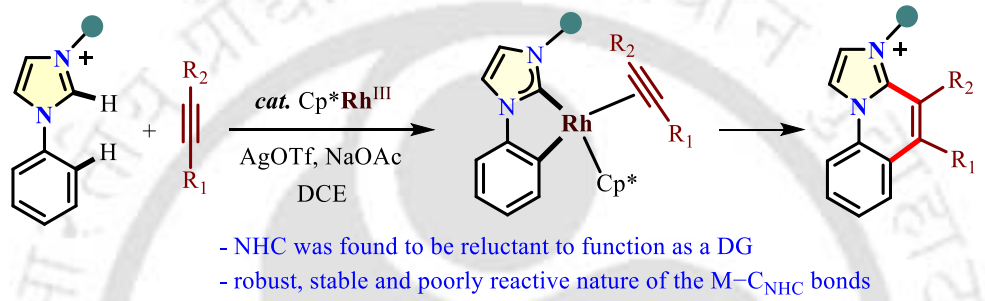
Scheme 4.2. Stoichiometric reaction between **Ru-5** and **4.2a**

The reaction between **Ru-5** (0.2 mmol) and alkyne **4.2a** (0.2 mmol) in EtOH (Scheme 4.2), leading to the formation of annulated product 1-methyl-8,9-diphenylbenzo[*ij*]imidazo[2,1,5-*de*]quinolizin-1-ium acetate **4.3a-OAc** in 98% yield. Notably, complex **Ru-5** can be considered

TH-3565_186122020

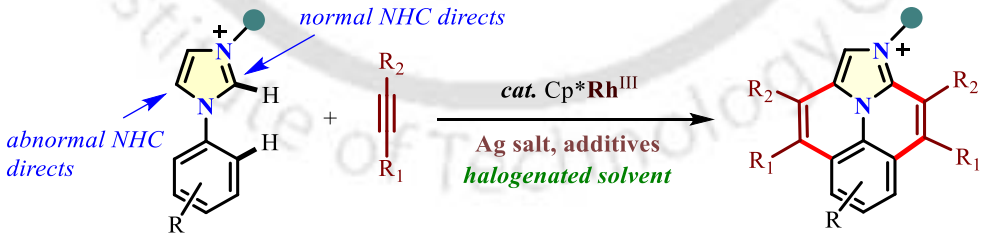
as a potential intermediate in the catalytic annulation reaction of **4.1a-OAc** and **4.2a** with Ru(*p*-cymene)$(OAc)_2$ catalyst. It is worth mentioning that progress has been made with the rhodium-catalyzed oxidative annulation reaction of alkyne *via* NHC-directed C–H bond activation; however cost-effective ruthenium-catalyzed annulative π-extension has not been systematically studied.

In 2014, Choudhury and co-workers first disclosed the prevalent *N*-heterocyclic carbene (NHC) ligands as a directing group with the help of Cp*Rh(III)-catalyst (Scheme 4.3).[3] The chemical strategy consists of cyclometalated species formation in the first step *via* imidazolium C(2)–H activation and aryl C–H activation, followed by alkyne insertion into cyclometalated species forming a seven-membered metalacyclic intermediate, and subsequently, it undergoes reductive elimination to provide the annulated product.



Scheme 4.3. Oxidative C–H activation/alkyne annulation *via* NHC-directed chelation

After a successful mono-annulation reaction, Choudhury[4] and Wang[5] independently reported a bis-annulation reaction by simply varying the reaction parameters. They showed the rhodium(III) catalyzed cascade oxidative annulation reaction of aryl imidazolium salts with alkynes, in which normal and abnormal NHCs participated as directing groups in double C–H bond activation. Control experiments suggested the proposed mechanistic sequence involves NHC and *a*NHC-directed C–H activation, alkyne insertion, and annulative reductive elimination. Then the Rh(I) will oxidize to regenerate the catalyst in the catalytic cycle.



Scheme 4.4. Bis-annulation reaction *via* NHC and *a*NHC-directed C–H activation

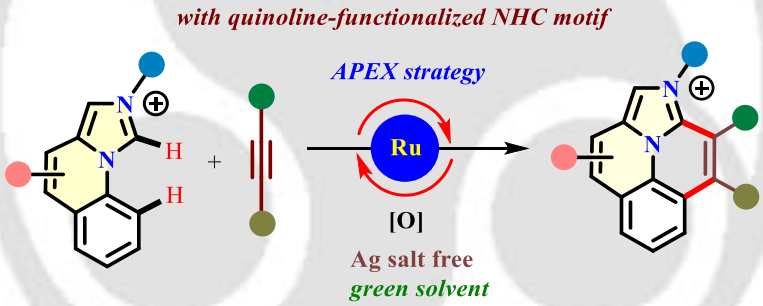
Despite these advances, these reactions require the use of stoichiometric excess oxidants,[4,5] such as silver(I) salts, thereby leading to the formation of a large amount of silver mirror in the reaction vessel. Thus, the method was restricted to scale-up synthesis. Besides, a halogenated solvent was used as the reaction medium in most cases. Therefore, in the context of green and sustainable chemistry, the development of an operationally simple, easy, and straightforward method with minimal chemical waste and good green metrics is highly desirable.[6]

TH-3565_186122020

The use of molecular oxygen as a sacrificial oxidant is certainly an attractive approach since it is inexpensive and produces only water as a by-product. Indeed, a variety of metal-catalyzed C−H functionalization catalysis with oxygen as the sole oxidant has been accomplished in the past few years including Pd-catalyzed indoles synthesis from simple anilines and alkynes,[7a] Ru and Rh-catalyzed oxidative alkyne annulation,[7b–7e] and Cu-catalyzed alkynylation of electron deficient polyfluoroarenes.[7f] These are mostly covered with a weak nitrogen- or oxygen-donor functional group as a directing group. In contrast, NHC directed C−H functionalization catalysis with oxygen as the sole oxidant has remained elusive until now. Due to inherently sluggish electron transfer processes, swapping common oxidants with molecular oxygen is still a great challenge.[8]

4.2. Present work

Herein, I report a one-pot efficient Ru(II)-catalyzed C–H bond activation and annulation reaction of imidazo[1,5-*a*]quinolin-2-ium salts with alkynes *via* newly designed quinoline functionalized NHCs as directing groups leading to access fluorescence active π-conjugated fused imidazo[1,5-*a*]quinolin-2-ium derivatives (Scheme 4.5). Like other aza-fused heterocycles,[3–5,9,10] these fused imidazo-quinolinium scaffolds could be useful in organic light-emitting diode (OLED) applications,[10a] and are important structural motifs with therapeutic potential.[10b]



Scheme 4.5. Ruthenium(II) catalyzed C−H activation-alkynes annulation using NHC as a directing and functionalizable group.

4.3. Results and discussion

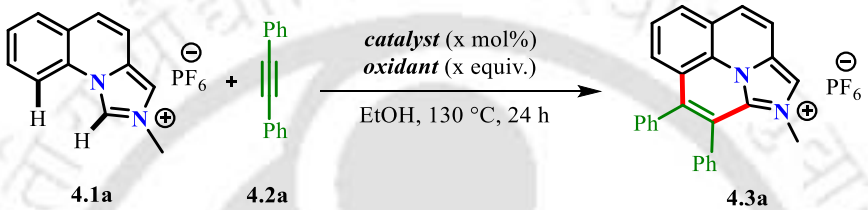
4.3.1. Optimization of reaction conditions

The optimization studies were initiated with the reaction of 2-methylimidazo[1,5-*a*]quinolin-2-ium hexafluoro phosphate **4.1a** (0.2 mmol) and diphenylacetylene **4.2a** (0.2 mmol) in the presence of $[Ru(p\text{-cymene})Cl_2]_2$ (1 mol%) as a catalyst and $Cu(OAc)_2 \cdot H_2O$ (2 equiv., 0.4 mmol) as an oxidant in ethanol at 130 ºC for 24 h. The annulated product 1-methyl-8,9-diphenylbenzo[*ij*] imidazo[2,1,5-*de*]quinolizin-1-ium hexafluoro phosphate, **4.3a** was obtained in 35% yield (entry 1, Table 4.1). On gradually increasing the catalyst loading to 5 mol%, the yield of the product was substantially increased to 98% (entry 3, Table 4.1). Other catalysts such as $RuCl_3.xH_2O$ and $Cp^*CoI_2(CO)$ were also employed in the annulation reaction, but no product was detected. On the other hand, the yield of **4.3a** decreased when the amount of

TH-3565_186122020

$Cu(OAc)_2•H_2O$ was reduced to 1 equiv. (entry 8, Table 4.1). A blank reaction suggests the necessity of a catalyst and oxidant in this oxidative annulation reaction (entries 7 and 9, Table 4.1). The use of copper(II) salts containing different counter anions, such as $Cu(BF_4)_2•6H_2O$, or $CuCl_2•2H_2O$ was also employed in the reaction, but no conversion was observed (entries 10-11, Table 4.1), indicating a critical role of acetate ligand in this transformation. Furthermore, the importance of the acetate ligand has been illustrated by the reaction of [Ru(*p*-cymene)$(OAc)_2$] (5 mol%) and $CuCl_2•2H_2O$ under identical conditions (entry 12, Table 4.1).[11] The formation of 44% of yields of **4.3a** suggested the importance of acetate ligand in this transformation.

Table 4.1. Screening of different catalyst and oxidant[a]



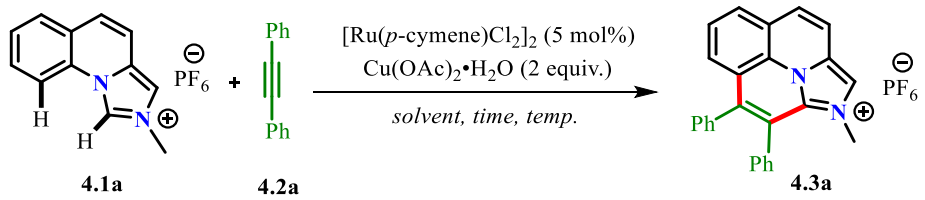
Entry	Catalyst (mol%)	Oxidant (equiv.)	Yield[b] (%)
1	[Ru(*p*-cymene)Cl_2]$_2$ (1)	$Cu(OAc)_2·H_2O$ (2)	35
2	[Ru(*p*-cymene)Cl_2]$_2$ (2)	$Cu(OAc)_2·H_2O$ (2)	47
3	**[Ru(*p*-cymene)Cl_2]$_2$ (5)**	**$Cu(OAc)_2·H_2O$ (2)**	**98**
4	[Ru(*p*-cymene)Cl_2]$_2$ (6)	$Cu(OAc)_2·H_2O$ (2)	98
5	$RuCl_3.xH_2O$ (5)	$Cu(OAc)_2·H_2O$ (2)	n.d.
6	$Cp^*CoI_2(CO)$ (5)	$Cu(OAc)_2·H_2O$ (2)	n.d.
7	–	$Cu(OAc)_2·H_2O$ (2)	n.d.
8	[Ru(*p*-cymene)Cl_2]$_2$ (5)	$Cu(OAc)_2·H_2O$ (1)	52
9	[Ru(*p*-cymene)Cl_2]$_2$ (5)	–	n.d.
10	[Ru(*p*-cymene)Cl_2]$_2$ (5)	$Cu(BF_4)_2•6H_2O$ (2)	6
11	[Ru(*p*-cymene)Cl_2]$_2$ (5)	$CuCl_2•2H_2O$ (2)	n.d.
12	Ru(*p*-cymene)$(OAc)_2$ (5)	$CuCl_2•2H_2O$ (2)	44
13	[Ru(*p*-cymene)Cl_2]$_2$ (5)	AgOAc (2)	11

[a]Reaction conditions: **4.1a** (0.2 mmol), **4.2a** (0.2 mmol), catalyst (x mol%), oxidant (x equiv.) in EtOH (2 mL) at 130 ºC in a preheated oil bath for 24 h in a closed 30 mL pressure tube; [b]isolated yields are reported. n.d. = not detected.

Next, I intended to find the best optimized conditions with respect to time, temperature, and solvent. The yield of **4.3a** decreased when the reaction time was decreased to 12 hours (entries 1-2, Table 4.2) or the reaction temperature was reduced to 100 °C (entries 4-5, Table 4.2). When the reaction was performed at room temperature, no product was detected. This suggested that the reaction temperature played a significant role in the reaction outcome. For further optimization, the reaction was examined with a series of other solvents (DCE, CH_3CN, and toluene) under identical reaction conditions (entries 9-11, Table 4.2). Ethanol was found to be the most efficient reaction medium in the current catalytic reaction.

Table 4.2. Screening of time, temperature and solvent[a]

TH-3565_186122020



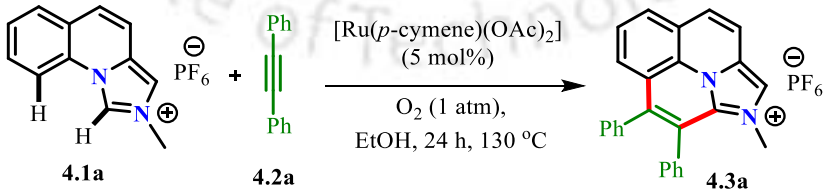
4.1a **4.2a** **4.3a**

Entry	Time (h)	Temperature (°C)	Solvent	Yield[b] (%)
1	12	130	EtOH	56
2	18	130	EtOH	80
3	**24**	**130**	**EtOH**	**98**
4	24	120	EtOH	87
5	24	100	EtOH	62
6	24	80	EtOH	40
7	24	25	EtOH	n.d.
8	24	130	MeOH	96
9	24	130	DCE	80
10	24	130	CH_3CN	87
11	24	130	toluene	54

[a]Reaction conditions: **4.1a** (0.2 mmol), **4.2a** (0.2 mmol), [Ru(*p*-cymene)Cl_2]$_2$ (5 mol%), $Cu(OAc)_2 \cdot H_2O$ (0.4 mmol), solvent (2 mL) at the indicated temperature and time in a closed 30 mL pressure tube; [b]isolated yields are reported. n.d. = not detected.

Since $Cu(OAc)_2$•H_2O is used as an oxidant for the given annulation process, a substantial amount of copper-containing byproducts are formed. To address this issue, molecular oxygen is used as an alternative oxidant which is certainly an attractive approach since it is inexpensive and produces only water as a by-product. To put the plan into practice, optimization studies were commenced by reacting imidazo[1,5-*a*]quinolin-2-ium salts **4.1a** (1 equiv.) and diphenylacetylene **4.2a** (1 equiv.) in the presence of [Ru(*p*-cymene)$(OAc)_2$] (5 mol %) in ethanol at 130 °C for 24 h under air. Gratifyingly, annulated product **4.3a** was obtained in 57% yield (entry 1, Table 4.3). To our delight, when the reaction was carried out under an oxygen atmosphere, the yield of product **4.3a** was substantially increased to 96%, indicating a key role of molecular oxygen in the current catalytic process (entry 2, Table 4.3).

Table 4.3. Optimization of reaction conditions with molecular oxygen[a]



4.1a **4.2a** **4.3a**

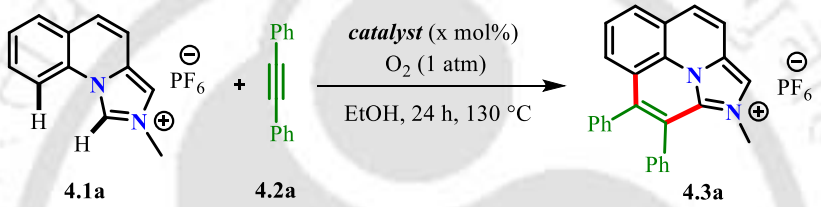
Entry	Deviation from above	Yield of **4.3a**
1	under air instead of oxygen atmosphere	57%
2	none	96%
3	DCE instead of EtOH	76%
4	2 mol% of [Ru(*p*-cymene)$(OAc)_2$]	43%
5	at 100 °C instead of 130 °C	62%
6	with 12 h instead of 24 h	52%

TH-3565_186122020

[a]Reaction conditions: **4.1a** (0.2 mmol), **4.2a** (0.2 mmol), catalyst (5 mol%) in EtOH (1.5 mL) at 130 °C for 24 h under 1 atm. of oxygen in a sealed tube, isolated yield.

For further optimization, the reaction was examined with a series of other solvents under the same reaction conditions. Ethanol was found to be the most efficient medium in the current catalytic reaction (entry 3, Table 4.3). Reducing the catalyst loading to 2 mol % (entry 4) or reaction temperature to 100 °C (entry 5) or shorter reaction time to 12 h (entry 6, Table 4.3), resulted in lower yields of **4.3a**. Furthermore, no product was formed when the reaction was carried out in the presence of [(*p*-cymene)$RuCl_2$]$_2$ (5 mol%) catalyst, suggesting the important role of coordinating and basic ligands in the catalytic process (entry 5, Table 4.4). Control experiments suggest the necessity of a catalyst in the reaction (entry 11, Table 4.4). For further detailed optimization studies see Table 4.4–4.6.

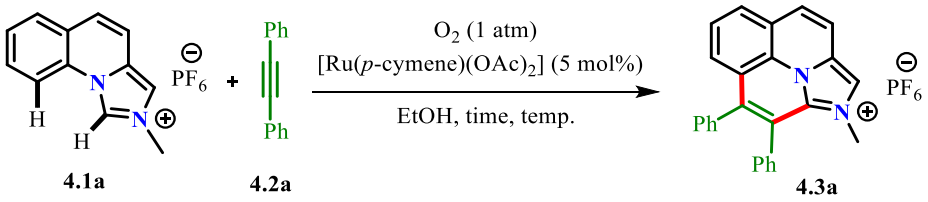
Table 4.4. Screening of catalyst with molecular oxygen[a]



Entry	Catalyst	Catalyst loading (mol%)	Yield [b] (%)
1	[Ru(*p*-cymene)$(OAc)_2$]	2.0	43
2	[Ru(*p*-cymene)$(OAc)_2$]	4.0	78
3	**[Ru(*p*-cymene)$(OAc)_2$]**	**5.0**	**96**
4	[Ru(*p*-cymene)$(OAc)_2$]	6.0	96
5	[Ru(*p*-cymene)$Cl_2]_2$	5.0	n.d.
6[c]	[Ru(*p*-cymene)$Cl_2]_2$	5.0	41
7[d]	[Ru(*p*-cymene)$Cl_2]_2$	5.0	57
8	$RuCl_3.xH_2O$	5.0	n.d.
9	[Ru(*p*-cymene)(OPiv)$_2$]	5.0	78
10[e]	[Ru(*p*-cymene)$(OAc)_2$]	2.0	n.d.
11	–	–	n.d.

[a]Reaction conditions: **4.1a** (0.2 mmol), **4.2a** (0.2 mmol), catalyst (x mol%), EtOH (2 mL) at 130 ºC in a preheated oil bath for 24 h under O_2 atmosphere (1 atm) in a closed 30 mL pressure tube; [b]isolated yields are reported. [c]2 equiv. NaOAc is used. [d]5 equiv. NaOAc is used. [e]under argon. n.d. = not detected.

Table 4.5. Screening of time and temperature[a]



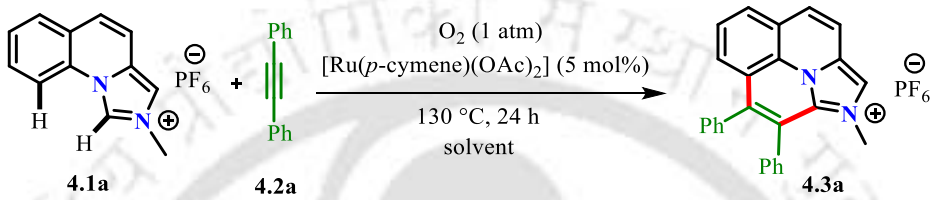
Entry	Time (h)	Temperature (ºC)	Yield[b] (%)
1	8	130	35

TH-3565_186122020

2	12	130	52
3	18	130	74
4	**24**	**130**	**96**
5	24	120	80
6	24	100	62
7	24	80	36
8	24	25	n.d.

[a]Reaction conditions: **4.1a** (0.2 mmol), **4.2a** (0.2 mmol), [Ru(*p*-cymene)(OAc)$_2$] (5 mol%), EtOH (2 mL) at the indicated temperature and time under O_2 atmosphere (1 atm) in a sealed tube; [b]isolated yields are reported. n.d. = not detected.

Table 4.6. Screening of solvent[a]



4.1a **4.2a** **4.3a**

Entry	Solvent	Yield[b] (%)
1	MeOH	92
2	**EtOH**	**96**
3	DCE	76
4	$CHCl_3$	82
5	CH_3CN	88
6	toluene	46
7[c]	EtOH	57
8[d]	EtOH	n.d.

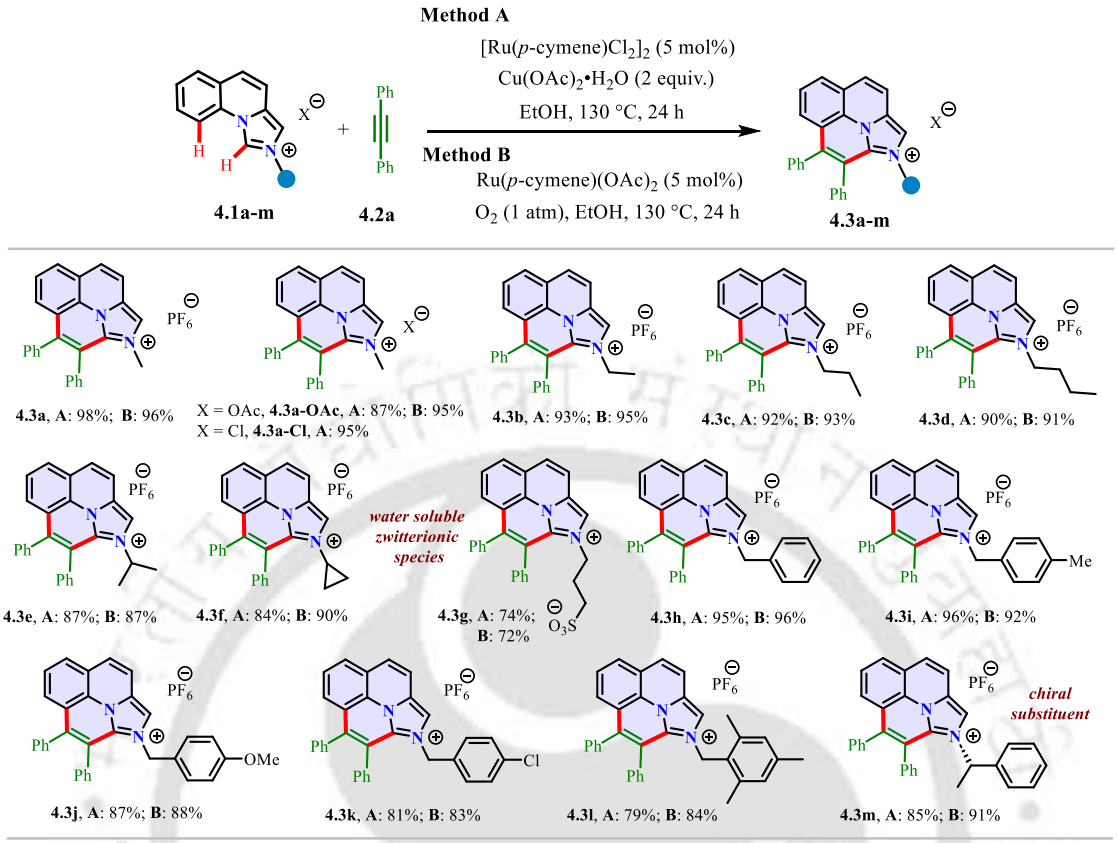
[a]Reaction conditions: **4.1a** (0.2 mmol), **4.2a** (0.2 mmol), [Ru(*p*-cymene)(OAc)$_2$] (5 mol%), solvent (2 mL) at 130 ºC in a preheated oil bath for 24 h under O_2 atmosphere (1 atm) in a sealed tube; [b]isolated yields are reported. [c]reaction was performed under air. [d]reaction was performed under O_2-free conditions. n.d. = not detected.

4.3.2. Substrate scope

With both optimized conditions in hand (Table 4.1, entry 3, for **Method A** and Table 4.4, entry 3, for **Method B**), the scope of the annulation reaction was investigated by using various types of fused-imidazo-quinolinium salts with wingtip substituents **4.1a-m** and alkyne **4.2a** as the standard substrate (Table 4.7). The reaction seems to be fairly effective for a wide pool of substrates with high to good yields of the annulated products. The *N*-substituted substrates such as *N*-alkyl (**4.1a-d**), *N*-isopropyl (**4.1e**), and *N*-cyclopropyl (**4.1f**) afforded the corresponding annulated products **4.3a-f** in 84-98% yields. Interestingly, the cyclopropyl group was retained under the oxidative conditions. A zwitterionic sulfonate salt of **4.1g** delivered the water-soluble annulated product **4.3g** with a good yield. Then, substrates bearing *N*-para-substituted benzyl groups (**4.1h-k**) and *N*-CH_2 mesityl group also provided the corresponding annulated products **4.3h-k** and **4.3l**, respectively in good yields. The protocol was successfully applied to the substrate having a chiral substituent at the nitrogen center to afford the annulated product **4.3m** in 85% yield in method A and 91% yield in method B.

TH-3565_186122020

Table 4.7. Substrate scope of imidazo-fused quinolinium salts with wingtip substituents[a]



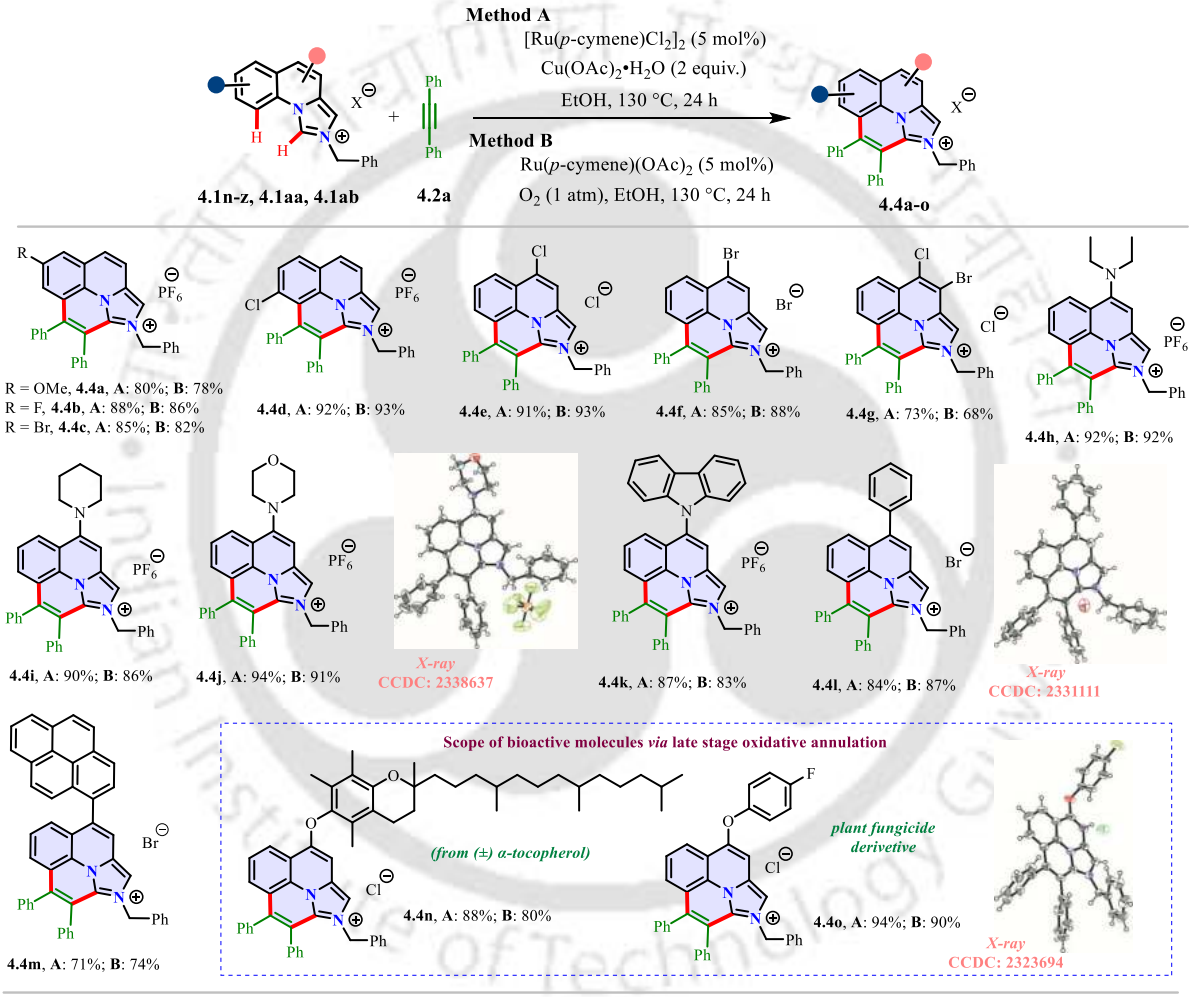
[a]Reaction condition: **Method A:** Substrate (0.2 mmol), alkyne (0.2 mmol), $Cu(OAc)_2•H_2O$ (0.4 mmol), $[Ru(p\text{-cymene})Cl_2]_2$ (5 mol%), EtOH (2 mL) were heated at 130 °C in a pressure tube for 24 h, isolated yield. **Method B:** Substrate (0.2 mmol), alkyne (0.2 mmol), $[Ru(p\text{-cymene})(OAc)_2]$ (5 mol%), EtOH (2 mL) were heated at 130 °C under O_2 atmosphere in a pressure tube for 24 h, isolated yield.

After inspecting the reactivities of imidazo-fused quinolinium salts with wingtip substituents, I then turned my attention to the scope of the reaction to various *N*-benzyl imidazoquinolinium salts **4.1n-z** with **4.2a** as the standard substrate (Table 4.8). The substrate containing electron-donating (e.g., −OMe) and electron-withdrawing (e.g., −F, −Cl, and −Br) groups were used in the annulation reactions and all of them provided the desired products in moderate to good yields. Slightly higher yields were observed for substrates containing an electron-withdrawing group. Interestingly, substrates with substituents near the annulation site of a quinolium moiety such as C8 substituted quinolium salt **4.1q** reacted efficiently with **4.2a** leading to the desired annulated product **4.4d**. In the case of *N*-benzyl-5-haloimidazo[1,5-*a*]quinolin-2-ium salt **4.1r** and **4.1s**, though C5 substituted halo functionality was susceptible to nucleophilic attack, desired annulated product **4.4e** and **4.4f** was obtained quantitatively, indicating impressive selectivity of the present protocol. Interestingly, disubstituted 4-bromo-5-chloroimidazo [1,5-*a*]quinolin-2-ium salt **4.1t** also afforded the product **4.4g** in 73% yield in method A and 68% yield in method B. The amine-bearing substituents at the 5-position in the quinolinium ring **4.1u-x** afforded the desired annulated products **4.4h-k** with good yield. Further, the scope of the reaction was expanded to phenyl- and pyrene-bearing quinolinium salt **4.1y** and **4.1z**, which successfully yielded the desired products **4.4l** and **4.4m** in good yield. Having the significance

TH-3565_186122020

of the quinolinium motif in various biologically and pharmacologically relevant molecular settings, a substrate containing (±) α-tocopherol modified quinolinium derivative **4.1aa** was effectively transformed into annulated product **4.4n**. To our pleasure, a plant fungicide derivative **4.1ab** was discovered to be susceptible to this approach, producing **4.4o** in good yield. The structure of **4.4j**, **4.4l** and **4.4o** was unambiguously confirmed by single-crystal X-ray diffraction investigations (SC-XRD).

Table 4.8. Substrate scope of *N*-benzyl imidazo-fused quinolinium salts with varying substituents in the backbone[a]



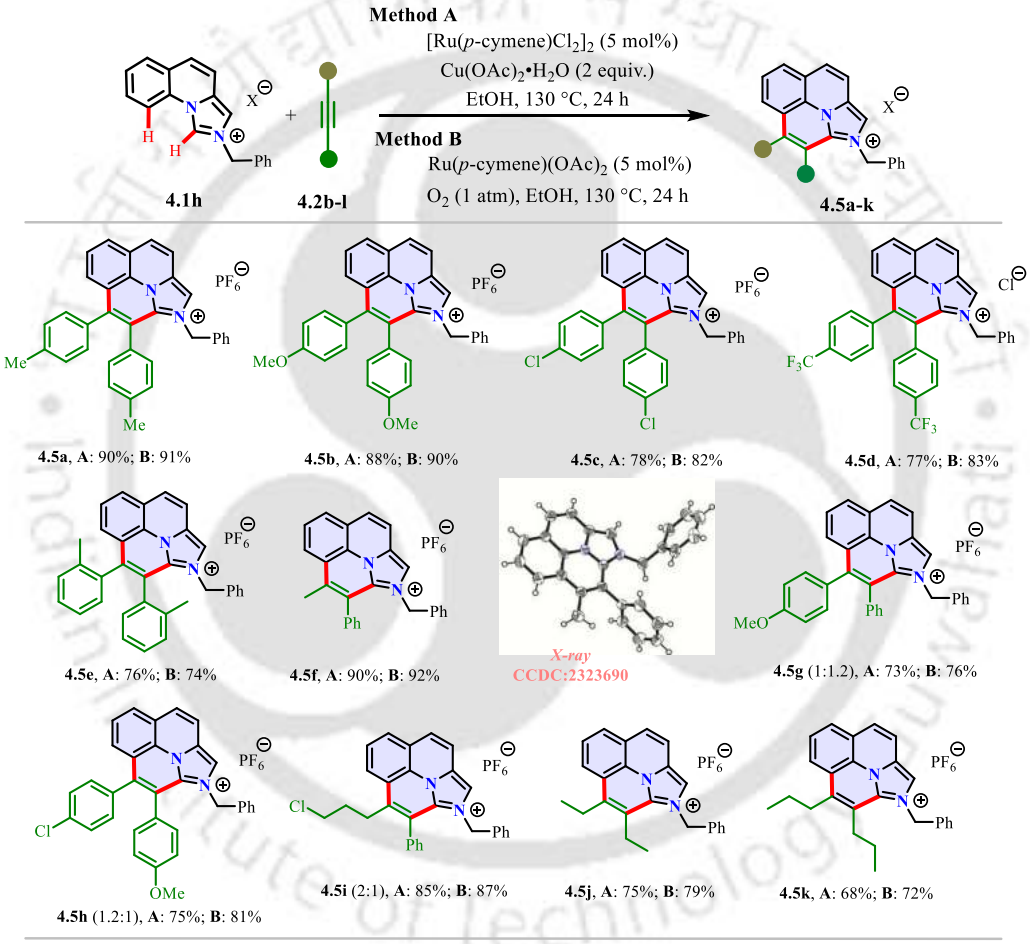
[a]Reaction condition: **Method A:** Substrate (0.2 mmol), alkyne (0.2 mmol), $Cu(OAc)_2•H_2O$ (0.4 mmol), $[Ru(p\text{-cymene})Cl_2]_2$ (5 mol%), EtOH (2 mL) were heated at 130 °C in a pressure tube for 24 h, isolated yield. **Method B:** Substrate (0.2 mmol), alkyne (0.2 mmol), $[Ru(p\text{-cymene})(OAc)_2]$ (5 mol%), EtOH (2 mL) were heated at 130 °C under O_2 atmosphere in a pressure tube for 24 h, isolated yield.

To further demonstrate the generality and practicability of this reaction, I expanded the substrate scope by varying the alkynes (Table 4.9). Other substituted symmetrical 1,2-diarylalkynes having electron-donating *p*-Me (**4.2b**), *p*-OMe (**4.2c**) and electron-withdrawing *p*-Cl (**4.2d**) and *p*-CF_3 (**4.2e**) groups, all efficiently provided the corresponding annulated

TH-3565_186122020

products **4.5a-d** in good to excellent yields. Notably, the sterically hindered *ortho*-substituted diphenyl acetylene **4.2f** was well tolerated to give **4.5e**. The regioselectivity of the annulation reaction was tested using 1-phenyl-1-propyne (**4.2g**) as an unsymmetrical alkyne. Interestingly, this yielded a single regioisomeric product **4.5f**. The structure of the regioisomer (**4.5f**) was unambiguously confirmed by single-crystal X-ray diffraction analyses (SC-XRD). On the other hand, alkynes bearing two different aromatic rings produced regioisomeric pairs, **4.5g** and **4.5h**. In addition to symmetrical and unsymmetrical aryl alkynes, the aliphatic alkyne such as 3-hexyne (**4.2k**) and 4-octyne (**4.2l**) were also compatible under the reaction conditions.

Table 4.9. Substrate scope of *N*-benzyl imidazo-fused quinolinium salts with various alkynes[a]



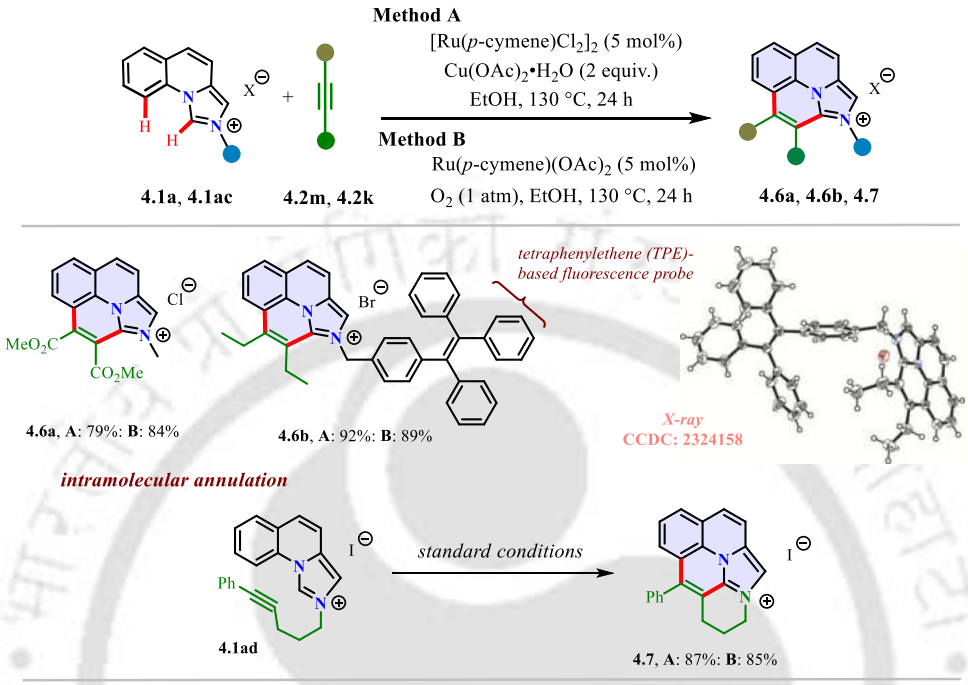
[a]Reaction condition: **Method A:** Substrate (0.2 mmol), alkyne (0.2 mmol), $Cu(OAc)_2•H_2O$ (0.4 mmol), $[Ru(p\text{-cymene})Cl_2]_2$ (5 mol%), EtOH (2 mL) were heated at 130 °C in a pressure tube for 24 h, isolated yield. **Method B:** Substrate (0.2 mmol), alkyne (0.2 mmol), $[Ru(p\text{-cymene})(OAc)_2]$ (5 mol%), EtOH (2 mL) were heated at 130 °C under O_2 atmosphere in a pressure tube for 24 h, isolated yield.

Additionally, the electron-deficient alkyne such as dimethyl acetylene dicarboxylate (DMAD) also proceeded smoothly to deliver the annulated product **4.6a** in 79% and 84% yield with method A and method B respectively. Then, the usefulness of the method has been showcased by synthesizing tetraphenylethene (TPE)-based fluorescent probe **4.6b**. The structure of **4.6b** was confirmed by SC-XRD. It was interesting to note that the alkyne-bearing substituent on

TH-3565_186122020

the nitrogen atom **4.1ad** gave an intramolecular annulated product **4.7** in quantitative yield. Unfortunately, terminal alkyne was not suited to this annulation process.

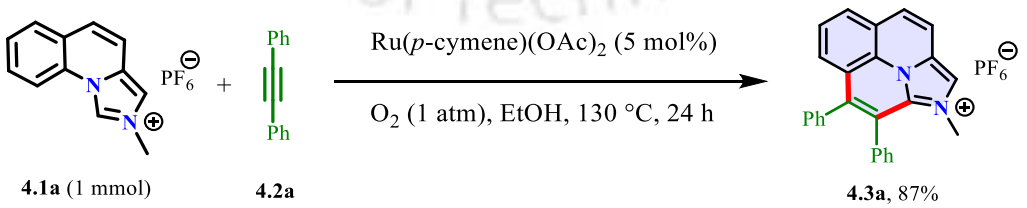
Table 4.10. Substrate scope with different wingtip substituents and different alkyne[a]



[a]Reaction condition: **Method A:** Substrate (0.2 mmol), alkyne (0.2 mmol), $Cu(OAc)_2•H_2O$ (0.4 mmol), $[Ru(p\text{-cymene})Cl_2]_2$ (5 mol%), EtOH (2 mL) were heated at 130 °C in a pressure tube for 24 h, isolated yield. **Method B:** Substrate (0.2 mmol), alkyne (0.2 mmol), $[Ru(p\text{-cymene})(OAc)_2]$ (5 mol%), EtOH (2 mL) were heated at 130 °C under O_2 atmosphere in a pressure tube for 24 h, isolated yield.

4.3.3. 1 mmol scale reaction

The efficiency of this process was studied by scaling up the reaction on a 1 mmol scale for bulk utilization. I have performed the 1 mmol-scale reaction with quinolinium salt **4.1a** (328.2 mg, 1 mmol) and alkyne **4.2a** (178.2 mg, 1 mmol), following the standard reaction conditions which provide **4.3a** in 87% yield. Hence, the process is overall very efficient from a practical perspective.

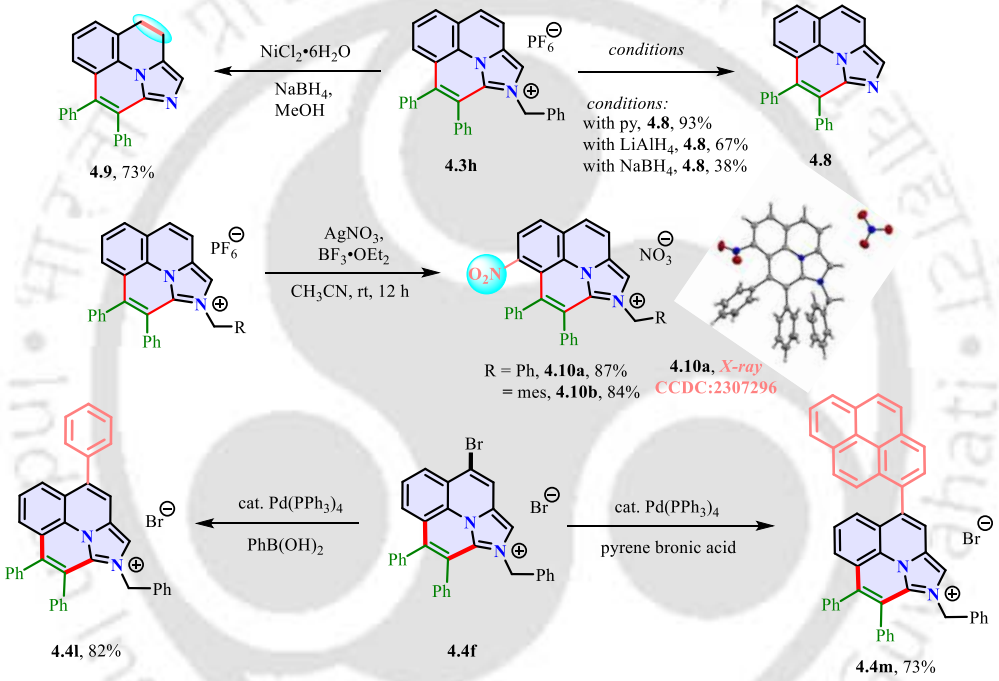


Scheme 4.6. 1 mmol scale reaction between **4.1a** and **4.2a**

4.3.4. Post-synthetic modification

TH-3565_186122020

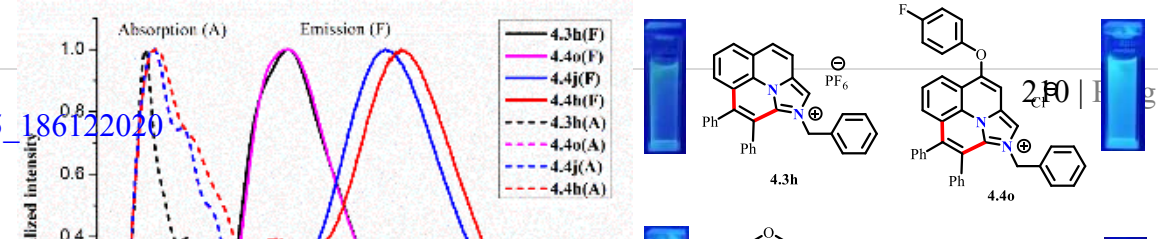
The synthesized annulated compounds can easily transform into other useful molecules (Scheme 4.7). For example, **4.3h** was easily debenzylated by treating with pyridine or under reductive conditions, yielding **4.8** in 38-93% yields. After the successful debenzylation of **4.3h**, the compound **4.9** can be obtained *via* one-pot tandem debenzylation of **4.3h**, followed by selective reduction at the less substituted double bond using $NiCl_2$-$NaBH_4$ combination to produce **4.9** in 73% yield. Moreover, by utilizing a mixture of $AgNO_3$ and BF_3•OEt_2, selective nitration was achieved at the backbone of the quinolinium moiety, affording **4.10a** and **4.1ab** with 87% and 84% yield respectively. The structure of the regioisomer **4.10a** was unambiguously confirmed by SC-XRD. Since the current reaction protocol tolerates the halogen functional groups, further functionalization was achieved in the backbone by using palladium-catalysis, delivering **4.4l** and **4.4m** in 82% and 73% yield respectively.



Scheme 4.7. Post-synthetic modification of annulated molecules

4.3.5. Photophysical properties

It is worth pointing out that benzo[*ij*]imidazo[2,1,5-*de*]quinolizin-1-ium salts exhibit intense fluorescence emission at a broad range. This class of ionic compounds has the potential to be useful, solution-processable, and new emitting materials in the near future. I have measured the absorption and emission properties of some selected molecules (Figure 4.1). Strong fluorescence emissions at 450-535 nm were observed upon an excitation at 350 nm. A significant bathochromic shift (~100 nm) was observed with amine-based electron donating group on the C5-position of the quinolium ring. Therefore, these new annulated molecules have the potential in the area of organic electronic materials.



TH-3565_186122020

Figure 4.1. Normalized emission and absorbance spectra of some selected molecules. Concentration: 20 μM in CH_2Cl_2. Excitation wavelength: 350 nm.

4.3.6. Mechanistic investigation

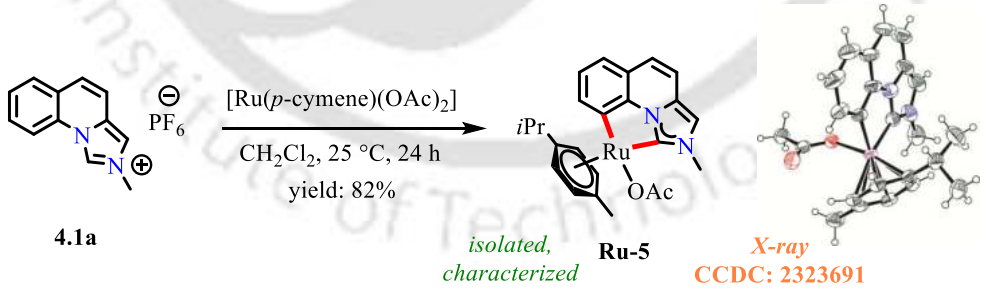
4.3.6.1. Proof of intermediate Ru-1/Ru-5 in the catalytic cycle

(i) Synthesis of cyclometalated Ru(II) intermediate **Ru-1**

The synthesis of cyclometalated Ru(II) complex **Ru-1** was already discussed in Chapter 2 (see details in section 2.3.1).

(ii) Synthesis of cyclometalated Ru(II) intermediate **Ru-5**

To gain insight into the mechanistic pathways, a series of control experiments were performed. Initial attempts were made to isolate the NHC-cyclometalated ruthenium(II) complex **Ru-5** by the reaction of 2-methylimidazo[1,5-*a*]quinolin-2-ium hexafluorophosphate **4.1a** and [Ru(*p*-cymene)$(OAc)_2$] in CH_2Cl_2 at room temperature for 24 h (Scheme 4.8). The structure of complex **Ru-5** was fully characterized by NMR, ESI-MS, and SC-XRD.



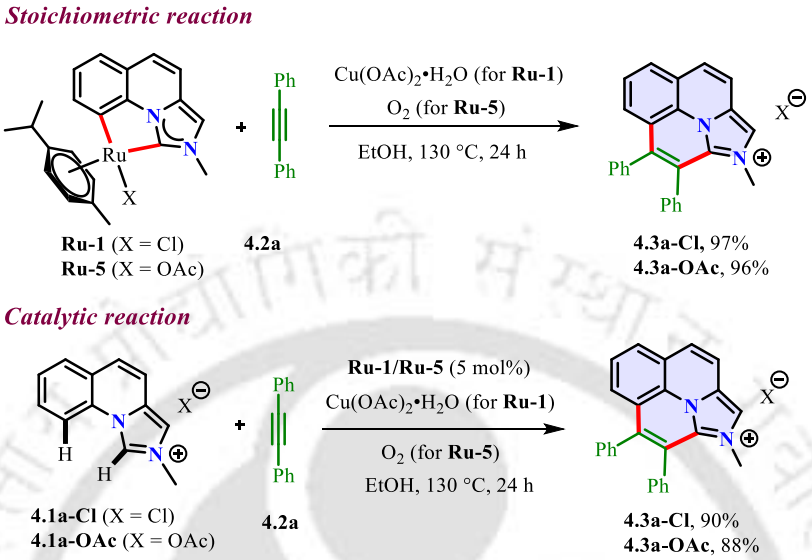
Scheme 4.8. Synthesis of cyclometalated Ru(II) intermediate **Ru-5**

(iii) Control experiments with cyclometalated Ru(II) intermediate, **Ru-1/Ru-5**

To prove the intermediacy of the complex **Ru-1**/**Ru-5** in the catalytic process, stoichiometric as well as catalytic reactions were performed as shown in Scheme 4.9. The stoichiometric reaction of the complexes **Ru-1** and **Ru-5** with **4.2a** under the standard reaction conditions, delivered the product **4.3a-Cl** in 97% and **4.3a-OAc** in 96% yield, respectively. Then annulation reaction between **4.1a-Cl** and **4.1a-OAc** with **4.2a** also proceeded smoothly in the

TH-3565_186122020

presence of **Ru-1**/**Ru-5** (5 mol%) as a catalyst, affording the annulated product **4.3a-Cl** in 90% and **4.3a-OAc** in 88% yield, respectively. These stoichiometric as well as catalytic reaction outcomes suggested that intermediate **Ru-1**/**Ru-5** is likely to be an active species in the catalytic cycle.



Scheme 4.9. Stoichiometric and catalytic reactions with **Ru-1**/**Ru-5**

4.3.6.2. Insertion of alkyne into M−C bonds (M−C_{aryl} *vs.* M−C_{NHC} bonds) of Ru-1/Ru-5

Since there is an equal chance of alkyne insertion into both M–C bonds of **Ru-1**/**Ru-5**, a theoretical calculation was performed to know the regioselectivity of the alkyne insertion into M–C bonds (M−C_{aryl} *vs.* M−C_{NHC} bonds). Mulliken charges were found to be 0.377 for C_{NHC} and −0.034 for C_{aryl}, suggesting that Ru−C_{aryl} is reasonably more electron-rich than Ru−C_{NHC} (Figure 4.2). Therefore, insertion of an alkyne may prefer to the Ru−C_{aryl} over the Ru−C_{NHC} moiety though there is an equal possibility of alkyne insertion into both the M−C bonds of the complex.

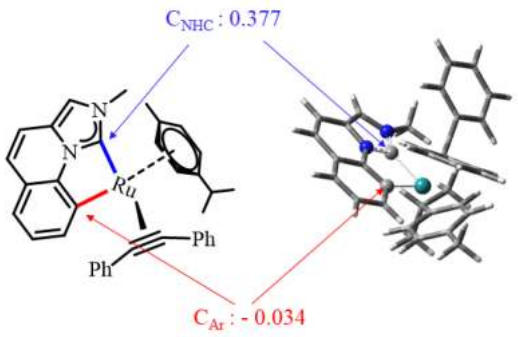
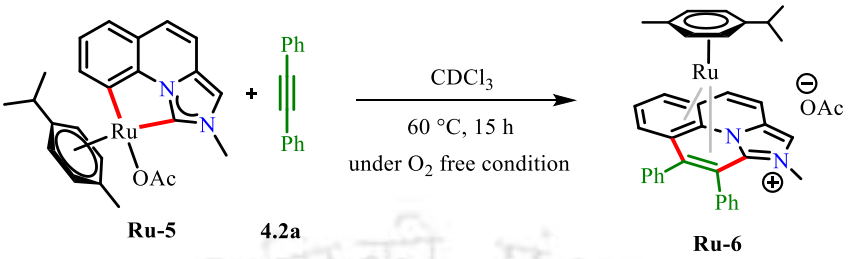


Figure 4.2. Natural bond orbital (NBO) analysis

4.3.6.3. Proof of ruthenium(0) sandwich species Ru-6 in the catalytic cycle

TH-3565_186122020

When I performed a reaction between the intermediate **Ru-5** and alkyne **4.2a** at 60 °C for 15 h in $CDCl_3$ under absolute oxygen-free conditions, fortunately, intermediate **Ru-6** was observed (Scheme 4.10). The NMR and ESI-MS spectroscopic data suggested that complex **Ru-6** is likely to be a ruthenium(0) sandwich complex (Figure 4.3).



Scheme 4.10. Spectroscopically characterized elusive Ru(0) sandwich species, **Ru-6**

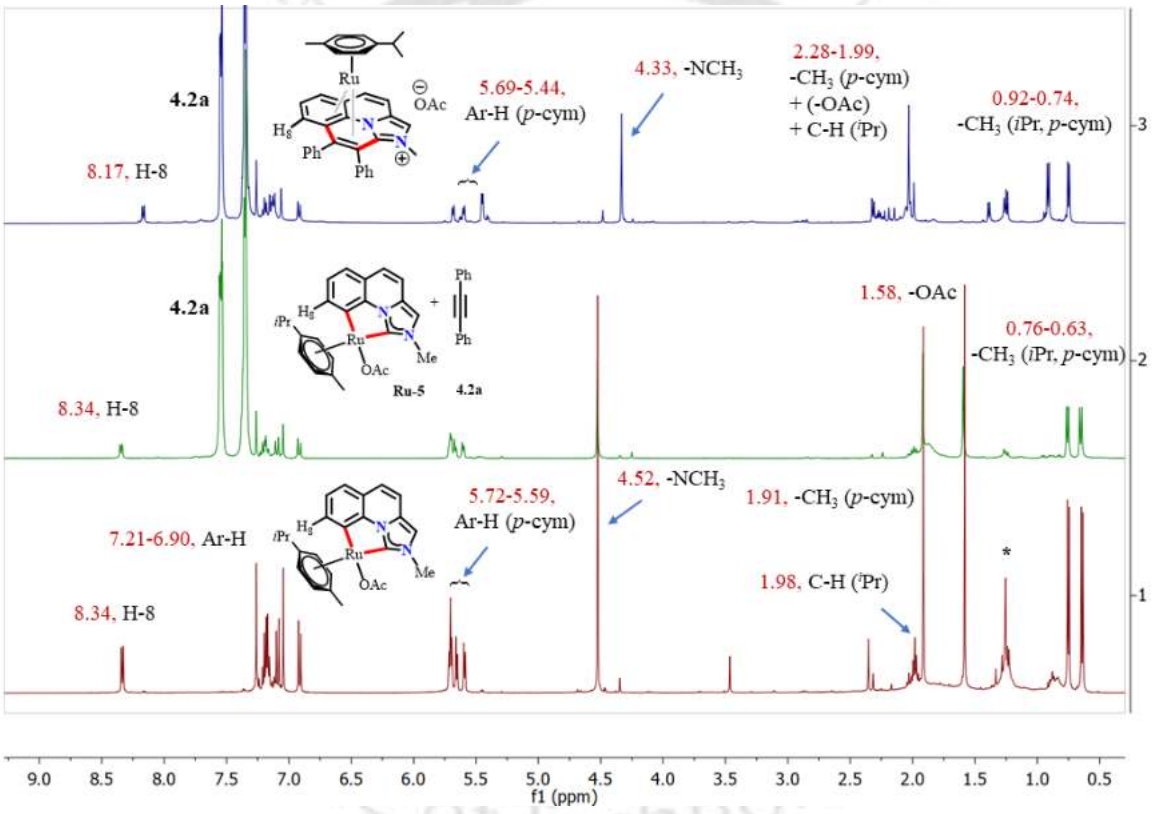
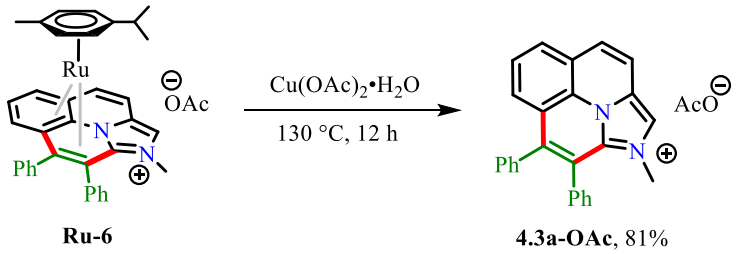


Figure 4.3. ^{1}H NMR spectra of **Ru-5**, a combination of **Ru-5** (23.8 mg, 0.05 mmol, 1 equiv.) and diphenylacetylene, **4.2a** (26.7 mg, 0.15 mmol, 3 equiv.) and formation of **Ru-6** in $CDCl_3$ at 298 K. *represents grease.

(i) Control experiment of **Ru-6** with $Cu(OAc)_2 \cdot H_2O$

TH-3565_186122020

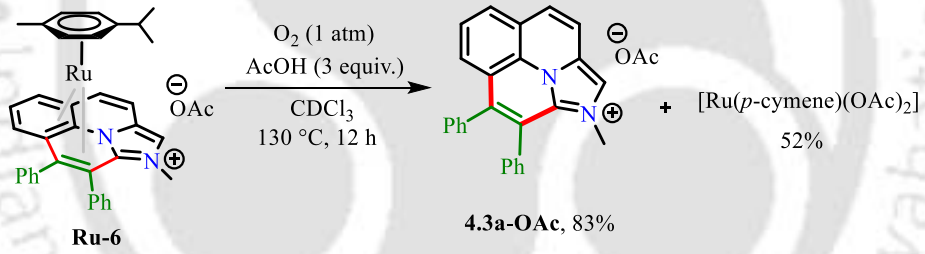


Scheme 4.11. Reaction of **Ru-6** with $Cu(OAc)_2•H_2O$

To know the intermediacy of ruthenium(0) sandwich complex **Ru-6** in the oxidation process, a control experiment was performed with **Ru-6** in the presence of $Cu(OAc)_2•H_2O$ in the identical reaction condition, compound **Ru-6** was completely transformed into product **4.3a-OAc** (81%) suggesting that compound **Ru-6** is the key reaction intermediate in the oxidation process.

(ii) Control experiment of **Ru-6** with molecular O_2 and AcOH

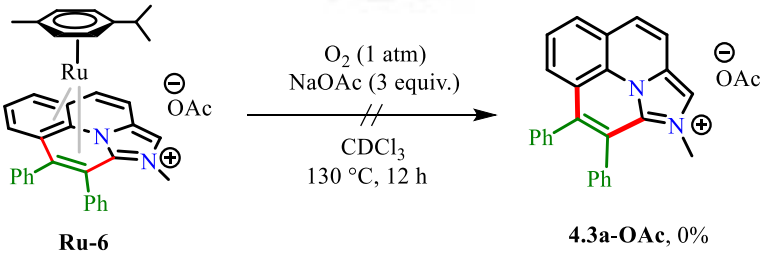
A control experiment was performed with **Ru-6** in the presence of acetic acid under an oxygen atmosphere. The formation of product **4.3a-OAc** (83%) along with [Ru(*p*-cymene)$(OAc)_2$] (52%) supports the ruthenium(0) sandwich complex **Ru-6** as the key reaction intermediate in the oxidative annulation reaction.



Scheme 4.12. Reaction of **Ru-6** and AcOH under molecular O_2

(iii) Control experiment of **Ru-6** with molecular O_2 and NaOAc

When a reaction was performed under identical reaction conditions with NaOAc instead of AcOH (Scheme 4.13), it failed to facilitate the oxidation process, suggesting the requirements of acid source in the oxidation process.



Scheme 4.13. Reaction of **Ru-6** and NaOAc under molecular O_2

TH-3565_186122020

4.3.6.4. Kinetic studies

(a) Order dependency of catalyst, substrate and alkyne

To investigate the rate-determining step of the reaction in detail, a series of kinetic experiments were performed. The initial rate of reaction was monitored to determine the order with respect to substrate **4.1h**. Reactions were performed with varying concentrations of **4.1h**. The initial rate varied linearly with the substrate concentration and the reaction was found to be first–order with respect to substrate. Similarly, the initial rate of the reaction was also monitored with respect to alkyne (diphenylacetylene) and catalyst [Ru(*p*-cymene)(OAc)$_2$]. The result suggested that first-order rate dependence on quinolinium salt **4.1h** and catalyst, and zero-order rate dependence on alkyne **4.2a** (Figure 4.4). These data suggested that substrate **4.1h** and catalyst [Ru(*p*-cymene)(OAc)$_2$] are kinetically relevant, and alkyne **4.2a** might not be involved in the rate-determining step (see details in experimental sections 4.5.5).

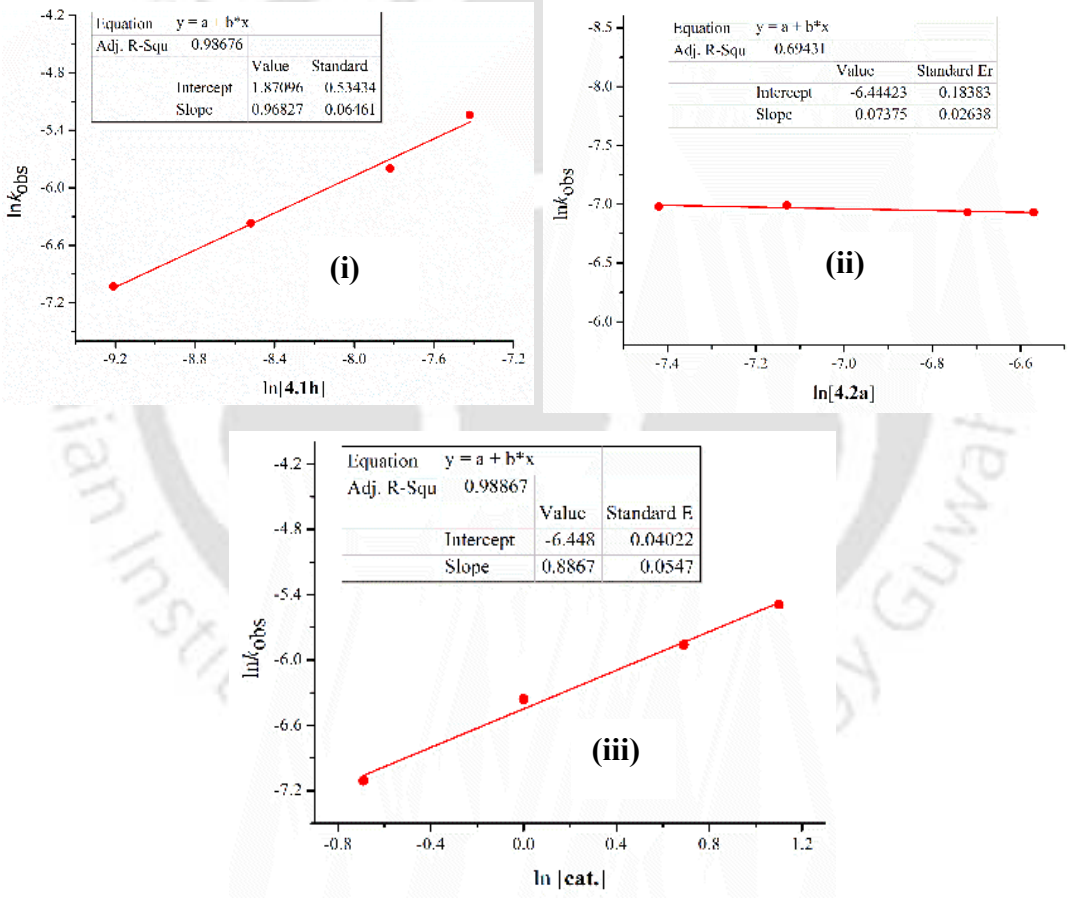


Figure 4.4. Dependence of initial rate (i) with respect to substrate **4.1h**, (ii) with respect to alkyne **4.2a** and (iii) with respect to catalyst [Ru(*p*-cymene)(OAc)$_2$].

(b) Entropy of activation

The effect of temperature on the rate of annulation reaction was examined by using Eyring analysis (Figure 4.5). The Eyring plot of ln(*k*/T) versus 1/T in the temperature range of 60 °C

TH-3565_186122020

to 120 °C was used to determine the activation parameters. The activation parameters were obtained using rate constants from these kinetic experiments and were found to be $\Delta H^{\ddagger}$ = 1.40 ± 0.21 kcal mol^{-1} and $\Delta S^{\ddagger}$ = -69.51 ± 2.4 cal K^{-1} mol^{-1} for Method A and $\Delta H^{\ddagger}$ = 2.29 ± 0.23 kcal mol^{-1} and $\Delta S^{\ddagger}$ = -66.98 ± 2.6 cal mol^{-1} K^{-1} for Method B (see details in experimental sections 4.5.5). The large negative entropy of activation indicates an associative mechanism was involved in the rate-determining step. Based on the thermodynamic activation parameters, and order dependence, one can postulate that fused imidazo-[1,5-*a*]quinolin-2-ium C(2)−H bond cleavage is the rate-determining step and ruling out the possibility of reductive elimination in the rate of the reaction.

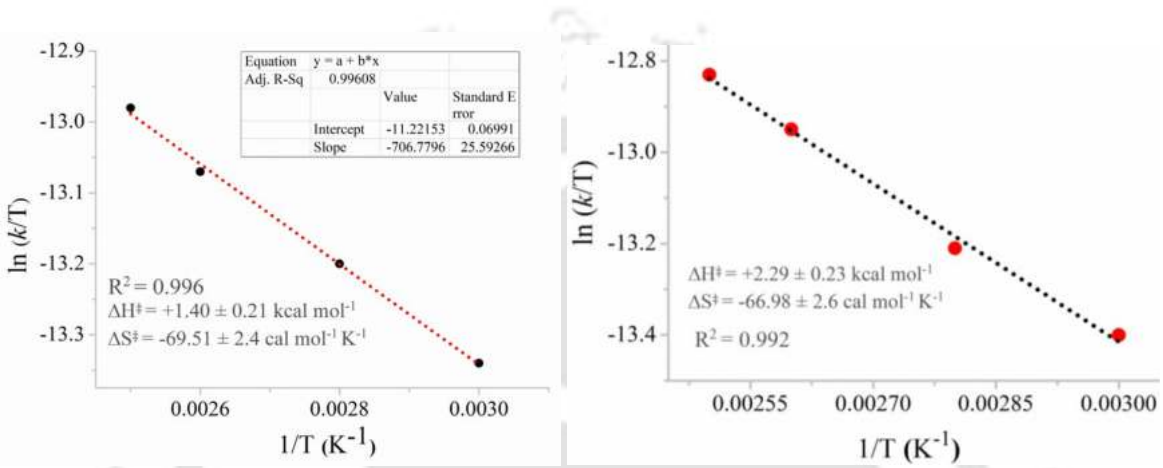


Figure 4.5. Arrhenius-Eyring plot for Method A (left), Method B (right)

(c) Deuterium kinetic isotope effect (DKIE) experiment

To further support the imidazo-[1,5-*a*]quinolin-2-ium C(2)−H bond cleavage is the rate-determining step, deuterium-labeling experiment was carried out with **4.1h** and **4.1h-[D$_1$]** as substrates under standard reaction conditions (Figure 4.6). The initial kinetics was monitored in two parallel experiments and the DKIE value was found to be 3.40 ± 0.28 for method A and 2.79 ± 0.24 for method B, suggesting that the fused imidazo-quinolium C(2)−H bond cleavage of **4.1h** as the turnover-limiting step.

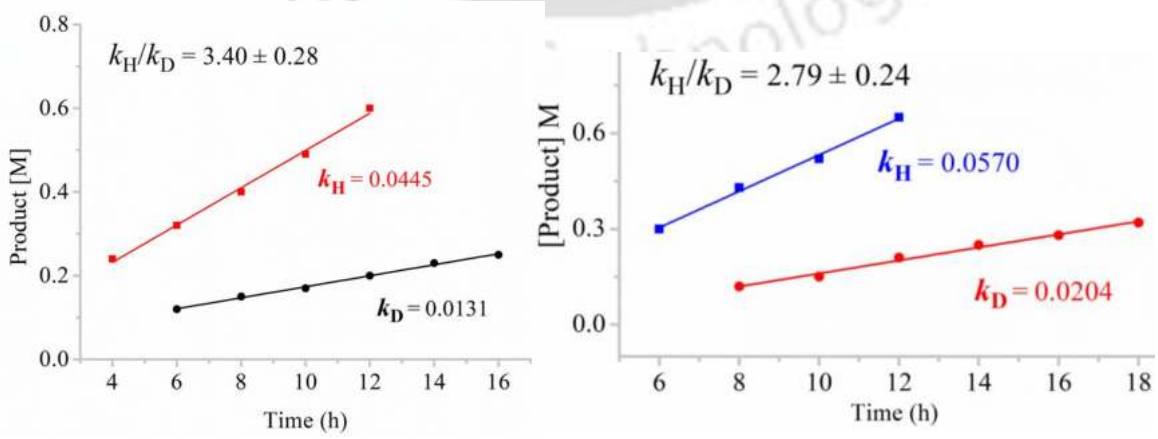


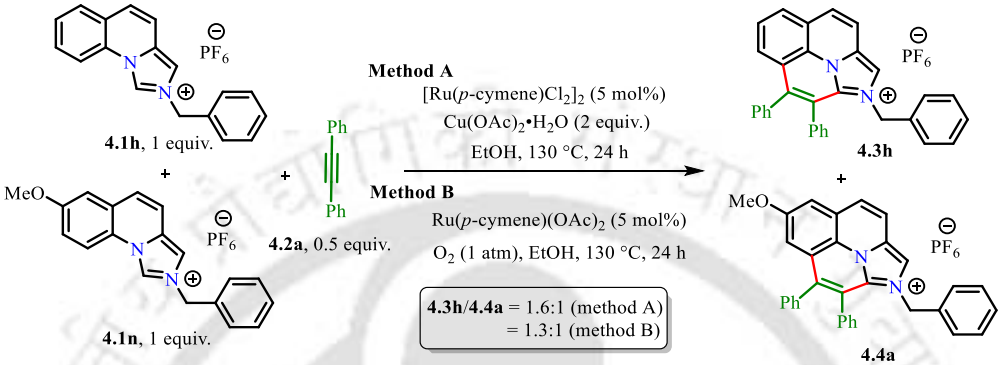
Figure 4.6. Concentration [Product] *vs* time plot for Method A (left), Method B (right)

TH-3565_186122020

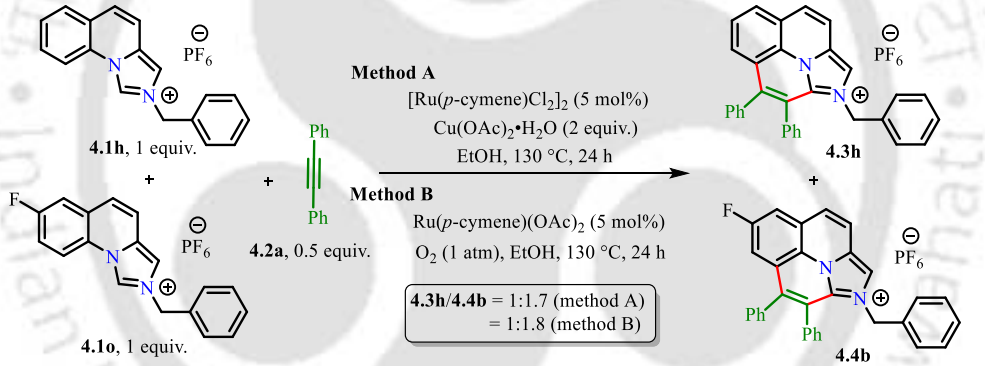
(d) Competitive annulation reactions with electronically different quinolinium salts

Furthermore, the electronic effect of the fused imidazo-quinolinium substrate on the reaction rate was examined. A competitive annulation reaction suggested that the electron-withdrawing group (-F) on the quinolinium salt enhanced the rate of the reaction with respect to an electron-donating group (-OMe) (see details in experimental section 4.5.5).

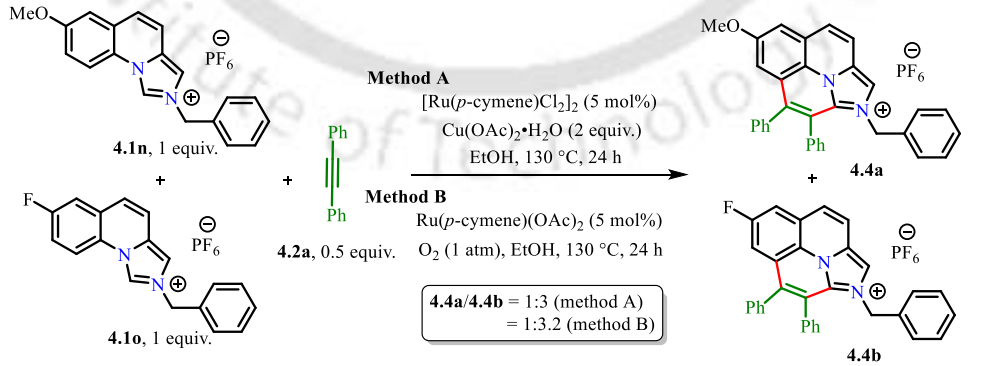
(i) competitive annulation reaction with **4.1h** and **4.1n**



(ii) competitive annulation reaction between **4.1h** and **4.1o**



(iii) competitive annulation reaction between **4.1n** and **4.1o**



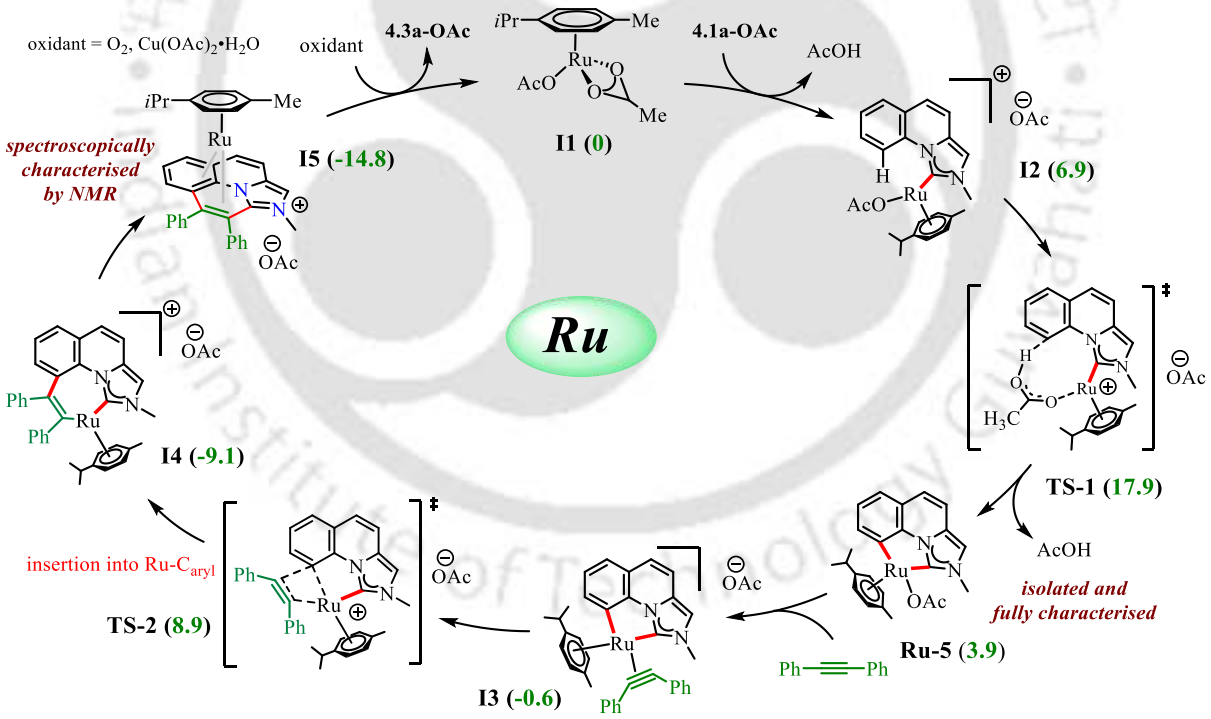
Scheme 4.14. Competitive annulation reactions between electronically different substrate

Therefore, the results based on thermodynamic activation parameters, DKIE experiments, and the electronic effect of the substrate, it is postulated that imidazo-fused quinolinium C(2)−H bond cleavage is likely to be a rate-determining step.

TH-3565_186122020

4.3.7. Proposed mechanism

For further understanding the mechanistic pathway for this annulation reaction, DFT calculations have been performed using M06L/BS1 level of theory (Figure 4.7). At first, nondirected fused imidazo-quinolium C(2)–H activation occurs *via* acetate-assisted concerted metalation-deprotonation (CMD) strategy[4,5,9,12] and generates intermediate **I2**. The process is energetically uphill (ΔG = 6.9 kcal/mol). Then the resulting intermediate **I2** takes part in another intramolecular aryl C–H activation and forms the five-membered cyclometalated complex **Ru-5** (ΔG = 3.9 kcal/mol) *via* another CMD process with an energy barrier of 11 kcal/mol. Next, the alkyne coordination takes place and produces complex **I3** (ΔG = -0.6 kcal/mol), followed by alkyne insertion into Ru–C_{aryl} to give seven-membered ruthenacyle intermediate **I4** (ΔG = -9.1 kcal/mol) with an energy barrier $\Delta G^{\ddagger}$ = 9.5 kcal/mol. Subsequently, intermediate **I4** undergoes reductive elimination to form ruthenium(0) sandwich complex **I5** (or **Ru-6**) with ΔG = -14.8 kcal/mol. Finally, the intermediate **I5** is oxidized by either molecular oxygen or copper acetate to regenerate the catalytically active ruthenium(II) bisacetate species[7b] and release the corresponding annulated product **4.3a-OAc** (ΔG = -33.8 kcal/mol). H_2O is formed as the only stoichiometric by-product in an overall process when molecular oxygen is used as an oxidant.



Scheme 4.15. Proposed mechanism

TH-3565_186122020

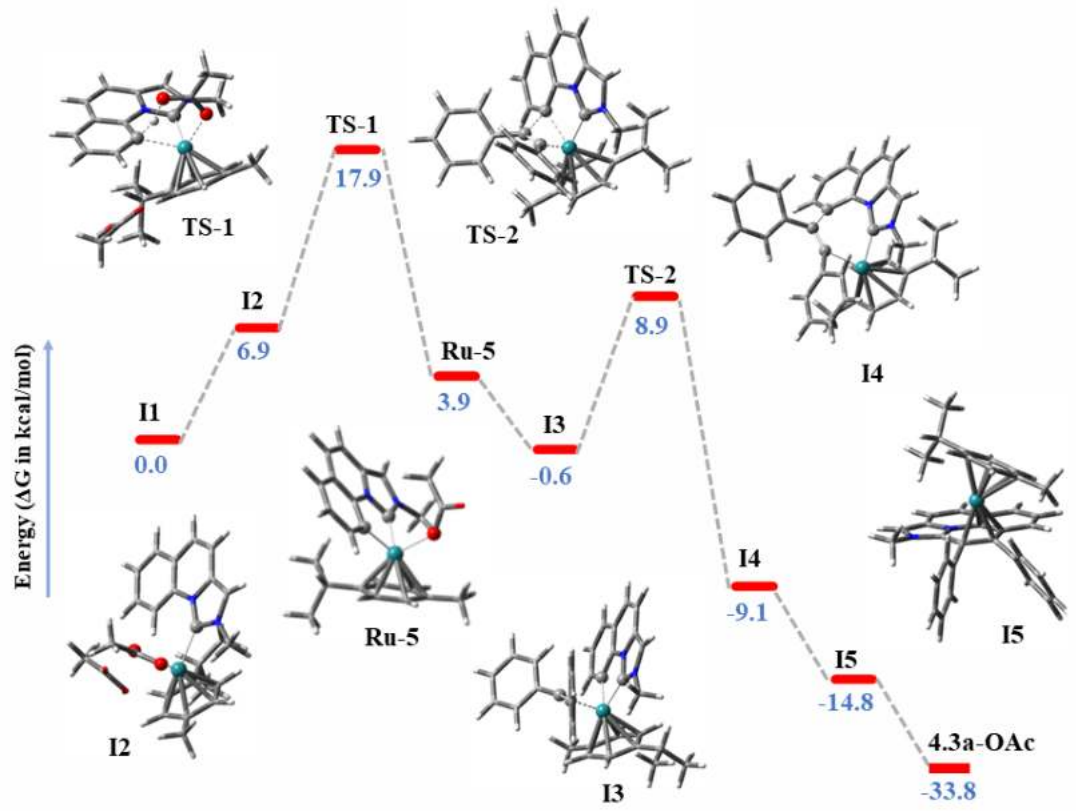


Figure 4.7. Reaction profile diagram based on DFT calculations

4.4. Summary

In conclusion, I have demonstrated a cost-effective Ru(II)-catalyzed C−H activation and oxidative annulation reaction of imidazo[1,5-*a*]quinolin-2-ium salts with alkynes to access fluorescence active π-conjugated fused imidazo[1,5-*a*]quinolin-2-ium derivatives. The reaction features broad substrate generality and tolerates pharmacophore-containing scaffolds. The post-transformations of the synthesized product have also been carried out to demonstrate the potential of the developed methodology. A detailed mechanistic investigation was done supported by isolation and full characterization of key reaction intermediates. The current user-friendly protocol appears to have the potential for synthesizing a new class of organic functional materials.

4.5. Experimental section

4.5.1. General information

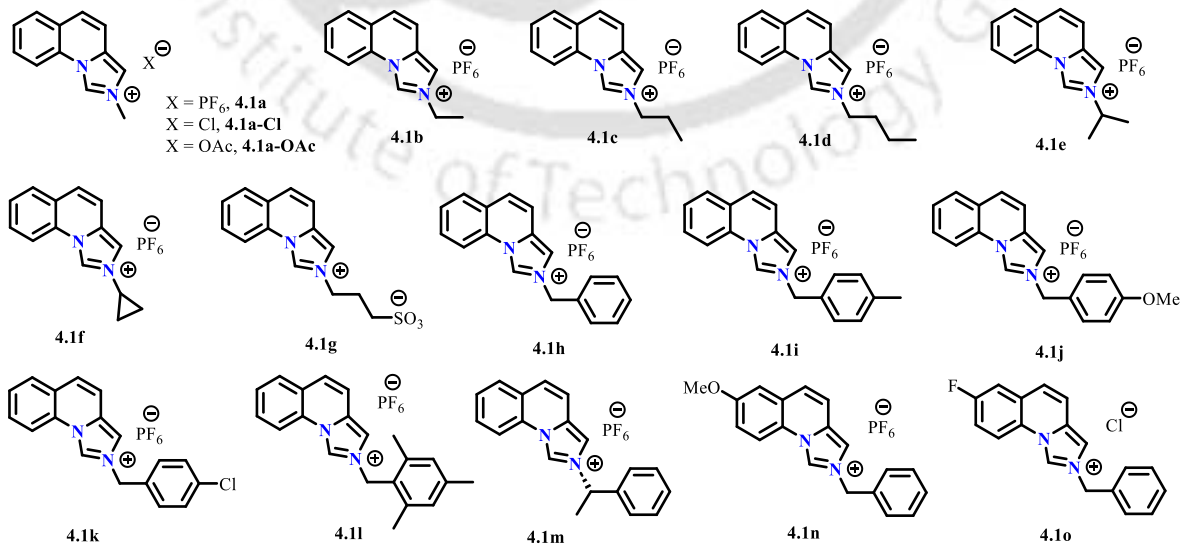
All the reagents and chemicals were purchased from common commercial suppliers like Sigma-Aldrich, Alfa Aesar, Merck, Spectrochem, Avra Synthesis Pvt. Ltd., BLD Pharma and directly used as received without any further purification unless otherwise mentioned. The following starting materials were synthesized according to the previously described procedure: $[Ru(OAc)_2(p\text{-cymene})]$,[13] $[Ru(OPiv)_2(p\text{-cymene})]$,[14] imidazo[1,5-*a*]quinoline,[15] 2-butylimidazo [1,5-*a*]quinolin-2-ium hexafluorophosphate (**4.1d**),[16] 2-benzylimidazo[1,5-

TH-3565_186122020

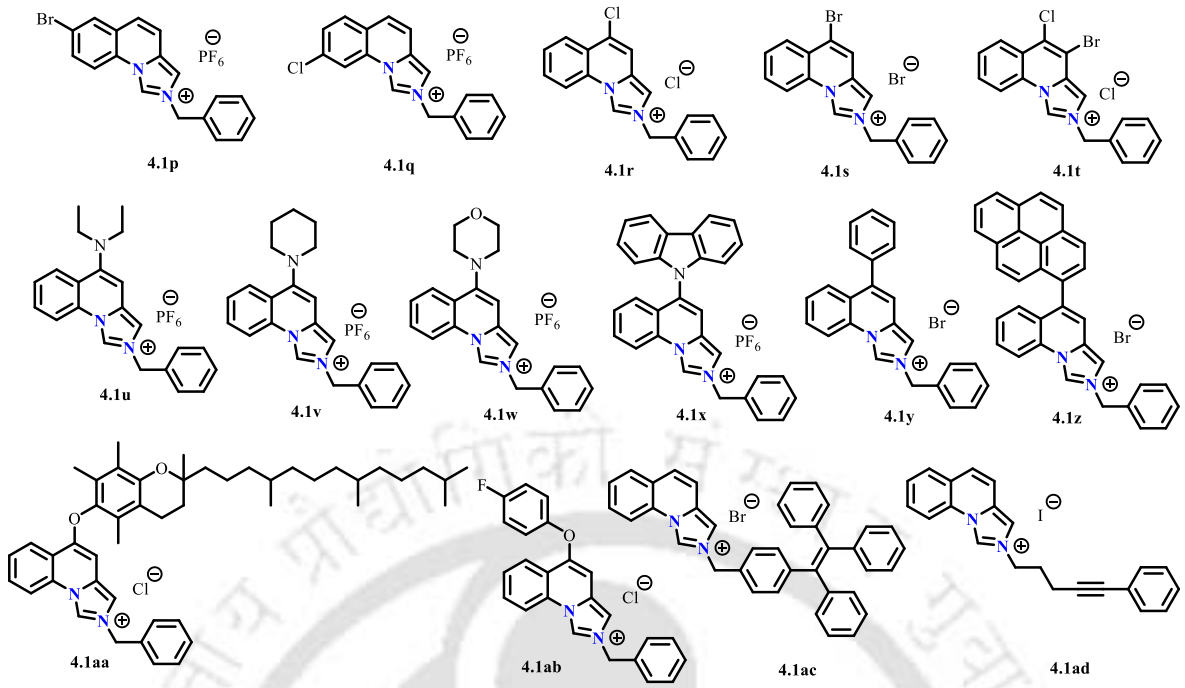
a]quinolin-2-ium hexafluorophosphate (**4.1h**),[17] (2-(4-(bromomethyl)phenyl)ethene-1,1,2-triyl)tribenzene.[18] Alkynes **4.2a**, **4.2g**, **4.2k**, **4.2l** and **4.2m** are commercially available and were used as supplied. Other alkynes **4.2b-f**,[19] **4.2h-i**[20] and **4.2j**[21] were synthesized through Sonogashira-coupling of terminal alkynes according to a previously described method. ^{1}H, $^{13}C\{^{1}H\}$, ^{19}F and ^{31}P NMR spectra of the compounds were measured in $CDCl_3$, D_2O and DMSO-d_6 as a solvent by using TMS as an internal standard. Chemical shifts, δ (in ppm), were reported relative to TMS δ (^{1}H) 0.0 ppm, δ (^{13}C) 0.0 ppm, which was used as the internal reference. Otherwise, the solvent's residual proton resonance and carbon resonance $CDCl_3$: δ (^{1}H) 7.26 ppm, δ (^{13}C) 77.16 ppm; D_2O: δ (^{1}H) 4.79 ppm; DMSO: δ (^{1}H) 2.5 ppm, δ (^{13}C) 39.52 ppm were used for calibration. Bruker Avance III 600, 500 and 400 spectrometers were used to record the NMR spectra. Chemical shift (δ) values were reported in ppm and spin-spin coupling constant (J) was expressed in Hz and other data were reported as follows: s = singlet, d = doublet, dd = doublet of doublet, dt = doublet of triplet, t = triplet, m = multiplet, q = quartet, p = pentet, br = broad, and brs = broad singlet. MS (ESI-HRMS): Mass spectra were recorded on an Agilent Accurate-Mass Q-TOF LC/MS 6546. Melting points were recorded in an open capillary tube and were uncorrected. Merck silica gel 60-120 mesh and neutral alumina 60-325 mesh were used for column chromatography. All the starting imidazolium salts, ligands, catalyst and their annulated products were characterized by spectroscopic methods and compared to literature wherever applicable, otherwise stated. All the annulation reactions were carried out in a preheated oil bath under a molecular O_2 atmosphere (1 atm) unless otherwise mentioned. Completion of reactions was examined by thin layer chromatography carried out on pre-coated Merck silica gel-60 F254 aluminium plates with ultraviolet light (UV) or iodine as visualizing agents.

4.5.2. Synthesis of starting materials

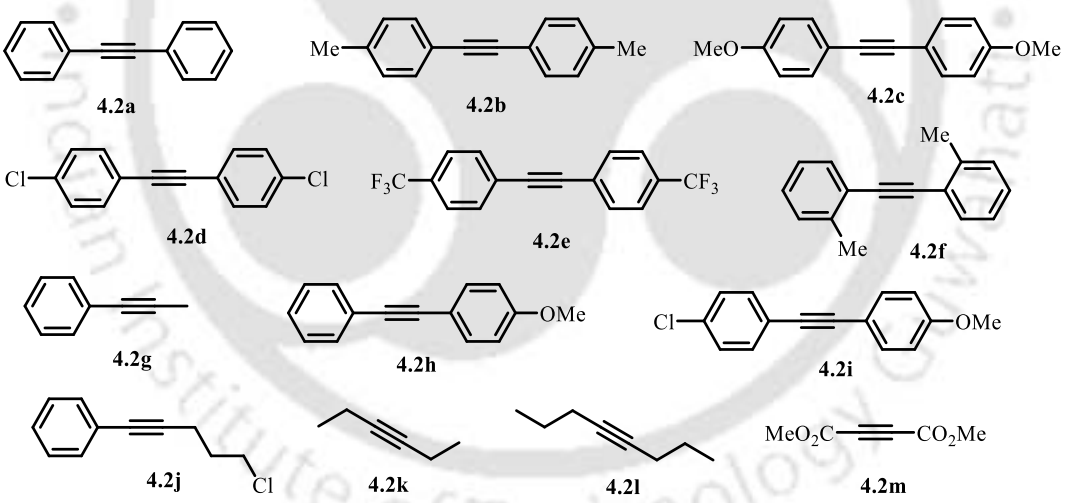
Substrates employed in the reaction:



TH-3565_186122020

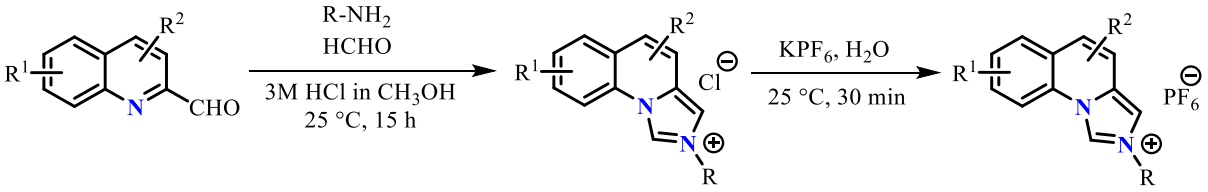


Alkynes employed in the reaction:



Experimental procedures for starting materials:

General procedure (GP-I)

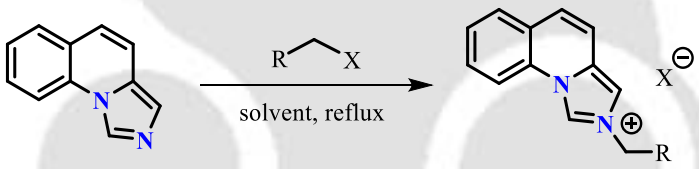


TH-3565_186122020

To a solution of aliphatic amine (1 equiv.) in dry methanol, formalin solution (1.5 equiv.) was added at room temperature and stirred for 10 minutes. At 0 ºC, 3M HCl in CH_3OH (prepared in another reaction tube by adding acetyl chloride (1.5 equiv.) to methanol at 0 ºC) was added to the reaction mixture, followed by the addition of substituted quinoline-2-carboxaldehyde (0.5 mmol, 1 equiv.) and stirred at room temperature for 15 h. Completion of the reaction was confirmed by TLC and the crude reaction mixture was concentrated under reduced pressure. Whenever the pure chloride salt was required, the crude reaction mixture was purified using neutral alumina column chromatography with ethyl acetate/methanol as the eluent to afford the desired product, otherwise for hexafluorophosphate counter-anion, the crude reaction mixture was subjected to salt metathesis by dissolving the crude reaction mixture in a minimal amount of water followed by slow addition of concentrated aqueous KPF_6 (1.5 equiv.) solution and stirring for 30 minutes. The resulting precipitate was filtered, washed with H_2O and diethyl ether (three times) to obtain the pure product.

- 1,4-dioxane was used as a solvent instead of methanol and 4M HCl in dioxane was used instead of 3M HCl in methanol in case of **4.1r**, **4.1t**.
- Concentrated HBr solution was used instead of HCl in MeOH in cases of **4.1s**, **4.1y**, and **4.1z**.

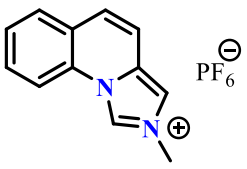
General procedure (GP-II)



A mixture of imidazo[1,5-*a*]quinoline (0.5 mmol, 1.0 equiv.) with corresponding halide (1.2 equiv.) was taken in a sealed tube with solvent and stirred under reflux condition for 12 h. After completion of the reaction, the reaction tube was brought to room temperature, white precipitate was observed. The resulting precipitate was filtered, washed three times with diethyl ether and dried under vacuum to obtain the desired product.

- Propane sultone (1.2 equiv.) was used instead of halide with toluene as a solvent for **4.1g**.
- THF was used as a solvent for **4.1ac**.
- NaI (5 equiv.) was used with acetone as a solvent for **4.1ad**.

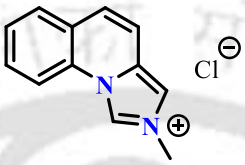
2-methylimidazo[1,5-*a*]quinolin-2-ium hexafluorophosphate (4.1a)



TH-3565_186122020

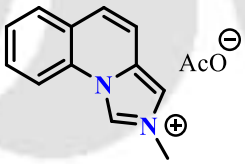
Following the general procedure GP-I, the title compound **4.1a** was obtained from quinoline-2-carbaldehyde on reaction with methylamine. White solid, 93% yield (153 mg). ^{1}H NMR (500 MHz, DMSO-d_6): δ 10.44 (s, 1H), 8.36 (d, J = 8.3 Hz, 1H), 8.19 (s, 1H), 7.99 (d, J = 7.8 Hz, 1H), 7.83 (t, J = 7.8 Hz, 1H), 7.71 (t, J = 7.6 Hz, 1H), 7.65 (q, J = 9.6 Hz, 2H), 4.16 (s, 3H). ^{13}C NMR (126 MHz, DMSO-d_6): δ 130.2, 129.5, 128.8, 128.7, 128.4, 128.0, 126.0, 124.0, 116.5, 116.3, 115.1, 36.9. ^{19}F NMR (565 MHz, DMSO): δ -69.4, -70.7. ^{31}P NMR (243 MHz, DMSO-d_6): δ -135.4, -138.3, -141.3, -144.2, -147.1, -150.0, -153.0. HRMS (ESI) *m/z*: calcd. for $C_{12}H_{11}N_2$ [M^+]: 183.0917; found: 183.0919.

2-methylimidazo[1,5-*a*]quinolin-2-ium chloride (4.1a-Cl)



Following the general procedure GP-I, the title compound **4.1a-Cl** was obtained from quinoline-2-carbaldehyde on reaction with methylamine. Compound **4.1a-Cl** was isolated by using neutral alumina column chromatography with ethyl acetate/ methanol (v/v = 10/1, R_f = 0.5) as the eluent to afford the desired product as brown solid, 91% yield (99.5 mg). ^{1}H NMR (600 MHz, CD_3OD): δ 10.30 (s, 1H), 8.36 – 8.32 (m, 1H), 8.09 (brs, 1H), 7.97 – 7.91 (m, 1H), 7.84 – 7.78 (m, 1H), 7.74 – 7.69 (m, 1H), 7.64 – 7.55 (m, 2H), 4.27 (s, 3H). ^{13}C NMR (151 MHz, CD_3OD): δ 131.7, 130.92, 130.87, 130.5, 129.9, 129.6, 128.0, 126.0, 117.7, 117.4, 115.8, 37.8.

2-methylimidazo[1,5-*a*]quinolin-2-ium acetate (4.1a-OAc)

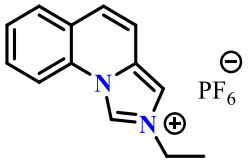


In a one-neck RB, salt **4.1a-Cl** (109.3 mg, 0.5 mmol, 1 equiv.) was dissolved in methanol (4.0 mL) with NaOAc (61.5 mg, 0.75 mmol, 1.5 equiv.) and stirred at room temperature for 2 h. After completion of the reaction, the solvent was removed in a rotary evaporator and extract the organic compound with $CHCl_3$. The solvent was evaporated under reduced pressure to get the pure compound **4.1a-OAc** as a white solid (104.2 mg, 86%).

^{1}H NMR (600 MHz, CD_3OD): δ 8.36 (d, J = 8.3 Hz, 1H), 8.09 (s, 1H), 7.97 (d, J = 7.8 Hz, 1H), 7.84 (t, J = 7.7 Hz, 1H), 7.74 (t, J = 7.6 Hz, 1H), 7.64 (d, J = 9.7 Hz, 1H), 7.60 (d, J = 9.7 Hz, 1H), 4.26 (s, 3H), 1.89 (s, 3H). ^{13}C NMR (151 MHz, CD_3OD): δ 180.2, 131.7, 130.9, 130.64, 130.58, 130.0, 128.1, 126.0, 117.6, 117.4, 115.8, 37.7, 24.1.

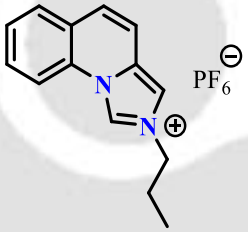
2-ethylimidazo[1,5-*a*]quinolin-2-ium hexafluorophosphate (4.1b)

TH-3565_186122020



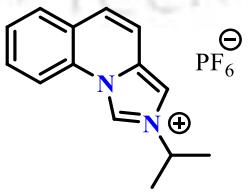
Following the general procedure GP-I, the title compound **4.1b** was obtained from quinoline-2-carbaldehyde on reaction with ethylamine. White solid, 90% yield (154 mg). ^{1}H NMR (500 MHz, DMSO-d_6): δ 10.48 (s, 1H), 8.43 – 8.41 (m, 1H), 8.29 (s, 1H), 8.00 – 7.99 (m, 1H), 7.86 – 7.82 (m, 1H), 7.73 – 7.65 (m, 3H), 4.50 (q, J = 7.5 Hz, 2H), 1.60 (t, J = 7.6 Hz, 3H). ^{13}C NMR (151 MHz, DMSO-d_6): δ 130.1, 129.5, 128.9, 128.4, 128.1, 127.9, 126.1, 124.0, 116.4, 115.2, 115.1, 45.7, 15.0. ^{19}F NMR (565 MHz, DMSO-d_6): δ -69.5, -70.7. ^{31}P NMR (243 MHz, DMSO-d_6): δ -135.4, -138.3, -141.2, -144.2, -147.1, -150.0, -153.0. HRMS (ESI) *m/z*: calcd. for $C_{13}H_{13}N_2$ [M^+]: 197.1079; found: 197.1077.

2-propylimidazo[1,5-*a*]quinolin-2-ium hexafluorophosphate (4.1c)



Following the general procedure GP-I, the title compound **4.1c** was obtained from quinoline-2-carbaldehyde on reaction with propylamine. White solid, 92% yield (164 mg). ^{1}H NMR (500 MHz, DMSO-d_6): δ 10.53 (s, 1H), 8.43 (d, J = 8.3 Hz, 1H), 8.30 (d, J = 1.6 Hz, 1H), 8.02 (dd, J = 7.9, 1.5 Hz, 1H), 7.88 – 7.85 (m, 1H), 7.75 – 7.72 (m, 1H), 7.71 – 7.66 (m, 2H), 4.43 (t, J = 7.1 Hz, 2H), 2.01 (h, J = 7.3 Hz, 2H), 0.96 (t, J = 7.4 Hz, 3H). ^{13}C NMR (126 MHz, DMSO-d_6): δ 130.2, 129.5, 129.1, 128.5, 128.3, 128.2, 126.1, 124.1, 116.6, 115.4, 115.3, 51.8, 22.9, 10.5. ^{19}F NMR (471 MHz, DMSO-d_6): δ -69.4, -70.9. ^{31}P NMR (202 MHz, DMSO-d_6): δ -133.6, -137.1, -140.7, -144.2, -147.7, -151.2, -154.7. HRMS (ESI) *m/z*: calcd. for $C_{14}H_{15}N_2$ [M^+]: 211.1230; found: 211.1231.

2-isopropylimidazo[1,5-*a*]quinolin-2-ium hexafluorophosphate (4.1e)

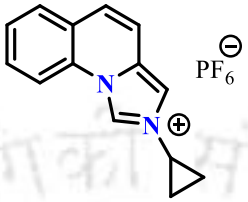


Following the general procedure GP-I, the title compound **4.1e** was obtained from quinoline-2-carbaldehyde on reaction with isopropyl amine. White solid, 86% yield (153 mg). ^{1}H NMR (500 MHz, DMSO-d_6): δ 10.53 (s, 1H), 8.52 (d, J = 8.2 Hz, 1H), 8.42 (d, J = 1.6 Hz, 1H), 8.03 (dd, J = 7.9, 1.4 Hz, 1H), 7.89 – 7.86 (m, 1H), 7.76 – 7.73 (m, 1H), 7.69 (s, 2H), 4.92 (hept, J

TH-3565_186122020

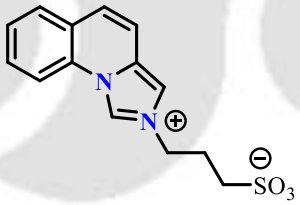
= 6.7 Hz, 1H), 1.66 (d, *J* = 6.7 Hz, 6H). ^{13}C NMR (126 MHz, DMSO-*d*$_6$): *δ* 130.1, 129.5, 129.2, 128.4, 128.2, 127.1, 126.1, 124.1, 116.7, 115.3, 113.8, 53.9, 22.6. ^{19}F NMR (471 MHz, DMSO-*d*$_6$): *δ* -69.4, -70.9. ^{31}P NMR (202 MHz, DMSO-*d*$_6$): *δ* -133.6, -137.2, -140.7, -144.2, -147.7, -151.2, -154.7. HRMS (ESI) *m/z*: calcd. for $C_{14}H_{15}N_2$ [M^+]: 211.1230; found: 211.1233.

2-cyclopropylimidazo[1,5-a]quinolin-2-ium hexafluorophosphate (4.1f)



Following the general procedure GP-I, the title compound **4.1f** was obtained from quinoline-2-carbaldehyde on reaction with cyclopropyl amine. White solid, 80% yield (141.6 mg). ^{1}H NMR (500 MHz, DMSO-*d*$_6$): *δ* 10.54 (s, 1H), 8.50 (d, *J* = 8.4 Hz, 1H), 8.35 (s, 1H), 8.01 (d, *J* = 7.9 Hz, 1H), 7.85 (t, *J* = 7.2 Hz, 1H), 7.73 (t, *J* = 7.6 Hz, 1H), 7.65 (q, *J* = 9.6 Hz, 2H), 4.15 – 4.11 (m, 1H), 1.40 – 1.36 (m, 2H), 1.28 – 1.24 (m, 2H). ^{13}C NMR (151 MHz, DMSO-*d*$_6$): *δ* 130.3, 129.6, 129.1, 128.9, 128.6, 128.1, 126.3, 124.1, 116.8, 116.0, 115.2, 32.1, 6.9. ^{19}F NMR (471 MHz, DMSO-*d*$_6$): *δ* -69.4, -70.9. ^{31}P NMR (202 MHz, DMSO-*d*$_6$): *δ* -137.2, -140.7, -144.2, -147.7, -151.2. HRMS (ESI) *m/z*: calcd. for $C_{14}H_{13}N_2$ [M^+]: 209.1074; found: 209.1083.

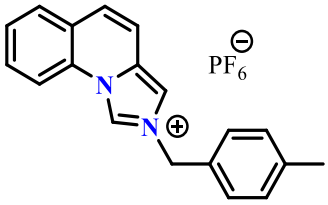
3-(imidazo[1,5-a]quinolin-2-ium-2-yl)propane-1-sulfonate (4.1g)



Following the general procedure GP-II, the title compound **4.1g** was obtained from imidazo[1,5-*a*]quinoline on reaction with propane sultone. Brown solid, 83% yield (120.5 mg). ^{1}H NMR (500 MHz, D_2O): *δ* 9.79 (s, 1H), 7.93 – 7.91 (m, 2H), 7.70 (d, *J* = 8.3 Hz, 1H), 7.62 (t, *J* = 7.8 Hz, 1H), 7.55 (t, *J* = 7.6 Hz, 1H), 7.37 – 7.33 (m, 2H), 4.62 (t, *J* = 7.2 Hz, 2H), 2.97 (t, *J* = 7.2 Hz, 2H), 2.44 (p, *J* = 7.2 Hz, 2H). ^{13}C NMR (151 MHz, D_2O): *δ* 130.0, 129.3, 129.0, 128.45, 128.39, 126.6, 126.3, 123.9, 115.6, 114.8, 114.3, 48.9, 47.1, 25.4. HRMS (ESI) *m/z*: calcd. for $C_{14}H_{15}N_2O_3S$ [M+H]$^+$: 291.0798; found: 291.0795.

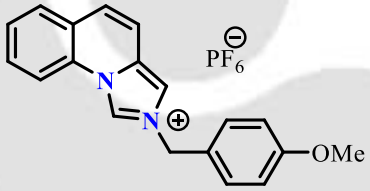
2-(4-methylbenzyl)imidazo[1,5-a]quinolin-2-ium hexafluorophosphate (4.1i)

TH-3565_186122020



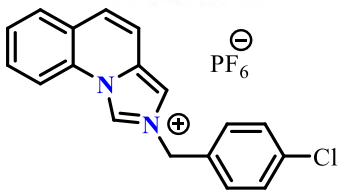
Following the general procedure GP-I, the title compound **4.1i** was obtained from quinoline-2-carbaldehyde on reaction with *p*-tolylmethanamine. Pale-yellow solid, 85% yield (178 mg). ^{1}H NMR (400 MHz, DMSO-d_6): δ 10.65 (brs, 1H), 8.45 (d, J = 8.3 Hz, 1H), 8.25 (d, J = 1.6 Hz, 1H), 8.04 – 8.02 (m, 1H), 7.89 – 7.84 (m, 1H), 7.74 (t, J = 7.6 Hz, 1H), 7.67 (s, 2H), 7.43 (d, J = 8.0 Hz, 2H), 7.26 (d, J = 8.0 Hz, 2H), 5.66 (s, 2H), 2.31 (s, 3H). ^{13}C NMR (151 MHz, DMSO-d_6): δ 138.4, 131.5, 130.3, 129.6, 129.5, 129.1, 128.6, 128.6, 128.5, 128.4, 126.4, 124.2, 116.8, 115.32, 115.29, 53.1, 20.7. ^{19}F NMR (377 MHz, DMSO-d_6): δ -69.2, -71.1. ^{31}P NMR (162 MHz, DMSO-d_6): δ -135.4, -139.8, -144.2, -148.6, -153.0. HRMS (ESI) *m/z*: calcd. for $C_{19}H_{17}N_2$ [M^+]: 273.1387; found: 273.1378.

2-(4-methoxybenzyl)imidazo[1,5-*a*]quinolin-2-ium hexafluorophosphate (4.1j):



Following the general procedure GP-I, the title compound **4.1j** was obtained from quinoline-2-carbaldehyde on reaction with (4-methoxyphenyl)methanamine. Pale-yellow solid, 86% yield (187 mg). ^{1}H NMR (500 MHz, DMSO-d_6): δ 10.65 (s, 1H), 8.45 (d, J = 8.3 Hz, 1H), 8.24 (d, J = 1.6 Hz, 1H), 8.01 – 7.99 (m, 1H), 7.87 – 7.83 (m, 1H), 7.74 – 7.71 (m, 1H), 7.66 (brs, 2H), 7.51 (d, J = 8.4 Hz, 2H), 7.02 – 7.00 (m, 2H), 5.64 (s, 2H), 3.77 (s, 3H). ^{13}C NMR (126 MHz, DMSO-d_6): δ 159.7, 130.3, 130.2, 129.5, 129.1, 128.5, 128.5, 128.2, 126.3, 126.2, 124.1, 116.7, 115.2, 115.1, 114.4, 55.2, 52.9. ^{19}F NMR (471 MHz, DMSO-d_6): δ -69.4, -70.9. ^{31}P NMR (202 MHz, DMSO-d_6): δ -133.6, -137.1, -140.6, -144.1, -147.7, -151.2, -154.7. HRMS (ESI) *m/z*: calcd. for $C_{19}H_{17}N_2O$ [M^+]: 289.1336; found: 289.1321.

2-(4-chlorobenzyl)imidazo[1,5-*a*]quinolin-2-ium hexafluorophosphate (4.1k)

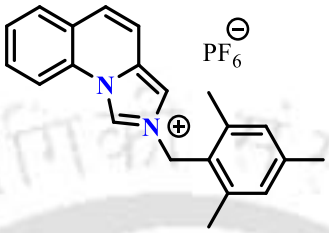


Following the general procedure GP-I, the title compound **4.1k** was obtained from quinoline-2-carbaldehyde on reaction with (4-chlorophenyl)methanamine. White solid, 79% yield (173 mg). ^{1}H NMR (500 MHz, DMSO-d_6): δ 10.61 (s, 1H), 8.43 (d, J = 8.3 Hz, 1H), 8.26 (s, 1H), 8.01 (d, J = 7.8 Hz, 1H), 7.86 (t, J = 7.9 Hz, 1H), 7.74 (t, J = 7.7 Hz, 1H), 7.67 (s, 2H), 7.56 –

TH-3565_186122020

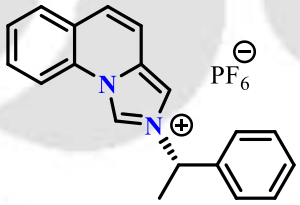
7.51 (m, 4H), 5.72 (s, 2H). ^{13}C NMR (151 MHz, DMSO-d_6): δ 133.6, 133.3, 130.5, 130.2, 129.5, 129.0, 128.9, 128.60, 128.56, 128.5, 126.4, 124.1, 116.7, 115.3, 115.2, 52.5. ^{19}F NMR (471 MHz, DMSO-d_6): δ -69.4, -70.9. ^{31}P NMR (202 MHz, DMSO-d_6): δ -137.2, -140.7, -144.2, -147.7, -151.2. HRMS (ESI) *m/z*: calcd. for $C_{18}H_{14}ClN_2$ [M^+]: 293.0841; found: 293.0836.

2-(2,4,6-trimethylbenzyl)imidazo[1,5-a]quinolin-2-ium hexafluorophosphate (4.1l)



Following the general procedure GP-I, the title compound **4.1l** was obtained from quinoline-2-carbaldehyde on reaction with mesitylmethanamine. White solid, 86% yield (192 mg).^{1}H NMR (600 MHz, DMSO-d_6): δ 10.57 (s, 1H), 8.60 (d, J = 8.4 Hz, 1H), 8.01 (d, J = 7.8 Hz, 1H), 7.95 (brs, 1H), 7.84 (t, J = 7.7 Hz, 1H), 7.73 (t, J = 7.6 Hz, 1H), 7.66 (d, J = 9.6 Hz, 1H), 7.61 (d, J = 9.5 Hz, 1H), 7.02 (s, 2H), 5.69 (s, 2H), 2.33 (s, 6H), 2.29 (s, 3H). ^{13}C NMR (151 MHz, DMSO-d_6): δ 138.8, 138.5, 130.1, 129.5, 129.4, 129.2, 128.54, 128.47, 128.1, 126.5, 126.2, 124.2, 117.1, 115.4, 114.8, 48.2, 20.7, 19.4. ^{19}F NMR (471 MHz, DMSO-d_6): δ -69.4, -70.9. ^{31}P NMR (202 MHz, DMSO-d_6): δ -133.6, -137.2, -140.7, -144.2, -147.7, -151.2, -154.7. HRMS (ESI) *m/z*: calcd. for $C_{21}H_{21}N_2$ [M^+]: 301.1700; found: 301.1705.

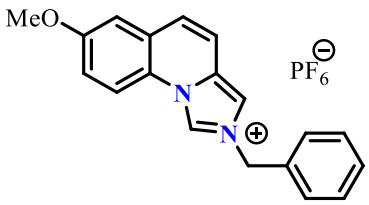
(*S*)-2-(1-phenylethyl)imidazo[1,5-a]quinolin-2-ium hexafluorophosphate (4.1m)



Following the general procedure GP-I, the title compound **4.1m** was obtained from quinoline-2-carbaldehyde on reaction with (*S*)-1-phenylethan-1-amine. White solid, 83% yield (173.6 mg). ^{1}H NMR (400 MHz, DMSO-d_6): δ 10.70 (brs, 1H), 8.56 (d, J = 8.3 Hz, 1H), 8.32 (d, J = 1.6 Hz, 1H), 8.02 (dd, J = 7.9, 1.5 Hz, 1H), 7.90 – 7.86 (m, 1H), 7.74 (t, J = 7.6 Hz, 1H), 7.66 (q, J = 9.7 Hz, 2H), 7.52 – 7.50 (m, 2H), 7.48 – 7.38 (m, 3H), 6.07 (q, J = 7.0 Hz, 1H), 2.07 (d, J = 7.0 Hz, 3H). ^{13}C NMR (151 MHz, DMSO-d_6): δ 139.4, 130.2, 129.6, 129.3, 129.0, 128.8, 128.6, 128.5, 127.6, 126.7, 126.4, 124.2, 117.0, 115.3, 114.4, 60.2, 20.8. ^{19}F NMR (377 MHz, DMSO-d_6): δ -69.2, -71.1. ^{31}P NMR (162 MHz, DMSO-d_6): δ -131.0, -135.4, -139.8, -144.2, -148.6, -153.0, 157.3. HRMS (ESI) *m/z*: calcd. for $C_{19}H_{17}N_2$ [M^+]: 273.1387; found: 273.1385. $[\alpha]_D^{20.0}$ = +188.22° (0.005 M, $CHCl_3$).

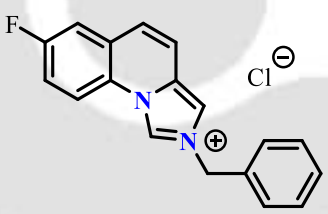
2-benzyl-7-methoxyimidazo[1,5-*a*]quinolin-2-ium hexafluorophosphate (4.1n)

TH-3565_186122020



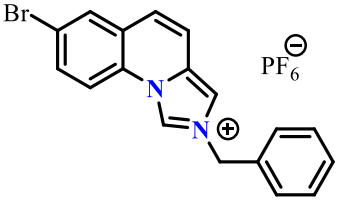
Following the general procedure GP-I, the title compound **4.1n** was obtained from 6-methoxyquinoline-2-carbaldehyde on reaction with benzylamine. White solid, 93% yield (202 mg). ^{1}H NMR (500 MHz, DMSO-d_6): δ 10.55 (s, 1H), 8.45 – 8.25 (m, 2H), 8.02 (m, 1H), 7.65 – 7.58 (m, 2H), 7.53 – 7.45 (m, 6H), 5.69 (s, 2H), 3.17 (s, 3H). ^{13}C NMR (126 MHz, DMSO-d_6): δ 193.5, 158.8, 136.4, 134.6, 131.3, 129.1, 128.5, 127.7, 126.3, 125.8, 123.7, 123.1, 118.3, 117.7, 115.7, 111.4, 105.9, 55.9, 53.3. ^{19}F NMR (471 MHz, DMSO-d_6): δ -69.4, -70.9. ^{31}P NMR (202 MHz, DMSO-d_6): δ -133.6, -137.2, -140.7, -144.2, -147.7, -151.2, -154.7. HRMS (ESI) *m/z*: calcd. for $C_{19}H_{17}N_2O$ [M^+]: 289.1336; found: 289.1333.

2-benzyl-7-fluoroimidazo[1,5-*a*]quinolin-2-ium chloride (4.1o)



Following the general procedure GP-I, the title compound **4.1o** was obtained from 6-fluoroquinoline-2-carbaldehyde on reaction with benzylamine. Compound **4.1o** was isolated by using neutral alumina column chromatography with ethyl acetate/ methanol (v/v = 10/1, R_f = 0.3) as the eluent to afford the desired product as yellow solid, 83% yield (129.8 mg). ^{1}H NMR (500 MHz, DMSO-d_6): δ 10.65 (s, 1H), 8.52 (dd, J = 9.2, 4.6 Hz, 1H), 8.31 (s, 1H), 7.92 (dd, J = 9.1, 2.9 Hz, 1H), 7.81 – 7.77 (m, 1H), 7.74 (d, J = 9.7 Hz, 1H), 7.64 (d, J = 9.7 Hz, 1H), 7.54 – 7.52 (m, 2H), 7.48 – 7.41 (m, 3H), 5.72 (s, 2H). ^{13}C NMR (101 MHz, DMSO-d_6): δ 162.0, 159.5, 134.4, 129.0, 128.9, 128.7, 128.5, 128.3, 126.2, 126.1, 125.9 (d, C-F, $J_{C\text{-}F}$ = 2.2 Hz), 125.6 (d, C-F, $J_{C\text{-}F}$ = 2.7 Hz), 119.5 – 119.4 (d, C-F, $J_{C\text{-}F}$ = 9.3 Hz), 118.1 – 117.8 (d, C-F, $J_{C\text{-}F}$ = 24.9 Hz), 116.6, 115.8, 114.8 – 114.6 (d, C-F, $J_{C\text{-}F}$ = 23.7 Hz), 53.3. ^{19}F NMR (471 MHz, DMSO-d_6): δ -112.1. HRMS (ESI) *m/z*: calcd. for $C_{18}H_{14}FN_2$ [M^+]: 277.1136; found: 277.1139.

2-benzyl-7-bromoimidazo[1,5-*a*]quinolin-2- ium hexafluorophosphate (4.1p)

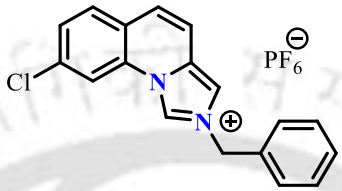


Following the general procedure GP-I, the title compound **4.1p** was obtained from 6-bromoquinoline-2-carbaldehyde on reaction with benzylamine. Yellow solid, 85% yield (205.4 mg). ^{1}H NMR (500 MHz, DMSO-d_6): δ 10.70 (s, 1H), 8.40 (d, J = 9.2 Hz, 1H), 8.31 – 8.30

TH-3565_186122020

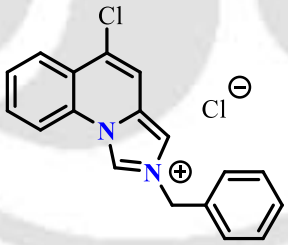
(m, 2H), 8.05 (d, J = 9.2 Hz, 1H), 7.72 (d, J = 9.7 Hz, 1H), 7.62 (d, J = 9.7 Hz, 1H), 7.53 (d, J = 7.4 Hz, 2H), 7.47 – 7.41 (m, 3H), 5.72 (s, 2H). ^{13}C NMR (126 MHz, DMSO-d_6): δ 134.4, 132.7, 131.6, 129.04, 129.01, 128.97, 128.6, 128.4, 126.1, 125.2, 121.1, 119.1, 116.7, 115.8, 53.4. ^{19}F NMR (471 MHz, DMSO-d_6): δ -69.4, -70.9. ^{31}P NMR (202 MHz, DMSO-d_6): δ -133.6, -137.2, -140.7, -144.2, -147.7, -151.2, -154.7. HRMS (ESI) *m/z*: calcd. for $C_{18}H_{14}BrN_2$ [M^+]: 337.0335; found: 337.0338.

2-benzyl-8-chloroimidazo[1,5-*a*]quinolin-2-ium hexafluorophosphate (4.1q)



Following the general procedure GP-I, the title compound **4.1q** was obtained from 7-chloroquinoline-2-carbaldehyde on reaction with benzylamine. White solid, 92% yield (201.8 mg). ^{1}H NMR (500 MHz, DMSO-d_6): δ 10.67 (s, 1H), 8.69 (s, 1H), 8.32 (s, 1H), 8.05 (d, J = 8.5 Hz, 1H), 7.80 (d, J = 8.6 Hz, 1H), 7.71 – 7.67 (m, 2H), 7.53 – 7.42 (m, 5H), 5.72 (s, 2H). ^{13}C NMR (126 MHz, DMSO-d_6): δ 134.34, 134.28, 131.2, 129.9, 129.1, 129.03, 128.98, 128.7, 128.6, 128.5, 125.7, 123.1, 117.2, 115.7, 115.6, 53.5. ^{19}F NMR (565 MHz, DMSO-d_6): δ -69.5, -70.7. ^{31}P NMR (243 MHz, DMSO-d_6): δ -135.4, -138.4, -141.3, -144.2, -147.1, -150.1, -153.0. HRMS (ESI) *m/z*: calcd. for $C_{18}H_{14}ClN_2$ [M^+]: 293.0841; found: 293.0845.

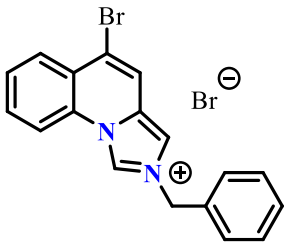
2-benzyl-5-chloroimidazo[1,5-*a*]quinolin-2-ium chloride (4.1r)



Following the general procedure GP-I, the title compound **4.1r** was obtained from 4-chloroquinoline-2-carbaldehyde on reaction with benzylamine. Compound **4.1r** was isolated by using neutral alumina column chromatography with ethyl acetate/ methanol (v/v = 10/1, R_f = 0.4) as the eluent to afford the desired product as white solid, 93% yield (153.1 mg). ^{1}H NMR (600 MHz, DMSO-d_6): δ 11.28 (s, 1H), 8.62 (d, J = 8.3 Hz, 1H), 8.33 (d, J = 1.6 Hz, 1H), 8.17 (dd, J = 8.2, 1.4 Hz, 1H), 8.06 (s, 1H), 7.96 (t, J = 7.7, 1H), 7.84 (t, J = 7.8 Hz, 1H), 7.60 (d, J = 7.0 Hz, 2H), 7.52 (d, J = 7.2 Hz, 1H), 7.45 – 7.43 (m, 1H), 7.42 – 7.39 (m, 1H), 5.77 (s, 2H). ^{13}C NMR (151 MHz, DMSO-d_6): δ 134.6, 134.1, 131.5, 129.8, 129.6, 129.2, 129.1, 129.0, 128.6, 128.5, 128.3, 127.6, 126.1, 121.8, 117.4, 115.5, 115.3, 53.2. HRMS (ESI) *m/z*: calcd. for $C_{18}H_{14}ClN_2$ [M^+]: 293.0841; found: 293.0836.

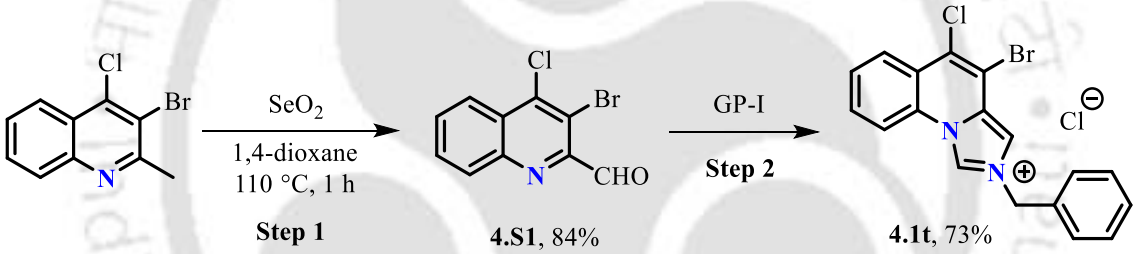
2-benzyl-5-bromoimidazo[1,5-*a*]quinolin-2-ium bromide (4.1s)

TH-3565_186122020



Following the general procedure GP-I, the title compound **4.1s** was obtained from 4-bromoquinoline-2-carbaldehyde on reaction with benzylamine. Compound **4.1s** was isolated by using neutral alumina column chromatography with ethyl acetate/ methanol (v/v = 10/1, R_f = 0.3) as the eluent to afford the desired product as brown solid, 87% yield (182 mg). ^{1}H NMR (600 MHz, $CDCl_3$): δ 12.64 (s, 1H), 8.93 (brs, 1H), 8.16 (d, J = 8.0 Hz, 1H), 7.90 – 7.88 (m, 1H), 7.75 – 7.73 (m, 1H), 7.66 – 7.63 (m, 2H), 7.58 (brs, 1H), 7.44 (s, 1H), 7.40 – 7.39 (m, 3H), 5.95 (s, 2H). ^{13}C NMR (126 MHz, $CDCl_3$): δ 133.0, 132.8, 132.5, 130.6, 129.9, 129.8, 129.7, 129.6, 128.1, 126.8, 122.4, 118.6, 113.5, 113.4, 55.0. HRMS (ESI) *m/z*: calcd. for $C_{18}H_{14}BrN_2$ [M^+]: 337.0335; found: 337.0340.

2-benzyl-4-bromo-5-chloroimidazo[1,5-*a*]quinolin-2-ium chloride (4.1t)



Scheme 4.16. Synthesis of **4.1t**

Step 1: Synthesis of 3-bromo-4-chloroquinoline-2-carbaldehyde (**4.S1**)

An oven dried pressure tube was charged with 3-bromo-4-chloro-2-methylquinoline (230 mg, 0.9 mmol, 1 equiv.), SeO_2 (120 mg, 1.08 mmol, 1.2 equiv.) with 1,4-dioxane (3 mL) and stirred at 110 ºC for 1 hour. After completion of the reaction, the reaction mixture was then passed through a bed of celite, the filtrate was collected and concentrated under reduced pressure. The crude reaction mixture was purified by column chromatography on silica gel using ethyl acetate/ pet ether (v/v = 1/10, R_f = 0.6) as the eluent to afford the desired product as a yellow solid (205 mg, 84%).

^{1}H NMR (600 MHz, $CDCl_3$): δ 10.31 (s, 1H), 8.26 (d, J = 8.4 Hz, 1H), 8.22 (d, J = 8.5 Hz, 1H), 7.86 (t, J = 8.4 Hz, 1H), 7.77 (t, J = 7.1 Hz, 1H). ^{13}C NMR (151 MHz, $CDCl_3$): δ 190.7, 146.4, 135.2, 132.5, 131.5, 131.3, 131.1, 128.3, 127.1, 124.8. HRMS (ESI) *m/z*: [M+H]$^+$ calcd. for $C_{10}H_6BrClNO$: 269.9316; found: 269.9315.

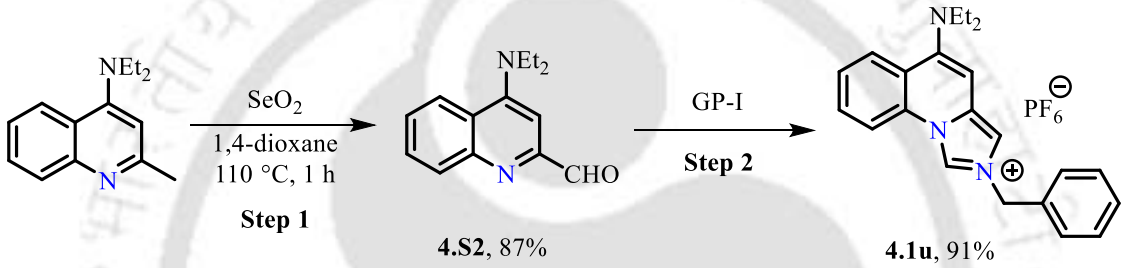
Step 2: Synthesis of **4.1t**

TH-3565_186122020

Following the general procedure GP-I, the title compound **4.1t** was obtained from 3-bromo-4-chloroquinoline-2-carbaldehyde **4.S1** (150 mg, 0.6 mmol, 1 equiv.) on reaction with benzylamine (64 mg, 0.6 mmol, 1 equiv.). Compound **4.1t** was isolated by using neutral alumina column chromatography with ethyl acetate/ methanol (v/v = 10/1, R_f = 0.4) as the eluent to afford the desired product as a white solid, 73% yield (179 mg).

^{1}H NMR (600 MHz, DMSO-d_6): δ 10.89 (s, 1H), 8.67 – 8.63 (m, 1H), 8.51 – 8.47 (m, 1H), 8.34 – 8.25 (m, 2H), 8.01 – 7.86 (m, 2H), 7.55 – 7.45 (m, 4H), 5.71 (s, 2H). ^{13}C NMR (151 MHz, DMSO-d_6): δ 134.3, 131.7, 130.9, 130.5, 129.7, 129.1, 128.6, 126.8, 123.8, 122.3, 122.0, 119.6, 118.2, 117.8, 117.4, 110.2, 108.7, 53.6. HRMS (ESI) *m/z*: calcd. for $C_{18}H_{13}BrClN_2$ [M^+]: 370.9946; found: 370.9947.

2-benzyl-5-(diethylamino)imidazo[1,5-*a*]quinolin-2-ium hexafluorophosphate (4.1u)



Scheme 4.17. Synthesis of **4.1u**

Step 1: Synthesis of 4-(diethylamino)quinoline-2-carbaldehyde (**4.S2**)

Compound **4.S2** was prepared in a similar method described above for **4.S1**, using *N,N*-diethyl-2-methylquinolin-4-amine (170 mg, 0.8 mmol, 1 equiv.) as a starting material. The crude reaction mixture was purified by column chromatography on silica gel using ethyl acetate/ pet ether (v/v = 1/10, R_f = 0.8) as the eluent to afford the desired product as a brown viscous liquid (159 mg, 87%).

^{1}H NMR (500 MHz, $CDCl_3$): δ 10.14 (s, 1H), 8.14 (d, J = 8.2 Hz, 1H), 8.05 (d, J = 8.5 Hz, 1H), 7.70 – 7.67 (m, 1H), 7.55 – 7.52 (m, 1H), 7.42 (s, 1H), 3.41 (q, J = 7.1 Hz, 4H), 1.16 (t, J = 7.1 Hz, 6H). ^{13}C NMR (126 MHz, $CDCl_3$): δ 194.7, 157.2, 152.7, 149.8, 130.9, 129.8, 127.1, 126.1, 124.6, 105.6, 46.6, 12.3. HRMS (ESI) *m/z*: calcd. for $C_{14}H_{17}N_2O$ [M+H]$^+$: 229.1336; found: 229.1333.

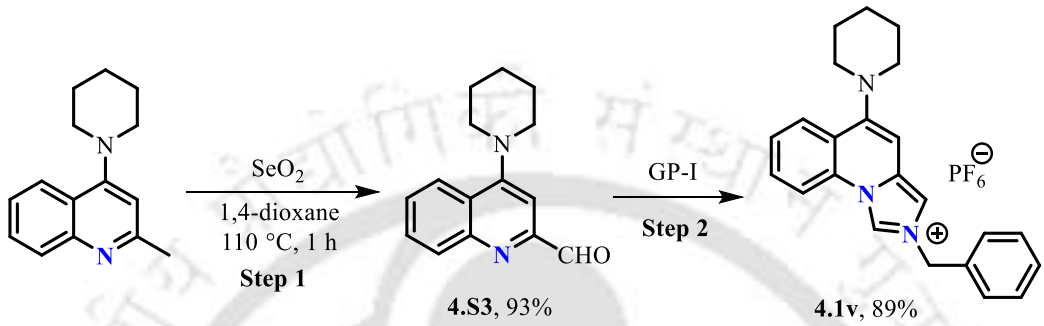
Step 2: Synthesis of **4.1u**

Following the general procedure GP-I, the title compound **4.1u** was obtained from 4-(diethylamino)quinoline-2-carbaldehyde **4.S2** (150 mg, 0.66 mmol, 1 equiv.) on reaction with benzylamine (71 mg, 0.66 mmol, 1 equiv.) as white solid, 91% yield (285.5 mg). ^{1}H NMR (500 MHz, DMSO-d_6): δ 10.55 (s, 1H), 8.43 (d, J = 8.3 Hz, 1H), 8.10 (d, J = 8.2 Hz, 1H), 7.98 (s, 1H), 7.86 (t, J = 7.4 Hz, 1H), 7.75 (t, J = 7.7 Hz, 1H), 7.52 (d, J = 7.3 Hz, 2H), 7.47 – 7.41 (m,

TH-3565_186122020

3H), 7.15 (s, 1H), 5.68 (s, 2H), 3.18 (q, J = 7.0 Hz, 4H), 1.06 (t, J = 7.0 Hz, 6H). ^{13}C NMR (126 MHz, DMSO-d_6): δ 144.8, 134.6, 130.2, 130.0, 129.6, 129.0, 128.8, 128.4, 128.2, 127.4, 126.0, 123.0, 117.2, 112.7, 103.1, 53.1, 45.7, 11.5. ^{19}F NMR (471 MHz, DMSO-d_6): δ -69.4, -70.9. ^{31}P NMR (202 MHz, DMSO-d_6): δ -133.6, -137.2, -140.7, -144.2, -147.7, -151.2, -154.7. HRMS (ESI) *m/z*: calcd. for $C_{22}H_{24}N_3$ [M^+]: 330.1965; found: 330.1968.

2-benzyl-5-(piperidin-1-yl)imidazo[1,5-*a*]quinolin-2-ium hexafluorophosphate (4.1v)



Scheme 4.18. Synthesis of **4.1v**

Step 1: Synthesis of 4-(piperidin-1-yl)quinoline-2-carbaldehyde (**4.S3**)

Compound **4.S3** was prepared in a similar method described above for **4.S1**, using 2-methyl-4-(piperidin-1-yl)quinoline (200 mg, 0.88 mmol, 1 equiv.) as a starting material. The crude reaction mixture was purified by column chromatography on silica gel using ethyl acetate/ pet ether (v/v = 1/10, R_f = 0.8) as the eluent to afford the desired product **4.S3** as a colourless oil (197 mg, 93%).

^{1}H NMR (500 MHz, $CDCl_3$): δ 10.13 (s, 1H), 8.14 (d, J = 9.4 Hz, 1H), 8.01 (d, J = 8.4 Hz, 1H), 7.71 – 7.68 (m, 1H), 7.57 – 7.54 (m, 1H), 7.42 (s, 1H), 3.22 (t, J = 5.4 Hz, 4H), 1.83 (p, J = 5.8 Hz, 4H), 1.71 – 1.66 (m, 2H). ^{13}C NMR (151 MHz, $CDCl_3$): δ 194.6, 159.2, 153.2, 149.5, 130.9, 129.9, 127.5, 125.4, 124.3, 104.5, 53.6, 26.1, 24.4. HRMS (ESI) *m/z*: calcd. for $C_{15}H_{17}N_2O$ [M+H]$^+$: 241.1336; found: 241.1341.

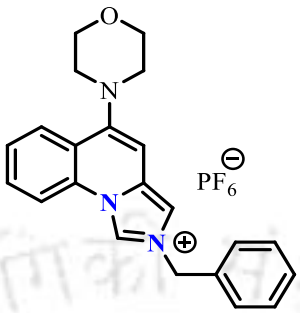
Step 2: Synthesis of **4.1v**

Following the general procedure GP-I, the title compound **4.1v** was obtained from 4-(piperidin-1-yl)quinoline-2-carbaldehyde **4.S3** (150 mg, 0.62 mmol, 1 equiv.) on reaction with benzylamine (66 mg, 0.62 mmol, 1 equiv.) as white solid, 89% yield (269 mg). ^{1}H NMR (400 MHz, DMSO-d_6): δ 10.53 (s, 1H), 8.42 (d, J = 8.3 Hz, 1H), 8.04 (d, J = 8.0 Hz, 1H), 7.99 (d, J = 1.7 Hz, 1H), 7.88 – 7.84 (m, 1H), 7.76 (t, J = 7.7 Hz, 1H), 7.52 – 7.49 (m, 2H), 7.47 – 7.41 (m, 3H), 7.06 (s, 1H), 5.67 (s, 2H), 2.99 (brs, 4H), 1.78 (p, J = 5.7 Hz, 4H), 1.64 – 1.62 (m, 2H). ^{13}C NMR (151 MHz, DMSO-d_6): δ 147.9, 134.7, 130.2, 130.1, 129.7, 129.0, 128.9, 128.4, 128.3, 127.5, 125.9, 121.9, 117.4, 113.0, 100.4, 53.24, 53.15, 25.6, 23.8. ^{19}F NMR (471 MHz,

TH-3565_186122020

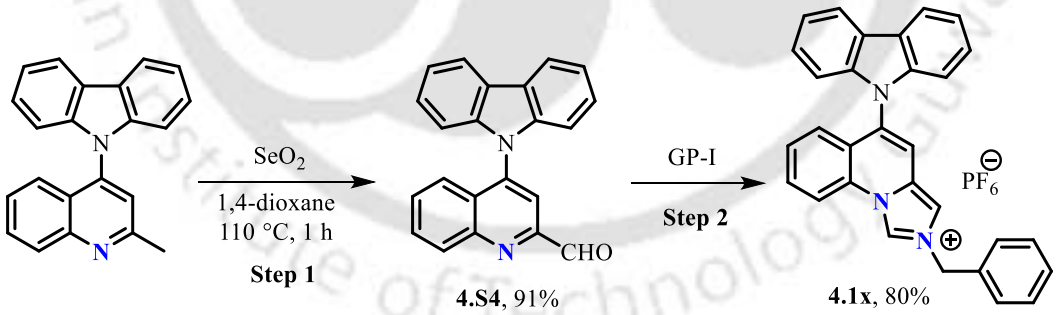
DMSO-d_6): δ -69.4, -70.9. ^{31}P NMR (162 MHz, DMSO-d_6): δ -126.3, -130.7, -135.0, -139.4, -143.8, -148.2, -152.6. HRMS (ESI) *m/z*: calcd. for $C_{23}H_{24}N_3$ [M^+]: 342.1965; found: 342.1962.

2-benzyl-5-morpholinoimidazo[1,5-*a*]quinolin-2-ium hexafluorophosphate (4.1w)



Following the general procedure GP-I, the title compound **4.1w** was obtained from 4-morpholinoquinoline-2-carbaldehyde (150 mg, 0.62 mmol, 1 equiv.) on reaction with benzylamine (66 mg, 0.62 mmol, 1 equiv.) as white solid, 90% yield (192 mg). ^{1}H NMR (500 MHz, DMSO-d_6): δ 10.55 (s, 1H), 8.44 (d, J = 8.4 Hz, 1H), 8.13 (d, J = 8.2 Hz, 1H), 8.04 (s, 1H), 7.88 (t, J = 7.8 Hz, 1H), 7.76 (t, J = 7.8 Hz, 1H), 7.52 – 7.50 (m, 2H), 7.46 – 7.41 (m, 3H), 7.14 (s, 1H), 5.68 (s, 2H), 3.88 (t, J = 4.4 Hz, 4H), 3.04 (t, J = 4.2 Hz, 4H). ^{13}C NMR (151 MHz, DMSO-d_6): δ 146.7, 134.7, 130.3, 130.1, 129.5, 129.0, 128.8, 128.4, 128.3, 127.7, 125.9, 121.4, 117.4, 113.4, 100.9, 66.1, 53.1, 52.4. ^{19}F NMR (377 MHz, DMSO-d_6): δ -69.2, -71.1. ^{31}P NMR (202 MHz, DMSO-d_6): δ -133.6, -137.1, -140.7, -144.2, -147.7, -151.2, -154.7. HRMS (ESI) *m/z*: calcd. for $C_{22}H_{22}N_3O$ [M^+]: 344.1758; found: 344.1768.

2-benzyl-5-(9*H*-carbazol-9-yl)imidazo[1,5-*a*]quinolin-2-ium hexafluorophosphate (4.1x)



Scheme 4.19. Synthesis of **4.1x**

Step 1: Synthesis of 4-(9*H*-carbazol-9-yl)quinoline-2-carbaldehyde (**4.S4**)

Compound **4.S4** was prepared in a similar method described above for **4.S1**, using 9-(2-methylquinolin-4-yl)-9*H*-carbazole (150 mg, 0.49 mmol, 1 equiv.) as a starting material. The crude reaction mixture was purified by column chromatography on silica gel using ethyl acetate/ pet ether (v/v = 1/20, R_f = 0.5) as the eluent to afford the desired product as a colourless oil (143 mg, 91%).

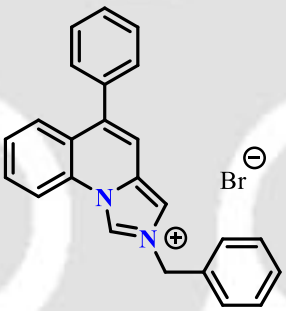
TH-3565_186122020

^{1}H NMR (500 MHz, $CDCl_3$): δ 10.34 (s, 1H), 8.45 (d, J = 8.6 Hz, 1H), 8.21 (brs, 1H), 8.20 (d, J = 2.2 Hz, 1H), 7.92 – 7.89 (m, 1H), 7.63 – 7.56 (m, 2H), 7.39 –7.34 (m, 5H), 7.07 – 7.05 (m, 2H). ^{13}C NMR (151 MHz, $CDCl_3$): δ 193.1, 153.7, 150.1, 144.7, 141.2, 131.4, 131.3, 129.9, 127.3, 126.5, 124.4, 124.2, 121.1, 120.7, 116.7, 110.3. HRMS (ESI) *m/z*: calcd. for $C_{22}H_{15}N_2O$ $[M+H]^+$: 323.1179; found: 323.1181.

Step 2: Synthesis of **4.1x**

Following the general procedure GP-I, the title compound **4.1x** was obtained from 4-(9*H*-carbazol-9-yl)quinoline-2-carbaldehyde **4.S4** (130 mg, 0.4 mmol, 1 equiv.) on reaction with benzylamine (43 mg, 0.4 mmol, 1 equiv.) as brown solid, 80% yield (182 mg). ^{1}H NMR (500 MHz, $CDCl_3$): δ 10.14 (s, 1H), 8.48 (d, J = 8.5 Hz, 1H), 8.16 (d, J = 6.8 Hz, 2H), 7.75 – 7.71 (m, 2H), 7.55 – 7.52 (m, 3H), 7.42 – 7.37 (m, 4H), 7.35 – 7.29 (m, 4H), 7.17 (d, J = 8.1 Hz, 1H), 7.06 (d, J = 7.8 Hz, 2H), 5.71 (s, 2H). ^{13}C NMR (151 MHz, $CDCl_3$): δ 141.2, 134.5, 132.5, 132.3, 130.4, 130.1, 129.8, 129.5, 129.4, 129.1, 127.3, 126.7, 126.3, 123.8, 122.5, 121.1, 120.8, 117.4, 115.5, 115.0, 110.1, 55.1. ^{19}F NMR (471 MHz, $CDCl_3$): δ -70.7, -72.3. ^{31}P NMR (202 MHz, $CDCl_3$): δ -136.9, -140.4, -144.0, -147.5, -151.0. HRMS (ESI) *m/z*: calcd. for $C_{30}H_{22}N_3$ $[M^+]$: 424.1809; found: 424.1815.

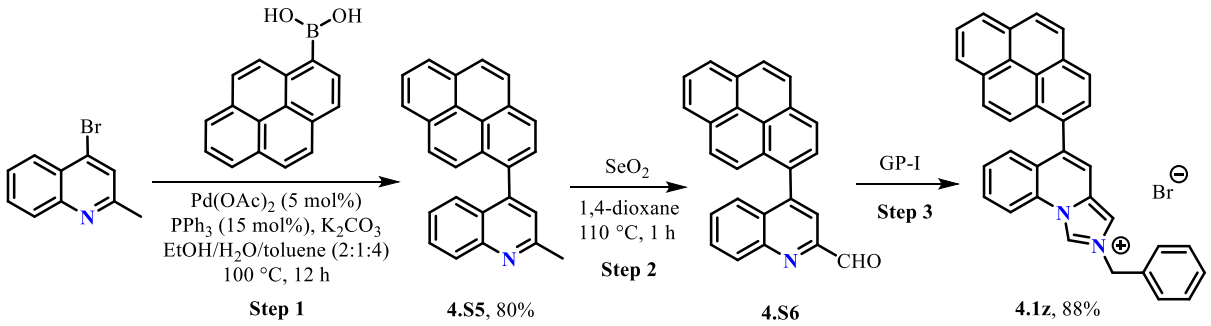
2-benzyl-5-phenylimidazo[1,5-*a*]quinolin-2-ium bromide (4.1y)



Following the general procedure GP-I, the title compound **4.1y** was obtained from 4-phenylquinoline-2-carbaldehyde on reaction with benzylamine. Compound **4.1y** was isolated by using neutral alumina column chromatography with ethyl acetate/ methanol (v/v = 10/1, R_f = 0.4) as the eluent to afford the desired product as a white solid, 85% yield (177 mg). ^{1}H NMR (500 MHz, $CDCl_3$): δ 12.45 (s, 1H), 8.92 (d, J = 8.2 Hz, 1H), 7.81 (t, J = 7.7 Hz, 1H), 7.71 – 7.67 (m, 4H), 7.56 (t, J = 7.7 Hz, 1H), 7.51 – 7.49 (m, 3H), 7.39 – 7.34 (m, 5H), 7.20 (s, 1H), 6.00 (s, 2H). ^{13}C NMR (151 MHz, $CDCl_3$): δ 140.2, 136.8, 133.3, 131.5, 129.7, 129.6, 129.5, 129.3, 129.1, 129.0, 128.9, 128.7, 128.3, 124.2, 118.4, 113.5, 113.4, 54.4. HRMS (ESI) *m/z*: calcd. for $C_{24}H_{19}N_2$ $[M^+]$: 335.1543; found: 335.1545.

2-benzyl-5-(pyren-1-yl)imidazo[1,5-*a*]quinolin-2-ium bromide (4.1z)

TH-3565_186122020



Scheme 4.20. Synthesis of **4.1z**

Step 1: Synthesis of 2-methyl-4-(pyren-1-yl)quinoline (**4.S5**)

4-bromo-2-methylquinoline (180 mg, 0.81 mmol, 1.0 equiv.), pyrene-1-boronic acid (239 mg, 0.97 mmol, 1.2 equiv.), anhydrous K_2CO_3 (448 mg, 3.24 mmol, 4.0 equiv.), PPh_3 (31.4 mg, 0.12 mmol, 15 mol%), $Pd(OAc)_2$ (9 mg, 0.04 mmol, 5 mol%), H_2O (1.0 mL), EtOH (0.5 mL) and toluene (2.0 mL) were added to an oven-dried Schlenk Tube. The reaction vessel was charged with argon and sealed. The mixture was heated to 100 °C using oil bath and stirred for 12 h. The mixture was diluted with CH_2Cl_2 and H_2O, and extracted with CH_2Cl_2. The organic layer was washed with brine solution, dried over anhydrous Na_2SO_4, concentrated, and then residues were purified by column chromatography on silica gel using ethyl acetate/ pet ether (v/v = 3/10, R_f = 0.3) as the eluent to afford the desired product **4.S5** as a yellow solid (222.5 mg, 80%).

^{1}H NMR (500 MHz, $CDCl_3$): δ 8.28 (d, J = 7.8 Hz, 1H), 8.23 (d, J = 7.6 Hz, 1H), 8.19 – 8.15 (m, 4H), 8.04 – 8.01 (m, 1H), 7.96 (d, J = 7.8 Hz, 1H), 7.92 (d, J = 9.2 Hz, 1H), 7.69 (t, J = 7.7 Hz, 1H), 7.61 (d, J = 9.2 Hz, 1H), 7.43 (s, 1H), 7.36 (d, J = 8.3 Hz, 1H), 7.29 – 7.25 (m, 1H), 2.86 (s, 3H). ^{13}C NMR (151 MHz, $CDCl_3$): δ 158.7, 148.2, 148.0, 136.3, 133.0, 131.5, 131.0, 129.7, 129.4, 129.1, 128.7, 127.6, 127.5, 126.7, 126.5, 126.4, 126.0, 125.7, 125.5, 125.2, 124.80, 124.76, 124.7, 124.0, 122.1, 25.6. HRMS (ESI) *m/z*: calcd. for $C_{26}H_{18}N$ $[M+H]^+$: 344.1434; found: 344.1436.

Step 2: Synthesis of 4-(pyren-1-yl)quinoline-2-carbaldehyde (**4.S6**)

Compound **4.S6** was prepared in a similar method described above for **4.S1**, using 2-methyl-4-(pyren-1-yl)quinoline (200 mg, 0.58 mmol, 1 equiv.) as a starting material. The crude reaction mixture was filtered, solvent was evaporated under reduced pressure and directly used for the next step without further purification.

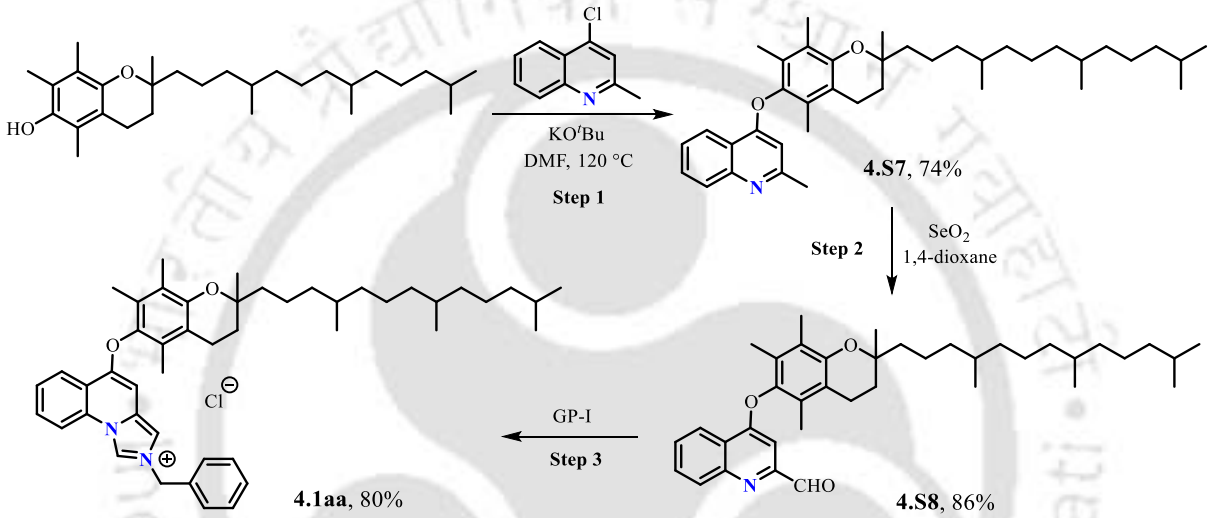
Step 3: Synthesis of **4.1z**

Following the general procedure GP-I, the title compound **4.1z** was obtained from 4-(pyren-1-yl)quinoline-2-carbaldehyde on reaction with benzylamine. Compound **4.1z** was isolated by using neutral alumina column chromatography with ethyl acetate/ methanol (v/v = 10/1, R_f= 0.3) as the eluent to afford the desired product as a brown solid, with 88% yield (275.3 mg).

TH-3565_186122020

^{1}H NMR (500 MHz, $CDCl_3$): δ 12.68 (s, 1H), 9.02 (d, J = 8.4 Hz, 1H), 8.28 (t, J = 7.2 Hz, 2H), 8.20 – 8.14 (m, 3H), 8.06 (t, J = 7.6 Hz, 1H), 7.96 (d, J = 9.2 Hz, 1H), 7.91 (d, J = 7.7 Hz, 1H), 7.81 (t, J = 7.8 Hz, 1H), 7.72 – 7.71 (m, 2H), 7.65 – 7.62 (m, 2H), 7.45 – 7.37 (m, 5H), 7.23 – 7.21 (m, 1H), 6.08 – 56.01 (m, 2H). ^{13}C NMR (151 MHz, $CDCl_3$): δ 139.5, 133.2, 132.0, 131.7, 131.4, 131.0, 130.8, 129.91, 129.87, 129.7, 129.65, 129.62, 129.4, 129.1, 128.9, 128.8, 128.7, 128.6, 127.45, 127.35, 126.7, 126.1, 125.9, 125.3, 124.9, 124.8, 124.6, 124.4, 118.4, 115.1, 113.3, 54.7. HRMS (ESI) *m/z*: calcd. for $C_{34}H_{23}N_2$ [M^+]: 459.1856; found: 459.1858.

2-benzyl-5-((2,5,7,8-tetramethyl-2-(4,8,12-trimethyltridecyl)chroman-6-yl)oxy)imidazo[1,5-*a*]quinolin-2-ium chloride (4.1aa)



Scheme 4.21. Synthesis of **4.1aa**

Step 1: Synthesis of 2-methyl-4-((2,5,7,8-tetramethyl-2-(4,8,12-trimethyltridecyl)chroman-6-yl)oxy)quinoline (**4.S7**)

In an oven-dried Schlenk tube, potassium *tert*-butoxide (191 mg, 1.7 mmol, 1.5 equiv.) was taken and dried under vacuum. Then, (±) α-tocopherol (560 mg, 1.3 mmol, 1.2 equiv.) in dry DMF (3 mL) was added and stirred at 120 °C for 2 hours. Then 4-chloro-2-methylquinoline (200 mg, 1.1 mmol, 1 equiv.) was added to the mixture and stirred at 120 °C for overnight. After completion of the reaction as confirmed by TLC, the reaction mixture was quenched with water and extracted with CH_2Cl_2 (3 × 15 mL). The reaction mixture was evaporated in a vacuum, and purified by using silica gel column chromatography with ethyl acetate/ pet ether (v/v = 1/10, R_f = 0.7) as the eluent to afford the desired product **4.S7** as a brown viscous liquid (465 mg, 74%).

^{1}H NMR (500 MHz, $CDCl_3$): δ 8.42 (d, J = 8.0, 1H), 8.03 (d, J = 8.5 Hz, 1H), 7.71 – 7.68 (m, 1H), 7.51 – 7.48 (m, 1H), 6.16 (d, J = 2.2 Hz, 1H), 2.67 – 2.63 (m, 2H), 2.56 (s, 3H), 2.18 (s, 3H), 2.02 (s, 3H), 1.97 (s, 3H), 1.92 – 1.79 (m, 2H), 1.75 – 1.60 (m, 2H), 1.57 – 1.50 (m, 2H), 1.46 – 1.40 (m, 2H), 1.35 – 1.25 (m, 12H), 1.18 – 1.09 (m, 6H), 0.91– 0.86 (m, 12H). ^{13}C NMR (126 MHz, $CDCl_3$): δ 161.5, 160.3, 149.4, 142.8, 129.9, 128.3, 127.6, 125.8, 125.0, 123.8,

TH-3565_186122020

123.7, 121.7, 119.5, 118.2, 102.9, 75.3, 39.5, 37.5, 37.4, 34.7, 32.9, 32.7, 31.6, 31.4, 31.2, 28.0, 25.8, 25.3, 24.9, 24.5, 22.8, 22.7, 20.7, 19.82, 19.76, 14.2, 12.8, 11.94, 11.89. HRMS (ESI) *m/z*: calcd. for $C_{39}H_{58}NO_2$ $[M+H]^+$: 572.4463; found: 572.4467.

Step 2: Synthesis of 4-((2,5,7,8-tetramethyl-2-(4,8,12-trimethyltridecyl)chroman-6-yl)oxy)quinoline-2-carbaldehyde (**4.S8**)

Compound **4.S8** was prepared in a similar method described above for **4.S1**, using **4.S7** (300 mg, 0.5 mmol, 1 equiv.) as a starting material. The crude reaction mixture was purified by column chromatography on silica gel using ethyl acetate/ pet ether (v/v = 1/20, R_f = 0.6) as the eluent to afford the desired product **4.S8** as a brown viscous liquid (252 mg, 86%).

^{1}H NMR (600 MHz, $CDCl_3$): δ 10.10 (s, 1H), 8.53 (d, J = 8.2 Hz, 1H), 8.25 (d, J = 8.5 Hz, 1H), 7.85 (t, J = 7.6 Hz, 1H), 7.72 (t, J = 7.7 Hz, 1H), 6.92 (d, J = 5.5 Hz, 1H), 2.64 (t, J = 7.3 Hz, 2H), 2.16 (s, 3H), 1.98 (s, 3H), 1.95 (s, 3H), 1.90 – 1.79 (m, 2H), 1.71 – 1.57 (m, 2H), 1.55 – 1.48 (m, 2H), 1.44 – 1.38 (m, 2H), 1.36 – 1.25 (m, 12H), 1.17 – 1.07 (m, 6H), 0.89 – 0.86 (m, 12H). ^{13}C NMR (151 MHz, $CDCl_3$): δ 194.1, 162.8, 154.3, 149.8, 149.4, 142.4, 130.9, 130.2, 128.5, 127.3, 125.5, 124.1, 122.6, 122.3, 118.4, 98.6, 75.4, 39.5, 37.7, 37.6, 37.5, 37.4, 32.9, 31.3, 31.0, 28.1, 24.9, 24.6, 24.4, 23.6, 22.8, 22.7, 21.2, 20.8, 19.9, 19.8, 12.8, 12.04, 11.96. HRMS (ESI) *m/z*: calcd. for $C_{39}H_{56}NO_3$ $[M+H]^+$: 586.4255; found: 586.4255.

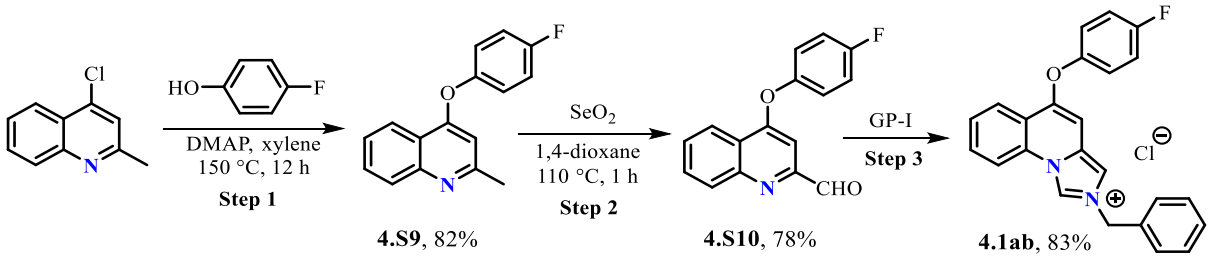
Step 3: Synthesis of **4.1aa**

Following the general procedure GP-I, the title compound **4.1aa** was obtained from **4.S8** (200 mg, 0.34 mmol, 1 equiv.) on reaction with benzylamine (36.6 mg, 0.34 mmol, 1 equiv.). Compound **4.1aa** was isolated as a white solid, 80% yield (197 mg) by using neutral alumina column chromatography with ethyl acetate/ methanol (v/v = 10/1, R_f = 0.3) as the eluent.

^{1}H NMR (500 MHz, DMSO-d_6): δ 11.19 (s, 1H), 8.64 (d, J = 8.4 Hz, 1H), 8.39 (dd, J = 11.8, 7.9 Hz, 1H), 7.96 (q, J = 8.5 Hz, 1H), 7.90 (d, J = 7.3 Hz, 1H), 7.86 – 7.81 (m, 1H), 7.55 (d, J = 7.2 Hz, 2H), 7.41 – 7.34 (m, 3H), 6.25 (d, J = 2.8 Hz, 1H), 5.69 (s, 2H), 2.59 (q, J = 6.2 Hz, 2H), 2.05 (s, 3H), 1.95 – 1.90 (m, 6H), 1.82 – 1.73 (m, 2H), 1.58 – 1.54 (m, 1H), 1.49 – 1.40 (m, 3H), 1.35 – 1.32 (m, 2H), 1.27 – 1.15 (m, 12H), 1.10 – 1.00 (m, 6H), 0.85 – 0.79 (m, 12H). ^{13}C NMR (151 MHz, DMSO-d_6): δ 150.7, 149.0, 141.8, 134.7, 131.3, 131.2, 130.1, 129.2, 128.9, 128.8, 128.7, 128.6, 128.2, 126.7, 125.4, 123.5, 123.4, 122.8, 119.3, 118.3, 117.4, 113.0, 92.2, 75.0, 53.0, 38.8, 36.8, 36.7, 36.6, 32.1, 32.0, 31.8, 29.0, 27.4, 24.2, 23.7, 22.7, 22.5, 22.4, 20.4, 20.0, 19.54, 19.49, 12.4, 11.7, 11.6. HRMS (ESI) *m/z*: calcd. for $C_{47}H_{63}N_2O_2$ $[M^+]$: 687.4885; found: 687.4899.

2-benzyl-5-(4-fluorophenoxy)imidazo[1,5-*a*]quinolin-2-ium chloride (4.1ab)

TH-3565_186122020



Scheme 4.22. Synthesis of **4.1ab**

Step 1: Synthesis of 4-(4-fluorophenoxy)-2-methylquinoline (**4.S9**)

4-chloro-2-methylquinoline (210 mg, 1.2 mmol, 1 equiv.), 4-fluorophenol (157 mg, 1.4 mmol, 1.2 equiv.), DMAP (29.3 mg, 20 mol%) was taken in an oven dried sealed tube with xylene (4 mL) and stirred at 115 ºC for 12 h. After the completion of the reaction as confirmed by TLC, the reaction mixture was evaporated under reduced pressure and purified by using silica gel column chromatography with ethyl acetate/ pet ether (v/v = 1/10, R_f = 0.5) as the eluent to afford the desired product **4.S9** as a yellow solid (249.2 mg, 82%).

^{1}H NMR (500 MHz, $CDCl_3$): δ 8.26 – 8.24 (m, 1H), 8.00 – 7.98 (m, 1H), 7.70 – 7.66 (m, 1H), 7.48 – 7.45 (m, 1H), 7.12 (d, J = 6.3 Hz, 4H), 6.36 (s, 1H), 2.57 (s, 3H). ^{13}C NMR (151 MHz, $CDCl_3$): δ 162.1, 160.9, 160.0, 159.3, 150.2 (d, C-F, $J_{C\text{-}F}$ = 2.7 Hz), 149.4, 130.2, 128.3, 125.4, 122.7 (d, C-F, $J_{C\text{-}F}$ = 8.5 Hz), 121.5, 119.8, 117.0 – 116.9 (d, C-F, $J_{C\text{-}F}$ = 23.6 Hz), 104.4, 25.7. ^{19}F NMR (471 MHz, $CDCl_3$): δ -116.8. HRMS (ESI) *m/z*: calcd. for $C_{16}H_{13}FNO$ $[M+H]^+$: 254.0976; found: 254.0961.

Step 2: 4-(4-fluorophenoxy)quinoline-2-carbaldehyde (**4.S10**)

Compound **4.S10** was prepared in a similar method described above for **4.S1**, using 4-(4-fluorophenoxy)-2-methylquinoline **4.S9** (180 mg, 0.71 mmol, 1 equiv.) as a starting material. The crude reaction mixture was purified by column chromatography on silica gel using ethyl acetate/ pet ether (v/v = 1/10, R_f = 0.6) as the eluent to afford the desired product as a brown solid (148.2 mg, 78%).

^{1}H NMR (500 MHz, $CDCl_3$): δ 10.10 (s, 1H), 8.43 (d, J = 8.4 Hz, 1H), 8.25 (d, J = 8.6 Hz, 1H), 7.88 – 7.85 (m, 1H), 7.74 – 7.71 (m, 1H), 7.19 (brs, 1H), 7.17 (brs, 1H), 7.11 (s, 1H), 6.90 – 6.86 (m, 1H), 6.79 – 6.76 (m, 1H). ^{13}C NMR (151 MHz, $CDCl_3$): δ 193.4, 163.3, 161.5, 159.6, 153.9, 149.7 (d, C-F, $J_{C\text{-}F}$ = 3.4 Hz), 149.4, 136.6, 131.4, 130.0, 129.0, 123.0 – 122.8 (C-F, $J_{C\text{-}F}$ = 14.1 Hz), 122.2, 117.5, 117.3, 116.4 (d, C-F, $J_{C\text{-}F}$ = 9.6 Hz), 116.1, 115.9, 99.7. ^{19}F NMR (471 MHz, $CDCl_3$): δ -116.8. HRMS (ESI) *m/z*: calcd. for $C_{16}H_{11}FNO_2$ $[M+H]^+$: 268.0769; found: 268.0751.

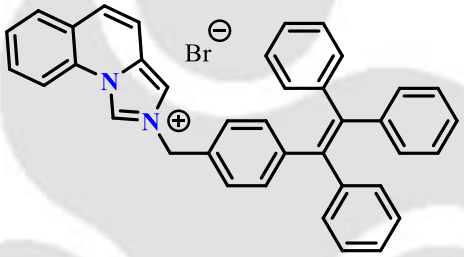
Step 3: Synthesis of **4.1ab**

TH-3565_186122020

Following the general procedure GP-I, the title compound **4.1ab** was obtained from **4.S10** (140 mg, 0.52 mmol, 1 equiv.) on reaction with benzylamine (56 mg, 0.52 mmol, 1 equiv.). Compound **4.1ab** was isolated by using neutral alumina column chromatography with ethyl acetate/ methanol (v/v = 10/1, R_f = 0.3) as the eluent to afford the desired product as an off-white solid, 83% yield (175 mg).

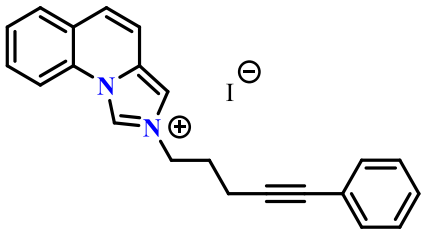
^{1}H NMR (500 MHz, DMSO-d_6): δ 10.61 (s, 1H), 8.51 (d, J = 8.4 Hz, 1H), 8.30 (d, J = 8.0 Hz, 1H), 7.99 (t, J = 7.2 Hz, 1H), 7.93 (s, 1H), 7.84 (t, J = 7.7 Hz, 1H), 7.49 – 7.48 (m, 2H), 7.45 – 7.40 (m, 3H), 7.38 – 7.36 (m, 4H), 6.76 (s, 1H), 5.68 (s, 2H). ^{13}C NMR (151 MHz, DMSO-d_6): δ 160.3, 158.7, 151.7, 150.0, 134.5, 131.4, 130.1, 129.1, 129.0, 128.9 (d, C-F, $J_{C\text{-}F}$ = 16.1 Hz), 128.4, 127.9, 123.8, 122.7 (d, C-F, $J_{C\text{-}F}$ = 8.6 Hz), 119.8, 117.2, 117.1, 116.1 (d, C-F, $J_{C\text{-}F}$ = 8.1 Hz), 115.7 – 115.5 (d, C-F, $J_{C\text{-}F}$ = 22.7 Hz), 113.9, 95.7, 53.2. ^{19}F NMR (471 MHz, DMSO-d_6): δ -117.1. HRMS (ESI) *m/z*: calcd. for $C_{24}H_{18}FN_2O$ [M^+]: 369.1398; found: 369.1395.

2-(4-(1,2,2-triphenylvinyl)benzyl)imidazo[1,5-*a*]quinolin-2-ium bromide (4.1ac)



Following the general procedure GP-II, the title compound **4.1ac** was obtained from imidazo[1,5-*a*]quinoline on reaction with (2-(4-(bromomethyl)phenyl)ethene-1,1,2-triyl)tribenzene. Brown solid, 86% yield (255 mg). ^{1}H NMR (400 MHz, $CDCl_3$): δ 12.52 (s, 1H), 8.82 (d, J = 8.4 Hz, 1H), 7.76 – 7.73 (m, 2H), 7.61 (t, J = 7.6 Hz, 1H), 7.50 (s, 1H), 7.43 (d, J = 9.5 Hz, 1H), 7.34 – 7.28 (m, 3H), 7.08 – 7.06 (m, 11H), 7.00 – 6.97 (m, 6H), 5.86 (s, 2H). ^{13}C NMR (126 MHz, $CDCl_3$): δ 145.5, 143.4, 143.3, 143.2, 142.2, 139.9, 132.4, 131.6, 131.34, 131.30, 130.9, 129.8, 129.4, 129.3, 129.1, 128.9, 128.8, 127.93, 127.91, 127.8, 127.7, 126.9, 126.8, 124.1, 118.2, 114.0, 113.3, 54.2. HRMS (ESI) *m/z*: calcd. for $C_{38}H_{29}N_2$ [M^+]: 513.2326; found: 513.2319.

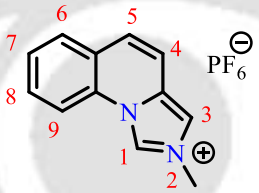
2-(5-phenylpent-4-yn-1-yl)imidazo[1,5-*a*]quinolin-2-ium iodide (4.1ad)



TH-3565_186122020

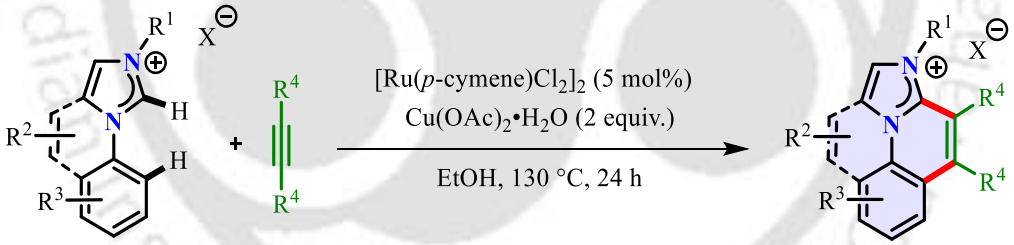
Following the general procedure GP-II, the title compound **4.1ad** was obtained from imidazo[1,5-*a*]quinoline on reaction with (5-chloropent-1-yn-1-yl)benzene **4.2j**. Compound **4.1ad** was isolated by using neutral alumina column chromatography with ethyl acetate/ methanol (v/v = 10/1, R_f = 0.2) as the eluent to afford the desired product as a brown solid, 63% yield (138 mg). ^{1}H NMR (400 MHz, $CDCl_3$): δ 11.56 (s, 1H), 8.63 (d, J = 8.3 Hz, 1H), 8.09 (d, J = 1.6 Hz, 1H), 7.70 – 7.65 (m, 2H), 7.55 (t, J = 7.7 Hz, 1H), 7.38 (d, J = 9.7 Hz, 1H), 7.31 (d, J = 9.7 Hz, 1H), 7.12 – 7.01 (m, 5H), 4.93 (t, J = 6.7 Hz, 2H), 2.65 (t, J = 6.6 Hz, 2H), 2.42 (p, J = 6.7 Hz, 2H). ^{13}C NMR (151 MHz, $CDCl_3$): δ 131.3, 131.0, 129.4, 129.0, 128.9, 128.61, 128.57, 128.1, 127.8, 127.3, 124.1, 122.6, 117.6, 115.1, 114.3, 87.0, 82.0, 50.4, 29.4, 16.9. HRMS (ESI) *m/z*: calcd. for $C_{22}H_{19}N_2$ [M^+]: 311.1543; found: 311.1547.

Compound numbering undertaken in this work: Representative for **4.1a**.



4.5.3. Annulation reaction of imidazoquinolinium salts with alkynes

General procedure for Ru(II)-catalyzed oxidative annulation reaction using $Cu(OAc)_2$•H_2O as an oxidant (GP-III)

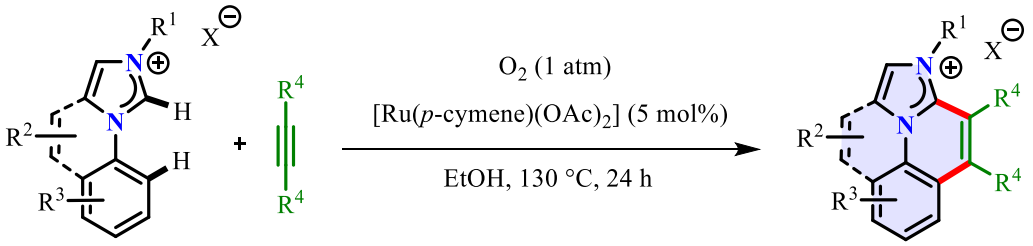


Scheme 4.23. Annulation reaction using copper salt as an oxidant

A mixture of imidazoquinolinium salt (0.2 mmol, 1 equiv.), alkyne (0.2 mmol, 1 equiv.), [Ru(*p*-cymene)Cl_2]$_2$ (5 mol%), $Cu(OAc)_2$·H_2O (0.4 mmol, 2 equiv.) in dry ethanol (2 mL) was taken in an oven-dried pressure tube equipped with a magnetic bar. The reaction mixture was stirred in a preheated oil bath at 130 ºC for 24 h. After completion of the reaction ethanol was added to the reaction mixture and the resulting mixture was passed through a plug of celite. The solvent was evaporated under reduced pressure and the residue was purified by column chromatography on neutral alumina (methanol/ethyl acetate as eluent) to get the pure product.

General procedure for Ru(II)-catalyzed oxidative annulation reaction using molecular oxygen as an oxidant (GP-IV)

TH-3565_186122020

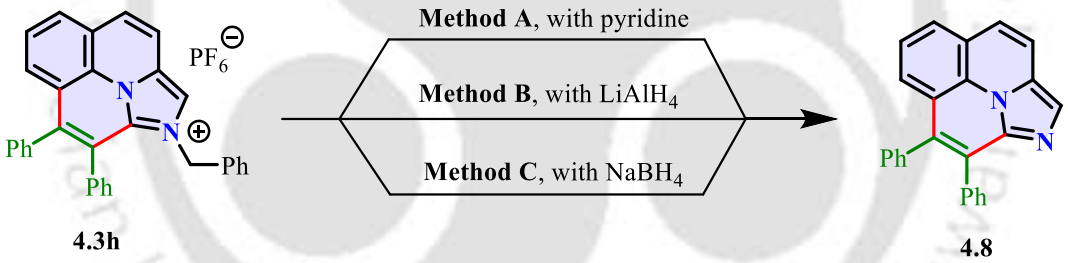


Scheme 4.24. Annulation reaction using molecular O_2 as an oxidant

A mixture of imidazolium salt (0.2 mmol, 1 equiv.), alkyne (0.2 mmol, 1 equiv.), [Ru(*p*-cymene)(OAc)$_2$] (5 mol%) and dry ethanol (2 mL) were taken in an oven-dried Schlenk tube equipped with a magnetic bar. The reaction mixture was degassed and purged with oxygen for 3 times and stirred in a preheated oil bath at 130 ºC for 24 h. After completion of the reaction, the resulting mixture was transferred to a round bottom flask. The solvent was evaporated under reduced pressure and the residue was absorbed onto small amounts of alumina. The purification was performed by column chromatography on neutral alumina (methanol: ethyl acetate = 1: 10) to get the pure product.

4.5.4. Post-synthetic modifications

i) Debenzylation reaction of 4.3h:



Scheme 4.25. Debenzylation of **4.3h**

Method A: In a sealed tube, compound **4.3h** (58 mg, 0.1 mmol, 1 equiv.) was taken with pyridine (1.5 mL) and stirred at 140 ºC in a preheated oil bath for 12 h. The reaction mixture was allowed to cool to room temperature, diluted with dichloromethane and transferred to a one neck round bottom flask. The pyridine was evaporated under reduced pressure, and the resulting residue was absorbed onto a small amount of alumina. The product was isolated by column chromatography on neutral alumina using pet ether/ethyl acetate (v/v = 10/1, R_f = 0.5) as eluent to afford the desired product **4.8** as a yellow oil (32 mg, 93%).

Method B: **4.3h** (58 mg, 0.1 mmol, 1 equiv.) was added to a Schlenk tube equipped with a magnetic stirring bar. After purging the tube with argon, THF (3 mL) and lithium aluminium hydride (4.2 mg, 0.11 mmol, 1.1 equiv.) were added. After stirring at room temperature for 18 h, the reaction was quenched with water and extracted with three portions of CH_2Cl_2. The organic layers were dried over Na_2SO_4 and the solvent was removed in vacuo. The crude

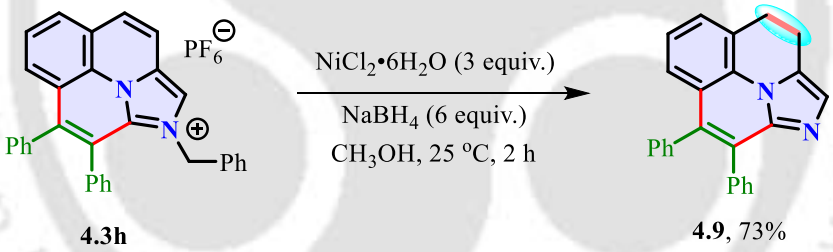
TH-3565_186122020

product was purified by neutral alumina column chromatography using pet ether/ethyl acetate (v/v = 10/1) as an eluent to afford compound **4.8** as a yellow oil (23.1 mg, 67%).

Method C: In a one-neck round bottom flask, **4.3h** (58 mg, 0.1 mmol, 1 equiv.) was taken with $NaBH_4$ (19 mg, 0.5 mmol, 5 equiv.) with methanol (4 mL) at 0 ºC and stirred the reaction mixture at room temperature for 2 hours. After completion of the reaction as confirmed by TLC, the solvent was removed under vacuum. The organic phase was extracted with ethyl acetate and washed with brine solution. The organic layer was dried over anhydrous Na_2SO_4, concentrated, and then residues were purified by column chromatography on neutral alumina using ethyl acetate/ pet ether (v/v = 1/10, R_f = 0.5) as the eluent to afford the desired product **4.8** as a yellow oil (13.1 mg, 38%).

^{1}H NMR (500 MHz, $CDCl_3$): δ 7.89 (s, 1H), 7.59 (d, J = 7.6 Hz, 1H), 7.52 – 7.50 (m, 1H), 7.49 – 7.45 (m, 1H), 7.39 – 7.36 (m, 4H), 7.35 – 7.33 (m, 2H), 7.31 – 7.29 (m, 2H), 7.28 – 7.27 (m, 1H), 7.26 – 7.25 (m, 1H), 7.24 – 7.23 (m, 2H). ^{13}C NMR (126 MHz, $CDCl_3$): δ 139.2, 137.0, 135.7, 135.3, 131.7, 130.9, 130.7, 129.7, 128.7, 128.0, 127.64, 127.63, 125.7, 125.5, 125.4, 125.2, 124.9, 122.2, 121.8, 120.9, 117.9. HRMS (ESI) *m/z*: calcd. for $C_{25}H_{17}N_2$ $[M+H]^+$: 345.1387; found: 345.1390.

ii) Selective reduction of 4.3h:



4.3h **4.9**, 73%

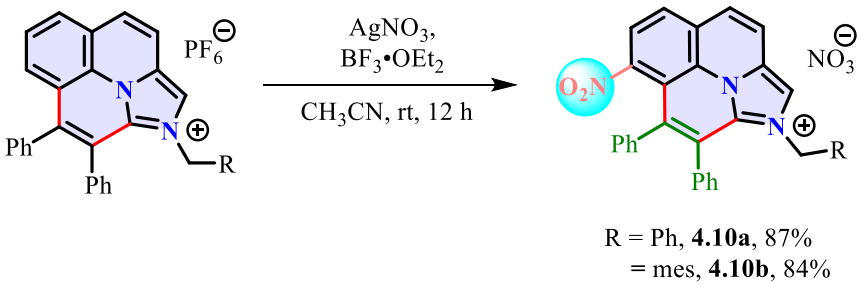
Scheme 4.26. Reduction of **4.3h** with $NaBH_4$

In a sealed tube, **4.3h** (58 mg, 0.1 mmol, 1 equiv.) was taken with $NiCl_2$•$6H_2O$ (39 mg, 0.3 mmol, 3 equiv.) in methanol and stirred at room temperature for 5 minutes. To this reaction mixture, $NaBH_4$ (22.8 mg, 0.6 mmol, 6 equiv.) was added in portions at 0 ºC and allowed to stir at room temperature for 2 h. After completion of the reaction as confirmed by TLC, the solvent was removed under vacuum. The organic phase was extracted with ethyl acetate and washed with brine solution. The organic layer was dried over anhydrous Na_2SO_4, concentrated, and then residues were purified by column chromatography on neutral alumina using ethyl acetate/ pet ether (v/v = 3/10, R_f = 0.5) as the eluent to afford the desired product **4.9** as a white solid (25.3 mg, 73%).

^{1}H NMR (400 MHz, $CDCl_3$): δ 7.44 – 7.41 (m, 2H), 7.38 – 7.36 (m, 1H), 7.33 – 7.28 (m, 6H), 7.24 – 7.19 (m, 5H), 3.40 – 3.36 (m, 2H), 3.34 – 3.30 (m, 2H). ^{13}C NMR (151 MHz, $CDCl_3$): δ 141.8, 137.1, 135.6, 134.2, 131.3, 130.9, 129.5, 128.8, 128.2, 128.1, 127.9, 127.4, 127.3, 126.7, 125.8, 124.52, 124.49, 123.1, 121.9, 25.3, 19.6. HRMS (ESI) *m/z*: calcd. for $C_{25}H_{19}N_2$ $[M+H]^+$: 347.1543; found: 347.1548.

TH-3565_186122020

iii) Nitration reaction:



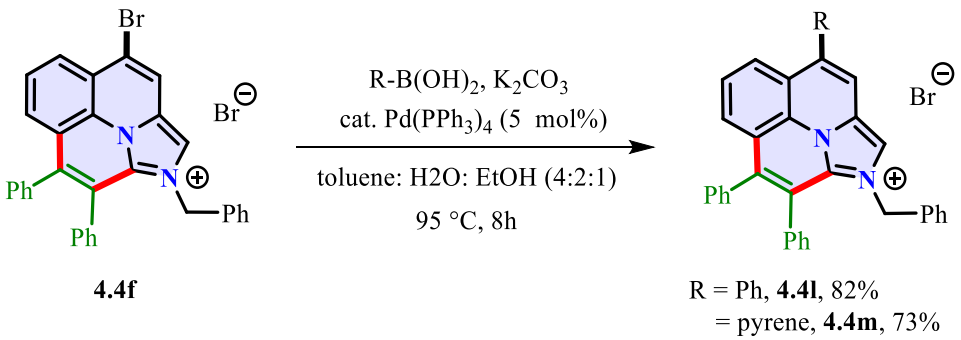
Scheme 4.27. Nitration reaction with $AgNO_3$

The imidazoquinolinium salt (0.2 mmol, 1 equiv.) was taken in a well dried Schlenk flask with $AgNO_3$ (0.4 mmol, 2 equiv.). At 0 °C, dry acetonitrile (3 mL) was added to it under argon atmosphere and $BF_3•Et_2O$ (0.6 mmol, 3 equiv.) was added slowly for certain interval of time and stirred at room temperature for 12 h. Full consumption of starting material was confirmed by TLC and the product was purified by column chromatography using neutral alumina with ethyl acetate/methanol (v/v = 20:1, R_f = 0.6) as a yellow solid.

Compound **4.10a** (99 mg, 87%); m.p. = 245–248 °C. ^{1}H NMR (600 MHz, $CDCl_3$): δ 9.15 (s, 1H), 8.69 (d, J = 10.1 Hz, 1H), 8.51 (d, J = 9.0 Hz, 1H), 8.28 (d, J = 10.1 Hz, 1H), 7.63 (d, J = 9.0 Hz, 1H), 7.34 – 7.30 (m, 6H), 7.27 – 7.20 (m, 5H), 7.17 – 7.16 (m, 2H), 6.85 (d, J = 7.4 Hz, 2H), 5.53 (s, 3H). ^{13}C NMR (151 MHz, $CDCl_3$): δ 145.7, 141.4, 133.7, 133.3, 132.1, 130.8, 130.7, 129.7, 129.5, 129.04, 128.98, 128.9, 128.7, 127.6, 127.5, 124.4, 124.2, 123.6, 122.9, 122.3, 121.8, 120.6, 54.5. HRMS (ESI) *m/z*: calcd. for $C_{32}H_{22}N_3O_2$ [M^+]: 480.1707; found: 480.1705.

Compound **4.10b** (98.2 mg, 84%); m.p. = 240–243 °C. ^{1}H NMR (600 MHz, $CDCl_3$): δ 8.76 (d, J = 10.3 Hz, 1H), 8.54 (d, J = 9.1 Hz, 1H), 7.86 (d, J = 10.3 Hz, 1H), 7.67– 7.64 (m, 3H), 7.45 (s, 1H), 7.41 – 7.39 (m, 2H), 7.38 – 7.37 (m, 2H), 7.36 – 7.34 (m, 2H), 7.32 – 7.31 (m, 2H), 6.95 (s, 2H), 4.94 (s, 2H), 2.31 (s, 3H), 2.15 (s, 6H). ^{13}C NMR (151 MHz, $CDCl_3$): δ 146.0, 141.5, 140.6, 139.0, 133.7, 132.7, 131.9, 131.0, 130.1, 130.0, 129.8, 129.4, 129.0, 128.92, 128.87, 127.7, 125.5, 124.7, 124.3, 123.7, 122.9, 120.4, 120.3, 117.3, 49.6, 21.2, 19.7.

iv) Suzuki coupling reaction at C5 position of 4.4f:



Scheme 4.28. Suzuki coupling reaction of **4.4f**

TH-3565_186122020

Following the reported literature procedure,[22] a well dried Schlenk tube was charged with **4.4f** (59.4 mg, 0.1 mmol, 1 equiv.), aryl boronic acid (0.15 mmol, 1.5 equiv.), K_2CO_3 (70 mg, 0.5 mmol, 5 equiv.), and $Pd(PPh_3)_4$ (6 mg, 5 mol%). To this reaction mixture, toluene (2 mL), H_2O (1 mL) and EtOH (0.5 mL) were added under a nitrogen atmosphere, and the mixture was stirred in a preheated oil bath at 95 °C for 8 h. After completion of the reaction, the reaction mixture was cooled, and filtered through a plug of celite. The resulting mixture was diluted with water and extracted with ethyl acetate. The combined extracts were dried over Na_2SO_4, concentrated, and purified by column chromatography on neutral alumina (methanol/ethyl acetate, 1:10, R_f = 0.3) to afford the desired product **4.4l** as an off-white solid in 82% yield (48.5 mg) and **4.4m** as a pale-yellow solid in 73% yield (52.2 mg).

4.5.5. Mechanistic investigation

(a) Proof of intermediate Ru-1/Ru-5 in the annulation reaction

The synthesis of cyclometalated Ru(II) intermediate **Ru-1** was reported in Chapter 2 (section 2.3.1).

Synthesis of cyclometalated Ru(II) intermediate Ru-5 (Scheme 4.8)

[Ru (*p*-cymene)$(OAc)_2$] (177 mg, 0.50 mmol, 1 equiv.) was added to a 10 mL Schlenk tube and the tube was evacuated and purged with N_2 three times. Deoxygenated CH_2Cl_2 (4.0 mL) and 2-methylimidazo[1,5-*a*]quinolin-2-ium hexafluorophosphate **4.1a** (164 mg, 0.50 mmol, 1 equiv.) were added successively. The mixture was stirred at ambient temperature for 24 h. The solvent was removed and the residue was purified by column chromatography on neutral alumina (ethyl acetate/ pet ether: 8/10, R_f = 0.4) as eluent to afford the **Ru-5** complex as a yellowish-brown solid (195 mg, 82%). Slow diffusion of petroleum ether into a concentrated solution of complex **Ru-5** in CH_2Cl_2 gave reddish-brown crystals suitable for X-Ray diffraction analysis.

^{1}H NMR (500 MHz, $CDCl_3$): δ 8.33 (dd, J = 6.9, 1.3 Hz, 1H), 7.21 – 7.16 (m, 2H), 7.09 (d, J = 9.4 Hz, 1H), 7.04 (s, 1H), 6.91 (d, J = 9.4 Hz, 1H), 5.71 (t, J = 5.2 Hz, 2H), 5.65 (d, J = 5.8 Hz, 1H), 5.59 (d, J = 5.8 Hz, 1H), 4.52 (s, 3H), 2.01 – 1.95 (m, 1H), 1.91 (s, 3H), 1.58 (s, 3H), 0.75 (d, J = 6.8 Hz, 3H), 0.64 (d, J = 6.8 Hz, 3H). ^{13}C NMR (151 MHz, $CDCl_3$): δ 178.2, 177.1, 161.4, 141.7, 140.1, 129.2, 128.4, 126.9, 126.5, 124.9, 120.5, 120.2, 113.1, 112.0, 90.5, 87.2, 85.1, 84.6, 38.3, 31.3, 24.2, 23.3, 22.1, 19.1. HRMS (ESI): *m/z*: calcd. for $C_{22}H_{23}N_2Ru$ [M-OAc]$^+$: 417.0905; found: 417.0909. IR (neat, cm^{-1}): 2175, 1734, 1654, 1370, 1237, 1021, 803, 771.

TH-3565_186122020

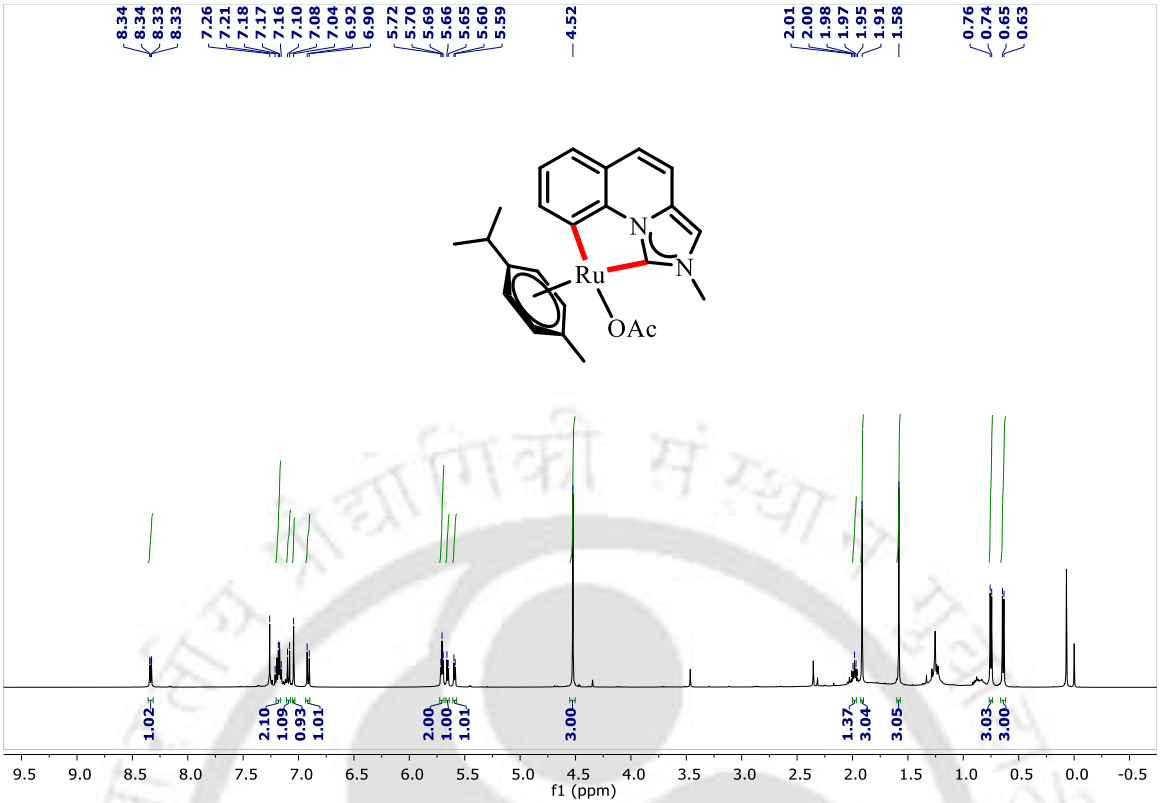


Figure 4.8. ^{1}H NMR spectrum of **Ru-5** ($CDCl_3$, 500 MHz, 298 K)

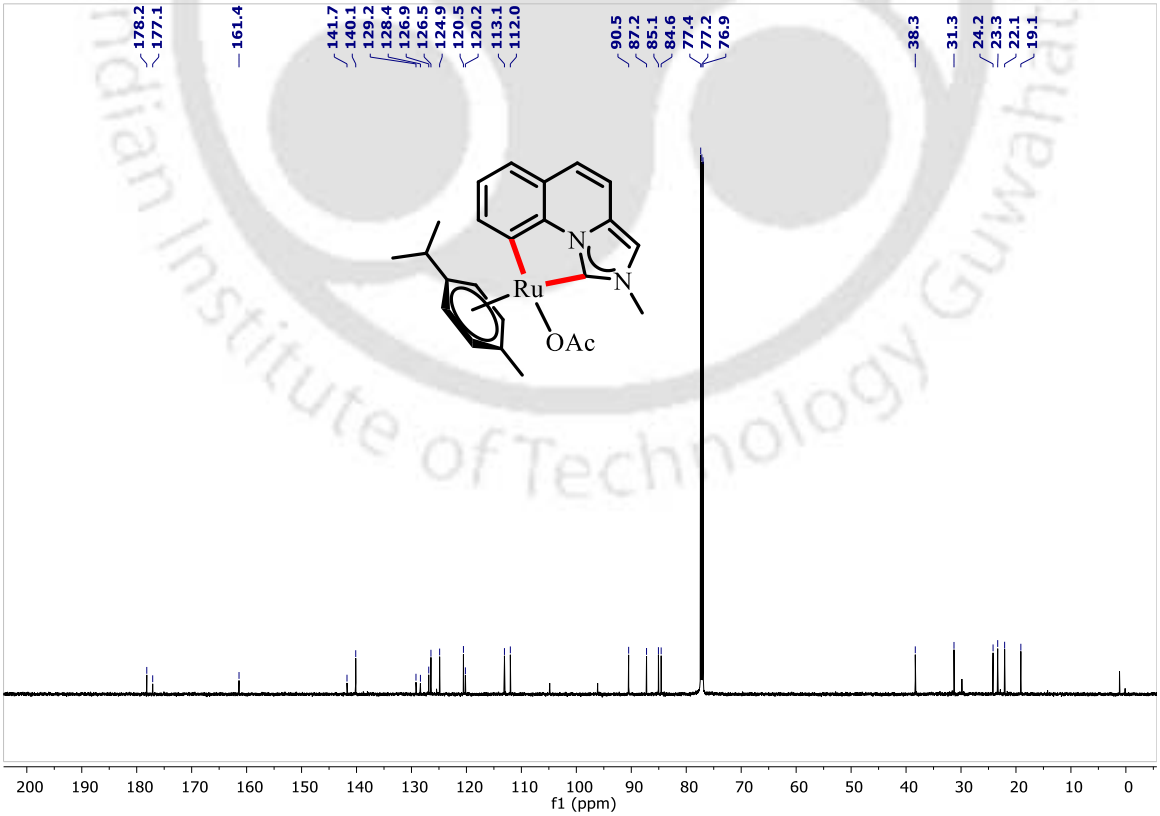


Figure 4.9. $^{13}C\{^{1}H\}$ NMR spectrum of **Ru-5** ($CDCl_3$, 151 MHz, 298 K)

TH-3565_186122020

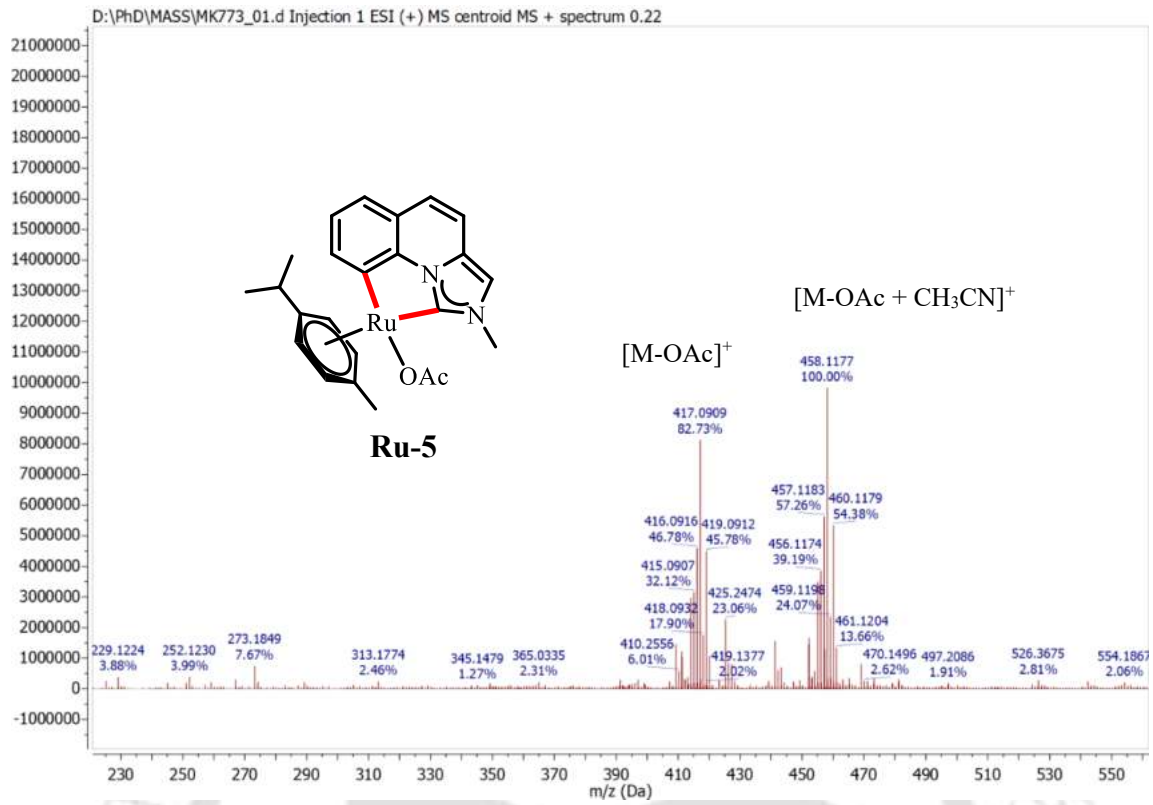


Figure 4.10. ESI-MS spectrum of [**Ru-5**]$^+$

Control experiments with cyclometalated Ru(II) intermediate Ru-1/Ru-5

i) Stoichiometric reaction (Scheme 4.9)

For Ru-1: A mixture of complex **Ru-1** (45.2 mg, 0.1 mmol, 1 equiv.), **4.2a** (17.8 mg, 0.1 mmol, 1 equiv.) and $Cu(OAc)_2 \cdot H_2O$ (40 mg, 0.2 mmol, 2 equiv.) in dry EtOH (2.0 mL) were stirred in an oven dried pressure tube at 130 ºC in a preheated oil bath. After 24 h stirring, the reaction mixture was allowed to cool and ethanol was added to it and the resulting mixture was passed through a celite plug. The solvent was evaporated under reduced pressure and the residue was absorbed onto small amounts of neutral alumina. Final product was separated by neutral alumina column chromatography with ethyl acetate/ methanol (v/v = 20/1, R_f = 0.3) in 97% yield (38.3 mg).

For Ru-5: A mixture of complex **Ru-5** (47.6 mg, 0.1 mmol, 1 equiv.) and **4.2a** (17.8 mg, 0.1 mmol, 1 equiv.) in dry and degassed EtOH (2.0 mL) were stirred in a dry Schlenk tube at 130 ºC in a preheated oil bath under molecular O_2 atmosphere. After 24 h stirring, the resulting mixture was transferred to a round bottom flask. The solvent was evaporated under reduced pressure and the residue was absorbed onto small amounts of alumina. Final product was separated by neutral alumina column chromatography with ethyl acetate/ methanol (v/v = 20/1, R_f = 0.3) in 96% yield (40.2 mg).

TH-3565_186122020

ii) Catalytic reaction (Scheme 4.9)

For Ru-1: To an oven dried Schlenk tube, **4.1a-Cl** (22 mg, 0.1 mmol, 1 equiv.), complex **Ru-1** (2.3 mg, 5 mol%), **4.2a** (17.8 mg, 0.1 mmol, 1 equiv.) and $Cu(OAc)_2 \cdot H_2O$ (40 mg, 0.2 mmol, 2 equiv.) were loaded with dry EtOH (2.0 mL). The reaction mixture was stirred in a preheated oil bath at 130 ºC in a pressure tube for 24 h. Then the reaction mixture was allowed to cool and ethanol was added to it and the resulting mixture was passed through a celite plug. The solvent was evaporated under reduced pressure and the residue was absorbed onto small amounts of alumina. The final compound was isolated by neutral alumina column chromatography with ethyl acetate/ methanol (v/v = 20/1, R_f = 0.3) in 90% yield (35.5 mg).

For Ru-5: To an oven dried Schlenk tube, **4.1a-OAc** (24.2 mg, 0.10 mmol, 1 equiv.), complex **Ru-5** (2.4 mg, 5 mol%) and **4.2a** (17.8 mg, 0.10 mmol, 1 equiv.) were loaded with dry and degassed EtOH (2.0 mL). The reaction mixture was stirred in a preheated oil bath at 130 ºC under a molecular O_2 atmosphere for 24 h. The resulting mixture was transferred to a round bottom flask. The solvent was evaporated under reduced pressure and the residue was absorbed onto small amounts of alumina. The final compound was isolated by neutral alumina column chromatography with ethyl acetate/ methanol (v/v = 20/1, R_f = 0.3) in 88% yield (36.8 mg).

(b) Proof of ruthenium(0) sandwich species, Ru-6 in the catalytic reaction (Scheme 4.10)

Ruthenacycle complex **Ru-5** (23.8 mg, 0.05 mmol, 1 equiv.) and diphenylacetylene **4.2a** (26.7 mg, 0.15 mmol, 3 equiv.) were taken in a Schlenk tube with $CDCl_3$ (1.0 mL). The reaction mixture was degassed and stirred in a preheated oil bath at 60 ºC under vacuum conditions for 15 hours with the aid of the Schlenk technique. Then, the reaction mixture was loaded into the NMR tube inside the glove box and recorded the NMR spectrum to obtain the Ru(0) sandwich complex, **Ru-6** (Figure 4.3). Additionally, the resulting reaction mixture was subjected to ESI-MS analysis, appeared a signal at *m/z* = 493.9045 corresponding to the ruthenium(0) intermediate, [(**Ru-6**) – (OAc^-) – (*p*-cymene) + $CH_3OH]^+$. Furthermore, to elucidate the Ru(0) intermediate, PPh_3 (52.5 mg, 0.2 mmol, 4 equiv.) was added into the reaction mixture, stirred at room temperature for 6 h, then recorded the $^{31}P\{^1H\}$ NMR. The result suggested the possible formation of Ru^0-PPh_3 adduct. ^{31}P NMR (243 MHz, $CDCl_3$): δ 43.4, 41.5. To our delight, when the reaction mixture was exposed to molecular oxygen (1 atm) and acetic acid (3 equiv.) under identical reaction conditions, these signals completely disappeared and raised a new signal at 29.7 ppm, which is likely to be Ru(II) species.

i) Control experiment of Ru-6 with $Cu(OAc)_2 \bullet H_2O$ (Scheme 4.11)

In a well dried Schlenk tube, **Ru-6** (32.7 mg, 0.05 mmol, 1 equiv.), $Cu(OAc)_2 \cdot H_2O$ (30 mg, 0.15 mmol, 3 equiv.) were taken and the reaction mixture was stirred in a preheated oil bath at 130 °C for 12 h. After completion of the reaction, ^{1}H-NMR was recorded which showed the formation of **4.3a-OAc**. The compound **4.3a-OAc** was isolated by neutral alumina column chromatography with ethyl acetate/ methanol (v/v = 20/1, R_f = 0.3) in 81% yield (16.9 mg).

TH-3565_186122020

ii) Control experiment of Ru-6 with molecular O_2 and AcOH (Scheme 4.12)

In a well dried Schlenk tube, **Ru-6** (32.7 mg, 0.05 mmol, 1 equiv.), acetic acid (9.0 µL, 0.15 mmol, 3 equiv.) were taken and the reaction mixture was degassed and purged with molecular oxygen for 3 times. The reaction mixture was stirred in a preheated oil bath at 130 °C for 12 h. After completion of the reaction, ^{1}H-NMR was recorded which showed the formation of **4.3a-OAc** along with [Ru(OAc)$_2$(*p*-cymene)] (52%). The compound **4.3a-OAc** was isolated by neutral alumina column chromatography with ethyl acetate/ methanol (v/v = 20/1, R_f = 0.3) in 83% yield (17.4 mg).

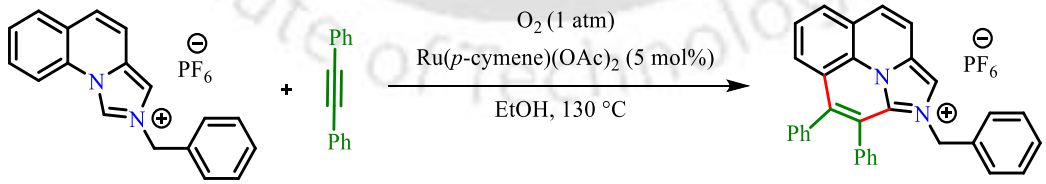
ii) Control experiment of Ru-2 with molecular O_2 and NaOAc (Scheme 4.13)

In a well dried Schlenk tube, **Ru-6** (32.7 mg, 0.05 mmol, 1 equiv.) and NaOAc (12.3 mg, 0.15 mmol, 3 equiv.) was added with $CDCl_3$ and the reaction mixture was degassed and purged with molecular oxygen for 3 times. The reaction mixture was stirred in a preheated oil bath at 130 °C for 12 h. After completion of the reaction, NMR analysis showed no conversion of **Ru-6**.

(c) Kinetic studies

Procedure: Substrate **4.1h** (42 mg, 0.1 mmol), diphenylacetylene **4.2a** (17.8 mg, 0.1 mmol) and [Ru(*p*-cymene)(OAc)$_2$] (5 mol%) were taken in an oven-dried Schlenk tube equipped with a magnetic bar. To this mixture, dry ethanol (1.0 mL) and 1,3,5-trimethylbenzene (internal standard) were added and the reaction mixture was degassed three times using the freeze-pump-thaw technique, flushed with molecular oxygen and properly closed with a teflon cap. The reaction tube was placed in an oil bath, heated at 130 ºC with continuous stirring for a particular time interval. Then aliquot (~100 µL) was withdrawn from the reaction mixture at different intervals, filtered by using a syringe filter, and the solvent was evaporated under a vacuum. The crude reaction mixture was subjected to ^{1}H NMR spectroscopy in $CDCl_3$ and calculated the yield by integrating the benzylic CH_2 peak of the product with respect to the internal standard.

i) Kinetic characterization of substrate 4.1h



4.1h, x mmol **4.2a**, 0.4 mmol **4.3h**

The general catalytic reaction procedure was followed by using catalyst [Ru(*p*-cymene)(OAc)$_2$] (5 mol%) and the concentration of substrate **4.1h** was varied from 0.1 mM to 0.6 mM. The product concentration (M) *vs* time (h) was plotted as shown in Figure 4.11 and plotting ln k_{obs} *vs* ln[**4.1h**], as shown in Figure 4.12. The order is determined from the slope (0.97) of the ln k_{obs} *versus* ln[**4.1h**] plot.

TH-3565_186122020

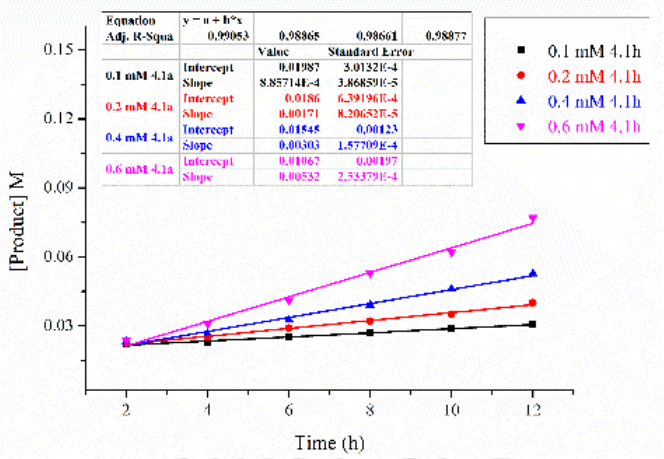


Figure 4.11. Concentration [Product] *vs* time plot at different **4.1h** concentrations.

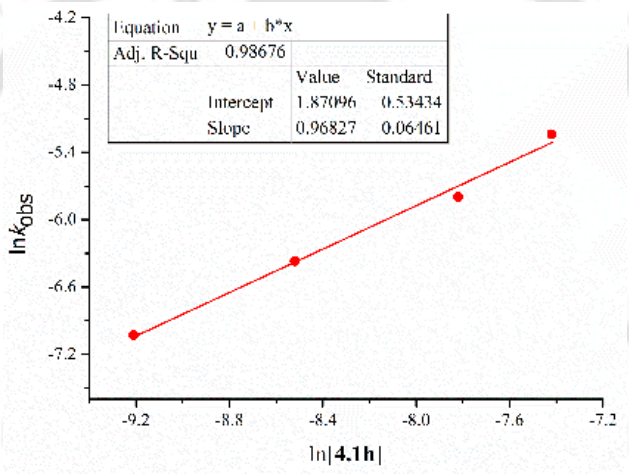
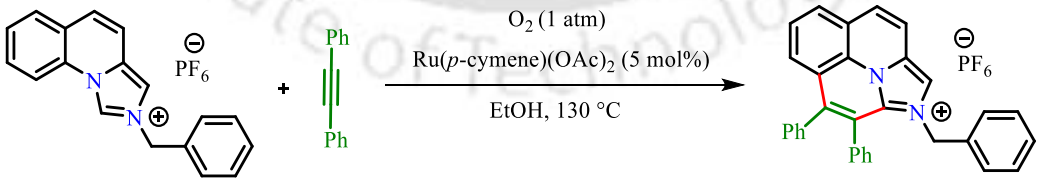


Figure 4.12. ln k_{obs} *vs* ln[**4.1h**]

ii) Kinetic characterization of diphenylacetylene 4.2a



4.1h, 1 mmol **4.2a,** x mmol **4.3h**

A standard catalytic reaction procedure was followed by using catalyst [Ru(*p*-cymene)$(OAc)_2$] (5 mol%) and the concentration of **4.2a** was varied from 0.6 mM to 1.4 mM. The product concentration (M) *vs* time (h) was plotted as shown in Figure 4.13 and plotting ln k_{obs} *vs* ln[**4.2a**], as presented in Figure 4.14. The order is determined from the slope (0.07) of the ln k_{obs} *vs* ln[**4.2a**] plot.

TH-3565_186122020

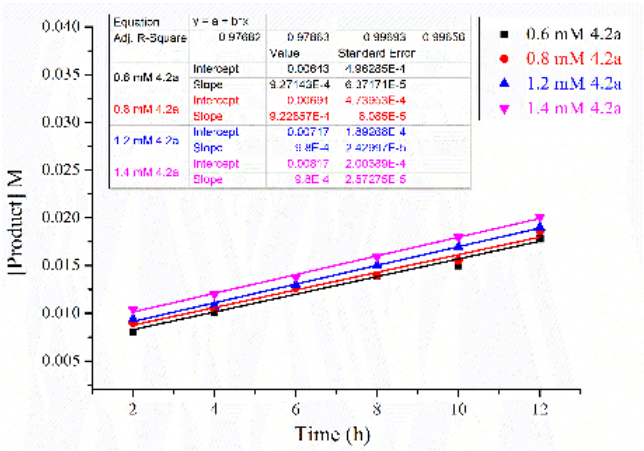


Figure 4.13. Concentration [Product] *vs* time plot at different **4.2a** concentrations.

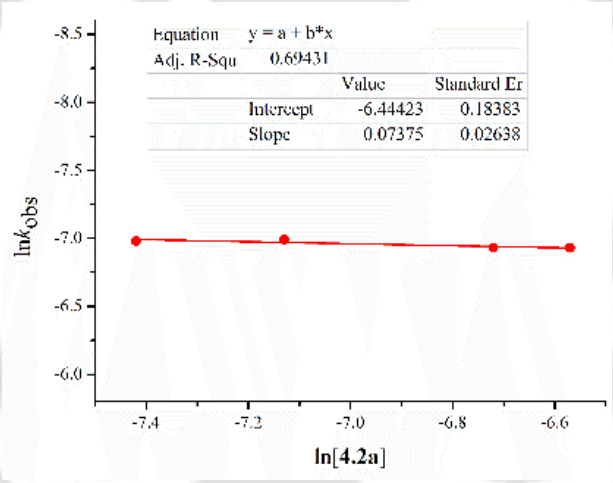
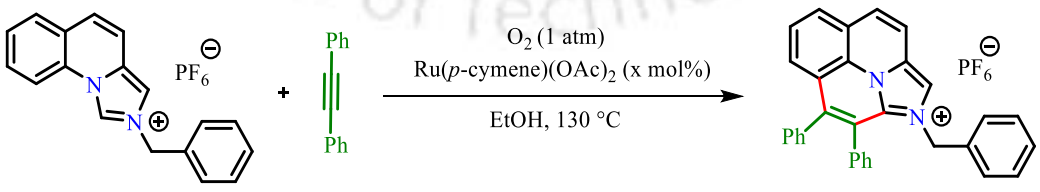


Figure 4.14. ln k_{obs} *vs* ln[**4.2a**].

iii) Kinetic characterization of catalyst [Ru(*p*-cymene)(OAc)$_2$]



4.1h, 1 mmol **4.2a**, 1 mmol **4.3h**

A standard catalytic reaction procedure was followed by varying the amount of catalyst loading of [Ru(*p*-cymene)(OAc)$_2$] from 2 mol% (0.5 M) to 12 mol% (3 M). The product concentration (M) *vs* time (h) was plotted as shown in Figure 4.15 and plotting ln k_{obs} *vs* ln[**cat**], as presented in Figure 4.16. The order is determined from the slope (0.89) of the ln k_{obs} *vs* ln[**cat**] plot.

TH-3565_186122020

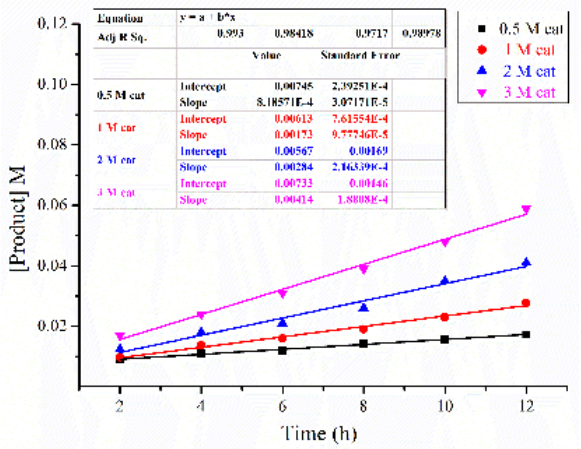


Figure **4.15.** Concentration [Product] *vs* time plot at different **cat.** concentrations.

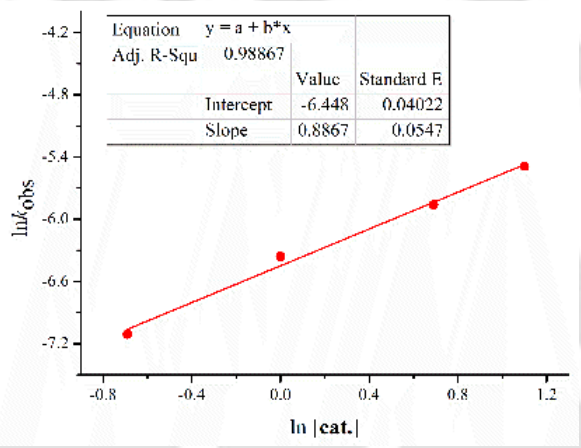
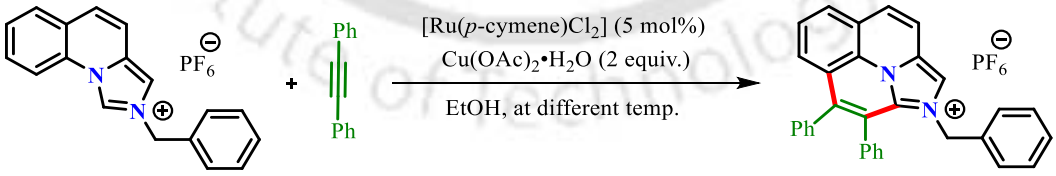


Figure **4.16.** ln k_{obs} *vs* ln[**cat.**].

(d) Entropy of activation

For method A:



4.1h, 0.4 mmol **4.2a**, 0.4 mmol **4.3h**

By following the standard catalytic procedure, annulation reactions of **4.1h** with **4.2a** were performed at different temperatures between 60 °C to 120 °C. The product concentration (M) *vs* time (h) is shown in Figure 4.17.

TH-3565_186122020

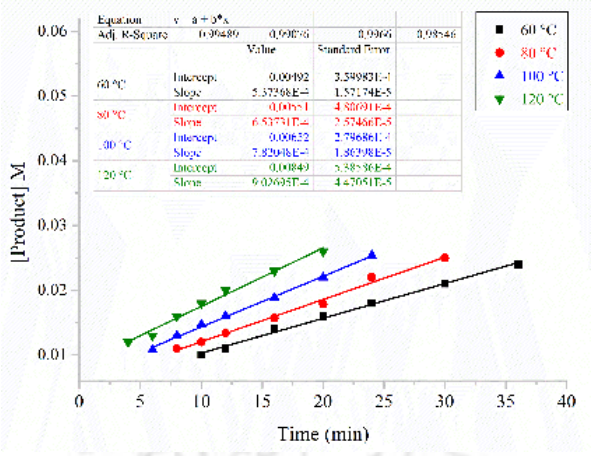


Figure 4.17. Concentration [Product] *vs* time plot at different temperatures.

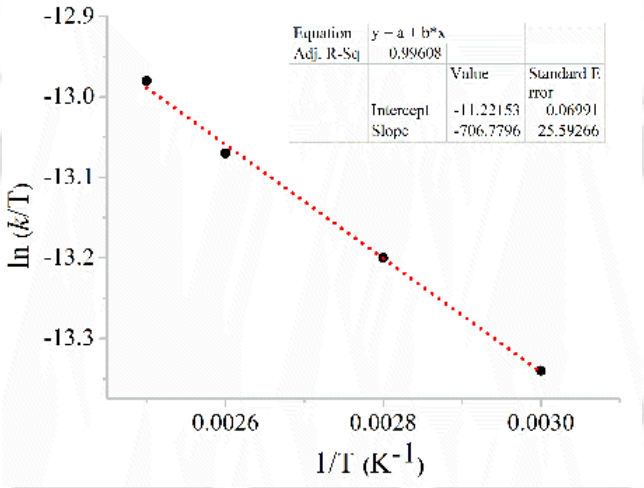


Figure 4.18. Arrhenius-Eyring plot

Activation enthalpy ($\Delta H^{\#}$) and activation entropy ($\Delta S^{\#}$) values were obtained from the slope and intercept of plots of ln(k/T) vs 1/T (Figure 4.18) using the following equation:

$$\ln(k/T) = -\Delta H^{\#}/R.(1/T) + \ln k_B/h + \Delta S^{\#}/R$$

where k_B = Boltzmann constant, R = universal gas constant, and h = Planck's constant.

From the plot of ln(k/T) vs 1/T,

$$\text{Slope} = -706.78$$
$$Or, -\Delta H^{\ddagger}/R = -706.78$$
$$Or, \Delta H^{\ddagger} = -(-706.78) \times (1.987 \text{ cal K}^{-1}\text{mol}^{-1})$$
$$= 1404.37 \text{ cal mol}^{-1}$$
$$= 1.40 \text{ kcal mol}^{-1}$$

And,

$$\text{Intercept} = -11.22$$
$$Or, \ln (k_B/h) + \Delta S^{\#}/R = -11.22$$
$$Or, \ln (1.38\times10^{-23} \text{ J K}^{-1}/6.626\times10^{-34} \text{ J s}) + \Delta S^{\#}/1.987 \text{ cal K}^{-1} \text{ mol}^{-1} = -11.22$$
$$Or, \ln (2.083\times10^{10} \text{ K}^{-1} \text{ s}^{-1}) + \Delta S^{\#}/1.987 \text{ cal K}^{-1} \text{ mol}^{-1} = -11.22$$

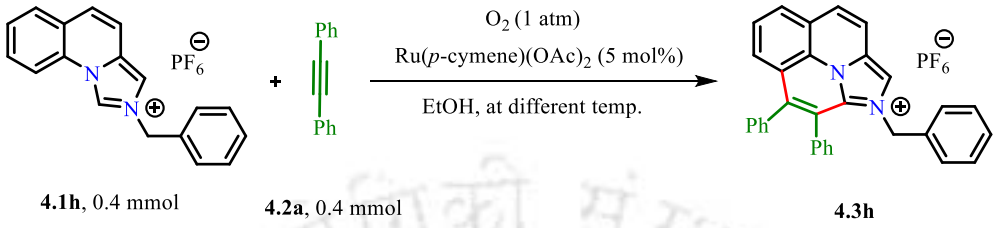
TH-3565_186122020

Or, $23.76 + \Delta S^{\#}/1.987$ cal K^{-1} $mol^{-1} = -11.22$

Or, $\Delta S^{\#}/1.987$ cal K^{-1} $mol^{-1} = -34.98$

Or, $\Delta S^{\#} = -69.51$ cal K^{-1} mol^{-1}

For Method B:



4.1h, 0.4 mmol **4.2a**, 0.4 mmol **4.3h**

Similarly, applying method B, the effect of temperature on the reaction rate was also studied by using Eyring analysis (Figure 4.19). The activation parameters were found to be $\Delta H^{\ddagger} = 2.29 \pm 0.23$ kcal mol^{-1} and $\Delta S^{\ddagger} = -66.98 \pm 2.6$ cal mol^{-1} K^{-1}. The results obtained are in accordance with the previous observation for method A.

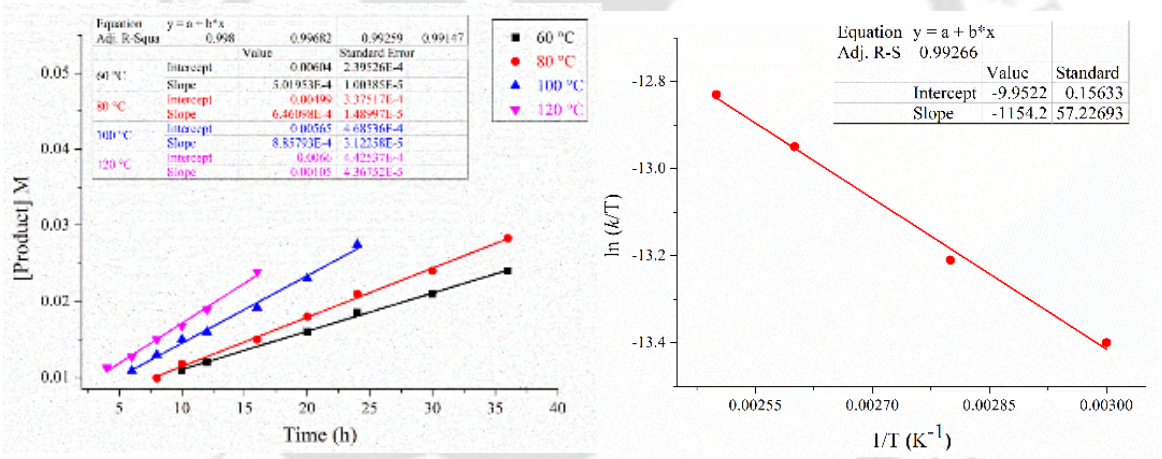
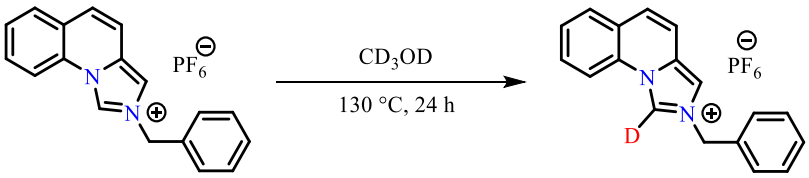


Figure 4.19. Concentration [Product] *vs* time plot at different temperatures (left) and Arrhenius-Eyring plot (right).

(e) k_H/k_D study for imidazo-fused quinolinium C(2)-H bond cleavage

i) Synthesis of C(2)-D substituted 2-benzylimidazo[1,5-*a*]quinolin-2-ium hexafluoro phosphate, 4.1h-[D_1]



4.1h **4.1h-[D_1]** (100% D)

TH-3565_186122020

2-benzylimidazo[1,5-*a*]quinolin-2-ium hexafluorophosphate (202 mg, 0.5 mmol) was taken in a Schlenk tube in CD_3OD (1.0 mL) under an inert atmosphere and stirred at 130 ºC in a preheated oil bath for 24 hours. The reaction mixture is directly injected into an NMR tube to check the crude ^{1}H-NMR and 100% deuteration was observed at the C(2) position of **4.1h**. For the DKIE experiments, the solvent was evaporated, dried in vacuo and used directly without further purification. (yield = 190.5 mg, 94%).

^{1}H NMR (600 MHz, CD_3OD): δ 8.39 (d, J = 8.4 Hz, 1H), 8.08 (s, 1H), 7.91 (d, J = 7.8 Hz, 1H), 7.78 (t, J = 7.8 Hz, 1H), 7.69 (t, J = 7.6 Hz, 1H), 7.59 – 7.57 (m, 3H), 7.52 (d, J = 9.7 Hz, 1H), 7.47 – 7.42 (m, 3H), 5.74 (s, 2H).

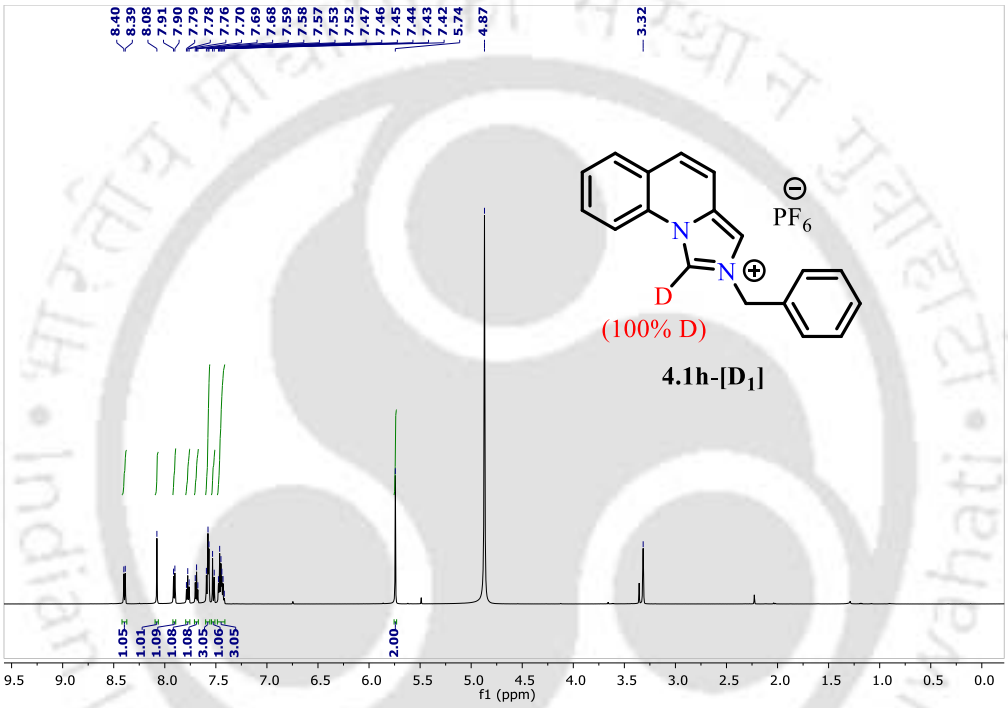
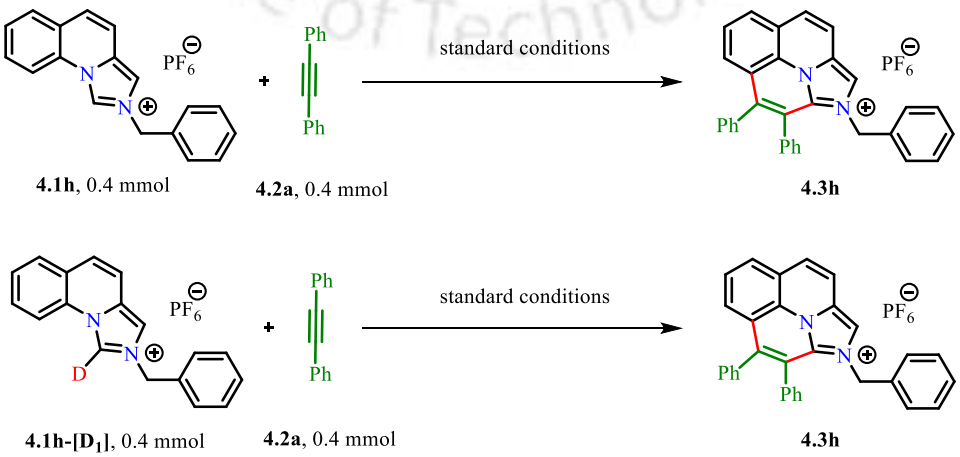


Figure 4.20. ^{1}H NMR spectrum of **4.1h-[D$_1$]** (CD_3OD, 600 MHz, 298 K)

ii) Deuterium kinetic isotope effect (DKIE) experiment



TH-3565_186122020

Procedure: By following the standard catalytic procedure (i.e. for both method A and method B), two parallel reactions were performed by using **4.1h** in CH_3OH (1.0 mL) and **4.1h-[D$_1$]** in CD_3OD (1.0 mL) as substrates. Then aliquot (~100 µL) was withdrawn from the reaction mixture at different intervals, filtered by using a syringe filter, and the solvent was evaporated under a vacuum. This crude mixture was subjected to ^{1}H NMR spectroscopy in $CDCl_3$ and calculated the yield by integrating the benzylic CH_2 peak of the product with respect to an internal standard (1,3,5-trimethylbenzene). Then the initial rates of product formation were obtained from the plot of the concentration of product *vs.* time. Reactions were performed in triplicate and an average $k_H/k_D = 3.40 \pm 0.28$ for method A and $k_H/k_D = 2.79 \pm 0.24$ for method B were obtained by comparing the initial rates of these two reactions.

(f) Competitive annulation reactions with electronically different quinolinium salts (Scheme 4.14)

i) Intermolecular competition experiment between **4.1h** and **4.1n**:

Procedure: A standard catalytic reaction procedure was followed for both method A and method B by using **4.1h** (80.9 mg, 0.2 mmol, 1 equiv.), **4.1n** (86.9 mg, 0.2 mmol, 1 equiv.), diphenylacetylene **4.2a** (17.8 mg, 0.1 mmol, 0.5 equiv.) with EtOH (2 mL) and stirred in a preheated oil bath at 130 °C for 24 h. After completion of the reaction, the solvent was evaporated under reduced pressure and the residue was absorbed onto small amounts of alumina. The purification was performed by column chromatography on neutral alumina (EtOAc/MeOH: 20/1 → 5/1) to get the isolated product **4.3h**, 58%; **4.4a**, 36% in 1.6:1 ratio for method A and **4.3h**, 48%; **4.4a**, 36% in 1.3:1 ratio for method B.

ii) Intermolecular competition experiment between **4.1h** and **4.1o**:

Procedure: A standard catalytic reaction procedure was followed for both method A and method B by using **4.1h** (80.9 mg, 0.2 mmol, 1 equiv.), **4.1o** (84.5 mg, 0.2 mmol, 1 equiv.), diphenylacetylene **4.2a** (17.8 mg, 0.1 mmol, 0.5 equiv.) with EtOH (2 mL) and stirred in a preheated oil bath at 130 °C for 24 h. After completion of the reaction, the solvent was evaporated under reduced pressure and the residue was absorbed onto small amounts of alumina. The purification was performed by column chromatography on neutral alumina (EtOAc/MeOH: 20/1 → 5/1) to get the isolated product **4.3h**, 26%; **4.4b**, 44% in 1:1.7 ratio for method A and **4.3h**, 25%; **4.4b**, 45% in 1:1.8 ratio for method B.

c) Intermolecular competition experiment between **4.1n** and **4.1o**:

Procedure: A standard catalytic reaction procedure was followed for both method A and method B by using **4.1n** (86.9 mg, 0.2 mmol, 1 equiv.), **4.1o** (84.5 mg, 0.2 mmol, 1 equiv.), diphenylacetylene **4.2a** (17.8 mg, 0.1 mmol, 0.5 equiv.) with EtOH (2 mL) and stirred in a preheated oil bath at 130 °C for 24 h. After completion of the reaction, the solvent was evaporated under reduced pressure and the residue was absorbed onto small amounts of alumina. The purification was performed by column chromatography on neutral alumina

TH-3565_186122020

(EtOAc/MeOH: 20/1 → 5/1) to get the isolated product **4.4a**, 15%; **4.4b**, 45% in 1:3 ratio for method A and **4.4a**, 15%; **4.4b**, 47% in 1:3.2 ratio for method B.

4.5.6. Crystallographic data

Crystallographic data of Ru-5

Single crystals of compound **Ru-5** suitable for X-ray diffraction were obtained by slow evaporation of the saturated solution of the compound in CH_2Cl_2 at room temperature. X-ray crystallographic data were collected using Bruker D8 QUEST diffractometer. Data refinement and cell reduction were carried out by *APEX4*. Structures were solved by direct methods using Olex2 v1.5 and refined by a full-matrix least-squares method using Olex2 v1.5. All of the non-H atoms were refined anisotropically. The ORTEP diagram was obtained with ORTEP3 software with 40% thermal ellipsoid. The crystallographic parameters and refinement data are listed below.

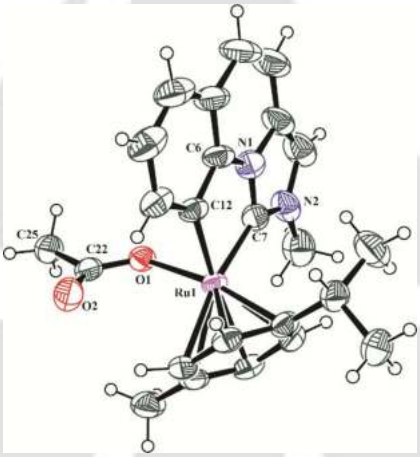


Figure 4.21. Molecular structure of compound **Ru-5** (thermal ellipsoid 40% probability level). Selected Bond lengths (in Å): Ru1-O1 2.114(3), Ru1-C7 2.051(4), Ru1-C12 2.089(4), O1-C22 1.279(5), O2-C22 1.222(5), N1-C7 1.344(6), N2-C7 1.354(6). Selected Bond Angles (in °): N1-C7-N2 103.5(4), N1-C7-Ru1 113.2(3), N2-C7-Ru1 143.3(4), C6-C12-Ru1 113.1(3), N1-C6-C12 114.1(4), C7-N1-C6 120.7(4), C22-O1-Ru1 125.3(3), O2-C22-O1 126.6(4), O2-C22-C25 119.7(4).

Table 4.11. Crystal data and structure refinement for **Ru-5**

Identification code	MK_Ru_OAC_B_0m_a
CCDC	2323691
Empirical formula	$C_{48}H_{54}N_4O_5Ru_2$
Formula weight	969.09
Temperature	297 K
Wavelength	0.71073 Å
Crystal system	monoclinic

TH-3565_186122020

Space group	$P2_1/c$	
Unit cell dimensions	a = 12.1365(15) Å	α = 90°
	b = 15.951(2) Å	β = 91.336(3)°
	c = 22.337(3) Å	γ = 90°
Volume	4323.0(9) $Å^3$	
Z	4	
Density (calculated)	1.489 g/cm^3	
Absorption coefficient	0.750 mm^{-1}	
F(000)	1992.0	
Crystal size	0.32 × 0.28 × 0.23 mm^3	
2Θ range for data collection	3.356 to 54.49°	
Index ranges	$-15 \leq h \leq 15$, $-20 \leq k \leq 20$, $-28 \leq l \leq 28$	
Reflections collected	110748	
Independent reflections	9646 [R_{int} = 0.0315, R_{sigma} = 0.0169]	
Completeness to theta = 27.245°	99.6%	
Data/restraints/parameters	9646/648/557	
Goodness-of-fit on F^2	1.133	
Final R indexes [I>=2σ (I)]	R_1 = 0.0465, wR_2 = 0.0813	
Final R indexes [all data]	R_1 = 0.0714, wR_2 = 0.0979	
Largest diff. peak and hole	1.01 and -0.63 e $Å^{-3}$	

Crystallographic data of 4.4j

Single crystals of compound **4.4j** suitable for X-ray diffraction were obtained by slow evaporation of the saturated solution of the compound in methanol at room temperature. X-ray crystallographic data were collected using Bruker D8 QUEST diffractometer. Data refinement and cell reduction were carried out by *APEX4*. Structures were solved by direct methods using Olex2 v1.5 and refined by a full-matrix least-squares method using Olex2 v1.5. All of the non-H atoms were refined anisotropically. The ORTEP diagram was obtained with ORTEP3 software with 40% thermal ellipsoid. The crystallographic parameters and refinement data are listed below.

TH-3565_186122020

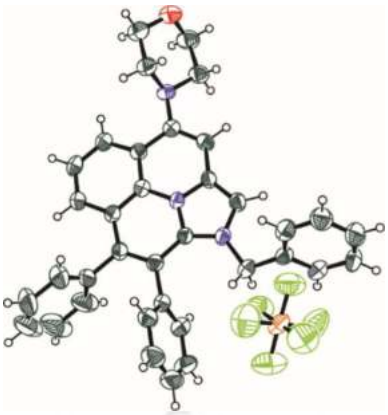


Figure 4.22. Molecular structure of compound **4.4j** (thermal ellipsoid 40% probability level).

Table 4.12. Crystal data and structure refinement for **4.4j**

Identification code	MK_522N_0ma_a	
CCDC	2338637	
Empirical formula	$C_{36}H_{30}F_6N_3OP$	
Formula weight	665.60	
Temperature	296.00 K	
Wavelength	0.71073 Å	
Crystal system	monoclinic	
Space group	C2/c	
Unit cell dimensions	a = 33.167(8) Å	α = 90°
	b = 9.943(3) Å	β = 126.884(6)°
	c = 26.394(11) Å	γ = 90°
Volume	6962(4) $Å^3$	
Z	8	
Density (calculated)	1.270 g/cm^3	
Absorption coefficient	0.143 mm^{-1}	
F(000)	2752.0	
Crystal size	0.31 × 0.28 × 0.21 mm^3	
2Θ range for data collection	3.07 to 49.996°	
Index ranges	$-39 \le h \le 39$, $-11 \le k \le 11$, $-31 \le l \le 31$	
Reflections collected	72544	
Independent reflections	6118 [R_{int} = 0.0947, R_{sigma} = 0.0624]	

TH-3565_186122020

Completeness to theta = 24.998°	99.7%
Data/restraints/parameters	6118/0/424
Goodness-of-fit on F^2	1.108
Final R indexes [I>=2σ (I)]	R_1 = 0.1126, wR_2 = 0.2716
Final R indexes [all data]	R_1 = 0.1839, wR_2 = 0.3379
Largest diff. peak and hole	0.49 and -0.35 e $Å^{-3}$

Crystallographic data of 4.4l

Single crystals of compound **4.4l** suitable for X-ray diffraction were obtained by slow evaporation of the saturated solution of the compound in $CHCl_3$ at room temperature. X-ray crystallographic data were collected using Bruker D8 QUEST diffractometer. Data refinement and cell reduction were carried out by *APEX4*. Structures were solved by direct methods using Olex2 v1.5 and refined by a full-matrix least-squares method using Olex2 v1.5. All of the non-H atoms were refined anisotropically. The ORTEP diagram was obtained with ORTEP3 software with 40% thermal ellipsoid. The crystallographic parameters and refinement data are listed below.

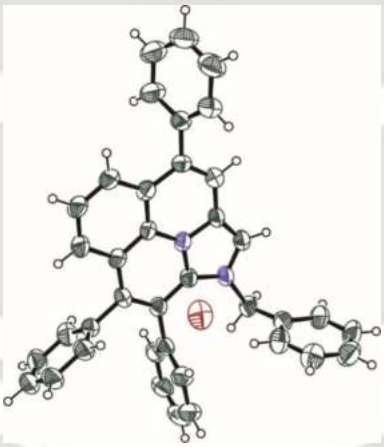


Figure 4.23. Molecular structure of compound **4.4l** (thermal ellipsoid 40% probability level).

Table 4.13. Crystal data and structure refinement for **4.4l**

Identification code	MK708_a
CCDC	2331111
Empirical formula	$C_{38}H_{27}BrN_2$
Formula weight	591.52
Temperature	297.00 K
Wavelength	0.71073 Å
Crystal system	monoclinic

TH-3565_186122020

Space group	C2/c	
Unit cell dimensions	a = 27.347(11) Å	α = 90°
	b = 9.409(3) Å	β = 90.629(17)°
	c = 26.256(9) Å	γ = 90°
Volume	6756(4) $Å^3$	
Z	8	
Density (calculated)	1.163 g/cm^3	
Absorption coefficient	1.243 mm^{-1}	
F(000)	2432.0	
Crystal size	0.35 × 0.27 × 0.23 mm^3	
2Θ range for data collection	2.978 to 49.998°	
Index ranges	$-32 \leq h \leq 32$, $-11 \leq k \leq 11$, $-31 \leq l \leq 31$	
Reflections collected	70297	
Independent reflections	5955 [R_{int} = 0.0564, R_{sigma} = 0.0291]	
Completeness to theta = 24.999°	100%	
Data/restraints/parameters	6252/0/446	
Goodness-of-fit on F^2	1.430	
Final R indexes [I>=2σ (I)]	R_1 = 0.0986, wR_2 = 0.2936	
Final R indexes [all data]	R_1 = 0.1473, wR_2 = 0.3776	
Largest diff. peak and hole	0.78 and -1.08 e $Å^{-3}$	

Crystallographic data of 4.4o

Single crystals of compound **4.4o** suitable for X-ray diffraction were obtained by slow evaporation of the saturated solution of the compound in CH_2Cl_2 at room temperature. X-ray crystallographic data were collected using Bruker D8 QUEST diffractometer. Data refinement and cell reduction were carried out by *APEX4*. Structures were solved by direct methods using Olex2 v1.5 and refined by a full-matrix least-squares method using Olex2 v1.5. All of the non-H atoms were refined anisotropically. The ORTEP diagram was obtained with ORTEP3 software with 40% thermal ellipsoid. The crystallographic parameters and refinement data are listed below.

TH-3565_186122020

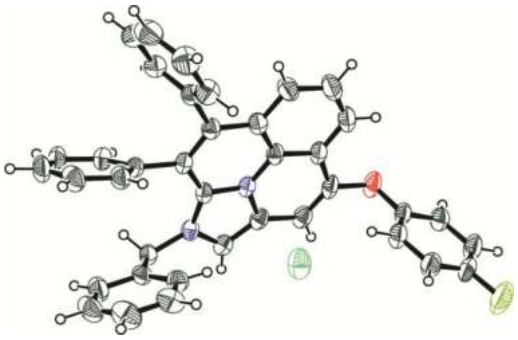


Figure 4.24. Molecular structure of compound **4.4o** (thermal ellipsoid 40% probability level).

Table 4.14. Crystal data and structure refinement for **4.4o**

Identification code	MK_512_ADAS_0m_a	
CCDC	2323694	
Empirical formula	$C_{38}H_{28}ClFN_2O_2$	
Formula weight	599.07	
Temperature	296.15 K	
Wavelength	0.71073 Å	
Crystal system	triclinic	
Space group	P-1	
Unit cell dimensions	a = 10.173(4) Å	α = 93.961(10)°
	b = 10.774(3) Å	β = 101.989(10)°
	c = 15.748(5) Å	γ = 90.046(10)°
Volume	1684.2(10) $Å^3$	
Z	2	
Density (calculated)	1.181 g/cm^3	
Absorption coefficient	0.153 mm^{-1}	
F(000)	624.0	
Crystal size	0.36 × 0.29 × 0.25 mm^3	
2Θ range for data collection	4.094 to 50.04°	
Index ranges	$-12 \le h \le 12$, $-12 \le k \le 12$, $-18 \le l \le 18$	
Reflections collected	20235	
Independent reflections	5823 [R_{int} = 0.0791, R_{sigma} = 0.0837]	
Completeness to theta = 25.02°	97.8%	

TH-3565_186122020

Data/restraints/parameters	5823/0/400
Goodness-of-fit on F^2	1.035
Final R indexes [I>=2σ (I)]	R_1 = 0.0668, wR_2 = 0.1578
Final R indexes [all data]	R_1 = 0.1308, wR_2 = 0.1863
Largest diff. peak and hole	0.40 and -0.36 e $Å^{-3}$

Crystallographic data of 4.5f

Single crystals of compound **4.5f** suitable for X-ray diffraction were obtained by slow evaporation of the saturated solution of the compound in a mixture of CH_2Cl_2 and methanol (4:1) at room temperature. X-ray crystallographic data were collected using Bruker D8 QUEST diffractometer. Data refinement and cell reduction were carried out by *APEX4*. Structures were solved by direct methods using Olex2 v1.5 and refined by a full-matrix least-squares method using Olex2 v1.5. All of the non-H atoms were refined anisotropically. The ORTEP diagram was obtained with ORTEP3 software with 40% thermal ellipsoid. The crystallographic parameters and refinement data are listed below.

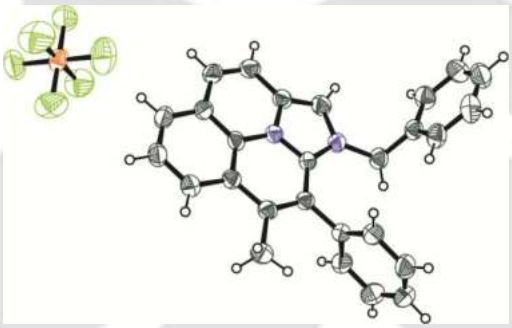


Figure 4.25. Molecular structure of compound **4.5f** (thermal ellipsoid 40% probability level).

Table 4.15. Crystal data and structure refinement for **4.5f**

Identification code	NH_365_0m_a
CCDC	2323690
Empirical formula	$C_{27}H_{21}F_6N_2P$
Formula weight	518.43
Temperature	298.0 K
Wavelength	0.71073 Å
Crystal system	orthorhombic
Space group	Pbca
Unit cell dimensions	a = 14.2843(16) Å α = 90°

TH-3565_186122020

	b = 16.6950(18) Å	β = 90°
	c = 19.642(2) Å	γ = 90°
Volume	4684.1(9) $Å^3$	
Z	8	
Density (calculated)	1.470 g/cm^3	
Absorption coefficient	0.185 mm^{-1}	
F(000)	2128.0	
Crystal size	0.29 × 0.27 × 0.19 mm^3	
2Θ range for data collection	4.288 to 52.14°	
Index ranges	$-17 \leq h \leq 17, -20 \leq k \leq 20, -24 \leq l \leq 24$	
Reflections collected	108956	
Independent reflections	4624 [R_{int} = 0.0774, R_{sigma} = 0.0289]	
Completeness to theta = 26.070°	99.6%	
Data/restraints/parameters	4624/0/327	
Goodness-of-fit on F^2	1.099	
Final R indexes [I>=2σ (I)]	R_1 = 0.0638, wR_2 = 0.1485	
Final R indexes [all data]	R_1 = 0.1158, wR_2 = 0.1975	
Largest diff. peak and hole	0.46 and -0.37 e $Å^{-3}$	

Crystallographic data of 4.6b

Single crystals of compound **4.6b** suitable for X-ray diffraction were obtained by slow evaporation of the saturated solution of the compound in $CHCl_3$ at room temperature. X-ray crystallographic data were collected using Bruker D8 QUEST diffractometer. Data refinement and cell reduction were carried out by *APEX4*. Structures were solved by direct methods using Olex2 v1.5 and refined by a full-matrix least-squares method using Olex2 v1.5. All of the non-H atoms were refined anisotropically. The ORTEP diagram was obtained with ORTEP3 software with 40% thermal ellipsoid. The crystallographic parameters and refinement data are listed below.

TH-3565_186122020

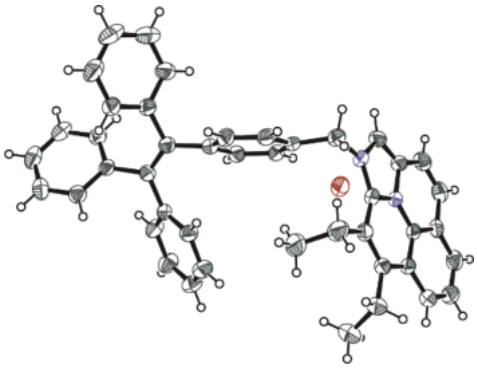


Figure 4.26. Molecular structure of compound **4.6b** (thermal ellipsoid 40% probability level).

Table 4.16. Crystal data and structure refinement for **4.6b**

Identification code	MK_782_0m_a	
CCDC	2324158	
Empirical formula	$C_{45}H_{41}BrN_2O$	
Formula weight	705.743	
Temperature	298.00 K	
Wavelength	0.71073 Å	
Crystal system	triclinic	
Space group	P-1	
Unit cell dimensions	a = 9.759(6) Å	α = 75.529(18)°
	b = 10.864(7) Å	β = 80.536(18)°
	c = 18.417(11) Å	γ = 71.454(18)°
Volume	1784.9(19) $Å^3$	
Z	2	
Density (calculated)	1.313 g/cm^3	
Absorption coefficient	1.189 mm^{-1}	
F(000)	736.0	
Crystal size	0.39 × 0.32 × 0.27 mm^3	
2Θ range for data collection	4.04 to 50.24°	
Index ranges	$-11 \leq h \leq 11$, $-12 \leq k \leq 12$, $-21 \leq l \leq 21$	
Reflections collected	33800	
Independent reflections	6252 [R_{int} = 0.0604, R_{sigma} = 0.0597]	

TH-3565_186122020

Completeness to theta = 25.12°	98.2%
Data/restraints/parameters	6252/0/446
Goodness-of-fit on F^2	1.168
Final R indexes [I>=2σ (I)]	R_1 = 0.0641, wR_2 = 0.0909
Final R indexes [all data]	R_1 = 0.1251, wR_2 = 0.1180
Largest diff. peak and hole	0.75 and -0.91 e $Å^{-3}$

Crystallographic data of 4.10a

Single crystals of compound **4.10a** suitable for X-ray diffraction were obtained by slow evaporation of the saturated solution of the compound in CH_2Cl_2 at room temperature. X-ray crystallographic data were collected using Bruker D8 QUEST diffractometer. Data refinement and cell reduction were carried out by *APEX4*. Structures were solved by direct methods using Olex2 v1.5 and refined by a full-matrix least-squares method using Olex2 v1.5. All of the non-H atoms were refined anisotropically. The ORTEP diagram was obtained with ORTEP3 software with 40% thermal ellipsoid. The crystallographic parameters and refinement data are listed below.

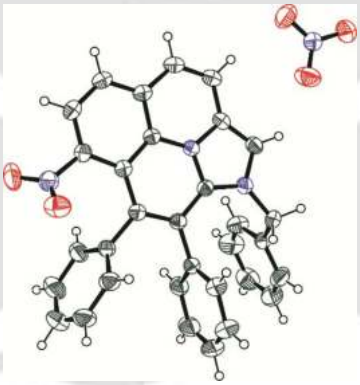


Figure 4.27. Molecular structure of compound **4.10a** (thermal ellipsoid 40% probability level).

Table 4.17. Crystal data and structure refinement for **4.10a**

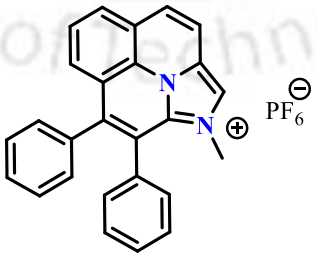
Identification code	NH_71_0m_a
CCDC	2307296
Empirical formula	$C_{32}H_{22}N_4O_5$
Formula weight	542.53
Temperature	297.00 K
Wavelength	0.71073 Å
Crystal system	triclinic
Space group	P-1

TH-3565_186122020

Unit cell dimensions	a = 6.8611(5) Å	α = 91.565(2)°
	b = 11.3399(8) Å	β = 90.724(2)°
	c = 17.1143(12) Å	γ = 104.814(2)°
Volume	1286.56(16) $Å^3$	
Z	2	
Density (calculated)	1.400 g/cm^3	
Absorption coefficient	0.097 mm^{-1}	
F(000)	564.0	
Crystal size	0.36 × 0.32 × 0.29 mm^3	
2Θ range for data collection	3.716 to 49.996°	
Index ranges	$-8 \leq h \leq 8, -13 \leq k \leq 13, -20 \leq l \leq 20$	
Reflections collected	28432	
Independent reflections	4502 [R_{int} = 0.0290, R_{sigma} = 0.0209]	
Completeness to theta = 24.998°	99.5%	
Data/restraints/parameters	4502/0/371	
Goodness-of-fit on F^2	1.108	
Final R indexes [I>=2σ (I)]	R_1 = 0.0433, wR_2 = 0.0893	
Final R indexes [all data]	R_1 = 0.0590, wR_2 = 0.1019	
Largest diff. peak and hole	0.15 and -0.15 e $Å^{-3}$	

4.5.7. Analytical data of the products

1-methyl-8,9-diphenylbenzo[*ij*]imidazo[2,1,5-*de*]quinolizin-1-ium hexafluorophosphate (4.3a)

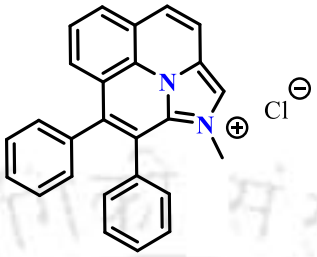


The title compound **4.3a** was isolated as a brown solid using neutral alumina column chromatography with ethyl acetate/ methanol (v/v = 10/1, R_f = 0.3) in 98% yield (99 mg) from GP-III; 96% yield (97 mg) from GP-IV. m.p. = 293–295 °C. ^{1}H NMR (400 MHz, DMSO-d_6): δ 8.50 (s, 1H), 8.18 (d, J = 7.5 Hz, 1H), 7.94 – 7.90 (m, 3H), 7.44 – 7.39 (m, 8H), 7.37 – 7.35 (m, 1H), 7.25 – 7.24 (m, 2H), 3.49 (s, 3H). ^{13}C NMR (101 MHz, DMSO-d_6): δ 144.0, 134.2,

TH-3565_186122020

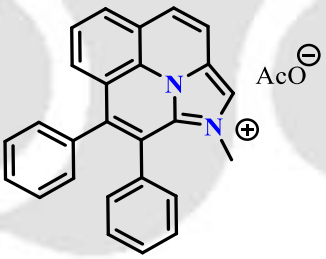
132.2, 131.8, 130.9, 129.4, 129.1, 128.8, 128.6, 128.4, 128.2, 127.9, 126.8, 125.4, 124.52, 124.48, 124.4, 123.7, 123.1, 119.8, 116.9, 37.4. HRMS (ESI) *m/z*: calcd. for $C_{26}H_{19}N_2$ [M^+]: 359.1543; found: 359.1545.

1-methyl-8,9-diphenylbenzo[*ij*]imidazo[2,1,5-*de*]quinolizin-1-ium chloride (4.3a-Cl)



The title compound **4.3a-Cl** was isolated as a brown solid using neutral alumina column chromatography with ethyl acetate/ methanol (v/v = 10/1, R_f = 0.3) in 95% yield (75 mg) from GP-III; m.p. = 280–283 °C. ^{1}H NMR (600 MHz, $CDCl_3$): δ 9.58 (s, 1H), 7.98 (d, J = 7.5 Hz, 1H), 7.86 – 7.84 (m, 1H), 7.80 (t, J = 7.8 Hz, 1H), 7.69 (d, J = 8.6 Hz, 1H), 7.54 (d, J = 8.2 Hz, 1H), 7.38 – 7.34 (m, 6H), 7.29 (brs, 2H), 7.17 (d, J = 7.0 Hz, 2H), 3.84 (s, 3H). ^{13}C NMR (151 MHz, $CDCl_3$): δ 145.5, 133.8, 131.5, 131.3, 130.8, 129.7, 129.5, 129.4, 128.9, 128.84, 128.82, 128.2, 127.0, 125.7, 125.1, 124.7, 124.4, 123.8, 122.2, 117.7, 38.6.

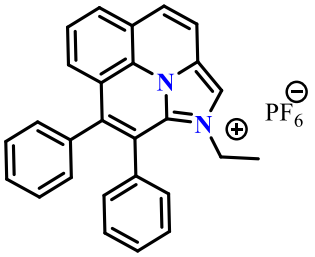
1-methyl-8,9-diphenylbenzo[*ij*]imidazo[2,1,5-*de*]quinolizin-1-ium acetate (4.3a-OAc)



The title compound **4.3a-OAc** was isolated as a brown solid using neutral alumina column chromatography with ethyl acetate/ methanol (v/v = 20/1, R_f = 0.3) in 87% yield (72.8 mg) from GP-III; 95% yield (79.5 mg) from GP-IV. m.p. = 292–294 °C. ^{1}H NMR (400 MHz, CD_3OD): δ 8.27 (s, 1H), 8.11 (d, J = 7.4 Hz, 1H), 7.89 – 7.85 (m, 2H), 7.78 (d, J = 9.8 Hz, 1H), 7.53 (dd, J = 8.2, 1.0 Hz, 1H), 7.45 – 7.34 (m, 8H), 7.30 – 7.28 (m, 2H), 3.59 (s, 3H), 1.90 (s, 3H). ^{13}C NMR (126 MHz, CD_3OD): δ 180.2, 146.9, 135.7, 134.0, 133.3, 132.4, 130.81, 130.77, 130.4, 129.7, 129.6, 129.0, 128.5, 126.9, 126.32, 126.26, 125.73, 125.66, 125.4, 120.7, 117.5, 38.4, 24.8. HRMS (ESI) *m/z*: calcd. for $C_{26}H_{19}N_2$ [M^+]: 359.1543; found: 359.1547.

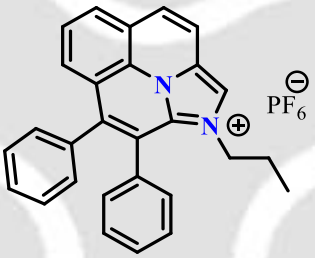
1-ethyl-8,9-diphenylbenzo[*ij*]imidazo[2,1,5-*de*]quinolizin-1-ium hexafluorophosphate (4.3b)

TH-3565_186122020



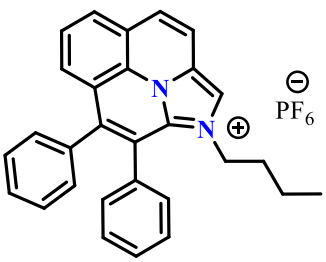
The title compound **4.3b** was isolated as a beige solid using neutral alumina column chromatography with ethyl acetate/ methanol (v/v = 20/1, R_f = 0.3) in 93% yield (96 mg) from GP-III; 95% yield (98.5 mg) from GP-IV. m.p. = 292–294 °C. ^{1}H NMR (600 MHz, $CDCl_3$): δ 8.44 (s, 1H), 7.94 (d, J = 7.6 Hz, 1H), 7.79 – 7.76 (m, 2H), 7.66 (d, J = 9.8 Hz, 1H), 7.50 (d, J = 8.1 Hz, 1H), 7.36 – 7.31 (m, 8H), 7.16 (d, J = 6.7 Hz, 2H), 3.97 (q, J = 7.2 Hz, 2H), 1.28 (t, J = 7.2 Hz, 3H). ^{13}C NMR (101 MHz, $CDCl_3$): δ 146.1, 134.2, 131.8, 131.5, 130.6, 129.7, 129.6, 129.0, 128.8, 128.7, 128.0, 127.2, 125.8, 125.2, 125.1, 124.85, 124.79, 124.3, 118.9, 117.4, 45.7, 16.4. HRMS (ESI) *m*/*z*: calcd. for $C_{27}H_{21}N_2$ [M^+]: 373.1700; found: 373.1708.

1-propyl-8,9-diphenylbenzo[*ij*]imidazo[2,1,5-*de*]quinolizin-1-ium hexafluorophosphate (4.3c)



The title compound **4.3c** was isolated as light-yellow solid using neutral alumina column chromatography with ethyl acetate/ methanol (v/v = 20:1, R_f = 0.3) in 92% yield (98 mg) from GP-III; 93% yield (99 mg) from GP-IV. m.p. = 289–291 °C. ^{1}H NMR (600 MHz, $CDCl_3$): δ 9.56 (s, 1H), 7.97 – 7.94 (m, 2H), 7.78 (t, J = 8.0 Hz, 1H), 7.65 (d, J = 9.8 Hz, 1H), 7.49 (d, J = 8.2 Hz, 1H), 7.40 – 7.30 (m, 6H), 7.27 – 7.26 (m, 2H), 7.13 (d, J = 6.6 Hz, 2H), 4.07 (t, J=7.9, 2H), 1.69 – 1.63 (m, 2H), 0.60 (t, J = 7.3 Hz, 3H). ^{13}C NMR (101 MHz, $CDCl_3$): δ 145.8, 134.0, 131.6, 131.0, 130.6, 129.7, 129.5, 129.0, 128.9, 128.8, 128.1, 126.8, 125.7, 125.3, 125.1, 124.7, 124.4, 124.2, 121.6, 118.2, 51.7, 25.5, 10.7. HRMS (ESI) *m*/*z*: calcd. for $C_{28}H_{23}N_2$ [M^+]: 387.1856; found: 387.1863.

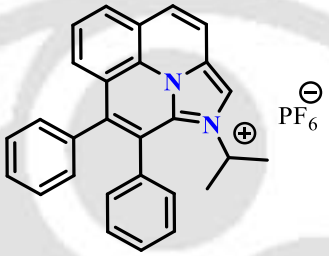
1-butyl-8,9-diphenylbenzo[*ij*]imidazo[2,1,5-*de*]quinolizin-1-ium hexafluorophosphate (4.3d)



TH-3565_186122020

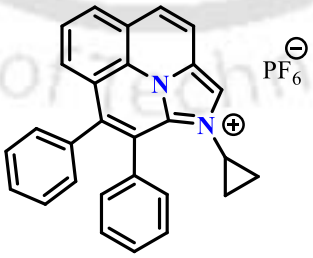
The title compound **4.3d** was isolated as brown solid using neutral alumina column chromatography with ethyl acetate/ methanol (v/v = 20:1, R_f = 0.3) in 90% yield (98.4 mg) from GP-III; 91% yield (99.5 mg) from GP-IV. m.p. = 236–238 °C. ^{1}H NMR (400 MHz, $CDCl_3$): δ 8.43 (s, 1H), 7.94 (d, J = 7.6 Hz, 1H), 7.81 – 7.75 (m, 2H), 7.66 (d, J = 9.8 Hz, 1H), 7.50 (d, J = 8.2 Hz, 1H), 7.37 – 7.32 (m, 8H), 7.17 – 7.15 (m, 2H), 3.93 (t, J = 8.0 Hz, 2H), 1.58 – 1.56 (m, 2H), 1.00 – 0.95 (m, 2H), 0.71 (t, J = 7.3 Hz, 3H). ^{13}C NMR (101 MHz, $CDCl_3$): δ 146.2, 134.2, 131.7, 131.4, 130.7, 129.7, 129.6, 128.9, 128.84, 128.76, 128.1, 127.2, 125.8, 125.19, 125.15, 124.8, 124.7, 124.3, 119.6, 117.5, 50.3, 33.5, 19.7, 13.4. HRMS (ESI) *m*/*z*: calcd. for $C_{29}H_{25}N_2$ [M^+]: 401.2013; found: 401.2021.

1-isopropyl-8,9-diphenylbenzo[*ij*]imidazo[2,1,5-*de*]quinolizin-1-ium hexafluorophosphate (4.3e)



The title compound **4.3e** was isolated as brown solid using neutral alumina column chromatography with ethyl acetate/ methanol (v/v = 20:1, R_f = 0.3) in 87% yield (92.6 mg) from GP-III; 87% yield (92.6 mg) from GP-IV. m.p. = 240–243 °C. ^{1}H NMR (600 MHz, DMSO-d_6): δ 8.82 (s, 1H), 8.20 – 8.19 (m, 1H), 7.96 – 7.95 (m, 1H), 7.93 – 7.88 (m, 2H), 7.46 – 7.40 (m, 7H), 7.37 – 7.34 (m, 2H), 7.22 – 7.21 (m, 2H), 3.97 – 3.95 (m, 1H), 1.33 (d, J = 5.8 Hz, 6H). ^{13}C NMR (101 MHz, DMSO-d_6): δ 144.4, 134.3, 132.4, 131.7, 130.1, 129.3, 128.8, 128.55, 128.52, 128.3, 127.9, 126.9, 125.5, 124.49, 124.47, 124.3, 124.2, 123.7, 116.9, 114.8, 50.8, 22.5. HRMS (ESI) *m*/*z*: calcd. for $C_{28}H_{23}N_2$ [M^+]: 387.1856; found 387.1858.

1-cyclopropyl-8,9-diphenylbenzo[*ij*]imidazo[2,1,5-*de*]quinolizin-1-ium hexafluorophosphate (4.3f)

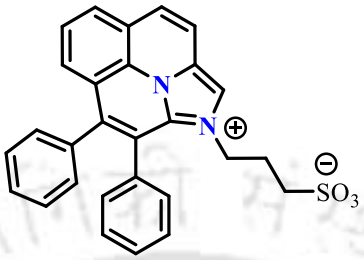


The title compound **4.3f** was isolated as light-yellow solid using neutral alumina column chromatography with ethyl acetate/ methanol (v/v = 20:1, R_f = 0.4) in 84% yield (89.1 mg) from GP-III; 90% yield (95.5 mg) from GP-IV. m.p. = 222–225 °C. ^{1}H NMR (500 MHz, $CDCl_3$): δ 8.06 (s, 1H), 7.93 (d, J = 7.6 Hz, 1H), 7.78 (t, J = 8.0 Hz, 1H), 7.68 – 7.64 (m, 2H), 7.54 (d, J = 8.2 Hz, 1H), 7.38 – 7.30 (m, 8H), 7.19 – 7.17 (m, 2H), 3.33 – 3.28 (m, 1H), 1.06 – 1.02 (m, 2H), 0.59 – 0.55 (m, 2H). ^{13}C NMR (151 MHz, $CDCl_3$): δ 146.8, 134.3, 133.6, 132.5,

TH-3565_186122020

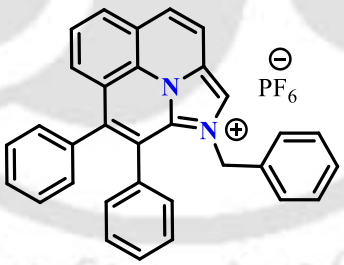
131.3, 129.7, 129.6, 129.0, 128.8, 128.7, 128.4, 128.2, 127.5, 125.9, 125.3, 125.1, 125.0, 124.7, 124.0, 118.3, 117.0, 51.1, 34.3, 9.0. HRMS (ESI) *m/z*: calcd. for $C_{28}H_{21}N_2$ [M^+]: 385.1700; found: 385.1698.

3-(8,9-diphenylbenzo[*ij*]imidazo[2,1,5-*de*]quinolizin-1-ium-1-yl)propane-1-sulfonate (4.3g)



The title compound **4.3g** was isolated as black solid using neutral alumina column chromatography with ethyl acetate/ methanol (v/v = 5:1, R_f = 0.2) in 74% yield (69 mg) from GP-III; 72% yield (67.2 mg) from GP-IV. m.p. = 327–330 °C. ^{1}H NMR (500 MHz, DMSO-d_6): δ 8.63 (s, 1H), 8.16 (d, J = 7.7 Hz, 1H), 7.94 – 7.88 (m, 3H), 7.46 – 7.45 (m, 2H), 7.40 – 7.32 (m, 7H), 7.24 (d, J = 7.4 Hz, 2H), 3.91 (t, J = 7.4 Hz, 2H), 2.09 (t, J = 7.3 Hz, 2H), 1.82 (p, J = 7.3 Hz, 2H). ^{13}C NMR (151 MHz, DMSO-d_6): δ 144.4, 134.4, 132.0, 131.9, 130.6, 129.4, 129.2, 129.0, 128.6, 128.4, 128.3, 127.8, 126.8, 125.4, 124.6, 124.2, 123.71, 123.67, 118.9, 117.1, 47.5, 31.2, 27.1. HRMS (ESI) *m/z*: calcd. for $C_{28}H_{23}N_2O_3S$ [M+H]$^+$: 467.1424; found: 467.1423.

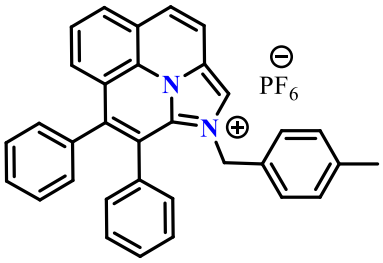
1-benzyl-8,9-diphenylbenzo[*ij*]imidazo[2,1,5-*de*]quinolizin-1-ium hexafluorophosphate (4.3h)



The title compound **4.3h** was isolated as brown solid using neutral alumina column chromatography with ethyl acetate/ methanol (v/v = 20:1, R_f = 0.3) in 95% yield (110.3 mg) from GP-III; 96% yield (111.5 mg) from GP-IV. m.p. = 90–95 °C. ^{1}H NMR (600 MHz, $CDCl_3$): δ 9.45 (s, 1H), 7.98 (d, J = 7.6 Hz, 1H), 7.89 (d, J = 9.0 Hz, 1H), 7.78 (t, J = 7.9 Hz, 1H), 7.69 (d, J = 9.5 Hz, 1H), 7.49 (d, J = 8.2 Hz, 1H), 7.30 (s, 1H), 7.29 – 7.27 (m, 3H), 7.19 – 7.15 (m, 3H), 7.13 – 7.11 (m, 2H), 7.07 – 7.06 (m, 3H), 7.05 (brs, 1H), 6.66 (d, J = 7.3 Hz, 2H), 5.54 (s, 2H). ^{13}C NMR (151 MHz, $CDCl_3$): δ 146.2, 134.6, 133.8, 131.3, 131.0, 130.8, 129.5, 129.3, 128.7, 128.65, 128.60, 128.58, 128.3, 128.1, 127.0, 126.6, 125.8, 125.1, 125.0, 124.7, 124.2, 121.8, 117.7, 53.5. HRMS (ESI) *m/z*: calcd. for $C_{32}H_{23}N_2$ [M^+]: 435.1856; found: 435.1858.

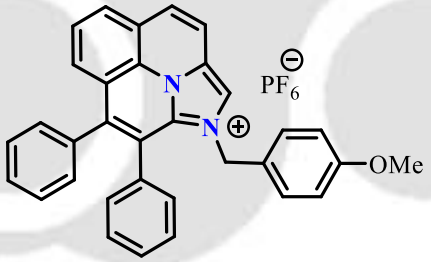
TH-3565_186122020

1-(4-methylbenzyl)-8,9-diphenylbenzo[*ij*]imidazo[2,1,5-*de*]quinolizin-1-ium hexafluorophosphate (4.3i)



The title compound **4.3i** was isolated as black solid using neutral alumina column chromatography with ethyl acetate/ methanol (v/v = 20:1, R_f = 0.4) in 96% yield (114.2 mg) from GP-III; 92% yield (109.4 mg) from GP-IV. m.p. = 112–115 °C. ^{1}H NMR (500 MHz, $CDCl_3$): δ 9.16 (s, 1H), 7.98 (d, J = 7.7 Hz, 1H), 7.89 (d, J = 9.7 Hz, 1H), 7.79 (t, J = 8.0 Hz, 1H), 7.70 (d, J = 9.7 Hz, 1H), 7.51 (d, J = 8.3 Hz, 1H), 7.32 – 7.28 (m, 4H), 7.24 (t, J = 7.7 Hz, 2H), 7.16 (d, J = 7.6 Hz, 2H), 7.10 (d, J = 6.5 Hz, 2H), 6.98 (d, J = 7.7 Hz, 2H), 6.70 (d, J = 7.7 Hz, 2H), 5.47 (s, 2H), 2.26 (s, 3H). ^{13}C NMR (151 MHz, $CDCl_3$): δ 146.2, 138.5, 134.0, 131.4, 131.2, 130.9, 129.6, 129.53, 129.49, 129.4, 128.8, 128.74, 128.70, 128.2, 127.2, 127.1, 125.9, 125.1, 124.8, 124.4, 124.2, 121.1, 117.7, 53.5, 21.2. HRMS (ESI) *m*/*z*: calcd. for $C_{33}H_{25}N_2$ [M^+]: 449.2013; found: 449.2026.

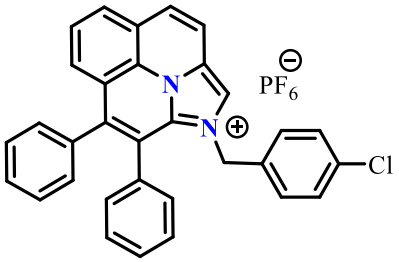
1-(4-methoxybenzyl)-8,9-diphenylbenzo[*ij*]imidazo[2,1,5-*de*]quinolizin-1-ium hexafluorophosphate (4.3j)



The title compound **4.3j** was isolated as brown solid using neutral alumina column chromatography with ethyl acetate/ methanol (v/v = 20:1, R_f = 0.35) in 87% yield (106 mg) from GP-III; 88% yield (107.4 mg) from GP-IV. m.p. = 133–135 °C. ^{1}H NMR (400 MHz, $CDCl_3$): δ 9.17 (s, 1H), 7.96 (d, J = 7.3 Hz, 1H), 7.89 (d, J = 9.8 Hz, 1H), 7.78 (t, J = 8.0 Hz, 1H), 7.68 (d, J = 9.8 Hz, 1H), 7.51 (d, J = 7.7 Hz, 1H), 7.34 – 7.28 (m, 6H), 7.22 – 7.19 (m, 2H), 7.12 – 7.10 (m, 2H), 6.82 (d, J = 8.7 Hz, 2H), 6.72 (d, J = 8.7 Hz, 2H), 5.44 (s, 2H), 3.73 (s, 3H). ^{13}C NMR (101 MHz, $CDCl_3$): δ 159.9, 146.2, 134.1, 131.42, 131.39, 131.0, 129.64, 129.59, 129.5, 129.1, 128.9, 128.8, 128.7, 128.1, 127.0, 126.5, 125.8, 125.2, 124.8, 124.5, 124.3, 121.1, 117.8, 114.3, 55.4, 53.3. HRMS (ESI) *m*/*z*: calcd. for $C_{33}H_{25}N_2O$ [M^+]: 465.1962; found: 465.1973.

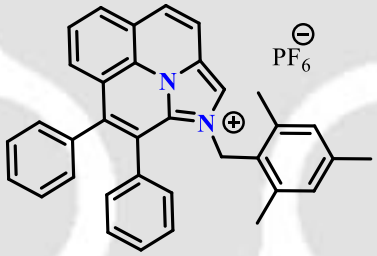
1-(4-chlorobenzyl)-8,9-diphenylbenzo[*ij*]imidazo[2,1,5-*de*]quinolizin-1-ium hexafluorophosphate (4.3k)

TH-3565_186122020



The title compound **4.3k** was isolated as brown solid using neutral alumina column chromatography with ethyl acetate/ methanol (v/v = 10:1, R_f = 0.25) in 81% yield (99.6 mg) from GP-III; 83% yield (102.1 mg) from GP-IV. m.p. = 125–128 °C. ^{1}H NMR (500 MHz, $CDCl_3$): δ 9.37 (s, 1H), 8.04 (d, J = 7.6 Hz, 1H), 7.85 – 7.80 (m, 2H), 7.76 (d, J = 9.8 Hz, 1H), 7.52 (d, J = 8.2 Hz, 1H), 7.34 – 7.30 (m, 4H), 7.22 (t, J = 7.6 Hz, 2H), 7.12 – 7.08 (m, 6H), 6.69 (d, J = 8.1 Hz, 2H), 5.62 (s, 2H). ^{13}C NMR (126 MHz, $CDCl_3$): δ 146.5, 134.1, 133.7, 133.1, 131.3, 130.9, 130.8, 129.4, 129.2, 128.7, 128.6, 128.2, 127.3, 126.0, 124.93, 124.91, 124.8, 124.1, 124.0, 120.9, 117.2, 52.8. HRMS (ESI) *m/z*: calcd. for $C_{32}H_{22}ClN_2$ [M^+]: 469.1467; found: 469.1469.

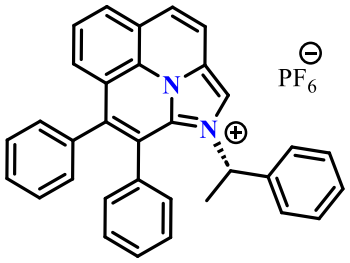
1-mesitylyl-8,9-diphenylbenzo[*ij*]imidazo[2,1,5-*de*]quinolizin-1-ium hexafluorophosphate (4.3l)



The title compound **4.3l** was isolated as brown solid using neutral alumina column chromatography with ethyl acetate/ methanol (v/v = 10:1, R_f = 0.35) in 79% yield (98.4 mg) from GP-III; 84% yield (104.6 mg) from GP-IV. m.p. = 138–140 °C. ^{1}H NMR (600 MHz, $CDCl_3$): δ 8.01 (d, J = 7.6 Hz, 1H), 7.80 (t, J = 8.0 Hz, 1H), 7.76 (d, J = 9.8 Hz, 1H), 7.71 (d, J = 9.8 Hz, 1H), 7.61 (d, J = 7.1 Hz, 2H), 7.55 (d, J = 8.2 Hz, 1H), 7.42 – 7.39 (m, 2H), 7.38 – 7.32 (m, 5H), 7.26 – 7.25 (m, 2H), 6.94 (s, 2H), 4.89 (s, 2H), 2.30 (s, 3H), 2.16 (s, 6H). ^{13}C NMR (151 MHz, $CDCl_3$): δ 146.2, 140.2, 138.5, 134.0, 132.10, 132.06, 131.1, 130.0, 129.7, 129.6, 129.5, 128.9, 128.73, 128.66, 128.2, 127.7, 126.0, 125.8, 125.1, 125.0, 124.9, 124.6, 124.4, 116.9, 115.5, 49.1, 21.1, 19.9. HRMS (ESI) *m/z*: calcd. for $C_{35}H_{29}N_2$ [M^+]: 477.2326; found: 477.2328.

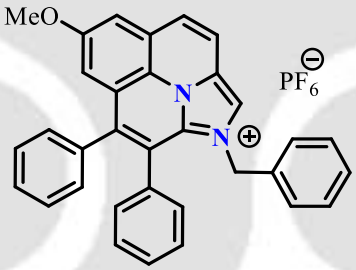
(*S*)-8,9-diphenyl-1-(1-phenylethyl)benzo[*ij*]imidazo[2,1,5-*de*]quinolizin-1-ium hexafluorophosphate (4.3m)

TH-3565_186122020



The title compound **4.3m** was isolated as viscous brown oil using neutral alumina column chromatography with ethyl acetate/ methanol (v/v = 10:1, R_f = 0.3) in 85% yield (101 mg) from GP-III; 91% yield (108.2 mg) from GP-IV. ^{1}H NMR (400 MHz, $CDCl_3$): δ 9.46 (s, 1H), 8.19 (d, J = 9.8 Hz, 1H), 8.01 (d, J = 7.6 Hz, 1H), 7.79 (t, J = 8.0 Hz, 1H), 7.73 (d, J = 9.8 Hz, 1H), 7.53 – 7.44 (m, 3H), 7.38 – 7.34 (m, 2H), 7.31 – 7.24 (m, 5H), 7.19 – 7.16 (m, 2H), 7.07 – 7.04 (m, 1H), 6.96 – 6.94 (m, 3H), 5.37 (q, J = 7.0 Hz, 1H), 1.98 (d, J = 7.0 Hz, 3H). ^{13}C NMR (151 MHz, $CDCl_3$): δ 146.6, 138.6, 134.0, 131.8, 131.0, 130.9, 130.3, 129.7, 129.5, 129.4, 129.3, 129.2, 129.1, 129.0, 128.92, 128.90, 128.7, 128.6, 128.3, 127.2, 126.4, 126.1, 125.30, 125.27, 125.1, 124.7, 124.1, 118.3, 118.1, 58.9, 22.5. HRMS (ESI) *m/z*: calcd. for $C_{33}H_{25}N_2$ [M^+]: 449.2013; found: 449.2014. $[\alpha]_D^{20.0}$ = +215.01º (0.005 M, $CHCl_3$).

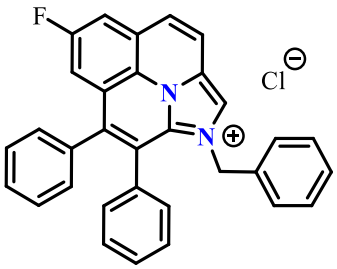
1-benzyl-6-methoxy-8,9-diphenylbenzo[*ij*]imidazo[2,1,5-*de*]quinolizin-1-ium hexafluorophosphate (4.4a)



The title compound **4.4a** was isolated as brown solid using neutral alumina column chromatography with ethyl acetate/ methanol (v/v = 20:1, R_f = 0.4) in 80% yield (97.7 mg) from GP-III; 78% yield (95.2 mg) from GP-IV. m.p. = 218–220 °C. ^{1}H NMR (400 MHz, $CDCl_3$): δ 8.05 (s, 1H), 7.67 – 7.59 (m, 2H), 7.51 – 7.50 (m, 1H), 7.31 – 7.22 (m, 11H), 7.15 – 7.13 (m, 2H), 6.93 – 6.92 (m, 1H), 6.85 – 6.84 (m, 2H), 5.16 (s, 2H), 3.83 (s, 3H). ^{13}C NMR (101 MHz, $CDCl_3$): δ 159.2, 145.8, 134.2, 134.0, 131.5, 131.2, 131.0, 129.5, 129.4, 129.2, 128.9, 128.81, 128.78, 128.7, 127.6, 127.2, 126.7, 126.5, 124.90, 124.86, 123.9, 119.4, 117.6, 112.6, 109.1, 56.1, 53.6. HRMS (ESI) *m/z*: calcd. for $C_{33}H_{25}N_2O$ [M^+]: 465.1962; found: 465.1963.

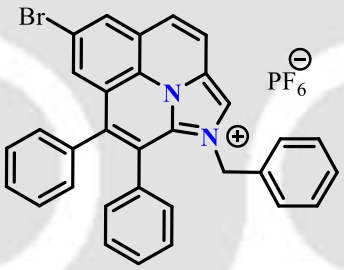
1-benzyl-6-fluoro-8,9-diphenylbenzo[*ij*]imidazo[2,1,5-*de*]quinolizin-1-ium chloride (4.4b)

TH-3565_186122020



The title compound **4.4b** was isolated as yellow oil using neutral alumina column chromatography with ethyl acetate/ methanol (v/v = 10:1, R_f = 0.4) in 88% yield (86 mg) from GP-III; 86% yield (84.1 mg) from GP-IV. ^{1}H NMR (600 MHz, $CDCl_3$): δ 9.16 (s, 1H), 8.07 (d, J = 9.6 Hz, 1H), 7.72 – 7.69 (m, 2H), 7.33 – 7.28 (m, 4H), 7.22 – 7.19 (m, 3H), 7.17 – 7.12 (m, 5H), 7.10 – 7.08 (m, 2H), 6.69 (d, J = 7.4 Hz, 2H), 5.49 (s, 2H). ^{13}C NMR (151 MHz, $CDCl_3$): δ 176.7, 162.1, 160.5, 145.5 (d, C-F, $J_{C\text{-}F}$ = 4.2 Hz), 134.5, 133.6, 131.0, 130.9, 130.8, 129.6, 129.3, 128.94, 128.88, 128.7, 128.5, 127.5 (d, C-F, $J_{C\text{-}F}$ = 10.0 Hz), 127.1 (d, C-F, $J_{C\text{-}F}$ = 9.7 Hz), 126.9, 126.4, 126.3 (d, C-F, $J_{C\text{-}F}$ = 2.6 Hz), 125.6, 124.0, 122.7, 119.5, 113.2 (d, C-F, $J_{C\text{-}F}$ = 26.1 Hz), 110.7 (d, C-F, $J_{C\text{-}F}$ = 26.5 Hz), 53.8. ^{19}F NMR (565 MHz, $CDCl_3$): δ -107.9. HRMS (ESI) m/z: calcd. for $C_{32}H_{22}FN_2$ [M^+]: 453.1762; found: 453.1761.

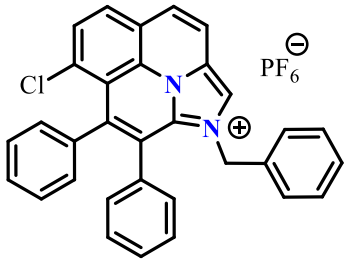
1-benzyl-6-bromo-8,9-diphenylbenzo[*ij*]imidazo[2,1,5-*de*]quinolizin-1-ium hexafluorophosphate (4.4c)



The title compound **4.4c** was isolated as yellow oil using neutral alumina column chromatography with ethyl acetate/ methanol (v/v = 10:1, R_f = 0.4) in 85% yield (112.1 mg) from GP-III; 82% yield (108.1 mg) from GP-IV. ^{1}H NMR (500 MHz, $CDCl_3$): δ 9.33 (s, 1H), 8.08 (s, 1H), 8.01 – 7.99 (m, 1H), 7.66 – 7.64 (m, 1H), 7.59 (s, 1H), 7.34 – 7.29 (m, 4H), 7.23 – 7.20 (m, 3H), 7.17 – 7.14 (m, 4H), 7.10 – 7.09 (m, 2H), 6.78 – 6.77 (m, 2H), 5.58 (s, 2H). ^{13}C NMR (151 MHz, $CDCl_3$): δ 145.2, 134.3, 133.4, 131.4, 130.9, 130.8, 129.6, 129.4, 129.01, 128.96, 128.9, 128.8, 128.6, 128.3, 127.1, 126.9, 126.8, 126.6, 125.9, 125.7, 124.0, 122.4, 122.3, 119.2, 53.9. HRMS (ESI) m/z: calcd. for $C_{32}H_{22}BrN_2$ [M^+]: 513.0961; found: 513.0970.

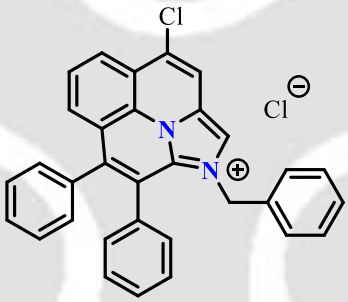
1-benzyl-7-chloro-8,9-diphenylbenzo[*ij*]imidazo[2,1,5-*de*]quinolizin-1-ium hexafluorophosphate (4.4d)

TH-3565_186122020



The title compound **4.4d** was isolated as brown solid using neutral alumina column chromatography with ethyl acetate/ methanol (v/v = 10:1, R_f = 0.3) in 92% yield (113.2 mg) from GP-III; 93% yield (114.4 mg) from GP-IV. m.p. = 230–233 °C. ^{1}H NMR (500 MHz, $CDCl_3$): δ 7.85 – 7.81 (m, 2H), 7.71 (s, 1H), 7.60 (d, J = 9.8 Hz, 1H), 7.52 (d, J = 9.8 Hz, 1H), 7.29 – 7.26 (m, 3H), 7.20 – 7.15 (m, 8H), 7.11 – 7.09 (m, 2H), 6.90 (d, J = 8.1 Hz, 2H), 4.95 (s, 2H). ^{13}C NMR (151 MHz, $CDCl_3$): δ 145.9, 135.8, 133.3, 132.0, 131.32, 131.29, 131.1, 130.5, 130.3, 129.4, 129.2, 128.6, 128.2, 127.9, 127.7, 127.5, 126.9, 126.4, 125.2, 124.5, 121.9, 118.2, 116.3, 53.6. HRMS (ESI) *m/z*: calcd. for $C_{32}H_{22}ClN_2$ [M^+]: 469.1467; found: 469.1466.

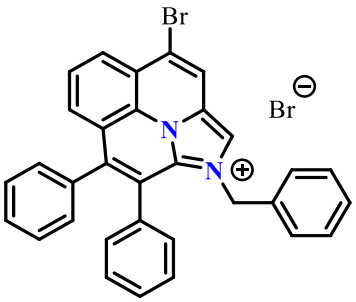
1-benzyl-4-chloro-8,9-diphenylbenzo[*ij*]imidazo[2,1,5-*de*]quinolizin-1-ium chloride (4.4e)



The title compound **4.4e** was isolated as off-white solid using neutral alumina column chromatography with ethyl acetate/ methanol (v/v = 8:1, R_f = 0.4) in 91% yield (92 mg) from GP-III; 93% yield (94.4 mg) from GP-IV. m.p. = 265–268 °C. ^{1}H NMR (500 MHz, $CDCl_3$): δ 8.26 (d, J = 7.9 Hz, 1H), 7.88 (t, J = 8.0 Hz, 1H), 7.79 (s, 1H), 7.73 (s, 1H), 7.63 (d, J = 8.2 Hz, 1H), 7.31 – 7.21 (m, 11H), 7.17 – 7.16 (m, 2H), 6.88 – 6.87 (m, 2H), 5.08 (s, 2H). ^{13}C NMR (126 MHz, $CDCl_3$): δ 147.0, 134.1, 133.4, 132.5, 132.3, 131.3, 131.0, 129.6, 129.5, 129.4, 129.3, 129.1, 128.8, 128.7, 128.2, 127.7, 126.5, 125.4, 124.6, 124.0, 123.7, 123.2, 118.2, 115.5, 53.8. HRMS (ESI) *m/z*: calcd. for $C_{32}H_{22}ClN_2$ [M^+]: 469.1467; found: 469.1468.

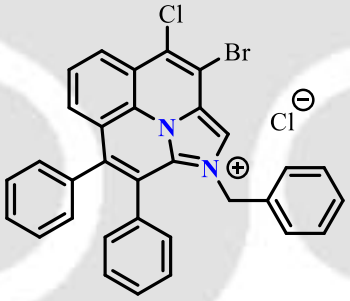
1-benzyl-4-bromo-8,9-diphenylbenzo[*ij*]imidazo[2,1,5-*de*]quinolizin-1-ium bromide (4.4f)

TH-3565_186122020



The title compound **4.4f** was isolated as white solid using neutral alumina column chromatography with ethyl acetate/ methanol (v/v = 8:1, R_f = 0.4) in 85% yield (101 mg) from GP-III; 88% yield (104.6 mg) from GP-IV. m.p. = 266–269 °C. ^{1}H NMR (400 MHz, $CDCl_3$): δ 9.03 (s, 1H), 8.28 (dd, J = 7.8, 1.0 Hz, 1H), 8.02 (s, 1H), 7.90 (t, J = 8.1 Hz, 1H), 7.64 (dd, J = 8.3, 1.0 Hz, 1H), 7.33 – 7.28 (m, 4H), 7.24 – 7.18 (m, 7H), 7.14 – 7.12 (m, 2H), 6.87 – 6.84 (m, 2H), 5.52 (s, 2H). ^{13}C NMR (151 MHz, $CDCl_3$): δ 146.4, 134.1, 133.9, 132.1, 131.8, 131.1, 131.0, 129.63, 129.55, 129.4, 129.1, 128.9, 128.86, 128.82, 128.3, 127.5, 126.3, 125.3, 124.9, 124.0, 123.5, 123.4, 120.9, 116.5, 54.1. HRMS (ESI) *m/z*: calcd. for $C_{32}H_{22}BrN_2$ [M^+]: 513.0961; found: 513.0965.

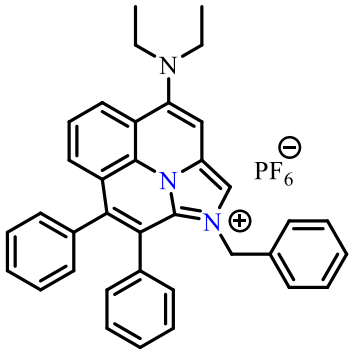
1-benzyl-3-bromo-4-chloro-8,9-diphenylbenzo[*ij*]imidazo[2,1,5-*de*]quinolizin-1-ium chloride (4.4g)



The title compound **4.4g** was isolated as brown solid using neutral alumina column chromatography with ethyl acetate/ methanol (v/v = 5:1, R_f = 0.4) in 73% yield (85.3 mg) from GP-III; 68% yield (79.5 mg) from GP-IV. m.p. = 168–170 °C. ^{1}H NMR (600 MHz, $CDCl_3$): δ 9.14 (s, 1H), 8.28 (d, J = 7.8 Hz, 1H), 8.03 (s, 1H), 7.90 (t, J = 8.0 Hz, 1H), 7.63 (d, J = 8.2 Hz, 1H), 7.31 – 7.29 (m, 3H), 7.23 – 7.21 (m, 5H), 7.19 – 7.17 (m, 2H), 7.12 – 7.11 (m, 2H), 6.81 (d, J = 7.4 Hz, 2H), 5.53 (s, 2H). ^{13}C NMR (151 MHz, $CDCl_3$): δ 146.3, 134.2, 133.9, 132.0, 131.8, 131.1, 131.0, 129.6, 129.5, 129.4, 129.0, 128.85, 128.81, 128.78, 128.7, 128.3, 127.3, 126.2, 125.3, 124.9, 123.9, 123.6, 123.4, 121.3, 116.6, 54.1. HRMS (ESI) *m/z*: calcd. for $C_{32}H_{21}BrClN_2$ [M^+]: 547.0572; found: 547.0578.

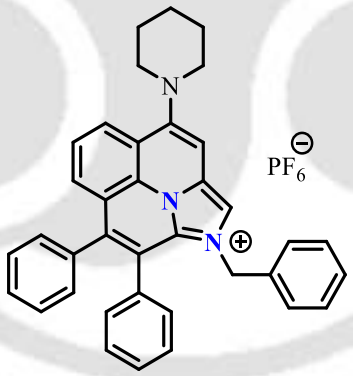
1-benzyl-4-(diethylamino)-8,9-diphenylbenzo[*ij*]imidazo[2,1,5-*de*]quinolizin-1-ium hexafluorophosphate (4.4h)

TH-3565_186122020



The title compound **4.4h** was isolated as black solid using neutral alumina column chromatography with ethyl acetate/ methanol (v/v = 20:1, R_f = 0.3) in 92% yield (120 mg) from GP-III; 92% yield (120 mg) from GP-IV. m.p. = 198–200 °C. ^{1}H NMR (500 MHz, $CDCl_3$): δ 9.21 (d, J = 10.0 Hz, 1H), 8.16 (d, J = 7.9 Hz, 1H), 7.83 (t, J = 8.1 Hz, 1H), 7.55 (d, J = 8.1 Hz, 1H), 7.32 – 7.27 (m, 5H), 7.21 – 7.13 (m, 5H), 7.09 – 7.06 (m, 4H), 6.74 (d, J = 7.7 Hz, 2H), 5.59 (s, 2H), 3.35 (q, J = 7.0 Hz, 4H), 1.22 (t, J = 6.9 Hz, 6H). ^{13}C NMR (151 MHz, $CDCl_3$): δ 146.5, 144.9, 135.0, 134.3, 131.3, 130.9, 130.3, 130.1, 129.6, 129.3, 128.75, 128.68, 128.64, 128.57, 128.3, 127.5, 126.9, 125.5, 125.1, 124.8, 123.95, 123.90, 123.4, 119.2, 104.2, 53.5, 45.3, 12.0. HRMS (ESI) *m/z*: calcd. for $C_{36}H_{32}N_3$ [M^+]: 506.2591; found: 506.2591.

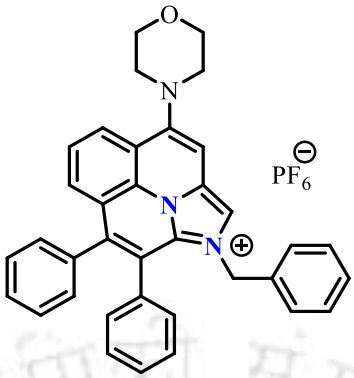
1-benzyl-8,9-diphenyl-4-(piperidin-1-yl)benzo[*ij*]imidazo[2,1,5-*de*]quinolizin-1-ium hexafluorophosphate (4.4i)



The title compound **4.4i** was isolated as brown solid using neutral alumina column chromatography with ethyl acetate/ methanol (v/v = 10:1, R_f = 0.3) in 90% yield (119.5 mg) from GP-III; 86% yield (114.1 mg) from GP-IV. m.p. = 196–198 °C. ^{1}H NMR (500 MHz, $CDCl_3$): δ 8.97 (s, 1H), 8.09 (d, J = 7.9 Hz, 1H), 7.85 (t, J = 8.0 Hz, 1H), 7.55 (d, J = 8.1 Hz, 1H), 7.31 – 7.26 (m, 5H), 7.21 – 7.14 (m, 5H), 7.11 – 7.09 (m, 4H), 6.73 (d, J = 7.2 Hz, 2H), 5.50 (s, 2H), 3.17 (brs, 4H), 1.89 (brs, 4H), 1.75 (brs, 2H). ^{13}C NMR (126 MHz, $CDCl_3$): δ 149.4, 145.0, 134.7, 134.2, 131.3, 130.9, 130.4, 129.9, 129.6, 129.3, 128.8, 128.61, 128.59, 128.5, 128.3, 127.5, 126.8, 125.4, 125.3, 124.9, 123.8, 123.2, 122.9, 119.1, 101.7, 53.5, 52.6, 26.1, 24.3. HRMS (ESI) *m/z*: calcd. for $C_{37}H_{32}N_3$ [M^+]: 518.2591; found: 518.2594.

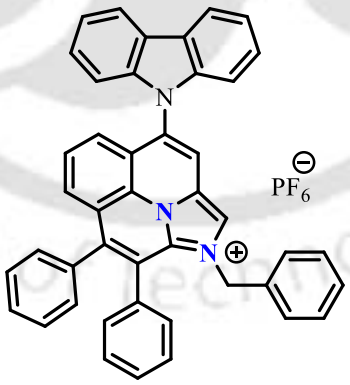
TH-3565_186122020

1-benzyl-4-morpholino-8,9-diphenylbenzo[*ij*]imidazo[2,1,5-*de*]quinolizin-1-ium hexafluorophosphate (4.4j)



The title compound **4.4j** was isolated as brown solid using neutral alumina column chromatography with ethyl acetate/ methanol (v/v = 10:1, R_f = 0.3) in 94% yield (125.1 mg) from GP-III; 91% yield (121.1 mg) from GP-IV. m.p. = 198–200 °C. ^{1}H NMR (500 MHz, $CDCl_3$): δ 9.11 (s, 1H), 8.11 (d, J = 7.9 Hz, 1H), 7.84 (t, J = 8.0 Hz, 1H), 7.56 (d, J = 8.2 Hz, 1H), 7.45 (s, 1H), 7.30 – 7.26 (m, 4H), 7.20 – 7.13 (m, 5H), 7.10 – 7.08 (m, 4H), 6.72 (d, J = 7.0 Hz, 2H), 5.50 (s, 2H), 4.01 (t, J = 4.5 Hz, 4H), 3.23 (t, J = 4.5 Hz, 4H). ^{13}C NMR (126 MHz, $CDCl_3$): δ 147.9, 145.2, 134.7, 134.2, 131.3, 130.9, 130.6, 130.1, 129.6, 129.4, 128.8, 128.70, 128.67, 128.6, 128.5, 127.6, 126.9, 125.6, 125.2, 125.1, 124.1, 122.9, 122.4, 119.9, 102.8, 66.9, 53.6, 51.7. HRMS (ESI) *m/z*: calcd. for $C_{36}H_{30}N_3O$ [M^+]: 520.2384; found: 520.2390.

1-benzyl-4-(9*H*-carbazol-9-yl)-8,9-diphenylbenzo[*ij*]imidazo[2,1,5-*de*]quinolizin-1-ium hexafluorophosphate (4.4k)

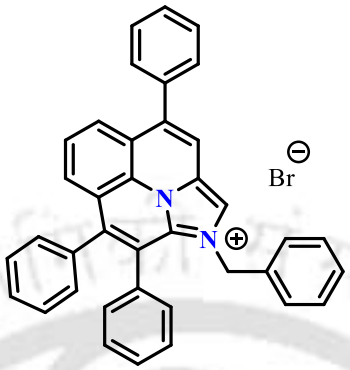


The title compound **4.4k** was isolated as black solid using neutral alumina column chromatography with ethyl acetate/ methanol (v/v = 5:1, R_f = 0.4) in 87% yield (129.8 mg) from GP-III; 83% yield (123.8 mg) from GP-IV. m.p. = 220–224 °C. ^{1}H NMR (500 MHz, $CDCl_3$): δ 9.38 (brs, 1H), 8.21 (d, J = 7.8 Hz, 2H), 8.06 (s, 1H), 7.60 (brs, 2H), 7.43 – 7.40 (m, 2H), 7.38 – 7.35 (m, 2H), 7.35 – 7.32 (m, 5H), 7.27 – 7.20 (m, 9H), 7.15 (d, J = 6.8 Hz, 2H), 6.87 (d, J = 7.0 Hz, 2H), 5.70 (s, 2H). ^{13}C NMR (151 MHz, $CDCl_3$): δ 146.5, 140.3, 134.5, 134.2, 133.9, 132.1, 131.09, 131.05, 130.7, 129.6, 129.5, 129.0, 128.83, 128.82, 128.7, 128.3,

TH-3565_186122020

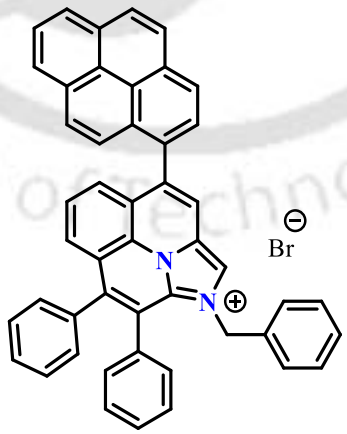
128.1, 127.3, 126.7, 126.0, 125.7, 124.9, 124.1, 123.7, 123.4, 122.9, 122.7, 121.2, 120.9, 117.9, 110.4, 54.1. HRMS (ESI) *m/z*: calcd. for $C_{44}H_{30}N_3$ [M^+]: 600.2435; found: 600.2438.

1-benzyl-4,8,9-triphenylbenzo[*ij*]imidazo[2,1,5-*de*]quinolizin-1-ium bromide (4.4l)



The title compound **4.4l** was isolated as off-white solid using neutral alumina column chromatography with ethyl acetate/ methanol (v/v = 20:1, R_f = 0.3) in 84% yield (99.4 mg) from GP-III; 87% yield (102.9 mg) from GP-IV. m.p. = 142–144 °C. ^{1}H NMR (500 MHz, $CDCl_3$): δ 9.10 (s, 1H), 7.93 (d, J = 7.9 Hz, 1H), 7.71 (t, J = 8.0 Hz, 1H), 7.67 (s, 1H), 7.56 – 7.52 (m, 6H), 7.30 – 7.25 (m, 4H), 7.21 – 7.15 (m, 7H), 7.11 – 7.09 (m, 2H), 6.80 – 6.78 (m, 2H), 5.57 (s, 2H). ^{13}C NMR (126 MHz, $CDCl_3$): δ 146.2, 139.9, 136.6, 134.6, 134.1, 131.5, 131.2, 131.0, 129.8, 129.52, 129.45, 129.44, 129.38, 128.9, 128.74, 128.70, 128.70, 128.6, 128.5, 127.9, 127.1, 125.5, 125.3, 125.2, 125.0, 124.5, 124.0, 121.0, 116.3, 53.8. HRMS (ESI) *m/z*: calcd. for $C_{38}H_{27}N_2$ [M^+]: 511.2169; found: 511.2167.

1-benzyl-8,9-diphenyl-4-(pyren-1-yl)benzo[*ij*]imidazo[2,1,5-*de*]quinolizin-1-ium bromide (4.4m)

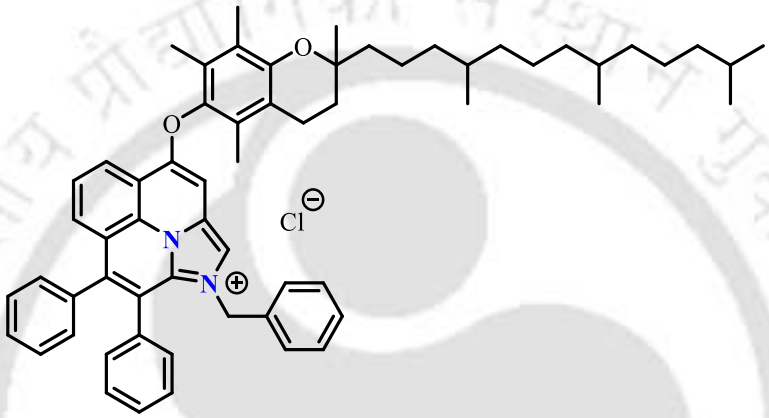


The title compound **4.4m** was isolated as pale-yellow solid using neutral alumina column chromatography with ethyl acetate/ methanol (v/v = 5:1, R_f = 0.4) in 71% yield (101.6 mg) from GP-III; 74% yield (105.9 mg) from GP-IV. m.p. = 145–148 °C. ^{1}H NMR (500 MHz, $CDCl_3$): δ 9.09 (s, 1H), 8.32 (d, J = 7.7 Hz, 1H), 8.25 (d, J = 7.6 Hz, 1H), 8.18 – 8.13 (m, 3H),

TH-3565_186122020

8.05 – 8.02 (m, 2H), 7.99 (d, J = 9.1 Hz, 1H), 7.87 – 7.84 (m, 2H), 7.54 (d, J = 4.4 Hz, 2H), 7.35 – 7.27 (m, 5H), 7.24 – 7.20 (m, 7H), 7.17 – 7.13 (m, 2H), 6.89 – 6.87 (m, 2H), 5.63 (s, 2H). ^{13}C NMR (151 MHz, $CDCl_3$): δ 146.4, 139.1, 134.6, 134.1, 132.1, 131.7, 131.3, 131.2, 131.1, 131.0, 130.9, 130.7, 129.54, 129.51, 129.46, 129.1, 128.9, 128.73, 128.71, 128.68, 128.6, 128.5, 127.9, 127.4, 127.2, 127.0, 126.5, 126.2, 126.0, 125.8, 125.7, 125.4, 125.2, 125.0, 124.7, 124.5, 124.3, 124.0, 121.0, 118.0, 53.9. HRMS (ESI) *m/z*: calcd. for $C_{48}H_{31}N_2$ [M^+]: 635.2482; found: 635.2481.

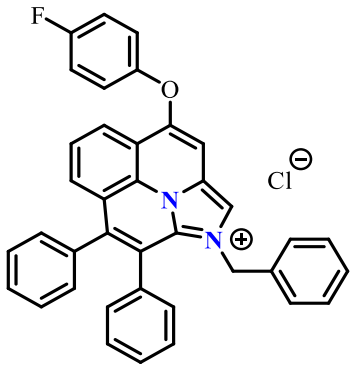
1-benzyl-8,9-diphenyl-4-((2,5,7,8-tetramethyl-2-(4,8,12-trimethyltridecyl)chroman-6-yl)oxy)benzo[*ij*]imidazo[2,1,5-*de*]quinolizin-1-ium chloride (4.4n)



The title compound **4.4n** was isolated as brown solid using neutral alumina column chromatography with ethyl acetate/ methanol (v/v = 10:1, R_f = 0.2) in 88% yield (158.3 mg) from GP-III; 80% yield (143.9 mg) from GP-IV. m.p. = 190–195 °C. ^{1}H NMR (500 MHz, $CDCl_3$): δ 9.14 – 9.06 (m, 1H), 8.53 (d, J = 7.8 Hz, 1H), 7.94 (t, J = 8.0 Hz, 1H), 7.67 (d, J = 8.2 Hz, 1H), 7.32 – 7.31 (m, 4H), 7.23 – 7.19 (m, 2H), 7.15 – 7.06 (m, 7H), 6.74 (t, J = 8.2 Hz, 2H), 6.49 (d, J = 6.5 Hz, 1H), 5.68 (d, J = 15.5 Hz, 1H), 5.57 (dd, J = 15.5, 6.5 Hz, 1H), 2.75 – 2.65 (m, 2H), 2.19 – 2.18 (m, 3H), 2.07 (s, 3H), 2.04 (s, 3H), 1.97 (s, 1H), 1.88 (t, J = 6.7 Hz, 1H), 1.70 – 1.58 (m, 2H), 1.56 – 1.49 (m, 2H), 1.48 – 1.42 (m, 2H), 1.34 – 1.22 (m, 12H), 1.18 – 1.06 (m, 6H), 0.91 – 0.86 (m, 12H). ^{13}C NMR (126 MHz, $CDCl_3$): δ 153.0, 150.0, 144.7, 141.9, 141.8, 134.9, 134.8, 134.0, 131.2, 131.1, 130.9, 130.8, 130.4, 129.8, 129.5, 129.3, 128.7, 128.64, 128.60, 128.58, 128.5, 128.2, 128.0, 127.0, 126.94, 126.89, 125.7, 125.3, 125.1, 124.7, 124.3, 121.1, 120.4, 119.1, 118.9, 118.6, 118.5, 93.5, 75.4, 53.4, 39.4, 37.5, 37.4, 37.3, 32.8, 27.9, 24.8, 24.4, 24.0, 23.6, 22.7, 22.6, 21.1, 21.0, 20.7, 19.75, 19.68, 19.6, 12.6, 11.9, 11.8. HRMS (ESI) *m/z*: calcd. for $C_{61}H_{71}N_2O_2$ [M^+]: 863.5511; found: 863.5517.

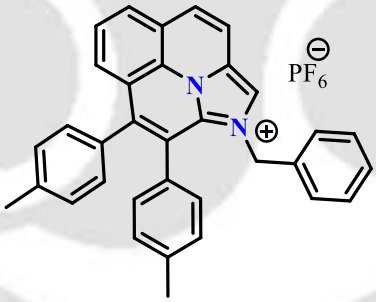
1-benzyl-4-(4-fluorophenoxy)-8,9-diphenylbenzo[*ij*]imidazo[2,1,5-*de*]quinolizin-1-ium chloride (4.4o)

TH-3565_186122020



The title compound **4.4o** was isolated as black solid using neutral alumina column chromatography with ethyl acetate/ methanol (v/v = 5:1, R_f = 0.3) in 94% yield (109.2 mg) from GP-III; 90% yield (104.6 mg) from GP-IV. m.p. = 215–218 °C. ^{1}H NMR (500 MHz, $CDCl_3$): δ 9.02 (s, 1H), 8.42 (d, J = 7.7 Hz, 1H), 7.90 (t, J = 8.0 Hz, 1H), 7.66 (d, J = 8.2 Hz, 1H), 7.33 – 7.20 (m, 11H), 7.17 – 7.12 (m, 6H), 6.80 – 6.77 (m, 3H), 5.57 (s, 2H). ^{13}C NMR (151 MHz, $CDCl_3$): δ 161.5, 159.9, 154.0, 149.2 (d, C-F, $J_{C\text{-}F}$ = 2.7 Hz), 145.0, 134.8, 134.1, 131.2, 131.0, 130.8, 129.9, 129.7, 129.5, 128.8, 128.7 (d, C-F, $J_{C\text{-}F}$ = 6.5 Hz), 128.5, 128.0, 127.1, 126.0, 125.1, 124.6, 124.3, 123.0 (d, C-F, $J_{C\text{-}F}$ = 8.7 Hz), 121.3, 120.7, 119.8, 117.6, 117.4, 95.8, 53.6. ^{19}F NMR (471 MHz, $CDCl_3$): δ -115.3. HRMS (ESI) *m/z*: calcd. for $C_{38}H_{26}FN_2O$ [M^+]: 545.2024; found: 545.2011.

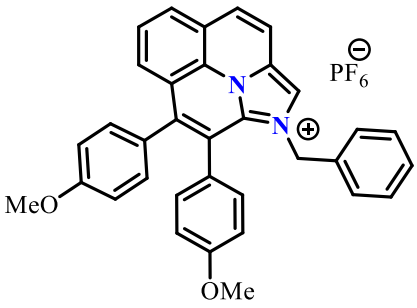
1-benzyl-8,9-di-*p*-tolylbenzo[*ij*]imidazo[2,1,5-*de*]quinolizin-1-ium hexafluorophosphate (4.5a)



The title compound **4.5a** was isolated as black solid using neutral alumina column chromatography with ethyl acetate/ methanol (v/v = 10:1, R_f = 0.4) in 90% yield (109.5 mg) from GP-III; 91% yield (110.8 mg) from GP-IV. m.p. = 234–237 °C. ^{1}H NMR (500 MHz, $CDCl_3$): δ 7.91 (d, J = 7.5 Hz, 1H), 7.78 (s, 1H), 7.74 (t, J = 8.0 Hz, 1H), 7.62 (d, J = 9.8 Hz, 1H), 7.55 – 7.51 (m, 2H), 7.27 – 7.26 (m, 3H), 7.13 – 7.11 (m, 4H), 7.05 – 7.02 (m, 4H), 6.90 – 6.88 (m, 2H), 5.08 (s, 2H), 2.32 (s, 3H), 2.29 (s, 3H). ^{13}C NMR (126 MHz, $CDCl_3$): δ 147.1, 139.5, 138.5, 133.8, 132.4, 131.2, 130.8, 129.8, 129.6, 129.5, 129.4, 129.2, 129.1, 128.4, 128.0, 127.8, 127.7, 125.9, 125.5, 125.2, 124.9, 124.49, 124.46, 118.2, 116.6, 53.6, 21.5, 21.4. HRMS (ESI) *m/z*: calcd. for $C_{34}H_{27}N_2$ [M^+]: 463.2169; found: 463.2179.

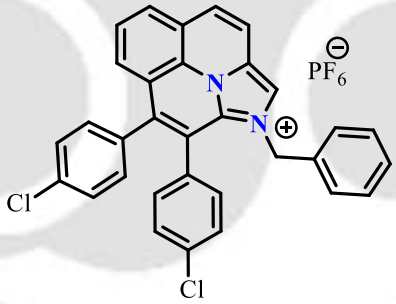
1-benzyl-8,9-bis(4-methoxyphenyl)benzo[*ij*]imidazo[2,1,5-*de*]quinolizin-1-ium hexafluorophosphate (4.5b)

TH-3565_186122020



The title compound **4.5b** was isolated as brown solid using neutral alumina column chromatography with ethyl acetate/ methanol (v/v = 10:1, R_f = 0.45) in 88% yield (113 mg) from GP-III; 90% yield (115.3 mg) from GP-IV. m.p. = 233–235 °C. ^{1}H NMR (500 MHz, $CDCl_3$): δ 9.14 (s, 1H), 7.94 – 7.92 (m, 1H), 7.83 (d, J = 9.8 Hz, 1H), 7.76 (t, J = 8.0 Hz, 1H), 7.65 (d, J = 9.8 Hz, 1H), 7.54 (d, J = 8.2 Hz, 1H), 7.19 – 7.14 (m, 3H), 7.02 – 6.99 (m, 4H), 6.84 – 6.79 (m, 4H), 6.73 – 6.71 (m, 2H), 5.57 (s, 2H), 3.78 (s, 3H), 3.77 (s, 3H). ^{13}C NMR (126 MHz, $CDCl_3$): δ 160.2, 159.7, 146.6, 134.8, 132.2, 132.0, 130.8, 129.6, 128.9, 128.5, 128.1, 127.1, 126.2, 125.7, 125.6, 125.2, 124.9, 124.5, 124.2, 123.2, 121.1, 117.7, 114.30, 114.26, 55.5, 55.4, 53.7. HRMS (ESI) *m/z*: calcd. for $C_{34}H_{27}N_2O_2$ [M^+]: 495.2068; found: 495.2069.

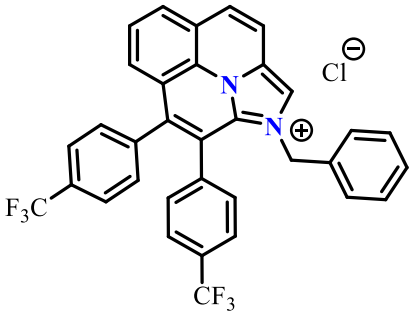
1-benzyl-8,9-bis(4-chlorophenyl)benzo[*ij*]imidazo[2,1,5-*de*]quinolizin-1-ium hexafluorophosphate (4.5c)



The title compound **4.5c** was isolated as off-white solid using neutral alumina column chromatography with ethyl acetate/ methanol (v/v = 8:1, R_f = 0.4) in 78% yield (101.3 mg) from GP-III; 82% yield (106.5 mg) from GP-IV. m.p. = 230–232 °C. ^{1}H NMR (500 MHz, $CDCl_3$): δ 8.95 (s, 1H), 7.97 (d, J = 7.7 Hz, 1H), 7.81 – 7.75 (m, 2H), 7.67 (d, J = 9.0 Hz, 1H), 7.43 (d, J = 8.2 Hz, 1H), 7.29 (d, J = 8.1 Hz, 2H), 7.20 – 7.14 (m, 7H), 7.05 (d, J = 8.2 Hz, 2H), 6.72 (d, J = 7.2 Hz, 2H), 5.55 (s, 2H). ^{13}C NMR (126 MHz, $CDCl_3$): δ 145.1, 135.8, 135.1, 134.3, 132.40, 132.36, 131.5, 130.9, 129.7, 129.4, 129.3, 129.0, 128.9, 128.6, 128.3, 127.3, 126.7, 126.2, 125.2, 125.0, 124.9, 124.5, 124.3, 123.8, 121.1, 117.6, 54.2. HRMS (ESI) *m/z*: calcd. for $C_{32}H_{21}Cl_2N_2$ [M^+]: 503.1077; found: 503.1081.

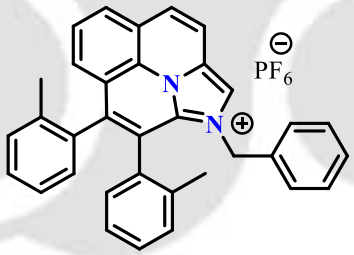
1-benzyl-8,9-bis(4-(trifluoromethyl)phenyl)benzo[*ij*]imidazo[2,1,5-*de*]quinolizin-1-ium chloride (4.5d)

TH-3565_186122020



The title compound **4.5d** was isolated as brown solid using neutral alumina column chromatography with ethyl acetate/ methanol (v/v = 10:1, R_f = 0.35) in 77% yield (93.5 mg) from GP-III; 83% yield (100.8 mg) from GP-IV. m.p. = 228–230 °C. ^{1}H NMR (600 MHz, $CDCl_3$): δ 8.89 (s, 1H), 8.00 (d, J = 7.6 Hz, 1H), 7.84 – 7.83 (m, 1H), 7.81 (d, J = 7.9 Hz, 1H), 7.71 (d, J = 9.8 Hz, 1H), 7.59 (d, J = 8.0 Hz, 2H), 7.40 – 7.39 (m, 5H), 7.29 (d, J = 8.0 Hz, 2H), 7.22 (t, J = 7.4 Hz, 1H), 7.16 (t, J = 7.7 Hz, 2H), 6.63 (d, J = 7.5 Hz, 2H), 5.56 (s, 2H). ^{13}C NMR (151 MHz, $CDCl_3$): δ 144.6, 137.6, 134.7, 134.1, 131.7, 131.5, 131.4, 131.3, 131.1, 130.1, 129.8, 129.1, 128.7, 128.5, 127.4, 126.4, 126.3, 126.0 (d, C-F, $J_{C\text{-}F}$ = 3.6 Hz), 125.5 (d, C-F, $J_{C\text{-}F}$ = 3.6 Hz), 125.3, 124.8, 124.5, 124.3, 123.9, 122.6, 121.2, 117.7, 54.6. ^{19}F NMR (565 MHz, $CDCl_3$): δ -62.9, -63.1. HRMS (ESI) *m/z*: calcd. for $C_{34}H_{21}F_6N_2$ [M^+]: 571.1604; found: 571.1605.

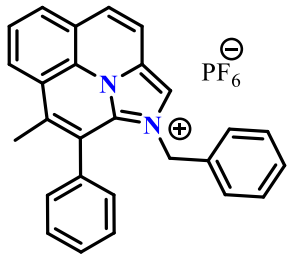
1-benzyl-8,9-di-o-tolylbenzo[*ij*]imidazo[2,1,5-*de*]quinolizin-1-ium hexafluorophosphate (4.5e)



The title compound **4.5e** was isolated as brown solid using neutral alumina column chromatography with ethyl acetate/ methanol (v/v = 10:1, R_f = 0.3) in 76% yield (92.5 mg) from GP-III; 74% yield (90.1 mg) from GP-IV. m.p. = 204–206 °C. ^{1}H NMR (600 MHz, $CDCl_3$): δ 9.41 (s, 1H), 7.95– 7.91 (m, 2H), 7.78 (t, J = 7.9 Hz, 1H), 7.66 (d, J = 9.7 Hz, 1H), 7.52 (d, J = 8.2 Hz, 1H), 7.20 – 7.16 (m, 4H), 7.13 – 7.08 (m, 3H), 6.94 – 6.86 (m, 3H), 6.79 – 6.75 (m, 1H), 6.72 – 6.70 (m, 2H), 5.72 – 5.68 (m, 1H), 5.53 – 5.49 (m, 1H), 2.26 – 2.25 (m, 3H), 2.13 – 2.11 (m, 3H). ^{13}C NMR (151 MHz, $CDCl_3$): δ 145.9, 137.3, 135.8, 134.5, 133.8, 131.2, 130.9, 130.8, 130.6, 130.2, 129.5, 129.3, 128.8, 128.7, 128.4, 127.6, 127.1, 127.03, 126.97, 126.4, 126.3, 125.8, 125.4, 124.7, 124.4, 124.3, 123.8, 122.2, 118.3, 53.3, 20.4, 20.1. HRMS (ESI) *m/z*: calcd. for $C_{34}H_{27}N_2$ [M^+]: 463.2169; found: 463.2167.

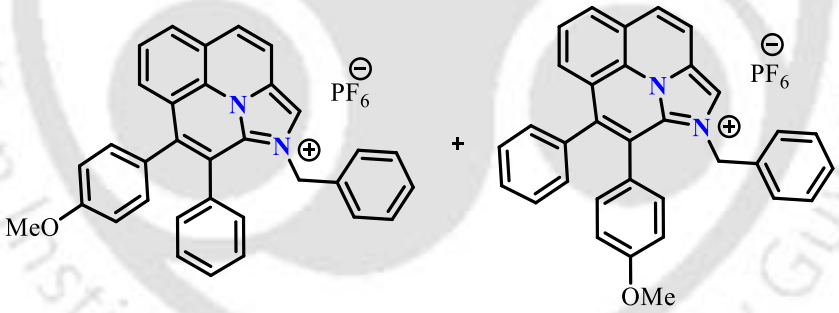
1-benzyl-8-methyl-9-phenylbenzo[*ij*]imidazo[2,1,5-*de*]quinolizin-1-ium hexafluorophosphate (4.5f)

TH-3565_186122020



The title compound **4.5f** was isolated as brown solid using neutral alumina column chromatography with ethyl acetate/ methanol (v/v = 10:1, R_f = 0.3) in 90% yield (93.3 mg) from GP-III; 92% yield (95.4 mg) from GP-IV. m.p. = 212–215 °C. ^{1}H NMR (600 MHz, DMSO-d_6): δ 8.42 (s, 1H), 8.32 – 8.29 (m, 1H), 8.25 – 8.24 (m, 1H), 8.09 (brs, 1H), 7.96 – 7.94 (m, 1H), 7.89 – 7.87 (m, 1H), 7.55 (brs, 1H), 7.45 (brs, 2H), 7.33 (brs, 2H), 7.28 – 7.25 (m, 3H), 6.80 (brs, 2H), 5.15 (s, 2H), 2.39 (s, 3H). ^{13}C NMR (126 MHz, DMSO-d_6): δ 141.0, 135.1, 132.1, 130.0, 129.6, 129.0, 128.53, 128.47, 128.0, 127.9, 127.0, 126.2, 125.7, 124.7, 124.0, 123.7, 123.4, 122.8, 118.3, 116.8, 51.9, 16.2. HRMS (ESI) *m/z*: calcd. for $C_{27}H_{21}N_2$ [M^+]: 373.1700; found: 373.1701.

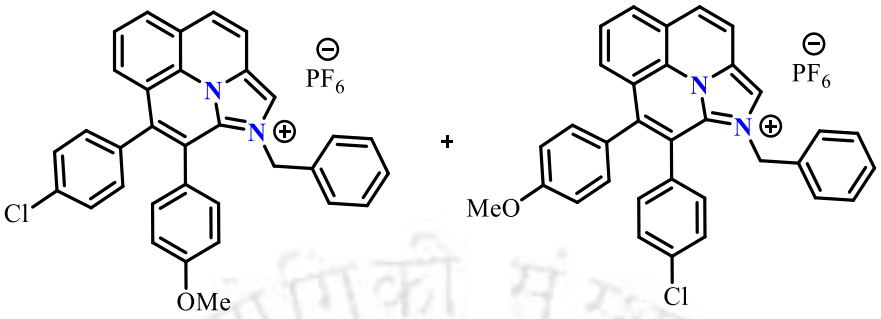
1-benzyl-9-(4-methoxyphenyl)-8-phenylbenzo[*ij*]imidazo[2,1,5-*de*]quinolizin-1-ium hexafluorophosphate and 1-benzyl-8-(4-methoxyphenyl)-9-phenylbenzo[*ij*]imidazo[2,1,5-*de*]quinolizin-1-ium hexafluorophosphate (4.5g + 4.5g′)



The title compound **4.5g** + **4.5g′** (1:1.2) was isolated as brown solid using neutral alumina column chromatography with ethyl acetate/ methanol (v/v = 10:1, R_f = 0.3) in 73% yield (89 mg) from GP-III; 76% yield (92.8 mg) from GP-IV. m.p. = 173–176 °C. ^{1}H NMR (500 MHz, $CDCl_3$): δ 9.26 – 7.20 (m, 1H), 7.99 – 7.97 (m, 1H), 7.87 – 7.76 (m, 2H), 7.71 – 7.69 (m, 1H), 7.58 – 7.56 (m, 0.5H), 7.50 – 7.49 (m, 0.5H), 7.33 – 7.29 (m, 2H), 7.24 – 7.14 (m, 4H), 7.11 – 7.09 (m, 2H), 7.04 – 7.00 (m, 2H), 6.83 – 6.81 (m, 2H), 6.74 – 6.71 (m, 2H), 5.62 (brs, 1.09H), 5.56 (brs, 0.91H), 3.78 – 3.76 (m, 3H). ^{13}C NMR (151 MHz, $CDCl_3$): δ 160.1, 159.6, 146.6, 146.3, 134.7, 134.6, 134.1, 132.1, 131.8, 131.6, 131.3, 130.9, 130.8, 129.6, 129.5, 129.4, 128.83, 128.81, 128.79, 128.76, 128.6, 128.5, 128.4, 128.2, 127.18, 127.17, 127.0, 126.8, 125.89, 125.85, 125.8, 125.4, 125.2, 125.10, 125.07, 124.9, 124.8, 124.5, 124.3, 124.2, 122.8, 121.2, 121.1, 117.60, 117.58, 114.2, 114.1, 55.4, 55.3, 53.7, 53.6. HRMS (ESI) *m/z*: calcd. for $C_{33}H_{25}N_2O$ [M^+]: 465.1962; found: 465.1966.

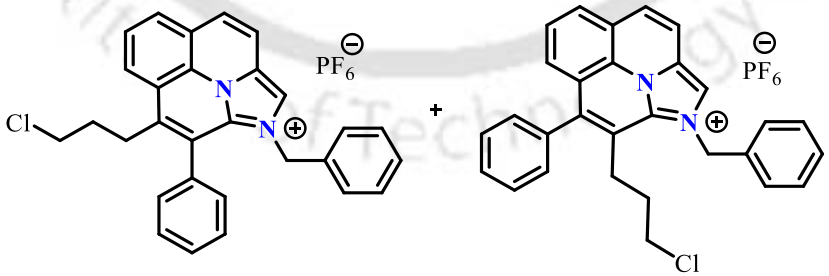
TH-3565_186122020

1-benzyl-8-(4-chlorophenyl)-9-(4-methoxyphenyl)benzo[*ij*]imidazo[2,1,5-*de*]quinolizin-1-ium hexafluorophosphate and 1-benzyl-9-(4-chlorophenyl)-8-(4-methoxyphenyl)benzo[*ij*]imidazo[2,1,5-*de*]quinolizin-1-ium hexafluorophosphate (4.5h + 4.5h′)



The title compound **4.5h** + **4.5h′** (1.2:1) was isolated as brown solid using neutral alumina column chromatography with ethyl acetate/ methanol (v/v = 10:1, R_f = 0.25) in 75% yield (96.7 mg) from GP-III; 81% yield (104.5 mg) from GP-IV. m.p. = 175–178 °C. ^{1}H NMR (600 MHz, $CDCl_3$): δ 8.88 (s, 1H), 7.95 (d, J = 8.2 Hz, 1H), 7.80 – 7.75 (m, 2H), 7.66 (d, J = 9.7 Hz, 1H), 7.52 (d, J = 9.3 Hz, 0.5H), 7.43 (d, J = 8.2 Hz, 0.5H), 7.29 – 7.26 (m, 1H), 7.19 – 7.11 (m, 4H), 7.06 – 7.03 (m, 3H), 6.97 (d, J = 8.7 Hz, 1H), 6.81– 6.78 (m, 2H), 6.71 (d, J = 8.6 Hz, 1H), 6.67 (d, J = 6.9 Hz, 1H), 5.52 (s, 1.08H), 5.49 (s, 0.92H), 3.76 (d, J = 4.0 Hz, 3H). ^{13}C NMR (126 MHz, $CDCl_3$): δ 160.3, 159.8, 146.6, 145.3, 135.5, 134.8, 134.45, 134.39, 132.7, 132.4, 132.1, 131.9, 131.6, 131.0, 130.8, 129.9, 129.6, 129.5, 129.2, 128.9, 128.8, 128.6, 128.5, 128.22, 128.17, 127.29, 127.27, 127.1, 126.6, 126.0, 125.9, 125.7, 125.4, 125.2, 125.1, 125.0, 124.7, 124.4, 124.3, 124.2, 123.5, 122.7, 120.9, 120.8, 117.6, 117.4, 114.4, 114.3, 55.42, 55.35, 54.1, 53.8. HRMS (ESI) *m/z*: calcd. for $C_{33}H_{24}ClN_2O$ [M^+]: 499.1572; found: 499.1579.

1-benzyl-8-(3-chloropropyl)-9-phenylbenzo[*ij*]imidazo[2,1,5-*de*]quinolizin-1-ium hexafluorophosphate and 1-benzyl-9-(3-chloropropyl)-8-phenylbenzo[ij]imidazo[2,1,5-de]quinolizin-1-ium hexafluorophosphate (4.5i + 4.5i′)

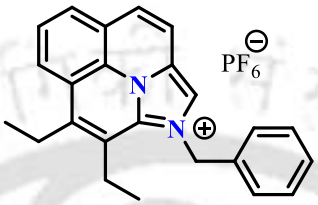


The title compound **4.5i** + **4.5i′** (2:1) was isolated as brown solid using neutral alumina column chromatography with ethyl acetate/ methanol (v/v = 10:1, R_f = 0.3) in 85% yield (98.8 mg) from GP-III; 87% yield (101.2 mg) from GP-IV. m.p. = 170–174 °C. ^{1}H NMR (400 MHz, $CDCl_3$): δ 9.09 (s, 0.36H), 9.03 (s, 0.64H), 8.19 – 8.14 (m, 1H), 7.99 – 7.96 (m, 2H), 7.86 – 7.83 (m, 1H), 7.67 – 7.64 (m, 1H), 7.58 – 7.54 (m, 1H), 7.49 – 7.47 (m, 1H), 7.45 – 7.43 (m, 1H), 7.28 (brs, 1H), 7.24 – 7.22 (m, 1H), 7.21 – 7.16 (m, 3H), 6.74 – 6.70 (m, 2H), 5.45 (s,

TH-3565_186122020

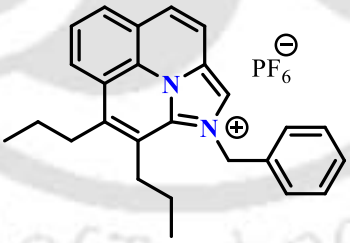
2H), 3.49 (t, J = 5.9 Hz, 1H), 3.31 – 3.26 (m, 1H), 3.00 – 2.96 (m, 1H), 2.91 – 2.87 (m, 1H), 2.02 – 1.97 (m, 1H), 1.81 – 1.74 (m, 1H). ^{13}C NMR (151 MHz, $CDCl_3$): δ 145.8, 144.4, 134.8, 134.7, 131.4, 131.2, 130.3, 130.2, 130.1, 129.7, 129.6, 129.5, 128.92, 128.87, 128.6, 128.52, 128.49, 128.4, 127.1, 127.0, 126.8, 126.7, 126.0, 125.8, 125.7, 125.6, 124.4, 124.0, 123.90, 123.88, 123.7, 122.8, 122.3, 121.3, 117.9, 117.8, 71.8, 58.8, 53.6, 53.5, 44.7, 31.7, 27.3, 26.8. HRMS (ESI) *m/z*: calcd. for $C_{29}H_{24}ClN_2$ [M^+]: 435.1623; found: 435.1622.

1-benzyl-8,9-diethylbenzo[*ij*]imidazo[2,1,5-*de*]quinolizin-1-ium hexafluorophosphate (4.5j)



The title compound **4.5j** was isolated as pale-yellow solid using neutral alumina column chromatography with ethyl acetate/ methanol (v/v = 20:1, R_f = 0.4) in 75% yield (72.7 mg) from GP-III; 79% yield (76.5 mg) from GP-IV. m.p. = 80–83 °C. ^{1}H NMR (600 MHz, $CDCl_3$): δ 8.36 (s, 1H), 8.07 – 8.05 (m, 1H), 7.94 – 7.91 (m, 2H), 7.69 (d, J = 9.7 Hz, 1H), 7.61 (d, J = 9.7 Hz, 1H), 7.40 – 7.36 (m, 3H), 7.17 (d, J = 7.1 Hz, 2H), 6.12 (s, 2H), 3.19 (q, J = 7.6 Hz, 2H), 3.13 (q, J = 7.6 Hz, 2H), 1.39 (q, J = 7.8 Hz, 6H). ^{13}C NMR (101 MHz, $CDCl_3$): δ 146.1, 134.8, 129.7, 129.2, 128.2, 127.2, 126.7, 125.6, 125.3, 124.23, 124.15, 124.1, 122.1, 120.3, 117.1, 54.5, 21.9, 20.6, 15.5, 13.7. HRMS (ESI) *m/z*: calcd. for $C_{24}H_{23}N_2$ [M^+]: 339.1856; found: 339.1854.

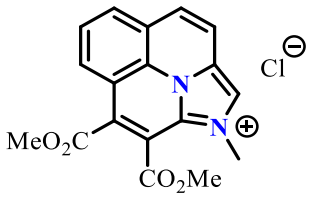
1-benzyl-8,9-dipropylbenzo[*ij*]imidazo[2,1,5-*de*]quinolizin-1-ium hexafluorophosphate (4.5k)



The title compound **4.5k** was isolated as pale-yellow solid using neutral alumina column chromatography with ethyl acetate/ methanol (v/v = 20:1, R_f = 0.4) in 68% yield (70 mg) from GP-III; 72% yield (73.8 mg) from GP-IV. m.p. = 81–84 °C. ^{1}H NMR (400 MHz, $CDCl_3$): δ 9.34 (s, 1H), 8.04 – 8.02 (m, 1H), 7.95 – 7.94 (m, 2H), 7.81 (d, J = 9.8 Hz, 1H), 7.65 (d, J = 9.8 Hz, 1H), 7.36 – 7.30 (m, 3H), 7.11 (d, J = 7.5 Hz, 2H), 6.36 (s, 2H), 3.10 – 3.06 (m, 2H), 3.00 – 2.96 (m, 2H), 1.74 – 1.67 (m, 4H), 1.19 – 1.12 (m, 6H). ^{13}C NMR (101 MHz, $CDCl_3$): δ 144.7, 135.3, 132.5, 129.5, 128.8, 128.7, 128.2, 127.0, 125.9, 125.4, 125.3, 124.2, 123.8, 122.9, 122.1, 121.5, 117.2, 54.2, 30.7, 29.1, 24.9, 22.8, 14.6, 14.1. HRMS (ESI) *m/z*: calcd. for $C_{26}H_{27}N_2$ [M^+]: 367.2169; found: 367.2171.

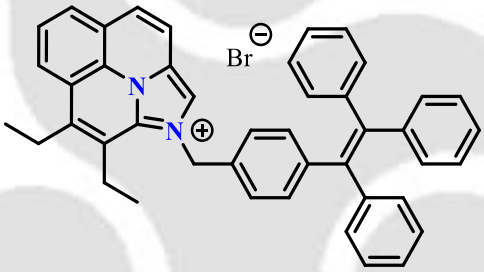
TH-3565_186122020

8,9-bis(methoxycarbonyl)-1-methylbenzo[*ij*]imidazo[2,1,5-*de*]quinolizin-1-ium chloride (4.6a)



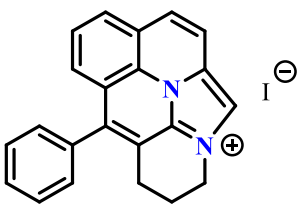
The title compound **4.6a** was isolated as black solid using neutral alumina column chromatography with ethyl acetate/ methanol (v/v = 4:1, R_f = 0.4) in 79% yield (56.6 mg) from GP-III; 84% yield (60.3 mg) from GP-IV. m.p. = 111–113 °C. ^{1}H NMR (600 MHz, DMSO-d_6): δ 8.76 (s, 1H), 8.31 (d, J = 7.7 Hz, 1H), 8.22 (d, J = 8.2 Hz, 1H), 8.09 (t, J = 7.9 Hz, 1H), 7.95 (s, 2H), 4.23 (s, 3H), 4.08 (s, 6H). ^{13}C NMR (151 MHz, DMSO-d_6): δ 164.4, 162.5, 134.6, 130.5, 129.1, 128.5, 127.5, 127.4, 124.8, 124.4, 123.5, 121.7, 119.7, 117.1, 117.0, 54.4, 54.1, 37.8. HRMS (ESI) *m/z*: calcd. for $C_{18}H_{15}N_2O_4$ [M^+]: 323.1027; found: 323.1031.

8,9-diethyl-1-(4-(1,2,2-triphenylvinyl)benzyl)benzo[*ij*]imidazo[2,1,5-*de*]quinolizin-1-ium bromide (4.6b)



The title compound **4.6b** was isolated as white solid using neutral alumina column chromatography with ethyl acetate/ methanol (v/v = 10:1, R_f = 0.3) in 92% yield (124 mg) from GP-III; 89% yield (120 mg) from GP-IV. m.p. = 240–242 °C. ^{1}H NMR (600 MHz, $CDCl_3$): δ 9.28 (s, 1H), 8.05 – 8.04 (m, 1H), 7.94 – 7.90 (m, 2H), 7.80 (d, J = 9.7 Hz, 1H), 7.61 (d, J = 9.8 Hz, 1H), 7.08 – 7.06 (m, 9H), 7.02 – 6.96 (m, 8H), 6.88 (d, J = 8.0 Hz, 2H), 6.35 (s, 2H), 3.19 (q, J = 7.6 Hz, 2H), 3.07 (q, J = 7.6 Hz, 2H), 1.39 (t, J = 7.6 Hz, 3H), 1.28 (t, J = 7.6 Hz, 3H). ^{13}C NMR (151 MHz, $CDCl_3$): δ 146.0, 144.6, 143.5, 143.3, 143.2, 141.9, 139.9, 133.0, 132.6, 132.4, 131.34, 131.31, 131.26, 129.1, 128.9, 128.3, 128.2, 127.8, 127.7, 127.0, 126.72, 126.69, 125.7, 125.4, 125.2, 124.1, 124.0, 123.7, 122.0, 121.3, 117.2, 54.5, 21.8, 20.4, 15.6, 13.7. HRMS (ESI) *m/z*: calcd. for $C_{44}H_{37}N_2$ [M^+]: 593.2952; found: 593.2954.

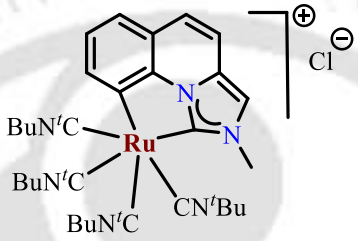
5-phenyl-3,4-dihydro-2*H*-1a,10a^1-diazabenzo[*mno*]aceanthrylen-1a-ium iodide (4.7)



TH-3565_186122020

The title compound **4.7** was isolated as black solid using neutral alumina column chromatography with ethyl acetate/ methanol (v/v = 10:1, R_f = 0.35) in 87% yield (76 mg) from GP-III; 85% yield (74.2 mg) from GP-IV. m.p. = 182–185 °C. ^{1}H NMR (600 MHz, $CDCl_3$ + DMSO-d_6): δ 8.51 (m, 1H), 8.06 (dd, J = 7.9, 3.1 Hz, 1H), 7.90 – 7.88 (m, 1H), 7.83 (dd, J = 9.9, 3.1 Hz, 1H), 7.77 – 7.74 (m, 2H), 7.71 – 7.69 (m, 2H), 7.67 – 7.64 (m, 1H), 7.51 – 7.48 (m, 2H), 4.84 – 4.82 (m, 2H), 2.63 – 2.62 (m, 2H), 2.51 – 2.49 (m, 2H). ^{13}C NMR (151 MHz, $CDCl_3$ + DMSO-d_6): δ 140.8, 132.2, 131.3, 129.1, 128.9, 128.3, 127.8, 127.5, 127.2, 124.63, 124.60, 123.9, 123.8, 123.3, 118.5, 116.0, 114.9, 45.7, 22.2, 21.4. HRMS (ESI) *m/z*: calcd. for $C_{22}H_{17}N_2$ [M^+]: 309.1387; found: 309.1388.

Analytical data of Ru-7



Complex **Ru-1** (50 mg, 0.11 mmol, 1 equiv.) and ^{t}BuNC (91.4 mg, 1.1 mmol, 10 equiv.) were taken with dry $CHCl_3$ (3 mL) in a 10 mL Schlenk tube and the tube was evacuated and purged with N_2 three times. The mixture was stirred at 60 °C for 16 h. After completion of the reaction, the solvent was removed and the residue was purified by column chromatography on neutral alumina (methanol/ ethyl acetate: 1/6, R_f = 0.6) as eluent to afford the **Ru-7** as a brown solid (45.4 mg, 76%). ^{1}H NMR (500 MHz, Chloroform-*d*): δ 7.68 – 7.67 (m, 1H), 7.52 (s, 1H), 7.17 – 7.13 (m, 2H), 7.09 (d, J = 9.3 Hz, 1H), 7.02 (d, J = 9.3 Hz, 1H), 4.16 (s, 3H), 1.62 (s, 9H), 1.56 (s, 9H), 1.01 (s, 18H). ^{13}C NMR (151 MHz, Chloroform-*d*): δ 173.5, 153.1, 142.6, 139.2, 128.2, 126.2, 125.2, 120.8, 120.5, 113.7, 113.5, 57.2, 57.1, 38.2, 31.2, 31.1, 30.4.

4.5.8. Computational details

All calculations were performed using the Gaussian-16 program package in the gas phase.[23] Full geometry optimizations were carried out using M06-L level[24] of theory and BS1 basis set. BS1 is defined as an SDD[25] basis set for Ru atom and 6-31G* Pople basis set for all other atoms. Frequency calculations at the same method and basis set were performed to distinguish transition state structures (one imaginary frequency) and minima structures (no imaginary frequency) on the potential energy surface. The transition states were verified by the intrinsic reaction coordinate (IRC) calculations, wherever necessary.[26] Free energies were calculated by using frequency calculations at 130 °C to match the experimental conditions. Mulliken charges were calculated by NBO analysis.

Table 4.18. Free Energies (G) and Total Energies (E) of all the optimized structures given in Hartree along with the number of imaginary frequencies[a]

TH-3565_186122020

Species	Free energy (G)	Total energy (E)	# Imaginary Frequency (NImag)
I1	-2053.434860	-2054.0223947	0
I2	-2053.423821	-2054.0094429	0
TS-1	-1514.150026	-1514.5653534	1
DPA	-539.256226	-539.3892217	0
Ru-5	-1595.348783	-1595.8326446	0
Acetic acid	-229.039902	-229.0627504	0
I3	-1595.356003	-1595.8424691	0
TS-2	-1595.340919	-1595.8272712	1
I4	-1595.369519	-1595.8624280	0
I5	-1595.378691	-1595.8669990	0
4.3a-OAc	-1112.329254	-1112.6361238	0
[Ru(*p*-cym)(OAc)$_2$]	-941.15956	-941.3981384	0

[a](G) is calculated at 130 °C to meet the experimental conditions. All the figures were generated using (G) values. All the transition states have one NImag and all the reactants, intermediates and products have zero NImag. All the calculations were performed at the M06-L level of DFT. (DPA = diphenyl acetylene)

4.6. References

1. (a) Stępień, M.; Gońka, E.; Żyła, M.; Sprutta, N. *Chem. Rev.* **2017**, *117*, 3479–3716. (b) Sucunza, D.; Cuadro, A. M.; Alvarez-Builla, J.; Vaquero, J. J. *J. Org. Chem.* **2016**, *81*, 10126–10135. (c) Bortolozzi, R.; von Gradowski, S.; Ihmels, H.; Schäfer, K.; Viola, G. *Chem. Commun.* **2014**, *50*, 8242–8245. (d) Viola, G.; Bressanini, M.; Gabellini, N.; Vedaldi, D.; Dall'Acqua, F.; Ihmels, H. *Photochem. Photobiol. Sci.* **2002**, *1*, 882–889. (e) Yang, L.; Steinbock, R.; Scheremetjew, A.; Kuniyil, R.; Finger, L. H.; Messinis, A. M.; Ackermann, L. *Angew. Chem. Int. Ed.* **2020**, *59*, 11130–11135. (f) Kong, W.-J.; Shen, Z.; Finger, L. H.; Ackermann, L. *Angew. Chem. Int. Ed.* **2020**, *59*, 5551–5556. (g) Ahmed, E.; Briseno, A. L.; Xia, Y.; Jenekhe, S. A. *J. Am. Chem. Soc.* **2008**, *130*, 1118–1119.

2. (a) Miao, Q. *Polycyclic Arenes and Heteroarenes: Synthesis, Properties, and Applications*; Wiley-VCH: New York, 2015. (b) Allard, S.; Forster, M.; Souharce, B.; Thiem, H.; Scherf, U. *Angew. Chem. Int. Ed.* **2008**, *47*, 4070–4098. (c) Wang, C.; Dong, H.; Hu, W.; Liu, Y.; Zhu, D. *Chem. Rev.* **2012**, *112*, 2208–2267. (d) Facchetti, A. *Chem. Mater.* **2011**, *23*, 733–758.

3. Ghorai, D.; Choudhury, J. *Chem. Commun.* **2014**, *50*, 15159–15162.

4. (a) Ghorai, D.; Choudhury, J. *ACS Catal.* **2015**, *5*, 2692–2696. (b) Thenarukandiyil, R.; Gupta, S. K.; Choudhury, J. *ACS Catal.* **2016**, *6*, 5132–5137.

5. Ge, Q.; Li, B.; Song, H.; Wang, B. *Org. Biomol. Chem.* **2015**, *13*, 7695–7710.

6. Sheldon, R. A. *Green Chem.* **2017**, *19*, 18–43.

TH-3565_186122020

7. (a) Shi, Z.; Zhang, C.; Li, S.; Pan, D.; Ding, S.; Cui, Y.; Jiao, N. *Angew. Chem. Int. Ed.* **2009**, *48*, 4572–4576. (b) Warratz, S.; Kornhaaß, C.; Cajaraville, A.; Niepötter, B.; Stalke, D.; Ackermann, L. *Angew. Chem. Int. Ed.* **2015**, *54*, 5513–5517. (c) Zhang, G.; Yang, L.; Wang, Y.; Xie, Y.; Huang, H. *J. Am. Chem. Soc.* **2013**, *135*, 8850–8853. (d) Sharma, R.; Kumar, R.; Sharma, U. *J. Org. Chem.* **2019**, *84*, 2786–2797. (e) Lu, Y.; Wang, H.-W.; Spangler, J. E.; Chen, K.; Cui, P.-P.; Zhao, Y.; Sun, W.-Y.; Yu, J.-Q. *Chem. Sci.* **2015**, *6*, 1923–1927. (f) Wei, Y.; Zhao, H.; Kan, J.; Su, W.; Hong, M. *J. Am. Chem. Soc.* **2010**, *132*, 2522–2523.

8. Stahl, S. S. *Science* **2005**, *309*, 1824–1826.

9. (a) Dutta, C.; Choudhury, J. *RSC Adv.* **2018**, *8*, 27881–27891. (b) Karak, P.; Rana, S. S.; Choudhury, J. *Chem. Commun.* **2022**, *58*, 133–154.

10. (a) Chou, H.-H.; Cheng, C.-H. *Adv. Mater.* **2010**, *22*, 2468−2471. (b) Hranjec, M.; Piantanida, I.; Kralj, M.; Šuman, L.; Pavelić, K.; Karminski-Zamola, G. *J. Med. Chem.* **2008**, *51*, 4899–4910.

11. Ackermann, L. *Chem. Rev.* **2011**, *111*, 1315–1345.

12. Li, L.; Brennessel, W. W.; Jones, W. D. *Organometallics* **2009**, *28*, 3492–3500.

13. Tocher, D. A.; Gould, R. O.; Stephenson, T. A. *J. Chem. Soc., Dalton Trans.,* **1983**, 1571−1581.

14. Arockiam, P. B.; Fischmeister, C.; Bruneau, C.; Dixneuf, P. H. *Angew. Chem., Int. Ed.* **2010**, *49*, 6629−6632.

15. Yan, Z. C.; Wan, C. F.; Zha, Z. G.; Wang, Z. Y. *RSC Adv.* **2018**, *8*, 23058−23065.

16. Hutt, J. T.; Jo, J.; Olasz, A.; Chen, C. -H.; Lee, D.; Aron, Z. D. *Org. Lett.* **2012**, *14*, 3162−3165.

17. lcarazo, M.; Roseblade, S. J.; Cowley, A. R.; Fernández, R.;Brown, J. M.; Lassaletta, J. M. *J. Am. Chem.Soc.* **2005**, *127*, 3290−3291.

18. Du, X. S.; Han, Y.; Chen. C. F. *Chem. Eur. J.* **2022**, *28*, e202104024.

19. Wang, W.; Bao, Z. -P.; Qi, X.; Wu, X. -F. *Org. Lett.* **2021**, *23*, 6589−6593.

20. Wu, H. -P.; Shao, C. -K.; Wu, D.; Jiang, L.; Yin, H. -Q.; Chen, F.-X. *J. Org. Chem*. **2021**, *86*, 5327−5335.

21. Luo, X. L.; Li, Y. B.; Chen, X. W.; Song, Z. Y.; Liang, J. Y.; Liao, C.S.; Zhu, Z. Z.; Chen, L. *Org. Biomol. Chem.* **2019**, *17*, 7315−7319.

22. Zhang, C.; Xu, K.; Liao, Y.; Zhao, L.; Jin, S.; Lu, X.; Wang, J.; Ding, L.; Zhang, J. *J. Org. Chem.* **2023**, *88*, 3436–3450.

23. Frisch, M. J.; Trucks, G. W.; Schlegel, H. B.; Scuseria, G. E.; Robb, M. A.; Cheeseman, J. R.; Scalmani, G.; Barone, V.; Petersson, G. A.; Nakatsuji, H.; Li, X.; Caricato, M.; Marenich, A. V.; Bloino, J.; Janesko, B. G.; Gomperts, R.; Mennucci, B.; Hratchian, H. P.; Ortiz, J. V.; Izmaylov, A. F.; Sonnenberg, J. L.; Williams-Young, D.; Ding, F.; Lipparini, F.; Egidi, F.;

TH-3565_186122020

Goings, J.; Peng, B.; Petrone, A.; Henderson, T.; Ranasinghe, D.; Zakrzewski, V. G.; Gao, J.; Rega, N.; Zheng, G.; Liang, W.; Hada, M.; Ehara, M.; Toyota, K.; Fukuda, R.; Hasegawa, J.; Ishida, M.; Nakajima, T.; Honda, Y.; Kitao, O.; Nakai, H.; Vreven, T.; Throssell, K.; Montgomery, J. A., Jr.; Peralta, J. E.; Ogliaro, F.; Bearpark, M. J.; Heyd, J. J.; Brothers, E. N.; Kudin, K. N.; Staroverov, V. N.; Keith, T. A.; Kobayashi, R.; Normand, J.; Raghavachari, K.; Rendell, A. P.; Burant, J. C.; Iyengar, S. S.; Tomasi, J.; Cossi, M.; Millam, J. M.; Klene, M.; Adamo, C.; Cammi, R.; Ochterski, J. W.; Martin, R. L.; Morokuma, K.; Farkas, O.; Foresman, J. B.; Fox, D. J. *Gaussian 16*, Revision C.01, Gaussian, Inc., Wallingford CT, 2016.

24. Wang, Y.; Jin, X.; Yu, H. S.; Truhlar, D. G.; He, X. *PNAS* **2017**, *114*, 8487–8492.

25. Dolg, M.; Wedig, U.; Stoll, H.; Preuss, H. *J. Chem. Phys*., **1987**, *86*, 866–872.

26. Fukui, K. *Acc. Chem. Res.* **1981**, *14*, 363–368

TH-3565_186122020

Chapter 5

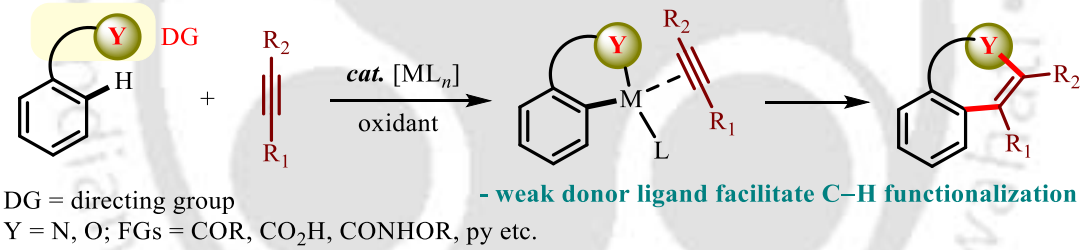
Carboxylic Acid Assisted Ru(II)-Catalyzed Annulation of Imidazo[1,5-a]quinoline with Alkynes via Double C−H Activation: A Direct Route to Functionalized Quinolizines

TH-3565_186122020

5.1. Introduction

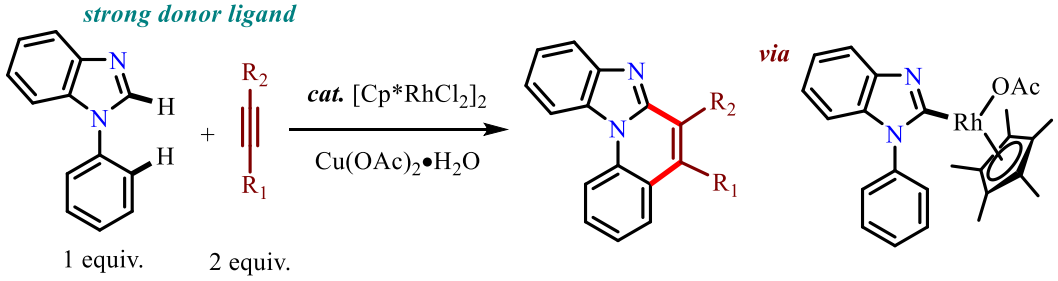
Fused polycyclic heteroaromatic compounds are common structural motifs found in a wide range of natural products, pharmaceuticals, agrochemicals, and DNA intercalators.[1] Additionally, its extended conjugated π-system has significant electrochemical and photochemical characteristics, indicating future applications as organic semiconductors and luminescent materials.[2] Therefore, many potential applications require improving present synthetic methods for extended π-systems. Various methods have been developed to synthesize fused (hetero)aromatics, particularly π-extended heteroarenes,[3] due to their importance and usefulness. Quinolizines are a kind of *N*-heterocycles that play important roles in many antihypertensive, antibacterial, and anticancer drugs.[4] They have recently been used as aggregation-induced emission luminogens (AIEgens) in photodynamic therapy studies.[5] However, a simple method to functionalize benzo-imidazo-quinolizine is quite rare.

Transition metal-catalyzed oxidative annulation reaction of alkyne *via* C–H bond activation emerged as one of the most powerful synthetic tools because it offers one-step construction of cyclic scaffolds from a wide variety of C−H bonds, thus leading to increasing atom and step economy.[6] A weak donor functional group containing substrate is strategically used as a directing group (DG) to promote such C−H functionalization chemistry.[7] Strong carbon donor-bearing functionality as a directing group in C−H functionalization catalysis has received less attention due to the robust, stable, and poorly reactive character of M−C bonds.[8]



Scheme 5.1. Oxidative C−H bond activation and alkyne annulation *via* weak chelation-assisted C−H activation

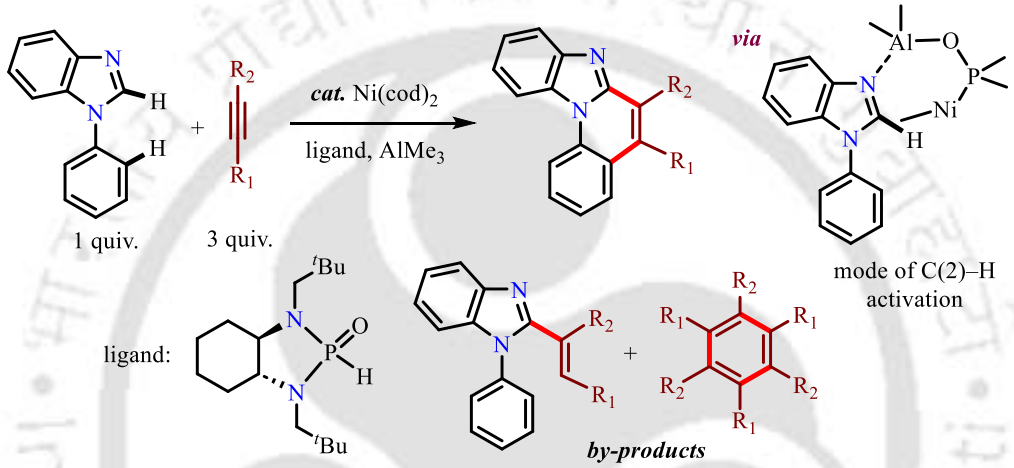
In 2012, Chen and coworkers demonstrated a $[Cp^*RhCl_2]_2$-catalyzed oxidative annulation of aryl benzimidazole with alkynes using benzimidazole ligand as a directing group and functionalizable group.[9] The reaction was initiated with the formation of 2-benzoimidazolyl-rhodium complex *via* copper acetate-assisted C(2)–H activation. Nevertheless, the use of $[RuCl_2(p\text{-cymene})]_2$ was found to be inefficient under the reaction condition.



Scheme 5.2. Rh-catalyzed annulation reaction of benzimidazole with alkynes

TH-3565_186122020

Very recently, Ye group reported a base-metal Ni-catalyzed annulation method to access π-conjugated polycyclic heteroaromatic molecules *via* dual C−H activation of *N*-aromatic benzimidazole and annulation with alkynes (Scheme 5.3).[10] The use of bifunctional phosphine oxide (PO) ligand and potent Lewis acid $AlMe_3$ played a key role in the activation of the C2–H bond. It has been documented that the *in situ* generated PO-bound Ni−Al bimetallic complex docked at the N atom of benzimidazole moiety, acting as a directing group to bring Ni to the proximity of the target C−H bond. Given the well-known air and moisture sensitivities and the expensive nature of phosphine ligands, the development of phosphine-free DGs for the activation of the C2−H bond is highly desired in this regard. Furthermore, high-loading $AlMe_3$ must be taken into account during synthetic transformation since these are potent Lewis acids and incompatible with several functional groups.



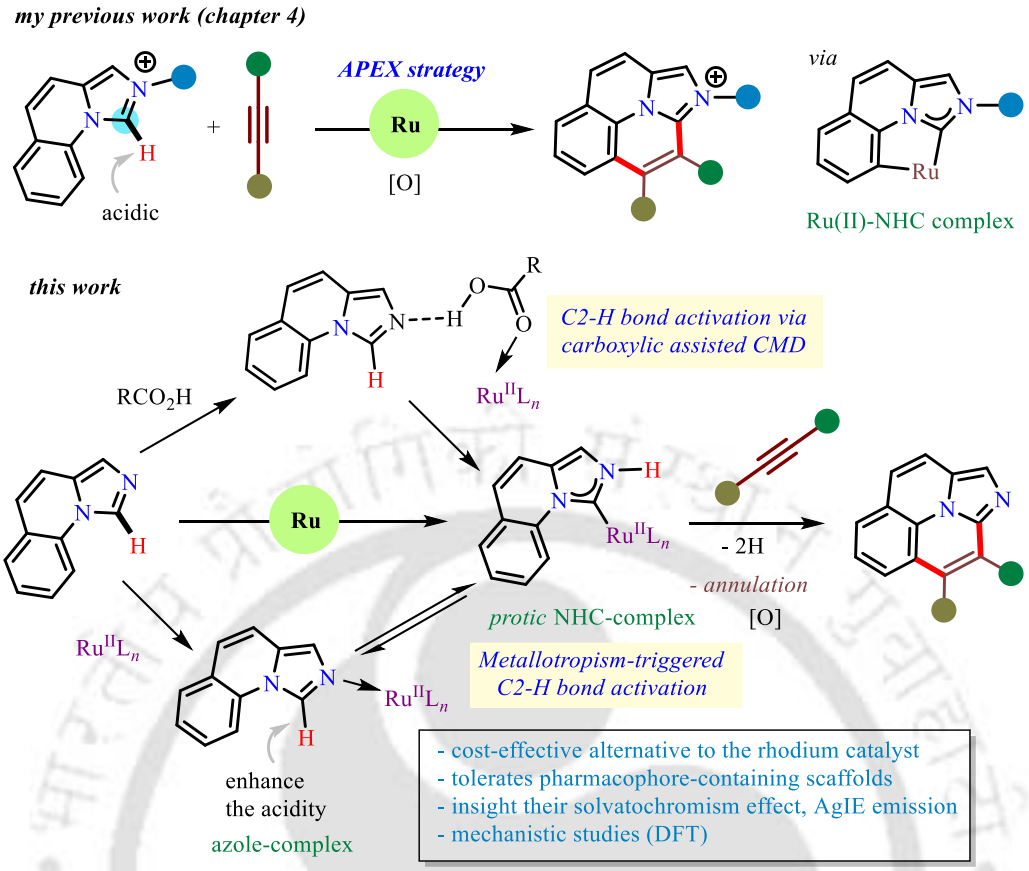
Scheme 5.3. Ni-catalyzed C-H annulation of benzimidazole with alkynes

5.2. Present work

In the previous chapter, I discussed about the Ru(II)-catalyzed annulation reaction of imidazo[1,5-*a*]quinolin-2-ium salts with alkynes. It has been proven that C2-proton of imidazo[1,5-*a*]quinolin-2-ium salts is acidic in nature which aids to generate *N*-heterocyclic carbene (NHC)-as a directing group in a catalytic C–H activation–alkyne insertion–annulation sequence.

Herein I hypothesized that imidazole moiety can coordinate to the metal ions by its *N*-donor site, resulting enhance the acidity at the C2-proton. This can open up the possibility of a potential metallotropism/tautomerization event as shown in Scheme 5.4, leading to the generation of a '*p*-NHC-M'.[11a] However, the stability/propensity of *p*-NHC-M is often less than the coordinated azole form.[11] Hence, a heteroatom chelation-assisted approach is often required to stabilize this. Notably, non-chelated *p*-NHC-M in catalysis is under explored. On the other hand, the carboxylic acid-assisted concerted metalation deprotonation (CMD) strategy is a privileged pathway to activate the C2-proton,[12] which can generate *p*-NHC-M complex. Subsequent aryl-CH bond activation leads to the formation of cyclometalated species. Next, alkyne insertion, followed by reductive elimination to provide the annulated product.

TH-3565_186122020



Scheme 5.4. *protic*-NHC directed oxidative annulation reaction with alkynes

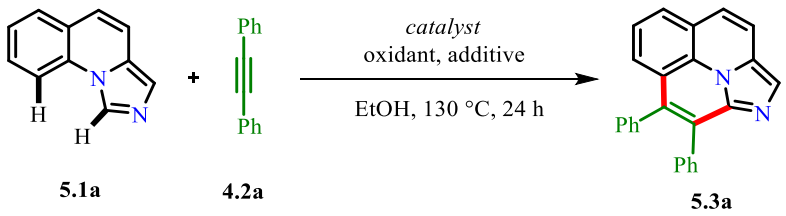
5.3. Results and discussion

5.3.1. Optimization of reaction conditions

I began the optimization study with the reaction between imidazo[1,5-*a*]quinoline (**5.1a**) and diphenylacetylene (**4.2a**) as model substrates for the annulation reaction using [(*p*-cymene)$RuCl_2$]$_2$ (2 mol%) as a catalyst and $Cu(OAc)_2$•H_2O (2 equiv.) as an oxidant in a closed pressure tube with dry ethanol at 130 °C for 24 h under air. The desired annulated product **5.3a** was obtained in 12% yield along with a recovered substantial amount of starting material. The formation of the annulated product **5.3a** was slightly increased to 26% when the catalyst loading was raised to 5 mol%. To our delight, the product yield was improved significantly to 62% upon adding one equivalent of pivalic acid as an additive indicating a key role of pivalic acid in the current catalytic process (entry 3, Table 5.1). Then an increase in the amount of pivalic acid to 2 equiv., under the same reaction conditions, product **5.3a** was obtained in 90% yield (entry 4, Table 5.1). Further, we investigated the efficacy of a series of alternative acids in the current catalytic process under the same reaction conditions. However, pivalic acid was found to be the best additive among the acids employed in this study. Interestingly, when the reaction was carried out with KOPiv and NaOPiv, product **5.3a** was obtained in 42% and 36%

TH-3565_186122020

Table 5.1. Optimization of the reaction conditions[a]



5.1a **4.2a** **5.3a**

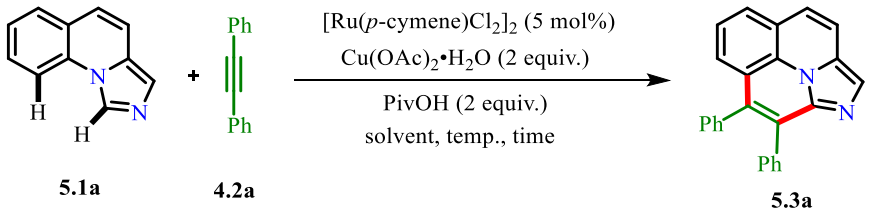
Entry	Catalyst (mol%)	Oxidant (equiv.)	Additive (equiv.)	Yield[b]
1	[Ru(*p*-cymene)Cl_2]$_2$ (2)	$Cu(OAc)_2$•H_2O (2)	–	12
2	[Ru(*p*-cymene)Cl_2]$_2$ (5)	$Cu(OAc)_2$•H_2O (2)	–	26
3	[Ru(*p*-cymene)Cl_2]$_2$ (5)	$Cu(OAc)_2$•H_2O (2)	PivOH (1)	62
4	**[Ru(*p*-cymene)Cl_2]$_2$ (5)**	**$Cu(OAc)_2$•H_2O (2)**	**PivOH (2)**	**90**
5	[Ru(*p*-cymene)Cl_2]$_2$ (5)	$Cu(OAc)_2$•H_2O (2)	PivOH (3)	89
6	[Ru(*p*-cymene)Cl_2]$_2$ (5)	$Cu(OAc)_2$•H_2O (2)	CH_3CO_2H (2)	81
7	[Ru(*p*-cymene)Cl_2]$_2$ (5)	$Cu(OAc)_2$•H_2O (2)	CF_3CO_2H (2)	40
8	[Ru(*p*-cymene)Cl_2]$_2$ (5)	$Cu(OAc)_2$•H_2O (2)	HCl (2)	52
9	[Ru(*p*-cymene)Cl_2]$_2$ (5)	$Cu(OAc)_2$•H_2O (2)	CF_3SO_3H (2)	32
10	[Ru(*p*-cymene)Cl_2]$_2$ (5)	$Cu(OAc)_2$•H_2O (2)	PhCOOH (2)	30
11	[Ru(*p*-cymene)Cl_2]$_2$ (5)	$Cu(OAc)_2$•H_2O (2)	KOPiv (2)	42
12	[Ru(*p*-cymene)Cl_2]$_2$ (5)	$Cu(OAc)_2$•H_2O (2)	NaOAc (2)	36
13	[Ru(*p*-cymene)Cl_2]$_2$ (5)	$Cu(OAc)_2$•H_2O (1)	PivOH (2)	48
14	[Ru(*p*-cymene)Cl_2]$_2$ (5)	–	PivOH (2)	n.d.
15	[Ru(*p*-cymene)Cl_2]$_2$ (5)	$Cu(BF_4)_2$•$6H_2O$ (2)	PivOH (2)	7
16	[Ru(*p*-cymene)Cl_2]$_2$ (5)	$CuCl_2$•$2H_2O$ (2)	PivOH (2)	n.d.
17	[Ru(*p*-cymene)Cl_2]$_2$ (5)	O_2 (1 atm)	PivOH (2)	4
18	–	$Cu(OAc)_2$•H_2O (2)	PivOH (2)	n.d.

[a]Reaction conditions: **5.1a** (0.5 mmol), **4.2a** (0.5 mmol), catalyst (x mol%), oxidant (x equiv.), additive (x equiv.), EtOH (2.0 mL) at 130 ºC in a preheated oil bath for 24 h in a sealed tube; [b]isolated yields are reported; n.d. = not detected.

yield, respectively indicating the impact of proton sources in the catalytic process (entries 11−12, Table 5.1). Furthermore, no product was formed when the reaction was carried out in the absence of $Cu(OAc)_2$•H_2O and only a trace amount of product **5.3a** was detected with O_2 as an oxidant, suggesting the role of $Cu(OAc)_2$•H_2O as an oxidant in the catalytic process. The use of copper(II) salts containing different counter anions, such as $Cu(BF_4)_2$•$6H_2O$, and $CuCl_2$•$2H_2O$, almost no conversion was acquired (entries 15−16, Table 5.1), indicating the importance of acetate ligand in this transformation. A blank reaction suggests the necessity of a catalyst in this oxidative annulation reaction (entry 18, Table 5.1). For detailed optimization studies of reaction time and reaction temperature, see entries 1−6 in Table 5.2. The reaction was performed in various solvents as a part of further optimization. A dramatic drop in yield has been observed in toluene, DCE, and DMF (entries 8−10, Table 5.2), whereas good results were attained in the polar protic solvents. Interestingly, EtOH was found to be an effective solvent for this transformation.

TH-3565_186122020

Table 5.2. Screening of time, temperature and solvent[a]



5.1a **4.2a** **5.3a**

Entry	Time (h)	Temperature (ºC)	Solvent	Yield[b]
1	12	130	EtOH	34
2	18	130	EtOH	73
3	**24**	**130**	**EtOH**	**90**
4	24	110	EtOH	68
5	24	80	EtOH	24
6	24	25	EtOH	n.d.
7	24	130	MeOH	87
8	24	130	DMF	58
9	24	130	DCE	65
10	24	130	toluene	30
11	24	130	water	n.d.

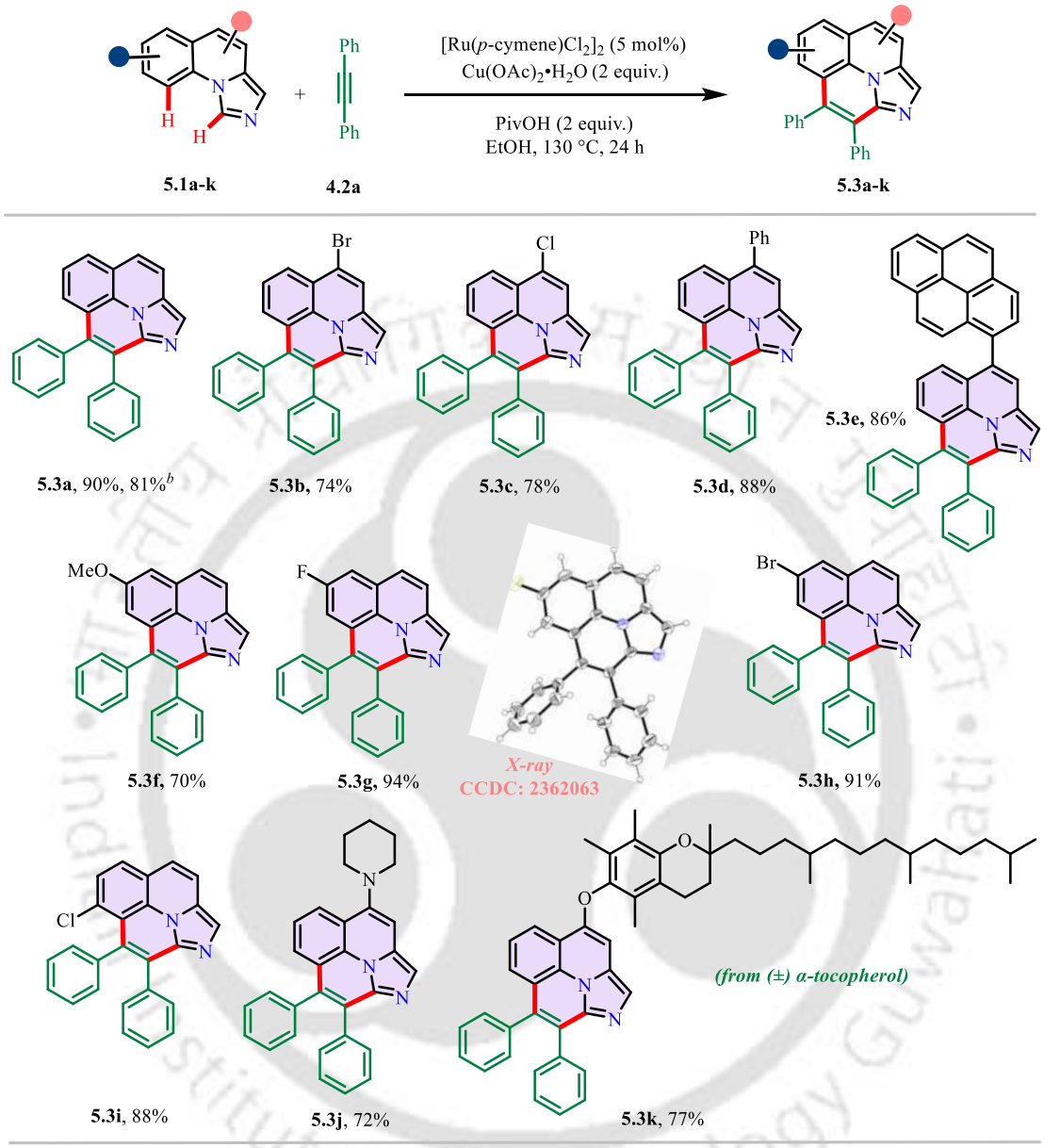
[a]Reaction conditions: **5.1a** (0.5 mmol), **4.2a** (0.5 mmol), [Ru(*p*-cymene)Cl_2]$_2$ (5 mol%), $Cu(OAc)_2$•H_2O (2 equiv.), PivOH (2 equiv.), solvent (2.0 mL) at the indicated time and temperature in a sealed tube; [b]isolated yields are reported. n.d. = not detected.

5.3.2. Substrate scope

With optimal reaction conditions in hand, I explored the substrate scope by employing varieties of imidazo[1,5-*a*]quinoline with varying substituents in the backbone, **5.1a-k** with alkyne **4.2a** as the standard substrate (Table 5.3). Under standard reaction conditions, when the model substrate imidazo[1,5-*a*]quinoline, **5.1a** was treated with diphenylacetylene **4.2a**, the desired annulated product **5.3a** was exclusively formed with 90% yield. In the case of 5-haloimidazo[1,5-*a*]quinoline **5.1b** and **5.1c**, though C5 substituted halo functionality was susceptible to nucleophilic attack, desired annulated products **5.3b** and **5.3c** was obtained in 74%, and 78% yield, respectively, indicating impressive selectivity of the present protocol. Further, the scope of the reaction was expanded to include C5-substituted phenyl- and pyrene-bearing imidazoquinoline **5.1d**, and **5.1e**. These are also successfully participated in the annulated reaction to provide the products **5.3d**, and **5.3e** in 88% and 86% respectively. Then the effects of electron-donating and electron-withdrawing groups on the C7 position of imidazo[1,5-*a*]quinoline were studied. The substrate containing electron-donating (e.g., −OMe) and electron-withdrawing (e.g., −F and −Br) groups were used in the annulation reactions and all of them provided the desired products in moderate to good yields (70-94%). It was found that the electron-withdrawing group containing substrate furnished higher yields than the electron-donating group containing substrate. It is interesting to note that substrates like C8 substituted imidazoquinoline **5.1i**, which has substituents close to the annulation site of the quinoline moiety, efficiently reacted with **4.2a** to produce the desired annulated product

TH-3565_186122020

Table 5.3. Substrate scope of imidazo[1,5-*a*]quinoline with varying substituents in the backbone[a]

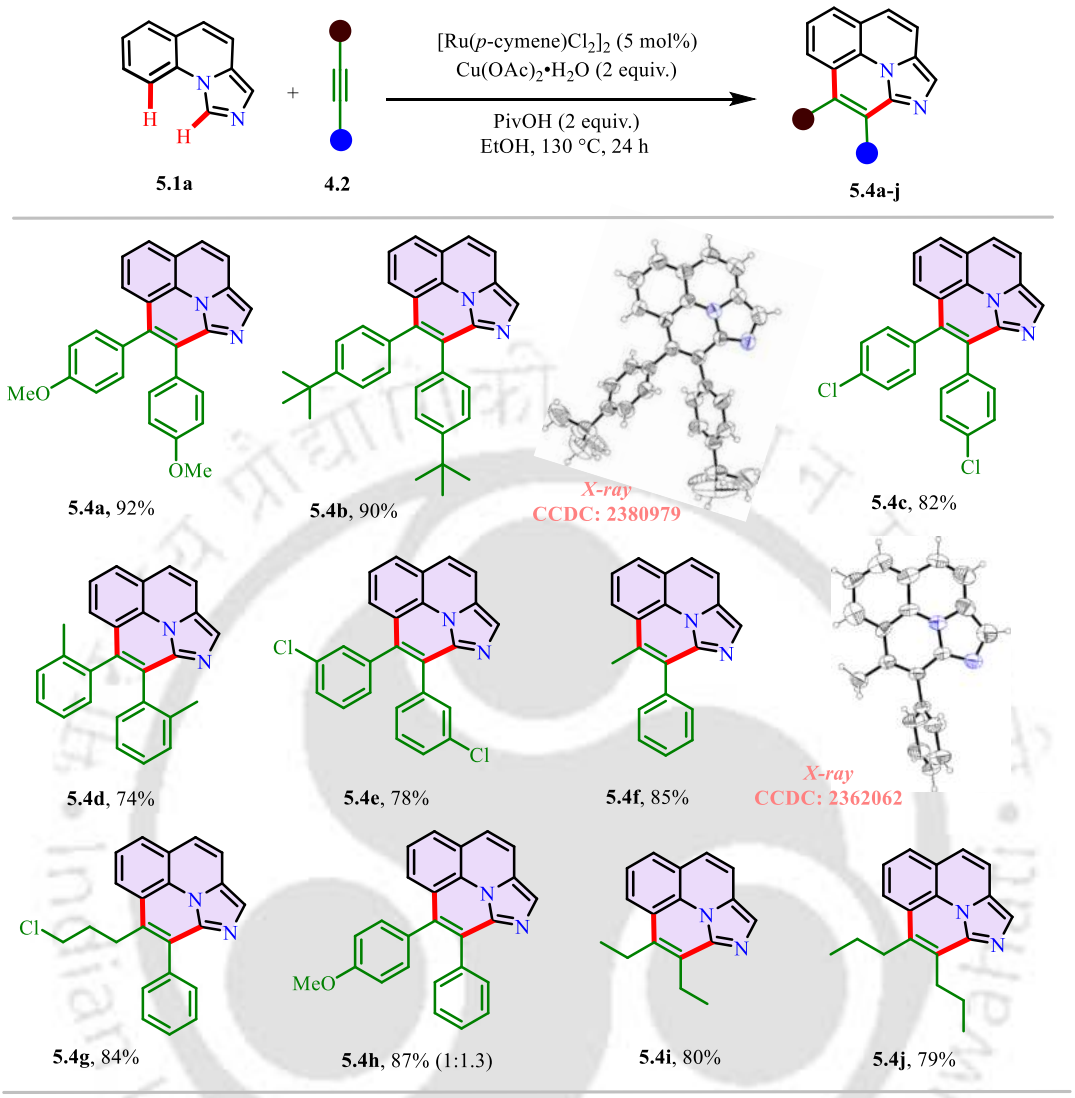


[a]Reaction condition: **5.1a-k** (0.5 mmol), **4.2a** (0.5 mmol), [Ru(*p*-cymene)Cl_2]$_2$ (5 mol%), Cu(OAc)$_2$•H_2O (2 equiv.), PivOH (2 equiv.), EtOH (2.0 mL) were heated at 130 °C in a pressure tube for 24 h, isolated yield. [b]2 mmol scale.

5.3i in 88% yield. The amine-bearing substituent at the C5-position of the quinoline moiety, **5.1j** was also well suited for this annulation reaction, affording the desired products **5.3j** with a 72% yield. Since the quinoline motif is important in various biologically and pharmacologically relevant molecular settings, a substrate containing (±) *α*-tocopherol modified quinoline derivative **5.1k** was successfully converted into an annulated product **5.3k** with a 77% yield.

TH-3565_186122020

Table 5.4. Substrate scope of imidazo[1,5-*a*]quinoline with various alkynes[a]



[a]Reaction condition: **5.1a** (0.5 mmol), **2b-2k** (0.5 mmol), [Ru(*p*-cymene)Cl_2]$_2$ (5 mol%), $Cu(OAc)_2$•H_2O (2 equiv.), PivOH (2 equiv.), EtOH (2.0 mL) were heated at 130 °C in a pressure tube for 24 h, isolated yield.

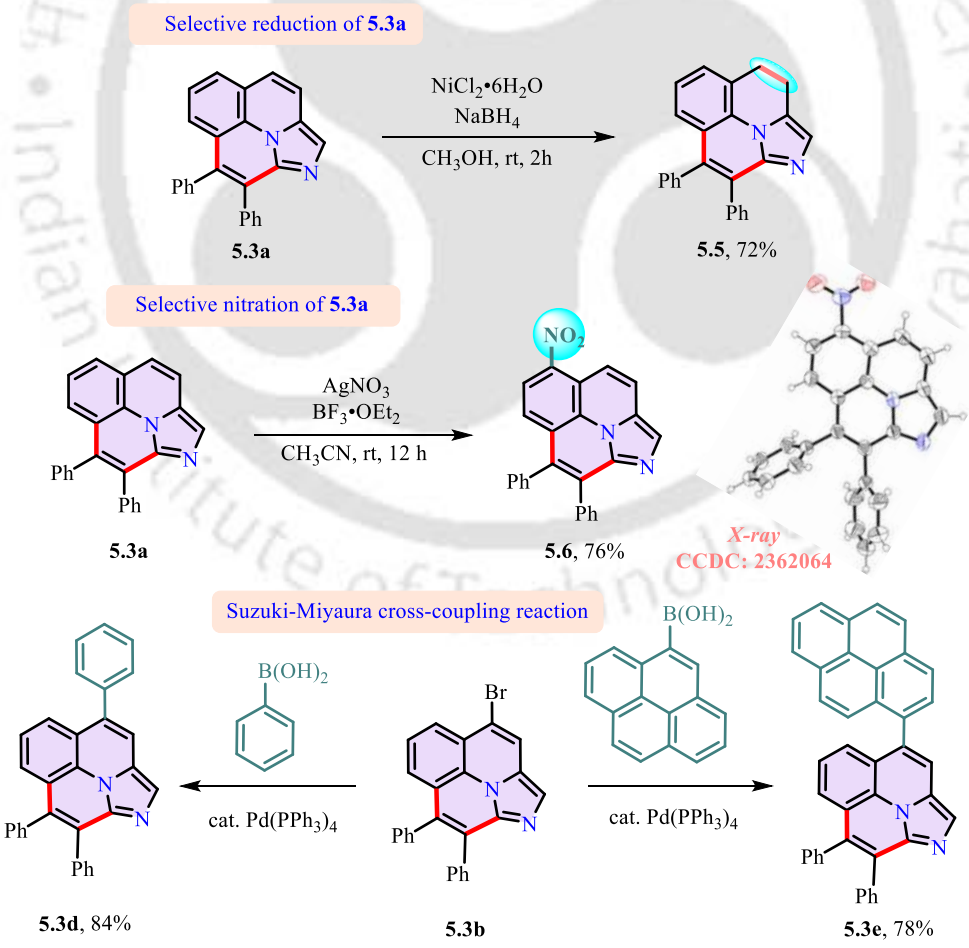
To further demonstrate the generality and practicability of this reaction, a range of alkynes were also tested (Table 5.4). Besides diphenylacetylene, other substituted symmetrical 1,2-diaryl alkynes having electron-donating *p*-OMe (**4.2c**), *p*-^{t}Bu (**4.2n**) and electron-withdrawing *p*-Cl (**4.2d**) efficiently produced the corresponding annulated products **5.4a-c** in 82-92% yields. Slightly higher yields were realized for electron-donating alkynes. Surprisingly, sterically hindered *ortho*-substituted diphenyl acetylene **4.2f** and *meta*-substituted diphenyl acetylene **4.2o** were well tolerated in this annulation reaction, yielding the products **5.4d** and **5.4e** in 74% and 78%, respectively. Next, unsymmetrical internal alkynes 1-phenyl-1- propyne (**4.2g**) and (5-chloropent-1-yn-1-yl)benzene (**4.2j**) were tested, which provided a single regioisomer of the corresponding product **5.4f** and **5.4g** in 85% and 84% yield respectively. The regioselectivity was consistent with previous reports[13] and primarily driven by electronic factors. The structure of the **5.4f** was confirmed by the SC-XRD study. In contrast, an alkyne with two different

TH-3565_186122020

aromatic rings produced the regioisomeric pairs **5.4h** in 87% yield. Besides symmetrical and unsymmetrical aryl alkynes, the aliphatic alkyne such as 3-hexyne (**4.2k**), and 4-octyne (**4.2l**) were also compatible under the reaction conditions to give the annulated products **5.4i** and **5.4j** with exclusive yield. Finally, to examine the efficiency of the catalytic process, a scale-up reaction was performed with a 2 mmol-scale reaction using imidazo-quinoline **5.1a** and alkyne **4.2a**, providing **5.3a** in 81% yield.

5.3.3. Post-synthetic modification

Furthermore, the synthesized compounds were easily modified into other useful molecules (Scheme 5.5). For example, compound **5.3a** can be selectively reduced at the least hindered double bond using a mixture of $NiCl_2$ and $NaBH_4$ to get the reduced compound **5.5** with a 72% yield. Using a mixture of $AgNO_3$ and BF_3•OEt_2, selective nitration of **5.3a** was achieved at the C6-position of imidazoquinoline moiety affording **5.6** in 76% yield. The structure of the regioisomer **5.6** was unambiguously confirmed by SC-XRD. Since the current reaction protocol tolerates the halogen functional groups, Suzuki-Miyaura cross-coupling was applied to functionalize the C5 position further, delivering **5.3d** and **5.3e** in 84%, 78% yield respectively.

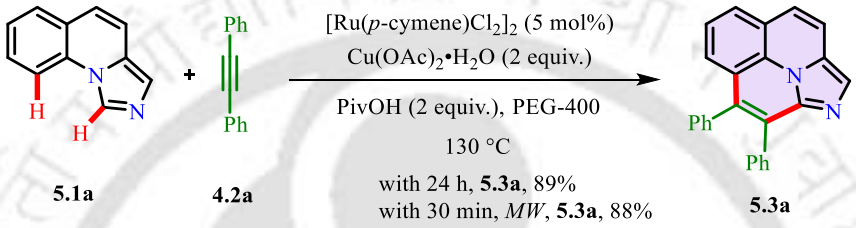


Scheme 5.5. Post-synthetic modification of annulated molecules

TH-3565_186122020

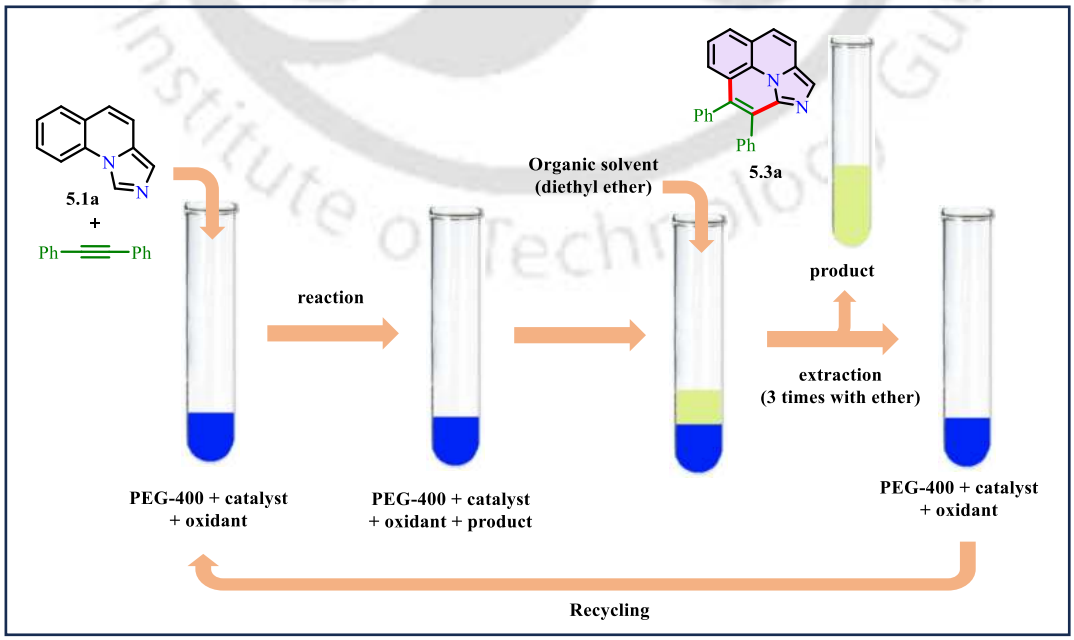
5.3.4. Recyclability and reusability of the catalytic system

While demonstrating the efficacy of the present protocol for synthesizing various quinolizine derivatives, I also focused my attention on developing an alternate reusable solvent medium for this transformation wherein the metal catalyst can also be recycled.[14] To our delight, when the reaction was carried out in biomass-derived solvent PEG-400 resulted in the formation of the desired product **5.3a** in 89% yield. The same reaction was examined under microwave irradiation (*μw*) since microwave condition is emerging as an alternative to conventional heating practices and leading to accelerated reaction rates. Gratifyingly, all the starting materials were entirely consumed within 30 minutes and provided the product **5.3a** with 88% yield (Scheme 5.6).



Scheme 5.6. Annulation reaction in PEG-400

After such observation, I decided to investigate the potential reuse of catalysts using given conditions. Once the first reaction is over, diethyl ether is added to the reaction mixture and the product extracted with diethyl ether 3-4 times. It was found that product **5.3a** is well soluble in the ether whereas catalyst and copper acetate are insoluble. Hence the respective PEG-400 layer can be reused for the next cycle by adding a fresh solution of substrates **5.1a**, **4.2a**, and PivOH.



TH-3565_186122020

Figure 5.1. Schematic diagram for the recycling of catalyst, oxidant, and solvent system

After 30 minutes of reaction time, the corresponding product **5.3a** was obtained in 86% yield. The following procedure will further examine for the next 3 cycles consistent in their yields of 85%, 82% and 77% respectively (see details in section 5.5.5). The recyclability of the catalyst, oxidant and solvent was accomplished successfully for a few times with minimal loss of catalytic activity. The result indicates that the catalytic system exhibits good recyclability.

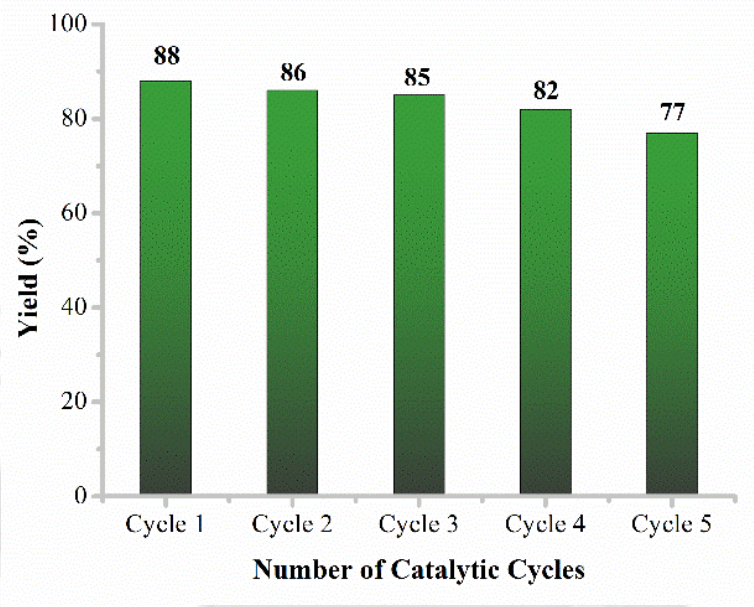


Figure 5.2. Recyclability study of the catalytic system for the annulation reaction of **5.1a**

5.3.5. Photophysical properties

Besides the substrate scope, functional group tolerance and recyclability of the catalyst, it is worth noting that the most of resulting quinolizine derivatives were found to have interesting photophysical properties and exhibit intense fluorescence emission at a broad range. Compound **5.4b** was chosen as a representative probe to investigate its photophysical properties in different solvents. As shown in Figure 5.3, the absorption maxima varied in the different solvents within the range from 277 nm to 368 nm. Notably, compound **5.4b** exhibited polarity-sensitive fluorescence properties with a solvatochromism effect. The maxima emission of **5.4b** red-shifted from 468 to 490 nm when varying the solvent from ethanol to acetonitrile. Significantly quenched emission intensity was observed in hexane and THF. In addition, the emission of **5.4b** could be tuned by restricting the intramolecular motion in aqueous media which might induce the aggregation-induced emission (AIE)-active property. To further investigate the AIE properties, the emission nature of **5.4b** was studied in EtOH/H_2O mixtures with different water fractions (f_w, volume %). The photoluminescence titration experiment shows that a gradual increase in the proportion of water to ethanol/water mixture causes an enhancement in fluorescence emission intensity. At f_w 60%, the maximum fluorescence intensity of **5.4b** was observed, while the emission intensity was largely quenched when the f_w was increased further.

TH-3565_186122020

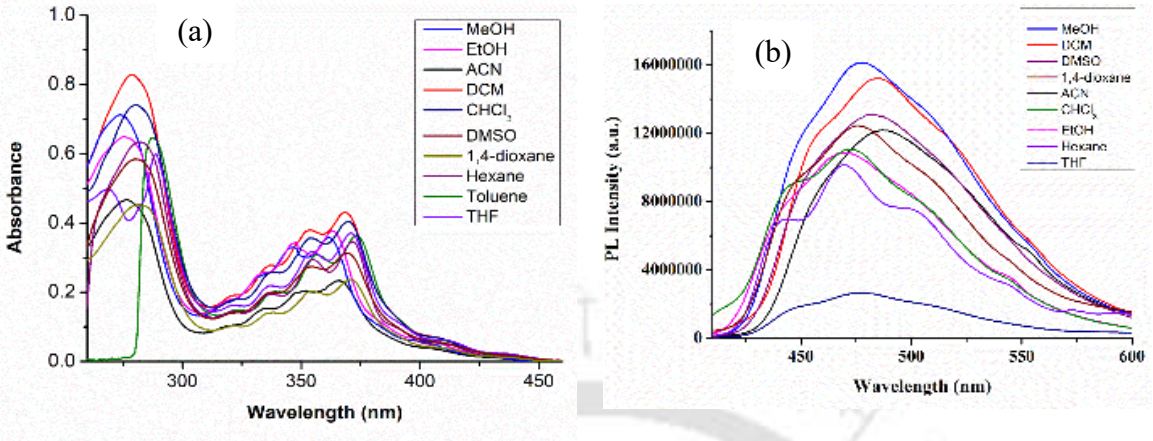


Figure 5.3. Spectroscopic properties of **5.4b** in various solvents. (a) UV–Vis absorption spectra, (b) PL emission spectra, concentration = 20 μM, λ_{ex} = 280 nm, slit = 2.

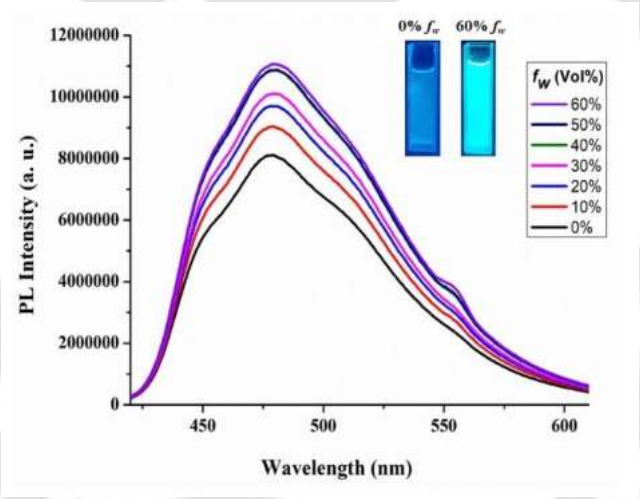


Figure 5.4. Photoluminescence spectra of **5.4b** in ethanol/water mixtures with different water fractions (f_w) with a concentration = 20 μM, λ_{ex} = 280 nm and slit = 2.

Selective Cu^{2+} detection using 5.3g

The synthesized product **5.3g** has been further studied for its ability to detect metal ions in methanol solution. The fluorescence response of the probe **5.3g** in the presence of different metal ions such as Li^{+}, Ca^{2+}, Ni^{2+}, Co^{2+}, Cu^{2+}, and Zn^{2+} were examined. Methanol solution of different chloride salts i.e., LiCl, $CaCl_2$, $NiCl_2$, $CoCl_2$, $CuCl_2$, $ZnCl_2$ were used for the measurement. There was a remarkable quenching in the fluorescence intensity of **5.3g** in the presence of $CuCl_2$, which is not observed for other metal ions. To explore the sensitivity of **5.3g** probe to Cu^{2+}, fluorescence titration experiments were performed by varying the concentration of Cu^{2+}. As shown in Figure 5.5(b), with the increase in the concentration of Cu^{2+}, the fluorescence intensity of **5.3g** gradually decreases. Reduction in emission intensity in

TH-3565_186122020

the presence of Cu^{2+} ion is due to the establishment of chelation enhanced quenching (CHEQ) process[15] upon coordination of **5.3g** to Cu^{2+} ion.

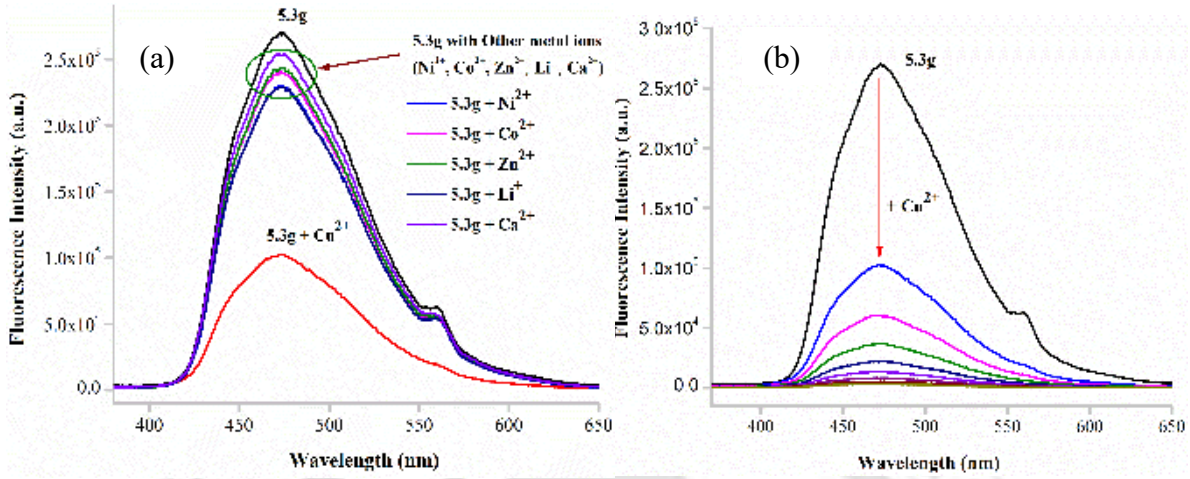


Figure 5.5. Fluorescence emission spectra (λ_{ex} = 280 nm) of **5.3g** in methanol (50 μM) (a) with different metal ions (100 μM). (b) with different concentrations of Cu^{2+} (100 μM→1 mM).

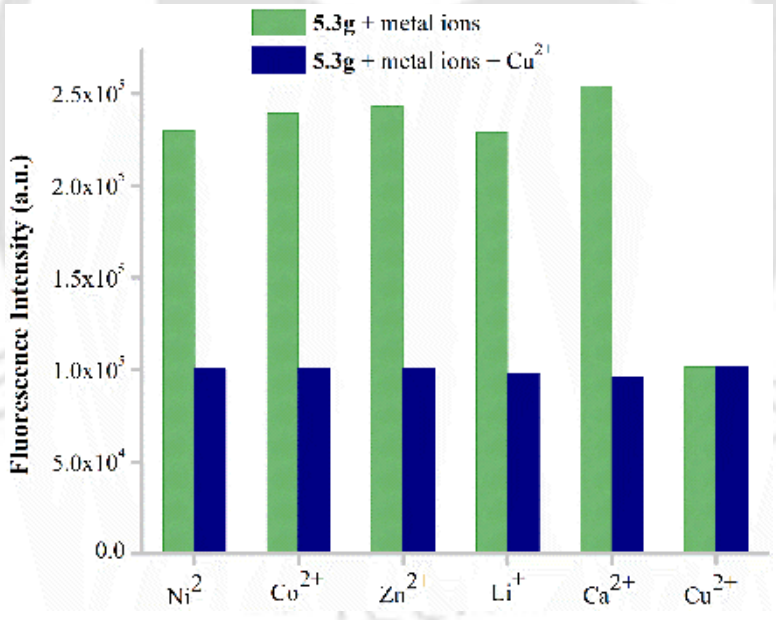


Figure 5.6. Bar diagram of **5.3g** by adding 2 equiv. of various metal chlorides and $CuCl_2$

The response of **5.3g** to Cu^{2+} ions in the presence of other metal ions was also measured to investigate the possible interference of these competing ions. (Figure 5.6, blue bars). It was observed that the fluorescence intensity of **5.3g** upon binding to Cu^{2+} ions significantly reduced in the presence of other metal ions. These ions have negligible influence on the sensing of Cu^{2+} ions and establish a good selectivity of **5.3g** in the presence of other metal salts. This selectivity can be explained by taking into account that with Cu^{2+} ions, **5.3g** forms a more stable complex than other metal ions analyzed, which is in accordance with the Irving-Williams series.

TH-3565_186122020

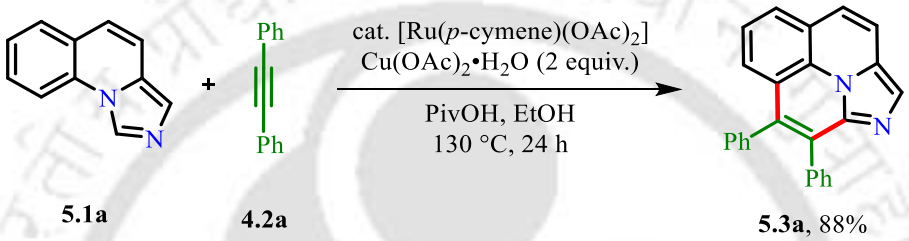
Therefore, **5.3g** could be applied to recognize Cu^{2+} in the environment; moreover, applications in biological systems may be achieved in the future.

5.3.6. Mechanistic investigation

5.3.6.1. Control experiments

(i) Proof of [Ru(*p*-cymene)$(OAc)_2$] in the annulation reaction

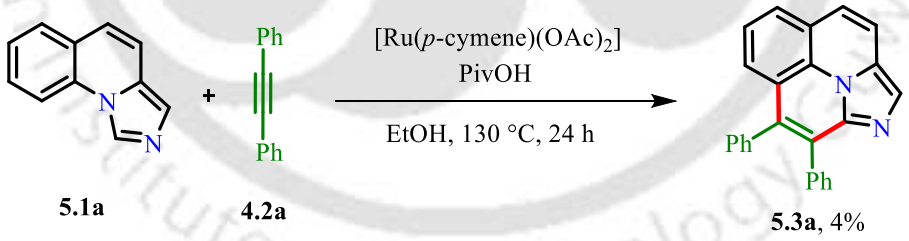
A series of control experiments were performed to gain insight into the mechanistic pathways. On performing a reaction with independently synthesized [Ru(*p*-cymene)$(OAc)_2$], the annulated product **5.3a** was formed in 88% yield, suggesting Ru(*p*-cymene)$(OAc)_2$ could be a possible intermediate in the catalytic reaction.



Scheme 5.7. Annulation reaction with [Ru(*p*-cymene)$(OAc)_2$] as a catalyst

(ii) Impact of $Cu(OAc)_2•H_2O$ in the annulation reaction

To know the role of $Cu(OAc)_2•H_2O$ in the annulation reaction, a control experiment was performed in the absence of $Cu(OAc)_2$, only a 4% yield of **5.3a** was obtained suggesting a necessity of $Cu(OAc)_2$ as an oxidant in the catalytic reaction.

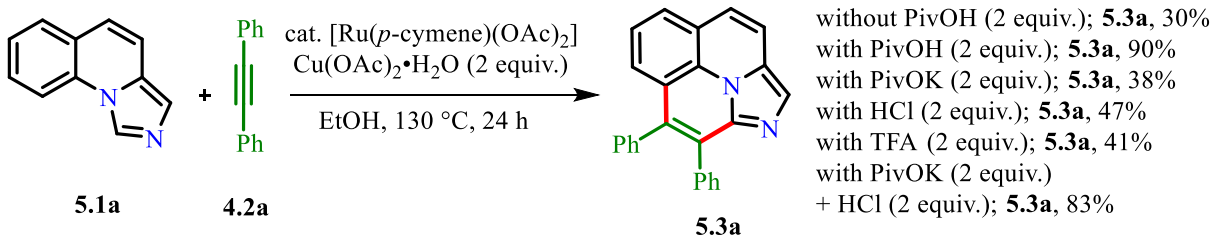


Scheme 5.8. Annulation reaction in absence of $Cu(OAc)_2•H_2O$

(iii) Importance of carboxylic acid in the annulation reaction

In the absence of PivOH, 30% product of **5.3a** was obtained which indicates the possible contribution by copper acetate C(2)–H activation, followed by transmetalation and/or metallotropism-tautomerization effect. Interestingly, when the reaction was carried out with Brønsted acid as a protic additive (such as HCl instead of carboxylic acid), obtained a 47% yield of **5.3a** indicating the important role of protic source in the reaction. With PivOK, only 38% yield of **5.3a** reveals that the carboxylate anion-assisted CMD pathway C−H bond activation as a minor pathway cannot be ruled out.

TH-3565_186122020



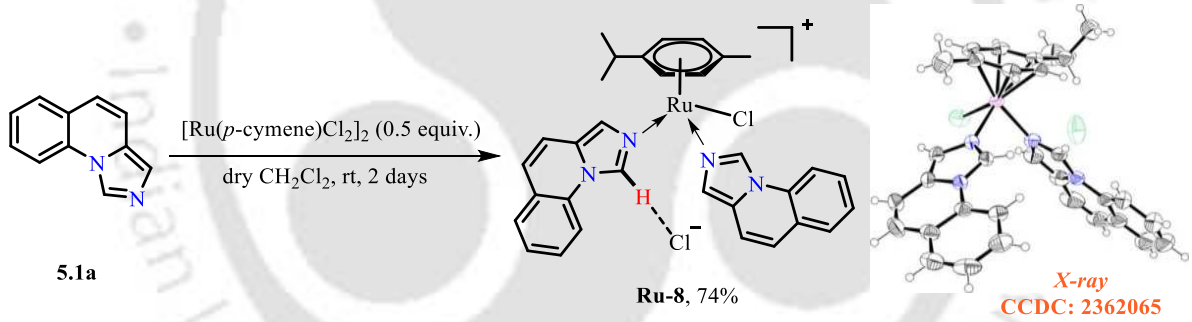
5.1a **4.2a** **5.3a**

Scheme 5.9. Importance of carboxylic acid

5.3.6.2. Proof of intermediate Ru-8 in the catalytic cycle

(i) Synthesis and characterization of intermediate **Ru-8**

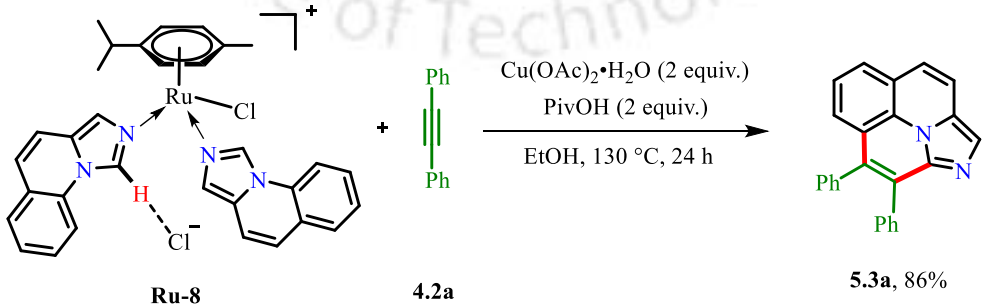
Then Ru(II)-azole complex **Ru-8** was synthesized in 74% yield by the reaction of **5.1a** with $[Ru(p\text{-cymene})Cl_2]_2$ in CH_2Cl_2 at room temperature. The structure analysis of **Ru-8** with ^1H, ^{13}C NMR spectroscopic and electron-spray ionization high-resolution mass spectrometry (ESI-HRMS) inferred **Ru-8** is a *N*-coordinated Ru^{II}-complex without undergoing any C−H activation. Upon X-ray structural analysis of **Ru-8**, it was realized that the Ru(II) binds with two imidazo-quinoline moieties through the N-center, halide and planar *p*-cymene forming piano-stool geometry.



5.1a **Ru-8**, 74%

Scheme 5.10. Synthesis of intermediate **Ru-8**

(ii) Stoichiometric and catalytic reaction with **Ru-8**

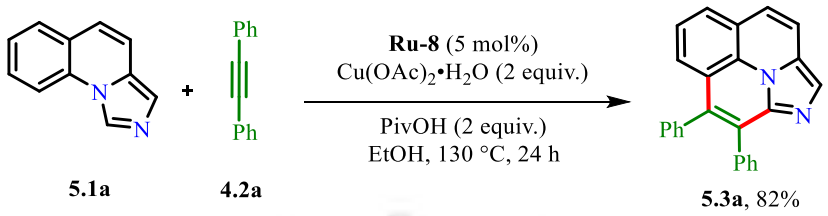


Ru-8 **4.2a** **5.3a**, 86%

Scheme 5.11. Stoichiometric reaction between **Ru-8** and **4.2a**

TH-3565_186122020

To probe the intermediacy of complex **Ru-8** in the catalytic process, a stoichiometric reaction was performed between **Ru-8** and **4.2a** with copper salt and pivalic acid under standard reaction conditions (Scheme 5.11). As expected, the desired annulated product **5.3a** was formed with 86% yield.

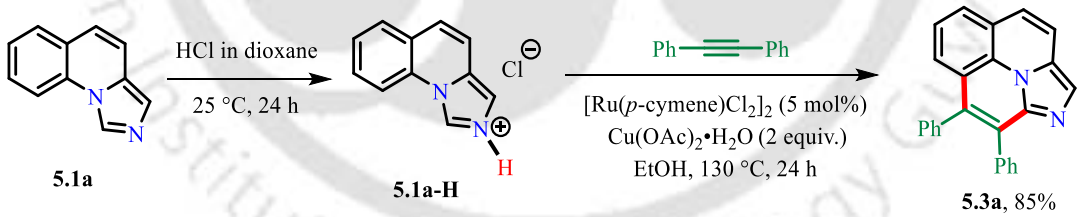


Scheme 5.12. Catalytic reaction with **Ru-8**

Then a successful annulation reaction between **5.1a** and **4.2a** in the presence of **Ru-8** as a catalyst also afforded the annulated product **5.3a** in 82% yield (Scheme 5.12). These stoichiometric and catalytic reaction outcomes suggested that **Ru-8** is likely to be an intermediate species in the catalytic process.

5.3.6.3. Proof of protonated imidazo-quinolinium salt as an intermediate in the catalytic cycle

To know the involvement of protonated imidazo-quinoline in the annulation reaction, a control experiment was performed under the standard reaction conditions with independently synthesized **5.1a-H**. The formation of annulated product **5.3a** in 85% yield suggests that direct protonated imidazo-quinolinium salt **5.1a-H** could be a possible intermediate while using Brønsted acid HCl as an additive.

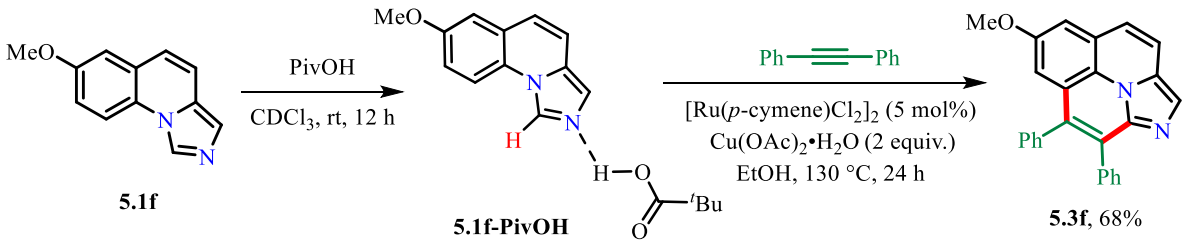


Scheme 5.13. Proof of protonated imidazo-quinolinium salt as an intermediate

5.3.6.4. Interaction of imidazoquinoline with carboxylic acid

On the other hand, in the presence of carboxylic acid, unlike direct pronation there is a possible involvement of hydrogen bonding interaction between azole **5.1f** and the carboxylic acid group, which is validated by the ^{1}H NMR (see Scheme 5.14 and Figure 5.14, the C(2)–H proton of **5.1f-PivOH** is shifted in downfield from δ 8.53 ppm to δ 8.64 ppm). The corresponding species have proven to be one of the important intermediates by performing the reaction with **4.2a** under standard conditions.

TH-3565_186122020

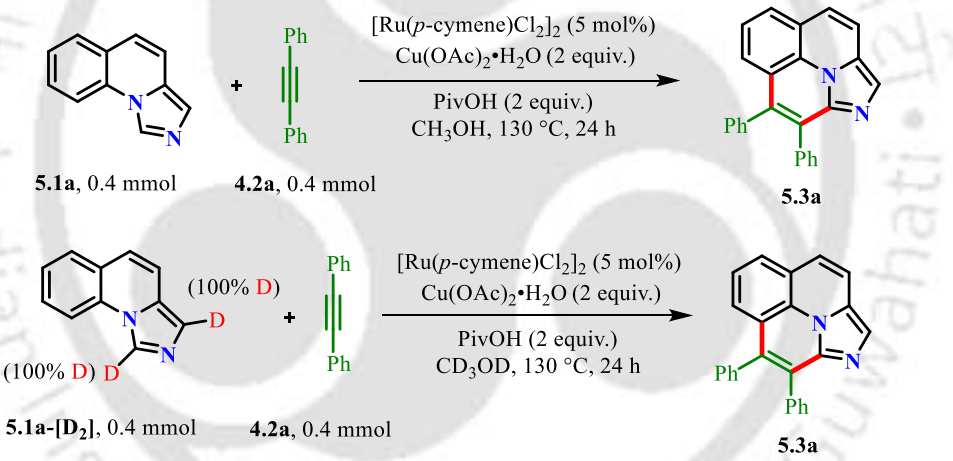


Scheme 5.14. Formation and reaction of imidazoquinoline-carboxylic acid adduct

5.3.6.5. Kinetic studies

(a) Deuterium kinetic isotope effect (DKIE) experiment

To check whether the azole C(2)−H bond cleavage step was rate-limiting, the deuterium kinetic isotope effect (DKIE) experiment was performed using **5.1a** and **5.1a-[D2]** as substrates. The initial kinetics were studied in two parallel reactions. The DKIE value was found to be 2.64 ± 0.18 indicating the fused imidazo-quinoline C(2)−H bond cleavage of **5.1a** as the turnover-limiting step (see details in section 5.5.6).



Scheme 5.15. Annulation reaction of **5.1a** and **5.1a-[D2]**

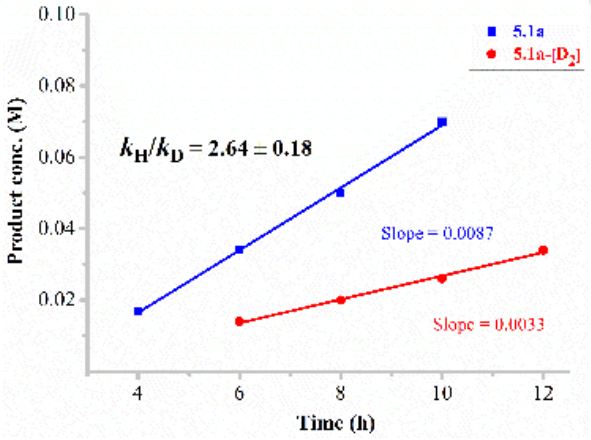


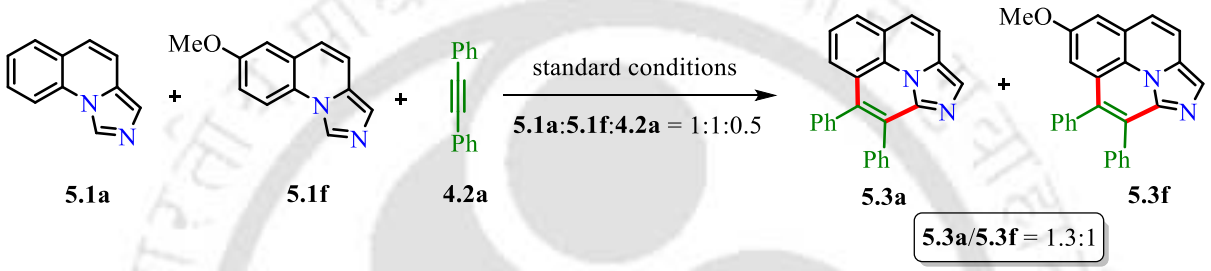
Figure 5.7. Concentration [Product] *vs* time plot of annulation reactions of **5.1a** and **5.1a-[D2]**

TH-3565_186122020

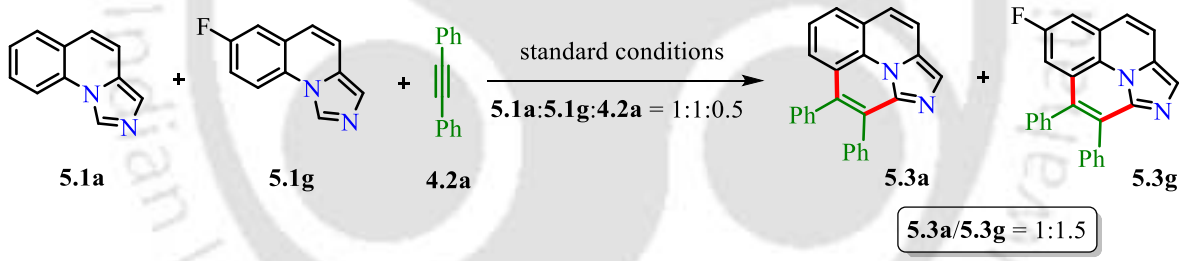
(b) Competitive annulation reactions with electronically different substrates

Furthermore, the electronic effect of the imidazo-quinoline substrate on the rate of the reaction was examined (Scheme 5.16). The reaction was examined with electron-donating and electron-withdrawing substituents at the C7-position in **5.1a** under standard reaction conditions. A competitive annulation reaction suggested that the electron-withdrawing group (−F) on the imidazo-quinoline moiety enhanced the reaction rate compared to an electron-donating group (−OMe). The study further supported that imidazo-quinoline C(2)−H bond cleavage could be the rate-limiting step, excluding the possibility of controlling the reaction rate through reductive elimination.

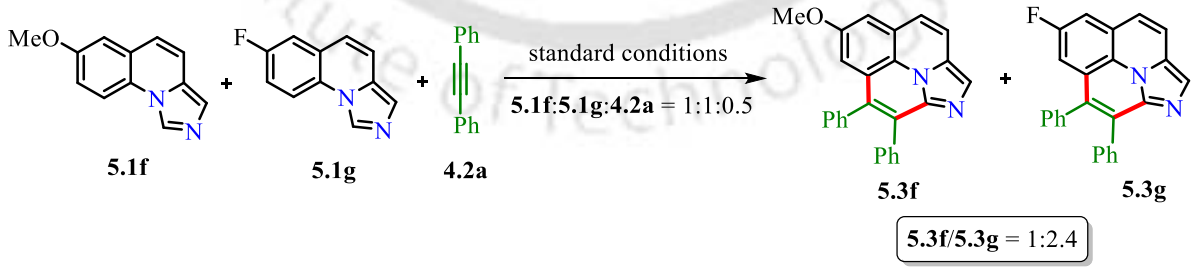
i) Intermolecular competition experiment between **5.1a** and **5.1f**:



ii) Intermolecular competition experiment between **5.1a** and **5.1g**:



iii) Intermolecular competition experiment between **5.1f** and **5.1g**:



Scheme 5.16. Competitive annulation reactions between electronically different substrate

5.3.6.6. Determination of regioselectivity of alkyne insertion into M−C bonds

To determine the regioselectivity of alkyne insertion into M−C bonds (M−C_{aryl} *vs.* M−C_{NHC} bonds of five-membered intermediate **Int5**, theoretical calculations were performed. The

TH-3565_186122020

Mulliken charges of C_{NHC} were found to be 0.310 and C_{aryl} was -0.033, suggesting that a higher electron density is in Ru−C_{aryl} than Ru−C_{NHC} (Figure 5.8). Hence, alkyne insertion may favour the Ru−C_{aryl} moiety over the Ru−C_{NHC} moiety, although there is an equal possibility of alkyne insertion into both the M−C bonds of the complex.

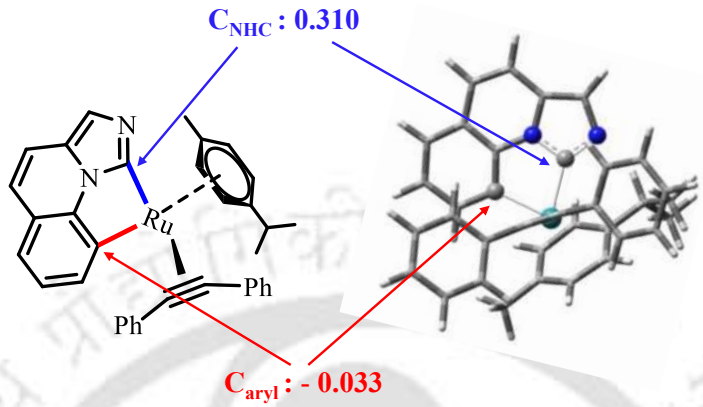
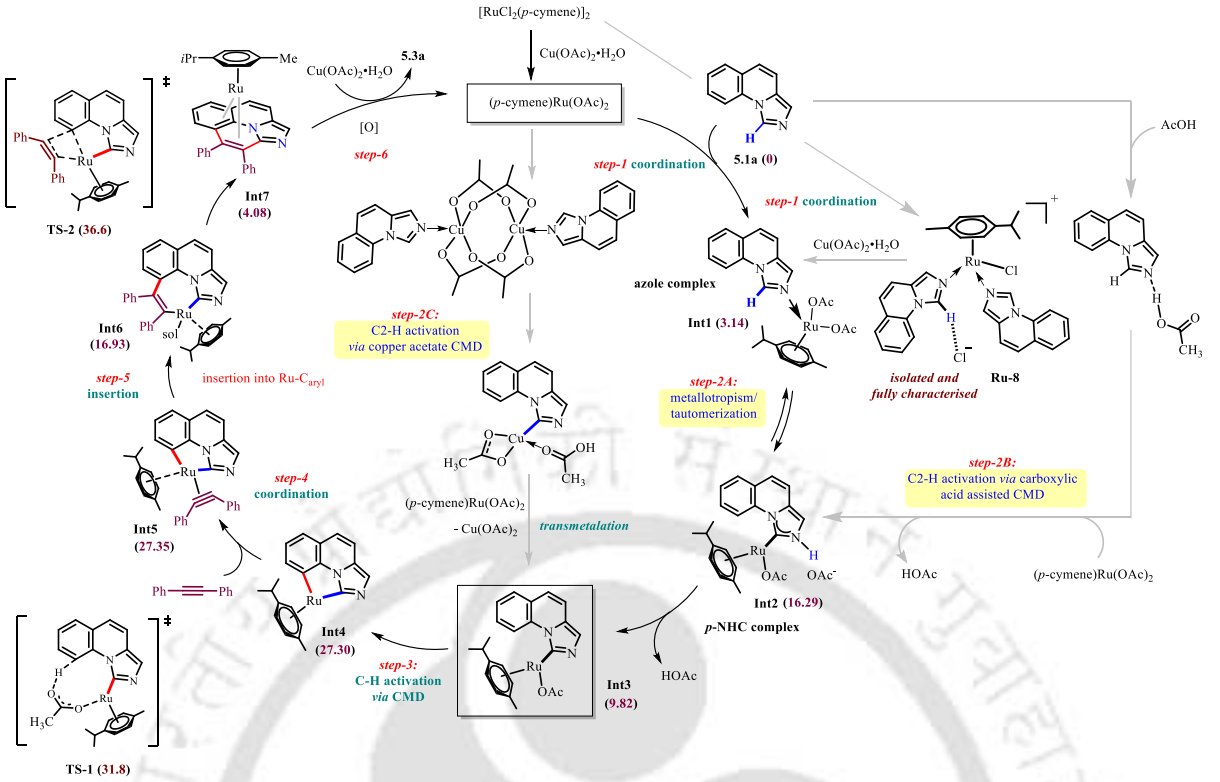


Figure 5.8. Natural bond orbital (NBO) analysis of **int5**

5.3.7. Proposed mechanism

On the basis of experimental observation, a plausible reaction mechanism has been proposed (Scheme 5.17). The C(2)−H bond activation of **5.1a** can occur in three possible pathways and lead to the formation of active imizadolyl-quinoline Ru(II) complex **Int3**. These likely proceed *via* metallotropism/tautomerization effect, carboxylic assisted CMD pathway, and copper acetate mediated transmetallation. The imidazo-quinoline **5.1a** interacts with Ru(*p*-cymene)$(OAc)_2$ to generate Ru(II)-azole complex **Int1**. Similar species can also be formed by the reaction of **5.1a** with $[Ru(p\text{-cymene})Cl_2]_2$ to form *N*-coordinated Ru^{II}-complex **Ru-8**, followed by ligand exchange reaction with copper acetate. Then corresponding azole complex **Int1** undergoes metallotropism triggered C(2)−H activation to form *p*-NHC complex **Int2**. Alternatively, the same *p*-NHC complex **Int2** can be formed *via* the carboxylic acid-assisted CMD pathway which is subsequently converted into imidazolyl-quinoline Ru(II) complex **Int3** by releasing acetic acid. The last possible pathway is the Lewis acid copper acetate-induced CMD pathway. Then intermediate **Int3** takes part in intramolecular aryl C−H activation and forms the five-membered cyclometalated complex **Int4** *via* CMD process. Next, alkyne coordination follows and produces complex **Int5**, followed by alkyne insertion into Ru−C_{aryl} to give seven-membered ruthenacyle intermediate **Int6**. Subsequently, intermediate **Int6** undergoes reductive elimination to form ruthenium(0) sandwich complex **Int7** which is oxidized by copper acetate to regenerate the catalytically active ruthenium(II)acetate species and release the corresponding annulated product **5.3a**.

TH-3565_186122020



Scheme 5.17. Proposed mechanism

5.3.8. Computational studies

To support the reaction pathway for this annulation reaction, I have executed DFT calculations using M06L/BS1 level of theory. The pathway for the formation of *p*-NHC Ru(II) complex **Int2** (ΔG = 16.3 kcal/mol) is energetically uphill, however, imidazolyl-fused-quinoline Ru(II) complex **Int3** (ΔG = 9.82 kcal/mol) is energetically downhill. The resulting complex subsequently participates in intramolecular aryl C−H activation *via* CMD process with an energy barrier of 22 kcal/mol to yield the cyclometalated intermediate **Int4** (ΔG = 27.30 kcal/mol). Subsequently, complex **Int5** (ΔG = 27.35 kcal/mol) is obtained by ligand exchange. This is followed by alkyne insertion into Ru−C_{aryl}, resulting in a seven-membered inserted intermediate **Int6** (ΔG = 16.9 kcal/mol) with an energy barrier of $\Delta G^{\ddagger}$ = 9.3 kcal/mol. After that, **Int6** leads to reductive elimination with ΔG = 4.1 kcal/mol to produce the Ru(0) species **Int7**. Finally, Ru(0) species was oxidized by copper acetate with ΔG = -25.9 kcal/mol and regenerated the catalyst.

TH-3565_186122020

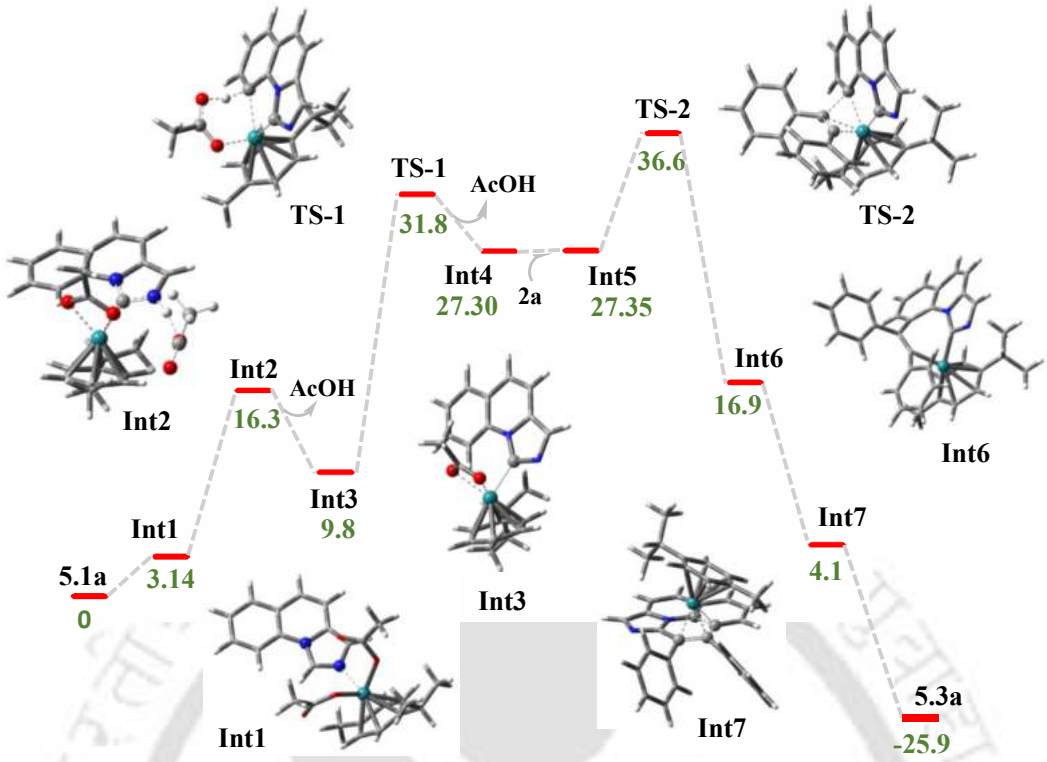


Figure 5.9. Energy profile diagram for the formation of annulated product

5.4. Summary

In summary, I have developed a Ru(II)-catalyzed oxidative annulation reaction of imidazo[1,5-*a*]quinoline with alkynes *via* double C−H activation, leading to the formation of highly functionalized quinolizines. The addition of carboxylic acid is the key to succeeding this goal. The reaction displays excellent regioselectivity and shows a wide range of substrate scope including bioactive (±)-*α*-tocopherol derivatives. The post-transformations of the synthesized product have also been carried out to demonstrate the potential of the developed methodology. Most of the annulated compounds show excellent polarity-sensitive fluorescence properties and aggregation-induced emission (AIE) properties. The important practical features are the use of a cheap catalytic system, aerobic reaction conditions, functional group diversity, biomass-derived solvent as a reaction medium, and catalyst recycling. Various control experiments, kinetic studies and DFT studies were demonstrated to support the reaction mechanism. The current protocol appears to have the potential for the synthesis of a new class of organic functional materials.

5.5. Experimental section

5.5.1. General information

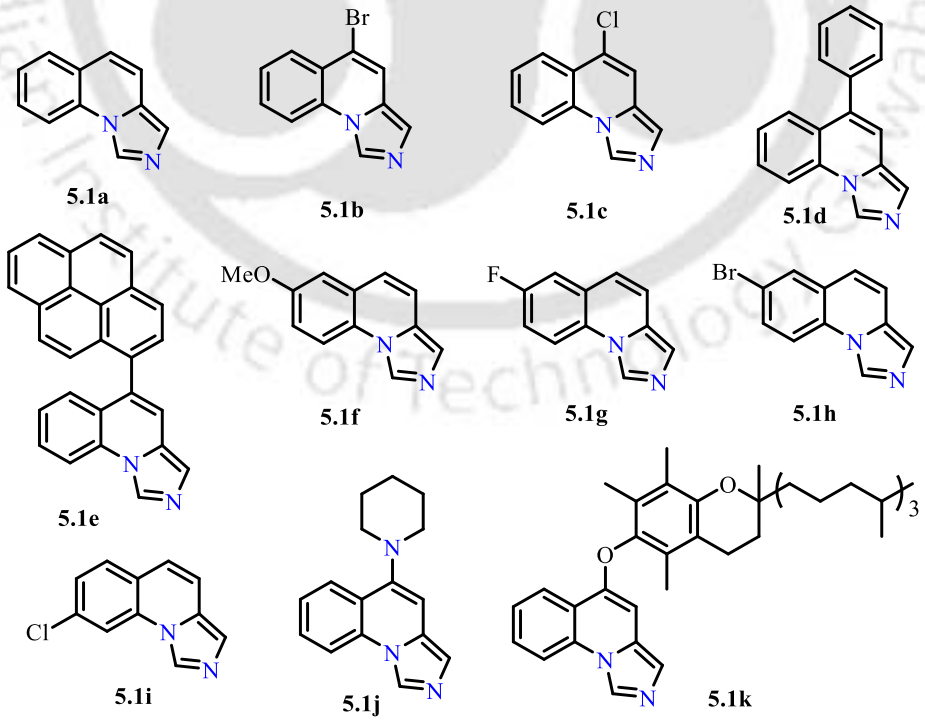
All the reagents and chemicals were purchased from common commercial suppliers like Sigma-Aldrich, Alfa Aesar, Merck, Spectrochem, Avra Synthesis Pvt. Ltd., BLD Pharma and directly used as received without any further purification unless otherwise mentioned. Alkynes **4.2a**, **4.2g**, **4.2k** and **4.2l** are commercially available and were used as supplied. Other alkynes

TH-3565_186122020

4.2c-d,[16a] **4.2f**,[16a] **4.2h**,[16b] **4.2j**,[16c] **4.2n**[16a] and **4.2o**[16a] were synthesized through Sonogashira-coupling of terminal alkynes according to a previously described method. The substituted quinoline-2-carboxaldehydes were synthesized according to the reported literature procedure.[17] ^{1}H, $^{13}C\{^{1}H\}$ and ^{19}F NMR spectra of the compounds were measured in $CDCl_3$ as a solvent by using TMS as an internal standard. Chemical shifts, δ (in ppm), were reported relative to TMS δ (^{1}H) 0.0 ppm, δ (^{13}C) 0.0 ppm, which was used as the internal reference. Otherwise, the solvent's residual proton resonance and carbon resonance $CDCl_3$: δ (^{1}H) 7.26 ppm, δ (^{13}C) 77.16 ppm were used for calibration. Bruker Avance III 600, 500 and 400 spectrometers were used to record the NMR spectra. Chemical shift (δ) values were reported in ppm and spin-spin coupling constant (J) was expressed in Hz and other data were reported as follows: s = singlet, d = doublet, dd = doublet of doublet, dt = doublet of triplet, t = triplet, m = multiplet, q = quartet, p = pentet, br = broad, and brs = broad singlet. MS (ESI-HRMS): Mass spectra were recorded on an Agilent Accurate-Mass Q-TOF LC/MS 6546. Merck silica gel 60-120 mesh and neutral alumina 60-325 mesh were used for column chromatography. All the starting materials and their annulated products were characterized by spectroscopic methods and compared to literature wherever applicable, otherwise stated. All the annulation reactions were carried out in a preheated oil bath under air unless otherwise mentioned. Completion of reactions was examined by thin layer chromatography carried out on pre-coated Merck silica gel-60 F254 aluminium plates with ultraviolet light (UV) or iodine as visualizing agents.

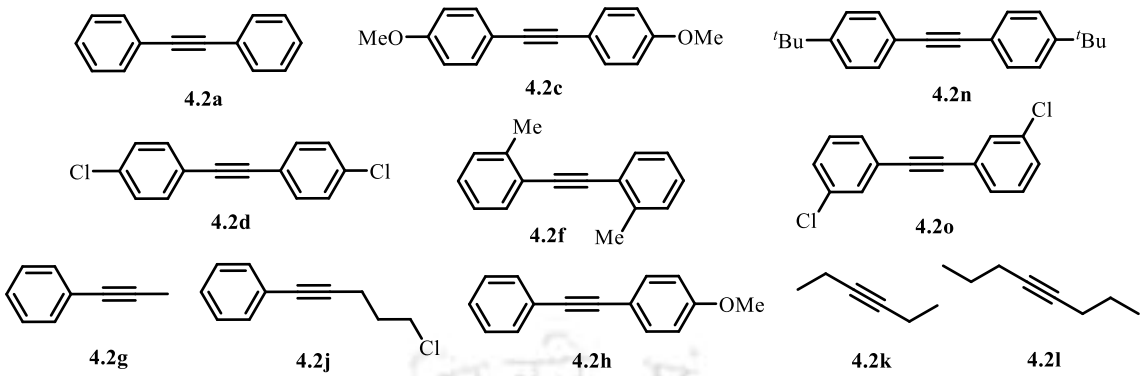
5.5.2. Synthesis of starting materials

Imidazo[1,5-*a*]quinoline employed in the reaction:



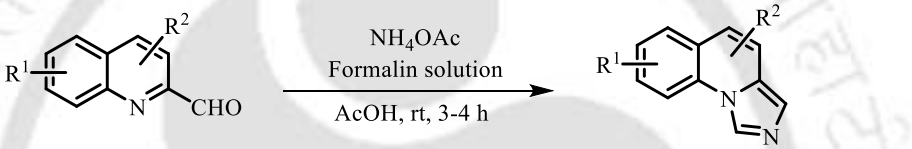
TH-3565_186122020

Alkynes employed in the reaction:



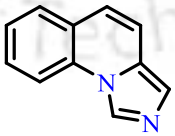
Experimental procedures for starting materials:

General procedure (GP-I)



To a stirred suspension of substituted quinoline-2-carboxaldehyde (0.5 mmol, 1 equiv.) in acetic acid (3.0 mL), ammonium acetate (1.15 mmol, 2.3 equiv.) was added and the reaction mixture was stirred at room temperature. Then 37% formalin solution (0.75 mmol, 1.5 equiv.) was added dropwise to the stirred solution and stirred for 3-4 hours at room temperature. After completion of the reaction as confirmed by TLC, the crude reaction mixture was concentrated under reduced pressure, quenched with aqueous $NaHCO_3$ solution and extracted with ethyl acetate (3 × 10 mL). The solvent was removed in a rotary evaporator and purified by using silica gel column chromatography with ethyl acetate/ pet ether as the eluent to obtain the desired pure product.

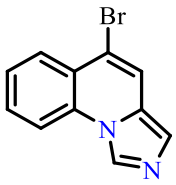
Imidazo[1,5-*a*]quinoline (5.1a)



Following the general procedure GP-I, the title compound **5.1a** was isolated as a brown oil using silica gel column chromatography with ethyl acetate/ pet ether (*v/v* = 3/5, R_f = 0.5) in 81% yield (68.1 mg). ^{1}H NMR (600 MHz, Chloroform-*d*): δ 8.65 (s, 1H), 7.96 (d, J = 8.3 Hz, 1H), 7.67 (d, J = 7.9 Hz, 1H), 7.56 (t, J = 7.8 Hz, 1H), 7.48 (br, 1H), 7.42 (t, J = 7.4 Hz, 1H), 7.33 (d, J = 9.4 Hz, 1H), 7.04 (d, J = 9.4 Hz, 1H). ^{13}C NMR (151 MHz, Chloroform-*d*): δ 130.8, 128.7, 128.6, 128.5, 127.8, 125.5, 124.1, 122.5, 121.1, 116.7, 114.5.

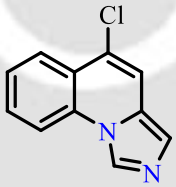
TH-3565_186122020

5-bromoimidazo[1,5-*a*]quinoline (5.1b)



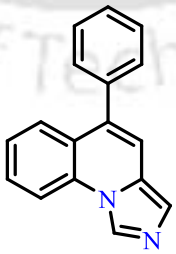
Following the general procedure GP-I, the title compound **5.1b** was isolated as a yellow oil using silica gel column chromatography with ethyl acetate/ pet ether (*v/v* = 3/10, R_f = 0.3) in 84% yield (103.8 mg). ^{1}H NMR (600 MHz, Chloroform-*d*): δ 8.63 (s, 1H), 8.07 (d, *J* = 8.0 Hz, 1H), 7.95 (d, *J* = 8.2 Hz, 1H), 7.68 (s, 1H), 7.64 – 7.61 (m, 1H), 7.51 (t, *J* = 7.4 Hz, 1H), 7.46 – 7.44 (m, 1H). ^{13}C NMR (151 MHz, Chloroform-*d*): δ 131.1, 129.9, 129.2, 126.6, 126.2, 126.1, 122.80, 122.75, 120.4, 115.4, 114.8. HRMS (ESI) *m/z*: calcd. for $C_{11}H_8BrN_2$ $[M+H]^+$: 246.9866; found: 246.9867.

5-chloroimidazo[1,5-*a*]quinoline (5.1c)



Following the general procedure GP-I, the title compound **5.1c** was isolated as a colourless oil using silica gel column chromatography with ethyl acetate/ pet ether (*v/v* = 3/10, R_f = 0.5) in 85% yield (86.1 mg). ^{1}H NMR (500 MHz, Chloroform-*d*): δ 8.61 (s, 1H), 8.12 – 8.10 (m, 1H), 7.98 (d, *J* = 8.2 Hz, 1H), 7.66 – 7.63 (m, 1H), 7.54 – 7.51 (m, 1H), 7.48 (s, 1H), 7.44 (s, 1H). ^{13}C NMR (126 MHz, Chloroform-*d*): δ 129.9, 128.3, 128.0, 126.6, 126.1, 125.4, 123.0, 122.2, 116.5, 114.8. HRMS (ESI) *m/z*: calcd. for $C_{11}H_8ClN_2$ $[M+H]^+$: 203.0371; found: 203.0369.

5-phenylimidazo[1,5-*a*]quinoline (5.1d)

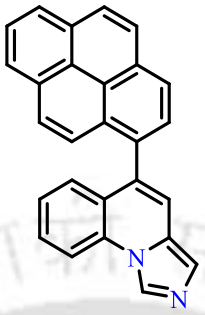


Following the general procedure GP-I, the title compound **5.1d** was isolated as a white solid using silica gel column chromatography with ethyl acetate/ pet ether (*v/v* = 3/10, R_f = 0.6) in 80% yield (97.7 mg). ^{1}H NMR (500 MHz, Chloroform-*d*): δ 8.67 (s, 1H), 8.03 (d, *J* = 8.2 Hz, 1H), 7.69 – 7.67 (m, 1H), 7.59 – 7.56 (m, 1H), 7.51 – 7.43 (m, 6H), 7.38 – 7.35 (m, 1H), 7.27 (s, 1H). ^{13}C NMR (126 MHz, Chloroform-*d*): δ 138.9, 133.5, 131.3, 129.7, 128.8, 128.7, 128.0,

TH-3565_186122020

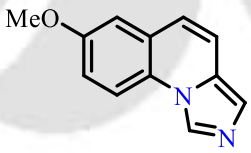
127.9, 125.4, 124.1, 123.2, 116.8, 114.9. HRMS (ESI) *m/z*: calcd. for $C_{17}H_{13}N_2$ $[M+H]^+$: 245.1074; found: 245.1073.

5-(pyren-1-yl)imidazo[1,5-*a*]quinoline (5.1e)



Following the general procedure GP-I, the title compound **5.1e** was isolated as a yellow solid using silica gel column chromatography with ethyl acetate/ pet ether (*v/v* = 4/10, R_f = 0.4) in 76% yield (140 mg). ^{1}H NMR (600 MHz, Chloroform-*d*): δ 8.79 (s, 1H), 8.29 (d, *J* = 7.7 Hz, 1H), 8.24 (d, *J* = 7.6 Hz, 1H), 8.17 – 8.16 (m, 3H), 8.11 (d, *J* = 8.3 Hz, 1H), 8.05 – 8.00 (m, 2H), 7.95 (d, *J* = 9.2 Hz, 1H), 7.83 (d, *J* = 9.2 Hz, 1H), 7.69 – 7.66 (m, 1H), 7.58 – 7.55 (m, 1H), 7.48 (s, 1H), 7.20 – 7.16 (m, 2H). ^{13}C NMR (151 MHz, Chloroform-*d*): δ 133.5, 132.31, 132.28, 132.2, 132.12, 132.10, 131.5, 131.4, 131.0, 130.1, 128.9, 128.7, 128.62, 128.57, 128.2, 128.0, 127.5, 126.4, 125.6, 125.5, 125.3, 124.94, 124.87, 124.8, 123.2, 118.5, 114.9. HRMS (ESI) *m/z*: calcd. for $C_{27}H_{17}N_2$ $[M+H]^+$: 369.1387; found: 369.1389.

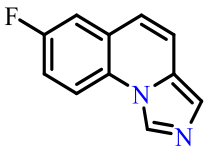
7-methoxyimidazo[1,5-*a*]quinoline (5.1f)



Following the general procedure GP-I, the title compound **5.1f** was isolated as a yellow solid using silica gel column chromatography with ethyl acetate/ pet ether (*v/v* = 9/10, R_f = 0.6) in 82% yield (81.3 mg). ^{1}H NMR (400 MHz, Chloroform-*d*): δ 8.53 (s, 1H), 7.85 (d, *J* = 8.9 Hz, 1H), 7.43 (s, 1H), 7.30 (d, *J* = 9.5 Hz, 1H), 7.14 – 7.08 (m, 2H), 6.95 (d, *J* = 9.5 Hz, 1H), 3.89 (s, 3H). ^{13}C NMR (151 MHz, Chloroform-*d*): δ 157.2, 128.5, 127.6, 125.5, 125.4, 122.7, 121.0, 117.5, 116.7, 115.9, 110.9, 55.8. HRMS (ESI) *m/z*: calcd. for $C_{12}H_{11}N_2O$ $[M+H]^+$: 199.0866; found: 199.0867.

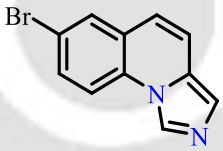
7-fluoroimidazo[1,5-*a*]quinoline (5.1g)

TH-3565_186122020



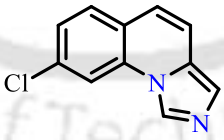
Following the general procedure GP-I, the title compound **5.1g** was isolated as a yellow oil using silica gel column chromatography with ethyl acetate/ pet ether (*v/v* = 3/5, R_f = 0.5) in 87% yield (81 mg). ^{1}H NMR (500 MHz, Chloroform-*d*): δ 8.58 (s, 1H), 7.94 – 7.91 (m, 1H), 7.48 (s, 1H), 7.38 – 7.33 (m, 2H), 7.30 – 7.27 (m, 1H), 6.96 (d, *J* = 9.5 Hz, 1H). ^{13}C NMR (126 MHz, Chloroform-*d*): δ 161.0, 159.1, 128.6, 128.1, 127.7, 126.0 (d, C-F, $J_{C\text{-}F}$ = 8.8 Hz), 123.5, 120.4 (d, C-F, $J_{C\text{-}F}$ = 2.8 Hz), 118.4, 116.4 (d, C-F, $J_{C\text{-}F}$ = 2.3 Hz), 116.3 (d, C-F, $J_{C\text{-}F}$ = 18.0 Hz), 114.1 (d, C-F, $J_{C\text{-}F}$ = 22.9 Hz). ^{19}F NMR (471 MHz, Chloroform-*d*): δ -116.1. HRMS (ESI) *m/z*: calcd. for $C_{11}H_8FN_2$ $[M+H]^+$: 187.0667; found: 187.0669.

7-bromoimidazo[1,5-*a*]quinoline (5.1h)



Following the general procedure GP-I, the title compound **5.1h** was isolated as a brown oil using silica gel column chromatography with ethyl acetate/ pet ether (*v/v* = 4/10, R_f = 0.3) in 85% yield (105 mg). ^{1}H NMR (400 MHz, Chloroform-*d*): δ 8.59 (s, 1H), 7.84 – 7.80 (m, 2H), 7.65 – 7.63 (m, 1H), 7.48 (s, 1H), 7.35 (d, *J* = 9.5 Hz, 1H), 6.93 (d, *J* = 9.5 Hz, 1H). ^{13}C NMR (151 MHz, Chloroform-*d*): δ 131.4, 131.2, 130.0, 128.6, 128.2, 126.1, 123.5, 120.0, 118.7, 118.3, 116.4. HRMS (ESI) *m/z*: calcd. for $C_{11}H_8BrN_2$ $[M+H]^+$: 246.9866; found: 246.9865.

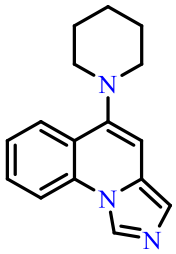
8-chloroimidazo[1,5-*a*]quinoline (5.1i)



Following the general procedure GP-I, the title compound **5.1i** was isolated as a yellow oil using silica gel column chromatography with ethyl acetate/ pet ether (*v/v* = 4/10, R_f = 0.5) in 78% yield (79 mg). ^{1}H NMR (600 MHz, Chloroform-*d*): δ 8.54 (s, 1H), 7.91 (s, 1H), 7.56 (d, *J* = 8.3 Hz, 1H), 7.46 (s, 1H), 7.36 – 7.35 (m, 1H), 7.30 (d, *J* = 9.4 Hz, 1H), 6.96 (d, *J* = 9.4 Hz, 1H). ^{13}C NMR (151 MHz, Chloroform-*d*): δ 134.2, 131.6, 129.9, 128.7, 128.2, 126.1, 123.2, 122.8, 120.4, 117.2, 115.0. HRMS (ESI) *m/z*: calcd. for $C_{11}H_8ClN_2$ $[M+H]^+$: 203.0371; found: 203.0374.

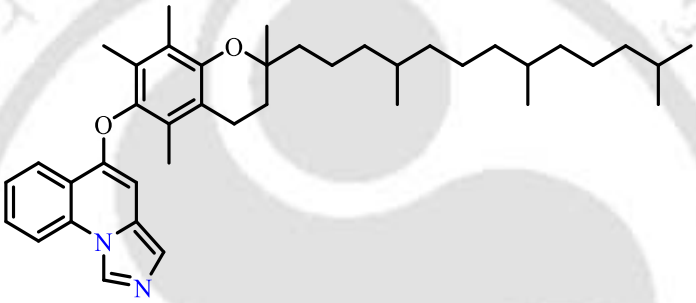
5-(piperidin-1-yl)imidazo[1,5-*a*]quinoline (5.1j)

TH-3565_186122020



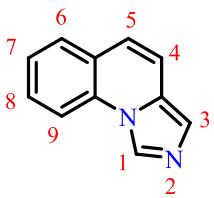
Compound **5.1j** was prepared in a similar method described above by following the general procedure GP-I. The crude reaction mixture was filtered and directly used for the next step without further purification.

5-((2,5,7,8-tetramethyl-2-(4,8,12-trimethyltridecyl)chroman-6-yl)oxy)imidazo[1,5-*a*]quinoline (5.1k)



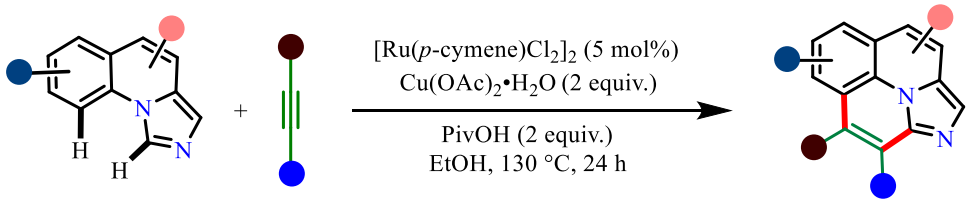
Following the general procedure GP-I, the title compound **5.1k** was isolated as a colourless oil using silica gel column chromatography with ethyl acetate/ pet ether (*v/v* = 4/10, R_f = 0.5) in 75% yield (223.8 mg). ^{1}H NMR (400 MHz, Chloroform-*d*): δ 8.51 (s, 1H), 8.35 (dd, *J* = 8.0, 1.5 Hz, 1H), 7.98 (d, *J* = 9.3 Hz, 1H), 7.67 – 7.63 (m, 1H), 7.55 – 7.51 (m, 1H), 7.09 (s, 1H), 6.05 (d, *J* = 3.7 Hz, 1H), 2.65 (t, *J* = 6.9 Hz, 2H), 2.16 (s, 3H), 2.05 (s, 3H), 2.01 (s, 3H), 1.90 – 1.80 (m, 2H), 1.68 – 1.62 (m, 2H), 1.56 – 1.49 (m, 2H), 1.33 – 1.32 (m, 2H), 1.30 – 1.26 (m, 12H), 1.16 – 1.07 (m, 6H), 0.90 – 0.84 (m, 12H). ^{13}C NMR (126 MHz, Chloroform-*d*): δ 149.4, 148.5, 142.7, 131.8, 129.5, 128.0, 126.9, 126.1, 125.5, 124.1, 123.8, 120.4, 119.7, 118.3, 114.7, 94.1, 75.4, 39.5, 37.63, 37.56, 37.5, 33.0, 32.8, 32.1, 29.8, 29.5, 28.1, 25.0, 24.6, 22.9, 22.84, 22.78, 21.2, 20.8, 19.9, 19.8, 14.3, 12.9, 12.04, 12.00. HRMS (ESI) *m/z*: calcd. for $C_{40}H_{57}N_2O_2$ $[M+H]^+$: 597.4415; found: 597.4416.

Compound numbering undertaken in this work: Representative for **5.1a**.



TH-3565_186122020

5.5.3. General procedure for oxidative annulation reaction (GP-II)



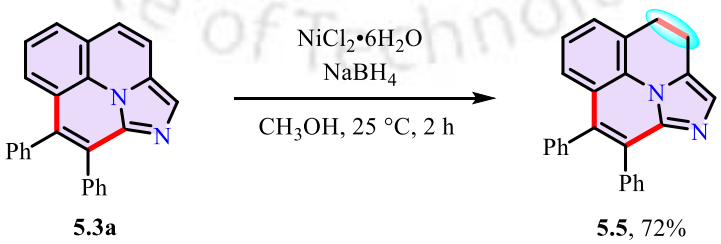
Scheme 5.18. Oxidative annulation reaction

A mixture of imidazo[1,5-*a*]quinoline (0.2 mmol, 1 equiv.), alkyne (0.2 mmol, 1 equiv.), [Ru(*p*-cymene)Cl_2]$_2$ (5 mol%), $Cu(OAc)_2$•H_2O (0.4 mmol, 2 equiv.) and PivOH (0.4 mmol, 2 equiv.) in dry ethanol (4.0 mL) were taken in an oven-dried pressure tube equipped with a magnetic bar. The reaction mixture was stirred in a preheated oil bath at 130 ºC for 24 h. After completion of the reaction, ethanol was added to the reaction mixture and the resulting mixture was passed through a plug of celite. The solvent was evaporated under reduced pressure and the residue was purified by silica gel column chromatography (ethyl acetate/ pet ether as eluent) to get the pure product.

2 mmol scale reaction of 5.1a: In an oven-dried 50 mL pressure tube **5.1a** (336.4 mg, 2 mmol, 1 equiv.), **4.2a** (356.5 mg, 2 mmol, 1 equiv.), [Ru(*p*-cymene)Cl_2]$_2$ (61.2 mg, 5 mol%), $Cu(OAc)_2$•H_2O (800 mg, 4 mmol, 2 equiv.) and PivOH (408.4 mg, 4 mmol, 2 equiv.) were taken with ethanol (8.0 mL). The reaction mixture was stirred in a preheated oil bath at 130 ºC for 24 h. After completion of the reaction, ethanol was added to the reaction mixture and the resulting mixture was passed through a plug of celite. The solvent was evaporated under reduced pressure. The purification was performed by column chromatography on silica gel by using ethyl acetate/ pet ether (*v*/*v* = 1/4, R_f = 0.5) to get the pure product **5.3a** as a yellow solid in 81% yield (558 mg).

5.5.4. Post-synthetic modifications

(i) Selective reduction of 5.3a



5.3a **5.5**, 72%

Scheme 5.19. Reduction reaction of **5.3a**

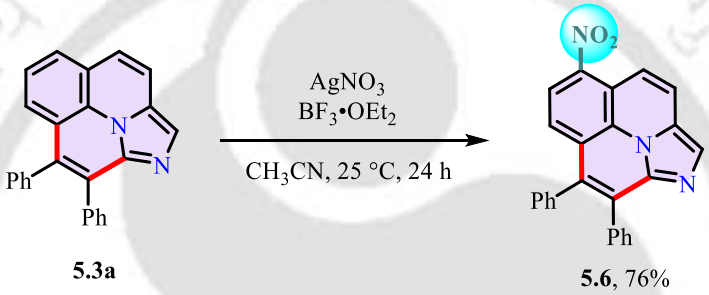
In a sealed tube, **5.3a** (34.4 mg, 0.1 mmol, 1 equiv.) was taken with $NiCl_2$•$6H_2O$ (26 mg, 0.2 mmol, 2 equiv.) in methanol and stirred at room temperature for 5 minutes. To this reaction mixture, $NaBH_4$ (12 mg, 0.3 mmol, 3 equiv.) was added in portions at 0 ºC and allowed to stir at room temperature for 2 h. After completion of the reaction as confirmed by TLC, the solvent

TH-3565_186122020

was removed under vacuum. The organic phase was extracted with ethyl acetate and washed with brine solution. The organic layer was dried over anhydrous Na_2SO_4, concentrated, and then residues were purified by column chromatography on neutral alumina using ethyl acetate/ pet ether (*v/v* = 3/10, R_f = 0.5) as the eluent to afford the desired product **5.5** as a white solid (25 mg, 72%).

^{1}H NMR (600 MHz, $CDCl_3$): δ 7.42 (d, *J* = 7.2 Hz, 1H), 7.40 (s, 1H), 7.37 (d, *J* = 8.2 Hz, 1H), 7.31 (d, *J* = 7.7 Hz, 2H), 7.29 – 7.27 (m, 3H), 7.26 – 7.22 (m, 3H), 7.20 – 7.17 (m, 3H), 3.37 (t, *J* = 7.3 Hz, 2H), 3.31 (t, *J* = 7.3 Hz, 2H). ^{13}C NMR (151 MHz, $CDCl_3$): δ 141.8, 137.1, 135.6, 134.2, 131.3, 130.9, 129.5, 128.8, 128.2, 128.1, 127.9, 127.4, 127.3, 126.7, 125.8, 124.52, 124.49, 123.1, 121.9, 25.3, 19.6. HRMS (ESI) *m/z*: calcd. for $C_{25}H_{19}N_2$ $[M+H]^+$: 347.1543; found: 347.1547.

(ii) Selective nitration of 5.3a



5.3a **5.6**, 76%

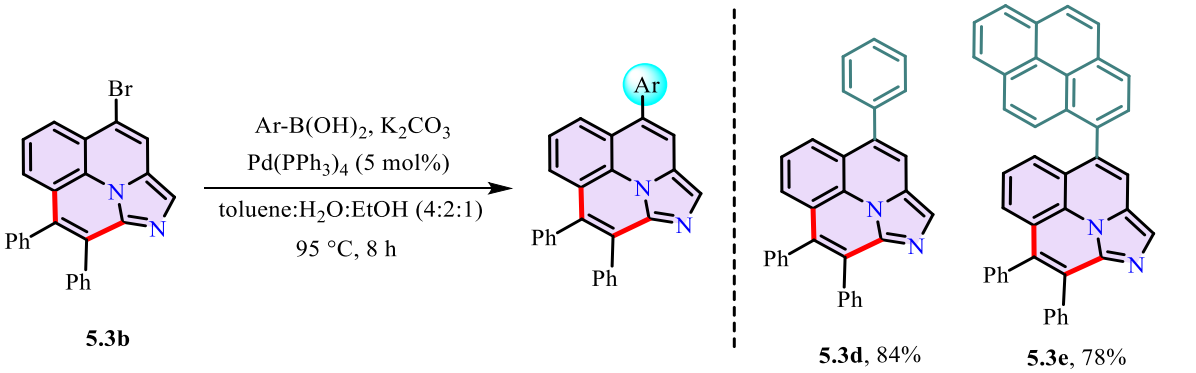
Scheme 5.20. Nitration reaction of **5.3a**

The 8,9-diphenylbenzo[*ij*]imidazo[2,1,5-*de*]quinolizine **5.3a** (72.3 mg, 0.21 mmol, 1 equiv.) was taken in a well dried Schlenk flask with $AgNO_3$ (72 mg, 0.42 mmol, 2 equiv.). At 0 °C, dry acetonitrile (3 mL) was added to it under argon atmosphere and BF_3•Et_2O (0.63 mmol, 3 equiv.) was added slowly for a certain interval of time and stirred at room temperature for 24 h. Full consumption of starting material was confirmed by TLC and the product was purified by silica gel column chromatography using ethyl acetate/ pet ether (*v/v* = 1/6, R_f = 0.6) to get the pure product **5.6** as a red solid (62.1 mg, 76%).

^{1}H NMR (400 MHz, Chloroform-*d*): δ 8.73 (d, *J* = 10.0 Hz, 1H), 8.44 (d, *J* = 9.2 Hz, 1H), 8.33 (s, 1H), 8.07 (d, *J* = 10.0 Hz, 1H), 7.50 (d, *J* = 9.2 Hz, 1H), 7.42 – 7.38 (m, 5H), 7.33 – 7.31 (m, 3H), 7.27 (brs, 1H), 7.25 – 7.24 (m, 1H). ^{13}C NMR (126 MHz, Chloroform-*d*): δ 139.2, 137.7, 136.0, 135.8, 134.3, 132.6, 131.2, 130.9, 130.6, 129.9, 129.7, 129.0, 128.35, 128.29, 128.2, 125.5, 122.6, 122.0, 121.3, 120.6, 118.4. HRMS (ESI) *m/z*: calcd. for $C_{25}H_{16}N_3O_2$ $[M+H]^+$: 390.1238; found: 390.1242.

(iii) Pd-catalyzed coupling reaction of 5.3b

TH-3565_186122020



Scheme 5.21. Suzuki coupling reaction of **5.3b**

Following the reported literature procedure,[18] a well dried Schlenk tube was charged with **5.3b** (42.3 mg, 0.1 mmol, 1 equiv.), aryl boronic acid (0.15 mmol, 1.5 equiv.), K_2CO_3 (70 mg, 0.5 mmol, 5 equiv.) and $Pd(PPh_3)_4$ (6 mg, 5 mol%). To this reaction mixture, toluene (2 mL), H_2O (1 mL) and EtOH (0.5 mL) were added under a nitrogen atmosphere, and the mixture was stirred in a preheated oil bath at 95 °C for 8 h. After completion of the reaction, the reaction mixture was cooled, and filtered through a plug of celite. The resulting mixture was diluted with water and extracted with ethyl acetate. The combined extracts were dried over Na_2SO_4, concentrated, and purified by column chromatography on silica gel (ethyl acetate/pet ether, 1:6, R_f = 0.6) to afford the desired product **5.3d** as a yellow solid in 84% yield (35.3 mg) and **5.3e** as a pale-yellow solid in 78% yield (42.5 mg).

5.5.5. Recyclability and reusability of the catalytic system (Scheme 5.6)

To investigate the reusability of the catalyst and solvent, imidazo[1,5-*a*]quinoline **5.1a** (84.1 mg, 0.5 mmol, 1 equiv.), alkyne **4.2a** (89.2 mg, 0.5 mmol, 1 equiv.), $Cu(OAc)_2$•H_2O (200 mg, 1 mmol, 2 equiv.) and PivOH (102.1 mg, 1 mmol, 2 equiv.) with PEG-400 (2.0 mL) were taken in a microwave tube and stirred under microwave irradiation (*μw*) for 30 minutes at 130 ºC. After completion of the reaction, the reaction mixture was cooled to room temperature, diluted with diethyl ether, and shaken well. Two layers were generated, the upper layer of diethyl ether contains product **5.3a**, which is directly used for further purification (88% yield of **5.3a** from 1st cycle). The lower layer contains PEG-400 with copper salt and the catalyst. Hence respective PEG-400 layer will be reused for the next cycle by adding a fresh solution of substrates **5.1a** (1 equiv.), **4.2a** (1 equiv.), and PivOH (2 equiv.) and stirred under the same reaction conditions. This process was repeated four times without any significant loss in catalytic activity. As depicted in Figure 5.1−5.2, the catalyst, oxidant, and solvent could be reused four times for the synthesis of **5.3a** with a slight loss of activity, indicating that the system exhibits good recyclability. Due to the presence of paramagnetic impurities (copper salt), the catalyst is not able to characterize spectroscopically.

5.5.6. Mechanistic studies

(a) Control experiments

TH-3565_186122020

(i) Proof of [Ru(*p*-cymene)$(OAc)_2$] in the annulation reaction (Scheme 5.7)

Procedure: A mixture of **5.1a** (33.6 mg, 0.2 mmol, 1 equiv.), alkyne **4.2a** (35.6 mg, 0.2 mmol, 1 equiv.), [Ru(*p*-cymene)$(OAc)_2$] (5 mol%), $Cu(OAc)_2$•H_2O (80 mg, 0.4 mmol, 2 equiv.) and PivOH (40.8 mg, 0.4 mmol, 2 equiv.) in dry ethanol (4.0 mL) were taken in an oven-dried pressure tube equipped with a magnetic bar and stirred in a preheated oil bath at 130 ºC for 24 h. After completion of the reaction, ethanol was added to the reaction mixture and the resulting mixture was passed through a plug of celite. The solvent was evaporated under reduced pressure and the residue was purified by silica gel column chromatography to get the pure product **5.3a** as a yellow solid (60.6 mg, 88%). The formation of product **5.3a** suggests that [Ru(*p*-cymene)$(OAc)_2$] is a possible intermediate in the catalytic reaction.

(ii) Impact of $Cu(OAc)_2$•H_2O in the annulation reaction (Scheme 5.8)

Procedure: A mixture of **5.1a** (33.6 mg, 0.2 mmol, 1 equiv.), alkyne **4.2a** (35.6 mg, 0.2 mmol, 1 equiv.), [Ru(*p*-cymene)$(OAc)_2$] (5 mol%) and PivOH (40.8 mg, 0.4 mmol, 2 equiv.) in dry ethanol (4.0 mL) were taken in an oven-dried pressure tube equipped with a magnetic bar. The reaction mixture was stirred in a preheated oil bath at 130 ºC for 24 h. After completion of the reaction, ethanol was added to the reaction mixture and the resulting mixture was passed through a plug of celite. The solvent was evaporated under reduced pressure and the residue was purified by silica gel column chromatography to get the pure product **5.3a** as a yellow solid (2.7 mg, 4%). The formation of only 4% product of **5.3a** implies the necessity of $Cu(OAc)_2$•H_2O in the annulation reaction, which acts as an oxidant in the catalytic reaction.

(iii) Importance of carboxylic acid in the annulation reaction (Scheme 5.9)

Procedure: A mixture of **5.1a** (33.6 mg, 0.2 mmol, 1 equiv.), alkyne **4.2a** (35.6 mg, 0.2 mmol, 1 equiv.), [Ru(*p*-cymene)$(OAc)_2$] (5 mol%), $Cu(OAc)_2$•H_2O (80 mg, 0.4 mmol, 2 equiv.) and acid source (0.4 mmol, 2 equiv.) in dry ethanol (4.0 mL) were taken in an oven-dried pressure tube equipped with a magnetic bar and stirred in a preheated oil bath at 130 ºC for 24 h. After completion of the reaction, ethanol was added to the reaction mixture and the resulting mixture was passed through a plug of celite. The solvent was evaporated under reduced pressure and the residue was purified by silica gel column chromatography to get the pure product **5.3a** as a yellow solid.

(b) Proof of intermediate Ru-8 in the catalytic cycle

(i) Synthesis and characterization of intermediate **Ru-8** (Scheme 5.10)

In an oven dried Schlenk tube **5.1a** (100 mg, 0.59 mmol, 1 equiv.) was taken with [Ru(*p*-cymene)$Cl_2]_2$ (184 mg, 0.30 mmol, 0.5 equiv.) in dry CH_2Cl_2 (4 mL). The reaction mixture was stirred at room temperature for two days under dark conditions. The yellow solution was filtered through a celite plug and reduced under vacuum. The resulting crude was purified on neutral alumina column chromatography (methanol: ethyl acetate = 1:10). The major yellow

TH-3565_186122020

band was collected, concentrated, and precipitated by the addition of Et_2O, which afforded the title complex **Ru-8** as a yellow solid (280.5 mg, 74%). Slow diffusion of petroleum ether into a concentrated solution of complex **Ru-8** in CH_2Cl_2 gave reddish-brown crystals suitable for X-ray diffraction analysis.

^{1}H NMR (500 MHz, Chloroform-*d*): δ 8.69 (d, J = 8.7 Hz, 1H), 8.65 (brs, 1H), 8.37 (d, J = 8.2 Hz, 1H), 8.17 (d, J = 8.2 Hz, 1H), 7.98 – 7.92 (m, 4H), 7.77 (t, J = 7.6 Hz, 1H), 7.68 (d, J = 7.8 Hz, 1H), 7.58 – 7.54 (m, 1H), 7.53 – 7.47 (m, 1H), 7.43 (t, J = 7.6 Hz, 1H), 7.33 (d, J = 9.4 Hz, 1H), 7.26 (s, 1H), 7.04 (d, J = 9.4 Hz, 1H), 5.75 (d, J = 6.0 Hz, 1H), 5.59 (d, J = 6.0 Hz, 1H), 5.55 (d, J = 5.8 Hz, 1H), 5.44 (d, J = 5.8 Hz, 1H), 2.67 – 2.61 (m, 1H), 2.28 (s, 3H), 1.13 (d, J = 6.9 Hz, 3H), 1.01 (d, J = 6.9 Hz, 3H). ^{13}C NMR (126 MHz, Chloroform-*d*): δ 171.3, 152.7, 147.7, 140.0, 131.7, 130.9, 129.2, 129.13, 129.09, 129.0, 128.7, 125.6, 124.4, 122.8, 121.3, 117.1, 114.7, 103.5, 100.3, 85.1, 81.2, 81.0, 80.9, 31.1, 22.7, 21.9, 18.9. HRMS (ESI) *m/z*: calcd. for $C_{32}H_{30}ClN_4Ru$ $[M]^+$: 607.1202; found: 607.1204.

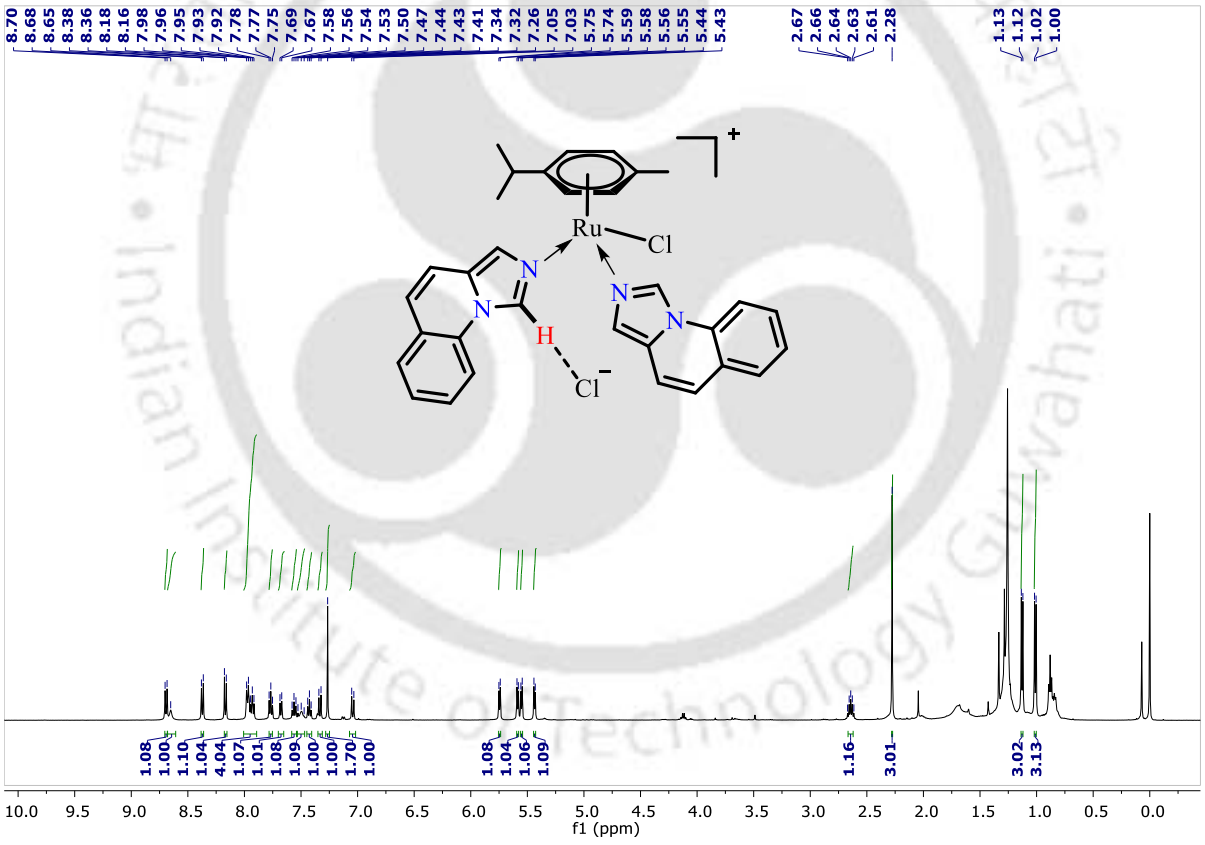


Figure 5.10. ^{1}H NMR spectrum of **Ru-8** ($CDCl_3$, 500 MHz, 298 K)

TH-3565_186122020

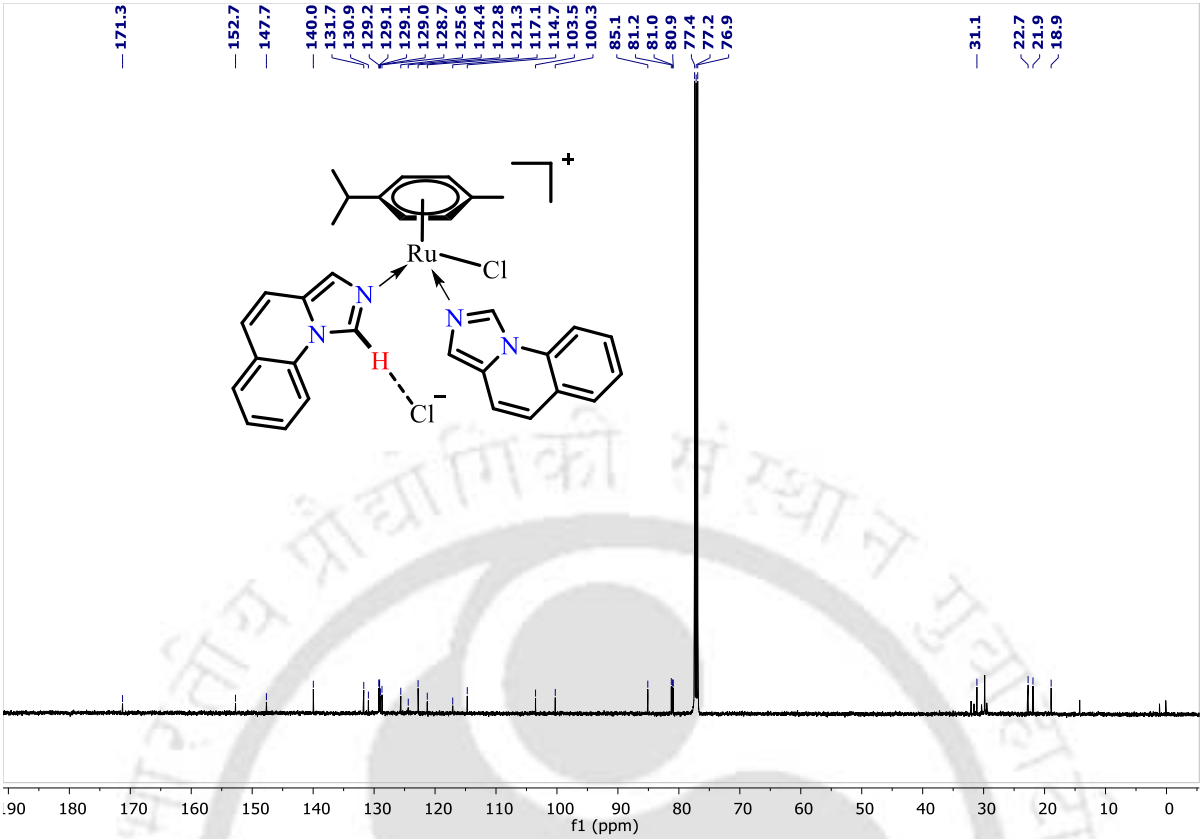


Figure 5.11. $^{13}C\{^{1}H\}$ NMR spectrum of **Ru-8** ($CDCl_3$, 126 MHz, 298 K)

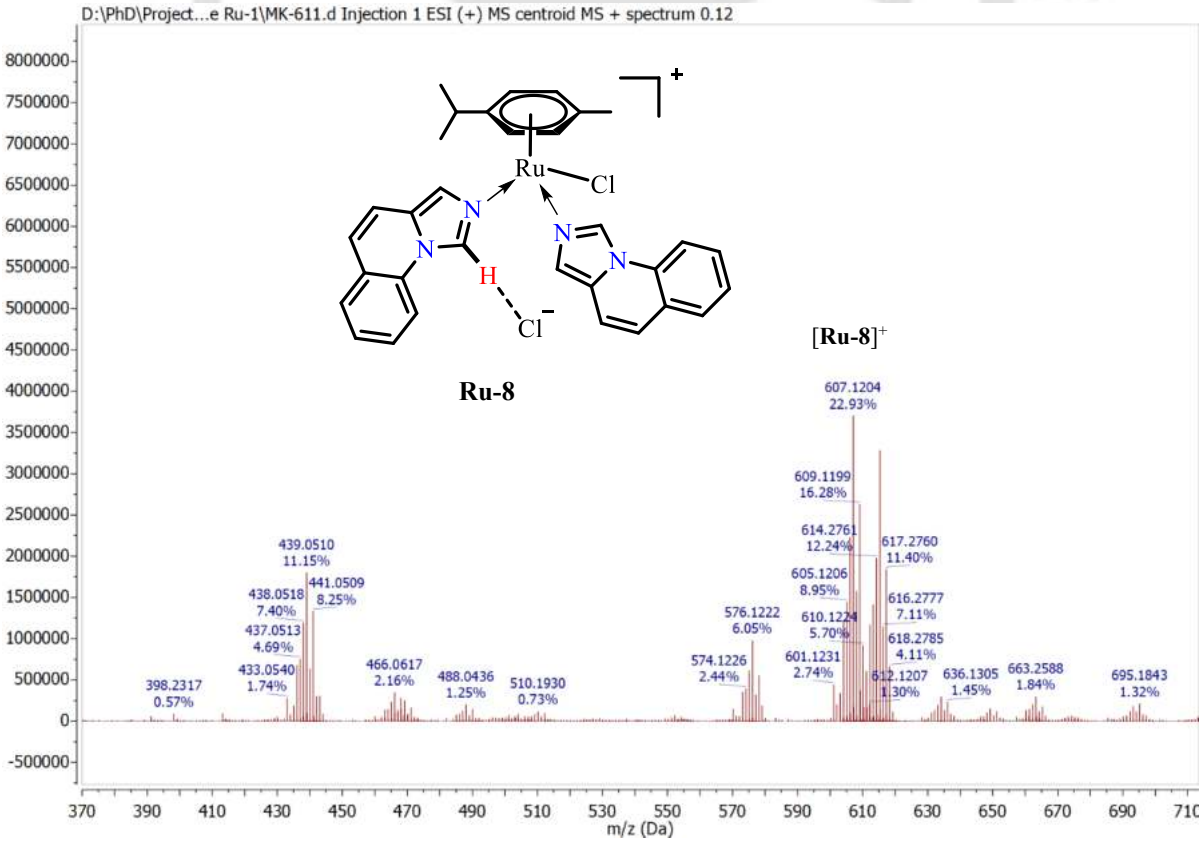


Figure 5.12. ESI-MS spectrum of [**Ru-8**]$^{+}$

TH-3565_186122020

(ii) Stoichiometric reaction with **Ru-8** (Scheme 5.11)

Procedure: A mixture of complex **Ru-8** (64.3 mg, 0.1 mmol, 1 equiv.), **4.2a** (17.8 mg, 0.1 mmol, 1 equiv.) $Cu(OAc)_2•H_2O$ (40 mg, 0.2 mmol, 2 equiv.) and PivOH (20.4 mg, 0.2 mmol, 2 equiv.) in dry EtOH (2.0 mL) were stirred in an oven dried pressure tube at 130 ºC in a preheated oil bath. After 24 h stirring, the reaction mixture was allowed to cool and ethanol was added to it and the resulting mixture was passed through a celite plug. The solvent was evaporated under reduced pressure. The purification was performed by column chromatography on silica gel by using ethyl acetate/ pet ether (*v/v* = 1/4, R_f = 0.5) to get the pure product **5.3a** as a yellow solid in 86% yield (29.6 mg).

(iii) Catalytic reaction with **Ru-8** (Scheme 5.12)

Procedure: To an oven dried pressure tube, **5.1a** (16.8 mg, 0.1 mmol, 1 equiv.), complex **Ru-8** (5 mol%), **4.2a** (17.8 mg, 0.1 mmol, 1 equiv.), $Cu(OAc)_2•H_2O$ (40 mg, 0.2 mmol, 2 equiv.) and PivOH (20.4 mg, 0.2 mmol, 2 equiv.) were loaded with dry EtOH (2.0 mL). The reaction mixture was stirred in a preheated oil bath at 130 ºC for 24 h. Then the reaction mixture was allowed to cool and ethanol was added to it and the resulting mixture was passed through a celite plug. The solvent was evaporated under reduced pressure. The purification was performed by column chromatography on silica gel by using ethyl acetate/ pet ether (*v/v* = 1/4, R_f = 0.5) to get the pure product **5.3a** as a yellow solid in 82% yield (28.2 mg).

(c) Proof of protonated imidazo-quinolinium salt as an intermediate in the catalytic cycle

(i) Synthesis of **5.1a-H** (Scheme 5.13)

Procedure: A mixture of **5.1a** (33.6 mg, 0.2 mmol) with HCl in dioxane (2.0 mL) were taken in a round bottom flask and stirred at room temperature for 24 h. The solvent was evaporated under reduced pressure and directly recorded the ^{1}H NMR spectrum to obtain the protonated species, **5.1a-H** (Figure 5.13). The C(2)–H proton of **5.1a-H** is downfield shifted from δ 8.65 ppm to δ 11.06 ppm and N–H proton is observed at δ 17.04 ppm; which confirms the formation of protonated species **5.1a-H**.

TH-3565_186122020

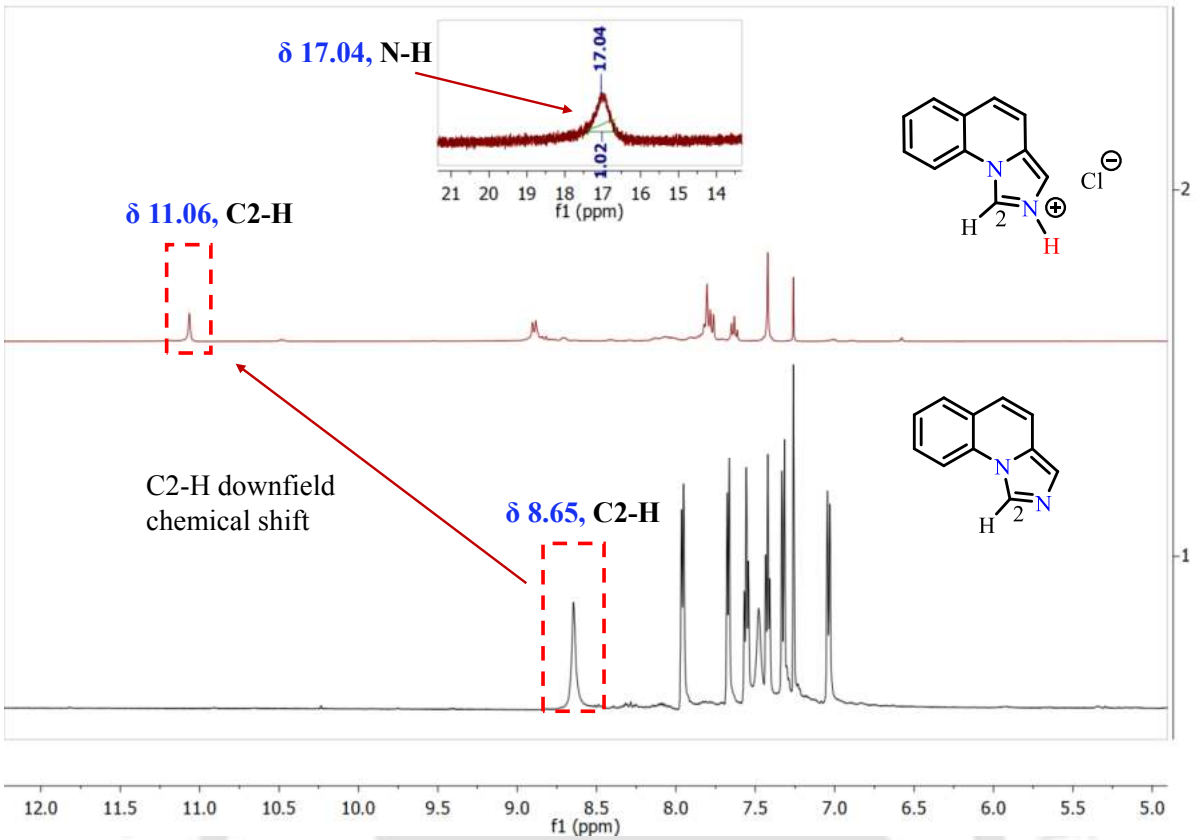


Figure 5.13. ^{1}H NMR spectra of **5.1a** and **5.1a-H** in $CDCl_3$ at 298 K

(ii) Control experiment with **5.1a-H** (Scheme 5.13)

Procedure: In an oven-dried 50 mL pressure tube **5.1a-H** (40.9 mg, 0.2 mmol, 1 equiv.), **4.2a** (35.6 mg, 0.2 mmol, 1 equiv.), $[Ru(p\text{-cymene})Cl_2]_2$ (6.1 mg, 5 mol%) and $Cu(OAc)_2{\bullet}H_2O$ (80 mg, 0.4 mmol, 2 equiv.) were taken with ethanol (4.0 mL). The reaction mixture was stirred in a preheated oil bath at 130 ºC for 24 h. After completion of the reaction, ethanol was added to the reaction mixture and the resulting mixture was passed through a plug of celite. The solvent was evaporated under reduced pressure. The purification was performed by column chromatography on silica gel by using ethyl acetate/ pet ether (v/v = 1/4, R_f = 0.5) to get the pure product **5.3a** as a yellow solid in 85% yield (58.5 mg). The formation of annulated product **5.3a** indicates that protonated imidazo-quinolinium salt **5.1a-H** is a possible intermediate in the annulation reaction.

(d) Interaction of imidazoquinoline with carboxylic acid (Scheme 5.14)

Procedure: In an oven dried sealed tube, a mixture of **5.1f** (19.8 mg, 0.1 mmol, 1 equiv.) and pivalic acid (10.2 mg, 0.1 mmol, 1 equiv.) was taken with $CDCl_3$ (1.0 mL) and stirred at room temperature for 12 h. After completion of the reaction, the reaction mixture was loaded in an NMR tube and recorded the ^{1}H NMR spectra of the solutions. The C(2)–H proton of **5.1f-PivOH** is downfield shifted from δ 8.53 ppm to δ 8.64 ppm which confirms the hydrogen

TH-3565_186122020

bonding interaction between 7-methoxyimidazo[1,5-*a*]quinoline **5.1f** and carboxylic acid (Figure 5.14).

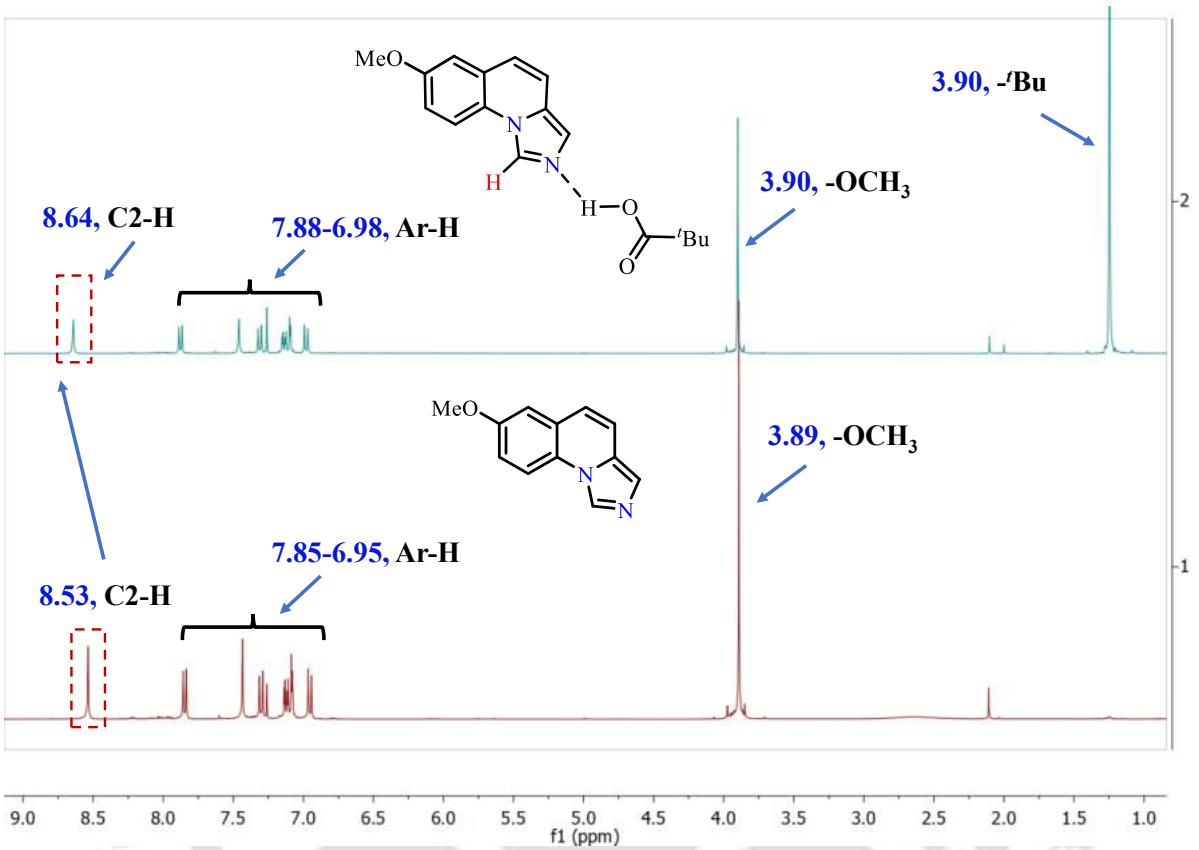


Figure 5.14. ^{1}H NMR spectra of **5.1f** and hydrogen bonding interaction between **5.1f** and pivalic acid in $CDCl_3$ at 298 K.

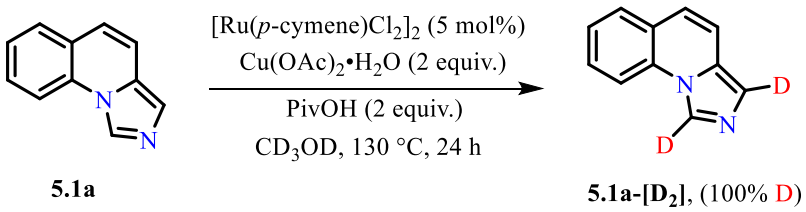
Control experiment with **5.1f-PivOH** (Scheme 5.14)

Procedure: In an oven-dried 50 mL pressure tube **5.1f-PivOH** (30 mg, 0.1 mmol, 1 equiv.), **4.2a** (17.8 mg, 0.1 mmol, 1 equiv.), $[Ru(p\text{-cymene})Cl_2]_2$ (3.1 mg, 5 mol%) and $Cu(OAc)_2 \cdot H_2O$ (40 mg, 0.2 mmol, 2 equiv.) were taken with ethanol (2.0 mL). The reaction mixture was stirred in a preheated oil bath at 130 ºC for 24 h. After completion of the reaction, ethanol was added to the reaction mixture and the resulting mixture was passed through a plug of celite. The solvent was evaporated under reduced pressure. The purification was performed by column chromatography on silica gel by using ethyl acetate/ pet ether (v/v = 4/10, R_f = 0.7) to get the pure product **5.3f** as a yellow solid in 68% yield (20.4 mg). The formation of annulated product **5.3f** indicates that the corresponding hydrogen-bonded species **5.1f-PivOH** might be a possible intermediate in the annulation reaction.

(e) Kinetic studies

(i) Synthesis of **5.1a-[D$_2$]**

TH-3565_186122020



5.1a **5.1a-[D$_2$]**, (100% D)

Scheme 5.22. Synthesis of **5.1a-[D$_2$]**

Procedure: In an oven-dried 50 mL pressure tube **5.1a** (168.2 mg, 1 mmol, 1 equiv.), [Ru(*p*-cymene)Cl$_2$]$_2$ (30.6 mg, 5 mol%), Cu(OAc)$_2$•H$_2$O (400 mg, 2 mmol, 2 equiv.) and PivOH (204.3 mg, 2 mmol, 2 equiv.) were taken with CD$_3$OD (3.0 mL). The reaction mixture was stirred in a preheated oil bath at 130 ºC for 24 h. After completion of the reaction, the solvent was evaporated under reduced pressure. The purification was performed by column chromatography on silica gel by using ethyl acetate/ pet ether (*v*/*v* = 3/5, R_f = 0.5) to get the pure product **5.1a-[D$_2$]** as a brown oil (yield = 153.2 mg, 90%) with 100% deuteration at the C(2) position of **5.1a-[D$_2$]**.

^{1}H NMR (600 MHz, Chloroform-*d*): δ 7.95 (d, J = 7.4 Hz, 1H), 7.66 (d, J = 7.7 Hz, 1H), 7.54 (t, J = 7.4 Hz, 1H), 7.41 (t, J = 7.4 Hz, 1H), 7.30 (d, J = 9.3 Hz, 1H), 7.04 (d, J = 8.5 Hz, 1H).

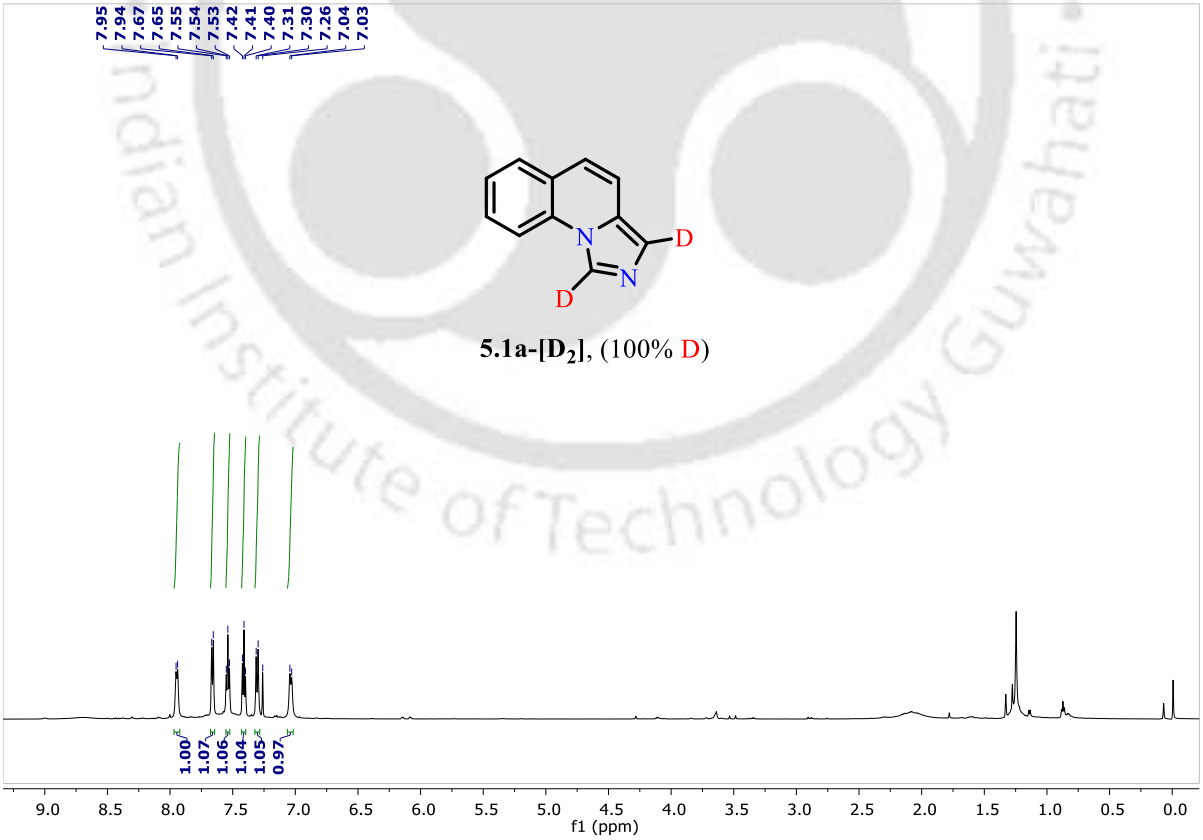


Figure 5.15. ^{1}H NMR spectrum of **5.1a-[D$_2$]** (CDCl$_3$, 600 MHz, 298 K)

TH-3565_186122020

(ii) Deuterium kinetic isotope effect (DKIE) experiment (Scheme 5.15)

Procedure: By following the standard catalytic procedure GP-II, two parallel reactions were performed by using **5.1a** in CH_3OH (2.0 mL) and **5.1a-[D$_2$]** in CD_3OD (2.0 mL) as substrates. After completion of the reaction, the solvent was evaporated under reduced pressure, and the residue was purified by column chromatography on silica gel using EtOAc/Petroleum ether as the eluent. The isolated yields of the products at different time intervals have been calculated. Then the initial rates of product formation were obtained from the plot of the concentration of product *vs* time (Figure 5.7). Reactions were performed in triplicate and an average k_H/k_D = 2.64 ± 0.18 was obtained by comparing the initial rates of these two reactions.

(f) Competitive annulation reactions with electronically different substrates (Scheme 5.16)

(i) Intermolecular competition experiment between **5.1a** and **5.1f**:

Procedure: A standard catalytic reaction procedure was followed by using **5.1a** (33.6 mg, 0.2 mmol, 1 equiv.), **5.1f** (39.6 mg, 0.2 mmol, 1 equiv.), diphenylacetylene **4.2a** (17.8 mg, 0.1 mmol, 0.5 equiv.), $Cu(OAc)_2$•H_2O (80 mg, 0.4 mmol, 2 equiv.), PivOH (40.8 mg, 0.4 mmol, 2 equiv.) and [Ru(*p*-cymene)Cl_2]$_2$ (6.1 mg, 5 mol%) were loaded in a pressure tube with EtOH (3.0 mL). The reaction mixture was stirred in a preheated oil bath at 130 °C for 24 h. After completion of the reaction, the resulting mixture was passed through a plug of celite. The solvent was evaporated under reduced pressure and the residue was absorbed onto small amounts of silica gel. The purification was performed by column chromatography on silica gel (EtOAc/Pet ether: 1/4 → 4/10) to get the isolated product **5.3a** (28 mg, 42%) and **5.3f** (24.7 mg, 33%) in 1.3:1 ratio.

(ii) Intermolecular competition experiment between **5.1a** and **5.1g**:

Procedure: A standard catalytic reaction procedure was followed by using **5.1a** (33.6 mg, 0.2 mmol, 1 equiv.), **5.1g** (37.2 mg, 0.2 mmol, 1 equiv.), diphenylacetylene **4.2a** (17.8 mg, 0.1 mmol, 0.5 equiv.), $Cu(OAc)_2$•H_2O (80 mg, 0.4 mmol, 2 equiv.), PivOH (40.8 mg, 0.4 mmol, 2 equiv.) and [Ru(*p*-cymene)Cl_2]$_2$ (6.1 mg, 5 mol%) were loaded in a pressure tube with EtOH (3.0 mL). The reaction mixture was stirred in a preheated oil bath at 130 °C for 24 h. After completion of the reaction, the resulting mixture was passed through a plug of celite. The solvent was evaporated under reduced pressure and the residue was absorbed onto small amounts of silica gel. The purification was performed by column chromatography on silica gel (EtOAc/Pet ether: 1/6 → 1/4) to get the isolated product **5.3a** (20.7 mg, 30%) and **5.3g** (32.6 mg, 45%) in 1:1.5 ratio.

(iii) Intermolecular competition experiment between **5.1f** and **5.1g**:

TH-3565_186122020

Procedure: A standard catalytic reaction procedure was followed by using **5.1f** (39.6 mg, 0.2 mmol, 1 equiv.), **5.1g** (37.2 mg, 0.2 mmol, 1 equiv.), diphenylacetylene **4.2a** (17.8 mg, 0.1 mmol, 0.5 equiv.), $Cu(OAc)_2•H_2O$ (80 mg, 0.4 mmol, 2 equiv.), PivOH (40.8 mg, 0.4 mmol, 2 equiv.) and $[Ru(p\text{-cymene})Cl_2]_2$ (6.1 mg, 5 mol%) were loaded in a pressure tube with EtOH (3.0 mL). The reaction mixture was stirred in a preheated oil bath at 130 °C for 24 h. After completion of the reaction, the resulting mixture was passed through a plug of celite. The solvent was evaporated under reduced pressure and the residue was absorbed onto small amounts of silica gel. The purification was performed by column chromatography on silica gel (EtOAc/Pet ether: 1/6 → 4/10) to get the isolated product **5.3f** (15 mg, 20%) and **5.3g** (34.8 mg, 48%) in 1:2.4 ratio.

5.5.7. Crystallographic data

Crystallographic data of Ru-8

Single crystals of compound **Ru-8** suitable for X-ray diffraction were obtained by slow evaporation of the saturated solution of the compound in CH_2Cl_2 at room temperature. X-ray crystallographic data were collected using Bruker D8 QUEST diffractometer. Data refinement and cell reduction were carried out by *APEX4*. Structures were solved by direct methods using Olex2 v1.5 and refined by a full-matrix least-squares method using Olex2 v1.5. All of the non-H atoms were refined anisotropically. The ORTEP diagram was obtained with ORTEP3 software with 40% thermal ellipsoid (see below, Figure 5.16). The crystallographic parameters and refinement data are listed in Table 5.5.

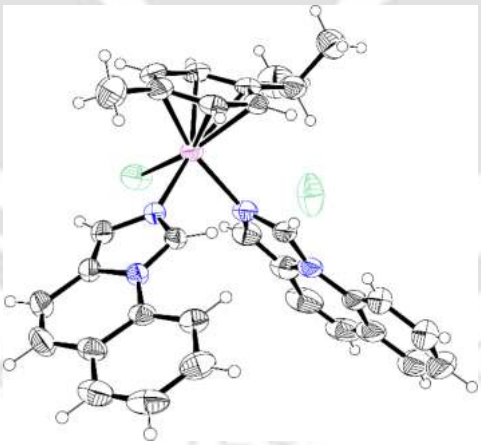


Figure 5.16. Molecular structure of compound **Ru-8** (thermal ellipsoid 40% probability level).

Table 5.5. Crystal data and structure refinement for **Ru-8**

Identification code	AD_1_0m_a
CCDC	2362065
Empirical formula	$C_{33}H_{33}Cl_5N_4ORu$
Formula weight	779.95

TH-3565_186122020

Temperature/K	297.00
Crystal system	monoclinic
Space group	$P2_1/c$
a/Å	10.4861(15)
b/Å	16.493(2)
c/Å	20.149(3)
α/°	90
β/°	101.462(4)
γ/°	90
Volume/Å^3	3415.2(8)
Z	4
ρ_{calc}g/cm^3	1.517
μ/mm^{-1}	0.883
F(000)	1584.0
Crystal size/mm^3	0.42 × 0.38 × 0.32
Radiation	MoKα (λ = 0.71073)
2Θ range for data collection/°	3.218 to 50.098
Index ranges	$-12 \leq h \leq 12$, $-19 \leq k \leq 19$, $-23 \leq l \leq 23$
Reflections collected	93445
Independent reflections	6042 [R_{int} = 0.0427, R_{sigma} = 0.0189]
Data/restraints/parameters	6042/0/403
Goodness-of-fit on F^2	1.068
Final R indexes [I>=2σ (I)]	R_1 = 0.0604, wR_2 = 0.1608
Final R indexes [all data]	R_1 = 0.0702, wR_2 = 0.1728
Largest diff. peak/hole / e Å^{-3}	2.02/-0.94

Crystallographic data of 5.3g

Single crystals of compound **5.3g** suitable for X-ray diffraction were obtained by slow evaporation of the saturated solution of the compound in CH_2Cl_2 at room temperature. X-ray crystallographic data were collected using Bruker D8 QUEST diffractometer. Data refinement and cell reduction were carried out by *APEX4*. Structures were solved by direct methods using

TH-3565_186122020

Olex2 v1.5 and refined by a full-matrix least-squares method using Olex2 v1.5. All of the non-H atoms were refined anisotropically. The ORTEP diagram was obtained with ORTEP3 software with 40% thermal ellipsoid (see below, Figure 5.17). The crystallographic parameters and refinement data are listed in Table 5.6.

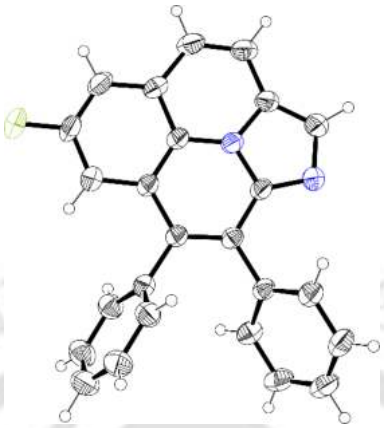


Figure 5.17. Molecular structure of compound **5.3g** (thermal ellipsoid 40% probability level).

Table 5.6. Crystal data and structure refinement for **5.3g**

Identification code	MK18_a
CCDC	2362063
Empirical formula	$C_{25}H_{15}FN_2$
Formula weight	362.39
Temperature/K	297.00
Crystal system	monoclinic
Space group	$P2_1/n$
a/Å	9.3531(12)
b/Å	16.590(2)
c/Å	11.7771(15)
α/°	90
β/°	91.926(4)
γ/°	90
Volume/Å^3	1826.4(4)
Z	4
ρ_{calc}g/cm^3	1.318
μ/mm^{-1}	0.085

TH-3565_186122020

F(000)	752.0
Crystal size/mm^3	0.3 × 0.24 × 0.2
Radiation	MoKα (λ = 0.71073)
2Θ range for data collection/°	4.91 to 49.986
Index ranges	-11 ≤ h ≤ 11, -19 ≤ k ≤ 19, -13 ≤ l ≤ 13
Reflections collected	43017
Independent reflections	3197 [R_{int} = 0.0556, R_{sigma} = 0.0255]
Data/restraints/parameters	3197/0/253
Goodness-of-fit on F^2	1.086
Final R indexes [I>=2σ (I)]	R_1 = 0.0566, wR_2 = 0.1214
Final R indexes [all data]	R_1 = 0.0798, wR_2 = 0.1486
Largest diff. peak/hole / e Å^{-3}	0.20/-0.25

Crystallographic data of 5.4b

Single crystals of compound **5.4b** suitable for X-ray diffraction were obtained by slow evaporation of the saturated solution of the compound in CH_2Cl_2 at room temperature. X-ray crystallographic data were collected using Bruker D8 QUEST diffractometer. Data refinement and cell reduction were carried out by *APEX4*. Structures were solved by direct methods using Olex2 v1.5 and refined by a full-matrix least-squares method using Olex2 v1.5. All of the non-H atoms were refined anisotropically. The ORTEP diagram was obtained with ORTEP3 software with 40% thermal ellipsoid (see below, Figure 5.18). The crystallographic parameters and refinement data are listed in Table 5.7.

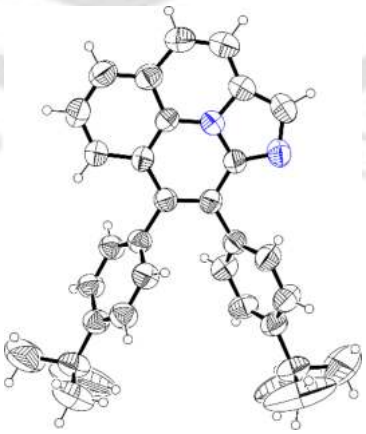


Figure 5.18. Molecular structure of compound **5.4b** (thermal ellipsoid 40% probability level).

Table 5.7. Crystal data and structure refinement for **5.4b**

TH-3565_186122020

Identification code	MK_4tBu_0ma_a
CCDC	2380979
Empirical formula	$C_{37}H_{44}N_2O_2$
Formula weight	548.74
Temperature/K	295.00
Crystal system	monoclinic
Space group	$P2_1/c$
a/Å	15.879(3)
b/Å	18.187(3)
c/Å	11.1543(17)
α/°	90
β/°	108.860(4)
γ/°	90
Volume/Å^3	3048.3(8)
Z	4
ρ_{calc}g/cm^3	1.196
μ/mm^{-1}	0.073
F(000)	1184.0
Crystal size/mm^3	0.39 × 0.11 × 0.1
Radiation	MoKα (λ = 0.71073)
2Θ range for data collection/°	2.71 to 50.084
Index ranges	$-18 \leq h \leq 18$, $-21 \leq k \leq 21$, $-13 \leq l \leq 13$
Reflections collected	83240
Independent reflections	5350 [R_{int} = 0.0433, R_{sigma} = 0.0194]
Data/restraints/parameters	5350/390/386
Goodness-of-fit on F^2	1.343
Final R indexes [I>=2σ (I)]	R_1 = 0.0857, wR_2 = 0.2682
Final R indexes [all data]	R_1 = 0.1259, wR_2 = 0.3437
Largest diff. peak/hole / e Å^{-3}	0.27/-0.35

TH-3565_186122020

Crystallographic data of 5.4f

Single crystals of compound **5.4f** suitable for X-ray diffraction were obtained by slow evaporation of the saturated solution of the compound in CH_2Cl_2/pet ether (1:10) at room temperature. X-ray crystallographic data were collected using Bruker D8 QUEST diffractometer. Data refinement and cell reduction were carried out by *APEX4*. Structures were solved by direct methods using Olex2 v1.5 and refined by a full-matrix least-squares method using Olex2 v1.5. All of the non-H atoms were refined anisotropically. The ORTEP diagram was obtained with ORTEP3 software with 40% thermal ellipsoid (see below, Figure 5.19). The crystallographic parameters and refinement data are listed in Table 5.8.

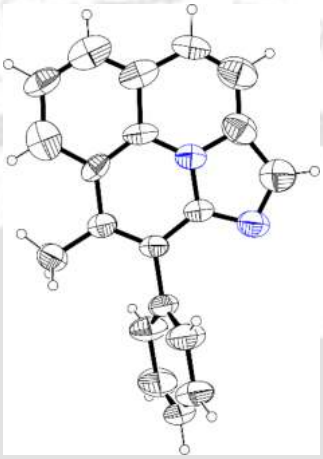


Figure 5.19. Molecular structure of compound **5.4f** (thermal ellipsoid 40% probability level).

Table 5.8. Crystal data and structure refinement for **5.4f**

Identification code	931_0m_a
CCDC	2362062
Empirical formula	$C_{20}H_{14}N_2$
Formula weight	282.33
Temperature/K	299.00
Crystal system	monoclinic
Space group	$P2_1/c$
a/Å	10.4641(14)
b/Å	6.9716(9)
c/Å	19.944(3)
α/°	90
β/°	101.929(4)

TH-3565_186122020

γ/°	90
Volume/Å^3	1423.6(3)
Z	4
ρ_{calc}g/cm^3	1.317
μ/mm^{-1}	0.078
F(000)	592.0
Crystal size/mm^3	0.08 × 0.066 × 0.05
Radiation	MoKα (λ = 0.71073)
2Θ range for data collection/°	4.174 to 49.984
Index ranges	-12 ≤ h ≤ 12, -8 ≤ k ≤ 8, -23 ≤ l ≤ 23
Reflections collected	25185
Independent reflections	2427 [R_{int} = 0.0865, R_{sigma} = 0.0554]
Data/restraints/parameters	2427/1208/404
Goodness-of-fit on F^2	1.151
Final R indexes [I>=2σ (I)]	R_1 = 0.0625, wR_2 = 0.1297
Final R indexes [all data]	R_1 = 0.1781, wR_2 = 0.2131
Largest diff. peak/hole / e Å^{-3}	0.11/-0.13

Crystallographic data of 5.6

Single crystals of compound **5.6** suitable for X-ray diffraction were obtained by slow evaporation of the saturated solution of the compound in ethyl acetate/pentane (1:10) at room temperature. X-ray crystallographic data were collected using Bruker D8 QUEST diffractometer. Data refinement and cell reduction were carried out by *APEX4*. Structures were solved by direct methods using Olex2 v1.5 and refined by a full-matrix least-squares method using Olex2 v1.5. All of the non-H atoms were refined anisotropically. The ORTEP diagram was obtained with ORTEP3 software with 40% thermal ellipsoid (see below, Figure 5.20). The crystallographic parameters and refinement data are listed in Table 5.9.

TH-3565_186122020

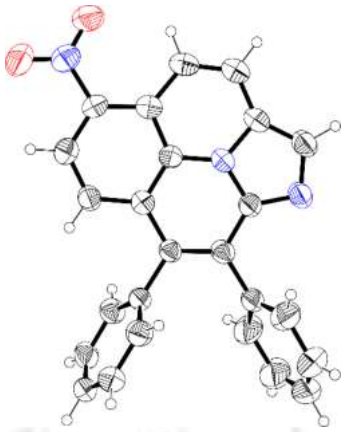


Figure 5.20. Molecular structure of compound **5.6** (thermal ellipsoid 40% probability level).

Table 5.9. Crystal data and structure refinement for **5.6**

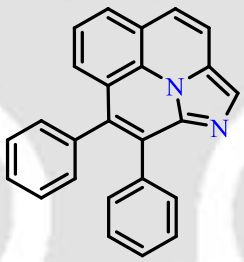
Identification code	NH_461_0ma_a
CCDC	2362064
Empirical formula	$C_{50}H_{30}N_6O_4$
Formula weight	778.80
Temperature/K	300.00
Crystal system	orthorhombic
Space group	$Pca2_1$
a/Å	30.862(14)
b/Å	6.739(3)
c/Å	17.832(8)
α/°	90
β/°	90
γ/°	90
Volume/Å^3	3708(3)
Z	4
ρ_{calc}g/cm^3	1.395
μ/mm^{-1}	0.091
F(000)	1616.0
Crystal size/mm^3	0.34 × 0.25 × 0.14
Radiation	MoKα (λ = 0.71073)

TH-3565_186122020

2Θ range for data collection/°	5.276 to 50.884
Index ranges	$-37 \leq h \leq 37, -8 \leq k \leq 8, -21 \leq l \leq 21$
Reflections collected	59714
Independent reflections	6815 [R_{int} = 0.0627, R_{sigma} = 0.0445]
Data/restraints/parameters	6815/1/542
Goodness-of-fit on F^2	1.112
Final R indexes [I>=2σ (I)]	R_1 = 0.0459, wR_2 = 0.0996
Final R indexes [all data]	R_1 = 0.1002, wR_2 = 0.1299
Largest diff. peak/hole / e $Å^{-3}$	0.16/-0.17
Flack parameter	0.1(6)

5.5.8. Analytical data of the products

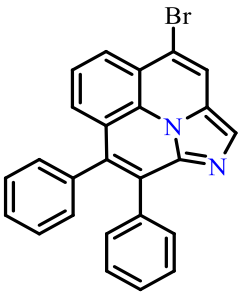
8,9-diphenylbenzo[*ij*]imidazo[2,1,5-*de*]quinolizine (5.3a)



Following the general procedure GP-II, the title compound **5.3a** was isolated as a yellow solid using silica gel column chromatography with ethyl acetate/ pet ether (*v/v* = 1/4, R_f = 0.5) in 90% yield (62 mg). ^{1}H NMR (500 MHz, Chloroform-*d*): δ 7.89 (s, 1H), 7.59 (d, *J* = 7.6 Hz, 1H), 7.52 – 7.46 (m, 2H), 7.39 – 7.36 (m, 3H), 7.34 (d, *J* = 7.3 Hz, 2H), 7.31 – 7.28 (m, 3H), 7.26 – 7.22 (m, 4H). ^{13}C NMR (126 MHz, Chloroform-*d*): δ 139.2, 137.0, 135.7, 135.3, 131.7, 130.9, 130.7, 129.7, 128.7, 128.0, 127.64, 127.63, 125.7, 125.5, 125.4, 125.2, 124.9, 122.2, 121.8, 120.9, 117.9. HRMS (ESI) *m/z*: calcd. for $C_{25}H_{17}N_2$ $[M+H]^+$: 345.1387; found: 345.1390.

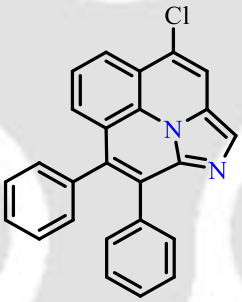
4-bromo-8,9-diphenylbenzo[*ij*]imidazo[2,1,5-*de*]quinolizine (5.3b)

TH-3565_186122020



Following the general procedure GP-II, the title compound **5.3b** was isolated as a yellow oil using silica gel column chromatography with ethyl acetate/ pet ether (*v/v* = 1/5, R_f = 0.5) in 74% yield (62.6 mg). ^{1}H NMR (600 MHz, Chloroform-*d*): δ 7.95 (s, 1H), 7.93 (d, *J* = 7.7 Hz, 1H), 7.73 (s, 1H), 7.62 (t, *J* = 7.9 Hz, 1H), 7.54 (d, *J* = 8.2 Hz, 1H), 7.39 – 7.36 (m, 4H), 7.34 – 7.33 (m, 1H), 7.31 – 7.28 (m, 2H), 7.27 – 7.25 (m, 3H). ^{13}C NMR (126 MHz, Chloroform-*d*): δ 139.2, 136.8, 135.8, 135.0, 131.2, 130.9, 130.7, 129.8, 128.7, 128.1, 127.8, 126.8, 125.9, 125.4, 125.2, 124.5, 123.2, 123.1, 119.2, 117.1. HRMS (ESI) *m/z*: calcd. for $C_{25}H_{16}BrN_2$ $[M+H]^+$: 423.0492; found: 423.0495.

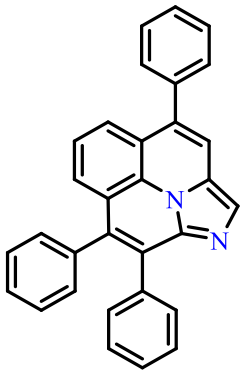
4-chloro-8,9-diphenylbenzo[*ij*]imidazo[2,1,5-*de*]quinolizine (5.3c)



Following the general procedure GP-II, the title compound **5.3c** was isolated as a white solid using silica gel column chromatography with ethyl acetate/ pet ether (*v/v* = 1/6, R_f = 0.4) in 78% yield (59.1 mg). ^{1}H NMR (500 MHz, Chloroform-*d*): δ 7.94 (s, 1H), 7.91 (d, *J* = 7.8 Hz, 1H), 7.71 (s, 1H), 7.61 (t, *J* = 8.0 Hz, 1H), 7.52 (d, *J* = 8.1 Hz, 1H), 7.38 – 7.34 (m, 4H), 7.33 – 7.31 (m, 1H), 7.30 – 7.24 (m, 5H). ^{13}C NMR (151 MHz, Chloroform-*d*): δ 139.1, 136.6, 135.8, 134.9, 131.0, 130.9, 130.7, 129.6, 128.7, 128.1, 127.8, 126.7, 125.8, 125.3, 125.2, 124.4, 123.1, 123.0, 119.1, 117.0. HRMS (ESI) *m/z*: calcd. for $C_{25}H_{16}ClN_2$ $[M+H]^+$: 379.0997; found: 379.1006.

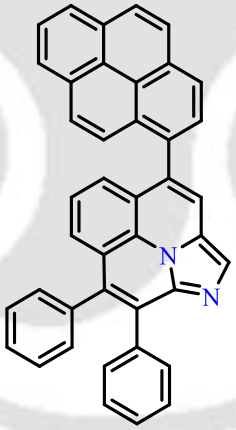
4,8,9-triphenylbenzo[*ij*]imidazo[2,1,5-*de*]quinolizine (5.3d)

TH-3565_186122020



Following the general procedure GP-II, the title compound **5.3d** was isolated as a yellow solid using silica gel column chromatography with ethyl acetate/ pet ether (*v/v* = 1/5, R_f = 0.5) in 88% yield (74 mg). ^{1}H NMR (600 MHz, Chloroform-*d*): δ 7.95 (s, 1H), 7.64 – 7.60 (m, 3H), 7.55 (t, *J* = 7.4 Hz, 2H), 7.50 – 7.47 (m, 2H), 7.44 – 7.43 (m, 2H), 7.41 – 7.39 (m, 2H), 7.37 – 7.35 (m, 2H), 7.32 – 7.24 (m, 6H). ^{13}C NMR (151 MHz, Chloroform-*d*): δ 139.1, 137.1, 135.7, 135.3, 134.8, 131.8, 130.9, 130.8, 129.6, 129.1, 128.9, 128.7, 128.4, 128.0, 127.7, 127.6, 125.9, 125.7, 125.3, 125.0, 124.7, 122.1, 120.2, 117.5. HRMS (ESI) *m/z*: calcd. for $C_{31}H_{21}N_2$ $[M+H]^+$: 421.1700; found: 421.1705.

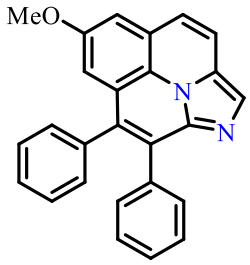
8,9-diphenyl-4-(pyren-1-yl)benzo[*ij*]imidazo[2,1,5-*de*]quinolizine (5.3e)



Following the general procedure GP-II, the title compound **5.3e** was isolated as a yellow solid using silica gel column chromatography with ethyl acetate/ pet ether (*v/v* = 1/8, R_f = 0.6) in 86% yield (93.7 mg). ^{1}H NMR (600 MHz, Chloroform-*d*): δ 8.34 (d, *J* = 7.6 Hz, 1H), 8.25 (d, *J* = 7.6 Hz, 1H), 8.19 – 8.17 (m, 3H), 8.10 (d, *J* = 7.6 Hz, 1H), 8.05 – 8.03 (m, 2H), 7.98 (s, 2H), 7.71 (s, 1H), 7.47 – 7.44 (m, 3H), 7.39 – 7.28 (m, 9H), 7.05 (d, *J* = 7.8 Hz, 1H). ^{13}C NMR (126 MHz, Chloroform-*d*): δ 139.3, 137.1, 135.8, 135.3, 133.70, 133.65, 131.6, 131.5, 131.4, 131.1, 131.0, 130.81, 130.77, 129.7, 129.6, 128.7, 128.1, 128.0, 127.72, 127.68, 127.6, 127.5, 126.4, 126.2, 126.1, 125.63, 125.61, 125.5, 125.4, 125.3, 125.23, 125.17, 125.0, 124.8, 122.1, 121.0, 119.2. HRMS (ESI) *m/z*: calcd. for $C_{41}H_{25}N_2$ $[M+H]^+$: 545.2013; found: 545.2015.

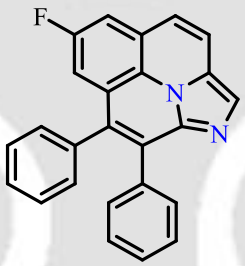
6-methoxy-8,9-diphenylbenzo[*ij*]imidazo[2,1,5-*de*]quinolizine (5.3f)

TH-3565_186122020



Following the general procedure GP-II, the title compound **5.3f** was isolated as a yellow solid using silica gel column chromatography with ethyl acetate/ pet ether (*v/v* = 4/10, R_f = 0.7) in 70% yield (52.4 mg). ^{1}H NMR (400 MHz, Chloroform-*d*): δ 7.88 (s, 1H), 7.52 (d, J = 9.6 Hz, 1H), 7.38 – 7.32 (m, 4H), 7.30 – 7.23 (m, 7H), 7.16 (d, J = 2.4 Hz, 1H), 6.90 (d, J = 2.4 Hz, 1H), 3.81 (s, 3H). ^{13}C NMR (126 MHz, Chloroform-*d*): δ 157.1, 138.7, 137.0, 135.3, 135.2, 130.9, 130.6, 130.2, 129.9, 128.7, 128.0, 127.7, 127.6, 127.1, 126.8, 126.4, 125.9, 125.0, 121.8, 118.5, 106.9, 55.9. HRMS (ESI) *m/z*: calcd. for $C_{26}H_{19}N_2O$ $[M+H]^+$: 375.1492; found: 375.1493.

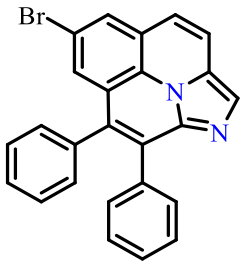
6-fluoro-8,9-diphenylbenzo[*ij*]imidazo[2,1,5-*de*]quinolizine (5.3g)



Following the general procedure GP-II, the title compound **5.3g** was isolated as a yellow solid using silica gel column chromatography with ethyl acetate/ pet ether (*v/v* = 1/6, R_f = 0.5) in 94% yield (68.1 mg). ^{1}H NMR (500 MHz, Chloroform-*d*): δ 7.95 (s, 1H), 7.57 (d, J = 9.6 Hz, 1H), 7.38 – 7.34 (m, 4H), 7.32 – 7.21 (m, 8H), 7.06 (dd, J = 10.7, 2.4 Hz, 1H). ^{13}C NMR (126 MHz, Chloroform-*d*): δ 161.1, 159.1, 138.8, 136.5, 135.21 (d, C-F, $J_{C\text{-}F}$ = 3.8 Hz), 135.0, 130.9, 130.7, 130.5, 128.8, 128.4, 128.0, 127.86 (d, C-F, $J_{C\text{-}F}$ = 6.3 Hz), 127.10 (d, C-F, $J_{C\text{-}F}$ = 10.1 Hz), 126.80 (d, C-F, $J_{C\text{-}F}$ = 10.1 Hz), 126.5, 125.1, 121.47 (d, C-F, $J_{C\text{-}F}$ = 2.5 Hz), 119.0, 107.79 (d, C-F, $J_{C\text{-}F}$ = 11.3 Hz), 107.58 (d, C-F, $J_{C\text{-}F}$ = 10.1 Hz). ^{19}F NMR (471 MHz, Chloroform-*d*): δ -114.3. HRMS (ESI) *m/z*: calcd. for $C_{25}H_{16}FN_2$ $[M+H]^+$: 363.1293; found: 363.1303.

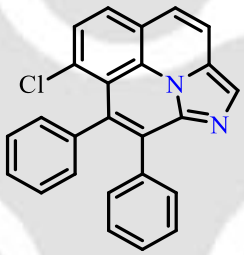
6-bromo-8,9-diphenylbenzo[*ij*]imidazo[2,1,5-*de*]quinolizine (5.3h)

TH-3565_186122020



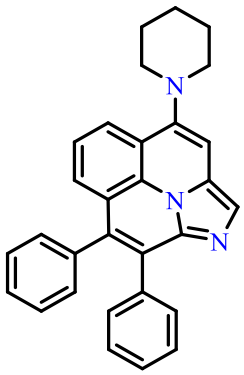
Following the general procedure GP-II, the title compound **5.3h** was isolated as a yellow oil using silica gel column chromatography with ethyl acetate/ pet ether (*v/v* = 1/6, R_f = 0.4) in 91% yield (77 mg). ^{1}H NMR (500 MHz, Chloroform-*d*): δ 7.96 (s, 1H), 7.72 (s, 1H), 7.58 (d, *J* = 9.5 Hz, 1H), 7.49 (s, 1H), 7.37 – 7.35 (m, 4H), 7.28 – 7.22 (m, 7H). ^{13}C NMR (151 MHz, Chloroform-*d*): δ 138.9, 136.1, 134.8, 134.7, 130.7, 130.6, 130.5, 130.1, 128.8, 127.9, 127.84, 127.76, 126.9, 126.7, 126.6, 125.1, 123.7, 123.1, 120.9, 119.0, 118.7. HRMS (ESI) *m/z*: calcd. for $C_{25}H_{16}BrN_2$ $[M+H]^+$: 423.0492; found: 423.0491.

7-chloro-8,9-diphenylbenzo[*ij*]imidazo[2,1,5-*de*]quinolizine (5.3i)



Following the general procedure GP-II, the title compound **5.3i** was isolated as a colorless oil using silica gel column chromatography with ethyl acetate/ pet ether (*v/v* = 1/6, R_f = 0.6) in 88% yield (66.7 mg). ^{1}H NMR (600 MHz, Chloroform-*d*): δ 7.95 (s, 1H), 7.59 – 7.55 (m, 3H), 7.32 (d, *J* = 9.5 Hz, 1H), 7.29 – 7.18 (m, 10H). ^{13}C NMR (151 MHz, Chloroform-*d*): δ 139.0, 138.1, 135.1, 134.8, 133.1, 132.7, 131.4, 130.5, 128.9, 127.9, 127.5, 127.3, 127.2, 126.8, 126.3, 125.9, 124.6, 122.2, 121.8, 121.5, 117.7. HRMS (ESI) *m/z*: calcd. for $C_{25}H_{16}ClN_2$ $[M+H]^+$: 379.0997; found: 379.0999.

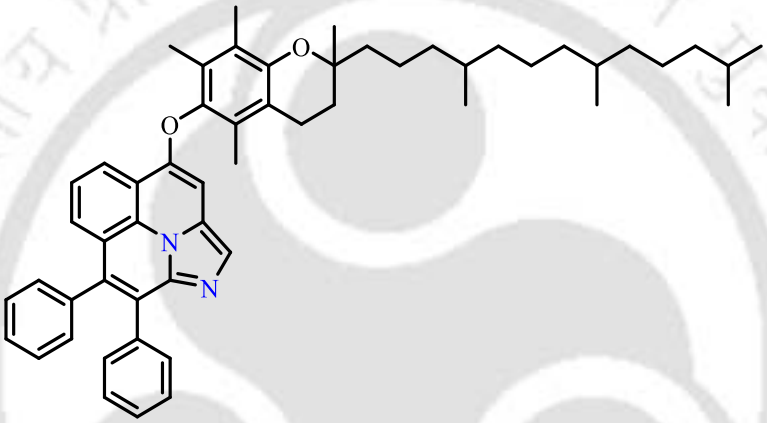
8,9-diphenyl-4-(piperidin-1-yl)benzo[*ij*]imidazo[2,1,5-*de*]quinolizine (5.3j)



TH-3565_186122020

Following the general procedure GP-II, the title compound **5.3j** was isolated as a yellow solid using silica gel column chromatography with ethyl acetate/ pet ether (*v/v* = 1/4, R_f = 0.5) in 72% yield (61.6 mg). ^{1}H NMR (500 MHz, Chloroform-*d*): δ 7.85 (s, 1H), 7.77 (d, *J* = 7.8 Hz, 1H), 7.56 (t, *J* = 8.0 Hz, 1H), 7.46 (d, *J* = 8.0 Hz, 1H), 7.38 (d, *J* = 6.8 Hz, 2H), 7.34 (d, *J* = 7.3 Hz, 2H), 7.31 – 7.27 (m, 4H), 7.25 – 7.21 (m, 2H), 7.11 (s, 1H), 3.12 (br, 4H), 1.89 (p, *J* = 5.6 Hz, 4H), 1.63 (br, 2H). ^{13}C NMR (126 MHz, Chloroform-*d*): δ 146.2, 137.9, 137.2, 135.3, 131.7, 131.0, 130.9, 128.9, 128.6, 128.0, 127.62, 127.56, 125.8, 125.7, 124.5, 123.8, 122.5, 122.1, 118.6, 103.2, 52.8, 26.5, 24.7. HRMS (ESI) *m/z*: calcd. for $C_{30}H_{26}N_3$ $[M+H]^+$: 428.2122; found: 428.2129.

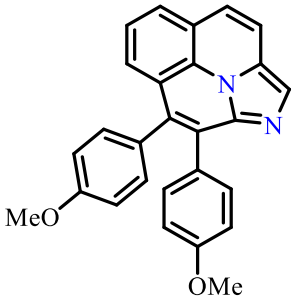
8,9-diphenyl-4-((2,5,7,8-tetramethyl-2-(4,8,12-trimethyltridecyl)chroman-6-yl)oxy)benzo[*ij*]imidazo[2,1,5-*de*]quinolizine (5.3k)



Following the general procedure GP-II, the title compound **5.3k** was isolated as a yellow solid using silica gel column chromatography with ethyl acetate/ pet ether (*v/v* = 1/6, R_f = 0.6) in 77% yield (119.1 mg). ^{1}H NMR (400 MHz, Chloroform-*d*): δ 8.15 (d, *J* = 8.8 Hz, 1H), 7.69 (s, 1H), 7.64 (t, *J* = 8.0 Hz, 1H), 7.57 – 7.55 (m, 1H), 7.40 – 7.36 (m, 3H), 7.34 – 7.31 (m, 2H), 7.29 – 7.22 (m, 5H), 6.40 (d, *J* = 4.2 Hz, 1H), 2.68 (t, *J* = 6.4 Hz, 2H), 2.19 (s, 3H), 2.10 (s, 3H), 2.06 (s, 3H), 1.92 – 1.81 (m, 2H), 1.70 – 1.62 (m, 2H), 1.58 – 1.50 (m, 2H), 1.35 (s, 2H), 1.29 – 1.26 (m, 12H), 1.17 – 1.06 (m, 6H), 0.89 – 0.85 (m, 12H). ^{13}C NMR (126 MHz, Chloroform-*d*): δ 150.3, 149.5, 142.9, 138.1, 137.2, 135.5, 133.9, 131.7, 131.02, 130.96, 129.5, 128.6, 128.0, 127.6, 126.1, 125.32, 125.30, 124.8, 124.1, 123.89, 123.87, 122.7, 119.9, 118.3, 116.6, 94.9, 75.4, 39.5, 37.63, 37.56, 37.5, 33.0, 32.9, 32.1, 29.8, 29.5, 28.1, 25.0, 24.6, 22.9, 22.83, 22.77, 21.2, 20.8, 19.9, 19.8, 14.3, 12.8, 12.1, 12.0. HRMS (ESI) *m/z*: calcd. for $C_{54}H_{65}N_2O_2$ $[M+H]^+$: 773.5041; found: 773.5046.

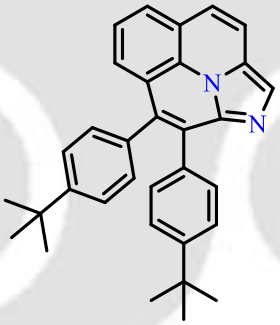
8,9-bis(4-methoxyphenyl)benzo[*ij*]imidazo[2,1,5-*de*]quinolizine (5.4a)

TH-3565_186122020



Following the general procedure GP-II, the title compound **5.4a** was isolated as a yellow solid using silica gel column chromatography with ethyl acetate/ pet ether (*v/v* = 1/5, R_f = 0.6) in 92% yield (74.4 mg). ^{1}H NMR (500 MHz, Chloroform-*d*): δ 7.86 (s, 1H), 7.56 – 7.54 (m, 1H), 7.47 (d, *J* = 9.4 Hz, 1H), 7.43 (d, *J* = 7.5 Hz, 1H), 7.41 – 7.39 (m, 1H), 7.31 – 7.29 (m, 2H), 7.24 (d, *J* = 3.0 Hz, 1H), 7.15 – 7.13 (m, 2H), 6.89 – 6.87 (m, 2H), 6.82 – 6.80 (m, 2H), 3.81 (s, 3H), 3.77 (s, 3H). ^{13}C NMR (126 MHz, Chloroform-*d*): δ 158.9, 139.4, 135.2, 132.2, 131.9, 131.5, 129.29, 129.27, 127.7, 125.8, 125.3, 125.1, 124.8, 122.1, 121.8, 120.8, 117.8, 114.2, 113.6, 55.4, 55.3. HRMS (ESI) *m/z*: calcd. for $C_{27}H_{21}N_2O_2$ $[M+H]^+$: 405.1598; found: 405.1592.

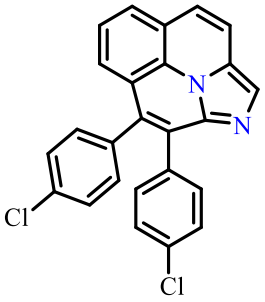
8,9-bis(4-(tert-butyl)phenyl)benzo[*ij*]imidazo[2,1,5-*de*]quinolizine (5.4b)



Following the general procedure GP-II, the title compound **5.4b** was isolated as a yellow solid using silica gel column chromatography with ethyl acetate/ pet ether (*v/v* = 1/10, R_f = 0.6) in 90% yield (82.2 mg). ^{1}H NMR (600 MHz, Chloroform-*d*): δ 7.89 (s, 1H), 7.57 – 7.56 (m, 1H), 7.50 – 7.46 (m, 3H), 7.33 (d, *J* = 7.9 Hz, 2H), 7.29 – 7.24 (m, 5H), 7.15 (d, *J* = 7.9 Hz, 2H), 1.32 (s, 9H), 1.26 (s, 9H). ^{13}C NMR (151 MHz, Chloroform-*d*): δ 150.4, 150.1, 139.4, 135.7, 134.0, 132.3, 131.6, 130.5, 130.4, 129.7, 125.6, 125.5, 125.3, 125.1, 124.8, 124.7, 122.0, 121.8, 120.7, 117.8, 34.7, 34.6, 31.44, 31.38. HRMS (ESI) *m/z*: calcd. for $C_{33}H_{33}N_2$ $[M+H]^+$: 457.2639; found: 457.2646.

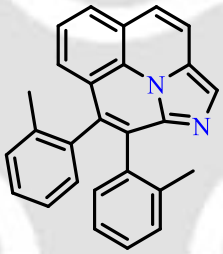
8,9-bis(4-chlorophenyl)benzo[*ij*]imidazo[2,1,5-*de*]quinolizine (5.4c)

TH-3565_186122020



Following the general procedure GP-II, the title compound **5.4c** was isolated as a yellow solid using silica gel column chromatography with ethyl acetate/ pet ether (*v/v* = 1/4, R_f = 0.6) in 82% yield (67.8 mg). ^{1}H NMR (400 MHz, Chloroform-*d*): δ 7.89 (s, 1H), 7.64 – 7.62 (m, 1H), 7.53 – 7.48 (m, 2H), 7.38 – 7.27 (m, 8H), 7.19 – 7.17 (m, 2H). ^{13}C NMR (126 MHz, Chloroform-*d*): δ 138.7, 135.1, 134.4, 133.93, 133.88, 133.5, 132.2, 132.1, 131.7, 129.3, 128.7, 128.5, 125.8, 125.6, 125.2, 125.09, 125.07, 122.4, 121.5, 121.3, 118.0. HRMS (ESI) *m/z*: calcd. for $C_{25}H_{15}Cl_2N_2$ $[M+H]^+$: 413.0607; found: 413.0606.

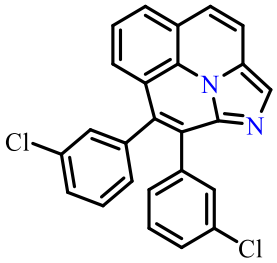
8,9-di-*o*-tolylbenzo[*ij*]imidazo[2,1,5-*de*]quinolizine (5.4d)



Following the general procedure GP-II, the title compound **5.4d** was isolated as a yellow solid using silica gel column chromatography with ethyl acetate/ pet ether (*v/v* = 3/10, R_f = 0.6) in 74% yield (55.1 mg). (two sets of isomers are present). ^{1}H NMR (400 MHz, Chloroform-*d*): δ 7.89 (s, 2H), 7.64 – 7.61 (m, 2H), 7.54 (dd, *J* = 9.6, 1.8 Hz, 2H), 7.51 – 7.45 (m, 2H), 7.35 – 7.32 (m, 2H), 7.24 – 7.16 (m, 11H), 7.10 – 7.07 (m, 4H), 7.03 – 7.02 (m, 2H), 6.99 – 6.96 (m, 1H), 2.24 (s, 3H), 2.19 (s, 3H), 2.15 (s, 3H), 2.03 (s, 3H). ^{13}C NMR (126 MHz, Chloroform-*d*): δ 138.74, 138.69, 136.84, 136.82, 136.75, 136.6, 136.5, 136.0, 135.9, 135.7, 135.2, 134.3, 131.77, 131.75, 131.4, 130.4, 130.3, 130.13, 130.09, 130.0, 129.8, 129.1, 128.9, 128.2, 128.1, 128.0, 127.9, 126.2, 125.8, 125.7, 125.62, 125.59, 125.24, 125.16, 125.13, 125.10, 125.0, 124.7, 122.1, 122.0, 121.8, 121.5, 120.9, 117.94, 117.92, 20.5, 20.4, 20.0, 19.7. HRMS (ESI) *m/z*: calcd. for $C_{27}H_{21}N_2$ $[M+H]^+$: 373.1700; found: 373.1705.

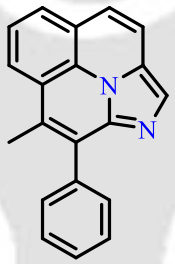
8,9-bis(3-chlorophenyl)benzo[*ij*]imidazo[2,1,5-*de*]quinolizine (5.4e)

TH-3565_186122020



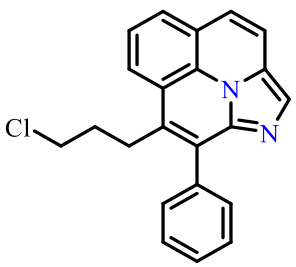
Following the general procedure GP-II, the title compound **5.4e** was isolated as a yellow solid using silica gel column chromatography with ethyl acetate/ pet ether (*v/v* = 1/4, R_f = 0.5) in 78% yield (64.5 mg). ^{1}H NMR (400 MHz, Chloroform-*d*): δ 7.91 (s, 1H), 7.66 – 7.64 (m, 1H), 7.54 (d, *J* = 4.8 Hz, 1H), 7.53 – 7.50 (m, 2H), 7.38 – 7.34 (m, 3H), 7.33 – 7.32 (m, 1H), 7.32 – 7.31 (m, 1H), 7.27 (s, 1H), 7.26 – 7.25 (m, 2H), 7.13 – 7.10 (m, 1H). ^{13}C NMR (151 MHz, Chloroform-*d*): δ 138.5, 138.4, 136.6, 134.7, 134.4, 134.1, 131.7, 130.9, 130.5, 130.2, 129.5, 129.1, 128.9, 128.5, 128.2, 126.0, 125.6, 125.21, 125.17, 124.9, 122.5, 121.6, 121.4, 118.0. HRMS (ESI) *m/z*: calcd. for $C_{25}H_{15}Cl_2N_2$ $[M+H]^+$: 413.0607; found: 413.0609.

8-methyl-9-phenylbenzo[*ij*]imidazo[2,1,5-*de*]quinolizine (5.4f)



Following the general procedure GP-II, the title compound **5.4f** was isolated as a yellow solid using silica gel column chromatography with ethyl acetate/ pet ether (*v/v* = 1/3, R_f = 0.7) in 85% yield (48 mg). ^{1}H NMR (400 MHz, Chloroform-*d*): δ 7.85 (s, 1H), 7.79 – 7.74 (m, 1H), 7.66 – 7.65 (m, 2H), 7.56 – 7.55 (m, 4H), 7.52 (d, *J* = 9.5 Hz, 1H), 7.49 – 7.45 (m, 1H), 7.30 (d, *J* = 9.6 Hz, 1H), 2.47 (s, 3H). ^{13}C NMR (126 MHz, Chloroform-*d*): δ 139.2, 135.9, 130.9, 130.5, 129.8, 129.6, 128.7, 128.2, 125.25, 125.18, 124.99, 124.96, 121.7, 120.9, 119.7, 117.8, 16.2. HRMS (ESI) *m/z*: calcd. for $C_{20}H_{15}N_2$ $[M+H]^+$: 283.1230; found: 283.1236.

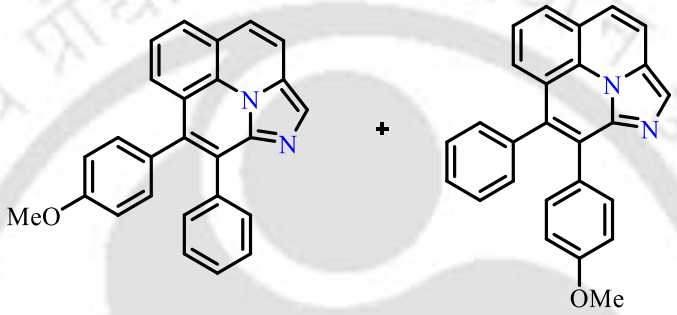
8-(3-chloropropyl)-9-phenylbenzo[*ij*]imidazo[2,1,5-*de*]quinolizine (5.4g)



TH-3565_186122020

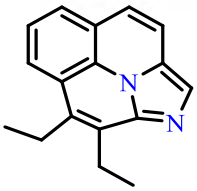
Following the general procedure GP-II, the title compound **5.4g** was isolated as a yellow solid using silica gel column chromatography with ethyl acetate/ pet ether (*v/v* = 1/3, R_f = 0.6) in 84% yield (57.9 mg). ^{1}H NMR (400 MHz, Chloroform-*d*): δ 7.88 – 7.86 (m, 1H), 7.83 (s, 1H), 7.65 – 7.64 (m, 2H), 7.57 – 7.48 (m, 6H), 7.29 (d, *J* = 9.6 Hz, 1H), 3.36 (t, *J* = 6.2 Hz, 2H), 2.99 – 2.95 (m, 2H), 1.94 – 1.87 (m, 2H). ^{13}C NMR (126 MHz, Chloroform-*d*): δ 139.3, 135.8, 134.3, 131.5, 130.0, 129.8, 128.8, 128.3, 125.5, 125.2, 125.1, 125.0, 124.3, 122.0, 120.9, 120.0, 117.8, 72.4, 58.7, 26.1. HRMS (ESI) *m/z*: calcd. for $C_{22}H_{18}ClN_2$ $[M+H]^+$: 345.1154; found: 345.1161.

8-(4-methoxyphenyl)-9-phenylbenzo[*ij*]imidazo[2,1,5-*de*]quinolizine and 9-(4-methoxyphenyl)-8-phenylbenzo[*ij*]imidazo[2,1,5-*de*]quinolizine (5.4h + 5.4h′, 1:1.3)



Following the general procedure GP-II, the title compound **5.4h + 5.4h′** was isolated as a yellow solid using silica gel column chromatography with ethyl acetate/ pet ether (*v/v* = 1/6, R_f = 0.4) in 87% yield (65.2 mg). ^{1}H NMR (500 MHz, Chloroform-*d*): δ 7.89 (d, *J* = 3.6 Hz, 1H), 7.59 – 7.57 (m, 1H), 7.51 – 7.42 (m, 3H), 7.39 – 7.35 (m, 2H), 7.33 – 7.24 (m, 5H), 7.16 (d, *J* = 8.2 Hz, 1H), 6.88 (d, *J* = 8.3 Hz, 0.84H), 6.81 (d, *J* = 8.3 Hz, 1.10H), 3.81 – 3.77 (m, 3H). ^{13}C NMR (126 MHz, Chloroform-*d*): δ 159.01, 158.99, 137.2, 135.5, 135.44, 135.37, 132.2, 131.9, 131.6, 131.5, 131.0, 130.8, 129.7, 129.3, 129.1, 128.7, 128.1, 127.6, 127.5, 125.8, 125.59, 125.56, 125.42, 125.37, 125.2, 125.1, 124.83, 124.80, 122.1, 121.8, 121.7, 120.9, 120.7, 117.9, 114.1, 113.6, 55.34, 55.31. HRMS (ESI) *m/z*: calcd. for $C_{26}H_{19}N_2O$ $[M+H]^+$: 375.1492; found: 375.1502.

8,9-diethylbenzo[*ij*]imidazo[2,1,5-*de*]quinolizine (5.4i)

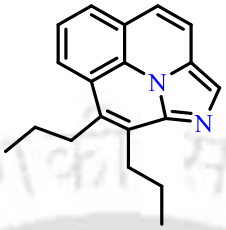


Following the general procedure GP-II, the title compound **5.4i** was isolated as a yellow oil using silica gel column chromatography with ethyl acetate/ pet ether (*v/v* = 1/5, R_f = 0.5) in 80% yield (39.7 mg). ^{1}H NMR (500 MHz, Chloroform-*d*): δ 7.84 (s, 1H), 7.74 (dd, *J* = 7.9, 1.3 Hz, 1H), 7.61 – 7.54 (m, 2H), 7.46 (d, *J* = 9.6 Hz, 1H), 7.24 (d, *J* = 9.6 Hz, 1H), 3.24 (q, *J* =

TH-3565_186122020

7.6 Hz, 2H), 3.07 (q, *J* = 7.6 Hz, 2H), 1.42 (t, *J* = 7.6 Hz, 3H), 1.34 (t, *J* = 7.6 Hz, 3H). ^{13}C NMR (126 MHz, Chloroform-*d*): *δ* 139.1, 134.8, 130.9, 129.7, 125.4, 125.0, 124.9, 124.4, 124.1, 121.8, 120.2, 119.2, 117.6, 21.30, 21.26, 14.8, 13.6. HRMS (ESI) *m/z*: calcd. for $C_{17}H_{17}N_2$ $[M+H]^+$: 249.1387; found: 249.1389.

8,9-dipropylbenzo[*ij*]imidazo[2,1,5-*de*]quinolizine (5.4j)



Following the general procedure GP-II, the title compound **5.4j** was isolated as a yellow oil using silica gel column chromatography with ethyl acetate/ pet ether (*v/v* = 1/10, R_f = 0.6) in 79% yield (43.7 mg). ^{1}H NMR (600 MHz, Chloroform-*d*): *δ* 7.87 (s, 1H), 7.72 – 7.71 (m, 1H), 7.59 (t, *J* = 7.7 Hz, 1H), 7.56 – 7.55 (m, 1H), 7.46 (d, *J* = 9.5 Hz, 1H), 7.24 (d, *J* = 9.5 Hz, 1H), 3.18 – 3.15 (m, 2H), 3.01 – 2.98 (m, 2H), 1.85 – 1.78 (m, 2H), 1.75 – 1.68 (m, 2H), 1.15 – 1.12 (m, 6H). ^{13}C NMR (151 MHz, Chloroform-*d*): *δ* 139.2, 130.7, 128.5, 128.4, 125.3, 124.85, 124.82, 124.6, 123.8, 121.9, 120.2, 119.4, 117.6, 30.4, 30.2, 23.6, 22.3, 14.74, 14.70. HRMS (ESI) *m/z*: calcd. for $C_{19}H_{21}N_2$ $[M+H]^+$: 277.1700; found: 277.1695.

5.5.9. Computational details

All calculations were performed using the Gaussian-16 program package in the gas phase.[19] Full geometry optimizations were carried out using M06L level[20] of theory and BS1 basis set. BS1 is defined as an SDD[21] basis set for Ru atom and 6-31G* Pople basis set for all other atoms. Frequency calculations at the same method and basis set were performed to distinguish transition state structures (one imaginary frequency) and minima structures (no imaginary frequency) on the potential energy surface. The transition states were verified by the intrinsic reaction coordinate (IRC) calculations, wherever necessary.[22] Free energies were calculated by using frequency calculations at 130 °C to match the experimental conditions. Mulliken charges were calculated by NBO analysis.

Table 5.10. Free Energies (G) and Total Energies (E) of all the optimized structures given in Hartree along with the number of imaginary frequencies[a]

Species	Free energy (G)	Total energy (E)	# Imaginary Frequency (NImag)
5.1a	-1474.466037	-1474.8453987	0
Int1	-1474.461029	-1474.8440936	0
Int2	-1474.440075	-1474.8251848	0
Int3	-1245.417527	-1245.7492624	0

TH-3565_186122020

TS-1	-1245.382501	-1245.7117191	1
Int4	-1016.356822	-1016.633771	0
DPA	-539.251210	-539.3862217	0
Int5	-1555.607949	-1556.0545539	0
TS-2	-1555.593173	-1556.0414389	1
Int6	-1555.624554	-1556.0783074	0
Int7	-1555.645025	-1556.0967867	0
5.3a	-1071.442430	-1071.7089523	0
[Ru(*p*-cym)(OAc)$_2$]	-941.141092	-941.3805389	0
Acetic acid	-229.032857	-229.0560845	0

[a](G) is calculated at 130 °C to meet the experimental conditions. All the figures were generated using (G) values. All the transition states have one NImag and all the reactants, intermediates and products have zero NImag. All the calculations were performed at the M06L level of DFT. (DPA = diphenyl acetylene)

5.6. References

1. (a) Balaban, A. T.; Oniciu, D. C.; Katritzky, A. R. *Chem. Rev.* **2004**, *104*, 2777−2812. (b) Joule, J. A.; Mills, K. Heterocyclic Chemistry, 5th ed., John Wiley & Sons, Chichester, 2010. (c) Banik, B. K.; Becker, F. F. *Curr. Med. Chem.* **2001**, *8*, 1513−1533. (d) Knölker, H.-J.; Reddy, K. R. *Chem. Rev.* **2002**, *102*, 4303−4427. (e) Singh, K.; Vellakkaran, M.; Banerjee, D. *Green Chem.* **2018**, *20*, 2250−2256.

2. (a) Facchetti, A. *Chem. Mater.* **2011**, *23*, 733−758. (b) Wang, C.; Dong, H.; Hu, W.; Liu, Y.; Zhu, D. *Chem. Rev.* **2012**, *112*, 2208−2267. (c) Forrest, S. R.; Thompson, M. E. *Chem. Rev.* **2007**, *107*, 923−925. (d) Mishra, A.; Bauerle, P. *Angew. Chem., Int. Ed.* **2012**, *51*, 2020−2067. (e) Itoh, T. *Chem. Rev.* **2012**, *112*, 4541−4568. (f) Dong, Y.; Yang, J.; Zhang, H.; Zhan, X. Y.; He, S.; Shi, Z. C.; Zhang, X. M.; Wang, J. Y. *Org. Lett.* **2020**, *22*, 5151−5156. (g) Lai, M.-Y.; Chen, C.-H.; Huang, W.-S.; Lin, J. T.; Ke, T.-H.; Chen, L.-Y.; Tsai, M.-H.; Wu, C.-C. *Angew. Chem., Int. Ed.* **2008**, *47*, 581−585. (h) Ge, Z.; Hayakawa, T.; Ando, S.; Ueda, M.; Akiike, T.; Miyamoto, H.; Kajita, T.; Kakimoto, M. *Adv. Funct. Mater.* **2008**, *18*, 584−590.

3. (a) Douglass, J. E.; Hunt, D. A. *J. Org. Chem.* **1977**, *42*, 3974. (b) Huang, J.; Dong, L.; Han, B.; Peng, C.; Chen, Y. *Chem. −Eur. J.* **2012**, *18*, 8896−8900. (c) Ghorai, D.; Choudhury, J. *Chem. Commun.* **2014**, *50*, 15159−15162. (d) Ge, Q.; Li, B.; Song, H.; Wang, B. *Org. Biomol. Chem.* **2015**, *13*, 7695−7710. (e) Yu, H.; Zhang, G.; Huang, H. *Angew. Chem., Int. Ed.* **2015**, *54*, 10912−10916. (f) Li, X.; Chen, X.; Wang, H.; Chen, C.; Sun, P.; Mo, B.; Peng, J. *Org. Biomol. Chem.* **2019**, *17*, 4014−4023. (g) Hu, Y.; Wang, T.; Liu, Y.; Nie, R.; Yang, N.; Wang, Q.; Li, G.-B.; Wu, Y. *Org. Lett.* **2020**, *22*, 501−504. (h) Ackermann, L. *Chem. Rev.* **2011**, *111*, 1315−1345. (h) Wencel-Delord J.; Glorius, F. *Nat. Chem.* **2013**, *5*, 369−375.

4. (a) Hranjec, M.; Kralj, M.; Piantanida, I.; Sedic´, M.; Suman, L.; Pavelic, K.; Karminski-Zamola, G. *J. Med. Chem.* **2007**, *50*, 5696−5711. (b) Kuduk, S. D.; Chang, R. K.; Di Marco, C. N.; Ray, W. J.; Ma, L.; Wittmann, M.; Seager, M. A.; Koeplinger, K. A.; Thompson, C. D.; Hartman, G. D.; Bilodeau, M. T. *ACS Med. Chem. Lett.* **2010**, *1*, 263−267. (c) Kuduk, S. D.; Di Marco, C. N. Pat. Appl. Publ. WO 2010/042347A1, 2010. (d) Xu, Y.-S.; Zeng, C.-C.; Jiao, Z.-G.; Hu, L.-M.; Zhong, R.-G. *Molecules* **2009**, *14*, 868−883. (e) Fujii, T.; Shindo, Y.; Hotta,

TH-3565_186122020

K.; Citterio, D.; Nishiyama, S.; Suzuki, K.; Oka, K. *J. Am. Chem. Soc.* **2014**, *136*, 2374−2381. (f) Sedic, M.; Poznic, M.; Gehrig, P.; Scott, M.; Schlapbach, R.; Hranjec, M.; Karminski-Zamola, G.; Pavelic, K.; Pavelic, S. K. *Mol. Cancer Ther.* **2008**, *7*, 2121−2132.

5. He, B.; Huang, J.; Zhang, J.; Sung, H. H. Y.; Lam, J. W. Y.; Zhang, Z.; Yan, S.; Wang, D.; Zhang, J.; Tang, B. Z. *Angew. Chem., Int. Ed.* **2022**, *61*, e202117709.

6. (a) Arockiam, P. B.; Bruneau, C.; Dixneuf, P. H. *Chem. Rev.* **2012**, *112*, 5879–5918. (b) Docherty, J. H.; Lister, T. M.; Mcarthur, G.; Findlay, M. T.; Domingo-Legarda, P.; Kenyon, J.; Choudhary, S.; Larrosa, I. *Chem. Rev.* **2023**, *123*, 7692–7760. (c) Song, L.; Van der Eycken, E. V. *Chem. –Eur. J.* **2021**, *27*, 121–144. (d) Jin, T.; Zhao, J.; Asao, N.; Yamamoto, Y. *Chem. –Eur. J.* **2014**, *20*, 3554 –3576. (e) Kong, W.-J.; Finger, L. H.; Messinis, A. M.; Kuniyil, R.; Oliveira, J. C. A.; Ackermann, L. *J. Am. Chem. Soc.* **2019**, *141*, 17198–17206.

7. (a) Ackermann, L. *Acc. Chem. Res.* **2014**, *47*, 281–295. (b) Hyster, T. K.; Rovis, T. *J. Am. Chem. Soc.* **2010**, *132*, 10565–10569. (c) Patureau, F. W.; Glorius, F. *Angew. Chem. Int. Ed.* **2011**, *50*, 1977–1979. (d) Stuart, D. R.; Bertrand-Laperle, M.; Burgess, K. M. N.; Fagnou, K. *J. Am. Chem. Soc.* **2008**, *130*, 16474–16475. (e) Ackermann, L.; Lygin, A. V.; Hofmann, N. *Angew. Chem. Int. Ed.* **2011**, *50*, 6379–6382.

8. (a) Zhao, Q.; Meng, G.; Nolan, S. P.; Szostak, M. *Chem. Rev.* **2020**, *120*, 1981–2048. (b) Dutta, C.; Choudhury, J. *RSC Adv.* **2018**, *8*, 27881–27891. (c) Karak, P.; Rana, S. S.; Choudhury, J. *Chem. Commun.* **2021**, *58*, 133–154.

9. Huang, J. R.; Dong, L.; Han, B.; Peng, C.; Chen, Y. C. *Chem. –Eur. J.* **2012**, *18*, 8896−8900.

10. Qi, S.-L.; Li, Y.; Li, J.-F.; Zhang, T.; Luan, Y.-X.; Ye, M. *Org. Lett.* **2021**, *23*, 4034−4039.

11. (a) Kuwata, S.; Hahn, F. E. *Chem. Rev.* **2018**, *118*, 9642−9677. (b) Karmakar, S.; Datta, A. *Angew. Chem., Int. Ed.* **2014**, *53*, 9587−9591. (c) Amyes, T. L.; Diver, S. T.; Richard, J. P.; Rivas, F. M.; Toth, K. *J. Am. Chem. Soc.* **2004**, *126*, 4366−4374. (d) Maier, G.; Endres, J.; Reisenauer, H. P. *Angew. Chem., Int. Ed. Engl.* **1997**, *36*, 1709−1712. (e) McGibbon, G. A.; Heinemann, C.; Lavorato, D. J.; Schwarz, H. *Angew. Chem., Int. Ed. Engl.* **1997**, *36*, 1478−1481.

12. (a) Ryabov, A. D.; Sakodinskkaya, I. K.; Yatsimirsky, J. *Chem. Soc., Dalton Trans.* **1985**, 2629–2638. (b) Kurzeev, A. A.; Kazankov, G. M.; Ryabov, A. D. *Inorg. Chim. Acta* **2002**, *340*, 192–196. (c) Davies, D. L.; Donald, S. M. A.; Macgregor, S. A. *J. Am. Chem. Soc.* **2005**, *127*, 13754–13755. (d) Lafrance, M.; Fagnou, K. *J. Am. Chem. Soc.* **2006**, *128*, 16496–16497.

13. (a) Ghorai, D.; Choudhury, J. *Chem. Commun.* **2014**, *50*, 15159−15162. (b) Ma, C.; Ai, C.; Li, Z.; Li, B.; Song, H.; Xu, S.; Wang, B. *Organometallics* **2014**, *33*, 5164−5172.

14. (a) Yedage, S. L.; Bhanage, B. M. *Green Chem.* **2016**, *18*, 5635−5642. (b) Konda, S. G.; Humne, V. T.; Lokhande, P. D. *Green Chem.* **2011**, *13*, 2354−2358. (c) Cecchini, M. M.;

TH-3565_186122020

Charnay, C.; De Angelis, F.; Lamaty, F.; Martinez, J.; Colacino, E. *ChemSusChem* **2014**, *7*, 45−65.

15. Mahata, S.; Dey, S.; Mandal, B. B.; Manivannan, V. *J. Photochem. Photobiol., A* **2022**, *427*, 113795.

16. (a) Wang, W.; Bao, Z. -P.; Qi, X.; Wu, X. -F. *Org. Lett.* **2021**, *23*, 6589−6593. (b) Wu, H. -P.; Shao, C. -K.; Wu, D.; Jiang, L.; Yin, H. -Q.; Chen, F.-X. *J. Org. Chem*. **2021**, *86*, 5327−5335. (c) Luo, X. L.; Li, Y. B.; Chen, X. W.; Song, Z. Y.; Liang, J. Y.; Liao, C.S.; Zhu, Z. Z.; Chen, L. *Org. Biomol. Chem.* **2019**, *17*, 7315−7319.

17. Konwar, M.; Hazarika, N.; Das, A. *Org. Lett.* **2024**, *26*, 2965−2970.

18. Zhang, C.; Xu, K.; Liao, Y.; Zhao, L.; Jin, S.; Lu, X.; Wang, J.; Ding, L.; Zhang, J. *J. Org. Chem.* **2023**, *88*, 3436–3450.

19. Frisch, M. J.; Trucks, G. W.; Schlegel, H. B.; Scuseria, G. E.; Robb, M. A.; Cheeseman, J. R.; Scalmani, G.; Barone, V.; Petersson, G. A.; Nakatsuji, H.; Li, X.; Caricato, M.; Marenich, A. V.; Bloino, J.; Janesko, B. G.; Gomperts, R.; Mennucci, B.; Hratchian, H. P.; Ortiz, J. V.; Izmaylov, A. F.; Sonnenberg, J. L.; Williams-Young, D.; Ding, F.; Lipparini, F.; Egidi, F.; Goings, J.; Peng, B.; Petrone, A.; Henderson, T.; Ranasinghe, D.; Zakrzewski, V. G.; Gao, J.; Rega, N.; Zheng, G.; Liang, W.; Hada, M.; Ehara, M.; Toyota, K.; Fukuda, R.; Hasegawa, J.; Ishida, M.; Nakajima, T.; Honda, Y.; Kitao, O.; Nakai, H.; Vreven, T.; Throssell, K.; Montgomery, J. A., Jr.; Peralta, J. E.; Ogliaro, F.; Bearpark, M. J.; Heyd, J. J.; Brothers, E. N.; Kudin, K. N.; Staroverov, V. N.; Keith, T. A.; Kobayashi, R.; Normand, J.; Raghavachari, K.; Rendell, A. P.; Burant, J. C.; Iyengar, S. S.; Tomasi, J.; Cossi, M.; Millam, J. M.; Klene, M.; Adamo, C.; Cammi, R.; Ochterski, J. W.; Martin, R. L.; Morokuma, K.; Farkas, O.; Foresman, J. B.; Fox, D. J. *Gaussian 16*, Revision C.01, Gaussian, Inc., Wallingford CT, 2016.

20. Wang, Y.; Jin, X.; Yu, H. S.; Truhlar, D. G.; He, X. *PNAS* **2017**, *114*, 8487–8492.

21. Dolg, M.; Wedig, U.; Stoll, H.; Preuss, H. *J. Chem. Phys*., **1987**, *86*, 866–872.

22. Fukui, K. *Acc. Chem. Res.* **1981**, *14*, 363–368.

TH-3565_186122020

Annexure I

Selected ^{1}H and ^{13}C NMR spectra of the products (*Chapter 2*)

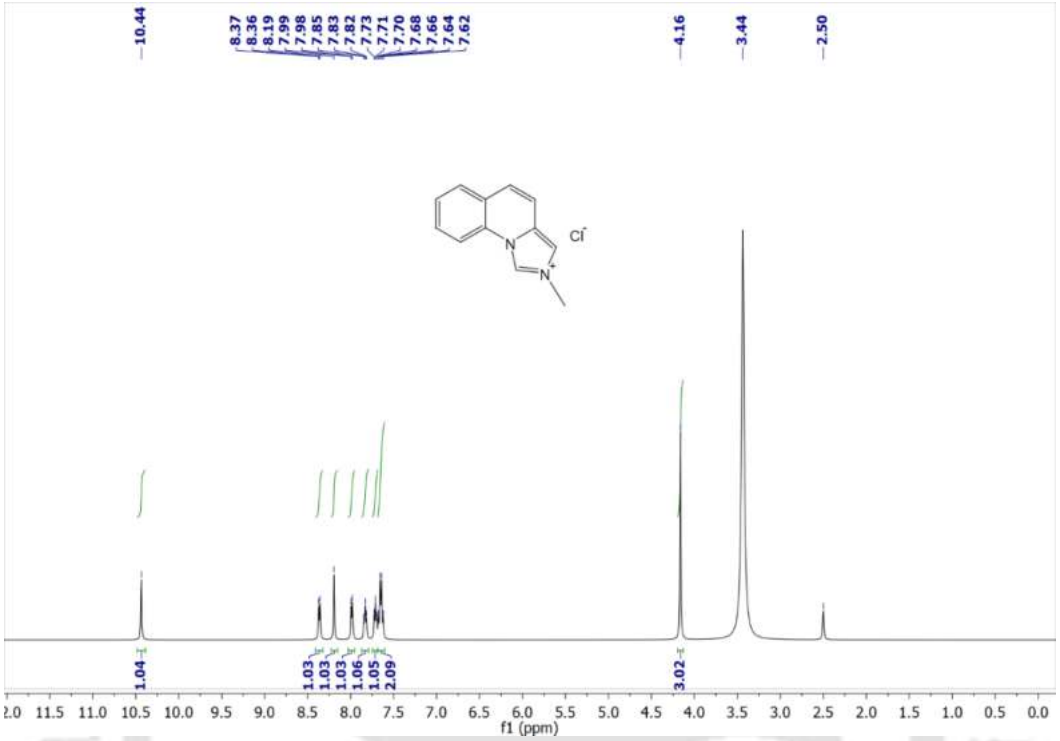


Figure S1. ^{1}H NMR Spectrum of **L¹** (DMSO-d_6, 500 MHz, 298 K)

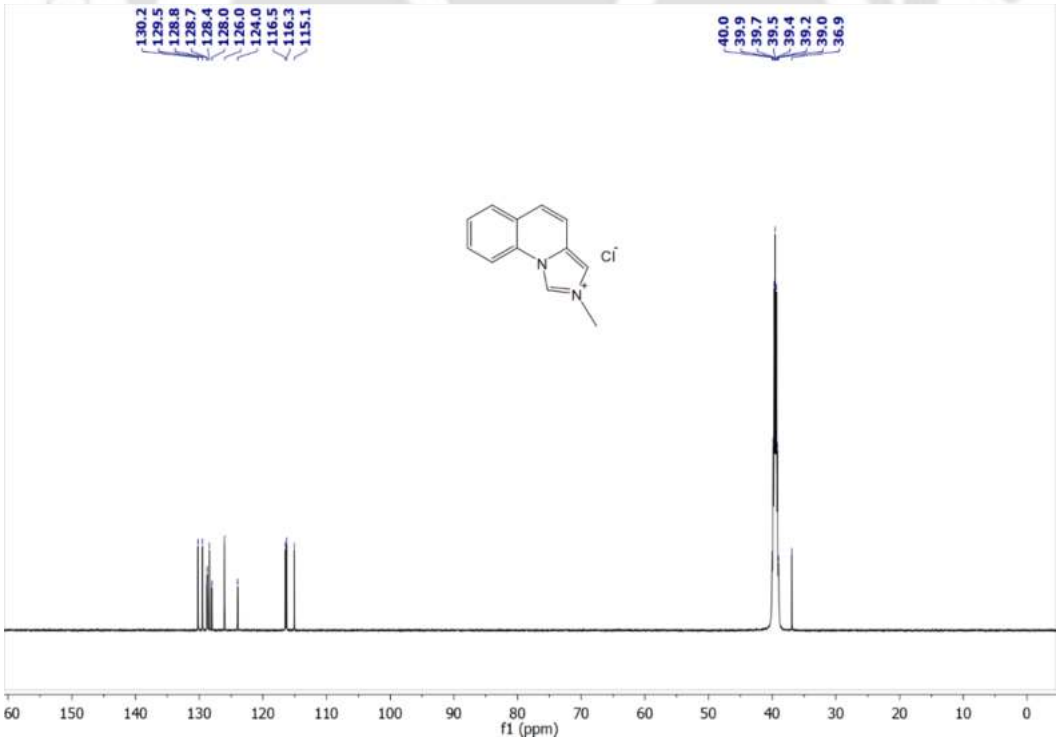


Figure S2. $^{13}C\{^{1}H\}$ NMR Spectrum of **L¹** (DMSO-d_6, 126 MHz, 298 K)

TH-3565_186122020

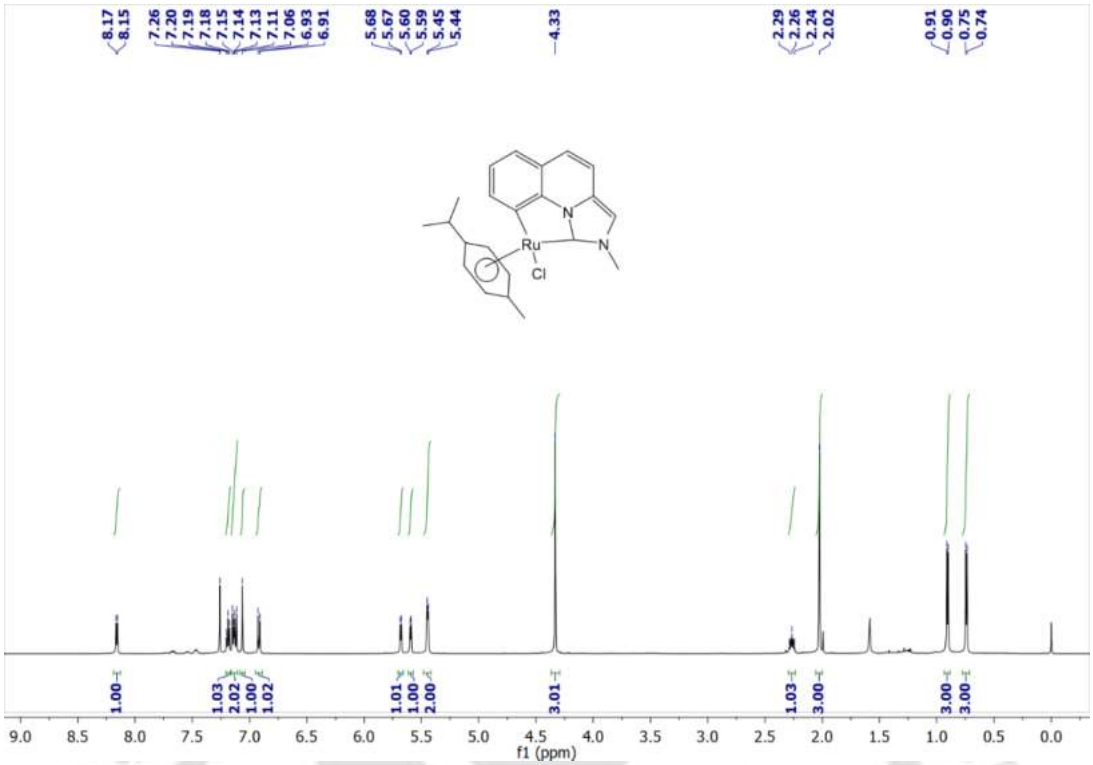


Figure S3. ^{1}H NMR Spectrum of **Ru-1** ($CDCl_3$, 600 MHz, 298 K)

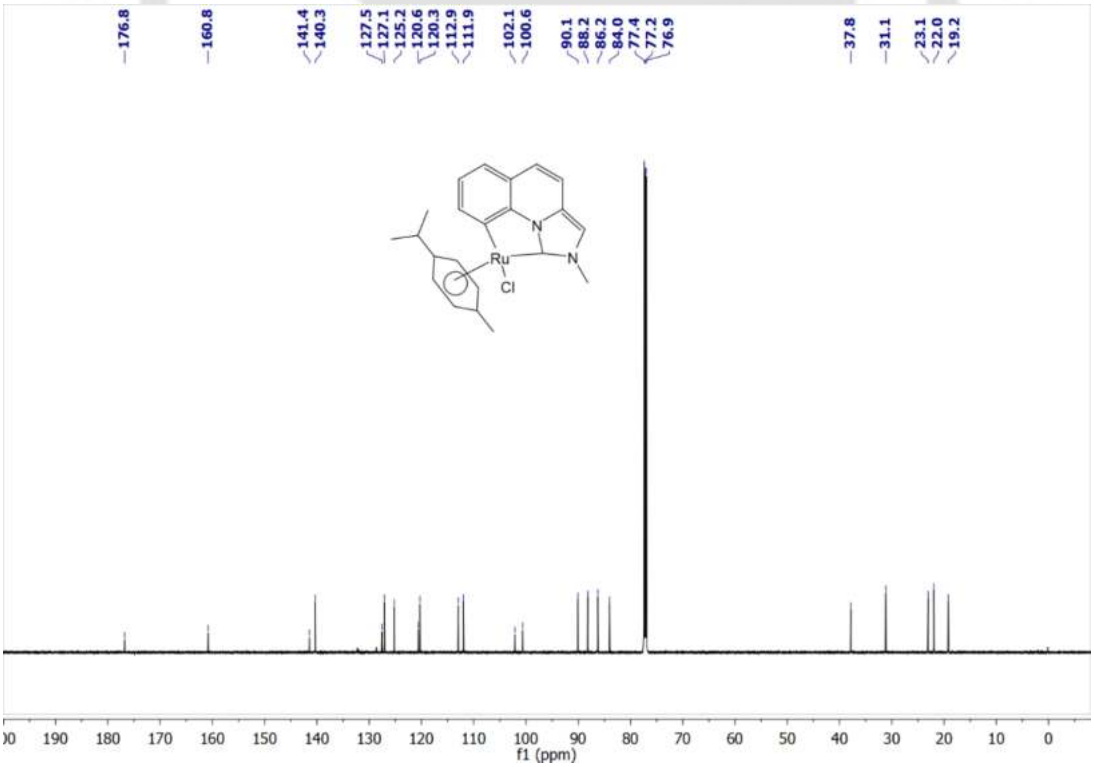


Figure S4. $^{13}C\{^{1}H\}$ NMR Spectrum of **Ru-1** ($CDCl_3$, 151 MHz, 298 K)

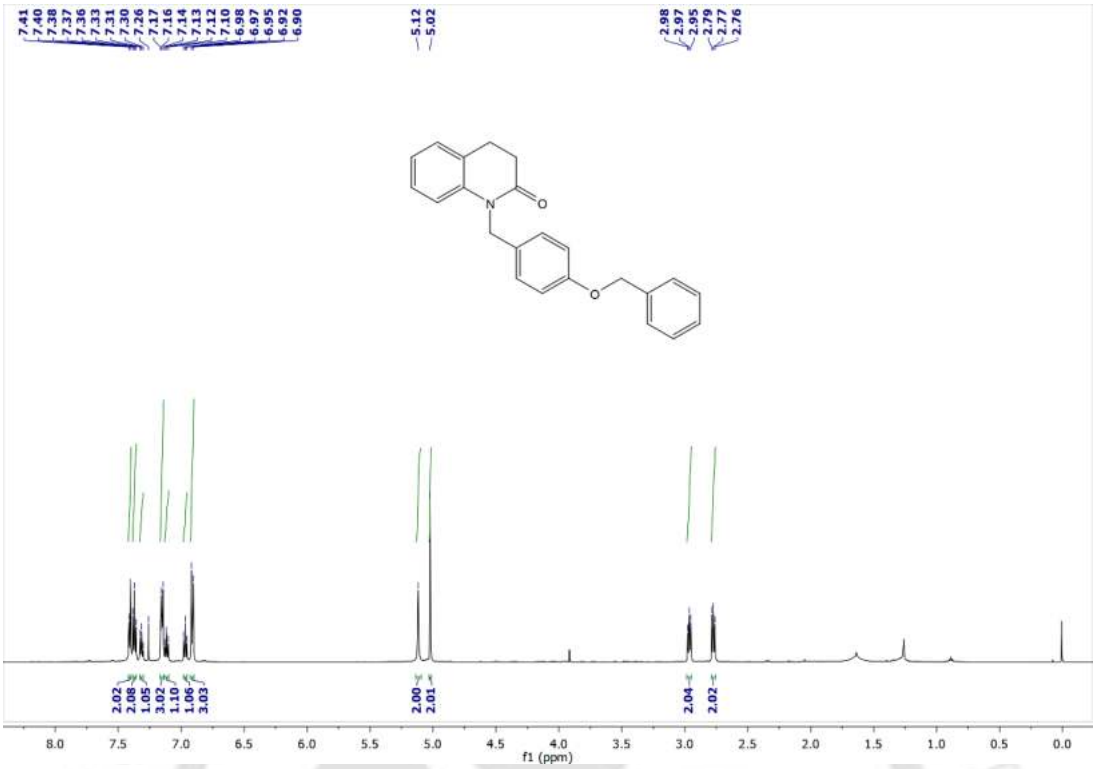


Figure S5. ^{1}H NMR Spectrum of **2.10e** ($CDCl_3$, 600 MHz, 298 K)

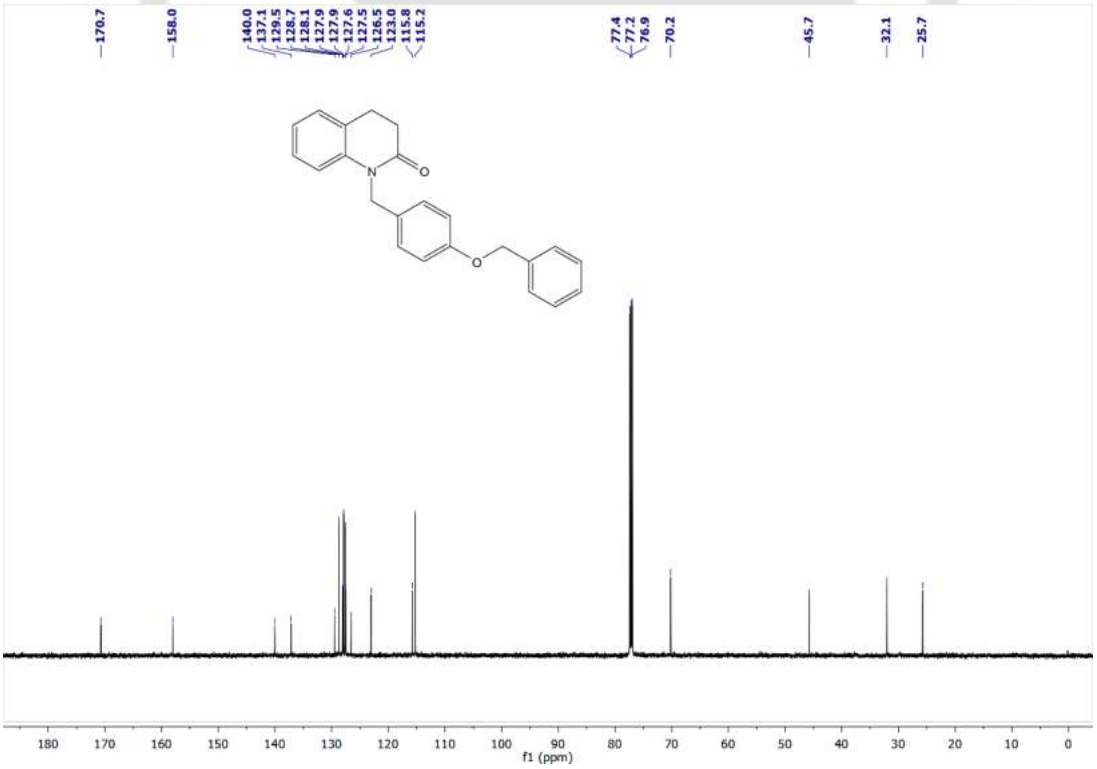


Figure S6. $^{13}C\{^{1}H\}$ NMR Spectrum of **2.10e** ($CDCl_3$, 151 MHz, 298 K)

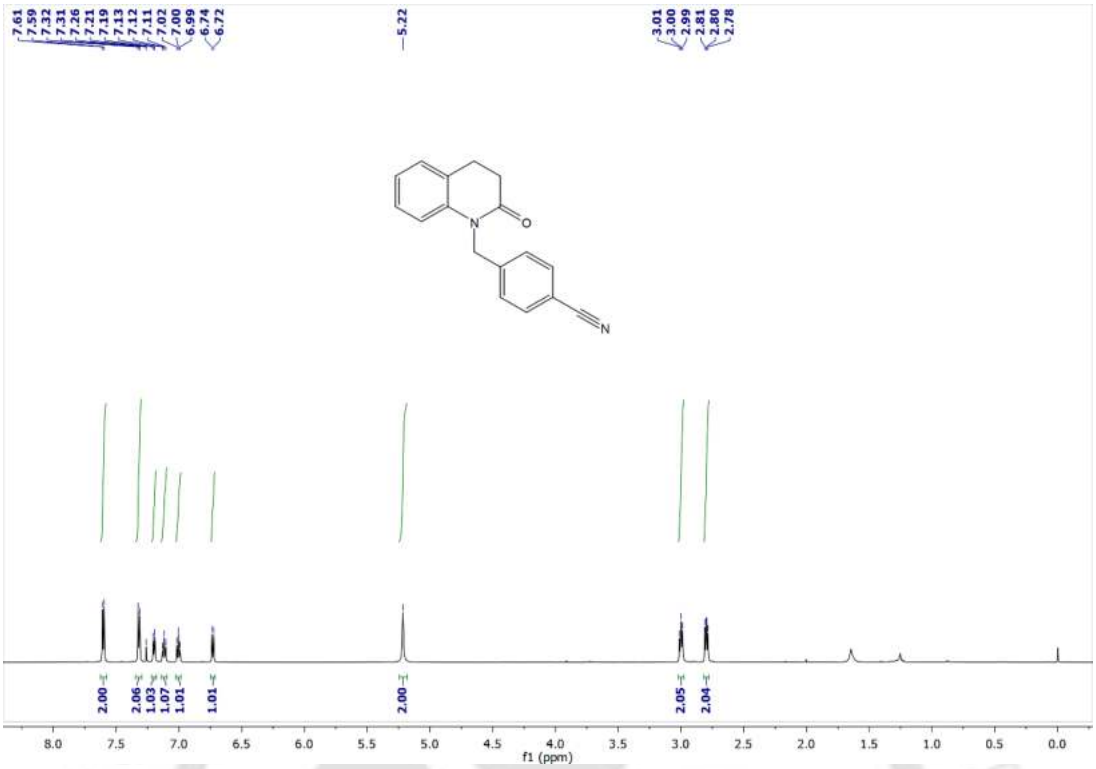


Figure S7. ^{1}H NMR Spectrum of **2.10h** ($CDCl_3$, 600 MHz, 298 K)

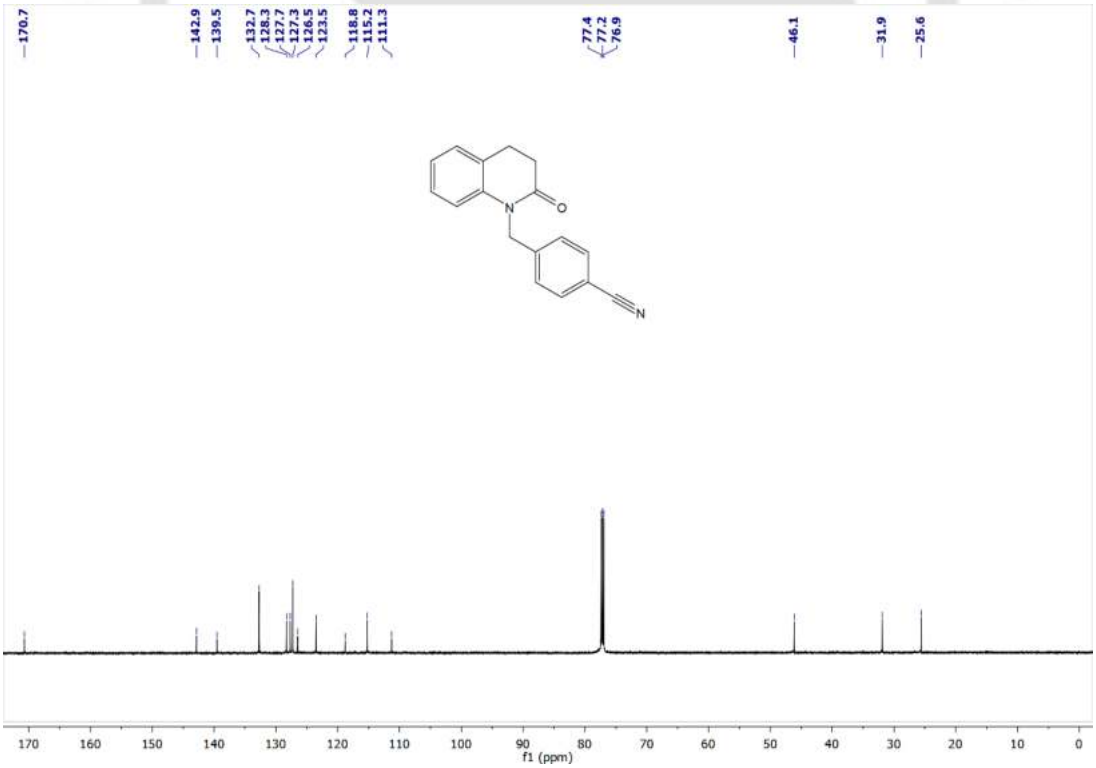


Figure S8. $^{13}C\{^{1}H\}$ NMR Spectrum of **2.10h** ($CDCl_3$, 151 MHz, 298 K)

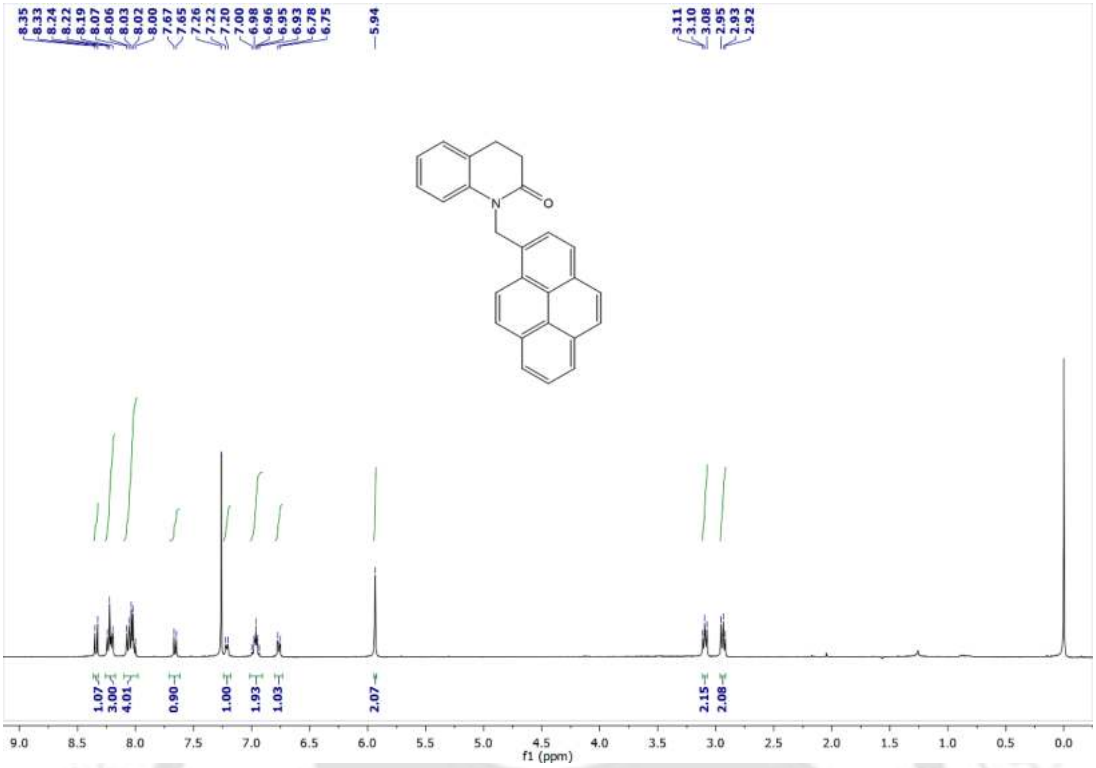


Figure S9. ^{1}H NMR Spectrum of **2.10n** ($CDCl_3$, 400 MHz, 298 K)

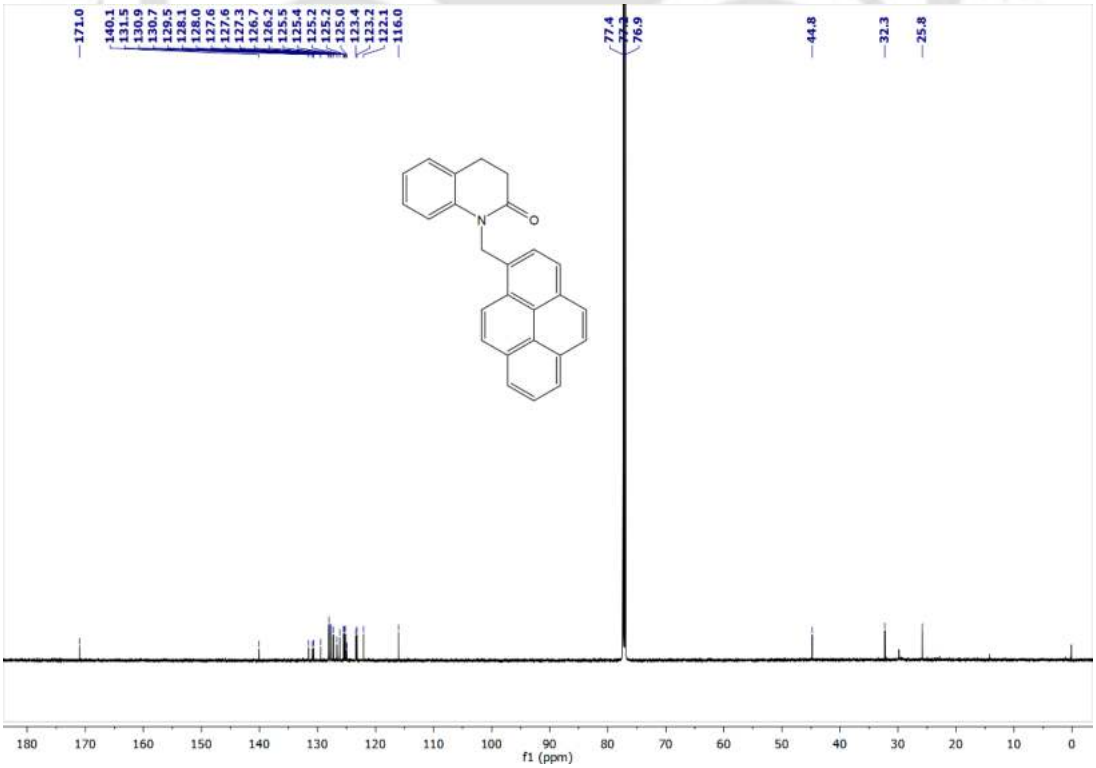


Figure S10. $^{13}C\{^{1}H\}$ NMR Spectrum of **2.10n** ($CDCl_3$, 151 MHz, 298 K)

TH-3565_186122020

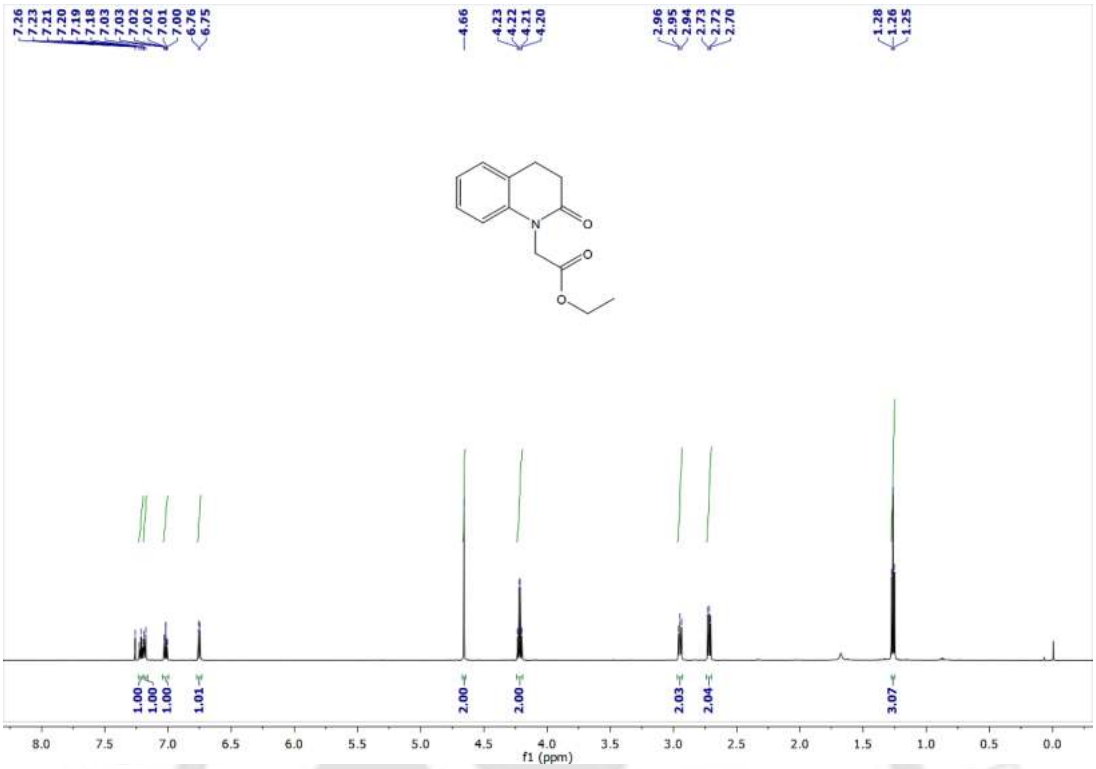


Figure S11. ^{1}H NMR Spectrum of **2.10u** ($CDCl_3$, 600 MHz, 298 K)

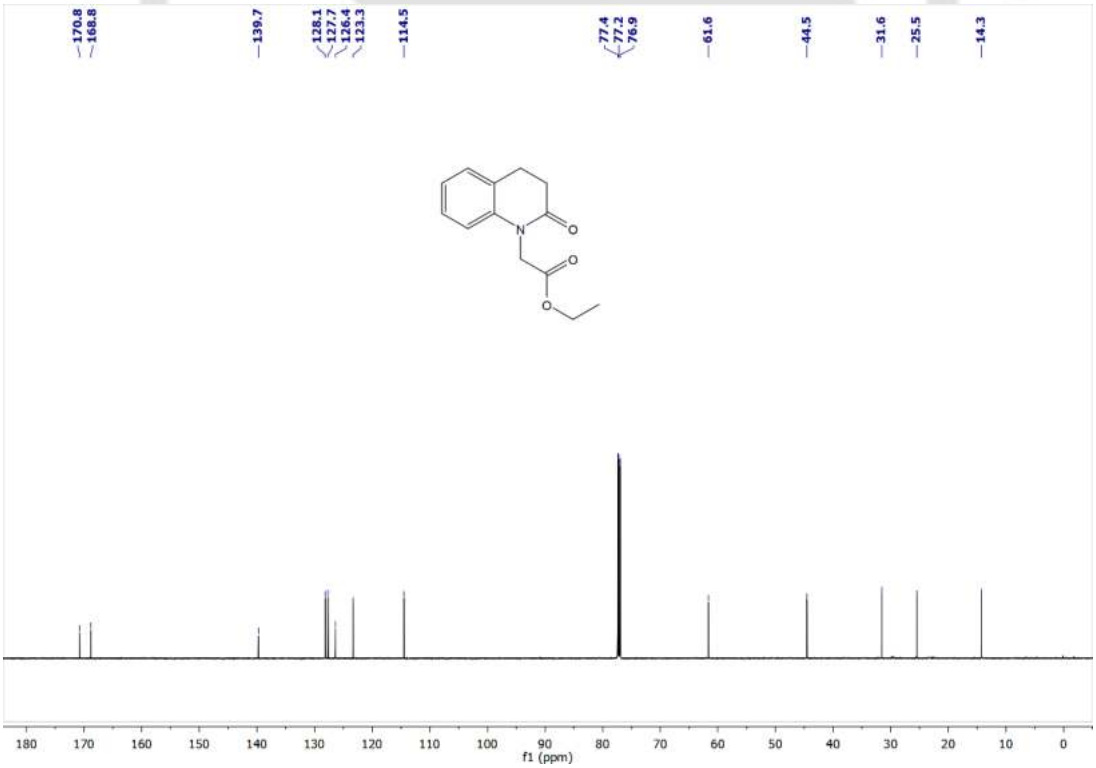


Figure S12. $^{13}C\{^{1}H\}$ NMR Spectrum of **2.10u** ($CDCl_3$, 151 MHz, 298 K)

TH-3565_186122020

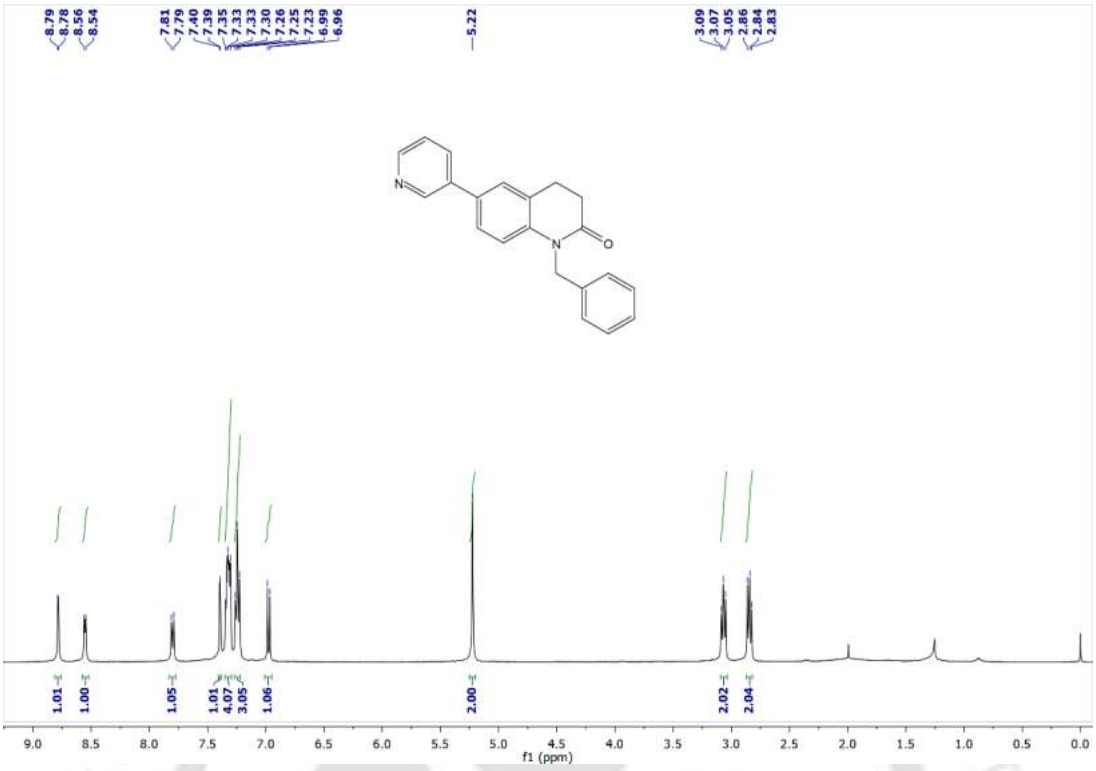


Figure S13. ^{1}H NMR Spectrum of **2.12c** ($CDCl_3$, 400 MHz, 298 K)

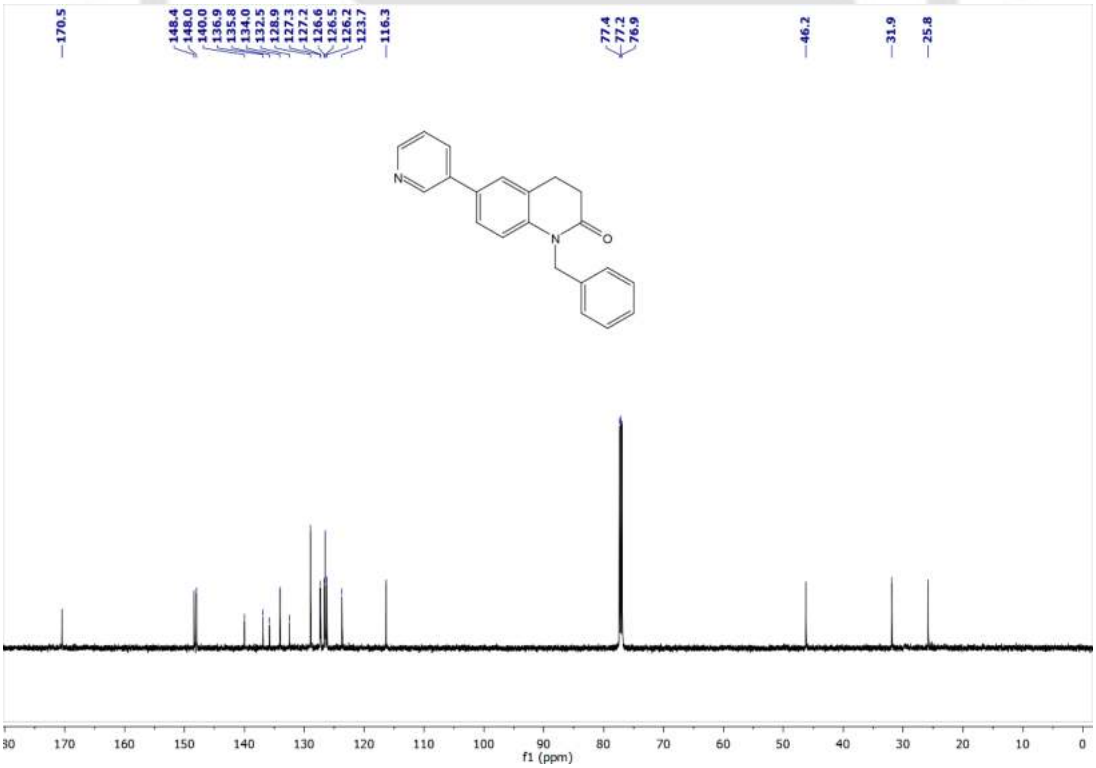


Figure S14. $^{13}C\{^{1}H\}$ NMR Spectrum of **2.12c** ($CDCl_3$, 151 MHz, 298 K)

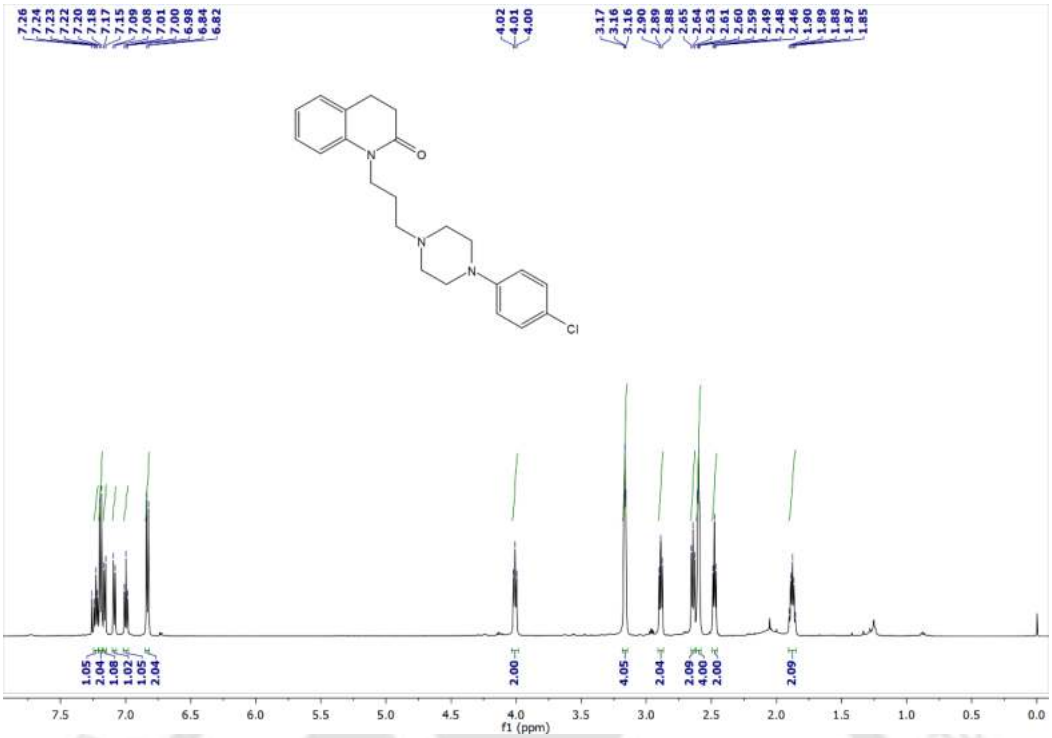


Figure S15. ^{1}H NMR Spectrum of **2.12d** ($CDCl_3$, 600 MHz, 298 K)

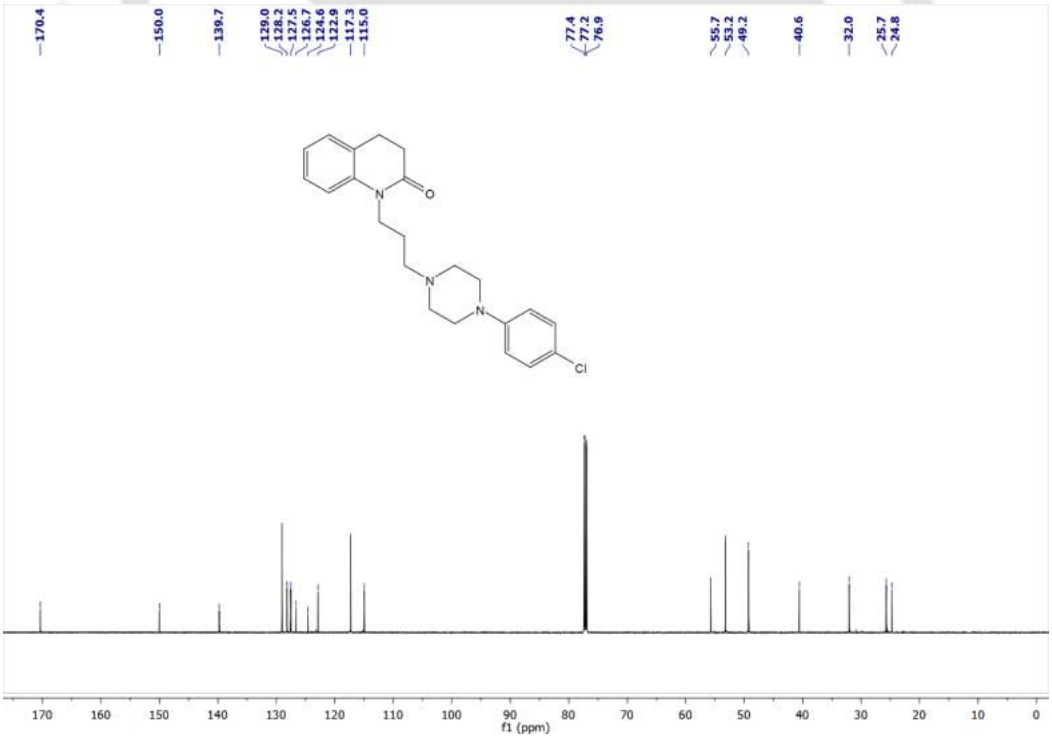


Figure S16. $^{13}C\{^{1}H\}$ NMR Spectrum of **2.12d** ($CDCl_3$, 151 MHz, 298 K)

The supporting information and all other product spectra for Chapter 2 are available at https://pubs.acs.org/doi/10.1021/acs.orglett.3c04263

Annexure II

Selected ^{1}H and ^{13}C NMR spectra of the products (*Chapter 3*)

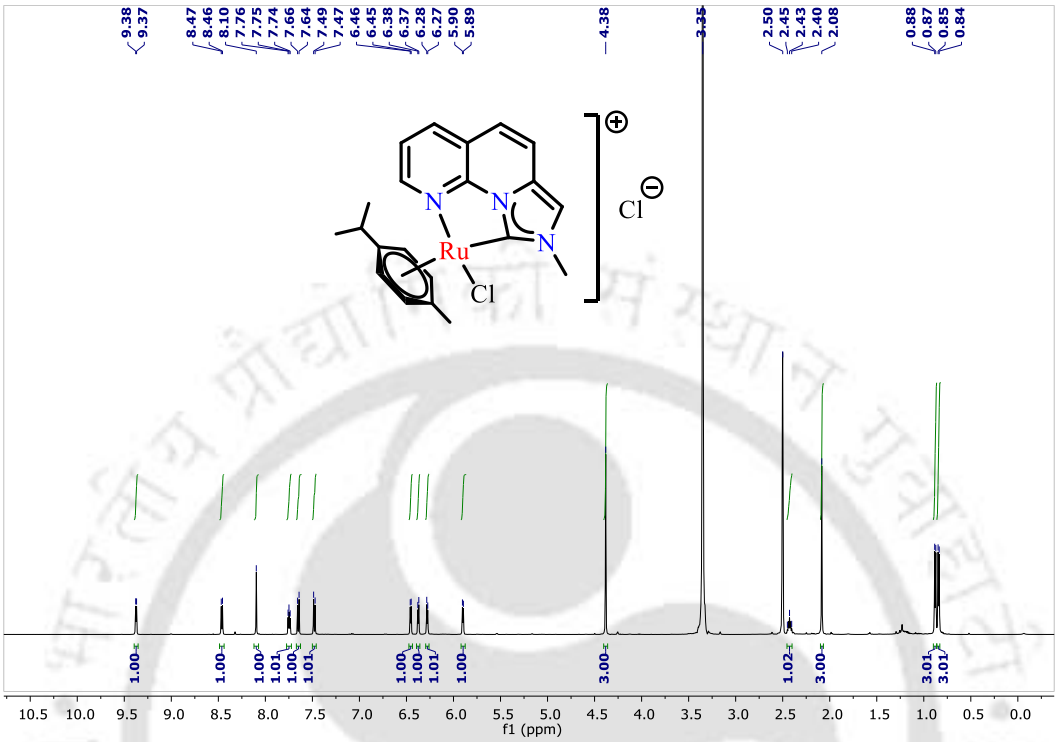


Figure S17. ^{1}H NMR Spectrum of **Ru-4** (DMSO-d_6, 600 MHz, 298 K)

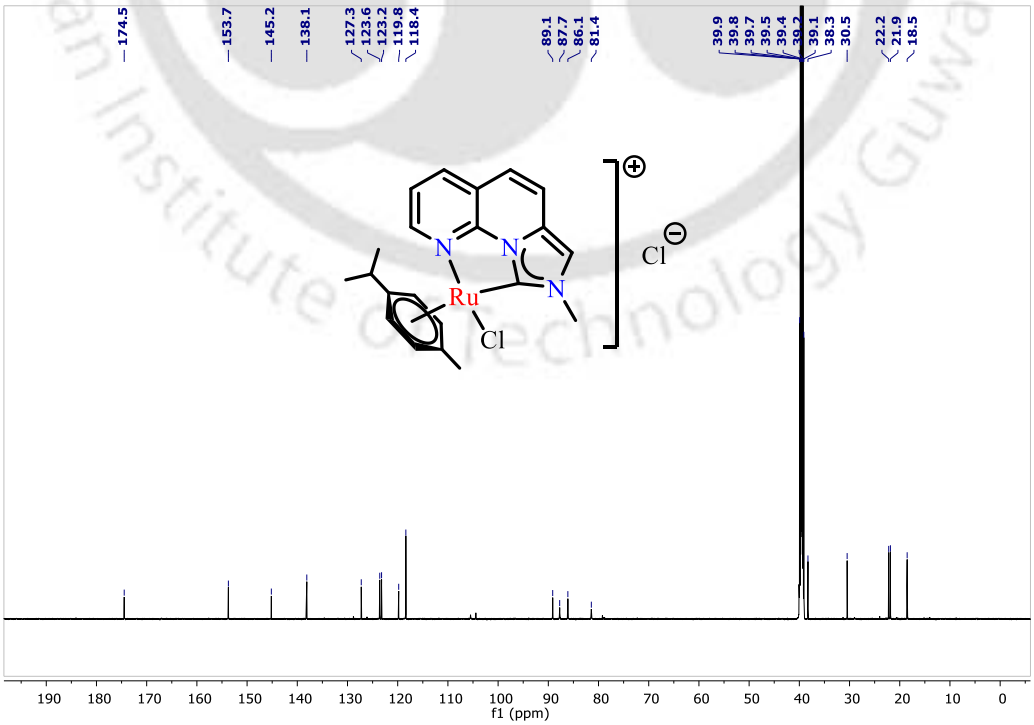


Figure S18. $^{13}C\{^{1}H\}$ NMR Spectrum of **Ru-4** (DMSO-d_6, 151 MHz, 298 K)

TH-3565_186122020

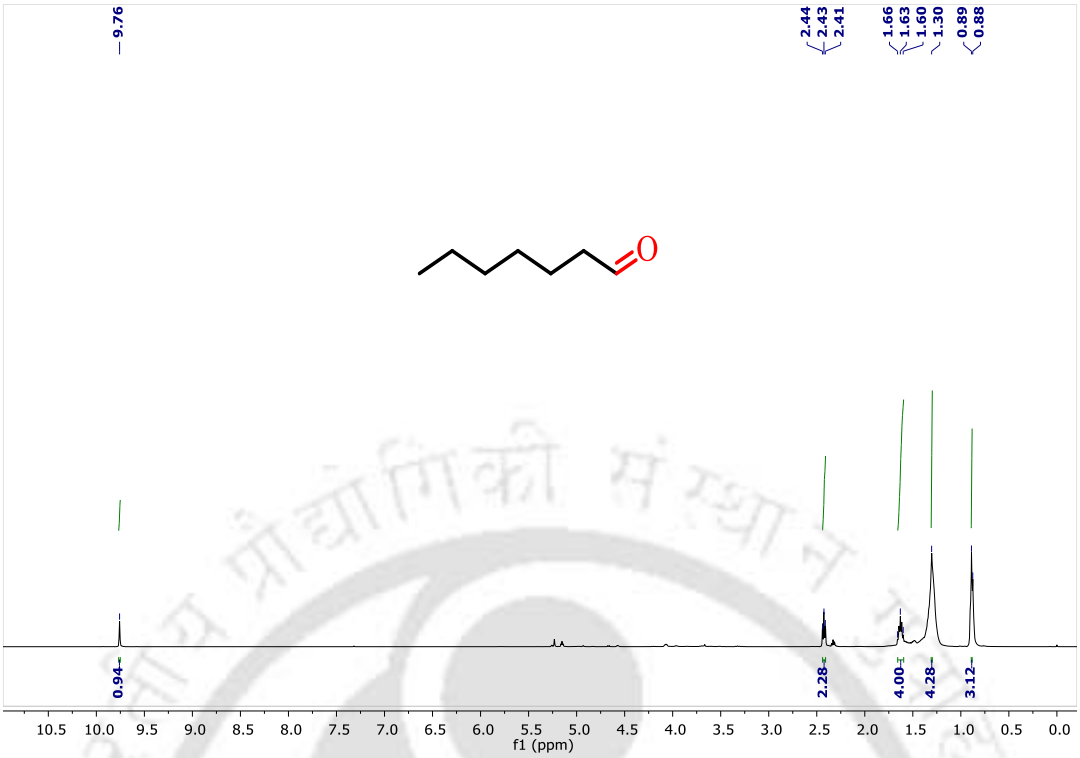


Figure S19. ^{1}H NMR Spectrum of **3.53** ($CDCl_3$, 500 MHz, 298 K)

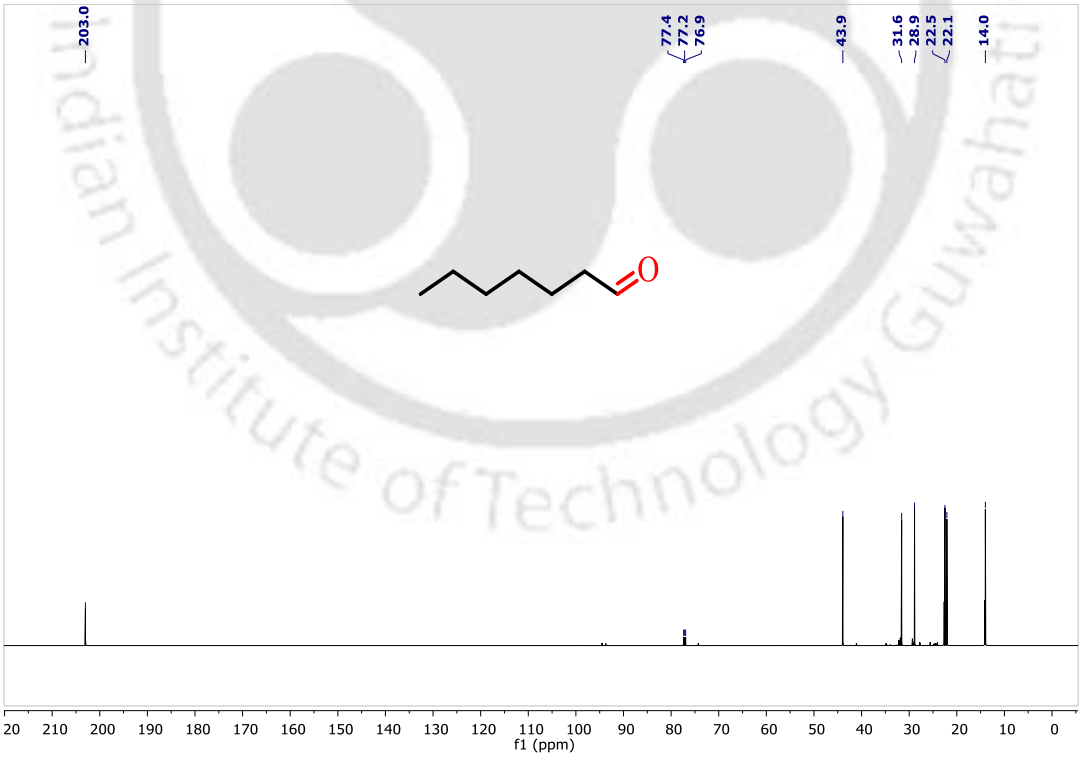


Figure S20. $^{13}C\{^{1}H\}$ NMR Spectrum of **3.53** ($CDCl_3$, 151 MHz, 298 K)

TH-3565_186122020

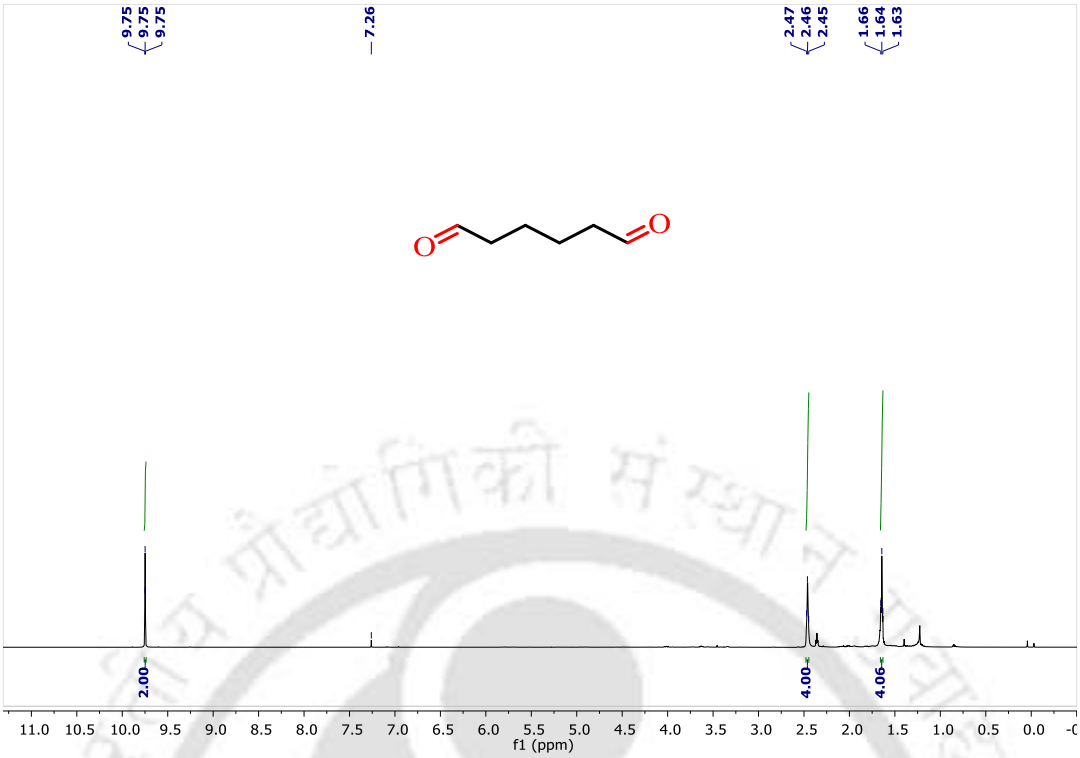


Figure S21. ^{1}H NMR Spectrum of **3.57** ($CDCl_3$, 600 MHz, 298 K)

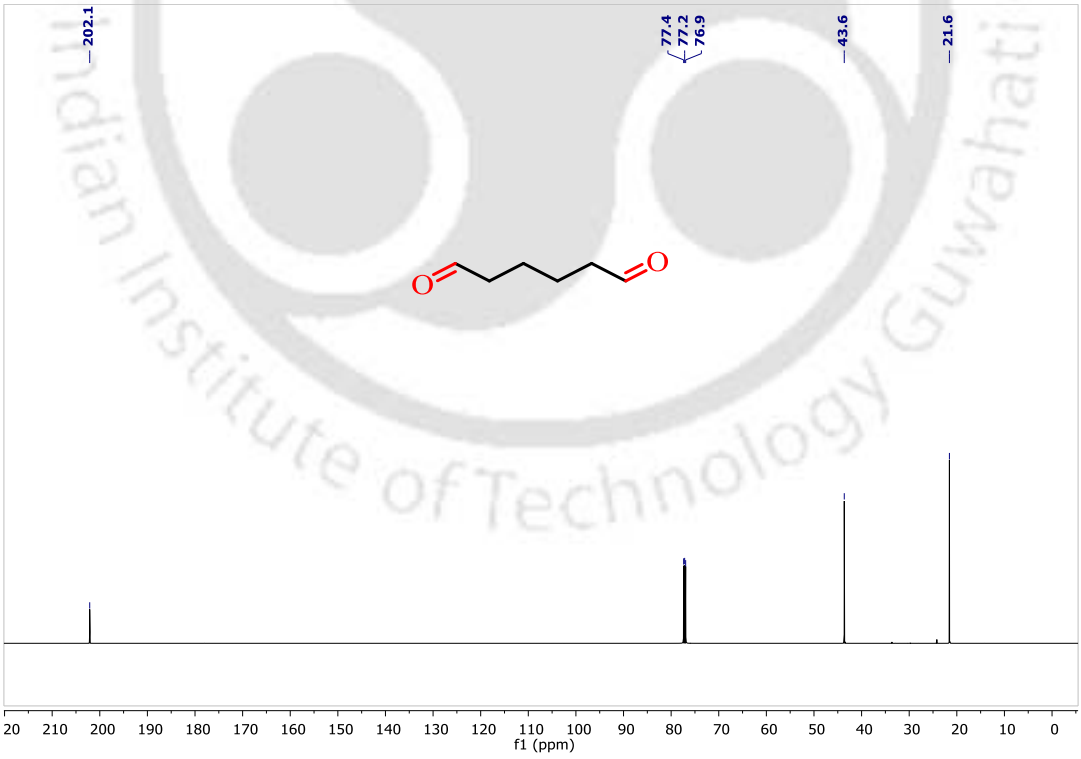


Figure S22. $^{13}C\{^{1}H\}$ NMR Spectrum of **3.57** ($CDCl_3$, 151 MHz, 298 K)

TH-3565_186122020

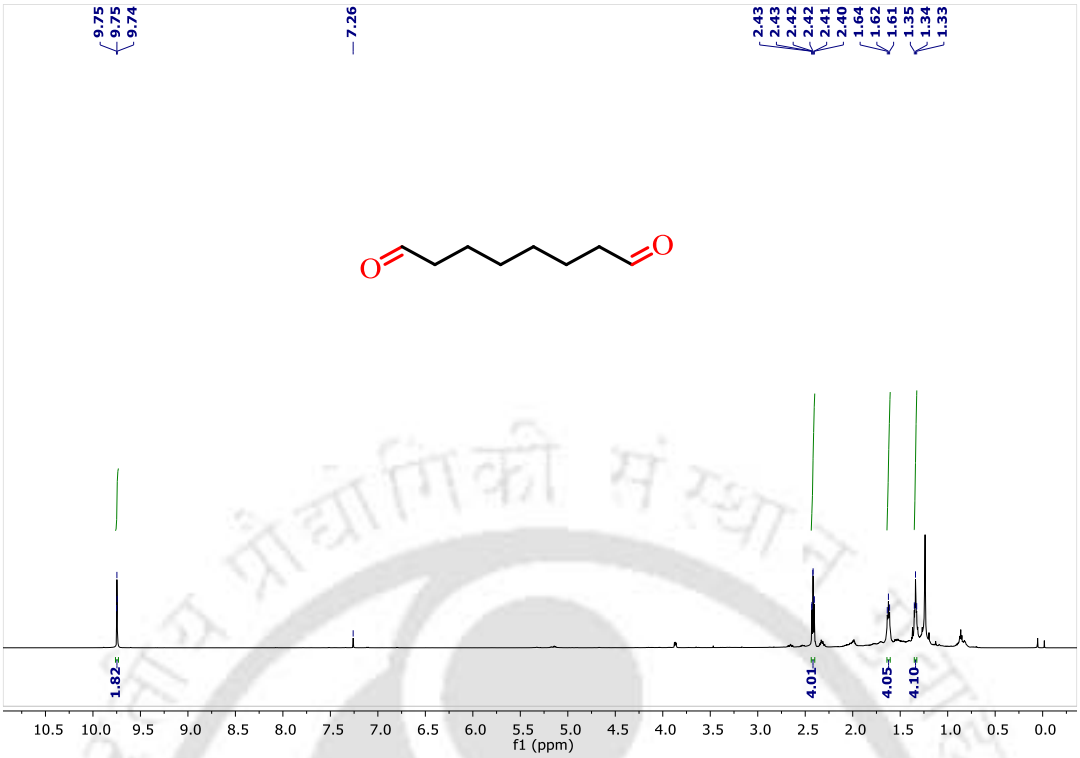


Figure S23. ^{1}H NMR Spectrum of **3.59** ($CDCl_3$, 600 MHz, 298 K)

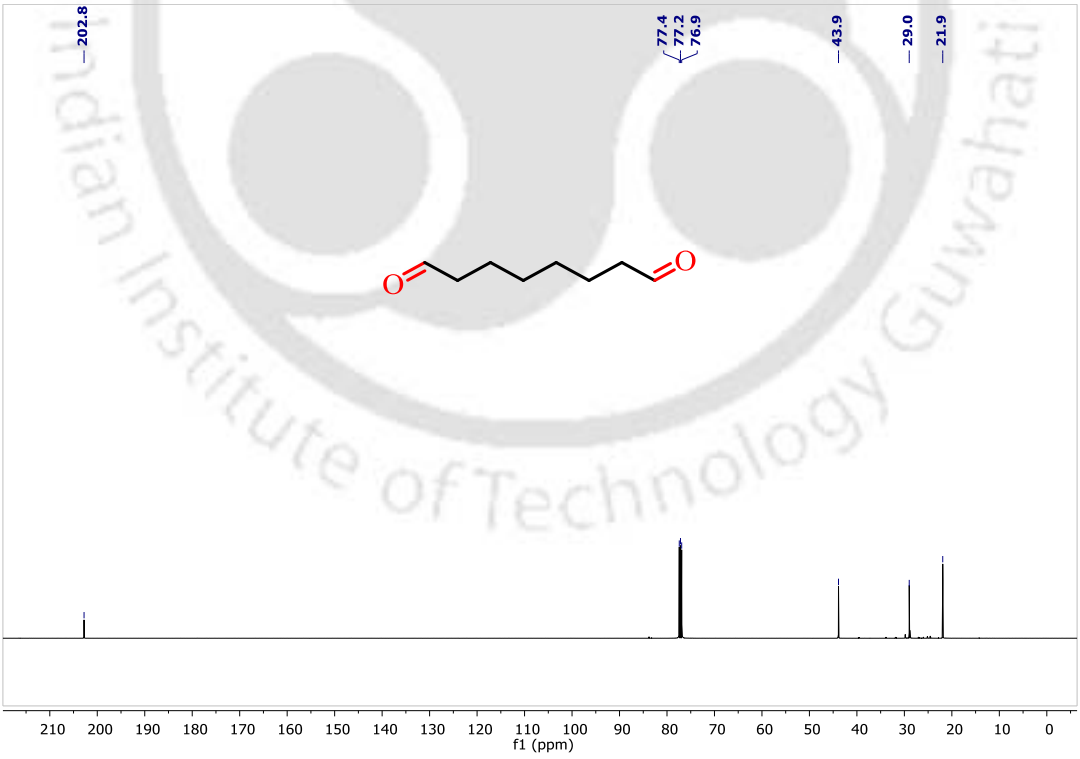


Figure S24. $^{13}C\{^{1}H\}$ NMR Spectrum of **3.59** ($CDCl_3$, 151 MHz, 298 K)

TH-3565_186122020

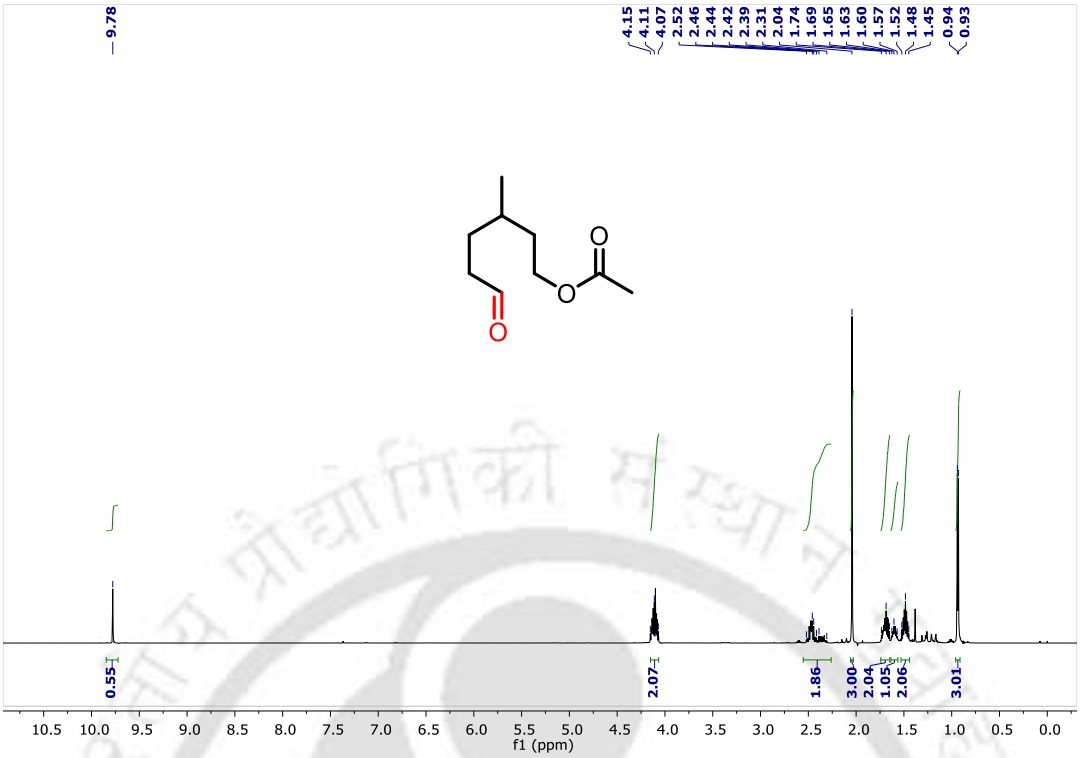


Figure S25. ^{1}H NMR Spectrum of **3.67** ($CDCl_3$, 600 MHz, 298 K)

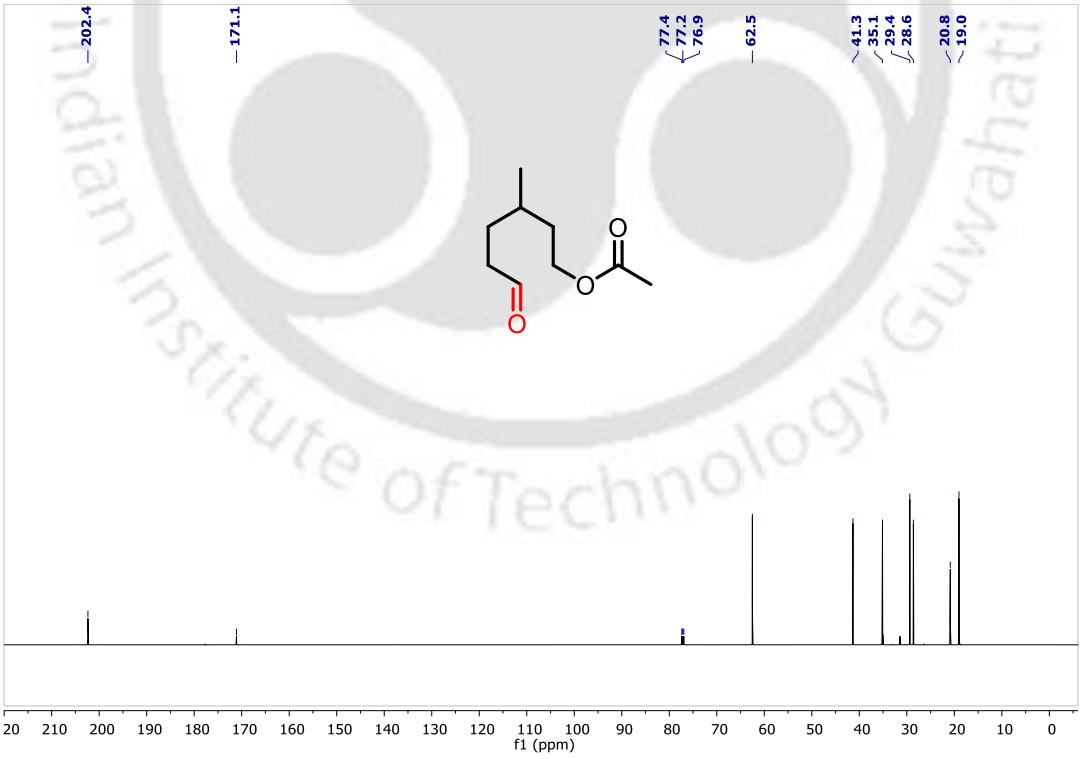


Figure S26. $^{13}C\{^{1}H\}$ NMR Spectrum of **3.67** ($CDCl_3$, 151 MHz, 298 K)

TH-3565_186122020

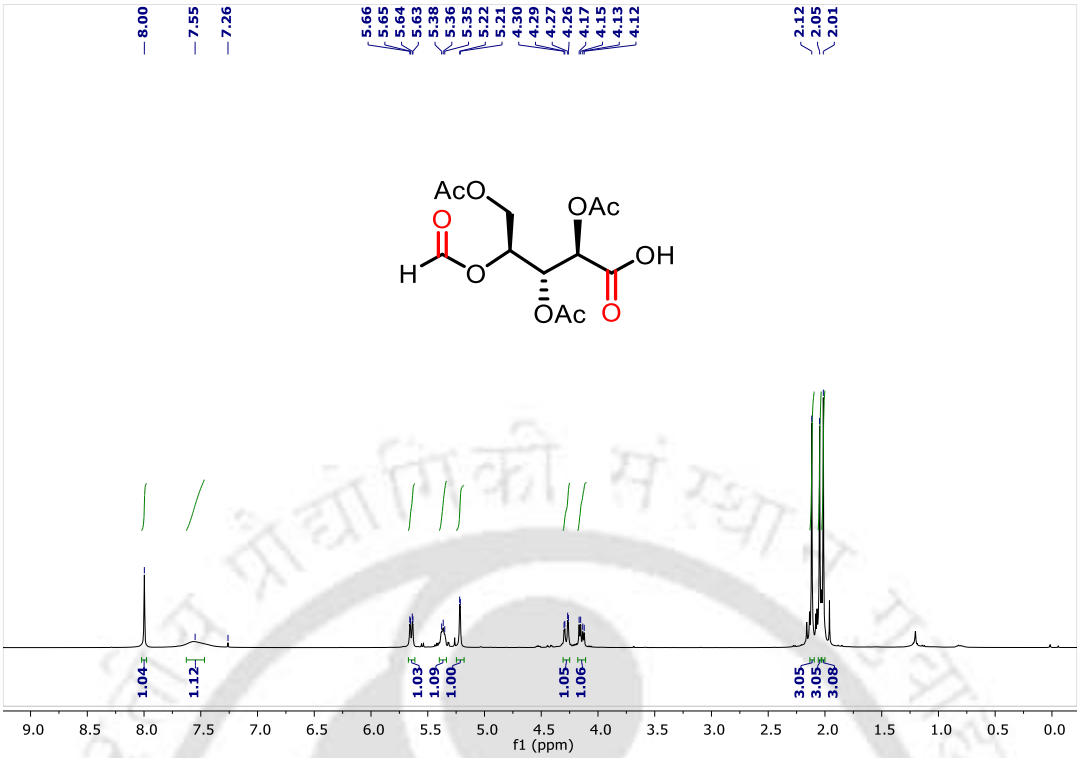


Figure S27. ^{1}H NMR Spectrum of **3.69** ($CDCl_3$, 400 MHz, 298 K)

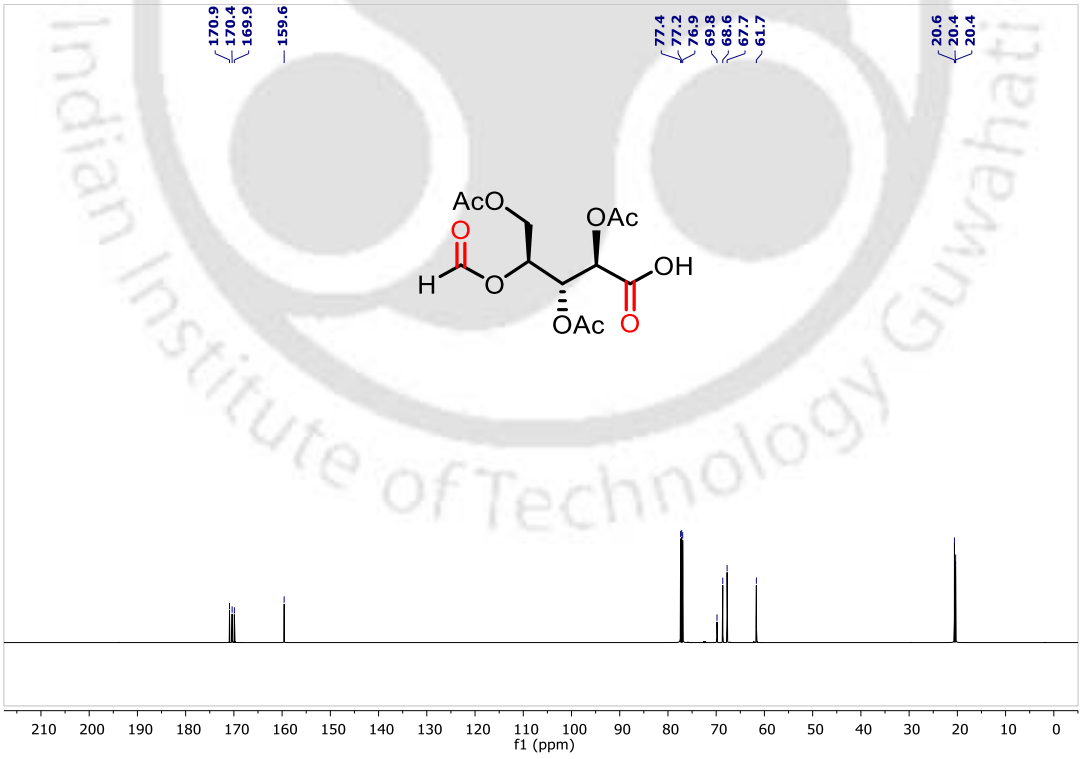


Figure S28. ^{13}C{^{1}H} NMR Spectrum of **3.69** ($CDCl_3$, 151 MHz, 298 K)

TH-3565_186122020

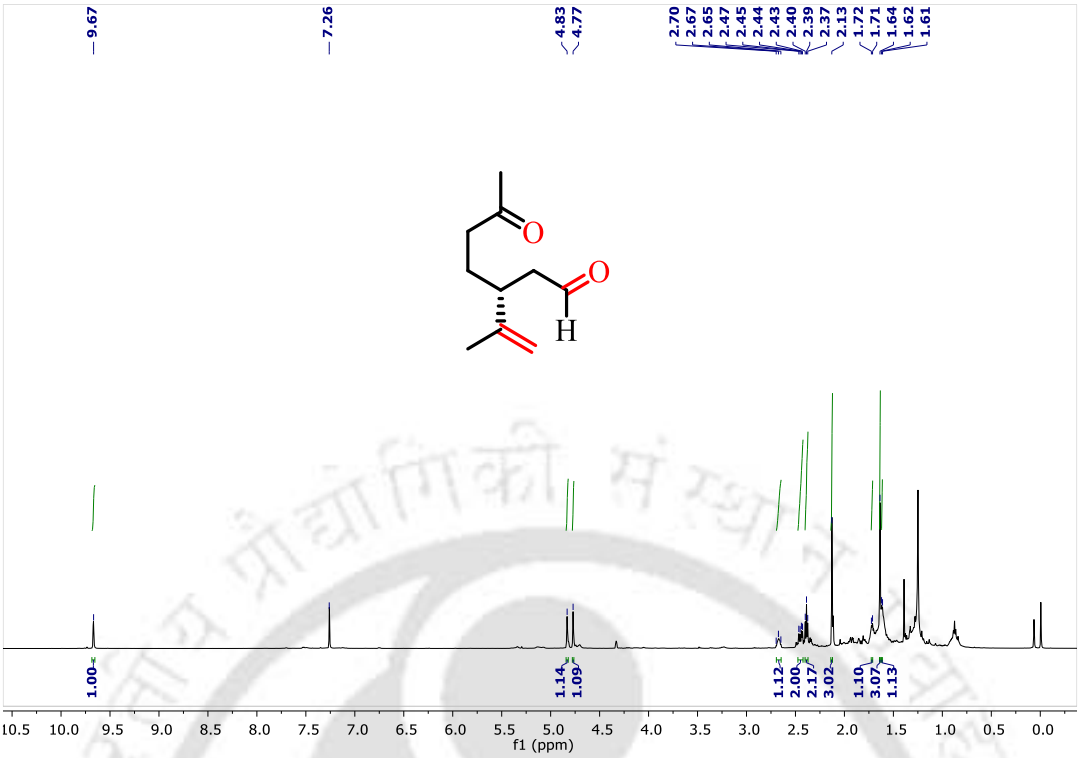


Figure S29. ^{1}H NMR Spectrum of **3.71** ($CDCl_3$, 600 MHz, 298 K)

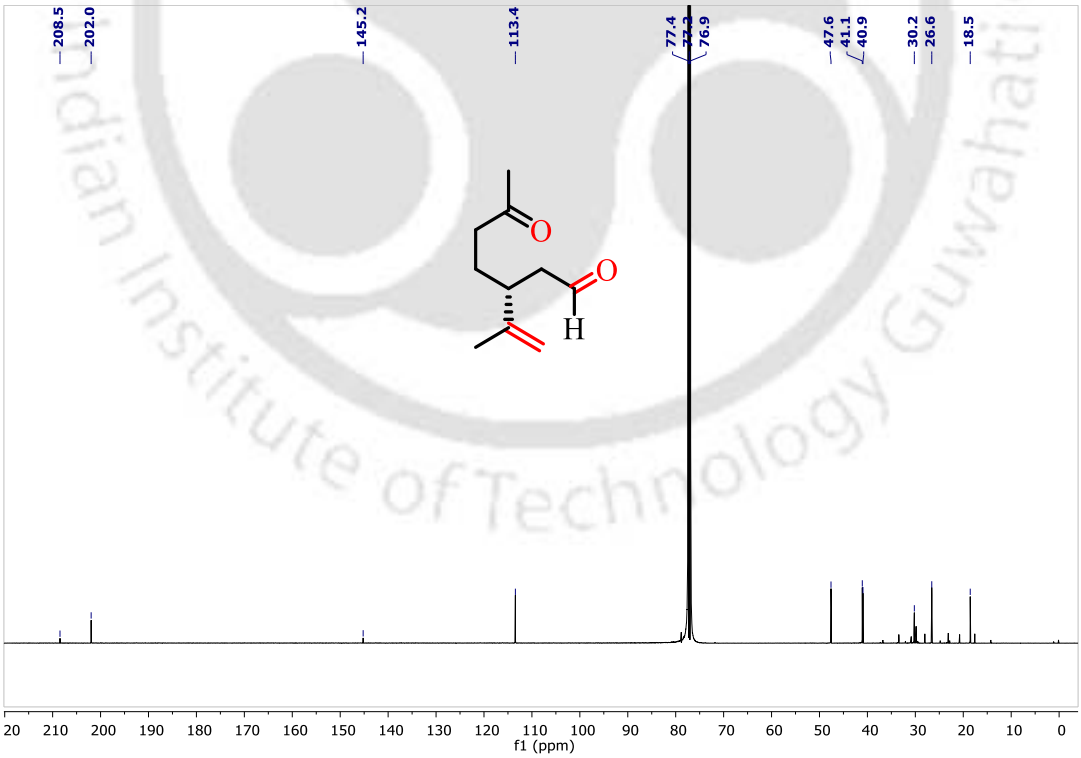


Figure S30. $^{13}C\{^{1}H\}$ NMR Spectrum of **3.71** ($CDCl_3$, 151 MHz, 298 K)

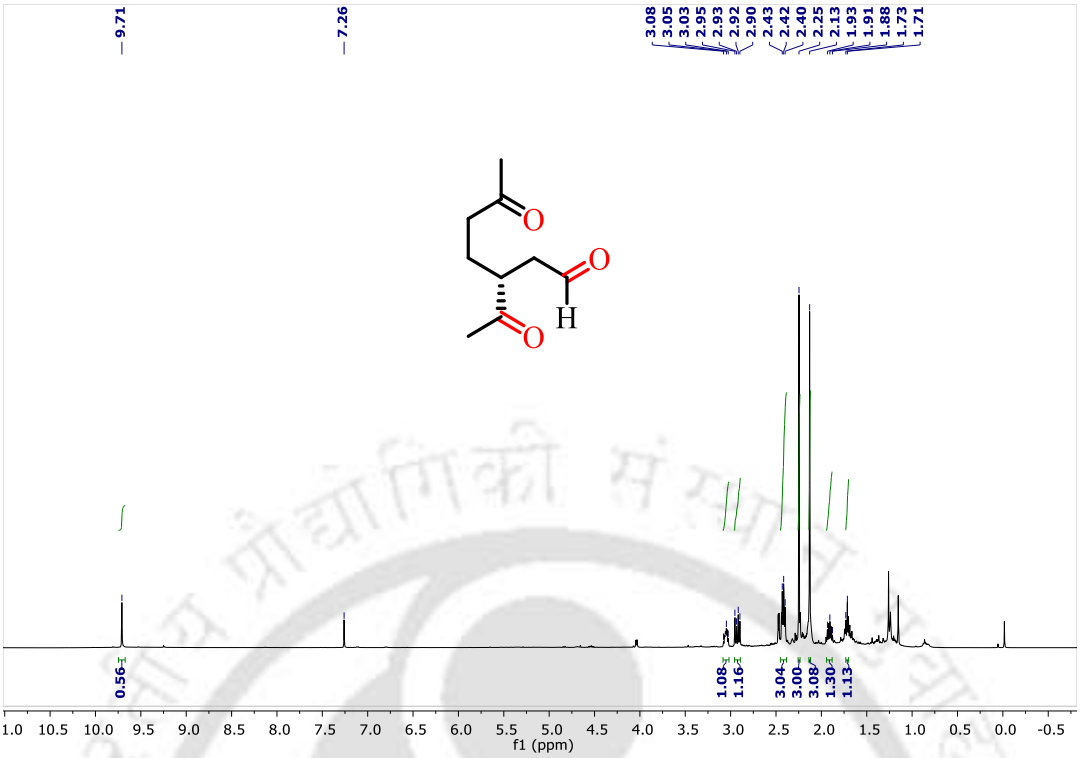


Figure S31. ^{1}H NMR Spectrum of **3.72** ($CDCl_3$, 500 MHz, 298 K)

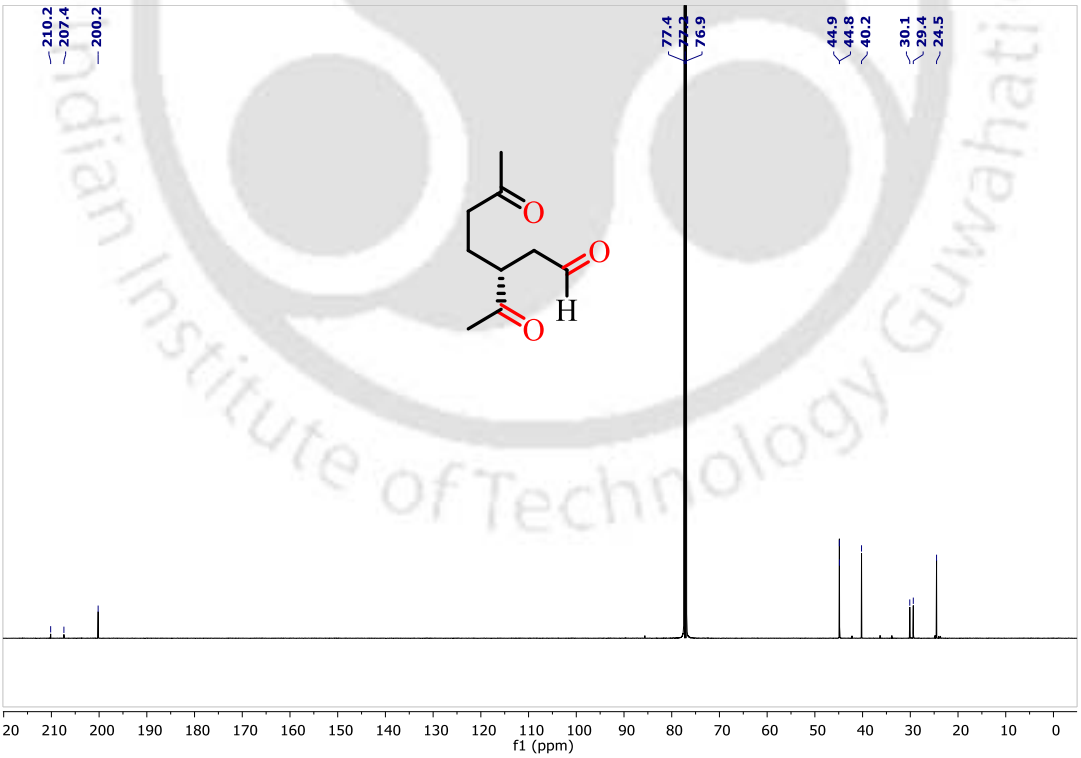


Figure S32. $^{13}C\{^{1}H\}$ NMR Spectrum of **3.72** ($CDCl_3$, 151 MHz, 298 K)

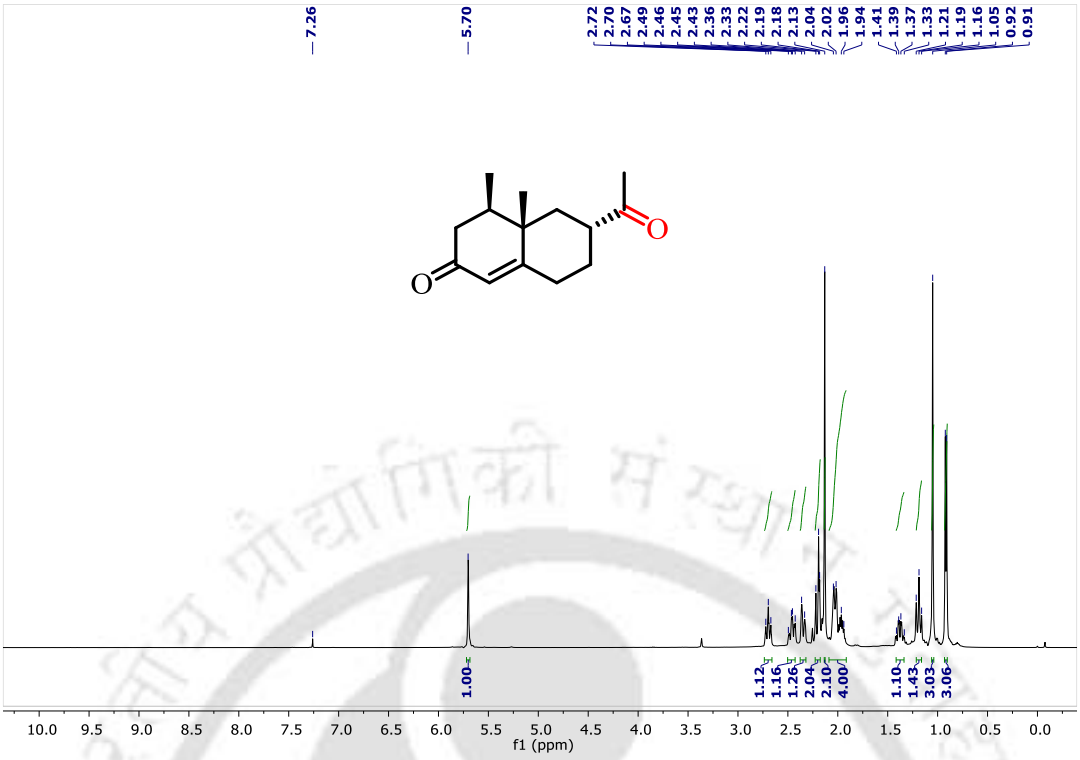


Figure S33. ^{1}H NMR Spectrum of **3.74** ($CDCl_3$, 500 MHz, 298 K)

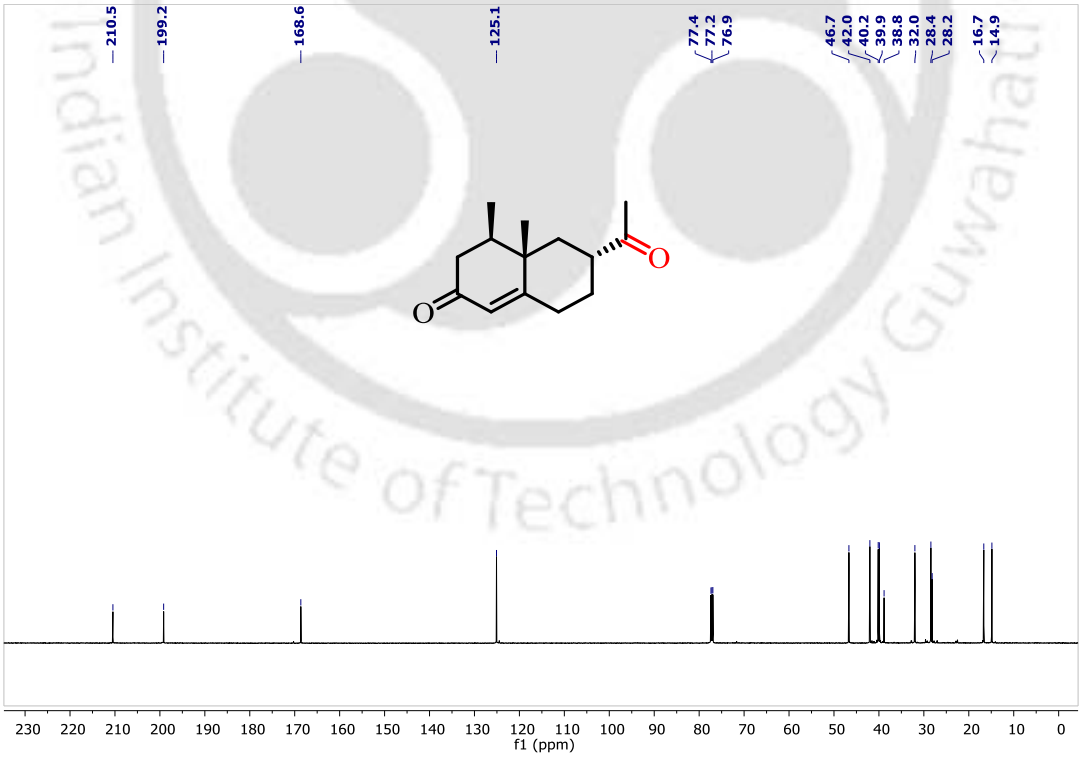


Figure S34. $^{13}C\{^{1}H\}$ NMR Spectrum of **3.74** ($CDCl_3$, 151 MHz, 298 K)

TH-3565_186122020

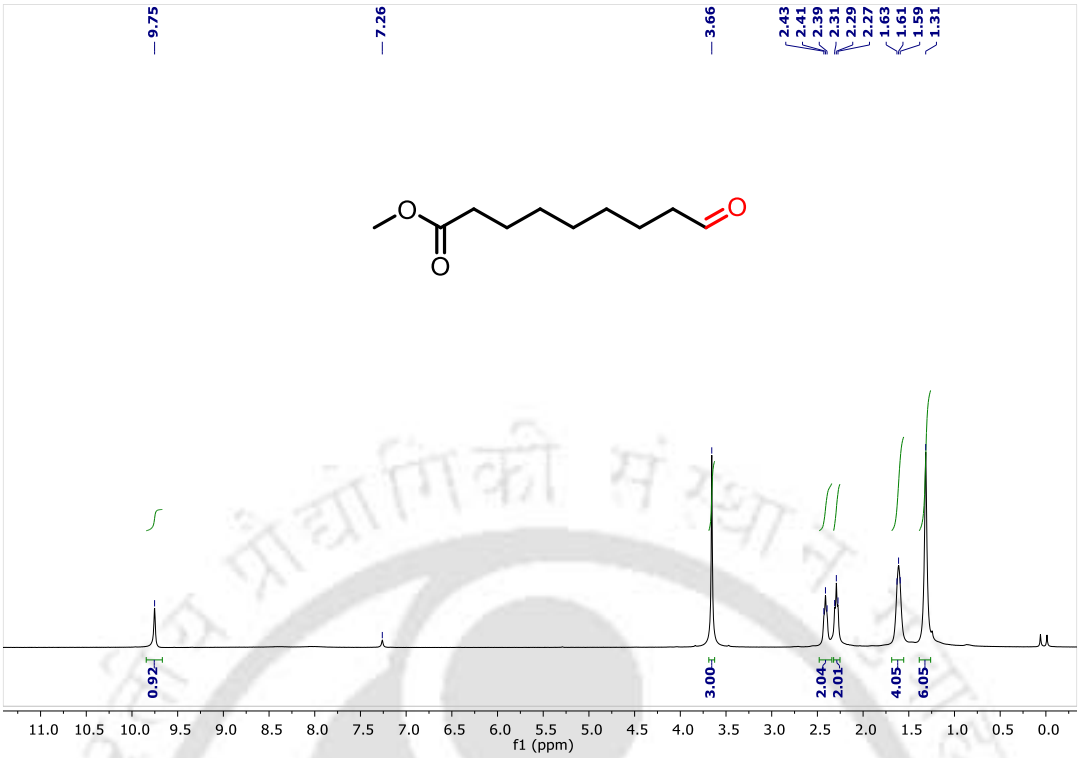


Figure S35. ^{1}H NMR Spectrum of **3.76** ($CDCl_3$, 400 MHz, 298 K)

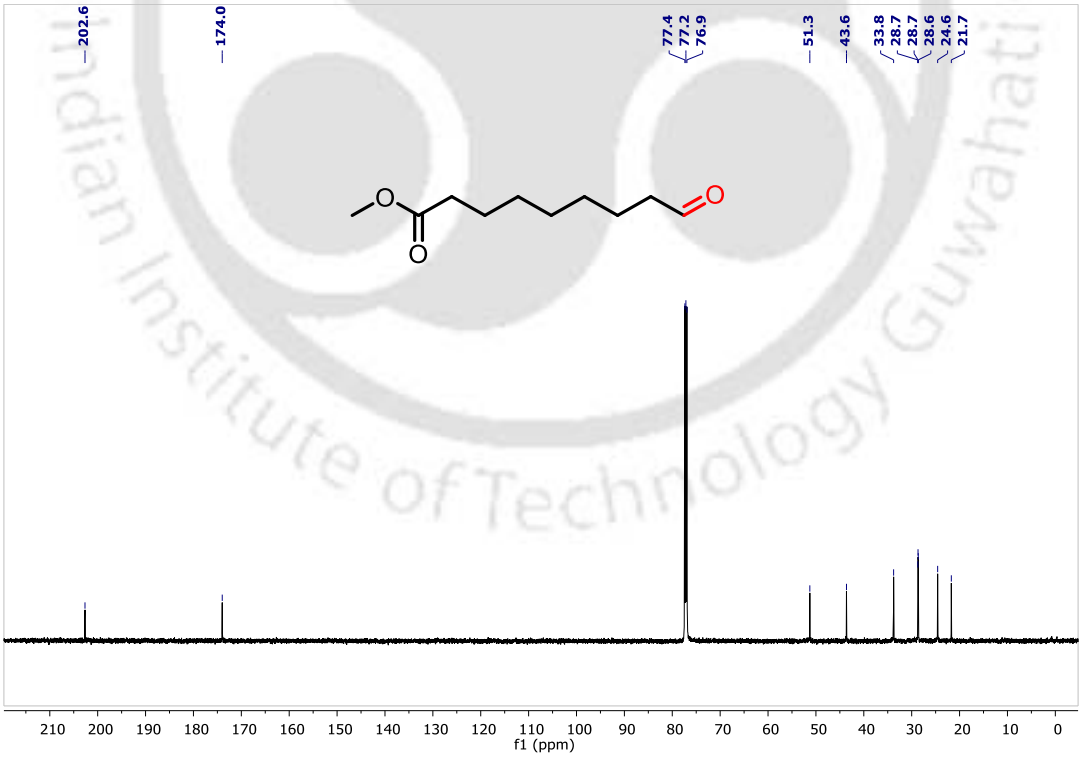


Figure S36. $^{13}C\{^{1}H\}$ NMR Spectrum of **3.76** ($CDCl_3$, 151 MHz, 298 K)

TH-3565_186122020

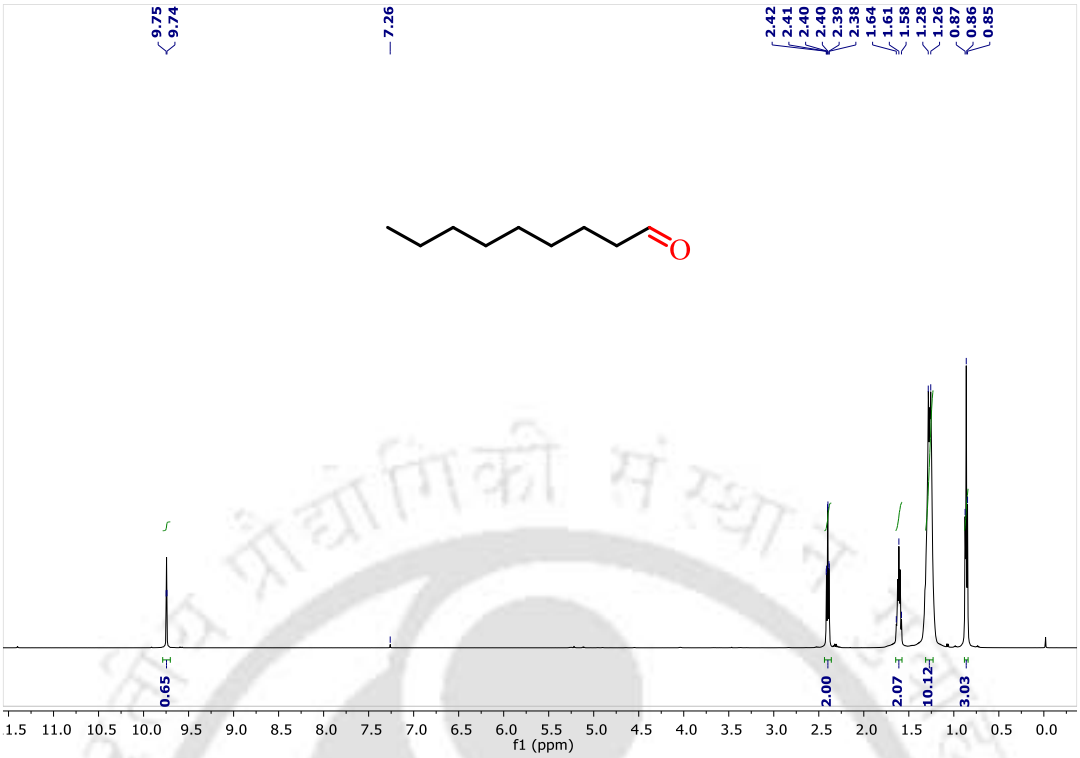


Figure S37. ^{1}H NMR Spectrum of **3.77** ($CDCl_3$, 500 MHz, 298 K)

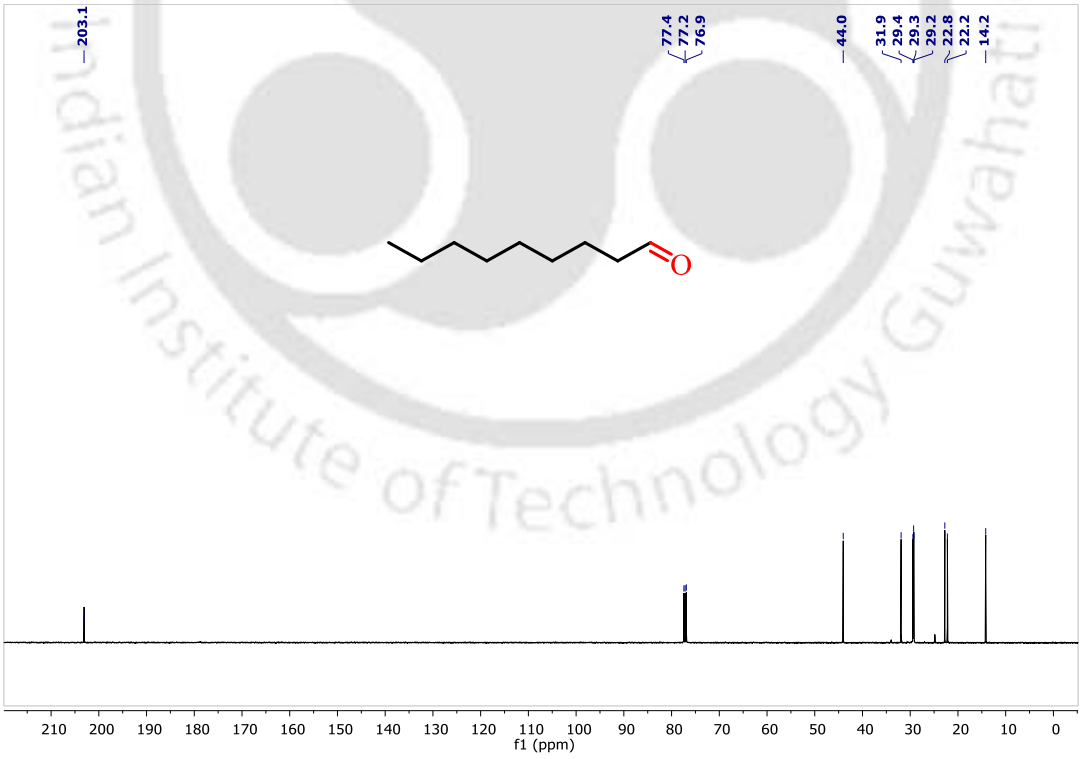


Figure S38. $^{13}C\{^{1}H\}$ NMR Spectrum of **3.77** ($CDCl_3$, 126 MHz, 298 K)

TH-3565_186122020

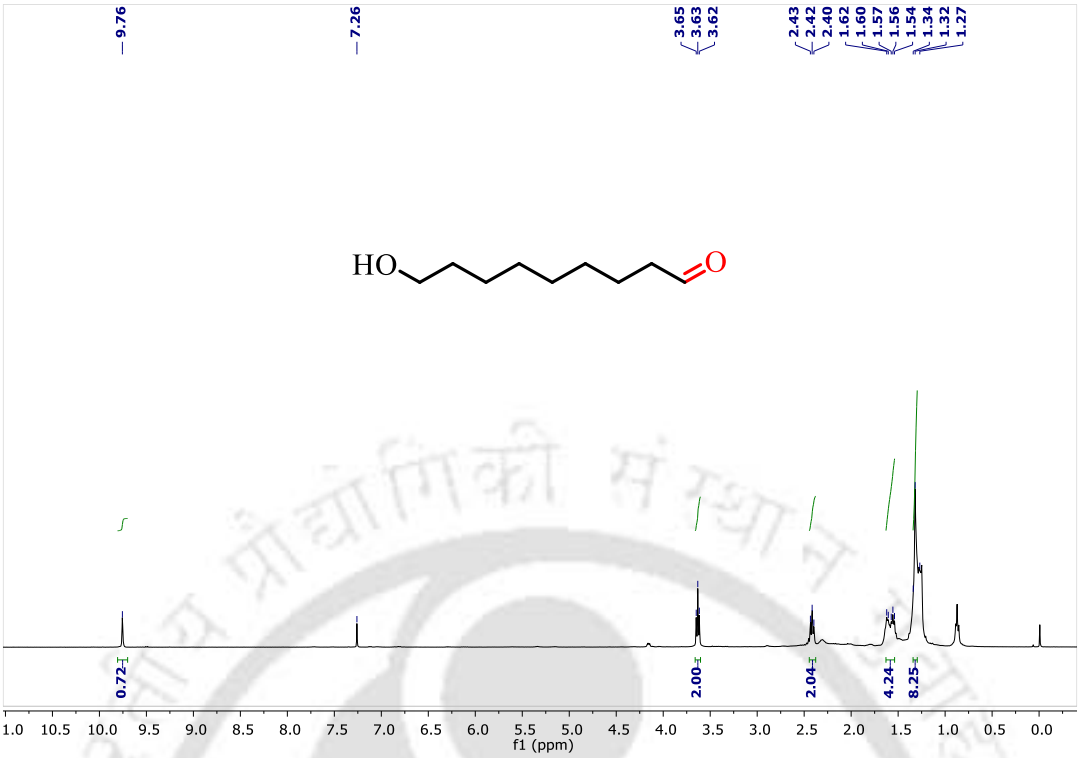


Figure S39. ^{1}H NMR Spectrum of **3.79** ($CDCl_3$, 400 MHz, 298 K)

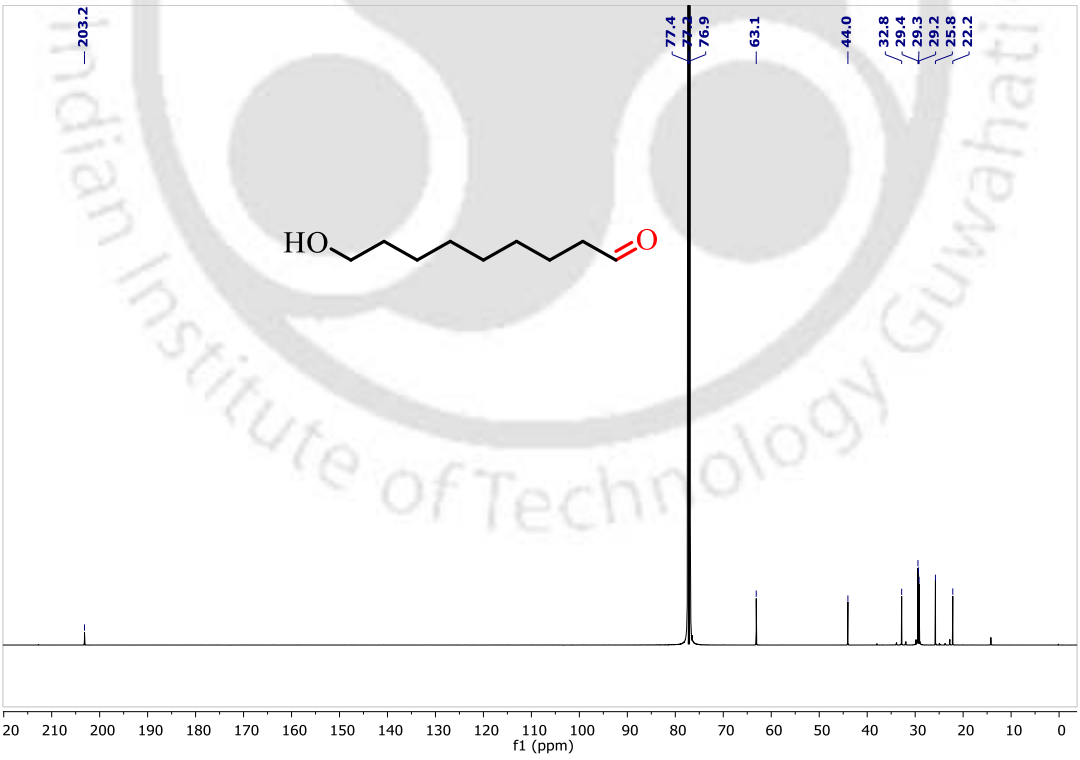


Figure S40. $^{13}C\{^{1}H\}$ NMR Spectrum of **3.79** ($CDCl_3$, 151 MHz, 298 K)

TH-3565_186122020

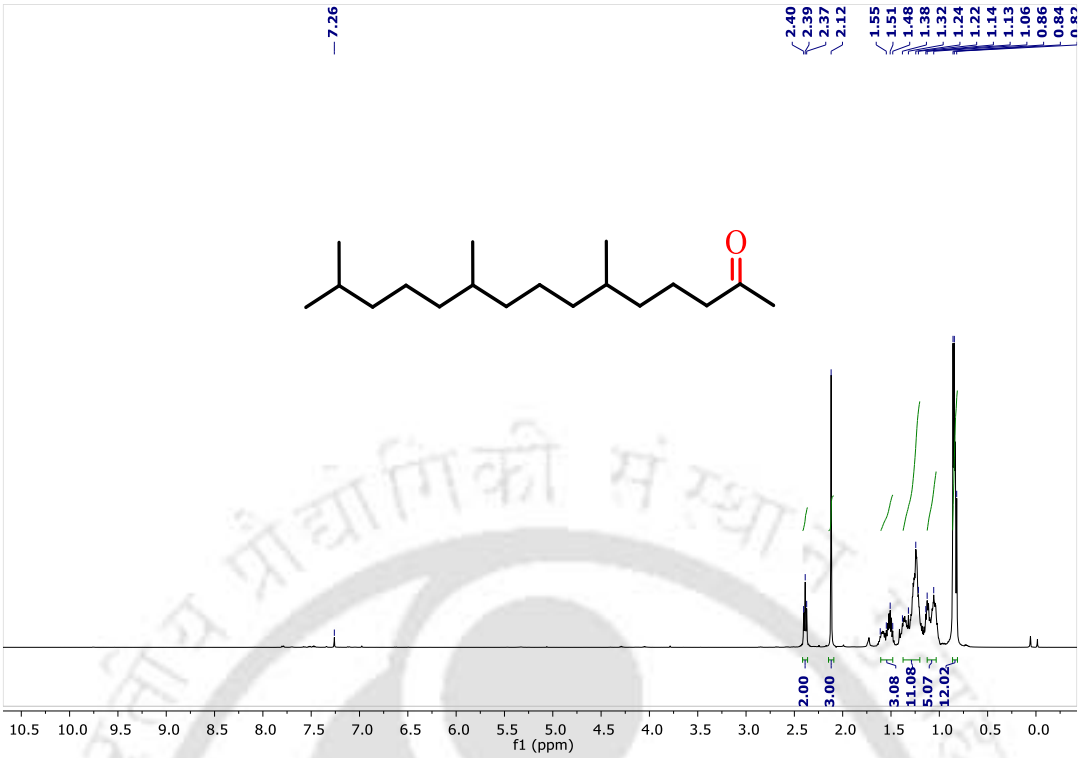


Figure S41. ^{1}H NMR Spectrum of **3.82** ($CDCl_3$, 500 MHz, 298 K)

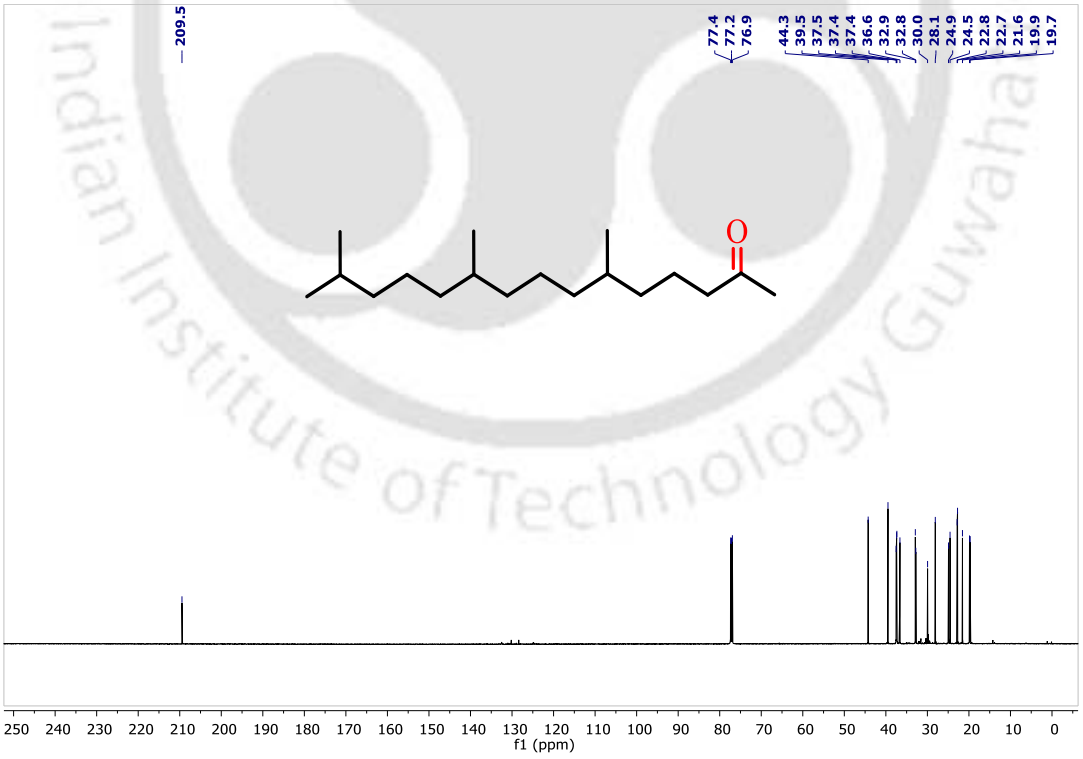


Figure S42. $^{13}C\{^{1}H\}$ NMR Spectrum of **3.82** ($CDCl_3$, 151 MHz, 298 K)

TH-3565_186122020

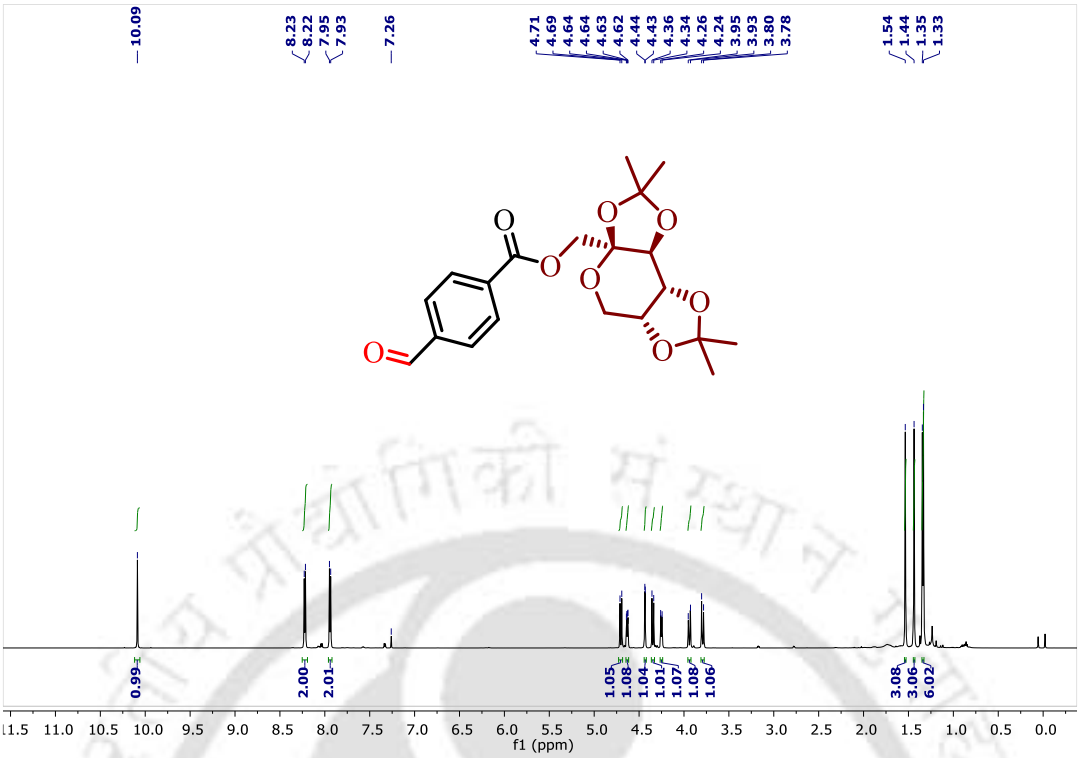


Figure S43. ^{1}H NMR Spectrum of **3.84** ($CDCl_3$, 600 MHz, 298 K)

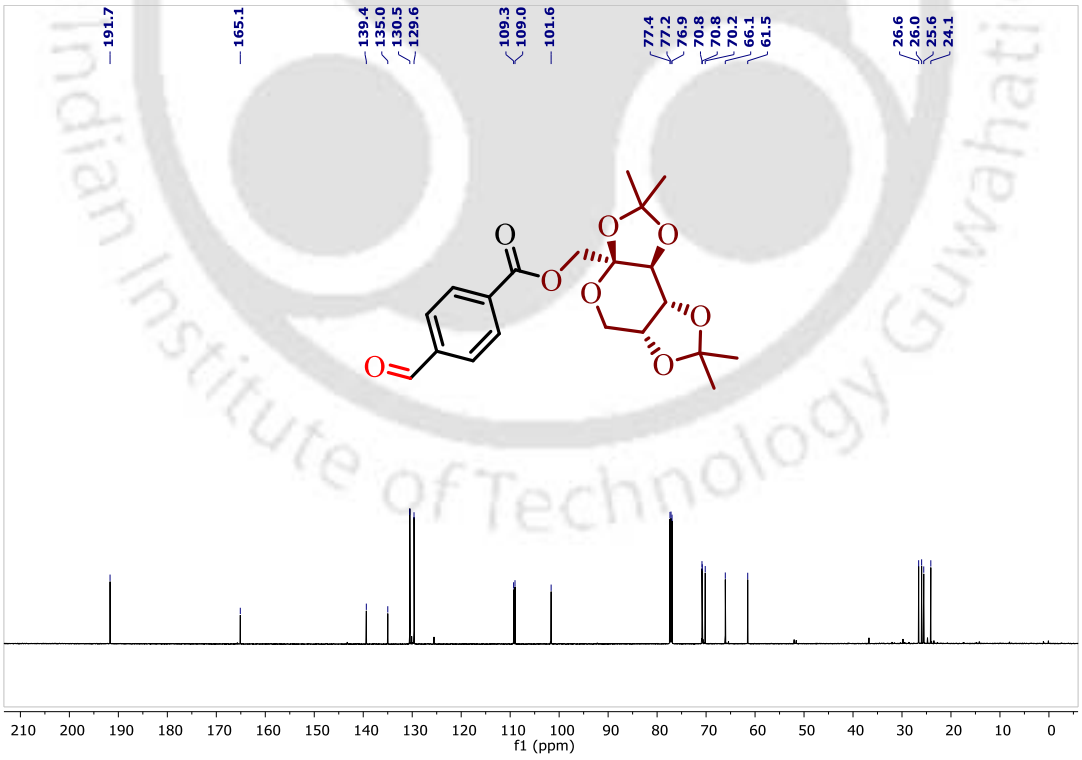


Figure S44. $^{13}C\{^{1}H\}$ NMR Spectrum of **3.84** ($CDCl_3$, 151 MHz, 298 K)

TH-3565_186122020

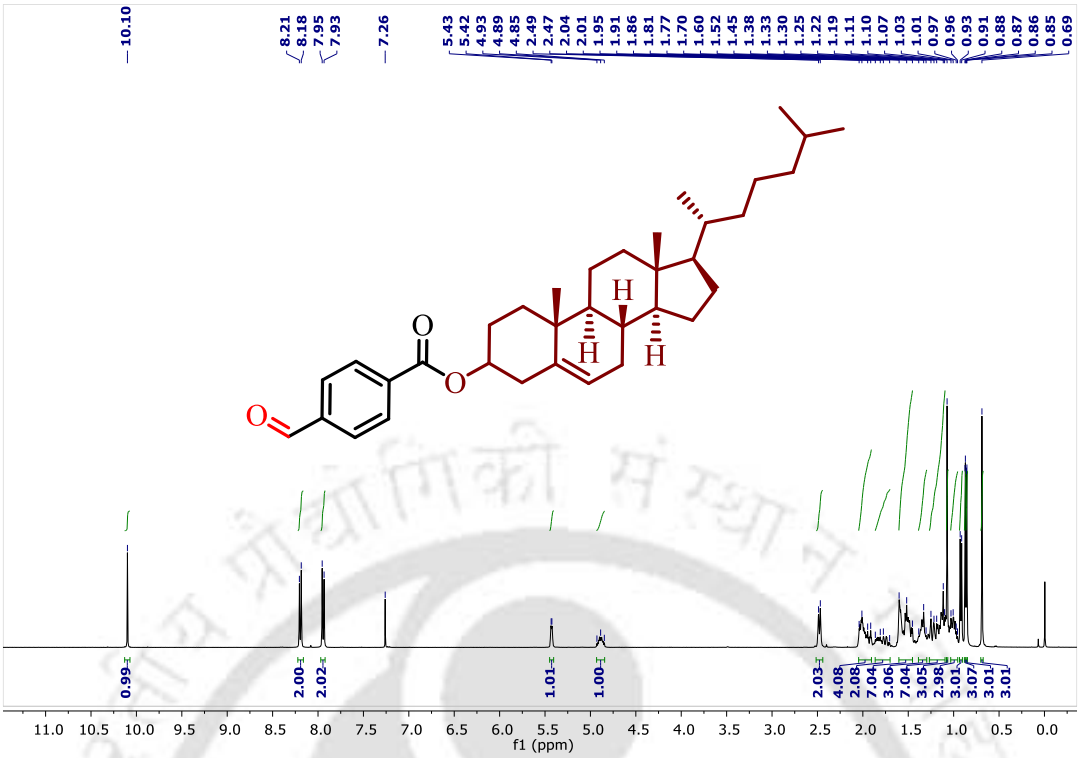


Figure S45. ^{1}H NMR Spectrum of **3.86** ($CDCl_3$, 400 MHz, 298 K)

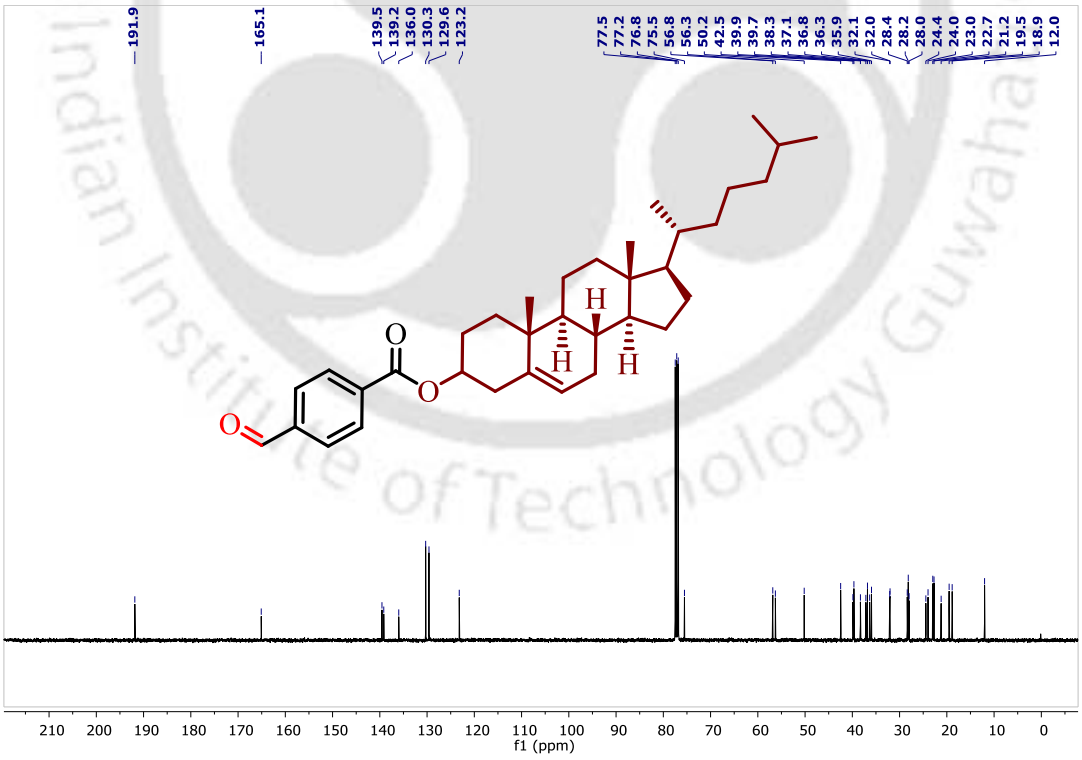


Figure S46. $^{13}C\{^{1}H\}$ NMR Spectrum of **3.86** ($CDCl_3$, 101 MHz, 298 K)

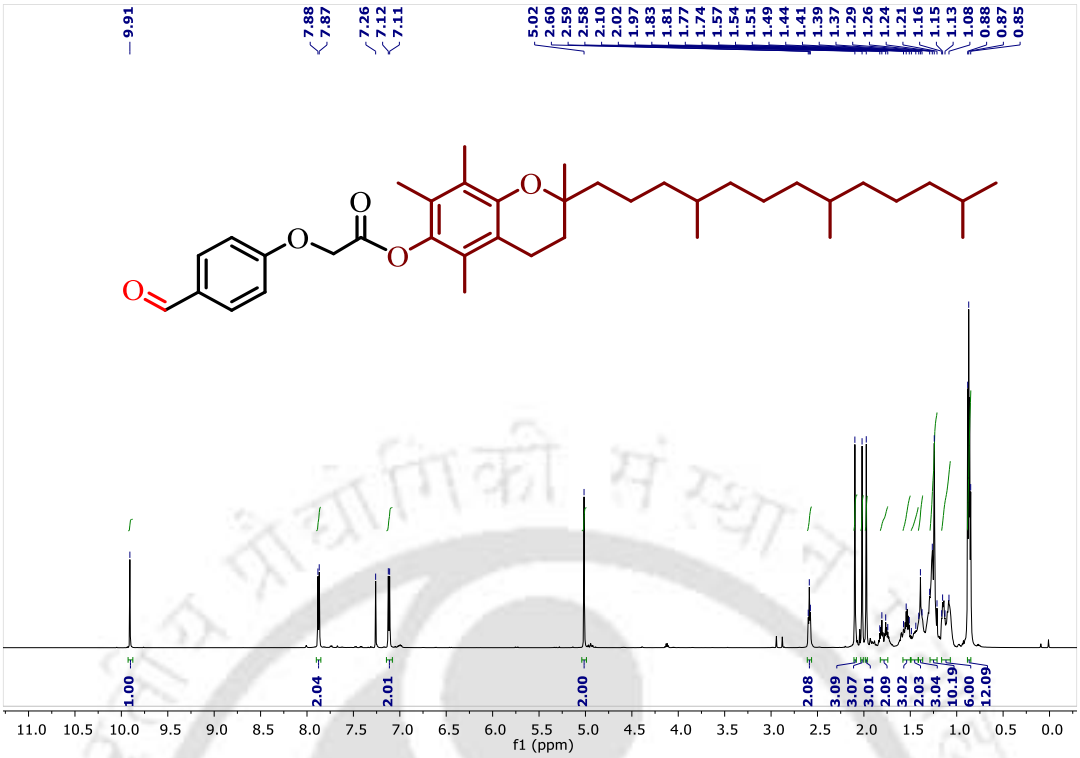


Figure S47. ^{1}H NMR Spectrum of **3.88** ($CDCl_3$, 600 MHz, 298 K)

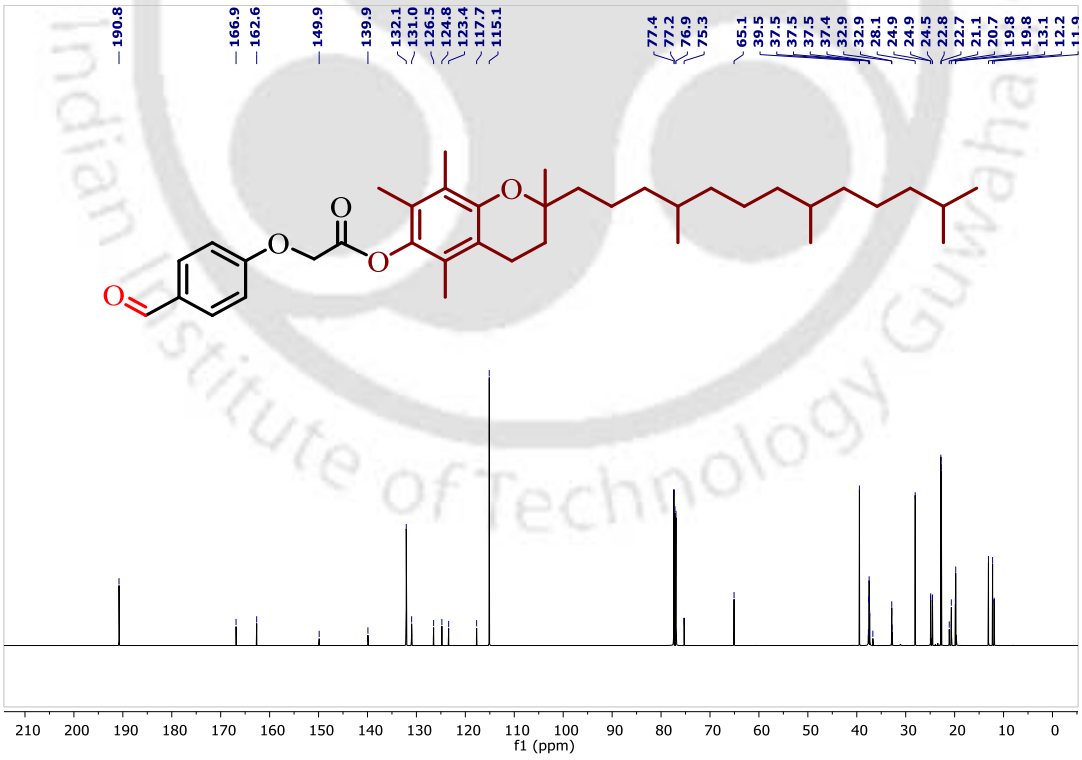


Figure S48. $^{13}C\{^{1}H\}$ NMR Spectrum of **3.88** ($CDCl_3$, 151 MHz, 298 K)

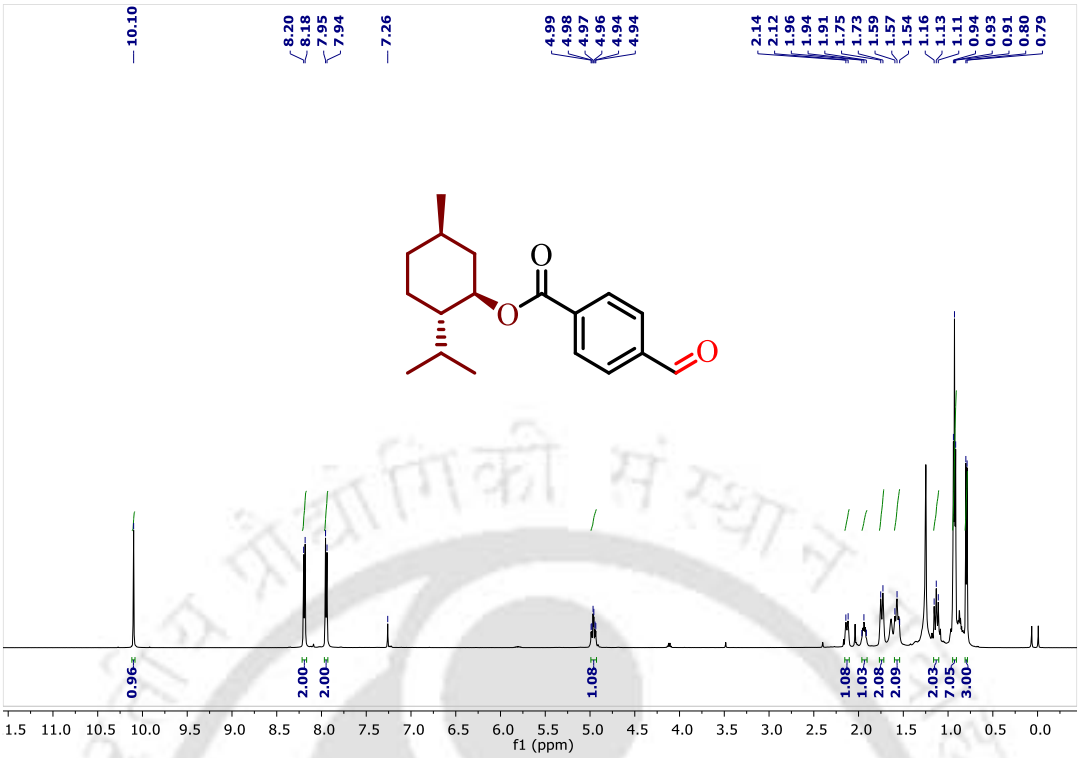


Figure S49. ^{1}H NMR Spectrum of **3.90** ($CDCl_3$, 500 MHz, 298 K)

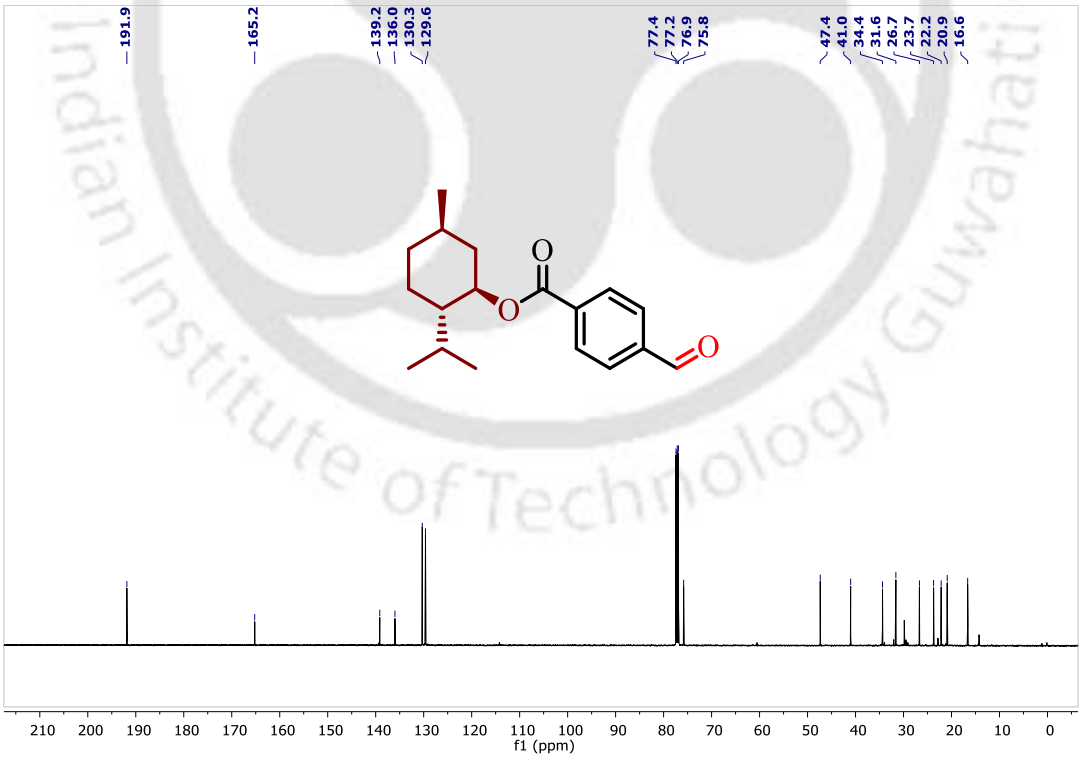


Figure S50. $^{13}C\{^{1}H\}$ NMR Spectrum of **3.90** ($CDCl_3$, 126 MHz, 298 K)

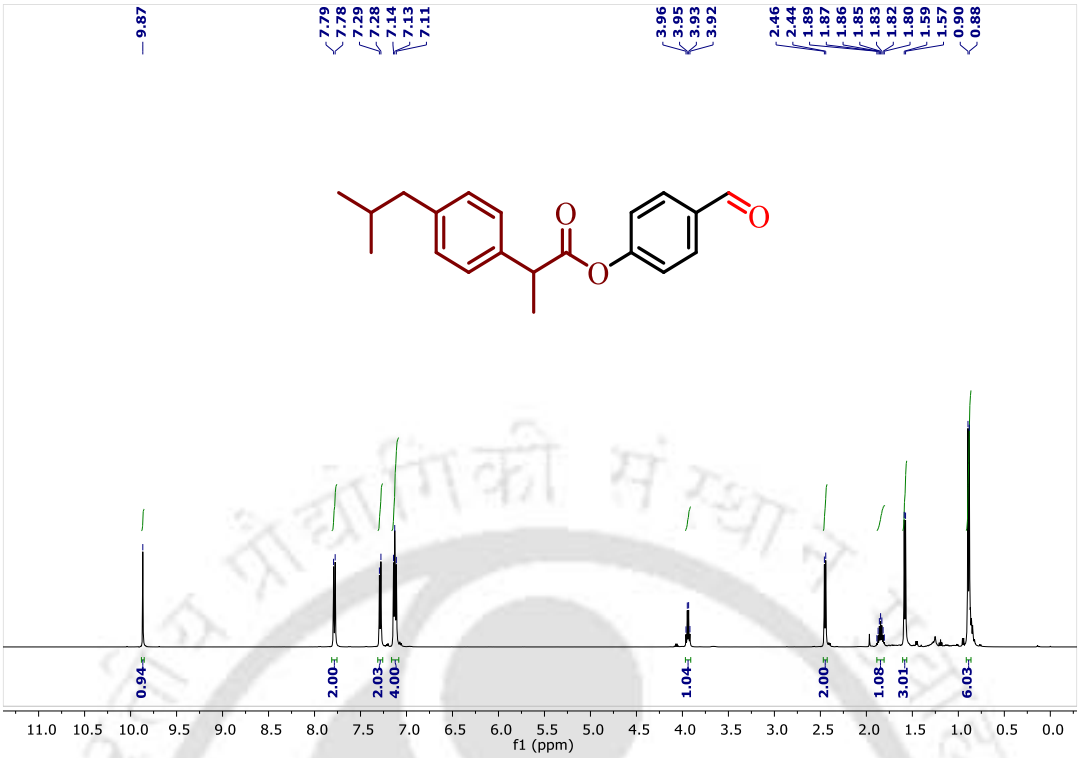


Figure S51. ^{1}H NMR Spectrum of **3.92** ($CDCl_3$, 500 MHz, 298 K)

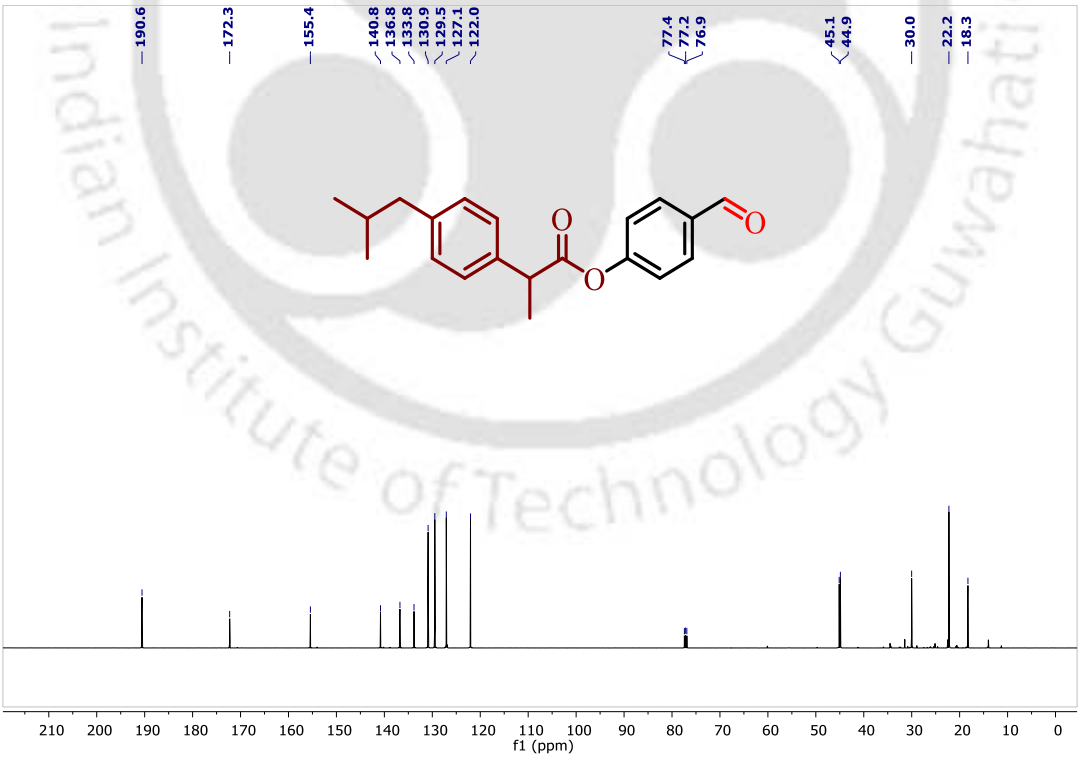


Figure S52. $^{13}C\{^{1}H\}$ NMR Spectrum of **3.92** ($CDCl_3$, 126 MHz, 298 K)

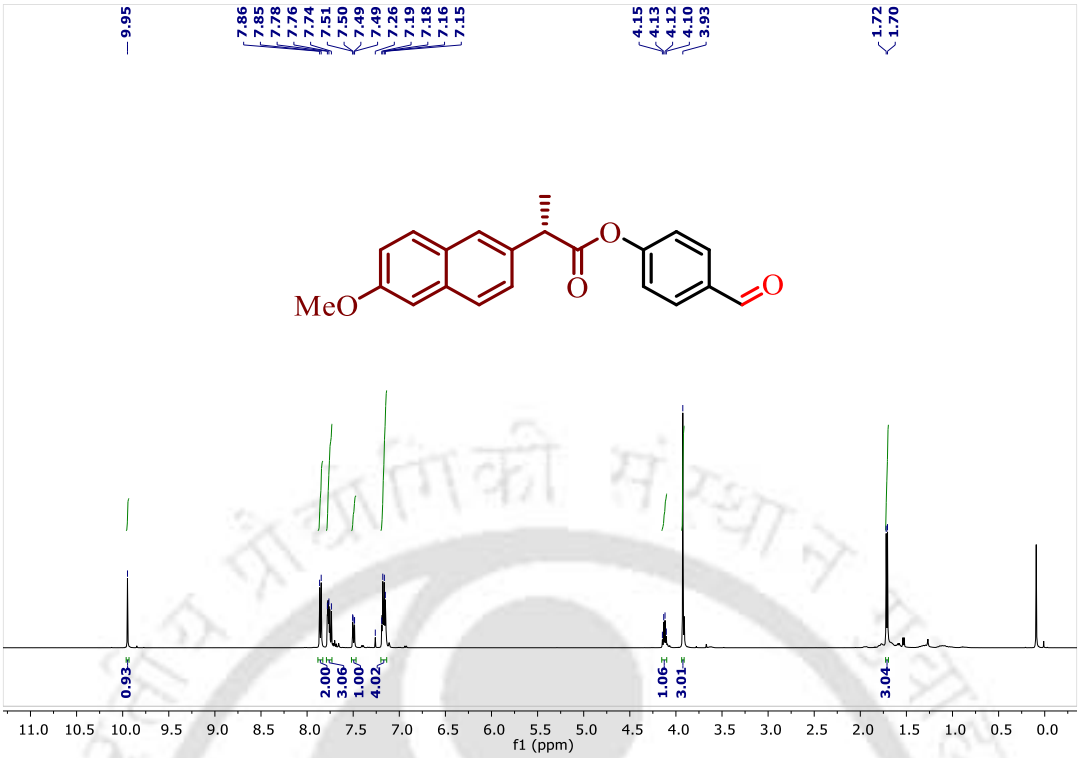


Figure S53. ^{1}H NMR Spectrum of **3.94** ($CDCl_3$, 500 MHz, 298 K)

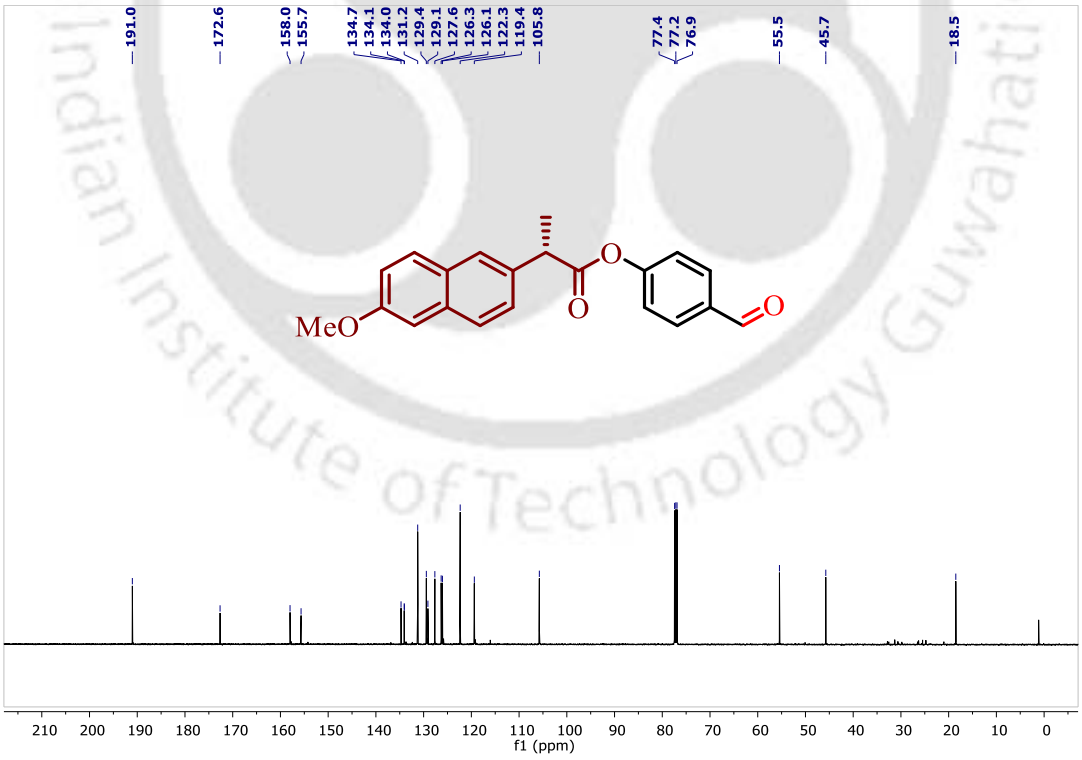


Figure S54. $^{13}C\{^{1}H\}$ NMR Spectrum of **3.94** ($CDCl_3$, 126 MHz, 298 K)

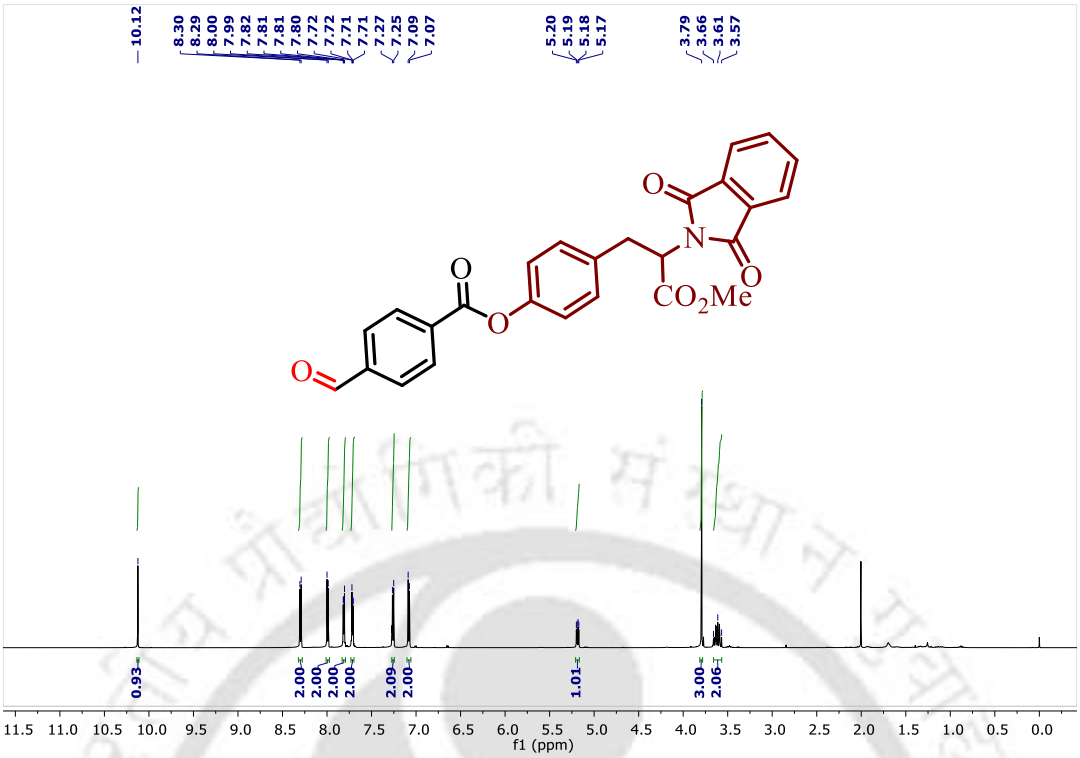


Figure S55. ^{1}H NMR Spectrum of **3.96** ($CDCl_3$, 600 MHz, 298 K)

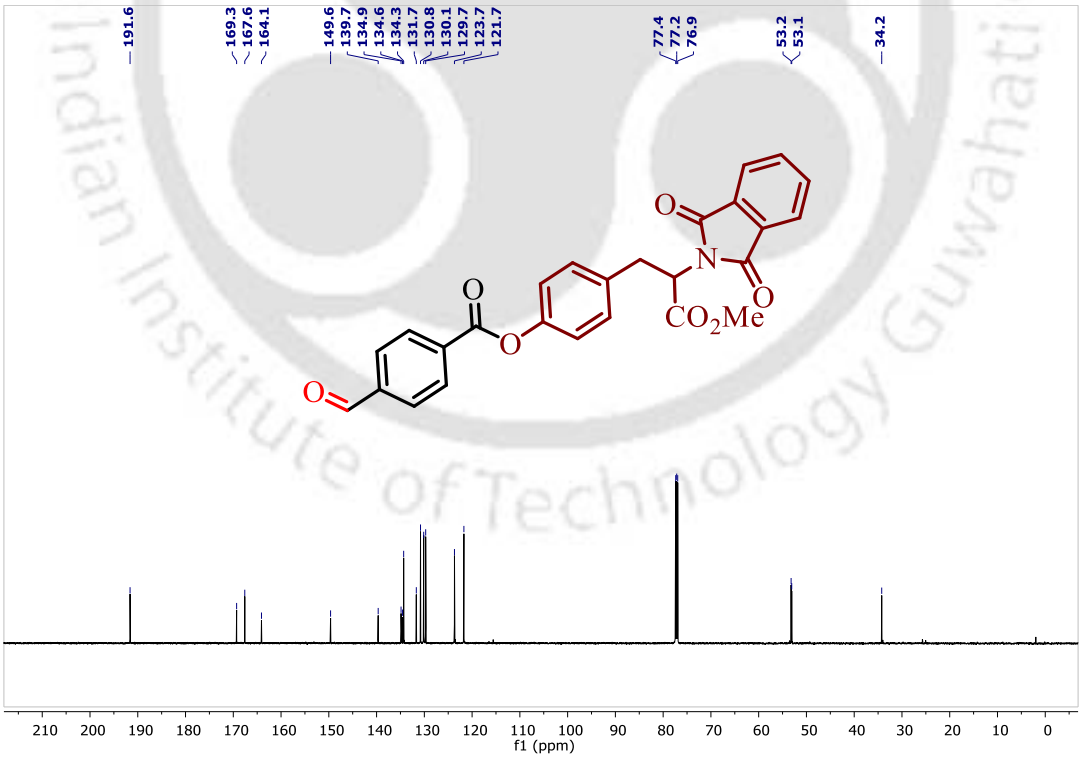


Figure S56. $^{13}C\{^{1}H\}$ NMR Spectrum of **3.96** ($CDCl_3$, 151 MHz, 298 K)

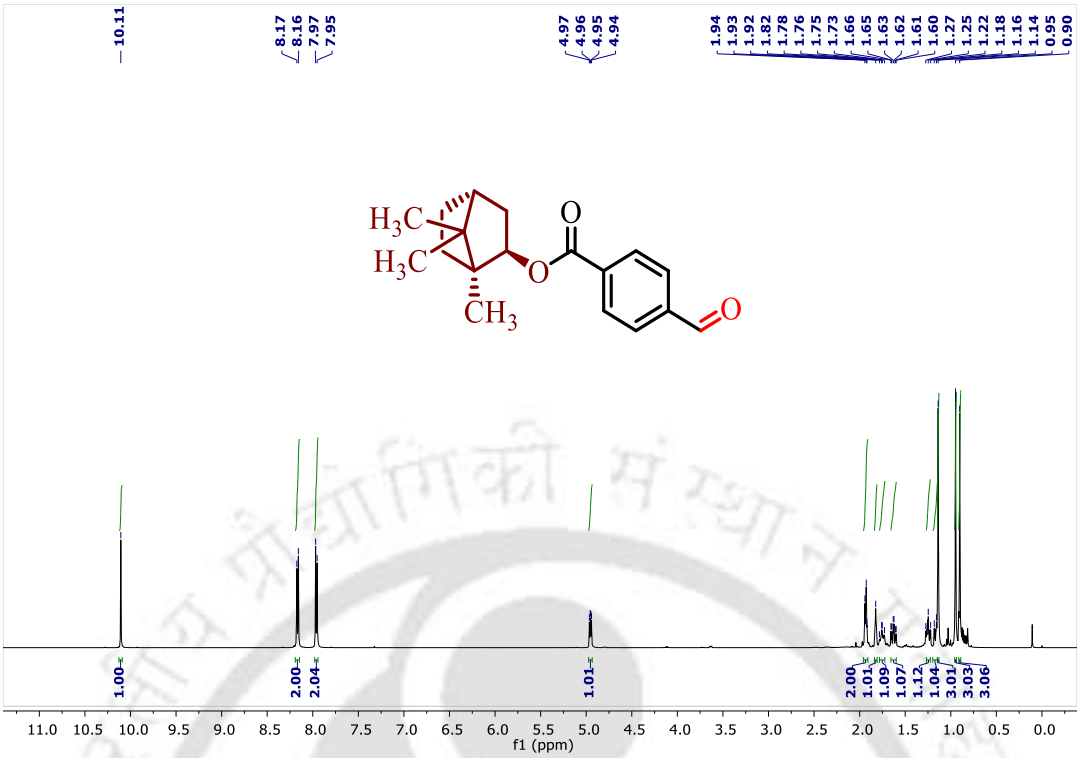


Figure S57. ^{1}H NMR Spectrum of **3.98** ($CDCl_3$, 500 MHz, 298 K)

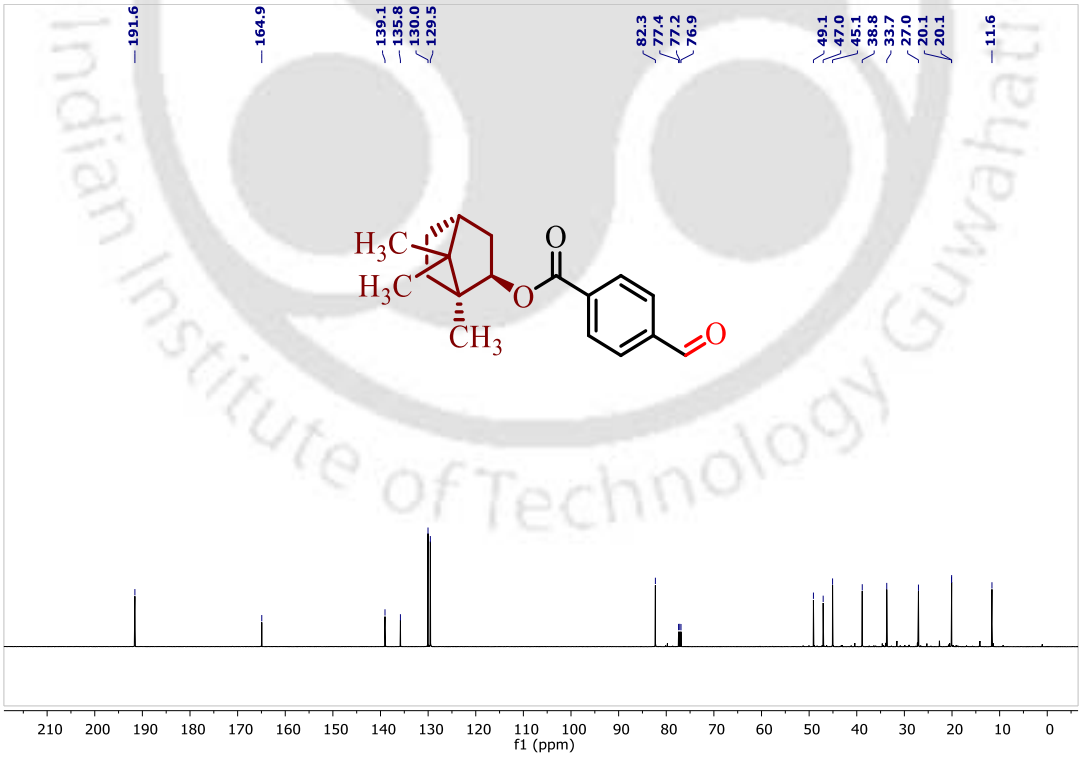


Figure S58. ^{13}C{^{1}H} NMR Spectrum of **3.98** ($CDCl_3$, 126 MHz, 298 K)

TH-3565_186122020

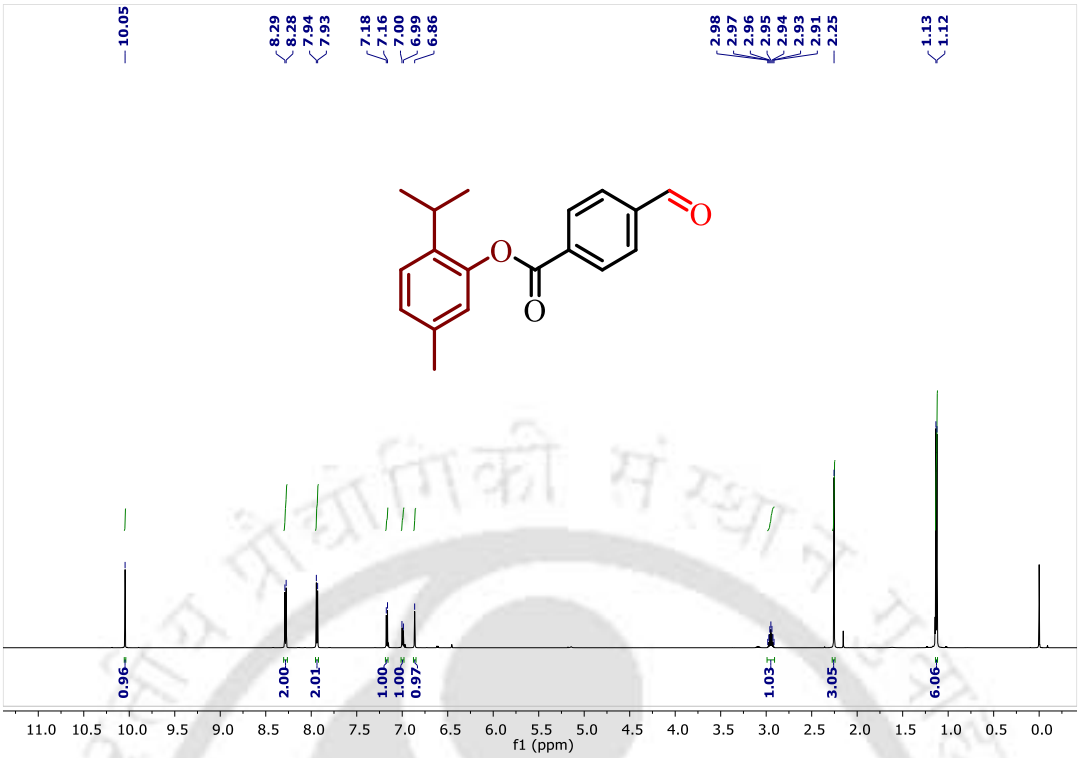


Figure S59. ^{1}H NMR Spectrum of **3.100** ($CDCl_3$, 600 MHz, 298 K)

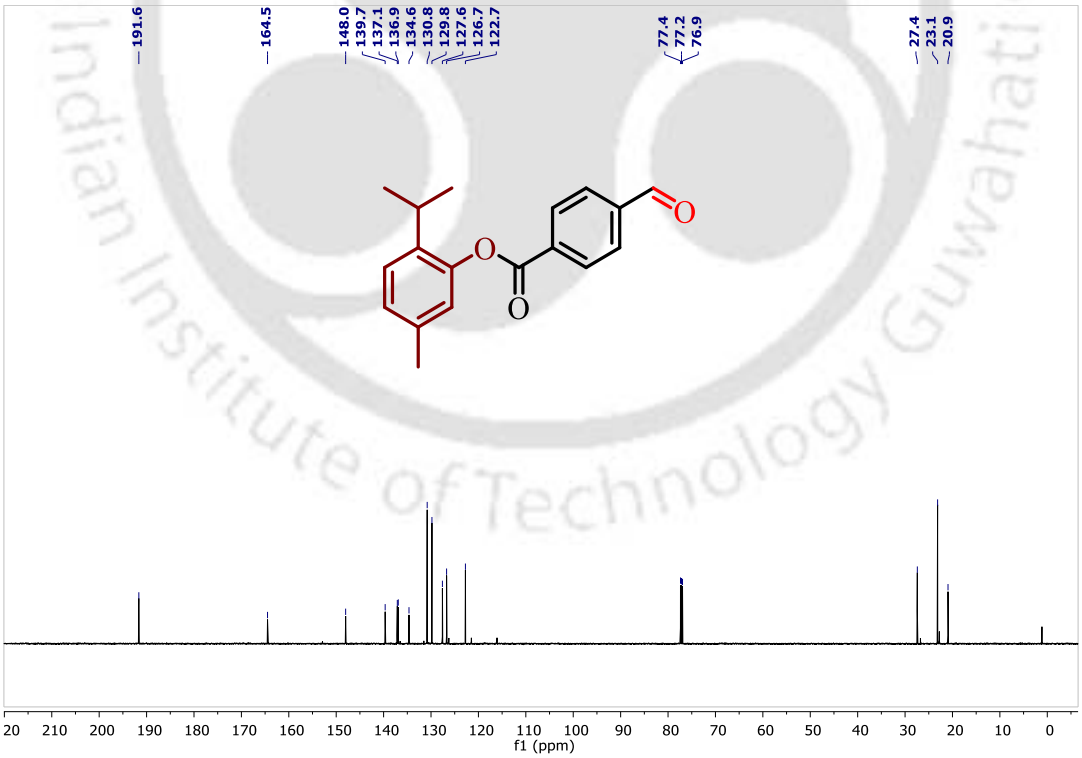


Figure S60. ^{13}C{^{1}H} NMR Spectrum of **3.100** ($CDCl_3$, 151 MHz, 298 K)

TH-3565_186122020

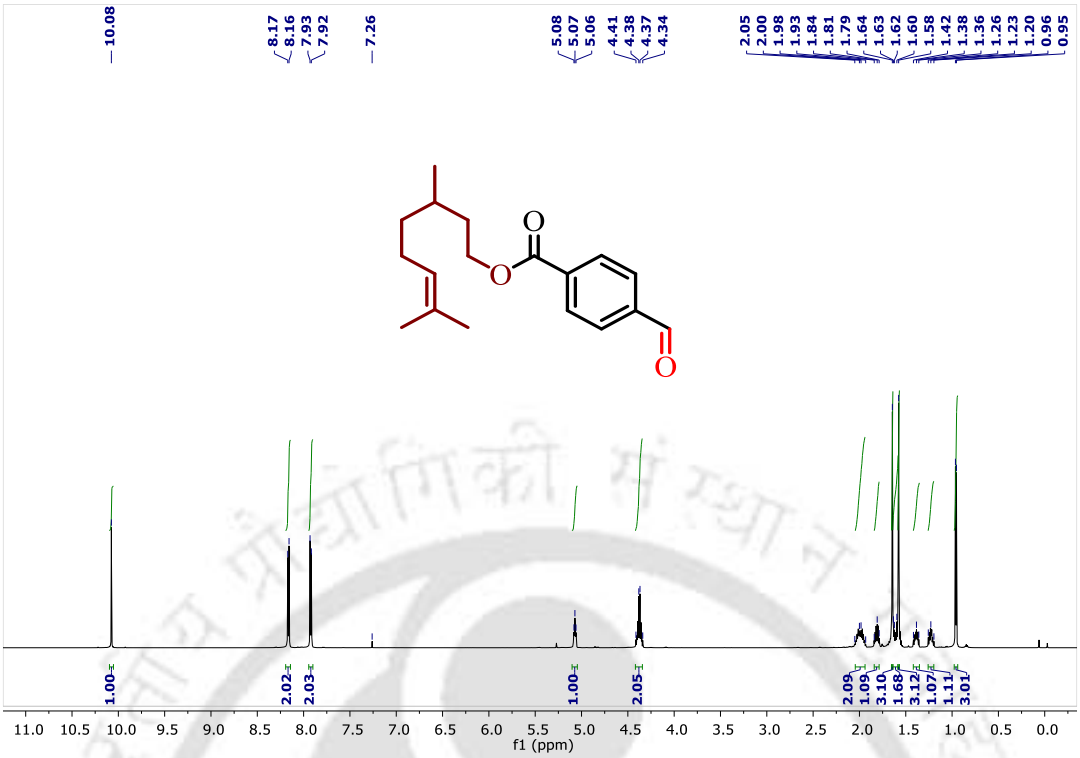


Figure S61. ^{1}H NMR Spectrum of **3.102** ($CDCl_3$, 600 MHz, 298 K)

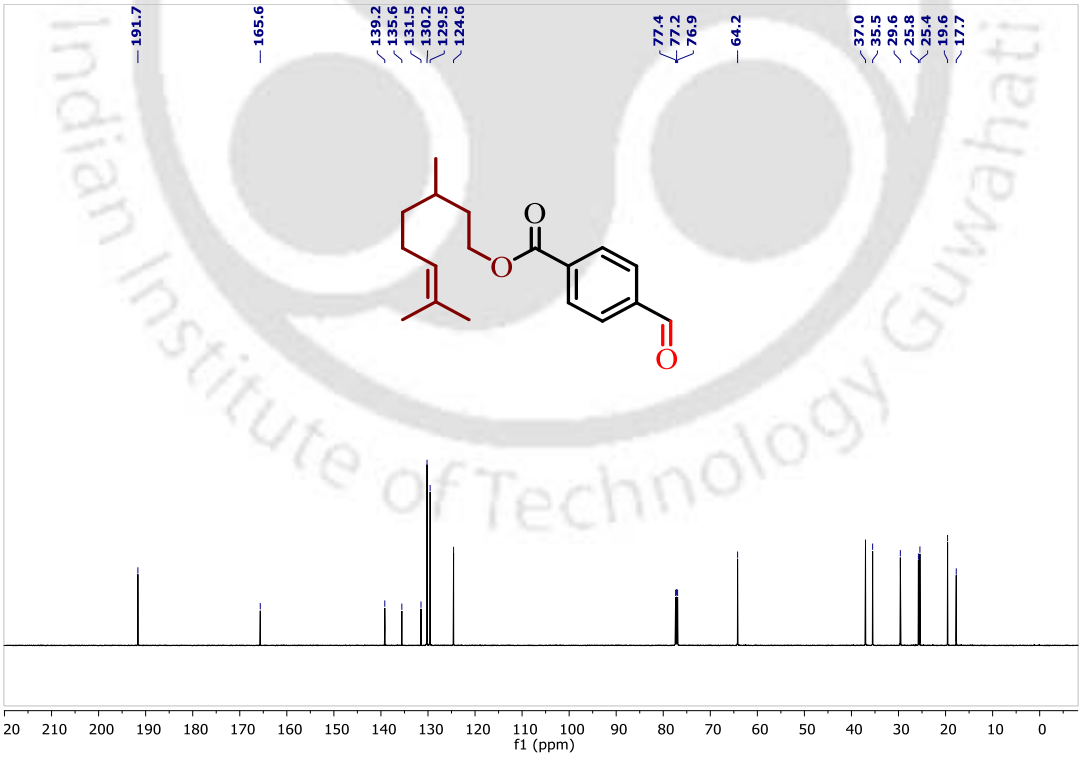


Figure S62. $^{13}C\{^{1}H\}$ NMR Spectrum of **3.102** ($CDCl_3$, 151 MHz, 298 K)

TH-3565_186122020

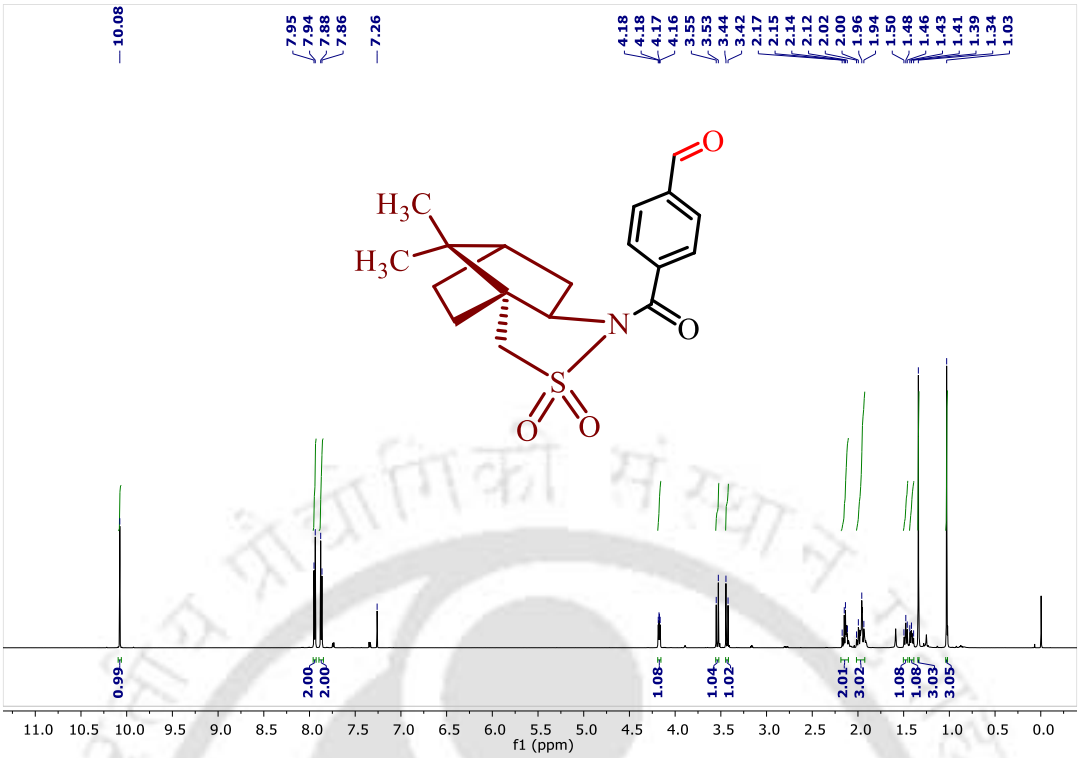


Figure S63. ^{1}H NMR Spectrum of **3.104** ($CDCl_3$, 600 MHz, 298 K)

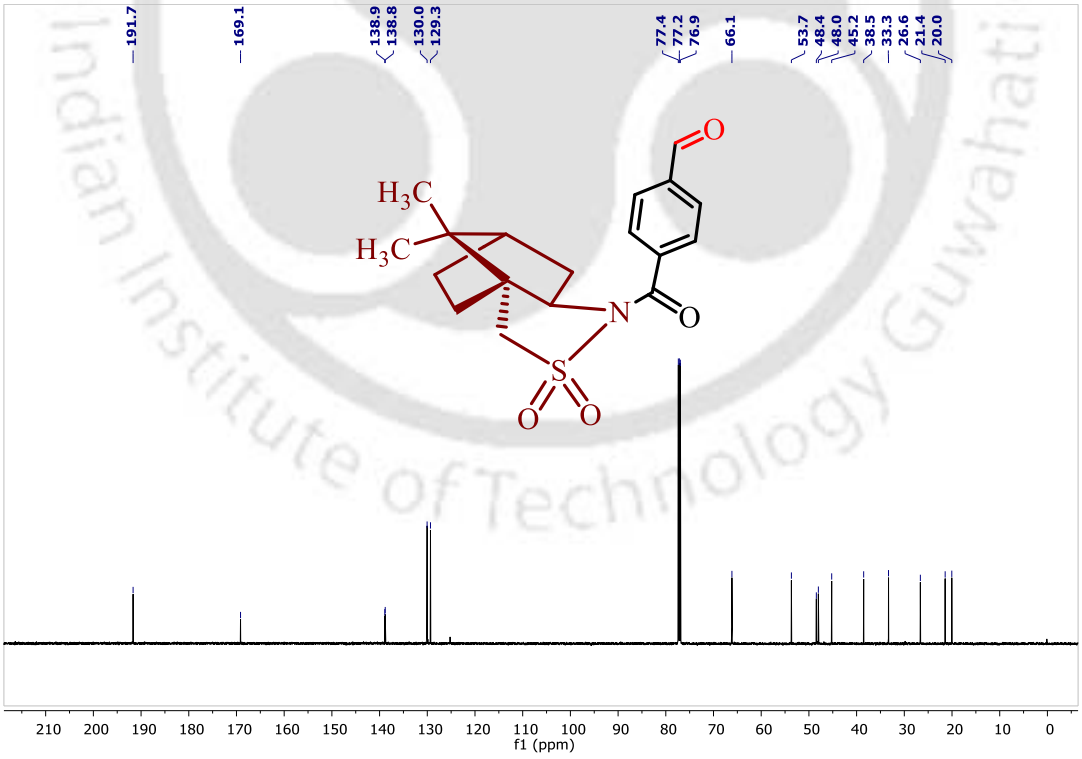


Figure S64. $^{13}C\{^{1}H\}$ NMR Spectrum of **3.104** ($CDCl_3$, 151 MHz, 298 K)

TH-3565_186122020

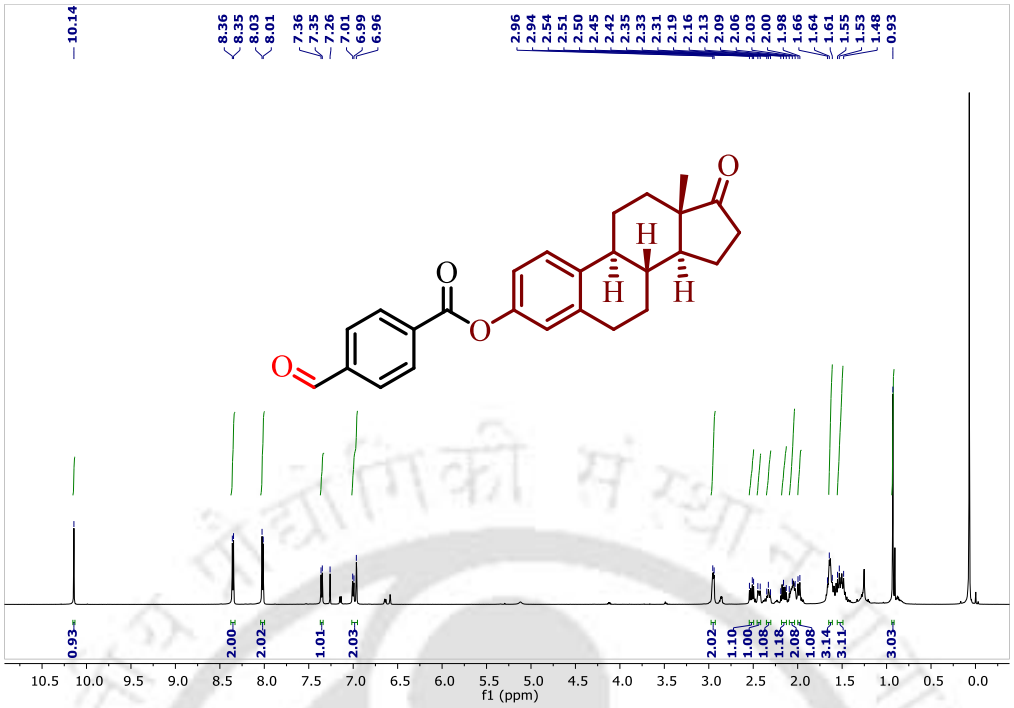


Figure S65. ^{1}H NMR Spectrum of **3.106** ($CDCl_3$, 600 MHz, 298 K)

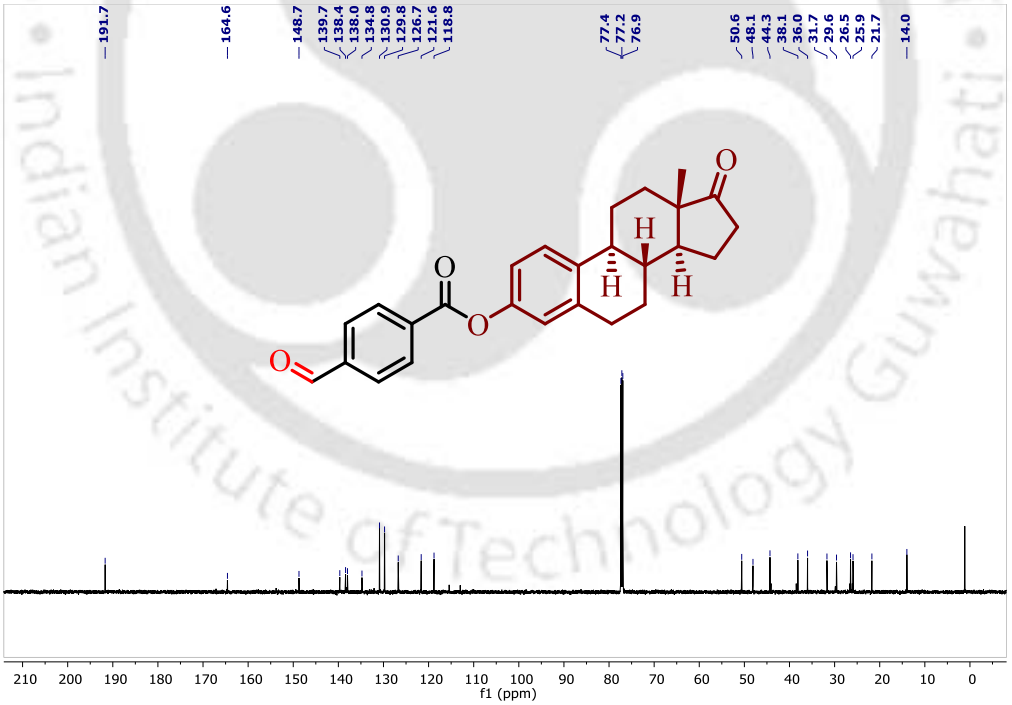


Figure S66. $^{13}C\{^{1}H\}$ NMR Spectrum of **3.106** ($CDCl_3$, 151 MHz, 298 K)

The supporting information and all other product spectra for Chapter 3 are available at

https://pubs.acs.org/doi/full/10.1021/acs.orglett.4c03595
https://chemistry-europe.onlinelibrary.wiley.com/doi/epdf/10.1002/chem.202403135

Annexure III

Selected ^{1}H and ^{13}C NMR spectra of the products (*Chapter 4*)

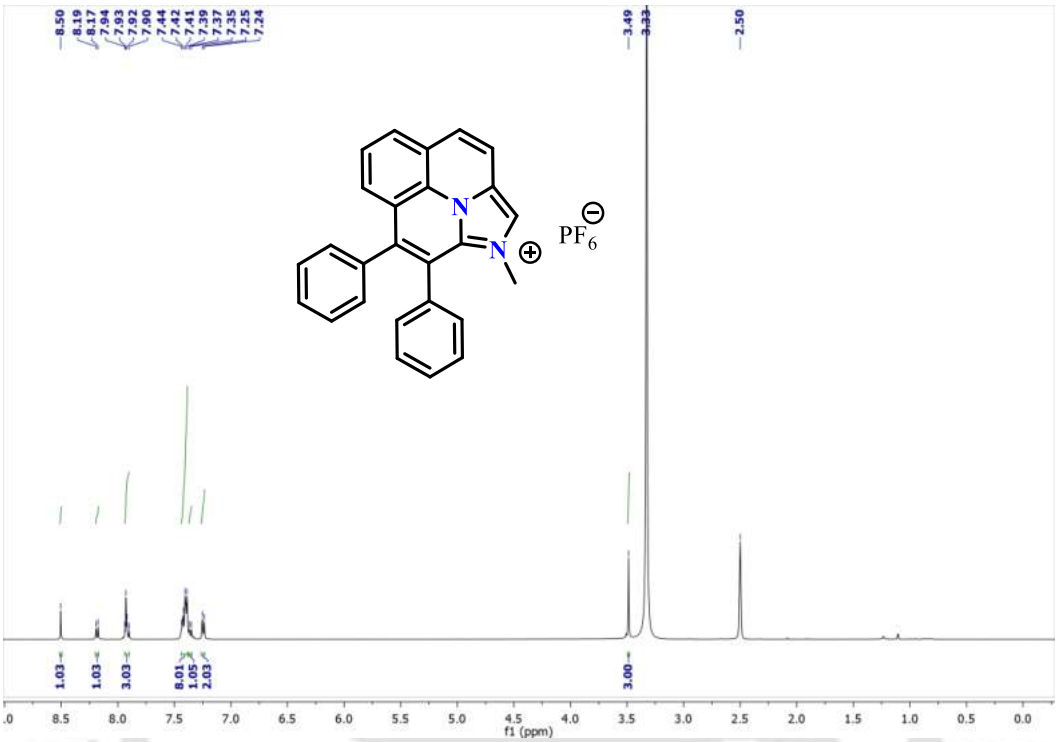


Figure S67. ^{1}H NMR spectrum of **4.3a** (DMSO-d_6, 400 MHz, 298 K)

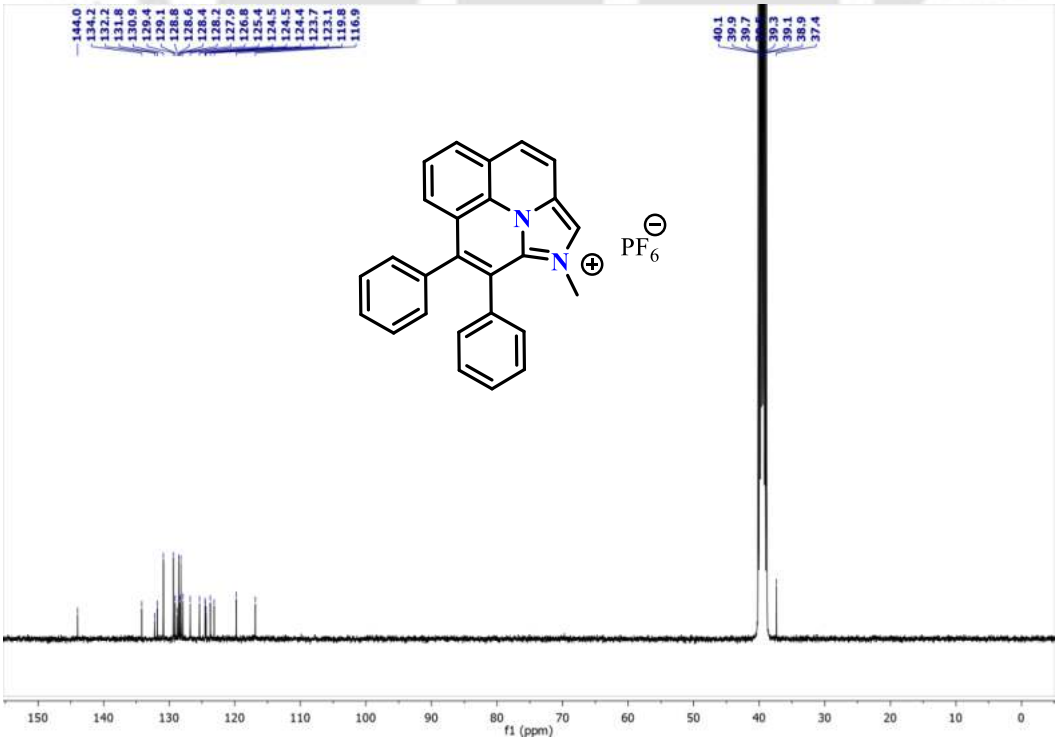


Figure S68. $^{13}C\{^{1}H\}$ NMR spectrum of **4.3a** (DMSO-d_6, 101 MHz, 298 K)

TH-3565_186122020

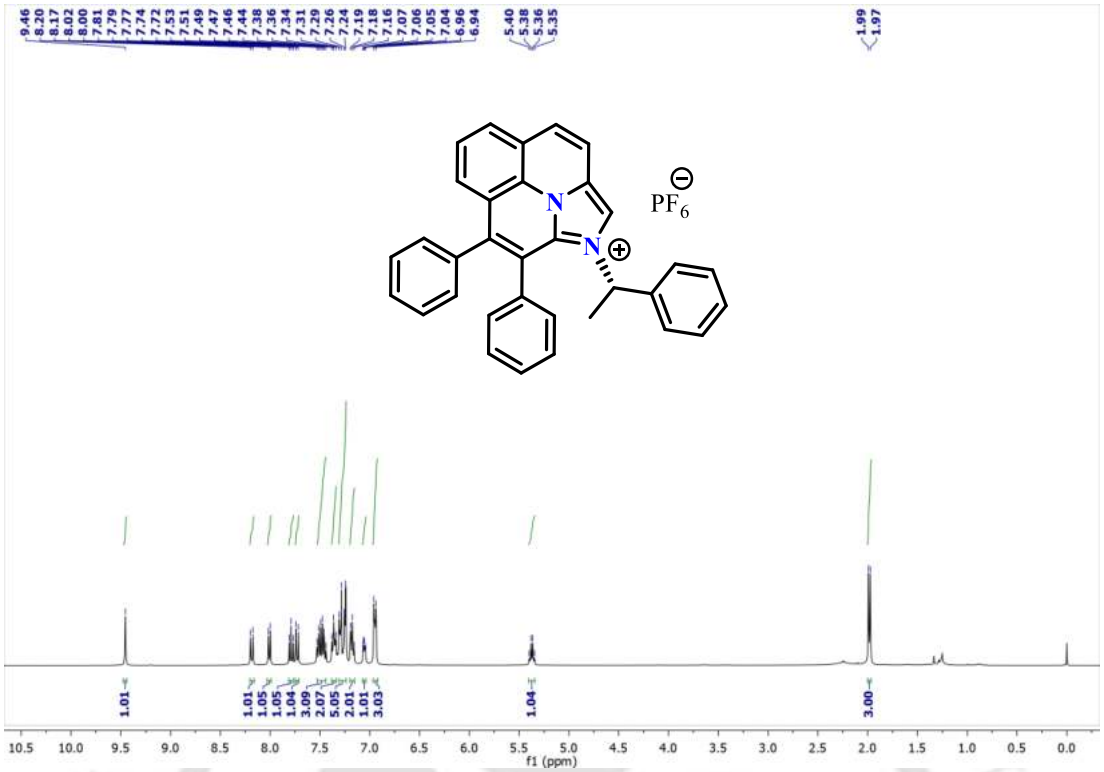


Figure S69. ^{1}H NMR spectrum of **4.3m** ($CDCl_3$, 400 MHz, 298 K)

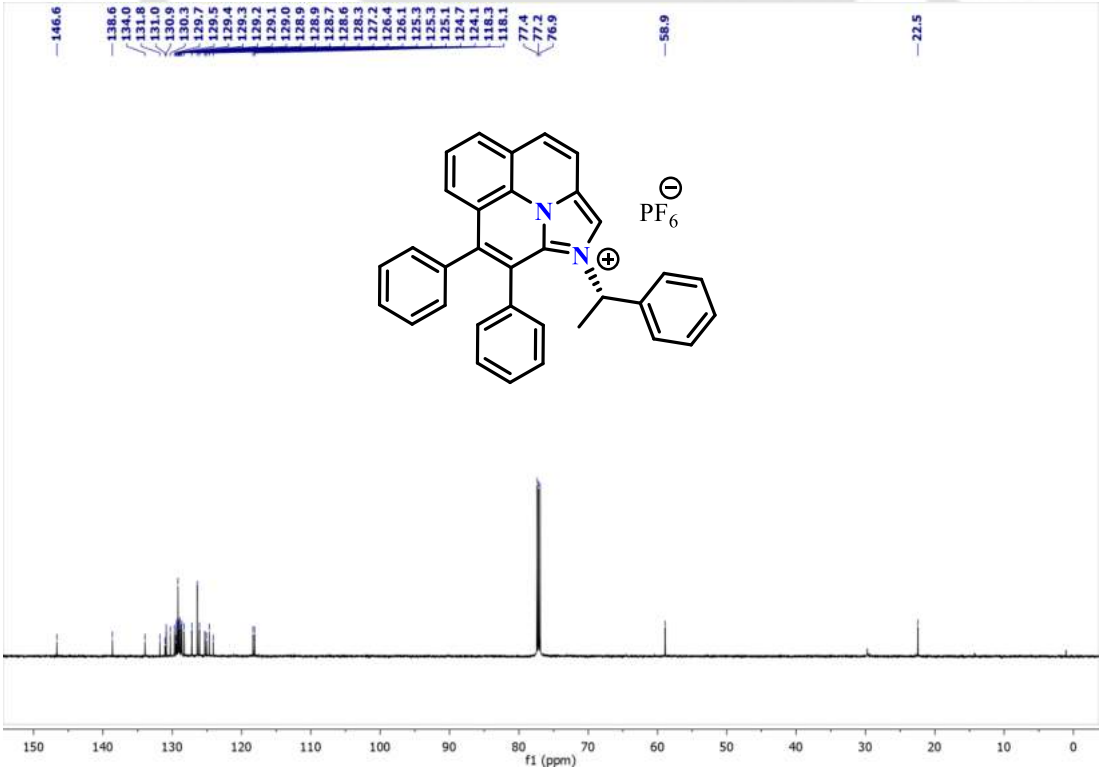


Figure S70. $^{13}C\{^{1}H\}$ NMR spectrum of **4.3m** ($CDCl_3$, 151 MHz, 298 K)

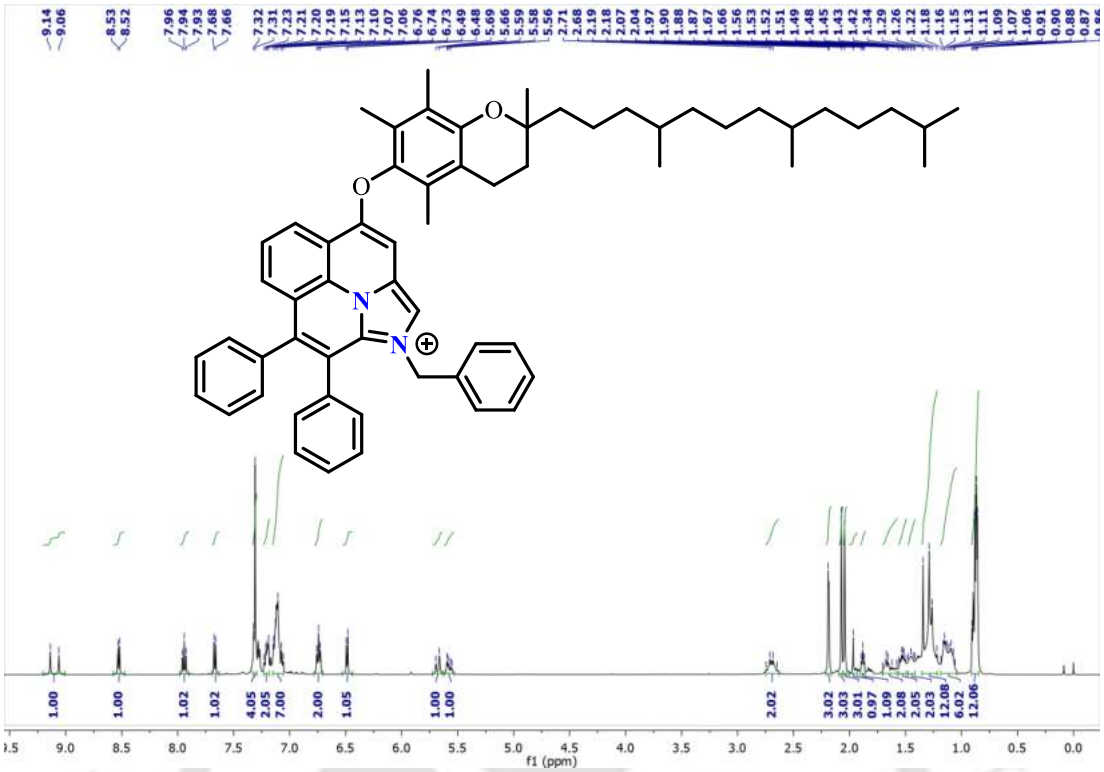


Figure S71. ^{1}H NMR spectrum of **4.4n** ($CDCl_3$, 500 MHz, 298 K)

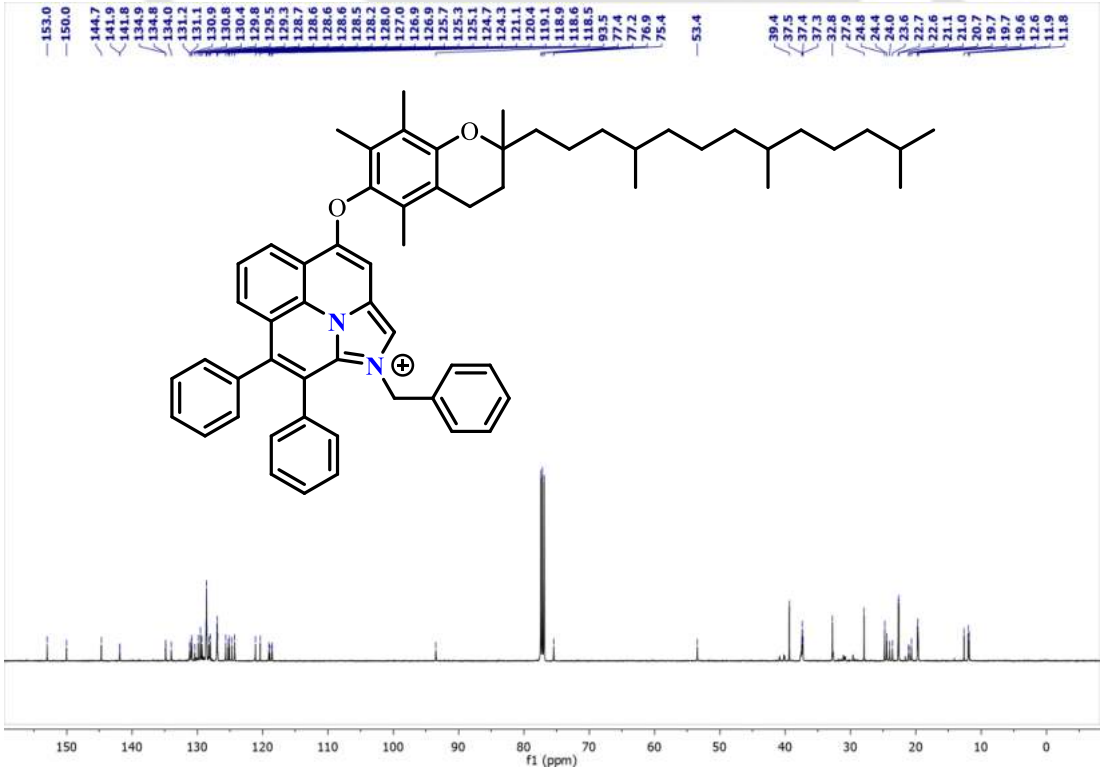


Figure S72. $^{13}C\{^{1}H\}$ NMR spectrum of **4.4n** ($CDCl_3$, 126 MHz, 298 K)

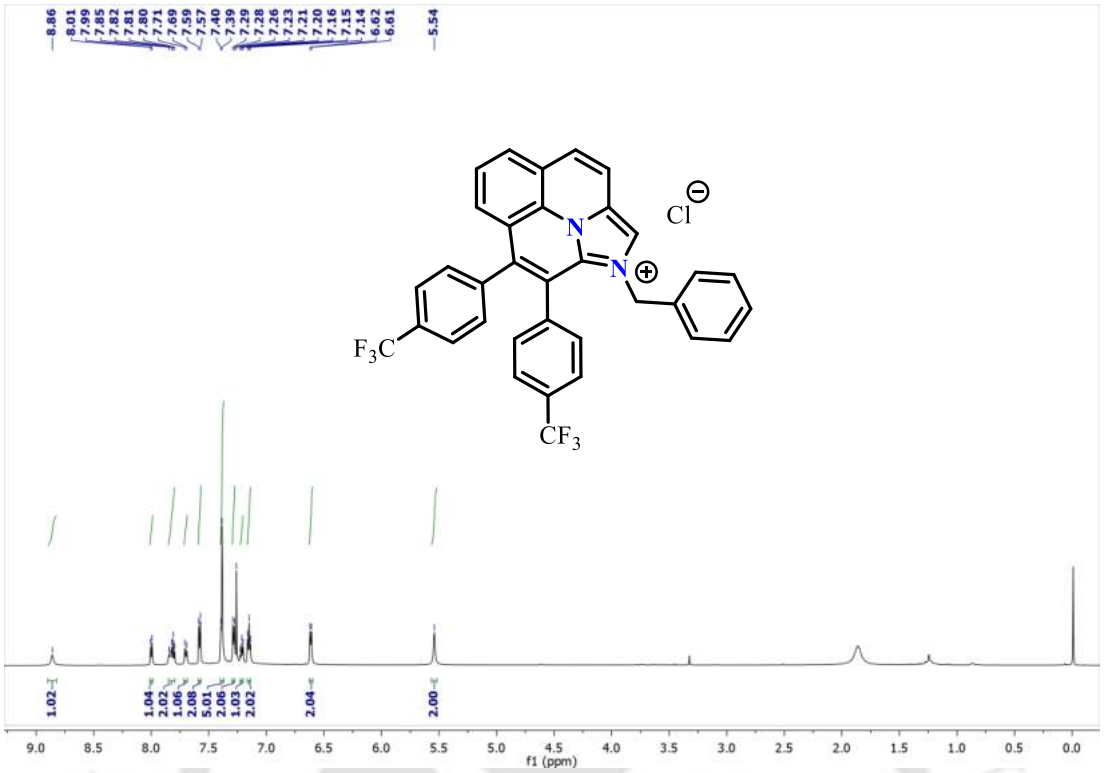


Figure S73. ^{1}H NMR spectrum of **4.5d** ($CDCl_3$, 600 MHz, 298 K)

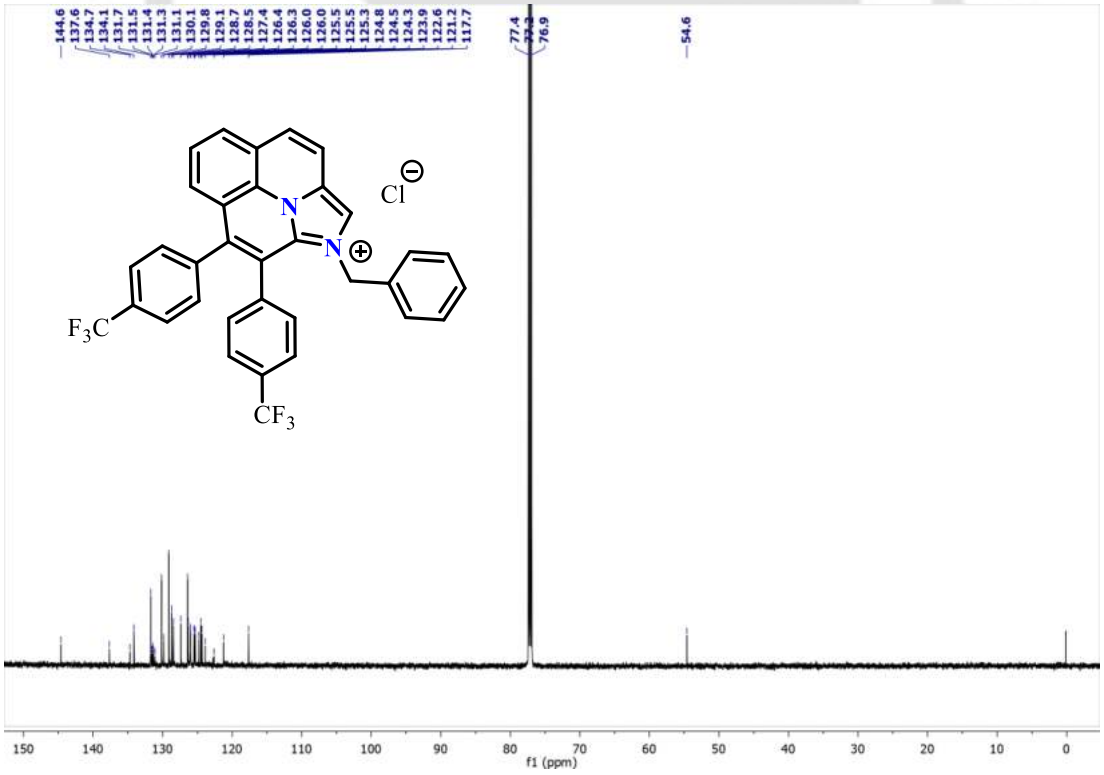


Figure S74. $^{13}C\{^{1}H\}$ NMR spectrum of **4.5d** ($CDCl_3$, 151 MHz, 298 K)

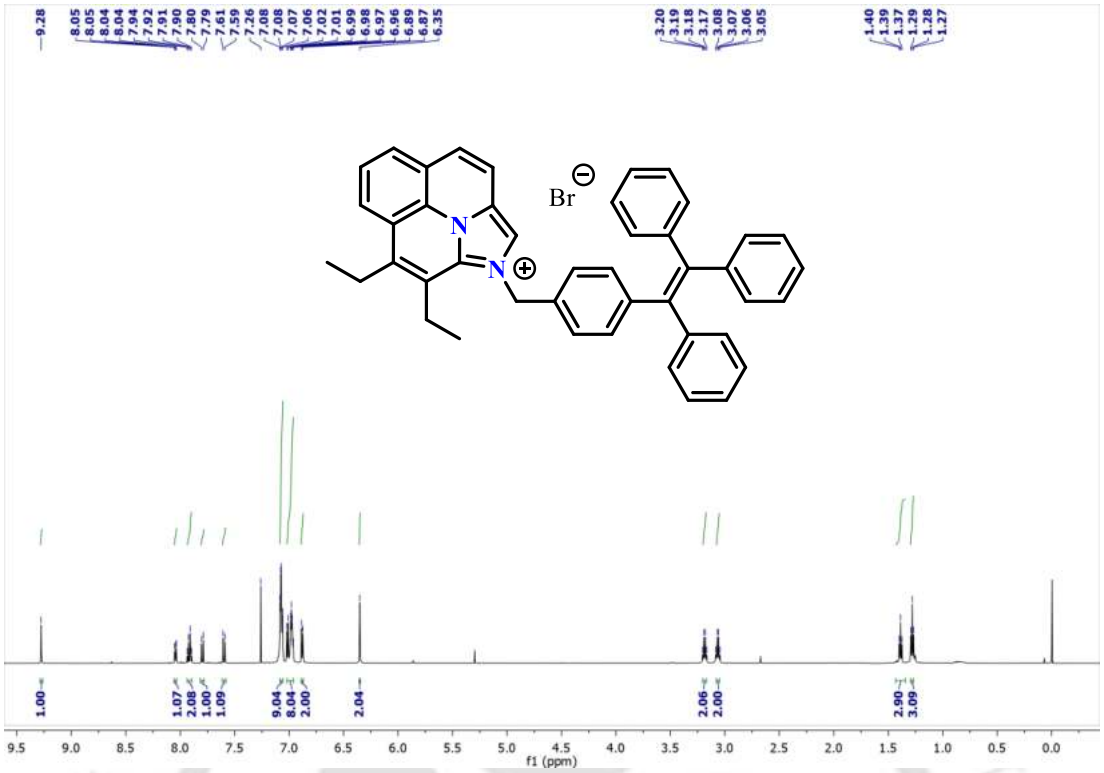


Figure S75. ^{1}H NMR spectrum of **4.6b** ($CDCl_3$, 600 MHz, 298 K)

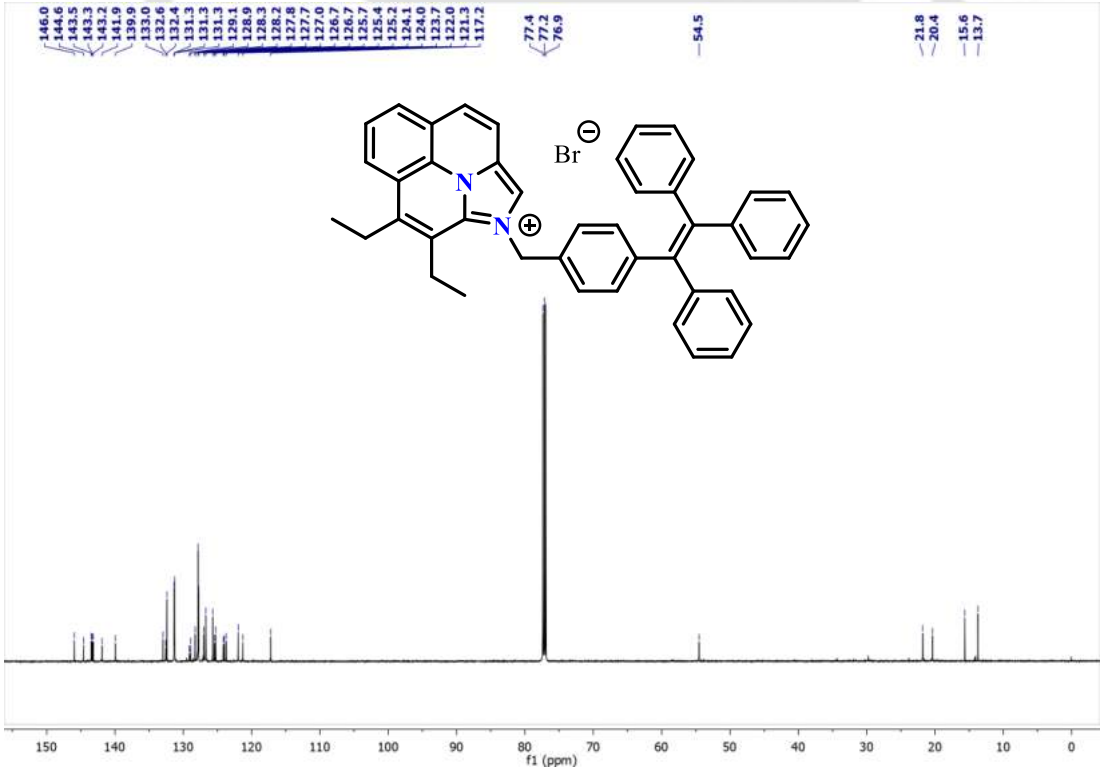


Figure S76. $^{13}C\{^{1}H\}$ NMR spectrum of **4.6b** ($CDCl_3$, 151 MHz, 298 K)

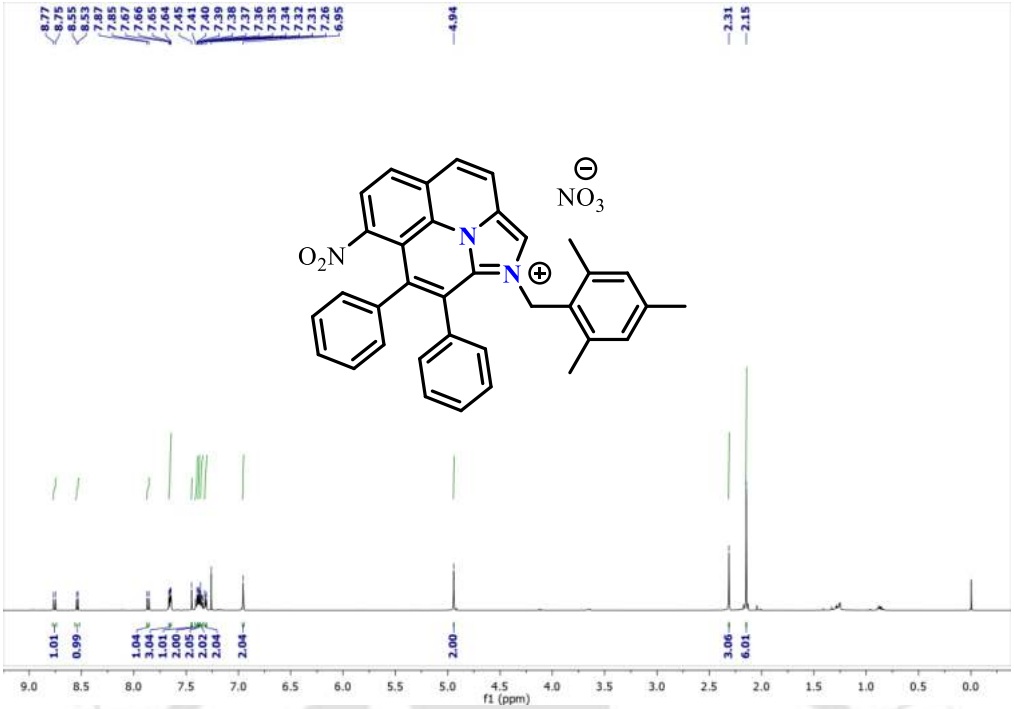


Figure S77. ^{1}H NMR spectrum of **4.10b** ($CDCl_3$, 600 MHz, 298 K)

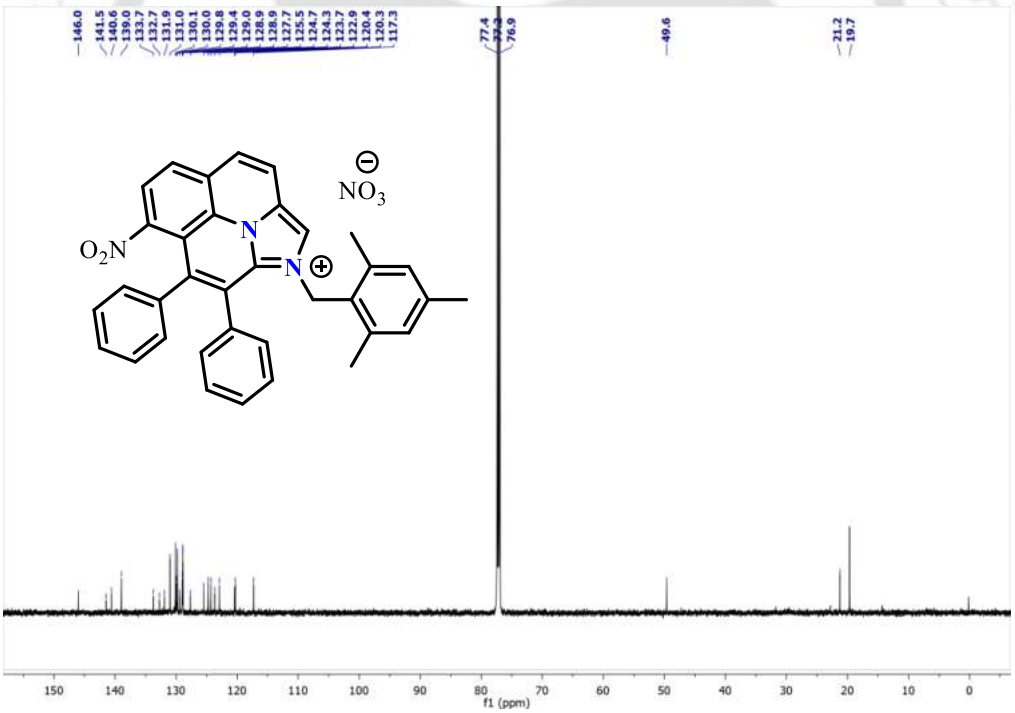


Figure S78. $^{13}C\{^{1}H\}$ NMR spectrum of **4.10b** ($CDCl_3$, 151 MHz, 298 K)

The supporting information and all other product spectra for Chapter 4 are available at https://pubs.acs.org/doi/10.1021/acs.orglett.4c00542
https://chemistry-europe.onlinelibrary.wiley.com/doi/10.1002/chem.202401133

Annexure IV

^{1}H, ^{13}C and ^{19}F NMR spectra of the products (*Chapter 5*)

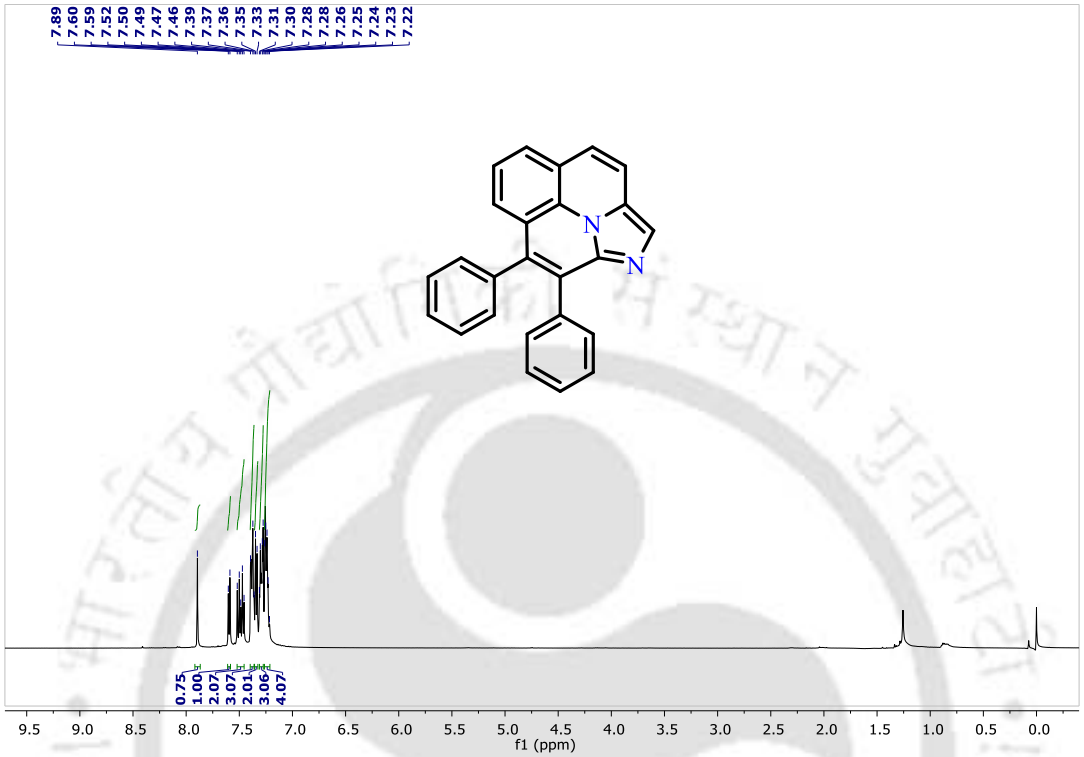


Figure S79. ^{1}H NMR spectrum of **5.3a** ($CDCl_3$, 500 MHz, 298 K)

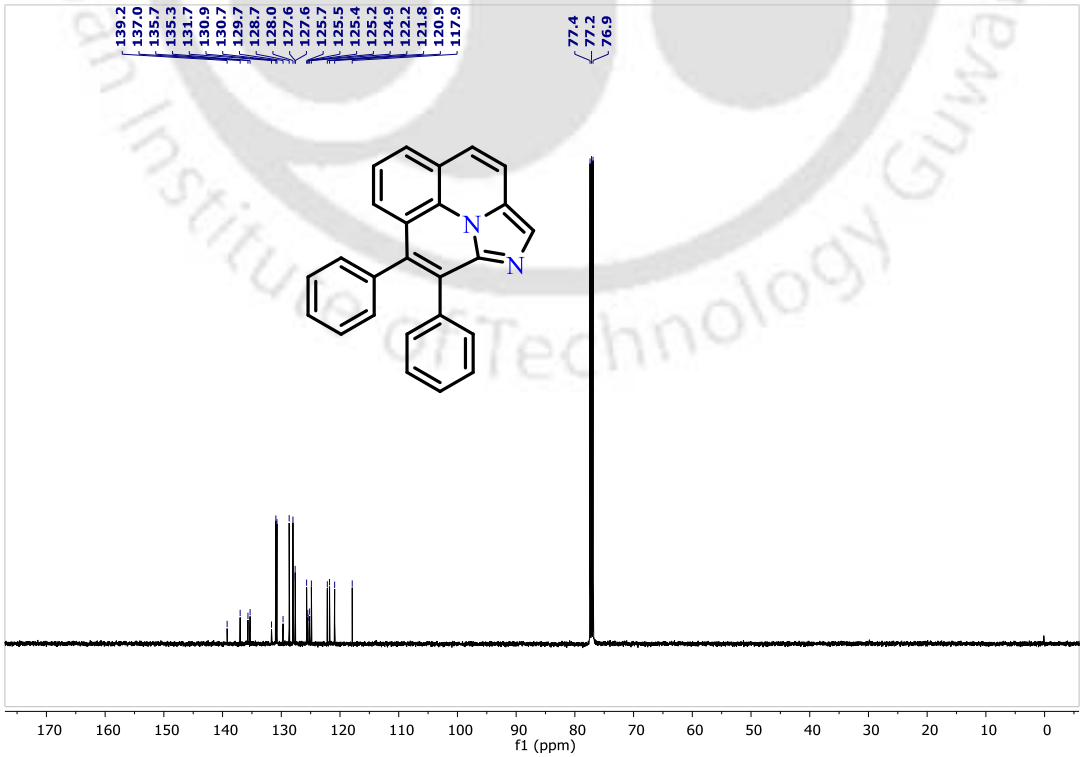


Figure S80. $^{13}C\{^{1}H\}$ NMR spectrum of **5.3a** ($CDCl_3$, 126 MHz, 298 K)

TH-3565_186122020

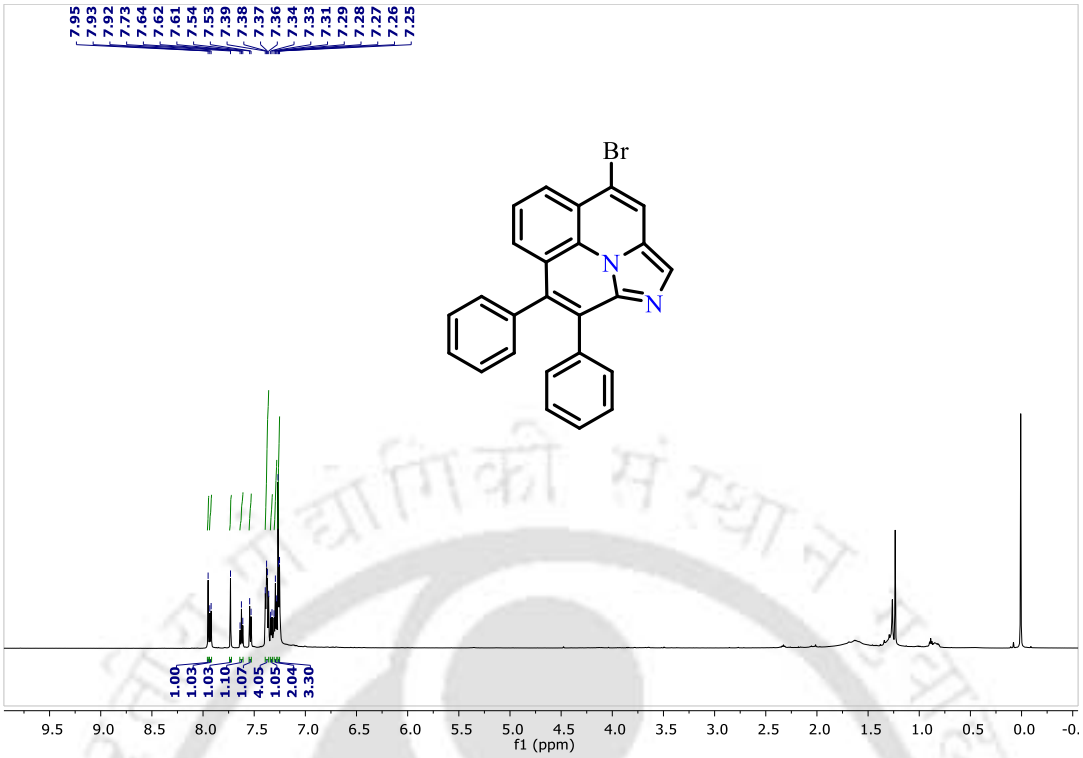


Figure S81. ^{1}H NMR spectrum of **5.3b** ($CDCl_3$, 600 MHz, 298 K)

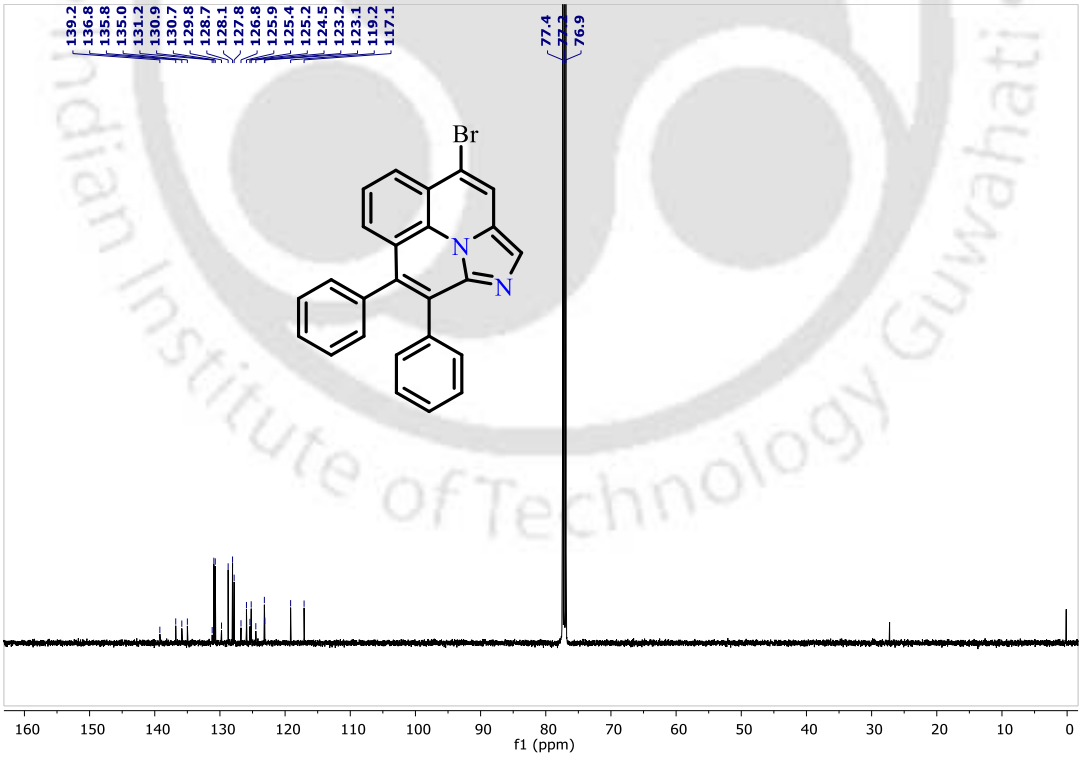


Figure S82. $^{13}C\{^{1}H\}$ NMR spectrum of **5.3b** ($CDCl_3$, 126 MHz, 298 K)

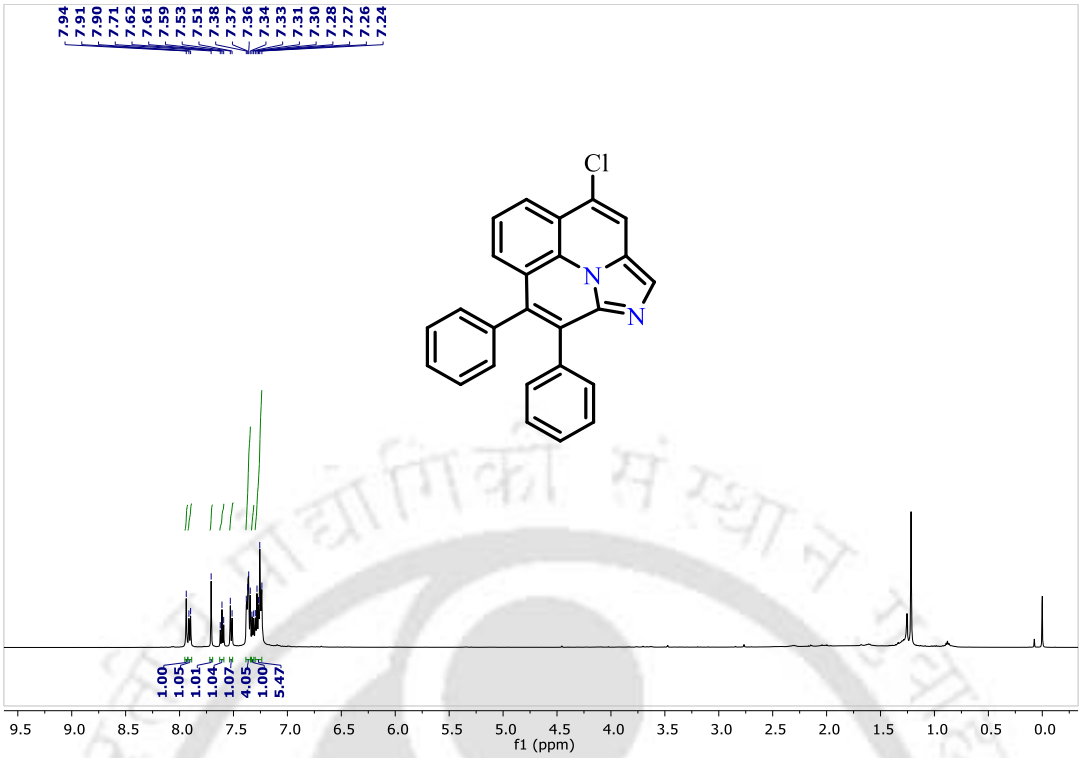


Figure S83. ^{1}H NMR spectrum of **5.3c** ($CDCl_3$, 500 MHz, 298 K)

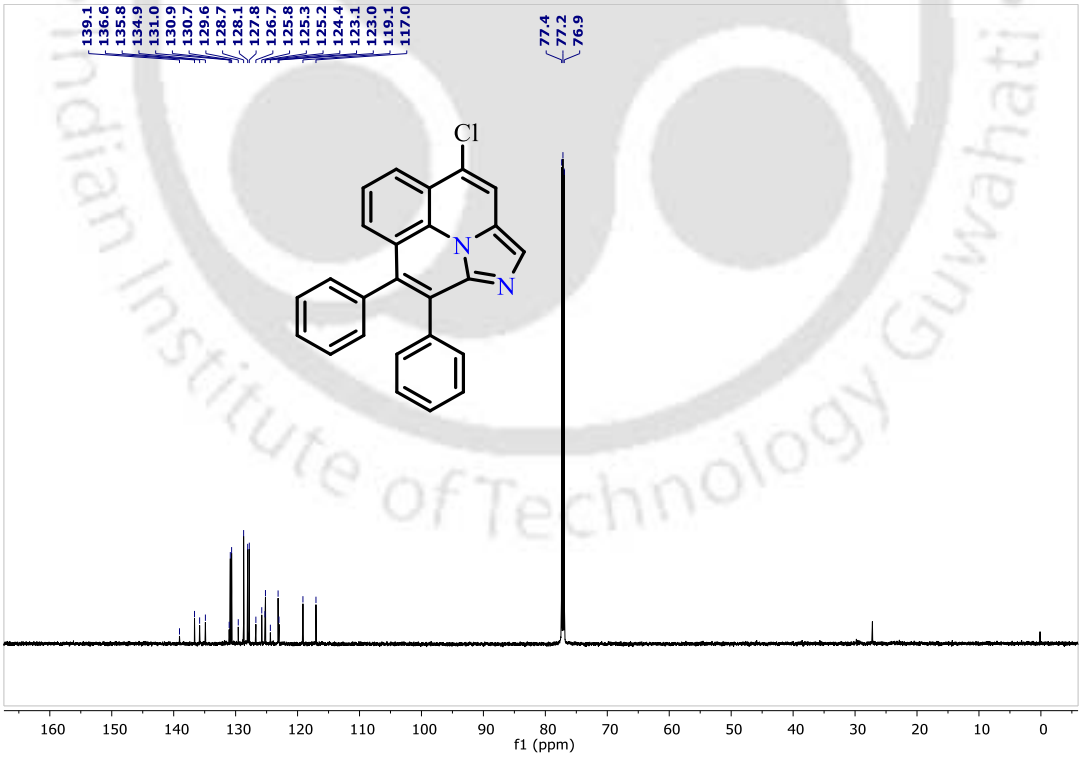


Figure S84. $^{13}C\{^{1}H\}$ NMR spectrum of **5.3c** ($CDCl_3$, 151 MHz, 298 K)

TH-3565_186122020

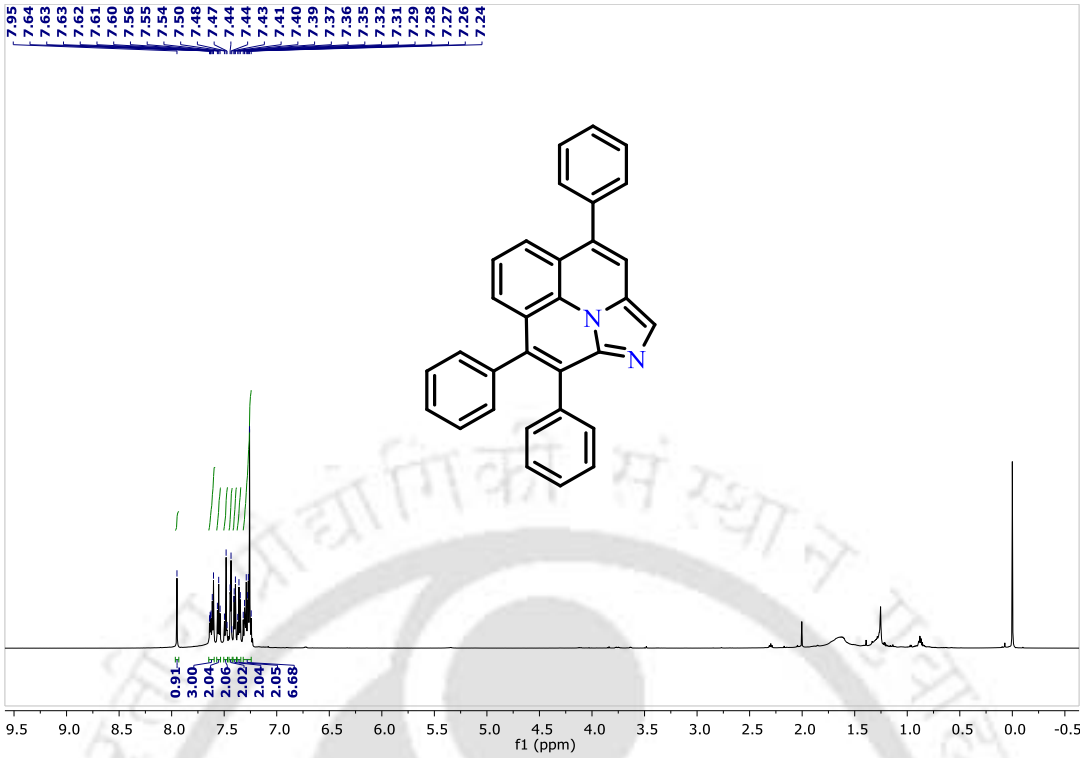


Figure S85. ^{1}H NMR spectrum of **5.3d** ($CDCl_3$, 600 MHz, 298 K)

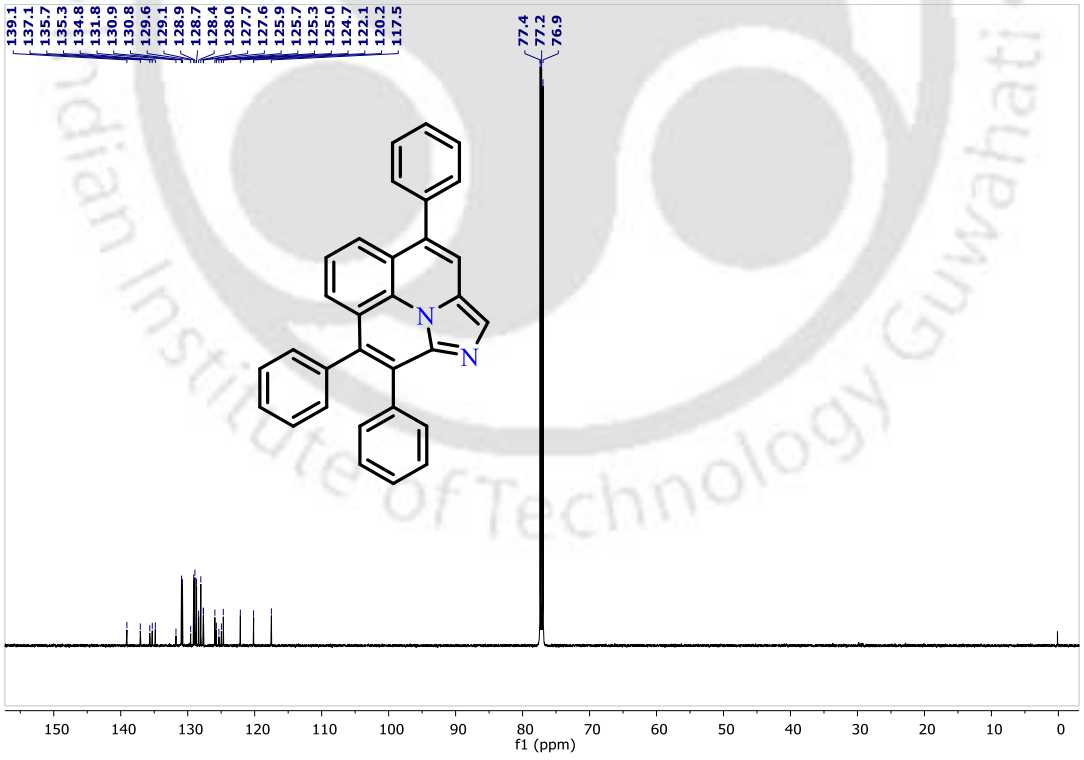


Figure S86. $^{13}C\{^{1}H\}$ NMR spectrum of **5.3d** ($CDCl_3$, 151 MHz, 298 K)

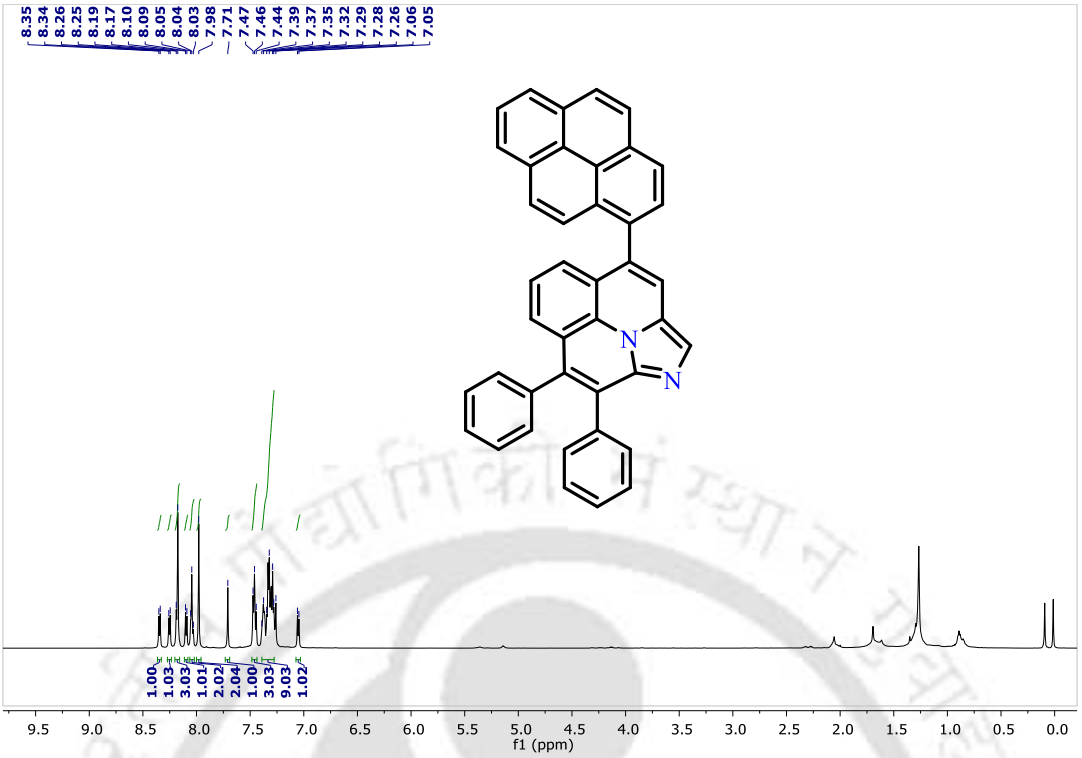


Figure S87. ^{1}H NMR spectrum of **5.3e** ($CDCl_3$, 600 MHz, 298 K)

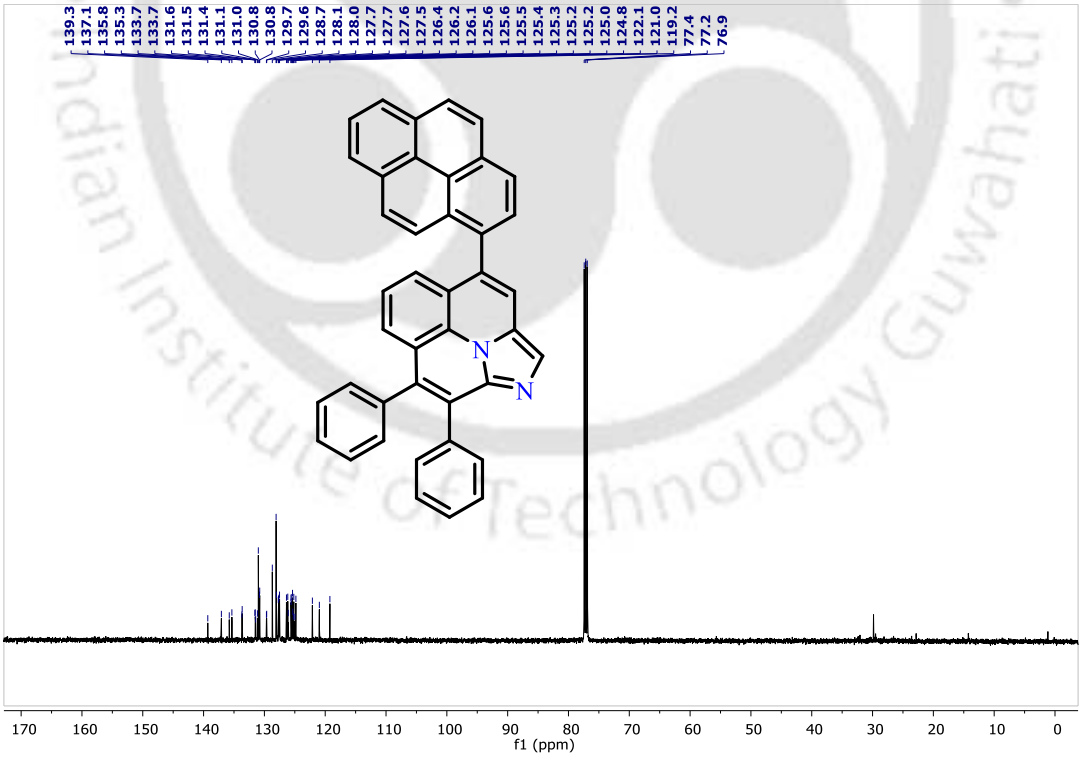


Figure S88. ^{13}C{^{1}H} NMR spectrum of **5.3e** ($CDCl_3$, 126 MHz, 298 K)

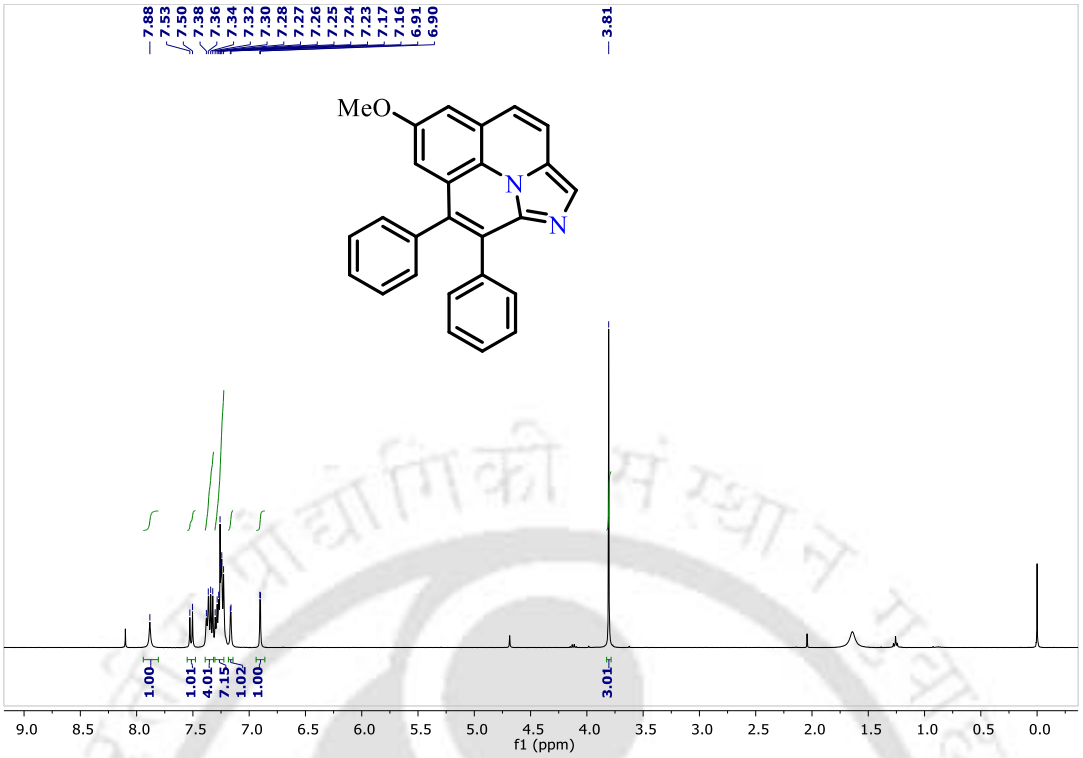


Figure S89. ^{1}H NMR spectrum of **5.3f** ($CDCl_3$, 400 MHz, 298 K)

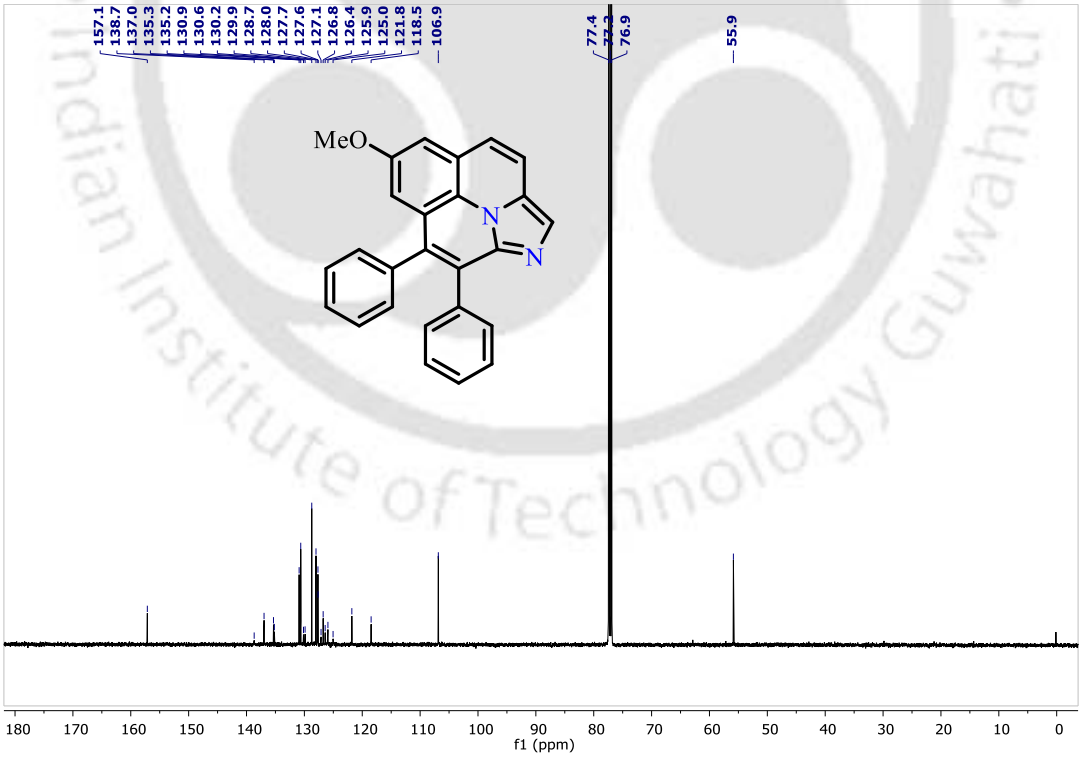


Figure S90. $^{13}C\{^{1}H\}$ NMR spectrum of **5.3f** ($CDCl_3$, 126 MHz, 298 K)

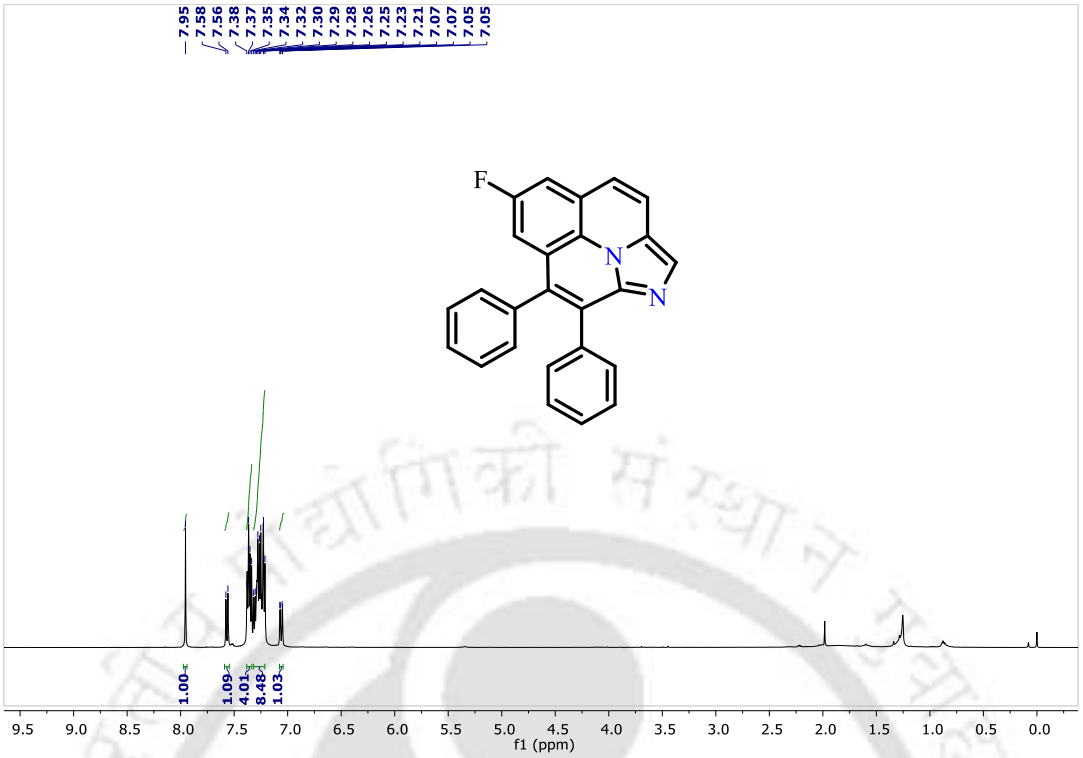


Figure S91. ^{1}H NMR spectrum of **5.3g** ($CDCl_3$, 500 MHz, 298 K)

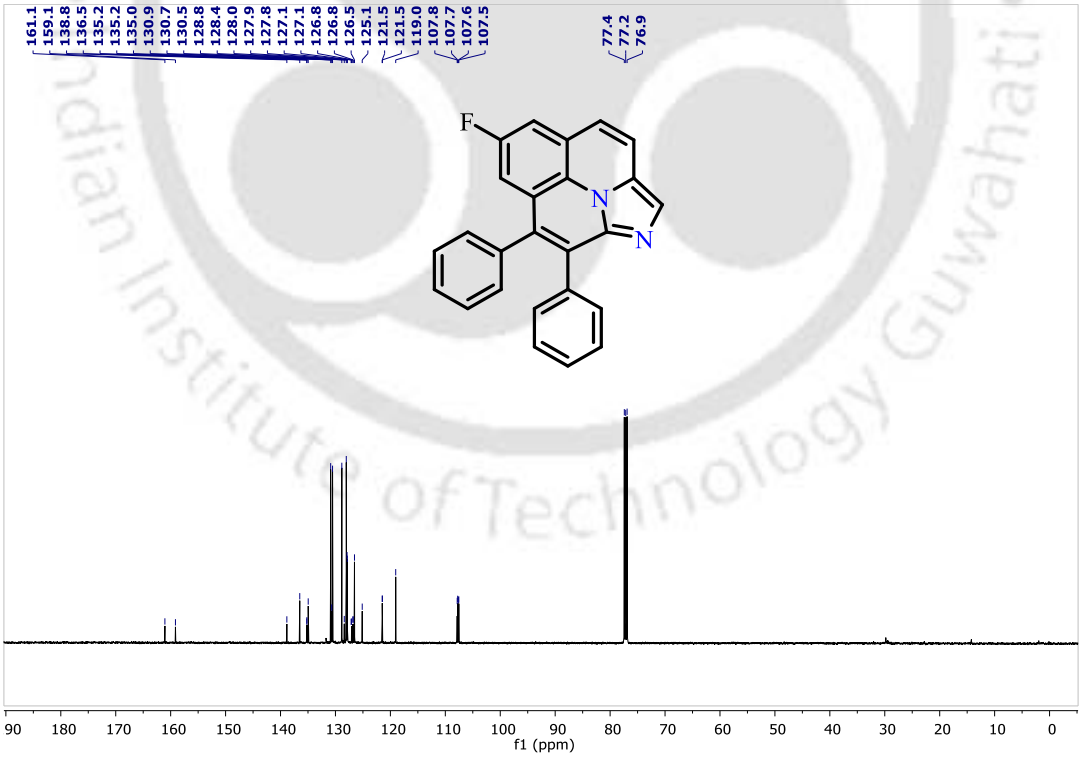


Figure S92. $^{13}C\{^{1}H\}$ NMR spectrum of **5.3g** ($CDCl_3$, 126 MHz, 298 K)

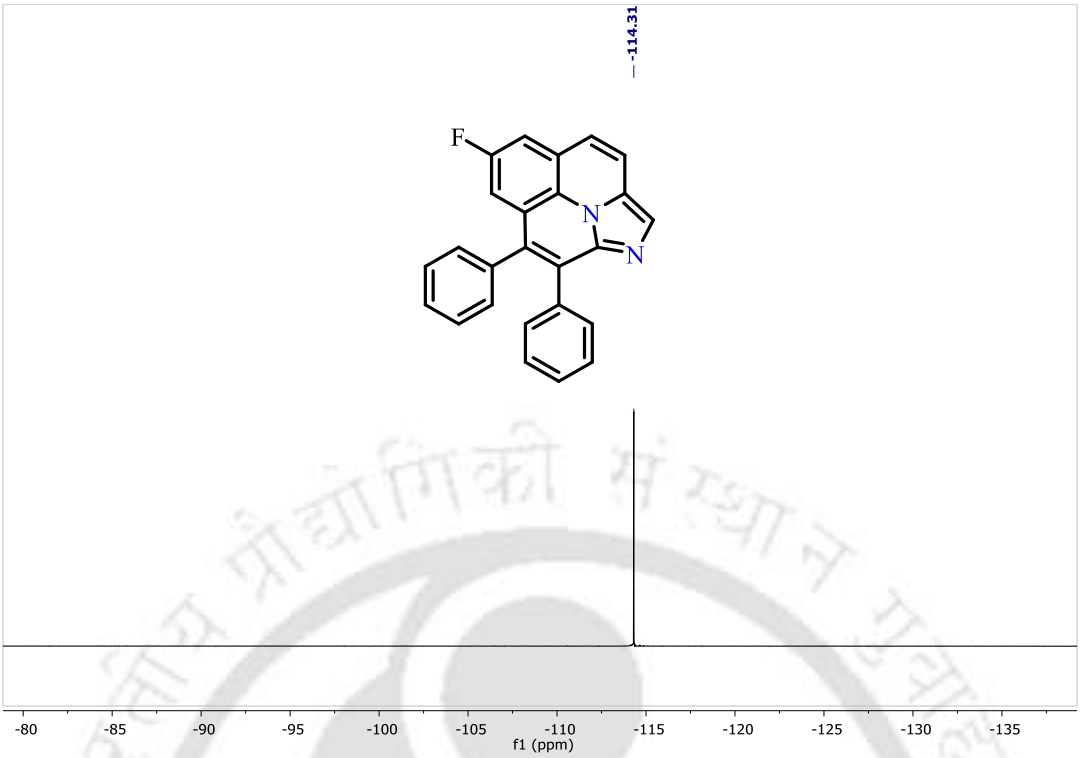


Figure S93. ^{19}F NMR spectrum of **5.3g** ($CDCl_3$, 471 MHz, 298 K)

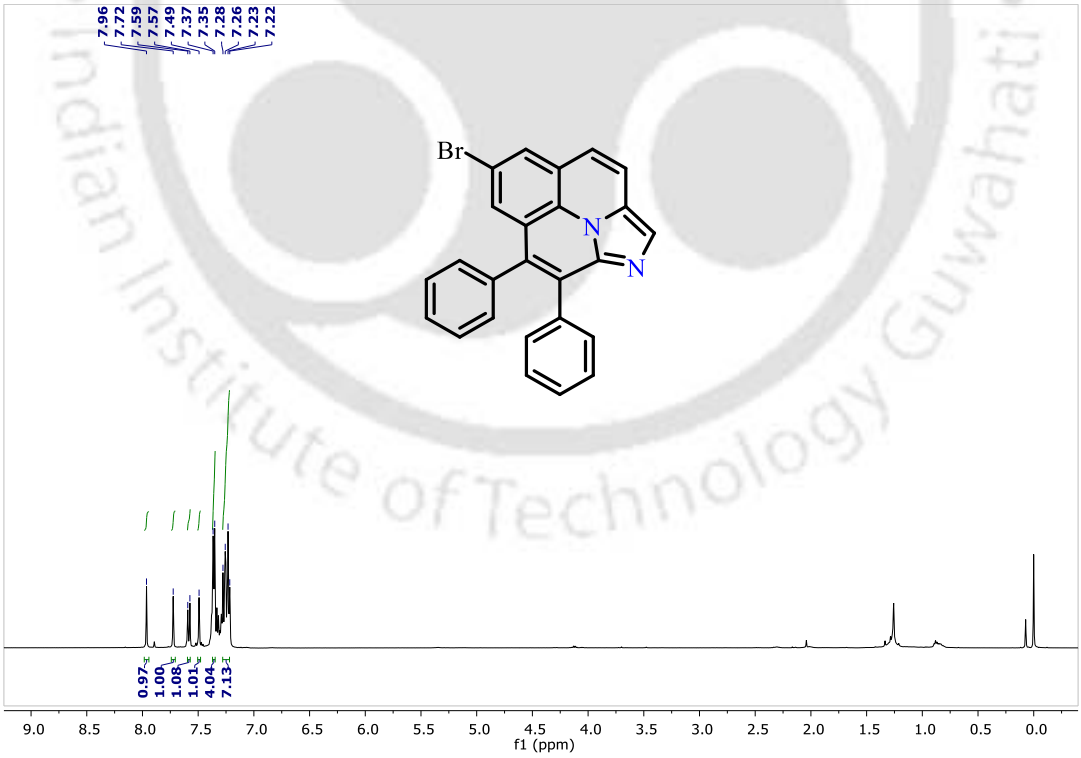


Figure S94. ^{1}H NMR spectrum of **5.3h** ($CDCl_3$, 500 MHz, 298 K)

TH-3565_186122020

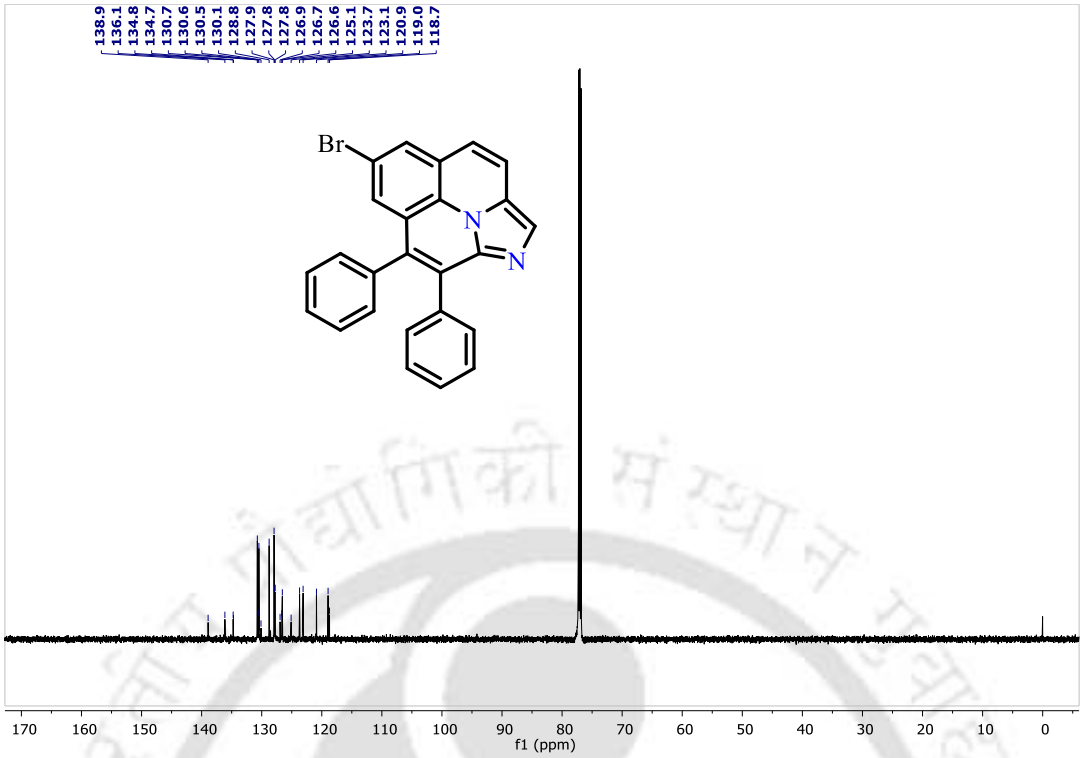


Figure S95. $^{13}C\{^{1}H\}$ NMR spectrum of **5.3h** ($CDCl_3$, 151 MHz, 298 K)

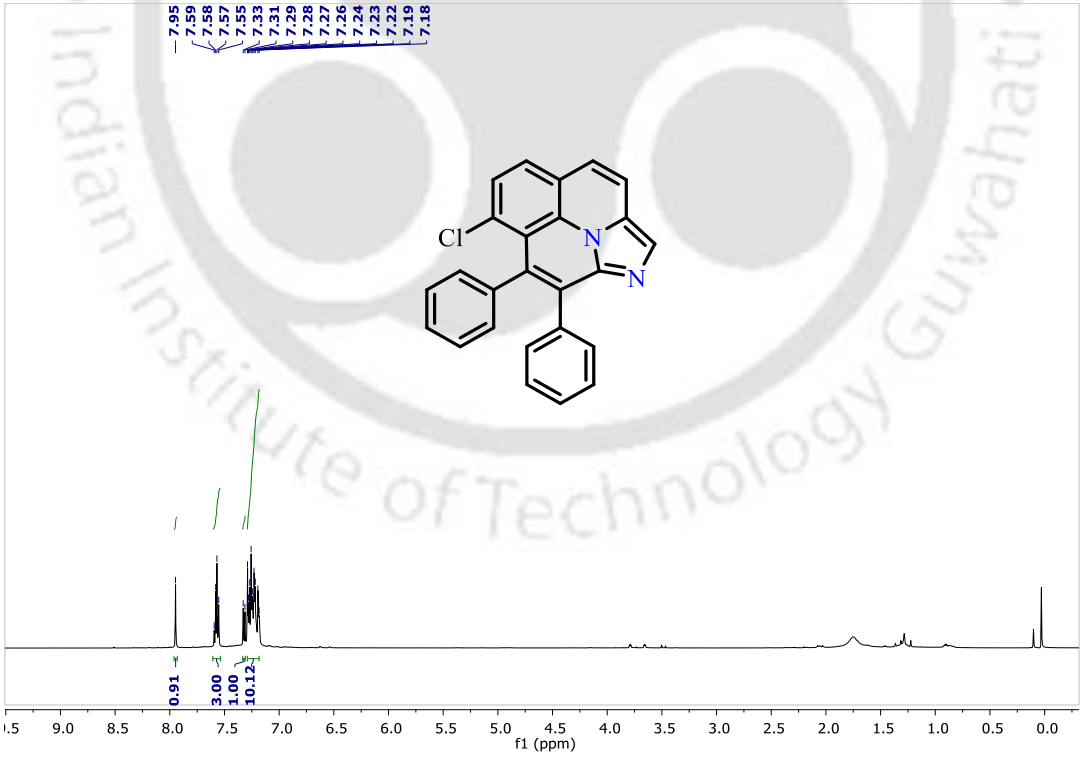


Figure S96. ^{1}H NMR spectrum of **5.3i** ($CDCl_3$, 600 MHz, 298 K)

TH-3565_186122020

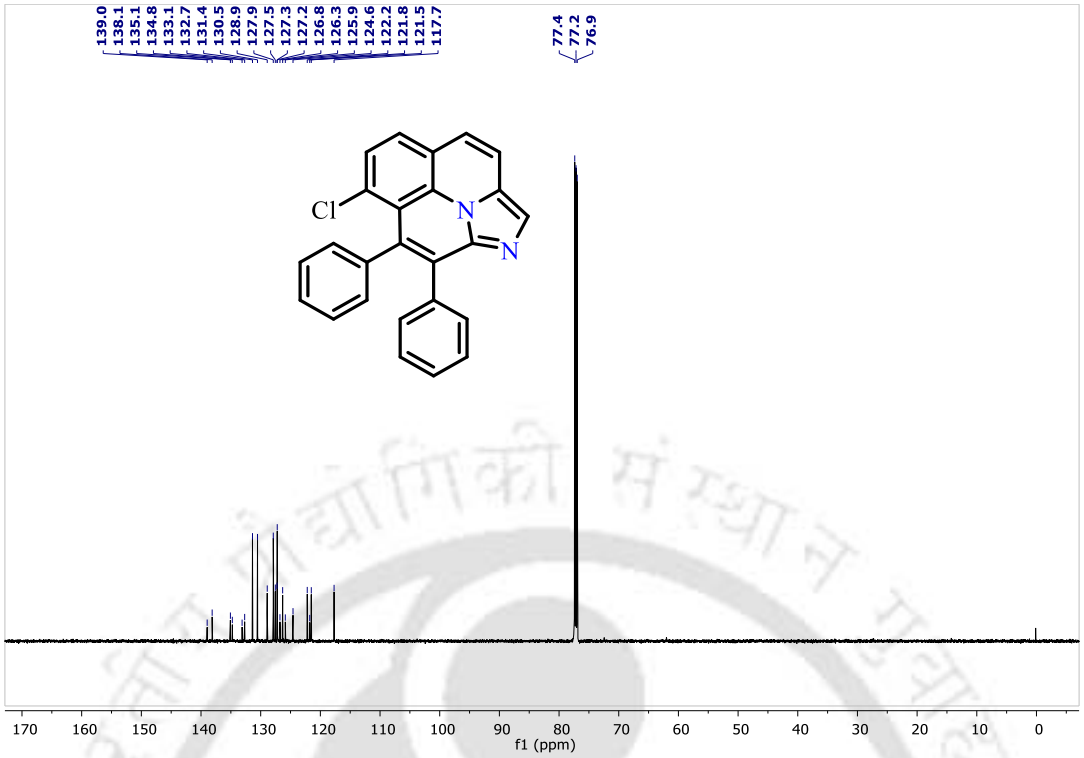


Figure S97. $^{13}C\{^{1}H\}$ NMR spectrum of **5.3i** ($CDCl_3$, 151 MHz, 298 K)

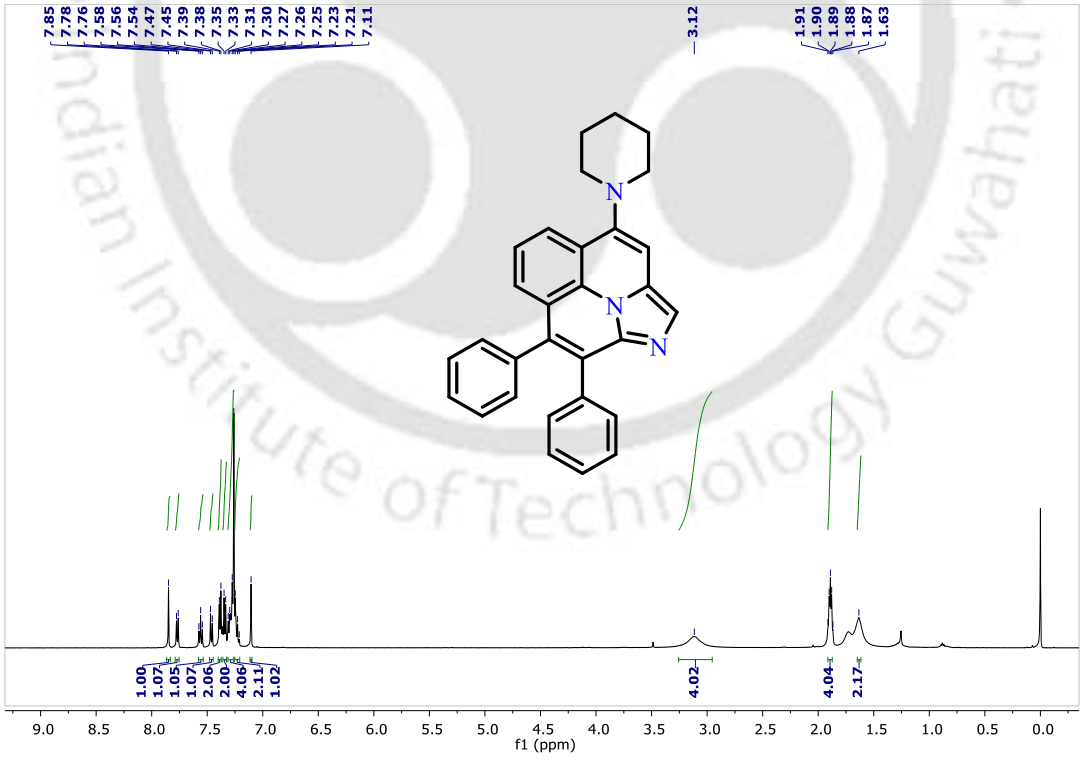


Figure S98. ^{1}H NMR spectrum of **5.3j** ($CDCl_3$, 500 MHz, 298 K)

TH-3565_186122020

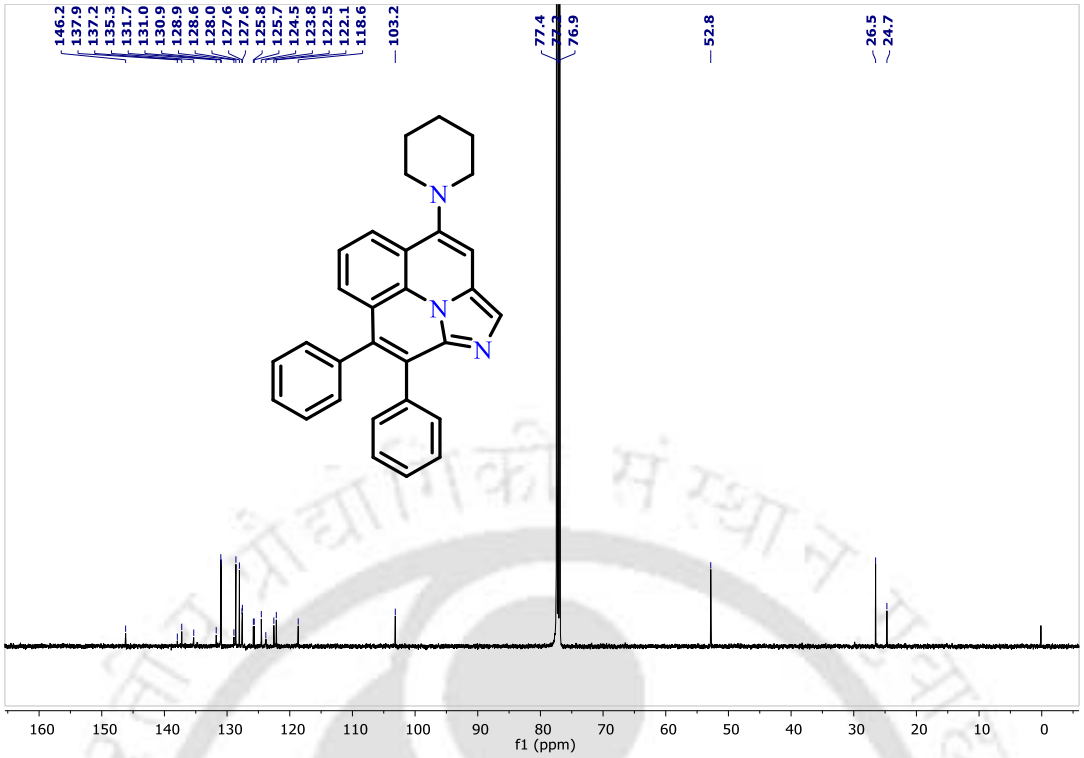


Figure S99. $^{13}C\{^{1}H\}$ NMR spectrum of **5.3j** ($CDCl_3$, 126 MHz, 298 K)

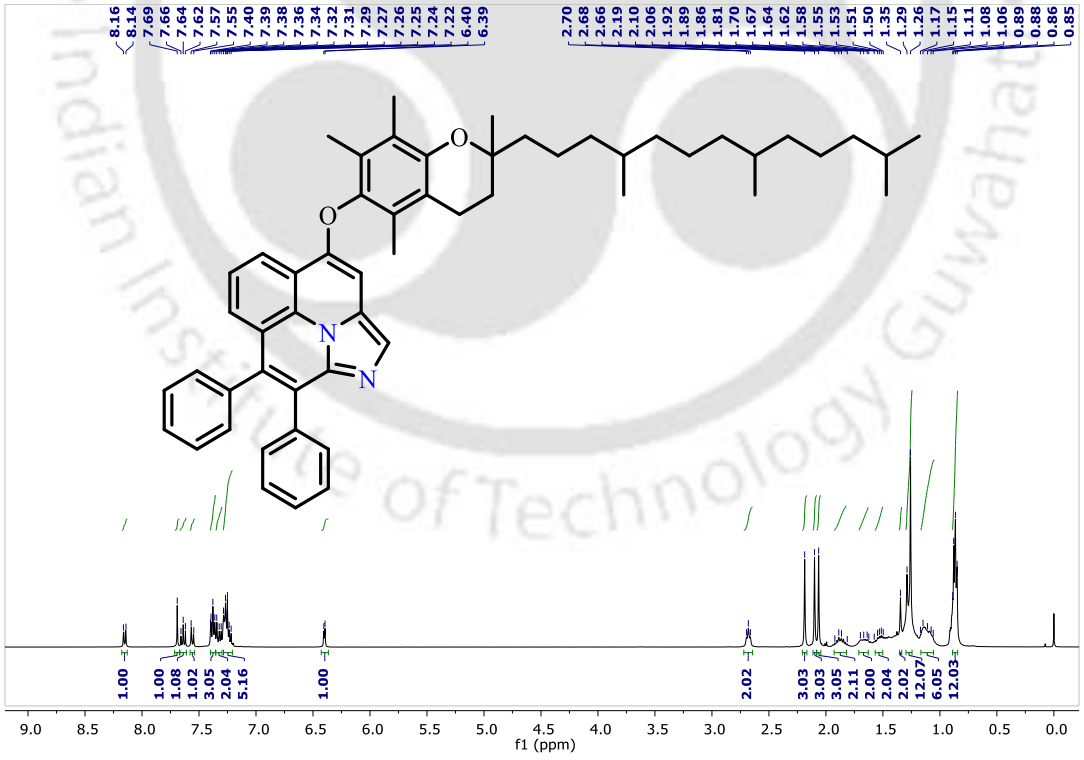


Figure S100. ^{1}H NMR spectrum of **5.3k** ($CDCl_3$, 400 MHz, 298 K)

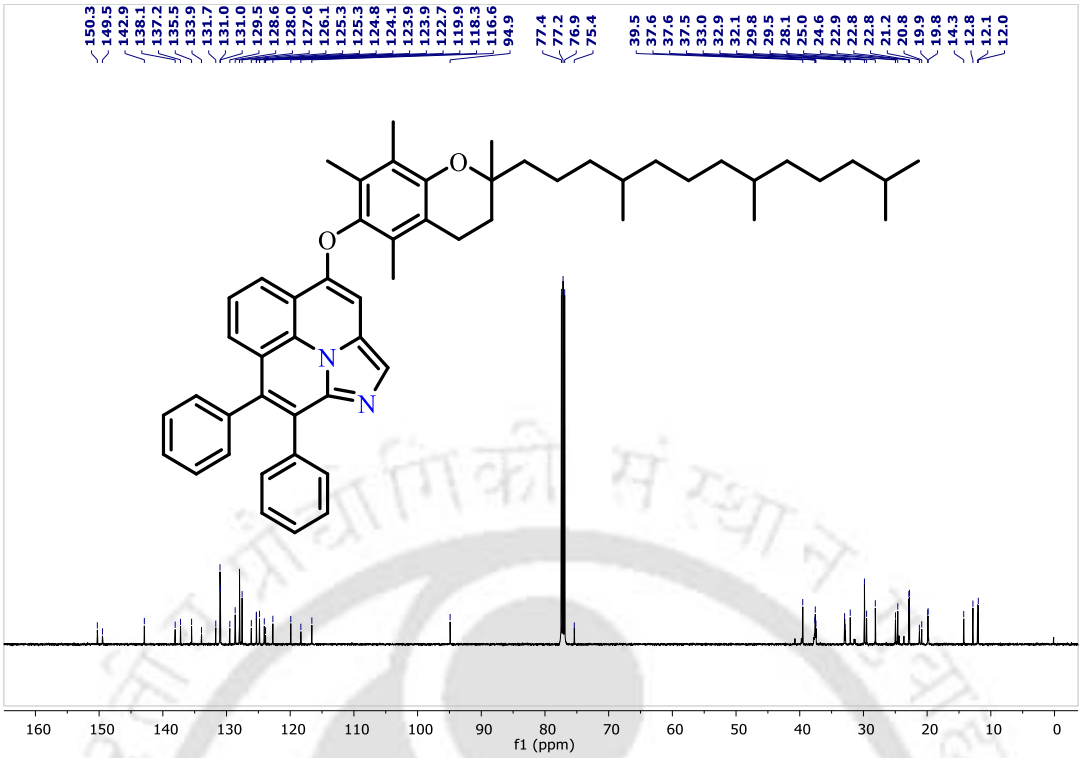


Figure S101. $^{13}C\{^{1}H\}$ NMR spectrum of **5.3k** ($CDCl_3$, 126 MHz, 298 K)

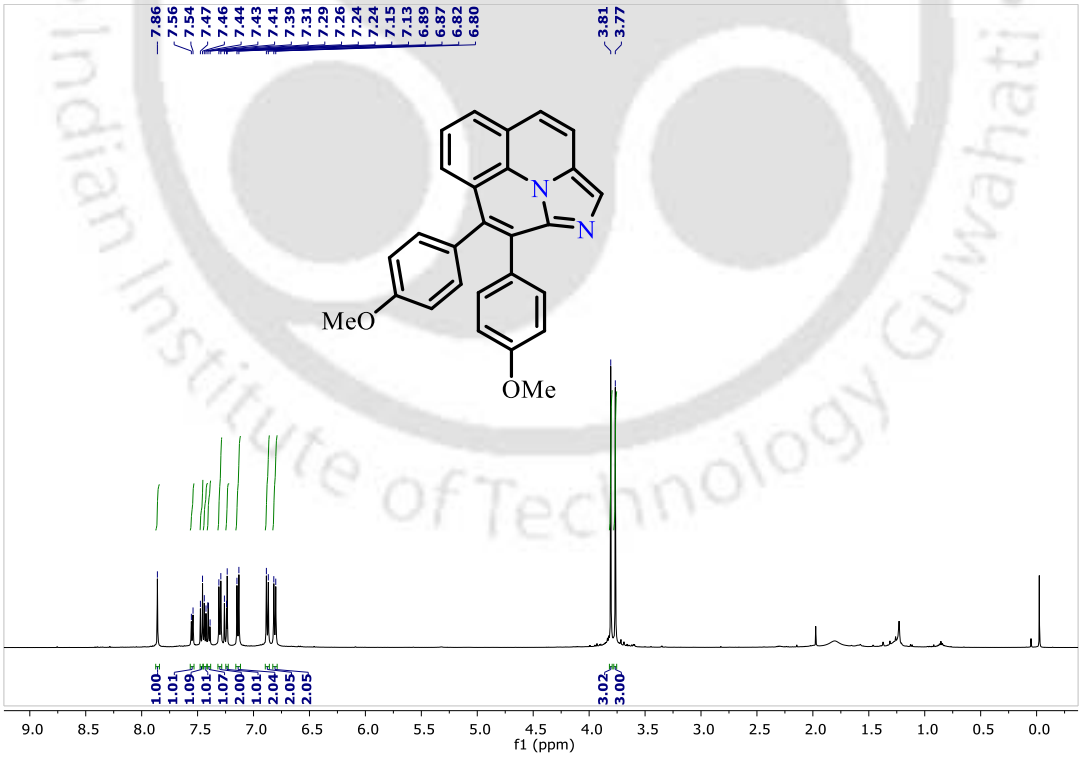


Figure S102. ^{1}H NMR spectrum of **5.4a** ($CDCl_3$, 500 MHz, 298 K)

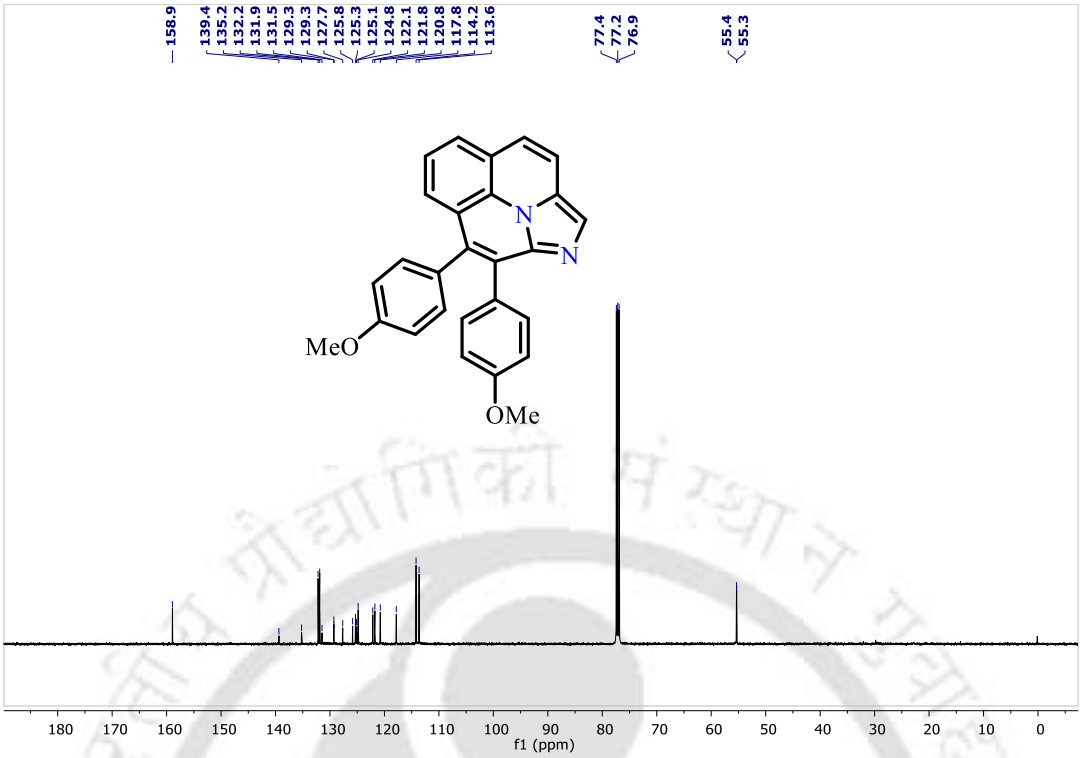


Figure S103. $^{13}C\{^{1}H\}$ NMR spectrum of **5.4a** ($CDCl_3$, 126 MHz, 298 K)

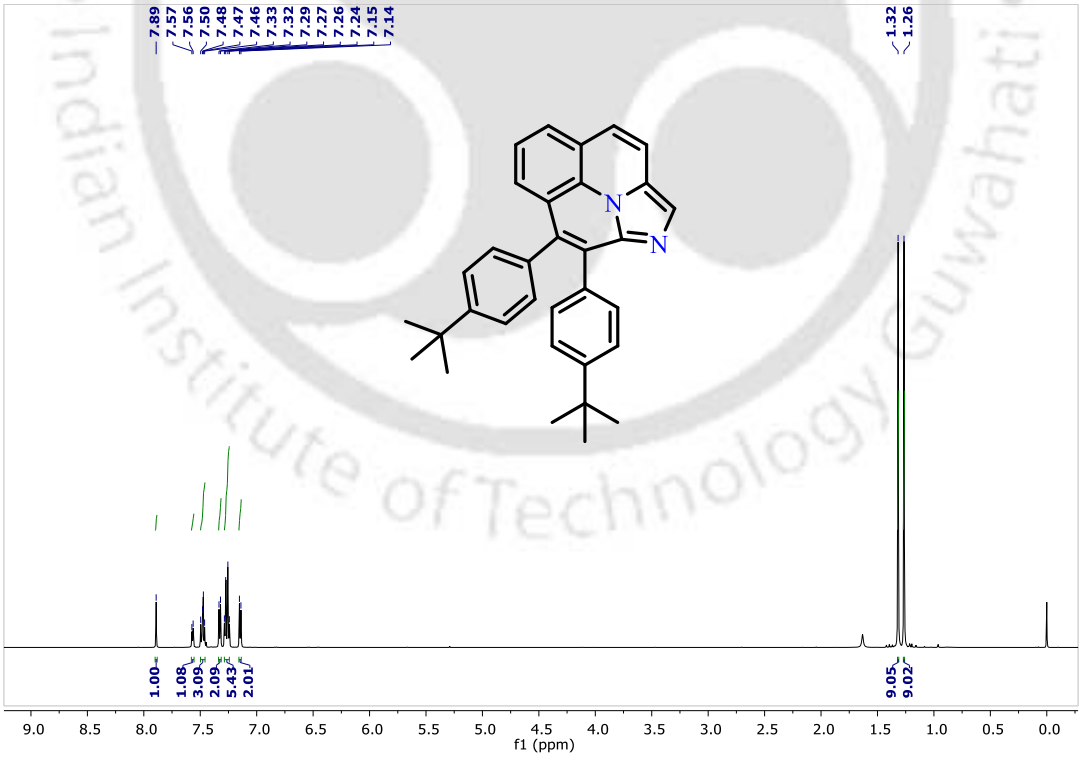


Figure S104. ^{1}H NMR spectrum of **5.4b** ($CDCl_3$, 600 MHz, 298 K)

TH-3565_186122020

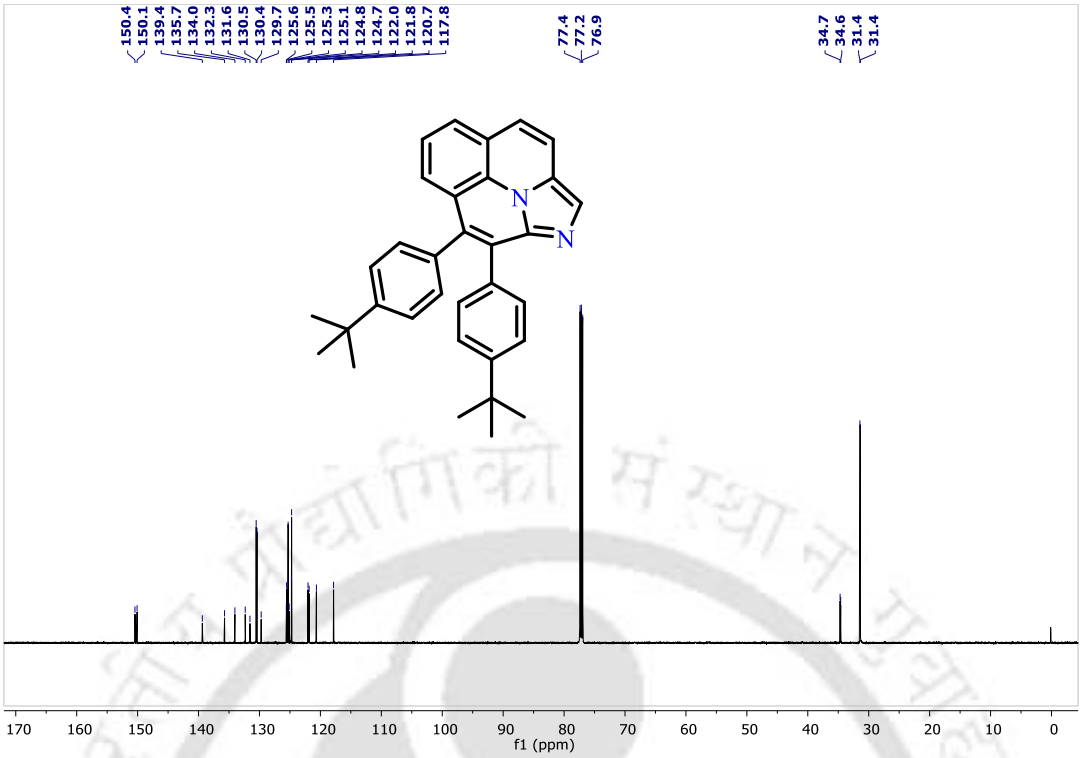


Figure S105. $^{13}C\{^{1}H\}$ NMR spectrum of **5.4b** ($CDCl_3$, 151 MHz, 298 K)

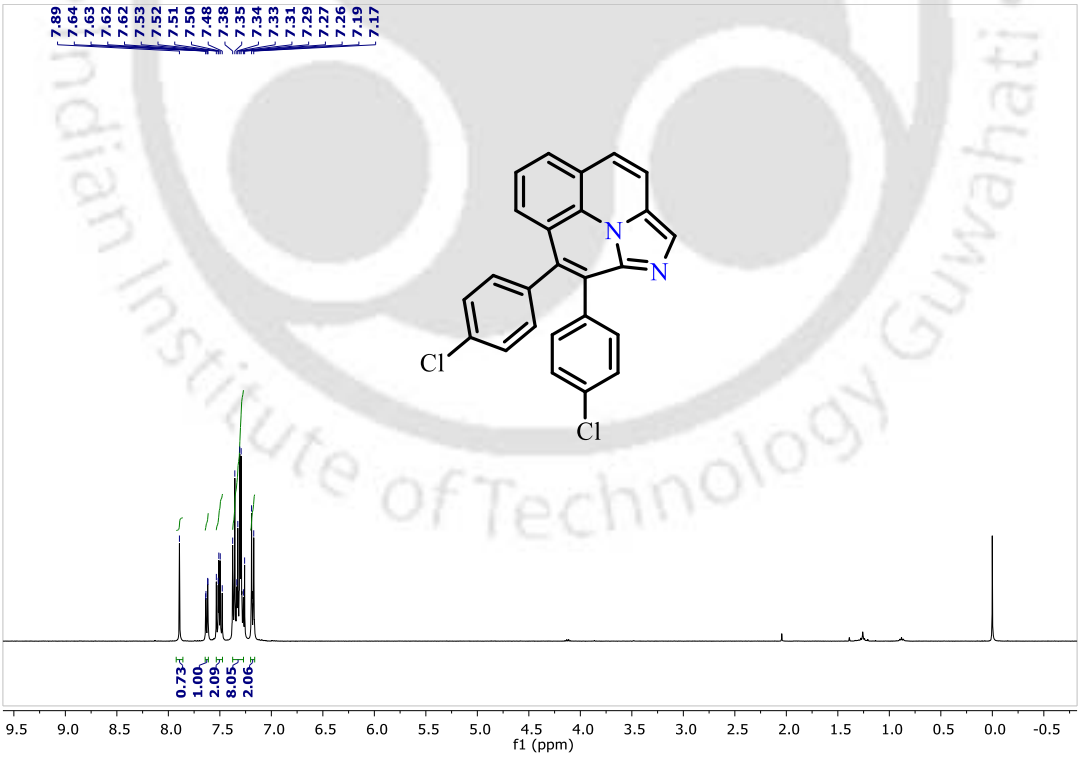


Figure S106. ^{1}H NMR spectrum of **5.4c** ($CDCl_3$, 400 MHz, 298 K)

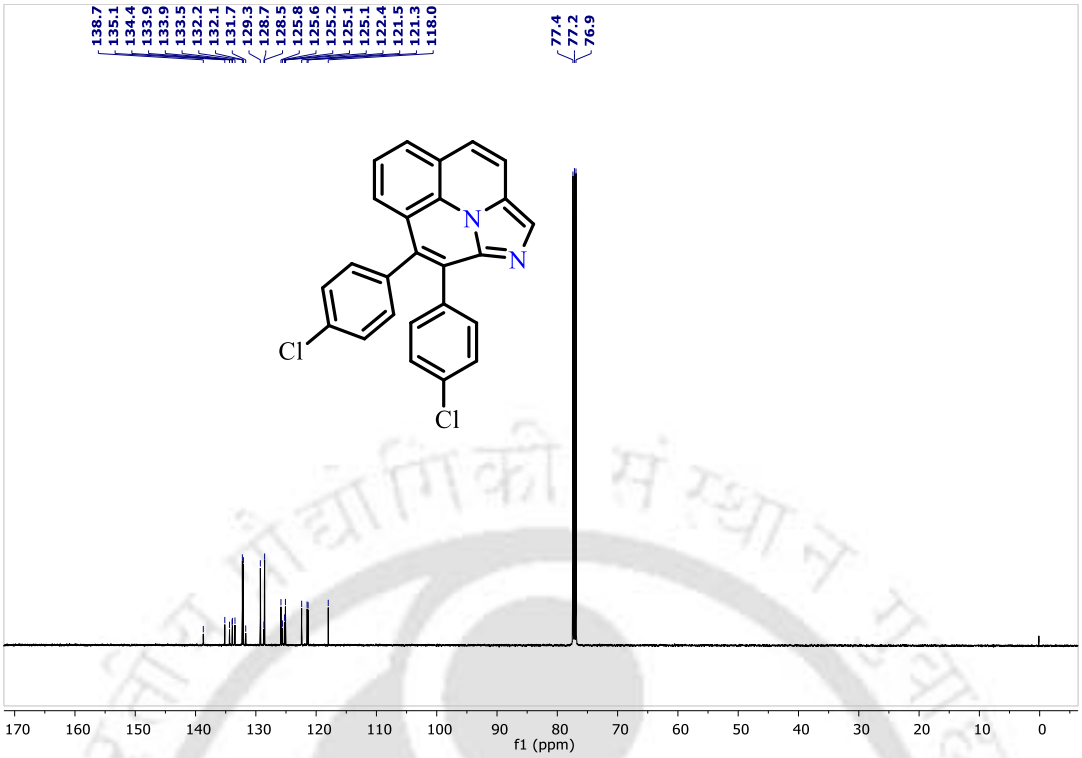


Figure S107. $^{13}C\{^{1}H\}$ NMR spectrum of **5.4c** ($CDCl_3$, 126 MHz, 298 K)

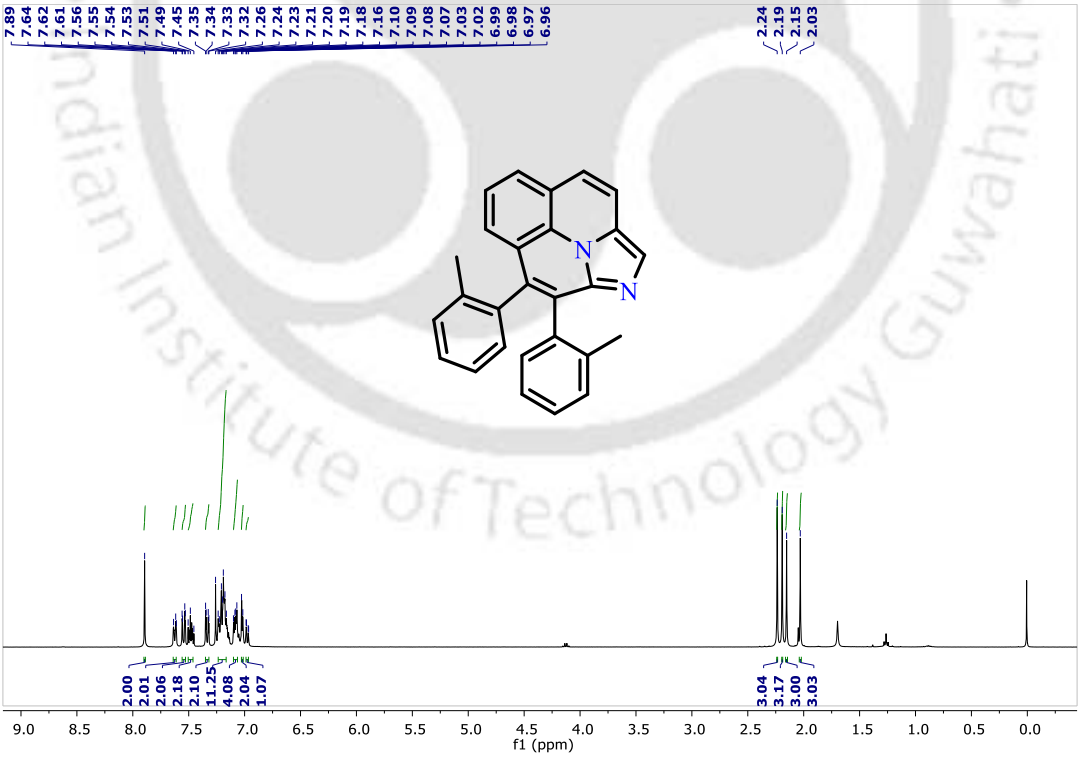


Figure S108. ^{1}H NMR spectrum of **5.4d** ($CDCl_3$, 400 MHz, 298 K)

TH-3565_186122020

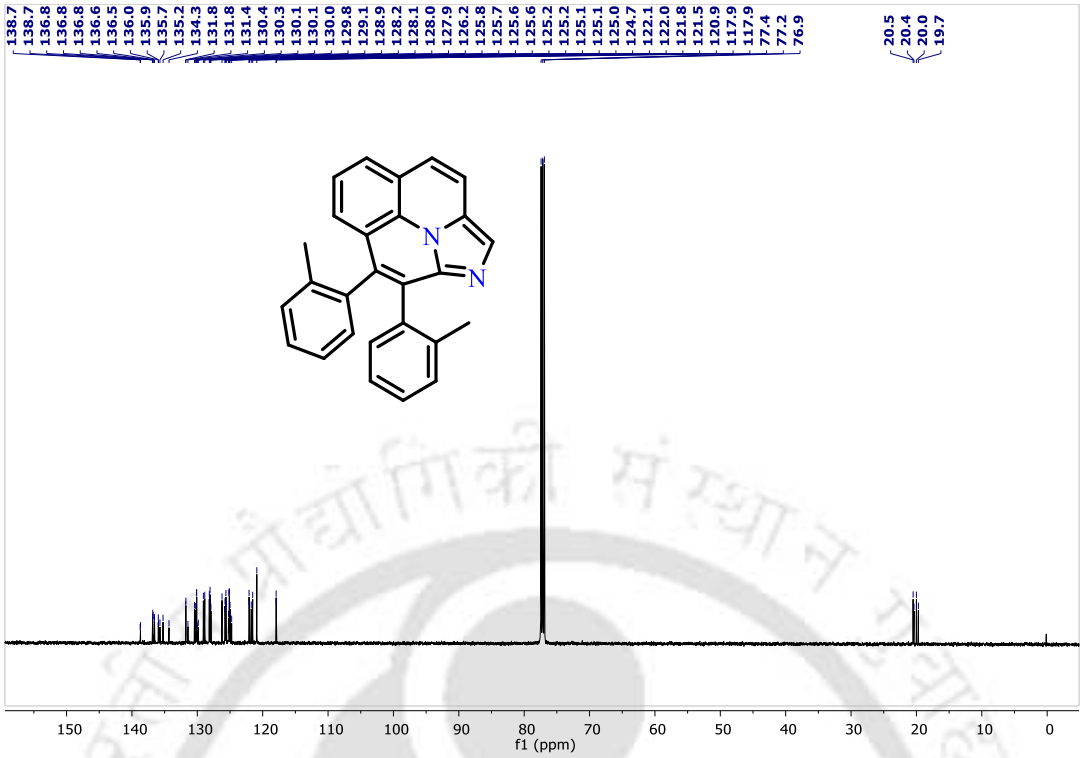


Figure S109. $^{13}C\{^{1}H\}$ NMR spectrum of **5.4d** ($CDCl_3$, 126 MHz, 298 K)

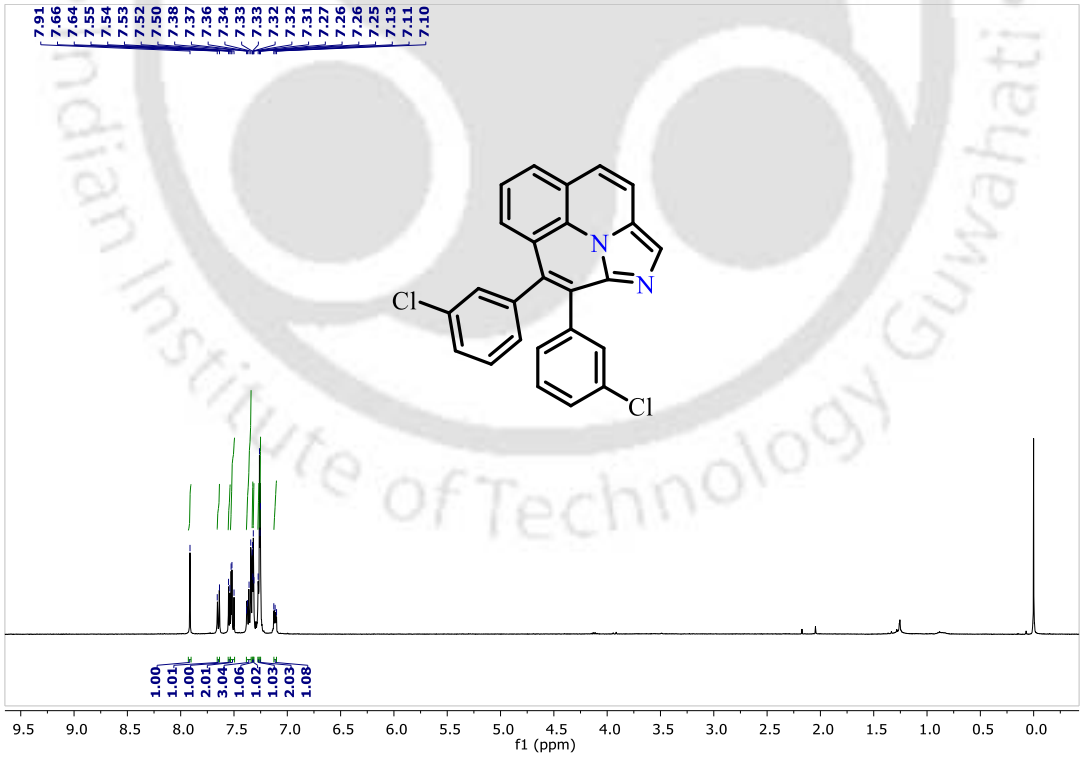


Figure S110. ^{1}H NMR spectrum of **5.4e** ($CDCl_3$, 400 MHz, 298 K)

TH-3565_186122020

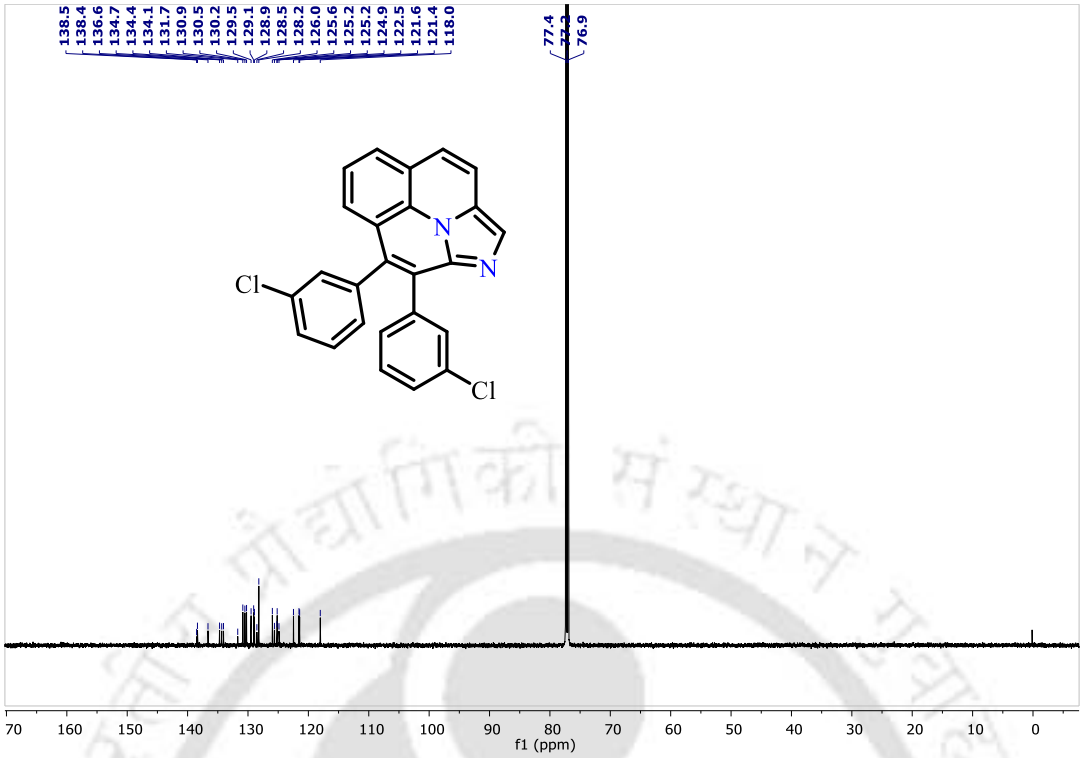


Figure S111. $^{13}C\{^{1}H\}$ NMR spectrum of **5.4e** ($CDCl_3$, 151 MHz, 298 K)

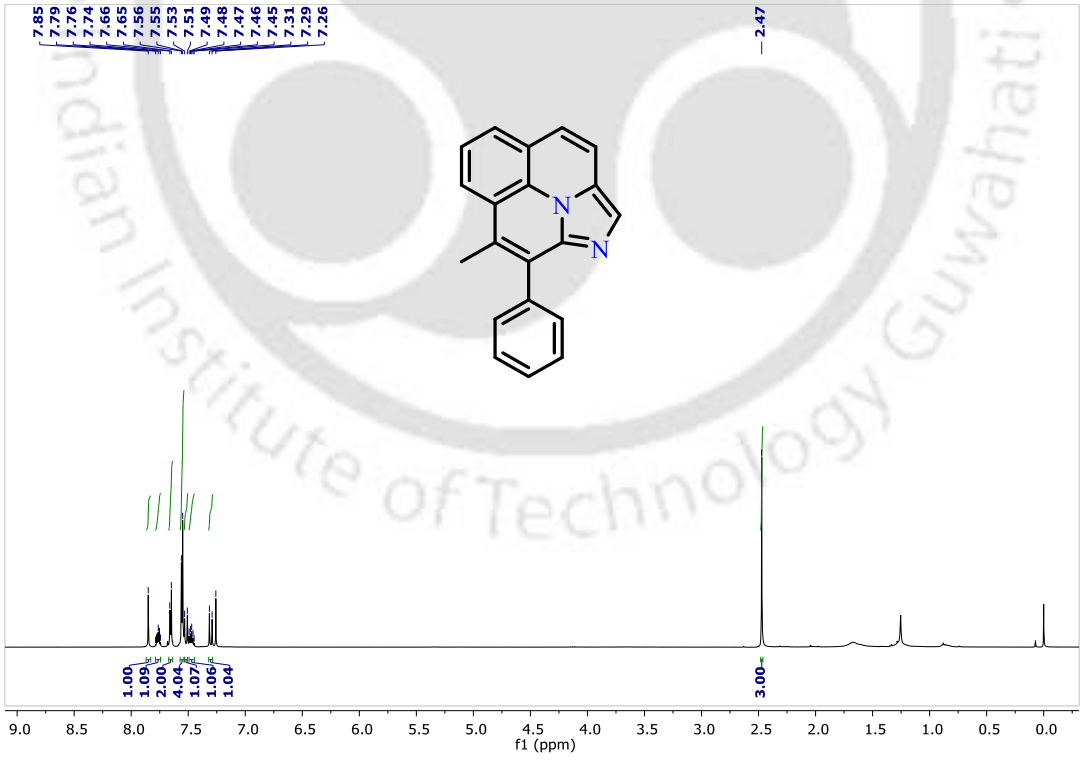


Figure S112. ^{1}H NMR spectrum of **5.4f** ($CDCl_3$, 400 MHz, 298 K)

TH-3565_186122020

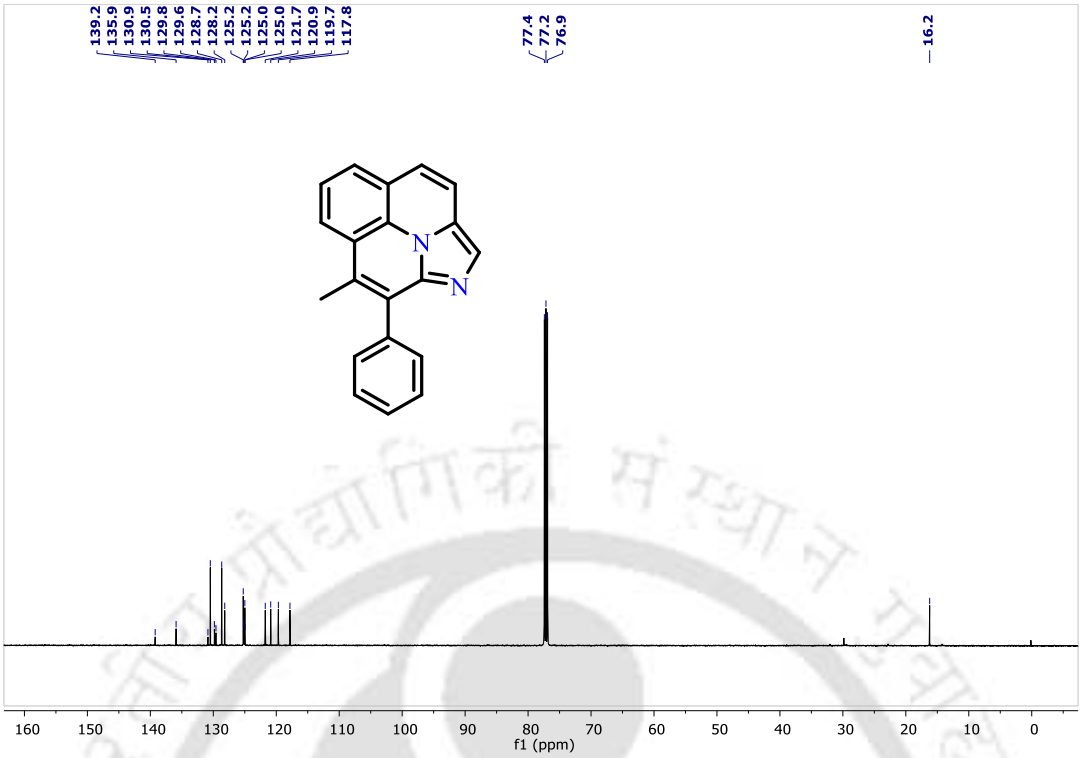


Figure S113. $^{13}C\{^{1}H\}$ NMR spectrum of **5.4f** ($CDCl_3$, 126 MHz, 298 K)

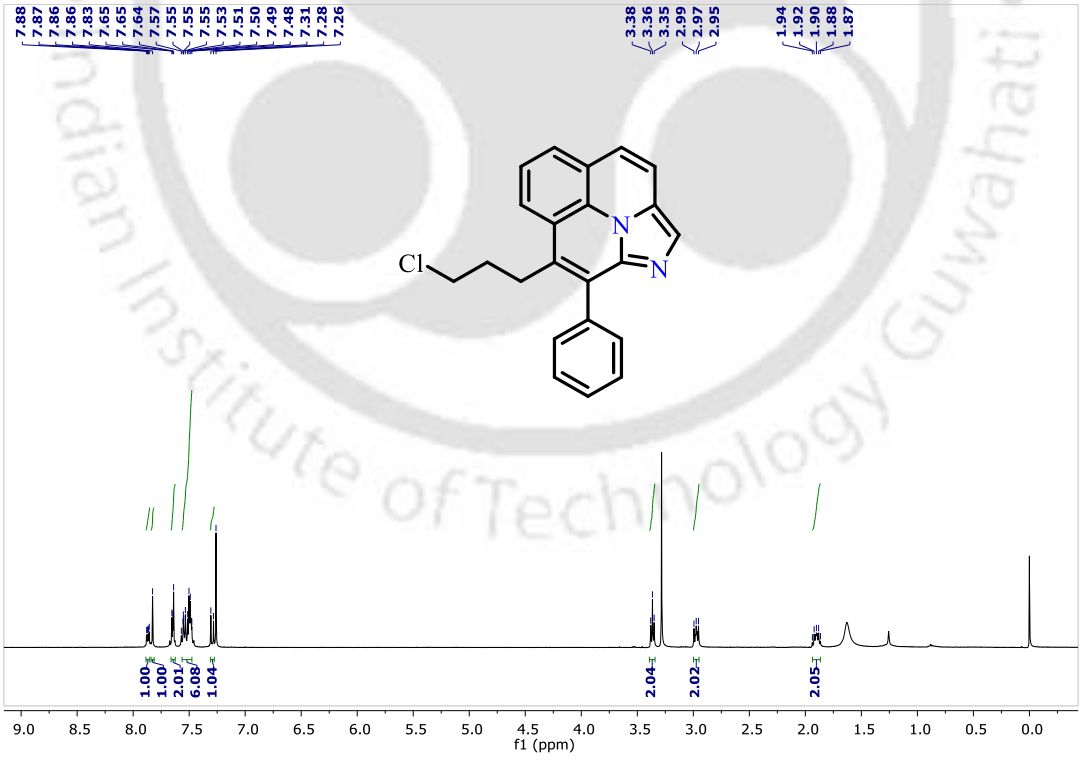


Figure S114. ^{1}H NMR spectrum of **5.4g** ($CDCl_3$, 400 MHz, 298 K)

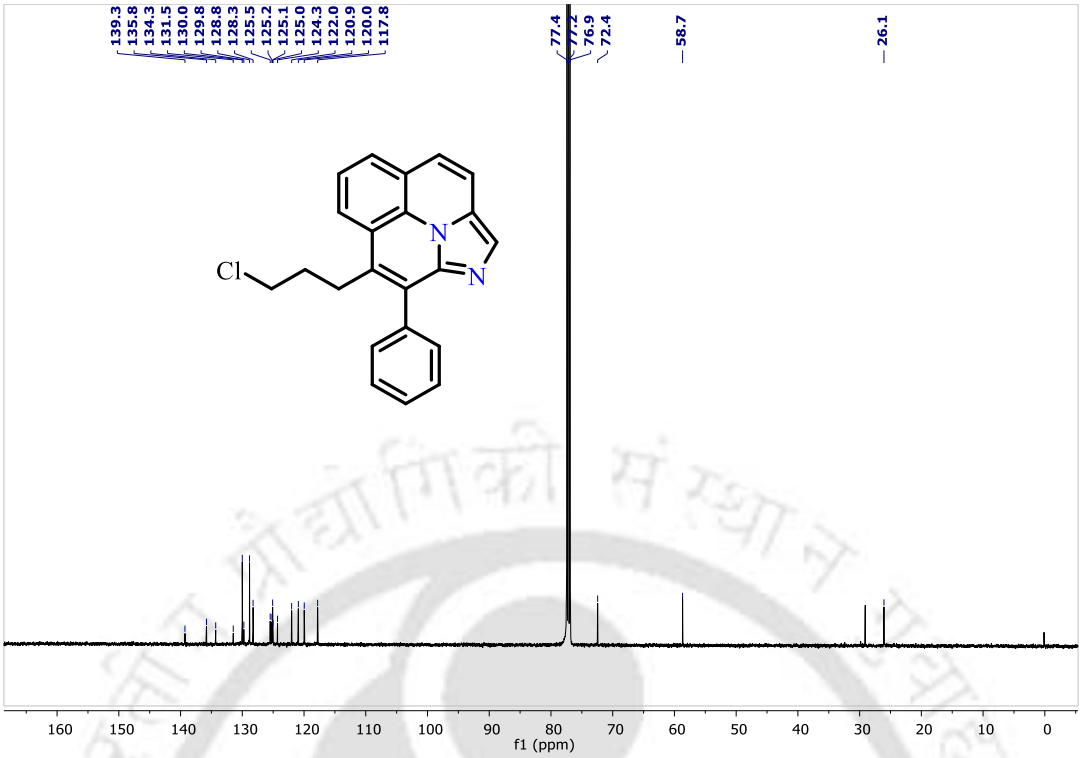


Figure S115. $^{13}C\{^{1}H\}$ NMR spectrum of **5.4g** ($CDCl_3$, 126 MHz, 298 K)

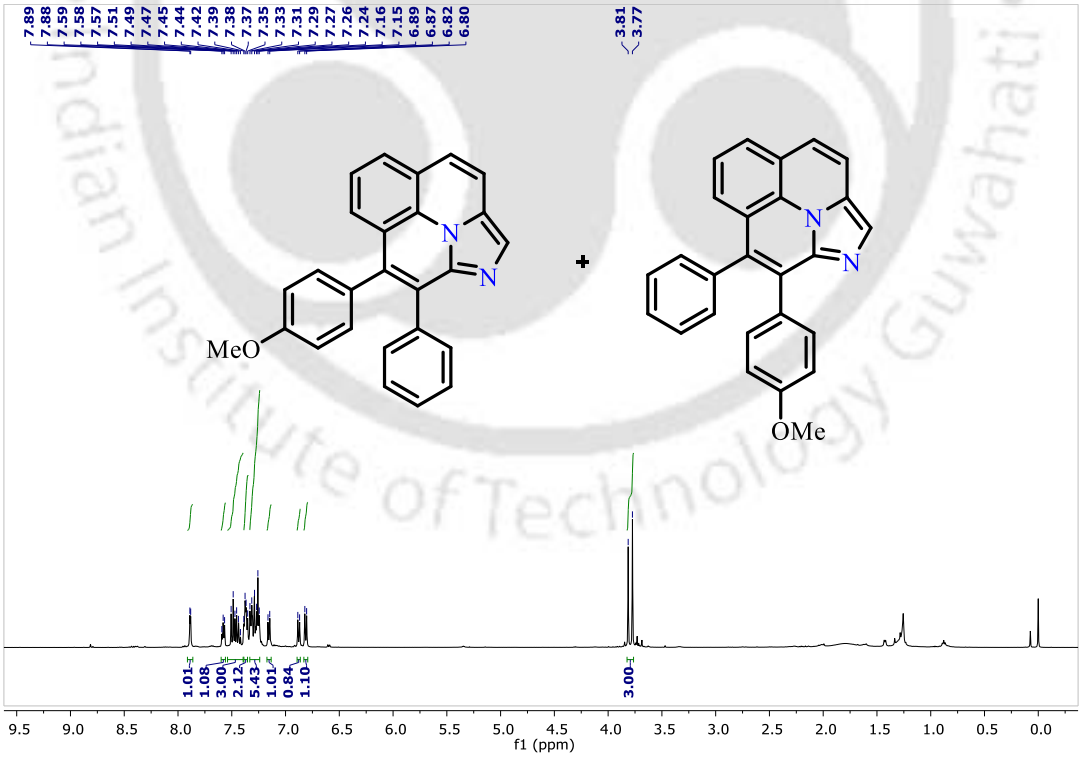


Figure S116. ^{1}H NMR spectrum of **5.4h** + **5.4h′** ($CDCl_3$, 500 MHz, 298 K)

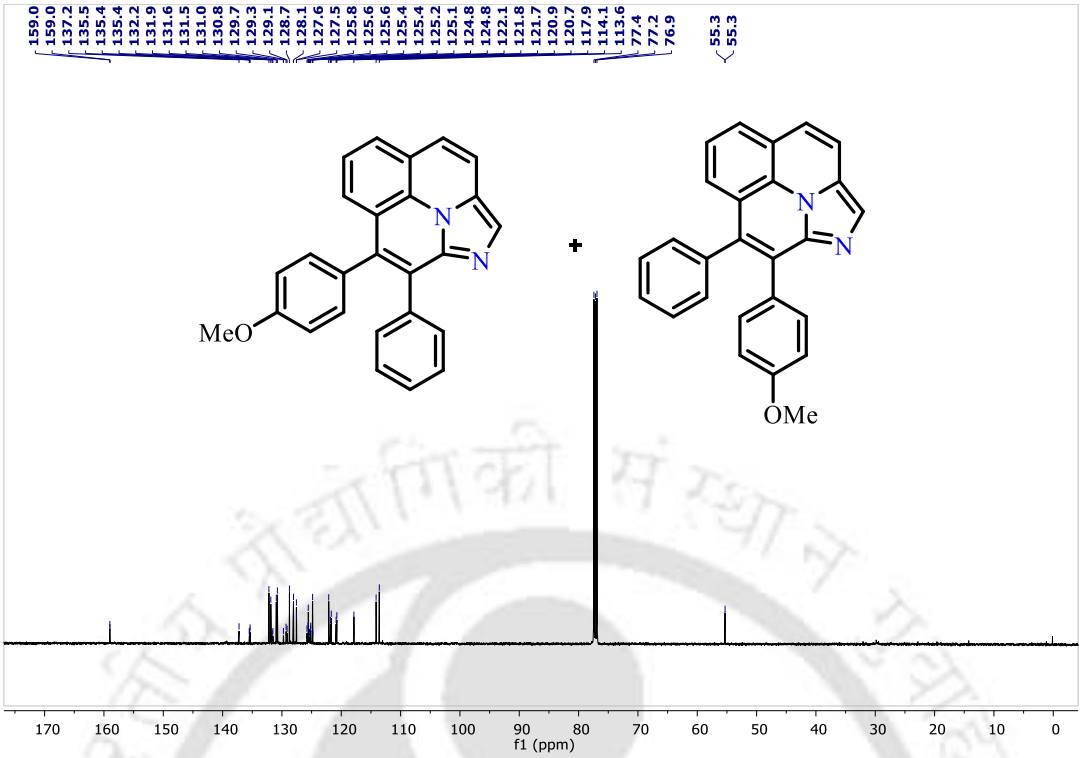


Figure S117. $^{13}C\{^{1}H\}$ NMR spectrum of **5.4h + 5.4h′** ($CDCl_3$, 126 MHz, 298 K)

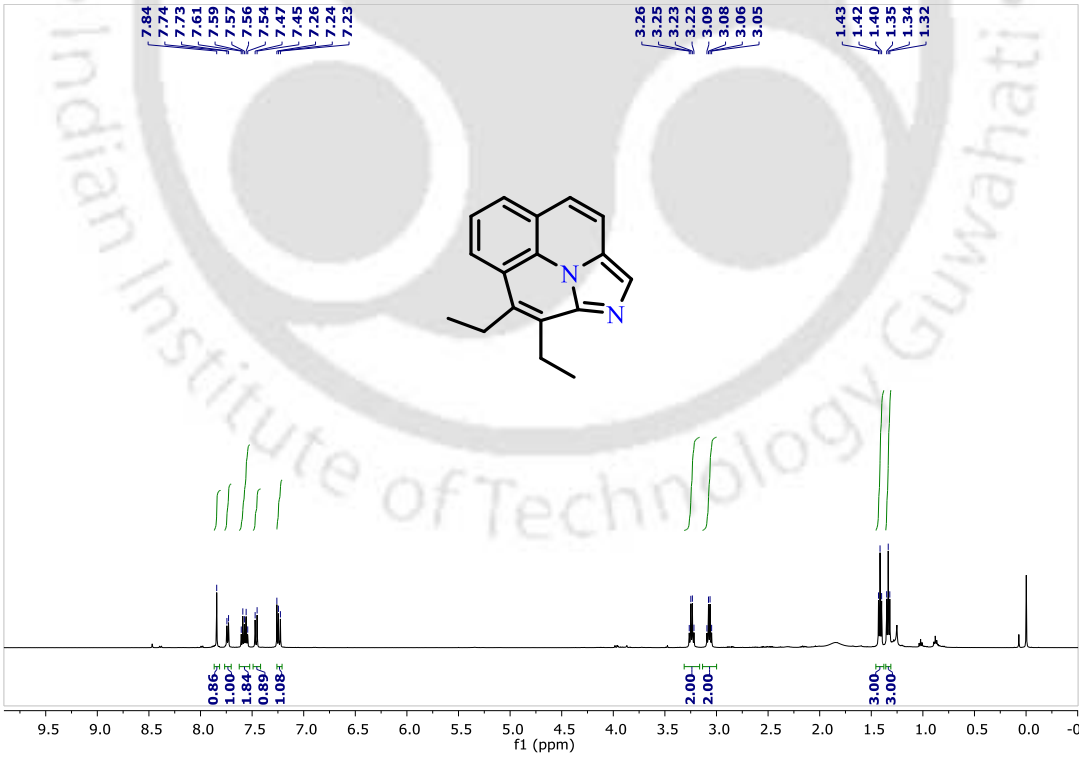


Figure S118. ^{1}H NMR spectrum of **5.4i** ($CDCl_3$, 500 MHz, 298 K)

TH-3565_186122020

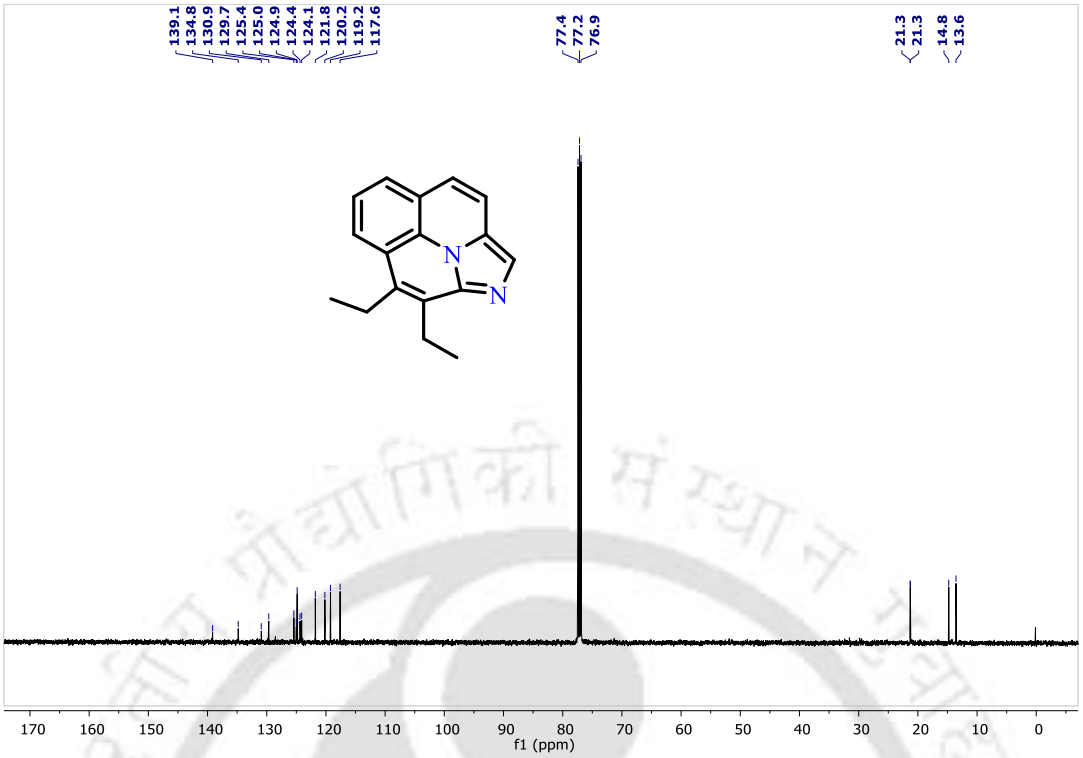


Figure S119. $^{13}C\{^{1}H\}$ NMR spectrum of **5.4i** ($CDCl_3$, 126 MHz, 298 K)

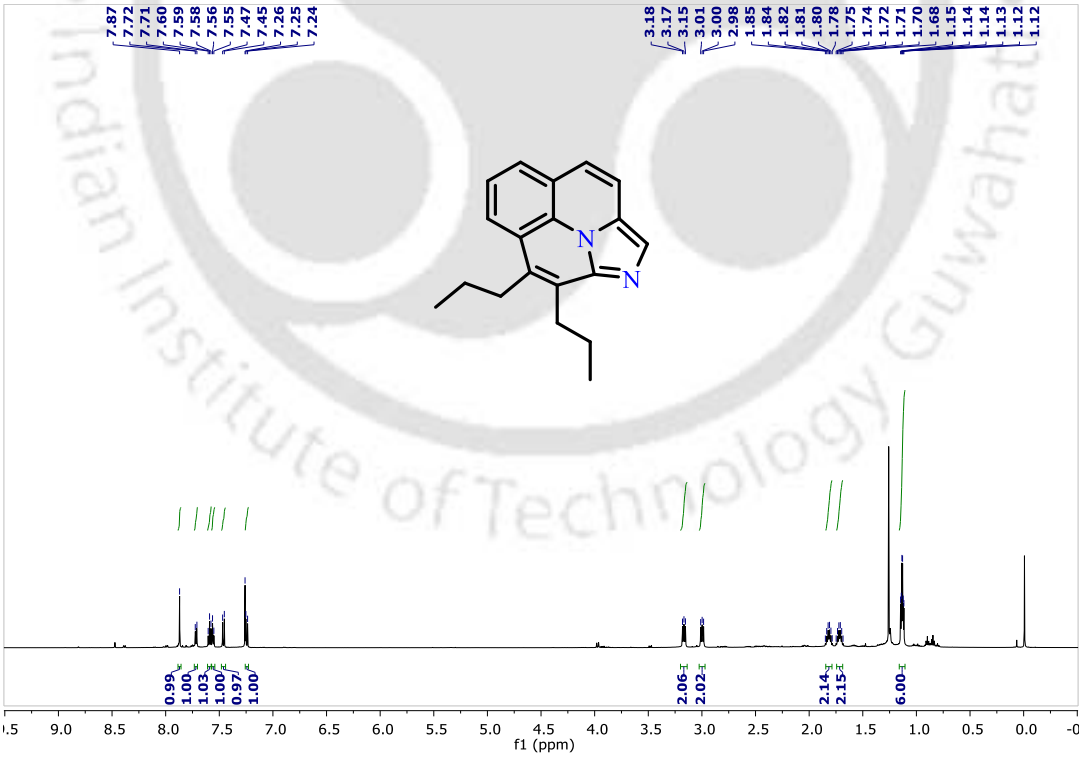


Figure S120. ^{1}H NMR spectrum of **5.4j** ($CDCl_3$, 600 MHz, 298 K)

TH-3565_186122020

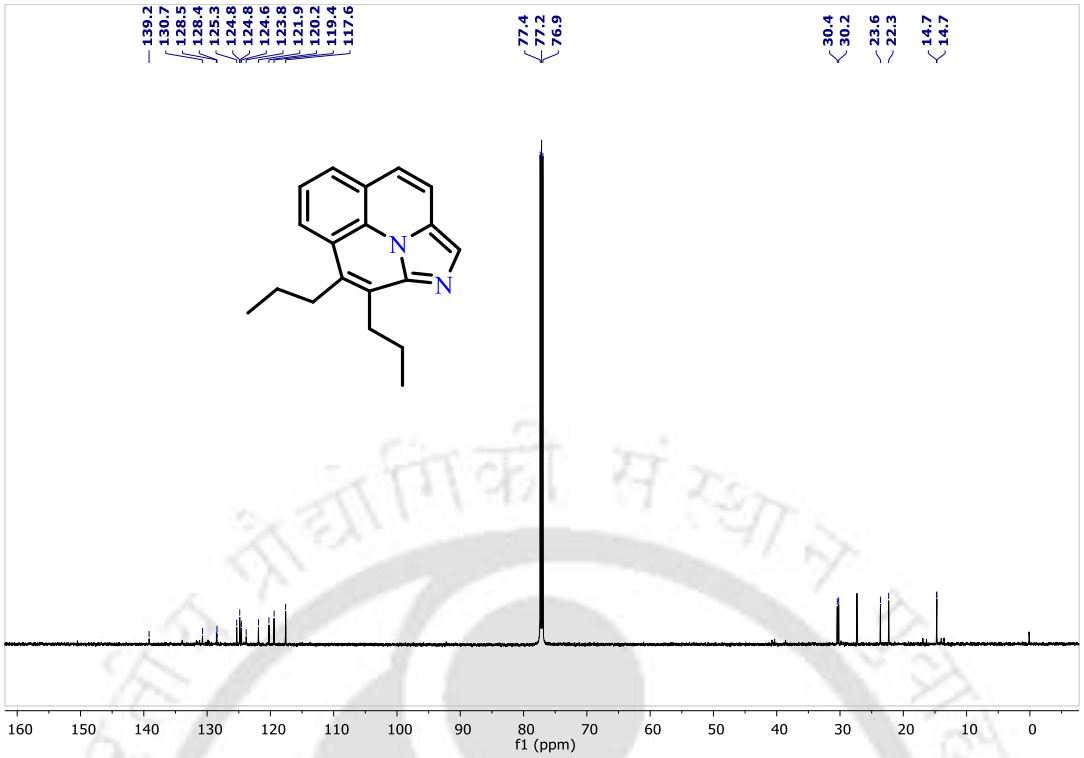


Figure S121. $^{13}C\{^{1}H\}$ NMR spectrum of **5.4j** ($CDCl_3$, 151 MHz, 298 K)

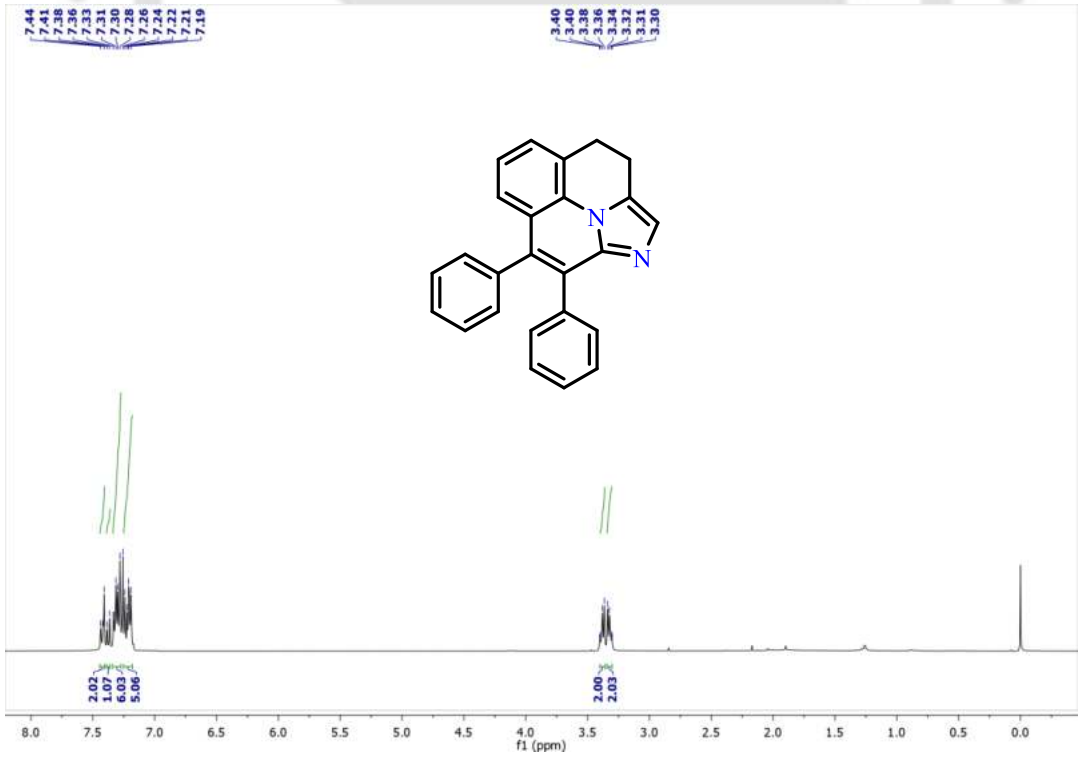


Figure S122. ^{1}H NMR spectrum of **5.5** ($CDCl_3$, 600 MHz, 298 K)

TH-3565_186122020

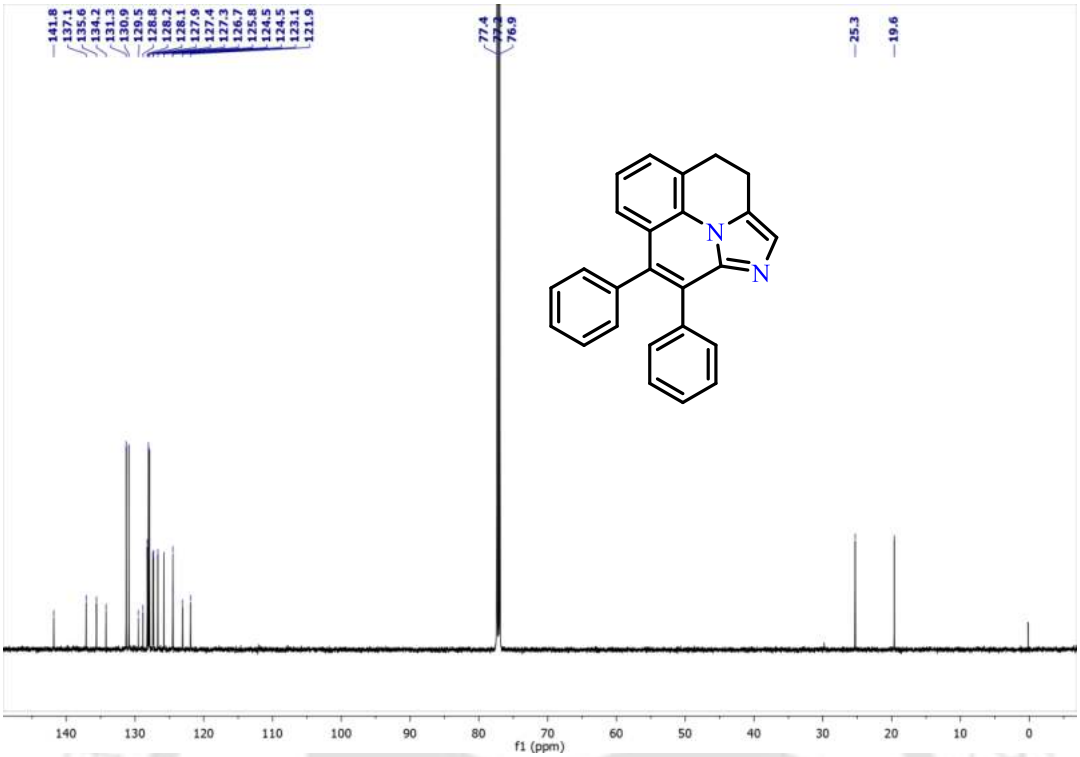


Figure S123. $^{13}C\{^{1}H\}$ NMR spectrum of **5.5** ($CDCl_3$, 151 MHz, 298 K)

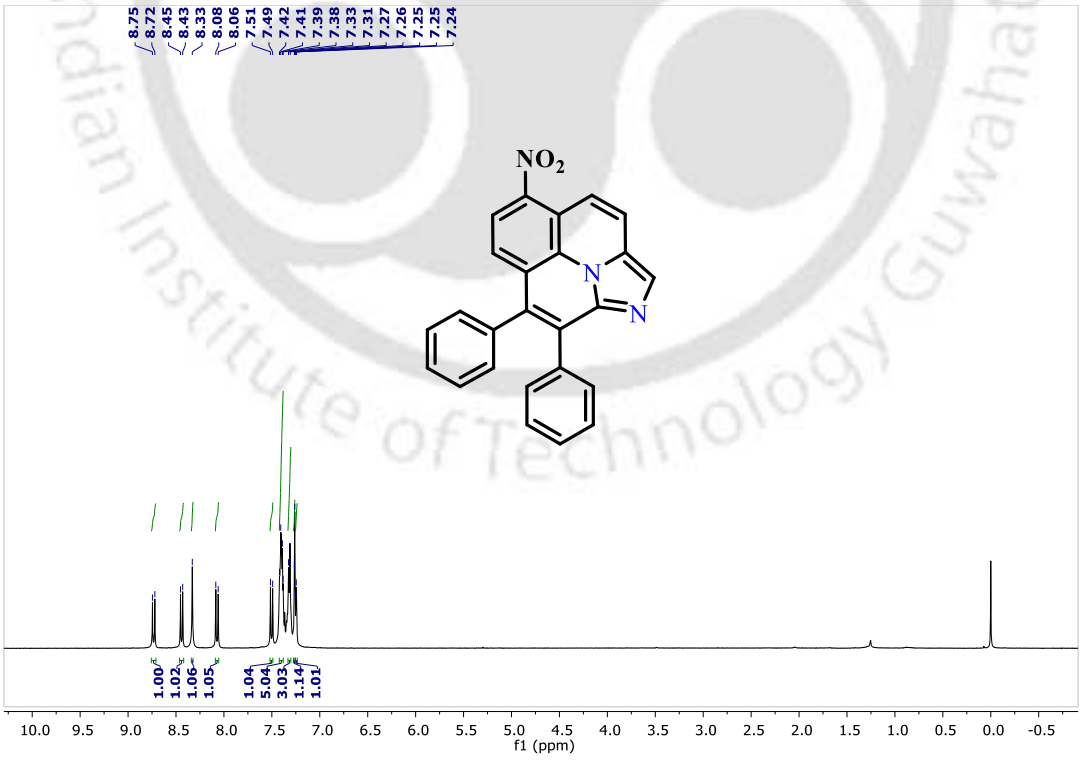


Figure S124. ^{1}H NMR spectrum of **5.6** ($CDCl_3$, 400 MHz, 298 K)

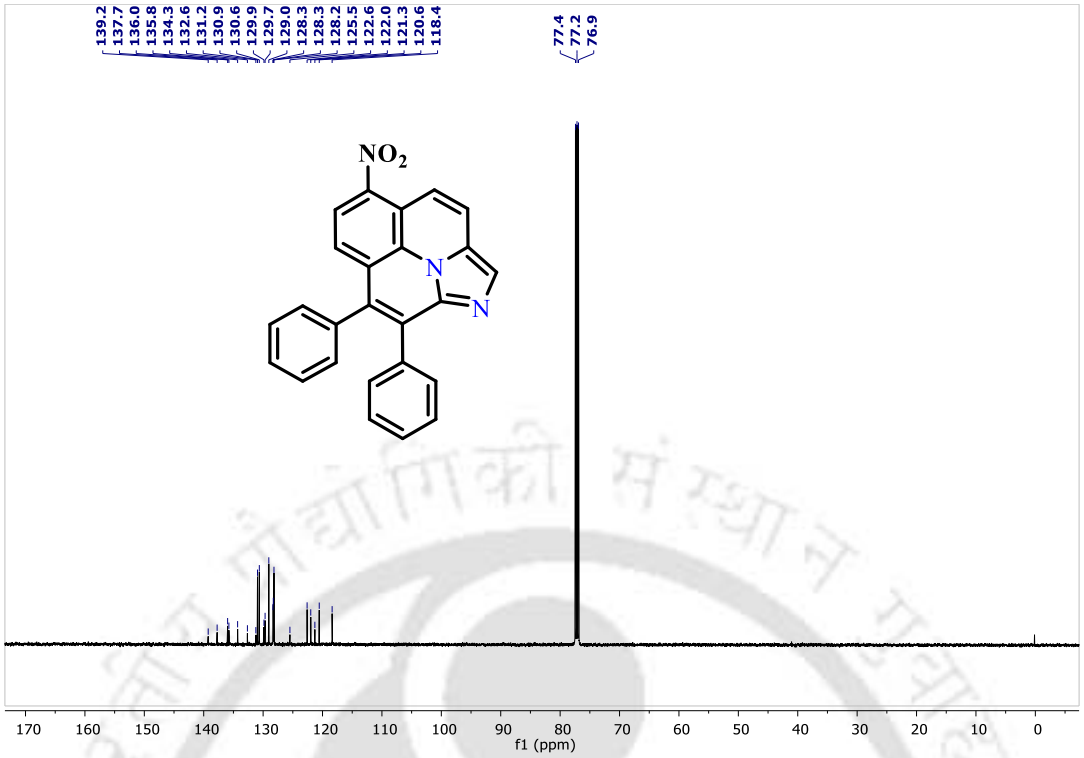
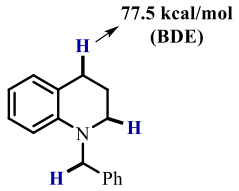


Figure S125. $^{13}C\{^{1}H\}$ NMR spectrum of **5.6** ($CDCl_3$, 126 MHz, 298 K)

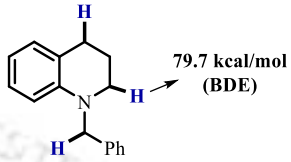
TH-3565_186122020

Annexure V

The cartesian coordinates (xyz) of all the optimized structures (*Chapter 2*)



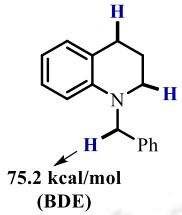
C	-1.33209600	-2.59020900	-0.47994400
C	-0.62586700	-1.39851100	-0.64596800
C	-1.19183000	-0.17052400	-0.28582400
C	-2.51526000	-0.14986200	0.27988100
C	-3.20297900	-1.38434500	0.41932200
C	-2.62889200	-2.58462200	0.04809400
H	-0.86352800	-3.52619100	-0.76838400
H	0.38141200	-1.44112900	-1.04422400
C	-3.08261800	1.05965200	0.71354300
H	-4.20540400	-1.36136000	0.84041000
H	-3.17574200	-3.51448200	0.17011100
C	-2.33115400	2.34145900	0.57330500
C	-1.34021700	2.23183100	-0.57899700
H	-3.01205900	3.18150100	0.39189700
H	-0.67966800	3.10264300	-0.59328600
N	-0.50945900	1.03916600	-0.42731400
C	0.73921600	1.03724100	-1.16565600
H	0.63371100	0.50449800	-2.12618600
H	0.96892700	2.07906300	-1.41326900
C	1.91613600	0.46178300	-0.39616900
C	3.05075100	0.04281800	-1.09538300
C	1.90493700	0.37159000	0.99576000
C	4.16347200	-0.44776900	-0.41555100
H	3.06199300	0.09776500	-2.18270900
C	3.01544800	-0.12404300	1.67794300
H	1.01377700	0.67771700	1.53671000
C	4.14839600	-0.53227400	0.97635600
H	5.03875900	-0.76981500	-0.97251000
H	2.99241100	-0.19624000	2.76161100
H	5.01148200	-0.92033300	1.50924400
H	-4.05571300	1.04958400	1.19521000
H	-1.77971500	2.57508900	1.49856900
H	-1.88908900	2.20224700	-1.53627900



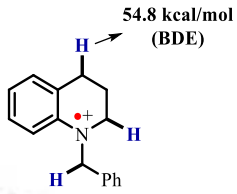
C	-1.68228000	-2.57502100	-0.18455100
C	-0.83463400	-1.51902500	-0.50399600
C	-1.27350400	-0.19068800	-0.36805400
C	-2.57884000	0.06263700	0.11385700
C	-3.39593400	-1.01473000	0.44088400
C	-2.96927000	-2.33406200	0.28993700
H	-1.32128900	-3.59345900	-0.29533800
H	0.17772100	-1.73333800	-0.82989000
C	-3.04841000	1.48914900	0.25720600
H	-4.39578400	-0.80892200	0.81781700
H	-3.62776600	-3.15743000	0.54747900
C	-1.86499500	2.38327800	0.64373500
C	-0.76445300	2.18644800	-0.34025400
H	-3.46437800	1.84485900	-0.69496500
H	-2.15583900	3.43777700	0.66672900
H	0.03431600	2.90860500	-0.46205000
N	-0.44867600	0.88610300	-0.70641400
C	0.79883000	0.65985000	-1.40659300
H	0.64154900	-0.09774700	-2.18337400
H	1.04700600	1.59116600	-1.92797400
C	1.96012200	0.25416800	-0.51317000
C	3.15855900	-0.15952400	-1.10165400
C	1.86681900	0.29923800	0.87753300
C	4.24922100	-0.51821000	-0.31395400
H	3.23722500	-0.20210800	-2.18674400
C	2.95794000	-0.06133900	1.66859100
H	0.93319200	0.60685200	1.34193300

TH-3565_186122020

C	4.15115500	-0.46918900	1.07690400
H	5.17417800	-0.83872700	-0.78475800
H	2.87150000	-0.02648500	2.75076700
H	4.99898900	-0.75133200	1.69405600
H	-3.84684800	1.54560700	1.00514100
H	-1.54500500	2.11408300	1.66753100

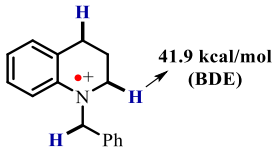


C	-2.98709200	-2.23649600	0.44262900
C	-1.72457300	-1.68557800	0.25744200
C	-1.57137000	-0.31972200	-0.03767300
C	-2.71701700	0.50423800	-0.08436100
C	-3.96913500	-0.07390800	0.11914400
C	-4.12408600	-1.43566200	0.36467400
H	-3.07601700	-3.29554200	0.66682500
H	-0.84508100	-2.30943900	0.37413900
C	-2.59378400	1.99439400	-0.30973800
H	-4.84446100	0.57205700	0.08735000
H	-5.11231200	-1.85837600	0.51534400
C	-1.19915500	2.47813300	0.07510500
C	-0.17008300	1.62164200	-0.64228000
H	-2.77846100	2.23276700	-1.36642000
H	-1.05740700	3.52742000	-0.20232600
H	0.84733700	1.95547700	-0.43442100
N	-0.28536300	0.21176800	-0.23779400
C	0.75348700	-0.63577400	-0.58811400
C	2.11072500	-0.40407300	-0.22541300
C	3.14357900	-1.12125600	-0.87908300
C	2.48482300	0.49442200	0.80545600
C	4.47304400	-0.93118400	-0.53769300
H	2.87834900	-1.82296000	-1.66653100
C	3.81955400	0.67875900	1.13702300
H	1.70866800	1.00776200	1.36741600
C	4.82536500	-0.02334900	0.46696500
H	5.24540900	-1.49108900	-1.05759500
H	4.08102000	1.36599200	1.93706400
H	5.86763500	0.12555100	0.73111500
H	-3.36398200	2.51554000	0.26920700
H	-1.05283300	2.39359000	1.15911900
H	-0.32300200	1.69083900	-1.73092400
H	0.49698600	-1.51948800	-1.16931600

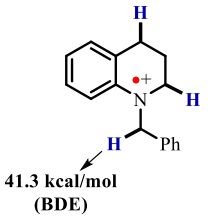


C	-2.87807600	-2.10200900	-0.21975300
C	-1.66107200	-1.57497000	-0.53653700
C	-1.43318600	-0.16602000	-0.38349800
C	-2.48792400	0.61782300	0.28473100
C	-3.77082300	-0.00693600	0.55462400
C	-3.96755200	-1.31898400	0.30369800
H	-3.03271800	-3.16682200	-0.37024500
H	-0.88449800	-2.22431000	-0.91837200
C	-2.18163000	1.84096100	0.78399000
H	-4.54840600	0.61185600	0.99330200
H	-4.91615800	-1.79845800	0.51581700
C	-0.81991500	2.42175000	0.60888700
C	-0.20721900	1.90880600	-0.67953500
H	-0.85674100	3.51446800	0.59135200
H	0.85756800	2.14547900	-0.72489000
N	-0.33565300	0.44490200	-0.79373200
C	0.79413400	-0.21384500	-1.46893600
H	0.47818500	-1.19152500	-1.83063600
H	1.02730500	0.39172100	-2.35168300
C	1.99878100	-0.30479700	-0.55723500
C	3.23858900	0.16735600	-0.98810200
C	1.87892400	-0.87296300	0.71495400
C	4.35483100	0.06571000	-0.15761700
H	3.33824000	0.60942700	-1.97700700
C	2.99193900	-0.97089200	1.54497100
H	0.91542300	-1.24456800	1.06090300
C	4.23192800	-0.50177200	1.10816400
H	5.31720100	0.43210100	-0.50068600

H	2.89482800	-1.41710000	2.52977000
H	5.09985500	-0.58010400	1.75515300
H	-0.20700600	2.14152500	1.48058600
H	-0.70411600	2.35203700	-1.55395600
H	-2.91976900	2.37465400	1.37987100



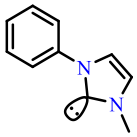
C	-1.41782400	-2.60557100	0.02486100
C	-0.65514200	-1.49082600	-0.30814500
C	-1.24997800	-0.22978900	-0.26278500
C	-2.59015400	-0.05647900	0.11248700
C	-3.33105200	-1.18933100	0.43509900
C	-2.75336600	-2.45707300	0.39251200
H	-0.96132900	-3.58914800	0.00044100
H	0.38978400	-1.61298800	-0.56880800
C	-3.18411300	1.32885800	0.11742500
H	-4.37227300	-1.07403000	0.72293500
H	-3.34594600	-3.32846100	0.65144100
C	-2.11403600	2.34202400	0.52277300
C	-0.88128800	2.12653400	-0.28052400
H	-3.56976300	1.57297600	-0.88145100
H	-2.44783300	3.37528100	0.40722000
N	-0.49487100	0.94659900	-0.63357200
C	0.76686200	0.78906100	-1.40194400
H	0.56927700	0.06403100	-2.19497400
H	0.96052300	1.75651200	-1.87317600
C	1.93030900	0.35681800	-0.53416800
C	2.89446300	-0.48864900	-1.08742300
C	2.08396000	0.81817000	0.77376300
C	4.00842100	-0.86340900	-0.33967300
H	2.77915500	-0.85315300	-2.10603700
C	3.19427900	0.43525700	1.52381000
H	1.34060800	1.47113800	1.22678100
C	4.15808600	-0.40388300	0.96779600
H	4.75528800	-1.51778000	-0.77776800
H	3.30559200	0.79355100	2.54221900
H	5.02242900	-0.70066200	1.55306800
H	-4.02821300	1.38171100	0.80868300
H	-1.83760900	2.20668700	1.58141600
H	-0.25215900	2.95786700	-0.59216300



C	1.18087600	2.47864900	-0.97106300
C	0.58509000	1.23225500	-1.07445000
C	1.14859200	0.14970000	-0.39188700
C	2.33882500	0.25998700	0.33223900
C	2.91176400	1.53422600	0.42655500
C	2.33871000	2.63250900	-0.20086000
H	0.75431000	3.32567800	-1.49772400
H	-0.30566000	1.09278600	-1.67939800
C	3.04629000	-0.93802400	0.93051100
H	3.83210500	1.65165500	0.99298500
H	2.80579500	3.60818200	-0.11336600
C	2.30014100	-2.26112500	0.72275500
C	1.54656500	-2.25202400	-0.60458300
H	4.03519200	-0.99790000	0.45966600
H	3.00081300	-3.10043400	0.73047100
H	1.01684100	-3.18874200	-0.78531200
N	0.55094400	-1.15749400	-0.51812800
C	-0.71904600	-1.43056600	-0.47737600
C	-1.84399300	-0.59508600	-0.10284600
C	-3.10091200	-1.00049800	-0.58698400
C	-1.75642200	0.49208300	0.78901200
C	-4.24640200	-0.29578900	-0.23877300
H	-3.17429500	-1.86315300	-1.24473600
C	-2.90908500	1.16685400	1.15886800
H	-0.80076200	0.79095600	1.20638900
C	-4.14927700	0.78673900	0.63417100
H	-5.21088300	-0.59983100	-0.63111900
H	-2.84656800	1.99227100	1.86021300
H	-5.04421200	1.32973700	0.92208800

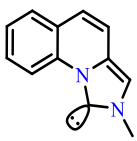
H	3.22537000	-0.76932600	1.99707000
H	1.57786900	-2.43509100	1.52833300
H	2.20617900	-2.03339200	-1.44961000
H	-0.95900600	-2.46028400	-0.74078600

2.7



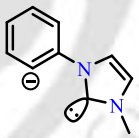
C	-1.13570	-1.41795	-0.04349
C	-2.28435	-0.59544	-0.03463
C	-3.61461	-1.08173	-0.06624
C	-3.77753	-2.46998	-0.12151
C	-2.66127	-3.31285	-0.14761
C	-1.36494	-2.80866	-0.11070
H	-4.77901	-2.88891	-0.14772
H	-2.80938	-4.38684	-0.19997
H	-0.51890	-3.48459	-0.13681
C	-3.13300	1.70476	0.04854
N	-2.10114	0.76414	0.00708
C	-2.5004	2.92255	0.111630
C	-0.87924	1.37301	0.03126
N	-1.13442	2.71316	0.10633
H	-2.91376	3.91729	0.16342
C	-0.11375	3.76904	0.17139
H	-0.24052	4.43895	-0.65327
H	-0.21756	4.30939	1.08908
H	0.85976	3.32736	0.12572
H	-4.45441	-0.41892	-0.04869
H	-4.18640	1.51757	0.03427
H	-0.14766	-1.00938	-0.00159

2.8



C	-1.38745	-1.65236	0.00049
C	-0.82606	-0.37059	0.00008
C	-1.63470	0.79146	-0.00027
C	-3.03565	0.61799	-0.00049
C	-3.59761	-0.64939	-0.00028
C	-2.77122	-1.78563	0.00027
H	-3.67036	1.49974	-0.00078
H	-4.67692	-0.76533	-0.00045
H	-3.21089	-2.77822	0.00059
C	-1.03007	2.10295	-0.00006
C	0.31864	2.26581	0.00037
C	1.15621	1.10891	0.00026
N	0.57681	-0.17144	0.00014
C	2.52290	0.91232	0.00021
C	1.56709	-1.08840	-0.00010
C	4.06179	-1.09146	-0.00032
H	4.61163	-0.79252	0.89470
H	3.92634	-2.17342	-0.00037
H	4.61140	-0.79236	-0.89541
N	2.74194	-0.44391	-0.00017
H	-1.68467	2.96934	-0.00008
H	0.78298	3.24573	0.00078
H	3.33287	1.62548	-0.00019
H	-0.76521	-2.54151	0.00105

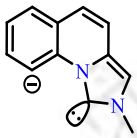
1.76



C	-1.57303	1.06742	0. 00000
C	-0.17787	1.06742	0. 00000
C	0.51966	2.27517	0. 00000
C	-0.17799	3.48368	-0.00120
C	-1.57281	3.48360	-0.00168
C	-2.27042	2.27539	-0.00068
H	-2.12279	0.11510	0.00045
H	0.37221	4.43582	-0.00126
H	-2.12294	4.43588	-0.00263
H	-3.37002	2.27557	-0.00086
N	0.55670	-0.20589	0.00176
C	0.96239	-0.90868	-1.12899
C	0.96117	-0.90652	1.13429

C	1.63080	-2.06685	0.72150
H	0.74863	-0.53807	2.13704
H	2.06711	-2.82276	1.36574
N	1.6316	-2.06813	-0.71338
C	2.22375	-3.09404	-1.58388
H	3.15940	-3.41273	-1.17413
H	1.56034	-3.93085	-1.65125
H	2.38252	-2.68528	-2.55990

1.77



C	-1.1357	-1.41795	-0.04349
C	-2.28435	-0.59544	-0.03463
C	-3.61461	-1.08173	-0.06624
C	-3.77753	-2.46998	-0.12151
C	-2.66127	-3.31285	-0.14761
C	-1.36494	-2.80866	-0.11070
H	-4.77901	-2.88891	-0.14772
H	-2.80938	-4.38684	-0.19997
H	-0.51890	-3.48459	-0.13681
C	-4.70108	-0.12254	-0.03697
C	-4.47956	1.21773	0.02157
C	-3.13300	1.70476	0.04854
N	-2.10114	0.76414	0.00708
C	-2.50040	2.92255	0.11163
C	-0.87924	1.37301	0.03126
N	-1.13442	2.71316	0.10633
H	-5.71762	-0.50275	-0.05937
H	-5.29588	1.93037	0.04823
H	-2.91376	3.91729	0.16342
C	-0.11375	3.76904	0.17139
H	-0.24052	4.43895	-0.65327
H	-0.21756	4.30939	1.08908
H	0.85976	3.32736	0.12572

2.9a + Ru-1-I2

Ru	-0.54528100	-0.49927600	0.02024600
C	-3.19397600	3.12511100	0.94627600
C	-4.44450200	2.60363000	0.62234200
C	-4.54192800	1.27494500	0.15410600
C	-3.32633000	0.57826600	0.05061200
C	-2.05335900	1.05009000	0.37918400
C	-2.00680800	2.36396500	0.83264500
H	-6.70621800	1.10620400	-0.13201600
H	-3.12496200	4.15523700	1.30579400
H	-5.34663900	3.21045200	0.72988800
C	-5.75677200	0.57076700	-0.21111100
H	-1.05548800	2.81479200	1.11479400
C	-4.50841700	-1.44086000	-0.73890300
C	-5.75498400	-0.73072600	-0.63626900
H	-6.68221000	-1.24305500	-0.89457500
C	-2.24418500	-1.45827700	-0.51179400
C	-4.03719000	-2.69879000	-1.07761400
N	-3.36864400	-0.72684800	-0.40616000
N	-2.65268700	-2.67644300	-0.92670600
H	-4.55960000	-3.59176000	-1.40522700
C	-1.77471100	-3.81085900	-1.18109100
H	-0.76269000	-3.53744100	-0.85822500
H	-2.11936600	-4.67878700	-0.60183300
H	-1.77996800	-4.05715500	-2.25311900
O	0.32236000	-2.04141100	0.19138200
Cl	-1.15859300	-0.86349500	2.37249500
C	1.34578800	1.33670800	2.08061800
C	1.80093300	0.65715800	0.93361700
C	2.18866800	1.37819000	-0.23398600
C	1.96691200	2.79013600	-0.25129400
C	1.52363500	3.41962100	0.90510500
C	1.22147400	2.71621900	2.08366000
H	1.07214400	0.74619300	2.95464200
H	2.04757500	-0.39662600	1.03025600
C	2.21798400	3.57868900	-1.51390500
H	1.39424100	4.50603900	0.88039000
H	0.87203700	3.24523100	2.97184500
C	3.28356000	2.90829800	-2.37477600
C	2.92589500	1.44337100	-2.57890000
H	1.27731100	3.64169100	-2.09118000

H	3.37219800	3.40398400	-3.35399000
N	2.77071700	0.74665800	-1.30699400
C	2.91913500	-0.70081900	-1.32873400
H	1.95571600	-1.20188600	-1.14883600
H	3.21688200	-0.97272700	-2.35277700
C	3.95328300	-1.24041100	-0.35872500
C	5.17279500	-0.57899300	-0.16596700
C	3.70162400	-2.42478200	0.34583900
C	6.13153700	-1.09909500	0.70525200
H	5.36056200	0.35990700	-0.69265300
C	4.66121700	-2.94787800	1.21707500
H	2.73213600	-2.91667700	0.23200000
C	5.87965300	-2.28828600	1.39714100
H	7.07829400	-0.57240400	0.84961100
H	4.44895100	-3.86738400	1.76807300
H	6.62773300	-2.69307500	2.08313400
H	2.50133800	4.61311800	-1.26434100
H	4.26702200	2.97647200	-1.87933500
H	3.72047700	0.93558100	-3.14561800
O	-0.18044900	0.24715500	-1.48649300
H	1.99439000	1.35977700	-3.17245900

int-1

Ru	-0.77264100	-0.27840700	0.03482600
C	-3.77920100	3.17218000	-0.37801300
C	-4.96041900	2.44241900	-0.47012200
C	-4.90665500	1.03189500	-0.43190600
C	-3.62406800	0.47368700	-0.29799000
C	-2.40121500	1.15248700	-0.18344200
C	-2.52009700	2.54296100	-0.24127300
H	-7.03796600	0.56532200	-0.61417100
H	-3.82297400	4.26387000	-0.41243600
H	-5.92344300	2.94805600	-0.57309300
C	-6.04085000	0.12990000	-0.51180600
H	-1.63530200	3.17649100	-0.18089200
C	-4.59394600	-1.80399900	-0.31800800
C	-5.90490700	-1.23035000	-0.45718400
H	-6.77173600	-1.88959500	-0.51209100
C	-2.34583400	-1.52407000	-0.12523700
C	-3.99906900	-3.04931400	-0.21050600
N	-3.53490500	-0.91014700	-0.26229600
N	-2.62564200	-2.84304900	-0.09685800
H	-4.42704200	-4.04646800	-0.20923800
C	-1.64330300	-3.90007300	0.10110300
H	-0.64547200	-3.48130400	-0.07717400
H	-1.70078900	-4.27416500	1.13389100
H	-1.84140200	-4.72019100	-0.60249600
O	0.50000900	-1.64670300	-0.00450400
Cl	-1.15024000	-0.39478300	2.37647800
C	1.88154100	0.99581400	2.73016700
C	2.42249300	0.40581900	1.60089700
C	2.08261800	0.86579000	0.30078500
C	1.12501400	1.92790900	0.18299300
C	0.63570600	2.52481100	1.36533400
C	0.98679100	2.07125800	2.62591900
H	2.16417100	0.61527600	3.71417500
H	3.14772100	-0.39768900	1.71419500
C	0.91477600	2.59151600	-1.16681900
H	-0.04383900	3.37415000	1.26952300
H	0.56404200	2.53268500	3.51903900
C	2.16020000	2.41620100	-2.03561400
C	2.52313300	0.94179800	-2.13285800
H	0.05269900	2.15783000	-1.69507000
H	1.99090100	2.81549400	-3.04737800
N	2.69656000	0.34672800	-0.81372200
C	3.40035700	-0.91547000	-0.76893400
H	2.91273900	-1.57266800	-0.03303700
H	3.25043000	-1.41886500	-1.73862900
C	4.88970700	-0.81430700	-0.48523800
C	5.49658600	0.40323800	-0.15826700
C	5.68260000	-1.97052500	-0.54050500
C	6.86820700	0.46617200	0.10782500
H	4.88383800	1.30495800	-0.10841900
C	7.05091900	-1.91115000	-0.27446000
H	5.21923900	-2.92850200	-0.79560100
C	7.64992700	-0.68918300	0.05105000
H	7.32615700	1.42505300	0.36332400

H	7.65446400	-2.82110600	-0.32216400
H	8.72140300	-0.64053500	0.25946200
H	0.69597700	3.65984400	-1.01497900
H	3.00617900	2.97465800	-1.59859500
H	3.47084100	0.82096400	-2.68321500
O	-0.43197000	-0.16810700	-1.75273800
H	1.73697900	0.39692500	-2.68668400

TS-1

Ru	0.78323300	0.31143600	0.11607800
C	3.81270100	-3.16247200	-0.07007500
C	4.99012400	-2.43096200	-0.20018500
C	4.92770500	-1.01892700	-0.23426300
C	3.63875700	-0.46749200	-0.13569700
C	2.41937500	-1.14420300	0.00037700
C	2.54788200	-2.53398900	0.02934100
H	7.05513700	-0.53812700	-0.42255700
H	3.86708300	-4.25426700	-0.04206600
H	5.95674700	-2.93529100	-0.27260100
C	6.05176700	-0.11078000	-0.34855400
H	1.66049500	-3.16348600	0.13766700
C	4.58446200	1.81655700	-0.25822900
C	5.90157300	1.25084800	-0.36047300
H	6.76223900	1.91542100	-0.44207700
C	2.33740800	1.52902400	-0.06087300
C	3.97669000	3.06371300	-0.21872700
N	3.53632500	0.91799900	-0.16007900
N	2.60777900	2.85310700	-0.09817500
H	4.39826900	4.06271800	-0.26343700
C	1.60410300	3.90429600	-0.00161500
H	0.61540100	3.42628700	0.02499900
H	1.75925500	4.48323800	0.92037300
H	1.68077200	4.57067900	-0.87276300
O	-0.49554200	1.60761400	0.15366900
Cl	0.90365600	0.10684500	2.46621700
C	-2.22960900	-1.57311400	2.42164000
C	-2.57942200	-0.69340000	1.40706700
C	-2.21075800	-0.95537400	0.06782800
C	-1.50629400	-2.15429900	-0.24096300
C	-1.17336700	-3.01718000	0.80943100
C	-1.51732600	-2.74013900	2.13081400
H	-2.50015500	-1.33475800	3.45174300
H	-3.12272300	0.21394200	1.65615500
C	-1.12604300	-2.50362500	-1.66061600
H	-0.63382400	-3.93742500	0.57051100
H	-1.22824300	-3.42568700	2.92941000
C	-1.89634600	-1.66325100	-2.67949000
C	-1.95326600	-0.21483700	-2.22631600
H	-0.04810000	-2.31539900	-1.78952700
H	-1.41508100	-1.71761700	-3.66674900
N	-2.51901300	-0.04601600	-0.94803400
C	-3.22528300	1.18834100	-0.63759800
H	-2.71177500	1.70154100	0.18827300
H	-3.10876600	1.84634300	-1.51098800
C	-4.69753100	0.98855000	-0.33709000
C	-5.42515700	-0.06742600	-0.90000400
C	-5.35947700	1.89570900	0.50109900
C	-6.78923200	-0.21005100	-0.63558700
H	-4.91499000	-0.79045600	-1.53984400
C	-6.72450300	1.75850200	0.76292400
H	-4.79625300	2.71488400	0.95724700
C	-7.44414000	0.70358600	0.19474000
H	-7.34285600	-1.04186700	-1.07797300
H	-7.22606600	2.47294100	1.42027100
H	-8.51045700	0.59016500	0.40391500
H	-1.29716900	-3.57800800	-1.83237700
H	-2.92763500	-2.04753000	-2.79583300
H	-2.39883500	0.47914900	-2.94902600
O	0.53473900	-0.07142200	-1.70428800
H	-0.69484700	0.09223400	-2.08038100

***endo*-int-2**

Ru	-3.24642500	-0.24972900	-0.39870200
C	-1.59719800	3.44265400	-2.21460700
C	-0.61569700	3.79447900	-1.29102700
C	-0.41766600	3.00809400	-0.13293600
C	-1.26305900	1.89519300	0.01082700
C	-2.24882900	1.50281500	-0.90184000

TH-3565_186122020

C	-2.41039500	2.30313800	-2.03050200
H	1.23899100	4.11032700	0.78397300
H	-1.73800200	4.05895100	-3.10592100
H	0.01121400	4.67376700	-1.45711700
C	0.58953500	3.23773500	0.88508300
H	-3.16149800	2.03407300	-2.77615200
C	-0.09266200	1.23826600	2.07144200
C	0.75303100	2.39324000	1.94774300
H	1.51851900	2.57759000	2.70056600
C	-1.80381400	-0.06973600	1.26960600
C	-0.23077800	0.13781300	2.89734500
N	-1.07441000	1.06509100	1.10605300
N	-1.26584600	-0.63140400	2.37859500
H	0.30735700	-0.15068400	3.79492400
C	-1.69770400	-1.90191400	2.94585300
H	-2.15418100	-1.74142900	3.93405400
H	-2.42551900	-2.35352400	2.25860900
H	-0.82958900	-2.56836700	3.05271200
O	-3.98578100	-0.33411600	-1.99540000
O	-4.59486600	0.65884900	0.54614000
Cl	-3.76608400	-2.54140300	0.21673500
C	5.28440100	-1.81356200	-2.15951400
C	4.30655500	-1.74121200	-1.16936200
C	4.40237700	-0.78522400	-0.13647700
C	5.50619100	0.10976600	-0.12091500
C	6.45974700	0.02123300	-1.13640700
C	6.36794300	-0.93194200	-2.15467000
H	5.18620000	-2.56147300	-2.94995400
H	3.45428800	-2.41682600	-1.21971400
C	5.63627200	1.11460700	0.99849800
H	7.30186700	0.71920400	-1.12059600
H	7.12896900	-0.98072200	-2.93601900
C	4.24859500	1.55249200	1.48798000
C	3.41548300	0.35513300	1.76754700
H	6.18356700	0.65959300	1.84405300
H	4.32480000	2.17663900	2.39199900
N	3.43560100	-0.70154600	0.87298900
C	2.38530400	-1.69595300	0.96619200
H	2.82260200	-2.70271800	0.86544200
H	1.97350200	-1.64050500	1.98634900
C	1.25509400	-1.53881600	-0.03621700
C	0.31038200	-2.56606100	-0.16328900
C	1.14057500	-0.40227300	-0.84761900
C	-0.73468500	-2.46366200	-1.08114700
H	0.39455000	-3.46071700	0.46074400
C	0.10564900	-0.30188000	-1.77666700
H	1.87457900	0.39931000	-0.75837900
C	-0.84627000	-1.32442500	-1.89136000
H	-1.47974500	-3.25490100	-1.15348200
H	0.03052100	0.58267000	-2.41036800
H	-1.64183800	-1.25556200	-2.63572800
H	6.23093100	1.97870100	0.66260800
H	3.78165700	2.19125600	0.70483400
H	-4.37262600	0.64732900	1.49167400
H	2.63250800	0.32714400	2.51855800

***endo*-int-3**

Ru	-3.56647700	-0.22089000	-0.12724600
C	-2.17017100	3.87232800	-1.21655800
C	-1.02008700	3.96891600	-0.43648600
C	-0.64972600	2.89236600	0.40297800
C	-1.51395400	1.78757300	0.38138700
C	-2.68368700	1.64828500	-0.37457800
C	-2.99969600	2.72468500	-1.19687800
H	1.19958900	3.67046100	1.27965200
H	-2.44208200	4.70869600	-1.86543000
H	-0.39865100	4.86665800	-0.47341800
C	0.52361500	2.81258100	1.24858000
H	-3.88334000	2.68414300	-1.83746100
C	-0.06430500	0.56764700	1.94495700
C	0.81360600	1.70254500	1.99785600
H	1.70504500	1.65712100	2.61996200
C	-1.93505500	-0.44232100	1.10146000
C	-0.15409400	-0.72083100	2.45876200
N	-1.17691800	0.68243900	1.13840500
N	-1.29052800	-1.30323800	1.92777200
H	0.48923500	-1.25552400	3.14979000

C	-1.72780800	-2.66156100	2.22742100
H	-2.15251500	-2.70343200	3.24111700
H	-2.48814500	-2.95054900	1.48947900
H	-0.86517300	-3.33891400	2.16239900
O	-3.78522200	-0.22236200	-2.00480100
O	-4.81541500	0.32998800	0.84644900
Cl	-3.95368500	-2.64534800	-0.38568900
C	5.74530300	-0.81058900	-2.50699900
C	4.67764800	-1.07040900	-1.64968100
C	4.72497900	-0.65454300	-0.30307500
C	5.86902000	0.04423900	0.16773500
C	6.91350400	0.30455000	-0.72038900
C	6.87074000	-0.11900900	-2.05211600
H	5.68555800	-1.14198000	-3.54642700
H	3.79453900	-1.57421300	-2.04005800
C	5.92750700	0.46787900	1.61444800
H	7.78733000	0.84911700	-0.35111100
H	7.70252300	0.09467600	-2.72630900
C	4.51794500	0.83888200	2.10601300
C	3.56292900	-0.25820800	1.79375800
H	6.31373100	-0.36245200	2.23378100
H	4.51248300	1.04428700	3.18733600
N	3.67311200	-0.91960800	0.58345400
C	2.60685400	-1.83107800	0.21393400
H	3.04245600	-2.68378900	-0.33129700
H	2.19093000	-2.24553700	1.14686100
C	1.47989400	-1.22674100	-0.60642700
C	0.36549300	-2.01863100	-0.91284100
C	1.52785600	0.08860500	-1.08471800
C	-0.67912000	-1.51314800	-1.69009300
H	0.30806700	-3.04464600	-0.53597400
C	0.48862500	0.59313100	-1.87117200
H	2.38328100	0.71912000	-0.84103500
C	-0.61530700	-0.20421000	-2.18038500
H	-1.55438400	-2.13353100	-1.88836300
H	0.53365800	1.62272300	-2.23204800
H	-1.44639500	0.19047200	-2.76456800
H	6.62767100	1.30936800	1.73615600
H	4.21585200	1.78182900	1.60207200
H	2.91859400	-0.72453000	2.53774500
H	-4.09182800	-1.12525100	-2.21927400

***endo*-int-4**

Ru	1.60643100	0.69987600	-1.38688500
C	0.26295900	3.14416000	2.00377100
C	0.79908000	2.42775400	3.07306300
C	1.58102900	1.27714400	2.82891800
C	1.74957800	0.92509900	1.48106800
C	1.19700300	1.59461500	0.37755900
C	0.45625700	2.74156100	0.66532400
H	2.08793400	0.69987400	4.88176500
H	-0.32667000	4.04191100	2.20422300
H	0.62571400	2.75641500	4.10030000
C	2.22311800	0.44014300	3.82926200
H	0.00777300	3.33419400	-0.13347400
C	3.16252900	-0.99219900	2.11013300
C	2.98005100	-0.64887800	3.49556200
H	3.45015400	-1.26413900	4.26352400
C	2.74111300	-0.53985000	-0.10160000
C	3.80694200	-1.93976000	1.33706800
N	2.53316200	-0.17240500	1.18350600
N	3.52488000	-1.63559800	0.00486400
H	4.42807500	-2.78463100	1.61726000
C	4.00746300	-2.39369600	-1.13683500
H	3.72941600	-3.45238500	-1.03255900
H	3.54049700	-1.98438900	-2.04029100
H	5.10089300	-2.30846300	-1.22221500
O	0.40665700	1.75034100	-2.51891800
O	0.38117800	-0.75625200	-1.39991300
Cl	3.50017700	1.95615200	-1.83807600
C	-3.07785800	-2.75645800	2.14427000
C	-2.78959800	-1.63892000	1.36141500
C	-2.12171600	-1.77132300	0.12577700
C	-1.74779500	-3.07041500	-0.30891500
C	-2.05618100	-4.17093000	0.49413900
C	-2.71431500	-4.03470300	1.71873800
H	-3.60019700	-2.61918900	3.09454700

H	-3.10704800	-0.65736700	1.70794800	C	3.26905000	2.85838500	0.41824700
C	-0.99728000	-3.24932700	-1.60733800	H	1.26835000	-0.41426000	-3.36268700
H	-1.76551400	-5.16559400	0.14223100	C	2.64118300	1.17305500	2.04472500
H	-2.94395100	-4.91306000	2.32575300	C	3.23390800	2.44204600	1.71996100
C	-1.23531100	-2.07395700	-2.54914200	H	3.63541700	3.06351000	2.52107200
C	-0.98216700	-0.76655900	-1.80828200	C	1.60537200	-0.75403200	1.34375600
H	0.08474400	-3.30995000	-1.39515600	C	2.37064000	0.38974500	3.15290600
H	-0.57157700	-2.12045300	-3.42475000	N	2.15458500	0.42845400	0.98129500
N	-1.85366600	-0.65182100	-0.66751300	N	1.74386700	-0.76640900	2.68857900
C	-2.05710400	0.68046300	-0.13770500	H	2.57041000	0.55451000	4.20683200
H	-1.60378300	0.78183800	0.86315800	C	1.29522700	-1.87530400	3.51749500
H	-1.49572800	1.36363100	-0.78971000	H	1.63780700	-1.72320700	4.54846300
C	-3.50121000	1.14153900	-0.08458000	H	0.19784600	-1.93961300	3.50138600
C	-3.86132100	2.18305700	0.78187500	H	1.71557100	-2.81243800	3.12762300
C	-4.48098500	0.57986600	-0.91041600	O	0.36716417	-2.96469766	-2.33326798
C	-5.17269700	2.66208300	0.81520100	O	-0.82671065	-1.40629060	-0.08848867
H	-3.10296700	2.61816200	1.44001200	Cl	3.10856000	-2.86234900	-0.22214400
C	-5.79486000	1.05376700	-0.87640100	C	-5.39013000	1.62872900	0.45776900
H	-4.20448800	-0.24335400	-1.57207500	C	-4.24103500	1.38524700	-0.29336600
C	-6.14528600	2.09767200	-0.01580300	C	-3.62728300	0.11480500	-0.29002800
H	-5.43887000	3.47415000	1.49667300	C	-4.19470700	-0.90991500	0.51255100
H	-6.55094600	0.60216000	-1.52365000	C	-5.35046300	-0.63865600	1.24829400
H	-7.17348200	2.46641300	0.01223500	C	-5.95889400	0.61867500	1.23477800
H	-1.28366700	-4.20071400	-2.08271100	H	-5.83984800	2.62457000	0.43288500
H	-2.27611300	-2.06824900	-2.91334100	H	-3.81368200	2.19845700	-0.87707000
H	-1.15303500	0.10412600	-2.46014700	C	-3.53200900	-2.26404900	0.56613000
H	0.23492700	2.65432500	-2.22142800	H	-5.77959100	-1.44357100	1.85260600
	***endo*-TS-2**			H	-6.85984000	0.80546000	1.82294000
Ru	1.36993052	-1.90621540	-0.43954811	C	-2.80211800	-2.54647400	-0.74085200
C	2.19245500	1.50918900	-2.97356700	C	-1.83242300	-1.41424100	-1.04795700
C	2.72357800	2.39569200	-2.03908600	H	-2.79570500	-2.28605400	1.38952000
C	2.74049700	2.05323200	-0.66893900	H	-2.22908100	-3.48329000	-0.70313100
C	2.18933500	0.80671900	-0.34454700	N	-2.49339100	-0.13597300	-1.06735800
C	1.66092200	-0.12415600	-1.25416200	C	-1.78772900	0.95213200	-1.70831100
C	1.66920500	0.25245200	-2.59720300	H	-1.00875300	0.50124500	-2.34014400
H	3.70529200	3.82961700	0.17445300	H	-4.27709200	-3.04483300	0.78357400
H	2.18436500	1.78909700	-4.02970900	H	-3.52061100	-2.62221700	-1.57418200
H	3.12607600	3.35912700	-2.35972100	H	-1.45448107	-2.06112557	-2.41627723

H	1.13679900	-2.62529800	-2.75610200
H	-2.46219300	1.49163400	-2.39745200
C	-1.13057000	1.96169200	-0.78053800
C	-0.73000700	3.20247500	-1.29236700
C	-0.91055500	1.68703600	0.57464700
C	-0.12035800	4.15238200	-0.47062200
H	-0.89855600	3.42816500	-2.34946200
C	-0.31186900	2.64003700	1.40077800
H	-1.20365700	0.71564300	0.97151000
C	0.08650700	3.87489700	0.88293700
H	0.18976300	5.11388900	-0.88755000
H	-0.15049600	2.41254600	2.45694200
H	0.55871500	4.61688100	1.53068100

2.10a + Ru-1-I1

Ru	1.06822900	-0.99013300	0.13887600
C	1.11039000	3.39358300	-0.47801800
C	2.48443600	3.63181500	-0.48100300
C	3.37016700	2.54118500	-0.32162900
C	2.76913200	1.28796200	-0.14625300
C	1.38968500	0.97808100	-0.12468900
C	0.56438100	2.09960500	-0.30943300
H	5.31119000	3.55114600	-0.47832100
H	0.42509900	4.23322800	-0.62583200
H	2.87661900	4.64168900	-0.62203900
C	4.82536100	2.58039800	-0.34964400
H	-0.51845400	1.98832300	-0.35653500
C	4.97156300	0.16814100	-0.08136000
C	5.59924300	1.45518900	-0.24037100
H	6.68758900	1.51789400	-0.28160600
C	3.01823500	-1.04391200	0.10843200
C	5.29938800	-1.16964100	0.02227000
N	3.58732700	0.18614300	-0.01850900
N	4.09557000	-1.87979300	0.13468300
H	6.26158700	-1.67147400	0.02150900
C	3.99365500	-3.32197700	0.22929900
H	4.50778300	-3.69176300	1.12997700
H	2.93050100	-3.58708100	0.28426900
H	4.43115600	-3.79960000	-0.66042200
O	1.08167000	-0.60270200	2.30745700
Cl	0.83335700	-1.75558200	-2.06889700
C	-4.22274000	1.72417500	-2.34978600
C	-3.54073800	0.87363900	-1.47794000
C	-3.05161800	1.36552200	-0.25997600
C	-3.25139000	2.71783300	0.08603600
C	-3.94317900	3.54760300	-0.79878200
C	-4.42789900	3.06331900	-2.01598900
H	-4.59775300	1.32754100	-3.29561600
H	-3.40376900	-0.17210900	-1.74682500
C	-2.68781200	3.21095100	1.39224500
H	-4.09675300	4.59501800	-0.52566500
H	-4.96315200	3.72789000	-2.69727500
C	-2.76883000	2.09789900	2.43239100
C	-2.10413900	0.83400700	1.93367500
H	-1.63092100	3.50488300	1.25468400
H	-2.28821700	2.36175400	3.38280200
N	-2.30850400	0.52225500	0.61589100
C	-1.73498300	-0.71083400	0.08619800
H	-1.30213500	-0.51172100	-0.90284000
H	-0.92016400	-0.99285300	0.79152700
C	-2.68754800	-1.88696700	0.02658800
C	-2.40050000	-2.94721600	-0.84626400
C	-3.82149100	-1.95697600	0.84349800
C	-3.24076700	-4.06155300	-0.89350200
H	-1.51325200	-2.88773500	-1.48267300
C	-4.66268500	-3.07146700	0.79032500
H	-4.05645300	-1.13409100	1.52129100
C	-4.37424000	-4.12771800	-0.07728700
H	-3.00971200	-4.88164400	-1.57773800
H	-5.54736400	-3.11317800	1.43039800
H	-5.03274100	-4.99863800	-0.11962700
H	-3.22639400	4.10661100	1.73404500
H	-3.82590500	1.85669000	2.64566000
O	-1.43453400	0.12315100	2.68438100
H	1.53750300	0.24630500	2.41434900
H	0.14666400	-0.40602000	2.56987700

***exo*-int-2**

TH-3565_186122020

Ru	-2.85453600	-0.50029600	0.01315500
C	-0.55975000	-0.56224800	-3.77054700
C	0.22362100	0.58149800	-3.64402500
C	0.10844000	1.39290300	-2.49232000
C	-0.81269400	0.96424200	-1.52090400
C	-1.61648600	-0.17928300	-1.61185400
C	-1.47807400	-0.94332900	-2.76891900
H	1.54823500	2.96013000	-3.00394500
H	-0.46566900	-1.17780100	-4.66858200
H	0.92557700	0.86334100	-4.43256100
C	0.84488200	2.61609400	-2.24161700
H	-2.08652000	-1.84127500	-2.89016300
C	-0.23157700	2.88260700	-0.08889800
C	0.68547500	3.34248700	-1.09392500
H	1.25039300	4.25912900	-0.92152900
C	-1.77311700	1.34135500	0.63913900
C	-0.65299900	3.24751600	1.17692300
N	-0.94308700	1.72247600	-0.36541700
N	-1.58115000	2.29332500	1.58370800
H	-0.38055000	4.09232300	1.80193200
C	-2.27545800	2.31560300	2.86586100
H	-2.97705700	3.16254900	2.90234500
H	-2.82238900	1.36829600	2.97294100
H	-1.54430900	2.41932900	3.68068400
O	-3.53816700	-1.97593600	-0.69761900
O	-4.26313700	0.58935100	-0.64482300
Cl	-3.60081000	-0.89897400	2.30992400
C	4.76345400	-2.69646000	1.03254100
C	3.70199800	-1.82554600	1.25023600
C	3.78735300	-0.47505200	0.85562000
C	4.98558100	0.00484500	0.27623300
C	6.03878700	-0.89574600	0.06985400
C	5.93985000	-2.23895700	0.42869700
H	4.67246000	-3.73962200	1.34398100
H	2.79506700	-2.18421000	1.73343100
C	5.17141200	1.46795800	-0.07106500
H	6.96074700	-0.52175900	-0.38496100
H	6.77419100	-2.92048900	0.25032600
C	3.86998600	2.26474000	-0.00101500
C	3.06161700	1.82406000	1.21585300
H	5.90221200	1.90043700	0.63627900
H	4.07575800	3.34610300	0.04725700
N	2.70978600	0.41241300	1.07098200
C	1.39958900	0.03339100	1.25581500
C	0.73462000	-1.05093500	0.62523900
C	-0.48966500	-1.53286900	1.19386300
C	1.21842000	-1.70907500	-0.53573300
C	-1.12135500	-2.66811800	0.67861200
H	-0.87063500	-1.09186100	2.11526600
C	0.55282700	-2.81598000	-1.05886600
H	2.11449900	-1.33699100	-1.03106700
C	-0.60149500	-3.31989500	-0.45551000
H	-2.00224500	-3.05823200	1.18824500
H	0.94555400	-3.29219100	-1.96044000
H	-1.11387500	-4.19181300	-0.86373900
H	5.62959000	1.56055000	-1.06914000
H	3.25642700	2.08824000	-0.89727500
H	-4.12521900	1.49441600	-0.32308600
H	2.13235900	2.39878100	1.30383400
H	3.65147600	1.97392100	2.14010300
H	0.82740700	0.66462100	1.94122300

***exo*-int-3**

Ru	-3.54449500	-0.72957300	0.18500200
C	-3.47473100	3.43499500	-1.41931700
C	-2.30715400	3.91752700	-0.83260200
C	-1.54839100	3.07515200	0.01321000
C	-2.06505900	1.78400200	0.20001200
C	-3.23783900	1.25886500	-0.35503800
C	-3.94290900	2.11800700	-1.19173600
H	0.09019500	4.41806200	0.56701400
H	-4.04940300	4.09353300	-2.07545300
H	-1.97107400	4.93919700	-1.02435500
C	-0.30897900	3.40779600	0.68560000
H	-4.85664300	1.77587100	-1.68265800
C	-0.14457600	1.16900200	1.60297500
C	0.36884700	2.50312600	1.45985800

H	1.29271900	2.77699600	1.96887300
C	-1.74839500	-0.38818900	1.12344400
C	0.20967500	-0.03898300	2.19051100
N	-1.34087200	0.89683300	0.97244200
N	-0.77597100	-0.95686700	1.87952500
H	1.07831700	-0.31320300	2.77991900
C	-0.74997400	-2.35194800	2.30266000
H	-0.93905500	-2.41778000	3.38406100
H	-1.52873300	-2.89535400	1.75118900
H	0.23781500	-2.77522600	2.07419200
O	-4.03697100	-1.01816000	-1.61652700
O	-4.72948900	-0.39011800	1.32230300
Cl	-3.36251100	-3.19026800	0.22330400
C	6.85289800	-2.01495100	-1.09129100
C	5.51755800	-1.62856600	-1.00426800
C	5.13936900	-0.48979800	-0.26184500
C	6.15106700	0.29606700	0.34797700
C	7.48408300	-0.10856600	0.23045600
C	7.84911400	-1.26229800	-0.46540100
H	7.11494000	-2.90357600	-1.67059500
H	4.75783700	-2.19663200	-1.54031900
C	5.79721100	1.57000400	1.08101500
H	8.25601000	0.50920100	0.69855400
H	8.89822800	-1.55621500	-0.53679400
C	4.47148100	2.12858300	0.57219600
C	3.41411700	1.04059600	0.63726500
H	5.71365800	1.37321700	2.16609100
H	4.14475400	2.99098700	1.17435500
N	3.78367900	-0.13094500	-0.16409800
C	2.79598000	-1.05965600	-0.45826300
C	1.53447300	-0.76517900	-1.04635700
C	0.53899400	-1.78224000	-1.08512900
C	1.21224700	0.48348200	-1.65581100
C	-0.69755500	-1.56374700	-1.67880200
H	0.75914100	-2.75508300	-0.63715000
C	-0.03140200	0.69386500	-2.23854500
H	1.96876800	1.26749100	-1.70802600
C	-1.00015700	-0.32029100	-2.25465600
H	-1.44466000	-2.35854800	-1.66873200
H	-0.25458000	1.66022500	-2.69693800
H	-1.98265400	-0.15439600	-2.69495200
H	6.60984300	2.30381900	0.96357500
H	4.57830900	2.47563600	-0.46943000
H	3.27616100	0.72624500	1.69174100
H	-4.13098200	-1.98782500	-1.69617000
H	2.44464700	1.40825400	0.28826200
H	3.04078800	-2.10598000	-0.25251800

***exo*-int-4**

Ru	0.77050000	-0.82690400	-1.40035700
C	1.69317800	3.29263000	-0.20804600
C	2.52143000	3.07210200	0.88947700
C	2.82443700	1.75086000	1.29113100
C	2.24434500	0.73058400	0.52321100
C	1.39321900	0.90964300	-0.58140600
C	1.12478500	2.22994600	-0.94248000
H	4.12185700	2.14756000	3.01152000
H	1.45441600	4.31517500	-0.50562700
H	2.93981300	3.91514700	1.44421800
C	3.67177400	1.35862000	2.40426300
H	0.46319100	2.46868100	-1.77484500
C	3.33627600	-0.99217200	1.90662500
C	3.92186700	0.04850600	2.70909700
H	4.56295500	-0.22202100	3.54883200
C	2.01257600	-1.59890400	0.12989600
C	3.31574500	-2.37220900	1.82440900
N	2.52642100	-0.57977400	0.85667400
N	2.50335500	-2.70121500	0.73874800
H	3.80208600	-3.12906300	2.43167700
C	2.22034200	-4.05670300	0.29912100
H	1.75667200	-4.63238900	1.11343600
H	1.52649500	-4.00302400	-0.54795600
H	3.14584100	-4.55660700	-0.02237700
O	-0.46468300	-0.10689500	-2.71967000
O	-0.68291600	-1.25725100	-0.23458000
Cl	2.54145500	-1.09193500	-2.87226300
C	-2.45299600	3.31922200	-1.96856000

C	-2.43950500	2.05556200	-1.38129200	C	2.52559153	0.64522210	0.77901170
C	-1.96663800	1.86329900	-0.06278900	C	1.67446553	0.82428110	-0.32560530
C	-1.58213400	3.01385600	0.67791700	C	1.40603153	2.14458410	-0.68667930
C	-1.62934800	4.27133900	0.07067900	H	4.40310353	2.06219810	3.26732070
C	-2.03669200	4.44447200	-1.25287500	H	1.73566253	4.22981310	-0.24982630
H	-2.81180300	3.42085300	-2.99605800	H	3.22105953	3.82978510	1.70001870
H	-2.79774300	1.21093700	-1.96541300	C	3.95302053	1.27325810	2.66006370
C	-1.10783100	2.87498600	2.10445000	H	0.74443753	2.38331910	-1.51904430
H	-1.32483100	5.13967400	0.66282600	C	3.61752253	-1.07753390	2.16242570
H	-2.05303200	5.43709900	-1.70724900	C	4.20311353	-0.03685590	2.96489770
C	-1.70014100	1.62714800	2.75108100	H	4.84420153	-0.30738290	3.80463270
C	-1.39350400	0.42410500	1.87580600	C	2.29382253	-1.68426590	0.38569670
H	-0.00506100	2.80102700	2.11904900	C	3.59699153	-2.45757090	2.08020970
H	-1.28218000	1.46397200	3.75677700	N	2.80766753	-0.66513590	1.11247470
N	-1.91062600	0.59784200	0.52153400	N	2.78460153	-2.78657690	0.99454870
C	-1.94137500	-0.62336900	-0.25676600	H	4.08333253	-3.21442490	2.68747770
H	-2.16434900	-0.36914800	-1.30180000	C	2.50158853	-4.14206490	0.55492170
C	-3.00466700	-1.58881600	0.25249100	H	2.03791853	-4.71775090	1.36923670
C	-2.78512700	-2.97066000	0.25715500	H	1.80774153	-4.08838590	-0.29215530
C	-4.24739300	-1.09377400	0.67103700	H	3.42708753	-4.64196890	0.23342370
C	-3.79141500	-3.84530800	0.67721500	O	-0.52738849	-0.07991837	-2.62354303
H	-1.81556800	-3.34916700	-0.06744500	O	-0.64318808	-1.41412498	0.21494145
C	-5.25378500	-1.96684400	1.08855200	Cl	2.82270153	-1.17729690	-2.61646230
H	-4.41544600	-0.01456100	0.67402600	C	-2.40499773	3.15818227	-1.51889275
C	-5.02841700	-3.34700400	1.09391100	C	-2.39150673	1.89452227	-0.93162475
H	-3.60775900	-4.92288400	0.67945200	C	-1.91863973	1.70225927	0.38687825
H	-6.21816400	-1.56820800	1.41352800	C	-1.53413573	2.85281627	1.12758425
H	-5.81485000	-4.03097700	1.42242500	C	-1.58134973	4.11029927	0.52034625
H	-1.36628500	3.78222500	2.67337300	C	-1.98869373	4.28343227	-0.80320775
H	-2.79229500	1.73780700	2.86076400	H	-2.76380473	3.25981327	-2.54639075
H	-1.84392100	-0.49075400	2.28978300	H	-2.74974473	1.04989727	-1.51574575
H	-0.43250500	0.84946700	-2.86135100	C	-1.05983273	2.71394627	2.55411725
H	-0.30155500	0.25436600	1.84808900	H	-1.27683273	4.97863427	1.11249325
		***exo*-TS-2**		H	-2.00503373	5.27605927	-1.25758175
Ru	1.05174653	-0.91226590	-1.14455630	C	-1.65214273	1.46610827	3.20074825
C	1.97442453	3.20726810	0.04775470	C	-1.34550573	0.26306527	2.32547325
C	2.80267653	2.98674010	1.14527770	H	0.04293727	2.63998727	2.56871625
C	3.10568353	1.66549810	1.54693170	H	-1.23418173	1.30293227	4.20644425

TH-3565_186122020

N	-1.86262773	0.43680227	0.97120125
C	-1.89337673	-0.78440873	0.19290125
H	-2.10164351	-0.39612463	-1.39792697
C	-2.95666873	-1.74985573	0.70215825
C	-2.73712873	-3.13169973	0.70682225
C	-4.19939473	-1.25481373	1.12070425
C	-3.74341673	-4.00634773	1.12688225
H	-1.76756973	-3.51020673	0.38222225
C	-5.20578673	-2.12788373	1.53821925
H	-4.36744773	-0.17560073	1.12369325
C	-4.98041873	-3.50804373	1.54357825
H	-3.55976073	-5.08392373	1.12911925
H	-6.17016573	-1.72924773	1.86319525
H	-5.76685173	-4.19201673	1.87209225
H	-1.31828673	3.62118527	3.12304025
H	-2.74429673	1.57676727	3.31043125
H	-1.79592273	-0.65179373	2.73945025
H	-0.49521049	0.87644363	-2.76522403
H	-0.25355673	0.09332627	2.29775625

2.10a′ + Ru-1-I1

Ru	-1.07048200	0.87749200	0.54822100
C	-1.19094200	-3.46984900	-0.33469500
C	-2.55071000	-3.64409500	-0.58575200
C	-3.40840700	-2.52133800	-0.52040400
C	-2.79826600	-1.31037700	-0.17176000
C	-1.43384700	-1.06163500	0.10852400
C	-0.63390800	-2.21112400	-0.00267500
H	-5.33268700	-3.41962100	-1.07220300
H	-0.52165300	-4.33137700	-0.41100100
H	-2.94964400	-4.62653600	-0.84949700
C	-4.83534300	-2.48234900	-0.80885500
H	0.44560100	-2.14774300	0.12246100
C	-4.92013200	-0.07827400	-0.45166700
C	-5.56599800	-1.32302500	-0.78321900
H	-6.63023700	-1.32738900	-1.02342300
C	-2.96962700	1.00816000	0.14289100
C	-5.19021900	1.27288500	-0.35484000
N	-3.57533000	-0.17834500	-0.13680100
N	-3.99026500	1.90671100	0.00157200
H	-6.10768200	1.83121100	-0.51053400
C	-3.83242100	3.33516500	0.17355300
H	-4.43373500	3.69995400	1.02148400
H	-2.77176600	3.53959100	0.36666400
H	-4.13372300	3.87025200	-0.73979700
O	-1.32809300	0.34506800	2.68156100
Cl	-0.45975600	1.63657600	-1.59368300
C	2.91897600	-1.45444300	-2.58560000
C	2.42382800	-0.79405300	-1.46645300
C	2.80364100	-1.21889800	-0.18104000
C	3.61145300	-2.35896900	-0.00979100
C	4.08687800	-3.01018300	-1.15726100
C	3.76488200	-2.55965500	-2.43604600
H	2.61988800	-1.11610500	-3.57985500
H	1.71758000	0.03128400	-1.58382200
C	3.89782500	-2.92800800	1.36524400
H	4.71892900	-3.89433500	-1.03378400
H	4.15046700	-3.08280200	-3.31392400
C	3.45698400	-2.00998400	2.50761200
C	2.12317500	-1.34230600	2.17850500
H	3.36578000	-3.89283800	1.44926500
H	3.37190800	-2.57778400	3.44735800
N	2.30108700	-0.54457700	0.96424900
C	1.93694100	0.77888400	0.96772900
C	2.75138600	1.75985500	0.20626500
C	2.17712900	2.98337300	-0.17159600
C	4.11825800	1.53386700	-0.03928900
C	2.95156900	3.95274000	-0.80834100
H	1.11821700	3.15231800	0.00663600
C	4.89067200	2.50973500	-0.66355900
H	4.57945600	0.59511000	0.26757600
C	4.30616400	3.71890500	-1.05760000
H	2.49134100	4.89399200	-1.11659300
H	5.95249900	2.32801900	-0.84413000
H	4.91063300	4.48022100	-1.55686800
H	4.96918000	-3.16916400	1.45818700
H	4.20479700	-1.21702400	2.67512900

H	-1.45488000	-0.61697800	2.64498700
H	-0.37944700	0.47255400	2.87966000
H	1.32734700	-2.09214700	2.03257500
H	1.80728500	-0.66679700	2.98171600
O	1.00228500	1.16945000	1.70471300

***endo*-int-4_6-Me**

Ru	-1.93391700	-0.83028700	-1.20398700
C	-0.62343900	-2.90209700	2.43707900
C	-0.88761800	-1.92981000	3.40112600
C	-1.49095200	-0.70952600	3.02437400
C	-1.77156600	-0.56052800	1.65754600
C	-1.48279100	-1.49388500	0.64927300
C	-0.91671200	-2.69707500	1.07238400
H	-1.62227100	0.28534100	4.97313600
H	-0.17257200	-3.84915300	2.74293700
H	-0.63976200	-2.10999400	4.44964800
C	-1.84753400	0.38768000	3.90905100
H	-0.68049500	-3.48753800	0.35821600
C	-2.74660900	1.66676300	2.05286100
C	-2.44639900	1.52953300	3.45344400
H	-2.70140100	2.34167400	4.13514400
C	-2.69998200	0.78254500	-0.06628100
C	-3.31445200	2.57889300	1.18343800
N	-2.39297800	0.59957000	1.23852100
N	-3.26456000	2.01010100	-0.08972600
H	-3.74077600	3.56123500	1.36055000
C	-3.74505600	2.65205100	-1.30127000
H	-3.23893800	3.61782200	-1.44444200
H	-3.51703700	1.99527800	-2.14885700
H	-4.83197300	2.81218200	-1.24727900
O	-1.02750700	-2.23212400	-2.22101300
O	-0.50607100	0.37631100	-1.56294800
Cl	-4.03696600	-1.79554000	-1.28659700
C	3.37974600	2.53493200	1.33256200
C	2.90529000	1.32980600	0.81382400
C	2.19737800	1.29172500	-0.40268000
C	1.97532900	2.51488000	-1.08799400
C	2.46949600	3.70014900	-0.54294000
C	3.17649700	3.74808500	0.66734300
H	3.92826400	2.52240700	2.27873500
H	3.10837800	0.40969100	1.35841500
C	1.17766200	2.53272500	-2.37092000
H	2.28881100	4.63141700	-1.09073000
C	1.18226100	1.16551800	-3.04658700
C	0.80629300	0.09175900	-2.03257800
H	0.13186800	2.80274900	-2.14116000
H	0.46979300	1.12989200	-3.88356700
N	1.74074900	0.08096700	-0.93689600
C	1.78029000	-1.12187500	-0.13200400
H	1.36455800	-0.94018700	0.87420800
H	1.09948600	-1.83979500	-0.60937600
C	3.14658000	-1.76724000	-0.00089400
C	3.39803500	-2.63834200	1.06831300
C	4.15484500	-1.54688000	-0.94547000
C	4.62988300	-3.28569900	1.18599200
H	2.61776800	-2.80509400	1.81716200
C	5.38985600	-2.18948700	-0.82805800
H	3.96397600	-0.85451100	-1.76773200
C	5.63140700	-3.06273600	0.23607700
H	4.81203500	-3.96165500	2.02542300
H	6.17022100	-2.00411900	-1.57052800
H	6.59825900	-3.56331300	0.32880500
H	1.56621600	3.30909200	-3.04875300
H	2.18303900	0.92789600	-3.44379500
H	0.79914200	-0.90886300	-2.49201300
H	-0.93879100	-3.08384300	-1.77177600
C	3.70989900	5.05190900	1.20549700
H	4.07144400	4.94176300	2.23897900
H	4.55337500	5.42609600	0.59909700
H	2.93848300	5.83975600	1.20045400

***endo*-TS-2_6-Me**

Ru	-1.18986900	0.66416200	-1.10097400
C	-1.67286400	-3.44006000	0.39252300
C	-2.66174900	-3.25095400	1.35774200
C	-3.19163200	-1.95858300	1.57809700
C	-2.64718000	-0.93961700	0.78627300

C	-1.64489400	-1.07519400	-0.19199600
C	-1.16624500	-2.37416200	-0.38420800
H	-4.67276500	-2.36440700	3.14480300
H	-1.27227000	-4.44268400	0.22655600
H	-3.03569500	-4.09775100	1.93826300
C	-4.23958900	-1.58326400	2.51526500
H	-0.39778500	-2.58857900	-1.12765400
C	-4.14346400	0.73701800	1.79559300
C	-4.70199900	-0.29884500	2.62582600
H	-5.49467800	-0.04812400	3.33190200
C	-2.63395600	1.33233400	0.15785100
C	-4.28367000	2.08794400	1.54196000
N	-3.13333400	0.33752700	0.93371100
N	-3.35522800	2.41469400	0.54703500
H	-4.94758100	2.82997600	1.97379100
C	-3.20443900	3.73352100	-0.03906100
H	-3.09640400	4.49144300	0.75055900
H	-2.30253500	3.73033800	-0.66288200
H	-4.07357200	3.98073500	-0.66720900
O	0.39393600	0.00340900	-2.30626400
O	0.28954900	1.38995200	-0.04647900
Cl	-2.74964600	0.54207600	-2.82258800
C	5.89693000	0.42882800	1.71306600
C	4.63111600	-0.00993800	1.32329500
C	3.68861800	0.90141200	0.80764200
C	4.04465600	2.26838300	0.68186100
C	5.32237300	2.67687700	1.06204200
C	6.25367800	1.77241800	1.58359200
H	6.61321900	-0.29453600	2.11020900
H	4.38315400	-1.06809100	1.40042100
C	3.00900900	3.21140000	0.13038600
H	5.58782300	3.73249700	0.95507100
C	2.25323700	2.49338300	-0.98846000
C	1.58927800	1.22843800	-0.46303300
H	2.29217800	3.49654300	0.92216900
H	1.46455700	3.11544500	-1.43292700
N	2.39984200	0.49239400	0.45010000
C	1.85428000	-0.74328700	0.97500700
H	2.18798200	-0.86508900	2.01715100
H	0.76138800	-0.62496400	1.01131500
C	2.17731600	-1.99734900	0.18355000
C	1.80290700	-3.24410200	0.70474200
C	2.78613800	-1.94944300	-1.07572200
C	2.01270300	-4.41511300	-0.02396900
H	1.32237500	-3.29305100	1.68544700
C	2.99112600	-3.12111600	-1.81243000
H	3.11131500	-0.98975100	-1.47963700
C	2.59991000	-4.35700800	-1.29243700
H	1.71146400	-5.37789500	0.39640300
H	3.46410000	-3.06515200	-2.79583700
H	2.75923200	-5.27180500	-1.86786900
H	3.48111700	4.13807500	-0.23021900
H	2.96171500	2.23024500	-1.79188500
H	1.29840400	0.50124800	-1.50857200
H	0.56760900	-0.95011600	-2.31671300
C	7.65515625	2.25455207	2.00192854
H	8.23122342	2.47737741	1.12820348
H	7.56468584	3.13476185	2.60354790
H	8.14331345	1.48650603	2.56469654

2.10ae + Ru-1-I1

Ru	-1.33885500	0.96473700	0.07192300
C	-0.83216600	-3.42638100	-0.16892300
C	-2.16650500	-3.82966800	-0.21095600
C	-3.18164900	-2.84571200	-0.18414200
C	-2.74242100	-1.51868100	-0.09090000
C	-1.41218700	-1.04251300	-0.03565700
C	-0.45187600	-2.06631800	-0.08818400
H	-4.97934700	-4.09348400	-0.33720000
H	-0.04583500	-4.18542200	-0.21432900
H	-2.42907600	-4.88779600	-0.28165000
C	-4.61854600	-3.06369300	-0.27148100
H	0.61128700	-1.82817400	-0.09779800
C	-5.06156600	-0.67346200	-0.21767900
C	-5.52415300	-2.03586800	-0.29252500
H	-6.59383900	-2.23362200	-0.37502300
C	-3.27706900	0.77843000	-0.04790900

C	-5.54951600	0.61849900	-0.24280900
N	-3.69011200	-0.51791400	-0.09396000
N	-4.44529100	1.47645600	-0.13911600
H	-6.56269200	0.99790400	-0.32763000
C	-4.51849000	2.92316100	-0.16738800
H	-5.14138500	3.29833700	0.65926500
H	-3.50082000	3.31946500	-0.06299100
H	-4.93654300	3.27126700	-1.12414300
O	-1.42239300	0.75756900	2.26333300
Cl	-1.07696800	1.56948800	-2.18237000
C	4.35507900	-1.30291400	-1.92918400
C	3.53602300	-0.46662600	-1.16818400
C	3.03899600	-0.90475400	0.06410200
C	3.37420400	-2.19209400	0.53169000
C	4.20016600	-3.00208200	-0.24587500
C	4.70358300	-2.58365200	-1.48725800
H	4.73158400	-0.94106400	-2.88898900
H	3.29955700	0.52908900	-1.53903700
C	2.80205100	-2.64173300	1.85009900
H	4.45422000	-3.99848400	0.12855700
C	2.69728200	-1.44612200	2.79240800
C	1.91941200	-0.31404700	2.15817700
H	1.79513300	-3.07002800	1.69214100
H	2.19958800	-1.68822900	3.73983900
N	2.15765600	-0.08723500	0.83002800
C	1.47594700	1.02040200	0.16878900
H	1.12280200	0.68963000	-0.81669400
H	0.59771300	1.26210100	0.81008200
C	2.28990600	2.29183600	0.04563700
C	1.93143700	3.23358200	-0.93057300
C	3.36242900	2.56401500	0.90215900
C	2.64014800	4.43178900	-1.04043100
H	1.09259800	3.01607500	-1.59754000
C	4.07238400	3.76196500	0.78645300
H	3.65252700	1.83434000	1.66055600
C	3.71264200	4.70011100	-0.18418000
H	2.35437900	5.15844900	-1.80491900
H	4.91044600	3.96182400	1.45864000
H	4.26856300	5.63638200	-0.27525500
H	3.42100900	-3.43581900	2.29221400
H	3.70646200	-1.06423900	3.03078400
O	1.13225200	0.36946900	2.81545200
H	-1.78535500	-0.12676100	2.42489000
H	-0.48611900	0.69323400	2.58294900
C	5.58587500	-3.49193400	-2.30446300
H	6.48906600	-3.78439000	-1.74366600
H	5.05918300	-4.42230000	-2.57483400
H	5.90981500	-3.00664100	-3.23635100

***endo*-int-4_6-CO_2Me**

Ru	1.89701500	1.91907900	-0.20925900
C	-0.17595200	1.16954700	3.58519600
C	0.00406500	-0.20761000	3.71836600
C	0.73851200	-0.92239100	2.74757500
C	1.24826900	-0.16124400	1.68483200
C	1.05868600	1.21678600	1.48734600
C	0.34162200	1.88404700	2.48515100
H	0.58446100	-2.95586200	3.55295100
H	-0.73594800	1.71170800	4.35087900
H	-0.42062600	-0.73827200	4.57374700
C	0.97625000	-2.35645600	2.72798200
H	0.16547500	2.95901300	2.42461400
C	2.14549700	-2.18291900	0.61264300
C	1.63246600	-2.97160200	1.69892600
H	1.76138100	-4.05287900	1.66874200
C	2.47935200	-0.11987500	-0.34190600
C	2.78667500	-2.36009600	-0.59618000
N	1.97561200	-0.80779800	0.70820300
N	2.97121900	-1.09173300	-1.14531200
H	3.07636000	-3.27142500	-1.10824200
C	3.59821100	-0.82968000	-2.42931600
H	3.15735200	-1.47972800	-3.19817200
H	3.41271200	0.21812900	-2.69260400
H	4.68216600	-1.01127700	-2.37733700
O	1.01995400	3.66990700	-0.18581800
O	0.85182400	1.48558400	-1.74724000
Cl	3.86411700	2.53729200	0.81567800

C	-1.52722700	-2.27980100	0.43436200
C	-1.71903300	-0.91447300	0.27100500
C	-1.28808900	-0.25740300	-0.90233200
C	-0.72760100	-1.03677800	-1.95562000
C	-0.50499900	-2.39102100	-1.74120300
C	-0.88937900	-3.04038200	-0.55724000
H	-1.81894800	-2.73834300	1.37928300
H	-2.17505300	-0.34562400	1.07833100
C	-0.33966600	-0.40864400	-3.27903200
H	-0.01210400	-2.97998600	-2.51856800
C	-0.76457800	1.05762100	-3.38424900
C	-0.49997600	1.72400800	-2.03331600
H	0.75417100	-0.47023200	-3.38931300
H	-0.19864600	1.57202600	-4.17429500
N	-1.36222800	1.11782800	-1.03244200
C	-1.97644300	1.93906500	-0.01046900
H	-1.56944000	1.69996000	0.98383600
H	-1.66537900	2.97610100	-0.20685000
C	-3.48894800	1.84333600	0.04417800
C	-4.15426000	2.07410900	1.25595500
C	-4.24707500	1.54739700	-1.09480300
C	-5.54838300	2.02669200	1.32668200
H	-3.56991000	2.28867300	2.15580000
C	-5.64131400	1.49475900	-1.02758400
H	-3.73342300	1.34610700	-2.03672000
C	-6.29737000	1.73660800	0.18268000
H	-6.05164400	2.20903400	2.27951600
H	-6.21914200	1.26070100	-1.92523100
H	-7.38783100	1.69322400	0.23582400
H	-0.77369300	-0.99615200	-4.10418400
H	-1.83637000	1.15192400	-3.62075500
H	-0.71152600	2.80528400	-2.04375600
H	0.80644900	3.99228600	0.70007200
C	-0.43727900	-4.43869600	-0.33903400
O	0.62822800	-4.84992900	-0.74181600
O	-1.21363800	-5.27598500	0.39375500
C	-2.62565200	-5.13812000	0.48634200
H	-3.05432400	-6.14711800	0.39559500
H	-2.91623200	-4.71862600	1.46251100
H	-3.03037100	-4.49748100	-0.31063700

***endo*-TS-2_6-CO_2Me**

Ru	-1.62135600	-0.66310600	1.12303000
C	-2.44838100	3.25034300	-0.69573700
C	-3.32207800	2.88213800	-1.71871100
C	-3.67739900	1.52366100	-1.88564000
C	-3.08809400	0.63006200	-0.98241100
C	-2.19611800	0.94778900	0.05836900
C	-1.88996500	2.30477300	0.19316700
H	-5.05593300	1.64749700	-3.58783300
H	-2.18311800	4.30276000	-0.57196400
H	-3.74077100	3.63916900	-2.38613800
C	-4.59060300	0.96580900	-2.87169700
H	-1.21852000	2.65712200	0.97691800
C	-4.28805300	-1.27582900	-1.98042700
C	-4.88976800	-0.36964500	-2.92436100
H	-5.58469300	-0.75863500	-3.66966400
C	-2.86547400	-1.57975900	-0.19221900
C	-4.29233200	-2.61516000	-1.64083500
N	-3.40820200	-0.70347900	-1.07432800
N	-3.42093200	-2.76376600	-0.55598300
H	-4.82676600	-3.45783900	-2.06762300
C	-3.17000000	-4.01501500	0.13494200
H	-2.33081200	-3.86368400	0.82447600
H	-4.05529300	-4.32436700	0.71074200
H	-2.90906500	-4.80304000	-0.58648000
O	-0.23328700	0.25898800	2.39643800
O	0.01922100	-1.26810100	0.24445600
Cl	-3.32665800	-0.62083000	2.70278100
C	5.59060900	0.27943800	-1.17835100
C	4.25509700	0.57441700	-0.90765400
C	3.38758300	-0.40997300	-0.39512800
C	3.89472900	-1.71155700	-0.14823300
C	5.23545000	-1.98858100	-0.40513000
C	6.07948600	-1.00185100	-0.92389100
H	6.25606600	1.04780000	-1.57404200
H	3.89469300	1.58813400	-1.07888200

C	2.94064300	-2.74128200	0.39489300	C	-1.62229800	-1.18830000	0.12343000
H	5.62944600	-2.98801400	-0.21128700	C	-0.45770800	-1.93951000	0.35167400
C	2.01848600	-2.05409000	1.40334800	H	-4.31094100	-5.04215600	-0.07916500
C	1.25002400	-0.91828600	0.74344200	H	0.43580200	-3.88914300	0.62314000
H	2.32862500	-3.16019000	-0.42459200	H	-1.68584200	-5.16321400	0.39834500
H	1.27875100	-2.74233000	1.83389200	C	-4.20931200	-3.95563800	-0.14252200
N	2.03775200	-0.14219300	-0.15849100	H	0.51193100	-1.44846100	0.42597000
C	1.39352300	0.98427300	-0.80395900	C	-5.18959300	-1.76504100	-0.53267800
H	1.78560000	1.07979800	-1.82849800	C	-5.31194500	-3.19725200	-0.43549000
H	0.32746700	0.73319500	-0.90338800	H	-6.28320100	-3.66371200	-0.60627700
C	1.51080500	2.31450000	-0.08308200	C	-3.83125600	0.09425500	-0.40063200
C	1.04355500	3.47400100	-0.71834800	C	-5.95076800	-0.64995000	-0.82426500
C	2.01659700	2.41656900	1.21786800	N	-3.92460300	-1.25829500	-0.28071500
C	1.06176400	4.70468100	-0.06153200	N	-5.10068000	0.46164900	-0.73714100
H	0.64224800	3.40526700	-1.73289500	H	-6.99941800	-0.54904300	-1.08467600
C	2.02981500	3.64800500	1.88195200	C	-5.49889600	1.82810300	-1.00872000
H	2.41235800	1.52859900	1.71266900	H	-6.30739400	2.14061600	-0.32997700
C	1.54707300	4.79481100	1.24752000	H	-4.62691000	2.47602800	-0.85574900
H	0.69069100	5.59769000	-0.57062900	H	-5.83831600	1.93275100	-2.05039000
H	2.42492000	3.70929100	2.89880800	O	-2.38702200	0.83946300	2.07892800
H	1.55674300	5.75621500	1.76608100	Cl	-1.57618900	1.11339900	-2.37383500
H	3.49061600	-3.57772000	0.85201900	C	4.23793200	-0.23905000	-1.09270100
H	2.62454900	-1.65524400	2.23412100	C	3.14980900	0.45087300	-0.56430300
H	0.78528400	-0.16885100	1.71193500	C	2.60951500	0.07173700	0.67395600
H	-0.17554700	1.22581500	2.35869000	C	3.17079800	-1.01041300	1.38765600
C	7.55530584	-1.33122027	-1.21556151	C	4.26193700	-1.68174900	0.84572000
O	7.85357646	-2.37933822	-1.84488968	C	4.80472800	-1.31091700	-0.39231600
O	8.58676610	-0.44602003	-0.77125275	H	4.65576000	0.05777100	-2.05434600
C	9.86439070	-1.02008486	-1.05939324	H	2.73317400	1.29193200	-1.11481300
H	9.96508646	-1.15399729	-2.11619399	C	2.54224200	-1.40651900	2.69701100
H	10.63607495	-0.36777832	-0.70739947	H	4.71169400	-2.52165300	1.37908500
H	9.94799513	-1.96802384	-0.57018777	C	2.02558700	-0.16068300	3.40951100
	2.10ac + Ru-1-I1			C	1.10252800	0.63699100	2.51642000
Ru	-2.02664800	0.77111300	-0.09462200	H	1.69894200	-2.09635500	2.50996600
C	-0.50036800	-3.34981200	0.45257900	H	1.46909800	-0.38980900	4.32687300
C	-1.68545800	-4.07329500	0.32399400	N	1.46884600	0.73532800	1.19667500
C	-2.89030600	-3.37754600	0.07181800	C	0.64981400	1.54409500	0.29766900
C	-2.78486000	-1.98269800	-0.00488600	H	0.52216300	1.00917800	-0.65249400

H	-0.34103500	1.64113000	0.79711100	H	3.26446800	-1.94735900	3.32485700
C	1.16072000	2.94929600	0.05710900	H	2.87091100	0.49563500	3.68481300
C	0.74191800	3.63343000	-1.09395700	O	0.09326200	1.18304600	2.95943300
C	2.00714300	3.59053200	0.96846000	H	-2.55427200	-0.07933400	2.33966200
C	1.16704700	4.94385000	-1.32214900	H	-1.52258100	1.05641200	2.50893300
H	0.08056000	3.12771200	-1.80293200	C	5.96876300	-2.08331400	-0.90538700
C	2.43441400	4.90018700	0.73451200	O	6.48803500	-3.00816300	-0.32232100
H	2.34318700	3.06477700	1.86430200	O	6.39161500	-1.64076900	-2.10461600
C	2.01466100	5.58118700	-0.41075700	C	7.50176800	-2.33200000	-2.67128000
H	0.83700100	5.46803800	-2.22233600	H	7.26400300	-3.39601800	-2.82109900
H	3.09840800	5.38934100	1.45133600	H	7.70565300	-1.84723800	-3.63367600
H	2.34986300	6.60482200	-0.59421100	H	8.38163100	-2.26389900	-2.01364400

Annexure VI

The cartesian coordinates (xyz) for all the optimized structures (*Chapter 3*)

2.7

C	0.82215	-0.3892	0.00001
C	1.59918	0.79638	-0.00003
C	3.00195	0.6699	-0.00003
C	3.59581	-0.58389	0.00001
C	2.80296	-1.74457	0.00005
H	3.5909	1.58142	-0.00006
H	4.67785	-0.6708	0.00001
H	3.27255	-2.72332	0.00008
C	-0.23433	2.21199	-0.00007
C	-1.12909	1.08616	-0.00003
N	-0.57978	-0.20098	0.00001
C	-2.49899	0.92733	-0.00001
C	-1.58477	-1.09482	0.00004
C	-4.08419	-1.04167	0.00003
H	-4.62632	-0.73084	-0.89545
H	-3.97112	-2.12611	0.00003
H	-4.62629	-0.73085	0.89554
N	-2.74885	-0.42188	0.00002
H	-0.65226	3.21655	-0.00009
H	-3.29163	1.6604	-0.00002
C	1.41428	-1.65488	0.00005
H	0.81463	-2.56006	0.00008
N	1.05291	2.07367	-0.00007

3

C	-1.1357	-1.41795	-0.04349
C	-2.28435	-0.59544	-0.03463
C	-3.61461	-1.08173	-0.06624
C	-3.77753	-2.46998	-0.12151
C	-2.66127	-3.31285	-0.14761
C	-1.36494	-2.80866	-0.1107
H	-4.77901	-2.88891	-0.14772
H	-2.80938	-4.38684	-0.19997
H	-0.5189	-3.48459	-0.13681
C	-3.133	1.70476	0.04854
N	-2.10114	0.76414	0.00708
C	-2.5004	2.92255	0.11163
C	-0.87924	1.37301	0.03126
N	-1.13442	2.71316	0.10633
H	-2.91376	3.91729	0.16342
C	-0.11375	3.76904	0.17139
H	-0.24052	4.43895	-0.65327
H	-0.21756	4.30939	1.08908
H	0.85976	3.32736	0.12572
H	-4.45441	-0.41892	-0.04869
H	-4.1864	1.51757	0.03427
H	-0.14766	-1.00938	-0.00159

Ru-2

C	-2.8712	0.47037	1.13373
C	-2.22382	1.56684	0.54572
C	-1.69082	1.47989	-0.7851
C	-1.91754	0.26577	-1.49882
C	-2.68115	-0.80717	-0.93528
C	-3.12385	-0.74042	0.39341
H	-3.15092	0.51246	2.18458
H	-2.02649	2.45905	1.13836
H	-1.49246	0.14155	-2.49288
H	-2.84182	-1.71518	-1.51226
Ru	-0.88413	-0.18892	0.32864
C	-3.79145	-1.896	1.06178
H	-3.33469	-2.09074	2.03931
C	-0.95771	2.65778	-1.37921
H	-0.45882	3.16657	-0.53873
C	2.279	2.60249	1.88145
C	3.43126	2.01906	1.36883
C	3.32474	0.84991	0.59039
C	2.02221	0.3728	0.3905
C	0.82248	0.90725	0.87859

TH-3565_186122020

C	0.99771	2.06024	1.64994
H	2.36612	3.50637	2.48362
H	4.40983	2.45381	1.56692
H	0.13675	2.56345	2.0947
C	2.88056	-1.5222	-0.93235
C	4.20972	-1.03701	-0.72791
H	5.04583	-1.585	-1.15309
C	0.62276	-1.25834	-0.57939
C	2.22141	-2.57095	-1.53488
N	1.86482	-0.76412	-0.37
N	0.86327	-2.38745	-1.30002
H	2.58614	-3.41481	-2.10157
C	-0.17337	-3.28375	-1.77096
H	0.17381	-4.31716	-1.70612
H	-1.05147	-3.15282	-1.13376
H	-0.4425	-3.05656	-2.80797
H	-4.85526	-1.68559	1.23036
H	-3.71611	-2.80767	0.45997
C	-1.96463	3.63069	-1.99366
H	-1.45639	4.52427	-2.37434
H	-2.49511	3.16306	-2.83366
H	-2.71436	3.95444	-1.26189
C	0.11251	2.26035	-2.38567
H	-0.32489	1.84115	-3.30102
H	0.69782	3.13778	-2.68228
H	0.8	1.5159	-1.96371
Cl	-0.4189	-1.64614	2.32473
N	4.41172	0.10257	-0.00058

Ru-4

C	2.29508	1.17862	-1.25015
C	1.37371	2.03217	-0.63024
C	0.95204	1.80675	0.72302
C	1.57392	0.73014	1.42436
C	2.60931	-0.05926	0.82809
C	2.94062	0.11651	-0.52138
H	2.50363	1.29142	-2.3122
H	0.89052	2.81712	-1.2103
H	1.2605	0.50385	2.44181
H	3.07547	-0.85963	1.3978
Ru	0.62543	-0.05181	-0.3394
C	3.89935	-0.78713	-1.22257
H	3.46129	-1.16106	-2.15588
C	-0.07186	2.71837	1.35435
H	-0.74355	3.03782	0.54121
C	-3.13312	1.73017	-1.86618
C	-4.0999	0.92463	-1.26811
C	-3.70688	-0.13034	-0.44478
C	-2.34782	-0.33782	-0.24217
C	-1.33161	0.45231	-0.81487
C	-1.77218	1.49096	-1.64407
H	-3.43692	2.55248	-2.51309
H	-5.158	1.10956	-1.44134
H	-1.04262	2.133	-2.14066
C	-2.43406	-2.41401	1.24757
C	-0.47236	-1.43139	0.66122
C	-1.42268	-3.1454	1.78246
N	-1.83321	-1.37387	0.56596
N	-0.23215	-2.53668	1.41168
H	-1.43725	-4.03785	2.39099
C	1.08402	-3.02375	1.77167
H	1.02979	-4.0976	1.96067
H	1.77154	-2.83859	0.94196
H	1.45641	-2.52135	2.67076
H	4.82041	-0.25022	-1.48266
H	4.16972	-1.64709	-0.60148
C	0.62156	3.96053	1.91469
H	-0.1138	4.66445	2.32155
H	1.31018	3.68884	2.72573
H	1.20056	4.48418	1.14467
C	-0.91879	2.03225	2.41688
H	-0.32856	1.77944	3.30726
H	-1.72606	2.69641	2.74514
H	-1.3693	1.10823	2.0322
Cl	0.55703	-1.67893	-2.25334
H	-4.45024	-0.77427	0.02385
H	-3.50444	-2.54958	1.29012

TH-3565_186122020

For the oxidation reaction catalyzed by **Ru-1**

I2_Cl

Ru	0.78782	-0.83143	0.01675
C	-3.56648	-1.87797	-0.66996
C	-4.14754	-0.62006	-0.60072
C	-3.34425	0.5119	-0.36427
C	-1.97481	0.25817	-0.21456
C	-1.34778	-0.98617	-0.26959
C	-2.18127	-2.07438	-0.49665
H	-4.8547	2.08335	-0.36895
H	-4.19801	-2.74469	-0.85747
H	-5.22267	-0.50134	-0.72707
C	-3.79109	1.8792	-0.25644
H	-1.76379	-3.07854	-0.54803
C	-1.53662	2.6589	0.12736
C	-2.93454	2.9159	-0.01557
H	-3.29814	3.93603	0.06661
C	0.18334	1.15915	0.14576
C	-0.35804	3.3374	0.36594
N	-1.14371	1.33642	0.00507
N	0.66289	2.39902	0.37847
H	-0.15791	4.38696	0.52331
C	2.07353	2.69548	0.56187
H	2.18084	3.50461	1.28836
H	2.56601	1.79269	0.93099
H	2.5302	2.98412	-0.38946
O	1.42999	-0.68969	-1.58119
O	-0.25605	-1.22075	2.24907
H	-0.32834	-2.18535	2.1199
H	0.62733	-1.1042	2.64665
Cl	0.85603	-3.25439	0.15228
O	2.04573	-0.49499	1.24532
C	4.4414	0.55752	-1.13334
H	3.89971	0.01843	-0.35564
H	4.2433	0.24058	-2.15566
C	5.29064	1.54197	-0.85223
H	5.83682	2.07629	-1.62851
H	5.49235	1.85174	0.17341

TS_Cl

Ru	1.05595	-0.34711	0.05791
C	-2.6935	-2.93493	-0.44398
C	-3.67965	-1.95989	-0.40997
C	-3.31703	-0.60717	-0.26102
C	-1.94031	-0.35943	-0.15691
C	-0.90373	-1.29487	-0.18984
C	-1.32484	-2.61518	-0.33169
H	-5.2862	0.32571	-0.28655
H	-2.98461	-3.97812	-0.56071
H	-4.73127	-2.23026	-0.49704
C	-4.21678	0.51682	-0.20615
H	-0.58295	-3.41375	-0.36187
C	-2.37846	2.06109	0.04601
C	-3.77883	1.80243	-0.05836
H	-4.47667	2.63396	-0.01947
C	-0.23374	1.27795	0.10075
C	-1.52204	3.13293	0.20215
N	-1.54105	0.95946	-0.0106
N	-0.23328	2.62423	0.23647
H	-1.71284	4.19203	0.29452
C	0.97429	3.41884	0.34892
H	0.81912	4.22208	1.07405
H	1.77872	2.75983	0.68627
H	1.23629	3.85177	-0.62281
O	1.53841	-0.12274	-1.62652
O	0.54109	-0.75102	2.32678
H	0.63858	-1.72209	2.27602
H	1.40136	-0.45115	2.67
Cl	2.02701	-2.56773	0.34941
O	2.45524	0.58558	0.79532
C	3.88878	1.08869	-0.50512
C	3.44278	0.80176	-1.77801
H	3.74005	-0.11509	-2.27478
H	3.01582	1.574	-2.41095
H	4.56644	0.4079	0.00064
H	3.89808	2.11268	-0.14197

I3_Cl

TH-3565_186122020

Ru	1.08505	-0.24256	0.18144
C	-2.32131	-3.14623	-0.32722
C	-3.40408	-2.27702	-0.38247
C	-3.18634	-0.89235	-0.26628
C	-1.84862	-0.50311	-0.10157
C	-0.7168	-1.32614	-0.03474
C	-1.00047	-2.69031	-0.15774
H	-5.22951	-0.14958	-0.42808
H	-2.49927	-4.21699	-0.42015
H	-4.41591	-2.65787	-0.51474
C	-4.18893	0.1442	-0.29567
H	-0.18402	-3.41167	-0.12916
C	-2.52183	1.86658	0.00943
C	-3.88336	1.46938	-0.16283
H	-4.65964	2.22902	-0.18644
C	-0.31436	1.27482	0.19319
C	-1.77378	3.01068	0.18859
N	-1.58618	0.84498	0.02323
N	-0.44501	2.6214	0.29909
H	-2.06165	4.04982	0.25251
C	0.66329	3.53515	0.49857
H	0.45291	4.19267	1.34737
H	1.55919	2.94181	0.70073
H	0.81716	4.14396	-0.39869
O	1.32788	0.0324	-1.72902
O	1.00105	-0.51037	2.41152
H	0.19687	-1.03401	2.56338
H	1.72749	-1.1641	2.4756
Cl	2.34214	-2.30251	0.37095
O	2.64933	1.03804	0.29205
C	3.13655	1.35468	-0.9805
C	2.70129	0.25902	-1.9483
H	3.27847	-0.65774	-1.7401
H	2.84332	0.53975	-3.00289
H	4.23332	1.45852	-0.9437
H	2.72741	2.33027	-1.31244

I4_Cl

Ru	-1.05286	-0.01162	-0.13634
C	1.95444	-3.28624	-0.1131
C	3.13164	-2.55359	-0.02967
C	3.06916	-1.14572	0.01173
C	1.78296	-0.59594	-0.03399
C	0.55213	-1.27413	-0.12125
C	0.68726	-2.66934	-0.15954
H	5.19098	-0.64621	0.12814
H	2.0121	-4.37413	-0.14718
H	4.09793	-3.05585	0.00171
C	4.1842	-0.23093	0.09082
H	-0.20695	-3.29168	-0.23254
C	2.70897	1.68728	0.06729
C	4.02315	1.1265	0.11587
H	4.88301	1.78908	0.17168
C	0.42151	1.3408	-0.0452
C	2.08686	2.91533	0.05764
N	1.66626	0.77798	0.00423
N	0.71503	2.67803	-0.0136
H	2.4846	3.91908	0.09353
C	-0.28802	3.71748	-0.0429
H	-0.09399	4.4117	-0.86764
H	-1.26178	3.24542	-0.18947
H	-0.29278	4.27774	0.89911
O	-1.28189	-0.10215	1.89988
O	-1.16052	-0.10139	-2.34233
H	-0.34865	-0.57584	-2.58684
H	-1.85221	-0.8016	-2.335
Cl	-2.75025	-1.82985	-0.40271
O	-2.76953	1.40823	-0.17177
C	-3.83868	1.16339	0.37656
C	-1.32952	-1.18039	2.50524
H	-4.67269	1.88468	0.30746
H	-4.00062	0.22351	0.93235
H	-1.12402	-2.13365	1.99735
H	-1.58493	-1.17012	3.57444
C	2.19302	-2.30634	1.01054
C	0.13979	0.65724	2.86771
H	2.9358	-3.109	0.88499

H	2.18003	-1.77549	1.97637
H	0.12947	1.65628	2.40956
H	0.28729	0.5512	3.95184
O	1.60722	1.06784	0.4284
I	3.35633	0.66126	-0.30361
O	4.01312	-0.7731	0.69771
O	2.91696	-0.00963	-1.99627

For the oxidation reaction catalyzed by **Ru-4**

I2_Cl

Ru	0.0563	0.17218	-0.42821
C	-2.70187	-3.43611	-0.71816
C	-3.91528	-2.84746	-0.3825
C	-3.9591	-1.47252	-0.09022
C	-2.73552	-0.7993	-0.17503
C	-1.49563	-1.34006	-0.50193
C	-1.49549	-2.70433	-0.76832
H	-2.67799	-4.50086	-0.94477
H	-4.83381	-3.42771	-0.33427
H	-0.56511	-3.20997	-1.02499
C	-3.87725	1.2454	0.50069
C	-5.08058	0.46075	0.55655
H	-6.015	0.94211	0.84813
C	-1.63885	1.29187	0.06335
C	-3.41313	2.52824	0.71807
N	-2.75383	0.54619	0.1079
N	-2.05502	2.52173	0.44967
H	-3.92088	3.42899	1.03084
C	-1.17152	3.67362	0.54695
H	-1.23828	4.1037	1.54984
H	-0.14615	3.34285	0.35795
H	-1.4556	4.42463	-0.19596
O	0.14681	0.74141	-2.05872
O	-0.11839	-0.80085	1.80086
H	-0.19965	-1.75771	1.66429
H	0.83125	-0.68453	2.06649
O	1.05865	1.19518	0.62742
C	2.12131	3.54496	-1.39337
H	2.0571	2.48992	-1.65321
H	1.80163	4.25908	-2.15299
C	2.58409	3.93248	-0.20724
H	2.67045	4.98462	0.06622
H	2.90883	3.19933	0.52852
N	-5.12692	-0.81174	0.27632
Cl	1.40961	-1.38669	-0.66444

TS_Cl

Ru	0.0284	-0.49987	0.59906
C	1.58195	3.79777	0.17707
C	2.88819	3.58862	-0.24632
C	3.35071	2.27293	-0.41709
C	2.41989	1.26069	-0.14378
C	1.10864	1.41294	0.27705
C	0.69829	2.73124	0.44322
H	1.22826	4.81869	0.31383
H	3.56431	4.41693	-0.44442
H	-0.3126	2.94522	0.79061
C	4.13502	-0.37546	-0.69427
C	5.0084	0.73497	-0.95194
H	6.03289	0.54062	-1.27294
C	2.05602	-1.08478	-0.05966
C	4.12863	-1.75467	-0.69685
N	2.85482	-0.03581	-0.30054
N	2.86304	-2.15194	-0.30373
H	4.89731	-2.47475	-0.93803
C	2.43231	-3.53553	-0.2095
H	3.22603	-4.13493	0.24379
H	1.53354	-3.56129	0.40981
H	2.20498	-3.92774	-1.20666
O	-0.61236	-0.60896	-1.05881
O	0.99468	-0.3538	2.82392
H	0.33639	0.31409	3.08935
H	0.64492	-1.19104	3.17063
O	-0.12003	-2.23271	1.00253
C	-1.2723	-3.37056	-0.45013
C	-1.38837	-2.58874	-1.56355
H	-2.30462	-2.03552	-1.73976
H	-0.68015	-2.65742	-2.3856

H	-2.07537	-3.40157	0.27898
H	-0.50809	-4.13839	-0.37131
N	4.64647	1.98046	-0.8253
Cl	-1.42911	0.84181	1.623

I3_Cl

Ru	0.21144	-0.92739	0.67344
C	0.13498	3.58504	0.75195
C	1.35529	3.9039	0.17043
C	2.22522	2.86481	-0.19902
C	1.75994	1.56262	0.03274
C	0.54477	1.1815	0.59624
C	-0.2685	2.25221	0.97012
H	-0.53192	4.38978	1.05764
H	1.66018	4.93471	0.00756
H	-1.2203	2.06058	1.46779
C	3.88919	0.72237	-0.797
C	4.25722	2.09156	-1.0246
H	5.23704	2.31531	-1.44933
C	2.29155	-0.74772	-0.06116
C	4.39677	-0.55644	-0.89956
N	2.6203	0.53684	-0.28272
N	3.41427	-1.41754	-0.44488
H	5.3528	-0.92111	-1.24715
C	3.56079	-2.86152	-0.36631
H	4.42207	-3.11315	0.25947
H	2.64322	-3.2623	0.07148
H	3.70909	-3.27705	-1.36793
O	-0.44222	-0.8624	-1.16606
O	1.1162	-1.18919	2.78352
H	1.47735	-0.31735	3.01114
H	0.25629	-1.21606	3.24315
O	0.50606	-2.83111	0.22606
C	0.06715	-3.16576	-1.06844
C	-0.9564	-2.13991	-1.50704
H	-1.92066	-2.31092	-0.99707
H	-1.13382	-2.14932	-2.59245
H	-0.35769	-4.18041	-1.0434
H	0.93051	-3.17761	-1.76287
N	3.48144	3.10117	-0.7467
Cl	-1.57972	-0.42176	1.90186

I4_Cl

Ru	-1.05286	-0.01162	-0.13634
C	1.95444	-3.28624	-0.1131
C	3.13164	-2.55359	-0.02967
C	3.06916	-1.14572	0.01173
C	1.78296	-0.59594	-0.03399
C	0.55213	-1.27413	-0.12125
C	0.68726	-2.66934	-0.15954
H	2.0121	-4.37413	-0.14718
H	4.09793	-3.05585	0.00171
H	-0.20695	-3.29168	-0.23254
C	2.70897	1.68728	0.06729
C	4.02315	1.1265	0.11587
H	4.88301	1.78908	0.17168
C	0.42151	1.3408	-0.0452
C	2.08686	2.91533	0.05764
N	1.66626	0.77798	0.00423
N	0.71503	2.67803	-0.0136
H	2.4846	3.91908	0.09353
C	-0.28802	3.71748	-0.0429
H	-0.09399	4.4117	-0.86764
H	-1.26178	3.24542	-0.18947
H	-0.29278	4.27774	0.89911
O	-1.28189	-0.10215	1.89988
O	-1.16052	-0.10139	-2.34233
H	-0.34865	-0.57584	-2.58684
H	-1.85221	-0.8016	-2.335
Cl	-2.75025	-1.82985	-0.40271
O	-2.76953	1.40823	-0.17177
C	-3.83868	1.16339	0.37656
C	-1.32952	-1.18039	2.50524
H	-4.67269	1.88468	0.30746
H	-4.00062	0.22351	0.93235
H	-1.12402	-2.13365	1.99735
H	-1.58493	-1.17012	3.57444
N	4.1842	-0.23093	0.09082

I2_IO3

Ru	0.04817	0.17864	-0.42136
C	-2.64297	-3.44852	-0.73755
C	-3.86838	-2.8844	-0.40908
C	-3.95504	-1.51141	-0.10561
C	-2.74774	-0.80469	-0.17075
C	-1.49561	-1.3263	-0.49307
C	-1.4566	-2.68664	-0.76985
H	-2.59484	-4.51092	-0.97131
H	-4.76642	-3.49986	-0.37986
H	-0.50892	-3.16241	-1.02071
C	-3.88723	1.27361	0.50236
C	-5.11839	0.55138	0.57069
H	-6.02476	1.07481	0.86115
C	-1.6459	1.28131	0.0678
C	-3.3987	2.54756	0.71017
N	-2.77432	0.54557	0.11476
N	-2.03742	2.51618	0.44317
H	-3.89071	3.45948	1.01475
C	-1.14065	3.65676	0.53
H	-1.20228	4.09684	1.52914
H	-0.11884	3.31398	0.34453
H	-1.41621	4.4055	-0.21878
O	0.14117	0.74723	-2.052
O	-0.11623	-0.80682	1.80835
H	-0.18645	-1.76305	1.66212
H	0.83309	-0.68315	2.07096
O	1.05146	1.19865	0.63718
C	2.15143	3.5299	-1.40317
H	2.07234	2.47371	-1.6541
H	1.83966	4.24208	-2.16793
C	2.62018	3.92084	-0.22066
H	2.71975	4.97393	0.0446
H	2.93528	3.18932	0.52086
O	1.40827	-1.38548	-0.65992
I	3.15776	-1.11774	0.21185
O	2.61952	-1.07651	1.99471
O	3.76551	0.54215	-0.30558
N	-5.14143	-0.78166	0.27248

TS_IO3

Ru	0.03346	-0.51128	0.59204
C	1.5088	3.79709	0.20243
C	2.81818	3.61771	-0.22013
C	3.32173	2.31606	-0.40096
C	2.42023	1.27378	-0.13616
C	1.10285	1.4008	0.28301
C	0.65661	2.70525	0.45885
H	1.13047	4.80834	0.34513
H	3.46174	4.47576	-0.40877
H	-0.36005	2.88605	0.80805
C	4.14638	-0.38903	-0.68987
C	5.06212	0.67202	-0.96154
H	6.07263	0.43113	-1.27911
C	2.05645	-1.07073	-0.05354
C	4.11679	-1.76668	-0.68825
N	2.86817	-0.02414	-0.2955
N	2.84394	-2.14691	-0.29304
H	4.87428	-2.49839	-0.92886
C	2.40486	-3.52718	-0.20563
H	3.1953	-4.13146	0.24755
H	1.50416	-3.55344	0.40999
H	2.1809	-3.91537	-1.20545
O	-0.61201	-0.6107	-1.06453
O	0.98674	-0.38185	2.82867
H	0.30908	0.27063	3.08465
H	0.64175	-1.22974	3.15362
O	-0.12077	-2.24748	0.98556
C	-1.28054	-3.36972	-0.4638
C	-1.39938	-2.58119	-1.57273
H	-2.31546	-2.02546	-1.7421
H	-0.69584	-2.64888	-2.39876
H	-2.08175	-3.40394	0.26725
H	-0.51933	-4.14132	-0.39409
O	-1.12432	0.54941	1.41784
I	-3.3763	0.72548	-0.24843
O	-4.83377	1.42013	-1.22474

O	-3.64734	-1.12062	0.04774
N	4.65547	1.96764	-0.82102

I3_IO3

Ru	0.21145	-0.92259	0.65845
C	0.10839	3.57195	0.75626
C	1.3252	3.90335	0.17804
C	2.21787	2.88125	-0.19323
C	1.77611	1.56849	0.0326
C	0.55789	1.17757	0.59013
C	-0.27219	2.23314	0.96756
H	-0.56973	4.36709	1.06245
H	1.60112	4.94525	0.02362
H	-1.22019	2.02185	1.4641
C	3.92316	0.68183	-0.781
C	4.36126	2.01609	-1.03827
H	5.3517	2.17923	-1.45365
C	2.28415	-0.74625	-0.04749
C	4.39845	-0.60963	-0.86191
N	2.64024	0.53618	-0.27611
N	3.39026	-1.44501	-0.4079
H	5.34901	-1.00062	-1.19496
C	3.51521	-2.88874	-0.31062
H	4.36082	-3.14386	0.33533
H	2.58408	-3.27534	0.11027
H	3.68123	-3.31656	-1.30457
O	-0.44491	-0.83758	-1.17925
O	1.10498	-1.20586	2.7743
H	1.50964	-0.35061	2.99071
H	0.23619	-1.17701	3.21816
O	0.48391	-2.82759	0.19835
C	0.05043	-3.14593	-1.10164
C	-0.96413	-2.10931	-1.53477
H	-1.93167	-2.28041	-1.03066
H	-1.13717	-2.1069	-2.62104
H	-0.38109	-4.15811	-1.09043
H	0.9177	-3.15585	-1.79126
O	-1.19143	-0.51773	1.636
I	-3.20575	0.46464	-0.26106
O	-4.44918	1.59112	-1.11932
O	-3.84432	-1.31302	-0.25007
N	3.53327	3.06401	-0.75508

I4_IO3

Ru	-0.02425	-0.31465	0.1385
C	-2.17017	3.57622	0.05805
C	-3.48346	3.14282	-0.07011
C	-3.7512	1.76012	-0.13746
C	-2.63342	0.92166	-0.06465
C	-1.27972	1.28996	0.05478
C	-1.0862	2.67651	0.11883
H	-1.97118	4.64679	0.10949
H	-4.30317	3.85862	-0.11972
H	-0.07281	3.07153	0.21554
C	-4.06363	-1.07476	-0.28473
C	-5.20645	-0.21905	-0.35653
H	-6.19382	-0.65815	-0.47388
C	-1.77025	-1.28223	-0.06367
C	-3.7446	-2.41323	-0.33381
N	-2.84313	-0.44048	-0.12314
N	-2.36019	-2.50757	-0.20479
H	-4.36173	-3.29204	-0.45124
C	-1.62259	-3.75003	-0.22509
H	-1.90241	-4.34156	-1.10287
H	-0.55803	-3.51195	-0.2768
H	-1.82231	-4.3372	0.6788
O	-0.02119	-0.36496	2.18779
O	0.26905	-0.3278	-2.02257
H	-0.00667	0.55328	-2.31918
H	1.26914	-0.32335	-2.12025
O	1.34858	-2.0955	0.14382
C	2.19302	-2.30634	1.01054
C	0.13979	0.65724	2.86771
H	2.9358	-3.109	0.88499
H	2.18003	-1.77549	1.97637
H	0.12947	1.65628	2.40956
H	0.28729	0.5512	3.95184
O	1.60722	1.06784	0.4284

TH-3565_186122020

I	3.35633	0.66126	-0.30361
O	4.01312	-0.7731	0.69771
O	2.91696	-0.00963	-1.99627
N	-5.04611	1.13643	-0.28092

Annexure VII

Cartesian coordinates (xyz) for all the optimized structures (*Chapter 4*)

I1

C	3.42324	2.26046	-1.50319
C	3.09038	1.08267	-0.85124
C	3.5208	0.89055	0.46046
C	4.30179	1.85532	1.13664
C	4.63385	3.03019	0.43731
C	4.19546	3.23466	-0.85805
H	3.07009	2.41734	-2.52091
H	2.49525	0.32685	-1.36201
C	4.68968	1.64443	2.50185
H	5.23354	3.78426	0.94362
H	4.451	4.15415	-1.37843
C	4.29846	0.54071	3.1889
C	3.50766	-0.43961	2.53313
H	5.29657	2.40532	2.98741
H	4.5712	0.3794	4.22711
C	2.43015	-1.31673	0.78018
C	2.94268	-1.63748	2.91156
N	3.16466	-0.26208	1.18527
N	2.2919	-2.14671	1.8195
H	1.98764	-1.45798	-0.20059
H	2.96412	-2.15961	3.8564
C	1.55613	-3.40513	1.7893
H	2.2512	-4.24075	1.67406
H	0.99988	-3.50652	2.72333
H	0.85888	-3.397	0.94733
C	0.67564	-0.83089	-2.71686
C	0.68348	0.45942	-3.31243
C	1.66687	0.77586	-4.27078
C	-0.27089	1.43094	-2.95745
C	1.68789	2.03296	-4.86155
H	2.39738	0.01956	-4.55253
C	-0.22982	2.68855	-3.54889
H	-1.05236	1.18285	-2.23744
C	0.74352	2.99427	-4.49851
H	2.44038	2.2619	-5.61363
H	-0.97442	3.43243	-3.27156
H	0.76068	3.97688	-4.96545
C	0.71498	-1.96352	-2.25941
C	0.76914	-3.28434	-1.73748
C	2.00267	-3.96308	-1.6634
C	-0.40012	-3.92943	-1.28469
C	2.06359	-5.25406	-1.15252
H	2.90255	-3.47303	-2.03354
C	-0.31973	-5.21921	-0.76806
H	-1.35829	-3.40827	-1.34623
C	0.90431	-5.88497	-0.69962
H	3.01849	-5.77536	-1.11837
H	-1.22868	-5.71318	-0.42905
H	0.95353	-6.89918	-0.30844
C	-1.44142	1.09003	2.8225
C	-1.91839	-0.23568	2.91303
C	-1.54416	-1.24014	1.9544
C	-0.68595	-0.84214	0.89822
C	-0.21883	0.50565	0.77454
C	-0.6251	1.49724	1.71374
H	-1.83096	1.84948	3.49827
H	-2.67535	-0.47857	3.65755
H	-0.52648	-1.53681	0.07289
H	0.30727	0.80069	-0.13495
Ru	-2.36098	0.50365	0.94201
O	-2.77129	0.30672	-1.09527
O	-3.60348	2.23522	0.62501
C	-4.6497	1.51043	0.72473
C	-2.90284	-0.89943	-1.57643
C	-5.99756	2.05059	0.40232
H	-6.19773	1.89014	-0.66344
H	-6.77207	1.52939	0.96983

TH-3565_186122020

H	-6.04234 3.12554 0.59281	H	-0.37978 0.15107 -4.26935
C	-3.16064 -0.94326 -3.06356	O	0.47086 -0.21486 -1.75554
O	-2.81319 -1.93887 -0.91635	C	1.51476 -4.59975 -2.24804
O	-4.49166 0.29581 1.08194	H	1.65032 -4.11438 -3.21848
C	-0.28468 2.9586 1.54453	C	2.91554 -0.9592 2.16459
H	-1.08892 3.52318 2.03996	H	2.99142 0.04872 1.72894
C	1.02922 3.25453 2.26714	C	0.87915 3.59755 1.77921
H	1.263 4.32442 2.22524	C	-0.34279 3.39468 2.3934
H	0.99836 2.95583 3.32235	C	-1.02597 2.17174 2.27862
H	1.85672 2.71583 1.78712	C	-0.43447 1.13312 1.51259
C	-0.23311 3.39986 0.08846	C	0.79358 1.34752 0.8889
H	-1.15826 3.13871 -0.4395	C	1.44124 2.56795 1.02427
H	-0.10286 4.48595 0.02744	H	-2.71839 2.81796 3.48077
H	0.61079 2.94442 -0.44854	H	1.38893 4.55414 1.86991
C	-2.14446 -2.60686 2.01548	H	-0.80722 4.18696 2.97888
H	-1.76845 -3.15626 2.88977	C	-2.2969 1.98721 2.91912
H	-3.23489 -2.5487 2.10668	H	1.24003 0.57084 0.27808
H	-1.92572 -3.17502 1.10796	H	2.38314 2.72036 0.5047
H	-4.03138 -1.57391 -3.26754	C	-2.36544 -0.25498 2.08689
H	-3.31668 0.04864 -3.49452	C	-2.94831 0.80465 2.82782
H	-2.30377 -1.41514 -3.56056	H	-3.91131 0.62852 3.29919
	I2	C	-0.79335 -1.25502 0.75307
C	2.75157 -2.58505 -1.3358	C	-2.78178 -1.52619 1.82063
C	2.99379 -1.67174 -0.27203	N	-1.1328 -0.09598 1.41909
C	2.51207 -1.89289 1.05052	N	-1.83046 -2.09784 1.01854
C	1.68421 -3.03757 1.25095	H	-3.68793 -2.0429 2.10163
C	1.3804 -3.91907 0.18788	C	-1.95751 -3.46522 0.54201
C	1.92046 -3.70704 -1.12506	H	-3.02006 -3.71284 0.48941
H	3.09022 -2.3459 -2.34085	H	-1.52038 -3.55192 -0.45336
H	3.50498 -0.73189 -0.49063	H	-1.4661 -4.15627 1.23347
H	1.19513 -3.18732 2.21166	C	5.11784 3.21801 -0.55248
H	0.69279 -4.74543 0.34955	H	5.14608 3.55184 0.491
Ru	0.84756 -1.9051 -0.41188	H	6.13257 3.32189 -0.95249
O	-0.63699 -2.07436 -2.02011	H	4.44423 3.8652 -1.11612
C	-0.39646 -0.88122 -2.40622	C	4.6576 1.79473 -0.63819
C	-1.10449 -0.28037 -3.57149	O	3.67858 1.41471 -1.24904
H	-1.71534 -1.02244 -4.09032	O	5.39516 0.88436 0.03302
H	-1.74796 0.53881 -3.22514	H	6.14142 1.31101 0.48808

H	2.12681	-5.5102	-2.23457
H	0.46824	-4.90757	-2.15315
C	4.31198	-1.35644	2.65108
H	4.65301	-0.66279	3.42824
H	4.30379	-2.366	3.08184
H	5.04328	-1.33882	1.83553
C	1.92739	-0.9204	3.32093
H	1.94612	-1.85451	3.89682
H	2.18557	-0.10961	4.01077
H	0.89862	-0.75594	2.97914
C	-3.06628	1.44734	-0.94093
C	-2.23256	2.32377	-1.10931
C	-4.04663	0.44703	-0.71277
C	-5.14923	0.71497	0.12223
C	-3.92883	-0.83362	-1.28481
C	-6.09171	-0.27104	0.38288
H	-5.24357	1.70134	0.57268
C	-4.87995	-1.81257	-1.02269
H	-3.07507	-1.06286	-1.91902
C	-5.96197	-1.53859	-0.18658
H	-6.93397	-0.04968	1.03544
H	-4.77307	-2.79768	-1.47394
H	-6.70253	-2.3087	0.01919
C	-1.27571	3.35489	-1.29909
C	-0.06222	3.10023	-1.96584
C	-1.52486	4.65244	-0.81272
C	0.87099	4.11516	-2.13507
H	0.14916	2.09125	-2.31401
C	-0.58564	5.66082	-0.98902
H	-2.4587	4.85291	-0.29019
C	0.61473	5.39719	-1.64935
H	1.8102	3.89912	-2.64236
H	-0.79009	6.65865	-0.60558
H	1.34916	6.18922	-1.78297

TS-1

C	-1.17815000	-2.45886600	-0.58669400
C	-1.57084500	-1.16462400	-0.97475000
C	-0.78605600	-0.36753700	-1.87196500
C	0.42454000	-0.93550200	-2.34672000
C	0.83789600	-2.24838500	-1.96441600
C	0.05048900	-3.01290300	-1.06757900
H	-2.45655000	-0.72487500	-0.51534200
H	1.78898200	-2.64108700	-2.31510600
Ru	0.48229800	-0.99957000	-0.18070800
O	1.40586300	-2.11111300	1.41206500
C	1.33548100	-1.69936900	2.60989100
C	1.97607600	-2.52761600	3.68148600
H	2.30190900	-3.49450100	3.29472000
H	2.84375700	-1.99262000	4.08193900
H	1.27800000	-2.67349500	4.51060100
O	0.75896400	-0.62126700	2.95178300
C	0.52428300	-4.33860900	-0.57730500
H	0.23761600	-4.50265900	0.46554600
C	-1.26595900	1.01161600	-2.25442300
H	-1.69566100	1.45590300	-1.34275500
C	-1.83716100	2.55534900	1.53371500
C	-0.89028800	3.55693000	1.34328400
C	0.41903500	3.22846200	0.94092900
C	0.67115900	1.86466500	0.74818800
C	-0.22593100	0.80401900	0.97652600
C	-1.51582400	1.20069700	1.36938000
H	1.31601200	5.21699500	0.88040800
H	-2.84737000	2.82723300	1.83484200
H	-1.15498400	4.60069300	1.50365800
C	1.50002200	4.15846000	0.70887100
H	0.26507300	-0.07612700	1.83710000
H	-2.27176800	0.44298900	1.57586800
C	2.96689400	2.36653500	0.01961900
C	2.73338400	3.74914500	0.29141600
H	3.53533100	4.46230300	0.12612400
C	2.14013200	0.22974100	-0.15889200
C	3.94516300	1.56118200	-0.51651100
N	1.90258100	1.50170500	0.25320900
N	3.41769800	0.28032200	-0.60748600
H	4.94989100	1.78206700	-0.84480800
C	4.12958200	-0.85859700	-1.15949300

H	5.15876100	-0.85870000	-0.79515400
H	3.62852800	-1.77171900	-0.83097100
H	4.13265400	-0.81273800	-2.25295500
C	-6.31960600	0.08415800	1.08488100
H	-6.43636400	1.08455300	1.51651300
H	-6.99495600	0.02300300	0.22438400
H	-6.61392400	-0.66053400	1.82477600
C	-4.90083900	-0.14152500	0.66126400
O	-4.17441000	-1.01723200	1.08552800
O	-4.41140200	0.71339500	-0.26487700
H	-5.08455600	1.36504300	-0.52608300
H	0.06939400	-5.13664100	-1.17757600
H	1.61115100	-4.43252100	-0.65999400
C	-2.39229000	0.88621900	-3.28197600
H	-2.79452400	1.87552700	-3.52856000
H	-2.02653200	0.43047600	-4.21116500
H	-3.21689500	0.27209900	-2.90226200
C	-0.15810400	1.92436100	-2.76098300
H	0.20871900	1.60823300	-3.74609000
H	-0.53231900	2.94831100	-2.86725000
H	0.69976900	1.95184000	-2.07687800
H	1.09177600	-0.33737800	-2.96455100
H	-1.76461400	-3.00311600	0.14967700

DPA

C	-4.13381	1.20668	0.00016
C	-4.83342	-0.00007	0.00004
C	-4.13368	-1.20677	-0.00013
C	-2.74465	-1.21217	-0.00016
C	-2.02806	0.00008	-0.00002
C	-2.74475	1.21222	0.00013
H	-4.6748	2.1509	0.0003
H	-5.92146	-0.00014	0.00007
H	-4.67461	-2.15104	-0.00024
H	-2.19671	-2.15225	-0.00027
H	-2.19696	2.15239	0.00022
C	-0.60984	0.00009	-0.00004
C	0.60984	0.00005	-0.00003
C	2.02805	0.00002	-0.00003
C	2.74472	1.2122	-0.00015
C	2.74468	-1.21219	0.00014
C	4.13377	1.2067	-0.00013
H	2.19688	2.15233	-0.00027
C	4.13372	-1.20675	0.00016
H	2.19679	-2.1523	0.00023
C	4.83343	-0.00003	0.00003
H	4.67475	2.15094	-0.00023
H	4.67466	-2.151	0.00028
H	5.92147	-0.00006	0.00006

Ru-5

C	-2.53851	-0.73181	-2.07839
C	-2.40775	-2.0969	-1.68359
C	-2.97925	-2.54268	-0.47749
C	-3.76035	-1.6152	0.29769
C	-3.9328	-0.28967	-0.10987
C	-3.28456	0.19918	-1.29535
H	-2.01196	-0.38667	-2.96464
H	-1.79989	-2.7758	-2.27709
H	-4.18012	-1.94141	1.24771
Ru	-1.69822	-0.66775	-0.1168
C	-3.4632	1.64169	-1.70388
C	-2.80724	-3.95878	-0.02985
H	-1.81315	-4.34499	-0.27765
C	2.15013	-0.81181	-2.43309
C	2.70991	0.41775	-2.1108
C	2.03034	1.27631	-1.22627
C	0.80211	0.80189	-0.74833
C	0.18435	-0.41795	-1.03774
C	0.90935	-1.23164	-1.91051
H	3.45562	2.92193	-1.08422
H	2.68858	-1.47826	-3.10617
H	3.6797	0.70863	-2.51382
C	2.4922	2.55266	-0.73521
H	0.53218	-2.21573	-2.19456
C	0.51117	2.82078	0.62711
C	1.77346	3.29889	0.157
H	2.1447	4.25422	0.51627

C	-1.08497	1.16692	0.62457
C	-0.51065	3.19809	1.47323
N	0.10678	1.58947	0.14117
N	-1.45797	2.18511	1.44758
H	-0.64429	4.07733	2.08582
C	-2.69407	2.22216	2.20516
H	-3.41974	2.88617	1.72425
H	-3.0995	1.20926	2.25675
H	-2.49684	2.58233	3.2177
H	-3.51429	2.22806	-0.77301
C	-2.31947	2.18715	-2.54717
H	-1.34319	2.00277	-2.08133
H	-2.3055	1.73919	-3.54875
H	-2.43423	3.26806	-2.68
C	-4.80309	1.7915	-2.4273
H	-5.64103	1.44686	-1.81045
H	-4.9813	2.8417	-2.68361
H	-4.80841	1.21231	-3.35951
H	-2.9744	-4.08014	1.04487
H	-3.54184	-4.59584	-0.53846
C	-1.23532	-1.76558	2.29823
C	-1.53222	-0.86538	3.33612
C	-0.56991	0.04224	3.7509
C	0.6907	0.06205	3.14982
C	1.00961	-0.82828	2.11716
C	0.01791	-1.74686	1.67295
H	-1.93304	-2.56573	2.07147
H	-2.50669	-0.902	3.81879
H	-0.78789	0.73905	4.55793
H	1.44675	0.76702	3.48979
H	0.29053	-2.5174	0.95473
C	2.29919	-0.82198	1.5392
C	3.41129	-0.79293	1.03879
C	4.67478	-0.70061	0.40623
C	5.13775	-1.73282	-0.43131
C	5.46542	0.45269	0.56964
C	6.35255	-1.60651	-1.09171
H	4.5248	-2.62211	-0.56515
C	6.6774	0.57115	-0.09897
H	5.10768	1.25423	1.21321
C	7.12446	-0.45502	-0.93134
H	6.69882	-2.40919	-1.73961
H	7.27691	1.47014	0.02914
H	8.07347	-0.35798	-1.45455
H	-4.50649	0.39874	0.5082

Acetic acid

O	-0.76161	-1.0504	0.00001
H	-1.71124	-0.83137	0.00003
C	-0.09208	0.12324	-0.00003
O	-0.65489	1.19898	0.0
C	1.38655	-0.09876	0.0
H	1.68222	-0.68041	0.87904
H	1.68226	-0.68042	-0.87901
H	1.91197	0.85667	0.0

I3

C	1.84145700	-2.41016000	-0.29097600
C	0.54106200	-2.90688600	-0.01268500
C	-0.49558900	-2.89024300	-0.98594000
C	-0.22385500	-2.17660500	-2.17816100
C	1.01892400	-1.53867900	-2.40092800
C	2.10846900	-1.71762700	-1.48533600
H	2.62447000	-2.53972600	0.45110500
H	-1.01767000	-2.05335500	-2.91290100
H	1.16771000	-0.96964300	-3.31513700
Ru	0.18421800	-0.72419400	-0.49817900
C	3.48679600	-1.21581800	-1.85958400
C	-1.79639200	-3.58961900	-0.76009700
H	-2.29396400	-3.24432900	0.15439200
C	-3.73460900	0.74636200	-2.08111400
C	-3.50951500	2.11592600	-2.15197200
C	-2.25618000	2.63223900	-1.77247100
C	-1.31706000	1.68399600	-1.34238300
C	-1.49132400	0.30389900	-1.23332500
C	-2.75139300	-0.15229900	-1.62351200
H	-2.56823600	4.76607800	-2.10781500
H	-4.70552600	0.35185500	-2.37706100

H	-4.29185700	2.78857100	-2.49887000
C	-1.84743000	4.01800900	-1.78273100
H	-3.00647600	-1.21061600	-1.55473600
C	0.35970300	3.44292800	-0.97487200
C	-0.59690600	4.41569900	-1.40170000
H	-0.31308900	5.46383700	-1.41879900
C	0.86833800	1.23354800	-0.58309400
C	1.66182600	3.36694000	-0.53512500
N	-0.06932200	2.12503700	-0.97812000
N	1.94031700	2.02669600	-0.30528100
H	2.41010700	4.12914200	-0.37619000
C	3.21706500	1.55755500	0.19126000
H	3.46961500	2.07480000	1.12189200
H	3.12658200	0.49004300	0.39466300
H	4.00455400	1.72999100	-0.54899700
H	3.40783900	-0.12636000	-2.00406600
C	0.17636500	-0.18862900	1.63323900
C	-1.02843600	-0.45319900	1.36409200
C	1.22240100	0.33279700	2.47635100
C	2.29567100	-0.47099000	2.89179000
C	1.18019600	1.67811000	2.87948500
C	3.30135400	0.05850600	3.69210400
H	2.33024900	-1.51630000	2.58697400
C	2.19182100	2.20260100	3.67721400
H	0.35327600	2.30553300	2.54880800
C	3.25580200	1.39702500	4.08261500
H	4.12588400	-0.57596500	4.01034300
H	2.15007600	3.24669600	3.98080100
H	4.04808400	1.81132800	4.70236500
C	-2.40557500	-0.71639800	1.67577400
C	-3.41125800	0.22578200	1.40039700
C	-2.75976900	-1.92751500	2.29786300
C	-4.73353600	-0.04248300	1.73410600
H	-3.14297000	1.16775400	0.92588200
C	-4.08538100	-2.18796300	2.62786400
H	-1.98240800	-2.65408900	2.53041600
C	-5.07616000	-1.24950500	2.34262400
H	-5.50144500	0.69737100	1.51630300
H	-4.34390100	-3.12767200	3.11146000
H	-6.11312600	-1.45633200	2.59890700
C	4.55561200	-1.50980600	-0.81506000
H	4.31546100	-1.12686000	0.18363300
H	4.72179800	-2.59053400	-0.72114900
H	5.50498700	-1.05622800	-1.11789500
C	3.90561000	-1.82552500	-3.20209700
H	3.20893600	-1.58034000	-4.00996100
H	4.89368400	-1.45012800	-3.48851100
H	3.96907500	-2.91823800	-3.12909200
H	-2.48107000	-3.44052100	-1.59996900
H	-1.63208800	-4.66790800	-0.65094100
H	0.35027700	-3.36728400	0.95612300

TS-2

C	-2.13301500	1.63778200	-1.58699400
C	-0.91884300	1.93832000	-2.24955200
C	-0.21432300	0.94645500	-2.97427900
C	-0.76620900	-0.36486000	-2.97569300
C	-2.02701300	-0.65817900	-2.39159000
C	-2.71597800	0.33036300	-1.65983600
H	-2.65271500	2.42013700	-1.03598700
H	-0.49676600	2.93890600	-2.16722600
H	-0.21249300	-1.16681100	-3.46008000
Ru	-0.61390300	0.18562000	-0.81837200
C	-4.03587800	0.06134100	-0.97841000
C	1.06129700	1.24701300	-3.68809100
H	1.53124200	2.15865400	-3.30686600
C	1.31197900	-3.86828500	-0.69532500
C	0.97704900	-4.29243200	0.58991200
C	0.29972800	-3.41505200	1.45547200
C	0.01540300	-2.14328800	0.93819200
C	0.42461100	-1.62510900	-0.30562300
C	1.06560800	-2.56423800	-1.13828000
H	0.08952400	-4.67410900	3.22461900
H	1.81066800	-4.56275100	-1.36887000
H	1.21998300	-5.30027600	0.92026900
C	-0.15483200	-3.70396100	2.79652100
H	1.42189900	-2.26427700	-2.12354000

C	-1.23593000	-1.54884700	2.96171500
C	-0.87370900	-2.80720300	3.53338700
H	-1.20490100	-3.04521600	4.53973100
C	-1.24346400	-0.15393600	1.12943400
C	-2.00777600	-0.44940300	3.25221900
N	-0.77394500	-1.30461100	1.67449100
N	-1.99036600	0.37664100	2.13569300
H	-2.58338900	-0.19285200	4.12910200
C	-2.69182300	1.64472200	2.08739400
H	-2.29906200	2.31927800	2.85331000
H	-2.53215100	2.09038600	1.10515300
H	-3.76203000	1.49109100	2.25255600
H	-4.08966900	0.74198100	-0.11542000
C	0.83842700	1.05621000	0.38746100
C	1.47090100	0.00654900	-0.06710700
C	2.85571300	-0.24474400	-0.46299400
C	3.56418900	-1.37027300	-0.01596200
C	3.53702500	0.73031300	-1.20920900
C	4.91248400	-1.52064700	-0.32080400
H	3.05573300	-2.11573700	0.59210400
C	4.88258000	0.56985800	-1.52386600
H	2.99842400	1.61951900	-1.53238800
C	5.57273000	-0.55815900	-1.08412000
H	5.45210000	-2.39222700	0.04425500
H	5.39294700	1.33107400	-2.11054300
H	6.62591700	-0.68315400	-1.32752200
C	-5.17384200	0.43106200	-1.93278000
H	-5.10142600	1.47145700	-2.26945800
H	-5.16087400	-0.21418900	-2.82029300
H	-6.14190400	0.30149900	-1.43664600
C	-4.18575300	-1.36642600	-0.47081200
H	-3.33334000	-1.67236300	0.14935900
H	-5.09455700	-1.45475400	0.13375200
H	-4.27709200	-2.08304200	-1.29644600
H	1.77728500	0.42204700	-3.60249700
H	0.86686400	1.39908200	-4.75731200
H	-2.40619600	-1.67613400	-2.42862600
C	1.02582500	2.26096100	1.14105300
C	0.15011400	3.35261600	1.00788700
C	2.11690900	2.37700100	2.02762700
C	0.35918800	4.52400700	1.72534700
H	-0.69492000	3.26684100	0.32525400
C	2.31679400	3.54764700	2.74604600
H	2.79851900	1.53539300	2.14298700
C	1.44125700	4.62576500	2.59906800
H	-0.32755300	5.35962900	1.60578300
H	3.16179300	3.62151600	3.42794800
H	1.60151400	5.54027000	3.16615300

I4

C	2.44506600	-2.20388400	-1.16568600
C	3.25264600	-1.23189900	-0.50595500
C	3.04350000	0.14010600	-0.74136100
C	1.98270700	0.51467100	-1.63622200
C	1.23424600	-0.46307900	-2.33762800
C	1.49422400	-1.85111900	-2.15534500
H	0.44145600	-0.14639400	-3.01329900
C	0.74248800	-2.87946000	-2.93276800
C	3.92352900	1.16644500	-0.05988500
C	-2.52056500	2.94181000	-2.46651200
C	-1.85049600	3.92115400	-1.75361900
C	-1.09610700	3.58892000	-0.61761800
C	-0.96155700	2.22197100	-0.25416800
C	-1.77749800	1.24764500	-0.86593200
C	-2.52295200	1.63527500	-1.98683800
H	-0.77322800	5.65868900	-0.03734000
H	-3.09792700	3.20060700	-3.35088100
H	-1.92903000	4.96937500	-2.03604900
C	-0.60327400	4.62432300	0.25283600
H	-3.15283700	0.88449900	-2.46153400
C	0.26874500	2.96680800	1.73616400
C	-0.03945600	4.32372200	1.44695100
H	0.26788300	5.08716800	2.15538500
C	0.63666400	0.80140400	1.08801200
C	1.10384100	2.38748500	2.64802800
N	-0.07623100	1.94906300	0.82029600
N	1.31285500	1.09261500	2.23667000

C	2.20743000	0.19034900	2.94345200
H	1.70833700	-0.22856100	3.82317000
H	2.50304100	-0.61765800	2.27032900
H	3.09270400	0.74268500	3.26747100
H	1.20167600	-3.00445000	-3.92158600
C	-1.00181000	-0.91753500	-0.05168800
C	-2.03342000	-0.09841100	-0.28992000
H	3.98747900	0.88749600	1.00306500
Ru	1.01548600	-0.79075400	-0.17416200
C	-3.43883700	-0.42009200	0.05395900
C	-3.89470800	-1.74661000	0.12913000
C	-4.35502100	0.60316000	0.35650200
C	-5.20279300	-2.03860200	0.49793600
H	-3.21741100	-2.56105000	-0.11696600
C	-5.66398400	0.31027400	0.72591000
H	-4.03287100	1.64254100	0.31298600
C	-6.09703000	-1.01195900	0.79844800
H	-5.52836400	-3.07655900	0.54007500
H	-6.34856700	1.12334600	0.96124600
H	-7.12236900	-1.24093000	1.08188200
C	-0.63930200	-2.18487700	0.50907800
C	-0.79842600	-3.45117200	-0.14021800
C	0.22566700	-2.12128500	1.65581500
C	-0.12687100	-4.55888800	0.31281100
H	-1.45068600	-3.51644400	-1.00906800
C	0.91332900	-3.28561800	2.08359800
H	0.11505300	-1.29383000	2.35072500
C	0.75787100	-4.47722800	1.41513200
H	-0.27383100	-5.51532800	-0.18580500
H	1.53839200	-3.23007900	2.97356300
H	1.28243100	-5.36860800	1.75130200
H	1.62583000	2.81300800	3.49228100
H	0.75628600	-3.85480700	-2.43772900
H	-0.29971100	-2.58113400	-3.09434100
C	5.33614200	1.07367700	-0.64495800
H	5.32917900	1.31312100	-1.71583900
H	6.00014900	1.78801500	-0.14563000
H	5.76374100	0.07218900	-0.52558000
C	3.40785000	2.59510400	-0.15647400
H	4.02824200	3.25810000	0.45563900
H	3.45315500	2.96629600	-1.18826100
H	2.37368300	2.69743300	0.19109200
H	1.74379500	1.56522300	-1.78261900
H	3.99913000	-1.55245800	0.21816500
H	2.56639100	-3.25558300	-0.90731200

I5

C	0.22397	0.32118	-1.91173
C	1.25889	1.25217	-1.71685
C	2.28006	1.5201	-2.65236
C	2.2537	0.79526	-3.85253
C	1.24695	-0.13724	-4.07673
C	0.24624	-0.36889	-3.13303
H	3.02629	0.97004	-4.59815
H	1.2354	-0.69955	-5.00771
H	-0.53192	-1.10207	-3.33836
C	3.28034	2.50279	-2.32143
C	3.27614	3.17123	-1.13522
C	2.26112	2.89019	-0.17951
N	1.29996	1.93943	-0.5217
C	1.93606	3.2907	1.09406
C	0.4229	1.74447	0.49752
C	0.25401	2.62684	2.83008
H	-0.73765	3.08682	2.82212
H	0.17766	1.60537	3.21914
H	0.92365	3.20745	3.4648
N	0.81893	2.58673	1.49084
C	-0.78816	0.09134	-0.8609
C	-0.70044	0.85356	0.39265
C	-2.1568	-0.31129	-1.31798
C	-2.95657	-1.20716	-0.59789
C	-2.71373	0.298	-2.45328
C	-4.25984	-1.49085	-0.99535
H	-2.54094	-1.6942	0.28448
C	-4.01621	0.01637	-2.85426
H	-2.11987	1.01334	-3.02124
C	-4.7962	-0.88087	-2.12715

H	-4.85479	-2.1976	-0.41931
H	-4.42388	0.50622	-3.73665
H	-5.81396	-1.10376	-2.44138
C	-1.93919	1.24079	1.14857
C	-2.39951	0.54464	2.269
C	-2.65631	2.36101	0.70789
C	-3.55164	0.9548	2.93578
H	-1.84226	-0.32344	2.62454
C	-3.80909	2.77067	1.37177
H	-2.30435	2.90986	-0.16626
C	-4.25963	2.06775	2.48847
H	-3.89478	0.40231	3.80822
H	-4.35598	3.64163	1.01593
H	-5.15993	2.38841	3.0087
H	4.05978	2.7035	-3.05301
H	4.03479	3.90864	-0.89301
H	2.41433	3.99918	1.75305
Ru	0.17842	-1.10522	0.74246
C	2.10105	-2.02467	-0.13258
C	0.97969	-2.66606	-0.70598
C	-0.03574	-3.2811	0.08417
C	0.11741	-3.23426	1.49909
C	1.24626	-2.60339	2.07996
C	2.24037	-1.96555	1.28258
H	2.83604	-1.54732	-0.77965
H	0.84991	-2.63412	-1.78742
H	-0.64286	-3.68052	2.1371
H	1.3216	-2.5376	3.16413
C	-1.17148	-4.00788	-0.56044
H	-2.0423	-4.06994	0.10089
C	3.43537	-1.29971	1.92446
H	3.26756	-1.31609	3.01177
H	-1.48365	-3.52146	-1.49173
H	-0.87385	-5.03512	-0.8102
C	4.70613	-2.096	1.62882
H	5.56597	-1.65719	2.14814
H	4.61254	-3.13987	1.94953
H	4.92968	-2.09401	0.55403
C	3.58175	0.15489	1.49532
H	4.44794	0.62268	1.97825
H	3.72258	0.2438	0.40898
H	2.68708	0.72808	1.76812

4.3a-OAc

C	-2.36302300	3.52801100	0.18951700
C	-3.53461400	2.77373700	0.12318400
C	-3.47328500	1.38034900	0.02826800
C	-2.18396500	0.80087800	-0.00333800
C	-0.97945800	1.53545600	0.04009000
C	-1.10851600	2.93328300	0.15158500
H	-5.60690900	0.96289900	-0.01950400
H	-2.43222600	4.60962000	0.27558700
H	-4.50626400	3.26198200	0.14970100
C	-4.61880600	0.51007000	-0.04367900
H	-0.21484700	3.54771700	0.21483600
C	-3.19489100	-1.41997100	-0.17821400
C	-4.49349600	-0.84067300	-0.14806600
H	-5.35857200	-1.49262700	-0.21157200
C	-0.92990000	-1.25631800	-0.11994000
C	-2.64966500	-2.67616600	-0.29188600
N	-2.10187600	-0.56120300	-0.08436800
N	-1.28050100	-2.56418900	-0.26596000
C	0.27575100	0.81850200	0.01327100
C	0.30956300	-0.56961000	-0.04553000
C	1.54182300	1.58719000	0.07006300
C	2.43832000	1.41183400	1.13159800
C	1.86490000	2.49022100	-0.95109400
C	3.63497700	2.12022300	1.16715000
H	2.19012000	0.71810800	1.93326900
C	3.06829000	3.18888800	-0.91923900
H	1.17555000	2.62782500	-1.78350200
C	3.95550500	3.00596300	0.13965000
H	4.31976200	1.97881000	2.00075000
H	3.31260500	3.87710200	-1.72570400
H	4.89487200	3.55442200	0.16495900
C	1.58427400	-1.33046600	-0.04172000
C	2.45687900	-1.25817300	-1.13321000

TH-3565_186122020

C	1.93353100	-2.11068300	1.06617500
C	3.65534400	-1.96543800	-1.11892300
H	2.18896200	-0.64658800	-1.99355600
C	3.13488100	-2.81329500	1.07967900
H	1.26391100	-2.15490600	1.92517400
C	3.99607500	-2.74421300	-0.01380700
H	4.32497800	-1.90794500	-1.97441100
H	3.39911200	-3.41325300	1.94820700
H	4.93412900	-3.29523500	-0.00401400
C	-0.38979400	-3.70925000	-0.42129600
H	0.40716300	-3.46927800	-1.12634600
H	0.04531600	-3.99089600	0.54027400
H	-0.98114300	-4.53737500	-0.81178800
H	-3.12798900	-3.63902600	-0.39601800
H	-5.44024500	-3.53262300	2.38067800
H	-4.69584400	-3.52309500	2.34355200

[Ru(*p*-cym)(OAc)$_2$]

C	0.36676300	-0.31939400	2.14367600
C	-0.99853300	-0.70510100	1.94129600
C	-1.28036900	-1.65654100	0.91736600
C	-0.25553800	-2.10695000	0.06097200
C	1.10638600	-1.69024200	0.23807500
C	1.40348100	-0.83877800	1.33628000
H	0.59835500	0.47324300	2.85073500
H	-2.31519800	-1.87845500	0.67844100
H	-0.52713700	-2.69297700	-0.81320000
H	2.40209100	-0.42873800	1.44799600
Ru	-0.17392500	0.05663600	0.11340400
C	2.21030000	-2.06386800	-0.73335700
H	2.94412700	-2.62423800	-0.13105200
C	-2.09875300	-0.09557600	2.74132300
H	-3.00370100	-0.00083700	2.13465700
H	-2.32494500	-0.73488100	3.60497800
H	-1.81578100	0.89016900	3.12367300
C	1.74621800	-2.96698600	-1.86671500
H	2.60014900	-3.24330000	-2.49391600
H	1.29001300	-3.89417000	-1.50216800
H	1.01901200	-2.45719900	-2.51250200
C	2.91659800	-0.82785400	-1.29300800
H	3.27423400	-0.15270300	-0.50710100
H	3.78204300	-1.12820800	-1.89385000
H	2.23754100	-0.25624300	-1.93982900
O	0.72516600	1.81601800	-0.41594500
O	-1.58482300	0.85279700	-1.14336800
C	1.78247400	2.32561500	0.17589600
C	-2.86301900	0.55783100	-1.17036000
C	2.47793400	3.36303100	-0.67312100
H	1.76409700	4.10217900	-1.05030800
H	3.26569600	3.86734100	-0.10882600
H	2.92457800	2.87935200	-1.55027800
C	-3.53797500	1.01117300	-2.44377100
H	-3.08537600	0.51402300	-3.30887500
H	-4.60733400	0.78959300	-2.42080300
H	-3.39406600	2.08706100	-2.58932900
O	2.19032400	2.01683300	1.29448900
O	-3.48460300	-0.00079100	-0.26711500

Annexure VIII

The cartesian coordinates (xyz) for all the optimized structures (*Chapter 5*)

5.1a

C	3.17443	-0.83624	3.02544
C	3.10359	0.3033	2.23804
C	3.34967	0.21523	0.86535
C	3.68145	-1.0245	0.26524
C	3.74967	-2.15801	1.09601
C	3.49605	-2.07254	2.45402
H	2.97606	-0.76178	4.09224
H	2.8474	1.26012	2.68722
C	3.90636	-1.09602	-1.15146
H	4.00551	-3.11591	0.6429
H	3.54988	-2.96305	3.07626
C	3.76748	0.00428	-1.93829
C	3.41683	1.25032	-1.36052
H	4.17666	-2.05828	-1.58242
H	3.91883	-0.04317	-3.01392
C	2.90821	2.62786	0.30158
C	3.16939	2.53315	-1.81831
N	3.24554	1.32855	0.02917
N	2.86057	3.36755	-0.78854
H	2.70555	2.97972	1.30496
H	3.20798	2.88701	-2.84182
C	-0.41964	-0.45598	-2.04364
C	-0.55732	0.94376	-1.92861
C	-0.28618	1.62735	-0.6943
C	0.15552	0.84347	0.40105
C	0.27846	-0.57597	0.30158
C	-0.05002	-1.25066	-0.9056
H	-0.76132	-0.95722	-2.94834
H	-1.00251	1.50377	-2.74972
H	0.2223	1.3144	1.37813
H	0.47375	-1.14873	1.20544
Ru	-1.68683	0.01089	-0.34581
O	-2.6352	-0.13522	1.50125
O	-3.34539	-1.31634	-0.83247
C	-4.12249	-0.3111	-0.91538
C	-2.58561	0.86372	2.34074
C	-5.59976	-0.49422	-1.02197
H	-6.02101	-0.54521	-0.01106
H	-6.06302	0.35121	-1.53677
H	-5.84143	-1.43032	-1.53186
C	-3.46746	0.64167	3.55244
O	-1.94034	1.9031	2.20313
O	-3.61407	0.8562	-0.86945
C	-0.12767	-2.75678	-1.00538
H	-0.95988	-2.97109	-1.69414
C	1.15617	-3.31189	-1.62087
H	1.06326	-4.38971	-1.79906
H	1.39956	-2.82773	-2.5749
H	2.00422	-3.15419	-0.94199
C	-0.43838	-3.43153	0.32367
H	-1.32759	-2.99788	0.79727
H	-0.62224	-4.50059	0.16973
H	0.40371	-3.34701	1.0242
C	-0.57806	3.08217	-0.54015
H	0.3093	3.67708	-0.79464
H	-1.39877	3.38611	-1.19957
H	-0.87225	3.29771	0.49128
H	-4.50523	0.87758	3.28806
H	-3.44815	-0.40239	3.87916
H	-3.16706	1.30061	4.3709

Int1

C	-2.27345	-2.23516	0.91677
C	-1.47865	-1.71899	1.96623
C	-1.79606	-0.40181	2.44701
C	-2.84907	0.35881	1.88998
C	-3.64903	-0.16038	0.81007
C	-3.34338	-1.46715	0.35575

TH-3565_186122020

H	-1.96736	-3.15954	0.43367
H	-1.13349	0.06524	3.17578
H	-2.96755	1.39362	2.19992
H	-3.8362	-1.84944	-0.53427
Ru	-1.52405	-0.29831	0.31259
C	-4.71914	0.66719	0.12053
H	-5.68296	0.25865	0.47281
C	-0.28302	-2.46275	2.46358
H	-0.55407	-3.13541	3.28806
H	0.15185	-3.06089	1.65554
H	0.48488	-1.77433	2.83498
C	-4.67284	2.14361	0.49881
H	-5.46909	2.68466	-0.02461
H	-4.82479	2.30664	1.57266
H	-3.71141	2.58125	0.20469
C	-4.66962	0.51514	-1.3999
H	-4.8589	-0.51106	-1.73267
H	-5.43404	1.14944	-1.86339
H	-3.68626	0.81972	-1.77593
O	-1.11094	-0.95897	-1.63869
C	0.97306	1.40896	1.07177
C	2.34576	1.48299	0.96407
C	1.60803	-0.45192	0.14209
N	0.54614	0.21994	0.55847
N	2.73226	0.27459	0.36673
H	1.56005	-1.43415	-0.3115
C	3.34435	2.43205	1.30101
C	4.06617	-0.03843	0.08509
C	4.65072	2.16032	1.0435
C	5.04571	0.9222	0.4315
C	6.38939	0.6159	0.15174
C	4.42004	-1.2468	-0.51816
C	6.74348	-0.58161	-0.44332
C	5.75513	-1.51319	-0.77938
H	7.15201	1.34853	0.41321
H	7.7888	-0.79774	-0.6524
H	6.02894	-2.45408	-1.25134
H	3.65346	-1.97011	-0.78636
H	5.42661	2.88148	1.29249
H	3.03573	3.36837	1.7582
H	0.27183	2.15432	1.42333
C	-0.38088	-2.00164	-1.85593
C	-0.12618	-2.23918	-3.32857
H	-1.04137	-2.11335	-3.91499
H	0.58254	-1.48254	-3.68683
H	0.29646	-3.23273	-3.49821
O	0.12272	-2.74083	-0.99236
O	-1.65484	1.57926	-0.62586
C	-0.84834	2.0413	-1.55419
C	-1.44312	3.27541	-2.21601
H	-1.72956	4.02298	-1.46717
H	-0.73134	3.71585	-2.91865
H	-2.35879	3.0059	-2.75677
O	0.24419	1.60223	-1.88867

Int2

C	-1.45546	-2.66501	-0.88585
C	-0.2066	-2.64222	-0.18018
C	-0.08168	-2.01741	1.09104
C	-1.23391	-1.34431	1.6092
C	-2.44763	-1.32163	0.88315
C	-2.59258	-2.01967	-0.36369
H	-1.48435	-3.07215	-1.89577
H	0.68068	-3.07366	-0.64485
H	-1.16541	-0.71191	2.49114
H	-3.25505	-0.64643	1.20508
Ru	-0.86178	-0.60197	-0.38692
O	-1.9635	1.02808	-1.31695
C	-1.2739	0.9364	-2.37953
C	-1.46864	1.90183	-3.50126
H	-2.48819	2.29514	-3.49782
H	-0.78168	2.74685	-3.37411
H	-1.2438	1.43318	-4.46277
O	-0.38817	0.02047	-2.44839
C	-3.86923	-1.88638	-1.12669
H	-3.71291	-2.00985	-2.20423
C	1.25048	-2.04886	1.80668

H	2.02669	-1.86287	1.04654
C	4.8812	-0.93022	-1.66439
C	5.15335	0.15233	-0.84758
C	4.12263	0.88698	-0.23512
C	2.78345	0.4812	-0.46193
C	2.51106	-0.5886	-1.31656
C	3.55318	-1.29065	-1.90581
H	5.44839	2.32647	0.7141
H	5.69439	-1.48399	-2.12851
H	6.18185	0.4637	-0.66834
C	4.40848	2.03701	0.57678
H	1.4822	-0.84933	-1.5373
H	3.32282	-2.11885	-2.57327
C	2.06019	2.34051	0.9664
C	3.40553	2.7552	1.13842
H	3.59834	3.6378	1.74291
C	0.40529	0.93804	0.24828
C	0.8601	2.78043	1.46034
N	1.759	1.19599	0.19197
N	-0.10274	1.9283	1.0077
H	0.63566	3.61813	2.10482
H	-4.59052	-2.64749	-0.80186
H	-4.32043	-0.90657	-0.93287
C	1.47738	-3.45174	2.37533
H	2.45306	-3.51378	2.8712
H	0.70893	-3.6997	3.11889
H	1.44573	-4.2205	1.59443
C	1.38895	-1.00305	2.90485
H	0.73576	-1.23152	3.7569
H	2.41863	-0.98529	3.27998
H	1.14061	0.00642	2.55946
H	-1.15226	1.91016	1.32191
C	-3.70604	3.13631	0.60656
H	-3.57023	3.88626	1.39545
H	-2.92207	3.30962	-0.14232
H	-4.68052	3.28289	0.13205
C	-3.56465	1.7295	1.17197
O	-2.48558	1.49554	1.83357
O	-4.46869	0.89818	0.97346

Int3

C	-3.23941	0.28935	1.14534
C	-2.27593	1.33837	1.08888
C	-1.71159	1.80788	-0.13807
C	-2.07255	1.09265	-1.32053
C	-2.93362	-0.0292	-1.26677
C	-3.53243	-0.44255	-0.02466
H	-3.60861	-0.05843	2.10721
H	-1.9259	1.78483	2.02093
H	-1.55594	1.29917	-2.25558
H	-3.06668	-0.63892	-2.15779
Ru	-1.32334	-0.32337	0.1166
O	-1.11272	-2.49042	0.37169
C	-0.33681	-2.31305	1.36329
C	0.38269	-3.45802	1.99467
H	-0.14381	-4.39889	1.81748
H	1.38026	-3.53628	1.54523
H	0.5173	-3.29101	3.06664
O	-0.14528	-1.1233	1.7764
C	-4.36018	-1.68474	0.01545
H	-4.48719	-2.05133	1.03864
C	-0.79143	3.005	-0.14321
H	-0.24882	2.99479	0.81635
C	3.98878	1.40181	2.17625
C	4.61038	0.68447	1.16955
C	3.87371	0.06132	0.14623
C	2.4569	0.15564	0.18535
C	1.83967	0.90737	1.18814
C	2.59656	1.52207	2.17416
H	5.609	-0.67305	-0.94153
H	4.58093	1.88001	2.95404
H	5.6969	0.60292	1.14146
C	4.52229	-0.61054	-0.94409
H	0.75803	0.99546	1.19117
H	2.0945	2.10029	2.94813
C	2.38008	-1.02064	-1.95872
C	3.79209	-1.1045	-1.97891

H	4.26675	-1.57246	-2.83889
C	0.35447	-0.55764	-1.07282
C	1.36456	-1.37463	-2.82132
N	1.72477	-0.47658	-0.83252
N	0.15068	-1.08076	-2.28389
H	1.46107	-1.8373	-3.79775
H	-5.35576	-1.49812	-0.40767
H	-3.8915	-2.48028	-0.57367
C	-1.62826	4.28521	-0.19158
H	-0.98438	5.17154	-0.1478
H	-2.20467	4.33788	-1.12459
H	-2.33875	4.3408	0.64191
C	0.23642	2.98083	-1.26537
H	-0.23497	3.12784	-2.24596
H	0.96337	3.78964	-1.13224
H	0.78351	2.03132	-1.29366

TS-1

C	-1.17843	-2.45881	-0.58567
C	-1.57091	-1.16464	-0.97416
C	-0.78602	-0.36799	-1.87167
C	0.42447	-0.93632	-2.34626
C	0.83762	-2.24914	-1.96352
C	0.05011	-3.01322	-1.0664
H	-2.45653	-0.72458	-0.51487
Ru	0.48228	-0.99966	-0.18023
O	1.4057	-2.11081	1.4129
C	1.33543	-1.69865	2.61058
C	1.97591	-2.52664	3.68244
H	2.30157	-3.49371	3.296
H	2.84369	-1.99165	4.08269
H	1.27783	-2.67211	4.51163
O	0.7591	-0.62033	2.95212
C	0.52369	-4.33884	-0.57569
H	0.23703	-4.50248	0.46723
C	-1.2657	1.01111	-2.25458
H	-1.6953	1.45579	-1.34305
C	-1.83653	2.55624	1.53305
C	-0.8895	3.55759	1.34225
C	0.41976	3.22877	0.93997
C	0.67165	1.86486	0.74768
C	-0.22561	0.80445	0.97641
C	-1.51543	1.20148	1.36916
H	1.31707	5.21713	0.87874
H	-2.84669	2.82839	1.83411
H	-1.15401	4.60146	1.50227
C	1.5009	4.1585	0.70756
H	0.26527	-0.07549	1.83727
H	-2.27149	0.44397	1.57593
C	2.96745	2.3661	0.01888
C	2.73418	3.74884	0.29021
H	3.53624	4.46181	0.12465
C	2.14032	0.22938	-0.15888
C	3.94557	1.5604	-0.51701
N	1.903	1.50153	0.25279
N	3.41788	0.2796	-0.60753
H	4.95032	1.781	-0.84541
H	0.06865	-5.137	-1.17567
H	1.61054	-4.43296	-0.65838
C	-2.39208	0.88556	-3.28206
H	-2.79415	1.87485	-3.52897
H	-2.02642	0.42943	-4.2111
H	-3.21678	0.27171	-2.90211
C	-0.1577	1.9235	-2.76149
H	0.20904	1.60697	-3.74649
H	-0.53175	2.94748	-2.86809
H	0.70019	1.95107	-2.07741
H	1.09179	-0.33852	-2.96432
H	-1.76496	-3.00271	0.1509
H	1.74554	-2.65741	-2.35582

Int4

C	-2.25387	0.61605	1.14378
C	-1.93226	1.94677	0.74316
C	-1.82553	2.27838	-0.62245
C	-2.08503	1.23598	-1.57211
C	-2.58344	-0.04192	-1.17721
C	-2.64199	-0.3884	0.19029

H	-2.20356	0.35899	2.19996
H	-1.61344	2.66632	1.49526
H	-1.90864	1.43447	-2.62873
Ru	-0.63864	0.40565	-0.23253
C	-3.03007	-1.78754	0.60639
C	-1.35413	3.62168	-1.0772
H	-0.83305	4.15695	-0.27642
C	3.22301	2.47365	1.05527
C	4.11856	1.43907	0.86275
C	3.65183	0.18799	0.3886
C	2.27589	0.10894	0.14703
C	1.30794	1.11413	0.32343
C	1.83945	2.31269	0.79261
H	5.5236	-0.92892	0.32044
H	3.58649	3.43273	1.42252
H	5.17891	1.57619	1.07341
C	4.45034	-0.98013	0.13951
H	1.18372	3.16827	0.97509
C	2.4956	-2.21825	-0.55522
C	3.8937	-2.15125	-0.31673
H	4.51229	-3.02722	-0.49654
C	0.42732	-1.26753	-0.58299
C	1.49912	-3.13032	-0.98669
N	1.77618	-1.0835	-0.31735
N	0.28338	-2.55879	-0.99362
H	1.64648	-4.16383	-1.284
H	-2.77827	-2.44351	-0.24023
C	-2.26686	-2.29586	1.8222
H	-1.18453	-2.20343	1.67751
H	-2.54385	-1.75347	2.73618
H	-2.49795	-3.35283	1.99555
C	-4.54047	-1.84869	0.83857
H	-5.10242	-1.5328	-0.04842
H	-4.85299	-2.86864	1.09232
H	-4.83574	-1.19434	1.67004
H	-0.6667	3.53556	-1.92643
H	-2.198	4.24694	-1.39882
H	-2.74367	-0.81278	-1.92873

Int5

C	1.935	-1.53297	-1.5382
C	0.70799	-2.23273	-1.689
C	-0.35912	-1.73021	-2.48265
C	-0.18174	-0.42911	-3.02238
C	0.99307	0.32728	-2.79476
C	2.09122	-0.22839	-2.04903
H	2.71638	-1.95983	-0.91256
H	-1.01436	0.03662	-3.54991
H	1.0682	1.34179	-3.18136
Ru	0.18058	-0.21724	-0.81884
C	3.35829	0.57138	-1.87079
C	-1.59915	-2.52977	-2.72594
H	-2.00388	-2.94437	-1.79368
C	-3.98108	1.47077	-0.94646
C	-3.80967	2.65984	-0.24802
C	-2.53614	3.0023	0.24775
C	-1.5206	2.06726	-0.00656
C	-1.63421	0.85917	-0.69983
C	-2.91483	0.5771	-1.17434
H	-2.93213	4.9401	1.17557
H	-4.96983	1.21645	-1.32797
H	-4.65255	3.33251	-0.09118
C	-2.1593	4.20429	0.95582
H	-3.12114	-0.35858	-1.69904
C	0.16755	3.50891	1.04916
C	-0.86419	4.45249	1.33206
H	-0.61109	5.38043	1.84083
C	0.79071	1.52359	0.14751
C	1.54411	3.31534	1.13289
N	-0.25743	2.34708	0.42702
N	1.91023	2.11034	0.5792
H	2.28769	3.98239	1.55508
H	3.04554	1.60505	-1.66453
C	0.44194	-0.95506	1.25253
C	-0.76517	-1.16634	0.96086
C	1.66057	-1.05207	2.00915
C	2.42495	-2.22969	1.92998

TH-3565_186122020

C	2.11424 -0.00126 2.82051	H	-0.49587 2.93865 -2.16794
C	3.61637 -2.34789 2.63409	H	-0.21256 -1.16742 -3.4599
H	2.06496 -3.0529 1.31205	Ru	-0.61387 0.18567 -0.81852
C	3.30707 -0.12849 3.52321	C	-4.03586 0.06227 -0.97886
H	1.53009 0.91274 2.88145	C	1.06189 1.24602 -3.6883
C	4.06457 -1.29366 3.42871	H	1.53204 2.15762 -3.30722
H	4.19589 -3.26692 2.56502	C	1.31093 -3.86872 -0.69444
H	3.64987 0.69581 4.14573	C	0.97576 -4.29251 0.59086
H	5.00073 -1.38316 3.97673	C	0.29859 -3.41476 1.45617
C	-2.08571 -1.70156 1.13851	C	0.01465 -2.14303 0.9386
C	-3.1604 -0.89769 1.55081	C	0.42412 -1.62522 -0.30529
C	-2.31757 -3.06503 0.8865	C	1.06495 -2.5647 -1.13769
C	-4.42713 -1.44733 1.70539	H	0.08788 -4.67339 3.22556
H	-2.98974 0.16118 1.73477	H	1.8095 -4.56346 -1.36779
C	-3.58802 -3.60764 1.04223	H	1.2184 -5.30034 0.92145
H	-1.48184 -3.69485 0.58023	C	-0.15617 -3.70327 2.79724
C	-4.64794 -2.79925 1.44897	H	1.42141 -2.26504 -2.12298
H	-5.25024 -0.80924 2.0224	C	-1.23672 -1.54784 2.96187
H	-3.74971 -4.66686 0.84928	C	-0.87488 -2.80617 3.53384
H	-5.64325 -3.22335 1.56833	H	-1.20624 -3.04388 4.54021
C	4.20338 0.11231 -0.69265	C	-1.2437 -0.15331 1.1293
H	3.61907 0.11263 0.23477	C	-2.0083 -0.44813 3.25207
H	4.62643 -0.88939 -0.85513	N	-0.77454 -1.30399 1.67464
H	5.04459 0.79926 -0.54949	N	-1.99056 0.37768 2.13537
C	4.15568 0.54876 -3.17674	H	-2.58393 -0.19124 4.12885
H	3.56837 0.91789 -4.02659	H	-4.08955 0.7431 -0.11602
H	5.05013 1.17628 -3.08934	C	0.83858 1.05613 0.38727
H	4.48645 -0.47036 -3.41866	C	1.47082 0.00621 -0.06702
H	-2.38181 -1.9194 -3.18771	C	2.8556 -0.24554 -0.46272
H	-1.39722 -3.37176 -3.40115	C	3.56374 -1.37116 -0.01538
H	0.58098 -3.19166 -1.18438	C	3.53725 0.72918 -1.20907
	TS-2	C	4.91202 -1.52196 -0.32006
C	-2.13252 1.63808 -1.58759	H	3.05502 -2.11636 0.59279
C	-0.9182 1.93815 -2.2501	C	4.88279 0.5683 -1.52357
C	-0.21388 0.94595 -2.97455	H	2.99891 1.61846 -1.53249
C	-0.76611 -0.36522 -2.97574	C	5.5726 -0.5598 -1.08352
C	-2.02705 -0.65808 -2.3917	H	5.45137 -2.3936 0.04523
C	-2.71582 0.3308 -1.66022	H	5.39341 1.32926 -2.11035

H	6.62577	-0.68513	-1.32679
C	-5.17363	0.43209	-1.93342
H	-5.10091	1.4724	-2.27031
H	-5.16075	-0.21335	-2.82079
H	-6.14178	0.30289	-1.43735
C	-4.18616	-1.36535	-0.47098
H	-3.33389	-1.67139	0.14934
H	-5.09505	-1.45331	0.13352
H	-4.27761	-2.08212	-1.29647
H	1.77765	0.42088	-3.60246
H	0.8676	1.39792	-4.75757
H	-2.4065	-1.67594	-2.42855
C	1.02622	2.26099	1.14063
C	0.15082	3.35285	1.00715
C	2.11726	2.37693	2.02728
C	0.36013	4.52434	1.72438
H	-0.69418	3.26716	0.32445
C	2.31738	3.54767	2.74548
H	2.79863	1.53516	2.14289
C	1.44214	4.62599	2.59819
H	-0.32638	5.36012	1.60458
H	3.16233	3.62146	3.42744
H	1.60259	5.54057	3.16509
H	-2.62435	2.40158	-1.02185

Int6

C	-2.67016	-2.08727	1.02031
C	-3.37654	-1.07141	0.30761
C	-3.09104	0.28794	0.53132
C	-2.0509	0.60566	1.47213
C	-1.397	-0.41448	2.21638
C	-1.74731	-1.78539	2.04975
H	-0.61032	-0.13985	2.91878
C	-1.07754	-2.85482	2.84875
C	-3.82653	1.34854	-0.26167
C	2.46595	2.91643	2.43987
C	1.8466	3.89939	1.6854
C	1.11566	3.56862	0.53341
C	0.95368	2.19541	0.19506
C	1.72203	1.21132	0.85566
C	2.44164	1.59763	1.99378
H	0.82828	5.62667	-0.10732
H	3.02503	3.18024	3.33559
H	1.94671	4.95104	1.95237
C	0.64843	4.58594	-0.371
H	3.03915	0.84019	2.50001
C	-0.20839	2.89785	-1.84907
C	0.09685	4.2522	-1.56862
H	-0.18833	5.01006	-2.29524
C	-0.63595	0.77705	-1.20075
C	-1.02558	2.25272	-2.75401
N	0.09813	1.91478	-0.88357
N	-1.28177	0.97533	-2.35151
H	-1.59728	-3.01252	3.80332
C	0.90405	-0.92172	-0.00502
C	1.95643	-0.14323	0.28738
H	-3.67485	1.09973	-1.32351
Ru	-1.10669	-0.76973	0.0838
C	3.36014	-0.50187	-0.02485
C	3.77105	-1.83874	-0.15567
C	4.32786	0.49568	-0.24071
C	5.07966	-2.16392	-0.48924
H	3.05199	-2.63731	0.00951
C	5.63788	0.16952	-0.5735
H	4.04305	1.54321	-0.15998
C	6.02498	-1.16193	-0.69807
H	5.36493	-3.21123	-0.57862
H	6.36064	0.96662	-0.74189
H	7.05169	-1.41701	-0.95432
C	0.51562	-2.17883	-0.57611
C	0.65003	-3.44636	0.08117
C	-0.35553	-2.10492	-1.72017
C	-0.04204	-4.546	-0.35848
H	1.30382	-3.51462	0.95003
C	-1.06638	-3.26191	-2.12749
H	-0.29104	-1.2638	-2.40513
C	-0.92854	-4.45559	-1.45856

H	0.09116	-5.50242	0.14654
H	-1.70288	-3.19458	-3.00868
H	-1.46894	-5.34016	-1.79049
H	-1.48768	2.67401	-3.64062
H	-1.07127	-3.81088	2.31411
H	-0.03953	-2.5873	3.08168
C	-5.3236	1.28413	0.04846
H	-5.51661	1.51258	1.1051
H	-5.87144	2.01757	-0.55491
H	-5.7492	0.29586	-0.15988
C	-3.30341	2.7589	-0.03458
H	-3.82102	3.46185	-0.69688
H	-3.48035	3.09196	0.99758
H	-2.23203	2.84527	-0.24349
H	-1.74416	1.63917	1.61363
H	-4.08851	-1.35335	-0.4652
H	-2.84398	-3.13248	0.76303

Int7

C	0.26365	-1.82309	0.67329
C	1.38597	-2.0747	-0.14025
C	2.46829	-2.9066	0.22394
C	2.41977	-3.49878	1.49594
C	1.3374	-3.25399	2.33233
C	0.27607	-2.43991	1.93474
H	3.23484	-4.14587	1.81597
H	1.31012	-3.71058	3.32025
H	-0.55897	-2.27193	2.61291
C	3.53752	-3.08459	-0.72301
C	3.52897	-2.47445	-1.94669
C	2.45638	-1.62071	-2.30317
N	1.44836	-1.45206	-1.36141
C	2.05549	-0.80394	-3.35992
C	0.52703	-0.56594	-1.86434
N	0.88951	-0.16821	-3.09098
C	-0.79992	-0.91129	0.20422
C	-0.66643	-0.27307	-1.09892
C	-2.16217	-1.07692	0.80072
C	-3.00874	0.01353	1.04114
C	-2.67165	-2.36105	1.04882
C	-4.30474	-0.16568	1.5108
H	-2.63316	1.01941	0.84256
C	-3.96752	-2.54452	1.52167
H	-2.04424	-3.22931	0.85094
C	-4.79203	-1.4471	1.75604
H	-4.93726	0.70354	1.68546
H	-4.33571	-3.55367	1.70021
H	-5.80548	-1.58935	2.12707
C	-1.81365	0.27334	-1.88599
C	-1.71054	1.5267	-2.50397
C	-2.97993	-0.47506	-2.08798
C	-2.75154	2.02898	-3.27624
H	-0.79378	2.10268	-2.37495
C	-4.024	0.02992	-2.85683
H	-3.07164	-1.4602	-1.6337
C	-3.91742	1.28537	-3.44876
H	-2.6502	3.00551	-3.74686
H	-4.92444	-0.56627	-2.99576
H	-4.73589	1.68026	-4.04837
H	4.3671	-3.73104	-0.44196
H	4.34004	-2.62661	-2.65452
H	2.57328	-0.64868	-4.29964
Ru	0.08311	1.1591	0.40387
C	1.95493	1.1141	1.70332
C	0.82836	0.91023	2.53428
C	-0.26912	1.81931	2.55895
C	-0.19872	2.96051	1.71072
C	0.93882	3.18165	0.88757
C	2.02017	2.25383	0.84955
H	2.75279	0.37179	1.69214
H	0.76084	-0.01001	3.11478
H	-1.02728	3.66683	1.69138
H	0.95873	4.04075	0.21845
C	-1.42818	1.59667	3.47718
H	-2.33437	2.09487	3.1143
C	3.22617	2.50613	-0.02592
H	2.98755	3.3762	-0.65783

H	-1.65885	0.53002	3.58538
H	-1.21405	1.99205	4.48002
C	4.4375	2.8655	0.83442
H	5.30089	3.119	0.20736
H	4.23117	3.71981	1.48985
H	4.72827	2.02063	1.47262
C	3.52685	1.33032	-0.94659
H	4.40793	1.53259	-1.56853
H	3.73283	0.41289	-0.37773
H	2.67903	1.12801	-1.61167

5.3a

C	1.15579	1.23143	-0.05397
C	2.29242	0.39262	-0.00958
C	3.63158	0.85254	-0.01994
C	3.8228	2.23753	-0.09499
C	2.72397	3.09092	-0.17019
C	1.41862	2.61226	-0.15432
H	4.83544	2.6373	-0.105
H	2.88936	4.16397	-0.24729
H	0.58809	3.30904	-0.22931
C	4.67977	-0.13178	0.04005
C	4.41347	-1.47069	0.09519
C	3.07082	-1.92639	0.08984
N	2.08386	-0.95275	0.03291
C	2.34749	-3.11948	0.12332
C	0.8548	-1.57732	0.03499
N	1.01245	-2.90524	0.09347
C	-0.16216	0.62389	-0.03116
C	-0.31534	-0.75893	0.01293
C	-1.34254	1.52024	-0.09187
C	-2.28183	1.40427	-1.12371
C	-1.55061	2.49396	0.89423
C	-3.39999	2.22986	-1.16331
H	-2.13306	0.64652	-1.89207
C	-2.67236	3.31604	0.859
H	-0.82912	2.58985	1.70573
C	-3.60139	3.18633	-0.17064
H	-4.11953	2.12337	-1.97322
H	-2.82297	4.05812	1.64133
H	-4.47937	3.82911	-0.20001
C	-1.62687	-1.4418	0.07656
C	-1.89243	-2.53878	-0.75403
C	-2.61948	-1.02784	0.9755
C	-3.12334	-3.18381	-0.70455
H	-1.12123	-2.88628	-1.43724
C	-3.84506	-1.67997	1.031
H	-2.42291	-0.18716	1.63869
C	-4.10464	-2.75695	0.18626
H	-3.31356	-4.0293	-1.36344
H	-4.60025	-1.34585	1.74034
H	-5.06633	-3.26571	0.22729
H	5.71043	0.21838	0.03975
H	5.2185	-2.19975	0.14124
H	2.75137	-4.12469	0.16884

TH-3565_186122020

List of Publications

1. Cyclometalated Ruthenium-Complex-Catalyzed Selective Oxidation of Olefins to Carbonyls.

   Konwar, M.; Das, A. *Org. Lett*. **2024**, *26*, 10235−10240.

2. Parts-Per-Million Level Loading Cyclometalated Ru(II)-NHC Catalyzed Selective Oxidation of Olefins to Carbonyls.

   Konwar, M.; Das, T.; Das, A. *Chem. Eur. J.* **2024**, e202403135.

3. Ru/O_2-Catalyzed Oxidative C−H Activation/Alkyne Annulation Using Quinoline-Functionalized NHC as a Directing and Functionalizable Group.

   Konwar, M.; Hazarika, N.; Das A. *Org. Lett.* **2024**, *26*, 2965−2970.

4. Ruthenium(II)-Catalyzed Oxidative Annulation of Imidazo[1,5-*a*]quinolin-2-iums Salts and Internal Alkynes *via* C−H Bond Activation.

   Konwar, M.; Hazarika, N.; Sarmah, B. K.; Das A. *Chem. Eur. J.* **2024**, e202401133.

5. Cyclometalated Ruthenium Catalyst Enables Selective Oxidation of *N*-Substituted Tetrahydroquinolines to Lactams.

   Konwar, M.; Das, T.; Das A. *Org. Lett.* **2024**, *26*, 1184−1189.

6. Carboxylic Acid Assisted Ru(II)-Catalyzed Annulation of Imidazo[1,5-*a*]quinoline with Alkynes *via* Double C−H Activation: A Direct Route to Functionalized Quinolizines.

   Konwar, M.; Hazarika, N.; Das A. *ChemCatChem*. **2025** (just accepted).

7. Facile Installation of *β*-Hydroxyarylethylamino Motifs at the C2-Position of Quinoline Moiety *via* Copper Catalysed [3+3]-Cycloaddition Reaction of *N*-oxide with *N*-Ts Aziridine.

   Konwar, M.; Das, T.; Naskar, A.; Murmu, R.; Das A. *Synlett* **2024**, *35*, 1446–1452.

8. Synthesis of π-Extended Imidazo[1,2-a]quinolines via Carboxylic Acid-Assisted Ru(II)-Catalyzed Dual C−H Activation and Alkyne Annulation.

   Hazarika, N.; **Konwar, M.;** Das, A. *Org. Lett.* **2024**, *26*, 10447−10452.

9. Copper-Catalyzed Oxidative Dehydrogenative Reaction of Quinoline-*N*-Oxides with Donor−Acceptor Cyclopropanes: Installation of a Tertiary Alkyl Motif at C2 Position.

   Sarmah, B. K.; **Konwar, M.;** Das, A. *Org. Lett.* **2021**, *23*, 8390−8395.

TH-3565_186122020

10. Site-Selective Deoxygenative Amination of Azine *N*-Oxides with Carbodiimides under Catalyst-, Activator-, Base-, and Solvent-Free Conditions.

    Sarmah, B. K.;† **Konwar, M.;**† Das, A. *J. Org. Chem.* **2021**, *86*, 10762–10772.

11. Boric acid catalyzed chemoselective reduction of quinolines.

    Bhattacharyya, D.; Nandi, S.; Adhikari, P.; Sarmah, B. K.; **Konwar, M.;** Das, A. *Org. Biomol. Chem.* **2020**, *18*, 1214–1220.

12. Regioselective Cyanation of Six-Membered *N*-Heteroaromatic Compounds Under Metal-, Activator-, Base- and Solvent-Free Conditions.

    Sarmah, B. K.; **Konwar, M.;** Bhattacharyya, D.; Adhikari, P.; Das, A. *Adv. Syn. Cat.* **2019**, *361*, 5616–5625.

List of Conferences

---

1. **30th International Conference on Organometallic Chemistry (ICOMC 2024)** from 14th-18th July 2024, Agra. Poster presentation with entitled "Cyclometalated ruthenium(II) complex as a catalyst for selective oxidation of *N*-substituted tetrahydroquinoline to lactam and as intermediate in aerobic alkyne annulation reaction." (**Best Poster Award**).

2. **International Conference on Modern Trends in Inorganic Chemistry (MTIC-XIX)** from 15th-17th December 2022, BHU, Varanasi. Poster presentation with entitled "Ru(II)-catalyzed aerobic oxidative annulation of imidazo[1,5-*a*]quinolin-2-ium salts with alkynes *via* *N*-heterocyclic carbene directed double C-H activation."

3. **Frontiers in Chemical Sciences - 2022 (FICS-2022)** from 2nd-4th December 2022, IIT Guwahati. Poster presentation with entitled "Copper-Catalyzed Oxidative Dehydrogenative Reaction of Quinoline-*N*-Oxides with Donor−Acceptor Cyclopropanes: Installation of a Tertiary Alkyl Motif at C2 Position."

4. **North-East Research Conclave (NERC)** from 20th-22nd May 2022, IIT Guwahati. Poster presentation with entitled "Site-Selective Deoxygenative Amination of Azine *N*-oxides with Carbodiimides under Catalyst-, Activator-, Base- and Solvent-Free Conditions."

5. **Chemical Research Society of India 28th National Symposium in Chemistry (CRSI NSC-28)** from 4th-6th February 2022, IIT Guwahati. Poster presentation with entitled "Site-Selective Deoxygenative Amination of Azine *N*-oxides with Carbodiimides under Catalyst-, Activator-, Base- and Solvent-Free Conditions."

6. **International Conference on Progress and Challenges in Modern Day Science (PCMDS-2021)** from 17h-18th June 2021, B. Borooah College, Assam. Poster presentation with entitled "Regioselective Cyanation of Six-Membered *N*-Heteroaromatic Compounds Under Metal-, Activator-, Base- and Solvent-Free Conditions."

7. **The Present and Future of Excellence in Organic Synthesis (PFEOS-2021)** from 7th-8th January 2021, Tezpur University, Assam. Poster presentation with entitled "Regioselective Cyanation of Six-Membered *N*-Heteroaromatic Compounds Under Metal-, Activator-, Base- and Solvent-Free Conditions."

TH-3565_186122020

भारतीय प्रौद्योगिकी संस्थान गुवाहाटी
Indian Institute of Technology Guwahati